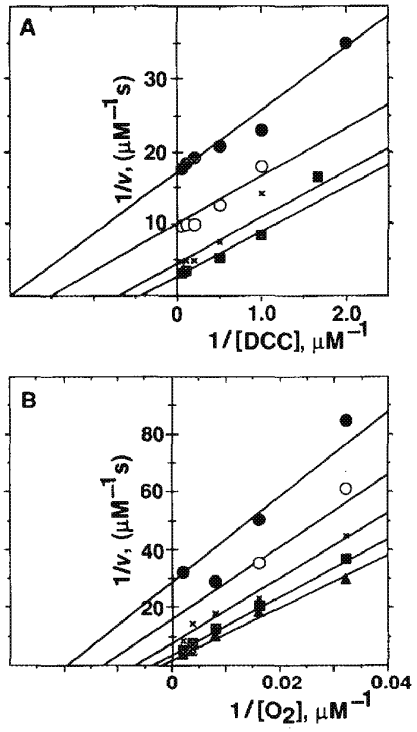


FIG. 6. Lineweaver–Burk plots of initial velocities of 3,5-dichlorocatechol 1,2-dioxygenase reaction in 0.05 M Tris–HCl buffer, pH 8.0, at 25°C. The amount of enzyme added was 3.6 μg. (A) 3,5-Dichlorocatechol concentrations, [DCC], were varied at fixed concentrations of O_2 (61.9, 124, 260, and 495 μM). (B) O_2 concentrations were varied at fixed concentrations of 3,5-dichlorocatechol (0.3, 0.5, 1.0, 2.0, and 10 μM).

was labile in the presence of higher $[O_2]$. Under the present conditions, the K_m values for 3,5-dichlorocatechol and oxygen were 4.40 and 652 μM, respectively. The k_{cat} value was 34.7 s^{-1} (Table II).

To examine the substrate specificity, catechol derivatives substituted at different positions were used as substrates. All the spectra of the products formed and their molar absorption coefficients (Table IV) were in good agreement with those of muconic acid derivatives, respectively (31). That is, no extradiol-cleaving activity was observed with any of the catechol derivatives. Using an air-saturated Tris–HCl buffer (pH 8.0), the apparent values of K_m and V_{max} were obtained from $[S]/v$ versus $[S]$ plots and specificity constants (k_{cat}/K_m) were calculated as given in Table IV. Chlorocatechols were good substrates and 3,5-dichlorocatechol had the highest specificity constant of 7.3 $\mu M^{-1}\ s^{-1}$. The specificity constant for catechol was 4% of that for 3,5-dichlorocatechol.

Inhibition studies. The results of inhibition studies are summarized in Table V. Heavy metal reagents used inhibited enzyme activity. Chelating agents, *o*-phenanthroline, tiron, and EDTA, showed a time-dependent inhibition, tiron being a more potent inhibitor than the others. Sulfhydryl reagents, iodoacetamide and *N*-ethylmaleimide, also time-dependently inhibited the activity.

DISCUSSION

No attempts have been made to purify 3,5-dichlorocatechol-degrading enzyme from any organism. This paper reports for the first time the purification and characterization of 3,5-dichlorocatechol-decomposing enzyme from a 2,4-D degrading bacterium, *P. cepacia* CSV90. This enzyme was found to be an intradiol-cleaving dioxygenase, named 3,5-dichlorocatechol 1,2-dioxygenase, and was deep red in color having a broad absorption with a peak at about 425 nm (Fig. 5A) which is a typical characteristic of ferric ion dioxygenases. This spectrum is similar to those of chlorocatechol 1,2-dioxygenase (11), protocatechuate 3,4-dioxygenase (29), and catechol 1,2-dioxygenase (30), all being intradiol-type nonheme ferric ion dioxygenases. The visible absorption spectrum of the anaerobic complex of the enzyme with the organic substrate is very similar to that reported for chlorocatechol dioxygenase (11), suggesting that the spectrum is due to a charge-transfer interaction of 3,5-dichlorocatechol with the ferric ion at the active site of the enzyme. Thus, these features indicated that the present enzyme was also a nonheme ferric ion dioxygenase.

The molecular weight of the native enzyme was determined to be 56,000 by light scattering method, while the

TABLE V

Inhibition Studies[a]

Reagent	Concentration (mM)	% Inhibition after incubation for 0 min	30 min	60 min
$HgCl_2$	1.0	90	100	100
$CuSO_4$	1.0	17	84	85
$MnCl_2$	1.0	8	34	41
$ZnCl_2$	1.0	57	100	100
$CoCl_2$	1.0	17	74	80
KCN	1.0	0	—[b]	9
o-Phenanthroline	0.1	0	—	12
Tiron	0.1	3	—	42
EDTA	0.1	3	—	17
Iodoacetamide	0.1	7	21	24
N-Ethylmaleimide	0.1	4	37	35

[a] The enzyme (10 μg) was incubated with each reagent as indicated in 0.05 M Tris–HCl buffer, pH 8.0, at 25°C in a volume of 2.8 ml. After 30 or 60 min, the remaining activity was polarographically measured by adding the substrate under the standard assay conditions. The activity at 0 min was measured by adding the enzyme to the mixture of the substrate and each reagent. As controls, the enzyme was incubated without any reagent under the same conditions, and the activity was taken as 100%, i.e., 0% inhibition.

[b] Not determined.

COR-AAD1-00002451
Bayer EX1008 (Part 5 of 9)

molecular weight of the enzyme denatured with 6 M guanidine–HCl or SDS was found to be ~30,000 (Fig. 3 and Table II). These results, together with the result of the determination of N-terminal sequence (Fig. 4), all suggest that native enzyme exists as a homodimer (α_2). Catechol 1,2-dioxygenase from *P. putida* mt-2 (32) and chlorocatechol dioxygenase from *P. putida* (11) are also homodimers; however, one of the catechol 1,2-dioxygenase isozymes from *P. arvilla* C-1 is a heterodimer (30) and protocatechuate 3,4-dioxygenase from *P. aeruginosa* is also composed of two different subunits (33).

The iron content of the enzyme was estimated to be ~1 mol/mol of enzyme (α_2Fe^{3+}), considering a molecular weight of 56,000. This stoichiometry of 1 iron/homodimer in the intradiol dioxygenases has also been reported for catechol 1,2-dioxygenases from *P. putida* mt-2 (32) and *Rhizobium leguminosarum* biovar *viceae* USDA2370 (34), and chlorocatechol dioxygenase from *P. putida* (11). We attempted to increase the specific activity of 3,5-dichlorocatechol 1,2-dioxygenase by providing external Fe^{3+} or Fe^{2+} in the assay buffer, or by adding iron by the method of Fujiwara and Nozaki (35), but these attempts failed to improve the specific activity.

The enzyme had only intradiol-cleaving activity and no extradiol-cleaving activity was observed. The substituents on the catechol ring had no effect on the intradiol cleavage activity, while catechol 1,2-dioxygenase cleaves 3-substituted catechols by both intradiol and extradiol cleavage (36). 3,5-Dichlorocatechol 1,2-dioxygenase showed a broad substrate specificity and cleaved catechol, 3-chloro-, 4-chloro-, 3-methyl-, 4-methyl-, and 3-methoxycatechol other than 3,5-dichlorocatechol by intradiol cleavage (Table IV). Among them, chloro-substituted catechols had high affinity for the enzyme (1.5–2.6 μM of K_m^a value in an air-saturated buffer), and 3,5-dichlorocatechol had the highest specificity constant (7.3 $\mu M^{-1}s^{-1}$) followed by 4-chloro- and 3-chloro-catechol. 3-Methoxycatechol, catechol, and 3-methycatechol had much lower specificity constants, the values being 2–7% of that of 3,5-dichlorocatechol. Similar results were obtained with chlorocatechol dioxygenase from *P. putida* (11). However, the specificity constants of 3-chloro-, 4-chloro-, and 3,5-dichloro-catechol for *P. putida* dioxygenase were similar to each other, 4-chlorocatechol having the highest k_{cat}/K_m value. That is, the present dioxygenase is more specific for 3,5-dichlorocatechol. In this connection, catechol 1,2-dioxygenase from *P. arvilla* C-1 and *P. putida* mt-2 showed negligible activity toward 4-chlorocatechol, the relative activity being 3–4% of that for catechol (30, 32). These results suggest that chlorocatechol dioxygenases may possess distinct steric and electronic properties around the substrate binding site and can easily accommodate the bulky chloro-substituted catechols.

The NH_2-terminal sequence up to 44 residues from the present dioxygenase (Fig. 4) did not reveal any similarity with those of catechol 1,2-dioxygenases from *P. arvilla* C-1 (30), *P. putida* mt-2 (32), and *Acinetobacter calcoaceticus* (37), and α- (38) and β-subunits (39) of protocatechuate 3,4-dioxygenase. However, a high degree of similarity was observed between chlorocatechol dioxygenases in the NH_2-terminal region. The DNA sequence of chlorocatechol dioxygenase (catechol 1,2-dioxygenase II) from *Alcaligenes eutrophus* JMP134 carrying the plasmid pJP4 revealed valine residue at the NH_2-terminal (40, 41), whereas in the present enzyme we found methionine residue at the NH_2-terminal. The remaining 43 amino acids from the NH_2-terminal were the same as those of the *A. eutrophus* enzyme. However, *A. eutrophus* enzyme has never been purified; therefore, the enzymatic properties including the substrate specificity are not known. On the other hand, the present sequence showed that 25 and 21 residues were the same as those of chlorocatechol dioxygenases from *P. putida* (pAC27) (40) and *Pseudomonas* sp. strain P51 (pP51) (42), respectively. However, as mentioned above, these enzymes did not have any preference for 3,5-dichlorocatechol (11, 42).

Purification of 3,5-dichlorocatechol 1,2-dioxygenase from *P. cepacia* CSV90 adds a new enzyme to the catechol 1,2-dioxygenase family. Recently a chlorocatechol dioxygenase activity in *Pseudomonas* sp. strain P51 which cleaves 3,4,6-trichlorocatechol has been reported (42); thus, we now have various halogenated-catechol dioxygenases. To investigate the mechanism of oxygen activation in the intradiol-type dioxygenases and to know how new enzymes evolve in response to the substrate availability, a family of chlorocatechol dioxygenases may be one of the best candidates, because we can comparatively analyze the structures and properties of these intradiol dioxygenases. Furthermore these studies may provide a clue to understand a detoxification mechanism of toxic pollutants, halogenated compounds. Gene cloning of 3,5-dichlorocatechol 1,2-dioxygenase, which would help us to elucidate the above problems, is now underway in our laboratory.

ACKNOWLEDGMENTS

We thank Drs. Seiki Kuramitsu and Hiroyuki Kagamiyama for the N-terminal amino acid sequence analysis of the dioxygenase, Dr. Hiromasa Tojo for his cooperation in determinations of molecular weight and amino acid composition, Drs. Hajime Sohmiya, Takahide Kimura, and Takashi Ando for their cooperation in measurements of ^1H and ^{13}C NMR, and Dr. Takehiro Kobayashi for his help and cooperation. Thanks are also due to Dr. Appaji Rao for his continuous encouragement during the course of this investigation.

REFERENCES

1. Schneider, M. J. (1979) Persistent Poisons: Chemical Pollutants in the Environment, N. Y. Acad. Sci., New York.
2. Hanify, J. A., Metcalf, P., Nobbs, C. L., and Worsley, K. J. (1981) *Science* **212**, 349–351.
3. Ghosal, D., You, I.-S., Chatterjee, D. K., and Chakrabarty, A. M. (1985) *Science* **228**, 135–142.

COR-AAD1-00002452
Bayer EX1008 (Part 5 of 9)

4. Evans, W. C., Smith, B. S. W., Fernley, H. N., and Davies, J. I. (1971) *Biochem. J.* **122,** 543–551.
5. Tiedje, J. M., and Alexander, M. (1969) *J. Agric. Food Chem.* **17,** 1080–1084.
6. Chaudhry, G. R., and Huang, G. H. (1988) *J. Bacteriol.* **170,** 3897–3902.
7. Don, R. H., Weightman, A. J., Knackmuss, H.-J., and Timmis, K. N. (1985) *J. Bacteriol.* **161,** 85–90.
8. Streber, W. R., Timmis, K. N., and Zenk, M. H. (1987) *J. Bacteriol.* **169,** 2950–2955.
9. Radjendirane, V., Bhat, M. A., and Vaidyanathan, C. S. (1991) *Arch. Biochem. Biophys.* **288,** 169–176.
10. Dorn, E., and Knackmuss, H.-J. (1978) *Biochem. J.* **174,** 73–84.
11. Broderick, J. B., and O'Halloran, T. V. (1991) *Biochemistry* **30,** 7349–7358.
12. Nakai, C., Hori, K., Kagamiyama, H., Nakazawa, T., and Nozaki, M. (1983) *J. Biol. Chem.* **258,** 2916–2922.
13. Dakin, H. D. (1909) *Am. Chem. J.* **42,** 477–498.
14. Nozaki, M., Kotani, S., Ono, K., and Senoh, S. (1970) *Biochim. Biophys. Acta* **220,** 213–223.
15. Lowry, O. H., Rosebrough, N. J., Farr, A. L., and Randall, R. J. (1951) *J. Biol. Chem.* **193,** 265–275.
16. Yonetani, T. (1961) *J. Biol. Chem.* **236,** 1680–1688.
17. Hayashi, Y., Matsui, H., and Takagi, T. (1989) *in* Methods in Enzymology (Fleischer, S., and Fleischer, B., Eds.), Vol. 172, pp. 514–528, Academic Press, San Diego.
18. Horiike, K., Tojo, H., Iwaki, M., Yamano, T., and Nozaki, M. (1982) *Biochem. Int.* **4,** 477–483.
19. Horiike, K., Tojo, H., Yamano, T., and Nozaki, M. (1983) *J. Biochem.* **93,** 99–106.
20. Ackers, G. K. (1967) *J. Biol. Chem.* **242,** 3237–3238.
21. Fish, W. W. (1975) *in* Methods in Membrane Biology (Korn, E. D., Ed.), Vol. 4, pp. 189–276, Plenum, New York.
22. Tojo, H., Horiike, K., Shiga, K., Nishina, Y., Miura, R., Watari, H., and Yamano, T. (1982) *J. Biochem.* **92,** 1741–1752.
23. Tojo, H., Horiike, K., Shiga, K., Nishina, Y., Nozaki, M., Watari, H., and Yamano, T. (1984) *J. Biochem.* **95,** 1–6.
24. Ui, N. (1979) *Anal. Biochem.* **97,** 65–71.
25. Laemmli, U. K. (1970) *Nature* **227,** 680–685.
26. Edelhoch, H. (1967) *Biochemistry* **6,** 1948–1954.
27. Ellman, G. L. (1959) *Arch. Biochem. Biophys.* **82,** 70–77.
28. Zimmerman, C. L., Appella, E., and Pisano, J. J. (1977) *Anal. Biochem.* **77,** 569–573.
29. Fujisawa, H., and Hayaishi, O. (1968) *J. Biol. Chem.* **243,** 2673–2681.
30. Nakai, C., Horiike, K., Kuramitsu, S., Kagamiyama, H., and Nozaki, M. (1990) *J. Biol. Chem.* **265,** 660–665.
31. Dorn, E., and Knackmuss, H.-J. (1978) *Biochem. J.* **174,** 85–94.
32. Nakai, C., Nakazawa, T., and Nozaki, M. (1988) *Arch. Biochem. Biophys.* **267,** 701–713.
33. Yoshida, R., Hori, K., Fujiwara, M., Saeki, Y., Kagamiyama, H., and Nozaki, M. (1976) *Biochemistry* **15,** 4048–4053.
34. Chen, Y. P., and Lovell, C. R. (1990) *Appl. Environ. Microbiol.* **56,** 1971–1973.
35. Fujiwara, M., and Nozaki, M. (1973) *Biochim. Biophys. Acta* **327,** 306–312.
36. Fujiwara, M., Golovleva, L. A., Saeki, Y., Nozaki, M., and Hayaishi, O. (1975) *J. Biol. Chem.* **250,** 4848–4855.
37. Neidle, E. L., Hartnett, C., Bonitz, S., and Ornston, L. N. (1988) *J. Bacteriol.* **170,** 4874–4880.
38. Kohlmiller, N. A., and Howard, J. B. (1979) *J. Biol. Chem.* **254,** 7309–7315.
39. Iwaki, M., Kagamiyama, H., and Nozaki, M. (1981) *Arch. Biochem. Biophys.* **210,** 210–223.
40. Ghosal, D., and You, I.-S. (1988) *Mol. Gen. Genet.* **211,** 113–120.
41. Perkins, E. J., Gordon, M. P., Caceres, O., and Lurquin, P. F. (1990) *J. Bacteriol.* **172,** 2351–2359.
42. van der Meer, J. R., Eggen, R. I. L., Zehnder, A. J. B., and de Vos, W. M. (1991) *J. Bacteriol.* **173,** 2425–2434.

COR-AAD1-00002453
Bayer EX1008 (Part 5 of 9)

JOURNAL OF BACTERIOLOGY, Sept. 1988, p. 3897–3902
0021-9193/88/093897-06$02.00/0
Copyright © 1988, American Society for Microbiology
Vol. 170, No. 9

Isolation and Characterization of a New Plasmid from a *Flavobacterium* sp. Which Carries the Genes for Degradation of 2,4-Dichlorophenoxyacetate†

G. RASUL CHAUDHRY* AND G. H. HUANG

Institute of Food and Agricultural Sciences, G159 McCarty Hall, University of Florida, Gainesville, Florida 32611

Received 19 February 1988/Accepted 7 June 1988

A *Flavobacterium* sp. (strain 50001), capable of degrading 2,4-dichlorophenoxyacetate (2,4-D), 2-methyl-4-chlorophenoxyacetate, and 2-chlorobenzoate and imparting resistance to mercury, harbored a degradative plasmid, pRC10. Cured strains of the *Flavobacterium* sp. lost the plasmid as well as the ability to degrade these chlorinated compounds. Comparison of this plasmid with the well-characterized 2,4-D-degradative plasmid pJP4 from *Alcaligenes eutrophus* showed regions of homology between the two plasmids. Restriction fragments of plasmid pRC10 which shared homology with the regions conferring 2,4-D-degradative genes (*tfd*) of plasmid pJP4 were cloned into a broad-host-range plasmid and studied in *Pseudomonas putida*. From the results obtained, the cloned DNA fragment expressed the genes for 2,4-D monooxygenase (*tfdA*) and 2,4-dichlorophenol hydroxylase (*tfdB*). In spite of the similarity in function, the size (45 kilobases) and restriction pattern of plasmid pRC10 were considerably different from those of pJP4 (80 kilobases). This may be due to the difference in the microbial background during evolution of the two plasmids.

Many of the microorganisms capable of metabolizing synthetic organic compounds harbor large degradative plasmids (15, 22, 36). The degradative plasmids which are involved in the catabolism of toluene and naphthalene are the best-characterized plasmids among this group (11, 16, 18, 26, 27, 35). Recently, plasmids involved in the degradation of 2,4-dichlorophenoxyacetic acid (2,4-D) have also been under considerable investigation (1, 8–10, 29). These plasmids range from 80 to 120 kilobase pairs (kb) in size and have been predominantly isolated from members of the genus *Alcaligenes*, obtained from soil or aquatic environments (1, 8). One of these plasmids, pJP4 from *Alcaligenes eutrophus*, has been investigated more extensively (9, 10, 29).

Several other microorganisms belonging to a variety of different bacterial genera, such as *Acinetobacter*, *Arthrobacter*, *Corynebacterium*, *Flavobacterium*, and *Pseudomonas*, have also been shown to degrade 2,4-D and related phenoxyacetates (2, 4, 8, 12, 14, 28, 30–32, 34; A. W. Ogram, M.S. thesis, University of Florida, Gainesville, 1984). Unlike *Alcaligenes*, little information is available on the mechanism of 2,4-D degradation by these microorganisms. Furthermore, the occurrence and nature of the 2,4-D-degradative plasmids in these microorganisms are not known. It should be of interest to isolate the plasmids from microorganisms other than *Alcaligenes* spp. and to compare them with the well-characterized plasmid pJP4. This may help us to understand how plasmids with the same function have evolved in different microbial backgrounds.

In this paper, we present initial results of a study designed to investigate the mechanism of degradation of 2,4-D in a previously isolated *Flavobacterium* sp. (Ogram, M.S. thesis). This bacterium resembles *A. eutrophus* in degradative properties (8) and was found to harbor a degradative plasmid, pRC10. This plasmid showed considerable differences in size and restriction patterns from plasmid pJP4 (from *A. eutrophus*). We report the physical map of pRC10 and compare its regions of homology with those of pJP4, as well as the cloning of its degradative genes.

* Corresponding author.

† Florida Agricultural Experiment Station Journal Series No. 7998.

MATERIALS AND METHODS

Bacterial strains and plasmids. The bacteria and plasmids used in this study are listed in Table 1.

Media and growth conditions. The *Flavobacterium* sp. and *Alcaligenes eutrophus* strains were grown at 28°C aerobically in minimal medium (MM) (5) supplemented with 2,4-D or other compounds as the sole source of carbon. *Escherichia coli* strains were grown in LB medium (5). The medium used for growing *Pseudomonas putida* has been described elsewhere (34). A nalidixic acid-resistant mutant of *P. putida* was obtained by selecting resistant colonies on heavily inoculated LB agar plates containing nalidixic acid (50 μg/ml) (Sigma Chemical Co.). The autoclaved medium was supplemented with antibiotics and metal salts by using sterile stock solutions as needed.

Detection and isolation of plasmid DNA. An estimated 10^8 exponentially growing cells were suspended in E buffer (21) containing 25% sucrose, lysozyme (2 mg/ml) and RNase (100 μg/ml). The cell suspension was then poured into the front wells of an 0.7% agarose gel in E buffer. A second series of wells immediately behind the front wells were filled with a lysis solution containing 1% sodium dodecyl sulfate (SDS) and 0.5% agarose in E buffer. Electrophoresis was first carried out for 30 min at 20 V for electrophoretic transfer of SDS into the front wells for cell lysis and then for 3 h at 100 V for fractionation of the DNA. *E. coli* plasmids were isolated by the method of Birnboim and Doly (3). Plasmid DNA from the *Flavobacterium* sp. and *A. eutrophus* was isolated by a previously described method (6).

The *Flavobacterium* sp. was cured of the plasmid by treating the exponentially growing cells (in LB) with streptomycin (100 μg/ml) overnight. The cells were then diluted, plated on LB agar plates, and checked for growth on MM containing 2,4-D and for the presence of the plasmid.

Analysis of DNA fragments and restriction mapping. Re-

Downloaded from http://jb.asm.org/ on September 3, 2020 at Corteva Agriscience

COR-AAD1-00002454

Bayer EX1008 (Part 5 of 9)

TABLE 1. Bacterial strains and plasmids

Strain or plasmid	Plasmid	Relevant traits	Source or reference
Flavobacterium sp.			
50001	pRC10	2,4-D$^+$ Hg^r	Ogram, thesis
50183	Cured	2,4-D$^-$ Hg^s	This study
Alcaligenes eutrophus			
50007 (JMP134)	pJP4	2,4-D$^+$ Hg^r	J. M. Pemberton (8)
50009 (JMP228)	Cured	2,4-D$^-$ Hg^s Str^r	J. M. Pemberton
Escherichia coli			
50008 (HB101)		*leu-6 pro thi-2 recA lacY hsdR rpsL*	21
S17-1		Mobilizing strain	R. Simon (23)
Pseudomonas putida			
PRS2015		Prototroph	A. M. Chakrabarty (33)
Plasmids			
pLOI193		Broad host range, *mob* (RSF1010), *mob* (RP4), Tc^r Cm^r	L. O. Ingram (7)
pKL400		Ap^r *galK*	K. McKenney
pRC220		*Hin*dIII-B of pJP4 cloned into pBR322	This study
pRC10EA		*Eco*RI-A of pRC10 cloned into pBR322	This study
pRC10AF		Ap^r *tfdA*	This study
pRC10PF		Tc^r *tfdB*	This study
pRC301		Tc^r *tfdA tfdB*	This study
pRC305		Cm^r *tfdA*	This study
pRC310		Cm^r *tfdB*	This study

striction endonucleases were purchased from U.S. Biochemical Corp., Cleveland, Ohio. Enzyme digestions were performed as specified by the manufacturer. Samples were subjected to agarose gel electrophoresis for fractionation of DNA. Sizes of restriction fragments were determined with reference to bacteriophage lambda DNA digested with *Hin*dIII or with both *Hin*dIII and *Eco*RI. Mapping of plasmid pRC10 was carried out by comparing the results of digestion with pairwise combinations of enzymes as well as partial digestions.

Ligation, transformation, and agarose gel electrophoreses were performed as described previously (21). For transfer of plasmids into microorganisms by conjugation, a procedure similar to that described by Simon et al. (23) was used. Overnight-grown cells were diluted 1:50 in 10 ml of the medium in a 250-ml flask and then incubated for 5 h at 30°C. Donor and recipient cells of approximately the same density were mixed in Eppendorf tubes (ratio, 1:1) and centrifuged for 30 s. The pellet was carefully suspended in 50 μl of medium, transferred onto nitrocellulose filters (pore size, 0.2 μm; diameter, 25 mm) which had been placed on prewarmed fresh plates, and incubated at 30°C for matings. After overnight incubation the cells were suspended, diluted in the medium, and plated on solid medium containing appropriate antibiotics for donor counter selection.

Southern hybridization. Hybridization was carried out by a modified Southern method (26). To prepare probes, DNA fragments were labeled by nick translation (21) with [^{32}P]dATP as the labeled precursor.

Oxygen uptake assays. Cell cultures (250 ml) were grown to late log phase in MM containing 2,4-D for the *Flavobacterium* sp. and *A. eutrophus* JMP134. Strains harboring recombinant plasmids were grown overnight in LB medium containing appropriate antibiotics, harvested by centrifugation, washed three times in cold MM, and suspended in MM to an optical density at 420 nm (A_{420}) of 30. Enzyme analysis was performed at 30°C (29). Protein was determined by the method of Lowry et al. (20). The assay was carried out in a volume of 1.5 ml. The reaction mixture contained MM saturated with oxygen and cell suspension (1:9) to a final A_{420} value of 3. After the background level of oxygen uptake was estimated, the reaction was started by adding a final concentration of 1 mM 2,4-D or 0.2 mM 2,4-dichlorophenol, and the linear decrease in oxygen concentration was measured over 15 min. Controls were run simultaneously with the strains without plasmids.

RESULTS

Properties of the *Flavobacterium* sp. The *Flavobacterium* sp. has been reported to degrade 2,4-D (Ogram, thesis). It was further observed that this bacterium was resistant to $HgCl_2$ (147 μM) and can also utilize additional chlorinated compounds, including 3-chlorobenzoate (3-CBA) and 2-methyl-4-chlorophenoxyacetic acid (MCPA), as a sole source of carbon. Such growth characteristics are similar to the properties of *A. eutrophus* (8). The *Flavobacterium* sp. was resistant to several antibiotics, including lincomycin (25 μg/ml), tetracycline (30 μg/ml), carbenicillin, kanamycin, mikamycin, and neomycin (50 μg/ml), and ampicillin (100 μg/ml), as well as to heavy metals such as cobalt, copper, and zinc (added as 40 μg of the chloride or sulfate salt per ml). Since *A. eutrophus* harbors a plasmid, pJP4 (9, 10, 29), coding for 2,4-D-degradative genes (Fig. 1), it was conceivable that the *Flavobacterium* sp. contained a similar plasmid. The presence of a single plasmid, pRC10 (Table 2), was confirmed by plasmid detection and isolation from this microorganism. The growth of the *Flavobacterium* sp. in the presence of streptomycin as a curing agent resulted in a putative cured strain (at a frequency of 1 to 2%) which had simultaneously lost both pRC10 and its ability to grow on the chlorinated compounds. However, the antibiotic resistance properties of the *Flavobacterium* sp. were not affected by curing of the plasmid. The cured strain (50183) did not revert to the 2,4-D$^+$ phenotype at detectable levels as tested (<1 in 10^{10}), nor did it retain the ability to utilize 3-CBA or MCPA or resistance to Hg. Also, enzyme activities for 2,4-D monooxygenase and 2,4-dichlorophenol hydroxylase were detected in wild-type but not in cured derivatives of the *Flavobacterium* sp. (Table 3).

Physical map of plasmid pRC10. By using a combination of restriction analysis, gene cloning, and Southern hybridization (as described below), a physical map of pRC10 was developed (Fig. 2). This map is relatively simpler than the

Downloaded from http://jb.asm.org/ on September 3, 2020 at Corteva Agriscience

COR-AAD1-00002455

Bayer EX1008 (Part 5 of 9)

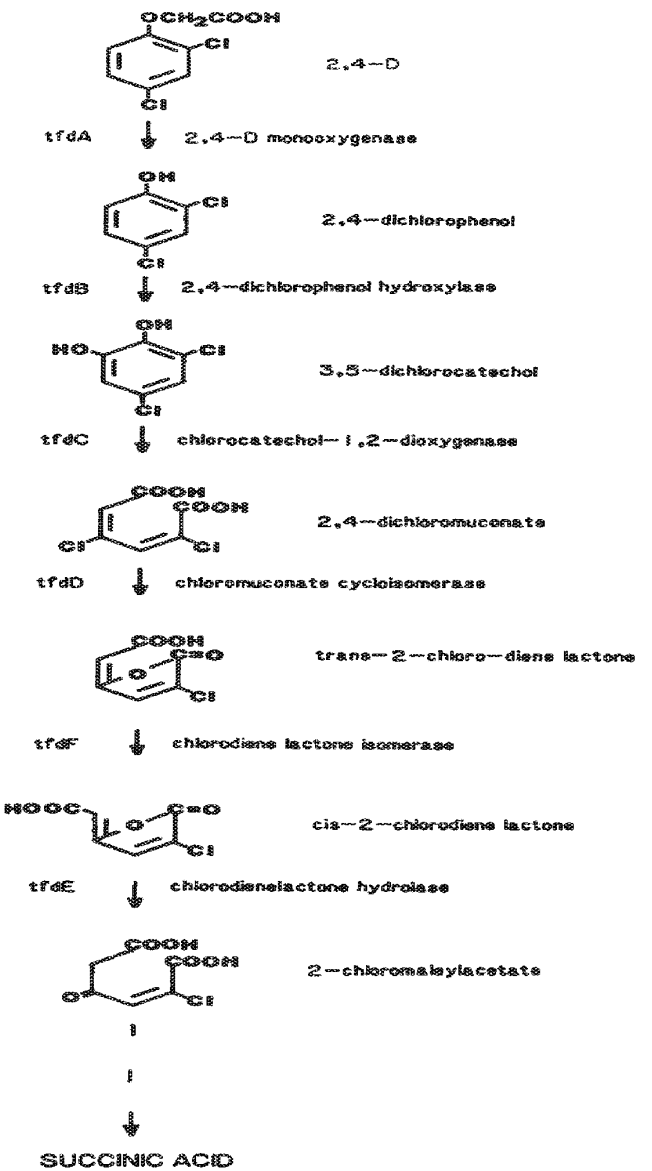


FIG. 1. Proposed 2,4-D-degradative pathway and the enzymes and genes encoding them (adapted from references 9, 10, 12, 14, 28, and 31).

TABLE 2. Comparison of restriction fragments of pRC10 and pJP4[a]

Fragment	Size (kb)					
	*Bam*HI		*Eco*RI		*Hin*dIII	
	pRC10	pJP4	pRC10	pJP4	pRC10	pJP4
A	35.0	39.4	31.0	28.8	23.0	34.7
B	8.0	14.4	9.6	14.5	16.0	22.2
C	2.0	11.9	4.5	10.6	3.5	8.0
D		6.5		9.9	3.0	6.4
E		3.6		8.3		4.1
F		3.3		3.2		2.0
G				1.9		1.6
H				1.7		1.4
I				1.2		
Total	45.0	79.1	45.1	80.1	45.5	80.4

[a] Sizes of DNA fragments of pRC10 were estimated by using bacteriophage lambda DNA cleared with restriction enzymes as standards as described in the text. Sizes of DNA fragments of pJP4 were taken from Don and Pemberton (9).

map of pJP4. As with its relative size, pRC10 has approximately half as many restriction sites as does pJP4.

DNA hybridization. The homology between pRC10 and pJP4, a well-characterized 2,4-D-degradative plasmid (10, 29), was investigated by Southern hybridization. First, pRC10 was used as a probe, and it hybridized to all of the restriction fragments of pJP4 except fragments *Bam*HI-D, *Eco*RI-A and -G, *Hin*dIII-A and -E to -H, and *Pst*I-C, -F, -G, and -H. This indicated that pRC10 had homology only with the regions of pJP4 encoding 2,4-D-degradative enzymes (data not shown). Subsequently, the location of the degradative genes on plasmid pRC10 was determined. This was accomplished by preparing two probes comprising isolated DNA fragments *Eco*RI-B and *Eco*RI-*Xba*I (from *Hin*dIII-B) of pJP4, which contain *tfdB-tfdF* genes and a part of the *tfdA* gene, respectively, and hybridizing them with the Southern blots of pRC10. It was found that the former probe hybridized with several of the restriction fragments of pRC10. However, the fragment *Eco*RI-A of pRC10 alone showed the most homology (Fig. 3A and B). This probe also hybridized weakly with fragments *Eco*RI-C and -D of pJP4, because the DNA used for preparation of the probe was slightly contaminated with these fragments. The fragments *Eco*RI-C and -D of pJP4 did not hybridize with pRC10 (data not shown). The

TABLE 3. Enzyme activities of microorganisms

Strain	Plasmid	Relative activity (%)[a]	
		2,4-D monooxygenase	2,4-Dichlorophenol hydroxylase
Flavobacterium sp.			
50001	pRC10	100	100
50183	None	<1	<1
A. eutrophus			
JMP134	pJP4	90	92
JMP228	None	<1	<1
P. putida (N1d")			
	pRC301	90	41
	pRC305	80	ND[b]
	pRC310	ND	65

[a] Expressed as percentages of the activities obtained with strain 50001 harboring plasmid pRC10.
[b] ND, Not determined.

Downloaded from http://jb.asm.org/ on September 3, 2020 at Corteva Agriscience

COR-AAD1-00002456

Bayer EX1008 (Part 5 of 9)

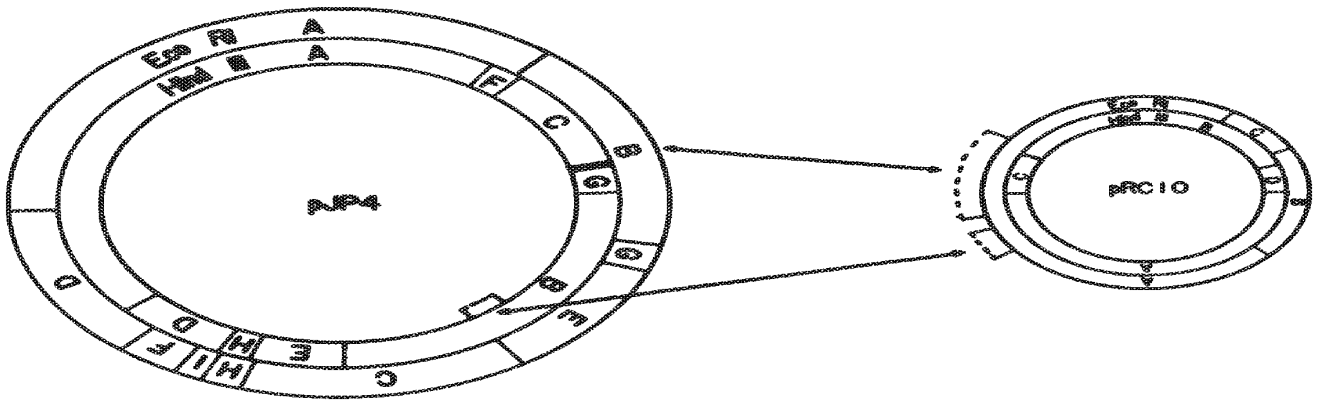


FIG. 2. Physical maps of plasmids pJP4 and pRC10, harboring 2,4-D-degradative genes in common. Regions of homology in pRC10 to *Eco*RI fragment B (*tfdB-tfdF*) and the *Eco*RI-*Xba*I segment from *Hin*dIII-B (part of *tfdA*) of pJP4 are shown by arrows.

second probe, (*Eco*RI-*Xba*I), which comprised only a part of *tfdA*, also hybridized to restriction fragments *Acc*I-F, *Eco*RI-A, *Hin*dIII-A, *Pst*I-C and -I, and *Pvu*I-F of pRC10 (Fig. 3A and C).

Cloning and location of *tfd* genes. The fragment *Eco*RI-A of pRC10 which showed homology with pJP4 was cloned into pKL400 (Fig. 4). The resulting plasmid, designated pRC10EA, contained *tfdA* and *tfdB* and possibly other degradative genes as well (see below). *E. coli* carrying pRC10EA exhibited low levels of 2,4-D monooxygenase (*tfdA*) activity as judged by the in vitro release of $^{14}CO_2$ from ^{14}C-labeled 2,4-D (data not presented). Since the fragment *Eco*RI-A of pRC10 is quite large (31 kb) and also hybridized to fragment *Eco*RI-B of pJP4, it was reasonable to presume that it also harbored other degradative genes. The fragment *Eco*RI-A was then cloned into plasmid pLOI193 (Fig. 4) in *E. coli* S17-1, and the resulting plasmid (pRC301) was transferred into *P. putida* (Nid^r) by conjugation to study expression of the degradative genes. The results (Table 3) show that *P. putida* harboring pRC301 exhibited 2,4-D monooxygenase and 2,4-dichlorophenol hydroxylase activities (*tfdB*).

To subclone the *tfdA* and *tfdB* genes, the following strategy was used. First, the 2.3-kb fragment (*Acc*I) isolated from fragment *Eco*RI-A of pRC10 which hybridized to the frag-

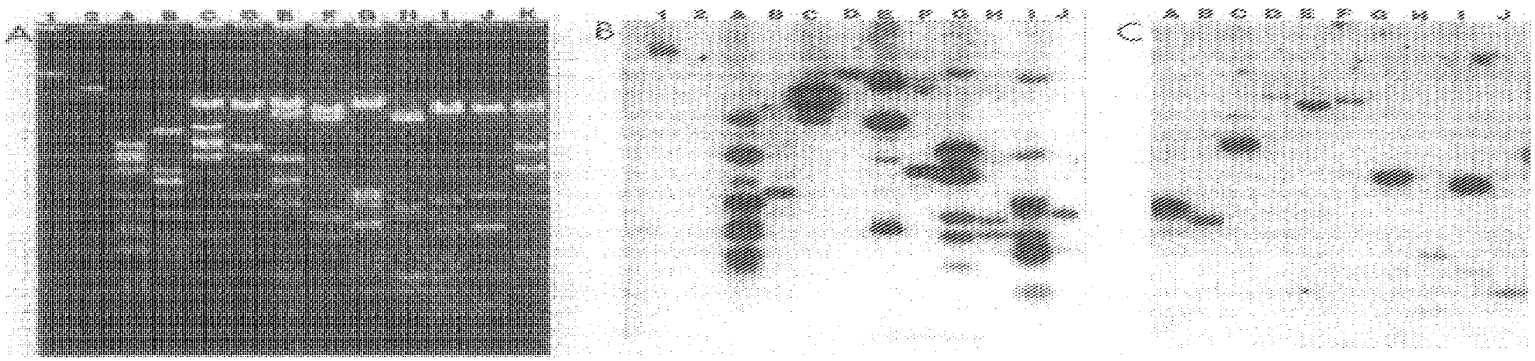


FIG. 3. Southern blot analysis for localization of degradative genes on pRC10. (A) DNA gel profile of plasmids pJP4 and pRC10. (B) Southern blot probed with *Eco*RI fragment B harboring the *tfdB-tfdF* genes of pJP4. To isolate probe DNA, *Eco*RI restriction digests of pJP4 were fractionated by agarose gel electrophoresis, and *Eco*RI fragment B was electroeluted. (C) Southern blot probed with the *Eco*RI-*Xba*I fragment containing part of the *tfdA* gene of pJP4. Plasmid pRC220 was used to isolate probe DNA by restriction digestion and electroelution. Plasmids: undigested (lanes 1, pJP4, and 2, pRC10) and digested with *Acc*I (lanes A, pJP4, and B, pRC10); *Eco*RI (lanes C, pJP4, and D, pRC10); *Hin*dIII (lanes E, pJP4, and F, pRC10); *Pst*I (lanes G, pJP4, and H, pRC10); and *Pvu*I (lanes I, pJP4, and J, pRC10). Molecular weight standards, bacteriophage lambda DNA cleaved with *Hin*dIII, are shown in lane K. Arrow in panel b, lane 2, indicates the low-intensity band of pRC10.

Downloaded from http://jb.asm.org/ on September 3, 2020 at Corteva Agriscience

COR-AAD1-00002457

Bayer EX1008 (Part 5 of 9)

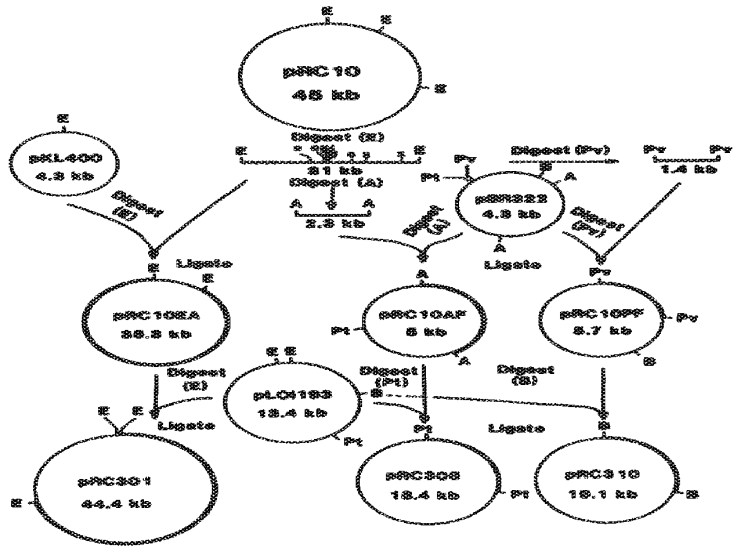


FIG. 4. Construction of plasmids. The inserts are represented by heavy lines. The restriction sites shown are: A, *Acc*I; B, *Bam*HI; E, *Eco*RI; H, *Hin*dIII; Pt, *Pst*I; Pv, *Pvu*I; and X, *Xba*I.

ment *Eco*RI-*Xba*I of pJP4 (Fig. 3C) was cloned into pBR322. The resulting plasmid, designated pRC10AF, was then digested with *Pst*I and cloned into the *Pst*I site of pLOI193 to generate plasmid pRC305 (Fig. 4). *P. putida* harboring pRC305 exhibited 2,4-D monooxygenase activity (Table 3). Second, the 1.4-kb fragment (*Pvu*I) again isolated from the digests of *Eco*RI-A of pRC10 was cloned into the *Pvu*I site of pBR322. The resulting plasmid, pRC10PF, was then digested with *Bam*HI and cloned into the *Bam*HI site of pLOI193 to generate plasmid pRC310 (Fig. 4). *P. putida* harboring pRC310 showed 2,4-dichlorophenol hydroxylase activity (Table 3).

DISCUSSION

We have isolated a new degradative plasmid, pRC10, from a *Flavobacterium* sp. capable of metabolizing 2,4-D and other chlorinated compounds such as 3-CBA and MCPA. The size and restriction pattern (Table 2 and Fig. 3A) of this plasmid were found to be considerably different from those of previously reported plasmids with similar functions isolated from species of *Alcaligenes* (1, 8). However, plasmid pRC10 showed homology (Fig. 2) with regions of pJP4 (fragments *Eco*RI-B and *Hin*dIII-B) coding for the degradative genes (*tfdABCDEF*) (9, 10, 29). When these fragments or their parts were used as probes containing the *tfd* genes, they all hybridized with fragment *Eco*RI-A of pRC10 (Fig. 3). Cloning of fragment A, first into pKL400 (plasmid pRC10EA) and then into pLOI193 (plasmid pRC301), revealed that it carried at least the first two genes (*tfdA* and *tfdB*) of the pathway of 2,4-D catabolism in this *Flavobacterium* sp. However, the restriction map of this fragment did not match the fragments (*Eco*RI-B and *Hin*dIII-B) of pJP4 which harbor the known *tfd* genes (Fig. 4). From this fragment, we were able to subclone two genes, *tfdA* and *tfdB*, by using a broad-host-range plasmid, pLOI193. The cloned genes were expressed in *P. putida* (Table 3). To determine whether the remaining *tfd* genes are also present on the same fragment requires further investigation. It would be interesting to determine differences in structure and expression of the gene (i.e., *tfdA*) coding for an identical function from the two different bacterial sources.

Plasmid pRC10 did not hybridize with regions of pJP4 (fragments *Eco*RI-A and *Hin*dIII-A) which have been reported to harbor the conjugative, incompatibility, replication, and maintenance functions (9). Unlike pJP4, the *tfd* genes on pRC10 were present in a region with fewer restriction sites (Table 2 and Fig. 3). This suggests that pRC10 may be different from pJP4 not only in the functions listed above, but also in the restriction map of its *tfd* genes. Interestingly, the cloning results support such an hypothesis. The DNA fragment encoding *tfdA* from pRC10 hybridized with the part of *tfdA* from pJP4 used as a probe. However, this fragment also had a different restriction map (manuscript in preparation) from that of the gene recently reported from pJP4 (29).

Degradative plasmids such as TOL, NAH, SAL, etc., of *Pseudomonas* spp. demonstrate appreciable homology with one another, suggesting evolutionary interrelationships (13, 17, 19). More recently, TOL genes have also been localized on the chromosome of a strain of *P. putida* (24). The chromosomal DNA segment conferring the degradative genes was reported to be almost identical to the same region found in the TOL plasmid pWW0. Relationships among the other isofunctional plasmids, such as those involved in the degradation of 2,4-D, evolved in different microbial backgrounds, are not well understood. A comparative study of pRC10 and pJP4 should further our understanding of the unique differences and evolutionary relationships between such plasmids.

ACKNOWLEDGMENTS

We thank L. T. Ou and J. M. Pemberton for providing the strains essential for our study, L. O. Ingram, K. T. Shanmugan, and G. Bitton for reviewing the manuscript, and T. Thomas for expert typing.

This work was partially supported by funds from the Center for Natural Resources, IFAS, University of Florida, and by the Florida Agricultural Experiment Station.

LITERATURE CITED

1. **Amy, P. S., J. W. Schulke, L. M. Frazier, and R. J. Seidler.** 1985. Characterization of aquatic bacteria and cloning of genes specifying partial degradation of 2,4-dichlorophenoxyacetic acid. Appl. Environ. Microbiol. 49:1237–1245.
2. **Bell, G. R.** 1957. Some morphological and biochemical characteristics of a soil bacterium which decomposes 2,4-dichlorophenoxyacetic acid. Can. J. Microbiol. 3:821–840.
3. **Birnboim, H. C., and J. Doly.** 1979. A rapid alkaline extraction procedure for screening recombinant plasmid DNA. Nucleic Acids Res. 7:1513–1523.
4. **Bollag, J. M., C. S. Helling, and M. Alexander.** 1968. 2,4-D metabolism: enzymatic hydroxylation of chlorinated phenols. J. Agric. Food Chem. 16:826–828.
5. **Chaudhry, G. R., and A. N. Ali.** 1988. Bacterial metabolism of carbofuran. Appl. Environ. Microbiol. 54:1414–1419.
6. **Chaudhry, G. R., and W. B. Wheeler.** 1988. Biodegradation of carbamates, p. 15-1 to 15-7. *In* Proceedings of the International Conference on Water and Wastewater Microbiology, New Port Beach, Calif.

Downloaded from http://jb.asm.org/ on September 3, 2020 at Corteva Agriscience

COR-AAD1-00002458

Bayer EX1008 (Part 5 of 9)

7. **Conway, T., M. O.-K. Byun, and L. O. Ingram.** 1987. Expression vector for *Zymomonas mobilis*. Appl. Environ. Microbiol. **53**:235–241.
8. **Don, R. H., and J. M. Pemberton.** 1981. Properties of six pesticide degradation plasmids isolated from *Alcaligenes eutrophus* and *Alcaligenes paradoxus*. J. Bacteriol. **145**:681–686.
9. **Don, R. H., and J. M. Pemberton.** 1985. Genetic and physical map of the 2,4-dichlorophenoxyacetic acid-degradative plasmid pJP4. J. Bacteriol. **161**:466–468.
10. **Don, R. H., A. J. Weightman, H. J. Knackmuss, and K. N. Timmis.** 1985. Transposon mutagenesis and cloning analysis of the pathways for degradation of 2,4-dichlorophenoxyacetic acid and 3-chlorobenzoate in *Alcaligenes eutrophus* JMP134(pJP4). J. Bacteriol. **161**:85–90.
11. **Dunn, N. W., and I. C. Gunsalus.** 1973. Transmissible plasmid coding early enzymes of naphthalene oxidation in *Pseudomonas putida*. J. Bacteriol. **114**:974–979.
12. **Evans, W. C., B. S. W. Smith, H. N. Fernley, and J. I. Davies.** 1971. Bacterial metabolism of 2,4-dichlorophenoxyacetate. Biochem. J. **122**:543–551.
13. **Farrell, R., and A. M. Chakrabarty.** 1979. Degradative plasmids: molecular nature and mode of evolution, p. 97–109. *In* K. N. Timmis and A. Puhler (ed.), Plasmids of medical, environmental and commercial importance. Elsevier/North-Holland Biomedical Press, Amsterdam.
14. **Gaunt, J. K., and W. C. Evans.** 1971. Metabolism of 4-chloro-2-methylphenoxyacetate by a soil pseudomonad: ring-fission, lactonizing and delactonizing enzymes. Biochem. J. **122**:533–542.
15. **Ghosal, D., I. S. You, D. K. Chatterjee, and A. M. Chakrabarty.** 1985. Microbial degradation of halogenated compounds. Science **228**:135–228.
16. **Harayama, S., R. A. Leppil, M. Rekik, N. Mermod, P. R. Lehrbach, W. Reineke, and K. N. Timmis.** 1986. Gene order of the TOL catabolic plasmid upper pathway operon and oxidation of both toluene and benzyl alcohol by the *xylA* product. J. Bacteriol. **167**:455–461.
17. **Heinaur, A. L., C. J. Duggleby, and P. Broda.** 1978. Molecular relationships of degradative plasmids determined by *in situ* hybridization of their endonuclease-generated fragments. Mol. Gen. Genet. **160**:347–351.
18. **Inouye, S., A. Nakazawa, and T. Nakazawa.** 1987. Overproduction of the *xylS* gene product and activation of the *xylDLEGF* operon on the TOL plasmid. J. Bacteriol. **169**:3587–3592.
19. **Lehrbach, P. R., I. McGregor, J. M. Ward, and P. Broda.** 1983. Molecular relationships between *Pseudomonas* IncP-9 degradative plasmids TOL, NAH and SAL. Plasmids **10**:164–174.
20. **Lowry, O. H., N. J. Rosebrough, A. L. Farr, and R. J. Randall.** 1951. Protein measurement with the Folin phenol reagent. J. Biol. Chem. **193**:265–275.
21. **Maniatis, T., E. F. Fritsch, and J. Sambrook.** 1982. Molecular cloning: a laboratory manual. Cold Spring Harbor Laboratory, Cold Spring Harbor, N.Y.
22. **Pemberton, J. M.** 1983. Degradative plasmids. Int. Rev. Cytol. **84**:155–183.
23. **Simon, R., U. Priefer, and A. Puhler.** 1983. A broad host range mobilization system for *in vivo* genetic engineering: transposon mutagenesis in gram-negative bacteria. Biotechnology **1**:784–791.
24. **Sinclair, M. I., P. C. Maxwell, B. R. Lyon, and B. W. Holloway.** 1987. Chromosomal location of TOL plasmid DNA in *Pseudomonas putida*. J. Bacteriol. **168**:1302–1308.
25. **Southern, E. M.** 1975. Detection of specific sequences among DNA fragments separated by gel electrophoresis. J. Mol. Biol. **98**:503–517.
26. **Spooner, R. A., M. Bagdasarian, and C. H. Franklin.** 1987. Activation of the *xylDLEGF* promoter of the TOL toluene-xylene degradation pathway by overproduction of the *xylS* regulatory gene product. J. Bacteriol. **169**:3581–3586.
27. **Spooner, R. A., K. Lindsay, and F. C. H. Franklin.** 1986. Genetic functional and sequence analysis of the *xylR* and *xylS* genes of the TOL plasmid pWW0. J. Gen. Microbiol. **132**:1347–1358.
28. **Steenson, T. I., and N. Walker.** 1957. The pathway of breakdown of 2,4-dichloro- and 4-chloro-2-methylphenoxyacetic acid by bacteria. J. Gen. Microbiol. **16**:146.
29. **Streber, W. R., K. N. Timmis, and M. H. Zenk.** 1987. Analysis, cloning, and high-level expression of 2,4-dichlorophenoxyacetate monooxygenase gene *tfdA* of *Alcaligenes eutrophus* JMP134. J. Bacteriol. **169**:2950–2955.
30. **Tiedje, J. M., and M. Alexander.** 1969. Enzymatic cleavage of the ether bond of 2,4-dichlorophenoxyacetate. J. Agric. Food Chem. **17**:1080–1084.
31. **Tiedje, J. M., J. M. Duxbury, M. Alexander, and J. E. Dawson.** 1969. 2,4-D metabolism: pathway of degradation of chlorocatechols by *Arthrobacter* species. J. Agric. Food Chem. **17**:1021–1026.
32. **Tyler, J. E., and R. K. Finn.** 1974. Growth rate of a pseudomonad on 2,4-dichlorophenoxyacetic acid and 2,4-dichlorophenol. Appl. Microbiol. **28**:181–184.
33. **Wheelis, M. L., and L. N. Ornston.** 1972. Genetic control of enzyme induction in the β-ketoadipate pathway of *Pseudomonas putida*: deletion mapping of *cat* mutations. J. Bacteriol. **109**:790–795.
34. **Williams, P. A., and K. Murray.** 1974. Metabolism of benzoate and the methyl benzoates by *Pseudomonas putida* (*arvilla*) mt-2: evidence for existence of a TOL plasmid. J. Bacteriol. **120**:416–423.
35. **Worsey, M. J., and P. A. Williams.** 1975. Metabolism of toluene and xylene by *Pseudomonas putida* (*arvilla*) mt-2: evidence for a new function of the TOL plasmid. J. Bacteriol. **124**:7–13.
36. **Yano, K.** 1980. Degradative plasmids: aspects of microbial evolution, p. 47–60. *In* K. Sakaguchi and M. Okanishi (ed.), Molecular breeding and genetics of applied microorganisms. Kodansha/Academic Press, Tokyo.

Downloaded from http://jb.asm.org/ on September 3, 2020 at Corteva Agriscience

COR-AAD1-00002459

Bayer EX1008 (Part 5 of 9)

Published April, 1989

Reasons for the Acclimation for 2,4-D Biodegradation in Lake Water

Shaojin Chen and Martin Alexander

ABSTRACT

A study was undertaken to determine reasons for the occurrence of an acclimation period for the biodegradation of 2,4-dichlorophenoxyacetate (2,4-D) in lake water. The length of the acclimation period was not affected by removal of larger protozoa from the water or the presence of cycloheximide and nystatin. The population of 2,4-D–degrading bacteria increased long before 2,4-D loss was detected, and herbicide loss was evident only when the population size was large. The acclimation phase was virtually eliminated if a culture of 2,4-D–utilizing bacteria was added to lake water. A culture of glucose-grown 2,4-D–degrading bacteria metabolized the herbicide in a time interval far shorter than the acclimation phase. The time for acclimation was identical in 14 replicate samples of the same lake water. These data suggest that the length of the acclimation phase is not mainly a result of the time for reduction of grazing pressure on 2,4-D–degrading bacteria, the destruction of antimicrobial compounds, the decomposition of alternative C sources used preferentially to the herbicide, induction of the requisite enzymes, or the appearance of a mutant able to utilize the pesticide. The acclimation for 2,4-D degradation in lake water appears chiefly to reflect the time for a small population of bacteria able to use the compound to become sufficiently large to cause a detectable loss of the chemical.

PRIOR TO THE BIODEGRADATION of some organic pollutants, a period of time elapses during which no significant decomposition is observed, but then breakdown of the compounds is rapid. Because the decomposition in these instances is mediated by the indigenous microorganisms, the phenomenon has been attributed to microbial acclimation. A long acclimation period could significantly increase the risk of sensitive species to organic pollutants because of the longer exposure period and the possibility of transport of the chemicals to sites distant from the point of discharge. Therefore, a better understanding of the reasons for acclimation is necessary to permit devising means of reducing the length of this period.

Several mechanisms have been postulated to explain acclimation. The acclimation period may reflect the time for an initially small population to reach a size sufficient to cause a detectable loss of the chemical (Wiggins et al., 1987; Ventullo and Larson, 1986). A deficiency of inorganic nutrients may limit the growth rate of the degrading microorganisms and thus increase the acclimation phase (Lewis et al., 1986). Acclimation may be the time for enzyme induction (Stephenson et al., 1984), or it may reflect the time for mutation or genetic exchange to yield a phenotype able to use the organic chemical (Schmidt et al., 1983; Varma et al., 1976). The time for the destruction or removal of microbial inhibitors or for the utilization of more readily metabolizable organic compounds may also result in an acclimation (Atlas and Bartha, 1972; Kim and Maier, 1986). However, few of these hypotheses have been tested experimentally. Hence, a study was initiated to determine why acclimation occurs in lake water. The test chemical was 2,4-dichlorophenoxyacetate (2,4-D).

Both authors, Dep. of Agronomy, Cornell Univ., Ithaca, NY 14853. Present address of senior author is Dep. of Plant and Soil Science, Montana State Univ., Bozeman, MT. 59717. Received 22 June 1988. *Corresponding author.

Published in J. Environ. Qual. 18:153–156 (1989).

MATERIALS AND METHODS

Water samples were taken from Cayuga Lake, Ithaca, NY, at a depth of 20 cm or from Beebe Lake, Ithaca, NY, at a depth of 15 cm. In some instances, the lake water was sterilized by passage through 0.22-μm pore-size membrane filters.

The biodegradation of 2,4-D was determined either by measuring the loss of UV absorbancy at 230 nm from solutions containing the herbicide or by measuring the disappearance of radioactivity from solutions containing the labeled compound by the procedure of Subba-Rao et al. (1982).

A 2,4-D–utilizing bacterium was isolated from Beebe Lake water amended with 10 μg 2,4-D/mL. When 80% of the UV absorbancy at 230 nm had disappeared, the lake water was streaked on agar containing 20 μg 2,4-D/mL and inorganic salts. A bacterium was isolated that is a short gram-negative rod, and it forms yellowish colonies on agar media containing 2,4-D. The organism is able to destroy totally the UV absorbancy of 2,4-D in liquid media when grown without shaking for 4 d at 29 °C in 500 mL liquid medium containing 20 μg 2,4-D, 0.17 mg NH_4NO_3, 0.8 mg of K_2HPO_4, 0.2 mg KH_2PO_4, 0.2 mg $MgSO_4$, 63 μg $CaCl_2$, and 0.17 g $FeCl_3$/mL. The cells were collected by passing the cultures through a 0.22-μm Millipore filter, washed with 0.1 *M* phosphate buffer, pH 6.8, and suspended in 150 mL fresh buffer. For studies of the possible role of toxins, portions (0.5 mL) of the suspension were added to duplicate 400-mL portions of the various test solutions and inorganic nutrients contained in 500-mL Erlenmeyer flasks.

To assess the possible role of protozoa, 400-mL samples of Beebe Lake water were passed through 3.0-μm pore-size filters (Millipore) or amended with 250 μg cycloheximide and 30 μg nystatin/mL. Each solution received 5.0 μg 2,4-D/mL, of which 0.1% was radiolabeled.

To make counts by the most-probable-number (MPN) procedure, duplicate 1.0-mL portions of various 10-fold dilutions were added to five replicate tubes containing 9.0 mL of a medium composed of autoclaved lake water containing 5.0 μg 2,4-D/mL. The UV absorbancy of each tube was measured after 52 d of incubation at 20 °C, and tubes in which the absorbancy was less than 50% of that in uninoculated tubes were considered positive. In a study in which the role of protozoa was investigated, counts after 10 d (when the population size was large) were made in duplicate by the spread-plate technique on a medium containing 250 μg 2,4-D, 150 μg yeast extract, and 20 mg Bacto agar (Difco)/mL. The three plates at each dilution were incubated for 7 d at 20 °C, and the 2,4-D-utilizing bacteria appeared as yellow colonies. The possible presence of protozoa was assessed by the procedure of Singh (1946) and examining the glass rings microscopically.

An isolate growing on 2,4-D-yeast extract agar was used to test whether the initial steps in 2,4-D degradation were inducible. The bacterium was grown in a medium containing inorganic salts and 32 μg 2,4-D/mL for 4 d or 32 μg glucose/mL for 2 d, and the cells were collected on 0.20-μm pore-

COR-AAD1-00002460
Bayer EX1008 (Part 5 of 9)

size filters, washed on the filters with 0.1 *M* phosphate buffer, pH 6.8, at 4 °C, and then suspended in the salts solution described above. The bacterial suspensions were adjusted to densities of 2.4×10^7 cells/mL, and 150-mL portions were amended with 1.8 mg 2,4-D and incubated at 20 °C. At intervals, 4.0-mL portions were removed, passed through 0.2-μm Acrodisc filter assemblies (Gelman) to remove the bacteria, and analyzed spectrophotometrically for 2,4-D metabolism.

In tests of the possible role of mutation, 14 samples (200 mL) of Cayuga Lake water contained in sterile 250-mL Erlenmeyer flasks were each amended with 1.0 mg 2,4-D, and 2,4-D loss was measured spectrophotometrically. The liquid was filtered to remove cells before analysis at the last two time periods.

Methylene-labeled 2,4-D (specific activity 1.04 MBq/μmol) was obtained from Amersham Corp., Arlington Heights, IL. Unlabeled 2,4-D was obtained from Aldrich Chemical Co., Milwaukee, WI. Cycloheximide and nystatin were from Sigma Chemical Co., St. Louis, MO.

RESULTS

Samples of Beebe Lake water were amended with 5.0 μg 2,4-D/mL and then treated as follows: (i) untreated, (ii) supplemented with 250 μg cycloheximide and 30 μg nystatin/mL, (iii) passed through 3.0-μm filters to remove larger protozoa, or (iv) filtered and supplemented with the two eucaryotic inhibitors. The 2,4-D also contained some radioactive chemical. Biodegradation was measured on duplicate samples. Counts were made of 2,4-D–degrading cells in treatments i and ii and in lake water receiving no herbicide. The herbicide was degraded in lake water with or without the two inhibitors and whether or not the water samples were filtered to remove larger protozoa (Fig. 1). The acclimation period was 18 d, and its length was not appreciably affected by treatments designed to suppress or physically remove protozoa. Examination of undiluted and 10- and 100-fold dilutions of the water samples failed to reveal the presence of protozoa at 0, 2, 6, 18, and 22 d.

The densities of 2,4-D degraders were estimated by the MPN procedure from 0 to 10 d and thereafter by spread plates on agar containing 2,4-D and yeast extract. The number of cells able to grow on 2,4-D increased whether the lake water received the compound or not, but the counts never exceeded 1700/mL if herbicide was not added to the water (Table 1). Addition of the two eucaryotic inhibitors did not affect the number of 2,4-D degraders in lake water amended with the compound.

To test whether the acclimation phase resulted from the presence in the lake water of toxins affecting the 2,4-D–degrading bacteria or organic nutrients that they used in preference to the herbicide, inorganic nutrients, and 12.5 ng 2,4-D/mL (containing radioactive 2,4-D) were added to nonsterile Beebe Lake water, lake water that had been sterilized by filtration, or sterile distilled water. The solutions were inoculated with a 2,4-D–utilizing bacterium to an initial density of 1800 cells/mL. In addition, the inorganic salts and 2,4-D but no inoculum were added to nonsterile lake water.

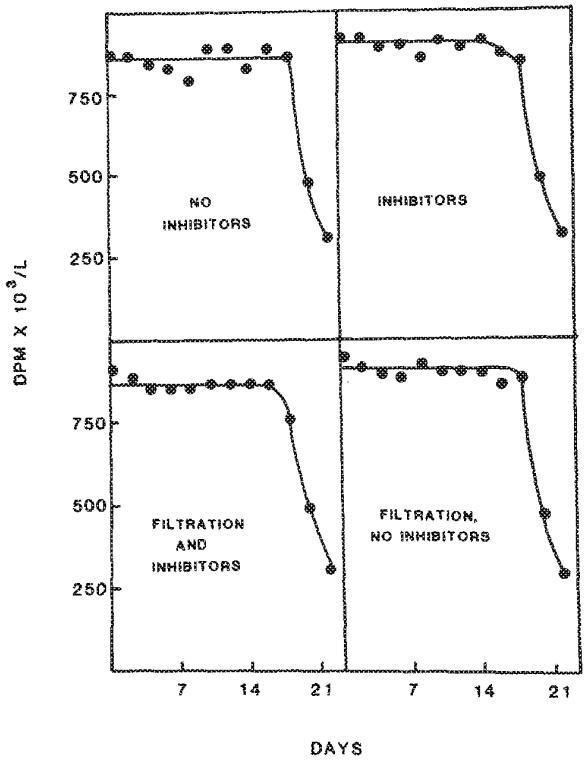


Fig. 1. Biodegradation of 2,4-D in lake water in the presence and absence of cycloheximide and nystatin and following filtration to remove large protozoa.

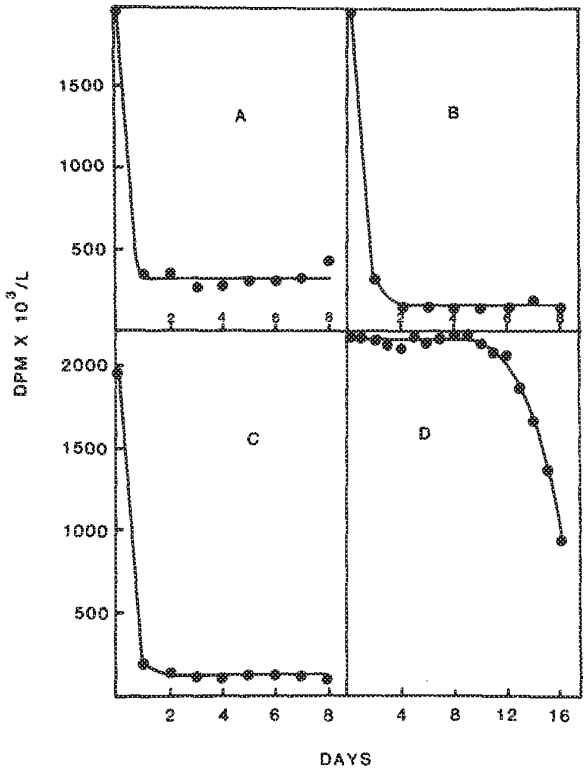


Fig. 2. Biodegradation of 2,4-D in (*A*) inorganic nutrient solution, (*B*) sterile lake water, and (*C*) nonsterile lake water inoculated with a 2,4-D–degrading bacterium, and (*D*) in uninoculated, nonsterile lake water. The samples of lake water also received theinorganic nutrients.

COR-AAD1-00002461
Bayer EX1008 (Part 5 of 9)

Table 1. Cell densities of 2,4-D degraders in lake water amended and not amended with eucaryotic inhibitors.

Days	No. of cells/mL		
	Untreated lake water	Lake water with 2,4-D	Lake water with 2,4-D, cycloheximide, and nystatin
0	<2	<2	<2
2	<2	<2	<2
4	<2	3	2
6	32	68	20
8	140	340	170
10	565	501	460
12	1400	1.0×10^4	3.0×10^4
14	830	4.2×10^4	4.2×10^4
16	1200	6.7×10^4	1.8×10^5
18	1000	1.9×10^5	3.6×10^5
20	1700	1.4×10^6	1.4×10^6
22	1000	1.8×10^6	1.6×10^6

In uninoculated Beebe Lake water, 2,4-D degradation was only detected after about 12 d, whereas the acclimation phase was less than 1 d in the inorganic salts solution or in sterile or nonsterile lake water inoculated with the pesticide-utilizing isolate (Fig. 2). The rapid degradation in all the inoculated solutions shows that the presence of inhibitors or organic nutrients used in preference to the herbicide does not result in an acclimation phase prior to the rapid biodegradation of 2,4-D by the isolate.

Because the acclimation period may reflect the time necessary for induction of the 2,4-D–degrading enzymes, a study was conducted to determine the rate of 2,4-D metabolism by 2,4-D- and glucose-grown cells. Bacterial cells grown on the herbicide metabolized the substrate linearly and with no lag phase, and all the UV absorbancy from 12 μg substrate/mL had disappeared in 3 h (Fig. 3). In contrast, no activity was evident in glucose-grown cells for about 15 h, but then 2,4-D was decomposed.

To evaluate whether the appearance of a mutant might explain the acclimation, comparisons were made

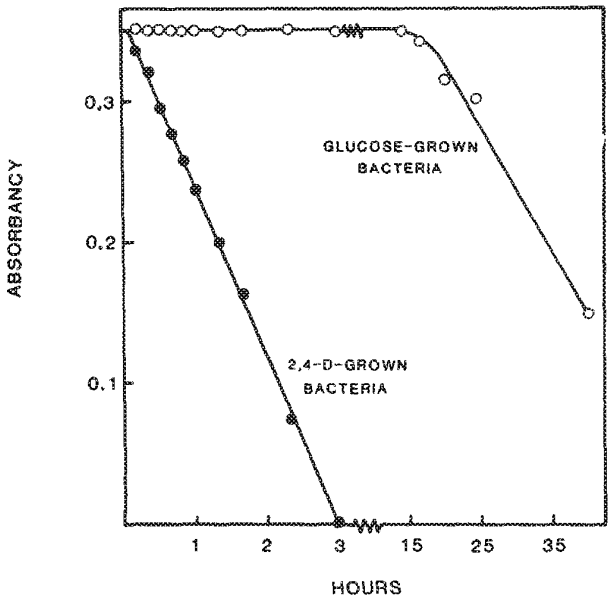


Fig. 3. Metabolism of 2,4-D by suspensions of cells grown on 2,4-D or glucose.

of the lengths of time for the loss of 5.0 μg 2,4-D/mL in 14 replicate samples of Cayuga Lake water. Because mutation is a random and often rare event, it was assumed that the appearance of a mutant would become evident if the lengths of the acclimation period differed among the replicates. The initiation of detectable 2,4-D loss, which was measured spectrophotometrically, following a mutation also requires that the mutant cells proliferate to reach the large population density required to cause a detectable loss of UV absorbancy. All 14 replicates had acclimation phases of about 10 d, although the subsequent rate in one replicate was somewhat delayed; nevertheless, 50 to 70% of the UV absorbancy in all replicates had disappeared at 16 d.

DISCUSSION

Several reasons have been proposed for the acclimation phase prior to the onset of detectable biodegradation. Thus, Atlas and Bartha (1972) suggested that part of the acclimation period prior to petroleum biodegradation in seawater at low temperature reflected the time for volatilization of toxic constituents. Our data provide no evidence of a role for inhibitors in the lake water that was studied. Other organic substrates may be used by the biodegrading bacteria in preference to the test compound, as indicated by the finding of Kim and Mayer (1986) that addition of nutrient broth reduced the acclimation period for the degradation of high concentrations of 2,4-D and 3,5-dichlorobenzoate. Nevertheless, our results suggest the preferential use of natural organic substrates in the water does not account for the delay prior to the onset of detectable biodegradation. Furthermore, although the 2,4-D–degrading enzyme system is inducible, enzyme induction does not account for most of the acclimation period, because only about 16 h was required for induction, whereas the acclimation period was at least several days. It is possible, however, that induction of enzymes takes a long period at low concentrations of the test compound (Button and Robertson, 1985).

Grazing by protozoa may affect the time for bacterial acclimation to biodegradation of organic chemicals (Wiggins et al., 1987). For example, if the potential growth rate of the biodegrading bacteria is slow and the rate of protozoan predation is rapid, a net increase in population size of the biodegraders may not occur until the grazing pressure abates. However, because the acclimation periods were unaffected by the addition of eucaryotic inhibitors, the removal of larger protozoa, or a combination of both treatments, and because the counts of biodegrading bacteria were unaffected by the treatment designed to eliminate the putative grazers, it appears that predation by protozoa was not an important contributor to the acclimation period.

The test for mutation, which is based on the method of Luria and Delbrück (1943), assumes that mutation is a random, rare event and thus should occur in individual water samples at different times. This would be reflected in different durations of the acclimation phase in replicate portions of the same water sample. Because the lengths of the acclimation periods were

COR-AAD1-00002462
Bayer EX1008 (Part 5 of 9)

reasonably similar among replicates, time for a mutation to occur followed by multiplication of the mutants does not account for the acclimation period for 2,4-D degradation. However, the time for mutants to appear seems to be a significant contributor to the acclimation phase prior to the destruction of several nitro compounds in waste waters (Wiggins and Alexander, 1988).

The data suggest that the acclimation phase reflects the time for a small population to multiply to reach a size sufficiently large for chemical loss to be detectable. Ventullo and Larson (1986) and Wiggins et al. (1987) previously noted that the cells of species carrying out a biodegradation multiply during acclimation. The present data confirm those observations but also demonstrate that the maximum cell density was approximately 1.7×10^6 cells/mL, indicating that one cell consumed about 3 pg of the substrate. A comparison of the data in Table 1 and Fig. 1 shows that the bacteria were multiplying long before 2,4-D biodegradation was detected, and increases in cell numbers were evident as early as 4 d. However, the loss of chemical was only first evident at 18 or 20 d; i.e., more than 10^5 active cells/mL had to develop before biodegradation was detected. Hence, when biodegradation is measured by disappearance of the organic chemical, the acclimation phase may simply be the time for the organisms to become sufficiently numerous to cause a detectable decrease in chemical concentration. On the other hand, no acclimation may be evident if the test for biodegradation is product formation, provided that the assay is both sensitive and precise (Scow et al., 1986).

ACKNOWLEDGMENTS

The research was supported by a fellowship awarded to the senior author by the government of the People's Republic of China, by a grant from the Army Research Office, and by grant 87-CRSR-2-2977 from the USDA.

REFERENCES

Atlas, R.M., and R. Bartha. 1972. Biodegradation of petroleum in sea water at low temperatures. Can. J. Microbiol. 18:1851–1855.
Button, D.K., and B.R. Robertson. 1985. Effect of toluene exposure time and concentration on induction of high affinity values for toluene oxidation by bacteria of estuarine seawater samples. Mar. Ecol. Prog. Ser. 26:187–193.
Kim, C.J., and W.J. Maier. 1986. Acclimation and biodegradation of chlorinated organic compounds in the presence of alternate substrates. J. Water Pollut. Control Fed. 58:157–164.
Lewis, D.L., H.P. Kollig, and R.E. Hodson. 1986. Nutrient limitation and adaptation of microbial populations to chemical transformations. Appl. Environ. Microbiol. 51:598–603.
Luria, S.E., and M. Delbrück. 1943. Mutations of bacteria from virus sensitivity to virus resistance. Genetics 28:491–511.
Schmidt, E., M. Hellwig, and H.-J. Knackmuss. 1983. Degradation of chlorophenols by a defined mixed microbial community. Appl. Environ. Microbiol. 46:1038–1044.
Scow, K.M., S. Simkins, and M. Alexander. 1986. Kinetics of mineralization of organic compounds at low concentrations in soil. Appl. Environ. Microbiol. 51:1028–1035.
Singh, B.N. 1946. A method of estimating the numbers of soil Protozoa, especially amoebae, based on their differential feeding on bacteria. Ann. Appl. Biol. 33:112–119.
Stephenson, T., J.N. Lester, and R. Perry. 1984. Acclimatization to nitrilotriacetic acid in the activated sludge process. Chemosphere 13:1033–1040.
Subba-Rao, R.V., H.E. Rubin, and M. Alexander. 1982. Kinetics and extent of mineralization of organic chemicals at trace levels in freshwater and sewage. Appl. Environ. Microbiol. 43:1139–1150.
Varma, M.M., L.W. Wan, and C. Prasad. 1976. Acclimation of wastewater bacteria by induction or mutation selection. J. Water Pollut. Control Fed. 48:832–834.
Ventullo, R.M., and R.J. Larson. 1986. Adaptation of aquatic microbial communities to quaternary ammonium compounds. Appl. Environ. Microbiol. 51:356–361.
Wiggins, B.A., and M. Alexander. 1988. Role of chemical concentration and second carbon sources in acclimation of microbial communities for biodegradation. Appl. Environ. Microbiol. 54:2803–2807.
Wiggins, B.A., S.H. Jones, and M. Alexander. 1987. Explanations for the acclimation period preceding the mineralization of organic chemicals in aquatic environments. Appl. Environ. Microbiol. 53:791–796.

COR-AAD1-00002463
Bayer EX1008 (Part 5 of 9)

JBIC (1999) 4:122–129 © SBIC 1999

ORIGINAL ARTICLE

Nathaniel J. Cosper · Christina M. V. Stålhandske
Ruth E. Saari · Robert P. Hausinger · Robert A. Scott

X-ray absorption spectroscopic analysis of Fe(II) and Cu(II) forms of a herbicide-degrading α-ketoglutarate dioxygenase

Received: 3 July 1998 / Accepted: 13 October 1998

Abstract The first step in the degradation of 2,4-dichlorophenoxyacetic acid (2,4-D) by *Ralstonia eutropha* JMP134 is catalyzed by the α-ketoglutarate (α-KG)-dependent dioxygenase TfdA. Previously, EPR and ESEEM studies on inactive Cu(II)-substituted TfdA suggested a mixture of nitrogen/oxygen coordination with two imidazole-like ligands. Differences between the spectra for Cu TfdA and α-KG- and 2,4-D-treated samples were interpreted as a rearrangement of the *g*–tensor principal axis system. Herein, we report the use of X-ray absorption spectroscopy (XAS) to further characterize the metal coordination environment of Cu TfdA as well as that in the active, wild-type Fe(II) enzyme. The EXAFS data are interpreted in terms of four N/O ligands (two imidazole-like) in the Cu TfdA sample and six N/O ligands (one or two imidazole-like) in the Fe TfdA sample. Addition of α-KG results in no significant structural change in coordination for Cu or Fe TfdA. However, addition of 2,4-D results in a decrease in the number of imidazole ligands in both Cu and Fe TfdA. Since this change is seen both in the Fe and Cu EXAFS, loss of one histidine ligand upon 2,4-D addition best describes the phenomenon. These XAS data clearly demonstrate that changes occur in the atomic environment of the metallocenter upon substrate binding.

Key words α-Ketoglutarate dioxygenase · TfdA · X-ray absorption spectroscopy · Extended X-ray absorption fine structure · 2,4-Dichlorophenoxyacetic acid

N.J. Cosper · C.M.V. Stålhandske · R.A. Scott (✉)
Center for Metalloenzyme Studies, University of Georgia, Athens, GA 30602-2556, USA
e-mail: rscott@arches.uga.edu
Tel.: +1-7065422726
Fax: +1-706-542-9454

R.E. Saari · R.P. Hausinger
Departments of Microbiology and Biochemistry and the Center for Microbial Ecology, Michigan State University, East Lansing, MI 48824-1101, USA

Abbreviations *BVS* bond valence sum · *2,4-D* 2,4-dichlorophenoxyacetic acid · *DAOCS* deacetoxycephalosporin C synthase · *EPR* electron paramagnetic resonance · *ESEEM* electron spin echo envelope modulation · *EXAFS* extended X-ray absorption fine structure · *FT* Fourier transform · *IPNS* isopenicillin N synthase · α-KG α-ketoglutarate · *MOPS* 3-(*N*–morpholino)propanesulfonic acid · *SSRL* Stanford Synchrotron Radiation Laboratory · *XAS* X-ray absorption spectroscopy

Introduction

α-Ketoglutarate-dependent dioxygenases couple the oxidative decarboxylation of α-ketoglutarate (α-KG) to hydroxylation of their respective substrates. The different members of this class of enzymes act on a variety of substances, ranging from amino acid residues of peptides (prolyl and lysyl hydroxylases) to pyrimidine catabolic products (thymine hydroxylase) to intermediates in the synthesis of plant products (giberellin and flavanone hydroxylases), antibiotics (clavaminate synthase), and other compounds (γ-butyrobetaine hydroxylase) (reviewed in [1–3]). The reactions require oxygen, ferrous ion, and often ascorbic acid. The only common sequence motif shared by enzymes in this family, and also conserved in isopenicillin N synthase (IPNS), is H-X-D-$X_{53–57}$–H [4]. There are two crystal structures available for this group of enzymes. The first was that determined for IPNS where the two histidines and the aspartic acid found in this motif are ligands to the iron [5]; however, IPNS is not an α-KG-dependent dioxygenase. Recently, deacetoxycephalosporin C synthase (DAOCS), an α-KG-dependent dioxygenase that catalyzes the reaction of penicillin N to deacetoxycephalosporin C, has been crystallographically characterized [6]. The structure of DAOCS complexed with iron revealed a ligand environment similar to that of IPNS. Addition of the cosubstrate α-KG results in bidentate ligation to the iron, replacing two of the three solvent molecules,

COR-AAD1-00002464
Bayer EX1008 (Part 5 of 9)

with no change in the endogenous ligands. A structural motif termed a facial triad, composed of two histidine residues and one carboxylate residue ligating the metallocenter, has been crystallographically observed in several families of iron-dependent oxygenases, as recently reviewed [7]. We seek to further characterize the non-heme iron metallocenter of 2,4-dichlorophenoxyacetic acid (2,4-D)/α-KG dioxygenase (TfdA) as a model system for this important class of enzymes.

2,4-D is a widely used broad-leaf herbicide that is readily degraded by soil microorganisms [8]. *Ralstonia eutropha* (formerly *Alcaligenes eutrophus* [9]) JMP134 is an extensively studied soil isolate capable of degrading 2,4-D [10]. TfdA (named in accordance with the gene designation [11]) carries out the first step (Scheme 1) of the biodegradative pathway using α-KG-dependent dioxygenase chemistry [12]. Chemical modification studies have established that multiple histidinyl residues are required for activity [possibly involved in Fe(II), α-KG, or substrate binding], while lysyl and cysteinyl residues are not involved in the catalysis [13]. Examination of the inactive Cu(II)-containing form of the protein by electron paramagnetic resonance (EPR) and electron spin echo envelope modulation (ESEEM) spectroscopies demonstrated the presence of two histidine ligands to the metal in native enzyme [14]. Addition of 2,4-D had no effect on the spectrum, whereas addition of α-KG perturbs this signal, consistent with ordered binding of α-KG prior to 2,4-D. Subsequent addition of 2,4-D to a sample containing α-KG leads to further changes in the signal, revealing the presence of a single equatorial histidine ligand in the ternary complex, which may reflect rearrangement of the principal axis of the g-tensor or displacement of one histidine ligand.

Here, we have probed the TfdA metallocenter using X-ray absorption spectroscopy (XAS). The active Fe(II)-containing TfdA was studied in the presence of substrate or cofactor. As well, the inactive Cu(II)-substituted form of the enzyme was studied to allow comparison with the EPR/ESEEM results.

Experimental

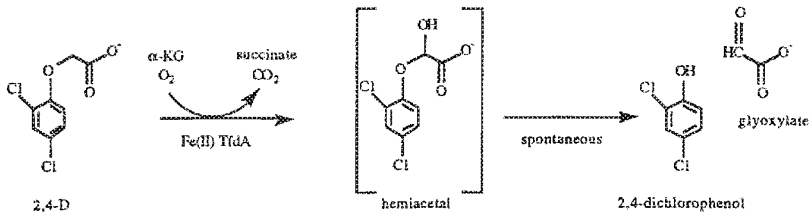
Sample preparation

TfdA was prepared from *Escherichia coli* DH5α cells carrying plasmid pUS311, as described earlier [13]. The stable apoprotein preparations possessed specific activities ranging from 11 to 17 μmol min^{-1}(U) mg^{-1}, consistent with the reported value of 16.9 U mg^{-1} [13], when assayed using standard conditions that immediately regenerate the active metallocenter by inclusion of 50 μM Fe(II). Protein was concentrated using ultrafiltration (Amicon centricon), and buffer exchange was carried out by repeated dilution and concentration with [3-(N-morpholino)propanesulfonic acid (MOPS) buffer (5 mM, pH 7.0). Protein concentrations were measured using the BioRad protein assay with bovine serum albumin as a standard, and are reported in terms of subunit concentrations. The Fe-containing samples contained 1.2 mM TfdA, 1 mM Fe (resting enzyme) or 0.7 mM Fe (substrates present) supplied as $(NH_4)_2Fe(SO_4)_2$, 1 mM ascorbate, 1 mM substrate (α-KG, or 2,4-D) when present, and 37–40% glycerol. The Cu-containing samples contained 1.4 mM TfdA, up to 1.4 mM Cu(II) supplied as $CuCl_2$, 5 mM 2,4-D (when present), 10 mM α-KG (when present), and 33–34% glycerol. Because TfdA is known to slowly lose activity in the presence of Fe and oxygen [15], in a process that is slowed by the presence of ascorbic acid, the TfdA apoprotein samples were mixed with the metal ions, substrates, and ascorbate [except for the Cu(II) samples] while on ice and immediately frozen (in an ethanol/dry ice bath) in polycarbonate cuvets, 24×3×1 mm for Fe and 24×3×2 mm for Cu, with a 0.025 mm Mylar window covering one 24×3 mm face. Representative samples that had been examined by XAS were thawed, diluted, and dialyzed against buffer containing EDTA to remove the added metal, and assayed for activity and protein content. The observed specific activity values ranged from 9.3 to 17.6 U mg^{-1} and demonstrated that little, if any, radiation damage had taken place.

X-ray absorption spectroscopy

XAS data were collected at Stanford Synchrotron Radiation Laboratory (SSRL) with the SPEAR storage ring operating in a dedicated mode at 3.0 GeV (Table 1). EXAFS analysis was performed with the EXAFSPAK software (courtesy of G. N. George; http://ssrl01.slac.stanford.edu/exafspak.html) according to standard procedures [16]. Both single- and multiple-scattering paths $\leq$4.5 Å from either the Cu or Fe atom were used to identify and quantify imidazole coordination due to histidine. Multiple-scattering paths were built by importing the crystal structure of tetrakis(imidazole)copper(II) sulfate [17] or bis(*N*-methylimidazole)bis(diphenylborondimethylglyoximato)iron(II) dichloromethane solvate [18] into Ball & Stick software (v. 3.5, Cherwell Scientific). The model was edited to only the metal atom and one imidazole and the coordinates were imported into FEFF v. 5.05 [19] to calculate scattering amplitudes and phase shifts for each scattering path containing four or fewer legs. A constrained fitting process was then used with the following parameters: coordination numbers were constrained to be integer values, the distances for outer-shell atoms of imidazole rings were constrained to be a constant difference with the first-shell (metal-nitrogen/oxygen) distance. Only a single ΔE_0 value was optimized. In fits containing *only* imidazole ligands, Debye-Waller values for the C_2, N_3, C_4, and C_5 atoms of imidazole rings were constrained to be a multiple of the N_1 (first-shell) value; scaling factors were determined from model compound analysis. In fits with first-shell mixtures of imidazoles and other (N,O)-containing ligands, Debye-Waller values for C_2, N_3, C_4, and C_5 atoms were similarly constrained to multiples of one another, but were not tied to the first shell [N_1, (N,O)] Debye-Waller values. This allows non-imidazole first-shell ligands to have Debye-Waller values independent of the imidazole ligand

Scheme 1



COR-AAD1-00002465
Bayer EX1008 (Part 5 of 9)

Table 1 X-ray absorption spectroscopic data collection for Fe(II) and Cu(II) TfdA samples

	Fe EXAFS	Cu EXAFS
SR facility	SSRL	SSRL
Beamline	7-3	7-3
Current in storage ring	40–80 mA	55–85 mA
Monochromator crystal	Si[220]	Si[220]
Detection method	Fluorescence	Fluorescence
Detector type	Solid state array[a]	Solid state array[a]
Scan length (min)	24	26
Scans in average	16	10
Temperature (K)	10	10
Energy standard	Fe foil, 1st inflection	Cu foil, 1st inflection
Energy calibration (eV)	7111.2	8980.3
E_0 (eV)	7120	8990
Pre-edge background		
Energy range (eV)	6852–7075	8657–8945
Gaussian center (eV)	6170	8040
Width (eV)	750	750
Spline background		
Energy range (eV)	7120–7353 (4)	8990–9224 (4)
(polynomial order)	7353–7586 (4)	9224–9458 (4)
	7586–7819 (4)	9458–9691 (4)

[a] The 13-element Ge solid-state X-ray fluorescence detector at SSRL is provided by the NIH Biotechnology Research Resource

values. The bond valence sum (BVS) method was applied to EXAFS-simulated coordination environments using standard procedures [20, 21]. Possible coordination numbers of histidyl imidazole ligands were chosen from fits that yielded chemically and physically reasonable Debye-Waller factors for the outer shell atoms, since goodness-of-fit values (f') were insensitive to these coordination numbers. In a number of metal-imidazole model compounds, we find that the following Debye-Waller factors are typical: M-N_1, $\sigma_{as}^2 = 0.001$–0.003 Å^2, M···(C_2, C_5), $\sigma_{as}^2 = 0.002$–0.004 Å^2, M···(N_3, C_4), $\sigma_{as}^2 = 0.003$–0.006 Å^2.

Results

Edge spectra

The Fe K-edge X-ray absorption spectrum for Fe(II) TfdA (Fig. 1a) is strikingly similar to that displayed by Fe(II) IPNS [22]. Of note is the intensity of the 1 $s \rightarrow 3$ d peak at 7113 eV, which has a peak area that is also very similar to that displayed by IPNS. Addition of α-KG (Fig. 1a) does not affect the shape of the Fe edge. By contrast, addition of 2,4-D causes a substantial change in the edge (Fig. 1b). Similar, but less obvious, changes are observed at the Cu K-edge (Fig. 1c,d), recorded on Cu(II)-substituted TfdA samples. Again, addition of α-KG causes only very slight changes in the edge (Fig. 1e), while addition of 2,4-D, either by itself (Fig. 1c) or in combination with α-KG (Fig. 1d), causes more noticeable changes.

Extended X-ray absorption fine structure

EXAFS data for the inactive Cu(II) TfdA samples are shown in Fig. 2. Addition of 2,4-D to either the Cu TfdA or the α-KG-treated Cu TfdA samples results in minor qualitative changes to the EXAFS, most notable at $k \approx 4.0$ Å^{-1} and 5.5 Å^{-1} (Fig. 2). Corresponding changes in the Cu EXAFS Fourier transforms (FTs) are most noticeable as a reduction in FT peaks at R' ≈ 3Å and 4 Å, features that result from scattering by the outer-shell atoms of histidine imidazole ligands.

The Cu EXAFS is best fit assuming four-coordination, which also yields reasonable BVS values (Ta-

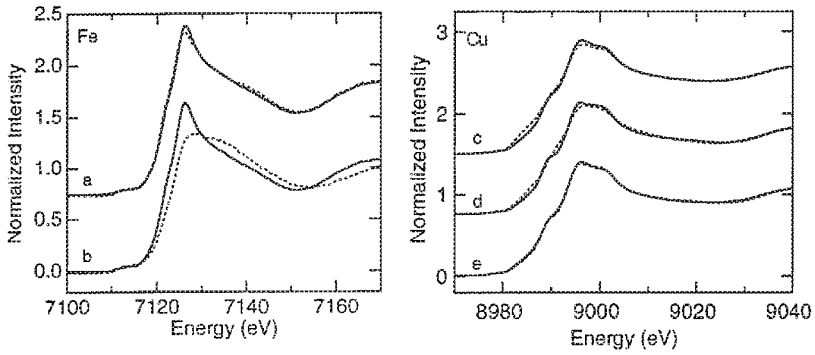


Fig. 1 Fe(II) X-ray absorption edge spectra of *a* TfdA (*solid line*) and TfdA with addition of α-KG (*dotted line*), *b* TfdA (*solid line*) and TfdA + 2,4-D (*dotted line*); and Cu(II) X-ray absorption edge spectra of *c* TfdA (*solid line*) and TfdA + 2,4-D (*dotted line*), *d* TfdA + α-KG (*solid line*) and TfdA + α-KG + 2,4-D (*dotted line*), and *e* TfdA (*solid line*) and TfdA + α-KG (*dotted line*)

COR-AAD1-00002466
Bayer EX1008 (Part 5 of 9)

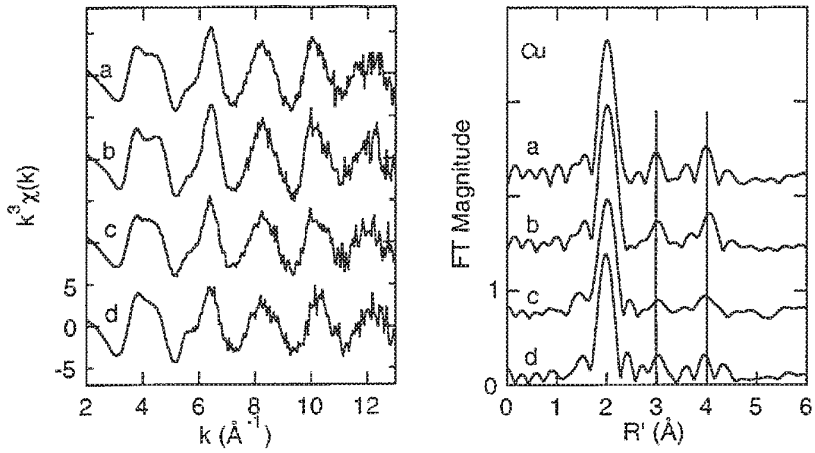


Fig. 2 k^3–weighted Cu(II) EXAFS (*left*) and Fourier transforms (*right*; over the range $k = 2$–13 Å^{-1}) of *a* TfdA, *b* TfdA + α-KG, *c* TfdA + 2,4-D, and *d* TfdA + α-KG + 2,4-D. The *vertical lines* on the *right* are a visual aid for comparing outer-shell features from histidine imidazole ligands

ble 2), while tri- and penta-coordinate fits were found to yield unreasonable values [e.g., BVS values of ca. 1.57(2) and ca. 2.64(4) result from tri- and penta-coordinate fits, respectively]. As expected from the change in the FTs, the EXAFS for Cu TfdA and α-KG-treated Cu TfdA are best fit by $Cu(N/O)_2(imid)_2$ coordination (fits 3 and 6, Table 2), while the EXAFS for the 2,4-D-treated samples are best fit by $Cu(N/O)_3(imid)_1$ coordination (fits 8 and 11, Table 2).

Lower S/N ratio EXAFS data were obtained for the Fe(II) protein samples (Fig. 3). As with the edge spectra, little change is seen between the native protein and samples containing α-KG. However, the extrema at 3.8, 5, and 6 Å^{-1} show modest yet noticeable shifts to higher k values in the 2,4-D treated sample (Fig. 3c) compared to the untreated Fe TfdA sample (Fig. 3a). The FTs of the Fe EXAFS show less obvious, but similar, trends as the edge and EXAFS. Of note is the marked decrease in intensity of the FT in the 3–4 Å region of the 2,4-D-treated Fe TfdA as opposed to untreated Fe TfdA (Fig. 3).

Quantitative analysis of the Fe EXAFS shows that either five- or six-coordinate $Fe(imid)_x(N/O)_y$ fits are best (Table 3). For untreated Fe TfdA, the Debye-Waller σ_{as}^2 and BVS values are most reasonable for fits with six N/O ligands, one or two of which are imidazoles (fits 4 and 6, Table 3). When α-KG is added, a significant increase is observed in the first-shell σ_{as}^2 values, but little change is seen in the σ_{as}^2 values for outer-shell imidazole atoms (implying no change in the number of histidine ligands; fits 9–12 compared to fits 3–6 in Table 3). Fits with lower coordination numbers yield more reasonable first-shell σ_{as}^2 values. Similar increases in the first-shell σ_{as}^2 values are seen upon addition of 2,4-D, but in this case, outer-shell imidazole interactions are essentially unnecessary for a satisfactory fit. Outer-shell imidazole σ_{as}^2 values for the $Fe(imid)_1(N/O)_4$ fit (fit 15, Table 3) for this sample are more reminiscent of the same σ_{as}^2 values for $Fe(imid)_2(N/O)_{3,4}$ fits to Fe TfdA ± α-KG (fits 5, 6, 11, and 12, Table 3).

Discussion

Edge spectra

The peak area of the $1s \rightarrow 3d$ transition in the preedge region of the Fe K-edge X-ray absorption spectrum has been shown to be inversely proportional to the coordi-

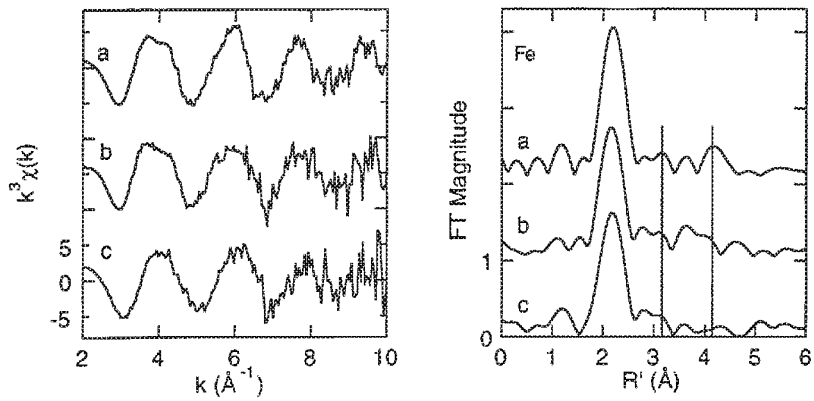


Fig. 3. k^3–weighted Fe(II) EXAFS (*left*) and Fourier transforms (*right*; over the range $k = 2$–10 Å^{-1}) of *a* TfdA, *b* TfdA + α-KG, and *c* TfdA + 2,4-D. *Vertical lines* are added to the FTs as in Fig. 2

COR-AAD1-00002467
Bayer EX1008 (Part 5 of 9)

Table 2 Curve fitting results for Cu EXAFS modeled as $Cu(imid)_x(N,O)_y$[a]

Sample k range	Fit	x, y	Shell	N_s	R_{as} (Å)	σ^2_{as} (Å^2)	ΔE_0 (eV)	f'[b]	BVS[c]
TfdA as isolated	1	0, 4	Cu-N/O	(4)[d]	1.99	0.0031	3.71	0.093 <0.080>[e]	2.10
k=2.0–13.0 Å^{-1}	2	1, 3	Cu-N/O	(4)	1.98	0.0030	−0.98	0.083	2.15
			Cu-N	(1)	[4.10][f]	0.0012	[−0.98]	<0.060>	
			Cu-C	(1)	[2.96]	[0.0009]	[−0.98]		
			Cu-C	(1)	[2.98]	[0.0009]	[−0.98]		
			Cu-C	(1)	[4.11]	[0.0012]	[−0.98]		
	3	2, 2	Cu-N/O	(4)	1.98	0.0030	−0.71	0.083	2.15
			Cu-N	(2)	[4.10]	0.0059	[−0.71]	<0.061>	
			Cu-C	(2)	[2.96]	[0.0042]	[−0.71]		
			Cu-C	(2)	[2.99]	[0.0043]	[−0.71]		
			Cu-C	(2)	[4.11]	[0.0059]	[−0.71]		
TfdA + α-KG	4	0, 4	Cu-N/O	(4)	1.99	0.0026	4.21	0.099 <0.073>	2.10
k=2.0–13.0 Å^{-1}	5	1, 3	Cu-N/O	(4)	1.98	0.0025	−0.08	0.088	2.15
			Cu-N	(1)	[4.09]	0.0013	[−0.08]	<0.062>	
			Cu-C	(1)	[2.95]	[0.0009]	[−0.08]		
			Cu-C	(1)	[2.98]	[0.0009]	[−0.08]		
			Cu-C	(1)	[4.10]	[0.0013]	[−0.08]		
	6	2, 2	Cu-N/O	(4)	1.98	0.0030	0.15	0.085	2.15
			Cu-N	(2)	[4.09]	0.0050	[0.15]	<0.060>	
			Cu-C	(2)	[2.95]	[0.0036]	[0.15]		
			Cu-C	(2)	[2.98]	[0.0036]	[0.15]		
			Cu-C	(2)	[4.10]	[0.0050]	[0.15]		
TfdA + 2,4-D	7	0, 4	Cu-N/O	(4)	1.99	0.0039	3.46	0.088 <0.059>	2.10
k=2.0–13.0 Å^{-1}	8	1, 3	Cu-N/O	(4)	1.98	0.0037	−1.46	0.080	2.15
			Cu-N	(1)	[4.09]	0.0050	[−1.46]	<0.051>	
			Cu-C	(1)	[2.95]	[0.0036]	[−1.46]		
			Cu-C	(1)	[2.98]	[0.0036]	[−1.46]		
			Cu-C	(1)	[4.10]	[0.0050]	[−1.46]		
	9	2, 2	Cu-N/O	(4)	1.98	0.0037	−1.11	0.079	2.15
			Cu-N	(2)	[4.09]	0.0096	[−1.11]	<0.051>	
			Cu-C	(2)	[2.95]	[0.0069]	[−1.11]		
			Cu-C	(2)	[2.98]	[0.0070]	[−1.11]		
			Cu-C	(2)	[4.10]	[0.0096]	[−1.11]		
TfdA + α-Kg + 2,4-D	10	0, 4	Cu-N/O	(4)	1.98	0.0038	3.25	0.099 <0.069>	2.15
k=2.0–13.0 Å^{-1}	11	1, 3	Cu-N/O	(4)	1.97	0.0037	−1.46	0.089	2.21
			Cu-N	(1)	[4.06]	0.0037	[−1.46]	<0.057>	
			Cu-C	(1)	[2.93]	[0.0027]	[−1.46]		
			Cu-C	(1)	[2.96]	[0.0027]	[−1.46]		
			Cu-C	(1)	[4.08]	[0.0038]	[−1.46]		
	12	2, 2	Cu-N/O	(4)	1.97	0.0036	−1.23	0.090	2.21
			Cu-N	(2)	[4.07]	0.0095	[−1.23]	<0.061>	
			Cu-C	(2)	[2.93]	[0.0069]	[−1.23]		
			Cu-C	(2)	[2.96]	[0.0069]	[−1.23]		
			Cu-C	(2)	[4.08]	[0.0095]	[−1.23]		

[a] Group is the chemical unit defined for the multiple scattering calculation. N_s is the number of scatterers (or groups) per metal. R_{as} is the metal-scatterer distance. σ^2_{as} is a mean square deviation in R_{as}. ΔE_0 is the shift in E_0 for the theoretical scattering functions

[b] f' is a normalized error (chi-squared):

$$f' = \frac{\left\{\sum_i [k^3(\chi_i^{obs} - \chi_i^{calc})]^2/N\right\}^{1/2}}{[(k^3\chi^{obs})_{max} - (k^3\chi^{obs})_{min}]}$$

[c] BVS = Σs, $s = \exp[(r_0 - r)/B]$, $B = 0.37$, r_0(Fe(II)-N) = 1.769, r_0(Cu(II)-N) = 1.751 [20]

[d] Numbers in parentheses were not varied during optimization

[e] Numbers in angle brackets are f' for the smoothed data

[f] Numbers in square brackets wire constrained to be either a multiple of the above value (σ^2_{as}) or to maintain a constant difference from the above value (R_{as}, ΔE_0)

COR-AAD1-00002468
Bayer EX1008 (Part 5 of 9)

Table 3 Curve fitting results for Fe EXAFS modeled as $Fe(imid)_x(N,O)_y$[a]

Sample *k* range	Fit	*x*, *y*	Shell	N_s	R_{as} (Å)	σ^2_{as} (Å^2)	ΔE_0 (eV)	*f'*	BVS
TfdA as isolated	1	0, 5	Fe-N/O	(5)	2.15	0.0033	2.59	0.114 <0.070>	1.79
k = 2.0–10.0 Å^{-1}	2	0, 6	Fe-N/O	(6)	2.15	0.0047	2.37	0.108 <0.063>	2.14
	3	1,4	Fe-N/O	(5)	2.15	0.0033	2.69	0.110	1.79
			Fe-N	(1)	[4.29]	0.0029	[2.69]	<0.064>	
			Fe-C	(1)	[3.13]	[0.0021]	[2.69]		
			Fe-C	(1)	[3.19]	[0.0022]	[2.69]		
			Fe-C	(1)	[4.32]	[0.0029]	[2.69]		
	4	1, 5	Fe-N/O	(6)	2.15	0.0046	2.38	0.104	2.14
			Fe-N	(1)	[4.28]	0.0033	[2.38]	<0.057>	
			Fe-C	(1)	[3.13]	[0.0024]	[2.38]		
			Fe-C	(1)	[3.19]	[0.0025]	[2.38]		
			Fe-C	(1)	[4.33]	[0.0033]	[2.38]		
	5	2, 3	Fe-N/O	(5)	2.15	0.0033	2.65	0.110	1.79
			Fe-N	(2)	[4.29]	0.0101	[2.65]	<0.065>	
			Fe-C	(2)	[3.13]	[0.0073]	[2.65]		
			Fe-C	(2)	[3.19]	[0.0075]	[2.65]		
			Fe-C	(2)	[4.32]	[0.0102]	[2.65]		
	6	2, 4	Fe-N/O	(6)	2.15	0.0046	1.99	0.104	2.14
			Fe-N	(2)	[4.28]	0.0098	[1.99]	<0.058>	
			Fe-C	(2)	[3.13]	[0.0071]	[1.99]		
			Fe-C	(2)	[3.19]	[0.0073]	[1.99]		
			Fe-C	(2)	[4.33]	[0.0099]	[1.99]		
TfdA + α-KG	7	0, 5	Fe-N/O	(5)	2.12	0.0055	1.10	0.101 <0.043>	1.88
k = 2.0–10.0 Å^{-1}	8	0, 6	Fe-N/O	(6)	2.12	0.0070	0.94	0.099 <0.040>	2.26
	9	1, 4	Fe-N/O	(5)	2.13	0.0049	2.26	0.101	1.88
			Fe-N	(1)	[4.25]	0.0019	[2.26]	<0.045>	
			Fe-C	(1)	[3.10]	[0.0014]	[2.26]		
			Fe-C	(1)	[3.17]	[0.0014]	[2.26]		
			Fe-C	(1)	[4.29]	[0.0020]	[2.26]		
	10	1, 5	Fe-N/O	(6)	2.13	0.0067	1.91	0.097	2.26
			Fe-N	(1)	[4.25]	0.0017	[1.91]	<0.040>	
			Fe-C	(1)	[3.10]	[0.0012]	[1.91]		
			Fe-C	(1)	[3.16]	[0.0012]	[1.91]		
			Fe-C	(1)	[4.29]	[0.0017]	[1.91]		
	11	2, 3	Fe-N/O	(5)	2.13	0.0049	2.24	0.100	1.88
			Fe-N	(2)	[4.25]	0.0103	[2.24]	<0.044>	
			Fe-C	(2)	[3.10]	[0.0075]	[2.24]		
			Fe-C	(2)	[3.17]	[0.0076]	[2.24]		
			Fe-C	(2)	[4.29]	[0.0103]	[2.24]		
	12	2, 4	Fe-N/O	(6)	2.13	0.0067	1.88	0.098	2.26
			Fe-N	(2)	[4.25]	0.0100	[1.88]	<0.038>	
			Fe-C	(2)	[3.10]	[0.0074]	[1.88]		
			Fe-C	(2)	[3.16]	[0.0075]	[1.88]		
			Fe-C	(2)	[4.29]	[0.0100]	[1.88]		
TfdA + 2,4-D	13	0, 5	Fe-N/O	(5)	2.10	0.0067	3.89	0.113 <0.053>	2.04
k = 2.0–10.0 Å^{-1}	14	0, 6	Fe-N/O	(6)	2.10	0.0086	3.39	0.110 <0.049>	2.45
	15	1, 4	Fe-N/O	(5)	2.10	0.0065	3.68	0.113	2.04
			Fe-N	(1)	[4.25]	0.0113	[3.68]	<0.053>	
			Fe-C	(1)	[3.09]	[0.0082]	[3.68]		
			Fe-C	(1)	[3.15]	[0.0082]	[3.68]		
			Fe-C	(1)	[4.29]	[0.0113]	[3.68]		
	16	1, 5	Fe-N/O	(6)	2.10	0.0084	3.12	0.110	2.45
			Fe-N	(1)	[4.24]	0.0096	[3.12]	<0.049>	
			Fe-C	(1)	[3.08]	[0.0075]	[3.12]		
			Fe-C	(1)	[3.14]	[0.0075]	[3.12]		
			Fe-C	(1)	[4.28]	[0.0096]	[3.12]		

[a] See footnotes to Table 2

COR-AAD1-00002469
Bayer EX1008 (Part 5 of 9)

nation number [23, 24]. This area can be used to quantify, with reasonable accuracy, the number of ligands, and the technique has been applied successfully by one of us (R.A.S.) to determine the number of ligands in IPNS [22]. Comparing our results to IPNS indicates that the area of this peak for all Fe TfdA samples[1] falls within the group of five-coordinate complexes investigated by Randall and coworkers [24].

Extended X-ray absorption fine structure

Cu(II) has a d^9 valence electronic configuration, making it highly susceptible to Jahn-Teller distortion [25]. This distortion results in longer axial bonds, making those ligands difficult to detect by EXAFS. Thus, EXAFS-derived coordination numbers of four for Cu(II) sites are expected, and this is what is observed for Cu(II)-substituted TfdA (Table 2). Addition of α-KG does not change the coordination (EXAFS), but does affect the electronic environment of the Cu(II) (EPR data from [14]). Taken together, these data are consistent with an axial ligand change, perhaps involving direct binding of α-KG. Addition of 2,4-D results in a reduction of the number of equatorial imidazoles from two to one, but EPR data show no change in electronic environment. Assuming both EPR and XAS data were collected on similarly prepared samples, this result would imply substitution of an imidazole by an electronically equivalent ligand. Of note, ESEEM analyses were not carried out with the 2,4-D-bound form of Cu TfdA; this spectroscopic approach should be pursued as an independent means to probe the number of equatorial imidazole ligands. The sample containing 2,4-D and α-KG shows both a reduction in the number of imidazoles and an alteration of the EPR signal, which could be explained either by a g–tensor rearrangement [14] or a loss of one histidine ligand.

Fe(II) is d^6, which should display little Jahn-Teller distortion. Thus, any rearrangement of the g–tensor should not affect the XAS-monitored coordination of the metal. There exists significant circumstantial evidence {Cu(II) ESEEM [14] and the presence of a H-X-D-X_{51}–H motif similar to that in several other α-KG dioxygenases and found in DAOCS and IPNS, for which the crystal structures are known [5, 6]} that the active site Fe(II) is bound by two histidine imidazoles. Curve-fitting of Fe EXAFS of untreated and α-KG-treated TfdA suggests coordination by a single histidine imidazole, but can accommodate two imidazoles if they exhibit Fe-N(imid) distances that differ by about 0.14 Å ($\Delta R_{as}{}^2$), to account for the large Debye-Waller factor value seen for the outer-shell imidazole atoms. Addition of α-KG has no significant effect on the XAS, whereas addition of 2,4-D results in an apparent reduction in the number of imidazole ligands, although the data do not distinguish whether the number decreases to one or zero. The decrease in imidazole content for the 2,4-D treated sample is assigned based on the increased outer-shell $\sigma_{as}{}^2$ values for the imidazole atoms in one imidazole fits of the same overall coordination number (cf. fits 3 and 4 with 15 and 16, Table 3). This reduction is consistent with either direct or indirect displacement of a histidine ligand.

If the Fe(II) active site of TfdA is homologous to that of IPNS and DAOCS, with two histidine imidazole ligands, then these two imidazoles are bound at very different distances in a distorted site. The alternative explanation of the Fe EXAFS, that only one of the conserved histidines coordinates the Fe(II), is less satisfying, especially since Cu EXAFS shows that Cu(II), in substitution for Fe(II), binds to two imidazoles. On the other hand, chemical modification studies [13] show that multiple histidines reside near the active site, and one should consider the possibility that Cu(II) adopts a slightly different ligand environment than Fe(II).

Little structural change at Fe(II) or Cu(II) results from α-KG addition, but addition of 2,4-D does result in coordination changes for both. While our Cu K-edge XAS data can be explained by the 2,4-D-induced g–tensor rearrangement suggested previously or by histidine imidazole displacement, the Fe K-edge XAS data suggest that the loss of a histidine ligand in 2,4-D-containing samples is more likely. Ligand displacement upon substrate addition has been observed in other dioxygenases. For example, protein structural studies were used to show that a tyrosinate ligand is displaced from the Fe(III) active site in protocatechuate 3,4-dioxygenase [26] and magnetic circular dichroism studies provide evidence for ligand dissociation from the active site Fe(II) of phthalate dioxygenase [27]. The apparent disparity in the XAS and EPR spectroscopic results regarding the order of substrate binding (i.e., 2,4-D addition leads to marked changes in the EXAFS while the addition of α-KG leads to negligible changes; yet, the reverse order was observed for samples monitored by EPR [14]) can be explained by the inherent differences in properties examined by the spectral techniques. The XAS results are based on atomic environment, while the EPR spectra reflect the electronic environment. While α-KG binding may greatly perturb the electronic environment of the metal center, the substitution of water molecules by the oxygen atoms in this substrate may not be apparent when monitored by XAS. Similarly, the atomic environmental changes seen by XAS upon binding 2,4-D may not greatly influence the electronic environment, especially if 2,4-D binds to an axial position. For either type of spectroscopy it is important to emphasize that the results were obtained for enzyme

[1] 1s→3 d peak areas are approximated as 0.11, 0.10, and 0.12 eV for TfdA, Tfda + α-KG, and TfdA + 2,4-D, respectively

[2] ΔR_{as} is estimated by the equation $\sigma_{stat} \approx \frac{(mn)^{1/2}}{(m+n)} |R_m - R_n|$ where $\sigma_{stat} = (\sigma_{as}^2 - \sigma_{vib}^2)^{1/2}$ and m and n are the number of atoms at a distance of R_m and R_n, respectively. With $m = n = 1$, and an estimated σ_{vib}^2 of 0.002 Å^2 for the ~3-Å shell, an observed σ_{as}^2 of 0.0073 Å^2 would require $|R_m - R_n|$ to be 0.14 Å

COR-AAD1-00002470
Bayer EX1008 (Part 5 of 9)

incubated separately with each substrate. To address the order of substrate binding during catalysis, steady state kinetic measurements will need to be carried out. For most other α-KG-dependent dioxygenases that have been examined, such as prolyl hydroxylase, deacetoxyvindoline hydroxylase and lysyl hydroxylase [28–31], α-KG binds first, followed by O_2, then the hydroxylatable substrate. In other cases, such as thymine 7-hydroxylase [32], the order of oxygen and substrate binding is switched, but α-KG continues to bind first.

Acknowledgements We thank Fumiyasu Fukumori for preparation of a sample of TfdA that was used in the initial studies. N.J.C. performed some of the data analysis and wrote (along with R.A.S.) the XAS portions of the manuscript. C.M.V.S. performed data collection, reduction, and initial analysis. R.E.S. prepared the samples and along with R.P.H. provided the biochemical portions of the manuscript. This research was supported by the National Institutes of Health (GM 42025 to R.A.S.) and the National Science Foundation (MCB 9603520 and DEB 9120006 to R.P.H.). The XAS data were collected at the SSRL, which is operated by the Department of Energy, Division of Chemical Sciences. The SSRL Biotechnology Program is supported by the National Institute of Health, Biomedical Resource Technology Program, Division of Research Resources. N.J.C. is supported by a National Science Foundation Research Training Group Award to the Center for Metalloenzyme Studies (DIR 90-14281).

References

1. De Carolis E, De Luca V (1994) Phytochemistry 36:1093–1107
2. Prescott AG (1993) J Exp Biol 44:849–861
3. Prescott AG, John P (1996) Annu Rev Plant Physiol Plant Mol Biol 47:245–247
4. Borovok I, Landman O, Kreisberg-Zakarin R, Aharonowitz Y, Cohen G (1996) Biochemistry 35:1981–1987
5. Roach PL, Clifton IJ, Hensgens CMH, Shibata N, Schofield CJ, Hajdu J, Baldwin JE (1997) Nature 387:827–830
6. Valegard K, Terwisscha van Scheltinga AC, Lloyd MD, Hara T, Ramaswamy S, Perrakis A, Thompson A, Lee HJ, Baldwin JE, Schofield CJ, Hajdu JL, Andersson I (1998) Nature 394:805–809
7. Hegg EL, Que L Jr (1997) Eur J Biochem 250:625–629
8. Hausinger RP, Fukumori F, Hogan DA, Sassanella TM, Kamagata Y, Takami H, Saari RE (1997) In: Horikoshi K, Fukada M, Kudo T (eds) Microbial diversity and genetics of biodegradation. Karger, Basel, pp 35–51
9. Yabuuchi E, Kosako Y, Yano I, Hotta H, Nishiuchi Y (1995) Microbiol Immunol 39:897–904
10. Don RH, Pemberton JM (1985) J Bacteriol 161:466–468
11. Streber WR, Timmis KN, Zenk MH (1987) J Bacteriol 169:2950–2955
12. Fukumori F, Hausinger RP (1993) J Bacteriol 175:2083–2086
13. Fukumori F, Hausinger RP (1993) J Biol Chem 268:24311–24317
14. Whiting AK, Que L Jr, Saari RE, Hausinger RP, Fredrick MA, McCracken J (1997) J Am Chem Soc 119:3413–3414
15. Saari RE, Hausinger RP (1998) Biochemistry 37:3035–3042
16. Scott RA (1985) Methods Enzymol 117:414–459
17. Fransson G, Lundberg BKS (1972) Acta Chem Scand 26:3969
18. Jansen JC, Verhage M, van Konigsveld H (1982) Cryst Struct Commun 11:305
19. Rehr JJ, Mustre de Leon J, Zabinsky SL, Albers RC (1991) J Am Chem Soc 113:5135–5140
20. Brown IDDA (1985) J Am Chem Soc 113:5135–5140
21. Liu W, Thorp HH (1993) Inorg Chem 31:1585–1588
22. Scott RA, Wang S, Eidsness MK, Kriauciunas A, Frolik CA, Chen VJ (1992) Biochemistry 31:4596–4601
23. Roe AL, Scheider DJ, Mayer RJ, Pyrz JW, Widom J, Que L Jr (1984) J Am Chem Soc 106:1676–1681
24. Randall CR, Shu L, Chiou YM, Hagen KS, Ito M, Kitajima N, Lachicotte RJ, Zang Y, Que L Jr (1995) Inorg Chem 34:1036–1039
25. Cotton FA, Wilkinson G (1988) Advanced inorganic chemistry. Wiley-Interscience, New York
26. Orville AM, Lipscomb JD, Ohlendorf DH (1997) Biochemistry 36:10052–10066
27. Gassner GT, Ballou DP, Landrum GA, Whittaker JW (1993) Biochemistry 32:4820–4825
28. De Carolis E, De Luca V (1993) J Biol Chem 268:5504–5511
29. Myllylä R, Tuderman L, Kivirikko KI (1977) Eur J Biochem 80:349–357
30. Puistola U, Turpeenniemi-Hujanen TM, Myllylä R, Kivirikko KI (1980) Biochim Biophys Acta 611:40–50
31. Puistola U, Turpeenniemi-Hujanen TM, Myllylä R, Kivirikko KI (1980) Biochim Biophys Acta 611:51–60
32. Holme E (1975) Biochemistry 14:4999–5003

COR-AAD1-00002471
Bayer EX1008 (Part 5 of 9)

APPLIED AND ENVIRONMENTAL MICROBIOLOGY, June 1999, p. 2376–2381 Vol. 65, No. 6
0099-2240/99/$04.00+0
Copyright © 1999, American Society for Microbiology. All Rights Reserved.

Earthworm Egg Capsules as Vectors for the Environmental Introduction of Biodegradative Bacteria

L. L. DAANE† AND M. M. HÄGGBLOM*

Biotechnology Center for Agriculture and the Environment, Cook College, Rutgers University, New Brunswick, New Jersey 08901-8520

Received 16 November 1998/Accepted 21 March 1999

Earthworm egg capsules (cocoons) may acquire bacteria from the environment in which they are produced. We found that *Ralstonia eutropha* (pJP4) can be recovered from *Eisenia fetida* cocoons formed in soil inoculated with this bacterium. Plasmid pJP4 contains the genes necessary for 2,4-dichlorophenoxyacetic acid (2,4-D) and 2,4-dichlorophenol (2,4-DCP) degradation. In this study we determined that the presence of *R. eutropha* (pJP4) within the developing earthworm cocoon can influence the degradation and toxicity of 2,4-D and 2,4-DCP, respectively. The addition of cocoons containing *R. eutropha* (pJP4) at either low or high densities (10^2 or 10^5 CFU per cocoon, respectively) initiated degradation of 2,4-D in nonsterile soil microcosms. Loss of 2,4-D was observed within the first week of incubation, and respiking the soil with 2,4-D showed depletion within 24 h. Microbial analysis of the soil revealed the presence of approximately 10^4 CFU *R. eutropha* (pJP4) g^{-1} of soil. The toxicity of 2,4-DCP to developing earthworms was tested by using cocoons with or without *R. eutropha* (pJP4). Results showed that cocoons containing *R. eutropha* (pJP4) were able to tolerate higher levels of 2,4-DCP. Our results indicate that the biodegradation of 2,4-DCP by *R. eutropha* (pJP4) within the cocoons may be the mechanism contributing to toxicity reduction. These results suggest that the microbiota may influence the survival of developing earthworms exposed to toxic chemicals. In addition, cocoons can be used as inoculants for the introduction into the environment of beneficial bacteria, such as strains with biodegradative capabilities.

Earthworms are saprotrophic invertebrates which contribute to the overall structure, drainage, and aeration of soil ecosystems (11). In addition, earthworms directly and indirectly influence soil microbial communities, mainly through the processes of feeding, burrowing, and fecal (cast) deposition. Several studies have shown that earthworms can transport bacteria into the environment (6, 7, 9, 13, 16, 23, 27, 28, 29). In particular, previous studies have assessed the importance of earthworms for the transport of beneficial bacteria for use in biological control (27). More recently, earthworms have been implicated as vectors and contributors for bacterial gene transfer (6, 7). To date, the majority of these studies have focused on adult earthworms, with little attention to how developing cocoons or juvenile earthworms affect microbial communities.

Several studies have shown that microorganisms are associated with earthworm egg capsules (cocoons) (8, 18, 32). Morgan and Burrows (18) reported that the internal fluid of *Eisenia fetida* cocoons contained bacteria of the genera *Nocardia*, *Pseudomonas*, and *Alcaligenes*. Zachmann and Molina (32) were the first to quantify the bacteria present in egg capsules of *E. fetida*, with up to 10^8 CFU g^{-1} of cocoon. Attempts to identify several of the morphologically diverse cocoon isolates were inconclusive. In addition, Zachmann and Molina (32) determined that cocoons may acquire bacteria from the environment from which they are formed; however, the location and function of the bacteria within the cocoon were not addressed in that study. Recently, Daane et al. (8), using scanning electron microscopy, determined the location of bacteria within the developing earthworm cocoon. Examination of cocoon fragments containing well-developed juvenile earthworms revealed the presence of numerous rod-shaped microorganisms within the developing tissues. The microorganisms present did not appear to be detrimental to the developing earthworm tissue, which suggests a mutualistic association.

Earthworm cocoon fluid has been found to elicit an immune response against several bacterial species, which indicates that earthworms may be able to control the cocoon microbiota (30). This is also suggested by Daane et al. (7), who reported consistent recovery of *Ralstonia eutropha* (formerly *Alcaligenes eutrophus*) from *Aporrectodea trapezoides* cocoons formed in inoculated soil. In addition, Zachmann and Molina (32) reported that *Escherichia coli* could not be recovered from cocoons formed in microcosms inoculated with this bacterium.

Although cocoons have been found to contain and acquire microorganisms from the environment, few if any studies have been performed to assess how the earthworm egg capsule microbiota influences juvenile development, terrestrial microbial communities, or the fate of toxic chemicals in the environment. The latter is of particular interest because it would determine whether earthworm egg capsules could be used as biovectors for the introduction of beneficial bacteria, such as biological control, biodegradative, or plant-growth-promoting strains, into the environment.

The objectives of the present study were to use the 2,4-dichlorophenoxyacetic acid (2,4-D)-degrading bacterium, *R. eutropha* JMP222N (pJP4), and the compost earthworm, *E. fetida* as a model system to determine whether bacterial strains acquired by earthworm egg capsules can be released from the cocoons into the soil for degradation of 2,4-D. In addition, we assessed the ability of a degradative strain within the cocoon to

* Corresponding author. Mailing address: Department of Biochemistry and Microbiology, Cook College, Rutgers University, 76 Lipman Drive, New Brunswick, NJ 08901-8525. Phone: (732) 932-9763. Fax: (732) 932-8965. E-mail: haggblom@aesop.rutgers.edu.

† Present address: Environmental Molecular Biology, M888, Life Sciences Division, Los Alamos National Laboratory, Los Alamos, NM 87545.

Downloaded from http://aem.asm.org/ on September 3, 2020 at Corteva Agriscience

COR-AAD1-00002472
Bayer EX1008 (Part 5 of 9)

influence the level of tolerance of the developing earthworm to 2,4-dichlorophenol (2,4-DCP).

MATERIALS AND METHODS

Bacterial strains and growth conditions. *R. eutropha* JMP222N is a nalidixic acid-resistant mutant of JMP222, a streptomycin-resistant, cured derivative of *R. eutropha* JMP134(pJP4) (21). *R. eutropha* JMP222N containing pJP4 was obtained by patch mating as previously described (7). Plasmid pJP4 is an IncP, broad-host-range plasmid containing genes for mercury resistance and 2,4-D and 2,4-DCP degradation (21). Strains were maintained on selective media at 4°C, and long-term storage was in 50% glycerol at −80°C. *R. eutropha* JMP222N(pJP4) was initially grown in minimal salts basal medium (26) containing 2,4-D and, thereafter, was routinely grown at 28°C on selective tryptone yeast (TY) agar medium (1) containing streptomycin, nalidixic acid, and $HgCl_2$. *R. eutropha* JMP222N was routinely grown at 28°C on selective (streptomycin and nalidixic acid) TY agar medium. Filter-sterilized streptomycin, nalidixic acid, 2,4-D, and $HgCl_2$ stock solutions were added to media after autoclaving to final concentrations of 500, 30, 400, and 10 μg ml^{-1}, respectively.

For the inoculation of earthworm-mating microcosms, bacteria were grown in selective TY broth medium to mid- to late-exponential growth and harvested by centrifugation at 5,000 × *g* for 10 min. Cells were washed three times in a 0.1× mineral salts solution (5) (pH 7.0) and resuspended in the same solution to obtain 10^9 cells ml^{-1}.

Chemicals. 2,4-DCP and 2,4-D (>98% purity) were purchased from Aldrich Chemical Co. (Milwaukee, Wis.). Streptomycin sulfate and nalidixic acid were obtained from Sigma Chemical Co. (St. Louis, Mo.). Mercuric chloride was obtained from EM Science (Gibbstown, N.J.).

Earthworms. *E. fetida* (Savigny, 1826) earthworms were purchased from Carolina Biological Supply Co. (Burlington, N.C.). Laboratory stock cultures of *E. fetida* were propagated and maintained at room temperature in nonsterile Canadian sphagnum peat moss bedding (Magic Products, Amhurst Junction, Wis.). Ground oatmeal was supplied to the surface as a food source every 2 to 3 days.

Earthworm mating microcosms. The microcosm design consisted of 1 liter Nalgene jars (Nalge Nunc International, Rochester, N.Y.) containing a sterile mixture of 128 g of bedding material, 32 g of microcrystalline cellulose (FMC Corp., Philadelphia, Pa.), and 280 ml of either 0.1× mineral salts solution (pH 7.0) or washed bacterial suspension at a final concentration of 10^8 cells g^{-1} of bedding (wet weight) as indicated below. The inoculated treatments received either R. eutropha JMP222N(pJP4) or R. eutropha JMP222N. All three mating microcosm treatments were established in three replications. Each microcosm received 40 adult (clitellate) earthworms (400 to 600 mg each) taken randomly from stock culture and was left undisturbed for 1-week intervals in continuous darkness at 24°C for the production of egg capsules.

Extraction and enumeration of bacteria from earthworm bedding. All microcosms were analyzed for inoculated strains after 1 week of incubation. Microcosms inoculated with the degradative strain were also analyzed after 2 and 3 weeks of incubation. A 5-g subsample of bedding was aseptically taken, and bacterial cells were extracted from the bedding with 90 ml of sterile extractant solution containing 0.1% sodium pyrophosphate (pH 7.0) and 0.03% (vol/vol) Tween 80 (Sigma Chemical Co.). Bedding suspensions were shaken for 30 min at 250 rpm on a wrist-action shaker and allowed to settle for 10 min. A 10-ml portion of the upper, bedding-free phase was serially diluted in 0.01 M phosphate-buffered saline (pH 7.1) containing 0.03% Tween 80 (PBS-T) and spread plated, in duplicate, onto appropriate selective TY agar media. Bacteria were enumerated after 1 week of incubation at 28°C, and counts are reported as CFU per gram of bedding (wet weight).

Collection and bacterial analysis of earthworm egg capsules. Cocoons were collected from earthworm mating microcosms at the end of a 1-week incubation period. Cocoons were also collected after the second and third weeks of incubation from microcosms inoculated with *R. eutropha* JMP222N(pJP4). The cocoons (age range, 0 to 7 days) were washed under running tap water, rinsed in distilled water, and incubated at room temperature for 12 days on water-saturated filter paper in petri dishes, yielding cocoons of ages ranging from 12 to 19 days. This age was chosen since viability can easily be assessed by observing either embryo movement or blood circulation. In addition, studies have shown bacterial numbers to increase with increasing cocoon age (8, 32). Therefore, an age range of 12 to 19 days provides for an accurate prediction of the bacterial numbers which will be released upon cocoon hatching, which usually begins around an age of 24 days but may take as long as 45 days for complete development. Prior to bacterial analyses, cocoons were examined for viability, weighed, and surface sterilized as previously described (6). A statistical analysis of the cocoon viability was performed by using a two-sample *t* test (Minitab release 11 computer package; Minitab, Inc., University Park, Pa.).

Five viable cocoons formed in each of the three earthworm mating microcosm treatments were analyzed for the presence of the inoculated bacterial strains. Each cocoon was homogenized by using a sterile tissue grinder in 2 ml of PBS-T and then analyzed as described for bedding analysis. Results are reported as CFU per cocoon.

2,4-D amended soil microcosms. A Hubbard loamy sand (Udorthentic Haploboroll) was used for all degradation experiments and was described previously (6). The microcosms consisted of 3 g (dry weight) of nonsterile soil in 7-ml glass serum vials. A filter-sterilized solution of 2,4-D was added to each of the microcosms to give a final concentration of approximately 100 ppm and a moisture content of 16.5% (gravimetric determination), which is conducive to earthworm survival. The experimental design included treatments of nonsterile soil with or without added earthworm egg capsules. A sufficient number of microcosms for each treatment were made for duplicate analyses of 2,4-D at each time point. The cocoon-containing treatments included uninoculated cocoons (formed in uninoculated sterile bedding), JMP222N cocoons (formed in *R. eutropha* JMP222N inoculated bedding), and JMP222N(pJP4) cocoons [formed in *R. eutropha* JMP222N(pJP4) inoculated bedding]. For microcosms containing cocoons, two surface-sterilized viable cocoons, ranging in age from 12 to 19 days, were added to the soil.

Quantification of 2,4-D biodegradation. The utilization of 2,4-D was determined by high-pressure liquid chromatography (HPLC). At each time point duplicate soil microcosms from each treatment were destructively sampled by vortexing for 2 min with 3 ml of distilled water. The soil slurry was transferred to a microcentrifuge tube and centrifuged at 16,000 × *g* for 5 min. The supernatant was filtered and analyzed by HPLC (Shimadzu model SCL-10A; Shimadzu, Columbia, Md.) equipped with a SphereClone ODS (2) column (250 by 4.6 mm; particle size, 5 μm; Phenomenex, Torrance, Calif.) with methanol-water-acetic acid (60:38:2, 1 ml min^{-1}) as the eluant with detection at 280 nm by using a Shimadzu SPD-10A UV-visible variable-wavelength detector. The results are reported in parts per million as the mean from duplicate soil microcosms.

Toxicity of 2,4-DCP to earthworm egg capsules and adults. Surface-sterilized cocoons containing viable embryos were exposed to various concentrations of 2,4-DCP. A filter-sterilized stock solution of 2,4-DCP in 0.1 N NaOH was added to molten 0.2% Nobie agar (Difco, Detroit, Md.) and poured into sterile glass petri dishes and allowed to cool. The final concentrations of 2,4-DCP tested included 0.1, 0.5, 1, 3, 5, 10, 15, 20, 25, 30, 40, and 50 ppm. In addition, a control was included which did not contain 2,4-DCP. The same concentration of NaOH was present in each of the petri dishes independent of the 2,4-DCP concentration. Several cocoons from each of the three earthworm mating microcosm treatments were fully submersed into the various concentrations of semisolid 2,4-DCP agar and checked for viability over time at room temperature. Viability was assessed with a stereoscope and was based on observing either movement or circulating blood in the developing worms. The experiment was halted after the hatching of remaining viable cocoons.

Adult earthworms, taken randomly from stock cultures, were also tested by the above methodology. The adults were tested in 10, 15, 20, 25, and 30 ppm 2,4-DCP. Three adults were added for each concentration, except for the 30-ppm concentration, which had six adults. Earthworms were assessed for mortality over time and were considered dead when the worms no longer responded to physical stimuli.

RESULTS

Enumeration of inoculated strains in earthworm bedding. Earthworm bedding was inoculated with either *R. eutropha* JMP222N(pJP4) or its plasmid-free derivative at an initial density of 10^8 cells g^{-1} (wet weight) of bedding. The bedding was analyzed for the inoculated strains after incubation for 1 week in the presence of 40 adult earthworms. Both inoculated strains decreased approximately 10-fold from the initial inoculation density to approximately 10^7 CFU g^{-1} of bedding at day 7. Neither of the *R. eutropha* strains could be isolated from the uninoculated control microcosms, with a level of detection of 9.0×10^1 CFU g^{-1} of soil.

To determine the survival of *R. eutropha* JMP222N(pJP4) over time, two earthworm mating microcosms were analyzed for 2 additional weeks. Each successive week revealed a decrease in the numbers of *R. eutropha* JMP222N(pJP4) recovered, with mean numbers of 1.4×10^7, 3.0×10^5, and 2.5×10^4 CFU g^{-1} for weeks 1, 2, and 3, respectively.

Egg capsule production. Replicate earthworm mating microcosms were set up for each treatment in order to perform both degradation and toxicity studies. None of the earthworms from the earthworm mating microcosms died or showed signs of loss of secondary sexual characteristics (presence of clitellum) during the course of the experiments. The average numbers of cocoons produced per worm in the uninoculated and the *R. eutropha* JMP222N- and *R. eutropha* JMP222N(pJP4)-inoculated mating microcosms over a 7-day mating period were 1.37 ± 0.49, 1.43 ± 0.42, and 1.48 ± 0.40, respectively. The average total numbers of cocoons produced weekly from

Downloaded from http://aem.asm.org/ on September 3, 2020 at Corteva Agriscience

COR-AAD1-00002473
Bayer EX1008 (Part 5 of 9)

40 adult earthworms over a 3-week period from two *R. eutropha* (pJP4)-inoculated mating microcosms were 51, 50, and 44 cocoons after weeks 1, 2, and 3, respectively. The greatest variability between the treatments was seen in the viability of the cocoons. The viabilities of cocoons collected from the uninoculated and the *R. eutropha* JMP222N(pJP4)-inoculated mating microcosms were 52 ± 8% and 92 ± 6%, respectively. The difference between the mean viabilities is significant ($P = 0.0056$).

Recovery of inoculated strains from earthworm egg capsules. Viable cocoons were analyzed after 12 days of incubation at room temperature. The average cocoon weight was 13.1 ± 1.5 mg (mean ± standard deviation for 24 cocoons), and the selective agar plates used for the evaluation of surface sterilization revealed no growth.

A total of five cocoons, collected from bedding after 1 week of egg capsule production from each treatment, were analyzed for the inoculated strains. Neither of the *R. eutropha* strains could be recovered from cocoons collected from the uninoculated treatments, with the level of detection being 1.0×10^1 CFU cocoon^{-1}. Cocoons formed in bedding inoculated with *R. eutropha* JMP222N had a mean number of 9.3×10^4 CFU cocoon^{-1}. Similar results were found with the cocoons formed in bedding inoculated with *R. eutropha* JMP222N(pJP4), with a mean number of 1.0×10^5 CFU cocoon^{-1} of the degradative strain. In addition, several cocoons collected after the second and third weeks of egg capsule production from two microcosms inoculated with *R. eutropha* JMP222N(pJP4) were analyzed for the degradative strain. The cocoons had 1.1×10^4 and 1.2×10^2 CFU cocoon^{-1} of recoverable *R. eutropha* JMP222N(pJP4) within earthworm cocoons collected at weeks 2 and 3, respectively.

Degradation of 2,4-D in earthworm egg capsule containing soil microcosms. Degradation of 2,4-D by bacteria introduced with developing earthworm egg capsules was examined by placing two earthworm cocoons, collected from earthworm mating microcosms, in 3 g of nonsterile soil amended with 100 ppm of 2,4-D. The cocoons were approximately 1 week from hatching, and juvenile earthworms were observed in the soil microcosms as early as 5 days after the start of the experiment; however, complete hatching of all cocoons required up to 25 days from the onset of the experiment. Microcosms were analyzed over time for loss of 2,4-D by HPLC. Figure 1 shows the loss of 2,4-D only in soil microcosms containing cocoons which were formed in bedding inoculated with the degradative strain, *R. eutropha* JMP222N(pJP4). The concentration of 2,4-D fell to below the level of detection within 4 days in the *R. eutropha* JMP222N(pJP4) treatments. 2,4-D was utilized within 24 h after the remaining experimental microcosms were respiked at day 10 and day 11. In contrast, no appreciable loss of 2,4-D occurred in nonsterile microcosms or in microcosms with cocoons containing *R. eutropha* JMP222N or with cocoons formed in uninoculated bedding. Analysis of the soil after complete hatching, on day 11 from two of the microcosms to which *R. eutropha* JMP222N(pJP4) cocoons had been added, showed the presence of 1.5×10^4 CFU of *R. eutropha* JMP222N(pJP4) g^{-1} (wet weight) of soil.

A comparative degradation experiment was set up with earthworm cocoons collected after 1 or 3 weeks from bedding initially inoculated with *R. eutropha* JMP222N(pJP4). The egg capsules collected after the first 7 days of cocoon production contained a mean density of 10^5 CFU of *R. eutropha* (pJP4) per cocoon and were considered high-inoculum cocoons. In contrast, cocoons collected after the third week of cocoon production contained a mean density of 10^2 CFU of *R. eutropha* (pJP4) per cocoon and were considered low-inoculum cocoons. Loss of 2,4-D was observed in both the high- and low-inoculum cocoon microcosms (Fig. 2). At the low-inoculum density of 10^2 CFU cocoon^{-1}, 2,4-D degradation occurred after 7 days from the start of the experiment.

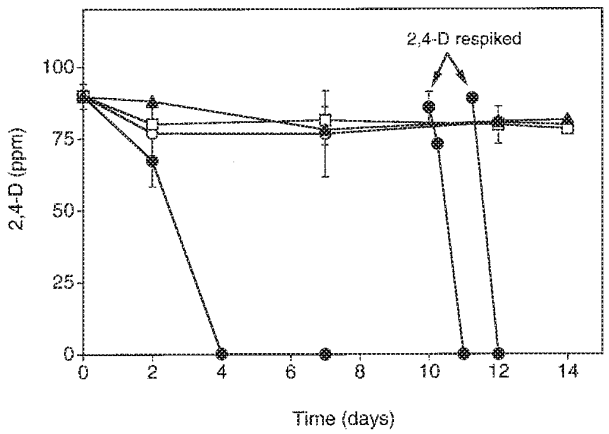


FIG. 1. Degradation of 2,4-D in nonsterile soil with or without added earthworm cocoons. Cocoons contained *R. eutropha* JMP222N(pJP4), *R. eutropha* JMP222N, or no degradative bacteria (nonsterile) and were about 1 week from hatching when added to the degradation microcosms at time zero. Juvenile worms containing microcosms were respiked with 100 ppm of 2,4-D on days 10 and 11. Data points represent the mean of two replicate samples. Error bars indicate the standard deviation, and where no standard bar is presented the value is less than the height of the symbol. Symbols: ▲, no cocoons; □, nonsterile cocoons; ○, JMP222N cocoons; ●, JMP222N(pJP4) cocoons.

Toxicity of 2,4-DCP to developing earthworms and adults. Preliminary studies revealed that 2,4-D was not toxic to adults or developing earthworms at concentrations of up to 1,000 ppm (data not shown). However, the first intermediate product of 2,4-D degradation, 2,4-DCP, has been found to be extremely toxic to earthworms (10). Therefore, toxicity studies were undertaken to determine the ability of a degradative bacterial strain to influence the tolerance of the developing earthworm to 2,4-DCP.

The toxicity of 2,4-DCP was assessed by embedding cocoons (12 to 19 days of age), with or without the degradative bacterial

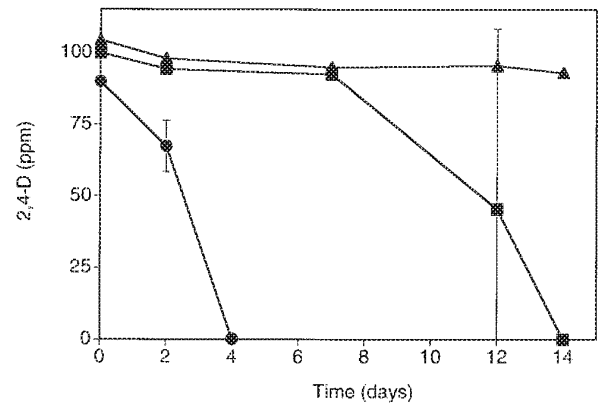


FIG. 2. Comparison of degradation of 2,4-D in nonsterile soil with cocoons containing high (~10^5 CFU cocoon^{-1}; ●) or low (~10^2 CFU cocoon^{-1}; ■) densities of *R. eutropha* JMP222N(pJP4) or without cocoons (▲). Data points represent the mean of two replicate samples. Error bars indicate the standard deviation, and where no standard bar is presented the value is less than the height of the symbol.

Downloaded from http://aem.asm.org/ on September 3, 2020 at Corteva Agriscience

COR-AAD1-00002474
Bayer EX1008 (Part 5 of 9)

TABLE 1. Viability of cocoons exposed to various concentrations of 2,4-DCP with or without *R. eutropha* JMP222N(pJP4)

Concn (ppm)[a]	Viability (%) after 23 days[b] in cocoons:	
	Without *R. eutropha* (pJP4)[c]	Containing *R. eutropha* (pJP4)[d]
0	100	100
5	100	100
10	100	100
15	60	100
20	0	100
25	0	83
30	0	67
40	0	0

[a] Exposure to 0.1, 0.5, 1, and 3 ppm of 2,4-DCP showed no mortality to developing earthworms with or without the degradative strain. Exposure to 50 ppm showed 100% mortality.

[b] Five to six cocoons ranging in age of 12 to 19 days were tested for each concentration. The cocoons were embedded in 0.2% Noble agar containing 2,4-DCP in glass petri dishes.

[c] Cocoons without *R. eutropha* (pJP4) were collected from nonsterile earthworm mating microcosms after 1 week of incubation.

[d] *R. eutropha* (pJP4)-containing cocoons were collected from earthworm mating microcosms inoculated with *R. eutropha* JMP222N(pJP4) after 1 week of incubation.

strain, into various concentrations of semisolid 2,4-DCP-containing agar. Cocoons which were formed in earthworm mating microcosms inoculated with *R. eutropha* JMP222N had results similar to those of cocoons formed in uninoculated bedding (data not shown). Table 1 shows the viability of cocoons after 23 days of continuous exposure to various concentrations of 2,4-DCP. Cocoons containing approximately 10^5 CFU of *R. eutropha* (pJP4) cocoon^{-1} showed a 33% mortality in 30 ppm of 2,4-DCP, with the remaining cocoons successfully hatching in this concentration. In contrast, cocoons formed in uninoculated bedding had a mortality of 40% at 15 ppm of 2,4-DCP. For cocoons with or without *R. eutropha* (pJP4), the mortality increased to 100% at 40 and 20 ppm of 2,4-DCP, respectively. Although the cocoons formed in uninoculated bedding were nonviable after long-term exposure to 20 ppm 2,4-DCP, viability was maintained for up to 15 days, with the greatest mortality (80%) occurring within the first 5 days (Fig. 3). The viability of cocoons containing the degradative strain *R. eutropha* (pJP4) exposed to 40 ppm of 2,4-DCP showed similar results in that the greatest mortality occurred within the first few days of incubation and 100% mortality occurring at 11 days (data not shown).

Adult earthworms taken randomly from laboratory stock were exposed to 2,4-DCP in the same manner as cocoons to determine whether adults and developing worms have similar tolerance levels. Adult earthworms died within 48 h of exposure to 25 and 30 ppm of 2,4-DCP and survived up to 7 days in 20 ppm of 2,4-DCP. All of the adult earthworms survived long-term exposure (2 weeks) in 10 and 15 ppm of 2,4-DCP.

DISCUSSION

In the present study we determined that a degradative bacterial strain associated with earthworm cocoons can be released into the soil upon hatching and can initiate the biodegradation of the herbicide 2,4-D. This suggests that earthworm cocoons can be used as biovectors for the delivery of beneficial bacteria into the environment. Our study showed that utilization of 2,4-D was seen only in soil that contained cocoons which were formed in bedding inoculated with the degradative

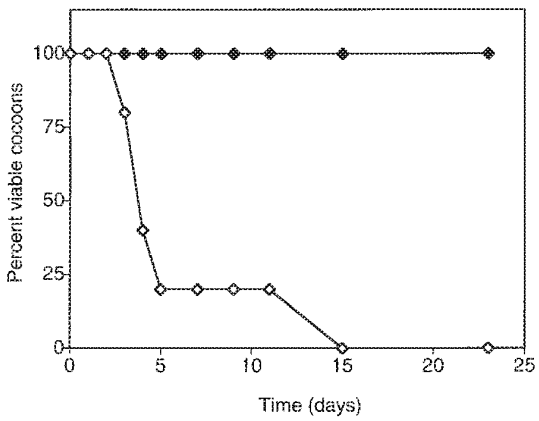


FIG. 3. Toxicity of 20 ppm of 2,4-DCP to cocoons formed in uninoculated or *R. eutropha* JMP222N(pJP4)-inoculated earthworm mating microcosms. Symbols: ◇, nonsterile cocoons; ◆, *R. eutropha* (pJP4) cocoons.

strain, *R. eutropha* JMP222N(pJP4). The number of days needed for complete loss of 2,4-D was significantly less when cocoons contained a higher density of *R. eutropha* (pJP4). Nevertheless, it should be noted that complete loss of 2,4-D was seen even when cocoons contained a mean density of ~10^2 CFU of *R. eutropha* (pJP4) cocoon^{-1}. Analysis of the soil, after complete hatching of the juvenile earthworms, revealed the presence of *R. eutropha* JMP222N(pJP4) at relatively high concentrations (~10^4 CFU g^{-1} of soil). The use of surface-sterilized cocoons determined that the inoculation of the soil with the degradative strain was solely due to cocoon hatching and not to carryover from the inoculated mating-microcosm bedding material. Our data also suggest that the semipermeable nature of the earthworm cocoon shell may initiate the degradation of 2,4-D in vivo. To our knowledge, this represents the first study demonstrating the degradation of 2,4-D by *R. eutropha* (pJP4) with an earthworm egg capsule as a delivery vehicle.

The number of earthworm egg capsules produced per worm per week was not different between the uninoculated and inoculated mating-microcosm treatments. However, our results are higher than those previously published by Zachmann and Molina (32), who used similar mating conditions. In the present study, the decreasing number of egg capsules produced from the same earthworms over a 3-week period suggests that necessary resources may become depleted from the medium over time. Resource depletion was suggested in studies by van Gestal et al. (31) and Hartenstein et al. (12); however, more work in this area with the present system is needed to support this hypothesis.

The viability of cocoons formed in uninoculated sterile bedding was significantly lower than for cocoons collected from inoculated mating microcosms. However, no difference was seen in cocoon viability between uninoculated or inoculated microcosms after a second consecutive week of cocoon production (data not shown). A possible reason for the increase in viability of cocoons collected from the sterile microcosm is that the earthworms added to the mating microcosms were reinoculating the sterilized bedding with bacteria. This suggests that a certain density or population of bacteria may be required for proper earthworm development, but this hypothesis remains to be proven.

In the present study, we isolated an average of 10^5 CFU of either *R. eutropha* strain per cocoon from egg capsules formed

Downloaded from http://aem.asm.org/ on September 3, 2020 at Corteva Agriscience

COR-AAD1-00002475
Bayer EX1008 (Part 5 of 9)

in bedding inoculated with these bacteria. These results are similar to those reported by Daane et al. (7) from *Aporrectodea trapezoides* cocoons collected from soil columns inoculated with the same bacterial strain. In addition, in the present study cocoons collected weekly from a microcosm inoculated with *R. eutropha* JMP222N(pJP4) showed decreasing numbers of this strain from weeks 1 to 3, a finding which directly corresponds to the same decline seen in the bedding material.

The majority of toxicity studies have focused on adult earthworms (for a review, see reference 10). Several studies have assessed sublethal effects (juvenile growth, cocoon production or hatching, and immune system effects) (2, 3, 14, 15, 17, 19, 25, 31); however, none have examined the toxicity of chemicals to developing earthworms in cocoons directly. Several studies have shown that 2,4-D is not toxic to adult earthworms even at high concentrations; however, the first intermediate of its degradation, 2,4-DCP, has been found to be highly toxic (20, 22, 24). Therefore, we focused our attention on the toxicity of 2,4-DCP to developing earthworms. Our results show that the presence of the 2,4-D-degrading bacterium, *R. eutropha* (pJP4), within the developing cocoon greatly increases the tolerance to this highly toxic compound. Indeed, the exposure level allowing the successful hatching of juvenile earthworms was twice that of cocoons devoid of the degrading bacterium.

Studies have shown that juvenile earthworms are more sensitive to agrochemicals than mature worms (17, 25). Contrary to these results, we found no difference in the level of tolerance to 2,4-DCP between developing worms within the cocoon and adults. However, our results cannot be directly compared to previous studies because we used a continual exposure contact test rather than an artificial soil or filter paper test of limited exposure time. The present method of using a semisolid agar medium was appropriate because it allowed for total immersion of the cocoon and daily assessment of viability without disturbance. In addition, the concentration of agar used here immobilized the cocoon without interfering with normal development and hatching.

Taken together, our results show that the presence of a degradative strain within the developing earthworm cocoon can increase the tolerance to toxic compounds, which indicates that the bacteria were metabolically active in vivo. In addition, we have shown that earthworm cocoons can release beneficial strains of bacteria into the soil upon hatching and initiate biodegradation. The present work with 2,4-D as the model system is currently being expanded to include degradation of more recalcitrant compounds such as polyaromatic hydrocarbons and polychlorinated biphenyls. We are also interested in including beneficial microbes such as plant pathogen antagonists and rhizobia. In addition, it will be interesting to determine if this model system can be extended to include other agriculturally relevant species of earthworms, such as *A. trapezoides*, *Lumbricus rubellus*, and *L. terrestris*. Furthermore, the influence of soil texture, pH, moisture, and temperature on the rate and degree of degradation will be important to determine in future studies.

ACKNOWLEDGMENTS

This work was supported in part by a grant from the New Jersey Commission on Science and Technology.

We thank Mervyn de Souza, Lisa Newman, and Michael Sadowsky for helpful discussions and suggestions regarding the manuscript. We also thank Gregory Flanagan and Quinn Im for technical assistance.

REFERENCES

1. **Beringer, J. E.** 1974. R factor transfer in *Rhizobium leguminosarum*. J. Gen. Microbiol. **84:**188–198.
2. **Bouwman, H., and A. J. Reinecke.** 1987. Effects of carbofuran on the earthworm, *Eisenia fetida*, using a defined medium. Bull. Environ. Contam. Toxicol. **38:**171–178.
3. **Bunn, K. E., H. M. Thompson, and K. A. Tarrant.** 1996. Effects of agrochemicals on the immune systems of earthworms. Bull. Environ. Contam. Toxicol. **57:**632–639.
4. **Clegg, C. D., J. M. Anderson, H. M. Lappin-Scott, J. D. van Elsas, and J. M. Jolly.** 1995. Interaction of a genetically modified *Pseudomonas fluorescens* with the soil-feeding earthworm *Octolasion cyaneum* (Lumbricidae). Soil Biol. Biochem. **27:**1423–1429.
5. **Cole, M. A., and G. H. Elkan.** 1973. Transmissible resistance to penicillin G, neomycin, and chloramphenicol in *Rhizobium japonicum*. Antimicrob. Agents Chemother. **4:**248–253.
6. **Daane, L. L., J. A. E. Molina, E. C. Berry, and M. J. Sadowsky.** 1996. Influence of earthworm activity on gene transfer from *Pseudomonas fluorescens* to indigenous soil bacteria. Appl. Environ. Microbiol. **62:**515–521.
7. **Daane, L. L., J. A. E. Molina, and M. J. Sadowsky.** 1997. Plasmid transfer between spatially separated donor and recipient bacteria in earthworm-containing soil microcosms. Appl. Environ. Microbiol. **63:**679–686.
8. **Daane, L. L., J. A. E. Molina, and M. J. Sadowsky.** 1998. Scanning electron microscopy of the microflora in egg capsules of the earthworm *Eisenia fetida*. Pedobiologia **42:**79–87.
9. **Doube, B. M., M. H. Ryder, C. W. Davoren, and P. M. Stephens.** 1994. Enhanced root nodulation of subterranean clover (*Trifolium subterraneum*) by *Rhizobium leguminosarum* biovar *trifolii* in the presence of the earthworm *Aporrectodea trapezoides* (Lumbricidae). Biol. Fertil. Soils **18:**169–174.
10. **Edwards, C. A., and P. J. Bohlen.** 1992. The effects of toxic chemicals on earthworms. Rev. Environ. Contam. Toxicol. **125:**23–99.
11. **Edwards, C. A., P. J. Bohlen, D. R. Linden, and S. Subler.** 1995. Earthworms in agroecosystems, p. 185–213. *In* P. F. Hendrix (ed.), Earthworm ecology and biogeography in North America. Lewis Publishers, Boca Raton, Fla.
12. **Hartenstein, R., E. F. Neuhauser, and D. L. Kaplan.** 1979. Reproductive potential of the earthworm *Eisenia foetida*. Oecologia (Berlin) **43:**329–340.
13. **Hendriksen, N. B.** 1995. Effects of detritivore earthworms on dispersal and survival of the bacterium *Aeromonas hydrophila*. Acta Zool. Fennica **196:** 115–119.
14. **Lofs-Holmin, A.** 1980. Measuring growth of earthworms as a method of testing sublethal toxicity of pesticides. Swed. J. Agric. Res. **10:**25–33.
15. **Lofs-Holmin, A.** 1982. Measuring cocoon production of the earthworm *Allolobophora caliginosa* (Sav.) as a method of testing sublethal toxicity of pesticides. Swed. J. Agric. Res. **12:**117–119.
16. **Madsen, E. L., and M. Alexander.** 1982. Transport of *Rhizobium* and *Pseudomonas* through soil. Soil Sci. Soc. Am. J. **46:**557–560.
17. **Martin, N. A.** 1986. Toxicity of pesticides to *Allolobophora caliginosa* (Oligochaeta: Lumbricidae). N. Z. J. Agric. Res. **29:**699–706.
18. **Morgan, M., and I. Burrows.** 1982. Earthworm/microorganism interactions. Rothamsted Exp. Stn. Rep. **1982:**104.
19. **Neuhauser, E. F., and C. A. Callahan.** 1990. Growth and reproduction of the earthworm *Eisenia fetida* exposed to sublethal concentrations of organic chemicals. Soil Biol. Biochem. **22:**175–179.
20. **Neuhauser, E. F., R. C. Loehr, M. R. Malecki, D. L. Milligan, and P. R. Durkin.** 1985. The toxicity of selected organic chemicals to the earthworm *Eisenia fetida*. J. Environ. Qual. **14:**383–388.
21. **Pemberton, J. M., B. Corney, and R. B. Don.** 1979. Evolution and spread of pesticide degrading ability among soil micro-organisms, p. 287–299. *In* K. N. Timmis and A. Pühler (ed.), Plasmids of medical, environmental and commercial importance. Elsevier/North-Holland Biomedical Press, Amsterdam, The Netherlands.
22. **Potter, D. A., P. G. Spicer, C. T. Redmond, and A. J. Powell.** 1994. Toxicity of pesticides to earthworms in Kentucky bluegrass turf. Bull. Environ. Contam. Toxicol. **52:**176–181.
23. **Reddell, P., and A. V. Spain.** 1991. Earthworms as vectors of viable propagules of mycorrhizal fungi. Soil Biol. Biochem. **23:**767–774.
24. **Roberts, B. L., and H. W. Dorough.** 1984. Relative toxicities of chemicals to the earthworm *Eisenia foetida*. Environ. Toxicol. Chem. **3:**67–78.
25. **Spurgeon, D. J., and S. P. Hopkin.** 1996. Effects of metal-contaminated soils on the growth, sexual development, and early cocoon production of the earthworm *Eisenia fetida*, with particular reference to zinc. Ecotox. Environ. Safety **35:**86–95.
26. **Stanier, R. Y., N. J. Palleroni, and M. Doudoroff.** 1966. The aerobic pseudomonads: a taxonomic study. J. Gen. Microbiol. **43:**159–271.
27. **Stephens, P. M., C. W. Davoren, M. H. Ryder, and B. M. Doube.** 1993. Influence of the lumbricid earthworm *Aporrectodea trapezoides* on the colonization of wheat roots by *Pseudomonas corrugata* strain 2140R in soil. Soil Biol. Biochem. **25:**1719–1724.
28. **Stephens, P. M., C. W. Davoren, M. H. Ryder, and B. M. Doube.** 1994. Influence of the earthworm *Aporrectodea trapezoides* (Lumbricidae) on the colonization of alfalfa (*Medicago sativa* L.) roots by *Rhizobium meliloti* L5-

Downloaded from http://aem.asm.org/ on September 3, 2020 at Corteva Agriscience

COR-AAD1-00002476
Bayer EX1008 (Part 5 of 9)

30R and the survival of *R. meliloti* L5-30R in soil. Biol. Fertil. Soils **18:**63–70.
29. **Thorpe, I. S., J. I. Prosser, L. A. Glover, and K. Killham.** 1996. The role of the earthworm *Lumbricus terrestris* in the transport of bacterial inocula through soil. Biol. Fertil. Soils **23:**132–139.
30. **Valembois, P., P. Roch, and M. Lassegues.** 1986. Antibacterial molecules in annelids, p. 74–93. *In* M. Brehélin (ed.), Immunity in invertebrates. Springer-Verlag, Berlin, Germany.
31. **van Gestel, C. A. M., W. A. van Dis, E. M. van Breemen, and P. M. Sparenburg.** 1989. Development of a standardized reproduction toxicity test with the earthworm species *Eisenia fetida andrei* using copper, pentachlorophenol, and 2,4-dichloroaniline. Ecotox. Environ. Safety **18:**305–312.
32. **Zachmann, J. E., and J. A. E. Molina.** 1993. Presence of culturable bacteria in cocoons of the earthworm *Eisenia fetida*. Appl. Environ. Microbiol. **59:** 1904–1910.

Downloaded from http://aem.asm.org/ on September 3, 2020 at Corteva Agriscience

COR-AAD1-00002477
Bayer EX1008 (Part 5 of 9)

ELSEVIER

FEMS Microbiology Ecology 35 (2001) 75–84

FEMS MICROBIOLOGY Ecology

www.fems-microbiology.org

Enhanced degradation of phenoxyacetic acid in soil by horizontal transfer of the *tfdA* gene encoding a 2,4-dichlorophenoxyacetic acid dioxygenase

Julia R. de Lipthay [a,b,*], Tamar Barkay [c], Søren J. Sørensen [a]

[a] *Department of General Microbiology, University of Copenhagen, Sølvgade 83H, DK-1307 Copenhagen K, Denmark*
[b] *Department of Geochemistry, Geological Survey of Denmark and Greenland, Thoravej 8, DK-2400 Copenhagen NV, Denmark*
[c] *Department of Biochemistry and Microbiology, Cook College, Rutgers University, New Brunswick, NJ 08901, USA*

Received 24 July 2000; received in revised form 23 October 2000; accepted 24 October 2000

Abstract

Few studies have investigated the possible impact of in situ gene transfer on the degradation of xenobiotic compounds in natural environments. In this work we showed that horizontal transfer of the *tfdA* gene, carried on plasmid pRO103, to phenol degrading recipient strains significantly increased the degradation rate of phenoxyacetic acid in sterile and non-sterile soil microcosms. The *tfdA* gene encodes a 2,4-dichlorophenoxyacetic acid/2-oxoglutarate dioxygenase and by complementation with the phenol degradation pathway an expanded catabolic substrate range, now including phenoxyacetic acid, is evolved. Presence of selective pressure had a positive effect on the emergence of transconjugants. However, even in the absence of phenoxyacetic acid transconjugant populations were detected and were kept at a constant level throughout the experimental period. The residuesphere (interface between decaying plant material and soil matrix) of dry leaves of barley was shown to be a hot-spot for gene transfer and presence of barley straw increased the conjugation frequencies in soil microcosms to the same extent as presence of organic nutrients. The results of this study indicate that dissemination of catabolic plasmids is a possible mechanism of genetic adaptation to degradation of xenobiotic compounds in natural environments, and that complementation of catabolic pathways possibly plays an important role in the evolution of new degradative capabilities. The application of horizontal gene transfer as a possible tool in bioremediation of contaminated sites is discussed. © 2001 Federation of European Microbiological Societies. Published by Elsevier Science B.V. All rights reserved.

Keywords: Genetic adaptation; Gene transfer; Phenoxyacetic acid; Complementation; Bioremediation; *tfdA*

1. Introduction

Genetic adaptation has been suggested to play an important role in microbial adaptation to degradation of xenobiotic compounds in natural environments, and to the evolution of new catabolic capabilities (for review see [1]). Horizontal gene transfer is one of the mechanisms of genetic adaptation and several studies have shown that plasmid conjugation is a process that occurs in terrestrial environments (for review see e.g. [2,3]). Likewise, a large number of studies have examined the potential for degradation of xenobiotic compounds by the indigenous soil microbial community as well as by inoculated biodegrading strains. However, only few studies have been designed to investigate the direct impact of horizontal transfer of catabolic genes on the degradation of xenobiotic compounds [4–6], and to elucidate the molecular events that take place during genetic adaptation in situ.

Dissemination of catabolic genes among endogenous microbial populations may be a valuable alternative to bioaugmentation in bioremediation scenarios. In situ transfer of catabolic genes to the indigenous populations of microorganisms can exploit the fact that these organisms are well adapted to the environment in question (as compared to inoculated strains) as well as to the constantly changing conditions, which prevail in nature. The use of this strategy, thus, has potential to ensure a more efficient maintenance as well as dispersal of the catabolic genes in the environment. Two different approaches have been suggested [7,8]: (i) the dissemination of plasmids encoding a complete degradation pathway, and (ii) the trans-

* Corresponding author. Tel.: +45 (38) 14 23 28; Fax: +45 (38) 14 20 50; E-mail: jli@geus.dk

0168-6496/01/$20.00 © 2001 Federation of European Microbiological Societies. Published by Elsevier Science B.V. All rights reserved.
PII: S0168-6496(00)00113-6

Downloaded from https://academic.oup.com/femsec/article/35/1/75/524663 by Pearson Hi-Ed International user on 03 September 2020

COR-AAD1-00002478
Bayer EX1008 (Part 5 of 9)

fer of a small number of genes which by complementation of existing pathways in the indigenous flora will expand the catabolic range of the indigenous community.

The approach presented here was to study the in situ complementation of the phenol degradation pathway with the *tfdA* gene, encoding a 2,4-dichlorophenoxyacetic acid/2-oxoglutarate dioxygenase [9], giving rise to a vertically expanded pathway, now including phenoxyacetic acid (PAA) (Fig. 1). We have previously shown that transfer of the *tfdA* gene resulted in the degradation of PAA by transconjugant strains of some phenol degraders [8]. Here we take this study one step further by testing the effect of such transfer on PAA degradation in sterile as well as non-sterile soil microcosms. The conjugative plasmid pRO103 [10] was used as a vector for transfer of the *tfdA* gene from *Escherichia coli* HB101 to the phenol degrading bacterium *Ralstonia eutropha* AEO106 as well as to indigenous soil bacteria. Plasmid pRO103 is a derivative of pJP4 having a deletion in the *Eco*RI E fragment, and harbours the transposon, Tn*1721*, encoding resistance to tetracycline [10]. Plasmid pJP4 is an 80 kb conjugative IncP-1 plasmid isolated from *R. eutropha* JMP134, harbouring catabolic genes (*tfd*) encoding a pathway for the degradation of 2,4-dichlorophenoxyacetic acid (2,4-D) [11,12]. However, the substrate range of the *tfdA* gene product is very broad and includes PAA [13]. The product of the *tfdB* gene, the enzyme 2,4-dichlorophenol hydroxylase, can not use non-substituted phenol as a substrate [14]. Thus only bacteria able to degrade phenol can use PAA as a growth substrate when complemented with pRO103. Such transconjugants carry a vertically expanded pathway that transforms PAA to CO_2 and water (Fig. 1).

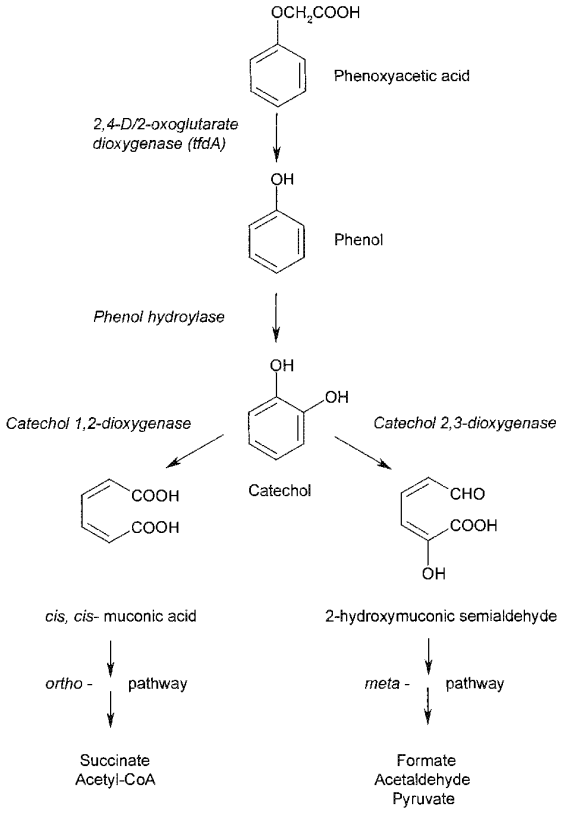


Fig. 1. Complementation of the pathway for phenol degradation with the *tfdA* gene, encoding a 2,4-D/2-oxoglutarate dioxygenase, results in a vertically expanded catabolic pathway now including phenoxyacetic acid. Phenol is degraded, via catechol, to intermediates of the tricarboxylic acid cycle. The two possible routes for ring cleavage, the *ortho*- and *meta*-cleavage pathways, are indicated in the figure.

The objective of this study was to elucidate whether in situ horizontal gene transfer is a mechanism that can directly influence the evolution of new catabolic capabilities of soil microbial communities. Furthermore, we studied the impact of selective pressure (presence of PAA) as well as micro-habitats (barley residuesphere) on gene transfer.

2. Materials and methods

2.1. Soil and barley straw

The soil used in the experiments was a sandy loam from a farm near Roskilde, Denmark. Soil characteristics were: pH: 6.5, cation-exchange capacity: 8.4 meq/100 g dry soil, organic matter: 2.4%, clay: 10.9%, silt: 30.7%, fine sand: 31.9%, coarse sand: 24.1%, water holding capacity: 24.4% [15]. Pesticides had not been applied to the field at Roskilde for the last few decades. Soil samples were collected from the upper 20 cm, dried at room temperature overnight (O.N.), sieved (2 mm grid), and stored in closed plastic boxes at 10°C.

Dry leaves of barley were cut into pieces of 1.5 cm and sterilised (121°C, 20 min). Sterilised barley straw was incubated O.N. (room temperature) in phosphate-buffered saline (PBS) [16] the day before set-up of soil microcosms.

2.2. Bacterial strains and growth conditions

The five phenol degrading bacterial strains: *R. eutropha* AEO106 (a plasmid cured derivative of *R. eutropha* JMP134), *Pseudomonas* sp. CF600, *Pseudomonas putida* DSM548, *P. putida* DSM549, and *Pseudomonas* sp. B13 were grown at 30°C in minimal medium (MM) supplemented with phenol (2 mM). Minimal medium consisted of (per l): 4.25 g $K_2HPO_4{\cdot}3H_2O$, 1.00 g $NaH_2PO_4{\cdot}H_2O$, 2.00 g NH_4Cl, 0.200 g $MgSO_4{\cdot}7H_2O$, 0.012 g $FeSO_4{\cdot}7H_2O$, 0.003 g $ZnSO_4{\cdot}7H_2O$, 0.003 g $MnSO_4{\cdot}H_2O$, 0.123 g nitrilotriacetic acid. Phenol degrading isolates from Roskilde soil were grown at 24°C in the same medium. Tetracycline (20 μg ml^{-1}) was added to the growth medium to select for transconjugants carrying pRO103. *E. coli* HB101 carrying pRO103 was grown at 37°C in Luria–Bertani (LB) medium [16] supplemented with streptomycin

Downloaded from https://academic.oup.com/femsec/article/35/1/75/524693 by Pearson Hubert International user on 03 September 2020

COR-AAD1-00002479
Bayer EX1008 (Part 5 of 9)

(Sm) (100 μg ml^{-1}) and tetracycline (Tc) (20 μg ml^{-1}). *E. coli* HB101 is an auxotroph [17] that does not grow in MM supplemented with single carbon sources (e.g. phenol or PAA). Agar–agar (Struers) was used for preparation of LB plates, and Noble Agar (Difco) for the preparation of MM plates. For plating soil and straw suspensions, the agar media were supplemented with cycloheximide (100 μg ml^{-1}) or natamycin (25 μg ml^{-1}) for inhibition of fungal growth. Natamycin was used for plates incubated for longer than 2 days.

2.3. Filter mating

Transfer of plasmid pRO103 on filters from *E. coli* HB101 to phenol degraders was performed as described by de Lipthay et al. [8]. Briefly, the donor and recipient strains were grown O.N. and washed twice in MM. Pairwise, 100 μl samples of the donor HB101/pRO103 and each recipient strain were deposited on cellulose nitrate filters (0.2 μm). Filters were placed on LB agar plates, and matings were performed at 30°C O.N. (24°C for matings with indigenous phenol degraders). After incubation, filters were washed in MM and dilutions were plated on donor, recipient and transconjugant agar media. Donors were enumerated on LB+Sm+Tc plates, recipients on MM+phenol plates, and transconjugants on MM+phenol+Tc plates.

2.4. Soil microcosms

Microcosms were set up in 100 ml glass flasks and all consisted of 15.0 g soil (wet weight). To some experiments, seven leaves of barley straw were added. Sterile soil microcosms were autoclaved (121°C, 20 min) twice with a 24 h period of incubation between treatments. Phenoxyacetic acid treated microcosms were amended to a final concentration of 250 ppm PAA (dissolved in PBS) and untreated microcosms were amended with a similar volume of PBS. Using PBS, the water content of the soil was adjusted to 15%. Microcosms were acclimated 20–24 h (24°C) before inoculation with bacterial strains.

Inocula cultures were grown to late-exponential phase, harvested (6000×*g*, 10 min, 20°C) and washed in PBS. The bacterial pellet was suspended in PBS and bacterial cultures were starved for 20–24 h by incubation while shaking (200 rpm) at 30°C (strain AEO106) or 37°C (strain HB101/pRO103). The bacterial cultures were starved to acclimate the strains grown under nutrient superfluous conditions prevailing in the growth medium to the more nutrient limited conditions in the soil microcosms. The bacterial biomass of the cultures was estimated using correlation curves of numbers of colony forming units (CFU) versus optical density (OD). Generally, bacterial strains were applied to a density of approximately 10^7 CFU g^{-1} soil (wet wt.). In gene transfer experiments, the recipient strain (AEO106) was inoculated to the soil, followed, 2 h later, by the inoculation of the donor (HB101/pRO103). Some microcosms were amended with 2% LB (vol/wt) broth 1 h before inoculation of the recipient strain. Finally, the water content of the soil was adjusted to 20% using PBS, equivalent to 82% of the water holding capacity. Control microcosms contained all ingredients, except amended donor and/or recipient strains. Microcosms were incubated at 24°C, and all treatments were set up in triplicate.

2.5. Sampling of microcosms

At each sampling day, three replicate microcosms were killed. Leaves of barley straw were carefully removed from the soil, transferred to Eppendorf tubes containing 1.4 ml PBS, and vortexed vigorously for 1 min. The barley leaves were dried (80°C, 24 h) and the dry wt. determined. Bulk soil was thoroughly mixed and 10.0 g (wet wt.) was added to 100 ml glass flasks. Ninety mililitre PBS was added and the flasks were shaken at room temperature (15 min, 300 rpm). Suspensions of straw and soil were serially diluted and 10 μl aliquots were drop-plated on donor (LB+Sm+Tc) and recipient plates (MM+phenol). For enumeration of transconjugant bacteria 300 μl aliquots were spread on MM+phenol+Tc plates. Occurrence of plate mating (the result of plasmid transfer on the surface of the transconjugant plates) was estimated by mixing and plating 150 μl aliquots of soil/straw suspensions, of separately incubated donors and recipients, on transconjugant selective plates. This control was necessary to assure that all detected transconjugants were the result of transfer events taken place in the soil and not after plating of soil suspensions.

2.6. Analysis of phenoxyacetic acid concentration

Soil suspensions in PBS (see Section 2.5) were shaken for 1 h (300 rpm) and 1 ml samples were filtered (0.2 μm) into HPLC vials. The filtrates were kept at 4°C until HPLC analysis for remaining PAA concentrations as described by de Lipthay et al. [8]. The concentration of PAA in MM+PAA medium of pure cultures was similarly determined.

2.7. Verification of transconjugant strains

The presence and identity of plasmids in transconjugants was verified by plasmid DNA preparation and by restriction endonuclease analysis using *Eco*RI [16]. The presence of *tfdA* was verified by dot-blot hybridisation (performed at high stringency) using a digoxigenin-labelled DNA probe (Boehringer Mannheim, Biochemica, Germany) consisting of the 1.6 kb *Sac*I-*Xba*I fragment of plasmid pKJS32 that carries *tfdA* [9].

Downloaded from https://academic.oup.com/femsec/article/35/1/75/524863 by Pearson Hi-Ered International user on 03 September 2020

COR-AAD1-00002480
Bayer EX1008 (Part 5 of 9)

2.8. Data analyses

Numbers of CFU were calculated as recommended by Niemlä [18]. Conjugation frequency is expressed as number of transconjugants (T) per geometric mean of donors (D) and recipients (R) ($= T/[D \times R]^{1/2}$) to describe transfer efficiencies that include both donor and recipient densities [19]. Student's t-test was performed for statistical analyses.

3. Results

3.1. Complementation of phenol degradation by tfdA

Our approach to the expansion of the catabolic profile of phenol degraders by complementation with the *tfdA* gene was initially tested using five characterised phenol degrading bacterial strains. Transfer of pRO103 was performed by filter mating. Presence of pRO103 as well as presence of the *tfdA* gene was verified in all transconjugants (data not shown), however, only transconjugants of four strains (AEO106, CF600, DSM548, B13) degraded PAA. Cultures of the transconjugant strains degraded 50% of the added PAA as follows: AEO106/pRO103: 16.8 h, CF600/pRO103: 36.2 h, DSM548/pRO103: 88.0 h, B13/pRO103: 116 h. Controls of donor and recipient strains did not grow on or degrade PAA when inoculated in MM+PAA.

R. eutropha AEO106 was chosen as the recipient organism in microcosm experiments because the transconjugant of this strain was the fastest PAA degrader among the tested strains. Furthermore, *R. eutropha* AEO106 was originally isolated from soil [11] and thus was expected to survive well in competition with the indigenous microorganisms.

3.2. Effect of nutrient addition on gene transfer frequency in soil

Preliminary experiments were performed to test the ability of transfer of plasmid pRO103 from *E. coli* HB101 to *R. eutropha* AEO106 in soil. Four microcosms containing non-sterile soil were set up with the addition of: (i) PBS, (ii) 2% LB (vol/wt), (iii) 5% LB (vol/wt), or (iv) barley straw. Phenoxyacetic acid was not added as it was the objective to measure gene transfer frequencies without the impact of selection of transconjugants. Two days later microcosms were killed and the result of gene transfer frequencies ($T/[D \times R]^{1/2}$) were: (i) PBS, 0.00; (ii) 2% LB, 1.11×10^{-6}; (iii) 5% LB, 7.50×10^{-7}; and (iv) barley straw, 1.56×10^{-6}. In microcosms containing barley straw, gene transfer only occurred in the residuesphere of the straw. Thus, transfer of pRO103 in non-sterile soil was enhanced by the addition of nutrients and leaves of barley. The stimulation by the three different amendments, however, did not differ significantly ($P > 0.05$).

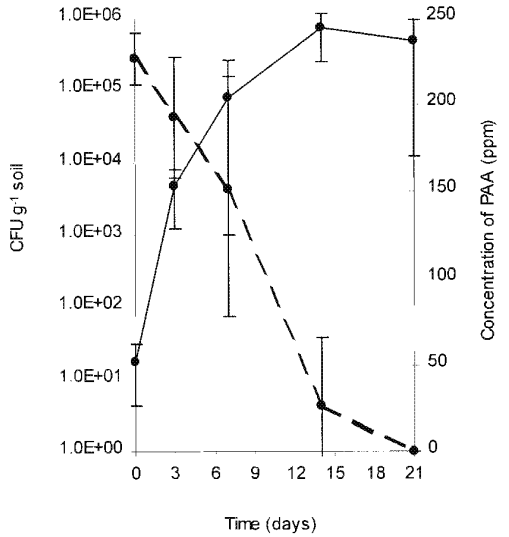


Fig. 2. Degradation of phenoxyacetic acid in non-sterile soil by the transconjugant strain, *R. eutropha* AEO106/pRO103. Strain AEO106/pRO103 was applied at a density of 10^1 CFU g^{-1}. The biomass of the strain is shown by the solid line, and the concentration of phenoxyacetic acid by the dashed line. Each data point represents the mean ± standard deviation of three replicate measurements.

Subsequent gene transfer experiments employing sterile soil were performed using 2% LB as nutrient amendment. However, microcosms containing non-sterile soil were amended with leaves of barley to approximate conditions more similar to those prevailing in nature.

3.3. Degradation of PAA in soil by AEO106/pRO103

The viability and activity of the transconjugant strain *R. eutropha* AEO106/pRO103 was studied in sterile and non-sterile soil microcosms. Experiments were performed using two inoculation densities, 10^1 and 10^4 CFU g^{-1} soil, respectively. Fig. 2 shows the results for inoculation of 10^1 CFU g^{-1} soil of strain AEO106/pRO103 in non-sterile soil microcosms. In all experiments AEO106/pRO103 survived well. In sterile soil PAA was degraded within 3 and 7 days, for high and low inoculation densities, respectively. In non-sterile soil, PAA was degraded within 14 and 21 days. Sterilisation thus had a significant effect on the PAA degradation rate ($P < 0.05$), pointing to the influence and significance of microbial competition.

3.4. Conjugation between HB101/pRO103 and AEO106: sterile soil microcosms

Initially, sterile soil microcosms were used to test the in situ complementation of the pathway for phenol degradation with the *tfdA* gene (Fig. 3). Two parallel experiments were performed, with and without addition of 2% LB (vol/wt), as preliminary experiments had shown a positive effect of LB amendment on gene transfer frequency (see

Downloaded from https://academic.oup.com/femsec/article/35/1/75/524693 by Pearson Hayward International user on 03 September 2020

COR-AAD1-00002481
Bayer EX1008 (Part 5 of 9)

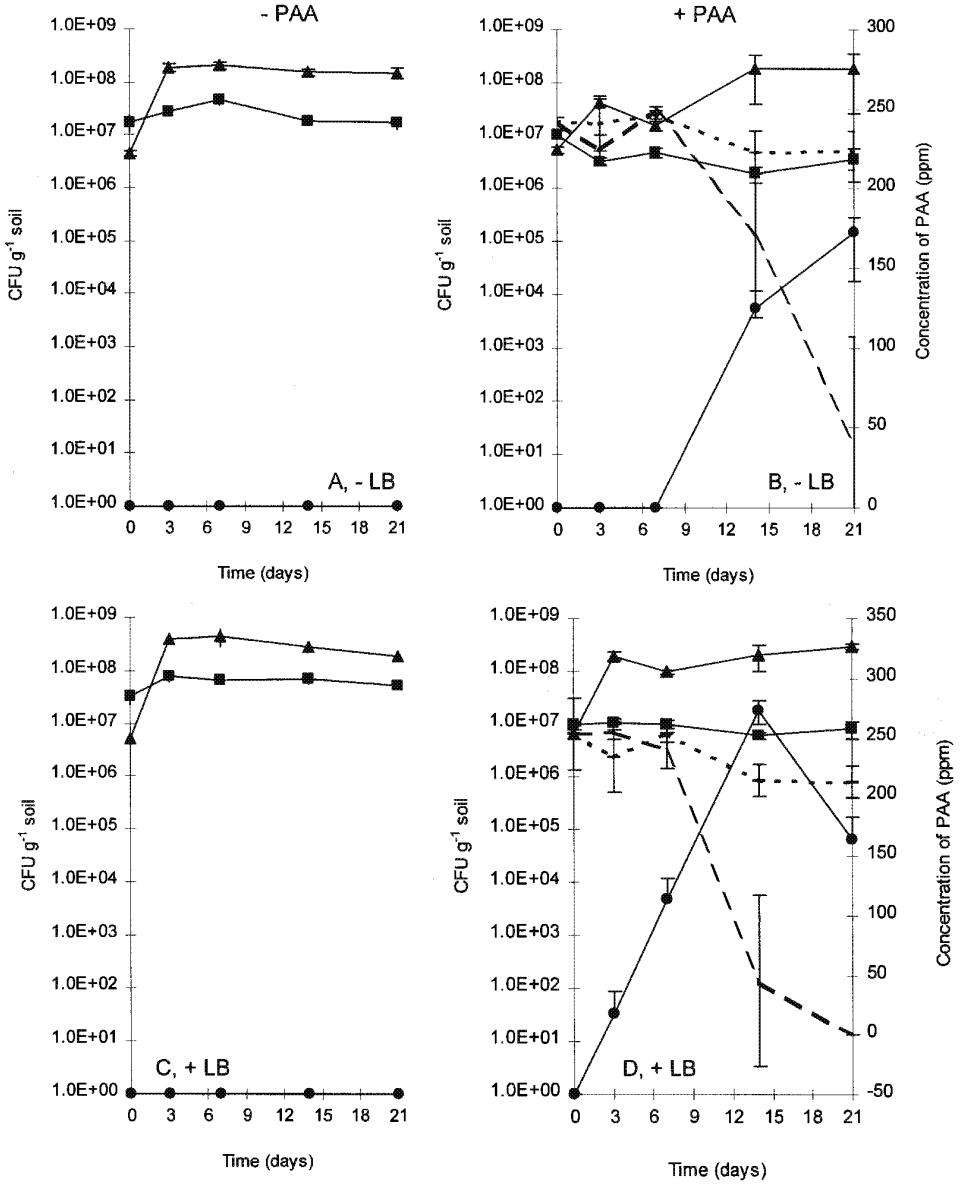


Fig. 3. Transfer of plasmid pRO103 from *E. coli* HB101/pRO103 (donor, ■) to *R. eutropha* AEO106 (recipient, ▲) in sterile soil resulting in appearance of transconjugants (AEO106/pRO103, ●). The figure represents four parallel experiments: with (B, D) and without (A, C) amendment of phenoxyacetic acid (PAA), and with (C, D) and without (A, B) addition of 2% LB. The concentration of PAA is indicated by the dashed lines. The concentration of PAA in control microcosms (without inoculation of bacterial strains) is indicated by the dotted lines. Each data point represents the mean ± standard deviation of three replicate measurements.

Section 3.2). Furthermore, each experiment was divided in two, adding PAA (250 ppm) to half the flasks. In microcosms without amendment of PAA, transfer of pRO103 could not be detected even though high densities of donor and recipient populations were maintained (Fig. 3A, C). This result, contradicting earlier observations in non-sterile soil (see Section 3.2), could be due to the release of toxic compounds when autoclaving the soil imposing a negative effect on plasmid transfer. Autoclaving is a very harsh sterilisation method and changes the original soil structure significantly [3]. In contrast, transconjugants were detected under selective conditions in the presence of PAA (Fig. 3B, D). In microcosms without the addition of LB, transconjugant strains appeared on day 14. Phenoxyacetic acid disappeared concomitantly with growth of transconjugants, and 83.8% of the added PAA was degraded in 21 days. In LB-amended microcosms, transconjugant strains appeared on day 3. Similarly, PAA disap-

Downloaded from https://academic.oup.com/femsec/article/35/1/75/524091 by guest on 03 September 2020

COR-AAD1-00002482
Bayer EX1008 (Part 5 of 9)

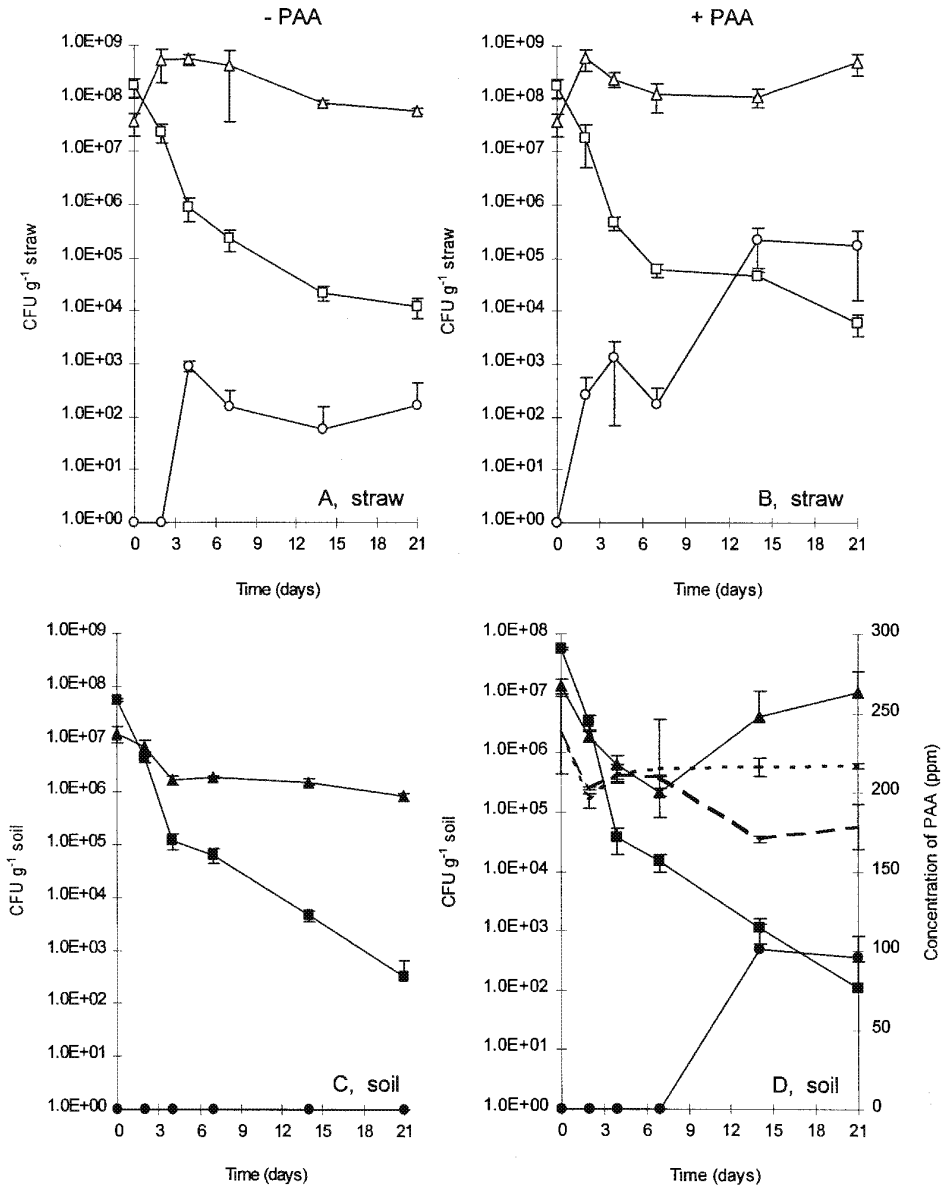


Fig. 4. Transfer of plasmid pRO103 from *E. coli* HB101/pRO103 (donor) to *R. eutropha* AEO106 (recipient) in non-sterile soil to which barley straw were added. The figure represents two parallel experiments, one with addition of phenoxyacetic acid (PAA) (B, D) and one without (A, C). Numbers of colony forming units of donor (□, ■), recipient (△, ▲), and transconjugant (○, ●) strains are shown separately for barley straw (A, B) (empty symbols) and bulk soil (C, D) (filled symbols). The concentration of PAA is indicated by the dashed line. The concentration of PAA in control microcosms (without inoculation of bacterial strains) is indicated by the dotted line. Each data point represents the mean ± standard deviation of three replicate measurements.

peared concomitantly with growth of transconjugants, and 100% of the added PAA was degraded in 21 days. In situ transfer of pRO103 resulted in a significantly decreased PAA concentration ($P < 0.01$), however, the addition of 2% LB did not significantly affect the PAA degradation rate ($P > 0.05$).

In control microcosms, no colonies appeared on transconjugant selective media on any sampling day. Plate mating controls were performed on each day of sampling and no transconjugant strains were detected (data not shown). This indicates that all of the detected transconjugants were the result of plasmid transfer that had taken place in the soil environment. Furthermore, HPLC analyses showed that PAA was not degraded in microcosms inoculated solely with *E. coli* HB101/pRO103 or *R. eutropha* AEO106 (data not shown). Thus, the disappearance of

Downloaded from https://academic.oup.com/femsec/article/35/1/75/524697 by guest on 03 September 2020

COR-AAD1-00002483
Bayer EX1008 (Part 5 of 9)

PAA was the result of the activity of transconjugant bacteria with the newly acquired capability to degrade PAA.

Selected transconjugant cells were isolated for each sampling day and verified for the presence of the *tfdA* gene (data not shown).

3.5. Conjugation between HB101/pRO103 and AEO106: non-sterile soil microcosms

In non-sterile soil microcosms in the absence of PAA, transconjugants of AEO106 were detected in the residuesphere of barley straw on day 4 (transfer frequency, 4.12×10^{-5}) and their number remained stable at approximately 10^2 CFU g^{-1} for the duration of the experiment (Fig. 4A). Transconjugants of AEO106 could easily be discriminated by colony morphology from potentially indigenous transconjugants, however, no indigenous transconjugants were detected in experiments described in this section. The recipient strain was kept at a constantly high density in the residuesphere while the population of donors declined quickly. Transconjugants survived well in the barley residuesphere even though the presence of pRO103 had no selective advantage in the absence of PAA. In bulk soil, however, no transconjugant bacteria were detected (Fig. 4C). This may be due to the fact that in addition to the poor survival of the donor, the density of the recipient strain dropped within the first couple of days.

For microcosms amended with PAA, transconjugants were detected in the residuesphere of barley straw as well as in bulk soil (Fig. 4B, D). During the first 7 days, the pattern of transconjugant biomass in the residuesphere was the same as for non-PAA-amended microcosms (Fig. 4A, B). However, following this initial period, the number of transconjugants rose and concomitantly with this rise transconjugants could be detected in bulk soil as well. The concentration of PAA decreased simultaneously with the appearance of transconjugant bacteria in bulk soil, and by the end of the experiment (day 21) 24.9% of the added PAA had disappeared. This increased degradation of PAA as compared to control experiments was significant ($P < 0.02$). The fact that only 25% of the PAA was degraded in this experiment while inoculation of transconjugants resulted in total disappearance of PAA (Fig. 2) could be due to the short period (7 days) during which a low number of transconjugants was present in the bulk soil of the microcosms. Generally, for the residuesphere and bulk soil, survival of HB101/pRO103 showed the same pattern in PAA-amended as in non-PAA-amended microcosms. The survival of the recipient strain, however, was improved in PAA-amended soil microcosms.

In control microcosms, no colonies appeared on transconjugant selective media on any sampling day. Plate mating controls showed that all detected transconjugants were a result of gene transfer processes that took place in the barley residuesphere/bulk soil and selected transconjugants from each day of sampling were verified for the presence of the *tfdA* gene (data not shown). No disappearance of PAA occurred in microcosms inoculated solely with *E. coli* HB101/pRO103 or *R. eutropha* AEO106 (data not shown). Thus, the in situ formation of PAA degrading populations

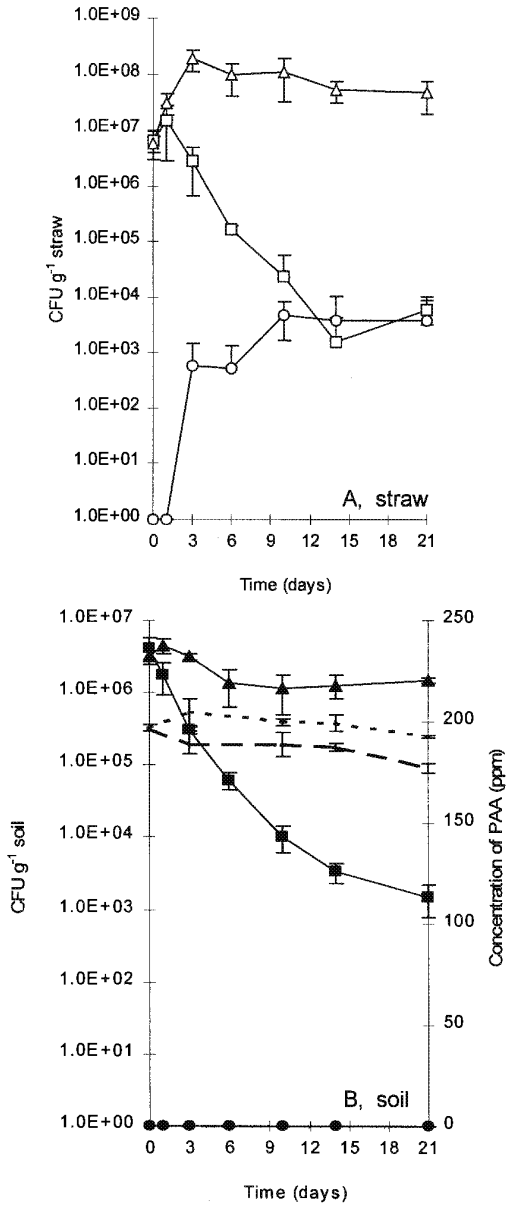


Fig. 5. Transfer of plasmid pRO103 from *E. coli* HB101/pRO103 (donor) to the indigenous population of phenol degraders (recipients) of Roskilde soil. Barley straw and phenoxyacetic acid (PAA) were added to microcosms. Numbers of colony forming units of donor (□, ■), recipient (△, ▲), and transconjugant (○, ●) strains are shown separately for barley straw (A) (empty symbols) and bulk soil (B) (filled symbols). The concentration of PAA in bulk soil is indicated by the dashed line. The concentration of PAA in control microcosms (without inoculation of strain HB101/pRO103) is indicated by the dotted line. Each data point represents the mean ± standard deviation of three replicate measurements.

Downloaded from https://academic.oup.com/femsec/article/35/1/75/524693 by Patents Ref Library user on 03 September 2020

COR-AAD1-00002484
Bayer EX1008 (Part 5 of 9)

significantly stimulated PAA degradation in both sterile and non-sterile soils.

3.6. Conjugation between HB101/pRO103 and indigenous phenol degraders

Finally, the ability of in situ complementation between the indigenous population of phenol degraders and the *tfdA* gene was examined. Microcosms consisting of soil and barley straw were inoculated with *E. coli* HB101/pRO103. The experiment was run in two parallels, with and without addition of PAA. The results were similar and only data from microcosms amended with PAA are shown (Fig. 5). The density of indigenous phenol degraders in bulk soil was approx. 10^6 CFU g^{-1}. However, in the residuesphere of barley straw the biomass rose to a level at 10^8 CFU g^{-1}. The donor strain survived poorly in soil. While a high number of transconjugant phenol degraders was detected in the residuesphere, none were present in bulk soil. Transconjugants appeared on day 3, showing a transfer frequency of 2.56×10^{-5} and 3.66×10^{-5} for PAA-amended and non-amended microcosms, respectively. The population of transconjugant phenol degraders remained at a constant level of approx. 10^3 CFU g^{-1}. In control microcosms, no colonies appeared on transconjugant selective plates on any sampling day. Controls for plate mating were impossible to perform, as this requires separate incubation of donor and recipient bacteria. However, no transconjugants were observed on days 0 and 1 when the donor density was at its highest. This strongly indicates that all the detected transconjugants had resulted from conjugation in the barley residuesphere and not on the transconjugant selective agar plates. Presence of plasmid pRO103 in selected transconjugant strains was verified by plasmid preparation (data not shown).

As illustrated in Fig. 5, the concentration of PAA declined slightly, however, significantly more PAA disappeared in donor-amended microcosms (10.0%) as compared to controls (2.3%) ($P<0.01$). This degradation could have been due to activities of non-culturable transconjugants of phenol degraders because culturable transconjugants (selected on MM+phenol+Tc) were not able to degrade PAA (data not shown). Alternatively, undefined synergistic interactions among soil bacteria could have resulted in PAA degradation. Furthermore, when plasmid pRO103 was transferred to several pure cultures of phenol degrading bacteria isolated from Roskilde soil, none of the transconjugants degraded PAA (data not shown).

4. Discussion

Horizontal transfer of plasmid pRO103 from *E. coli* HB101/pRO103 to *R. eutropha* AEO106 and to indigenous phenol degraders resulted in an increased rate of PAA degradation in soil. These findings demonstrate the role of in situ plasmid dissemination in the evolution of new catabolic pathways to otherwise undegraded xenobiotic compounds. Other studies have shown transfer of whole catabolic pathways to soil [5,6] and aquatic [20] bacteria and the complementation of a pathway in activated sludge [4]. To the best of our knowledge, results reported here are the first to show a direct impact of genetic complementation on the catabolic potential of soil microbial communities.

A sequential assembly of catabolic genes, which by complementation gives rise to horizontally or vertically expanded degradation pathways, has been suggested as an important mechanism of genetic adaptation to degradation of xenobiotic compounds and to the evolution of new catabolic pathways (e.g. [1,21,22]). The feasibility of complementing degradative pathways has been demonstrated by us [7,8] and others [23,24] with pure cultures but to the best of our knowledge only one other study has demonstrated an enhanced degradation rate of new compounds following complementation of existing pathways in situ [4]. Ravatn et al. [4] showed that in situ horizontal transfer of chlorocatechol degradative genes to a toluene degrading recipient strain resulted in a new metabolic pathway for degradation of chlorobenzene. These results together with those presented here suggest that complementing catabolic capabilities by horizontal transfer of additional genes to indigenous microbial communities in contaminated sites is a possible approach to bioremediation that warrants further investigation and development.

The residuesphere of barley straw was shown to be a hot-spot for gene transfer in comparison to bulk soil and imposed the same effect as addition of nutrients (LB). Sengeløv et al. [25] suggested that this hot-spot was the consequence of an increased biomass of donors and recipients in the micro-habitat. Like the rhizosphere [26–28], the phylloplane [29], and the spermosphere [28], the residuesphere thus seems to constitute a hot-spot for gene transfer in terrestrial environments.

The presence of a natural microbial population restricted PAA degradation as compared to experiments performed with sterile soil, demonstrating the significance of microbial competition to the survival and proliferation of transconjugant bacteria even though these organisms possess a selective advantage.

The presence of selective pressure (PAA) had a positive effect on the emergence of transconjugants. At present there is no basis to suggest that PAA could stimulate transfer of plasmid pRO103, rather the availability of PAA as a carbon source was likely to enhance the proliferation of transconjugants. Ravatn et al. [4] and Top et al. [5] likewise have demonstrated increased biomass of transconjugants when selective pressure was present. This is possibly one of the most significant factors determining survival and proliferation of genes in natural environments. However, data from experiments performed in non-sterile soil showed that even without selective pressure

Downloaded from https://academic.oup.com/femsec/article/35/1/75/524663 by Pearson Hubbard International user on 03 September 2020

COR-AAD1-00002485
Bayer EX1008 (Part 5 of 9)

a population of transconjugants appeared in the barley residuesphere and was kept at a constant level throughout the experimental period. The data thus suggest that acquisition of newly acquired genetic material might be sustained in microbial sub-populations for long periods of time until the appearance of selective pressure gives rise to proliferation of the transconjugant populations.

Although transfer of plasmid pRO103 to indigenous soil populations of phenol degraders took place, this transfer had a limited, though significant, effect on PAA degradation. However, culturable transconjugants did not degrade PAA suggesting that they could not express the *tfdA* gene. Likewise, in one of five well-known phenol degraders the acquisition of pRO103 did not result in the ability to degrade PAA. Other studies have found that catabolic genes when present in some host strains are not always properly expressed [8,11,30]. This could be due to e.g. a dependence on host-specified function(s) or a poor recognition of promoter regions [30,31].

The practical application of the results presented points to the ability of manipulating the degradative potential of the microbial community in contaminated sites. The success of the in situ complementation approach, however, is dependent on the type of indigenous recipients present, their relative distribution and on the expression of the transferred genes. As a tool in bioremediation, this strategy, though valid, is still at the very initial stages of development and requires additional experimentation and problem solving before its true potential can be evaluated. Especially, factors determining the proper expression of the newly established catabolic capabilities need to be understood. However, the idea of dissemination of catabolic plasmids encoding a complete catabolic pathway seems a promising tool in bioremediation as maintenance of foreign DNA in hot-spots of terrestrial environments can be high even without presence of selective pressure.

In conclusion, we have shown that (i) complementation of degradative pathways can result in acquisition of new catabolic capabilities of soil microbial communities, pointing to the significance of gene exchange in the evolution of catabolic pathways in situ, (ii) the residuesphere of barley straw is a hot-spot for gene transfer, (iii) selective pressure has a positive effect on the emergence of transconjugants, (iv) in the absence of selective pressure, however, new genetic material can be sustained in microbial sub-populations.

References

[1] van der Meer, J.R., de Vos, W.M., Harayama, S. and Zehnder, A.J.B. (1992) Molecular mechanisms of genetic adaptation to xenobiotic compounds. Microbiol. Rev. 56, 677–694.

[2] Stotzky, G. (1989) Gene transfer among bacteria in soil. In: Gene Transfer in the Environment (Levy, S.B. and Miller, R.V., Eds.), pp. 165–222. McGraw-Hill, New York.

[3] Cresswell, N. and Wellington, E.M.H. (1992) Detection of genetic exchange in the terrestrial environment. In: Genetic Interactions among Microorganisms in the Natural Environment (Wellington, E.M.H and van Elsas, J.D., Eds.), pp. 59–82. Pergamon Press, Oxford.

[4] Ravatn, R., Zehnder, A.J.B. and van der Meer, J.R. (1998) Low-frequency horizontal transfer of an element containing the chlorocatechol degradation genes from *Pseudomonas* sp. strain B13 to *Pseudomonas putida* F1 and to indigenous bacteria in laboratory-scale activated-sludge microcosms. Appl. Environ. Microbiol. 64, 2126–2132.

[5] Top, E.M., Van Daele, P., De Saeyer, N. and Forney, L.J. (1998) Enhancement of 2,4-dichlorophenoxyacetic acid (2,4-D) degradation in soil by dissemination of catabolic plasmids. Antonie van Leeuwenhoek 73, 87–94.

[6] Newby, D.T., Josephson, K.L. and Pepper, I.L. (2000) Detection and characterization of plasmid pJP4 transfer to indigenous soil bacteria. Appl. Environ. Microbiol. 66, 290–296.

[7] Barkay, T., Liebert, C. and Gillman, M. (1993) Conjugal gene transfer to aquatic bacteria detected by the generation of a new phenotype. Appl. Environ. Microbiol. 59, 807–814.

[8] de Lipthay, J.R., Barkay, T., Vekova, J. and Sørensen, S.J. (1999) Utilization of phenoxyacetic acid, by strains using either the *ortho* or *meta* cleavage of catechol during phenol degradation, after conjugal transfer of *tfdA*, the gene encoding a 2,4-dichlorophenoxyacetic acid/2-oxoglutarate dioxygenase. Appl. Microbiol. Biotechnol. 51, 207–214.

[9] Streber, W.R., Timmis, K.N. and Zenk, M.H. (1987) Analysis, cloning, and high-level expression of 2,4-dichlorophenoxyacetate monooxygenase gene *tfdA* of *Alcaligenes eutrophus* JMP134. J. Bacteriol. 169, 2950–2955.

[10] Harker, A.R., Olsen, R.H. and Seidler, R.J. (1989) Phenoxyacetic acid degradation by the 2,4-dichlorophenoxyacetic acid (TFD) pathway of plasmid pJP4: mapping and characterization of the TFD regulatory gene, *tfdR*. J. Bacteriol. 171, 314–320.

[11] Don, R.H. and Pemberton, J.M. (1981) Properties of six pesticide degradation plasmids isolated from *Alcaligenes paradoxus* and *Alcaligenes eutrophus*. J. Bacteriol. 145, 681–686.

[12] Don, R.H., Weightman, A.J., Knackmuss, H.-J. and Timmis, K.N. (1985) Transposon mutagenesis and cloning analysis of the pathway for degradation of 2,4-dichlorophenoxyacetic acid and 3-chlorobenzoate in *Alcaligenes eutrophus* JMP134(pJP4). J. Bacteriol. 161, 85–90.

[13] Fukumori, F. and Hausinger, R.P. (1993) Purification and characterisation of 2,4-dichlorophenoxyacetate/α-ketoglutarate dioxygenase. J. Biol. Chem. 268, 24311–24317.

[14] Liu, T. and Chapman, P.J. (1984) Purification and properties of a plasmid-encoded 2,4-dichlorophenol hydroxylase. FEBS Lett. 173, 314–318.

[15] Jacobsen, C.S. and Pedersen, J.C. (1992) Growth and survival of *Pseudomonas cepacia* DBO1(pRO101) in soil amended with 2,4-dichlorophenoxyacetic acid. Biodegradation 2, 245–252.

[16] Sambrook, J., Fritsch, E.F. and Maniatis, T. (1989) Molecular Cloning: A Laboratory Manual, 2nd Edn. Cold Spring Harbor Laboratory Press, Cold Spring Harbor, NY.

[17] Boyer, H.W. and Roulland-Dussoix, D. (1969) A complementation analysis of the restriction and modification of DNA in *Escherichia coli*. J. Mol. Biol. 41, 459–472.

[18] Niemelä, S. (1983) Mathematics of the colony count. In: Statistical Evaluation of Results from Quantitative Microbiological Examinations. Report no. 1. Nordic Committee on Food Analysis, Sweden.

[19] Smit, E. and van Elsas, J.D. (1990) Determination of plasmid transfer in soil: consequences of bacterial mating on selective agar media. Curr. Microbiol. 21, 151–157.

[20] Fulthorpe, R.R. and Wyndham, R.C. (1992) Involvement of a chlorobenzoate-catabolic transposon, Tn*5271*, in community adaptation to chlorobiphenyl, chloroaniline, and 2,4-dichlorophenoxyacetic acid in a freshwater ecosystem. Appl. Environ. Microbiol. 58, 314–325.

[21] van der Meer, J.R., Werlen, C., Nishino, S.F. and Spain, J.C. (1998)

Downloaded from https://academic.oup.com/femsec/article/35/1/75/524883 by Pearson Hubbard International user on 03 September 2020

COR-AAD1-00002486
Bayer EX1008 (Part 5 of 9)

Evolution of a pathway for chlorobenzene metabolism leads to natural attenuation in contaminated groundwater. Appl. Environ. Microbiol. 64, 4185–4193.
[22] Vallaeys, T., Courde, L., McGowan, C., Wright, A.D. and Fulthorpe, R.R. (1999) Phylogenetic analyses indicate independent recruitment of diverse gene cassettes during assemblage of the 2,4-D catabolic pathway. FEMS Microbiol. Ecol. 28, 373–382.
[23] Top, E.M., Holben, W.E. and Forney, L.J. (1995) Characterization of diverse 2,4-dichlorophenoxyacetic acid-degradative plasmids isolated from soil by complementation. Appl. Environ. Microbiol. 61, 1691–1698.
[24] Top, E.M., Maltseva, O.V. and Forney, L.J. (1996) Capture of a catabolic plasmid that encodes only 2,4-dichlorophenoxyacetic acid:α-ketoglutaric acid dioxygenase (TfdA) by genetic complementation. Appl. Environ. Microbiol. 62, 2470–2476.
[25] Sengeløv, G., Kowalchuk, G.A. and Sørensen, S.J. (2000) Influence of fungal–bacterial interactions on bacterial conjugation in the residuesphere. FEMS Microbiol. Ecol. 31, 39–45.
[26] van Elsas, J.D., Trevors, J.T. and Starodub, M.E. (1988) Bacterial conjugation between pseudomonads in the rhizosphere of wheat. FEMS Microbiol. Ecol. 53, 299–306.
[27] Kroer, N., Barkay, T., Sørensen, S. and Weber, D. (1998) Effect of root exudates and bacterial metabolic activity on conjugal gene transfer in the rhizosphere of a marsh plant. FEMS. Microbiol. Ecol. 25, 375–384.
[28] Sørensen, S.J. and Jensen, L.E. (1998) Transfer of plasmid RP4 in the spermosphere and rhizosphere of barley seedling. Antonie van Leeuwenhoek 73, 69–77.
[29] Normander, B., Christensen, B.B., Molin, S. and Kroer, N. (1998) Effect of bacterial distribution and activity on conjugal gene transfer on the phylloplane of the bush bean (Phaseolus vulgaris). Appl. Environ. Microbiol. 64, 1902–1909.
[30] Frantz, B. and Chakrabarty, A.M. (1986) Degradative plasmids in *Pseudomonas*. In: The Bacteria (Sokatch, J.R. and Ornston, L.N., Eds.), Vol. 10, pp. 295–323. Academic Press, New York.
[31] DeFlaun, M.F. and Levy, S.B. (1989) Genes and their varied hosts. In: Gene Transfer in the Environment (Levy, S.B. and Miller, R.V., Eds.), pp. 1–32. McGraw-Hill, New York.

Downloaded from https://academic.oup.com/femsec/article/35/1/75/524603 by Pearson Hi-Ered International user on 03 September 2020

COR-AAD1-00002487
Bayer EX1008 (Part 5 of 9)

ELSEVIER

FEMS Microbiology Ecology 40 (2002) 205–214

FEMS MICROBIOLOGY Ecology

www.fems-microbiology.org

Expression of *tfdA* genes in aquatic microbial communities during acclimation to 2,4-dichlorophenoxyacetic acid

Julia R. de Lipthay [a,b,*], Jens Aamand [a], Tamar Barkay [b]

[a] *Department of Geochemistry, Geological Survey of Denmark and Greenland, Thoravej 8, DK-2400 Copenhagen NV, Denmark*
[b] *Department of Biochemistry and Microbiology, Cook College, Rutgers University, New Brunswick, NJ 08901, USA*

Received 10 October 2001; received in revised form 8 February 2002; accepted 21 February 2002

First published online 24 April 2002

Downloaded from https://academic.oup.com/femsec/article/40/3/205/507750 by Cortava Agriscience user on 03 September 2020

Abstract

The role of gene expression during acclimation of aquatic microbial communities was examined by relating transcription of *tfdA* to the degradation of the herbicide 2,4-dichlorophenoxyacetic acid (2,4-D). The *tfdA* gene encodes for a 2,4-D/2-oxoglutarate dioxygenase that transforms 2,4-D to 2,4-dichlorophenol. Transcription of *tfdA*, the abundance of *tfdA* genes and 2,4-D degrading populations, and the rate of 2,4-D disappearance were followed in laboratory incubations of two pond water samples that were exposed to 0.11 mM 2,4-D. Both communities responded to 2,4-D exposure by induction of *tfdA* transcription but the dynamics of transcript abundance and the homology to the *tfdA* riboprobe suggested different populations of 2,4-D degraders in the two ponds. In one community, where *tfdA* transcripts were highly homologous to the *tfdA* gene of *Ralstonia eutropha* JMP134, transcription of *tfdA* was transient and dropped while 2,4-D degradation continued. In the other freshwater community, where *tfdA* genes with a lower similarity to the *tfdA* gene of strain JMP134 were transcribed, transcript levels remained high although 2,4-D degradation had ceased. Restriction fragment length polymorphism analysis of *tfdA* amplicons similarly demonstrated the presence of different *tfdA* loci in the two freshwater communities, and this difference in populations of *tfdA* genes probably explains the observed difference in dynamics of catabolic gene transcription. © 2002 Federation of European Microbiological Societies. Published by Elsevier Science B.V. All rights reserved.

Keywords: *tfdA*; Catabolic gene transcription; mRNA; Acclimation; 2,4-Dichlorophenoxyacetic acid

1. Introduction

When natural microbial communities are exposed to xenobiotic compounds a stress response characterised by changes in their metabolic activity and biomass production is often observed, and usually this response results in communities that are more able to survive and function under repeated applications of the stress compound [1]. Typically, however, a lag phase of varying length occurs before this response is expressed. During the lag phase, the microbial community is acclimating to the new conditions, and three mechanisms have been suggested to account for this process [2,3]: (i) enrichment of microorganisms bearing the required catabolic capabilities, (ii) genetic adaptation, e.g. gene transfer and genetic recombination, and (iii) induction of enzyme activity, i.e. gene expression. Several studies have reported on the enrichment of xenobiotic degrading microbial populations during microbial acclimation (e.g. [1,2]). Likewise, increases in the abundance of catabolic gene sequences have been found in DNA extracted from natural microbial communities exposed to xenobiotics [4,5]. Furthermore, experiments have recently shown that horizontal transfer of catabolic genes increased the rate of degradation of xenobiotic compounds [6–8]. However, the role of gene expression in acclimation of indigenous microbial communities to xenobiotic compounds has not been examined. A few studies have related the presence of catabolic gene transcripts of natural microbial communities to the transformation of a xenobiotic compound. Fleming et al. [9] and Sanseverino et al. [10] thus found increased *nahA* mRNA levels in soils showing high rates of naphthalene mineralisation, and Nazaret et al. [11] demonstrated a correlation between mercury volatilisation and transcription of *merA*, the gene encoding mercuric reductase. These studies, however, did not specifically address gene expression during acclimation. Here, we examined the transcription of *tfdA* in aquatic microbial

* Corresponding author. Present address: Department of General Microbiology, University of Copenhagen, Sølvgade 83H, DK-1307 Copenhagen K, Denmark. Tel.: +45 35 32 20 69; Fax: +45 35 32 20 40.
E-mail address: lipthay@mermaid.molbio.ku.dk (J.R. de Lipthay).

0168-6496/02/$22.00 © 2002 Federation of European Microbiological Societies. Published by Elsevier Science B.V. All rights reserved.
PII: S0168-6496(02)00228-3

COR-AAD1-00002488
Bayer EX1008 (Part 5 of 9)

communities at different stages during degradation of 2,4-dichlorophenoxyacetic acid (2,4-D). The *tfdA* gene was originally discovered on plasmid pJP4 [12] in *Ralstonia eutropha* JMP134, which is the best-characterised 2,4-D degrader [13]. The *tfdA* gene encodes a 2,4-D/2-oxoglutarate dioxygenase that transforms 2,4-D to 2,4-dichlorophenol [14,15], the first step in the 2,4-D degradation pathway. Fulthorpe et al. [16] studied the presence of *tfdA* genes in 2,4-D degrading bacteria by DNA:DNA hybridisation. Of 32 strains analysed, 26 possessed *tfdA*-homologous genes with either >90%, 75–90% or 60–75% homology to the *tfdA* gene of strain JMP134. Vallaeys et al. [17] used *tfdA*-specific PCR amplification to show that 17 of 25 isolates had *tfdA*-like sequences. The widespread abundance of *tfdA*-homologous genes in 2,4-D degrading bacteria implies that levels of *tfdA* genes and transcripts can be related to the presence and the activity of 2,4-D degrading microbial populations.

In this study, we examined the transcription of *tfdA* during different stages of 2,4-D degradation in laboratory incubations of two freshwater pond samples. Transcripts of *tfdA* were quantified by hybridisation of RNA extracts with a *tfdA*-specific ^{35}S-labelled riboprobe, and the transcription response was related to the dynamics of 2,4-D degradation and to the abundance of *tfdA* genes and indigenous 2,4-D degraders. The presence of transcripts was measured at both low and high stringency conditions, which allowed the detection of *tfdA* genes with >75% and approx. 100% similarity to the *tfdA* gene of *R. eutropha* JMP134. Both aquatic communities showed an increased *tfdA* transcript abundance concomitant with herbicide degradation; however, the dynamics of gene transcription was different. We suggest that this difference can be explained by differences in populations of *tfdA* loci in the two aquatic communities.

2. Materials and methods

2.1. Field sites

On 4 October 2000, water samples were collected from two ponds on the campus of Rutgers University (New Brunswick, NJ, USA), one located at the Rutgers Golf Course and the other, Passion Puddle, on the campus of Cook College. The Golf Course pond is continuously exposed to herbicides, including 2,4-D, originating from run-off water from the surrounding greens, whereas no source of 2,4-D to Passion Puddle is known. Samples were brought to the laboratory and experiments were set up within 12 h.

2.2. Bacterial strains and growth conditions

R. eutropha JMP134 was grown at 28°C in a minimal medium (MM) [18] supplemented with 1.1 mM 2,4-D (Merck, Darmstadt, Germany). Cells were harvested at early exponential phase for nucleic acid extraction analysis. *Escherichia coli* S17.1/pKJS32, *E. coli* JM83 carrying the cloning vector pGEM-3Z (Promega, Promega Corporation, Madison, WI, USA) and *E. coli* HB101 were grown at 37°C in Luria–Bertani (LB) medium [19]. Kanamycin (50 μg ml^{-1}) and ampicillin (50 μg ml^{-1}) were supplemented to LB for selection of pKJS32 and pGEM-3Z, respectively.

2.3. Construction of tfdA-specific ^{35}S-labelled riboprobe

Applying the software Vector NTI® (INforMax, Inc., Bethesda, MD, USA), primers for amplification of the largest possible *tfdA* fragment (819 bp = 95%) were constructed. A *Pst*I and *Sal*I site, as well as a 6-bp linker, were added to the forward and reverse primer, respectively. The final primer sequences were (i) forward: 5′-ATA-ATA-CTG-CAG-GTC-GTC-GCA-AAT-CCC-CTT-CA-3′, and (ii) reverse: 5′-GAC-CTA-GTC-GAC-CTC-ACG-CCT-GGC-CGA-GAT-GT-3′ (IDT®, Integrated DNA Technologies, Inc., Coralville, IA, USA). The *tfdA* containing plasmid pKJS32 [12] was purified from *E. coli* S17.1 with the Qiagen Plasmid Midi Kit (Qiagen, Hilden, Germany) and the *tfdA* gene was amplified using the PCR protocol described by Vallaeys et al. [17]. The *tfdA* PCR product was cloned into the pGEM-3Z vector, and propagated in *E. coli* HB101 by growth in LB medium supplemented with ampicillin. The pGEM-3Z:*tfdA* construct was purified by plasmid preparation (Qiagen Plasmid Midi Kit), and an in vitro transcription kit (RiboProbe® In Vitro Transcription Systems, Promega) was used to synthesise *tfdA* sense (riboprobe) and antisense (standard) RNA, transcribed from the Sp6 and T7 RNA polymerase promoters, respectively. ^{35}S-Labelled rUTP (NEN® Life Science Products, Inc., Boston, MA, USA) was used for the synthesis of the *tfdA* riboprobe. Non-radioactive nucleic acids were applied for the synthesis of antisense RNA that was used for the production of standard curves for quantification of microbial community *tfdA* transcripts. The in vitro transcribed *tfdA* products were finally purified on NucAway™ Spin Columns (Ambion, Austin, TX, USA).

2.4. Laboratory incubations

Experiments were set up in 300-ml Erlenmeyer flasks with 135 ml pond water. The samples were incubated at 28°C for 24 h before addition of 15 ml MM containing 2,4-D, resulting in a final herbicide concentration of 0.11 mM. Samples without 2,4-D served as non-exposed controls. Erlenmeyer flasks were incubated at 28°C. At each sampling time, three replicate flasks were sacrificed for the measurement of (i) 2,4-D disappearance, (ii) abundance of *tfdA* transcripts, (iii) numbers of culturable 2,4-D degraders, and (iv) abundance of *tfdA* genes.

Downloaded from http://academic.oup.com/femsec/article/40/3/205/507750 by Corteva Agriscience user on 03 September 2020

COR-AAD1-00002489
Bayer EX1008 (Part 5 of 9)

Sampling times were selected using a parallel set of triplicate Erlenmeyer flasks that were set up solely to measure 2,4-D mineralisation activity. In addition to the 0.11 mM 2,4-D, these flasks contained 33.8 nCi [U-^{14}C]2,4-D (Sigma, St. Louis, MO, USA; radiochemical purity >98%), corresponding to a concentration of 12.4 nM. The experimental flasks, to which only unlabelled 2,4-D was added, were sacrificed at different stages of the 2,4-D mineralisation course as indicated by the evolution of $^{14}CO_2$ accumulation.

2.5. Disappearance and mineralisation of 2,4-D

Disappearance of 2,4-D in water samples was measured by high performance liquid chromatography (HPLC) analyses. Ten millilitres of sample were filtered (0.22 μm), and the filtrate was analysed with a Hewlett Packard 1050 HPLC equipped with a Hypersil 5 C-18 column (25×0.2 cm, 5 μm particle size) (Hewlett Packard, Waldbronn, Germany). The detection of 2,4-D at 200 nm was performed by a variable wavelength monitor (Hewlett Packard, 1050). The mobile phase was composed of 63% KH_2PO_4 (5 mM, pH <1) and 37% acetonitrile:methanol (1:1, pH <1), and the analysis was run at isocratic conditions.

Mineralisation of [U-^{14}C]2,4-D was followed by the accumulation of $^{14}CO_2$ in NaOH traps. Test tubes containing 2 ml of 0.5 M NaOH were placed in the Erlenmeyer flasks, which were kept closed with airtight rubber stoppers. At each sampling time the NaOH was changed and Erlenmeyer flasks were left open for 5 min to replenish oxygen. Ten millilitres of EcoLume™ scintillation fluid (ICN Pharmaceuticals, Costa Mesa, CA, USA) were added to the NaOH and the content of $^{14}CO_2$ was estimated by liquid scintillation counting (LS 6500, Beckman Coulter, Fullerton, CA, USA).

2.6. RNA extraction

To prevent RNase activity, all glassware, centrifuge tubes and chemical solutions were treated with diethyl pyrocarbonate (DEPC) as recommended [20]. The treatment was performed overnight (37°C), and DEPC was inactivated by autoclaving for 45 min at 121°C. Furthermore, all plastic ware was autoclaved for 45 min at 121°C.

Bacterial cells were collected by filtering 100-ml (pond water) or 10-ml (JMP134 cultures) samples through 0.22-μm-pore-size cartridge filters (Sterivex™-GS, Milipore, Burlington, MA, USA) submerged in an ice bath. Filters were stored at −80°C.

RNA extractions, performed by modifications of the methods of Jeffrey et al. [21] and Wilson et al. [22], were optimised with 2,4-D grown JMP134 cells. Two millilitres lysis buffer (10 mM Tris–HCl (pH 8.0), 1 mM EDTA, 0.1 M NaCl, 1% sodium dodecyl sulfate (SDS)), pre-warmed to approx. 85°C, were added to frozen Sterivex filters. The filters were boiled for 5 min, and the cell lysate was transferred to centrifuge tubes and stored on ice. Filters were rinsed with another 2 ml of lysis buffer, and the 4 ml of lysate were combined. At this step, a 0.5-ml sample was removed and stored at −20°C for DNA extraction (see Section 2.9). Attempts to increase the RNA yield by introducing another cycle of freezing (−80°C, 1 h) and boiling were not successful (data not shown). From the remaining 3.5 ml lysate, RNA was extracted with an equal volume of freshly made GIPS solution (4 M guanidinium isothiocyanate, 0.5% *N*-lauryl sarcosine, 25 mM sodium citrate (pH 7.0), 0.1 M β-mercaptoethanol), 0.35 ml sodium acetate (2 M), 3.5 ml phenol (pH 4.5), and 0.7 ml chloroform:isoamyl alcohol (49:1). Samples were vortexed for 15 s, stored on ice for 5 min, and centrifuged for 15 min at 4°C (12 000 rpm, Sorvall SS34 rotor). One volume of isopropanol and 5 μl glycogen (20 mg ml^{-1}) were added to the aqueous layer and samples were stored overnight at −20°C. RNA was precipitated by centrifugation at 17 000 rpm for 30 min (4°C) and the pellet was resuspended in 0.5 ml TE buffer (10 mM Tris–HCl (pH 8.0), 1 mM EDTA). One volume of isopropanol and 50 μl 2 M NaCl were added, and samples were stored at −80°C for 30 min. RNA was precipitated by centrifugation (14 000×*g*, 4°C, 30 min), and the pellet was rinsed with 70% ethanol and finally resuspended in TE buffer containing 20% formamide. At this step RNA samples were stored at −80°C.

RNA samples of strain JMP134 were tested for the presence of DNA by spectrophotometric analysis at wavelengths of 260 and 280 nm. Treatment with DNase did not result in a significant drop in nucleic acid concentration, but following RNase treatment no nucleic acids could be measured (data not shown). This demonstrates that the applied RNA extraction protocol is selective to RNA, and extractions are virtually free of contaminating DNA. This selectivity of guanidine extraction methods has previously been demonstrated by Jeffrey et al. [21] and Wilson et al. [22]. To be sure that no DNA was present at all, all RNA extracts were treated with 5 U RNase-free DNase (Promega, Madison, MI, USA) (37°C, 30 min). The reaction was stopped by addition of EDTA (10 mM), and proteins were removed by phenol:chloroform:isoamyl alcohol (50:49:1) extraction. The organic phase was extracted with an equal volume of TE buffer, and the two aqueous phases were combined. RNA was precipitated and rinsed as described above and finally resuspended in TE buffer containing 20% formamide. RNA samples were finally stored at −80°C.

Quantification of RNA was performed by fluorometric analysis (Turner®Quantech™ Digital Filter Fluorometer, Turner Designs, Sunnyvale, CA, USA) of SYBR® Green (×1) (Molecular Probes, Eugene, OR, USA) stained samples in TE buffer. *E. coli* strain W rRNA (Sigma) was used to establish a standard calibration curve.

As an alternative to isopropanol and NaCl in RNA

Downloaded from https://academic.oup.com/femsec/article/40/3/205/507750 by Corteva Agriscience user on 03 September 2020

COR-AAD1-00002490
Bayer EX1008 (Part 5 of 9)

precipitation, we tried (i) 2 vols. of 100% ethanol+0.5 vol. of 7.5 M ammonium acetate, and (ii) 2 vols. of 95% ethanol+0.1 vol. of 3 M sodium acetate; however, these procedures did not significantly increase the RNA yield (data not shown).

2.7. Quantification of *tfdA* transcripts

Approximately 1.5 μg RNA was dot-blotted onto positively charged nylon membranes (Immobilon-Ny$^+$, Millipore) and covalently bound by UV cross-linking (254 nm, 40 000 μJ cm^{-2}) as described by standard protocols [20]. Transcripts of the *tfdA* gene were then detected by hybridisation with the *tfdA*-specific ^{35}S-labelled riboprobe at low and high stringency conditions (see below). Application of 1.5 μg *E. coli* rRNA (Sigma) was used as a control for non-specific hybridisation and corresponded to a level of 15 and 1.2 pg *tfdA* transcripts μg^{-1} RNA for low and high stringency hybridisation, respectively.

Hybridisation of RNA blots was performed at 55°C for 48 h in 10 ml hybridisation buffer (50% deionised formamide, 7% SDS, 0.25 M phosphate buffer (pH 7.4), 0.25 M NaCl, 1 mM EDTA, 10 mM DTT, 1 mg salmon sperm DNA) as modified after standard protocols [20]. Post-hybridisation washes were performed at low and high stringency. Low stringency washes consisted of (i) two washes of 5 min (room temperature) with 2×SSPE (1×SSPE is 0.18 M NaCl, 10 mM sodium phosphate buffer (pH 7.4), 1 mM EDTA)+2% SDS, (ii) two washes of 5 min (room temperature) with 1×SSPE+1% SDS, and (iii) two washes of 15 min (44°C) with 1×SSPE+1% SDS. High stringency washes consisted of two washes of 15 min (68°C) with 0.2×SSPE+0.1% SDS. Hybridisation results were visualised and quantified by phosphor imager analysis (PhosphorImager™SI, Molecular Dynamics, Sunnyvale, CA, USA).

As calculated according to [20], *tfdA* gene transcripts with >75% sequence similarity with *tfdA* from *R. eutropha* JMP134 would give signals at low stringency hybridisation, and only transcripts of approx. 100% similarity would give signals at high stringency.

2.8. Quantification of 2,4-D degraders

The numbers of culturable 2,4-D degraders were estimated by a most probable number (MPN) technique assaying the mineralisation of [U-^{14}C]2,4-D. Minimal medium containing 0.01 mM 2,4-D and 2.25 nCi [U-^{14}C]2,4-D were added to 20-ml glass vials equipped with test tubes containing 0.75 ml 0.5 M NaOH. Dilutions of water samples (10^0–10^{-7}) were added and the vials were incubated at 28°C. Five replicates of each sample dilution were set up. Following 4 weeks of incubation, NaOH samples were analysed by liquid scintillation counting, and samples showing a minimum of 25% mineralisation activity were scored as positive.

2.9. DNA extraction

The 0.5-ml cell lysate (see Section 2.6) of laboratory pond incubations was extracted with phenol:chloroform:isoamyl alcohol (50:49:1), and the aqueous phase was treated with RNase (3.5 μg ml^{-1}) for 1 h at 37°C. Proteins were removed by another phenol:chloroform:isoamyl alcohol extraction, and DNA was precipitated with isopropanol (14 000×*g*, 4°C, 30 min). The DNA samples were finally resuspended in TE buffer and stored at −20°C.

2.10. Analyses of *tfdA* genes

Primers for *tfdA* PCR analysis were derived from conserved regions of the *tfdA* gene sequences from *R. eutropha* JMP134 and *Burkholderia* sp. RASC [17], and they have been shown to amplify a 362-bp product from a diverse group of 2,4-D degraders [17]. The PCR reaction mixture contained (per 25 μl): 1×GeneAmp® PCR Buffer (Perkin-Elmer, Applied Biosystem, Foster City, CA, USA), 200 μM of each dNTP (Perkin-Elmer), 1.0 μM of each primer (DNA Technology A/S, Aarhus, Denmark), and 0.625 U AmpliTaq Gold™ DNA polymerase (Perkin-Elmer). A 2.5-μl aliquot of the DNA sample was added and PCR was performed applying the following programme, slightly modified after the method described by Vallaeys et al. [17]: 6 min at 94°C, followed by 40 cycles of 45 s at 94°C, 30 s at 59°C, and 2 min at 72°C; with a final extension of 6 min at 72°C. The presence of *tfdA* genes was confirmed by agarose gel (1.2%) electrophoresis. The abundance of *tfdA* genes in DNA samples was estimated by MPN-PCR, by analysing three replicates of each sample dilution (10^0–10^{-2}).

Restriction fragment length polymorphism (RFLP) patterns of *tfdA* amplicons were obtained by digestion with *Hae*III and *Cfo*I (an isoschizomer of *Hha*I) (Roche Molecular Biochemicals, Mannheim, Germany) followed by separation on 3.5% agarose gels. The molecular masses of the restriction fragments were calculated by the application of a standard curve derived from the 100–600-bp bands of a 100-bp ladder marker (Promega). Three lanes of the molecular mass marker were used for these calculations. The RFLP patterns were compared to the patterns of bacterial pure cultures (Table 1) [17].

2.11. Data analyses

Data were analysed by application of Student's *t*-tests. One-tailed tests were applied to evaluate whether the herbicide exposure had resulted in increased levels of *tfdA* transcript abundance, culturable 2,4-D degraders, and *tfdA* gene copies. The relation between *tfdA* transcript abundance and numbers of JMP134 cells was evaluated by Pearson correlation analysis.

Downloaded from http://academic.oup.com/femsec/article/40/2/205/507750 by Corteva Agriscience user on 03 September 2020

COR-AAD1-00002491
Bayer EX1008 (Part 5 of 9)

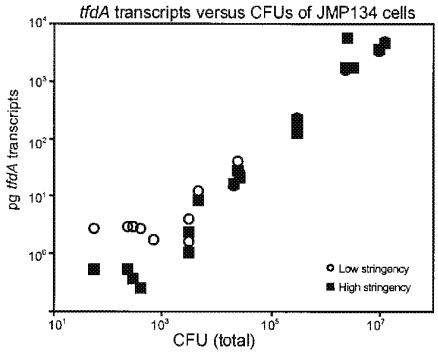


Fig. 1. Correlation of *tfdA* gene transcripts to numbers of colony forming units (CFU) of *R. eutropha* JMP134 cells. Data of low and high stringency hybridisation of *tfdA* gene transcripts are shown.

3. Results

3.1. Correlation between abundance of tfdA transcripts and numbers of JMP134 cells

The abundance of *tfdA* transcripts and cell numbers of *R. eutropha* JMP134 were linearly correlated ($r = 0.98$) in a range of approx. 10^3–10^7 colony forming units (CFU) (Fig. 1). This correlation was found with low as well as high stringency of post-hybridisation washes. At lower cell numbers the sensitivity of detection depended on the wash conditions as approx. 10 times higher background signals were apparent at low stringency washes. The detection limits for the measurement of *tfdA* transcripts corresponded to approx. 3×10^3 and 3×10^2 CFU, for low and high stringency hybridisation, respectively. Above the detection limits, the hybridisation signals of the two wash conditions were similar (Fig. 1), confirming that the

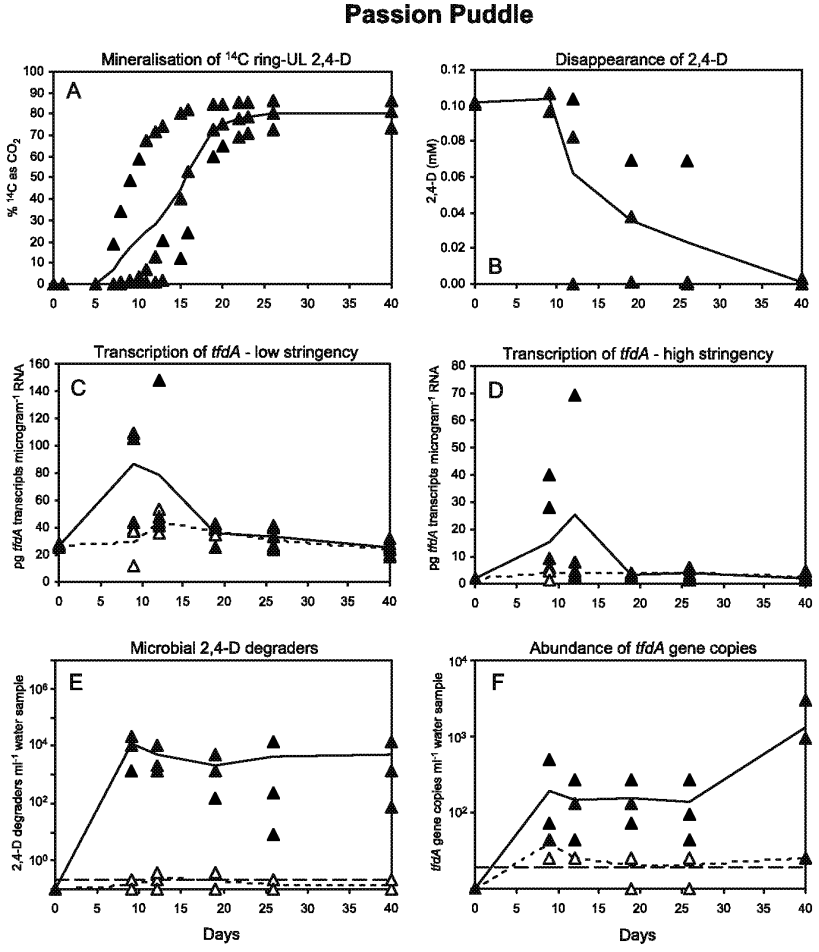


Fig. 2. Acclimation of the indigenous microbial community to 2,4-D in laboratory incubations of Passion Puddle water samples. The figure illustrates mineralisation of [U-^{14}C]2,4-D (A), disappearance of 2,4-D (B), pg of *tfdA* gene transcripts at low (C) and high (D) stringency of hybridisation conditions, numbers of culturable 2,4-D degraders (E), and abundance of *tfdA* gene copies (F). Filled and empty symbols represent 2,4-D exposed and non-exposed samples, respectively. All experiments were performed in triplicate, and mean values are represented by the continuous (2,4-D exposed) and broken (non-exposed) lines. The dashed lines in E and F indicate the limits of detection.

Downloaded from http://academic.oup.com/femsec/article/40/3/205/497150 by Corteva Agriscience user on 03 September 2020

COR-AAD1-00002492
Bayer EX1008 (Part 5 of 9)

tfdA riboprobe is highly similar to the *tfdA* gene of *R. eutropha* JMP134.

The utility of transcript quantification as a tool in studying gene expression depends on the sensitivity of detection. The number of 2,4-D degraders in Passion Puddle and Golf Course samples stabilised at approx. 10^4–10^5 cells ml^{-1} (see Section 3.4). At each sampling, 100 ml pond water were filtered suggesting that our sensitivity was sufficient to detect transcripts in all 2,4-D treated water samples.

3.2. Degradation of 2,4-D

The indigenous microbial communities of both Passion Puddle and the Golf Course quickly acclimated to 2,4-D, and generally, data of 2,4-D disappearance and mineralisation were congruent. In Passion Puddle samples, half the added 2,4-D was degraded in 14.3 days and within 16.5 days 50% of the [U-^{14}C]2,4-D was mineralised (Fig. 2A,B). The Golf Course samples showed a slightly faster response. Within 12.0 days half the added 2,4-D had disappeared and 50% of the [U-^{14}C]2,4-D was mineralised in 13.7 days (Fig. 3A,B). No residual concentrations of 2,4-D were measured in the pond samples prior to the laboratory setup (data not shown).

3.3. Transcription of tfdA

Passion Puddle samples showed an initial increased level of *tfdA* transcript abundance ($P < 0.05$) on day 9 (Fig. 2C,D), but this level quickly returned to that of the non-exposed controls (on day 18). The low hybridisation signals of the controls probably were due to non-specific binding of the *tfdA* riboprobe as demonstrated by the application of equal amounts of *E. coli* rRNA (see Section 2.7). The rise in transcript abundance occurred prior to the accelerated disappearance of 2,4-D (Fig. 2B) and in spite of a drop in *tfdA* mRNA levels degradation of 2,4-D con-

Downloaded from https://academic.oup.com/femsec/article/40/3/205/505750 by Cortava Agriscience user on 03 September 2020

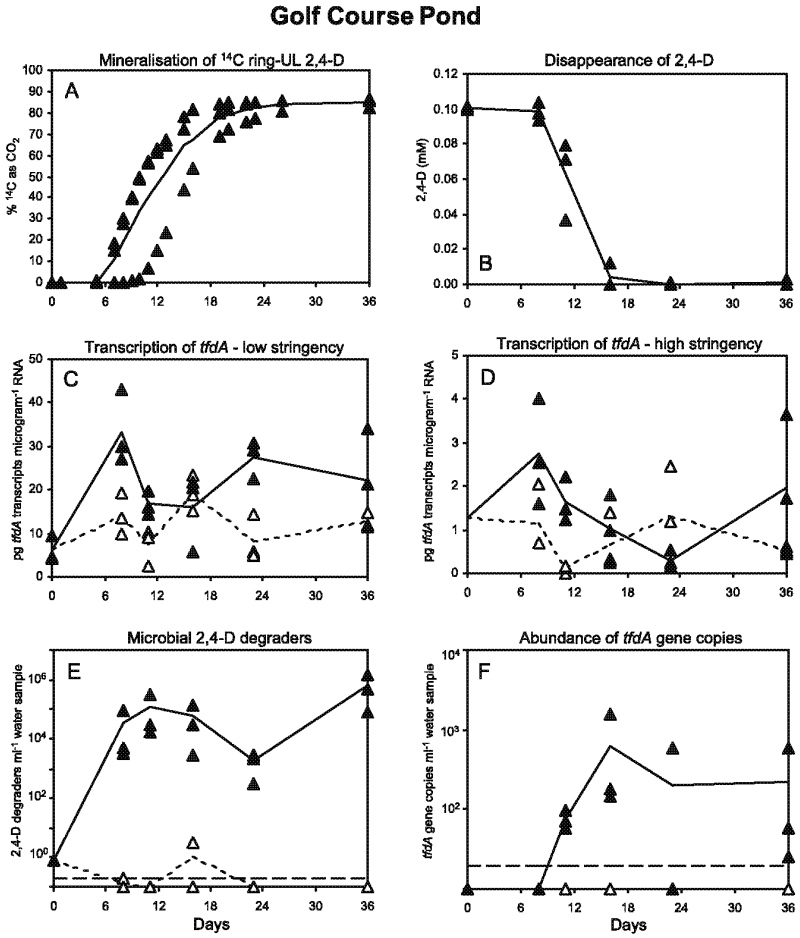


Fig. 3. Acclimation of the indigenous microbial community to 2,4-D in laboratory incubations of Golf Course water samples. The figure illustrates mineralisation of [U-^{14}C]2,4-D (A), disappearance of 2,4-D (B), pg of *tfdA* gene transcripts at low (C) and high (D) stringency of hybridisation conditions, numbers of culturable 2,4-D degraders (E), and abundance of *tfdA* gene copies (F). Filled and empty symbols represent 2,4-D exposed and non-exposed samples, respectively. All experiments were performed in triplicate, and mean values are represented by the continuous (2,4-D exposed) and broken (non-exposed) lines. The dashed lines in E and F indicate the limits of detection.

COR-AAD1-00002493
Bayer EX1008 (Part 5 of 9)

tinued for approx. 2 weeks. The observed rise in transcript abundance was similar for both low (Fig. 2C) and high (Fig. 2D) stringencies of hybridisation, although with a decrease in signal levels when high stringency washes were employed. The background level was reduced by a factor of 10, while the maximum transcript level was reduced only by a factor of 2–3. This indicates that the transcribed *tfdA* genes in Passion Puddle were highly homologous (close to 100%), although not identical, to the *tfdA* gene of *R. eutropha* JMP134. The high variation in transcript abundance on days 9 and 12 was most likely due to the short half-life (minutes) of mRNA molecules.

Measured by low stringency hybridisation, transcription of *tfdA* in the Golf Course samples similarly increased following 2,4-D exposure (Fig. 3C). In contrast to Passion Puddle, however, these significantly increased *tfdA* mRNA levels were found throughout most of the incubation period (day 8 ($P < 0.025$), 11 ($P < 0.025$), and 23 ($P < 0.005$)), even after 2,4-D was degraded (Fig. 3B). When high stringency hybridisation was used, a general reduction in *tfdA* mRNA abundance levels was observed, and 2,4-D exposed samples had significantly higher transcript levels only on sampling day 11 ($P < 0.005$) (Fig. 3D). These observations indicate that the *tfdA* transcripts of the Golf Course microorganisms predominantly had a lower similarity (> 75%) to the *tfdA* gene of strain JMP134.

3.4. Abundance of 2,4-D degraders

A significant increase in numbers of microbial 2,4-D degraders ($P < 0.05$) was detected in both ponds following 2,4-D exposure. In Passion Puddle, the biomass increased from below detection to approx. 10^4 cells ml^{-1} (Fig. 2E), and in the Golf Course the population increased from 0.8 to approx. 10^5 cells ml^{-1} (Fig. 3E). In contrast, numbers of 2,4-D degraders in non-exposed samples were at or below the detection limit during the entire incubation period (Figs. 2E and 3E). In the herbicide exposed samples, the numbers of 2,4-D degraders remained constant during the 6-week incubation, even 2 weeks after 2,4-D was depleted and mineralisation had ceased.

3.5. Abundance of tfdA genes

Initially, we attempted to quantify *tfdA* genes by hybridisation of DNA samples with the ^{35}S-labelled *tfdA* riboprobe. Results showed a high detection limit corresponding to approx. 10^6 CFU of JMP134 cells, and a high level of non-specific hybridisation (data not shown). Therefore, we chose to estimate *tfdA* gene copies by MPN-PCR (Figs. 2F and 3F). PCR is not a strict quantitative method, but the MPN technique can give an estimate of the relative abundance of the genes of interest [23]. For environmental samples it is generally observed that more than one gene copy is needed in order to detect PCR products [24]. Thus, titres obtained by MPN-PCR describe a relative gene abundance rather than an absolute gene copy number.

No *tfdA* genes could be detected in water samples prior to 2,4-D exposure. Following herbicide exposure, an abundance of 10^2 *tfdA* genes ml^{-1} was measured in samples from both aquatic sites and the gene levels were significantly higher than in the non-exposed controls ($P < 0.05$) (Figs. 2F and 3F). The abundance of *tfdA* genes remained elevated throughout the experiment indicating that, for at least a short period of time, *tfdA* genes were sustained in the community even after depletion of 2,4-D.

3.6. RFLP patterns of tfdA PCR products

The two ponds showed different *tfdA* RFLP patterns, indicating that different *tfdA* loci dominated in the two aquatic environments (Table 1). Vallaeys et al. [17] divided the *tfdA* genes of seventeen 2,4-D degraders into four RFLP groups, and the *tfdA* gene of *R. eutropha* JMP134 was classified as group I. Restriction analysis of Passion Puddle samples showed two different patterns illustrated by data collected on day 12 (similar to the results on days 9, 19 and 26) and day 40 indicative of a change in the

Table 1
RFLP patterns of *tfdA* PCR products

	Restriction fragment length (bp)	
	*Hae*III	*Cfo*I
*Samples**		
Passion Puddle (days 9, 12, 19, 26)	156[a], 119[b], 82[e]	272[a], 73[f]
Passion Puddle (day 40)	159[a], 107[c], 75[f]	272[a], 141[c], 101[d], 77[e]
Golf Course (days 11, 16, 23, 36)	107[c], 92[d], 74[f], 52[g]	222[b], 71[f]
R. eutropha JMP134	158[a], 105[c], 81[e]	139[c], 104[d], 78[e], 59[g]
tfdA PCR RFLP group#		
I	167, 107, 74, (11, 7)	145, 99, 63, 37, 20
II	164, 124, 74	274, 88
III	167, 107, 52, (22, 17, 7)	145, 99, 63, 37, 20
IV	164, 124, 74	274, 55, (20, 14)

*DNA bands considered of similar fragment size are stated by the same superior letter (a, b, c, etc.).
#Groupings as determined by Vallaeys et al. [17] by analysing *tfdA* PCR products of seventeen 2,4-D degrading bacteria. Values in parentheses indicate uncertain bands [17].

Downloaded from http://academic.oup.com/femsec/article/40/3/205/507750 by Corteva Agriscience user on 03 September 2020

COR-AAD1-00002494
Bayer EX1008 (Part 5 of 9)

degrading populations during later stages of 2,4-D utilisation. Data of the initial four samplings were similar to group II *tfdA* genes, which include the bacterial strains *Burkholderia* sp. RASC and *Burkholderia mallei* TFD6 [17]. On day 40, digestion with *Cfo*I resulted in larger fragments (total size equals 591 bp) than the size of the *tfdA* amplicon (362 bp), and the population of *tfdA* genes possibly was composed of group I as well as group II *tfdA* genes. The Golf Course samples, on the other hand, did not show any similarity with presently described *tfdA* groups.

In the present study the RFLP pattern of strain JMP134 was measured in order to have a control to compare the RFLP results of the pond community DNA with the RFLP groupings derived by Vallaeys et al. [17]. We found that our *tfdA* RFLP pattern of strain JMP134 deviated slightly from that obtained by Vallaeys et al. [17] (Table 1). This deviation probably resulted from the use of different standard curves (molecular mass markers) in the two studies, which should be taken into account when interpreting the RFLP results. Due to analytical limitations, we found that small restriction fragments (smaller than approx. 50 bp) were difficult to detect and their presence should not be ruled out.

4. Discussion

Laboratory incubations of Passion Puddle and Golf Course water samples both showed increased levels of *tfdA* mRNA following 2,4-D exposure and for both communities *tfdA* transcription was initiated prior to the commencement of herbicide disappearance. The observed transcription patterns, however, were different for the two microbial communities as evaluated by *tfdA* homology and dynamics of gene transcription. In Passion Puddle, the detected transcripts were highly homologous (close to 100%) to the *tfdA* gene of *R. eutropha* JMP134. In these pond samples, increased levels of *tfdA* mRNA were solely detected at initial stages of 2,4-D degradation, and despite a decrease in *tfdA* transcript abundance degradation of 2,4-D continued for an additional 2 weeks. This would be possible if the 2,4-D dioxygenase remained active for prolonged periods after *tfdA* mRNA could no longer be detected or if the expression of other *tfdA* genes with no similarity to our riboprobe was turned on during later stages of 2,4-D degradation. Leveau et al. [25] showed that chlorocatechol 1,2-dioxygenase activities remained constant for extended periods in chemostat cultures of *R. eutropha* JMP134 even though transcription of *tfdC* was only transient. On the other hand, other studies have demonstrated a tight relationship between the dynamics of gene transcription and of the activity of the corresponding gene product. For example Pichard and Paul [26] showed that the activity of catechol 2,3-dioxygenase in cultures of *Vibrio* sp. strain WJT-1C(pLV1013) was closely related to the transcription of *xylE*, and Wyman et al. [27] similarly found a close relation between nitrogenase activity and the dynamics of *nifH* transcription in natural populations of marine cyanobacteria. Selvaratnam et al. [28] likewise found a correlation between the transcription of *dmpN*, the gene encoding phenol hydroxylase, and the concentration of phenol in batch reactors inoculated with the phenol-degrading *Pseudomonas putida* ATCC 11172. It seems, therefore, that the relationships of transcripts to the activity of their gene products vary and are likely related to the relative stabilities of the mRNAs and their translation products. Indeed, the microbial communities of the Golf Course, where *tfdA* genes with a lower homology to the *tfdA* of JMP134 were dominating, showed increased transcript levels during most of the incubation period, also after 2,4-D was degraded. Thus, using mRNA patterns as indicators of activities in natural microbial communities requires caution in interpreting negative results, i.e. the absence of transcripts does not necessarily mean inactivity.

We attempted to study the composition of *tfdA* populations in Passion Puddle and Golf Course samples in order to evaluate whether the different dynamics of *tfdA* transcription could be ascribed to differences in the microbial populations of 2,4-D degraders. In Passion Puddle, the dynamics of *tfdA* transcription and the high homology to the employed riboprobe suggested a dominance of populations carrying JMP134-like genes. An RFLP analysis of *tfdA* PCR products only partly confirmed this observation, however (Table 1). During the initial 26 days, solely group II-like *tfdA* genes were detected. This *tfdA* group has only 60–75% homology to our riboprobe [16,29] and would therefore be expected to produce no or only very weak hybridisation signals when high stringency wash conditions were used. On day 40, however, the presence of group I *tfdA* genes was demonstrated, suggesting that JMP134-like *tfdA* genes were indeed present in Passion Puddle. The Golf Course samples did not show any similarity with presently described *tfdA* groups and hybridisation analyses of *tfdA* transcripts suggested a low homology to the *tfdA* gene of JMP134. In Passion Puddle microbial communities, analyses of *tfdA* genes and transcripts thus did not fully agree with each other. This discrepancy could have a true biological reason although it might have also arisen from the use of different methodological approaches when measuring presence (PCR) and transcript abundance (hybridisation) of *tfdA*. For example, if the dominating *tfdA* genes present in Passion Puddle were not the most actively transcribed ones, their gene products would be poorly represented among the extracted *tfdA* transcripts. Such observations of skewed patterns of related DNA and RNA data were reported by Delbès et al. [30] who monitored the dynamics of the microbial community in an anaerobic digester using 16S rDNA and rRNA analyses. Our data indicate that concomitant analyses of genes and their transcripts will give an understand-

Downloaded from https://academic.oup.com/femsec/article/40/2/205/540750 by Corteva Agriscience user on 03 September 2020

COR-AAD1-00002495
Bayer EX1008 (Part 5 of 9)

ing of what specific loci are expressed during acclimation to xenobiotic compounds.

The major goal of our research was to examine the role of catabolic gene expression in the acclimation of mixed microbial communities to 2,4-D. Increased transcript abundance can result from (i) increased numbers of transcriptional units (gene dosage effect), (ii) true increases in gene expression on a per cell or per gene basis, (iii) increased mRNA stability and turnover, and (iv) increased RNA polymerase pools [26]. Thus, a clear demonstration of induction during acclimation requires observations of increases in *tfdA* transcript abundance independent of enrichments of 2,4-D degrading populations and *tfdA* genes. Distinguishing among the mechanisms listed above might be difficult, especially in mixed microbial communities, and possibly several were involved in the observed dynamics of *tfdA* transcription in the two pond communities. Some indication, however, of the processes responsible for changes in transcript levels may be gleaned by comparing transcript dynamics with those of *tfdA* gene abundance and 2,4-D degraders. For example, in Passion Puddle the abundance of *tfdA* mRNA dropped after day 9 (Fig. 2C,D) although population levels of 2,4-D degraders and *tfdA* genes remained relatively constant (Fig. 2E,F). This suggests a true decline in *tfdA* transcription on a per cell basis during later stages of 2,4-D degradation. With Golf Course samples, the increase in numbers of *tfdA* genes, which was obvious on day 11 (Fig. 3F), lagged behind the increase in *tfdA* transcripts that was detected on the first day of sampling (day 8) (Fig. 3C). This observation indicates that the detected transcript levels were not solely the result of a gene dosage effect, but also the result of a true increase in *tfdA* transcription. Thus, the data suggest that induction of *tfdA* transcription played a role in acclimation of the two pond microbial communities to 2,4-D.

In summary, transcription of *tfdA* in natural microbial communities from two freshwater ponds in response to 2,4-D exposure demonstrated a role for induction of catabolic gene expression in microbial acclimation. By relating transcript abundance to the dynamics of 2,4-D degradation, *tfdA* gene levels, and presence of degrading populations, different patterns emerged for the two aquatic communities. In Passion Puddle, a transient transcription of *tfdA* was observed while a more stable transcript presence was evident in the Golf Course community. Different 2,4-D degrading populations, as suggested by the RFLP analysis of *tfdA* PCR products, might have been responsible for these two patterns. To the best of our knowledge, this is the first study to describe the dynamics of catabolic gene transcription in environmental samples during degradation of a xenobiotic compound. However, to distinguish induction from enrichment as a mechanism of acclimation, a more refined determination of the dynamics of the relationships between numbers of *tfdA* transcripts, genes and 2,4-D degraders in 2,4-D acclimation will be needed.

Acknowledgements

Jarek Letowski, Ruth Dorn and Jeffra Schaefer are acknowledged for valuable discussions and technical suggestions. We thank Jerry Kukor for plasmid pGEM-3Z, and Kaare Johnsen for critically reading the manuscript. This work was supported by the Danish Environmental Research Program, Pesticides and Groundwater.

References

[1] Barkay, T. and Pritchard, H. (1988) Adaptation of aquatic microbial communities to pollutant stress. Microbiol. Sci. 5, 165–169.
[2] Spain, J.C., Pritchard, P.H. and Bourquin, A.W. (1980) Effects of adaptation on biodegradation rates in sediment/water cores from estuarine and freshwater environments. Appl. Environ. Microbiol. 40, 726–734.
[3] van der Meer, J.R., de Vos, W.M., Harayama, S. and Zehnder, A.J.B. (1992) Molecular mechanisms of genetic adaptation to xenobiotic compounds. Microbiol. Rev. 56, 677–694.
[4] Ka, J.O., Holben, W.E. and Tiedje, J.M. (1994) Use of gene probes to aid in recovery and identification of functionally dominant 2,4-dichlorophenoxyacetic acid-degrading populations in soil. Appl. Environ. Microbiol. 60, 1116–1120.
[5] Stapleton, R.D., Sayler, G.S., Boggs, J.M., Libelo, E.L., Stauffer, T. and Macintyre, W.G. (2000) Changes in subsurface catabolic gene frequencies during natural attenuation of petroleum hydrocarbons. Environ. Sci. Technol. 34, 1991–1999.
[6] Ravatn, R., Zehnder, A.J.B. and van der Meer, J.R. (1998) Low-frequency horizontal transfer of an element containing the chlorocatechol degradation genes from *Pseudomonas* sp. strain B13 to *Pseudomonas putida* F1 and to indigenous bacteria in laboratory-scale activated-sludge microcosms. Appl. Environ. Microbiol. 64, 2126–2132.
[7] Top, E.M., Van Daele, P., De Saeyer, N. and Forney, L.J. (1998) Enhancement of 2,4-dichlorophenoxyacetic acid (2,4-D) degradation in soil by dissemination of catabolic plasmids. Antonie van Leeuwenhoek 73, 87–94.
[8] de Lipthay, J.R., Barkay, T. and Sørensen, S.J. (2001) Enhanced degradation of phenoxyacetic acid in soil by horizontal transfer of the *tfdA* gene encoding a 2,4-dichlorophenoxyacetic acid dioxygenase. FEMS Microbiol. Ecol. 35, 75–84.
[9] Fleming, J.T., Sanseverino, J. and Sayler, G.S. (1993) Quantitative relationship between naphthalene catabolic gene frequency and expression in predicting PAH degradation in soils at town gas manufacturing sites. Environ. Sci. Technol. 27, 1068–1074.
[10] Sanseverino, J., Werner, C., Fleming, J., Applegate, B., King, J.M.H. and Sayler, G.S. (1993) Molecular diagnostics of polycyclic aromatic hydrocarbon biodegradation in manufactured gas plant soils. Biodegradation 4, 303–321.
[11] Nazaret, S., Jeffrey, W.H., Saouter, E., von Haven, R. and Barkay, T. (1994) *merA* gene expression in aquatic environments measured by mRNA production and Hg(II) volatilization. Appl. Environ. Microbiol. 60, 4059–4065.
[12] Streber, W.R., Timmis, K.N. and Zenk, M.H. (1987) Analysis, cloning, and high-level expression of 2,4-dichlorophenoxyacetate monooxygenase gene *tfdA* of *Alcaligenes eutrophus* JMP134. J. Bacteriol. 169, 2950–2955.
[13] Don, R.H. and Pemberton, J.M. (1981) Properties of six pesticide degradation plasmids isolated from *Alcaligenes paradoxus* and *Alcaligenes eutrophus*. J. Bacteriol. 145, 681–686.
[14] Fukumori, F. and Hausinger, R.P. (1993) *Alcaligenes eutrophus* JMP134 '2,4-dichlorophenoxyacetate monooxygenase' is an α-ketoglutarate dioxygenase. J. Bacteriol. 175, 2083–2086.

Downloaded from https://academic.oup.com/femsec/article/40/3/205/507150 by Corteva Agriscience user on 03 September 2020

COR-AAD1-00002496
Bayer EX1008 (Part 5 of 9)

[15] Fukumori, F. and Hausinger, R.P. (1993) Purification and characterization of 2,4-D-dichlorophenoxyacetate/alpha-ketoglutarate dioxygenase. J. Biol. Chem. 268, 24311–24317.
[16] Fulthorpe, R.R., McGowan, C., Maltseva, O.V., Holben, W.E. and Tiedje, J.M. (1995) 2,4-Dichlorophenoxyacetic acid-degrading bacteria contain mosaics of catabolic genes. Appl. Environ. Microbiol. 61, 3274–3281.
[17] Vallaeys, T., Fulthorpe, R.R., Wright, A.M. and Soulas, G. (1996) The metabolic pathway of 2,4-dichlorophenoxyacetic acid degradation involves different families of *tfdA* and *tfdB* genes according to PCR-RFLP analysis. FEMS Microbiol. Ecol. 20, 163–172.
[18] de Lipthay, J.R., Barkay, T., Vekova, J. and Sørensen, S.J. (1999) Utilization of phenoxyacetic acid, by strains using either the *ortho* or *meta* cleavage of catechol during phenol degradation, after conjugal transfer of *tfdA*, the gene encoding a 2,4-dichlorophenoxyacetic acid/2-oxoglutarate dioxygenase. Appl. Microbiol. Biotechnol. 51, 207–214.
[19] Sambrook, J., Fritsch, E.F. and Maniatis, F. (1989) Molecular Cloning: a Laboratory Manual, 2nd edn. Cold Spring Harbor Laboratory Press, Cold Spring Harbor, NY.
[20] Ausubel, F.M., Brent, R., Kingston, R.E., Moore, D.D., Seidman, J.G., Smith, J.A. and Struhl, K. (2000) Current Protocols in Molecular Biology. John Wiley and Sons, New York.
[21] Jeffrey, W.H., Nazaret, S. and von Haven, R. (1994) Improved method for recovery of mRNA from aquatic samples and its application to detection of *mer* expression. Appl. Environ. Microbiol. 60, 1814–1821.
[22] Wilson, M.S., Bakermans, C. and Madsen, E.L. (1999) In situ, real-time catabolic gene expression: extraction and characterisation of naphthalene dioxygenase mRNA transcripts from groundwater. Appl. Environ. Microbiol. 65, 80–87.
[23] Rosado, A.S., Seldin, L., Wolters, A.C. and van Elsas, J.D. (1996) Quantitative 16S rDNA-targeted polymerase chain reaction and oligonucleotide hybridization for the detection of *Paenibacillus azotofixans* in soil and the wheat rhizosphere. FEMS Microbiol. Ecol. 19, 153–164.
[24] Sobecky, P.A., Mincer, T.J., Chang, M.C. and Helinsky, D.R. (1997) Plasmids isolated from marine sediment microbial communities contain replication and incompatibility regions unrelated to those of known plasmid groups. Appl. Environ. Microbiol. 63, 888–895.
[25] Leveau, J.H.J., König, F., Füchslin, H., Werlen, C. and van der Meer, J.R. (1999) Dynamics of multigene expression during catabolic adaptation of *Ralstonia eutropha* JMP134 (pJP4) to the herbicide 2,4-dichlorophenoxyacetate. Mol. Microbiol. 33, 396–406.
[26] Pichard, S.L. and Paul, J.H. (1993) Gene expression per gene dose, a specific measure of gene expression in aquatic microorganisms. Appl. Environ. Microbiol. 59, 451–457.
[27] Wyman, M., Zehr, J.P. and Capone, D.G. (1996) Temporal variability in nitrogenase gene expression in natural populations of the marine cyanobacterium *Trichodesmium thiebautii*. Appl. Environ. Microbiol. 62, 1073–1075.
[28] Selvaratnam, S., Schoedel, B.A., McFarland, B.L. and Kulpa, C.F. (1995) Application of reverse transcriptase PCR for monitoring expression of the catabolic *dmpN* gene in a phenol-degrading sequencing batch reactor. Appl. Environ. Microbiol. 61, 3981–3985.
[29] McGowan, C., Fulthorpe, R., Wright, A. and Tiedje, J.M. (1998) Evidence for interspecies gene transfer in the evolution of 2,4-dichlorophenoxyacetic acid degraders. Appl. Environ. Microbiol. 64, 4089–4092.
[30] Delbès, C., Moletta, R. and Godon, J.-J. (2000) Monitoring of activity dynamics of an anaerobic digester bacterial community using 16S rRNA polymerase chain reaction-single-strand conformation polymorphism analysis. Environ. Microbiol. 2, 506–515.

Downloaded from http://academic.oup.com/femsec/article/40/3/205/540750 by Cortava Agriscience user on 03 September 2020

COR-AAD1-00002497
Bayer EX1008 (Part 5 of 9)

APPLIED AND ENVIRONMENTAL MICROBIOLOGY, Jan. 2003, p. 461–467 Vol. 69, No. 1
0099-2240/03/$08.00+0 DOI: 10.1128/AEM.69.1.461–467.2003
Copyright © 2003, American Society for Microbiology. All Rights Reserved.

In Situ Exposure to Low Herbicide Concentrations Affects Microbial Population Composition and Catabolic Gene Frequency in an Aerobic Shallow Aquifer

Julia R. de Lipthay,[1]† Nina Tuxen,[2] Kaare Johnsen,[1,3] Lars H. Hansen,[4] Hans-Jørgen Albrechtsen,[2] Poul L. Bjerg,[2] and Jens Aamand[1]*

Department of Geochemistry, Geological Survey of Denmark and Greenland, Øster Voldgade 10, DK-1350 Copenhagen K,[1] Environment & Resources DTU, Technical University of Denmark, DK-2800 Lyngby,[2] Danish Veterinary Institute, DK-1790 Copenhagen V,[3] and Department of General Microbiology, University of Copenhagen, DK-1307 Copenhagen K,[4] Denmark

Received 13 May 2002/Accepted 30 October 2002

The aim of this study was to evaluate how the in situ exposure of a Danish subsurface aquifer to phenoxy acid herbicides at low concentrations (<40 μg l^{-1}) changes the microbial community composition. Sediment and groundwater samples were collected inside and outside the herbicide-exposed area and were analyzed for the presence of general microbial populations, *Pseudomonas* bacteria, and specific phenoxy acid degraders. Both culture-dependent and culture-independent methods were applied. The abundance of microbial phenoxy acid degraders (10^0 to 10^4 g^{-1} sediment) was determined by most probable number assays, and their presence was only detected in herbicide-exposed sediments. Similarly, PCR analysis showed that the 2,4-dichlorophenoxyacetic acid degradation pathway genes *tfdA* and *tfdB* (10^2 to 10^3 gene copies g^{-1} sediment) were only detected in sediments from contaminated areas of the aquifer. PCR-restriction fragment length polymorphism measurements demonstrated the presence of different populations of *tfd* genes, suggesting that the in situ herbicide degradation was caused by the activity of a heterogeneous population of phenoxy acid degraders. The number of *Pseudomonas* bacteria measured by either PCR or plating on selective agar media was higher in sediments subjected to high levels of phenoxy acid. Furthermore, high numbers of CFU compared to direct counting of 4′,6-diamidino-2-phenylindole-stained cells in the microscope suggested an increased culturability of the indigenous microbial communities from acclimated sediments. The findings of this study demonstrate that continuous exposure to low herbicide concentrations can markedly change the bacterial community composition of a subsurface aquifer.

During the past decade an increasing number of herbicides has been detected in groundwater aquifers (15). These include the phenoxy acids, which have been widely used for more than 50 years, such as mecoprop [2-(2-methyl-4-chlorophenoxy)propionic acid], dichlorprop [2-(2,4-dichlorophenoxy)propionic acid], and 2,4-D (2,4-dichlorophenoxyacetic acid). Groundwater is an important drinking water resource, and studies exploring the potential of the indigenous microbial communities to degrade herbicides and the impact of these chemicals on microbial community structure may contribute to our understanding of how and when microorganisms indigenous to aquifers acclimate to xenobiotic compounds.

Microbial acclimation is commonly defined as the processes taking place during the time period between entry of a chemical and the evidence of its detectable loss (2). With acclimated microbial communities this period is typically shortened following repeated exposure to the same chemical compound (2). Microbial acclimation is generally ascribed to the enrichment of specific degraders, enzyme induction, and genetic adaptation, but the presence of toxins, predation by protozoa, and diauxie also influence the process (2).

It is only in the past few years that microbial acclimation to herbicides in subsurface aquifer environments has been investigated (1, 24, 37). Most of these studies involved laboratory incubation and primarily focused on the activity and rate of herbicide degradation. None, however, dealt with the effects of herbicides on the indigenous subsurface microbial communities. In contrast, numerous studies have examined the effects of herbicides on surface soil microbial communities, e.g., microbial biomass and the abundance of specific degraders and catabolic genes (12, 19, 22, 36). Subsurface aquifers constitute environments that are physically, chemically, and biologically very different from surface soils. They have reduced concentrations and availability of oxygen, carbon, and inorganic nutrients and a 10^2 to 10^6 times lower bacterial density (17). Results from surface soil environments, thus, cannot readily be extrapolated to subsurface aquifer conditions. Furthermore, in agricultural fields herbicides are typically applied in concentrations in the milligrams per kilogram of soil range, and surface soil microbial communities may thus be naturally exposed to high contaminant concentrations. In contrast, herbicide concentrations in groundwater are low: typical concentrations measured from landfills are 10 to 250 μg l^{-1} (26, 43) (equivalent to 2 to 40 μg kg^{-1} of sediment), whereas herbicide concentrations in groundwater polluted due to agricultural use most often are <1 μg l^{-1} (15). To get a realistic picture of how

* Corresponding author. Mailing address: Department of Geochemistry, Geological Survey of Denmark and Greenland, Øster Voldgade 10, DK-1350 Copenhagen K, Denmark. Phone: 45 38 14 23 26. Fax: 45 38 14 20 50. E-mail: jeaa@geus.dk.

† Present address: Department of General Microbiology, University of Copenhagen, Sølvgade 83H, DK-1307 Copenhagen K, Denmark.

Downloaded from http://aem.asm.org/ on September 3, 2020 at Corteva Agriscience

COR-AAD1-00002498
Bayer EX1008 (Part 5 of 9)

herbicides affect subsurface microbial communities, studies need to be carried out at low contaminant concentrations. Besides, information retrieved from such studies is necessary in order to model the fate of real-world contaminant plumes properly and for suggesting possible actions for remediation of polluted groundwater.

In a natural gradient field injection experiment, a part of the Vejen aquifer (Denmark) was continuously exposed to herbicide concentrations of <40 μg l^{-1} (8) (equivalent to <7 μg kg^{-1} of sediment). After an initial lag phase of 80 to 100 days, fast degradation of mecoprop and dichlorprop was observed and herbicide concentrations decreased to below detection levels within the first meter from the injection wells (8). This indicated that the microbial community acclimated to the contamination. This was verified by laboratory experiments showing that sediments close to the injection wells had the highest potential for phenoxy acid herbicide degradation (38). The aim of the present study was to evaluate how the in situ herbicide exposure of the Vejen aquifer affected the indigenous microbial community composition. This was done by measuring the total microbial population density and the abundance of *Pseudomonas* bacteria and phenoxy acid degraders. Furthermore, the frequency and the composition of the 2,4-D degradation pathway genes *tfdA* and *tfdB* (14, 33) (Fig. 1) were estimated.

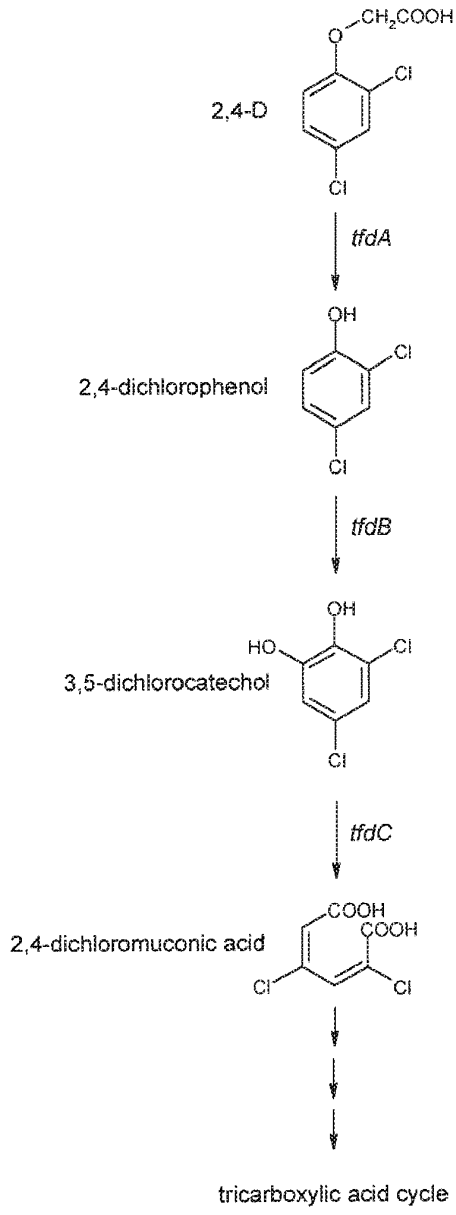


FIG. 1. Illustration of the 2,4-D degradation pathway in *R. eutropha* JMP134, the archetype 2,4-D degrader (13). The catabolic genes *tfdA*, *tfdB*, and *tfdC* were originally discovered in strain JMP134 and encode a 2,4-D/2-oxoglutarate dioxygenase, a chlorophenol hydroxylase, and a chlorocatechol 1,2-dioxygenase, respectively (14, 33). Other *tfd* genes are involved in the further transformation to products of the tricarboxylic acid cycle (14).

MATERIALS AND METHODS

Field site. Sediment and groundwater were collected from an unconfined shallow aerobic aquifer located at Vejen, Denmark (5, 8). Part of the aquifer was previously exposed to herbicides during a natural gradient field injection experiment (8). A mixture of the herbicides mecoprop, dichlorprop, DNOC (2-methyl-4,6-dinitrophenol), bentazone [3-(1-methylethyl)-1H-2,1,3-benzothiadiazin-4(3H)-one 2,2-dioxide], isoproturon {*N*,*N*-dimethyl-*N*′-[4-(1-methylethyl)phenyl]urea}, and 2,4-dichlorbenzamide (BAM; a degradation product of dichlobenil) was continuously injected into the aquifer for a period of 216 days, creating a contaminant plume. Bromide was included as a nonreactive tracer. The concentration of each herbicide was approximately 40 μg l^{-1} immediately down-gradient of the injection wells. Migration of bromide and the herbicides was monitored by using a dense network of multilevel samplers (8).

At the time of sampling (40 days after termination of the field injection), herbicides were no longer present in the aquifer due to advective flow and degradation (8). The field exposures of mecoprop and dichlorprop were expressed as the total amount (in micrograms) of each compound that passed through each sampling point during the whole injection period (38).

Sampling. Sediment and groundwater were sampled from the herbicide-exposed area (samples A1, A2, B1, B2, C1, and C2) and from nonexposed areas outside the contaminant plume (NX1 to -4) (Fig. 2). Herbicide-exposed aquifer sediment was collected as three intact cores at different distances from the injection wells (0.5 m for A sites, 1.5 m for B sites, and 4.5 m for C sites). Two subsamples from each core were obtained, an upper sample (number 1) and a lower sample (number 2). The distance between the upper and lower samples was approximately 0.5 m. The nonexposed samples were collected similarly at upper (NX1 and NX3) and lower (NX2 and NX4) depths. All sediment cores were collected with a stainless steel piston sampler from the saturated zone, 5 to 6.25 m below the surface, and were stored (4°C) until partitioning. Two centimeters of each core end and the outermost 0.5 cm were aseptically removed by using a paring device modified from that described by Wilson et al. (41). Individual sediment samples were homogenized thoroughly and were stored at 4°C for a maximum of 9 days until setup of laboratory experiments. Sediments for DNA analysis were stored at −20°C. Groundwater was sampled adjacent to each sediment core by using a peristaltic pump and were stored at 4°C.

Bacterial strains and culture conditions. *Pseudomonas putida* KT2442 was grown in Luria-Bertani medium (28). The *Ralstonia eutropha* strains JMP134 and AEO106 (a plasmid-cured derivative of *R. eutropha* JMP134) were grown in minimal medium (10) supplemented with 2 mM 2,4-D (>98%; Merck, Darmstadt, Germany) and 0.2% fructose, respectively. All bacterial strains were grown at 30°C.

Microbial populations. Microbial population sizes were estimated by analyzing three replicate subsamples of each sediment sample. One gram of sediment was diluted in 9.0 ml of sterile NaCl (0.9% [wt/vol]) and vortexed for 1 min, and 10-fold dilutions were prepared. Direct counting of bacteria was performed by using epifluorescence microscopy (Olympus BX50; Hamburg, Germany) after staining with 4′,6-diamidino-2-phenylindole (DAPI) (2 μg ml^{-1}) for 10 min in darkness. Three replicates of each subsample were enumerated. The number of

Downloaded from http://aem.asm.org/ on September 3, 2020 at Corteva Agriscience

COR-AAD1-00002499
Bayer EX1008 (Part 5 of 9)

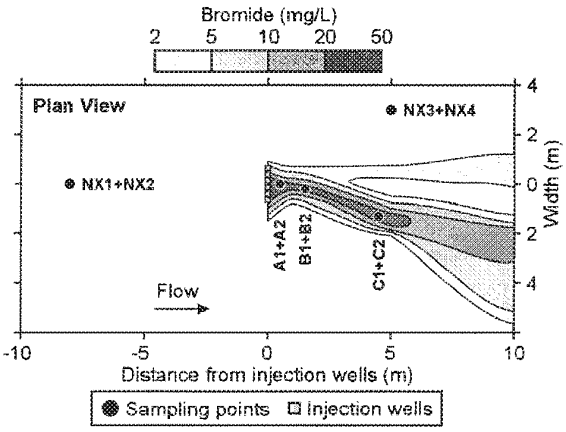


FIG. 2. Field plot of the Vejen aquifer. Plan view showing the bromide tracer plume and the location of aquifer sampling points inside (A1, A2, B1, B2, C1, and C2) and outside (NX1 to -4) the herbicide-exposed area. The groundwater velocity is approximately 0.5 m day^{-1} (8), and the temperature is 10°C (38). At sampling (40 days after the field injection had been terminated), bromide as well as herbicides were no longer present within the monitoring network (8).

culturable heterotrophs was estimated by plating on water agar (15.0 g l^{-1} of BiTek agar [Difco, Detroit, Mich.] in Milli-Q water). The number of culturable *Pseudomonas* bacteria was estimated by plating on the *Pseudomonas*-specific (18, 20) Gould's S1 agar medium (18). All agar media were supplemented with nystatin (50 μg ml^{-1}) to prevent fungal growth. Each subsample was plated in triplicate and was incubated at 20°C for 21 days (water agar) and 7 days (Gould's S1) before enumeration of CFU.

The number of mecoprop, dichlorprop, and 2,4-D degraders was estimated by a most probable number (MPN) assay relying on herbicide degradation. Two milliliters of a minimal medium (10) containing 2.5-mg $liter^{-1}$ concentrations of mecoprop (>99%; Riedel-de Haën, Seelze, Germany), dichlorprop (>99%; Riedel-de Haën), or 2,4-D (Merck) was added to 20-ml glass vials. The vials were then supplied with 200-μl aliquots of each sediment dilution (10^{-1} to 10^{-5}), set up in five replicates, and incubated at 20°C for 3 months. Samples were filter sterilized (0.2 μm) and stored at 4°C until high-performance liquid chromatography analyses were made for remaining concentrations of herbicides as previously described (11). A similar setup was used to determine the abundance of mecoprop- and 2,4-D-mineralizing bacteria, though these vials also included ^{14}C-labeled herbicides and a NaOH trap to collect $^{14}CO_2$ as described previously (11). MPN samples were scored as positive if more than 25% of the herbicides were degraded or mineralized.

DNA extraction. Whole-community DNA was extracted from three subsamples of each sediment sample by a combination of bead beating and freeze-thaw procedures. Bead beating was applied on 500 mg of sediment by using the FastDNA Spin Kit for Soil (BIO 101, Vista, Calif.) followed by two freeze-thaw cycles (1 h at −80°C, 30 min at 37°C). DNA was purified by the use of a GeneClean procedure (BIO 101), and the resulting samples were stored at −20°C.

Detection of *Bacteria*- and *Pseudomonas*-specific 16S rDNA. The DNA primers PRBA338f and PRUN518r (27) were used to amplify general bacterial 16S ribosomal DNA (rDNA) segments, while PSM_Gf (7) and 785r (3) were used to amplify *Pseudomonas*-specific 16S rDNA segments. The PSM_G primer has been shown to be specific to *Pseudomonas* (7, 21, 35). PCR mixtures (50 μl) consisted of 1× GeneAmp PCR Buffer (Perkin-Elmer, Applied Biosystem, Foster City, Calif.), 100 μM concentrations of each deoxynucleoside triphosphate (Perkin-Elmer), 0.5 μM concentrations of each primer (Gibco-BRL Custom Primers; Life Technologies, Paisley, Scotland), and 1.25 U of AmpliTaq Gold DNA polymerase (Perkin-Elmer). Five-microliter aliquots of the DNA extracts were added to the reaction mixtures, and PCR was performed with the following program: 10 min at 95°C; 35 cycles of 30 s at 95°C, 30 s at 55°C (*Bacteria*) or 59°C (*Pseudomonas*), and 1 min at 72°C; 6 min at 72°C. DNA extracts (1 μl) of *P. putida* KT2442 and *R. eutropha* JMP134 cultures were used as positive and negative controls, respectively, for *Pseudomonas*-specific PCR. The abundance of 16S rDNA genes in DNA samples was estimated by MPN-PCR by analyzing three replicates of each sample dilution (10^{0} to 10^{-4}).

Detection of *tfdA*, *tfdB*, and *tfdC* genes. PCR amplification of the 2,4-D degradation genes *tfdA*, *tfdB* (39), and *tfdC* (9) was performed with degenerate primers. PCR of *tfdA*- and *tfdB*-homologous genes was performed by using a program slightly modified from the methods described by Vallaeys et al. (39): 6 min at 94°C; 40 cycles of 45 s at 94°C, 30 s at 59°C (*tfdA*) or 49°C (*tfdB*), and 2 min at 72°C; 6 min at 72°C. PCR of *tfdC*-homologous genes was performed as described by Cavalca et al. (9). For all *tfd* PCRs, each tube contained a total of 50 μl of reaction mixture consisting of 1× GeneAmp PCR Buffer (Perkin-Elmer), 200 μM concentrations of each deoxynucleoside triphosphate (Perkin-Elmer), 1.0 μM concentrations of each primer (DNA Technology A/S, Aarhus, Denmark), and 2.5 U of AmpliTaq Gold DNA polymerase (Perkin-Elmer). Five-microliter aliquots of the DNA extracts were added to the reaction mixtures, and PCR was performed as described above. DNA extracts (1 μl) of 2,4-D-grown *R. eutropha* JMP134 and fructose-grown *R. eutropha* AEO106 cultures were used as positive and negative controls for the presence of *tfd* genes. The abundance of *tfd* genes in DNA samples was estimated by MPN-PCR by analyzing three replicates of each sample dilution (10^{0} to 10^{-2}).

The populations of *tfd* genes obtained from individual aquifer sediments were analyzed by restriction fragment length polymorphism (RFLP) by digestion of PCR products with *Hae*III and *Cfo*I (an isoschizomer of *Hha*I) (Roche Molecular Biochemicals, Mannheim, Germany) followed by separation on 3.5% agarose gels. The molecular sizes of the restriction fragments were calculated by using a standard curve derived from the 100- to 600-bp bands of a 100-bp molecular size marker.

Statistical analyses. All measurements of microbial population density and gene abundance are expressed per gram (dry weight) of sediment. The statistical significance of differences was determined by using a Student's *t* test at the 0.05 significance level. The level of linear correlation between data was expressed by Pearson correlation coefficients (*r*).

RESULTS AND DISCUSSION

General bacterial populations. We found a total bacterial density of approximately 10^7 DAPI-stained cells g^{-1} of sediment (Fig. 3A), with no significant differences between samples ($P > 0.05$). In contrast, the population density measured as CFU on water agar was significantly higher in sediments A1, A2, and B2 (approximately 10^7 CFU g^{-1}) than in any other sediment (approximately 10^3 to 10^5 CFU g^{-1}) (Fig. 3A). These three sediments have previously been shown to have a much higher potential for degradation of phenoxy acid herbicides than the nonexposed sediments (NX1 to -4) (38). The higher CFU numbers found in the highly acclimated sediments A1, A2, and B2 suggest an increased culturability of the microbial communities and not an increase in the total bacterial population density. Similar to the total bacterial counts, MPN-PCR of *Bacteria*-specific 16S rDNA gene segments showed an equal distribution of DNA (approximately 10^4 to 10^5 gene copies g^{-1}) (Fig. 3B). Only in B1 were significantly lower levels ($P < 0.05$) of 16S rDNA gene abundance recorded, and only in B2 were significantly higher levels ($P < 0.05$) of 16S rDNA gene abundance recorded. The MPN-PCR assay gave a lower estimate of bacterial populations compared to those from the classical microbiological methods. The true copy number, however, is probably several orders of magnitude higher: the calculation of MPNs is based on the capability of one gene copy to yield a positive reaction, and this is rarely enough to produce a visible PCR product (31). Furthermore, complete extraction of all bacterial DNA from the aquifer sediments may not be possible.

***Pseudomonas* populations.** It is generally known that *Pseudomonas* bacteria are able to degrade a wide range of xenobiotic compounds (29). In the Vejen aquifer, culturable *Pseudomo-*

Downloaded from http://aem.asm.org/ on September 3, 2020 at Corteva Agriscience

COR-AAD1-00002500
Bayer EX1008 (Part 5 of 9)

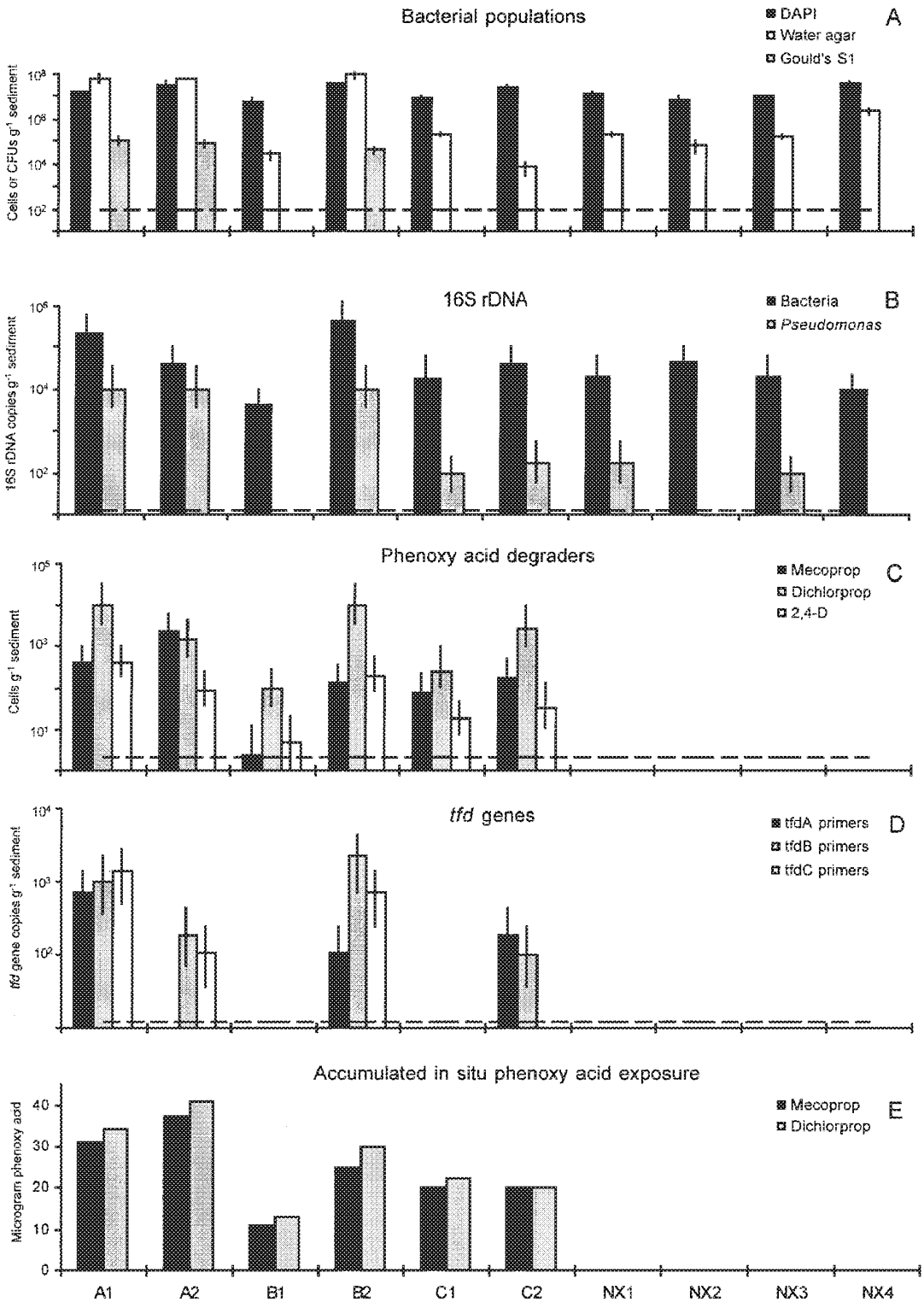


FIG. 3. Effect of in situ herbicide exposure on microbial community composition in the Vejen aquifer. A1, A2, B1, B2, C1, and C2 indicate sediment samples collected within the herbicide-exposed area of the aquifer, while NX1 to -4 indicate samples collected outside the contaminant plume. Field samples were collected in the saturated zone at two depths (1 = upper, 2 = lower) (see also Materials and Methods). (A) Bacterial population density estimated by DAPI staining (cells per gram of sediment) and by plating on water and Gould's S1 agar (CFU per gram of sediment). Each data point represents the means ± standard deviations of nine replicate measurements. The broken line indicates the detection

Downloaded from http://aem.asm.org/ on September 3, 2020 at Corteva Agriscience

COR-AAD1-00002501
Bayer EX1008 (Part 5 of 9)

nas organisms were only detected in the acclimated sediments A1, A2, and B2 (approximately 10^5 CFU g^{-1}) (Fig. 3A). Nevertheless, PCR analysis demonstrated that *Pseudomonas*-specific gene segments were present in both herbicide-exposed (A1, A2, B2, C1, and C2) and -nonexposed (NX1 and NX3) sediments (Fig. 3B). The abundance, though, was significantly higher in A1, A2, and B2 than in any other sediment ($P < 0.05$). Densities recorded as CFU on Gould's S1 agar and *Pseudomonas*-specific 16S rDNA gene segments were linearly correlated ($r = 0.92$), and data indicated that the microbial communities of the acclimated sediments A1, A2, and B2 were enriched in bacteria phylogenetically belonging to *Pseudomonas*. These results might suggest that *Pseudomonas* bacteria had a possible role in the phenoxy acid degradation in the Vejen aquifer. Therefore, we tested approximately 50 *Pseudomonas* isolates for the ability to mineralize ^{14}C-labeled mecoprop and 2,4-D, but only one bacterial morphotype had this capacity (data not shown). This suggests that only a few of the enriched *Pseudomonas* bacteria had a potential direct impact on the in situ herbicide degradation, although the involvement of nonculturable species or the dependence on codegrading microorganisms cannot be excluded. Nor can the possible existence of dichlorprop-degrading bacteria not detected by this assay be excluded.

Phenoxy acid degraders. Mecoprop, dichlorprop, and 2,4-D degraders were found in all herbicide-exposed sediments (Fig. 3C). In contrast, at the nonexposed sites the number of specific degraders was below the detection limit (2 cells g^{-1}). In general, the abundance of degraders was highest in sediments A1, A2, B2, and C2 (approximately 10^2 to 10^4 degraders g^{-1}), whereas B1 harbored the significantly lowest number of phenoxy acid degraders (approximately 10^0 to 10^2 g^{-1}) ($P < 0.05$). In correspondence with this, the mass of field-injected mecoprop and dichlorprop could at most explain increases in population densities of 2×10^5 cells g^{-1} sediment, assuming (i) a yield coefficient of 0.3 g of carbon in produced biomass per gram of carbon of degraded herbicide (38), (ii) a weight of 1.72×10^{-13} g of carbon per cell (4), and (iii) a homogenous distribution of produced biomass in the plume (2 m^3). The calculations included the first meter from the injection where the major part of the phenoxy acids was degraded (8). We found that the estimated density of mecoprop and 2,4-D degraders was identical irrespective of whether the MPN assay was performed by high-performance liquid chromatography or mineralization analyses (data not shown). The phenoxy acid degraders of the Vejen aquifer thus had the potential to degrade the herbicides completely to CO_2.

The Vejen aquifer had not been exposed to 2,4-D during the field injection, but the number of 2,4-D degraders corresponded well with the number of mecoprop and dichlorprop degraders (Fig. 3C). Most bacterial phenoxy acid degraders are able to transform several phenoxy acids. For example, mixed and pure bacterial cultures enriched on mecoprop typically show a broad substrate range, including dichlorprop, 2,4-D, and MCPA [2-(4-chloro-2-methylphenoxy)acetic acid] (23, 34, 42). However, isolates enriched on 2,4-D typically do not degrade phenoxypropionic acids (13, 40).

Increases in the density of specific degraders have also been observed in situ in subsurface environments and aquifers contaminated with fuel compounds (6, 25, 32), but they have been observed at much higher contaminant concentrations than the herbicide concentrations in the Vejen aquifer. Also, several studies have demonstrated an increased population density (10^4 to 10^8 g^{-1}) of 2,4-D degraders following exposure to 2,4-D (in milligrams per kilogram levels) in laboratory microcosms of surface soil (12, 19). However, no studies have reported on increases in the density of specific microbial degraders following in situ exposure to low herbicide concentrations (<40 μg l^{-1}) in groundwater aquifers.

***tfd* genes.** PCR amplification with *tfd*-specific primers was only seen in the herbicide-exposed sediments (Fig. 3D). *tfdA*-homologous genes were found in sediments A1, B2, and C2 (Fig. 3D), and RFLP analysis revealed a difference between the populations found in C2 and those in A1 and B2 (data not shown). *tfdB*-homologous genes were observed in sediments A1, A2, B2, and C2 (Fig. 3D). Here, RFLP patterns of the populations in B2 were different from those in the other three sediments (data not shown). The abundance of *tfd* gene copies was approximately 10^2 to 10^3 g^{-1} of sediment (Fig. 3D), which is lower than was estimated by the culture-dependent assay for measuring phenoxy acid degraders (Fig. 3C). However, as in the case of the MPN-PCR analysis of *Bacteria*-specific 16S rDNA gene segments, the copy number is probably several orders of magnitude higher. Although resulting in different abundance levels, the culture-dependent and the culture-independent MPN assays generally correlated: *tfdA* versus mecoprop ($r = 0.97$), dichlorprop ($r = 0.76$), and 2,4-D ($r = 0.91$) degraders; *tfdB* versus mecoprop ($r = 0.50$), dichlorprop ($r = 0.91$), and 2,4-D ($r = 0.70$) degraders. The lack of *tfd* genes in sediments B1 and C1 is probably due to a lower population density of phenoxy acid degraders in these samples. It cannot be excluded, however, that the sequence of the *tfd* genes in these sediments differs from those of the archetype 2,4-D degrader, *R. eutropha* JMP134. Several bacterial 2,4-D degraders have been reported not to have any homology with the *tfd* genes of strain JMP134 (9, 16, 39). This could also explain the lack of *tfdA* genes in sediment A2. Also, presently only *tfd* gene sequences from culturable 2,4-D degraders are known.

Amplification with *tfdC*-specific primers resulted in PCR products in sediments A1, A2, and B2 (Fig. 3D), but these were significantly shorter than the product of strain JMP134 (data not shown). Further characterization of the *tfdC* PCR

limit (10^2 CFU g^{-1}) for culturable estimates. (B) Abundance of *Bacteria*- and *Pseudomonas*-specific 16S rDNA gene segments determined by MPN-PCR. Each data point represents the mean ± 95% confidence interval of three replicate measurements. The broken line indicates the detection limit (40 gene copies g^{-1}, assuming that one gene copy can give rise to a PCR product). (C) Population density of phenoxy acid degraders as measured by an MPN assay relying on herbicide degradation. Each data point represents the mean ± 95% confidence interval of five replicate measurements. The broken line indicates the detection limit (2 cells g^{-1}). (D) Abundance of *tfd* genes determined by MPN-PCR. Each data point represents the mean ± 95% confidence interval of three replicate measurements. The broken line indicates the detection limit (40 gene copies g^{-1}, assuming that one gene copy can give rise to a PCR product). (E) Accumulated exposure levels of mecoprop and dichlorprop in the Vejen aquifer during the in situ natural field injection (reprinted from reference 38 with permission of the publisher).

Downloaded from http://aem.asm.org/ on September 3, 2020 at Corteva Agriscience

COR-AAD1-00002502
Bayer EX1008 (Part 5 of 9)

products by cloning and sequencing followed by a search for known DNA sequences at the GenBank database (http://www.ncbi.nlm.nih.gov/) revealed no homology to known *tfdC* genes or other DNA sequences (data not shown). At the protein level, however, significantly high homology with bacterial ferredoxin NADP reductases was found (data not shown).

The *tfd* genes are widespread among bacterial 2,4-D degraders (9, 16, 39), and the enrichment of these catabolic genes following application of 2,4-D to surface soil has previously been observed (19, 22). The detection of *tfdA* and *tfdB* genes in acclimated microbial communities of the Vejen aquifer suggests, however, that *tfd* genes are possibly also responsible for the transformation of phenoxypropionic acid compounds. This is in agreement with the recent finding of *tfdA*-homologous genes in three bacterial mecoprop degraders (30).

In general, the PCR analysis of *tfd* genes complemented the MPN measurements of culturable phenoxy acid degraders, although it failed to detect their presence in sediments B1 and C1. It may thus be concluded that the culture-dependent MPN assay is a better tool than PCR in the evaluation of in situ microbial acclimation. However, if nonculturable contaminant degraders need to be detected, the application of molecular analyses is necessary. Also, these analyses can give a more refined picture of the presence and distribution of the catabolic genes responsible for the observed in situ degradation.

The abundance of herbicide degraders as well as the presence of *tfd* genes correlated with the phenoxy acid field exposure (Fig. 3E). Furthermore, it has previously been shown that the sediments exposed to the highest amount of phenoxy acids also were the most acclimated to mecoprop, dichlorprop, and 2,4-D (38).

Concluding remarks. Continuous exposure to low herbicide concentrations ($< 40\ \mu g\ l^{-1}$) in the Vejen aquifer changed the microbial community composition toward a higher bacterial culturability, increased abundance of *Pseudomonas* bacteria, and increased abundance of phenoxy acid degraders as well as *tfd* genes. The most pronounced effects were observed with sediments A1, A2, and B2, which had been exposed to the highest levels of phenoxy acids in the field. Data suggest that the degradation of mecoprop and dichlorprop measured in situ (8) was attributable to acclimated microbial communities (38) enriched by a heterogeneous population of phenoxy acid degraders carrying *tfd* genes. To our knowledge, this is the first study to show that in situ exposure of subsurface aquifers to low herbicide concentrations can markedly change the indigenous microbial community composition, resulting in acclimated microbial communities. This information contributes to our understanding of the complex processes taking place in polluted aquifers and may be used to decide what actions should be taken for the remediation of polluted groundwater environments. Whether the continuous exposure to even smaller herbicide concentrations coming from agricultural use also will result in acclimated microbial communities is still to be investigated.

ACKNOWLEDGMENTS

This work was supported by the Danish Environmental Research Programme, Pesticides and Groundwater, and by the Technical University of Denmark.

We gratefully acknowledge the assistance of Spire Maja Kiersgaard and Rasmus Rune Hansen with the field sampling and of Spire Maja Kiersgaard and Pia Bach Jacobsen with the high-performance liquid chromatography analyses and measurements of DAPI-stained bacteria. We also thank Roger Garrett for access to the MegaBACE 1000 sequencer.

REFERENCES

1. **Albrechtsen, H.-J., M. S. Mills, J. Aamand, and P. L. Bjerg.** 2001. Degradation of herbicides in shallow Danish aquifers: an integrated laboratory and field study. Pest Manag. Sci. **57:**341–350.
2. **Alexander, M. (ed.).** 1999. Acclimation, p. 17–40. *In* Biodegradation and bioremediation. Academic Press, San Diego, Calif.
3. **Amann, R. I., W. Ludwig, and K.-H. Schleifer.** 1995. Phylogenetic identification and in situ detection of individual microbial cells without cultivation. Microbiol. Rev. **59:**143–159.
4. **Balkwill, D. L., F. R. Leach, J. T. Wilson, J. F. McNabb, and D. C. White.** 1988. Equivalence of microbial biomass measures based on membrane lipid and cell wall components, ATP and direct counts in subsurface aquifer sediments. Microb. Ecol. **16:**73–84.
5. **Bjerg, P. L., K. Hinsby, T. H. Christensen, and P. Gravesen.** 1992. Spatial variability of hydraulic conductivity of an unconfined sandy aquifer determined by a mini slug test. J. Hydrol. **136:**107–122.
6. **Braddock, J. F., and K. A. McCarthy.** 1996. Hydrologic and microbiological factors affecting persistence and migration of petroleum hydrocarbons spilled in a continuous-permafrost region. Environ. Sci. Technol. **30:**2626–2633.
7. **Braun-Howland, E. B., P. A. Vescio, and S. A. Nierzwicki-Bauer.** 1993. Use of a simplified cell blot technique and 16S rRNA-directed probes for identification of common environmental isolates. Appl. Environ. Microbiol. **59:**3219–3224.
8. **Broholm, M. M., K. Rügge, N. Tuxen, A. L. Højberg, H. Mosbæk, and P. L. Bjerg.** 2001. Fate of herbicides in a shallow aerobic aquifer: a continuous field injection experiment (Vejen, Denmark). Water Resour. Res. **37:**3163–3176.
9. **Cavalca, L., A. Hartmann, N. Rouard, and G. Soulas.** 1999. Diversity of *tfdC* genes: distribution and polymorphism among 2,4-dichlorophenoxyacetic acid degrading soil bacteria. FEMS Microbiol. Ecol. **29:**45–58.
10. **de Lipthay, J. R., T. Barkay, J. Vekova, and S. J. Sørensen.** 1999. Utilization of phenoxyacetic acid, by strains using either the *ortho* or *meta* cleavage of catechol during phenol degradation, after conjugal transfer of *tfdA*, the gene encoding a 2,4-dichlorophenoxyacetic acid/2-oxoglutarate dioxygenase. Appl. Microbiol. Biotechnol. **51:**207–214.
11. **de Lipthay, J. R., J. Aamand, and T. Barkay.** 2002. Expression of *tfdA* genes in aquatic microbial communities during acclimation to 2,4-dichlorophenoxyacetic acid. FEMS Microbiol. Ecol. **40:**205–214.
12. **DiGiovanni, G. D., J. W. Neilson, I. L. Pepper, and N. A. Sinclair.** 1996. Gene transfer of *Alcaligenes eutrophus* JMP134 plasmid pJP4 to indigenous soil recipients. Appl. Environ. Microbiol. **62:**2521–2526.
13. **Don, R. H., and J. M. Pemberton.** 1981. Properties of six pesticide degradation plasmids isolated from *Alcaligenes paradoxus* and *Alcaligenes eutrophus*. J. Bacteriol. **145:**681–686.
14. **Don, R. H., A. J. Weightman, H.-J. Knackmuss, and K. N. Timmis.** 1985. Transposon mutagenesis and cloning analysis of the pathways for degradation of 2,4-dichlorophenoxyacetic acid and 3-chlorobenzoate in *Alcaligenes eutrophus* JMP134(pJP4). J. Bacteriol. **161:**85–90.
15. **European Environment Agency.** 1999. Groundwater quality and quantity in Europe—environmental assessment report no. 3. European Environment Agency, Copenhagen, Denmark.
16. **Fulthorpe, R. R., C. McGowan, O. V. Maltseva, W. E. Holben, and J. M. Tiedje.** 1995. 2,4-Dichlorophenoxyacetic acid-degrading bacteria contain mosaics of catabolic genes. Appl. Environ. Microbiol. **61:**3274–3281.
17. **Ghiorse, W. C., and J. T. Wilson.** 1988. Microbial ecology of the terrestrial subsurface. Adv. Appl. Microbiol. **33:**107–172.
18. **Gould, W. D., C. Hagedorn, T. R. Bardinelli, and R. M. Zablotowicz.** 1985. New selective media for enumeration and recovery of fluorescent pseudomonads from various habitats. Appl. Environ. Microbiol. **49:**28–32.
19. **Holben, W. E., B. M. Schroeter, V. G. M. Calabrese, R. H. Olsen, J. K. Kukor, V. O. Biederbeck, A. E. Smith, and J. M. Tiedje.** 1992. Gene probe analysis of soil microbial populations selected by amendment with 2,4-dichlorophenoxyacetic acid. Appl. Environ. Microbiol. **58:**3941–3948.
20. **Johnsen, K., and P. Nielsen.** 1999. Diversity of *Pseudomonas* strains isolated with King's B and Gould's S1 agar determined by repetitive extragenic palindromic-polymerase chain reaction, 16S rDNA sequencing and Fourier transform infrared spectroscopy characterisation. FEMS Microbiol. Lett. **173:**155–162.
21. **Johnsen, K., Ø. Enger, C. S. Jacobsen, L. Thirup, and V. Torsvik.** 1999. Quantitative selective PCR of 16S ribosomal DNA correlates well with selective agar plating in describing population dynamics of indigenous *Pseudomonas* spp. in soil hot spots. Appl. Environ. Microbiol. **65:**1786–1788.
22. **Ka, J. O., W. E. Holben, and J. M. Tiedje.** 1994. Use of gene probes to aid

Downloaded from http://aem.asm.org/ on September 3, 2020 at Corteva Agriscience

COR-AAD1-00002503
Bayer EX1008 (Part 5 of 9)

in recovery and identification of functionally dominant 2,4-dichlorophenoxyacetic acid-degrading populations in soil. Appl. Environ. Microbiol. **60:**1116–1120.

23. **Kilpi, S.** 1989. Degradation of some phenoxy acid herbicides by mixed cultures of bacteria isolated from soil treated with 2-(2-methyl-4-chloro)phenoxypropionic acid. Microb. Ecol. **6:**261–270.
24. **Larsen, L., S. R. Sørensen, and J. Aamand.** 2000. Mecoprop, isoproturon, and atrazine in and above a sandy aquifer: vertical distribution of mineralization potential. Environ. Sci. Technol. **34:**2426–2430.
25. **Long, S. C., C. M. Aelion, D. C. Dobbins, and F. K. Pfaender.** 1995. A comparison of microbial community characteristics among petroleum-contaminated and uncontaminated subsurface soils. Microb. Ecol. **30:**297–307.
26. **Lyngkilde, J., and T. H. Christensen.** 1992. Fate of organic contaminants in the redox zones of a landfill leachate pollution plume (Vejen, Denmark). J. Contam. Hydrol. **10:**291–307.
27. **Muyzer, G., E. C. de Waal, and A. G. Uitterlinden.** 1993. Profiling of complex microbial populations by denaturing gradient gel electrophoresis analysis of polymerase chain reaction-amplified genes coding for 16S rRNA. Appl. Environ. Microbiol. **59:**695–700.
28. **Sambrook, J., E. F. Fritsch, and T. Maniatis.** 1989. Molecular cloning: a laboratory manual, 2nd ed. Cold Spring Harbor Laboratory Press, Cold Spring Harbor, N.Y.
29. **Sayler, G. S., S. W. Hooper, A. C. Layton, and J. M. H. King.** 1990. Catabolic plasmids of environmental and ecological significance. Microb. Ecol. **19:**1–20.
30. **Smejkal, C. W., T. Vallaeys, S. K. Burton, and H. M. Lappin-Scott.** 2001. Substrate specificity of chlorophenoxyalkanoic acid-degrading bacteria is not dependent upon phylogenetically related *tfdA* gene types. Biol. Fertil. Soils **33:**507–513.
31. **Sobecky, P. A., T. J. Mincer, M. C. Chang, and D. R. Helinsky.** 1997. Plasmids isolated from marine sediment microbial communities contain replication and incompatibility regions unrelated to those of known plasmid groups. Appl. Environ. Microbiol. **63:**888–895.
32. **Song, H.-G., and R. Bartha.** 1990. Effects of jet fuel spills on the microbial community of soil. Appl. Environ. Microbiol. **56:**646–651.
33. **Streber, W. R., K. N. Timmis, and M. H. Zenk.** 1987. Analysis, cloning, and high-level expression of 2,4-dichlorophenoxyacetate monooxygenase gene *tfdA* of *Alcaligenes eutrophus* JMP134. J. Bacteriol. **169:**2950–2955.
34. **Tett, V. A., A. J. Willetts, and H. M. Lappin-Scott.** 1994. Enantioselective degradation of the herbicide mecoprop [2-(2-methyl-4-chlorophenoxy)propionic acid] by mixed and pure bacterial cultures. FEMS Microbiol. Ecol. **14:**191–200.
35. **Thirup, L., K. Johnsen, and A. Winding.** 2001. Succession of indigenous *Pseudomonas* spp. and actinomycetes on barley roots affected by the antagonistic strain *Pseudomonas fluorescens* DR54 and the fungicide imazalil. Appl. Environ. Microbiol. **67:**1147–1153.
36. **Topp, E., T. Vallaeys, and G. Soulas.** 1997. Pesticides: microbial degradation and effects on microorganisms, p. 547–575. *In* J. D. van Elsas, J. T. Trevors, and E. M. H. Wellington (ed.), Modern soil microbiology. Marcel Dekker, New York, N.Y.
37. **Tuxen, N., P. L. Tuchsen, K. Rügge, H.-J. Albrechtsen, and P. L. Bjerg.** 2000. Fate of seven pesticides in aquifer materials using aerobic column experiments. Chemosphere **41:**1485–1494.
38. **Tuxen, N., J. R. de Lipthay, H.-J. Albrechtsen, J. Aamand, and P. L. Bjerg.** 2002. Effect of exposure history on microbial herbicide degradation in an aerobic aquifer affected by a point source. Environ. Sci. Technol. **36:**2205–2212.
39. **Vallaeys, T., R. R. Fulthorpe, A. M. Wright, and G. Soulas.** 1996. The metabolic pathway of 2,4-dichlorophenoxyacetic acid degradation involves different families of *tfdA* and *tfdB* genes according to PCR-RFLP analysis. FEMS Microbiol. Ecol. **20:**163–172.
40. **Vallaeys, T., L. Albino, G. Soulas, A. D. Wright, and A. J. Weightman.** 1998. Isolation and characterization of a stable 2,4-dichlorophenoxyacetic acid degrading bacterium, *Variovorax paradoxus*, using chemostat culture. Biotechnol. Lett. **20:**1073–1076.
41. **Wilson, J. T., J. F. McNabb, D. L. Balkwill, and W. C. Ghiorse.** 1983. Enumeration and characterization of bacteria indigenous to a shallow water-table aquifer. Ground Water **2:**134–142.
42. **Zipper, C., K. Nickel, W. Angst, and H.-P. Kohler.** 1996. Complete microbial degradation of both enantiomers of the chiral herbicide mecoprop [(*RS*)-2-(4-chloro-2-methylphenoxy)propionic acid] in an enantioselective manner by *Sphingomonas herbicidovorans* sp. nov. Appl. Environ. Microbiol. **62:**4318–4322.
43. **Zipper, C., M. J.-F. Suter, S. B. Haderlein, M. Gruhl, and H.-P. Kohler.** 1998. Changes in the enantiomeric ratio of (*R*)- to (*S*)-mecoprop indicate in situ biodegradation of this chiral herbicide in a polluted aquifer. Environ. Sci. Technol. **32:**2070–2076.

Downloaded from http://aem.asm.org/ on September 3, 2020 at Corteva Agriscience

COR-AAD1-00002504
Bayer EX1008 (Part 5 of 9)

APPLIED AND ENVIRONMENTAL MICROBIOLOGY, Apr. 1997, p. 1326–1331 Vol. 63, No. 4
0099-2240/97/$04.00+0
Copyright © 1997, American Society for Microbiology

Genetic Diversity through the Looking Glass: Effect of Enrichment Bias

JOHN DUNBAR,[1]† SCOTT WHITE,[2] AND LARRY FORNEY[1]*

NSF Center for Microbial Ecology and Department of Microbiology, Michigan State University, East Lansing, Michigan,[1] and Los Alamos National Laboratories, Los Alamos, New Mexico[2]

Received 26 August 1996/Accepted 16 January 1997

The effect of enrichment bias on the diversity of 2,4-dichlorophenoxyacetate (2,4-D)-degrading (2,4-D$^+$) bacteria recovered from soil was evaluated by comparing the diversity of isolates obtained by direct plating to the diversity of isolates obtained from 85 liquid batch cultures. By the two methods, a total of 159 isolates were purified from 1 g of soil and divided into populations based on repeated extragenic palindromic sequence PCR (rep-PCR) genomic fingerprints. Approximately 42% of the direct-plating isolates hybridized with the *tfdA* and *tfdB* genes from *Alcaligenes eutrophus* JMP134(pJP4), 27% hybridized with the *tfdA* and *tfdB* genes from *Burkholderia* sp. strain RASC, and 30% hybridized with none of the probes. In contrast, the enrichment isolates not only represented fewer populations than the isolates obtained by direct plating but also exhibited, almost exclusively, a single hybridization pattern with 2,4-D catabolic gene probes. Approximately 98% of the enrichment isolates possessed pJP4-type *tfdA* and *tfdB* genes, whereas isolates containing RASC-type *tfdA* and *tfdB* genes were obtained from only 2 of the 85 enrichment cultures. The skewed occurrence of the pJP4-type genes among the isolates obtained by enrichment suggests that the competitive fitness of 2,4-D$^+$ populations during growth with 2,4-D may be influenced either by specific *tfd* alleles or by genetic factors linked to these alleles. Moreover, the results indicate that evaluation of the diversity and distribution of catabolic pathways in nature can be highly distorted by the use of enrichment culture techniques.

Our understanding of the genetic diversity underlying specific bacterial phenotypes in nature is shaped by the organisms used for study. The use of cultured instead of uncultured bacteria is a well-known source of potential bias. Culturable bacteria represent only 0.1 to 5% of the bacteria observed in microbial communities (16, 29). Since culturable bacterial strains are the ones used for biochemical and genetic studies, it is possible that only a small portion of the biochemical and genetic diversity underlying particular phenotypes has been documented. Even within the culturable fraction of bacteria, obtaining organisms which are representative of the diversity in nature can be difficult as a result of inherent biases in the methods used for isolation. Batch culture enrichment is the most widely used method for isolation of bacteria expressing specific phenotypes. It has long been recognized that enrichment limits the number and relative growth rates of organisms obtained from the environment (13). These limitations may also affect the diversity of catabolic pathways obtained from the environment.

By design, enrichment in liquid batch culture yields only one or a few strains possessing a specific phenotype. This limitation is potentially overcome by establishing numerous enrichment cultures, but to our knowledge this has not been systematically evaluated. A more serious limitation is the fact that liquid batch culture enrichments typically select for fast-growing organisms (13). A number of researchers have demonstrated that both fast- and slow-growing organisms possessing the same phenotype are found simultaneously in natural communities and can be isolated from the same inoculum source by use of chemostats with different dilution rates (17, 32) or by direct plating (11). However, as a result of the high substrate concentrations ($\gg K_s$) commonly used in batch culture enrichments, slower-growing organisms are typically outcompeted by organisms with a higher maximum specific growth rate, μ_{max}. The genetic factors responsible for differences in growth rates and competitive fitness are poorly understood. Thus, the bias which enrichment might impose on the diversity of a particular catabolic pathway detected in environmental samples is unknown.

To evaluate the potential for bias due to the use of enrichment cultures, we compared the genetic diversity of 2,4-dichlorophenoxyacetate (2,4-D) catabolic pathways among 2,4-D-degrading bacteria obtained by enrichment and by direct plating. All of the isolates originated from just 1 g of soil. Gene probes representing different alleles for the first two genes in the 2,4-D catabolic pathway were used in Southern hybridization analyses to evaluate the diversity among the isolates obtained.

MATERIALS AND METHODS

Media and reagents. Defined aerobic basal (DAB) medium amended with 2,4-D at 250 μg ml^{-1} was used for specific cultivation of 2,4-D-degrading bacteria. DAB medium consists of a mineral salts base supplemented with amino acids and vitamins at low concentrations and has been described previously (11). Reagent grade 2,4-D and [UL-^{14}C]2,4-D were purchased from Sigma Chemical Co., St. Louis, Mo.

Soil. Soil was obtained from an experimental field plot at Kellogg Biological Station (Hickory Corners, Mich.) which had been treated with 2,4-D (100 μg/g of soil) from 1989 to 1992 (19). A 1-kg sample of soil was collected in October 1993 and stored at 4°C until used. For isolation of 2,4-D-degrading bacteria, 1 g of soil was mixed with 9 ml of 10 mM phosphate buffer (pH 7.0) containing 6.1 mM Na_2HPO_4 and 3.9 mM KH_2PO_4 and shaken for 20 min at 250 rpm on a rotary shaker, and aliquots were used for enrichment or direct plating.

Enrichment cultures. Enrichment cultures were established by transferring 0.1 ml of soil slurry to each of 74 test tubes containing 3 ml of DAB medium amended with 250 μg of 2,4-D ml^{-1}. After 1 week of incubation at 30°C on a rotary shaker set at 250 rpm, the disappearance of 2,4-D in each enrichment

* Corresponding author. Mailing address: Department of Microbiology, Michigan State University, East Lansing, MI 48824. Phone: (517) 432-1365. Fax: (517) 432-3770. E-mail: forney@pilot.msu.edu.

† Present address: Life Sciences Division M888, Los Alamos National Labs, Los Alamos, NM 87544.

Downloaded from http://aem.asm.org/ on September 3, 2020 at Corteva Agriscience

COR-AAD1-00002505
Bayer EX1008 (Part 5 of 9)

culture was confirmed spectrophotometrically with a Hewlett-Packard 8452A diode array spectrophotometer. A 0.03-ml aliquot of each culture was then transferred to 3 ml of fresh DAB–2,4-D medium, incubated for 1 week, and monitored spectrophotometrically for 2,4-D disappearance. After three serial transfers, each culture was streaked on one-quarter-strength Trypticase soy agar (TSA). 2,4-D-degrading bacteria on each plate were identified by transferring colonies representing different morphologies into 3 ml of DAB-2,4-D medium and monitoring the disappearance of 2,4-D. Cultures which tested positive were streaked on one-quarter-strength TSA to check for purity. Pure cultures were fingerprinted by rep-PCR (see below), and representatives of different rep-PCR patterns were regrown in DAB–2,4-D medium to establish 15% glycerol stocks, which were stored at −80°C.

Direct plating. To isolate 2,4-D-degrading bacteria by direct plating, the soil slurry was serially diluted and appropriate dilutions were spread directly on HATF nitrocellulose filters (Millipore, Bedford, Mass.) atop R2A agar medium (Difco, Detroit, Mich.). After 1 week of incubation at 30°C, colonies able to degrade 2,4-D were identified by autoradiography based on their ability to incorporate ^{14}C from [U-^{14}C]2,4-D. This procedure has been described previously with $^{35}SO_4^{2-}$ instead of a ^{14}C-labeled carbon source (11). The procedure was modified for [U-^{14}C]2,4-D as follows. Each master filter was replicated once, and each replica filter was incubated on DAB–2,4-D solid medium containing 1.5% agar and 0.1 μCi of [U-^{14}C]2,4-D ml^{-1}. After 3 days of incubation, the replica filters were transferred to 1% agar medium containing 10 mM phosphate buffer and 750 μg of 2,4-D ml^{-1} and incubated for 30 min to remove unincorporated [U-^{14}C]2,4-D. This washing step was repeated once. The replica filters were dried, mounted on paper, covered with a layer of Saran, and exposed to Kodak X-OMAT XAR (Eastman Kodak, Rochester, N.Y.) film overnight at −80°C. The film was developed as recommended by the manufacturer. The autoradiography films were aligned with appropriate master filters, and colonies corresponding to film signals were considered putative 2,4-D^+ colonies. Since the filters used for isolation of 2,4-D^+ bacteria were crowded with bacterial colonies unable to degrade 2,4-D (2,4-D^-), putative 2,4-D^+ colonies were transferred to 3 ml of DAB-2,4-D medium to reduce the relative abundance of 2,4-D^- bacterial contaminants. Cultures were transferred two or three times and purified as described above for enrichment cultures.

MPN estimation. The most probable number (MPN) of 2,4-D-degrading bacteria in the soil was determined by standard methods (6) with five tubes per dilution. For each 10-fold dilution of the soil slurry, 1 ml was transferred to each of five tubes containing 3 ml of DAB–2,4-D medium. The MPN tubes were incubated for 2 weeks at 30°C. The disappearance of 2,4-D in the tubes was determined spectrophotometrically, and MPN estimates of the 2,4-D degrading bacteria were obtained from statistical tables (6). 2,4-D-degrading bacteria were isolated from MPN tubes as described above for enrichment cultures.

rep-PCR. Genomic fingerprints of 2,4-D-degrading isolates were obtained with consensus primers for the repeated extragenic palindromic (REP) sequence (33). PCRs were performed by the method of de Bruijn (8) with colonies of pure cultures grown on one-quarter-strength TSA as the template. Approximately 1 μl of cells was added to each 24 μl of PCR mixture. PCR products were electrophoresed through 1.5% agarose gels containing one-half-strength TAE (26) and 0.25 μg of ethidium bromide ml^{-1} and then photographed. After fingerprints of all isolates were obtained, the reproducibility of the rep-PCR patterns was confirmed by retesting representative isolates regrown in DAB–2,4-D medium.

16S rDNA restriction analysis. 16S rDNA was amplified with primers 8-27 and 1541-1522 (4) under the reaction conditions described by Laguerre et al. (22). PCRs were performed in a Perkin-Elmer 9600 thermal cycler. Cells from broth cultures subjected to four freeze-thaw cycles were used as templates for PCR amplifications. For each 2,4-D^+ strain, 10 μl of amplified 16S rDNA was digested separately with *Cfo*I, *Hoe*III, *Msp*I, *Rsa*I, and *Hin*fI (Gibco). After a 3-h incubation, digested 16S rDNA was electrophoresed through 3% Metaphor agarose gels (FMC Bioproducts, Rockland, Maine) in TAE buffer. Following electrophoresis, the gels were stained with ethidium bromide and photographed.

Phylogenetic analysis. The restriction fragment profiles of all strains were compared and the presence or absence of fragments was recorded, resulting in 96 binary characters for each strain. The data were analyzed with PAUP version 3.1.1 (31). Excluding redundant taxa (i.e., strains with identical 16S restriction fragment length polymorphism data), the data matrix contained 45 phylogenetically informative characters. All characters were treated as Fitch (unordered) characters, and searches were unrooted. A bootstrap analysis with 1,000 replicates was performed by a heuristic search procedure with global branch swapping and 10 randomized taxon additions for each replicate. A 50% majority rule consensus tree (31) was computed from all minimal trees recovered in the bootstrap analysis. All nodes supported by bootstrap values of less than 50 were collapsed into polytomies.

2,4-D gene probe analysis. Genomic DNA was obtained by standard methods (2). Bacterial strains were grown overnight in 5 ml of 1/10-strength Trypticase soy broth (TSB), and 1.5 ml was transferred to an Eppendorf tube for DNA extraction. For each strain, approximately 5 μg of genomic DNA was digested with 10 U of *Eco*RI for 4 h and then electrophoresed in ethidium bromide-stained 0.8% agarose gels. Digested DNA was transferred to Hybond-N nylon membranes (Amersham, Arlington Heights, Ill.) by capillary blotting (28) and cross-linked with a UV Stratalinker 1800 (Stratagene, La Jolla, Calif.) for subsequent hybridization with gene probes.

Gene probes were derived from 2,4-D catabolic genes encoded on plasmid pJP4 from *Alcaligenes eutrophus* JMP134 and from the chromosomally encoded 2,4-D genes in *Burkholderia* sp. strain RASC. Four probes that consisted of internal fragments of *tfdA* and *tfdB* from pJP4 (14) and of *tfdA* (30) and *tfdB* from strain RASC were used. The RASC *tfdB* probe consisted of a 1-kb *Sac*I-*Kpn*I fragment from a 1.2-kb *Sac*I-*Sac*I fragment which had been cloned into pUC9 and was kindly provided by Yuichi Suwa. The RASC *tfdA* and *tfdB* genes have 73 and 65% DNA sequence similarity, respectively, to the corresponding pJP4 alleles (30). Gel-purified probes were labeled with digoxigenin-dUTP by using the DIG DNA labeling and detection kit (Boehringer Mannheim, Indianapolis, Ind.). Prehybridization and hybridization solutions contained 5× SSC (1× SSC is 0.15 M NaCl plus 0.015 M sodium citrate) (26), 0.1% *N*-lauroylsarcosine, 0.02% sodium dodecyl sulfate, 5% blocking reagent, and 50% formamide. Hybridizations were conducted at 62°C to achieve high-stringency conditions (90 to 100% similarity). Following hybridization, membranes were washed twice in 2× SSC and processed for probe detection.

RESULTS

Population diversity of 2,4-D^+ isolates. A total of 159 2,4-D^+ isolates were obtained from 1 g of soil. One 2,4-D^+ strain was obtained from each enrichment culture, yielding a total of 74 isolates; an additional 74 isolates were obtained by direct plating; and one 2,4-D^+ isolate was obtained from each of 11 MPN tubes representing 10^{-3}, 10^{-4}, and 10^{-5} dilutions of soil. These isolates exhibited 30 distinct rep-PCR patterns (Fig. 1). Isolates with identical rep-PCR patterns were considered to be members of a single population. Thus, at least 30 different 2,4-D^+ populations occurred in the original 1 g of soil.

The diversity of isolates obtained by direct plating was greater than the diversity of isolates obtained by enrichment (Fig. 2). Among the 74 isolates obtained by direct plating, 25 distinct populations were detected, while only 7 were identified among the 74 enrichment isolates. Similar results were obtained in previous experiments in which 2,4-D-degrading isolates were obtained from 1 g of soil either by direct plating or by enrichment (Table 1). The estimated population diversity, $E(S)$, for a standardized sample size of 50 isolates was calculated by rarefaction (15, 27) and used to compare the diversity of isolates obtained in different experiments since the actual number of isolates in each experiment varied (Table 1). The average population diversity, $E(S)$, among isolates obtained by direct plating from each of three separate 1-g samples of soil was 19 populations (standard deviation = 1.026). In contrast, the average value of $E(S)$ for isolates obtained from two separate 1-g samples of soil by enrichment was 8.6 populations (standard deviation = 3.182). These results demonstrate that numerous 2,4-D^+ populations can be obtained by establishing multiple enrichment cultures, but the population diversity of isolates from enrichment cultures is still significantly lower than that obtained by direct plating.

Catabolic diversity. Significant differences were also observed in the diversity of 2,4-D catabolic genes obtained by enrichment and by direct plating (Fig. 3). Hybridization of 2,4-D gene probes with genomic DNA from each of the 25 populations obtained by direct plating identified three groups of catabolic genes. Nine populations, representing approximately 42% of the isolates, belonged to catabolic group A_1B_1, since these populations hybridized with the *tfdA* and *tfdB* genes from *A. eutrophus* JMP134(pJP4). Nine populations representing 27% of the isolates belonged to group A_2B_2 based on hybridization with the *tfdA* and *tfdB* genes from *Burkholderia* sp. strain RASC, and seven populations representing 30% of the isolates belonged to group A_XB_X, since these populations hybridized with none of the probes. In contrast, six populations representing 98% of the isolates obtained by enrichment belonged to group A_1B_1. A population exhibiting the A_2B_2 hybridization pattern was obtained from only 1 of 74 enrichment

Downloaded from http://aem.asm.org/ on September 3, 2020 at Corteva Agriscience

COR-AAD1-00002506
Bayer EX1008 (Part 5 of 9)

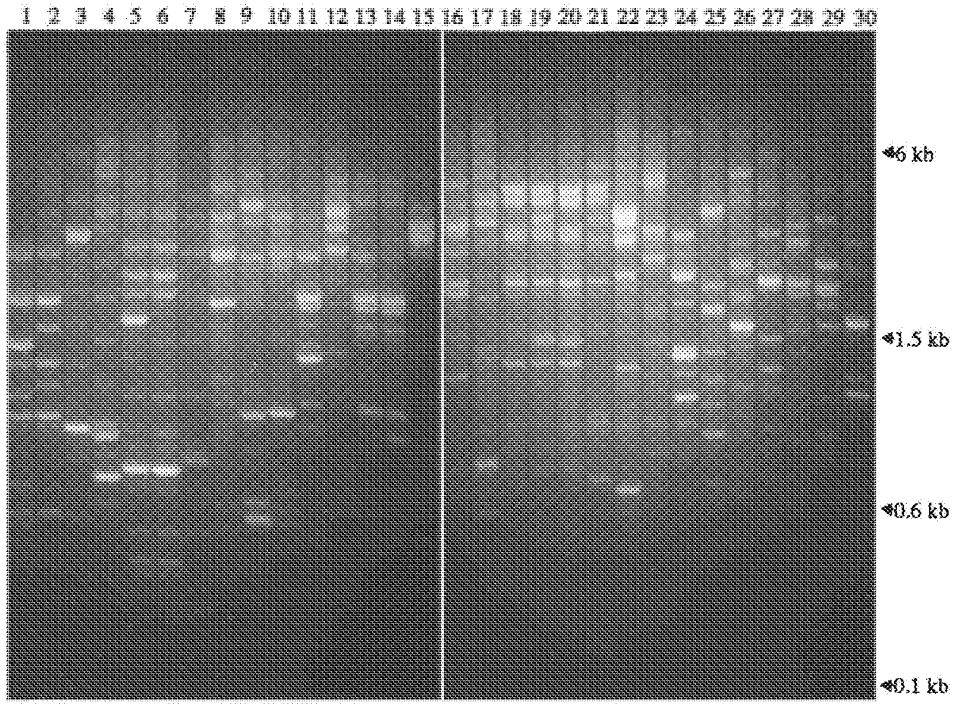


FIG. 1. Unique rep-PCR patterns of 2,4-D$^+$ strains obtained by direct plating and by enrichment. Strains 1 to 16, 18, and 20 to 27 were obtained by direct plating, whereas strains 9, 17 to 19, 21 to 23, and 28 to 30 were obtained by enrichment.

cultures. Similarly, a population representing group A_2B_2 was obtained from only 1 of 11 MPN tubes; the remaining tubes yielded populations exhibiting the A_1B_1 hybridization pattern. These data demonstrate a marked bias in the catabolic genes obtained from soil by use of enrichment.

Phylogenetic analysis. To determine if the skewed enrichment of the A_1B_1 group was due to outgrowth of populations representing a single species, an estimate of the phylogeny of the populations was constructed based on restriction analysis of 16S rDNA amplified from each population. The most parsimonious reconstruction (Fig. 4) had a rescaled consistency index of 0.531 (21). Each operational taxonomic unit (OTU) represents a unique, five-enzyme 16S restriction fragment length polymorphism pattern. While such patterns identify coherent phylogenetic units, the resolution of this approach is not always sufficient to delineate individual species (25). Nonetheless, the diversity of OTUs revealed by this approach provides an estimate of the minimum number of species present. The 25 populations obtained by direct plating represented 16 different OTUs, which were distributed among three catabolic groups (Fig. 4). The frequency distribution of the OTUs obtained from enrichment cultures and MPN tubes was highly skewed. The enrichment and MPN isolates (combined) represented seven OTUs, and one OTU (no. 5) accounted for 72%

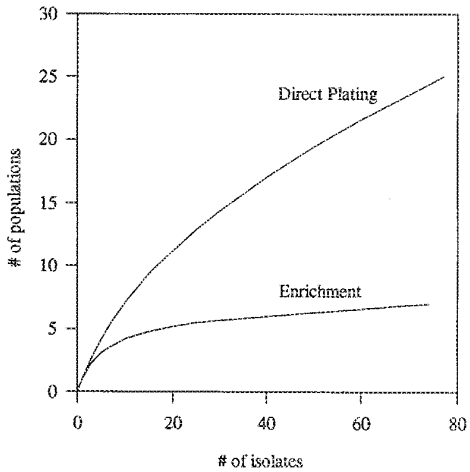


FIG. 2. Cumulative diversity curves for isolates obtained by direct plating and by enrichment. Rarefaction (15, 27) was used to estimate population diversity for numerous samples sizes between 0 and 74. The estimates were then plotted to construct the curves shown.

TABLE 1. Population diversity of 2,4-D$^+$ isolates obtained by enrichment and by direct plating

Expt[a]	Enrichment			Direct plating		
	No. of isolates[b]	$E(S)$[c]	Variance[d]	No. of isolates	$E(S)$	Variance
1				50	18	0.745
2	50	10.8	0.146	50	20	0.000
3	50	6.3	0.440	50	19.4	2.871

[a] For each experiment, 1 g of soil was used.
[b] The actual number of isolates collected in each experiment varied from 51 to 74. To standardize the diversity measure, $E(S)$, between experiments, $E(S)$ was calculated for a standardized sample size of 50 isolates for each experiment.
[c] The standardized population diversity, $E(S)$, was obtained by rarefaction (15, 27).
[d] The variance arises from inherent statistical uncertainty in the estimation of population diversity, $E(S)$, for sample sizes smaller than the actual sample size.

Downloaded from http://aem.asm.org/ on September 3, 2020 at Corteva Agriscience

COR-AAD1-00002507
Bayer EX1008 (Part 5 of 9)

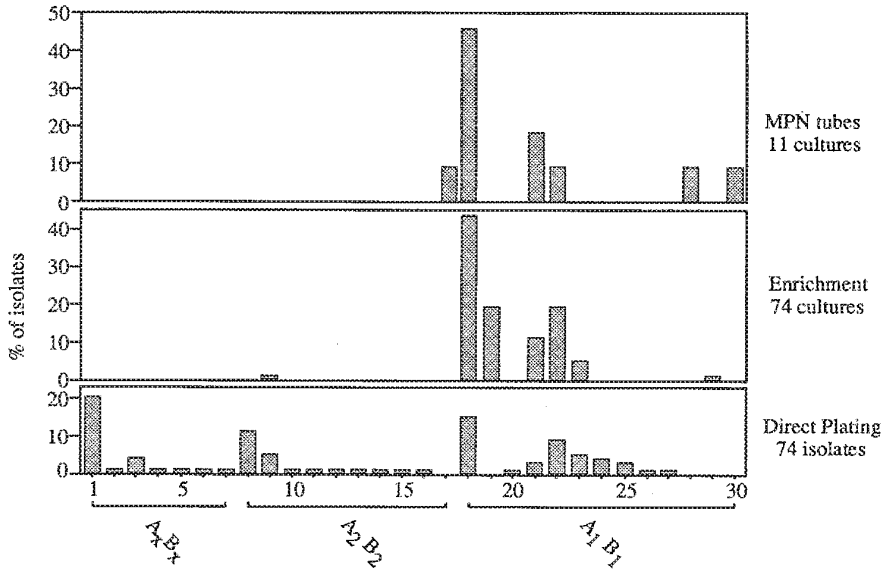


FIG. 3. Frequency distribution of populations obtained by direct plating and by enrichment. The numbers below the *x* axis correspond to lane numbers in Fig. 1. The hybridization pattern of each population with 2,4-D catabolic gene probes is indicated by the brackets below the *x* axis. Genotype A_1B_1 indicates hybridization with *tfdA* and *tfdB* gene probes from *A. eutrophus* JMP134(pJP4), genotype A_2B_2 indicates hybridization with *tfdA* and *tfdB* probes from *Burkholderia* sp. strain RASC, and genotype A_XB_X indicates lack of high-stringency (90 to 100% sequence similarity) hybridization with any of the probes used.

of the isolates. Populations belonging to the A_1B_1 group represented six OTUs (Fig. 4). The enrichment of multiple species possessing predominantly the pJP4-type *tfd* genes suggests that the competitive fitness of these species during competition for 2,4-D may be enhanced by pJP4-type *tfd* alleles or genetic factors linked to these alleles.

DISCUSSION

Bacteria expressing specific phenotypes are most commonly obtained from natural samples by enrichment. Competition among populations during the enrichment process typically results in dominance of one or a few populations with the highest growth rates. This phenotypic bias of enrichment culture techniques is well known. We have demonstrated the genetic consequences of this phenotypic bias among 2,4-D-degrading bacteria. Enrichment of 2,4-D-degrading bacteria from 1 g of soil resulted in the almost exclusive isolation of species possessing *tfdA* and *tfdB* genes that were highly similar, if not identical, to the genes from *A. eutrophus* JMP134(pJP4). In contrast, the species obtained by direct plating represented three different groups of 2,4-D genes in roughly equal abundance. These results suggest that there is an association between specific alleles of 2,4-D catabolic genes and the competitive fitness of the species obtained by enrichment. Furthermore, the data demonstrate that the direct-plating method facilitates the acquisition of strains with previously uncharacterized and genetically distinct catabolic genes.

It is not clear whether the association between specific 2,4-D alleles and competitive fitness in enrichment cultures is coincidental or causal. Preferential selection of specific *tfd* alleles may simply be a coincidental function of host range. It is conceivable that the pJP4-type *tfdA* and *tfdB* alleles are distributed among species which, in general, are better adapted to rapid exploitation of new resources than are species harboring other *tfd* alleles. In previous studies, the pJP4-type alleles have been identified primarily in species of *Alcaligenes* and *Burkholderia* (1, 3, 5, 9, 10, 12). However, the RASC-type alleles also occur primarily in *Burkholderia* species (12, 24, 30). Although the phylogenetic identities of the OTUs obtained in the present study were undetermined, restriction analysis of amplified 16S rDNA identified three cases in which the host range of pJP4-type alleles and RASC-type alleles overlapped (OTUs 10, 15, and 17). In these cases, the pJP4-type alleles and RASC-type alleles appeared in different populations belonging to the same (or very closely related) species (Fig. 4). Thus, host range seems unlikely to account for the differential abundance of pJP4-type and RASC-type alleles following enrichment. The fact that these two sets of alleles occur in the same or very similar organisms would suggest that both sets have a similar chance of being obtained by enrichment if, in fact, competitiveness during enrichment were primarily a result of host-specific factors. However, the overabundance of the pJP4-type alleles among the enrichment isolates in the present study suggests that host-specific factors alone are insufficient to account for differences in competitive fitness.

The predominance of the pJP4-type *tfdA* and *tfdB* alleles among the seven OTUs obtained by enrichment suggests that the competitive fitness of 2,4-D-degrading species may be strongly influenced by one or more of the pJP4-type alleles or by other genetic factors linked to these alleles. Plasmids encoding different sets of *tfd* alleles have been shown to confer different growth rates on *B. cepacia* DBO1 transconjugants (18). The growth rate of a transconjugant harboring pJP4 was twofold greater than the growth rate of a transconjugant harboring a different plasmid, which contained a pJP4-type *tfdA* allele and alleles for *tfdB* and *tfdC* with less than 90% DNA sequence similarity to the pJP4 alleles (18). At maximum growth rates, TfdB, the second enzyme in the pJP4 pathway, may limit the rate of 2,4-D metabolism based on the observed accumulation of 2,4-dichlorophenol in a chemostat culture (7). The fact that 2,4-dichlorophenol is toxic to bacterial cells would tend to magnify the effects of catalytic differences be-

Downloaded from http://aem.asm.org/ on September 3, 2020 at Corteva Agriscience

COR-AAD1-00002508
Bayer EX1008 (Part 5 of 9)

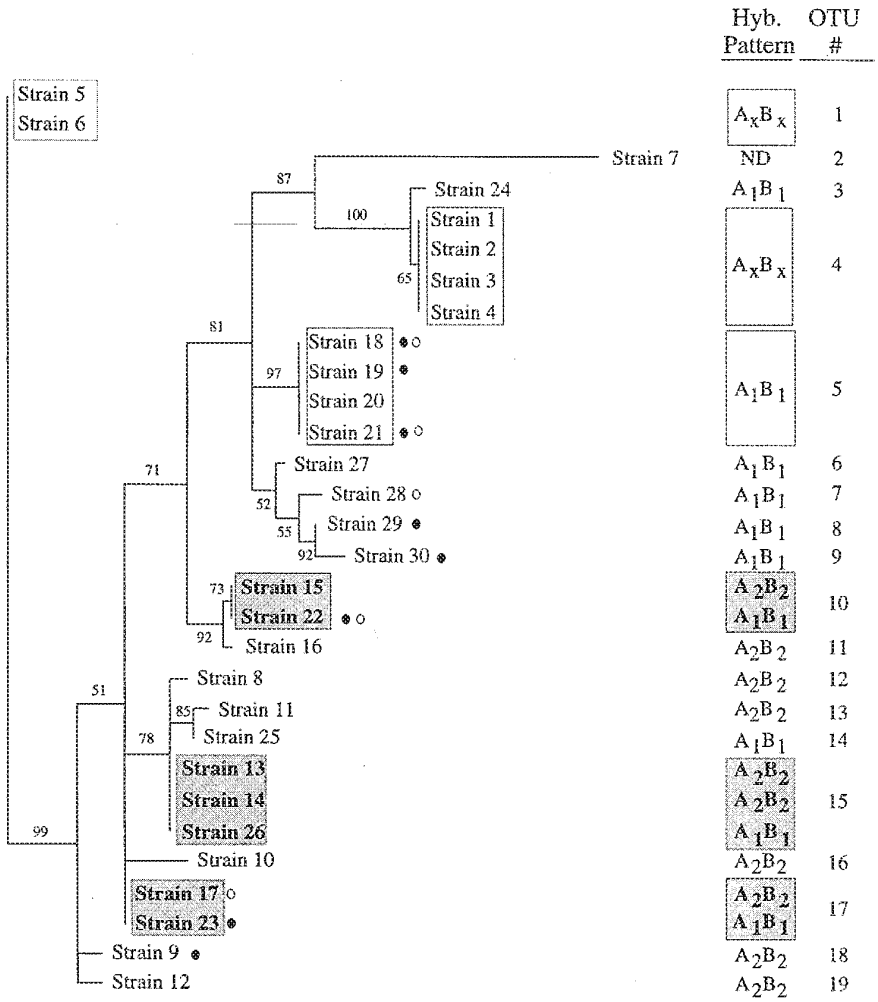


FIG. 4. Phylogenetic reconstruction of 2,4-D$^+$ strains. The number above each node indicates the bootstrap value for that node. Branch lengths are proportional to numbers of derived characters. Solid circles indicate strains obtained from standard enrichments. Open circles indicate strains obtained by enrichment in MPN tubes. All but five strains (strains 17, 19, 28, 29, and 30) were obtained by direct plating; these five strains were isolated only by standard enrichment or enrichment in MPN tubes. Strains enclosed by boxes belong to the same OTU. Boxes that are shaded include strains of the same OTU that have dissimilar 2,4-D catabolic genes.

tween TfdB isozymes. Although the kinetics of TfdB isozymes have not been measured, the deduced amino acid sequences of TfdB (pJP4) and TfdB (RASC) are 80.5% identical (29a). The isozymes encoded by different *tfdB* alleles may thus differ in catalytic efficiency and cause differences in the growth rates of 2,4-D-degrading populations. If the pJP4 *tfdB* allele is in fact optimal for rapid growth, genetic linkage with other pJP4 2,4-D genes could account for the frequent appearance of the genetic pathway encoded on pJP4 following selection for maximum growth rates. Alternatively, other genetically linked factors, such as *tfd* gene copy number per cell or elements involved in the regulation of transcription or translation of *tfd* genes, may affect the fitness of strains with different *tfd* genotypes.

In previous studies on the genetic basis of 2,4-D metabolism, the pJP4 alleles have been the most frequently encountered. The prototypical strain, *A. eutrophus* JMP134 containing the broad-host-range 2,4-D-degradative plasmid pJP4, was obtained in 1980 from an enrichment culture in Australia (10). Genes highly similar, if not identical, to the pJP4 alleles were subsequently identified in isolates obtained from India (3), Estonia (23), Florida (5), and Oregon (1) by standard enrichment techniques. While these studies established the widespread distribution of pJP4-type *tfd* alleles, enrichment bias may have obscured the presence of other 2,4-D catabolic genes in the environment. The existence of different alleles for 2,4-D catabolic genes was established only recently. Hybridization of the pJP4 alleles with DNA from pure cultures and from entire microbial communities known to contain 2,4-D-degrading populations has indicated that numerous other alleles occur in nature for each of the 2,4-D catabolic genes and may be widespread (12, 18, 19, 34). Recently, the RASC *tfdA* and *tfdB* alleles were cloned and sequenced (20, 24, 30). These alleles have 77.2 and 78.5% DNA sequence similarity, respectively, to the pJP4 alleles. Other alleles with even lower similarities have also been identified (12). In the present study, the use of direct plating instead of enrichment demonstrated that at least three groups of 2,4-D catabolic genes occurred in roughly equal abundance in a single 1-g sample of soil. Thus, isolation techniques which separate competing populations improve the as-

Downloaded from http://aem.asm.org/ on September 3, 2020 at Corteva Agriscience

COR-AAD1-00002509
Bayer EX1008 (Part 5 of 9)

sessment of the diversity and redundancy of catabolic genes and hosts in the environment.

It is conceivable that some strains are detected by enrichment and not by direct plating. Only the strains able to form colonies on a specific medium will be detected by direct plating. Furthermore, only the most abundant organisms expressing a specific phenotype within a community will be detected. By using enrichment culture techniques, strains may be obtained which are rare relative to other organisms expressing the same phenotype, provided that they are highly competitive in liquid batch cultures under the selective conditions used. In this study, strains 17, 19, 28, 29, and 30 were obtained only from enrichments (Fig. 3). However, three of these strains were obtained from MPN tubes representing 10^{-4} dilutions of the original sample. Based on MPN and autoradiographic plate counts, there were 10^4 to 10^5 2,4-D^+ organisms per g of soil (data not shown). The rarefaction curves (Fig. 2) suggest that additional isolates obtained by direct plating would reveal additional diversity. Thus, it is likely that the strains obtained from MPN enrichments would have been detected by direct plating if a larger collection of isolates had been examined.

Although populations with different 2,4-D catabolic alleles have occasionally been obtained by enrichment, this method severely distorts the apparent diversity of 2,4-D-degrading populations in individual samples from the environment. The limited number of populations obtained in a single enrichment culture can be partially overcome by establishing multiple enrichment cultures. However, although a larger number of populations may be obtained, the population diversity is still substantially lower than that obtained by other methods such as direct plating. Furthermore, specific alleles of catabolic genes may be exclusively obtained as a result of the enrichment bias for organisms with relatively high growth rates. Future use of alternative methods to obtain isolates exhibiting a specific phenotype may identify novel biochemical pathways or, at least, a broader array of isozymes. With a better understanding of the diversity and distribution of particular catabolic pathways, new insights into the evolution of catabolic pathways may be obtained.

ACKNOWLEDGMENT

This research was funded by a grant from the National Science Foundation (BIR 9120006).

REFERENCES

1. **Amy, P. S., J. W. Schulke, L. M. Frazier, and R. J. Seidler.** 1985. Characterization of aquatic bacteria and cloning of genes specifying partial degradation of 2,4-dichlorophenoxyacetic acid. Appl. Environ. Microbiol. **49:** 1237–1245.
2. **Ausubel, F. M., R. Brent, R. E. Kingston, D. D. Moore, J. A. Smith, J. G. Seidman, and K. Struhl.** 1987. Current protocols in molecular biology. John Wiley & Sons, Inc., New York, N.Y.
3. **Bhat, M. A., M. Tsuda, K. Horiike, M. Nozaki, C. S. Vaidyanathan, and T. Nakazawa.** 1994. Identification and characterization of a new plasmid carrying genes for degradation of 2,4-dichlorophenoxyacetate from *Pseudomonas cepacia* CSV90. Appl. Environ. Microbiol. **60:**307–312.
4. **Bruce, K. D., W. D. Hiorns, J. L. Hobman, A. M. Osboru, P. Strike, and D. A. Ritchie.** 1992. Amplification of DNA from native populations of soil bacteria by using the polymerase chain reaction. Appl. Environ. Microbiol. **58:**3413–3416.
5. **Chaudry, G. R., and G. H. Huang.** 1988. Isolation and characterization of a new plasmid from a *Flavobacterium* sp. which carries the genes for degradation of 2,4-dichlorophenoxyacetate. J. Bacteriol. **170:**3897–3902.
6. **Cochran, W. G.** 1950. Estimation of bacterial densities by means of the "most probable number." Biometrics **6:**105–116.
7. **Daugherty, D. D., and S. Karel.** 1994. Degradation of 2,4-dichlorophenoxyacetic acid by *Pseudomonas cepacia* DBO1(pRO101) in a dual-substrate chemostat. Appl. Environ. Microbiol. **60:**3261–3267.
8. **de Bruijn, F. J.** 1992. Use of repetitive (repetitive extragenic palindromic and enterobacterial repetitive intergenic consensus) sequences and the polymerase chain reaction to fingerprint the genomes of *Rhizobium meliloti* isolates and other soil bacteria. Appl. Environ. Microbiol. **58:**2180–2187.
9. **Ditzelmuller, G., M. Loidl, and F. Streichsbier.** 1989. Isolation and characterization of a 2,4-dichlorophenoxyacetic acid-degrading soil bacterium. Appl. Microbiol. Biotechnol. **31:**93–96.
10. **Don, R. H., and J. M. Pemberton.** 1981. Properties of six pesticide degradation plasmids from *Alcaligenes paradoxus* and *Alcaligenes eutrophus*. J. Bacteriol. **145:**681–686.
11. **Dunbar, J., D. C. L. Wong, M. J. Yarus, and L. J. Forney.** 1996. Autoradiography method for isolation of diverse bacterial species with unique catabolic traits. Appl. Environ. Microbiol. **62:**4180–4185.
12. **Fulthorpe, R. R., C. McGowan, O. V. Maltseva, W. H. Holben, and J. M. Tiedje.** 1995. 2,4-Dichlorophenoxyacetic acid-degrading bacteria are mosaics of catabolic genes. Appl. Environ. Microbiol. **61:**3274–3281.
13. **Harder, W., and L. Dijkhuizen.** 1982. Strategies of mixed substrate utilization in microorganisms. Philos. Trans. R. Soc. London Ser. B **297:**459–480.
14. **Holben, W. E., B. M. Schroeter, V. G. M. Calabrese, R. H. Olsen, J. K. Kukor, V. O. Biederbeck, A. E. Smith, and J. M. Tiedje.** 1992. Gene probe analysis of soil microbial populations selected by amendment with 2,4-dichlorophenoxyacetic acid (2,4-D)-degrading bacteria isolated from 2,4-D-treated field soils. Appl. Environ. Microbiol. **58:**3941–3948.
15. **Hurlbert, S. H.** 1971. The non-concept of species diversity: a critique and alternative parameters. Ecology **52:**577–586.
16. **Jannasch, H. W., and G. E. Jones.** 1959. Bacterial populations in seawater as determined by different methods of enumeration. Limnol. Oceanogr. **4:**128–139.
17. **Jannasch, H. W.** 1967. Enrichments of aquatic bacteria in continuous culture. Arch. Mikrobiol. **59:**165–173.
18. **Ka, J. O., W. E. Holben, and J. M. Tiedje.** 1994. Analysis of competition in soil among 2,4-dichlorophenoxyacetic acid-degrading bacteria. Appl. Environ. Microbiol. **60:**1121–1128.
19. **Ka, J. O., W. E. Holben, and J. M. Tiedje.** 1994. Genetic and phenotypic diversity of 2,4-dichlorophenoxyacetic acid (2,4-D)-degrading bacteria isolated from 2,4-D-treated field soils. Appl. Environ. Microbiol. **60:**1106–1115.
20. **Kamagata, Y., Y. Suwa, A. Wright, J. Tiedje, and L. Forney.** 1996. Unpublished data.
21. **Kluge, A. G., and J. S. Farris.** 1969. Quantitative phyletics and the evolution of anurans. Syst. Zool. **18:**1–32.
22. **Laguerre, G., M. Allard, F. Revoy, and N. Amarger.** 1994. Rapid identification of rhizobia by restriction fragment length polymorphism analysis of PCR-amplified 16S rRNA genes. Appl. Environ. Microbiol. **60:**56–63.
23. **Mae, A. A., R. O. Marits, N. R. Ausmees, V. M. Koiv, and A. L. Heinaru.** 1993. Characterization of a new 2,4-dichlorophenoxyacetic acid degrading plasmid pEST4011: physical map and localization of catabolic genes. J. Gen. Microbiol. **139:**3165–3170.
24. **Matheson, V. G., L. J. Forney, Y. Suwa, C. H. Nakatsu, A. J. Sexstone, and W. E. Holben.** 1996. Evidence for acquisition in nature of a chromosomal 2,4-dichlorophenoxyacetic acid/α-ketoglutarate dioxygenase gene by different *Burkholderia* spp. Appl. Environ. Microbiol. **62:**2457–2463.
25. **Moyer, C. L., J. M. Tiedje, F. C. Dobbs, and D. M. Karl.** 1996. A computer-simulated restriction fragment length polymorphism analysis of bacterial small-subunit rRNA genes: efficacy of selected tetrameric restriction enzymes for studies of microbial diversity in nature. Appl. Environ. Microbiol. **62:**2501–2507.
26. **Sambrook, J., E. F. Fritsch, and T. Maniatis.** 1989. Molecular cloning: a laboratory manual, 2nd ed. Cold Spring Harbor Laboratory Press, Cold Spring Harbor, N.Y.
27. **Simberloff, D.** 1978. Use of rarefaction and related methods in ecology, p. 150–165. *In* K. L. Dickson, J. Cairns, Jr., and R. J. Livingston (ed.), Biological data in water pollution assessment: quantitative and statistical analyses. American Society for Testing and Materials, Washington, D.C.
28. **Southern, E. M.** 1975. Detection of specific sequences among DNA fragments separated by gel electrophoresis. J. Mol. Biol. **98:**503–517.
29. **Staley, J. T., and A. Konopka.** 1985. Measurement of *in situ* activities of nonphotosynthetic microorganisms in aquatic and terrestrial habitats. Annu. Rev. Microbiol. **39:**321–346.

29a. **Suwa, Y.** Personal communication.

30. **Suwa, Y., A. D. Wright, F. Fukimori, K. A. Nummy, R. P. Hausinger, W. E. Holben, and L. J. Forney.** 1996. Characterization of a chromosomally encoded 2,4-dichlorophenoxyacetic acid (2,4-D)/α-ketoglutarate dioxygenase from *Burkholderia* sp. strain RASC. Appl. Environ. Microbiol. **62:**2464–2469.
31. **Swofford, D. L.** 1993. PAUP: phylogenetic analysis using parsimony, 3.1.1 ed. Smithsonian Institution, Washington, D.C.
32. **Veldkamp, H., and J. G. Kuenen.** 1973. The chemostat as a model system for ecological studies. Bull. Ecol. Res. Comm. NFR **17:**347–355.
33. **Versalovic, J., T. Koeuth, and J. R. Lupski.** 1991. Distribution of repetitive DNA sequences in eubacteria and application to fingerprinting of bacterial genomes. Nucleic Acids Res. **19:**6823–6831.
34. **Xia, X., J. Bollinger, and A. Ogram.** 1995. Molecular genetic analysis of the response of three soil microbial communities to the application of 2,4-D. Microb. Ecol. **4:**17–28.

Downloaded from http://aem.asm.org/ on September 3, 2020 at Corteva Agriscience

COR-AAD1-00002510
Bayer EX1008 (Part 5 of 9)

Biodegradation and Plant Protection from the Herbicide 2,4-D by Plant–Microbial Associations in Cotton Production Systems

L. Feng, and I. R. Kennedy

Cooperative Research Centre for Sustainable Cotton Production, Deparatment of Agricultural Chemistry and Soil Science, University of Sydney, NSW 2006, Australia; telephone: 61293513546; fax: 61293515108; e-mail: kennedy@spiro.biz.usyd.edu.au

Received 13 March 1996; accepted 18 October 1996

Abstract: A significant "biosafening" protection of plants from the effect of 2,4-D in plant–microbial associations has been demonstrated in this study. The 2,4-D-degrading plasmid, pJP4 was transferred into *Rhizobium* sp. CB1024, which nodulates *Dolichos lablab,* and *Azospirillum brasilense* Sp7 carrying a *nifA–lacZ* gene marker, which can colonize cotton roots. Both transconjugants degraded 2,4-D in pure culture via cometabolism up to 50 μg mL^{-1}. When the transconjugants were inoculated onto *Dolichos lablab* and cotton, respectively, such plants were resistant to this herbicide when the nutrient solution was treated with 2,4-D up to 10 μg mL^{-1} for *Dolichos lablab* and 0.5 μg mL^{-1} for cotton. Plants inoculated with wild-type strains were dead (*Dolichos lablab*) or dying (cotton). Because cotton is more sensitive to herbicides, only incomplete protection of plants was achieved with the transconjugant. Improving the effect of colonization of *Azospirillum* on cotton roots may be critical for a complete degradation and plant protection. The transconjugant of *Rhizobium* sp. CB1024 was still able to nodulate *Dolichos lablab,* and N_2-fixing activity was only slightly affected. Other pesticide-degrading capacities may also be inserted into those plant-associated bacterial strains for the degradation of these chemicals by plant–microbial associations. Whether such systems will be successful when applied in the field with competition from other bacteria is being examined. © 1997 John Wiley & Sons, Inc. *Biotechnol Bioeng* **53**: 513–519, 1997.
Keywords: plant–microbial associations; 2,4-D; biodegradation; plant protection; *Dolichos lablab*; cotton

INTRODUCTION

The persistence of pesticide residues is often considered to be an acute environmental problem. Apart from causing contamination of soil, water, and agricultural produce, there is also concern regarding the residual toxicity of herbicides to nontarget crops. Many herbicides exert their effects by inactivating "target proteins" essential for vital functions such as photosynthetic or other biosynthetic pathways unique to plants. Because crops usually share these processes with competing weeds, many herbicides are nonselective. Others can only be used selectively on tolerant crops, mainly as a consequence of a differential uptake of the chemicals. For example, studies on atrazine persistence and toxicity in Australian soils showed that sensitive crops such as the sunflower may be damaged when grown in rotation after tolerant crops, or if irrigated with contaminated water (Bowmer, 1981). Herbicide-induced declines in plant growth and N_2 fixation in legume plants were also reported (Clark and Mahanty, 1991; Eberbach and Douglas, 1989). Considerable damage to cotton could be caused by 2,4-D residue from previous application or from spray drift (Llewllyn et al., 1990).

Although application of microorganisms offers great potential for degradation of particular pesticides, the results from soil inoculation have been inconsistent, with success as enhanced biodegradation observed only spasmodically (Greer and Shelton, 1992). Most successful studies have been conducted in the laboratory under optimal conditions required for the growth or metabolism of degrading bacteria. Some conditions are unable to be replicated outside the lab. Soil acts as a strong biological buffer, often resisting attempts to increase populations of desired strains because of the presence of other microbes with superior competitive ability for available substrates.

However, enhanced populations in soil ecosystems of selected microorganisms may be more reliably achieved in plant–microbial associations. The best known example is *Rhizobium*–legume symbiosis. Other bacteria such as *Azospirillum* are also known to associate with many crops including nonlegumes. With the chemically induced nodular structure (*para*-nodules) of wheat, both colonization and N_2 fixation of azospirilla have been increased (Katupitiya et al., 1995; Kennedy and Tchan, 1992; Sriskandarajah et al., 1993). This suggests that induced associations between nonlegumes and microbes are also possible for an increased growth rate

Correspondence to: I. R. Kennedy
Contract grant sponsor: The Australian Cooperative Research Centre for Sustainable Cotton Production

© 1997 John Wiley & Sons, Inc. CCC 0006-3592/97/060513-07

COR-AAD1-00002511
Bayer EX1008 (Part 5 of 9)

for both microbes and plants. If pesticide-degrading abilities can be introduced into those microorganisms, enhanced biodegradation may also be possible in associations with plants.

Possible bioremediation by plant–microbial associations has been suggested and demonstrated previously (van Zwieten et al., 1995). van Zwieten et al. found that wheat and canola were colonized by the 2,4-D-degrading bacteria *Alcaligenes* or *Acinetobacter,* and those plants were less susceptible to damage by the herbicide after being treated with 2,4-D. In our previous study (Feng, 1994), the 2,4-D-degrading plasmid, pJP4, was transferred into *Rhizobium trifolii.* By inoculating the transconjugant onto white or subterranean clovers, plants were more resistant to 2,4-D and a significant "biosafening" protection was observed.

Cotton, a large export crop in Australia, is sensitive to many herbicides. There is a need to develop strategies to prevent herbicidal effects on the crop for sustained cotton production. In this study, using 2,4-D degradation as a model, we have investigated the possibility of plant protection in an *Azospirillum*–cotton association. A *Rhizobium–Dolichos lablab* symbiosis was also used because *Dolichos lablab* has potential for "clean-up" of pesticide residues from cotton fields as a rotation crop.

MATERIALS AND METHODS

Plasmid, Bacterial Strains, and Plant Species

The plasmid, bacterial strains, and plant species used in this study are listed in Table I.

Media and Growth Conditions for Bacteria

Azospirillum brasilense strains were grown in nutrient broth (Difco) as complete medium and NFB supplemented with 0.05% yeast extract as selective medium as shown by Sriskandarajah et al. (1993). *Rhizobium* strains were grown in YMA containing (per liter) 1.0 g of yeast extract, 0.2 g of $MgSO_4 \cdot 7H_2O$, 0.5 g of K_2HPO_4, and 10.0 g of mannitol as complete medium, and TMR (Innes, 1988) as selective medium. Tetracycline (Tc) and $HgCl_2$ at 5 $\mu g\ mL^{-1}$, each were added as required. The 2,4-D concentration used for the degradation test in pure culture was 50 $\mu g\ mL^{-1}$. All strains were incubated at 28°C with shaking.

Conjugation

Conjugation was performed as described previously (Feng et al., 1994), except that NB + $HgCl_2$ + Tc was used as the selective medium for *Azospirillum* containing the pJP4 plasmid.

Assay for 2,4-D Degradation

2,4-D degradation by the transconjugants in pure cultures was detected by either UV absorbance or gas chromatography as described previously (Feng et al., 1994), except growth media differed for each strain.

Seeds Sterilization and Germination

Dolichos lablab and cotton seeds were rinsed with pure ethanol, sterilized with 6% NaOCl (v/v) for 15 min, and rinsed with sterile deionized water at least eight times.

Table I. Plasmid, bacterial strains, and plant species.

Plasmid, bacterial strains or plant species	Relevant characteristics[a]	Reference or source
Plasmid		
pJP4	80 kb, IncP1, Hg^r, tfd^+ conjugative, broad-host	Don and Pemberton (1981)
Bacterial strains		
Alcaligenes eutrophus JMP134	Nature host of pJP4 Hg^r, tfd^+	Don and Pemberton (1981)
Azospirillum brasilense Sp7–S*nifA*	Sp7-S containing pAB576, Tc^r, *nifA–lacZ* transcriptional fusion	Katupitiya et al. (1995)
Azospirillum brasilense Sp7–S*nifA*pJP4	Transconjugant of Sp7-S*nifA* containing pJP4, Hg^r, tfd^+	This study
Rhizobium sp. CB1024	Wild-type, Nod^+ and Nif^+ on *Dolichos lablab*	Roughley[b]
Rhizobium sp. CB1024pJP4	Transconjugant containing pJP4, Nod^+ and Nif^+ on *Dolichos lablab* Hg^r, tfd^+	This study
Plant species		
Dolichos lablab		
Cotton (Sicala V-2)		Constable[c]

[a]Hg^r: resistance to $HgCl_2$; tfd^+: genes for degradation of 2,4-D; Nod^+: nodulation genes; Nif^+: N_2-fixing genes.
[b]NSW Horticultural Research and Advisory Station, Gosford, Australia.
[c]Australian Cotton Institute, Narrabri.

COR-AAD1-00002512
Bayer EX1008 (Part 5 of 9)

Cotton seeds were soaked for 1 to 2 days in sterile deionized water at room temperature, rinsed once more, and germinated on YMA plates at 28°C overnight. *Dolichos lablab* seeds were sowed into pots directly.

Growth, Inoculation, and 2,4-D Treatment for *Dolichos* lablab

Nitrogen-free Jensen's medium (Jensen, 1942) and Leonard jars (2-L Nalgene jar) with inserted pots were used to grow *Dolichos lablab.* Growth medium (Jensen's) was added to each Leonard jar (1.5 L). A 34 × 2.5 cm wick was inserted into each pot through one of the drain holes to within 2.5 cm of the potting mix surface with the other end of the wick reaching the bottom of jar. Any remaining holes were filled with paper tissue and the pots were filled with potting mix, a mixture of sand : perlite : vermiculite (2 : 2 : 1). Each pot was placed into the neck of the Leonard jars and the whole system (pot and jar) was autoclaved. Three seeds were planted in each pot and plants were grown in a glass-house at a temperature range of 22° to 26°C for 1 week. *Rhizobium* strains CB1024 and CB1024pJP4 were subcultured in YMA for 5 days. Culture (2 mL) was inoculated into each plant in the pot, plants were grown for another 2 to 3 weeks, and 2,4-D (5 or 10 $\mu g\ mL^{-1}$) was added to the growth medium. Plants were then assayed after 4 weeks.

Growth, Inoculation, and 2,4-D Treatment for Cotton

Cotton plants were grown hydroponically in modified Hoagland's nutrient solution (Epstein, 1972) in a growth chamber with continuous lighting and a 12-h cycle at 22° and 28°C. Individual plants were grown in a test-tube system as previously described (Zeman et al., 1992) for 6 days and then transferred into 100-mL bottles inoculated with 1 mL of overnight culture of *Azospirillum* in NFB + yeast, and 2,4-D (0.2 or 0.5 $\mu g\ mL^{-1}$) was added. Plants were assayed after 2 weeks.

Plant Assay

The growth of plants was assayed by size and dry weight. Nodulation and N_2-fixation activity (nitrogenase activity) were also performed for *Dolichos lablab.* The nitrogenase activity was assayed by the acetylene reduction test as described previously (Feng et al., 1994), except that 100-mL McCartney bottles were used. Reisolation of bacteria from nodules was as described by Rolfe et al. (1980).

Colonization of Cotton Roots

Colonization of cotton roots by bacteria was monitored by in situ staining of roots for β-galactosidase activity with X-gal (5-bromo-4-chloro-3-indolyl-β-galactopyranoside), as described by Arsène et al (1994), using a *nifA–lacZ* gene marker transconjugated with plasmid to the bacterial strain used in tests.

RESULTS

The 2,4-D-degrading plasmid, pJP4, was successfully transferred from its natural host *Alcaligenes eutrophus* JMP134 into *Rhizobium* sp. CB1024 and *Azospirillum brasilense* Sp7–*SnifA,* as shown by the transconjugants' acquired resistance to $HgCl_2$ up to 5 $\mu g\ mL^{-1}$. Both transconjugants degraded 2,4-D (50 $\mu g\ mL^{-1}$) in the presence of a second carbon source or with resting cells (data not shown). None of the transconjugants could grow on 2,4-D as a sole carbon and energy source indicating that both transconjugants degraded 2,4-D via cometabolism.

When the transconjugant *Rhizobium* CB1024pJP4 was inoculated onto *Dolichos lablab,* plants survived up to 4 weeks after treatment with 2,4-D at both 5 and 10 $\mu g\ mL^{-1}$ in the growth solution. By comparison, those inoculated with wild-type CB1024 lacking pJP4 died (Fig. 1). This result indicates that plants could be protected from toxicity of 2,4-D by the transconjugant. The dry weight for plants inoculated with the transconjugant was 20% higher at the 2,4-D level of 5 $\mu g\ mL^{-1}$ and slightly higher at the 2,4-D level of 10 $\mu g\ mL^{-1}$ than those inoculated with the wild-type (Table II). This indicates that plants were better protected at the lower 2,4-D level. In transconjugant nodulated plants, nodule size was smaller and the number was greater than those inoculated with the wild-type strain. However, the nitrogen fixing activity was slightly decreased (data not shown).

Transconjugants *Rhizobium* CB1024pJP4 were reisolated from the plant growth medium, root surface, and nodules on selective medium YMA + $HgCl_2$ agar plates. The results showed that the numbers of CB1024pJP4 were about 10^6 cells per milliliter of plant growth medium (200 to 500 mL), 10^6 cells per centimeter of root (about 300 to 600 cm of total length for three plants in each pot), and 10^7 cells per nodule (about 30 to 60 nodules for three plants in each pot) at 6 weeks. These data suggest that most 2,4-D degrading activity took place within the plants. The stability of the transconjugant CB1024pJP4 in nodules was also determined and results showed that 90% of viable bacteria reisolated from the nodules still contained the plasmid pJP4, as indicated by resistance to $HgCl_2$ after 6 weeks.

Both wild-type and transconjugant strains of *Azospirillum* were able to colonize cotton roots, as indicated by X-gal staining in which *Azospirillum* cells were stained a blue color (Fig. 2a, b). There was better colonization for cotton plants treated with 2,4-D, and the same result was observed in wheat (Katupitiya et al., 1995). Bacterial cells were found inside plant cells and on the root

COR-AAD1-00002513
Bayer EX1008 (Part 5 of 9)

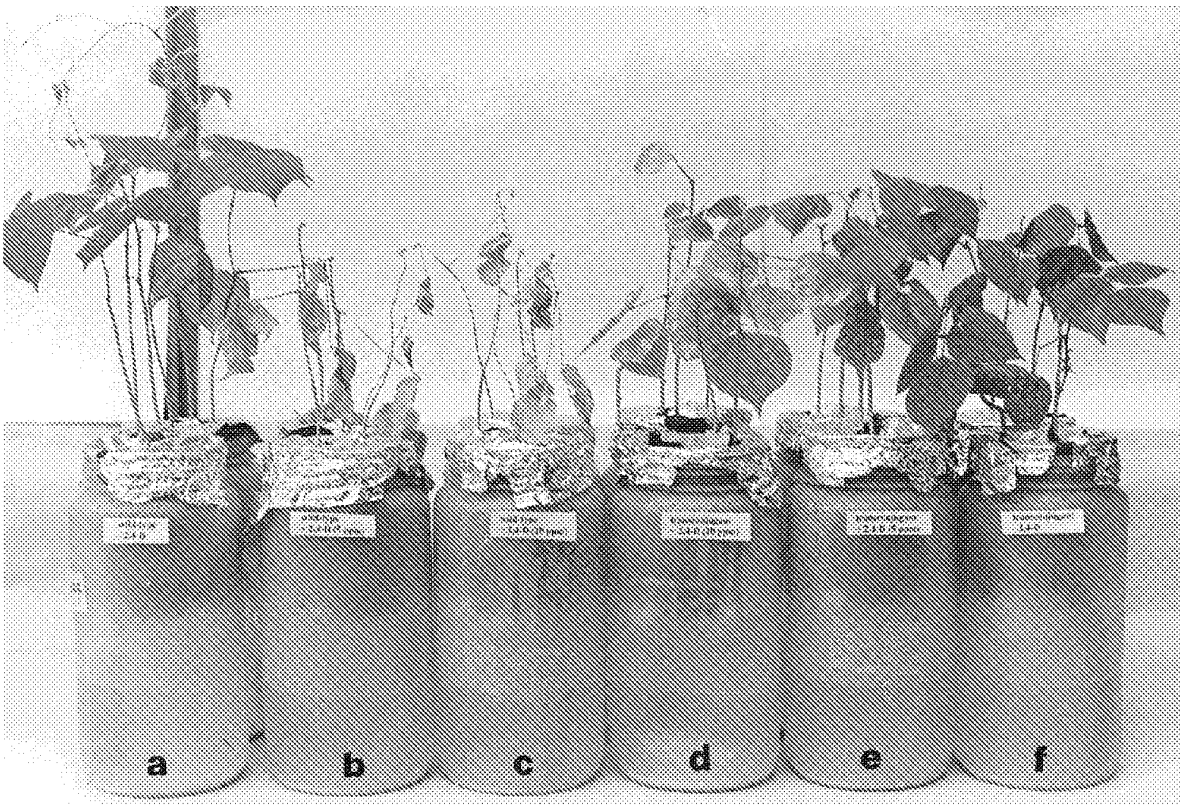


Figure 1. *Dolichos lablab* (7-week-old) inoculated with the wild-type or transconjugant strain of *Rhizobium* sp. CB1024 4 weeks after treatment with or without 2,4-D. (a) Wild-type without 2,4-D; (b) wild-type with 5 μg mL^{-1} 2,4-D; (c) wild-type with 10 μg mL^{-1} 2,4-D; (d) transconjugant with 10 μg mL^{-1} 2, 4-D; (e) transconjugant with 5 μg mL^{-1} 2, 4-D; and (f) transconjugant without 2,4-D.

surface, as well as at the base of the nodule-like structure, which developed from lateral roots of 2,4-D-treated plants.

When treated with 2,4-D (0.2 or 0.5 μg mL^{-1}), cotton plants inoculated with the transconjugant showed much better growth than those with the wild-type strain, which were dying (Fig. 3). Plants inoculated with the transconjugant had about a 2.5-fold increase in dry weight at a 2,4-D level of 0.2 μg mL^{-1} and a more than twofold increase at the 2,4-D level of 0.5 μg mL^{-1}, in comparison to those inoculated with the wild-type (Table III).

Table II. Dry weight of *Dolichos lablab* treated with 2,4-D.

Strains	2,4-D (μg mL^{-1})	Dry weight per plant (g)[a]	SD
No bacteria	0	0.382	0.102
No bacteria	5	0.384	0.024
R. CB1024	0	0.500	0.142
R. CB1024	5	0.320	0.042
R. CB1024	10	0.354	0.041
R. CB1024pJP4	0	0.465	0.119
R. CB1024pJP4	5	0.407	0.044
R. CB1024pJP4	10	0.368	0.021

[a]The mean of 4 to 6 plants

Compared with untreated plants, the growth of plants treated with 2,4-D was decreased. At the 2,4-D level of 0.2 μg mL^{-1}, there was an approximately 36% decrease of dry weight for transconjugant inoculated plants, and an almost 60% decrease for wild-type inoculated ones. At the 2,4-D level of 0.5 μg mL^{-1}, there was a 50% decrease for transconjugant inoculated plants, and an almost 80% decrease for wild-type inoculated ones. Severe damage to plant roots inoculated with the wild-type strain was indicated by shorter roots and a failure to develop new lateral roots. Less damage was shown in plants inoculated with the transconjugant, for the which main roots and lateral roots continued growing, but not as well as untreated ones. This result suggests that protection of plants from the effects of 2,4-D by the transconjugant was incomplete at either the 2,4-D level of 0.2 or 0.5 μg mL^{-1}.

When cotton plants inoculated with the transconjugant were transferred into fresh medium supplemented with 0.5 μg mL^{-1} 2,4-D after 1-week growth, protection of plants could still be observed. Plants inoculated with the transconjugant survived for 2 weeks after transfer, compared with those inoculated with wild-type, which were then dying. This indicates the effectiveness of colonization of cotton roots with the transconjugant, rather

COR-AAD1-00002514
Bayer EX1008 (Part 5 of 9)

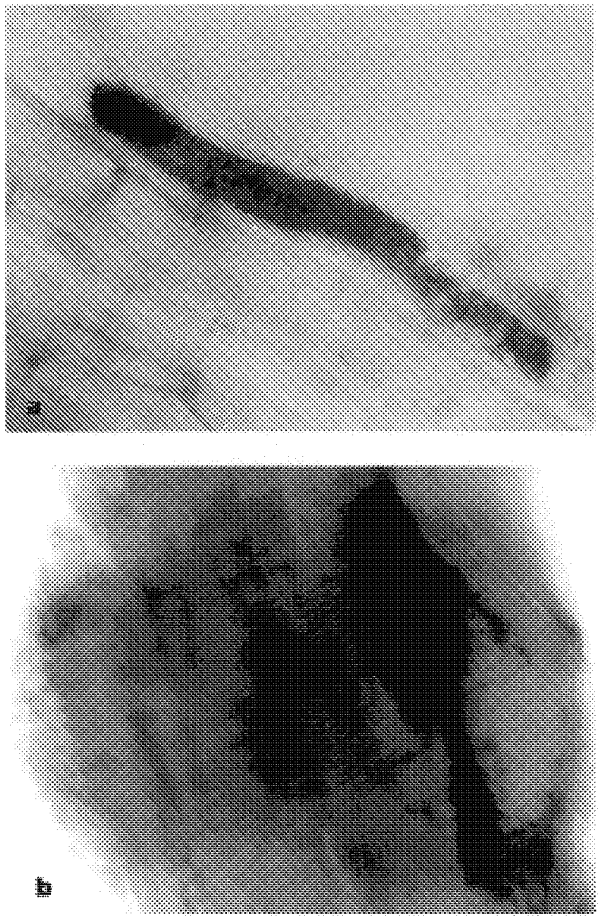


Figure 2. X-gal-stained cotton roots with wild-type or transconjugant of *A. brasilense* Sp7–*SnifA* (*nifA–lacZ* fusion). (a) Bacteria inside plant cell (wild-type without 2,4-D); (b) bacteria around base of nodule-like structure (transconjugant with 0.2 μg mL^{-1} 2,4-D). Azospirilla appear as blue color.

than 2,4-D degradation by bacteria in the liquid medium. However, much better growth by untreated plants also showed incomplete protection with the transconjugant.

DISCUSSION AND CONCLUSION

We have further investigated the concept of plant–microbial association as a means of increasing the specificity and total activity of biodegradation processes. Here the plant is used as a cometabolic source of substrates for pesticide-degrading bacteria, employing 2,4-D degradation by *Rhizobium–Dolichos lablab* or *Azospirillum*–cotton associations as models. Both rapid biodegradation and significant "bio-safening" protection of plants by plant–microbial associations have been shown in this study.

When the transconjugant *Rhizobium* CB1024pJP4 was inoculated into *Dolichos lablab,* plants were resistant to 2,4-D up to 10 μg mL^{-1} as shown by the survival of those plants, in comparison to those inoculated with wild-type, which died (Fig. 1). At a 2,4-D level of 5 μg mL^{-1}, almost complete protection was achieved and partial protection was achieved at the 2,4-D level of 10 μg mL^{-1}, as shown by dry weight results (Table II). The presence of transconjugant CB1024pJP4 inside nodules, on the root surface, and in growth solution suggests that the degradation of 2,4-D could have occurred in both the rhizoisphere and inside nodules. However, the majority of the bacteria would have been contained in roots or in nodules. The inoculum was added to the pot onto plants and bacteria apparently transferred to the growth medium by growh of roots into the medium. Bacteria isolated from surface-sterilized nodules still contained the 2,4-D-degrading plasmid.

When the transconjugant *A. brasilense* Sp7–*SnifA*pJP4 was inoculated into cotton plants, such plants were more resistant to 2,4-D up to 0.5 μg mL^{-1} as shown by better survival and growth of those plants, in comparison to those inoculated with wild-type, which were dying. Cotton was more sensitive to the herbicide than *Dolichos lablab,* in the 0.2 to 0.5 μg mL^{-1} 2,4-D range, and only incomplete protection was achieved with the transconjugant *A. brasilense* Sp7–*SnifA*pJP4 in the first 2 weeks, as indicated by dry weight results (Table III). Further recovery may be expected because large plants are more resistant to 2,4-D and the plants themselves may also have some ability to metabolize this herbicide. Better protection may also be achieved in the lower 2,4-D range, which was not examined. Both transconjugant in liquid solution and on the root surface may contribute to 2,4-D degradation, although some protection was still achieved when plants were transferred to fresh medium containing 2,4-D. Because colonization of *Azospirillum* on nonlegume plants is not as significant as in the *Rhizobium*–legume symbiosis, there is a need to develop techniques to improve colonization of roots, which is not only critical for the mutual benefits of both plants and microbes, but also for the success of biodegradation using such a system.

That *Azospirillum* can colonize cotton roots has been shown by X-gal staining. This is not surprising because there is little specificity of plants for colonization with *Azospirillum* species. There was better colonization for plants treated with 2,4-D, consistent with other reports (Katupitiya et al., 1995; Kennedy and Tchan, 1992; Sriskandarajah et al., 1993). These investigators found that colonization of *Azospirillum* on wheat was increased by addition of small amounts of 2,4-D and the induced *para*-nodules were suggested to be responsible for the changes. Based on our results, the increased colonization may also be due to formation of similar structures.

As a broad-host-range plasmid, pJP4 has now been transferred into many different bacterial strains (Don and Pemberton, 1981; Feng et al., 1994; Friedrich et al., 1983). Thus, it was not unexpected that the transfers of

COR-AAD1-00002515
Bayer EX1008 (Part 5 of 9)

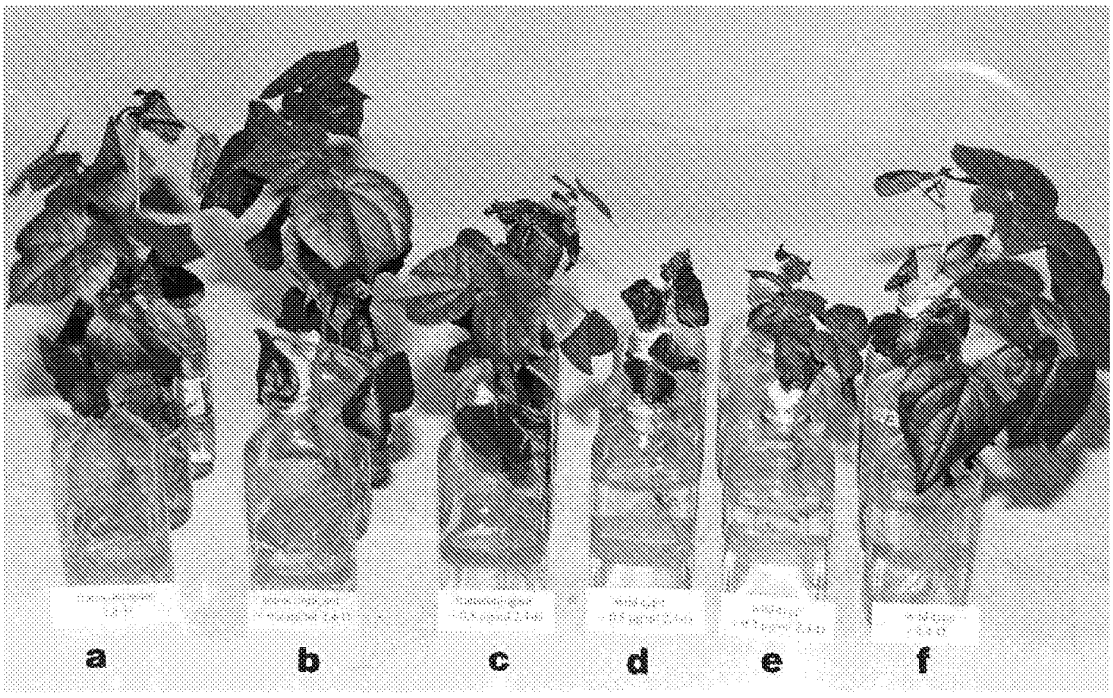


Figure 3. Cotton (3-week-old) inoculated with wild-type or transconjugant strain of *A. brasilense* Sp7–S*nifA* (*nifA–lacZ* fusion) 2 weeks after treatment with or without 2,4-D. (a) Transconjugant without 2,4-D; (b) transconjugant with 0.2 μg mL^{-1} 2,4-D; (c) transconjugant with 0.5 μg mL^{-1} 2,4-D; (d) wild-type with 0.5 μg mL^{-1} 2,4-D; (e) wild-type with 0.2 μg mL^{-1} 2,4-D; and (f) wild-type without 2,4-D.

pJP4 into *Rhizobium* CB1024 and *Azospirillum brasilense* Sp7–*SnifA* would be successful. Both transconjugants developed the ability to resist $HgCl_2$ (5 μg mL^{-1}) and to degrade 2,4,-D (50 μg mL^{-1}) via cometabolism. No transconjugant was able to grow on 2,4-D as a sole carbon source. The same results were also obtained in a previous study for the transconjugant of *Rhizobium trifolii* ANU843, which could not mineralize 2,4-D (Feng et al., 1994). The probable reason is that these transconjugants lack genes coding for enzymes needed to complete the degradation of this herbicide, which are carried on the chromosome of its natural host, *Alcaligenes* (Don et al., 1985; Kukor et al., 1989).

Table III. Dry weight of cotton treated with 2,4-D.

Strains	2,4-D (μg mL^{-1})	Dry weight per plant (g)[a]	SD
No bacteria	0	0.481	0.192
No bacteria	0.2	0.080	0.016
No bacteria	0.5	0.070	0.014
A. Sp7-S*nifA*	0	0.382	0.098
A. Sp7-S*nifA*	0.2	0.130	0.031
A. Sp7-S*nifA*	0.5	0.083	0.018
A. Sp7-S*nifA*pJP4	0	0.423	0.140
A. Sp7-S*nifA*pJP4	0.2	0.310	0.067
A. Sp7-S*nifA*pJP4	0.5	0.209	0.043

[a]The mean of 4 to 6 plants

The phenomenon of accelerated degradation of soil-applied pesticides is essentially unwanted bioremediation (Racke and Coats, 1990) in agricultural production. Herbicides are often required to be present in the fields for a certain period of time. Because of the nonselectiveness of the herbicides or low tolerance of nontarget plants, different degrees of side-effects of herbicides on crops may be inevitable. Avoiding side-effects on nontarget plants by application of pesticides was referred to by Nagy as "bio-safening" (Nagy, 1989; Nagy et al., 1990). Genetic engineering technology can be used for generation of resistant crops by inserting herbicide-resistant genes into plants. Our system also offers to provide herbicide-resistant crops, because biodegradation is probably most intense in the rhizosphere or inside the plants. Therefore, plants can possibly be protected from herbicidal damage at the same time as herbicides in soil act on weeds. Herbicide-resistant crops could allow the use of less expensive and more environmentally acceptable herbicides.

Success in 2,4-D degradation and plant protection by plant–microbial association in our model system indicates that other pesticide-degrading capacities could be inserted into microbial strains for decontamination and protection of plants in plant–microbial associations. Whether such systems will be as successful when applied in the field with competition is being examined. However, the approach appears to have significant advan-

COR-AAD1-00002516
Bayer EX1008 (Part 5 of 9)

tages related to control of bioremediative processes, which are desirable and perhaps more likely to win support from environmental agencies responsible for regulation of genetically engineered microbes. Using such a system could be considered as a distinct process on farms that when completed, leave little trace of the decontaminating system.

The authors thank Dr. R. J. Roughley of the NSW Horitcultural Research and Advisory Station, Gosford, for supplying *Rhizobium* sp. CB1024 and Dr. G. Constable of the Australian Cotton Institute, Narrabri, for providing cotton seeds. We also acknowledge the gift of *lacZ* fusions by Dr. Claudine Elmerich of the Institute Pasteur, Paris, France.

References

Arsène, F., Katutipiya, S., Kennedy, I. R. Elmerich, C. 1994. Use of *lac* Z fusions to study the expression of *nif* genes of *Azospirillum brasilense* in association with plants. Mol. Plant-Microbe Int. **7**: 748–757.

Bowmer, K. H. 1981. Atrazine persistence and toxicity in two irrigated soils of Australia. Austral. J. Soil Res. **29**: 339–350.

Clark, S. A., Mahanty, H. K. 1991. Influence of herbicides on growth and nodulation of white clover, *Trifolium repens.* Soil Biol. Biochem. **23**: 725–730.

Don, R. H., Pemberton, J. M. 1981. Properties of six pesticide degradation plasmids isolated from *Alcaligenes paradoxus* and *Alcaligenes eutrophus.* J. Bacteriol. **145**: 681–686.

Don, R. H., Weightman, A. J., Knackmuss, H. J., Timmis, K. N. 1985. Transposon mutagenesis and cloning analysis of the pathways for degradation of 2,4-dichlorophenoxyacetic acid and 3-chlorobenzoate in *Alcaligenes eutrophus* JPM134 (pJP4). J. Bacteriol. **161**: 85–90.

Eberbach, P. L., Douglas, L. A. 1989. Herbicide effects on the growth and nodulation potential of *Rhizobium trifolii* with *Trifolium subterraneum L.* Plant Soil **119**: 15–23.

Epstein, E. 1972. Mineral nutrition of plants: principles and perspectives. John Wiley & Sons, New York.

Feng, L., Rolfe, B. G., Gartner, E., van Zwieten, L., Kennedy, I. R. 1994. Expression of the 2,4-D degrading plasmid pJP4 of *Alcaligenes eutrophus* in *Rhizobium trifolii.* Acta Biotechnol. **14**: 119–129.

Feng, L. 1994. A study on pesticide breakdown by plant–microbial associations: 2,4-D degradation as a model, thesis, University of Sydney, Sydney, Australia.

Friedrich, B., Meyer, M., Schlegel, H. G. 1983. Transfer and expression of the herbicide-degrading plasmid pJP4 in aerobic autotrophic bacteria. Arch. Microbiol. **134**: 92–97.

Greer, L. E., Shelton, D. R. 1992. Effect of inoculant strain and organic matter content on kinetics of 2,4-dichlorophenoxyacetic acid and degradation in soil. Appl. Environ. Microbiol. **58**: 1459–1465.

Innes, R. W. 1988. A molecular genetic analysis of host-range control in *Rhizobium trifolii.* Ph.D. thesis, Humboldt State University, Humboldt, CA, USA.

Jensen, H. L. 1942. Nitrogen fixation in leguminous plants I. General characters of root-nodule bacteria isolated from species of *Medicago* and *Trifolium* in Australia. Proc. Linn. Soc. NSW **66**: 721–723.

Katupitiya, S., Millet, J., Vesk, M., Viccars, L., Zeman, A., Zhao, L., Elmerich, C., Kennedy, I. R. 1995. A mutant of *Azospirillum brasilense* Sp7 impaired in flocculation with a modified colonization pattern and superior nitrogen fixation in association with wheat. Appl. Environ. Microbiol. **61**: 1987–1995.

Kennedy, I. R., Tchan, Y. T. 1992. Biological nitrogen fixation in non-leguminous field crops: recent advances. Plant Soil **141**: 93–118.

Kukor, J. J., Olsen, R. H., Siak, J.-S. 1989. Recruitment of a chromosomal encoded maleylacetate reductase for degradation of 2,4-dichlorophenoxyacetic acid by plasmid pJP4. J. Bacteriol. **171**: 3385–3390.

Llewllyn, D., Lyon, B. R., Cousins, Y., Huppatz, J., Dennis, E. S., Peacock, W. J. 1990. Genetic engineering of plants for resistance of the herbicide 2,4-D, pp. 67–77. In: G. W. Lylett and D. Grierson (eds), Genetic engineering of crop plants. Butterworths, London.

Nagy, I. 1989. Investigations of interactions between thiocarbamates, extenders, soil microbes, and high plants, Ph.D. thesis, Hungarian Academy of Sciences, Budapest, Hungary.

Nagy, J., Kecskes, M., Nagy, I. 1990. Soil pretreatment with EPTC improves maize tolerance to this herbicide. International Conference on Herbicide Safeners Chemistry, Mode of Action and application, Budapest, August 12–15, 1990.

Racke, K. D., Coats, J. R. 1990. Enhanced biodegradation of pesticides in the environment. ACS Symp. Ser. **426**: 1–302.

Rolfe, B. G., Gresshoff, P. M., Shine, J. 1980. Rapid screening for symbiotic mutants of *Rhizobium* and white clover. Plant Sci. Lett. **19**: 277–284.

Sriskandarajah, S., Kennedy, I. R., Yu, D., Tchan, Y. T. 1993. Effects of plant growth regulators on acetylene-reducing associations between *Azospirillum brasilense* and wheat. Plant Soil **153**: 165–177.

Zeman, A. M. M., Tchan, Y. T., Elmerich, C., Kennedy, I. R. 1992. Nitrogenase activity in wheat seedlings bearing para-nodules induced by 2,4-dichlorophenoxyacetic acid (2,4-D) and inoculated with *Azospirillum.* Res. Microbiol. **143**: 847–855.

van Zwieten, L., Feng, L., Kennedy, I. R. 1995. Colonisation of seedling roots by 2,4-D degrading bacteria: a plant-microbial model. Acta Biotechnol. **15**: 27–39.

COR-AAD1-00002517
Bayer EX1008 (Part 5 of 9)

Environmental Microbiology (2003) 5(10), 878–887 doi:10.1046/j.1462-2920.2003.00479.x

Effect of integration of a GFP reporter gene on fitness of *Ralstonia eutropha* during growth with 2,4-dichlorophenoxyacetic acid

Hans Peter Füchslin, Irene Rüegg, Jan Roelof van der Meer and Thomas Egli*
Swiss Federal Institute for Environmental Science and Technology (EAWAG), Environmental Microbiology and Molecular Ecotoxicology, PO Box 611, CH-8600 Dübendorf, Switzerland.

Summary

Green fluorescent proteins (GFPs) are frequently used as marker and reporter systems to assess the fate and activity of microbial strains with the ability to degrade xenobiotic compounds. To evaluate the potential of this tool for tracking herbicide-degrading microorganisms in the environment a promoterless *gfp* was linked to the *tfd C* promoter, which is activated during degradation of the herbicide 2,4-dichlorophenoxyacetic acid (2,4-D), and integrated into the chromosome of the 2,4-D–degrading strain *Ralstonia eutropha* JMP 134. The effects of the inserted *gfp* gene on the kinetics of 2,4-D degradation by *R. eutropha* in batch and chemostat culture were compared to those of the wild-type strain. In batch culture with 2,4-D as the only carbon and energy source the maximum specific growth rate of the *gfp*-marked strain did not differ significantly from the wild type. However, compared to the wild type, the 2,4-D steady-state concentration in 2,4-D-limited chemostat cultures of the *gfp*-marked strain was higher at all dilution rates tested. The reduced competitiveness of the *gfp*-marked strain at low substrate concentrations was confirmed in a competition experiment for 2,4-D in continuous culture at a dilution rate of 0.075 h^{-1}. Reproducibly, the *gfp*-marked strain was displaced by the wild-type strain. The study clearly demonstrates that fitness of constructs cannot be assessed by measuring μ_{max} with selected substrates in batch cultures only but that a thorough kinetic analysis is needed, which also considers slow, carbon-limited growth conditions as they occur in the environment.

Received 10 February, 2003; accepted 14 May, 2003. *For correspondence. E-mail egli@eawag.ch; Tel. (+41) 1 823 51 58; Fax (+41) 1 823 55 47.

Introduction

Green fluorescent protein (GFP)-expressing strains are now frequently used for tracking specific microbial strains in ecosystems. Bacteria marked with *gfp* have been employed to study the distribution and dynamics of bacterial populations in soils (Errampalli *et al.*, 1998; Tresse *et al.*, 1998), aqueous systems (Stretton *et al.*, 1998), rhizospheres (Gage *et al.*, 1996; Bloemberg *et al.*, 1997; Tombolini *et al.*, 1997), activated-sludge (Eberl *et al.*, 1997; Olofsson *et al.*, 1998) and biofilms (Möller *et al.*, 1998; Skillman *et al.*, 1998). Furthermore, GFPs can be used to visualize gene expression (Cubitt *et al.*, 1995; Andersen *et al.*, 1998; Jaspers *et al.*, 2001). Very often, the *gfp* gene is placed behind a constitutive promoter, allowing constant visualization of the cells. In other constructs, the *gfp* gene is fused behind the promoter of a particular gene of interest, e.g. a promoter of a biodegradation operon, of a signalling pathway or of antibiotic resistance. In such cases of inducible *gfp* constructs the specific conditions leading to GFP induction can be followed and the fluorescence of individual cells detected and quantified by UV microscopy or flow cytometry. In either case, *gfp* constructs are introduced into the host cell, either on plasmid DNAs or integrated as monocopy into the chromosome at (usually) unspecified locations.

Even though the value of GFP for cellular localization and expression studies is beyond doubt, the limits of using *gfp* as a marker gene and the possible impact of the insertion and GFP expression on a *gfp* tagged strain have been neglected. Even in field studies, GFP has been used as marker and reporter gene to study the distribution and activity of specific introduced microbial strains in the environment and it has been assumed that GFP-tagged strains were not affected by the *gfp* insertion (Tombolini *et al.*, 1997; Andersen *et al.*, 1998; Errampalli *et al.*, 1999; Dandie *et al.*, 2001; Elväng *et al.*, 2001). However, usually only a few and very simple experiments are carried out to assess whether insertion of the *gfp* gene has any adverse effects. Control experiments are typically based on whether or not the μ_{max} of the *gfp*-tagged strain is reduced in batch culture with the carbon source of interest compared to the wild-type strain (Tombolini *et al.*, 1997; Dandie *et al.*, 2001). For some applications, in particular when

© 2003 Society for Applied Microbiology and Blackwell Publishing Ltd

COR-AAD1-00002518
Bayer EX1008 (Part 5 of 9)

using the marked bacteria in environmental systems, it is essential to assure that *gfp*-tagging does not constitute a discernible metabolic burden to the cells. Nevertheless, as far as the authors are aware of no detailed growth kinetic analysis in batch and continuous culture has ever been reported for a GFP-carrying strain.

2,4-D still is the most widely used synthetic herbicide to control broadleaf weeds (Bohmont, 1999). The herbicide is biologically degradable and several 2,4-D-degrading bacteria have been isolated. *Ralstonia eutropha* JMP134 is probably the best investigated organism with respect to the 2,4-D degradation pathway, the genetics as well as kinetics of growth and 2,4-D degradation. *Ralstonia eutropha* JMP 134 carries a 22 kb DNA region on plasmid pJP4 (Pemberton *et al.*, 1979) on which 15 genes responsible for degradation of 2,4-D are located (Streber *et al.*, 1987; Perkins *et al.*, 1990; Matrubutham and Harker, 1994; You and Ghosal, 1995; van der Meer, 1997; Leveau *et al.*, 1999; Laemmli *et al.*, 2000; Perez-Pantoja *et al.*, 2000). The enzymes for 2,4-D degradation are also responsible for part of the degradation of 3-chlorobenzoate (3CBA), phenoxyacetic acid and co-metabolic degradation of trichloroethylene (Don and Pemberton, 1981). The plasmid pJP4 is an 80 kb broad-host-range, P1 incompatibility group plasmid and further carries resistance determinants to mercury (Don and Pemberton, 1981).

A derivative of *R. eutropha* JMP 134 was constructed by integrating in single copy a fusion between the *tfdC* promoter and the gene for GFP –F64L, S65T (Miller and Lindow, 1997).This *R. eutropha* derivative still degrades 2,4-D and induces GFP during growth on 2,4-D.

In order to assess whether expression of GFP or the integration of the *tfdC'-gfp* construct would have negative physiological effects in the tagged strain, the kinetics of 2,4-D degradation was studied in batch and chemostat culture and was compared to that of the wild-type strain. Furthermore, direct competition experiments between the wild-type strain and the *gfp*-tagged strain were carried out in continuous culture and the chromosomal insertion site of the mini-Tn*5* construct was determined.

Results

Growth kinetics with 2,4-D in batch and chemostat culture

Determination of μ_{max} in batch culture. The maximum specific growth rate of *R. eutropha* JMP134 and strain 1265 (with the *tfdC'::gfp* insertion) was determined in batch culture with 2,4-D as the only carbon and energy source. *Ralstonia eutropha* was adapted to fast growth by transferring the culture from the exponential growth phase at least three times (approximately 12 generations) into new batch medium before the cells were used as an inoculum. Both wild-type and the *gfp*-containing strain exhibited perfect exponential growth (Fig. 1). The average μ_{max} calculated by linear regression from the logarithmized optical density data were slightly lower for the wild-type strain ($\mu_{max} = 0.225 \pm 0.013\ h^{-1}$) than for the GFP strain ($\mu_{max} = 0.228 \pm 0.010\ h^{-1}$), a difference that cannot be considered significant because of overlapping standard deviations.

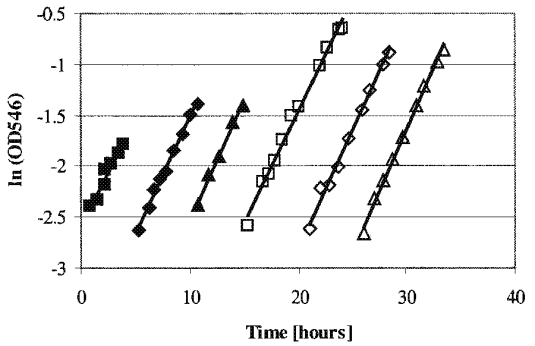


Fig. 1. Growth of *Ralstonia eutropha* wild type (■, ◆, ▲) and *gfp*-marked strain (□, ◇, △) in batch culture with 2,4-D as the only source of carbon and energy. Growth was followed by measuring optical density at 546 nm. The maximum specific growth rates determined by linear regression were $0.225 \pm 0.013\ h^{-1}$ and $0.228 \pm 0.010\ h^{-1}$ for the wild-type and the *gfp*-marked strain respectively.

Growth kinetics in 2,4-D limited continuous culture. Wild-type *R. eutropha* JMP134 and its *gfp* derivative strain 1265 were grown separately in carbon-limited continuous culture with 2,4-D as the only carbon and energy source and the 2,4-D steady-state concentration was measured as a function of dilution rate. After switching from batch culture to the continuous culture mode cells were always allowed to adapt first at $D = 0.075\ h^{-1}$ at least for one week (approximately 18.2 generations and 12.5 volume changes) to the low substrate concentration before sampling was started. At every dilution rate five samples distributed over a time period of 5 h were collected to measure the residual 2,4-D concentration. For a particular dilution rate each steady-state was measured at least twice in independent experiments.

After each change in dilution rate the culture was run for 3.5–5 volume changes before it was sampled again. Preliminary experiments had shown that this was sufficient time to establish the new steady-state (data not shown). The dilution rate was not changed in an increasing or decreasing order but D was set randomly within the range of $0.025\ h^{-1}$–$0.225\ h^{-1}$. As soon as slight wall growth, a decrease in the biomass concentration, or a decrease in the 2,4-D residual concentration in the outlet was observed the cultures were no longer used for kinetic experiments. The steady-state 2,4-D concentrations

COR-AAD1-00002519
Bayer EX1008 (Part 5 of 9)

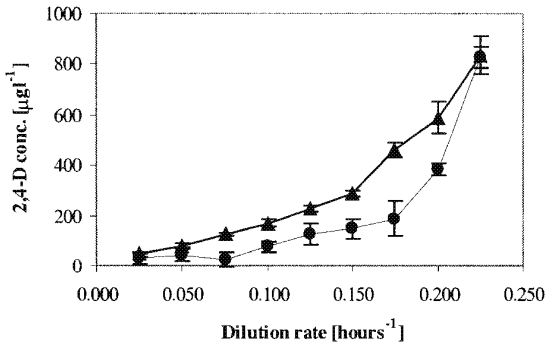


Fig. 2. Steady-state concentrations of 2,4-D in carbon–limited continuous cultures of *R. eutropha* wild type (●) and its *gfp* derivative (▲), as a function of dilution rate.

obtained for the wild type and the GFP clone as a function of the dilution rate are shown in Fig. 2. The steady-state 2,4-D concentrations increased with increasing dilution rate as expected for saturation type kinetics (Pirt, 1975). At virtually all dilution rates the steady-state 2,4-D concentrations in the cultures of strain 1265 were significantly higher than those observed in cultures of the wild type. Only when D was close to D_{crit} steady-state 2,4-D concentrations were similar in both cultures.

Modelling growth with 2,4-D in continuous culture

According to the model proposed by Monod (Monod, 1942) two parameters, K_s and μ_{max}, determine the competitive ability of a microbial strain under single-substrate limited growth conditions. Whereas μ_{max} is important for growth at high substrate concentrations in batch culture, K_s is the parameter that mainly affects the ability to compete for substrate at low concentrations and during slow growth (Jannasch, 1967; Veldkamp and Jannasch, 1972; Button, 1998; Kovárová-Kovar and Egli, 1998). The classical Monod equation (eqns 1 and 2) (Monod, 1942) does not consider effects of maintenance requirements on growth kinetics. Because a number of studies have given evidence for the existence of a minimum substrate concentration for growth, s_{min} (Boethling and Alexander, 1979; Rittmann and McCarty, 1980; Schmidt *et al.*, 1985; Alexander, 1994; Kovárová *et al.*, 1996; Tros *et al.*, 1996a), the original Monod equation was modified accordingly (eqns 3 and 4). In addition, the conversion factor ($Y_{x/s}$) relating substrate utilized (S) to the amount of biomass (X) formed (for data see Table 1) is needed for modelling the competition (eqn 5).

$$\mu = \mu_{max}*s/(K_s + s) \quad (1)$$

$$s = K_s*D/(\mu_{max}-D) \quad (2)$$

$$\mu = \mu_{max}*(s-s_{min})/(K_s + (s-s_{min})) \quad (3)$$

$$s = K_s*D/(\mu_{max}-D) + s_{min} \quad (4)$$

$$Y_{x/s} = dX/dS \quad (5)$$

Parameter estimation with the models given in eqn 2 and 4 was carried out to obtain the best fit to the experimentally determined 2,4-D steady-state concentrations (Fig. 2). The μ_{max} and $Y_{x/s}$ were directly derived from experimental data as previously described, whereas s_{min} and K_s were variables and were determined by parameter estimation. The resulting values are listed in Table 1.

For the wild type both models described the experimental data well (Fig. 3A). Nevertheless, the relative residual plot (Fig. 3B) indicated that the extended Monod model fitted the data slightly better over the whole range of dilution rates tested and showed a systematically deviation of the original Monod model at low dilution rates.

A more complex pattern was observed for the kinetics of the GFP strain (Fig. 4). Obviously, insertion of the GFP gene had a negative effect on the uptake of 2,4-D and residual 2,4-D steady-state concentrations were negatively affected at low rather than at high dilution rates. Possible reasons for this discrepancy to the Monod kinetics will be given in the discussion. Neither the original nor the extended Monod model was able to predict the steady-state 2,4-D concentration reasonably well over the whole range of dilution rates up to μ_{max} of 0.238 h^{-1}. Other models such as that used by Shehata and Marr (1971) were also unable to fit the data over the whole range of growth rates tested. The residual plot (Fig. 4B) visualizes the superior fit of the extended Monod model to the experimental data at low dilution rates (≤0.175 h^{-1}). A reasonable fit was only found with the Monod model extended

Table 1. Kinetic parameters obtained from parameter estimation by fitting the model to the steady-state 2,4-D concentrations over the whole range of dilution rates for the *R. eutropha* wild type and, for fitting the experimental data obtained between D = 0.025 h^{-1} and D = 0.175 h^{-1} for its *gfp* derivative.

		R. eutropha (wild type)	Strain *R. eutropha* 1265 (*gfp*-marked strain)
Experimentally determined	$Y_{X/2,4\text{-}D}$:	0.226 ± 0.022 g g^{-1}	0.226 ± 0.022 g g^{-1}
	μ_{max}:	0.225 ± 0.013 h^{-1}	0.228 ± 0.010 h^{-1}
Estimated using original Monod model (eq. 2)	K_s	71.4 µg·l^{-1}	211.9 µg·l^{-1}
Estimated using extended Monod model (eq. 4)	K_s	56.7 µg·l^{-1}	167.1 µg·l^{-1}
	s_{min}:	16.5 µg·l^{-1}	31.6 µg·l^{-1}

COR-AAD1-00002520
Bayer EX1008 (Part 5 of 9)

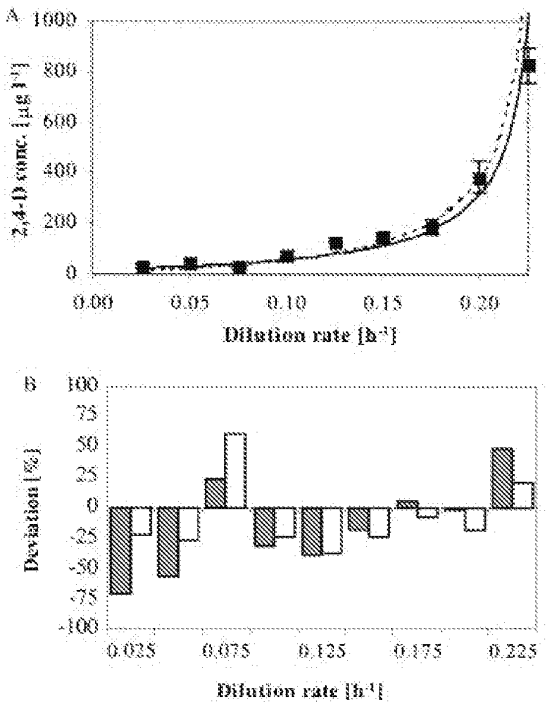


Fig. 3. A. Comparison of model predictions [Monod model (---), Monod model extended by s_{min} (–)] and experimentally determined 2,4-D steady-state concentrations (▩) for growth of *R. eutropha* (wild type) in 2,4-D-limited chemostat culture as a function of dilution rate. For kinetic parameters used see Table 1.
B. Relative deviations of model predictions (▨ Monod model, □ Monod model extended by s_{min}) from steady-state 2,4-D concentrations for growth of *R. eutropha* (wild type) in 2,4-D-limited chemostat culture, as a function of dilution rate. For the simulation by the classical Monod kinetics a weighed deviation (χ^2) of 138.5 was determined compared to the lower χ^2 (77.5) of the extended Monod model.

by s_{min} and multiplied with a fitting variable (K_i) including the impact of changing dilution rate ($\mu = \mu_{max}\cdot(s\text{-}s_{min})/(K_s + (s\text{-}s_{min}))\text{-}D/(D + K_i)$). However, there is no defined physiological meaning for the fitting variable therefore this model was not considered further.

Competition between R. eutropha *JMP134 and its derivative strain 1265 in continuous culture*

To verify the observed kinetic handicap of the GFP derivative competition experiments were set up between wild-type and GFP derivative and with 2,4-D as the only carbon and energy source. Wild type and GFP derivative were first cultivated separately for at least seven days (18.2 generations) in 2,4-D-limited (s_o = 115 mg l^{-1}) continuous culture at a dilution rate of 0.075 h^{-1} in order to allow the cells to adapt to low 2,4-D concentrations. Then 100 ml of wild-type culture was removed and injected into the culture of strain 1265 (total working volume 2.8 l) to start the competition on 2,4-D. This resulted in an initial mixture consisting of 96% GFP- expressing plus 4% wild-type cells. Both, total cell number on non-selective complex medium agar plates and the number of GFP cells on kanamycin-containing TS plates were determined as a function of time to follow the competition between the two strains. Two competition experiments were carried out, both at the same D and with the same result (Fig. 5). Although some outlying data points were obtained within the first 50 h of the competition experiment the data demonstrate that after some 140 h, corresponding to approximately 15 generations, the GFP derivative was displaced by the wild type.

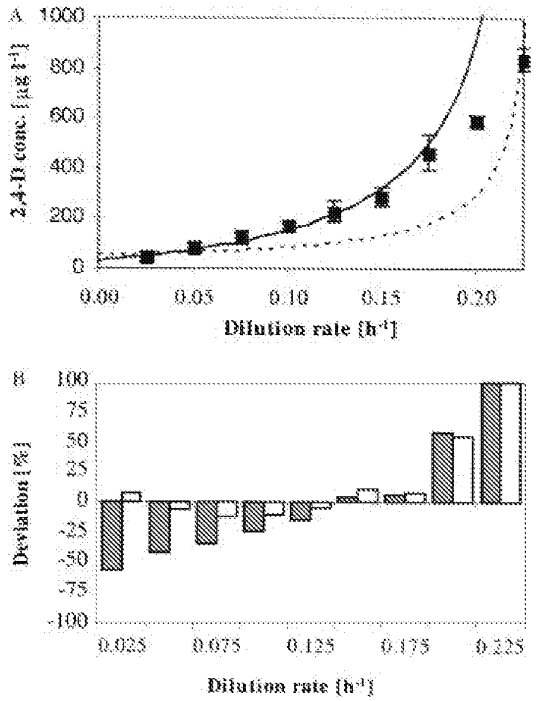


Fig. 4. A. Comparison of model predictions and experimentally determined 2,4-D steady-state concentrations (▩) for growth of *R. eutropha* (*gfp*-tagged strain) in 2,4-D-limited chemostat culture, as a function of dilution rate.
Simulations for two different models are shown: (-) Monod kinetics expanded with s_{min} optimized only for low dilution rates (0.025 h^{-1}–0.175 h^{-1}); (---) Monod kinetics expanded by s_{min} optimized for the steady-state data at the highest dilution rate 0.225 h^{-1} and kinetic parameter values of μ_{max} = 0.238 h^{-1}, K_s = 45.33 µg·l^{-1}, s_{min} = 50.47 µg·l^{-1}.
B. Relative deviations of model predictions (▨ Monod model, □ Monod model extended by s_{min}) from steady-state 2,4-D concentrations for growth of *R. eutropha* (*gfp* derivative) in 2,4-D-limited chemostat culture, as a function of dilution rate. The parameter estimation for the kinetic parameters for both models was carried out only for the data at low dilution rates between 0.025 h^{-1} and 0.175 h^{-1}. The deviations at the dilution rate of 0.225 h^{-1} were 265% for the Monod kinetics and 250% for the extended Monod kinetics respectively. For the simulation by the classical Monod kinetics a weighed deviation (χ^2) 101.5 was determined, which is considerably higher than the χ^2 (10.8) for the extended Monod model.

COR-AAD1-00002521
Bayer EX1008 (Part 5 of 9)

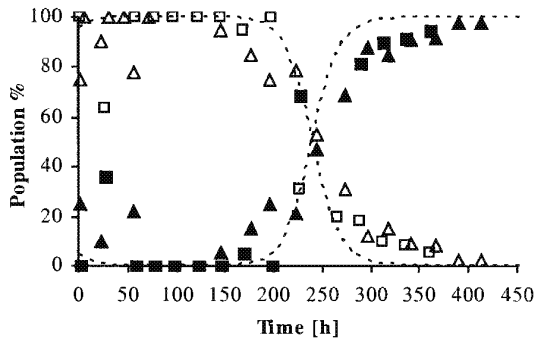


Fig. 5. Population dynamics of *R. eutropha* wild type (■, ▲) and *gfp*-marked strain (□, △) during competition for 2,4-D in two independent 2,4-D-limited continuous cultures at a dilution rate of 0.075 h^{-1}. At time zero the *gfp*-tagged culture was inoculated with 100 ml of wild-type cells precultivated under exactly the same conditions. Additionally the model prediction for the competition is shown. It was assumed that the inoculated wild-type cells exhibited a lag of 100 h before they started to compete successfully (see text).

Simulation of the competition between wild-type and gfp-marked strain

The comparison between the experimental data and a simulation based on the Monod model extended by s_{min} is shown in Fig. 5. A significant delay of about 100 h in growth of the wild-type strain was experimentally observed. A simulation was carried out based on the kinetic parameters of Table 1 and when a lag time of 100 h for growth of the inoculated wild-type cells was included it was possible to predict the experimental outcome. Taking into account that the modelling was based on parameters (μ_{max}, K_s and s_{min}) determined in preceding independent kinetic experiments it can be stated that the experimental data can be simulated with good agreement (Fig. 5). At the end of the competition the complete elimination of the GFP clone from the culture proceeded slower than predicted by the model. This can be explained by wall growth that started to develop with small portions of the GFP strain sticking to the bioreactor wall, or by its splashing to the bioreactor lid and the subsequent reinoculation from the lid.

In a control experiment it was checked whether growth of the wild type was affected by the excretion of an inhibiting compound by the GFP strain and whether or not this was the reason for the lag in competition observed. Wild-type cells were grown in batch culture on 2,4-D as the only carbon and energy source with and without supernatant collected from a batch culture of the GFP strain. No difference in μ_{max} was observed, suggesting that excretion of an inhibitor compound by the GFP clone is not likely.

Gene analysis

Because the growth kinetic behaviour of the GFP derivative of *R. eutropha* was different from that of the wild-type strain, it was important to analyse the site of insertion of the *tfdC'::gfp* fusion on the chromosome. By using the kanamycin resistance gene rescuing strategy, cloning the fragment into *E. coli* and subsequent DNA sequencing, it was found that the transposon fragment carrying the *tfdC'::gfp* fusion had integrated into a pyruvate kinase-like gene (Fig. 6). A region of 400 basepairs outside the I-end of the transposon was translated and found to exhibit 50% identical amino acid residues in a 128 residue overlap with the C-terminal end (residues 300–429) of pyruvate kinases from among others, *Mezorhizobium loti* (GenBank entry AP003002), *Ralstonia solanacearum* (AL646084) and *Brucella melitensis* (AE009472). This strongly suggests that the transposon inserted into a gene for pyruvate kinase in *R. eutropha* and, possibly, interrupted this gene function. In fact, the maximum specific growth rate of the GFP-expressing strain with fructose in batch culture (0.262 ± 0.006 h^{-1}) was significantly lower than that of the wild type (0.44 h^{-1}) (Leveau *et al.*, 1999) suggesting that most probably the *tfdC'::gfp* insertion disturbed an intact functional gene for pyruvate kinase on the chromosome of *R. eutropha* JMP134. However, as far as we know, pyruvate kinase is not involved in 2,4-D degradation. Moreover, many bacterial strains, like *R. solanacearum* and *E. coli* carry two copies for pyruvate kinase.

Discussion

Increased 2,4-D steady-state concentrations in 2,4-D-limited continuous cultures, and displacement by the wild-type strain during competition for 2,4-D in chemostat cultivation clearly demonstrated that a *tfdC'::gfp*-marked strain of *R. eutropha* JMP134 was less competitive during slow growth. In contrast, the μ_{max} with 2,4-D was not significantly affected by the chromosomal insertion of the *tfdC'::gfp* fusion. The μ_{max} of both the wild-type and the *gfp*-tagged strain was approximately 0.23 h^{-1}, which corresponds well with the values of 0.21–0.215 h^{-1} reported earlier (Greer *et al.*, 1992; Müller and Babel, 1996). Whereas the kinetics of the wild type could well be described with the extended Monod model (eqn 4), the kinetics of the *gfp*-marked derivative were more difficult to simulate over the whole range of dilution rates tested. A reasonable fit with simple Monod models was obtained

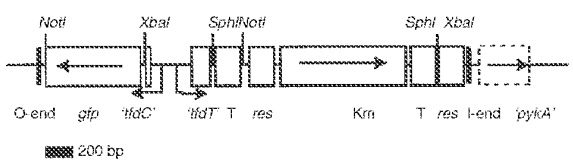


Fig. 6. Position of insertion of the *tfdC::gfp* fusion on the chromosome.

COR-AAD1-00002522
Bayer EX1008 (Part 5 of 9)

only at dilution rates lower than 0.175 h^{-1}. The consequences of the integration of the *tfdC'::gfp* gene fusion into the chromosome on the growth kinetic behaviour of *R. eutropha* JMP 134 seem to be twofold. On one hand, insertion results in a significantly reduced affinity for 2,4-D, from K_{sWT} (56.7 $\mu g \cdot l^{-1}$) to K_{sGFP} (167.1 $\mu g \cdot l^{-1}$). On the other hand, insertion led to a considerable increase of the minimum 2,4-D concentration from s_{minWT} (16.5 $\mu g \cdot l^{-1}$) to s_{minGFP} (31.6 $\mu g \cdot l^{-1}$). Whereas the value of μ_{max} is consistent with earlier reports those of K_s and s_{min} determined here are approximately one order of magnitude lower than those published earlier. For example, the K_s value reported for *R. eutropha* JMP 134 growing on 2,4-D by Müller and Babel (Müller and Babel, 1996) was 2830 $\mu g \cdot l^{-1}$ (recycling-mode fermenter), whereas Greer (Greer *et al.*, 1992) reported a K_s of 2200 $\mu g \cdot l^{-1}$ (batch culture) for growth with 2,4-D. This difference in K_s values may be explained by the longer adaptation time used in our study. The phenomenon that microorganisms can improve their kinetic parameters during long-term cultivation on a single substrate has already been reported to occur in different experimental systems (Höfle, 1983; Rutgers *et al.*, 1987; Senn *et al.*, 1994; Ferenci, 1999; Wick *et al.*, 2001). Similarly, the s_{min} determined for growth of *R. eutropha* JMP134 in a recycling reactor was 272 $\mu g \cdot l^{-1}$ (Müller and Babel, 1996) in contrast to the 20 $\mu g \cdot l^{-1}$ observed in our study. This discrepancy might be due to the different cultivation systems used as already observed by Tros *et al.* (1996a) in the case of *Pseudomonas* sp. strain B13 growing with 3-chlorobenzoate.

Heterotrophic microbial growth in natural environments is generally limited by the availability of carbon and energy sources (Morita, 1997). In natural water bodies or soil contaminated by xenobiotic compounds the concentrations of available carbon are usually very low (Alexander, 1994; Tros *et al.*, 1996b). Hence, our kinetic study suggests that under environmental growth conditions the *gfp*-expressing derivative of *R. eutropha* has a disadvantage compared to the wild type in using low 2,4-D concentrations. The observed handicap must be caused by the additional genetic and/or metabolic burden of the *tfdC'::gfp* gene fusion and kanamycin marker, inserted randomly into the genome. Several explanations can be put forward for the reduced competitiveness of the *gfp*-marked strain. One possible reason could be that the addition of another promoter out-titrates the number of activated tfdR (tfdS) regulatory proteins. Addition of the *tfdC'::gfp* fusion increases the number of *tfdR*-binding sites to four (i.e. *tfdA-tfdS*, *tfdR-tfdDII*, *tfdT-tfdC* and *tfdC'::gfp*) (Leveau *et al.*, 1999). Assuming that in the presence of 2,4-D the concentration of the inducer was the same in both strains a competition for free inducer by the regulatory protein could occur. As a result, the frequency of transcription from the *tfdR*-regulated promoters might decline, leading to a smaller amount of *tfd* gene products. This again might result in a higher residual 2,4-D concentration needed for supporting a particular specific growth rate of the *gfp*-marked strain. Competition of multiple promoters for the inducer could also explain why at higher dilution rates the difference between the 2,4-D residual concentration of wild type and *gfp*-tagged strain decreased and became virtually equal. At specific growth rates close to μ_{max} the metabolic pools should be virtually saturated and the intracellular concentration of the inducers (McFall *et al.*, 1997) is probably high enough to saturate all promoters. Furthermore, it is also possible that during fast growth several copies of the plasmid pJP4 are present in the cell to support a high growth rate. This implies that the effect of adding an additional promoter on the chromosome is outnumbered by the promoters of the *tfd* operons on plasmid pJP4 and an increased number of the regulatory genes, leading to a reduced influence on 2,4-D utilisation kinetics. Another explanation for the lower competitiveness of the *gfp*-marked strain could be that expression of the GFP protein itself led to an increased requirement of maintenance energy reflected in the enhanced s_{min}. Not only the additionally expressed GFP but also the aminoglycoside phosphotransferase (product of the kanamycin resistance gene) might account for an increased metabolic burden and a reduced competitiveness.

A third reason for the reduced competitive ability of the GFP expressing derivative could stem from the fact that the continuous production and presence of the GFP in the cell might slightly disturb intracellular metabolism and nutrient transport mechanisms (Tombolini *et al.*, 1997). Once formed, the GFP protein appears to be stable and to remain in the cell for long periods of time, diluted only by cell growth and division or in the absence of growth persist until the cell lyses (Tombolini *et al.*, 1997). Last but not least the site of insertion of the transposon might affect the metabolic behaviour of the construct. For this reason, we analysed the exact insertion site of the *tfdC'::gfp* fusion, which turned out to be in/near a putative gene for pyruvate kinase. However, we assume that this should have no or only a moderate effect on the kinetic behaviour observed with 2,4-D as growth substrate. First of all, several bacterial strains are known to harbour two copies for pyruvate kinase, such as *R. solanacearum* and *E. coli* and this might also be the case for *R. eutropha* because it still grows on fructose as sole carbon and energy source. This confirms that at least one functional pyruvate kinase is still present. Second, pyruvate kinase is not directly involved in 2,4-D degradation, which proceeds via the metabolites 3-oxoadipate, acetyl- and succinyl-CoA, and the TCA cycle (Kaschabek *et al.*, 2002). Therefore, a defect in pyruvate kinase is unlikely to affect the residual 2,4-D concentration during growth. It would be interesting to see

COR-AAD1-00002523
Bayer EX1008 (Part 5 of 9)

whether or not the negative effect of the insertion is restricted to growth with 2,4-D and fructose. Competition of the wild type and the *gfp*-marked strain, e.g. in a carbon-limited continuous culture for acetate, a substrate in whose degradation pyruvate kinase is not involved, might give an answer to this question. Hence, there are a number of reasons why the GFP-expressing strain might not behave in a similar way as the original wild-type strain. Certainly, the worst mutants, in which even the maximum specific growth rate was affected, were eliminated by the initial screening of *gfp*-marked strains for μ_{max} with 2,4-D in batch culture. As far as the authors are aware, this is the first time that the effect of the integration of a *gfp* gene into a reporter strain and its expression has been demonstrated clearly under conditions of slow growth. Our experiments allowed us to quantify the effect of chromosomal insertion of the *tfdC'::gfp* gene fusion on the kinetics of 2,4-D degradation by *R. eutropha*. The data clearly demonstrate that changes in kinetic properties have to be considered in field experiments with strains containing reporter systems. The work presented suggests that a profound kinetic continuous culture study including testing of growth with a wide spectrum of nutrients is needed if one wants to investigate and test the fitness of wild-type and genetically engineered strains under environmentally relevant conditions. Our results indicate that the *gfp*-marked strain investigated here can be used for monitoring the metabolic activity when inoculated into soil containing high 2,4-D concentrations in the range of mg or $g \cdot l^{-1}$, e.g. at the beginning of the bioremediation process. However, the use of this clone for assessing the survival and activity of 2,4-D degrading *R. eutropha* cells in low polluted environments (range of µg or $ng \cdot l^{-1}$) is clearly not feasible. It is very likely that this genetically engineered strain will be out competed by the indigenous 2,4-D degrader populations under carbon-limited oligotrophic conditions. Definitively, more information is needed in order to construct marker and reporter systems without a significant impact on the host cell. Green fluorescent proteins are a tool of enormous potential for the investigation of microbial processes in the environment, but as always, their advantages and limitations have to be evaluated critically.

Experimental procedures

Organism and cultivation conditions

Strains. The strain *R. eutropha* JMP134(pJP4) was used as a wild type. *Ralstonia eutropha* strain 1265 is a derivative of strain JMP 134 with the *tfdC'::gfp* insertion and kanamycin resistance.

Construction of gfp-tagged R. eutropha. A 486 bp fragment containing the intergenic region between *tfdT* and *tfdC* (nucleotides 260 and 367, sequence numberings according to GenBank entries U16782 and M35097 respectively) was amplified in the PCR by using primers 990702f (5′-CTA GCG GCA GCA TGC GAT CGC-3′, *Sph*I site underlined) and 990703r (5′-CAT CGA CAA CAT TCT AGA CTC-3′, *Xba*I site underlined) and *R. eutropha* JMP134 chromosomal DNA as template. This fragment was cloned into vector pGEM-T-Easy (Promega, Madison, WI, USA) and its sequence was determined to exclude any undesired mutations. The *tfdT-C* intergenic region was retrieved by cutting with *Sph*I and *Xba*I. This fragment was inserted into plasmid pJAMA23, cut with the same two enzymes. Plasmid pJAMA23 (Jaspers *et al.*, 2001) contains the *gfp*-mut3 gene encoding the GFP-F64L, S65T mutant protein (Cormack and Falkow, 1996) behind the *rrnB* transcription terminator. This yielded plasmid pCBA204. Plasmid pCBA204 was digested with *Not*I, the 1.5 kb fragment isolated and ligated with the 7 kb *Not*I vector part of the mini transposon plasmid pCK218 (Kristensen *et al.*, 1995). After transformation into *Escherichia coli* CC118λpir this yielded plasmid pCBA206. The fragment containing the *tfdT-C* intergenic region transcriptionally fused to the *gfp* gene plus the gene for kanamycin resistance was subsequently introduced into *R. eutropha* JMP134 by triparental mating with the help of *E. coli* HB101 (pRK2013) (Ditta *et al.*, 1980) and transposase activity. Transconjugants of *R. eutropha* JMP134 containing the *tfdC'::gfp* fusion were selected for kanamycin resistance and subsequently checked for chromosomal integration by Southern hybridisation (not shown). One of the transconjugants, strain 1265, which had the highest GFP expression when grown on 2,4-D, was used for further studies.

In order to determine the exact site of insertion of the *tfdC'::gfp* fragment on the chromosome of *R. eutropha* strain 1265, we used the strategy to rescue the kanamycin resistance gene. Therefore, total DNA of strain 1265 was partially digested with *Sau*3AI. Fragments in the range between 2.5 and 3.5 kb were isolated and ligated with pUC18, digested with *Bam*HI. After transformation in *E. coli* DH5α, selection was made for kanamycin-resistant colonies. The plasmid of one such kanamycin-resistant transformants was isolated and found to contain an approximately 0.4 kb overlap with the chromosomal insertion site. The insert of this plasmid was completely sequenced and the result indicated that the *tfdC'::gfp* fusion had been inserted in a *pykA* homologous gene for pyruvate kinase.

Growth media

Batch medium. The mineral medium contained, per litre: 275 mg NH_4Cl, 75 mg $MgSO_4 \cdot 7H_2O$, 5 mg $CaCl_2 \cdot H_2O$, 35 mg KCl, 1.5 mg $FeCl_2$, 60 µg H_3BO_3, 100 µg $MnCl_2 \cdot 4H_2O$, 120 µg $CoCl_2 \cdot 6H_2O$, 70 µg $ZnCl_2$, 25 µg $NiCl_2 \cdot 6H_2O$, 15 µg $CuCl_2 \cdot 2H_2O$, 25 µg $Na_2MoO_4 \cdot 2H_2O$, 5.2 mg EDTA·$Na_4(H_2O)_4$. The mineral medium was supplemented with 2,4-D (99%, Aldrich, Steinheim, Germany) or with fructose (Fluka, Buchs, Switzerland) as the only source of carbon and energy. The total 2,4-D concentration was always 500 mg of carbon per litre. After heat sterilization and cooling to room temperature 100 ml of phosphate buffer ($Na_2HPO_4 \cdot 2H_2O/KH_2PO_4$, 0.56 M with respect to phosphate and a pH of 7.5) was added by filtration to one litre of medium using sterile disposable filters (0.22 µm, type GVWP, Millipore, Bedford, USA). 0.05 ml of

COR-AAD1-00002524
Bayer EX1008 (Part 5 of 9)

filter sterilized vitamin stock solution (containing per litre: pyrodoxin·HCl, 100 mg; 50 mg of each, thiamine·HCl, riboflavin, nicotinic acid, D-Ca-pantothenic acid, p-amino benzoic acid, lipoic acid, nicotinamide and vitamin B12; biotin 20 mg, and folic acid 20 mg) were also added per litre of mineral medium.

Chemostat medium. The acidic mineral medium for continuous cultivation contained per litre: 275 mg NH_4Cl, 1.25 ml H_3PO_4 (85%), 75 mg $MgSO_4{\cdot}7H_2O$, 5 mg $CaCl_2{\cdot}H_2O$, 35 mg KCl, 1.5 mg $FeCl_2$, 60 µg H_3BO_3, 100 µg $MnCl_2{\cdot}4H_2O$, 120 µg $CoCl_2{\cdot}6H_2O$, 70 µg $ZnCl_2$, 25 µg $NiCl_2{\cdot}6H_2O$, 15 µg $CuCl_2{\cdot}2H_2O$, 25 µg $Na_2MoO_4{\cdot}2H_2O$, 5.2 mg EDTA·$Na_4(H_2O)_4$ and 0.025 ml of silicon antifoam (Fluka, Buchs, Switzerland). The mineral medium was supplemented with 2,4-D as the only source of carbon and energy. The total 2,4-D concentration was always 50 mg of 2,4-D carbon per litre. After autoclaving, 0.25 ml of vitamin stock solution was added per 1 litre of medium by sterile filtration as described above. Chemicals were purchased from either Fluka (Buchs, Switzerland) or Merck (Darmstadt, Germany) if not mentioned otherwise.

Cultivation conditions

Continuous cultivation at a dilution rate of 0.075 h^{-1} was performed in a 3.5 litre bioreactor (MBR, Wetzikon, Switzerland) with a working volume of 2.8 litre and equipped with both pH (7.50 ± 0.05) and temperature control (30 ± 0.1°C). To adjust pH in the reactor an equimolar mixture of 0.5 M NaOH and KOH was used. The impeller speed was controlled at 750 revolutions per minute and the oxygen saturation was always >90% air saturation. The bioreactors were regularly checked for wall growth to avoid artefacts as reported by Pirt (1975). In our bioreactors with glass walls already the slightest wall growth could be observed at baffles before it started at the glass walls. In case of clearly visible wall growth at the glass surfaces the residual concentration of 2,4-D in the bulk liquid decreased significantly compared to the steady-state concentration and this was the most sensitive indication of wall growth effects. Subsequently also the biomass concentration decreased.

Biomass and growth yield determination

Biomass measured as cell dry weight was determined by filtration through 0.2 µm pore size polycarbonate membrane filters (Sterico AG, Dietikon, Switzerland). Cells collected on filters were washed once with 50 ml distilled water and filters were dried at 100°C to constant weight. The growth yield was calculated as gram of dry cell weight formed per gram of substrate consumed. Optical density was determined in a 1-cm cuvette at 546 nm with an Uvikon 860 spectrophotometer (Kontron, Zürich, Switzerland). The correlation factor between dry weight and OD_{546} equalled 308.1 ± 29.1 [$mg{\cdot}l^{-1}{\cdot}OD_{546}^{-1}$].

Analytical procedures

The concentration of 2,4-D in the culture medium was determined by using a Gynkotek HPLC system consisting of a Gina 50 automated injection module, a M480 G gradient pump, on-line degasser, and a UVD 340S photodiode array detector (Dionex, Germering, Germany). Samples collected from the bioreactor were immediately filtered (0.22 µm, type GVWP, Millipore, Bedford, USA) and acidified before analysis. An amount of 50 µl was injected and the compounds were separated on a Nucleosil column (CC 250/4 Nucleosil 100–5 C18 HD from Macherey Nagel, Düren, Germany) using an eluent consisting of 60% (v/v) methanol, 40% (v/v) 50 mM NaH_2PO_4 and pH 4, at a flow rate of 0.7 ml min^{-1}, and 2,4-D was subsequently detected at a wavelength of 205 nm. The detection limit was 10 $µg{\cdot}l^{-1}$.

Population composition

In competition experiments the population dynamics of *R. eutropha* JMP 134 and strain 1265 was determined by plating on non-selective and kanamycin-containing agar plates. The culture from the chemostat was diluted (factor 2×10^5) in autoclaved phosphate-buffered saline (PBS; 14.4 g l^{-1} $Na_2HPO_4{\cdot}2H_2O$, 3.2 g l^{-1} $NH_2PO_4{\cdot}2H_2O$, 5.9 g l^{-1} NaCl, pH 7.5) and five 100 µl aliquots were plated on complex medium agar plates (containing per litre 4 g of tryptic soy agar (Biolife, Milano, Italy) plus 15 g technical agar (Biolife, Milano, Italy)) either with or without 50 mg l^{-1} of kanamycin (Fluka, Buchs, Switzerland).

The fraction (P) of strain 1265 (as percentage of the total population) was calculated using the following (eqn 6).

$$P(\%) = [(\text{Number of colonies growing on kanamycin – containing plates})/(\text{Number of colonies growing on kanamycin – free plates})]^*100\% \quad (6)$$

For each measurement five samples were taken and the average was calculated.

Continuous culture

The dilution rate [D (h^{-1})], corresponding to the specific growth rate [µ (h^{-1})] of the culture in chemostat at steady state is defined as

$$D = F/V \quad (7)$$

F: flow rate ($l{\cdot}h^{-1}$)

V: volume (l)

Simulation software

AQUASIM, a program developed at our institute (Reichert, 1998) allows estimating parameters by fitting calculated values (s_{pred}) to experimental data (s_{obs}). This feature was used to estimate kinetic parameters that resulted in the best fit of simulations and experimental data. The program estimated the best fit by minimizing χ^2-values ($\chi^2 = \Sigma((s_{obs}-s_{pred})/\sigma)^2$). If not experimentally determined the standard deviation (σ) was set to 10%.

Acknowledgements

We thank Bettina Baumgartner for the construction of the strain *R. eutropha* 1265, A.J.B. Zehnder for support through-

COR-AAD1-00002525
Bayer EX1008 (Part 5 of 9)

out this study and acknowledge the financial support of the Swiss Federal Institute for Environmental Science and Technology (EAWAG).

References

Alexander, M. (1994) *Biodegradation and Bioremedation.* San Diego, California: Academic Press.

Andersen, J.B., Sternberg, C., Kongsbak, P.L., Bjorn Petersen, S., Givskov, M., and Molin, S. (1998) New unstable variants of green fluorescent protein for studies of transient gene expression in bacteria. *Appl Environ Microbiol* **64:** 2240–2246.

Bloemberg, G.V., O'Toole, G.A., Lugtenberg, B.J.J., and Kolter, R. (1997) Green fluorescent protein as a marker for *Pseudomonas spp. Appl Environ Microbiol* **63:** 4543–4551.

Boethling, R.S., and Alexander, M. (1979) Effect of concentration of organic chemicals on their biodegradation by natural microbial communities. *Appl Environ Microbiol* **37:** 1211–1216.

Bohmont, B.L. (1999) *The Standard Pesticide User's Guide.* Trenton, New Jersey: Prentice Hall.

Button, D.K. (1998) Nutrient uptake by microorganisms according to kinetic parameters from theory as related to cytoarchitecture. *Microbiol Mol Biol Rev* **62:** 636–645.

Cormack, B.P., and Falkow, S. (1996) FACS-optimized mutants of the green fluorescent protein (GFP). *Gene* **173:** 33–38.

Cubitt, A.B., Heim, R., Adams, S.R., Boyd, A.E., Gross, L.A., and Tsien, R.Y. (1995) Understanding, improving and using green fluorescent proteins. *TIBS* **20:** 448–455.

Dandie, C.E., Thomas, S.M., and McClure, N.C. (2001) Comparison of a range of green fluorescent protein-tagging vectors for monitoring a microbial inoculant in soil. *Lett Appl Microbiol* **32:** 26–30.

Ditta, G., Stanfield, S., Corbin, D., and Helinski, D.R. (1980) Broad host range DNA cloning system for Gram-negative bacteria: construction of gene bank of *Rhizobium meliloti. Proc Natl Acad Sci USA* **77:** 7347–7351.

Don, R.H., and Pemberton, J.M. (1981) Properties of six pesticide degradation plasmids isolated from *Alcaligenes paradoxus* and *Alcaligenes eutrophus. J Bacteriol* **145:** 681–686.

Eberl, L., Schulze, R., Ammendola, A., Geisenberger, O., Earhart, R., Steinberg, C., *et al.* (1997) Use of green fluorescent protein as a marker for ecological studies of activated sludge communities. *FEMS Microbiol Lett* **149:** 77–83.

Elväng, A.M., Westerberg, K., Jernberg, C., and Jansson, J.K. (2001) Use of green fluorescent protein and luciferase biomarkers to monitor survival and activity of *Arthrobacter chlorophenolicus* A6 cells during degradation of 4-chlorophenol in soil. *Environ Microbiol* **1:** 32–42.

Errampalli, D., Okamura, H., Lee, H., Trevors, J.T., and van Elsas, J.D. (1998) Green fluorescent protein as a marker to monitor survival of phenanthrene-mineralizing *Pseudomonas sp.* UG14Gr in creosote-contaminated soil. *FEMS Microbiol Ecol* **26:** 181–191.

Errampalli, D., Tresse, O., Lee, H., and Trevors, J.T. (1999) Bacterial survival and mineralization of p-nitrophenol in soil by green fluorescent protein-marked *Moraxella* sp. G21 encapsulated cells. *FEMS Microbiol Ecol* **30:** 229–236.

Ferenci, T. (1999) Growth of bacterial cultures 50 years on: towards an uncertainty principle instead of constants in bacterial growth kinetics. *Res Microbiol* **150:** 431–438.

Gage, D.J., Bobo, T., and Long, S.R. (1996) Use of green fluourescent protein to visualize early events of symbiosis between *Rhizobium meliloti* and alfalfa (*Medicago sativa*). *J Bacteriol* **178:** 7159–7166.

Greer, L.E., Robinson, J.A., and Shelton, D.R. (1992) Kinetic comparison of seven strains of 2,4-dichlorophenoxyacetic acid-degrading bacteria. *Appl Environ Microbiol* **58:** 1027–1030.

Höfle, M.G. (1983) Long-term changes in chemostat cultures of *Cytophaga johnsonae. Appl Environ Microbiol* **46:** 1045–1053.

Jannasch, H.W. (1967) Enrichments of aquatic bacteria in continuous culture. *Arch Microbiol* **59:** 165–173.

Jaspers, M.C., Meier, C., Zehnder, A.J., Harms, H., and van der Meer, J.R. (2001) Measuring mass transfer processes of octane with the help of an alkSalkB:: gfp-tagged *Escherichia coli. Environ Microbiol* **3:** 512–524.

Kaschabek, S.R., Kuhn, B., Muller, D., Schmidt, E., and Reineke, W. (2002) Degradation of aromatics and chloroaromatics by *Pseudomonas sp.* strain B13. purification and characterization of 3-oxoadipate: succinyl-coenzyme A (CoA) transferase and 3-oxoadipyl-CoA thiolase. *J Bacteriol* **184:** 207–215.

Kovárová, K., Zehnder, A.J.B., and Egli, T. (1996) Temperature-dependent growth kinetics of *Escherichia coli* ML30 in glucose-limited continuous culture. *J Bacteriol* **178:** 4530–4539.

Kovárová-Kovar, K., and Egli, T. (1998) Growth kinetics of suspended microbial cells: From single-substrate-controlled growth to mixed-substrate kinetics. *Microbiol Mol Biol Rev* **62:** 646–666.

Kristensen, C.S., Eberl, L., Sanchez-Romero, J.M., Givskov, M., Molin, S., and de Lorenzo, V. (1995) Site-specific deletions of chromosomally located DNA segments with the multimer resolution system of broad-host-range plasmid RP4. *J Bacteriol* **177:** 52–58.

Laemmli, C.M., Leveau, J., Zehnder, A.J.B., and Van der Meer, J.R. (2000) Characterization of a second *tfd* gene cluster for chlorophenol and chlorocatechol metabolism on plasmid pJP4 in *Ralstonia eutropha* JMP134 (pJP4). *J Bacteriol* **182:** 4165–4172.

Leveau, J.H.J., König, F., Füchslin, H.P., Werlen, C., and van der Meer, J.R. (1999) Dynamics of multigene expression during catabolic adaptation of *Ralstonia eutropha* JMP134 (pJP4) to the herbicide 2,4-dichlorophenoxyacetate. *Mol Microbiol* **2:** 389–395.

Matrubutham, U., and Harker, A.R. (1994) Analysis of duplicated gene sequences associated with *tfdR* and *tfdS. Alcaligenes eutrophus* JMP134. *J Bacteriol* **176:** 2348–2353.

McFall, S.M., Parsek, M.R., and Chakrabarty, A.M. (1997) 2-Chloromuconate and ClcR-mediated activation of the *clcABD* operon: *in vitro* transcriptional and DNase I footprint analyses. *J Bacteriol* **179:** 3655–3663.

van der Meer, J.R. (1997) Evolution of novel metabolic pathways for the degradation of chloroaromatic compounds. *Antonie Van Leeuwenhoek* **71:** 159–178.

COR-AAD1-00002526
Bayer EX1008 (Part 5 of 9)

Miller, W.G., and Lindow, S.E. (1997) An improved GFP cloning cassette designed for prokaryotic transcriptional fusions. *Gene* **191:** 149–153.

Möller, S., Steinberg, C., Andersen, J.B., Christensen, B.B., Ramos, J.L., Givskov, M., and Molin, S. (1998) *In situ* gene expression in mixed-culture biofilms evidence of metabolic interaction between community members. *Appl Environ Microbiol* **64:** 721–732.

Monod, J. (1942) Recherche sur la croissance des cultures bactériennes. Paris, France: Hermann et Cie.

Morita, R.Y. (1997) *Bacteria in Oligotrophic Environments.* New York, NY: Chapman & Hall.

Müller, R.H., and Babel, W. (1996) Measurement of growth at very low rates ($\mu \geq 0$), an approach to study the energy requirement for the survival of *Alcaligenes eutrophus* JMP 134. *Appl Environ Microbiol* **62:** 147–151.

Olofsson, A.C., Zita, A., and Hermansson, M. (1998) Floc stability and adhesion of green-fluorescent-protein-marked bacteria to flocs in activated sludge. *Microbiology* **144:** 519–528.

Pemberton, J.M., Conrney, B., and Don, R.H. (1979) Evolution and spread of pesticide degrading ability among soil micro-organisms. In *Plasmids of Medical, Environmental and Commercial Importance.* Timmis, K.N., and Puhler, A. (eds). Amsterdam, Netherlands: Elsevier/North-Holland Biomedical Press.

Perez-Pantoja, D., Guzman, L., Manzano, M., Pieper, D.H., and Gonzalez, B. (2000) Role of tfdC (I) D (I) E (I) F (I) and tfdD (II) C (II) E (II) F (II) gene modules in catabolism of 3-chlorobenzoate by *Ralstonia eutropha* JMP134 (pJP4). *Appl Environ Microbiol* **66:** 1602–1608.

Perkins, E.J., Gordon, M.P., Caceres, O., and Lurquin, P.F. (1990) Organization and sequence analysis of the 2,4-dichlorophenol hydroxylase and dichlorocatechol oxidative operons of plasmid pJP4. *J Bacteriol* **172:** 2351–2359.

Pirt, J.S. (1975) *Principles of Microbe and Cell Cultivation.* Oxford: Blackwell Scientific Publications.

Reichert, P. (1998) *aquasim 2.0 – Tutorial, Computer Program for the Identification and Simulation of Aquatic Systems.* Dübendorf, Switzerland: EAWAG.

Rittmann, B.E., and McCarty, P.L. (1980) Evaluation of steady-state-biofilm kinetics. *Biotechnol Bioeng* **22:** 2359–2373.

Rutgers, M., Teixeira De Mattos, M.J., Postma, P.W., and Van Dam, K. (1987) Establishment of steady state in glucose-limited chemostat cultures of *Klebsiella pneumoniae. J Gen Microbiol* **133:** 445–451.

Schmidt, S.K., Alexander, M., and Shuler, M.L. (1985) Predicting threshold concentrations of organic substrates for bacterial growth. *J Theor Biol* **114:** 1–8.

Senn, H., Lendenmann, U., Snozzi, M., Hamer, G., and Egli, T. (1994) The growth of *Escherichia coli* in glucose-limited chemostat cultures: a re-examination of the kinetics. *Biochim Biophys Acta* **1201:** 424–436.

Shehata, T., and Marr, A.G. (1971) Effect of nutrient concentration on the growth of *Escherichia coli. J Bacteriol* **107:** 210–216.

Skillman, L.C., Sutherland, I.W., Jones, M.V., and Goulsbra, A. (1998) Green fluorescent protein as a novel species-specific marker in enteric dual-species biofilms. *Microbiology* **144:** 2095–2101.

Streber, W.R., Timmis, K.N., and Zenk, M.H. (1987) Analysis, cloning, and high-level expression of 2,4-dichlorophenoxyacetate monooxygenase gene *tfdA* of *Alcaligenes eutrophus* JMP134. *J Bacteriol* **169:** 2950–2955.

Stretton, S., Techkarnjanaurk, S., McLennan, A.M., and Goodman, A.E. (1998) Use of green fluorescent protein to tag and investigate gene expression in marine bacteria. *Appl Environ Microbiol* **64:** 2554–2559.

Tombolini, R., Unge, A., Ellen, D., de Bruijn, F., and Jansson, J.K. (1997) Flow cytometric and microscopic analysis of GFP-tagged *Pseudomonas fluorescens* bacteria. *FEMS Microbiol Ecol* **22:** 17–28.

Tresse, O., Errampalli, D., Kostrzynska, M., Leung, K.T., Lee, H., Trevors, J.T., and van Elsas, J.D. (1998) Green fluorescent protein as a visual marker in a *p*-nitrophenol degrading *Moraxella sp. FEMS Microbiol Lett* **164:** 187–193.

Tros, M., Bosma, T., Schraa, G., and Zehnder, A.J.B. (1996a) Measurement of minimum substrate concentration (s_{min}) in a recycling fermenter and its prediction from the kinetic parameters of *Pseudomonas sp.* strain B13 from batch and chemostat cultures. *Appl Environ Microbiol* **62:** 3655–3661.

Tros, M.E., Schraa, G., and Zehnder, A.J.B. (1996b) Transformation of low concentration of 3-chlorobenzoate by *Pseudomonas* spl strain B13: Kinetics and residual concentrations. *Appl Environ Microbiol* **62:** 437–442.

Veldkamp, H., and Jannasch, H.W. (1972) Mixed culture studies with the chemostat. *J Appl Chem Biotechnol* **22:** 105–123.

Wick, L., Quadroni, M., and Egli, T. (2001) Short- and long-term changes in proteome composition and kinetic properties in a culture of *Escherichia coli* during transition from glucose-excess to glucose-limited growth conditions in continuous culture, and vice versa. *Environ Microbiol* **3:** 588–599.

You, I.S., and Ghosal, D. (1995) Genetic and molecular analysis of a regulatory region of the herbicide 2,4-dichlorophenoxyacetate catabolic plasmid pJP4. *Mol Microbiol* **16:** 321–331.

COR-AAD1-00002527
Bayer EX1008 (Part 5 of 9)

JOURNAL OF BACTERIOLOGY, Jan. 1989, p. 314–320
0021-9193/89/010314-07$02.00/0
Copyright © 1989, American Society for Microbiology
Vol. 171, No. 1

Phenoxyacetic Acid Degradation by the 2,4-Dichlorophenoxyacetic Acid (TFD) Pathway of Plasmid pJP4: Mapping and Characterization of the TFD Regulatory Gene, *tfdR*

ALAN R. HARKER,[1]† RONALD H. OLSEN,[2]* AND RAMON J. SEIDLER[3]

Corvallis Environmental Research Laboratory, U.S. Environmental Protection Agency,[3] and Department of Microbiology, Oregon State University,[1] Corvallis, Oregon 97333, and Department of Microbiology and Immunology, University of Michigan Medical School, Ann Arbor, Michigan 48109[2]

Received 23 March 1988/Accepted 28 September 1988

Plasmid pJP4 enables *Alcaligenes eutrophus* JMP134 to degrade 3-chlorobenzoate and 2,4-dichlorophenoxyacetic acid (TFD). Plasmid pRO101 is a derivative of pJP4 obtained by insertion of Tn*1721* into a nonessential region of pJP4. Plasmid pRO101 was transferred by conjugation to several *Pseudomonas* strains and to *A. eutrophus* AEO106, a cured isolate of JMP134. AEO106(pRO101) and some *Pseudomonas* transconjugants grew on TFD. Transconjugants with a chromosomally encoded phenol hydroxylase also degraded phenoxyacetic acid (PAA) in the presence of an inducer of the TFD pathway, namely, TFD or 3-chlorobenzoate. A mutant of one such phenol-degrading strain, *Pseudomonas putida* PPO300(pRO101), grew on PAA as the sole carbon source in the absence of inducer. This isolate carried a mutant plasmid, designated pRO103, derived from pRO101 through the deletion of a 3.9-kilobase DNA fragment. Plasmid pRO103 constitutively expressed the TFD pathway, and this allowed the metabolism of PAA in the absence of the inducer, TFD. Complementation of pRO103 in *trans* by a DNA fragment corresponding to the fragment deleted in pRO101 indicates that a negative control-regulatory gene (*tfdR*) is located on the *Bam*HI E fragment of pRO101. Other subcloning experiments resulted in the cloning of the *tfdA* monooxygenase gene on a 3.5-kilobase fragment derived from pRO101. This subclone, in the absence of other pRO101 DNA, constitutively expressed the *tfdA* gene and allowed PPO300 to grow on PAA. Preliminary evidence suggests that the monooxygenase activity encoded by this DNA fragment is feedback-inhibited by phenols.

Xenobiotic compounds have been used extensively in agriculture as herbicides and pesticides and in the manufacturing industry. Chlorinated derivatives of phenoxyacetic acid (PAA) have been released to the environment as herbicides over the past 40 years. Unlike many of the recalcitrant synthetic compounds that have been released over the last several decades, 2,4-dichlorophenoxyacetic acid (TFD) is rapidly degraded by soil bacteria (13). Several strains in multiple genera that are capable of degrading TFD have been isolated from the soil (2, 9, 21). Those that have been most thoroughly studied are strains identified as *Alcaligenes eutrophus* (4). In these strains the genes which encode the degradative pathway for TFD are plasmid encoded (4). Plasmid pJP4 from the strain *A. eutrophus* JMP134 is an 80-kilobase, broad-host-range, P1 incompatibility group plasmid (4). Several restriction maps for this plasmid, and similar plasmids, have been published (Fig. 1) (5, 6, 11). Plasmid pJP4 carries genes essential for the degradation of 3-chlorobenzoate (3CB) and expression of mercury resistance, as well as the degradation of TFD (4). The metabolic pathways for 3CB and TFD degradation utilize enzymes common to the degradation of chlorocatechol to chloromaleylacetic acid (6–8, 18, 21). The *tfdA* and *tfdB* gene products are TFD monooxygenase and 2,4-dichlorophenol (TFP) hydroxylase, respectively, and are apparently unique to the TFD pathway. These two gene products convert chlorophenoxyacetic acid to chlorocatechol. Most of the catabolic functions of plasmid pJP4 have been mapped by transposon mutagenesis in a region corresponding to the *Bam*HI C fragment shown in Fig. 1 (6). However, this analysis failed to identify the position of the *tfdA* gene. Amy et al. (2) cloned the *Hin*dIII B fragment into *Escherichia coli* HB101 and demonstrated the release of radiolabeled CO_2 from cultures grown with TFD labeled on the alkyl side chain reflecting the cloning of a presumptive TFD monooxygenase. Don et al. (6) reported that a plasmid containing the *Eco*RI B fragment cloned into a cured derivative of JMP134 enabled the strain to grow on TFD as the sole carbon source. Recently, the *tfdA* gene has been cloned as a subfragment of the *Hin*dIII B fragment of pJP4 (20). Oxygen uptake assays performed with this subclone showed monooxygenase activity in the presence of either TFD or PAA (20). In contrast to these oxygen uptake studies, however, bacterial strains carrying the parental plasmid, pJP4, are incapable of utilizing PAA as the sole carbon source for growth. However, Pemberton et al. (17) described mutants of JMP134 which are able to degrade PAA as a sole carbon source for growth.

In this work we describe the transfer of a derivative of plasmid pJP4, designated pRO101, into various pseudomonads and its expression in these strains. A deletion mutant of plasmid pRO101, designated pRO103, occurred in *Pseudomonas putida* PPO300 and rendered this strain capable of growth on PAA as the sole carbon source, leading to the identification by complementation of a TFD-regulatory gene (*tfdR*). To demonstrate unregulated expression of the *tfdA* gene in the absence of the *tfdR* gene, we describe here the cloning and expression of the *tfdA* gene from plasmid pRO101 into *P. putida* PPO300 and growth of this constructed strain on PAA as the sole carbon source.

* Corresponding author.
† Present address: Department of Botany and Microbiology, Oklahoma State University, Stillwater, OK 74078.

Downloaded from http://jb.asm.org/ on September 3, 2020 at Corteva Agriscience

COR-AAD1-00002528

Bayer EX1008 (Part 5 of 9)

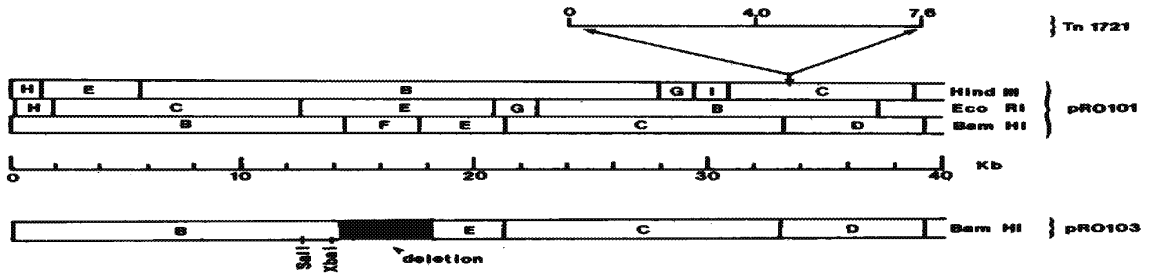


FIG. 1. Restriction digest map of the plasmids pRO101 and pRO103. The locations of the *Eco*RI, *Hin*dIII, and *Bam*HI restriction sites are from data reported elsewhere (5). We have represented here only those fragments in the regions implicated in catabolic pathways. The insert at the top indicates the position of the Tn*1721* transposon (1) and its *Eco*RI restriction sites.

MATERIALS AND METHODS

Bacterial strains and plasmids. Bacterial strains and plasmids used or constructed in this study are described in Table 1.

Media. Complex medium (TN) used to maintain cultures has been described previously (16). The use of antibiotic supplements in either complex or minimal medium is described below and in the tables. Screening for mercury resistance was done by using brain heart infusion medium (Difco Laboratories, Detroit, Mich.) with 25 μg of $HgCl_2$ per ml. Phosphate-buffered minimal medium (MMO) was used extensively to test cultures for growth on single carbon substrates or depletion of such substrates. This medium (MMO) has been described elsewhere (19). Carbon substrates (TFD, PAA, etc.) were added at a final concentration of 0.05%. Casamino Acids (CAA; Difco) when used as a supplemental carbon source were added to a final concentration of 0.3%.

Genetic techniques. Isolation of plasmid DNA, restriction endonuclease digestion and cloning, transformation, and plasmid matings were as described previously (3, 12, 14–16). Plasmid pRO101 (i.e., pJP4::Tn*1721*) was constructed by mating R388::Tn*1721* (1) into *P. putida* PPO2034(pJP4). A transconjugant containing both plasmids pJP4 and R388::Tn*1721* was then used as a donor for mating with *E. coli* HB101, with selection of transconjugants for their acquisition of both mercury and tetracycline resistance. Such transconjugants were subsequently mated into *A. eutrophus* AEO106 (strain JMP134 spontaneously cured of plasmid pJP4) with selection for growth on TFD and the nonselective acquisition of tetracycline resistance. One such transconjugant plasmid was designated pRO101.

Oxygen uptake assays. Cells grown on plates containing an appropriate test medium were harvested by scraping the plate with an inoculation loop. The cell mass was suspended in 2 ml of MMO. The electrode chamber (Gilson Medical Electronics, Middleton, Wis.) was filled with 1.4 ml of the MMO and 0.4 ml of the cell suspension. The concentration of dissolved oxygen was measured with a Clark oxygen electrode (Yellow Springs Instrument Co., Yellow Springs, Ohio) interfaced with a strip chart recorder. A base-line rate of endogenous oxygen consumption was established for the culture in MMO alone. A suitable carbon source (e.g., TFD) was then injected into the chamber (ca. 20 μl of a stock

TABLE 1. Bacterial strains and plasmids

Strain or plasmid	Relevant markers[a]	Source or reference
P. aeruginosa PAO1c	Prototroph	Laboratory stock (3)
P. putida PPO2034	*leu-34*	Laboratory stock
P. putida PPO300	Prototroph	ATCC 17514
P. cepacia DBO1	Prototroph	Laboratory stock
E. coli HB101		Laboratory stock
A. eutrophus JMP134	Prototroph, Tfd^+	4
A. eutrophus AEO106	Prototroph, Tfd^-	This study (JMP134 cured of plasmid pJP4)
Alcaligenes sp. strain EML159	Prototroph, Tfd^+	2
Plasmids		
pJP4	Plasmid from JMP134 (Tfd^+ Hg^r)	4
pRO101	pJP4::Tn*1721* Tfd^+ Hg^r Tc^r	This study
pRO103	Constitutive mutant of pRO101 (Tfd^+ Hg^r Tc^r)	This study
pRO1727	cloning vector (Tc^r Cb^r)	3
pRO2321	cloning vector (Tc^r Tp^r)	—[c]

[a] Gene designations are as described previously (12).
[b] Abbreviations: Cb^r, Hg^r, Tc^r, Tp^r, resistance to carbenicillin, mercury, tetracycline, and trimethoprim, respectively; other abbreviations as in text or references.
[c] —, Cloning vector derived from plasmid R388 (G. J. Zylstra and R. H. Olsen, manuscript in preparation).

Downloaded from http://jb.asm.org/ on September 3, 2020 at Corteva Agriscience

COR-AAD1-00002529

Bayer EX1008 (Part 5 of 9)

solution resulting in a final concentration of 0.05%), and any change in the rate of oxygen consumption was recorded. The optical density of representative samples from each culture was recorded at 425 nm. All assay data was normalized to represent a culture optical density within the chamber of 1.0 determined spectrophotometrically at 425 nm.

Spectroscopy. All spectrophotometric measurements were performed on a model DU8B spectrophotometer (Beckman Instruments, Inc., Fullerton, Calif.). Optical densities of all cultures were recorded at 425 nm. UV-absorbing carbon substrates (TFD, PAA, and phenol [PHL]) were identified by scanning spectra between 320 nm and 240 nm. Samples (1 ml) of liquid cultures were centrifuged in an Eppendorf microcentrifuge for 5 min at maximum speed to remove cells. A 100-μl portion of the supernatant was removed, added to 200 μl of MMO, and placed in a microcuvette (path length, 10 mm). Under these conditions TFD exhibits a maximum absorbance at 293 nm; that of TFP is 294 nm. Addition of supernatant samples to 200 μl of 0.1 M NaOH shifts the TFP maximum to 315 nm, while the TFD maximum remains at 293 nm. Rates of TFD (or other carbon source) removal were measured by changes in peak height relative to the absorbance minima.

RESULTS

Transfer of the pRO101 plasmid into strains listed in Table 1 conferred tetracycline and mercury resistance. *A. eutrophus* AEO106(pRO101) achieved rapid growth on TFD as the sole carbon source, similar to the growth characteristics of the parent strain, JMP134. *P. cepacia* DBO1(pRO101) also grew on TFD as the sole carbon source. All other *Pseudomonas* strains carrying the plasmid pRO101 could degrade TFD only in cultures of relatively high density (A_{425} = 1.5) and then only for short and inconsistent periods relative to JMP134 or AEO106(pRO101). Low-density liquid cultures (A_{425} = 0.02) and solid-medium cultures of these transconjugant *Pseudomonas* strains were unable to grow in the presence of 0.05% TFD as the sole carbon source.

MMO with TFD (0.05%) was supplemented with an additional carbon source (0.3%) to identify a substrate for rapid growth without inhibiting the expression of the TFD-degradative pathway. Lactate, succinate, and citrate supplements were similar to glucose as the primary carbon source for growth with respect to their inhibitory effect on TFD degradation. CAA, however, allowed more rapid growth and complete utilization of 0.05% TFD in overnight cultures of all strains carrying pRO101 except *E. coli* HB101(pRO101). No TFD utilization was observed for HB101(pRO101). Growth characteristics and rates of TFD utilization for *Pseudomonas* and *Alcaligenes* strains were almost identical in the presence of 0.3% CAA and 0.05% TFD.

The TFD-degradative pathway is induced in the presence of TFD or 3CB and Casamino acids. Data in Table 2 represent relative rates of substrate-dependent oxygen consumption by cultures previously grown in the presence or absence of various aromatic compounds. It is clear that CAA alone and PAA do not induce any of the degradative activities encoded by pJP4 or pRO101.

TFD induces activities related to TFD and TFP degradation with concomitant 4-chlorocatechol consumption. As reported elsewhere (6), 3CB induces the TFD pathway as well as a pathway involved in 3CB degradation. PAA did not induce oxygen uptake but was metabolized by cultures grown in the presence of TFD or 3CB. Clearly, PAA is not an inducer of the pathway but may function as a substrate in the TFD pathway. The data in Table 2 also show that PAA is not readily degraded to the extent of the other substrates in the TFD pathway, even when the TFD pathway has been induced.

TABLE 2. Oxygen uptake for cells grown on solid medium with CAA and inducer

Strain	Inducer	Rate of oxygen uptake in presence of[a]:				
		TFD	PAA	TFP	3CB	4CC[b]
JMP134	None	−	−	−	−	−
	PAA	−	−	−	−	−
	TFD	++	+	++	−	+
	3CB	++	+	++	++	++
AEO106	None	−	−	−	−	−
	PAA	−	−	−	−	−
	TFD	−	−	−	−	−
	3CB	ND	ND	ND	ND	ND
AEO106(pRO101)	None	−	−	−	−	−
	PAA	−	−	−	−	−
	TFD	++	+	++	−	+
	3CB	++	+	++	++	++
PAO1c	None	−	−	−	−	−
	PAA	−	−	−	−	−
	TFD	−	−	−	−	−
	3CB	−	−	−	+	+
PAO1c(pRO101)	None	−	−	−	−	−
	PAA	−	−	−	−	−
	TFD	++	+	++	−	++
	3CB	+	+	++	++	+

[a] Symbols: −, no increase over basal oxygen consumption rates; +, approximately twice the basal rate; ++, five times the basal rate or greater; ND, not done (growth inhibited). All strains were grown on solid medium with 0.3% CAA plus the indicated inducer. Inducing substrates (when present) were at 0.05% (wt/vol).
[b] 4CC, 4-Chlorocatechol.

Since PAA is not an inducing substrate, we thought that the simultaneous presence of TFD during growth might allow the subsequent metabolism of PAA. Results of these experiments are shown in Table 3. In repeated trials, strain JMP134 exhibited high rates of substrate-dependent oxygen uptake for both PAA and TFD if cells were grown in the presence of both TFD and PAA. The complete degradation of both substrates was confirmed by spectrophotometric scans of supernatant from liquid cultures grown overnight. However, *P. aeruginosa* PAO1c(pRO101) cells showed little oxygen consumption in the presence of PAA. In addition, spectrophotometric scans of liquid cultures grown overnight showed no detectable degradation of PAA by PAO1c (pRO101) and reduced utilization of TFD, although the utilization of TFP was similar to that by JMP134.

One clear difference between these *Alcaligenes* and *Pseudomonas* strains which is relevant to their degradation of aromatic compounds is the absence of a chromosomally encoded PHL hydroxylase in PAO1c. *P. aeruginosa* PAO1c is unable to grow on PHL, whereas both *A. eutrophus* AEO106 and *P. putida* PPO300 can do so (data not shown). Simultaneous degradation of TFD and PAA by *A. eutrophus* JMP134 and *P. putida* PPO300(pRO101) can thus be explained if TFD and PAA are both suitable substrates for the first enzyme in the pathway, TFD monooxygenase (*tfdA* gene product). PHL, the product of monooxygenase activity on PAA, is not a substrate for the plasmid-encoded 2,4-dichlorophenol hydroxylase (*tfdB* gene product). However,

Downloaded from http://jb.asm.org/ on September 3, 2020 at Corteva Agriscience

COR-AAD1-00002530

Bayer EX1008 (Part 5 of 9)

TABLE 3. Induction of PAA utilization

Strain	Inducer	Rate of oxygen uptake in presence of[a]:				
		TFD	PAA	TFP	PHL	4CC[b]
JMP134(pJP4)	TFD	++	+	++	−	+
	TFD-PAA	++	++	++	++	++
	TFD-PHL	++	++	++	++	++
	PHL	−	−	−	++	+
PAO1c(pRO101)	TFD	++	+	++	−	+
	TFD-PAA	++	+	++	−	+
	TFD-PHL	++	+	++	−	+
	PHL	−	−	−	−	−
PPO300(pRO101)	TFD	++	+	++	−	+
	TFD-PAA	++	++	++	++	++
	TFD-PHL	++	++	++	++	++
	PHL	−	−	−	++	++

[a] Symbols: −, no increase over basal oxygen consumption rates; +, approximately twice basal rates; ++, five times the basal rate or greater. Culture medium was MMO–0.3% CAA plus the indicated inducer(s).
[b] 4CC, 4-Chlorocatechol.

PHL produced from PAA degradation may be utilized if a chromosomal PHL hydroxylase is induced. Simultaneous induction of PAA utilization by both TFD and PHL for cultures carrying plasmid pRO101 in the absence of PAA supports this hypothesis. When plasmid pRO101 was transferred by conjugation to *P. putida* PPO300 (ATCC 17514) (known to express a chromosomally encoded phenol hydroxylase), a metabolic pattern similar to JMP134 was obtained. Thus, growth of PPO300(pRO101) in the presence of TFD and PHL resulted in significant oxygen consumption in the presence of PAA. This observation contrasts with no PAA utilization for TFD-grown liquid cultures (Table 3). Analogously, AEO106(pRO101) shows similar PHL-dependent induction patterns for PAA utilization (data not shown). It is noteworthy that the Tfd^+ strain of *Alcaligenes* sp. strain EML159 isolated by Amy et al. (2), which contains a plasmid identical to pJP4, is incapable of PAA or PHL utilization and does not respond to PHL induction (data not shown). This is a significant difference from *A. eutrophus* JMP134.

In the absence of PHL hydroxylase activity, PHL accumulation apparently inhibits the activity of the first enzyme, TFD monooxygenase, of the pJP4-encoded TFD pathway. This is indicated in Table 3 for PAO1c(pRO101). When TFD-induced strains are subsequently fed PAA, insignificant quantities of PAA are consumed and detectable quantities of PHL do not accumulate. This suggests that the presence of feedback inhibition by PHL on the TFD-PAA monooxygenase (*tfdA* gene product) occurs for overnight cultures of PAO1c(pRO101) grown on TFD and PAA. Not only is there no detectable reduction in the concentration of PAA as determined spectrophotometrically, but utilization of TFD in the presence of PAA is less than 30% of that measured for cultures grown on TFD alone as the inducing substrate. In further experiments designed to demonstrate the inhibition of the first enzyme by PHL, TFD-induced cells of PAO1c(pRO101) were exposed to either CAA or TFD, and oxygen uptake was measured with an oxygen electrode. After a linear rate of oxygen consumption was established, PHL was added to 0.05%. The rate of oxygen consumption in the presence of TFD was abruptly inhibited 34% by added phenol and 28% by added TFP. These results suggest feedback inhibition of the TFD-PAA monooxygenase by its product, TFP or PHL produced metabolically from TFD or PAA, respectively. When either PHL or TFP was added, the rate of oxygen consumption for CAA utilization was not affected (data not shown). Thus, PHL and TFP were apparently not toxic to other degradative metabolism of the cells.

TABLE 4. Induction profile of the plasmid pRO103

Strain	Inducer	Rate of oxygen uptake in presence of[a]:				
		TFD	PAA	TFP	PHL	4CC[b]
AEO106(pRO103)	None	++	+	++	−	++
	PAA	++	++	++	++	++
	TFD	++	+	++	−	++
	PHL	++	++	++	++	++
	3CB	++	+	++	−	++
PPO300(pRO103)	None	++	+	++	−	+
	PAA	+	++	++	++	++
	TFD	++	+	+	−	++
	PHL	+	++	++	++	++
	3CB	++	+	+	−	++
PAO1c(pRO103)	None	++	+	+	−	++
	PAA	++	+	++	−	++
	TFD	++	+	++	−	++
	PHL	++	+	++	−	++
	3CB	++	+	++	−	++

[a] Symbols: −, no increase over basal oxygen consumption rates; +, approximately twice basal rates; ++, five times the basal rate or greater. Culture medium was MMO–0.3% CAA plus the indicated inducer.
[b] 4CC, 4-Chlorocatechol.

The degradation of PAA requires the simultaneous expression of the TFD pathway and a chromosomally encoded phenol hydroxylase. This suggests that plasmid pRO101, when maintained in a Phl^+ strain (i.e., PPO300) might be mutated to allow growth on PAA in the absence of TFD. Such a strain would reflect a mutation in either a TFD pathway regulatory gene which now recognized PAA in addition to TFD as an inducer, or a mutation that now showed constitutive expression of the TFD pathway. When we did this experiment, we obtained no PAA^+ mutants. However, in previous experiments we noted that 3CB inhibited the rate of growth, when used to induce the TFD pathway in cells growing on CAA; i.e., the growth of discrete colonies on such a medium was slower than in the absence of 3CB. From this observation we surmised that 3CB was an effective inducer of the pathway but that it was also inhibitory to growth. Thus, we reasoned that rapid growth on combined CAA-3CB medium might indicate a constitutive mutation in the plasmid, resulting in higher levels of TFD pathway enzymes and more efficient detoxification of the growth medium. When cultures of PPO300(pRO101) were plated on CAA-3CB medium, several fast-growing colonies were observed. One of these colonies, when transferred to PAA medium, grew on PAA as the sole carbon source. This isolate was designated PPO300(pRO103).

Plasmid pRO103 was mated into AEO106 and PAO1c. The induction and substrate utilization profiles of transconjugants from these matings are shown in Table 4. The TFD pathway is now constitutively expressed in strains containing plasmid pRO103 when they are grown on CAA as the sole source of carbon. In most cases TFD, TFP, and 4-chlorocatechol are degraded by these strains at comparable rates independent of prior growth in the presence of an inducer (TFD or 3CB). PAA degradation, however, occurs at substantial rates only in AEO106(pRO103) or PPO 300(pRO103), reflecting induction of their chromosomal

Downloaded from http://jb.asm.org/ on September 3, 2020 at Corteva Agriscience

COR-AAD1-00002531

Bayer EX1008 (Part 5 of 9)

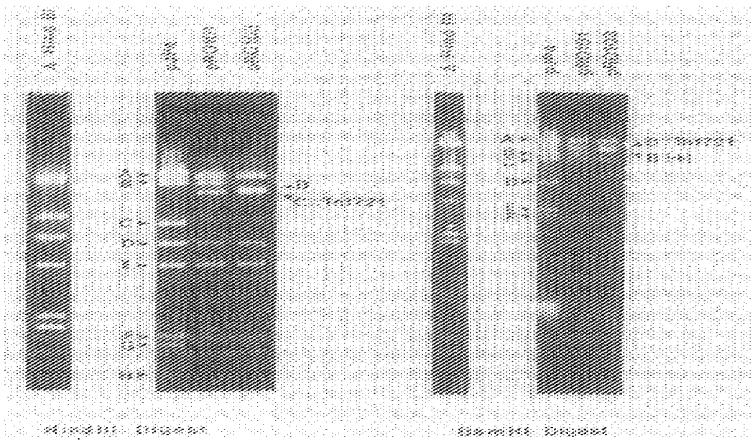


FIG. 2. Electrophoresis of TFD plasmids digested with restriction endonucleases *Hin*dIII and *Bam*HI. The plasmids are pJP4, pRO101, and pRO103. Letters to the right of the gel lanes indicate fragments altered by the insertion of the transposon Tn*1721* in pRO101 or by the deletion in pRO103. The symbol B[+] indicates the fusion of the *Bam*HI B and E fragments owing to the deletion of the two *Bam*HI sites that define the *Bam*HI F fragment (Fig. 1).

PHL hydroxylase activities by prior growth of the cells in the presence of either PAA or PHL. Rates of PAA-dependent oxygen consumption for PAO1c(pRO103), which lacks a chromosomally encoded phenol hydroxylase, are low, suggesting feedback inhibition by PHL produced from PAA. In this case, all the oxygen consumed is probably attributable only to residual feedback-inhibited activity of the first enzyme alone (i.e., the *tfdA* gene product). Some of the results in Table 4 for strain PPO300(pRO103) show less activity of the TFD pathway intermediates than expected (for example, cells grown with PAA or PHL and then reacted with TFD). This was consistent for repeated trials and may reflect the interaction of TFD pathway metabolites with chromosomal gene products in PPO300. However, the results in Table 4 for strain AEO106(pRO103) conform to those expected for the constitutive expression of the TFD pathway and direct feedback inhibition of the *tfdA* gene product by PHL. These data also show that the results corresponding to prior growth of cells on CAA (noninducing conditions) are equivalent to oxygen uptakes for cells grown in the presence of inducers.

Mapping of pRO103 with restriction endonucleases in comparison with pRO101 indicates that there has been a deletion within the *Eco*RI E fragment of pRO101 (Fig. 1). This is confirmed by digestion of pRO103 with restriction endonuclease *Bam*HI, which shows the deletion of the *Bam*HI F fragment and part of the *Bam*HI E fragment (Fig. 2). This deletion apparently eliminates a regulatory gene (*tfdR*) that imposes negative control on the TFD pathway, since in its absence, the TFD pathway is constitutive.

The TFD pathway is constitutively expressed in the three *Pseudomonas*(pRO103) species tested. It is repressed in *trans* by the presence of the *Bam*HI E but not the *Bam*HI F fragments cloned from pRO101. This was observed when the *Bam*HI E or the *Bam*HI F fragment was subcloned into plasmid pRO1727 (3), a cloning vector compatible with plasmid pRO103. Recombinant plasmids containing the *Bam*HI E or *Bam*HI F fragment were transformed into PAO1c(pRO101) and PAO1c(pRO103). The parent strain, PAO1c, was also transformed with these subclones to provide control constructions for subsequent experiments. The oxygen uptake profiles resulting from these various constructions are shown in Table 5. The negative control imposed in *trans* by the presence of the *Bam*HI E fragment is clearly demonstrated by data collected for the double construction PAO1c(pRO103, pRO1727:*Bam*HI-E), but not for the PAO1c(pRO103, pRO1727*Bam*HI-F) combination. We have recently subcloned a 1.9-kilobase fragment from the *Bam*HI E fragment extending from kilobase coordinates 17.8 to 19.7 which also imposes negative control in *trans* on the TFD pathway as described above for the *Bam*HI E

TABLE 5. Regulation of the TFD plasmids pRO101 and pRO103 in *P. aeruginosa* PAO1c

Plasmid	Inducer	Rate of O_2 uptake in presence of[a]:			
		TFD	PAA	TFP	4CC[b]
Singles					
pRO1727:*Bam*HI-E	None	0	10	0	0
	TFD	16	1	0	0
pRO1727:*Bam*HI-F	None	0	0	0	0
	TFD	7	0	0	0
Doubles					
pRO101 and pRO1727:*Bam*HI-E	None	0	0	3	0
	TFD	92	23	23	23
pRO101 and pRO1727:*Bam*HI-F	None	0	0	3	0
	TFD	78	28	20	27
pRO103 and pRO1727:*Bam*HI-E	None	0	4	9	3
	TFD	46	51	15	35
pRO103 and pRO1727:*Bam*HI-F	None	54	15	27	0
	TFD	48	9	37	26

[a] Units are nanomoles of O_2 per minute normalized to a culture optical density at 425 nm of 1.0. Culture medium was MMO with 0.3% CAA plus 0.05% TFD where indicated. Double constructions were maintained by the addition of tetracycline at 50 μg/ml and carbenicillin at 500 μg/ml.
[b] 4CC, 4-Chlorocatechol.

Downloaded from http://jb.asm.org/ on September 3, 2020 at Corteva Agriscience

COR-AAD1-00002532

Bayer EX1008 (Part 5 of 9)

fragment (B. Kaphammer, J. J. Kukor, and R. H. Olsen, Abstr. Annu. Meet. Am. Soc. Microbiol. 1988, K1, p. 206).

We noted that on solid medium containing TFD, PAO1c(pRO2321:*Bam*HI-B) accumulated an odorous phenolic compound, suggesting the accumulation of TFP. Also, overnight liquid cultures of this strain accumulated a compound detectable by UV spectroscopy under alkaline conditions. This compound exhibited an alkaline shift and peak absorption identical to those of TFP. This suggests that the *tfdA* gene, which encodes the first enzyme in the pathway, is located on the *Bam*HI B fragment. To confirm this, the *Bam*HI B fragment was subcloned into pRO1727 and transformed into *P. putida* PPO300. Since PPO300 encodes a PHL hydroxylase and the *tfdA* gene would be constitutive in the absence of the *Bam*HI E fragment, we expected that PPO300(pRO1727, pJP4:*Bam*HI-B) would grow on PAA. This was confirmed by selecting PPO300 transformants on solid medium containing PAA. We next subcloned a *Hin*dIII-*Bam*HI fragment into vector pRO1727 and again obtained PPO300 transformants growing on PAA. From these observations we conclude that the *tfdA* locus is within the kilobase coordinates 5.5 to 14.2 (Fig. 1). Accordingly, the *tfdA* locus has been mapped in this region of pJP4.

DISCUSSION

Plasmid pJP4, which encodes TFD degradation, has been transferred to numerous bacterial strains. Growth on TFD as the sole carbon source has been reported for *A. eutrophus*, *A. paradoxus*, *P. putida* (4), *P. oxalaticus* (10), and *P. cepacia* (this study). *E. coli*, *Rhodopseudomonas sphaeroides*, *Rhizobium* sp., *Agrobacterium tumefaciens*, *P. fluorescens*, and *Acinetobacter calcoaceticus* were unable to grow on TFD as the sole carbon source (4). In this study, *P. putida* and *P. aeruginosa* also were unable to grow on TFD as the sole source of carbon. However, the data presented here indicate that the enzymes encoded by the pJP4 plasmid are expressed in these *Pseudomonas* strains when grown in the presence of an additional carbon source (CAA). The previous report of Don et al. (6) suggests that the ability or inability of a particular bacterial strain to grow on TFD is determined by the presence of complementary enzymes encoded on the chromosome. Plasmid-encoded enzymes, if expressed, degrade TFD to chloromaleylacetic acid, which may be a nondegradable substrate for some bacteria. However, strains growing on TFD chromosomally encode a chloromaleylacetic acid reductase which reductively dechlorinates the substrate, producing β-ketoadipate. This is further metabolized by other chromosomally encoded enzymes.

Our data indicate that the *tfdA* gene product, TFD monooxygenase, recognizes both TFD and PAA as substrates, although their conversion to TFP and PHL, respectively may inhibit this conversion. PAA, however, is not an inducer of the TFD pathway. PAA degradation requires the presence of an inducing compound (TFD, 3CB) or the absence of the negative control gene (*tfdR*) which regulates the synthesis of the TFD monooxygenase (*tfdA* gene product). *A. eutrophus* AEO106(pRO103) and *P. putida* PPO300(pRO103) are able to degrade PAA because this regulatory gene has been deleted and the TFD monooxygenase is constitutively expressed. Furthermore, AEO106 (pRO103) and PPO300(pRO103) are able to grow on PAA as the sole carbon source because they express a chromosomally encoded PHL hydroxylase. The TFP hydroxylase encoded on the plasmid does not accept PHL as a substrate. This is demonstrated by the inability of *P. aeruginosa* PAO1c(pRO103) to metabolize or grow on PAA (data not shown) because it lacks PHL hydroxylase.

In our strains in which PHL cannot be further degraded, the accumulation of PHL inhibits the function of the TFD monooxygenase. It is not known whether this feedback inhibition occurs by simple equilibrium effects on the enzyme or by a more complicated mechanism(s) involving a binding site on the enzyme, resulting in allosteric transitions as for feedback inhibition. In any case, PHL and TFP clearly are not toxic to the metabolism of unrelated substrates.

P. aeruginosa PAO1c grows on glyoxylate as the sole source of carbon (data not shown), and glyoxylate and TFP are the products of TFD monooxygenase activity on TFD. However, PAO1c(pRO103) will not grow on the glyoxylate produced from TFD, although TFP is not toxic to growth. This enigma suggested to us initially that TFD monooxygenase might be inhibited by the product(s) of its catalysis. Such a circumstance would diminish glyoxylate production from TFD to levels insufficient to support growth. Our observations reported here correspond to this expectation and support feedback inhibition as an additional regulatory mechanism influencing TFD degradation. We believe that this is a rare example of feedback inhibition inherent to a plasmid-encoded degradative pathway.

The deletion of the regulatory gene, *tfdR*, encoded within the *Bam*HI E fragment of pRO101 and the coupling of the TFD and PHL pathways produce a hybrid pathway enabling the complete degradation of PAA (without inducing the TFD pathway). The same result could be obtained by mutation of the TFP hydroxylase to accept PHL as a substrate, but we have been unable to isolate such a mutant. Other mechanisms for PAA degradation have been proposed (17) which involve duplication of the *tfdA* gene and its mutation to accept the nonchlorinated PAA substrate (PAA). Our data suggest that a simpler explanation can be invoked.

On the basis of product accumulation (TFP) and the constitutive metabolism of PAA in PPO300(pRO1727:*Bam*HI-B), we have assigned the *tfdA* gene to a position on the *Bam*HI B fragment of plasmid pRO101. This location is congruent with the finding of Amy et al. (2) that the *tfdA* gene was on the *Hin*dIII B fragment which overlaps the *Bam*HI B fragment for a plasmid similar if not identical to pJP4 (Fig. 1). Streber et al. (20) have recently subcloned this region, identifying a 1.4 Kb subfragment which encoded the TFD monooxygenase.

ACKNOWLEDGMENT

This study was funded by the U.S. Environmental Protection Agency, Cooperative Agreement no. CR-812679.

LITERATURE CITED

1. **Altenucher, J., K. Schmid, and R. Schmitt.** 1983. Tn*1721*-encoded tetracycline resistance: mapping of structural and regulatory genes mediating resistance. J. Bacteriol. **153**:116–123.
2. **Amy, P. S., J. W. Schulke, L. M. Frazier, and R. J. Seidler.** 1985. Characterization of aquatic bacteria and cloning of genes specifying partial degradation of 2,4-dichlorophenoxyacetic acid. Appl. Environ. Microbiol. **49**:1237–1245.
3. **Cuskey, S. M., V. Pecoraro, and R. H. Olsen.** 1987. Initial Catbolism of aromatic biogenic amines by *Pseudomonas aeruginosa*: pathway description, mapping of mutations, and cloning of essential genes. J. Bacteriol. **169**:2398–2404.
4. **Don, R. H., and J. M. Pemberton.** 1981. Properties of six pesticide degradation plasmids isolated from *Alcaligenes paradoxus* and *Alcaligenes eutrophus*. J. Bacteriol. **145**:681–686.

Downloaded from http://jb.asm.org/ on September 3, 2020 at Corteva Agriscience

COR-AAD1-00002533

Bayer EX1008 (Part 5 of 9)

5. **Don, R. H., and J. M. Pemberton.** 1985. Genetic and physical map of the 2,4-dichlorophenoxyacetic acid degradative plasmid pJP4. J. Bacteriol. **161**:466–468.
6. **Don, R. H., A. J. Weightman, H.-J. Knackmuss, and K. N. Timmis.** 1985. Transposon mutagenesis and cloning analysis of the pathways for degradation of 2,4-dichlorophenoxyacetic acid and 3-chlorobenzoate in *Alcaligenes eutrophus* JMP134(pJP4). J. Bacteriol. **161**:85–90.
7. **Dorn, E., and H. J. Knackmuss.** 1978. Chemical structure and biodegradability of halogenated aromatic compounds. Two catechol 1,2-dioxygenase from a 3-chlorobenzoate grown pseudomonad. Biochem. J. **174**:73–84.
8. **Evans, W. C., B. S. W. Smith, H. N. Zernley, and J. I. Davies.** 1971. Bacterial metabolism of 2,4-dichlorophenoxyacetate. Biochem. J. **122**:543–551.
9. **Fisher, P. R., J. Appleton, and J. M. Pemberton.** 1978. Isolation and characterization of the pesticide-degrading plasmid pJP1 from *Alcaligenes paradoxus*. J. Bacteriol. **135**:798–804.
10. **Friedrich, B., M. Meyer, and H. G. Schlegel.** 1983. Transfer and expression of the herbicide-degrading plasmid pJP4 in the aerobic autotrophic bacteria. Arch. Microbiol. **134**:92–97.
11. **Ghosal, D., I.-S. You, D. K. Chatterjee, and A. M. Chakrabarty.** 1985. Microbial degradation of halogenated compounds. Science **228**:135–142.
12. **Holloway, B. W., V. Krishnapillai, and A. F. Morgan.** 1979. Chromosomal genetics of *Pseudomonas*. Microbiol. Rev. **43**: 73–102.
13. **Kaufman, D. D., and P. C. Kearney.** 1976. Microbial transformation in the soil, p. 26–64. *In* L. J. Audus (ed.), Herbicides: physiology, biochemistry, and ecology. Academic Press, Inc. (London), Ltd., London.
14. **Maniatis, T., E. F. Fritsch, and J. Sambrook.** 1982. Molecular cloning: a laboratory manual. Cold Spring Harbor Laboratory, Cold Spring Harbor, N.Y.
15. **Olsen, R. H., G. DeBusscher, and W. R. McCombie.** 1982. Development of broad-host-range vectors and gene banks: self-cloning of the *Pseudomonas aeruginosa* PAO chromosome. J. Bacteriol. **150**:60–69.
16. **Olsen, R. H., and P. Shipley.** 1973. Host range and properties of the *Pseudomonas aeruginosa* R factor R1822. J. Bacteriol. **113**: 772–780.
17. **Pemberton, J. M., B. Corney, and R. H. Don.** 1979. Evolution and spread of pesticide degrading ability among soil microorganisms, p. 287–299. *In* K. N. Timmis and A. Puhler (ed.), Plasmids of medical, environmental, and commercial importance. Elsevier Biomedical Press, Amsterdam.
18. **Schmidt, E., and H.-J. Knackmuss.** 1980. Chemical structure and biodegradability of halogenated aromatic compounds. Conversion of chlorinated muconic acids into maleylacetic acid. Biochem. J. **192**:339–347.
19. **Stanier, R. N., N. Palleroni, and M. Doudoroff.** 1966. The aerobic pseudomonads: a taxonomic study. J. Gen. Microbiol. **43**:159–271.
20. **Streber, W. R., K. N. Timmis, and M. H. Zenk.** 1987. Analysis, cloning, and high-level expression of the 2,4-dichlorophenoxyacetate monooxygenase gene *tfdA* of *Alcaligenes eutrophus* JMP134. J. Bacteriol. **169**:2950–2955.
21. **Tiedje, J. M., J. M. Duxbury, M. Alexander, and J. E. Dawson.** 1969. 2,4-D metabolism: pathway of degradation of chlorocatechols by *Arthrobacter* sp. J. Agr. Food Chem. **17**:1021–1026.

Downloaded from http://jb.asm.org/ on September 3, 2020 at Corteva Agriscience

COR-AAD1-00002534

Bayer EX1008 (Part 5 of 9)

APPLIED AND ENVIRONMENTAL MICROBIOLOGY, Feb. 2002, p. 968–972 Vol. 68, No. 2
0099-2240/02/$04.00+0 DOI: 10.1128/AEM.68.2.968–972.2002
Copyright © 2002, American Society for Microbiology. All Rights Reserved.

Chemotaxis of *Ralstonia eutropha* JMP134(pJP4) to the Herbicide 2,4-Dichlorophenoxyacetate

Andrew C. Hawkins and Caroline S. Harwood*

Department of Microbiology and Center for Biocatalysis and Bioprocessing, The University of Iowa, Iowa City, Iowa 52242

Received 29 August 2001/Accepted 22 November 2001

***Ralstonia eutropha* JMP134(pJP4) and several other species of motile bacteria can degrade the herbicide 2,4-dichlorophenoxyacetate (2,4-D), but it was not known if bacteria could sense and swim towards 2,4-D by the process of chemotaxis. Wild-type *R. eutropha* cells were chemotactically attracted to 2,4-D in swarm plate assays and qualitative capillary assays. The chemotactic response was induced by growth with 2,4-D and depended on the presence of the catabolic plasmid pJP4, which harbors the *tfd* genes for 2,4-D degradation. The *tfd* cluster also encodes a permease for 2,4-D named TfdK. A *tfdK* mutant was not chemotactic to 2,4-D, even though it grew at wild-type rates on 2,4-D.**

Most motile bacteria can sense and respond to low concentrations of organic compounds in their environment by the process of chemotaxis. There is evidence that chemotaxis can enhance biodegradation (11), presumably by rapidly bringing cells into close contact with degradable substrates. 2,4-Dichlorophenoxyacetate (2,4-D) is a widely used herbicide (Industry Task Force on 2,4-D research data [http://www.24d.org]) that can be degraded by a number of species of motile bacteria (12).

The bacterium *Ralstonia eutropha* JMP134(pJP4) grows on 2,4-D by using genes present on a self-transmissible plasmid called pJP4 (3). Plasmid pJP4 also encodes a permease for 2,4-D named TfdK (10). The predicted TfdK protein has 12 membrane-spanning regions and is a member of the aromatic acid:H^+ symporter family of the major facilitator superfamily of transport proteins (15). It is 33% identical in amino acid sequence to PcaK, a 4-hydroxybenzoate permease from *Pseudomonas putida* that is also required for chemotaxis to 4-hydroxybenzoate (2, 7, 13). The similarity of TfdK to PcaK led us to investigate if *R. eutropha* is chemotactically attracted to 2,4-D and, if so, whether *tfdK* is required for the chemotactic response.

Bacterial strains and experimental procedures. Wild-type *R. eutropha* [strain JMP134(pJP4)], a plasmid pJP4-cured derivative (strain JMP289), and a *tfdK* mutant [strain JMP134(pJP4::cba79)] (10) were obtained from J. R. van der Meer. Strains were grown on mineral salts medium (7) at 30°C with shaking at 250 rpm. Analysis by gas chromatography-mass spectrometry as previously described (17) indicated that the 2,4-D (Sigma-Aldrich, St. Louis, Mo.) used in these studies contained no detectable contaminants. Bacterial transformations were carried out according to the method of Hanahan (6).

Plasmid DNA was prepared from *Escherichia coli* with a QIAprep spin miniprep kit (Qiagen Inc., Chatsworth, Calif.). Plasmid DNA was prepared from *R. eutropha* as described previously (18). DNA fragments were purified from agarose gels with the QIAquick gel extraction kit (Qiagen Inc.).

Plasmid pHAH108, a broad-host-range plasmid designed for expression of TfdK, was constructed in several steps. First, a 1,388-bp fragment of DNA encompassing the *tfdK* gene was amplified from pJP4 by PCR and cloned into pAF7 (A. Ferrandez and C. S. Harwood, unpublished data) to form pHAH107. Plasmid pAF7 is a derivative of pT7–6 (20) that carries the *P. putida pcaK* gene fused at its predicted N terminus to a hemagglutinin (HA) epitope sequence derived from the X47 virus hemagglutinin (14) behind a transcriptional enhancer and a ribosome-binding site (RBS).

The PCR-amplified *tfdK* gene was cloned into the *Nae*I and *Bam*HI sites of pAF7, replacing the *pcaK* gene. An *Eco*RI/*Hin*dIII fragment from pHAH107 containing HA-*tfdK*, the transcriptional enhancer, and the consensus RBS was then subcloned into the broad-host-range vector pBBR1MCS-5 (9) to create pHAH108. Plasmids were introduced into *R. eutropha* by conjugation (1) from *Escherichia coli* DH5α in triparental matings using *E. coli* CC118(pRK600) (8) to provide the transfer functions. Gentamicin (20 μg per ml), chloramphenicol (100 μg per ml), and ampicillin (100 μg per ml) were added to growth media to select for plasmids in *E. coli* and *R. eutropha*. Western blot analysis (20) with anti-HA antiserum (Roche Molecular Biochemicals, Indianapolis, Ind.) was used to show that HA-TfdK was expressed in *R. eutropha* JMP134(pJP4::cba79, pHAH108).

***R. eutropha* JMP134(pJP4) cells are attracted to 2,4-D, and this is a plasmid-encoded, inducible trait.** Chemotaxis was tested with a soft agar swarm plate assay and a modified capillary assay. For the soft agar swarm plate assay, an *R. eutropha* colony was stabbed into the center of a mineral salts medium plate that contained 0.25 mM 2,4-D or 1.0 mM succinate and was solidified with 0.3% Noble agar (Difco Laboratories, Detroit, Mich.). Wild-type cells had a positive chemotactic response to succinate and to 2,4-D, as evidenced by a sharp ring of growth that formed when cells responded to the gradient of attractant that was created as they metabolized the carbon source in the plates (Fig. 1A).

Modified capillary assays allowed qualitative assessment of chemotaxis with a phase contrast microscope (5). With this

* Corresponding author. Mailing address: Department of Microbiology, 3-432 BSB, The University of Iowa, Iowa City, IA 52242. Phone: (319) 335-7783. Fax: (319) 335-7679. E-mail: caroline-harwood@uiowa.edu.

Downloaded from http://aem.asm.org/ on September 3, 2020 at Corteva Agriscience

COR-AAD1-00002535
Bayer EX1008 (Part 5 of 9)

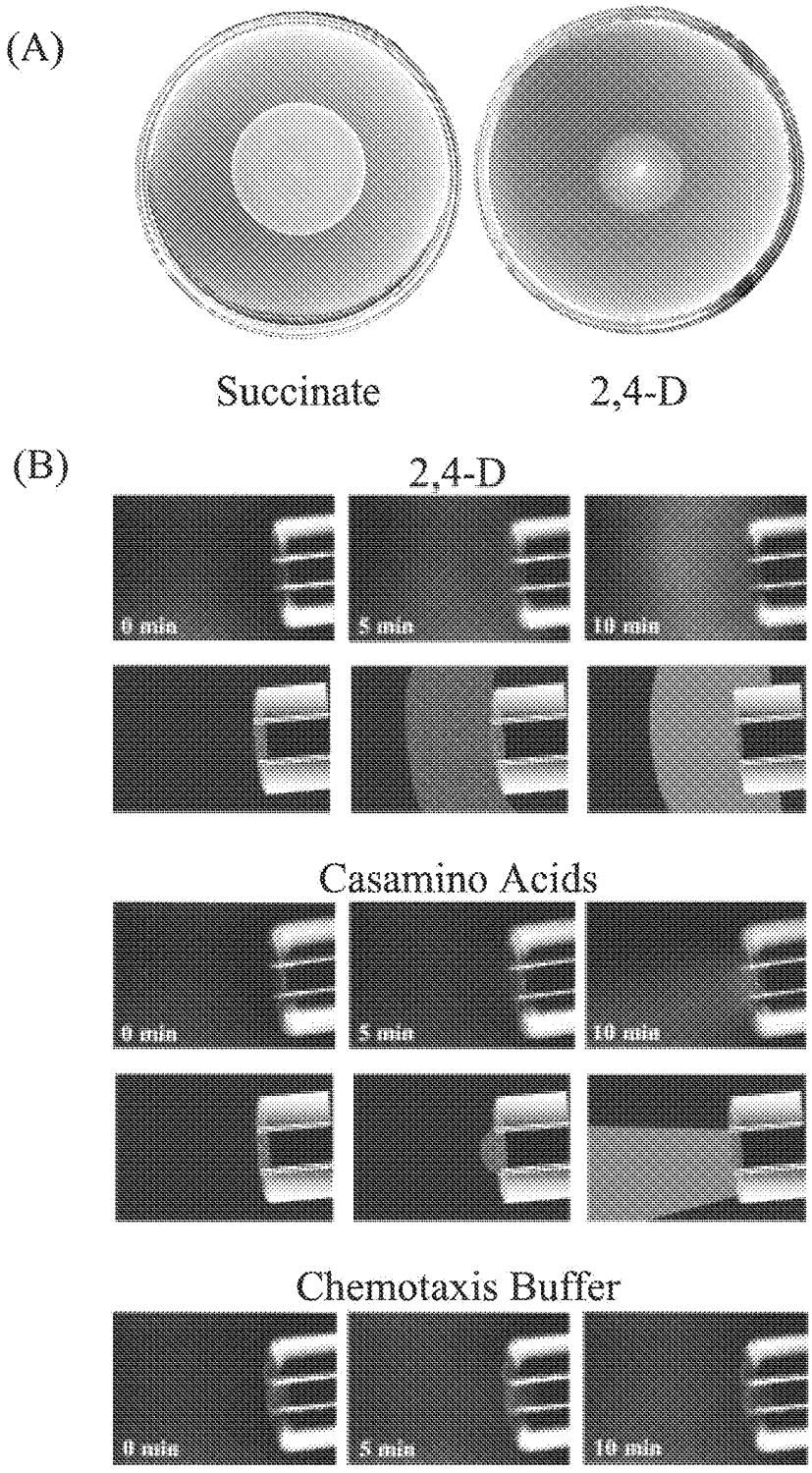


FIG. 1. Chemotactic response of *R. eutropha* JMP134(pJP4). (A) Chemotactic rings formed by wild-type cells on soft agar swarm plates containing 0.5 mM succinate (left) or 0.25 mM 2,4-D (right). Plates were inoculated by stabbing motile cells in the center of the plate at a point corresponding to the center of the swarm ring and incubated for 24 to 48 h at 30°C. (B) Attraction of wild-type cells in a modified capillary assay. Cells were grown on 3 mM 2,4-D. Capillaries contained 10 mM 2,4-D, 1% Casamino Acids, or no attractant (chemotaxis buffer). Chemotactic responses are shown in photographic form (top) and illustrative form (bottom). Illustrations for chemotaxis buffer were omitted because no response was observed.

Downloaded from http://aem.asm.org/ on September 3, 2020 at Corteva Agriscience

COR-AAD1-00002536
Bayer EX1008 (Part 5 of 9)

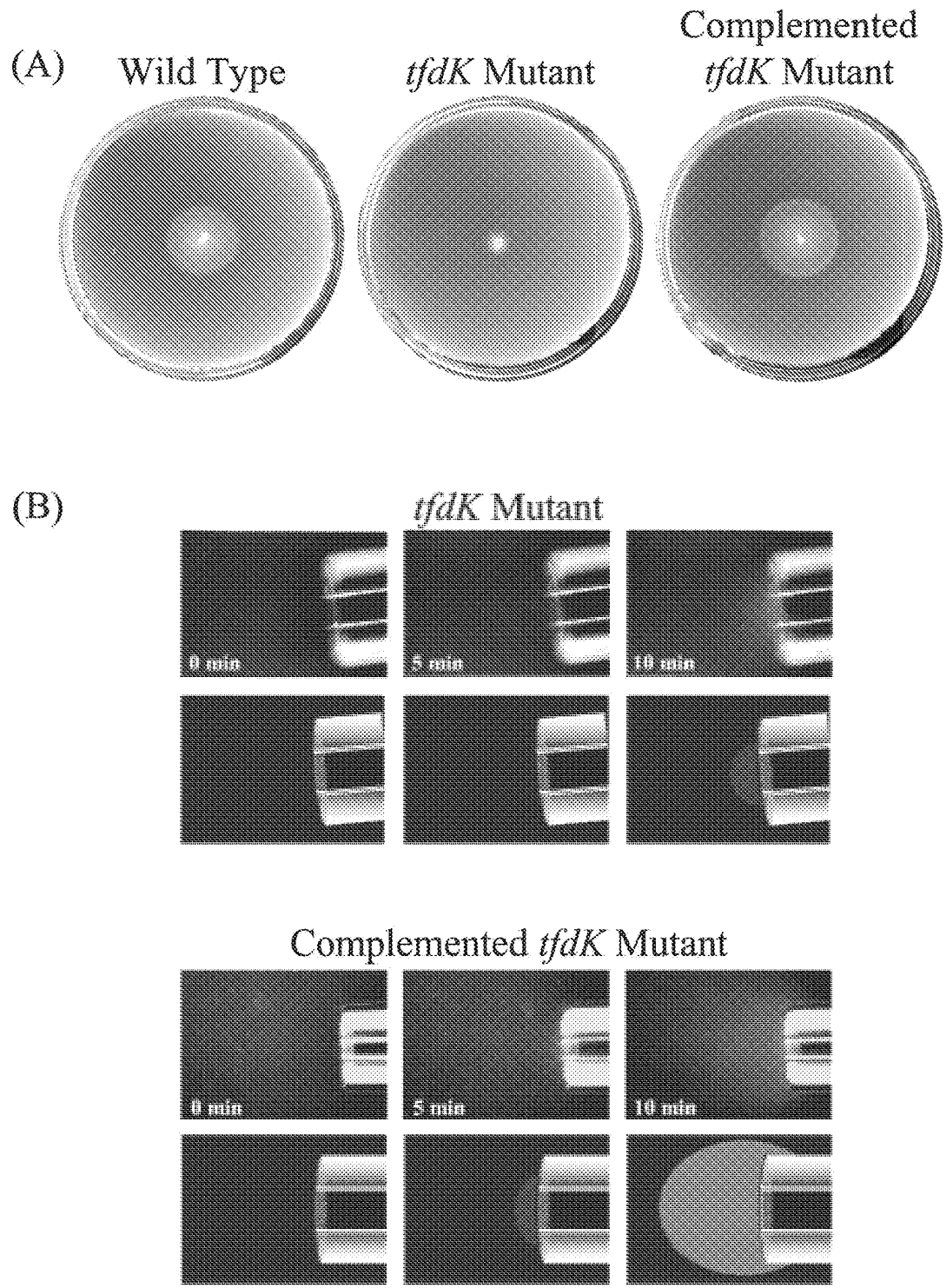


FIG. 2. Response of a *tfdK* mutant to 2,4-D. (A) Chemotactic swarms formed by wild-type cells, the *tfdK* mutant, and the *tfdK* mutant expressing the *tfdK* gene in *trans* on swarm plates containing 0.25 mM 2,4-D. (B) Modified capillary assays showing the response of *tfdK* mutant cells and complemented *tfdK* mutant cells to 2,4-D. Both strains were grown on 3 mM 2,4-D. Results are shown in photographic form (top) and illustrative form (bottom).

Downloaded from http://aem.asm.org/ on September 3, 2020 at Corteva Agriscience

COR-AAD1-00002537
Bayer EX1008 (Part 5 of 9)

method, chemotaxis can be visualized in the absence of metabolism of the attractant. Capillaries (1 μl) contained attractant in 1% low-melting-temperature agarose dissolved in chemotaxis buffer (50 mM potassium phosphate [pH 7.0], 20 μM EDTA, 0.05% glycerol). Cells that had been grown in mineral medium (7) containing 3 mM 2,4-D, 10 mM succinate, or 10 mM succinate plus 0.5 mM 2,4-D were harvested in the midlogarithmic phase of growth and suspended in chemotaxis buffer to a final A_{660} of approximately 0.1. Samples of the cell suspension were placed in a chamber formed by a microscope slide, a glass U-tube, and a cover slip, and the capillary containing the attractant was inserted into the suspension. Cell behavior around the tip of the capillary was observed at a final magnification of ×40 and photographed at 0 min, 5 min, and 10 min. Modified capillary assays were repeated at least five times for each condition tested with reproducible results.

R. eutropha wild-type cells formed visible clouds of turbidity as they accumulated around the open tips of capillaries that contained either 10 mM 2,4-D or 1% Casamino Acids (Fig. 1B). Wild-type cells also accumulated around the open tips of capillaries that contained 1 mM 2,4-D, but this response was less dramatic and difficult to photograph (data not shown). Chemotaxis buffer, used as a control, did not elicit a chemotactic response from *R. eutropha* in the modified capillary assay. *R. eutropha* JMP134(pJP4) cells that had been grown in 10 mM succinate did not respond to 2,4-D in modified capillary assays. However, these cells were attracted to 2,4-D when grown on 10 mM succinate plus 0.5 mM 2,4-D (data not shown). This indicates that chemotaxis to 2,4-D was induced by growth with 2,4-D. *R. eutropha* cells that had been cured of the pJP4 plasmid (strain JMP289) and grown on 10 mM succinate plus 0.5 mM 2,4-D showed little or no attraction to 2,4-D in a modified capillary assay (data not shown). This indicates that 2,4-D chemotaxis is a plasmid-encoded trait.

***tfdK* gene is required for chemoattraction to 2,4-D.** TfdK is a membrane-spanning protein that catalyzes the active transport of 2,4-D into cells. The TfdK permease allows cells to take up very low concentrations of 2,4-D, but it is not essential for entry of 2,4-D into cells, as 2,4-D can cross the cell membrane of *R. eutropha* by simple diffusion (10). When 2,4-D was supplied at a concentration of 3 mM, the *tfdK* mutant had a specific growth rate with 2,4-D ($0.324 \pm 0.064\ h^{-1}$) that was nearly identical to that of the wild type ($0.333 \pm 0.044\ h^{-1}$). A *tfdK* mutant did not form chemotactic rings in soft agar swarm plates containing 2,4-D, even after incubation for 2 days (Fig. 2A). Instead, the cells formed a fuzzy, slow-moving ring that reflected random movement of motile cells.

tfdK mutant cells that had been grown on 3 mM 2,4-D were attracted to 1% Casamino Acids but not to 10 mM 2,4-D in modified capillary assays (Fig. 2B). The *tfdK* mutant sometimes had a slight positive response to 2,4-D, but this response was no greater than that exhibited by cells of the pJP4-cured strain, JMP289, that had been grown under the same conditions (10 mM succinate plus 0.5 mM 2,4-D).

When the TfdK protein was expressed in *trans* from plasmid pHAH108 in the *tfdK* mutant, cells formed chemotactic rings on 2,4-D swarm plates (Fig. 2A) and were attracted to 2,4-D in modified capillary assays (Fig. 2B). The vector pBBR1MCS-5 did not complement the *tfdK* mutant in chemotaxis assays.

Conclusions. The coordinate regulation of 2,4-D chemotaxis with 2,4-D degradation suggests that chemotaxis may be an integral feature of the biodegradation of 2,4-D by *R. eutropha*. Various strains of *Pseudomonas* can sense and swim towards the pollutants benzene, toluene, trichloroethylene, and naphthalene as well as to the aromatic acid 4-hydroxybenzoate (4, 5, 7, 16). Chemotaxis to these compounds requires prior growth with toluene (for the benzene, toluene, and trichloroethylene responses), naphthalene, or 4-hydroxybenzoate. The coregulation of chemotaxis and degradation often reflects the coordinate induction of a chemoreceptor gene with degradation genes.

Recently, a methyl-accepting chemotaxis protein (MCP) gene required for chemotaxis to naphthalene was found to be cotranscribed with *meta*-cleavage pathway genes present on the NAH7 catabolic plasmid for naphthalene degradation (5). MCPs have been well studied in *E. coli* and *Salmonella* spp., in which they serve as cell surface receptors for chemoattractants. On binding an attractant, an MCP undergoes a conformational change that initiates sensory signal transduction by altering the activity of CheA, an associated sensor kinase. CheA-P then acts as a phosphodonor for the response regulator, CheY, which interacts with rotational switch proteins in the flagellar motors. This causes a change in swimming behavior so that cells migrate towards chemoattractants (19).

The data presented here suggest that plasmid pJP4 for 2,4-D degradation also encodes a chemoreceptor protein that is coordinately regulated with 2,4-D degradation genes. However, this protein, TfdK, does not resemble an MCP. Instead, it is homologous to PcaK, a protein that in *P. putida* functions in the transport of 4-hydroxybenzoate as well as in chemotaxis to 4-hydroxybenzoate (2, 13). TfdK is thus a second example of a major facilitator superfamily transport protein that has dual roles in transport and in chemotaxis.

We do not understand how either PcaK or TfdK functions in chemotaxis. These permeases could play a direct role in signaling and communicate a conformational change in protein structure that occurs on ligand binding or transport to a physically associated MCP or other chemosensory protein. Alternatively, they may have a more indirect role in chemotaxis. Since 2,4-D can diffuse into *R. eutropha* at rates sufficient to support wild-types rates of growth under the conditions in which 2,4-D chemotaxis was measured, simple accumulation of this aromatic acid within cells does not appear to be sufficient for chemotaxis to occur; TfdK must be present. A more likely scenario for an indirect role is that TfdK functions in chemotaxis by delivering a high local concentration of chemoattractant to chemosensory proteins present on the cytoplasmic side of the cell membrane.

We thank Jan Roelof van der Meer for supplying strains used in this study, Rebecca Parales for helpful discussions, and Juan Parales for assistance with GC-MS analysis.

This work was supported by Public Health Service grant GM56665 from the National Institute of General Medical Sciences. A.C.H. has been supported by a National Science Foundation Research Training Grant (DBI9602247) and by a fellowship from the University of Iowa Center for Biocatalysis and Bioprocessing.

REFERENCES

1. **de Lorenzo, V., and K. N. Timmis.** 1994. Analysis and construction of stable phenotypes in gram-negative bacteria with Tn *5*- and Tn *10*-derived minitransposons. Methods Enzymol. 235:386–405.

Downloaded from http://aem.asm.org/ on September 3, 2020 at Corteva Agriscience

COR-AAD1-00002538
Bayer EX1008 (Part 5 of 9)

2. **Ditty, J. L., and C. S. Harwood.** 1999. Conserved cytoplasmic loops are important for both the transport and chemotaxis functions of PcaK, a protein from *Pseudomonas putida* with 12 membrane-spanning regions. J. Bacteriol. **181:**5068–5074.
3. **Don, R. H., and J. M. Pemberton.** 1985. Genetic and physical map of the 2,4-dichlorophenoxyacetic acid-degradative plasmid pJP4. J. Bacteriol. **161:** 466–468.
4. **Grimm, A. C., and C. S. Harwood.** 1997. Chemotaxis of *Pseudomonas* spp. to the polyaromatic hydrocarbon naphthalene. Appl. Environ. Microbiol. **63:** 4111–4115.
5. **Grimm, A. C., and C. S. Harwood.** 1999. NahY, a catabolic plasmid-encoded receptor required for chemotaxis of *Pseudomonas putida* to the aromatic hydrocarbon naphthalene. J. Bacteriol. **181:**3310–3316.
6. **Hanahan, D.** 1983. Studies on transformation of *Escherichia coli* with plasmids. J. Mol. Biol. **166:**557–580.
7. **Harwood, C. S., N. N. Nichols, M. K. Kim, J. L. Ditty, and R. E. Parales.** 1994. Identification of the *pcaRKF* gene cluster from *Pseudomonas putida*: involvement in chemotaxis, biodegradation, and transport of 4-hydroxybenzoate. J. Bacteriol. **176:**6479–6488.
8. **Kessler, B., V. de Lorenzo, and K. N. Timmis.** 1992. A general system to integrate *lacZ* fusions into the chromosomes of gram-negative eubacteria: regulation of the *Pm* promoter of the *TOL* plasmid studied with all controlling elements in monocopy. Mol. Gen. Genet. **233:**293–301.
9. **Kovach, M. E., P. H. Elzer, D. S. Hill, G. T. Robertson, M. A. Farris, R. M. Roop, 2nd, and K. M. Peterson.** 1995. Four new derivatives of the broad-host-range cloning vector pBBR1MCS, carrying different antibiotic-resistance cassettes. Gene **166:**175–176.
10. **Leveau, J. H., A. J. Zehnder, and J. R. van der Meer.** 1998. The *tfdK* gene product facilitates uptake of 2,4-dichlorophenoxyacetate by *Ralstonia eutropha* JMP134(pJP4). J. Bacteriol. **180:**2237–2243.
11. **Marx, R. B., and M. D. Aitken.** 2000. Bacterial chemotaxis enhances naphthalene degradation in a heterogeneous aqueous system. Environ. Sci. Technol. **34:**3379–3383.
12. **McGowan, C., R. Fulthorpe, A. Wright, and J. M. Tiedje.** 1998. Evidence for interspecies gene transfer in the evolution of 2,4-dichlorophenoxyacetic acid degraders. Appl. Environ. Microbiol. **64:**4089–4092.
13. **Nichols, N. N., and C. S. Harwood.** 1997. PcaK, a high-affinity permease for the aromatic compounds 4-hydroxybenzoate and protocatechuate from *Pseudomonas putida*. J. Bacteriol. **179:**5056–5061.
14. **Niman, H. L., R. A. Houghten, L. E. Walker, R. A. Reisfeld, I. A. Wilson, J. M. Hogle, and R. A. Lerner.** 1983. Generation of protein-reactive antibodies by short peptides is an event of high frequency: implications for the structural basis of immune recognition. Proc. Natl. Acad. Sci. USA **80:**4949–4953.
15. **Pao, S. S., I. T. Paulsen, and M. H. Saier, Jr.** 1998. Major facilitator superfamily. Microbiol. Mol. Biol. Rev. **62:**1–34.
16. **Parales, R. E., J. L. Ditty, and C. S. Harwood.** 2000. Toluene-degrading bacteria are chemotactic towards the environmental pollutants benzene, toluene, and trichloroethylene. Appl. Environ. Microbiol. **66:**4098–4104.
17. **Resnick, S. M., and D. T. Gibson.** 1996. Regio- and stereospecific oxidation of 9,10-dihydroanthracene and 9,10-dihydrophenanthrene by naphthalene dioxygenase: structure and absolute stereochemistry of metabolites. Appl. Environ. Microbiol. **62:**3355–3359.
18. **Sambrook, J., E. F. Fritsch, and T. Maniatis.** 1989. Molecular cloning: a laboratory manual, 2nd ed. Cold Spring Harbor Laboratory Press, Cold Spring Harbor, N.Y.
19. **Stock, J. B., and M. G. Surette.** 1996. Chemotaxis, p. 1103–1129. *In* F. C. Neidhardt, R. Curtiss III, J. L. Ingraham, E. C. C. Lin, K. B. Low, B. Magasanik, W. S. Reznikoff, M. Riley, and M. Schaechter (ed.), *Escherichia coli* and *Salmonella*: cellular and molecular biology, 2nd ed., vol. 1. American Society for Microbiology, Washington, D.C.
20. **Tabor, S., and C. C. Richardson.** 1985. A bacteriophage T7 RNA polymerase/promoter system for controlled exclusive expression of specific genes. Proc. Natl. Acad. Sci. USA **82:**1074–1078.

Downloaded from http://aem.asm.org/ on September 3, 2020 at Corteva Agriscience

COR-AAD1-00002539
Bayer EX1008 (Part 5 of 9)

Herbicide-Degrading α-Keto Acid-Dependent Enzyme TfdA: Metal Coordination Environment and Mechanistic Insights†

Eric L. Hegg,‡,§ Adam K. Whiting,‡ Ruth E. Saari,‖ John McCracken,*,⊥ Robert P. Hausinger,*,‖ and Lawrence Que, Jr.*,‡

Department of Chemistry and Center for Metals in Biocatalysis, University of Minnesota, Minneapolis, Minnesota 55455, Departments of Microbiology and Biochemistry, Michigan State University, East Lansing, Michigan 48824, and Department of Chemistry, Michigan State University, East Lansing, Michigan 48824

Received August 3, 1999; Revised Manuscript Received October 12, 1999

ABSTRACT: TfdA is a non-heme iron enzyme which catalyzes the first step in the oxidative degradation of the widely used herbicide (2,4-dichlorophenoxy)acetate (2,4-D). Like other α-keto acid-dependent enzymes, TfdA utilizes a mononuclear Fe(II) center to activate O_2 and oxidize substrate concomitant with the oxidative decarboxylation of α-ketoglutarate (α-KG). Spectroscopic analyses of various Cu(II)-substituted and Fe(II)-reconstituted TfdA complexes via electron paramagnetic resonance (EPR), electron spin−echo envelope modulation (ESEEM), and UV−vis spectroscopies have greatly expanded our knowledge of the enzyme's active site. The metal center is coordinated to two histidine residues as indicated by the presence of a five-line pattern in the Cu(II) EPR signal, for which superhyperfine splitting is attributed to two equivalent nitrogen donor atoms from two imidazoles. Furthermore, a comparison of the ESEEM spectra obtained in H_2O and D_2O demonstrates that the metal maintains several solvent-accessible sites, a conclusion corroborated by the increase in multiplicity in the EPR superhyperfine splitting observed in the presence of imidazole. Addition of α-KG to the Cu-containing enzyme leads to displacement of an equatorial water on copper, as determined by ESEEM analysis. Subsequent addition of 2,4-D leads to the loss of a second water molecule, with retention of a third, axially bound water. In contrast to these results, in Fe(II)-reconstituted TfdA, the cosubstrate α-KG chelates to the metal via a C-1 carboxylate oxygen and the α-keto oxygen as revealed by characteristic absorption features in the optical spectrum of Fe−TfdA. This binding mode is maintained in the presence of substrate, although the addition of 2,4-D does alter the metal coordination environment, perhaps by creating an O_2-binding site via solvent displacement. Indeed, loss of solvent to generate an open binding site upon the addition of substrate has also been suggested for the α-keto acid-dependent enzyme clavaminate synthase 2 [Zhou et al. (1998) *J. Am. Chem. Soc. 120*, 13539−13540]. Nitrosyl adducts of various Fe−TfdA complexes have also been investigated by optical and EPR spectroscopy. Of special interest is the tightly bound NO complex of Fe−TfdA·(α-KG)·(2,4-D), which may represent an accurate model of the initial oxygen-bound species.

Downloaded via CORTEVA AGRISCIENCE on September 3, 2020 at 18:40:01 (UTC).
See https://pubs.acs.org/sharingguidelines for options on how to legitimately share published articles

α-Keto acid-dependent enzymes are the largest class of mononuclear non-heme iron oxygen-activating enzymes, catalyzing the oxidation of aliphatic C−H bonds in reactions that are even more diverse and varied (*1*−*3*) than those performed by the cytochromes P-450 and methane monooxygenase. The array of reactions catalyzed includes the posttranslational hydroxylation of amino acid side chains during collagen biosynthesis, the conversion of thymine to 5-hydroxymethyluracil in pyrimidine catabolism, the oxidative cyclization of proclavaminate in the biosynthesis of a clinically important β-lactamase inhibitor, and the synthesis of carnitine, a substance critical for both fatty acid anabolism and catabolism (*1*−*3*). The general reaction catalyzed by α-keto acid-dependent enzymes (Scheme 1) involves the oxidative decarboxylation of an α-keto acid cosubstrate, typically α-ketoglutarate (α-KG),[1] concomitant with the oxidation of the primary substrate (*2*). Detailed kinetic data on a number of α-keto acid-dependent enzymes indicate that they utilize an ordered binding mechanism, whereby iron binds first, followed by α-KG, and then either substrate or O_2, the order of which is enzyme dependent (*4*−*7*). The exact

† Financial support was provided by NIH grants GM33162 (L. Q.) and GM54065 (J. M.), an NIH postdoctoral fellowship for E. L. H. (GM18639), NSF grant MCB 9603520 (R. P. H.), and the Michigan State University Agricultural Experiment Station (R. P. H.).

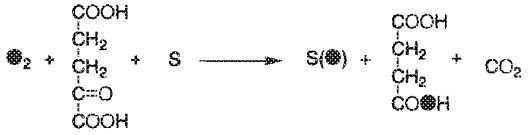
* To whom correspondence should be addressed.
‡ University of Minnesota.
§ Present address: Department of Chemistry, University of Utah, Salt Lake City, UT 84112.
‖ Departments of Microbiology and Biochemistry, Michigan State University.
⊥ Department of Chemistry, Michigan State University.

[1] Abbreviations: CS2, clavaminate synthase 2; 2,4-D, (2,4-dichlorophenoxy)acetate; DAOCS, deacetoxycephalosporin C synthase; EDTA, ethylenediaminetetraacetic acid; EPR, electron paramagnetic resonance; ESEEM, electron spin−echo envelope modulation; EXAFS, extended X-ray absorption fine structure; fwhm, full width at half-maximum; HPPD, 4-hydroxyphenylpyruvate dioxygenase; IPNS, isopenicillin N synthase; α-KG, α-ketoglutarate; MLCT, metal-to-ligand charge transfer; Mops, 4-morpholinepropanesulfonic acid; TauD, taurine/α-KG dioxygenase; TfdA, (2,4-dichlorophenoxy)acetate/α-KG dioxygenase.

10.1021/bi9917961 CCC: $18.00 © 1999 American Chemical Society
Published on Web 11/18/1999

COR-AAD1-00002540
Bayer EX1008 (Part 5 of 9)

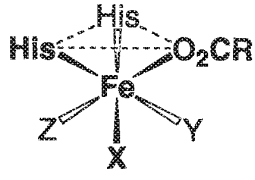
Scheme 1: General Reaction Performed by α-Keto Acid-Dependent Enzymes



mechanism utilized by this class of enzymes, however, is currently unknown.

The crystal structures of two α-keto acid-dependent enzymes have recently been reported. Deacetoxycephalosporin C synthase (DAOCS), which catalyzes the transformation of penicillin N to deacetoxycephalosporin (*8*, *9*), contains a mononuclear iron center ligated to two histidines and an aspartate, while the structure of 4-hydroxyphenylpyruvate dioxygenase (HPPD), an enzyme involved in the catabolism of tyrosine, reveals a mononuclear iron coordinated to two histidines and a glutamate (*10*). These are the only endogenous ligands, which, in both cases, occupy a single face of the polyhedron. Interestingly, the active site of DAOCS and HPPD contain a number of structural features which are common to other crystallographically characterized mononuclear, non-heme iron enzymes including the extradiol ring-cleaving catechol dioxygenases 2,3-dihydroxybiphenyl 1,2-dioxygenase (*11*, *12*), catechol 2,3-dioxygenase (*13*), and protocatechuate 4,5-dioxygenase (*14*), the pterin-dependent tyrosine (*15*) and phenylalanine (*16*) hydroxylases, the Rieske-type naphthalene 1,2-dioxygenase (*17*), and isopenicillin N synthase (IPNS) (*18*). These common features include a "2-His−1-carboxylate facial triad" as the endogenous ligand set and the availability of three cis-oriented coordination sites for the binding of exogenous ligands (*19*) (Figure 1). An attractive hypothesis for the prevalence of this conserved structural motif in non-heme iron oxygen-activating enzymes is that the Fe(II) center has the flexibility to coordinate both substrate and O_2 (*19*). Furthermore, in contrast to heme enzymes, the cis-orientation of the available coordination sites on non-heme iron enzymes may allow intramolecular attack by the reactive oxygen species on the coordinated substrate (*19*).

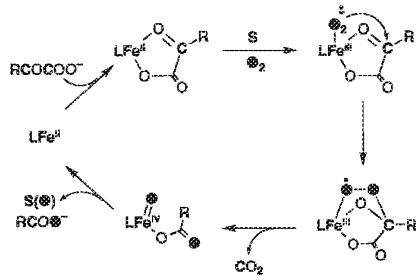
The crystal structure of the DAOCS·(α-KG) complex has also been reported and reveals α-KG to be ligated to the iron center through a C-1 carboxylate oxygen and the α-keto oxygen (*9*). This binding motif, which was anticipated by biomimetic complexes (*20*−*22*) and has recently been proposed for α-KG binding to clavaminate synthase 2 (CS2) (*23*, *24*), maintains one available coordination site on the iron, presumably for coordinating O_2. Binding of O_2 to the Fe(II) center is proposed to generate a metal-coordinated



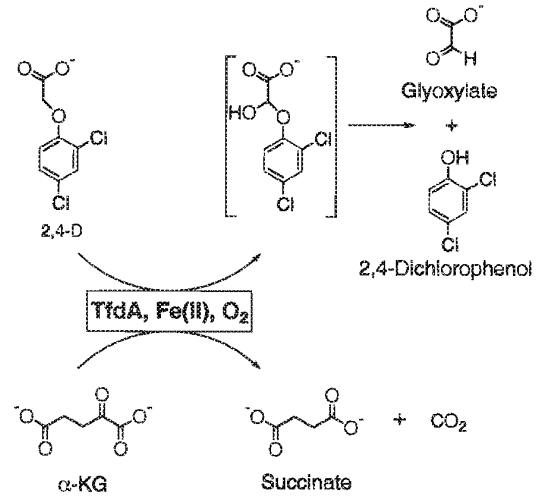
R = Glu or Asp

FIGURE 1: The 2-His-1-carboxylate facial triad utilized by many O_2-activating mononuclear non-heme iron enzymes.

Scheme 2: Proposed Reaction Mechanism for α-Keto Acid-dependent Enzymes



Scheme 3: Reaction Catalyzed by TfdA



superoxide which may then attack the α-carbon of α-KG to initiate oxidative decarboxylation and formation of a putative high valent iron−oxo species (*20*, *21*, *25*, *26*), the species postulated to be responsible for the subsequent oxidation reaction (Scheme 2).

To gain further insight into the iron coordination environment and the mechanism of oxygen activation by α-keto acid-dependent enzymes, we have performed extensive spectroscopic studies on 2,4-dichlorophenoxyacetate/α-KG dioxygenase (TfdA). This enzyme catalyzes the first step in the biodegradation of the widely used herbicide 2,4-dichlorophenoxyacetate (2,4-D), as illustrated in Scheme 3 (*27*, *28*). TfdA possesses a His-X-Asp-$X_{(51)}$-His sequence motif (*29*), much like that found in IPNS and DAOCS; for the latter two enzymes these residues are known to function in metal ligation (*9*, *18*, *30*). While it is tempting to assume from the presence of this motif that TfdA also utilizes these same endogenous ligands, caution is warranted since TfdA displays very limited sequence homology to either of the other two enzymes. DAOCS, on the other hand, exhibits considerable sequence (20.6% identity and 32.2% similarity according to the comparison program GAP) and structural homology with IPNS (*9*). Therefore, understanding the iron coordination environment and mechanism of the herbicide-degrading TfdA has obvious importance not only in the area of bioremediation but also in the general understanding of how this varied and ubiquitous class of enzymes binds and activates dioxygen. We describe herein our spectroscopic studies on TfdA and place these results in perspective with

COR-AAD1-00002541
Bayer EX1008 (Part 5 of 9)

other data recently obtained on this class of enzymes (*8*, *9*, *18*, *23*, *24*, *31*, *32*).

EXPERIMENTAL SECTION

Chemicals. Ferrous ammonium sulfate [$Fe(NH_4)_2(SO_4)_2$] and Mops were purchased from Sigma (St. Louis, MO), while 2,4-D, $CuCl_2 \cdot 2H_2O$ and the monosodium salt of α-KG were all obtained from Aldrich (Milwaukee, WI). Isotopically pure cupric oxide (^{63}CuO) was purchased from Cambridge Isotope Laboratories (Andover, MA). Argon and nitric oxide gas cylinders were obtained from Airgas, Inc. (Radnor, PA) and Matheson Gas Products, Inc. (Parsippany, NJ), respectively. All solutions were prepared with water, which was purified by passage through a Millipore (Bedford, MA) purification system.

Enzyme Isolation. The homodimeric 64 kDa enzyme TfdA was purified from *Escherichia coli* DH5α cells carrying the *Ralstonia eutropha* (formerly *Alcaligenes eutrophus*) JMP134 *tfdA* gene on a pUS311 plasmid as previously described (*27*). TfdA apoprotein was concentrated via centrifugation using Centricon-10 or Centricon-30 concentrators from Amicon. Buffer exchange was accomplished either via repeated concentration/dilution steps or using PD-10 desalting columns from Amersham Pharmacia Biotech (Wikströms, Sweden). Protein concentrations were ascertained using the Bio-Rad (Hercules, CA) assay utilizing bovine serum albumin as a standard. Alternatively, protein concentrations were assessed from the absorbance at 280 nm using a calculated (*33*) ϵ_{280} of 30 600 M^{-1} cm^{-1} per subunit (or 1.0 $AU_{280} \approx 0.96$ mg/mL) based on the amino acid sequence which contains 7 tyrosines, 4 tryptophans, and 13 phenylalanines (*29*).

Activity Assays. The specific activity of TfdA was assessed by reacting the product 2,4-dichlorophenol with 4-aminoantipyrine to give a colored product that was monitored spectrophotometrically (*27*). Alternatively, the activity was assayed by measuring O_2 uptake using a Gilson (Middleton, WI) model K-ICT C Oxygraph containing a 1.5 mL cell equipped with a YSI (Yellow Springs, OH) model 5331 Oxygen Probe, which reduces O_2 to water at the electrode surface; the oxygraph was calibrated by adding concentrated protocatechuate 3,4-dioxygenase to a known quantity of the substrate protocatechuate. Oxygen-uptake reactions were performed with an enzyme concentration of 1−10 μM subunit at 25 °C in 25 mM Mops buffer at pH 6.9. In a typical assay, anaerobic concentrated iron(II)-reconstituted TfdA was added to a stirring aerobic solution containing 66 μM α-KG, 0.33 mM 2,4-D, and 50 μM sodium ascorbate as a reductant.

Preparation of Cu−TfdA Samples. TfdA was reconstituted with copper by the slow addition of an aqueous $CuCl_2$ solution to TfdA apoprotein in 25 mM Mops buffer at pH 6.9 (rapid addition leads to some precipitation of protein). Substoichiometric amounts of copper (0.9 equiv/subunit) were added relative to the enzyme concentration, and electron paramagnetic resonance (EPR) spin quantitation indicated that all of the Cu^{2+} ions were bound to the enzyme. Samples containing α-KG and/or 2,4-D were prepared by the addition of 10 equiv of the appropriate substrate (in 25 mM Mops buffer at pH 6.9) to the Cu−TfdA solution. Typical sample concentrations were 500 μM TfdA subunit, 450 μM Cu^{2+}, 5.0 mM α-KG, and 5.0 mM 2,4-D. In cases where exogenous imidazole was added to the solution, the imidazole/copper ratio was maintained at 15. Isotopically pure [^{63}Cu]TfdA samples were prepared in an identical fashion except that $^{63}CuCl_2$ was prepared from ^{63}CuO by dissolving the cupric oxide in a minimal volume of concentrated HCl, then diluted with H_2O and adjusted to approximately pH 4 using NaOH(aq), yielding a final $^{63}CuCl_2$ stock concentration of 12 mM. Dual samples for electron spin−echo envelope modulation (ESEEM) spectroscopy were prepared in H_2O/D_2O at pH/pD 7.0 using $CuCl_2$ as described above except that the concentration of buffer was 50 mM and only 5 equiv of α-KG and 2,4-D were utilized.

Preparation of Fe−TfdA Samples. All samples were prepared anaerobically in an ice bath to prevent enzyme turnover, oxidative inactivation (*34*), and autoxidation of Fe^{2+}. TfdA solutions were made anaerobic by placing a small volume of concentrated TfdA (approximately 50−100 μL in 100 mM Mops buffer, pH 6.9 at 4 °C) in a heart-shaped Schlenk flask followed by two rapid vacuum/argon cycles. The enzyme was then allowed to equilibrate under Ar while stirring for approximately 15 min, followed by an additional 15 min of stirring under an Ar stream. All other solutions were prepared using standard Schlenk vacuum line techniques and contained 100 mM Mops buffer, pH 6.9, at 4 °C. TfdA apoprotein was reconstituted by the addition of a substoichiometric quantity of iron (0.8−0.9 equiv) from an ice-cold $Fe(NH_4)_2(SO_4)_2$ solution using gastight Hamilton syringes (Reno, NV). Samples containing α-KG and/or 2,4-D (5.0 equiv) were prepared by anaerobic addition of a concentrated buffered solution of the appropriate substrate to the Fe−TfdA solution. Typical TfdA concentrations ranged from 0.3 to 0.6 mM subunit for optical spectroscopy and 0.1 to 0.4 mM for EPR spectroscopy.

Preparation of NO Samples. Fe−TfdA solutions were briefly incubated with nitric oxide (NO) gas in either a Schlenk flask or Schlenk cuvette via headspace diffusion using standard Schlenk vacuum line techniques. The solutions were gently mixed until the samples exhibited the brillant yellow color characteristic of iron−nitrosyl complexes. Excess NO was removed by vacuum. To ensure that adventitous nitric acid was not introduced into the sample, the gas line was equipped with a column of NaOH pellets to "scrub" the NO and the line was purged with Ar for 30 min before using. ***Caution***: NO is a poisonous gas and should only be used with proper ventilation.

Electron Paramagnetic Resonance (EPR) Spectroscopy. X-band EPR spectra were recorded using either a Varian E−109 spectrometer or a Bruker E-500 spectrometer, both of which were equipped with an Oxford Instruments ESR-10 liquid helium cryostat. Samples were placed into 0.3 mm i.d. quartz tubes and frozen in liquid nitrogen. Cu−TfdA spectra were acquired at 20 K using a power of 0.20 mW. In general, the spectra were obtained as 4.0 min scans from 2200 to 2800 G using a time constant of 0.128 s, a modulation amplitude of 10 G, and a modulation frequency of 100 kHz. To obtain high-resolution spectra of the farthest downfield $g_{\parallel}$ hyperfine line of Cu−TfdA, 4.0 min scans were obtained from 2560 to 2640 G using a time constant of 2.0 s, a modulation amplitude of 2.0 G, and a modulation

COR-AAD1-00002542
Bayer EX1008 (Part 5 of 9)

frequency of 100 kHz. The high-resolution EPR spectra were fit using the program QPOWA (*35*). Nitrosyl Fe−TfdA spectra were collected as 168 s scans at 8.0 K from 0 G to 5000G at a power of 0.20 mW using a time constant of 0.164 s, a modulation amplitude of 10 G, and a modulation frequency of 100 kHz. Spin quantification of both Cu−TfdA and Fe−TfdA samples was performed by integrating the EPR absorption spectra and comparing the results with that of an aqueous CuEDTA solution of known concentration (*36*). In performing the spin quantifications, appropriate corrections were made for different EPR parameters between the standard and samples. In all cases, power saturation studies were performed to ensure that the signals were not saturated under the conditions utilized.

Electron Spin−Echo Envelope Modulation (ESEEM) Spectroscopy. Pulsed EPR data were collected on a home-built spectrometer as previously described (*37*). ESEEM data were collected in the usual point-by-point fashion using a Tektronix 620 B digital oscilloscope to perform signal averaging and numerical integration of the echo amplitudes. Data acquisition was controlled by a Power Computing model 200 computer, using software created with the LabView, version 5.0, programming package (National instruments). The microwave probe utilized a folded stripline resonant element (*38*) and a Gordon coupling scheme suitable for liquid helium immersion experiments (*39*). For two-pulse ESEEM experiments (90°−τ−180°), τ was varied from 150 ns to ~2.5 μs for each data set containing 512 points. Spectra were collected at 4.2 K using a microwave pulse power of 20 W, a pulse width of 20 ns (fwhm), and a repetition rate of 40 Hz. The magnetic field strength was set to 3050 G with a microwave frequency of approximately 8.8 GHz. Data analysis was performed using Matlab version 5.2 (Mathworks); dead time reconstruction (*40*) was used to process the data for the ESEEM envelopes prior to Fourier transformation. Computer simulations of deuterium ESEEM spectra were done using software based on the density matrix treatment of Mims (*41*).

Electronic Absorption Spectroscopy. Anaerobic Fe−TfdA samples were prepared as described above and placed in a 0.8 mL dual path length (2.0 mm × 1.0 cm) quartz cuvette (Wilmad Glass; Buena, NJ) which had been modified to contain a Schlenk-type fitting. Spectra were recorded on a scanning Beckman DU 640 spectrophotometer equipped with a refrigerated circulating bath. Typical enzyme concentrations (expressed as the number of active sites) were 0.3−0.6 mM. The reference sample contained only 100 mM Mops buffer. Spectra were obtained at 4 °C to stabilize the enzyme.

RESULTS

EPR Studies of Cu(II)-Substituted TfdA. To provide a means to probe the spectroscopically inaccessible Fe(II) active site and to circumvent the oxygen reactivity of Fe−TfdA, we replaced the native Fe(II) ion with Cu(II), an ion that possesses rich EPR properties and whose coordination chemistry is well characterized (*42*). Significantly, Cu(II) is a very strong competitive inhibitor of TfdA activity (K_i = 0.1−0.3 μM) with respect to Fe(II), suggesting that the Cu(II) ion replaces Fe(II) at the active site. In fact, the K_i of Cu(II) is significantly lower than the concentration of Fe(II) required for TfdA to achieve half-maximal activity (10−30 μM). Thus, while Cu(II) coordination is unlikely to exactly model that of Fe(II) due to the preference of Cu(II) for tetragonal geometries as opposed to the octahedral geometry common for Fe(II), analysis of the TfdA-bound copper environment is likely to reflect the important features of the native TfdA metallocenter.

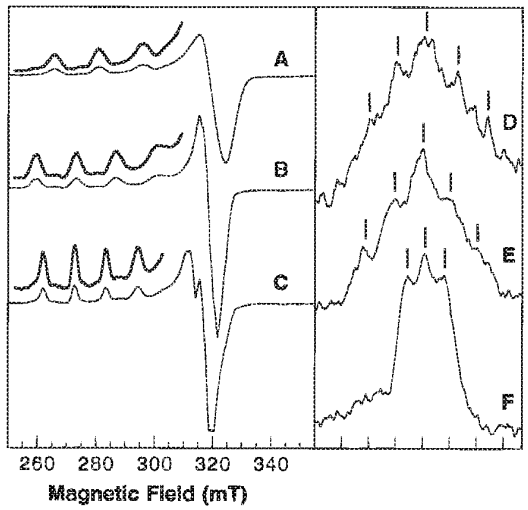


FIGURE 2: EPR spectra of Cu−TfdA complexes. (A) Cu−TfdA ($g_\perp$ = 2.07, $g_\parallel$ = 2.29, $A_\parallel$ = 16.1 mK, 4.2 mT fwhm at 281 mT); (B) Cu−TfdA·(α-KG) ($g_\perp$ = 2.07, $g_\parallel$ = 2.36, $A_\parallel$ = 14.9 mK, 4.2 mT fwhm at 273 mT); (C) Cu−TfdA·(α-KG)·(2,4-D) (g_x = 2.07, g_y = 2.11, g_z = 2.37, A_z = 12.0 mK, 2.2 mT fwhm at 273 mT). Insets show $g_\parallel$ with the intensity magnified 5 times. Spectra D−F display superhyperfine splitting of the $g_\parallel$ region in [^{63}Cu]TfdA EPR spectra due to ^{14}N-containing (I = 1) ligands. While the spectra utilize different x-axes in order to align the peaks, each tick mark represents 1 mT for all three spectra. (D) [^{63}Cu]TfdA; (E) [^{63}Cu]-TfdA·(α-KG); (F) [^{63}Cu]TfdA·(α-KG)·(2,4-D). Spectra D−F were simulated with QPOWA (*35*) as described in the Experimental Section. Spectra D and E display 5-fold splitting (A = 1.0 mT) while spectrum F displays 3-fold splitting (A = 0.7 mT).

The EPR spectra of various copper-substituted TfdA complexes were obtained and have provided considerable insight into the nature of the endogenous ligands coordinated to the metal in the active site (*32*). In the absence of either the cosubstrate α-KG or the primary substrate 2,4-D (Figure 2A), Cu−TfdA exhibits an axial spectrum with g- and A-values ($g_\perp$ = 2.07; $g_\parallel$ = 2.29; $A_\parallel$ = 16.1 mK)[2] consistent with the Cu(II) ion possessing tetragonal geometry (*43*) and a ligation environment containing a mixture of N and O donors (*44*). This EPR spectrum is perturbed by the addition of the cosubstrate α-KG (Figure 2B), with $g_\perp$ = 2.07, $g_\parallel$ = 2.36, and $A_\parallel$ = 14.9 mK. While the addition of 2,4-D to Cu−TfdA has no effect on the EPR spectrum in the absence of α-KG, addition of 2,4-D to the binary Cu−TfdA·(α-KG) complex results in a more rhombic signal and a considerable sharpening of the spectrum from 4.2 mT (fwhm at 273 mT) to 2.2 mT (fwhm at 273 mT) with g_x = 2.07, g_y = 2.11, g_z = 2.37, and A_z = 12.0 mK (Figure 2C). A comparison of the three spectra shows a progressive movement to lower field for $g_\parallel$ and a decrease in the $A_\parallel$ values in the binary and ternary complexes. This is a significant trend since an

[2] A keiser (K) is equivalent in energy to a reciprocal centimeter (cm^{-1}). Therefore, using the units of K, $A_\parallel$ = (g-value) × (splitting in gauss) × (β_e).

COR-AAD1-00002543
Bayer EX1008 (Part 5 of 9)

increase in $g_{\parallel}$ is usually indicative of a shift to a more oxyanion-rich environment (*44*), while small $A_{\parallel}$ values suggest a significant distortion from planarity (*45*, *46*). For example, the $g_{\parallel}$ and $A_{\parallel}$ values of the ternary Cu−TfdA·(α-KG)·(2,4-D) complex are comparable to those of Cu-substituted ribulose-1,5-bisphosphate carboxylase/oxygense complexed to the transition-state analogue 2-carboxyarabinitol bisphosphate [$g_{\parallel} = 2.41$, $A_{\parallel} = 11.59$ mK (*47*)] and Cu(II)-substituted enolase complexed to 2-phosphoglycerate [$g_{\parallel} = 2.40$, $A_{\parallel} = 12.0$ mK (*48*)], both with crystallographically determined structures which reveal an oxyanion-rich environment at a distorted metal center (*49*, *50*).

In a previous communication (*32*), we incorrectly reported that the EPR spectra of Cu−TfdA·(pyruvate) complexes were identical to those with α-KG. This observation led to the erroneous conclusion that the C-5 carboxylate was not important in eliciting the characteristic spectrum of the Cu−TfdA·(α-KG) species. We have since discovered, however, that the pyruvate utilized in the experiments contained small quantities of a "pyruvate dimer" (2-hydroxy-2-methyl-4-oxoglutaric acid), which mimics α-KG in possessing the second carboxyl functional group. On the basis of its structural similarity to α-KG ($K_m = 3.2$ μM), this "dimer" is presumed to have a much lower K_m than pyruvate ($K_m =$ 1.0 mM). Experiments using authentic "pyruvate dimer" (synthesized by treating pyruvate with concentrated NaOH for at least 30 min) yielded the EPR spectrum characteristic of the α-KG-bound state, whereas those using ultrapure pyruvate failed to reproduce this spectroscopic feature. Thus, the C-5 carboxylate is, in fact, important in the binding of α-KG despite the fact that this carboxylate presumably does not coordinate to the metal center.

Further information about the coordination environment of the metal center was obtained from analysis of the superhyperfine splitting in the EPR spectra. This phenomenon arises from the interaction of the unpaired electron on the Cu(II) ion with the nuclear spin (I) of an atom directly bound to the metal and lying in the principal tetragonal plane (superhyperfine splitting is not observed for axial ligands). In an ideal situation, one can determine the number of nitrogen-containing ligands (while ^{16}O does not have a nuclear spin, ^{14}N has $I = 1$) since the number of superhyperfine lines is equal to $2nI + 1$, where n is the number of equivalent nuclei. An excellent example of such an analysis of superhyperfine splitting was recently reported by Ballou and co-workers in their study of Cu(II)-substituted phthalate dioxygenase (*51*).

Although not readily apparent from Figure 2, superhyperfine splitting is present in the $g_{\perp}$ region of the Cu−TfdA EPR spectra, and this splitting can be discerned in the second derivative spectra. Figure 3A shows the EPR second derivative spectrum of Cu−TfdA in the $g_{\perp}$ region. Unfortunately, the resolution of ligand superhyperfine features is poor, indicating that the structure about the metal center may be somewhat heterogeneous prior to substrate addition. When α-KG binds to the holoenzyme, however, the resolution of the superhyperfine features is greatly enhanced, and an apparent 1:2:3:2:1 quintet is observed (Figure 3C), consistent with two nitrogen-containing endogenous ligands. Enhanced resolution of the ligand superhyperfine features at $g_{\perp}$ is also observed in the presence of a 15-fold excess of imidazole (Figure 3B). The appearance of at least nine features in this spectrum is commensurate with the addition of 1−2 exogenous imidazole ligands to the Cu(II) tetragonal plane, in addition to the two derived from the protein (*32*). These results suggest that TfdA maintains solvent-accessible sites on the metal ion which are presumably available for the binding of exogenous ligands.

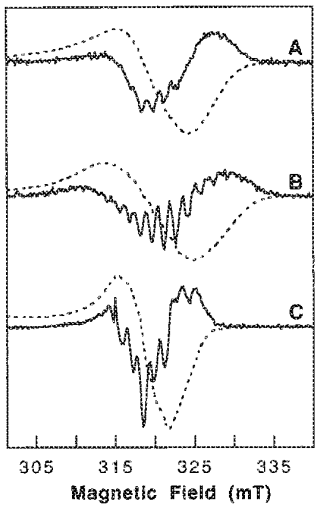


FIGURE 3: Superhyperfine splitting of the $g_{\perp}$ region in Cu−TfdA EPR spectra due to ^{14}N-containing ($I = 1$) ligands. (A) Cu−TfdA; (B) Cu−TfdA in the presence of 15 equivalents of imidazole; (C) Cu−TfdA·(α-KG). The dashed lines are the expanded first derivative $g_{\perp}$ signals, while the solid lines are the second derivative $g_{\perp}$ signal in which the superhyperfine splitting is more easily observed.

The breadth of the $g_{\perp}$ feature as shown in the second derivative spectra of Figure 3, however, indicates that $A_{\perp}^{Cu}$ is similar in magnitude to the nitrogen superhyperfine splitting of the equatorially bound histidyl or imidazole ligands. This renders an analysis of the number of nitrogen-based ligands based on counting superhyperfine features at $g_{\perp}$ tenuous and led us to a detailed examination of ligand superhyperfine structure in the $g_{\parallel}$ region. Splitting in this region is often difficult to resolve because natural abundance copper contains a mixture of ^{63}Cu (69%) and ^{65}Cu (31%), both of which are $I = 3/2$ nuclei but give rise to slightly different $A_{\parallel}$ values. To increase the likelihood of observing the superhyperfine splitting, isotopically pure Cu(II) was utilized. The farthest downfield $g_{\parallel}$ signal of samples prepared with [^{63}Cu]TfdA (Figure 2) exhibits improved resolution relative to that obtained using natural abundance copper and provides information complementary to that derived from the $g_{\perp}$ region. For Cu−TfdA, a 1:2:3:2:1 pattern expected from two equivalent nitrogens may be discerned (Figure 2D). This five-line pattern is more clearly resolved in the Cu−TfdA·(α-KG) complex (Figure 2E), supporting the coordination of two nitrogen-containing ligands to the metal center. In the presence of both α-KG and 2,4-D (Figure 2F), however, the EPR spectrum displays only 3-fold splitting, indicating a loss of one of the nitrogen ligands from the tetragonal plane of Cu(II). These results suggest that 2,4-D binding either displaces one of the His ligands or causes a reorientation of the principal tetragonal plane of the Cu(II) ion such that one of the nitrogen ligands shifts to an axial position.

ESEEM Spectroscopy of Cu(II)-Substituted TfdA. To gain further information on the number and identity of the

COR-AAD1-00002544
Bayer EX1008 (Part 5 of 9)

metallocenter ligands, Cu−TfdA samples were also studied by the ESEEM method of pulsed EPR spectroscopy. Previous ESEEM studies on this system provided evidence for the equatorial ligation of two His ligands for Cu−TfdA and the Cu−TfdA·(α-KG) adduct (*32*), in agreement with the results of continuous wave EPR experiments presented above. The ESEEM from one of these His ligands was lost upon the addition of 2,4-D to the Cu−TfdA·(α-KG) complex, consistent with the observed decrease in the multiplicity of the superhyperfine splitting in the ternary Cu−TfdA·(α-KG)·(2,4-D) complex. Because the model for Fe(II) coordination in this class of enzymes calls for the coordination of multiple water ligands that are displaced as the cosubstrates bind to the metal, ESEEM experiments were performed on samples exchanged against D_2O. The overall strategy for these measurements makes use of the product rule for ESEEM, which states that the modulation function for a discrete paramagnetic center consists of a product of a background decay function, governed by spin relaxation processes, with the individual modulation functions due to all of the coupled nuclei (*52*, *53*). If ESEEM data collected for samples exchanged against D_2O-based buffer are divided by ESEEM data collected under identical conditions for like samples in aqueous buffer, the resulting modulation function will contain only contributions arising from exchangeable deuterons that are magnetically coupled to the paramagnet (*54*). This technique thus provides a method to study coordinated water molecules in the presence of substantial ESEEM from the remote nitrogens of the coordinated histidyl ligands (*55*).

ESEEM ratios taken for Cu−TfdA, Cu−TfdA·(α-KG), and Cu−TfdA·(α-KG)·(2,4-D) are shown as solid lines in panels A−C of Figure 4, respectively. These data were collected using a two-pulse (90°−τ−180°−τ−echo) microwave excitation scheme because this method provides the most reliable measure of amplitudes for dividing data sets (*54*). Also, the two-pulse data feature a sum combination frequency component that provides an "internal" line width, or damping standard for distinguishing bound D_2O molecules from ambient waters (*55*). For all three enzyme samples, the data of Figure 4 show intense modulations that consist of major frequency components at 2.0 MHz (modulation period = 500 ns), the Larmor frequency of deuterium in a 0.305 T magnetic field, and a sum combination frequency centered at 4.1 MHz (modulation period ≈ 250 ns). In agreement with the proposal that the cosubstrates displace water ligands when they bind to Cu(II), the depth, or amplitude, of the modulations decreases as one goes from the Cu−TfdA data (Figure 4A) to the data for the Cu−TfdA·(α-KG)·(2,4-D) ternary complex (Figure 4C). Some caution needs to be taken when considering these results, however, since the ^{2}H-ESEEM shown in Figure 4 originates from D_2O molecules bound to the metal, ambient D_2O molecules close enough to the Cu(II) to magnetically couple to it, and deuterons that have exchanged with the exchangeable protons of TfdA near the metal site.

A useful means to differentiate the different populations of deuterons that contribute to the ESEEM is to make use of the relative amplitudes of the ^{2}H fundamental and sum combination frequency components. Figure 5 shows two-pulse ESEEM simulations for D_2O molecules bound to Cu(II) at an equatorial position (trace A) and an axial position (trace B). Figure 5C shows the predicted two pulse ESEEM

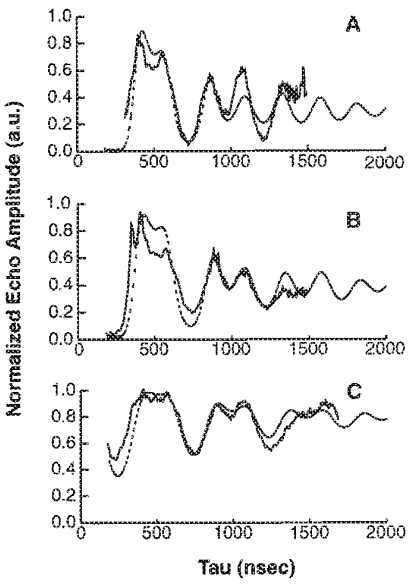


FIGURE 4: The solid lines are deuterium ESEEM data collected for (A) Cu−TfdA, (B) Cu−TfdA·(α-KG), and (C) Cu−TfdA·(α-KG)·(2,4-D). These data were obtained by dividing the two-pulse ESEEM data collected for each sample exchanged against D_2O-based buffer with the identical sample in H_2O-based buffer. Prior to division, each data set was normalized so that the ordinate ranged 0−1, where 0 amplitude was measured directly for each scan and 1 was assigned to the maximum amplitude found experimentally. Conditions common to these measurements were microwave frequency, 8.78 GHz; magnetic field strength, 0.305 T; microwave pulse power, 25 W; pulse width, 20 ns (fwhm); pulse sequence repetition rate, 40 Hz; 40 events were averaged at each time point and four complete scans were averaged to arrive at each ESEEM trace. The dashed lines are ESEEM simulations for (A) two equatorial and one axial bound D_2O molecules, (B) one equatorial and one axial bound D_2O, and (C) one axially bound D_2O. Simulations used the Hamiltonian parameters for equatorial and axial bound D_2O molecules given in the captions for Figure 5, respectively.

for a D_2O molecule with both deuterons positioned 4 Å away from the Cu(II) and coupled by a dipolar, or through-space mechanism. The hyperfine splitting constants used for these simulations were taken from a single-crystal ENDOR study of $Cu(II)(H_2O)_6$ in Tutton salts and are given in the figure caption (*56*). Figure 5A shows a deuterium ESEEM pattern that features intense modulation at the deuterium Larmor frequency (2.0 MHz) which damps quickly and leaves only modulations at the sum combination frequency (4.1 MHz) at longer times. The axially bound D_2O (Figure 5B) shows deep modulations, but the fundamental frequency is less damped than it was for the equatorial case so that the second harmonic is less prominent at longer values of τ. The ambient water shows modulations that are a factor of 7−8 less intense than those of the bound waters with a substantially reduced contribution of the sum combination frequency (Figure 5C). These effects are conveniently viewed in the frequency domain as shown in Figure 6 where Fourier transforms of the simulations for equatorial (Figure 6A), axial (Figure 6B), and ambient (Figure 6C) D_2O molecules are provided. For equatorially bound D_2O, the anisotropic contribution to the hyperfine splitting is large (the effective dipole−dipole distance is about 2.4 Å), and that serves to broaden the width of the 2.0 MHz peak. Because the deuterium hyperfine splitting is of opposite sign in the two-electron spin manifolds

COR-AAD1-00002545
Bayer EX1008 (Part 5 of 9)

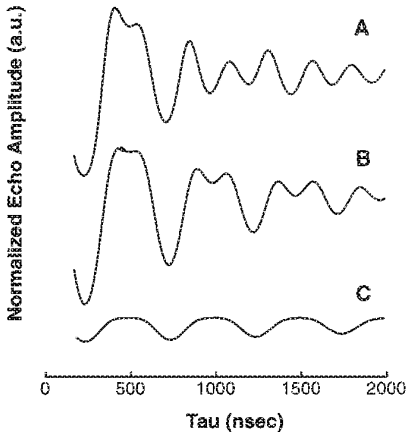


FIGURE 5: ^{2}H-ESEEM simulations for (A) a D_2O molecule bound equatorially to Cu(II), (B) an axially bound D_2O, and (C) a D_2O molecule coupled through space to Cu(II) so that the deuterium−copper distance was 4 Å. Hamiltonian parameters for the ESEEM simulations were for equatorially bound D_2O; $A_{xx} = -1.4$ MHz, $A_{yy} = -0.6$ MHz, $A_{zz} = 1.4$ MHz, nuclear g-value = 0.857 44, magnetic field = 0.305 T, starting $\tau = 180$ ns, $e^2qQ = 0.2$ MHz, nqi asymmetry parameter = 0.5 and the nqi and hyperfine tensors were taken as coaxial. Parameters were the same for the axially bound D_2O except for the hyperfine splitting, $A_{xx} = -0.5$ MHz, $A_{yy} = -0.5$ MHz, and $A_{zz} = 1.1$ MHz. For ambient D_2O (trace C), $A_{xx} = -0.2$ MHz, $A_{yy} = -0.2$ MHz, and $A_{zz} = 0.4$ MHz.

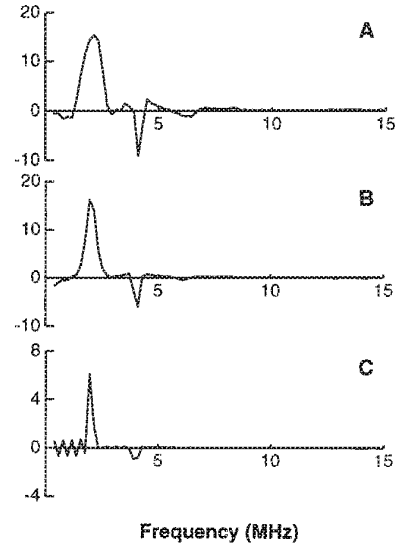


FIGURE 6: Fourier transforms of the ESEEM simulations shown in Figure 5. Trace A is for an equatorially bound D_2O, trace B an axially bound D_2O, and trace C ambient D_2O.

that combine to yield the sum combination peak, the width of the 4.1 MHz line remains narrow for all three of the splitting cases depicted in Figures 5 and 6. This feature is broadened only by the small nuclear quadrupole interaction that is intrinsic to the D_2O molecule.

The simulations of Figures 5 and 6 suggest that a simple method to gauge the relative contributions of equatorial and axial water coordination to Cu(II) ESEEM data is to determine the ratio of the amplitudes of first and second harmonics of the deuterium modulation frequencies as measured from the ESEEM spectra. For the simulation of equatorially bound D_2O (Figures 5A and 6A), this ratio is 1.5; for axially bound D_2O (Figures 5B and 6B), the 2/4 MHz intensity ratio climbs to 2.5; and for ambient water at 4 Å, a ratio of >5 is found. Table 1 shows the results of determining these ratios for simulations carried out for several cases of mixed equatorial/axial D_2O ligation. It is apparent that if both equatorial and axial D_2O ligands are present, the 2/4 MHz amplitude ratio is close to 2.0, a value that is intermediate to those representing pure axial or equatorial ligation. The chief source of errors in measuring peak amplitudes and computing these ratios comes from the reduced frequency resolution realized for 2-pulse ESEEM and difficulties in estimating the position of the baseline for each peak. The sum combination frequency can be measured more reliably because of its narrow line width and negative phase. In contrast, it is often difficult to estimate the baseline position for the low ^{2}H fundamental frequency because the baseline "roll", which stems from shortcomings of the dead-time reconstruction procedure (*40*), is most severe near "0" MHz. The error for computing these peak ratios from the FT is probably ±0.1, for the simulations, and ± 0.2, for the experimental data of Figure 4.

Table 1: Ratios of ^{2}H-ESEEM Fundamental (2 MHz) and Sum-Combination (4 MHz) Frequencies for Various D_2O Coordination Schemes

(A) Computer Simulations	
coordinated D_2O molecules	2/4 MHz ratio
2 equatorial, 0 axial	1.5 (±0.1)
1 equatorial, 0 axial	1.5
2 equatorial, 1 axial	1.7
1 equatorial, 1 axial	1.7
2 equatorial, 2 axial	2.0
1 equatorial, 2 axial	2.0
0 equatorial, 1 axial	2.5
0 equatorial, 2 axial	2.5
(B) TfdA Data	
sample	2/4 MHz ratio
Cu-TfdA	1.7 (±0.2)
Cu-TfdA•(α-KG)	1.8
Cu-TfdA•(α-KG)•(2,4-D)	2.5

The 2/4 MHz amplitude ratios measured from Fourier analysis of the three TfdA ^{2}H-ESEEM traces of Figure 4 are also listed in Table 1. The ternary complex Cu−TfdA•(α-KG)•(2,4-D) gives a ratio of 2.5, indicating that it has at least one axially bound D_2O ligand and no equatorial waters. For the other two complexes, Cu−TfdA and Cu−TfdA•(α-KG), more ^{2}H second harmonic is observed with these 2/4 MHz peak ratios being 1.7 and 1.8, respectively. These results favor a model for Cu(II) water coordination that begins with two equatorial waters and one axial water for the protein in the absence of the cosubstrates (Cu−TfdA). The addition of α-KG displaces one of the equatorial water molecules to leave one equatorial and one axial water. Finally, formation of the ternary complex leads to the displacement of the remaining equatorial water to yield a Cu(II) site with a single, axially bound water molecule. To test this idea, ^{2}H-ESEEM calculations were carried out using the model simulations of Figure 5, curves A and B, together with the spherical model approximation to the ESEEM product rule (*57*) to produce simulations of the two-equatorial/one-axial, one-equatorial/one-axial, and one-axial cases. The results are superimposed on the data of panels A−C of Figure 4, respectively (dashed lines) and show that

COR-AAD1-00002546
Bayer EX1008 (Part 5 of 9)

there is good agreement between the measured ^{2}H-ESEEM functions (solid lines) and the amplitudes predicted theoretically. No attempt was made to adjust the hyperfine parameters from the values determined in the single-crystal ENDOR studies of Cu(II)$(H_2O)_6$ in Tutton salts (*56*).

There are several features of the ^{2}H-ESEEM data shown in Figure 4 that need to be kept in mind when judging the quality of the simulations. These data were obtained by dividing two sets of 2-pulse ESEEM data that featured deep ^{14}N modulations from His coordination and background decay functions due to electron spin−spin relaxation that left only small amplitudes at longer τ. As a result, one is forced to take the ratios of small numbers adding considerable noise to the result that gets worse at longer times. The data shown in Figure 4 are truncated at 1500 ns because the noise in the ratio becomes too severe at higher τ values. The agreement between experiment and theory is worst for the Cu−TfdA sample (solid line of Figure 4A) because the deeper ^{2}H modulation that results from the additional bound water molecule leads to greater uncertainty in the ratio, and additional ambient water, that likely has access to the site when the cosubstrates are absent, is not being considered in the calculation. As a result of these problems, emphasis was placed on comparison between experiment and theory for the first 1 μs of the ^{2}H-ESEEM function of Figure 4A, providing strong evidence that there are two equatorial and one axial D_2O molecules bound to the Cu(II) of TfdA in the absence of the cosubstrates.

In principle, further verification of our ^{2}H-ESEEM modeling of water coordination to Cu−TfdA could be obtained by taking another set of ESEEM ratios. By dividing the ratio of Figure 4A with that of Figure 4B, it should be possible to obtain the ^{2}H-ESEEM pattern of the water displaced by α-KG binding. In a similar fashion, division of Figure 4B by Figure 4C should reveal the ^{2}H-ESEEM function of the D_2O molecule displaced by 2,4-D addition to the protein. Unfortunately, this procedure is only accurate when the continuous wave EPR spectrum remains unchanged as a result of substrate addition. Because there are large changes that occur when adding α-KG to Cu−TfdA, particularly with respect to narrowing the distribution of coordination environments that likely exists for the holo-enzyme, the ratio of trace B in Figure 4 with trace A gave a deep ^{2}H-ESEEM pattern with a 2/4 MHz ratio of 1.1 and an appearance that was much different from the model calculations of Figure 5, traces A and B (data not shown). However, the changes in the EPR spectrum that occur when 2,4-D is added to the Cu−TfdA·(α-KG) complex are more subtle, and a good ratio was obtained by dividing the ^{2}H-ESEEM data of Figure 4, trace B, with that of trace C. The result provides the ^{2}H-ESEEM spectrum of the D_2O displaced by 2,4-D addition and is shown in Figure 7 (solid line). The dashed line superimposed on these data is from the model calculation of the ^{2}H-ESEEM for a D_2O molecule bound equatorially to Cu(II).

Binding of α-KG and 2,4-D to Fe(II)-Reconstituted TfdA. Binding of α-KG to the metal center was assessed directly via optical spectroscopy. In the absence of α-KG, the optical spectrum of Fe−TfdA does not exhibit any absorption features in the visible region, while the UV region is dominated by protein $\pi-\pi^*$ transitions. Lack of a visible chromophore is typical of high-spin Fe(II) species. Upon the anaerobic addition of α-KG, however, the enzyme solution

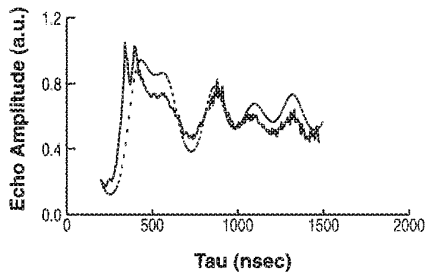


FIGURE 7: The solid line is a ^{2}H-ESEEM trace obtained by dividing the experimental ratios for Figure 4B by that of Figure 4C. The dashed curve is a simulation for a single D_2O molecule bound equatorially to Cu(II) and was obtained by truncating the trace of Figure 5A at 1.5 μs.

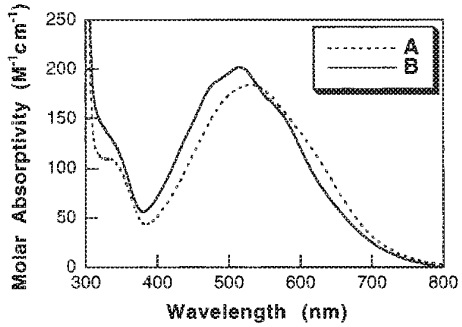


FIGURE 8: Optical absorption spectra of (A) Fe−TfdA·(α-KG) (λ_{max} = 530 nm) and (B) Fe−TfdA·(α-KG)·(2,4-D) (λ_{max} = 515 nm with shoulders at approximately 475 and 560 nm). The spectrum of the Fe−TfdA sample has been subtracted to minimize protein scattering effects.

becomes pinkish and a broad absorption is observed in the visible region centered at approximately 530 nm (Figure 8). Analogous spectra are obtained from synthetic Fe(II)·(α-keto acid) complexes (*20*−*22*, *25*) where the energy of this spectral feature is easily tuned by varying the substituent on the α-keto acid. Electron-donating groups shift the transition to shorter wavelengths (higher energy), while electron-withdrawing groups shift it to longer wavelengths (lower energy) (*20*, *21*), consistent with its assignment as a metal-to-ligand charge transfer (MLCT) transition from the Fe(II) center to the α-keto acid. Significantly, this feature is only observed when the α-keto acid chelates via the carboxylate oxygen and the α-keto oxygen; when the α-keto acid binds in a monodentate fashion, the model iron complexes remain colorless (*21*, *22*). Thus, this broad absorption feature is diagnostic of an α-keto acid chelated to an Fe(II) metal center, indicating that α-KG chelates to the iron in TfdA.

The MLCT transition observed in the presence of α-KG is a convenient probe for monitoring the binding of the primary substrate 2,4-D. As shown in Figure 8, upon the addition of 2,4-D, the absorption is blue-shifted and the optical spectrum sharpens significantly, revealing the presence of at least three different charge-transfer transitions (λ_{max} = 515 nm with shoulders at approximately 475 and 560 nm). These results indicate that α-KG remains chelated to the Fe(II) center in the presence of substrate [i.e., in the Fe−TfdA·(α-KG)·(2,4-D) complex], and that 2,4-D binding affects the coordination environment of the iron(II) center.

Binding of NO to Fe(II)-Reconstituted TfdA. In an effort to gain insight into O_2 binding at the active site, various

COR-AAD1-00002547
Bayer EX1008 (Part 5 of 9)

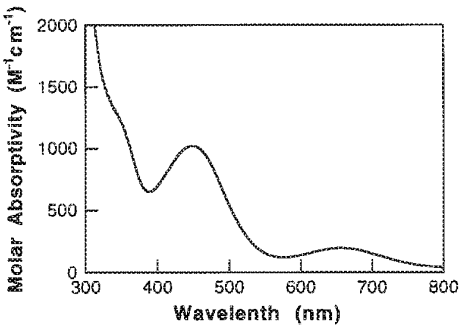


FIGURE 9: Optical absorption spectrum of Fe—TfdA·(α-KG)·(2,4-D)·(NO) (λ_{max} = 449 and 657 nm).

complexes of TfdA were incubated with the O_2 analogue NO. Such an approach has been applied successfully to both model complexes and other iron(II) oxygenases (*58*—*61*). Nitric oxide has an advantage over other O_2-mimics (such as azide) because the radical NO converts the usually nonchromophoric and effectively EPR-silent high-spin (S = 2) Fe(II) ion into an $\{FeNO\}^7$ system (*62*), which is EPR active (S = 3/2) and contains a visible chromophore. Thus, the use of NO provides additional spectroscopic techniques with which to probe the metal center.

Nitric oxide reacts readily with Fe—TfdA, the binary complex Fe—TfdA·(α-KG), and the ternary complex Fe—TfdA·(α-KG)·(2,4-D), as assessed by the formation of characteristic bright yellow iron-nitrosyl species (*58*, *63*). The electronic structure of these complexes appears to be dominated by Fe—NO interactions, since the spectra exhibit only slight variations in the presence/absence of α-KG and 2,4-D [only the Fe—TfdA·(α-KG)·(2,4-D)·(NO) spectrum is shown in Figure 9]. On the basis of detailed spectroscopic analysis of small inorganic Fe—NO model complexes, the absorptions observed at 449 and 657 nm have been assigned by Solomon and co-workers to $NO^- \rightarrow Fe^{3+}$ and Fe^{3+} ligand field transitions, respectively (*63*). The assignment of the TfdA complexes as Fe—NO species was corroborated by EPR spectroscopy (Figure 10), which yielded signals very close to g = 4, 4, and 2 as expected for axial S = 3/2 systems (*58*). The spectra of Fe—TfdA·(NO) and Fe—TfdA·(α-KG)·(NO) are essentially identical with g_x = 4.09, g_y = 3.98, and g_z = 2.00 and a peak-to-peak width of 6.4 mT in the g = 4 region. In the presence of both α-KG and 2,4-D, however, the $\{Fe—NO\}^7$ center becomes more rhombic, with signals at g_x = 4.12, g_y = 3.96, and g_z = 2.00 and a peak-to-peak width of 8.9 mT. This change is mirrored in the copper EPR data of the ternary Cu—TfdA·(α-KG)·(2,4-D) complex which indicates that the copper ion also is in a more rhombic environment. The binding of NO directly to the ternary Fe—TfdA·(α-KG)·(2,4-D) complex indicates that even in the presence of both α-KG and 2,4-D, an available coordination site is maintained on the iron atom for the binding of NO and, by analogy, O_2. In addition, the fact that NO binds directly to the metal ion implies that O_2 activation occurs via direct ligation of O_2 to the Fe(II) center, not via some outer-sphere electron-transfer pathway. The Fe—TfdA·(α-KG)·(2,4-D)·(NO) complex is the best model to date of the active quaternary Fe—TfdA·(α-KG)·(2,4-D)·(O_2) complex, i.e., the species which ultimately gives rise to catalysis.

NO binding appears to be reversible under certain circumstances as evidenced by the frequent presence of free

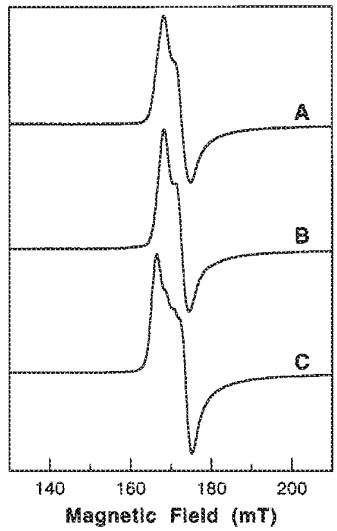


FIGURE 10: EPR spectra of Fe—TfdA-nitrosyl complexes. Only the expanded g = 4 region is displayed since the g = 2 region is relatively uninformative and there was frequent overlap with the signal of free NO. (A) Fe—TfdA·(NO) (g_x = 4.09, g_y = 3.98, g_z = 2.00, g_x to g_y peak-to-peak width of 6.4 mT); (B) Fe—TfdA·(α-KG)·(NO) (g_x = 4.09, g_y = 3.98, g_z = 2.00, g_x to g_y peak-to-peak width of 6.4 mT); (C) Fe—TfdA·(α-KG)·(2,4-D)·(NO) (g_x = 4.12, g_y = 3.96, g_z = 2.00, g_x to g_y peak-to-peak width of 8.9 mT).

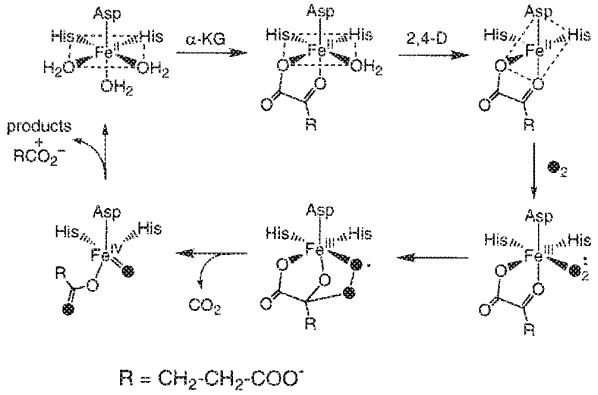
NO in the EPR spectra of both Fe—TfdA·(NO) and Fe—TfdA·(α-KG)·(NO). To further characterize the reversibility of NO binding, optical spectra of various nitrosyl complexes were monitored as the complexes were placed under gentle vacuum followed by incubation under an argon atmosphere. The results demonstrated that NO does, in fact, bind reversibly to both the Fe—TfdA and Fe—TfdA·(α-KG) complexes (most NO exchanged within 10 min). Under these same conditions, however, NO was *not* released from the ternary Fe—TfdA·(α-KG)·(2,4-D) complex. This increased affinity for NO, and by analogy O_2, in the presence of substrate(s) was observed previously in other O_2-activating non-heme Fe(II) enzymes (*59*, *60*) and presumably protects the enzyme from self-inactivation since the formation of reactive Fe—O_2 species is controlled.

DISCUSSION

TfdA exhibits many features associated with the emerging class of mononuclear non-heme iron enzymes that possess a 2-His-1-carboxylate facial triad (*19*). While these enzymes activate dioxygen to catalyze a diverse array of oxidative transformations, they share a common structural motif in which two histidines and one carboxylate occupy a trigonal face of the metal coordination sphere (Figure 1). This facial triad is proposed to anchor the iron(II) center in the active site, leaving the remaining coordination sites available for binding exogenous ligands such as cofactor, substrate, and/or O_2 (*19*). Such an arrangement allows the enzyme to juxtapose reactants to facilitate catalysis. In addition, it has been suggested that ligating anionic exogenous ligands may prime the iron center for binding and activating O_2, presumably by altering the redox potential of the metal center (*19*). Scheme 4 shows a proposed mechanistic scheme for TfdA based on our results as well as information from other mechanistically related enzymes and model systems (*2*, *8*,

COR-AAD1-00002548
Bayer EX1008 (Part 5 of 9)

Scheme 4: Proposed Reaction Scheme for TfdA Based on Current TfdA Studies and Published Work with Related Enzymes



9, *20*−*25*, *31*). Evidence supporting this scheme is discussed in the following sections.

2-His-1-Carboxylate Facial Triad. Our EPR and ESEEM studies of Cu−TfdA and the binary Cu−TfdA·(α-KG) complex demonstrate that two histidine ligands coordinate the metal center in the equatorial plane. In the EPR spectra, both the lowest $g_{||}$ feature and the $g_\perp$ signal exhibit 5-fold splitting, indicative of superhyperfine splitting from two nitrogen ligands. These two nitrogen ligands were identified on the basis of characteristic ESEEM features as arising from the distal nitrogens of two or more coordinated histidine ligands (*32*). The present results are consistent with extended X-ray absorption fine structure (EXAFS) spectroscopic data (*31*) that identified two histidine ligands to both the Cu−TfdA and the Fe−TfdA metallocenters.

Sequence comparisons show that IPNS and a subset of the α-keto acid-dependent enzymes share a common His-X-Asp-$X_{(53-57)}$-His motif (*30*). On the basis of numerous spectroscopic and biochemical studies, it was proposed that this motif provides the endogenous ligands to the metal center (*19*), a notion later confirmed crystallographically for IPNS (*18*) and DAOCS (*8*, *9*). TfdA also contains a His-X-Asp-X_{51}-His sequence (His113, Asp115, and His167) (*29*), although it does *not* possess obvious overall sequence similarity to IPNS or DAOCS. Furthermore, mutagenesis studies on TfdA have demonstrated that the residues associated with this motif are essential for enzyme activity.[3] Together with the EPR, ESEEM, and EXAFS data, these results provide very strong evidence that TfdA utilizes the 2-His-1-carboxylate facial triad as the endogenous metal ligand set.

Exogenous Ligands. A key aspect of the 2-His-1-carboxylate facial triad is that this endogenous ligand set maintains three cis-oriented sites which are available for the binding of exogenous ligands and are proposed to play a critical role in the catalytic mechanisms of these enzymes (*19*). By analogy to DAOCS (*9*), these sites are presumably occupied by solvent molecules in the resting state of TfdA. Indeed, ESEEM spectroscopic results of Cu−TfdA in H_2O and D_2O are consistent with the presence of one axial and two equatorial water molecules. Significantly, the EPR spectrum of Cu−TfdA obtained in the presence of imidazole buffer shows evidence for imidazole binding to the metal center, presumably displacing one or two solvent molecules from the principal tetragonal plane.

The addition of the cosubstrate α-KG to Fe(II)-reconstituted TfdA results in the displacement of two coordinating solvent ligands as shown by the development of MLCT transitions that are diagnostic of an α-keto acid moiety chelated to an Fe(II) center (*20*−*22*, *25*). Indeed, the crystal structure of the Fe-DAOCS·(α-KG) complex reveals just such a chelated α-KG (*9*). A chelated α-KG was also recently deduced for the Fe(II)-reconstituted α-keto acid-dependent enzymes CS2 (*23*) and TauD (*64*).[4] Thus, the chelate binding mode of α-KG appears to be general to all α-keto acid-dependent enzymes. The proposed binding orientation for α-KG shown in Scheme 4 corresponds to that observed in the crystal structure of DAOCS.

The optical spectrum of the ternary Fe−TfdA·(α-KG)·(2,4-D) complex retains MLCT transitions characteristic of an α-keto acid chelated to an Fe(II) ion, indicating that α-KG remains chelated to the iron center in the presence of the substrate 2,4-D. The addition of substrate does, however, alter the coordination environment of the active site as evidenced by the blue-shift in the MLCT transitions and the sharpening of the optical spectrum. Analogous perturbations to the MLCT transitions also occur in the spectra of both Fe−CS2·(α-KG) (*24*) and Fe−TauD·(α-KG) (*64*) upon addition of the appropriate substrate, suggesting that this perturbation may be a feature common to all α-keto acid-dependent enzymes. We interpret the sharpening of the optical features as an indication that the iron is in a more homogeneous environment in the presence of both α-KG and 2,4-D, and that the Fe(II) ion is now "locked" in position and primed for catalysis.

In contrast to the Fe(II)-reconstituted enzyme, addition of α-KG to Cu(II)-substituted TfdA results in the displacement of only a single equatorial water molecule according to ESEEM analysis, suggesting that α-KG binds in a monodentate fashion to Cu−TfdA. This difference in α-keto acid-binding mode between Cu(II) and Fe(II) adducts, which has also been observed in model complexes (*65*), is not surprising given the preference of Cu(II) to maintain a tetragonal coordination environment. Upon the addition of 2,4-D to the Cu−TfdA·(α-KG) complex, a second equatorial water molecule is lost. It remains unclear whether the water is displaced by the α-keto group or by direct ligation of the substrate, but we favor the former interpretation which would allow the primary substrate to bind identically in the Cu- and Fe-enzymes.

Creation of an O_2-Binding Site. As illustrated in Scheme 4, one feature associated with priming the Fe(II) site for reaction with O_2 may entail the loss of a ligand to form a coordinately unsaturated metal center. Our EPR studies of various Cu−TfdA and nitrosyl-Fe−TfdA complexes indicate that a significant change occurs in the metal environment upon formation of the Cu/(Fe−NO)−TfdA·(α-KG)·(2,4-D) complex, with both spectra exhibiting more rhombicity. In addition, for Cu−TfdA·(α-KG)·(2,4-D), we observe a low field shift of $g_{||}$ to 2.37, a decrease of $A_{||}$ to 12.0 mK, and a

[3] Hogan, D. A., Smith, S. R., Saari, E. A., McCracken, J., and Hausinger, R. P., manuscript in preparation.

[4] TauD catalyzes the conversion of taurine to aminoacetaldehyde and sulfite [Eichhorn et al. (1997) *J. Biol. Chem. 272*, 23031−23036].

COR-AAD1-00002549
Bayer EX1008 (Part 5 of 9)

sharpening of the $g_{\parallel}$ signals by a factor of 2 due to the loss of superhyperfine splitting from one nitrogen ligand. The first two spectral changes indicate a Cu(II) ion with more oxyanionic ligands in the principal tetragonal plane (*44*), while the third indicates the displacement of one His ligand from this plane (shown by the shift in position of the dotted lines in Scheme 4). Two options can be considered for this His displacement: complete loss of a His ligand from the coordination sphere or a reorientation of the principal g-tensor axis.

In support of a model in which one His ligand is lost upon addition of the substrate 2,4-D, EXAFS spectra of the ternary Cu−TfdA·(α-KG)·(2,4-D) and binary Fe−TfdA·(2,4-D) complexes show decreases in the intensity of outer-sphere features due to imidazole coordination (*31*). It should be stressed, however, that precise numbers of ligands are difficult to assign by this method, especially involving second-shell atoms, and that EXAFS spectra for the ternary Fe−TfdA·(α-KG)·(2,4-D) complex were not reported (*31*). The EXAFS data suggest that 2,4-D binding leads to His displacement but do not define whether the ligand changes arise from protein conformational changes associated with substrate binding or whether the carboxylate of 2,4-D replaces the endogenous ligands. In the latter case, this proposed displacement would be specific only for substrates with carboxylate groups and not apply to either prolyl hydroxylase or lysyl hydroxylase, two α-keto acid-dependent enzymes involved in collagen formation (*1*). A further argument against this model is the crystal structure reported for DAOCS. If the active site of DAOCS is representative of that in TfdA, the displacement of a histidine in the facial triad would appear to require substantial side-chain rearrangements (*8*, *9*).

We currently favor an alternative interpretation in which the endogenous 2-His-1-carboxylate facial triad is maintained upon 2,4-D binding. According to this alternative proposal, α-KG binds iron in a chelate fashion while 2,4-D binds in a pocket near the iron center and induces the loss of a solvent molecule from the metal coordination sphere, resulting in a 5-coordinate iron(II) metallocenter. This interpretation is in agreement with the perturbation observed at the iron(II) center upon addition of 2,4-D to Fe−TfdA·(α-KG), as well as the crystal structure (*9*) and modeled substrate binding pocket (*8*) of DAOCS. Further support of this model is provided by detailed spectroscopic studies of CS2 (*23*, *24*) in which Solomon and co-workers demonstrated a shift from a 6- to 5-coordinate Fe(II) center upon substrate binding. In the case of Cu−TfdA, we propose that the interactions with α-KG and 2,4-D cause a reorientation of the principal tetragonal plane in Cu−TfdA, resulting in a shift of one of the histidines from the tetragonal plane to an axial position (Scheme 4). This reorientation increases the number of oxygen ligands in this plane and decreases the multiplicity of the superhyperfine splitting, consistent with the Cu−TfdA EPR data.

As Scheme 4 illustrates, having formed the ternary Fe−TfdA·(α-KG)·(2,4-D) complex, the next step is to bind O_2. Evidence that the addition of substrate to the binary complex primes the iron to bind and activate O_2 can be derived from studies with the O_2 mimic NO. Nitric oxide binding is reversible unless both α-KG and 2,4-D are present, suggesting that the ternary complex has a much higher affinity than the binary or free enzyme for NO and, by analogy, O_2. An energetic coupling of NO/O_2 and substrate binding has been observed previously in other non-heme iron enzymes that activate O_2, including three different extradiol dioxygenases (*59*, *60*) and IPNS (*61*). The increased affinity for NO/O_2 only in the presence of a properly "primed" active site presumably serves to protect the enzyme since the potent oxidizing species will only be generated when the catalytic cycle can be completed (*19*). This hypothesis is consistent with the ordered binding mechanism established for the α-keto acid-dependent enzyme thymine 7-hydroxylase (*4*), where O_2 binds after both α-KG and the primary substrate and the fact that the oxidative decarboxylation of α-KG cannot be uncoupled from 2,4-D oxidation in TfdA (*27*). In addition, stopped-flow studies with TauD demonstrate an enhanced rate of reaction with O_2 for the ternary complex relative to Fe−TauD·(α-KG), suggesting a similar priming of the active site upon the addition of both α-KG and the primary substrate (*64*).

Mechanistic Considerations. Understanding the coordination environment of the iron(II) center in TfdA ultimately leads to the question of how α-keto acid-dependent enzymes activate O_2. Cytochrome P-450, the prototypical heme oxygenase, utilizes an electron from NADH and one from the porphyrin ring itself to generate compound I, the putative high valent iron−oxo species involved in oxidation (*66*). In the non-heme methane monooxygenase, the dinuclear iron activates O_2 to form intermediate Q, proposed to be a diiron-(IV)-oxo species (*67*). Mononuclear, non-heme iron enzymes, however, must utilize the exogenous ligands themselves to supply the additional electrons necessary to activate and reduce O_2 (*19*). Thus, the extra electrons are furnished by the cosubstrate α-KG in α-keto acid-dependent enzymes. Still left unanswered, however, is how these enzymes overcome the energy required to break the O−O bond. In heme enzymes, it is generally accepted that O−O bond cleavage is induced by the "push−pull" mechanism, with the respective involvement of the proximal and distal residues (*66*). No such mechanism is available in the α-keto acid-dependent oxygenases. Analysis of the reactivity of model complexes suggests that the oxidative decarboxylation itself may provide the necessary driving force; that is, the loss of CO_2 may be coupled to O−O bond cleavage as depicted in Scheme 4 and, therefore, provides the energy required to overcome this key activation barrier (*20*). Thus, the α-keto acid cosubstrate would have a unique role, providing both electrons and an energetic boost.

In conclusion, the spectroscopic results reported herein have greatly expanded our knowledge of the iron coordination environment in α-keto acid-dependent enzymes. Our current working model for TfdA, shown in Scheme 4, builds on a hypothetical mechanism first proposed for prolyl hydroxylase by Hanauske-Abel in 1982 (*26*). The scheme consists of an iron coordinated to the active site via the widely used 2-His-1-carboxylate facial triad with the remaining sites filled with solvent molecules and available for the binding of exogenous ligands. α-KG chelates to the iron via the α-keto oxygen and a carboxylate oxygen forming a stable five-membered ring. This binding mode is maintained even in the presence of the primary substrate 2,4-D, the binding of which induces the loss of a solvent ligand to generate a 5-coordinate iron(II) center. Upon the binding of O_2 at the

COR-AAD1-00002550
Bayer EX1008 (Part 5 of 9)

vacant site, α-KG is oxidatively decarboxylated, releasing both the electrons and the driving force necessary to form the putative high valent iron−oxo intermediate. Thus, the unique coordination environment of α-keto acid-dependent enzymes affords an oxygen activation mechanism, which is distinct from those utilized by oxygenases which require a porphyrin ring or a second metal ion.

REFERENCES

1. Abbott, M. T., and Udenfriend, S. (1974) in Molecular Mechanisms of Oxygen Activation (Hayaishi, O., Ed.) pp 167−214, Academic Press, New York.
2. Que, L., Jr., and Ho, R. Y. N. (1996) *Chem. Rev. 96*, 2607−2624.
3. Prescott, A. G., and John, P. (1996) *Annu. Rev. Plant Physiol. Plant Mol. Biol. 47*, 245−271.
4. Holme, E. (1975) *Biochemistry 14*, 4999−5003.
5. De Carolis, E., and De Luca, V. (1993) *J. Biol. Chem. 268*, 5504−5511.
6. Myllylä, R., Tuderman, L., and Kivirikko, K. I. (1977) *Eur. J. Biochem. 80*, 349−357.
7. Puistola, U., Turpeenniemi-Hujanen, T. M., Myllylä, R., and Kivirikko, K. I. (1980) *Biochim. Biophys. Acta 611*, 51−60.
8. Lloyd, M. D., Lee, H.-J., Harlos, K., Zhang, Z.-H., Baldwin, J. E., Schofield, C. J., Charnock, J. M., Garner, C. D., Hara, T., van Scheltinga, A. C. T., Valegård, K., Viklund, J. A. C., Hajdu, J., Andersson, I., Danielsson, Å., and Bhikhabhai, R. (1999) *J. Mol. Biol. 287*, 943−960.
9. Valegård, K., van Scheltinga, A. C. T., Lloyd, M. D., Hara, T., Ramaswamy, S., Perrakis, A., Thompson, A., Lee, H.-J., Baldwin, J. E., Schofield, C. J., Hajdu, J., and Andersson, I. (1998) *Nature 394*, 805−809.
10. Serre, L., Sailland, A., Sy, D., Boudec, P., Rolland, A., Pebay-Peyroula, E., and Cohen-Addad, C. (1999) *Structure 7*, 977−988.
11. Senda, T., Sugiyama, K., Narita, H., Yamamoto, T., Kimbara, K., Fukuda, M., Sato, M., Yano, K., and Mitsui, Y. (1996) *J. Mol. Biol. 255*, 735−752.
12. Han, S., Eltis, L. D., Timmis, K. N., Muchmore, S. W., and Bolin, J. T. (1995) *Science 270*, 976−980.
13. Kita, A., Kita, S., Fujisawa, I., Inaka, K., Ishida, T., Horiike, K., Nozaki, M., and Miki, K. (1999) *Structure 7*, 25−34.
14. Sugimoto, K., Senda, T., Aoshima, H., Masai, E., Fukuda, M., and Mitsui, Y. (1999) *Structure 7*, 953−965.
15. Goodwill, K. E., Sabatier, C., and Stevens, R. C. (1998) *Biochemistry 37*, 13437−13445.
16. Erlandsen, H., Flatmark, T., Stevens, R. C., and Hough, E. (1998) *Biochemistry 37*, 15638−15646.
17. Kauppi, B., Lee, K., Carredano, E., Parales, R. E., Gibson, D. T., Eklund, H., and Ramaswamy, S. (1998) *Structure 6*, 571−586.
18. Roach, P. L., Clifton, I. J., Hensgens, C. M. H., Shibata, N., Schofield, C. J., Hajdu, J., and Baldwin, J. E. (1997) *Nature 387*, 827−830.
19. Hegg, E. L., and Que, L., Jr. (1997) *Eur. J. Biochem. 250*, 625−629.
20. Hegg, E. L., Ho, R. Y. N., and Que, L., Jr. (1999) *J. Am. Chem. Soc. 121*, 1972−1973.
21. Chiou, Y.-M., and Que, L., Jr. (1995) *J. Am. Chem. Soc. 117*, 3999−4013.
22. Hikichi, S., Ogihara, T., Fujisawa, K., Kitajima, N., Akita, M., and Moro-oka, Y. (1997) *Inorg. Chem. 36*, 4539−4547.
23. Pavel, E. G., Zhou, J., Busby, R. W., Gunsior, M., Townsend, C. A., and Solomon, E. I. (1998) *J. Am. Chem. Soc. 120*, 743−753.
24. Zhou, J., Gunsior, M., Bachmann, B. O., Townsend, C. A., and Solomon, E. I. (1998) *J. Am. Chem. Soc. 120*, 13539−13540.
25. Ha, E. H., Ho, R. Y. N., Kosiel, J. F., and Valentine, J. S. (1995) *Inorg. Chem. 34*, 2265−2266.
26. Hanauske-Abel, H. M., and Günzler, V. (1982) *J. Theor. Biol. 94*, 421−455.
27. Fukumori, F., and Hausinger, R. P. (1993) *J. Biol. Chem. 268*, 24311−24317.
28. Fukumori, F., and Hausinger, R. P. (1993) *J. Bacteriol. 175*, 2083−2086.
29. Streber, W. R., Timmis, K. N., and Zenk, M. H. (1987) *J. Bacteriol. 169*, 2950−2955.
30. Borovok, I., Landman, O., Kreisberg-Zakarin, R., Aharonowitz, Y., and Cohen, G. (1996) *Biochemistry 35*, 1981−1987.
31. Cosper, N. J., Stålhandske, C. M. V., Saari, R. E., Hausinger, R. P., and Scott, R. A. (1999) *J. Biol. Inorg. Chem. 4*, 122−129.
32. Whiting, A. K., Que, L., Jr., Saari, R. E., Hausinger, R. P., Fredrick, M. A., and McCracken, J. (1997) *J. Am. Chem. Soc. 119*, 3413−3414.
33. Fasman, G. D., Ed. (1976) *Handbook of Biochemistry and Molecular Biology*, CRC Press, Inc, CRC Press, Inc, Boca Raton, FL.
34. Saari, R. E., and Hausinger, R. P. (1998) *Biochemistry 37*, 3035−3042.
35. Belford, R. L., and Belford, G. G. (1973) *J. Chem. Phys. 59*, 853−854.
36. Cammack, R., and Cooper, C. E. (1993) *Methods Enzymol. 227*, 353−384.
37. McCracken, J., Shin, D.-H., and Dye, J. L. (1992) *Appl. Magn. Reson. 3*, 305−316.
38. Lin, C. P., Bowman, M. K., and Norris, J. R. (1985) *J. Magn. Reson. 65*, 369−374.
39. Britt, R. D., and Klein, M. P. (1987) *J. Magn. Reson. 74*, 535−540.
40. Mims, W. B. (1984) *J. Magn. Reson. 59*, 291−306.
41. Mims, W. B. (1972) *Phys. Rev. B 5*, 2409−2419.
42. Bertini, I., and Scozzafava, A. (1981) *Metal Ions Biol. Sys. 12*, 31−74.
43. Solomon, E. I., Baldwin, M. J., and Lowery, M. D. (1992) *Chem. Rev. 92*, 521−542.
44. Peisach, J., and Blumberg, W. E. (1974) *Arch. Biochem. Biophys. 165*, 691−708.
45. Rosenberg, R. C., Root, C. A., Bernstein, P. K., and Gray, H. B. (1975) *J. Am. Chem. Soc. 97*, 2092−2096.
46. Addison, A. W. (1983) in *Copper Coordination Chemistry: Biochemical and Inorganic Perspectives* (Karlin, K. D., and Zubieta, J., Eds.) pp 109−128, Adenine Press, New York.
47. Styring, S., and Brändén, R. (1985) *Biochemistry 24*, 6011−6019.
48. Dickinson, L. C., Rose, S. L., and Westhead, E. W. (1980) *J. Inorg. Biochem. 13*, 353−366.
49. Andersson, I. (1996) *J. Mol. Biol. 259*, 160−174.
50. Larsen, T. M., Wedekind, J. E., Rayment, I., and Reed, G. H. (1996) *Biochemistry 35*, 4349−4358.
51. Coulter, E. D., Moon, N., Batie, C. J., Dunham, W. R., and Ballou, D. P. (1999) *Biochemistry 38*, 11062−11072.
52. Rowan, L. G., Hahn, E. L., and Mims, W. B. (1965) *Phys. Rev. 137*, A61−A71.
53. Dikanov, S. A., Shubin, A. A., and Parmon, V. N. (1981) *J. Magn. Reson. 42*, 474−487.
54. Mims, W. B., Davis, J. L., and Peisach, J. (1984) *Biophys. J. 45*, 755−766.
55. McCracken, J., Peisach, J., and Dooley, D. M. (1987) *J. Am. Chem. Soc. 109*, 4064−4072.
56. Atherton, N. M., and Horsewill, A. J. (1979) *Mol. Phys. 37*, 1349−1361.
57. Kevan, L., Bowman, M. K., Narayana, P. A., Boeckman, R. K., Yudanov, V. F., and Tsvetkov, L. (1975) *J. Chem. Phys. 63*, 409−416.
58. Chiou, Y.-M., and Que, L., Jr. (1995) *Inorg. Chem. 34*, 3270−3278.
59. Wolgel, S. A., Dege, J. E., Perkins-Olson, P. E., Juarez-Garcia, C. H., Crawford, R. L., Münck, E., and Lipscomb, J. D. (1993) *J. Bacteriol. 175*, 4414−4426.

COR-AAD1-00002551
Bayer EX1008 (Part 5 of 9)

60. Arciero, D. M., Orville, A. M., and Lipscomb, J. D. (1985) *J. Biol. Chem. 260*, 14035−14044.
61. Chen, V. J., Orville, A. M., Harpel, M. R., Frolik, C. A., Surerus, K. K., Münck, E., and Lipscomb, J. D. (1989) *J. Biol. Chem. 264*, 21677−21681.
62. Feltham, R. D., and Enemark, J. H. (1981) *Top. Stereochem. 12*, 155−215.
63. Brown, C. A., Pavlosky, M. A., Westre, T. E., Zhang, Y., Hedman, B., Hodgson, K. O., and Solomon, E. I. (1995) *J. Am. Chem. Soc. 117*, 715−732.
64. Ryle, M. J., Padmakumar, R., and Hausinger, R. P. (1999) *Biochemistry 46*, 15278−15286.
65. Zheng, H., and Que, L., Jr. (1997) *Inorg. Chim. Acta 263*, 301−307.
66. Sono, M., Roach, M. P., Coulter, E. D., and Dawson, J. H. (1996) *Chem. Rev. 96*, 2841−2887.
67. Wallar, B. J., and Lipscomb, J. D. (1996) *Chem. Rev. 96*, 2625−2657.

BI991796L

COR-AAD1-00002552
Bayer EX1008 (Part 5 of 9)

Microbiology (2003), **149**, 2545–2556 DOI 10.1099/mic.0.26260-0

A transposon encoding the complete 2,4-dichlorophenoxyacetic acid degradation pathway in the alkalitolerant strain *Delftia acidovorans* P4a

Doreen Hoffmann, Sabine Kleinsteuber, Roland H. Müller and Wolfgang Babel

UFZ Centre for Environmental Research, Department of Environmental Microbiology, Permoserstrasse 15, 04318 Leipzig, Germany

Correspondence
Doreen Hoffmann
hoffmann@umb.ufz.de

Received 27 January 2003
Revised 16 April 2003
Accepted 9 May 2003

The bacterial strain *Delftia acidovorans* P4a, isolated from an extreme environment (heavily contaminated with organochlorines, highly alkaline conditions in an aqueous environment), was found to mineralize 2,4-dichlorophenoxyacetic acid (2,4-D) and 2-methyl-4-chlorophenoxyacetic acid under alkaline conditions. Screening a genomic DNA library of the alkalitolerant strain for 2,4-D genes revealed the presence of the two 2,4-D gene clusters *tfdCDEF* and $tfdC_{II}E_{II}BKA$, *tfdR* genes being located in the vicinity of each *tfd* gene cluster. The results showed that the putative genes of the complete 2,4-D degradation pathway are organized in a single genomic unit. Sequence similarities to homologous gene clusters indicate that the individual *tfd* elements of strain P4a do not share a common origin, but were brought together by recombination events. The entire region is flanked by insertion elements of the IS*1071* and IS*1380* families, forming a transposon-like structure of about 30 kb, of which 28·4 kb were analysed. This element was shown to be located on the bacterial chromosome. The present study provides the first reported case of a chromosomally located catabolic transposon which carries the genes for the complete 2,4-D degradation pathway.

INTRODUCTION

Pollution of the environment with compounds derived from fossil sources and the anthropogenic production of xenobiotics is a global problem. Organochlorines are one group of compounds having a most serious impact on the environment; these compounds were applied extensively as herbicides, pesticides and solvents in the past. Some of them prove recalcitrant, as shown, for example, for polychlorinated biphenyl or dioxin, whereas others have been shown to be fairly well degradable by micro-organisms. Nevertheless, these compounds are known to accumulate in the environment. Therefore, a challenge in solving pollution problems is to better exploit and stabilize degradative performance. A metabolic route pivotal for catalysing organochlorine degradation is the modified *ortho* cleavage pathway. It contributes to the mineralization of haloaromatic compounds by converting chlorocatechols to intermediates of the general cell metabolism. The genes of the *ortho* cleavage pathway are homologous and clustered in operons of similar structure. In many cases, the modified *ortho* cleavage pathway is encoded on catabolic plasmids (Don & Pemberton, 1981; Chatterjee *et al.*, 1981; van der Meer *et al.*, 1991c; Mäe *et al.*, 1993; Bhat *et al.*, 1994; Ogawa & Miyashita, 1995; Poh *et al.*, 2002), which hints to the distribution of these genes by horizontal gene transfer. High similarity has also been observed for the genes and their products which are required to catalyse steps of certain upper pathways. This is the case for TfdA [2,4-dichlorophenoxyacetic acid (2,4-D)/2-oxoglutarate dioxygenase] and TfdB (2,4-dichlorophenol hydroxylase), respectively, which are responsible for the degradation of the commonly used herbicide 2,4-D to 3,5-dichlorocatechol via 2,4-dichlorophenol. Moreover, the genes and operons of the various steps/sequences are organized in a mosaic-like manner (Fulthorpe *et al.*, 1995; Vallaeys *et al.*, 1999).

2,4-D can be used as a carbon and energy source by various soil bacteria and therefore has become a model compound to study the distribution and evolution of catabolic genes for chloroaromatic compounds (Ka *et al.*, 1994; Fulthorpe *et al.*, 1995, 1996; Top *et al.*, 1995; Vallaeys *et al.*, 1996, 1999; Hogan *et al.*, 1997; Kamagata *et al.*, 1997; McGowan *et al.*, 1998; Itoh *et al.*, 2002). Although micro-organisms capable of mineralizing 2,4-D have been investigated intensively, knowledge on the microbial degradation of chloroaromatics in extreme environments such as highly alkaline habitats is still very limited (Maltseva *et al.*, 1996). However, in addition to contaminated soils and (ground)water,

Abbreviation: 2,4-D, 2,4-dichlorophenoxyacetic acid.

The GenBank/EMBL/DDBJ accession number for the sequence reported in this article is AY078159.

COR-AAD1-00002553
Bayer EX1008 (Part 5 of 9)

pollution problems in the chemical industry often extend to the facilities themselves. One special problem in this context is toxic residues in pesticide factories and the microbial decontamination of building rubble obtained after their demolition, since aqueous eluates from this material are very alkaline. Microbes occupying such an ecological niche have to face both extreme pH values and toxic substrates.

In the case described here, the building rubble of a former herbicide production plant was heavily contaminated with organochlorines, especially chlorinated and methylated phenoxyalkanoates and phenols, and generated pH values of up to 12 in an aqueous environment (Müller *et al.*, 1999a). A microbial consortium was enriched from this material which was able to mineralize the cocktail of contaminants under alkaline conditions. One of the strains isolated from this consortium was *Delftia* [formerly *Comamonas* (Wen *et al.*, 1999)] *acidovorans* P4a, which can utilize 2,4-D as sole sources of carbon and energy at pH values of up to 10, and has also exhibited degradative activity on concrete material *in situ* at overall pH values of up to 11·5 (Hoffmann *et al.*, 1996; Müller *et al.*, 1996).

Biodegradation of 2,4-D is catalysed sequentially by six degradative enzymes, encoded by *tfdA*, *tfdB*, *tfdC*, *tfdD*, *tfdE* and *tfdF* in the case of the well-characterized strain *Ralstonia eutropha* JMP134 (Don & Pemberton, 1985; Pieper *et al.*, 1988, 1993). Enzymes with regulatory or transport functions encoded by *tfdR*, *tfdS* and *tfdK*, respectively, are also known (Kaphammer *et al.*, 1990; Kaphammer & Olsen, 1990; Leveau & van der Meer, 1996; Leveau *et al.*, 1998). The presence of *tfd* genes in *D. acidovorans* P4a has been revealed by analysis of PCR products generated using *tfd*-specific primers and genomic DNA of *D. acidovorans* P4a as a template (Hoffmann *et al.*, 2001). In the present study, the organization of the genes of the entire 2,4-D degradative pathway in strain P4a was elucidated, and the relationships of the individual genes to those of other strains were probed. In addition, the localization of the respective genes was looked for. Both these aspects were considered essential to understand the function and stability of 2,4-D biodegradation. These aspects are of special interest if one intends to use strains such as *D. acidovorans* P4a to initiate or improve bioremediation efficiency in such problematic biotopes as building rubble.

METHODS

Genomic library. Genomic DNA of *D. acidovorans* P4a was isolated according to the protocol supplied with the Supercos 1 Cosmid Vector Kit (Stratagene), which was used to construct a genomic DNA library of *D. acidovorans* P4a. The library was amplified in *Escherichia coli* XL-1 Blue MR according to the Supercos 1 Cosmid Library (Stratagene) instruction manual.

Screening of recombinant library clones. To prepare DNA of the recombinant *E. coli* clones, the biomass of each freshly grown single colony was suspended in 50 µl sterile distilled water, boiled for 10 min, left on ice for 10 min and sedimented by centrifugation at 23 000 *g* and 4 °C for 10 min. From each supernatant, 4 µl was dripped onto a nylon membrane (Roche Diagnostics) and the DNA was fixed by UV irradiation. Clones were screened for genes encoding the 2,4-D degradation pathway with probes specific for the *tfdA*, *tfdB*, *tfdC*, *tfdD* and *tfdF* genes, obtained by PCR using genomic DNA from *D. acidovorans* P4a as a template and primers derived from conserved amino acid sequence motifs of corresponding homologous enzymes (Hoffmann *et al.*, 2001). Oligonucleotides were synthesized by MWG BIOTECH. PCR and purification of the PCR products were performed as described by Hoffmann *et al.* (2001). The PCR products were digoxigenin (DIG)-labelled using the DIG DNA Labelling Kit (Roche). For hybridization with the DIG-labelled probes and immunodetection, the DIG Easy Hyb Wash and Block Buffer Set and DIG Nucleic Acid Detection Kit (Roche) were used. Hybridizations with *tfdA*, *tfdB* and *tfdC* probes were performed at 50 °C; *tfdD* and *tfdF* probes were hybridized at 60 °C. Two library clones, 59 and 1183, which showed hybridization signals with various *tfd* probes, were selected for further investigation.

Characterization of positive library clones and subcloning. Cosmid DNA of the *tfd*-positive *E. coli* clones was isolated with the NucleoBond PC Kit and NucleoBond AX columns as recommended by the manufacturer (Macherey-Nagel). Restriction analyses were initiated by digesting the cosmid DNA with various restriction endonucleases (Roche; New England Biolabs). DNA fragments were then separated electrophoretically in 0·8 % agarose gels, blotted onto nylon membranes by standard procedures according to Sambrook *et al.* (1989) and fixed as described above. Southern blotting was performed with an Appligene vacuum blotter. Hybridizations with the *tfdA*, *tfdB*, *tfdC*, *tfdD* and *tfdF* probes were carried out as described above. The positive DNA fragments of the two library clones 59 (subclones A34, B108 and C93) and 1183 (subclone N11) were subcloned using pUC18 and pGEM3-Zf(+) as vectors and *E. coli* DH5α as a host strain. Recombinant subclones were screened by blue/white selection and plasmidal DNA of selected clones was isolated as described above. The presence of the expected insert was verified by restriction analysis.

DNA sequencing and sequence analysis. The nucleotide sequences of the *tfd*-positive and subcloned restriction fragments of *D. acidovorans* P4a (inserts of A34, B108, C93 as well as N11 subclones) were determined according to the method of Sanger *et al.* (1977) using an ABI PRISM 310 Genetic Analyser (PE Applied Biosystems). To complete the sequence data, sequencing was extended to neighbouring regions in the cosmid DNA of the library clones 59 and 1183 applying the primer-walking technique (Alphey, 1998; Strauss *et al.*, 1986). Special primers were derived from respective insert sequences. Each sequence was determined twice. Sequence data were analysed by the SEQUENCE NAVIGATOR software (PE Applied Biosystems) and contigs were assembled by the AUTO ASSEMBLER software (PE Applied Biosystems).

The comparison of sequences with DNA and protein sequences in sequence databases was performed with BLAST (Altschul *et al.*, 1997; http://www.ncbi.nlm.nih.gov/blast). The sequence determined will appear in the GenBank/EMBL/DDBJ sequence databases under accession number AY078159.

Location of the *tfdCDEF* and *tfdC*$_{II}$*E*$_{II}$*BKA* operons. Chromosomal DNA of *D. acidovorans* P4a was isolated by using the NucleoSpin C&T Kit (Macherey-Nagel), while plasmidal DNA was isolated by using the NucleoBond PC Kit (Macherey-Nagel) following the standard protocol of the supplier. DNA was digested with *Eco*RI and *Bgl*II (double digestion). DNA fragments were separated electrophoretically, blotted and fixed as described above, and subjected to Southern blot hybridization with the labelled PCR fragments *tfdDEF* (3·4 kb) and *tfdAKB* (2·5 kb) as probes at 60 °C. The *tfdCDF* probe was obtained by PCR carried out with genomic DNA of strain P4a

COR-AAD1-00002554
Bayer EX1008 (Part 5 of 9)

using the specific *tfdD* forward and *tfdF* reverse primers described by Hoffmann *et al.* (2001). To prepare the *tfdAKB* probe, PCR was carried out with genomic DNA of strain P4a as template using 5′-CAT (A/G)TC (A/G)CA GAA CTC CGT-3′ as the *tfdA* primer and 5′-GA(A/G) ATG AA(C/T) CAG CGC TAT-3′ as the *tfdB* primer (complementary reverse sequences to the *tfdA2* and *tfdB1* primers described by Vallaeys *et al.*, 1996).

RESULTS

Characterization of the *tfd*-positive subclones

The respective *tfd* genes of library clone 59 were found on three different DNA fragments subcloned in A34 (2 kb), B108 (1·1 kb) and C93 (4·6 kb). Sequence analysis of these inserts revealed *tfdA* (partial) and a further open reading frame (ORF), *orfL*, on the A34 insert, *tfdK* and *tfdA* (partial) on the B108 insert as well as *tfdB*, $tfdE_{II}$, $tfdC_{II}$ and also a partial *tfdK* gene on the C93 insert. The *tfd*-positive DNA fragment of library clone 1183 subcloned in N11 (8·2 kb) revealed the presence of genes encoding putative enzymes of the chlorocatechol pathway: *tfdR*, *tfdC*, *tfdD*, *tfdE* as well as *tfdF* (partial). Two further ORFs, *orfI* and *orfII*, were detected in this fragment in addition to a partial IS*1380* sequence.

The 2,4-D degradation pathway of strain P4a

The genome fragments of library clones 59 and 1183 were found to carry different *tfd* genes and several ORFs; nevertheless, in both library clones *orfL*, *tfdA*, *tfdK* and *tfdB* occurred. Based on these data, the sequences were assembled, resulting in a 28·4 kb segment of the genome of strain P4a, suggesting the organization of the degradative genes of the entire 2,4-D degradation pathway in P4a (Fig. 1). Accordingly, the degradation pathway apparently consists of the two different gene clusters *tfdCDEF* and $tfdC_{II}E_{II}BKA$, arranged in opposite transcriptional directions. The *tfdR* genes evidently associated with each of the two clusters are transcribed in the opposite direction to the respective clusters. Furthermore, the *tfdE* and *tfdC* genes occur twice, once in each cluster.

The *tfdCDEF* cluster. Some of the genes in the *tfdCDEF* cluster overlap in their coding regions, as this applies to the *tfdC* and *tfdD* as well as to the *tfdE* and *tfdF* genes in their start and stop codons, respectively. Other genes are separated from each other by intergenic regions: 1 bp between *tfdD* and *orfI*, 21 bp between the stop and start codons of *orfI* and *tfdE*, and 149 bp between *tfdR* and *tfdC*. The intergenic region of *tfdR* and *tfdC* has a typical characteristic of a divergent promoter region subjected to regulation by a LysR-type transcriptional regulator, as the nucleotide sequence differs in only one nucleotide compared with the homologous region in *Pseudomonas* sp. P51 (van der Meer *et al.*, 1991b). Downstream of *tfdF*, the additional ORFs *orfIII* (1029 bp) and *orfL* (720 bp) were located, whereof *orfL* is transcribed divergently. Upstream of *tfdC*, another ORF, *orfII*, was detected which is transcribed in the same direction as the *tfdCDEF* operon.

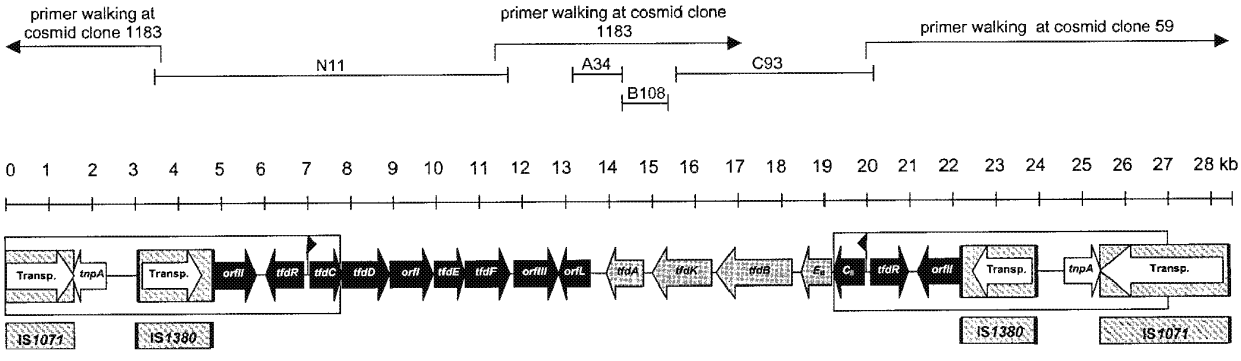


Fig. 1. Graphical presentation of the genetic organization of the 2,4-D degradation pathway in *D. acidovorans* P4a within a transposon-like structure. The sequenced chromosomal DNA segment of 28·4 kb carries the complete sequences of the degradative genes and regulatory elements required for the 2,4-D degradation pathway. The 2,4-D genes are organized in two clusters: *tfdCDEF* (black) and $tfdC_{II}E_{II}BKA$ (grey). The two *tfd* gene clusters are arranged in opposite transcriptional directions. A *tfdR* gene is located upstream of each *tfdC* gene and is transcribed in the opposite direction to the respective cluster. Coding regions and the direction of transcription are indicated by arrows. The black arrows in the intergenic region between *tfdR* and *tfdC* point to the location of TfdR/TfdC-binding sites. The ORFs *orfI*, *orfII*, *orfIII* as well as *orfL* were also detected. The genes of the 2,4-D degradation pathway are flanked by insertion elements (represented as boxes with grey diagonal hatching) of the IS*1071* and IS*1380* families as well as by a part of a *tnpA* gene. Complete sequencing of insertion element IS*1380* showed that the transposase gene is flanked on either side by inverted and direct repeats (black colouring at the ends of this insertion element). Both DNA segments indicated in the open boxes (0–7·8 kb, 19·2–27 kb) have identical nucleotide sequences. The positions of the subcloned DNA fragments (N11, A34, B108 and C93) within the contig are represented by black bars in the upper part of the graph. Their positions relative to each other were verified by primer walking.

COR-AAD1-00002555
Bayer EX1008 (Part 5 of 9)

The *tfdC*$_{II}$*E*$_{II}$*BKA* cluster. The second gene cluster comprises five ORFs. An additional *tfdC* gene was detected which is identical in nucleotide sequence to that within the *tfdCDEF* cluster except for a short sequence of 19 bp at the 3′ terminus. By contrast, a further *tfdE* gene was found, the sequence of which differs substantially compared to *tfdE* in the *tfdCDEF* cluster, corresponding to gene products with only 28 % identity. For differentiation, the *tfdC* and *tfdE* genes in this cluster were indexed. The gene cassette is arranged in the order *tfdC*$_{II}$*E*$_{II}$*BKA* and transcribed in the opposite direction to the *tfdCDEF* cluster. The *tfdR* gene, which presumably encodes the positive regulator of the *tfdC*$_{II}$*E*$_{II}$*BKA* cluster, is located upstream of *tfdC*$_{II}$. Downstream of *tfdR*, another ORF is located which is identical to *orfII* in the vicinity of the *tfdCDEF* cluster.

IS sequences. Sequence data from the 28·4 kb contig show that the genes of the 2,4-D degradation pathway are flanked by insertion elements of the IS*1071* and IS*1380* families (Mahillon & Chandler, 1998). This indicates that the *tfd* genes of strain P4a are located within a transposon-like structure.

The insertion elements belonging to the IS*1380* families were completely sequenced and found to be 1744 bp long. The transposase gene (1·4 kb) is flanked on either side by inverted and direct repeats. The inverted repeats consist of 17 bp and their nucleotide sequences are nearly identical: 5′-CCCG**GA**T**G**TTTCATAAA-3′ and 5′-CCCG**AA**TT**T**TTCATAAA-3′. The nucleotide sequence of the direct repeat is CTAG; it is located in front of the inverted repeat.

The insertion element belonging to the IS*1071* family was completely sequenced in the right part of the segment (Fig. 1); the one on the left was only partially sequenced. A fragment of a further transposase gene, *tnpA*, is located in the intergenic region of the insertion elements IS*1380* and IS*1071* and showed high similarity to the transposase gene of Tn*21*.

Comparison of the sequence with sequence databases. The chlorocatechol degradative operon of strain P4a exhibits high similarity in both its nucleotide sequence and in the arrangement of the genes to the homologous operons in other strains such as *R. eutropha* NH9(pENH91) [99 % identity (Ogawa & Miyashita, 1995, 1999)], *Pseudomonas chlororaphis* RW71 [99 % identity (Potrawfke *et al.*, 1998, 2001)] and *Pseudomonas* sp. P51(pP51) [97 % identity (van der Meer *et al.*, 1991a); Fig. 2]. The lengths of the homologous ORFs, their overlaps and the lengths of the intervening sequences are identical in these gene clusters. Comparison of the nucleotide sequences of the complete operons indicated that the *D. acidovorans* P4a sequence differs in only five nucleotides in relation to *R. eutropha* NH9.

The *tfdR* and *tfdC*$_{II}$ genes of the *tfdC*$_{II}$*E*$_{II}$*BKA* cluster (except for a short nucleotide sequence at the 3′ end of

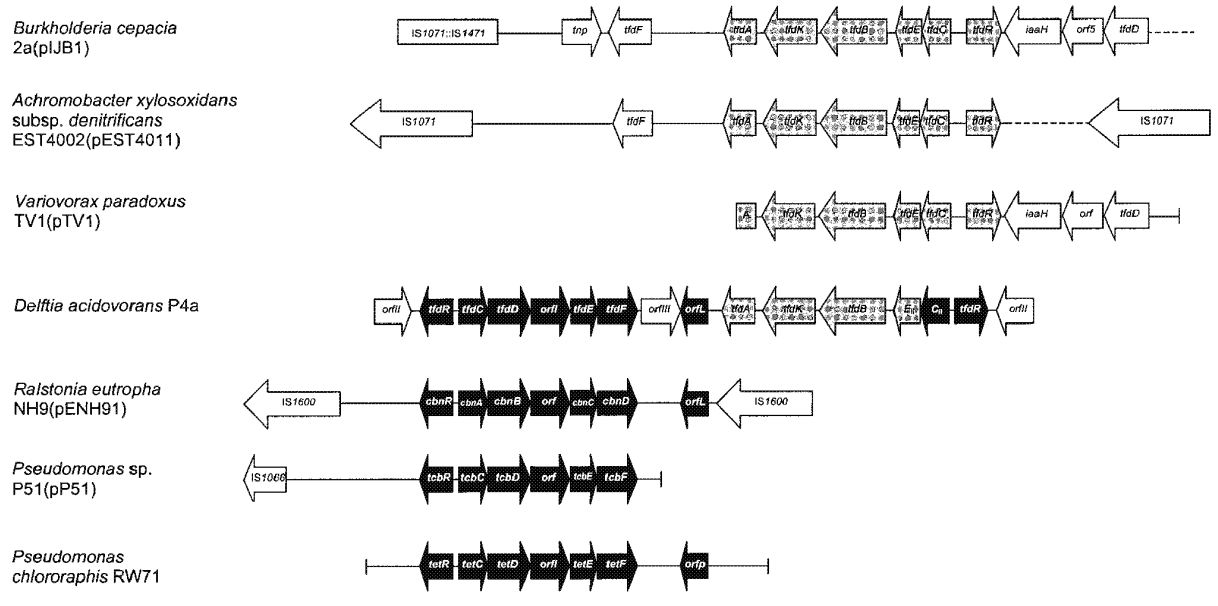


Fig. 2. Comparison of the arrangement of genes in various organochlorine-degrading bacterial strains. The genes of strain P4a that are most similar to the homologous genes in *R. eutropha* NH9, *Pseudomonas* sp. P51 and *P. chlororaphis* RW71 are shown in black, whereas the genes most similar to the homologous genes in *A. xylosoxidans* subsp. *denitrificans* EST4002, *B. cepacia* 2a and *V. paradoxus* TV1 are shown in grey.

COR-AAD1-00002556
Bayer EX1008 (Part 5 of 9)

tfdC$_{II}$) are highly similar to the homologous coding regions of the *cbn*, *tcb* and *tet* genes in *R. eutropha* NH9(pENH91) (Ogawa & Miyashita, 1995, 1999), *Pseudomonas* sp. P51(pP51) (van der Meer *et al.*, 1991a, b) and *P. chlororaphis* RW71 (Potrawfke *et al.*, 1998, 2001), respectively, while the remaining nucleotide sequence including the genes *tfdE*$_{II}$*BKA* is highly similar to plasmid segments of the bacterial strains *Burkholderia cepacia* 2a(pIJB1) [99 % identity (Poh *et al.*, 2002)], *Achromobacter xylosoxidans* subsp. *denitrificans* EST4002(pEST4011) [98–99 % identity (Vedler *et al.*, 2000)] and *Variovorax paradoxus* TV1(pTV1) [98–99 % identity (Vallaeys *et al.*, 1999)]. The strains *B. cepacia* 2a, *A. xylosoxidans* subsp. *denitrificans* EST4002 and *V. paradoxus* TV1 are known to degrade 2,4-D. The similarity of the putative gene products of strain P4a to those of other bacterial strains is listed in Table 1.

Rearrangements within the transposon-like structure

Sequence analysis of the transposon-like structure revealed that a nucleotide sequence of 7·8 kb upstream of *tfdD*, including IS*1071* and IS*1380* insertion elements as well as the *orfII*, *tfdR* and *tfdC* genes (Fig. 1; 0–7·8 kb, DNA segment in the box), is identical to another 7·8 kb nucleotide sequence located immediately upstream of the *tfdE*$_{II}$*BKA* cluster (Fig. 1; 19·2–27 kb). The sequences are oriented in opposite directions to each other. The *tfdC* gene and the sequence upstream of it are highly similar to homologous sequences of *R. eutropha* NH9(pENH91), *Pseudomonas* sp. P51(pP51) and *P. chlororaphis* RW71. This is also true for the nucleotide sequence of *tfdC*$_{II}$. However, a short sequence upstream of the stop codon of *tfdC*$_{II}$ (19 nt) is identical to the corresponding sequences of *A. xylosoxidans* subsp. *denitrificans* EST4002(pEST4011) and *V. paradoxus* TV1(pTV1) (Fig. 3). The latter also applies to a further 5 kb sequence (98–99 % identity) in the downstream direction. These facts are considered indications of rearrangements that took place in the formation of this transposon-like structure, probably by recombination of DNA fragments (Fig. 1). If this hypothesis is correct, the 7·8 kb DNA fragment (Fig. 1, in the box, on the left side of the transposon-like structure) was presumably transferred into the intragenic region of an ancient *tfdC* gene by recombination. Hence, the nucleotide sequence of *tfdC*$_{II}$ represents a combination of two genes rearranged without any frame shifts.

Chromosomal localization of the *tfd* genes in *D. acidovorans* P4a

In the hybridization experiment with a *tfdAKB* probe (2·5 kb), in which both chromosomal and plasmidal DNA from *D. acidovorans* P4a were tested (Fig. 4), a strong signal was generated from a 6 kb DNA fragment derived from the chromosomal moiety (lane 2). No signals were obtained, by contrast, with the plasmidal DNA (lane 1). On the basis of the hybridization results, a chromosomal localization of the *tfd* genes clustered in *tfdC*$_{II}$*E*$_{II}$*BKA* in *D. acidovorans* P4a is highly probable. This was confirmed by the results of another hybridization experiment using the *tfdDEF* (3·4 kb) probe (not shown).

2,4-D-negative mutants

After prolonged cultivation under non-selective conditions, mutants occurred repeatedly which were unable to degrade 2,4-D. PCR was performed by using the genomic DNA as a template and by applying the appropriate primers specific for the *tfd* genes. The results of the PCR experiments were negative; no PCR products were detected with any of the *tfd* primers. Moreover, no signals were obtained by hybridizing the genomic DNA of these 2,4-D-negative mutants using the labelled PCR products of the *tfd* genes as probes, indicating that all the *tfd* genes are completely lost in these mutants.

DISCUSSION

Micro-organisms are able to adapt to changing environmental conditions and to protect themselves from potentially damaging agents such as toxicants (Loffhagen *et al.*, 1997, 2001). They may even exploit such agents by acquiring novel genetic capacity to open up new metabolic niches. This is frequently found with the utilization of xenobiotic compounds, a well-established example being the degradation of chloroaromatics via the modified *ortho* pathway. The genes of these pathways are arranged in mosaic-like structures (Fulthorpe *et al.*, 1995; van der Meer, 1997). For instance, the ability to utilize chlorocatechols by means of the *tfdCDEF* genes can be extended to the degradation of chlorophenols and chlorophenoxyalkanoates by acquiring the genes *tfdB* and *tfdA* (Top *et al.*, 1995; McGowan *et al.*, 1998; Vallaeys *et al.*, 1996, 1999). In many cases, the metabolic versatility of micro-organisms can be quickly and conveniently extended using appropriate plasmids (Don & Pemberton, 1981, 1985; Chaudhry & Huang, 1988; van der Meer *et al.*, 1991c; Mäe *et al.*, 1993; Bhat *et al.*, 1994; Ka & Tiedje, 1994; Vallaeys *et al.*, 1998; Xia *et al.*, 1998; Vedler *et al.*, 2000) and other mobile elements such as transposons and integrons (van der Meer *et al.*, 1991d, 2001; Nakatsu *et al.*, 1991, 1995, 1997; Springael *et al.*, 1993; Nakatsu & Wyndham, 1993; Wyndham *et al.*, 1994a, b; Merlin *et al.*, 1997; Xia *et al.*, 1998; Ogawa & Miyashita, 1999; Müller *et al.*, 2003).

Assuming that the *tfd* genes detected in the present study were adequately expressed, *D. acidovorans* P4a provides an excellent example of this kind of adaptation. Indeed, implication of the *tfd* genes in the metabolism of 2,4-D is highly reliable as this strain exhibits growth on this substrate being accompanied, moreover, by expressing respective enzyme activities as measured for TfdA, TfdB, TfdC and TfdD (D. Hoffmann, unpublished data). The genes of the chlorocatechol pathway (i.e. the *tfdCDEF* genes encoding the enzymes of the modified *ortho* pathway and the regulatory unit *tfdR*, controlling their transcriptional activity as shown for *R. eutropha* JMP134 by Leveau &

COR-AAD1-00002557
Bayer EX1008 (Part 5 of 9)

Table 1. Putative gene products of strain P4a compared to gene products in other bacterial strains

Comparisons were performed with BLAST (Altschul *et al.*, 1997). The percentage identity represents the ratio of identical amino acids to the total number of amino acids in common. The full lengths of the putative gene products of strain P4a are shown in parentheses. Hyp. prot., hypothetical protein; Put. reg. prot., putative regulatory protein; Tnp., transposase.

D. acidovorans P4a putative gene product	Gene product (product, percentage identity, no. identical amino acids/total no. amino acids in common) from		
	Ralstonia eutropha NH9(pENH91) (Ogawa & Miyashita, 1999)	*Pseudomonas chlororaphis* RW71 (Potrawfke *et al.*, 2001)	*Pseudomonas* sp. P51(pP51) (van der Meer *et al.*, 1991a)
TfdR (294 aa)	CbnR, 99 %, 293/294	TetR, 98 %, 291/294	TcbR, 99 %, 292/294
TfdC (251 aa)	CbnA, 99 %, 250/251	TetC, 98 %, 248/251	TcbC, 95 %, 238/250
TfdD (370 aa)	CbnB, 100 %, 370/370	TetD, 89 %, 332/371	TcbD, 97 %, 359/370
OrfI (336 aa)	Orf, 99 %, 335/336	Orf1, 100 %, 336/336	Orf, 97 %, 327/336
TfdE (238 aa)	CbnC, 100 %, 238/238	TetE, 100 %, 238/238	TcbE, 99 %, 237/238
TfdF (352 aa)	CbnD, 100 %, 352/352	TetF, 99 %, 350/352	TcbF, 100 %, 352/352
OrfL (240 aa)	OrfL, 100 %, 240/240	Orfp, 99 %, 239/240	–
$TfdC_{II}$ (249 aa)	CbnA, 99 %, 246/248	TetC, 98 %, 244/248	TcbC, 94 %, 235/248
	Variovorax paradoxus TV1(pTV1) (Vallaeys *et al.*, 1999)	*Achromobacter xylosoxidans* subsp. *denitrificans* EST4002(pEST4011) (Vedler *et al.*, 2000)	*Burkholderia cepacia* 2a(pIJB1) (Poh *et al.*, 2002)
$TfdE_{II}$ (235 aa)	TfdE, 99 %, 233/235	Hyp. prot., 95 %, 202/212	TfdE, 97 %, 229/235
TfdB (586 aa)	TfdB, 99 %, 582/586	TfdB, 98 %, 580/586	TfdB, 99 %, 582/586
TfdK (463 aa)	TfdK, 98 %, 456/463	TfdK, 98 %, 456/463	TfdK, 98 %, 458/463
TfdA (287 aa)	TfdA, 98 %, 104/106	TfdA, 98 %, 282/287	TfdA, 98 %, 283/287
	Pseudomonas putida (Cowles *et al.*, 2000)	*Pseudomonas* sp. IC(pWW110) (Odgen, 1998)	*Pseudomonas putida* 01G3 (Chablain *et al.*, 2001)
OrfII (336 aa)	BenR, 26 %, 69/262	BphS, 26 %, 70/263	EbdR, 27 %, 85/313
	Pseudomonas resinovorans pCAR1 (Maeda *et al.*, 2003))	*Pseudomonas aeruginosa* JB2 (Hickey *et al.*, 2001)	*Pseudomonas resinovorans* (Nojiri *et al.*, 2001)
OrfIII (343 aa)	Put. reg. prot., 38 %, 132/339	Unknown protein, 37 %, 123/325	Put. reg. prot., 34 %, 117/341
	Sphingomonas paucimobilis UT26 (Miyauchi & Nagata, BAA36333)	*Sphingomonas* sp. CF06 (Feng *et al.*, 1997)	*Acetobacter pasteurianus* 1–6, 4–12 and NC11380 (Takemura *et al.*, 1991)
Tnp. IS*1380* (463 aa)	Tnp. IS*sp1*, 39 %, 183/462	Tnp. IS*1412*, 38 %, 179/465	Put. Tnp. IS*1380*, 40 %, 181/445
	Alcaligenes sp. (Nakatsu *et al.*, 1991)	*Comamonas testosteroni* (Nakatsu *et al.*, 1991)	*Pseudomonas putida* UCC22 (Fukumori, BAA12804)
Tnp. IS*1071* (956 aa)	Tnp. IS*1071*, 99 %, 932/936	Tnp. IS*1071*, 99 %, 932/936	TnpA, 100 %, 531/531

COR-AAD1-00002558
Bayer EX1008 (Part 5 of 9)

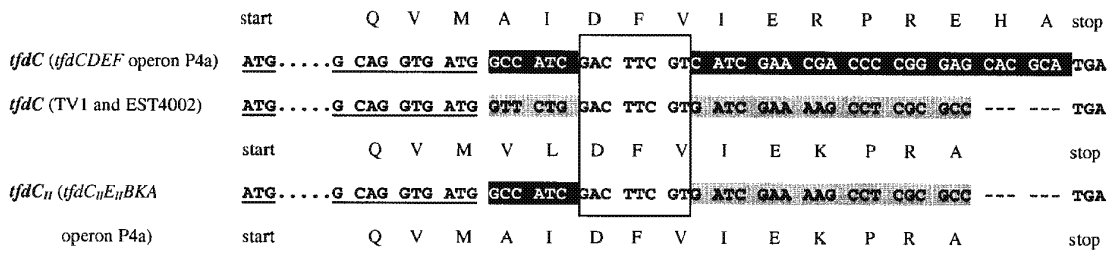


Fig. 3. Alignment of the 3′ termini of the *tfdC* and *tfdC*$_{II}$ genes of *D. acidovorans* P4a as well as the *tfdC* genes of *V. paradoxus* TV1 and *A. xylosoxidans* subsp. *denitrificans* EST4002 (49 and 43 nt upstream of the stop codon, respectively). The *tfdC*$_{II}$ gene of strain P4a is composed of nucleotide sequences descending from two different *tfdC* genes. The 5′ terminus of *tfdC*$_{II}$ is identical to the *tfdC* gene in the chlorocatechol operon of strain P4a. However, the 19 nt at the end 3′ terminus are identical to homologous regions in *V. paradoxus* TV1 and *A. xylosoxidans* subsp. *denitrificans* EST4002. Black underlined, identical regions; black framed, putative target region of recombination events; white with black background, nucleotide sequence of *tfdC* in the *tfdCDEF* operon of *D. acidovorans* P4a; black with grey background, nucleotide sequence of *tfdC* in *V. paradoxus* TV1 and *A. xylosoxidans* subsp. *denitrificans* EST4002.

van der Meer, 1996) are clustered (Fig. 2), as they are in a range of other strains (van der Meer *et al.*, 1991a, b, c, d; Leveau *et al.*, 1994; Potrawfke *et al.*, 1998, 2001; Ogawa & Miyashita, 1999). Sequence similarity even extends to the overlapping regions of some genes as well as to their intergenic regions. Clearly this kind of arrangement has emerged during the course of evolution, enabling the effective use of chlorocatechols, and is distributed as a module for the recruitment of degradative pathways.

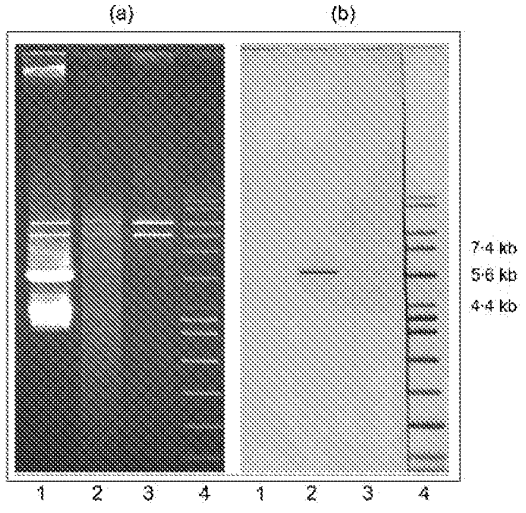


Fig. 4. Southern blot hybridization of chromosomal and plasmidal DNA of *D. acidovorans* P4a. Chromosomal and plasmidal DNA were digested with *Eco*RI and *Bgl*II. The DNA fragments were separated electrophoretically in an 0·8% agarose gel (a), blotted onto a nylon membrane and fixed by UV irradiation. Southern blot hybridization was performed with a *tfdAKB*-specific probe (2·5 kb) at 60 °C (b). Raoul size marker was hybridized with labelled pBR322 fragments. Lanes: 1, plasmid DNA 1 (containing all plasmids) of strain P4a, digested with *Eco*RI and *Bgl*II; 2, genomic DNA of strain P4a, digested with *Eco*RI and *Bgl*II; 3, plasmid DNA 2 (containing the 21 kb plasmid only) of strain P4a, digested with *Eco*RI and *Bgl*II; 4, Raoul marker (Appligene).

A second cluster found in some organisms is distinguished by the presence of *tfdA*, encoding a 2,4-D/2-oxoglutarate dioxygenase (Streber *et al.*, 1987; Fukumori & Hausinger, 1993), in addition to *tfdK*, which was shown to encode a transport protein (Leveau *et al.*, 1998). The combination of these genes seems logical if active transport is required for exploiting phenoxyalkanoates as carbon and energy sources. Active transport of these compounds has been found to play a significant role in *Sphingomonas herbicidovorans* MH, in which inducible and substrate-specific uptake systems have been observed (Zipper *et al.*, 1998). By contrast, the lack of *tfdK* appears to have only minor negative effects in a mutant strain of *R. eutropha* JMP134 (Leveau *et al.*, 1998). Accordingly, uptake may also proceed by simple diffusion, which is a mechanism known for (uncharged) organic acids. In these two studies, the strains were grown under neutral pH conditions. With strain P4a, which is adapted to alkaline conditions, the uptake characteristics remain to be proven. One should take into account, however, that the dissociation equilibrium is shifted strongly towards the anion of the target compounds during growth under alkaline conditions, which means pH values of up to 10 with this strain (Hoffmann *et al.*, 1996). Hence, uptake by simple diffusion ought to be limited by the concentration of the free acid of 2,4-D, making it likely or even essential to support utilization of this compound by a specific uptake system.

The second *tfd* cluster, *tfdC*$_{II}$*E*$_{II}$*BKA*, also includes *tfdB*, which is known to encode a chlorophenol hydroxylase (Perkins *et al.*, 1990). This apparently completes the 2,4-D degradative pathway in strain P4a. The structure of this gene

COR-AAD1-00002559
Bayer EX1008 (Part 5 of 9)

cassette appears to be identical to that found in other strains (Fig. 2; Vallaeys *et al.*, 1996; Vedler *et al.*, 2000; Poh *et al.*, 2002) and, again, transcription of the genes is presumably governed by *tfdR*. Two sets of *tfdC* and *tfdE* genes are found in strain P4a. It remains to be elucidated whether the expression of both these genes is essential for the proper function of the 2,4-D pathway in this strain or whether one of each is merely rudimentary. In *R. eutropha* JMP134, two complete sets of the chlorocatechol genes were also found, the expression of which was shown to speed up growth of this organism on 2,4-D (Leveau *et al.*, 1999; Laemmli *et al.*, 2000; Pérez-Pantoja *et al.*, 2000). According to the differences in their nucleotide sequences, both *tfd* modules must have been acquired from different evolutionary origins in *R. eutropha* JMP134. This can also be concluded for strain P4a when the differences between *tfdE* and $tfdE_{II}$ are considered: their gene products share only 28 % identity with each other but are highly similar to TfdE homologues in different bacterial strains (Table 1).

This high degree of coincidence between the *tfd* genes and their arrangement suggests horizontal gene transfer as the likely explanation for the acquisition of the 2,4-D cassettes in strain P4a rather than being a feature evolved in this strain itself. The two different cassettes (*tfdCDEF* and $tfdC_{II}E_{II}BKA$) hint at two origins, although it cannot be excluded that a complete arrangement was captured by *D. acidovorans* from any strain. With special reference to building rubble, from which strain P4a was isolated, some questions regarding the generation of the ability to degrade 2,4-D remain obscure. These refer to the fact that the highly alkaline environmental conditions, which exceed pH 11·5 in aqueous surroundings of this material, preclude growth of *D. acidovorans* on this material. Thus, any conjugative processes are rather unlikely to occur in this very habitat. One can speculate, however, that micro-niches with moderate pH conditions, for example, mixing zones between building rubble and soil, are appropriate breeding areas for this characteristic. Starting from any primitive strain carrying and expressing the genetic information for 2,4-D degradation, strain P4a might have evolved in one of these micro-niches by gene transfer, genetic rearrangements and selection of the fittest. This also applies to the strains *D. acidovorans* MC1 and *Rhodoferax* sp. P230, which were isolated from the same habitat and are highly similar to strain P4a with reference to some of their *tfd* genes (Müller *et al.*, 2001).

The nucleotide sequences found outside the 2,4-D degradation genes, i.e. downstream of the *tfdR* genes, are indicative of possible maturation processes and complete the picture of the 'recent' strain *D. acidovorans* P4a. The *tfd* genes are flanked by transposons of the IS*1380* and IS*1071* families, each comprising a transposase gene in this DNA segment. Remarkably, the two segments are identical in structure. Moreover, the identity is extended to an ORF with unknown function, named *orfII*, and to both *tfdR* and *tfdC*. A further observation that may help elucidate the evolution of the 2,4-D degradation pathway in strain P4a is that a short sequence of $tfdC_{II}$ (19 bp, located downstream) deviates from that of *tfdC* in P4a and is identical to homologous sequences of other *tfdC* genes found in the *tfdCEBKA* cassettes of some other strains (Fig. 2). This implies that recombination events took place at this position with a gene descending from a different ancestor.

Another finding that should be emphasized is that the complete set of *tfd* genes is located on the chromosome in strain P4a, while in other strains known to carry chromosomally located *tfd* genes only parts of the 2,4-D degradation pathway are encoded on the chromosome (Ka *et al.*, 1994; Matheson *et al.*, 1996; Suwa *et al.*, 1996). When we started investigating strain P4a we noted plasmids of various sizes ranging from 5 to about 60 kb, and found indications that *tfd* genes were located on them (Hoffmann *et al.*, 1996). However, we have had serious problems assigning the *tfd* genes to the respective plasmids. Recent investigations have shown that strain P4a now carries only one plasmid of about 21 kb, which is not associated with 2,4-D degradation. Therefore, under the selective pressure applied during laboratory cultivation, events occurred in the genetic structure that stabilized the degradative activities, leading to the emergence of the strain we describe as 'recent'. The transposon structure is likely to have promoted these events in a kind of evolutionary optimization process, similar to phenomena observed in various other strains, raising questions about the pros and cons of carrying plasmids (Deutz *et al.*, 1991; Stouthamer & Kooijman, 1993).

The chromosomal location of the genes of a pathway should certainly have consequences. Genes localized in the chromosomal matrix of the genome can be considered established, in contrast to plasmid-derived properties which can be classed as temporary or transitional. Taking into account that transposons are elements appropriate to quickly spread genetic information to suitable carriers, and plasmids are carriers capable of distributing genetic information into respective host strains, strains with plasmids harbouring respective information on transposons are fragile for this characteristic as they include 2 d.f. of losing this information. When it becomes localized on the chromosome, by contrast, even as a transposon, the d.f. is accordingly reduced. This prompts the question of whether P4a, as a strain of a species that prefers organic acids as carbon and energy sources (Tamaoka *et al.*, 1987; Wen *et al.*, 1999), is in the process of adding a further acid, i.e. 2,4-D, to its spectrum of preferred substrates. Only a few mutation events which prevent this genetic element from transposing, for example, by changing target sites of transposase attack, avoiding expression of transposases or leading to inactive transposases, would be required to stabilize this property, making the ability to use the compound an inherent property of the strain. Stability of the degradative performance is by no means under selective pressure but becomes decisive if any strain is intended

COR-AAD1-00002560
Bayer EX1008 (Part 5 of 9)

to be used for bioaugmentation as effective production of biomass will rely more on conventional carbon and energy sources. Even in recent times we have observed the occasional loss of the 2,4-D degradative capability in some clones, accompanied by the lack of all *tfd* genes.

The metabolic constellation of this alkalitolerant strain (P4a) enables the productive degradation of 2,4-D at pH values up to 10 in laboratory cultures (Hoffmann *et al.*, 1996). Moreover, we have detected activity at up to pH 11·5 when strain P4a has been applied as an inoculum in a bioremediation process with building rubble (Müller *et al.*, 1996, 2000). The capacity of the species to metabolize phenoxyalkanoates was also demonstrated with another strain, *D. acidovorans* MC1, which was isolated from the same alkaline environment and was able to utilize an even wider spectrum of compounds (Müller *et al.*, 1999b, 2001). In contrast to these alkalitolerant strains, true alkaliphiles are unlikely to be able to degrade 2,4-D productively. This conclusion is consistent with results obtained with a soda lake isolate, *Halomonas* sp. EF43, supplied with plasmid pJP4 by conjugative transfer (Kleinsteuber *et al.*, 2001). Despite the expression of the *tfd* genes, this strain was unable to use 2,4-D as a sole source of carbon and energy, even though it was able to degrade the compound, at least in the presence of an additional carbon source (Kleinsteuber *et al.*, 2001). This may well also apply to another alkaliphilic strain belonging to the *Halomonadaceae* described by Maltseva *et al.* (1996), since the published data do not indicate that this isolate can make productive use of 2,4-D.

The property of catching and getting rid of genetic information is considered a mechanism to effectively settle niches and contributes to the metabolic resilience of biotopes. The present results suggest that the uptake of any genetic information for completing a degradative pathway, even as preformed and 'optimized' cassettes, is only a precondition to enable the degradation of a given compound but may not be sufficient to do this in an effective, ultimately competitive, way. This refers to growth rate first but may include stability too, both of which are an expression of adaptation. The latter also applies for *D. acidovorans* MC1, a further strain isolated in this laboratory in 1999. In this case, we observed loss of the degradative trait under non-selective conditions in almost all overnight cultures. Today, derivatives of this strain exist which harbour this activity for at least 80 generations during growth on complex medium. Thus, stability is gained at the expense of flexibility.

REFERENCES

Alphey, L. (1998). *DNA-Sequenzierung.* Heidelberg, Berlin: Spektrum Akademischer Verlag GmbH.

Altschul, S. F., Madden, T. L., Schaffer, A. A., Zhang, J., Zhang, Z., Miller, W. & Lipman, D. J. (1997). Gapped BLAST and PSI-BLAST: a new generation of protein database search programs. *Nucleic Acids Res* **25**, 3389–3402.

Bhat, M. A., Tsuda, M., Horiike, K., Nozaki, M., Vaidyanathan, C. S. & Nakazawa, T. (1994). Identification and characterization of a new plasmid carrying genes for degradation of 2,4-dichlorophenoxyacetate from *Pseudomonas cepacia* CSV90. *Appl Environ Microbiol* **60**, 307–312.

Chablain, P. A., Zgoda, A. L., Sarde, C. O. & Truffaut, N. (2001). Genetic and molecular organization of the alkylbenzene catabolism operon in the psychrotrophic strain *Pseudomonas putida* 01G3. *Appl Environ Microbiol* **67**, 453–458.

Chatterjee, D. K., Kellogg, S. T., Hamada, S. & Chakrabarty, A. M. (1981). Plasmid specifying total degradation of 3-chlorobenzoate by a modified *ortho* pathway. *J Bacteriol* **146**, 639–646.

Chaudhry, G. R. & Huang, G. H. (1988). Isolation and characterization of a new plasmid from a *Flavobacterium* sp. which carries the genes for degradation of 2,4-dichlorophenoxyacetate. *J Bacteriol* **170**, 3897–3902.

Cowles, C. E., Nichols, N. N. & Harwood, C. S. (2000). BenR, a XylS homologue, regulates three different pathways of aromatic acid degradation in *Pseudomonas putida*. *J Bacteriol* **182**, 6339–6346.

Deutz, W. A., Winson, M. K., van Andel, J. G. & Williams, P. A. (1991). Mathematical analysis of catabolic function loss in a population of *Pseudomonas putida* mt-2 during non-limited growth on benzoate. *J Gen Microbiol* **137**, 1363–1368.

Don, R. H. & Pemberton, J. M. (1981). Properties of six pesticide degradation plasmids isolated from *Alcaligenes paradoxus* and *Alcaligenes eutrophus*. *J Bacteriol* **145**, 681–686.

Don, R. H. & Pemberton, J. M. (1985). Genetic and physical map of the 2,4-dichlorophenoxyacetic acid-degradative plasmid pJP4. *J Bacteriol* **161**, 466–468.

Feng, X., Ou, L. T. & Ogram, A. (1997). Cloning and sequence analysis of a novel insertion element from plasmids harbored by the carbofuran-degrading bacterium, *Sphingomonas* sp. CF06. *Plasmid* **37**, 169–179.

Fukumori, F. & Hausinger, R. P. (1993). *Alcaligenes eutrophus* JMP134 "2,4-dichlorophenoxyacetate monooxygenase" is an α-ketoglutarate-dependent dioxygenase. *J Bacteriol* **175**, 2083–2086.

Fulthorpe, R. R., McGowan, C., Maltseva, O. V., Holben, W. E. & Tiedje, J. M. (1995). 2,4-Dichlorophenoxyacetic acid-degrading bacteria contain mosaics of catabolic genes. *Appl Environ Microbiol* **61**, 3274–3281.

Fulthorpe, R. R., Rhodes, A. N. & Tiedje, J. M. (1996). Pristine soils mineralize 3-chlorobenzoate and 2,4-dichlorophenoxyacetate via different microbial populations. *Appl Environ Microbiol* **62**, 1159–1166.

Hickey, W. J., Sabat, G., Yuroff, A. S., Arment, A. R. & Perez-Lesher, J. (2001). Cloning, nucleotide sequencing, and functional analysis of a novel, mobile cluster of biodegradation genes from *Pseudomonas aeruginosa* strain JB2. *Appl Environ Microbiol* **67**, 4603–4609.

Hoffmann, D., Müller, R. H., Kiesel, B. & Babel, W. (1996). Isolation and characterization of an alkaliphilic bacterium capable of growing on 2,4-dichlorophenoxyacetic acid and 4-chloro-2-methylphenoxyacetic acid. *Acta Biotechnol* **16**, 121–131.

Hoffmann, D., Kleinsteuber, S., Müller, R. H. & Babel, W. (2001). Development and application of PCR primers for the detection of the *tfd* genes in *Delftia acidovorans* P4a involved in the degradation of 2,4-D. *Acta Biotechnol* **21**, 321–331.

Hogan, D. A., Buckley, D. H., Nakatsu, C. A., Schmidt, T. M. & Hausinger, R. P. (1997). Distribution of the *tfdA* gene in soil bacteria that do not degrade 2,4-dichlorophenoxyacetic acid, 2,4-D. *Microb Ecol* **34**, 90–96.

Itoh, K., Kanda, R., Sumita, Y., Kim, H., Kamagata, Y., Suyama, K., Yamamoto, H., Hausinger, R. P. & Tiedje, J. M. (2002). *tfdA*-like

COR-AAD1-00002561
Bayer EX1008 (Part 5 of 9)

genes in 2,4-dichlorophenoxyacetic acid-degrading bacteria belonging to the *Bradyrhizobium-Agromonas-Nitrobacter-Afipia* cluster in α-*Proteobacteria*. *Appl Environ Microbiol* **68**, 3449–3454.

Ka, J. O. & Tiedje, J. M. (1994). Integration and excision of a 2,4-dichlorophenoxyacetic acid-degradative plasmid in *Alcaligenes paradoxus* and evidence of its natural intergeneric transfer. *J Bacteriol* **176**, 5284–5289.

Ka, J. O., Holben, W. E. & Tiedje, J. M. (1994). Genetic and phenotypic diversity of 2,4-dichlorophenoxyacetic acid (2,4-D)-degrading bacteria isolated from 2,4-D-treated field soils. *Appl Environ Microbiol* **60**, 1106–1115.

Kamagata, Y., Fulthorpe, R. R., Tamura, K., Takami, H., Forney, L. J. & Tiedje, J. M. (1997). Pristine environments harbor a new group of oligotrophic 2,4-dichlorophenoxyacetic acid-degrading bacteria. *Appl Environ Microbiol* **63**, 2266–2272.

Kaphammer, B. & Olsen, R. H. (1990). Cloning and characterization of *tfdS*, the repressor-activator gene of *tfdB*, from the 2,4-dichlorophenoxyacetic acid catabolic plasmid pJP4. *J Bacteriol* **172**, 5856–5862.

Kaphammer, B., Kukor, J. J. & Olsen, R. H. (1990). Regulation of *tfdCDEF* by *tfdR* of the dichlorophenoxyacetic acid degradation plasmid pJP4. *J Bacteriol* **172**, 2280–2286.

Kleinsteuber, S., Müller, R. H. & Babel, W. (2001). Expression of the 2,4-D degradative pathway of pJP4 in an alkaliphilic, moderately halophilic soda lake isolate, *Halomonas* sp. EF43. *Extremophiles* **5**, 375–384.

Laemmli, C. M., Leveau, J. H. J., Zehnder, A. J. B. & van der Meer, J. R. (2000). Characterization of a second *tfd* gene cluster for chlorophenol and chlorocatechol metabolism on plasmid pJP4 in *Ralstonia eutropha* JMP134(pJP4). *J Bacteriol* **182**, 4165–4172.

Leveau, J. H. J. & van der Meer, J. R. (1996). The *tfdR* gene product can successfully take over the role of the insertion element-inactivated TfdT protein as a transcriptional activator of the *tfdCDEF* gene cluster, which encodes chlorocatechol degradation in *Ralstonia eutropha* JMP134(pJP4). *J Bacteriol* **178**, 6824–6832.

Leveau, J. H. J., de Vos, W. M. & van der Meer, J. R. (1994). Analysis of the binding site of the LysR-type transcriptional activator TcbR on the *tcbR* and *tcbC* divergent promotor sequences. *J Bacteriol* **176**, 1850–1856.

Leveau, J. H. J., Zehnder, A. J. B. & van der Meer, J. R. (1998). The *tfdK* gene product facilitates uptake of 2,4-dichlorophenoxyacetate by *Ralstonia eutropha* JMP134(pJP4). *J Bacteriol* **180**, 2237–2243.

Leveau, J. H. J., König, F., Füchslin, H., Werlen, C. & van der Meer, J. R. (1999). Dynamics of multigene expression during catabolic adaptation of *Ralstonia eutropha* JMP134(pJP4) to the herbicide 2,4-dichlorophenoxyacetate. *Mol Microbiol* **33**, 396–406.

Loffhagen, N., Härtig, C. & Babel, W. (1997). The toxicity of substituted phenolic compounds to a detoxifying and an acetic acid bacterium. *Ecotoxicol Environ Saf* **36**, 269–274.

Loffhagen, N., Härtig, C. & Babel, W. (2001). Suitability of the *trans*/*cis* ratio of unsaturated fatty acids in *Pseudomonas putida* NCTC 10936 as an indicator of the acute toxicity of chemicals. *Ecotoxicol Environ Saf* **50**, 65–71.

Mäe, A. A., Marits, R. O., Ausmess, N. R., Kõiv, V. M. & Heinaru, A. L. (1993). Characterization of a new 2,4-dichlorophenoxyacetic acid degrading plasmid pEST4011: physical map and localization of catabolic genes. *J Gen Microbiol* **139**, 3165–3170.

Maeda, K., Nojiri, H., Shintani, M., Yoshida, T., Habe, H. & Omori T. (2003). Complete nucleotide sequence of carbazole/dioxin-degrading plasmid pCAR1 in *Pseudomonas resinovorans* strain CA10 indicates its mosaicity and the presence of large catabolic transposon Tn*4676*. *J Mol Biol* **326**, 21–33.

Mahillon, J. & Chandler, M. (1998). Insertion sequences. *Microbiol Mol Biol Rev* **62**, 725–774.

Maltseva, O., McGowan, C., Fulthorpe, R. & Oriel, P. (1996). Degradation of 2,4-dichlorophenoxyacetic acid by haloalkaliphilic bacteria. *Microbiology* **142**, 1115–1122.

Matheson, V. G., Forney, L. J., Suwa, Y., Nakatsu, C. H., Sextone, A. J. & Holben, W. E. (1996). Evidence for acquisition in nature of a chromosomal 2,4-dichlorophenoxyacetic acid/α-ketoglutarate dioxygenase gene by different *Burkholderia* spp. *Appl Environ Microbiol* **62**, 2457–2463.

McGowan, C., Fulthorpe, R., Wright, A. & Tiedje, J. M. (1998). Evidence for interspecies gene transfer in the evolution of 2,4-dichlorophenoxyacetic acid degraders. *Appl Environ Microbiol* **64**, 4089–4092.

Merlin, C., Springael, D., Mergeay, M. & Toussaint, A. (1997). Organization of the *bph* gene cluster of transposon Tn*4371*, encoding enzymes for the degradation of biphenyl and 4-chlorobiphenyl compounds. *Mol Gen Genet* **253**, 499–506.

Müller, R. H., Müller, R. A. & Babel, W. (1996). Degradation von Phenoxyalkansäure-Herbiziden durch alkaliphile Mikroorganismen – Dekontamination von belastetem Bauschutt. In *Neue Techniken der Bodenreinigung*, pp. 373–384. Edited by R. Stegmann. Bonn: Economia Verlag.

Müller, R. H., Müller, R. A., Jahn, Y. & Babel, W. (1999a). A biotechnological approach of detoxifying herbicide-contaminated building rubble. In *Bioremediation of Nitroaromatic and Haloaromatic Compounds*, pp. 143–148. Edited by B. C. Alleman & A. Leeson. Columbus, Richland: Battelle Press.

Müller, R. H., Jorks, S., Kleinsteuber, S. & Babel, W. (1999b). *Comamonas acidovorans* strain MC1: a new isolate capable of degrading the chiral herbicides dichlorprop and mecoprop and the herbicides 2,4-D and MCPA. *Microbiol Res* **154**, 241–246.

Müller, R. H., Müller, R. A., Jahn, Y. & Babel, W. (2000). Bioremediation of building material contaminated with herbicides. In *Remediation of Hazardous Waste Contaminated Soils*, 2nd edn, pp. 121–131. Edited by D. L. Wise, D. J. Trantolt & E. J. Cichon. New York: Marcel Dekker.

Müller, R. H., Kleinsteuber, S. & Babel, W. (2001). Physiological and genetic characteristics of two bacterial strains utilizing phenoxypropionate and phenoxyacetate herbicides. *Microbiol Res* **156**, 121–131.

Müller, T. A., Werlen, C., Spain, J. & van der Meer, J. R. (2003). Evolution of a chlorobenzene degradative pathway among bacteria in a contaminated groundwater mediated by a genomic island in *Ralstonia*. *Environ Microbiol* **5**, 163–173.

Nakatsu, C. H. & Wyndham, R. C. (1993). Cloning and expression of the transposable chlorobenzoate-3,4-dioxygenase genes of *Alcaligenes* sp. strain BR60. *Appl Environ Microbiol* **59**, 3625–3633.

Nakatsu, C., Ng, J., Singh, R., Straus, N. & Wyndham, C. (1991). Chlorobenzoate catabolic transposon Tn*5271* is a composite class I element with flanking class II insertion sequences. *Proc Natl Acad Sci U S A* **88**, 8312–8316.

Nakatsu, C. H., Straus, N. A. & Wyndham, R. C. (1995). The nucleotide sequence of the Tn*5271* 3-chlorobenzoate 3,4-dioxygenase genes (*cbaAB*) unites the class IA oxygenases in a single lineage. *Microbiology* **141**, 485–495.

Nakatsu, C. H., Providenti, M. & Wyndham, R. C. (1997). The *cis*-diol dehydrogenase *cbaC* gene of Tn*5271* is required for growth on 3-chlorobenzoate but not on 3,4-dichlorobenzoate. *Gene* **196**, 209–218.

Nojiri, H., Sekiguchi, H., Maeda, K., Urata, M., Nakai, S., Yoshida, T., Habe, H. & Omori, T. (2001). Genetic characterization and evolutionary implications of a *car* gene cluster in the carbazole degrader *Pseudomonas* sp. strain CA10. *J Bacteriol* **183**, 3663–3679.

COR-AAD1-00002562
Bayer EX1008 (Part 5 of 9)

Odgen, R. (1998). *The bphS regulatory gene found in Pseudomonas sp. strain IC: a molecular analysis.* PhD Thesis, University of Wales.

Ogawa, N. & Miyashita, K. (1995). Recombination of a 3-chlorobenzoate catabolic plasmid from *Alcaligenes eutrophus* NH9 mediated by direct repeat elements. *Appl Environ Microbiol* **61**, 3788–3795.

Ogawa, N. & Miyashita, K. (1999). The chlorocatechol-catabolic transposon Tn*5707* of *Alcaligenes eutrophus* NH9, carrying a gene cluster highly homologous to that in the 1,2,4-trichlorobenzene-degrading bacterium *Pseudomonas* sp. strain P51, confers the ability to grow on 3-chlorobenzoate. *Appl Environ Microbiol* **65**, 724–731.

Pérez-Pantoja, D., Guzmán, L., Manzano, M., Pieper, D. H. & González, B. (2000). Role of $tfdC_ID_IE_IF_I$ and $tfdD_{II}C_{II}E_{II}F_{II}$ gene modules in catabolism of 3-chlorobenzoate by *Ralstonia eutropha* JMP134(pJP4). *Appl Environ Microbiol* **66**, 1602–1608.

Perkins, E. J., Gordon, M. P., Caceres, O. & Lurquin, P. F. (1990). Organization and sequence analysis of the 2,4-dichlorophenol hydroxylase and dichlorocatechol oxidative operons of plasmid pJP4. *J Bacteriol* **172**, 2351–2359.

Pieper, D. H., Reineke, W., Engesser, K.-H. & Knackmuss, H.-J. (1988). Metabolism of 2,4-dichlorophenoxyacetic acid, 4-chloro-2-methylphenoxyacetic acid and 2-methylphenoxyacetic acid by *Alcaligenes eutrophus* JMP134. *Arch Microbiol* **150**, 95–102.

Pieper, D. H., Stadler-Fritzsche, K., Engesser, K.-H. & Knackmuss, H. J. (1993). Metabolism of 2-chloro-4-methylphenoxyacetate by *Alcaligenes eutrophus* JMP134. *Arch Microbiol* **160**, 169–178.

Poh, R. P.-C., Smith, A. R. W. & Bruce, I. J. (2002). Complete characterization of Tn*5530* from *Burkholderia cepacia* strain 2a(pIJB1) and studies of 2,4-dichlorophenoxyacetate uptake by the organism. *Plasmid* **48**, 1–12.

Potrawfke, T., Timmis, K. N. & Wittich, R. M. (1998). Degradation of 1,2,3,4-tetrachlorobenzene by *Pseudomonas chlororaphis* RW71. *Appl Environ Microbiol* **64**, 3798–3806.

Potrawfke, T., Armengaud, J. & Wittich, R. M. (2001). Chlorocatechols substituted at positions 4 and 5 are substrates of the broad-spectrum chlorocatechol 1,2-dioxygenase of *Pseudomonas chlororaphis* RW71. *J Bacteriol* **183**, 997–1011.

Sambrook, J., Fritsch, E. F. & Maniatis, T. (1989). *Molecular Cloning: a Laboratory Manual*, 2nd edn. Cold Spring Harbor, NY: Cold Spring Harbor Laboratory.

Sanger, F., Nicklen, S. & Coulson, A. R. (1977). DNA sequencing with chain-terminating inhibitors. *Proc Natl Acad Sci U S A* **74**, 5463–5467.

Springael, D., Kreps, S. & Mergeay, M. (1993). Identification of a catabolic transposon, Tn*4371*, carrying biphenyl and 4-chlorobiphenyl degradation genes in *Alcaligenes eutrophus* A5. *J Bacteriol* **175**, 1674–1681.

Stouthamer, A. H. & Kooijman, S. A. (1993). Why it pays for bacteria to delete disused DNA and to maintain megaplasmids. *Antonie Van Leeuwenhouk* **63**, 39–43.

Strauss, E. C., Kobori, J. A., Siu, G. & Hood, L. E. (1986). Specific-primer-directed DNA sequencing. *Anal Biochem* **154**, 353–360.

Streber, W. R., Timmis, K. N. & Zenk, M. H. (1987). Analysis, cloning and high-level expression of 2,4-dichlorophenoxyacetate monooxygenase gene *tfdA* of *Alcaligenes eutrophus* JMP134. *J Bacteriol* **169**, 2950–2955.

Suwa, Y., Wright, A. D., Fukimori, F., Nummy, K. A., Hausinger, R. P., Holben, W. E. & Forney, L. J. (1996). Characterization of a chromosomally encoded 2,4-dichlorophenoxyacetic acid/α-ketoglutarate dioxygenase from *Burkholderia* sp. strain RASC. *Appl Environ Microbiol* **62**, 2464–2469.

Takemura, H., Horinouchi, S. & Beppu, T. (1991). Novel insertion sequence IS*1380* from *Acetobacter pasteurianus* is involved in loss of ethanol-oxidizing ability. *J Bacteriol* **173**, 7070–7076.

Tamaoka, J., Ha, D.-M. & Komagata, K. (1987). Reclassification of *Pseudomonas acidovorans* den Dooren de Jong 1926 and *Pseudomonas testosteroni* Marcus and Talalay 1956 as *Comamonas acidovorans* comb. nov. and *Comamonas testosteroni* comb. nov., with an emended description of the genus *Comamonas*. *Int J Syst Bacteriol* **37**, 52–59.

Top, E. M., Holben, W. E. & Forney, L. J. (1995). Characterization of diverse 2,4-dichlorophenoxyacetic acid-degradative plasmids isolated from soil by complementation. *Appl Environ Microbiol* **61**, 1691–1698.

Vallaeys, T., Fulthorpe, R. R., Wright, A. M. & Soulas, G. (1996). The metabolic pathway of 2,4-dichlorophenoxyacetic acid degradation involves different families of *tfdA* and *tfdB* genes according to PCR-RFLP analysis. *FEMS Microbiol Ecol* **20**, 163–172.

Vallaeys, T., Albino, L., Soulas, G., Wright, A. D. & Weightman, A. J. (1998). Isolation and characterization of a stable 2,4-dichlorophenoxyacetic acid degrading bacterium, *Variovorax paradoxus*, using chemostat culture. *Biotechnol Lett* **20**, 1073–1076.

Vallaeys, T., Courde, L., McGowan, C., Wright, A. D. & Fulthorpe, R. R. (1999). Phylogenetic analyses indicate independent recruitment of diverse gene cassettes during assemblage of the 2,4-D catabolic pathway. *FEMS Microbiol Ecol* **28**, 373–382.

van der Meer, J. R. (1997). Evolution of novel metabolic pathways for the degradation of chloroaromatic compounds. *Antonie Van Leeuwenhoek* **71**, 159–178.

van der Meer, J. R., Eggen, R. I. L., Zehnder, A. J. B. & de Vos, W. M. (1991a). Sequence analysis of the *Pseudomonas* sp. strain P51 *tcb* gene cluster, which encodes metabolism of chlorinated catechols: evidence for specialization of catechol 1,2-dioxygenases for chlorinated substrates. *J Bacteriol* **173**, 2425–2434.

van der Meer, J. R., Frijters, A. C. J., Leveau, J. H. J., Eggen, R. I. L., Zehnder, A. J. B. & de Vos, W. M. (1991b). Characterization of the *Pseudomonas* sp. strain P51 gene *tcbR*, a LysR-type transcriptional activator of the *tcbCDEF* chlorocatechol oxidative operon, and analysis of the regulatory region. *J Bacteriol* **173**, 3700–3708.

van der Meer, J. R., Neerven, A. R. W., de Vries, E. J., de Vos, W. M. & Zehnder, A. J. B. (1991c). Cloning and characterization of plasmid-encoded genes for the degradation of 1,2-dichloro-, 1,4-dichloro-, and 1,2,4-trichlorobenzene of *Pseudomonas* sp. strain P51. *J Bacteriol* **173**, 6–15.

van der Meer, J. R., Zehnder, A. J. B. & de Vos, W. M. (1991d). Identification of a novel composite transposable element, Tn*5280*, carrying chlorobenzene dioxygenase genes of *Pseudomonas* sp. strain P51. *J Bacteriol* **173**, 7077–7083.

van der Meer, J. R., Ravatn, R. & Sentchilo, V. (2001). The *clc* element of *Pseudomonas* sp. B13 and other mobile degradative elements employing phage-like integrases. *Arch Microbiol* **175**, 79–85.

Vedler, E., Kõiv, V. & Heinaru, A. (2000). Analysis of the 2,4-dichlorophenoxyacetic acid-degradative plasmid pEST4011 of *Achromobacter xylosoxidans* subsp. *denitrificans* strain EST4002. *Gene* **255**, 281–288.

Wen, A., Fegan, M., Hayward, C., Chakraborty, S. & Sly, L. I. (1999). Phylogenetic relationships among members of the *Comamonadaceae*, and description of *Delftia acidovorans* (den Dooren de Jong 1926 and Tamaoka *et al.*, 1987) gen. nov., comb. nov. *Int J Syst Bacteriol* **49**, 567–576.

Wyndham, R. C., Cashore, A. E., Nakatsu, C. H. & Peel, M. C. (1994a). Catabolic transposons. *Biodegradation* **5**, 323–342.

COR-AAD1-00002563
Bayer EX1008 (Part 5 of 9)

Wyndham, R. C., Nakatsu, C., Peel, M., Cashore, A., Ng, J. & Szilagy, F. (1994b). Distribution of the catabolic transposon Tn*5271* in a groundwater bioremediation system. *Appl Environ Microbiol* **60**, 86–93.

Xia, X.-S., Aathithan, S., Oswiecimska, K., Smith, A. R. W. & Bruce, I. J. (1998). A novel plasmid pIJB1 possessing a putative 2,4-dichlorophenoxyacetate degradative transposon Tn*5530* in *Burkholderia cepacia* strain 2a. *Plasmid* **39**, 154–159.

Zipper, C., Bunk, M., Zehnder, A. J. & Kohler, H. P. (1998). Enantioselective uptake and degradation of the chiral herbicide dichlorprop [(RS)-2-(2,4-dichlorophenoxy)propanoic acid] by *Sphingomonas herbicidovorans* MH. *J Bacteriol* **13**, 3368–3374.

COR-AAD1-00002564
Bayer EX1008 (Part 5 of 9)

MICROBIAL ECOLOGY

Microb Ecol (1997) 34:90–96
© 1997 Springer-Verlag New York Inc.

Distribution of the *tfdA* Gene in Soil Bacteria That Do Not Degrade 2,4-Dichlorophenoxyacetic Acid (2,4-D)

D.A. Hogan,[1] D.H. Buckley,[1] C.H. Nakatsu,[1*] T.M. Schmidt,[1] R.P. Hausinger[1,2]

[1] Center for Microbial Ecology and Department of Microbiology, Giltner Hall, Michigan State University, East Lansing, MI 48824, USA
[2] Department of Biochemistry,[2] Michigan State University, East Lansing, MI 48824, USA

Received: 15 July 1996; Accepted: 3 October 1996

ABSTRACT

The *tfdA* gene encodes an α-ketoglutarate-dependent dioxygenase that catalyzes the initial step in the degradation of the widely used herbicide, 2,4-dichlorophenoxyacetic acid (2,4-D). Since its description in *Alcaligenes eutrophus* JMP134, *tfdA* has been found on plasmids or on the chromosomes of phylogenetically diverse 2,4-D–degrading microorganisms. To assess its distribution in more diverse microbial populations, including bacteria that do not degrade 2,4-D, a collection of 76 soil bacteria that had been isolated on nonselective medium was screened for the presence of this gene by PCR amplification of an internal fragment of *tfdA*. PCR amplification products of the expected size were generated from the genomic DNA of 37% of these isolates. The products were shown to be highly similar to previously described *tfdA* sequences, either by hybridization of *tfdA* gene probes or by DNA sequence analyses. None of the isolates were able to degrade 2,4-D in liquid medium, or incorporate radiolabeled carbon from ring- or chain-labeled ^{14}C-2,4-D. Characterization of these isolates by analysis of 16S rDNA partial sequence data showed the extensive distribution of *tfdA* in soil isolates from the same soil community. Microorganisms containing *tfdA* were found in many different phylogenetic groups, including α, β, and γ Proteobacteria, and both the Bacillus-Lactobacillus-Streptococcus subdivision and high G+C group of the Gram-positive phylum. These data suggest that *tfdA*, or closely related homologs, are widespread among soil isolates and are likely to exist in these organisms for a purpose other than the degradation of 2,4-D.

Introduction

The *tfdA* gene [26] encodes 2,4-dichlorophenoxyacetic acid (2,4-D)/α-ketoglutarate dioxygenase [10]; this catalyzes removal of the acetate side chain of 2,4-D, yielding 2,4-dichlorophenol. Thus far, the *tfdA* gene is uniquely associated with 2,4-D degradation and is most often found with the other *tfd* genes that encode the enzymes necessary to complete the degradation of 2,4-D (Fig. 1). While *tfdA* shows no obvious similarity to previously characterized genes, the other 2,4-D degradation genes are related to genes

* *Present Address:* Department of Agronomy, Purdue University, West Lafayette, Indiana, USA.
Correspondence to: R.P. Hausinger.

COR-AAD1-00002565
Bayer EX1008 (Part 5 of 9)

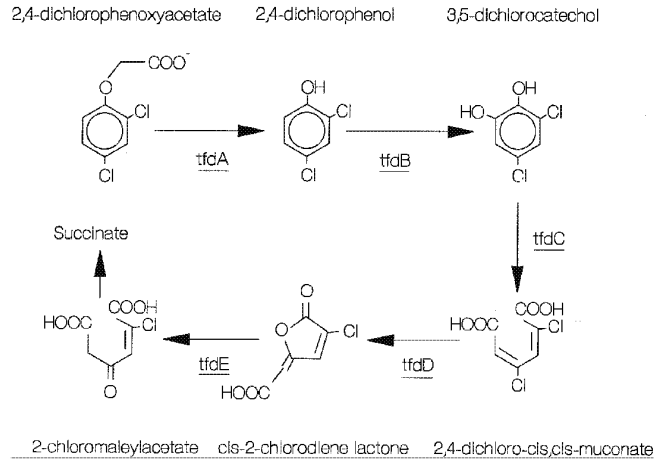


Fig. 1. 2,4-D degradative pathway encoded by plasmid pJP4 in *Alcaligenes eutrophus* JMP134. The genes *tfdA, B, C, D,* and *E* encode 2,4-dichlorophenoxyacetic acid/α-ketoglutarate dioxygenase, 2,4-dichlorophenol hydroxylase, 3,5-dichlorocatechol dioxygenase chloromuconate cycloisomerase, and chlorodiene-lactone hydrolase, respectively.

involved in other degradative pathways. For instance, genes similar in sequence to *tfdB* encode hydroxylases that act on various substituted or unsubstituted phenols in a variety of microorganisms [15, 34]. Likewise, the *tfdCDEF* operon is homologous to other catechol degradation genes involved in many different aromatic degradative pathways [34]. Because the downstream *tfd* genes are closely related to known bacterial genes, it is likely that homologs to *tfdA* can also be identified.

Several pieces of evidence suggest that the assembly of the *tfd* genes to form 2,4-D degradation plasmids has occurred numerous times. First, *tfd* genes have been identified on plasmids from different incompatibility (Inc) groups, as well as on diverse plasmids from the same Inc group [30, 31]. Second, plasmids within the same Inc group can have different alleles of the gene that encode the first three enzymes of the 2,4-D degradative pathway [11, 31]. Third, on some plasmids, *tfdA* is physically distant from the *tfdCDEFB* gene cluster [8]. Furthermore, evidence for *tfdA* or TfdA-like activity has been found in diverse phylogenetic groups, including the β-subdivision of Proteobacteria [3, 7, 11, 27], a γ-Proteobacterium [19], a member of the Flexibacter-Cytophaga-Bacteroides phylum [4], and *Arthrobacter* sp. in the High G+C Subdivision of the Gram-positive phylum [29]. For there to be a "source" of *tfd* genes in the environment prior to their incorporation in 2,4-D degradative pathways, these genes must either be maintained without selection, or serve an alternate purpose.

To assess the natural distribution of *tfdA*, we used PCR primers internal to the *tfdA* gene to screen a collection of soil microorganisms, isolated on a nonselective medium, for the presence of *tfdA* or *tfdA*-like genes. We provide evidence that *tfdA* is present in phylogenetically diverse soil microbes that do not degrade 2,4-D. These data suggest that *tfdA* is maintained in natural populations for a purpose other than 2,4-D degradation.

Materials and Methods

Bacterial Strains

Bacterial strains were isolated from soils obtained from a Long Term Ecological Research (LTER) plot [21] at the Kellogg Biological Research Station in Hickory Corners, Michigan, USA. Soil extracts were serially diluted in 50 mM phosphate buffer (pH 7), then plated on R2A medium (Difco, Detroit, Mich.) and incubated at 28°C for 10 days. Plates with 30–150 colonies were divided into quadrants. All colonies from one quadrant were purified on R2A agar and incubated at 28°C for 3–4 days. Additional colonies were chosen to include several isolates with similar morphologies, as well as a representation of distinctive types. The origins of *Alcaligenes eutrophus* JMP134 (pJP4) [7], JMP228 [1], and *Burkholderia* sp. RASC [27] have been described previously.

16S rDNA Partial Sequence Analyses

Total DNA was obtained from these isolates by detergent lysis [2], and 16S rDNA was amplified by PCR using the eubacterial primers complementary to *Escherichia coli* nucleotide positions 8–27 and 1510-1492 [9]. Amplified rDNA was purified with Ultra-free MC (30,000 MWCO) centrifugal filter units (Millipore, Bedford, Mass.), then sequenced with primers complementary to *E. coli* positions 536–519 or 8–27 [24]. The rDNA sequence was determined by automated fluorescent sequencing performed by the MSU-DOE-PRL Plant Biochemistry Facility, using an ABI Catalyst 800 for *Taq* cycle sequencing and the ABI 373A Sequencer for the analysis of products. Partial 16S rDNA sequences were manually aligned against a collection of 16S rRNA sequences [18] on the basis of conserved regions of sequence and secondary structure of 16S rRNA. Regions of ambiguous alignment were omitted from the subsequent analysis. Phylogenetic trees were generated using the Neighbor Joining method, and the topology was confirmed by Parsimony and Maximum likelihood analyses [28].

PCR Amplification of the tfdA *Gene*

Total DNA samples were isolated from each of the LTER strains [2]. Primers were derived from conserved regions of sequence in the *tfdA* genes of pJP4 and *Burkholderia* strain RASC (79% iden-

COR-AAD1-00002566
Bayer EX1008 (Part 5 of 9)

tical to *tfdA*-pJP4). The sequence of the forward primer, TVU, was 5′-ACG GAG TTC TG(C/T) GA(C/T) ATG-3′; the sequence of the reverse primer, TVL, was 5′-AAC GCA GCG (G/A)TT (G/A)TC CCA-3′ [33]. The PCR mix contained 5 µl 10 × PCR buffer (Gibco, Gaithersberg, MD), 1.5 mM $MgCl_2$, 1 µM primer TVU, 1 µM primer TVL, 1 mM dNTPs (Boehringer Mannheim, Indianapolis, Ind.), 1.5 units of *Taq* polymerase (Gibco), 10–100 ng template DNA, and distilled water, to bring the final volume to 50 µl. The PCR amplification protocol consisted of 35 cycles with a 1-min denaturation step at 94°C, a 1-min annealing step at 55°C, and a 1-min extension step at 72°C. The predicted product size is 360 bp. Amplified products were separated on a 1% agarose gel, and compared to PCR products generated from JMP134 and RASC genomic DNA as template. Generation of PCR products was confirmed by at least one additional PCR amplification reaction. Products were purified with Promega PCR mini-prep columns (Promega, Madison, Wis.). Selected PCR products were sequenced with either primer TVL or TVU, by the method described for 16S rDNA, above.

Dot Blot of PCR Products

PCR products were applied to a Hybond N nylon membrane (Amersham, Arlington Heights, Ill.) in 1-µl aliquots, and UV cross-linked to the membrane with a Stratalinker (Stratagene, La Jolla, Calif.). To create probes, PCR products obtained using DNA from JMP134 and RASC were labeled with digoxigenin, using the DIG High Prime labeling mix (Boehringer Mannheim), according to the manufacturer's instructions. Hybridization, detection, and probe removal were performed according to protocols in the Genius Detection System manual (Boehringer Mannheim). To assure high stringency, the hybridization solution contained 50% formamide, and hybridizations and stringency washes were at 68°C. Hybridization signals were detected by the colorimetric detection system (Boehringer Mannheim).

Analysis of 2,4-D Degradation

Isolates were streaked on R2A agar and incubated at 30°C for three days to allow for growth of all cultures. Isolated colonies were transferred to tubes containing 3 ml of A + N medium [36] amended with 0.1% yeast extract and 1 mM 2,4-D. Cultures were incubated for 2 weeks at 30°C, on a shaker. After incubation, cells

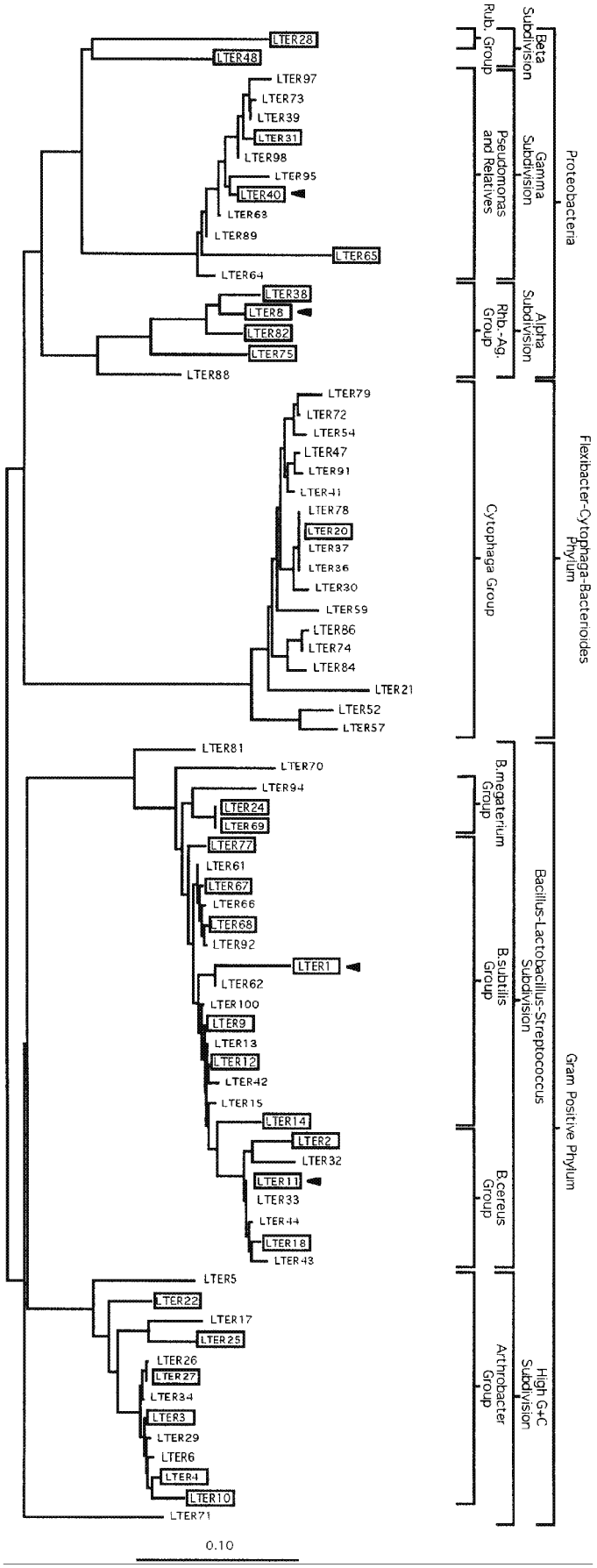


Fig. 2. 16S rDNA phylogeny of the LTER isolates as determined by analyses of 16S rDNA sequences between *E. coli* positions 27–519. Names of phylogenetic divisions are derived from the RDP 5.0 release [18]. The *scale bar* indicates the number of nucleotide changes per base position analyzed. Isolates that produce a PCR amplification product with primers internal to the *tfdA* gene are enclosed in *boxes*. *Arrows* indicate isolates for which *tfdA* amplification products were sequenced. The abbreviation Rub. indicates Rubrivivax, Rhb. indicates Rhizobium, and Ag. signifies Agrobacterium.

COR-AAD1-00002567
Bayer EX1008 (Part 5 of 9)

were removed by centrifugation. The supernatant was filtered (0.45 μm) into an autosampler vial. Duplicate samples of each culture were either analyzed immediately or frozen for later analysis. 2,4-D and 2,4-dichlorophenol concentrations were determined by HPLC, with 70/30 methanol-0.1% phosphoric acid as eluent, with a Lichrosorb RP-18 column (EM Separations, Gibbstown, N.J.) and monitored with a UV detector at 230 nm.

Incorporation of Radiolabel from ^{14}C-2,4-D

Single colonies from cultures grown on R2A medium were transferred to sterile nylon membranes overlaid on R2A agar. After overnight incubation at 30°C, all cultures had visible growth. Each filter was replicated [22]; then both master and replica filters were transferred to minimal agar containing either ^{14}C-ring-labeled or chain-labeled 2,4-D and incubated for three days at room temperature. The filters were exposed to X-ray film (Kodak, Rochester, N.Y.) for 18 h to detect incorporation of radiolabeled carbon.

Results and Discussion

Composition of the LTER Collection

The analysis of 16S rDNA partial sequence from strains in the LTER collection showed that these isolates represent diverse phylogenetic divisions (Fig. 2). The taxonomic divisions used to describe the isolates are defined in the Ribosomal Database Project [18]. Among the 76 isolates analyzed, 27 were found to cluster within the Bacillus-Lactobacillus-Streptococcus subdivision, and 13 strains fall within the High G+C subdivision of the Gram-positive phylum. The remaining isolates included 5 α-Proteobacteria, 2 β-Proteobacteria, 11 γ-Proteobacteria, and 18 members of the Cytophaga group. In a polyphasic taxonomy study, more than 95% of these isolates were found to be distinct taxa based on BIOLOG analyses (Biolog, Hayward, Calif.), fatty acid methyl ester (FAME) profiles [14], and genomic fingerprints from rep-PCR analyses [35]. The polyphasic taxonomy study of the LTER isolates, including refined phylogenetic analyses based on complete 16S rDNA sequence, is currently underway. Because the LTER collection includes both closely related isolates and organisms from several different phyla, this collection provides a good opportunity to test for the distribution of *tfdA* among distantly related bacteria, as well as the presence of *tfdA* in similar strains within a bacterial species.

Identification of tfdA *in LTER Collection*

PCR amplification with internal *tfdA* primers generated products using genomic DNA from 28 of the 76 isolates. The products were similar in size to the *tfdA* product amplified from JMP134 and RASC (360 bp), and hybridized at high stringency to labeled products from PCR amplification of *tfdA* from JMP134 (Fig. 3) and *Burkholderia* RASC. When primers TVU and TVL were applied directly to the membrane, hybridization to the probe was not detected.

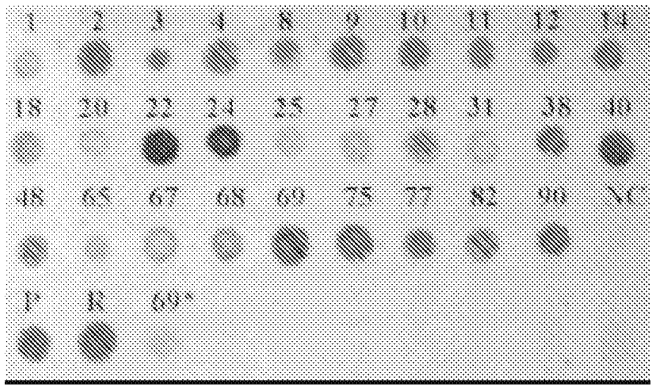


Fig. 3. Hybridization of amplified products from LTER isolates to a digoxigenin-labeled fragment internal to the *tfdA* gene. The numbers correspond to the LTER isolates that yielded the template DNA for the PCR reaction; *69** is an amplified product that is 40 bp longer than the predicted product size; as a negative control (*NC*), PCR primers were applied directly to the membrane; *P* is the amplified product from JMP134 (pJP4); *R*, amplified product from *Burkholderia* strain RASC.

The high percentage of isolates that yield the expected PCR product demonstrates that *tfdA* or *tfdA*-like genes are found in a significant number of organisms in this soil community. Most remarkable is evidence that these *tfdA*-like genes are found among diverse phylogenetic taxa (Fig. 2, Table 1). Previous research has shown evidence for *tfdA*-like genes in 2,4-D degraders from only a small number of Gram-positive organisms, such as *Arthrobacter* sp. [29],

Table 1. Distribution of isolates with *tfdA* among the different phylogenetic groups within the LTER collection

Phylogenetic subdivision	Total no. of isolates	No. of isolates with *tfdA*	% of isolates with *tfdA*
α-Proteobacteria	5	4	60
β-Proteobacteria	2	2	100
γ-Proteobacteria	11	3	27
Cytophaga	18	1	6
High G+C gram-positives	13	6	46
Bacillus-Lactobacillus-Streptococcus	27	12	40
Total	76	28	37

COR-AAD1-00002568
Bayer EX1008 (Part 5 of 9)

compared to a vast collection of Gram-negative organisms [3, 7, 19, 27, 30]. This is the first report of a *tfdA*-like gene in *Bacillus* or *Cytophaga*.

Amplified PCR products from four isolates were sequenced to assess the similarity of the gene in organisms from different phylogenetic divisions. Three of the isolates, LTER 1, LTER 11 (Bacillus-Lactobacillus-Streptococcus subdivision) and LTER 8 (Rhizobium-Agrobacterium group of the α-Proteobacteria) were identical to the *tfdA* partial sequence (Genbank Accession number U22499) from a *Halomonas* sp., a moderate halophile [19]. The *Halomonas* sp. *tfdA* sequence is 77.9% identical to the *tfdA* from pJP4, in the amplified region. The sequence of the PCR product from LTER 40, a member of the β-Proteobacteria division, was identical to the sequence of *tfdA* found on pJP4 (M16730). The high identity of the PCR products amplified from isolates representing distant phylogenetic taxa suggests extensive horizontal transfer of this gene. The *tfdA* gene is most often found on self-transmissible, broad host-range plasmids that confer the ability to degrade 2,4-D [3, 7, 31]. The widespread use of 2,4-D in agriculture may have driven the extensive transfer of these plasmids, however, there may be other forces that influence the transfer of plasmids carrying the *tfd* genes. Several studies [5–7] have shown that plasmid pJP4, which encodes enzymes catalyzing 2,4-D degradation, can be maintained in a number of different bacteria. It is worth noting, however, that some of the organisms harboring pJP4 do not express the 2,4-D–degrading phenotype [7]. Top et al. [32] have identified a plasmid that has *tfdA* but does not appear to have the other genes required for 2,4-D degradation. The function of this plasmid in soil microorganisms is unknown.

Ka et al. [16, 17] did not detect *tfdA* by gene probe hybridization it to total DNA extracted from LTER soils from the Kellogg Biological Station prior to exposure to 2,4-D, while our research indicates that *tfdA* is present in isolates from these soils. The disparity between these studies may be explained by the use of different sampling and detection methods. If the *tfdA* gene is present in a small proportion of the microbial population, or if the bacteria with the *tfdA* gene are not efficiently lysed, the *tfdA* gene may not be detectable by gene probe hybridization of total community DNA. In addition, PCR amplification of *tfdA* may detect concentrations of the gene that are below the detectable limit of gene probe hybridization. Because the PCR primers used in this study anneal to conserved regions in at least three different *tfdA* alleles, this method may detect genes with lower sequence similarity that are missed by other methods.

2,4-D Degradation by LTER Isolates

HPLC analyses showed that 2,4-D was not degraded to a significant extent by any of the LTER isolates after a 2-week incubation. In contrast, JMP134 (pJP4) or *Burkholderia* sp. RASC completely consumed the 2,4-D during this time period. Uptake experiments provided additional evidence that none of the LTER isolates utilized 2,4-D for cellular carbon. Neither ring- nor chain-labeled ^{14}C-2,4-D was incorporated into the LTER cultures after a 3-day incubation period, while JMP134 (pJP4) produced a strong positive signal after incubation on medium with either radiolabeled substrate.

Although 2,4-D is readily degraded by microbial communities in many different environments [23], the isolation of axenic cultures that degrade 2,4-D has proven to be difficult [12, 17]. It is possible that axenic 2,4-D degraders are difficult to isolate due to certain nutritional requirements that are not met in pure culture, or because 2,4-D degraders are present only in very low numbers prior to enrichment with 2,4-D. Alternatively, it is also possible that, in many microbial communities, 2,4-D is not degraded by individual isolates but by the concerted activities of several organisms. The presence of *tfdA* in isolates that do not degrade 2,4-D identifies a source of the 2,4-D-degradation potential of microbial communities. In such a case the genes for the partial degradation of 2,4-D may be present in a microorganism, but 2,4-D degradation is difficult to detect in pure culture due to the accumulation of toxic products such as 2,4-dichlorophenol. Furthermore, induction of *tfdA* may be dependent on products of further catabolism normally produced by other organisms that are not present in pure culture.

Conclusions

Three interesting conclusions can be drawn from this study: (1) a *tfdA*-like gene is present in a significant proportion of culturable heterotrophs; (2) this gene is found in bacteria that do not degrade 2,4-D; and (3) the microorganisms that carry this gene represent diverse phylogenetic groups. The high percentage of phylogenetically diverse microorganisms that do not degrade 2,4-D, but possess genes very similar to *tfdA*, suggests that this gene serves an important cellular role that is unrelated to herbicide metabolism. This hypothesis is supported by a study by Xia et al. [37] which shows that *tfdA* gene probes hybridize at a low level to total community DNA from soils without a history of 2,4-D application. The addition of 2,4-D to these soils did not change the concentration of target *tfdA* sequence, suggesting that the *tfdA* gene

COR-AAD1-00002569
Bayer EX1008 (Part 5 of 9)

is maintained for another function. There are several naturally occurring compounds that bear structural resemblance to 2,4-D and are potential substrates of the native TfdA. Some examples include the numerous aryl-ether compounds that are released during fungal degradation of lignin [20], or the different halogenated aromatic metabolites produced by fungi and bacteria [13, 25]. Alternatively, it is possible that the natural substrate for TfdA bears little resemblance to 2,4-D, and the ability to degrade this compound is fortuitous.

More research is necessary to discover the role of these *tfdA* or *tfdA*-like genes in organisms that do not alone degrade 2,4-D. To examine the role that horizontal transfer plays in the distribution of *tfdA*, it is important to know the location of this gene in these isolates (e.g., whether it is on self-transmissible plasmids or chromosomally encoded). Furthermore, it is important to determine if the downstream *tfd* genes are present in these isolates. A study of the growth conditions under which these *tfdA*-like genes are expressed may provide insight into the natural substrate of the enzyme. Research on the natural role of *tfdA* may ultimately shed light on the evolution of the 2,4-D degradation pathway and on how microorganisms may recruit existing genes to degrade other xenobiotic compounds.

Note added in proof

A *tfdA* homologue in *E. coli* has been shown to be part of a gene cluster involved in taurine utilization as a sulfur source (33a). *Alcaligenes eutrophus* has been renamed *Ralstonia eutropha* (38).

Acknowledgments

This work was partially supported by the NSF-Center for Microbial Ecology (DEB-9120006), the Michigan State University Biotechnology Training Program, and the Michigan State Agricultural Experiment Station. We are grateful to Helen Corlew-Newman and Frank Lowes for providing the LTER strains. We thank our coworkers associated with the Research on Microbial Evolution (ROME) Laboratory for helpful suggestions and discussions.

References

1. Amy PS, Schulke JW, Frazier LM, Seidler RJ (1985) Characterization of aquatic bacteria and cloning of genes specifying partial degradation of 2,4-dichlorophenoxyacetic acid. Appl Environ Microbiol 49:1237–1245
2. Ausubel FM, Brent R, Kingston RE, Moore DD, Seidman JG, Smith JA, Struhl K (1987) Current protocols in molecular biology. John Wiley and Sons, New York
3. Bhat MA, Tsuda M, Horiike K, Nozaki M, Vaidyanathan CS, Nakazawa T (1994) Identification and characterization of a new plasmid carrying genes for degradation of 2,4-dichlorophenoxyacetate from *Pseudomonas cepacia* CSV90. Appl Environ Microbiol 60:307–312
4. Chaudry GR, Huang GH (1988) Isolation and characterization of a new plasmid from a *Flavobacterium* sp. which carries the genes for the degradation of 2,4-dichlorophenoxyacetate. J Bacteriol 170:3897–3902
5. Daane LL, Molina JAE, Berry EC, Sadowsky MJ (1996) Influence of earthworm activity on gene transfer from *Pseudomonas fluorescens* to indigenous soil bacteria. Appl Environ Microbiol 62:515–521
6. DiGiovanni GD, Neilson JW, Pepper IL, Sinclair NA (1996) Gene transfer of *Alcaligenes eutrophus* JMP134 plasmid pJP4 to indigenous soil recipients. Appl Environ Microbiol 62:2521–2526
7. Don RH, Pemberton JM (1981) Properties of six pesticide degradation plasmids isolated from *Alcaligenes paradoxus* and *Alcaligenes eutrophus*. J Bacteriol 145:681–686
8. Don RH, Weightman AJ, Knackmuss HJ, Timmis KN (1985) Transposon mutagenesis and cloning analysis of the pathways for degradation of 2,4-dichlorophenoxyacetic acid and 3-chorobenzoate in *Alcaligenes eutrophus* JMP134 (pJP4). J Bacteriol 161:85–90
9. Eden PA, Schmidt TM, Blakemore RP, Pace NR (1991) Phylogenetic analysis of *Aquaspirillum magnetotacticum* using polymerase chain reaction–amplified 16S rRNA–specific DNA. Int J Syst Bacteriol 42:166–170
10. Fukumori F, Hausinger RP (1993) Purification and characterization of 2,4-dichlorophenoxyacetate/α-ketoglutarate dioxygenase. J Biol Chem 268:24311–24317
11. Fulthorpe RR, McGowan C, Maltseva OV, Holben WE, Tiedje JM (1995) 2,4-Dichlorophenoxyacetic acid–degrading bacteria contain mosaics of catabolic genes. Appl Environ Microbiol 61:3274–3281
12. Fulthorpe RR, Rhodes AN, Tiedje JM (1996) Pristine soils mineralize 3-chlorobenzoate and 2,4-dichlorophenoxyacetate via different microbial populations. Appl Environ Microbiol 62:1159–1166
13. Gribble GW (1992) Naturally occurring organohalogen compounds-a survey. J Nat Prod 55:1353–1395
14. Haack SK, Garchow H, Oldelson DA, Forney LJ, Klug MJ (1994) Accuracy, reproducibility, and interpretation of fatty acid methyl ester profiles of model bacterial communities. Appl Environ Microbiol 60:2483–2493
15. Häggblom MM (1992) Microbial breakdown of halogenated aromatic pesticides and related compounds. FEMS Microbiol Rev 103:29–72
16. Ka JO, Holben WE, Tiedje JM (1994) Analysis of competition in soil among 2,4-dichlorophenoxyacetic acid–degrading bacteria. Appl Environ Microbiol 60:1121–1128
17. Ka JO, Holben WE, Tiedje JM (1994) Use of gene probes to

COR-AAD1-00002570
Bayer EX1008 (Part 5 of 9)

aid in recovery and identification of functionally dominant 2,4-dichlorophenoxyacetic acid–degrading populations in soil. Appl Environ Microbiol 60:1116–1120

18. Larsen N, Olsen GJ, Maidak BL, McCaughey MJ, Overbeek R, Macke TJ, Marsh TL, Woese CR (1993) The ribosomal database project. NAR 21:3021–3023
19. Maltseva OV, McGowan C, Fulthorpe R, Oriel PJ (1996) Degradation of 2,4-dichlorophenoxyacetic acid by haloalkaliphilic bacteria. Microbiol 142:1115–1122
20. Ribbons DW (1987) Chemicals from lignin. In: Hartley BC, Broda PMA, Senior PJ (eds) Technology in the 1990s: utilization of lignocellulosic wastes, Royal Society, London, England U.K. pp 485–494
21. Robertson GP, Freckman DW (1995) The spatial distribution of nematode trophic groups across a cultivated ecosystem. Ecology 76:1425–1432
22. Sambrook J, Fritsch EF, Maniatis T (1989) Molecular cloning: a laboratory manual, 2nd edn., Cold Spring Harbor Laboratory Press, Cold Spring Harbor, N.Y.
23. Sandmann E, Loos MA, van Dyk LP (1988) Microbial degradation of 2,4-dichlorophenoxyacetic acid in soil. Rev Environ Contamin Toxic 101:1–53
24. Schmidt TM, DeLong EF, Pace NR (1991) Analysis of a marine picoplankton community by 16S rRNA gene cloning and sequencing. J Bacteriol 173:4371–4378
25. Siuda JF, deBernardis JF (1973) Naturally occurring halogenated compounds. Lloydia 36:107–143
26. Streber WR, Timmis KN, Zenk MH (1987) Analysis, cloning, and high-level expression of 2,4-dichlorophenoxyacetate monooxygenase gene of *tfdA* of *Alcaligenes eutrophus* JMP134. J Bacteriol 169:2950–2955
27. Suwa Y, Wright AD, Fukumori F, Nummy KA, Hausinger RP, Holben WE, Forney LJ (1996) Characterization of a chromosomally encoded 2,4-dichlorophenoxyacetic acid/α-ketoglutarate dioxygenase from *Burkholderia* sp. strain RASC. Appl Environ Microbiol 62:2464–2469
28. Swofford DL, Olsen GJ (1990) Phylogeny reconstruction. In: Hillis D, Moritz C (eds), Molecular systematics, Sinaur Associates, Sunderland, Mass.
29. Tiedje JM, Alexander M (1969) Enzymatic cleavage of the ether bond of 2,4-dichlorophenoxyacetate. J Agric Food Chem 17:1080–1084
30. Tonso NL, Matheson VG, Holben WE (1995) Polyphasic characterization of a suite of bacterial isolates capable of degrading 2,4-D. Microbiol Ecol 3:3–24
31. Top EM, Holben WE, Forney LJ (1995) Characterization of diverse 2,4-dichlorophenoxyacetic acid–degradative plasmids isolated from soil by complementation. Appl Environ Microbiol 61:1691–1698
32. Top EM, Maltseva OV, Forney LJ (1996) Capture of a catabolic plasmid that encodes only 2,4-D/α-ketoglutarate dioxygenase (TfdA) by genetic complementation. Appl Environ Microbiol 62:2470–2476
33. Vallaeys T, Fulthorpe RR, Wright AM, Soulas G (1996) The metabolic pathway of 2,4-dichlorophenoxyacetic acid degradation involves different families of *tfdA* and *tfdB* genes according to PCR-RFLP analysis. FEMS Microbiol Ecol 20:163–172

33a. van der Ploeg JR, Weiss MA, Saller E, Nashimoto H, Saito N, Kertesz MA, Leisinger T (1996) Identification of sulfate starvation-regulated genes in *Escherichia coli*: a gene cluster involved in the utilization of taurine as a sulfur source. J Bacteriol 178:5438–5446

34. van der Meer JR, de Vos WM, Harayama S, Zehnder AJB (1992) Molecular mechanisms of genetic adaption to xenobiotic compounds. Microbiol Rev 56:677–694
35. Versalovic J, Schneider M, de Bruijn FJ, Lupski JR (1994) Genomic fingerprinting of bacteria using repetitive sequence–based polymerase chain reaction. Meth Mol Cell Biol 5:25–40
36. Wyndham RC (1986) Evolved aniline catabolism in *Acinetobacter calcoaceticus* during continuous culture of river water. Appl Environ Microbiol 51:781–789
37. Xia X, Bollinger J, Ogram A (1995) Molecular genetic analysis of the response of three soil microbial communities to the application of 2,4-D. Mol Ecol 4:17–28
38. Yabuuchi E, Kosako Y, Yano I, Hotta H, Nishiuchi Y (1995) Transfer of two *Burkholderia* and an *Alcaligenes* species to *Ralstonia* gen. nov.: proposal of Ralstonia pickettii (Ralston, Palleroni and Doudoroff 1973) comb. nov., *Ralstonia solanacearum* (Smith 1896) comb. nov. and *Ralstonia eutropha* (Davis 1969) comb. nov. Microbiol Immunol 39:897–904

COR-AAD1-00002571
Bayer EX1008 (Part 5 of 9)

THE JOURNAL OF BIOLOGICAL CHEMISTRY
Vol. 275, No. 17, Issue of April 28, pp. 12400–12409, 2000
© 2000 by The American Society for Biochemistry and Molecular Biology, Inc.
Printed in U.S.A.

Site-directed Mutagenesis of 2,4-Dichlorophenoxyacetic Acid/α-Ketoglutarate Dioxygenase

IDENTIFICATION OF RESIDUES INVOLVED IN METALLOCENTER FORMATION AND SUBSTRATE BINDING*

(Received for publication, January 18, 2000)

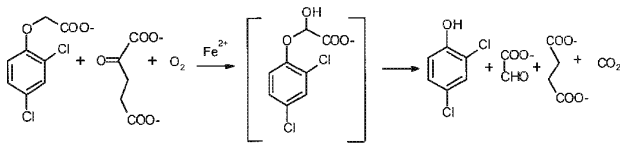
Deborah A. Hogan‡§¶, Sheila R. Smith‖, Eric A. Saari‖, John McCracken‖, and Robert P. Hausinger‡§‡‡**

*From the ‡Center for Microbial Ecology and Departments of §Microbiology, ‖Chemistry, and **Biochemistry, Michigan State University, East Lansing, Michigan 48824*

2,4-Dichlorophenoxyacetic acid (2,4-D)/α-ketoglutarate (α-KG) dioxygenase (TfdA) is an Fe(II)-dependent enzyme that catalyzes the first step in degradation of the herbicide 2,4-D. The active site structures of a small number of enzymes within the α-KG-dependent dioxygenase superfamily have been characterized and shown to have a similar $HXDX_{50-70}HX_{10}RXS$ arrangement of residues that make up the binding sites for Fe(II) and α-KG. TfdA does not have obvious homology to the dioxygenases containing the above motif but is related in sequence to eight other enzymes in the superfamily that form a distinct consensus sequence $(HX(D/E)X_{138-207}HX_{10}R/K)$. Variants of TfdA were created to examine the roles of putative metal-binding residues and the functions of the other seven histidines in this protein. The H167A, H200A, H213A, H245A, and H262A forms of TfdA formed inclusion bodies when overproduced in *Escherichia coli* DH5α; however, these proteins were soluble when fused to the maltose-binding protein (MBP). MBP-TfdA exhibited kinetic parameters similar to the native enzyme. The H8A and H235A variants were catalytically similar to wild-type TfdA. MBP-H213A and H216A TfdA have elevated K_m values for 2,4-D, and the former showed a decreased k_{cat}, suggesting these residues may affect substrate binding or catalysis. The H113A, D115A, MBP-H167A, MBP-H200A, MBP-H245A and MBP-H262A variants of TfdA were inactive. Gel filtration analysis revealed that the latter two proteins were highly aggregated. The remaining four inactive variants were examined in their Cu(II)-substituted forms by EPR and electron spin-echo envelope modulation (ESEEM) spectroscopic methods. Changes in EPR spectra upon addition of substrates indicated that copper was present at the active site in the H113A and D115A variants. ESEEM analysis revealed that two histidines are bound equatorially to the copper in the D115A and MBP-H167A TfdA variants. The experimental data and sequence analysis lead us to conclude that His-113, Asp-115, and His-262 are likely metal ligands in TfdA and that His-213 may aid in catalysis or binding of 2,4-D.

2,4-Dichlorophenoxyacetic acid (2,4-D)[1]/α-ketoglutarate (α-KG) dioxygenase (TfdA) is an Fe(II)- and α-KG-dependent enzyme that catalyzes the first step in degradation of the herbicide 2,4-D. This enzyme couples the oxidative decarboxylation of α-KG to the hydroxylation of a side chain carbon atom. The resultant hemiacetal spontaneously decomposes to form 2,4-dichlorophenol and glyoxalate (1). Mechanistically, TfdA resembles numerous other α-KG-dependent dioxygenases from plants, animals, fungi, and bacteria that catalyze similar hydroxylation reactions at unactivated carbon centers (2, 3).

Members of the α-KG-dependent dioxygenase superfamily are not closely related by their sequences but rather appear to fall into one of three groups of related enzymes or fall into a fourth group of unrelated sequences (4). The best studied α-KG-dependent hydroxylases, including prolyl and lysyl hydroxylase (5) and flavanone hydroxylase (3, 6), have an $HXDX_{\sim55}HX_{10}RXS$ motif in common (7, 8), and this motif is present in the more than 20 enzymes, defined here as Group I, within the α-KG dependent dioxygenase superfamily (8, 9). Site-directed mutagenesis studies have confirmed the importance of these residues for activity (8, 10–13), and the crystal structures of two Group I enzymes, isopenicillin *N* synthase (IPNS) and deacetoxycephalosporin C synthase (DAOCS), indicate that these residues comprise the metallocenter and α-KG-binding site (14–17). TfdA is not closely related in sequence to the Group I α-KG-dependent dioxygenases described above but is clearly homologous (25–30% identity) to *Escherichia coli* taurine/α-KG dioxygenase (TauD) (18) and sulfonate/α-KG dioxygenase from *Saccharomyces cerevisiae* (19). Furthermore, PSI-BLAST analyses (20) find additional rela-



SCHEME 1

* This research was supported in part by National Science Foundation Grants DEB9120006 and MCB 9603520 (to R. P. H), National Institutes of Health Grant GM 54065 (to J. M.), and the Michigan State University Agricultural Experiment Station. The costs of publication of this article were defrayed in part by the payment of page charges. This article must therefore be hereby marked "*advertisement*" in accordance with 18 U.S.C. Section 1734 solely to indicate this fact.

¶ Supported in part by National Institutes of Health Biotechnology Training Grant T32-GM08350.

‡‡ To whom correspondence should be addressed: 160 Giltner Hall, Dept. of Microbiology, Michigan State University, East Lansing, MI 48824. Tel.: 517-353-9675; Fax.: 517-353-8957; E-mail: Hausinge@pilot.msu.edu.

[1] The abbreviations used are: 2,4-D, 2,4-dichlorophenoxyacetic acid; α-KG, α-ketoglutarate; TfdA, 2,4-D/α-KG dioxygenase; TauD, taurine/α-KG dioxygenase; cw-EPR, continuous wave electron paramagnetic resonance; ESEEM, electron spin echo envelope modulation; IPNS, isopenicillin *N* synthase; DAOCS, deacetoxycephalosporin synthase; MBP, maltose-binding protein; FT, Fourier transform; MOPS, 4-morpholinepropanesulfonic acid.

This paper is available on line at http://www.jbc.org

Downloaded from http://www.jbc.org/ by guest on September 3, 2020

COR-AAD1-00002572
Bayer EX1008 (Part 5 of 9)

TABLE I
Consensus motifs for subgroups within the α-KG-dependent dioxygenase superfamily

Group I (IPNS, DAOCS, and related enzymes)	HXD	X_{50-70}	HX_{10}(R/K)XS
Group II (TfdA, TauD, clavaminate synthase and related enzymes)	HX(D/E)	$X_{138-207}$	HX_{10-13}R
Group III (Phytanoyl-CoA hydroxylase, proline hydroxylase and related enzymes)	HXD	X_{72-101}	HX_{10}(R/K)XS

tionships to γ-butyrobetaine hydroxylase and clavaminate synthase. Alignment of these Group II sequences indicates the conservation of two histidines and one aspartate (His-113, His-262, and Asp 115 in TfdA) as well as an invariant arginine that may be analogous to the α-KG-binding arginine in DAOCS and related enzymes (Table I). A third set of enzyme sequences (Group III) from members of the α-KG-dependent dioxygenase superfamily, including phytanoyl-CoA hydroxylase and proline hydroxylase, exhibit the presence of a third related motif despite the lack of overall sequence similarity to Group I or Group II enzymes.

In this study, we used site-directed mutagenesis methods to examine the roles of potential metal-binding residues in the above motif (His-113, His-262, and Asp-115) and the remaining seven histidines in TfdA. Previously published work showed that TfdA was inactivated by diethylpyrocarbonate, a histidine-selective reagent, and provided evidence consistent with the presence of multiple histidines in the active site (21). Spectroscopic studies of TfdA showed the presence of two equatorially bound imidazole nitrogens as ligands to the active site metal and indicated that one imidazole ligand may be displaced or shifted to an axial position upon substrate binding (22–24). Based on analyses of different TfdA variants, we identify several likely metal ligands and provide evidence that another one or two histidines may aid in substrate binding.

EXPERIMENTAL PROCEDURES

Recombinant Plasmids—All plasmids were constructed from pUS311 (21), a pUC19 derivative that contains the *Ralstonia eutropha* JMP134 *tfdA* gene (Fig. 1). The H8A, D115A, H213A, H216A, H235A, H245A, and H262A TfdA variants were created by direct mutation of *tfdA* in pUS311 by the Stratagene Quickchange System (Stratagene, La Jolla, CA). All mutagenic primers are listed in Table II. Two alternative approaches were used to construct the three remaining variants. Plasmids encoding H113A and H167A TfdA variants were created by CLONTECH mutagenesis of pXHtfdA, a pUC19 plasmid containing the 5′-*Xba*I-*Hin*dII fragment of the *tfdA* gene (Fig. 1). To create the complete gene containing the indicated mutations, the *Xba*I-*Hin*dII fragment was cloned into pHKtfdA, which contains the 3′ end of the *tfdA* gene. pHKtfdA was constructed in two steps. First, the 1.4-kilobase pair *Xba*I-*Sal*I fragment from pUS311, containing the complete *tfdA* gene, was cloned into pBC KS$^-$ (Stratagene) cut with *Xba*I and *Xho*I to create pBCtfdA. This step had the benefit of eliminating a *Hin*dII site that interfered with further cloning steps. The 727-base pair *Hin*dII-*Kpn*I fragment of pBCtfdA was subcloned into pBC KS$^-$ cut with the same enzymes to give pHKtfdA. Similarly, the gene encoding H200A TfdA was made by mutagenesis of pXXtfdA, a pUC19 plasmid containing the 5′-*Xba*I-*Xho*I fragment of *tfdA*. The altered *Xba*I-*Xho*I fragment was then inserted into pHKtfdA cut with *Xba*I and *Xho*I to give the complete H200A *tfdA* gene. The identity of all final constructs was confirmed by sequence analysis. To insert the genes encoding H167A and H262A variants of TfdA into a plasmid that would allow for isopropyl-1-thio-β-D-galactopyranoside-controlled expression, the *Xba*I-*Sal*I fragments from the corresponding plasmids described above were cloned into pET23a (Novagen) prepared with the same enzymes.

To create the maltose-binding protein (MBP)-TfdA fusion proteins, the wild-type *tfdA* gene was amplified from pUS311 with TfdA-MBPF and TfdA-MBPR primers (Table II) to create an *Xba*I site directly upstream of the GTG start codon of the *tfdA* gene and a *Hin*dIII restriction site 54 base pairs downstream of the stop codon. The polymerase chain reaction product was cloned directly into the pGEM-T vector according to the manufacturer's instructions (Promega, Madison, WI). The *Xba*I-*Hin*dIII fragment was isolated from the resulting plasmid and cloned into the pMAL-c2 vector that had been digested with the same enzymes. The identity of the newly created *malE-tfdA* gene fusion was confirmed by sequencing. Substitution of the mutation-containing internal *Nru*I fragment for the same fragment of the wild-type *malE-tfdA* gene created MBP-fusion forms of altered TfdAs. First, pMAL-*tfdA* was digested with *Nru*I, and the vector fragment was purified and religated to create pMAL-*tfdA*Δ*Nru*I. The resultant plasmid was linearized with *Nru*I and dephosphorylated with calf intestine alkaline phosphatase prior to ligation with the *Nru*I fragments isolated from the previously described mutant genes. Constructs were confirmed by restriction analysis.

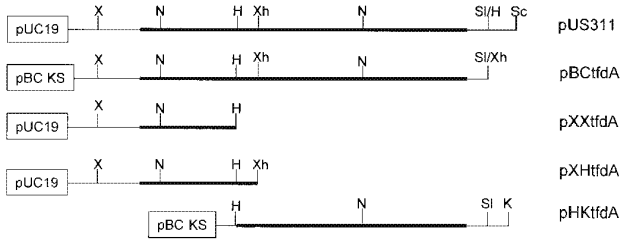


FIG. 1. **Restriction maps of the plasmids used in construction of *tfdA* mutants.** The abbreviations for the restriction enzyme sites are as follows: *H*, *Hin*dII; *X*, *Xba*I; *Xh*, *Xho*I; *Sl*, *Sal*I; *K*, *Kpn*I; *Sc*, *Sac*I; and *N*, *Nru*I. The vector backbone is indicated in the *box* on the *left*. The *tfdA* open reading frame is shown as a *wide*, *solid line*.

TABLE II
Sequences of mutagenic primers used to create altered tfdA genes

Mutant	Primer sequence[a]
H8A	5′-CGC AAA TCC CCT TGC TCC TCT TTT CGC C-3′
H113A	5′-GTC GCT GGC CCA AGC TGG-3′
D115A	5′-GCA CAG CGC CAG CTC CTT TCA-3′
H167A	5′-GCG TGC CGA GCA GTA CGC ACT G-3′
H200A	5′-GGT TCG AAC CGC CGC CGG CTC-3′
H213A	5′-GCT CGC GGC CGC GCC GAT-3′
H216A	5′-CCT TCG ACG GCG CTC GCG-3′
H235A	5′-GCT TCT CGA GGC GAC ACA G-3′
H245A	5′-GTG TAC CGG GCT CGC TGG AAC-3′
H262A	5′-CGT TCT TGC ACG CGG ACG CAG-3′
Tfda-MBPF	5′-TCT CTA GAG TGA GCG TCG TCG CAA ATC C-3′
Tfda-MBPR	5′-GTC AAG CTT GGT TGC GTA CAT CTT GTG G-3′

[a] The reverse primer used for the creation of all mutants was the complement of the forward primer.

Protein Purification—H8A, H113A, D115A, H216A, H235A, and wild-type TfdA proteins were purified from *E. coli* DH5α cells carrying pUS311 and its mutated derivatives according to a previously described protocol (21). In addition, the non-mutated enzyme and the TfdA variants H167A, H200A, H213A, H245A, and H262A were purified as MBP-TfdA fusion proteins from *E. coli* DH5α by the protocol described in the pMAL Protein Fusion and Purification System Manual (New England Biolabs, Beverly, MA).

Analysis of Kinetic Parameters—Specific activities of the wild-type and variant TfdA proteins were determined by a previously described spectrophotometric assay (21). The typical assay mixture contained 1 mM 2,4-D, 1 mM α-KG, 100 μM $(NH_4)_2Fe(SO_4)_2$, and 100 μM ascorbic acid in 10 mM MOPS buffer (pH 6.75) at 30 °C. The reactions were quenched by the addition of EDTA to a concentration of 5 mM. 2,4-Dichlorophenol was quantified by reaction with 4-aminoantipyrene followed by measurement of the absorbance at 510 nm. One unit of activity was defined as the amount of enzyme required to produce 1 μmol of dichlorophenol·min^{-1}. Protein concentrations were determined using

Downloaded from http://www.jbc.org/ by guest on September 3, 2020

COR-AAD1-00002573
Bayer EX1008 (Part 5 of 9)

the Bio-Rad Protein Assay with bovine serum albumin as a standard. For calculation of the k_{cat} values, the TfdA variants were assumed to have M_r = 31,600 and the MBP-TfdA variants were assigned M_r = 74,500.

The low K_m values for α-KG (~2–5 μM for the wild-type enzyme) precluded use of the 4-aminoantipyrene assay for accurate determination of this value. The alternative method used to measure the K_m values for α-KG quantified the amount of $^{14}CO_2$ liberated from α-[1-^{14}C]KG during the course of the reaction (21).

Native Protein Analysis by Gel Filtration—Size exclusion chromatography was used to estimate the native molecular weights of TfdA, MBP-TfdA, and mutant proteins. The proteins were chromatographed on a Superose 6 gel filtration column (1.0 × 30 cm, Amersham Pharmacia Biotech) in 20 mM Tris buffer (pH 7.5), 1 mM EDTA, and 200 mM NaCl at a flow rate of 0.2 ml·min^{-1}. The elution volumes were compared with those for gel filtration standards (Bio-Rad) including thyroglobulin, 670 kDa; bovine gamma globulin, 158 kDa; chicken ovalbumin, 44 kDa; myoglobin, 17 kDa; and vitamin B_{12}, 1350 Da.

Spectroscopic Analysis—Proteins for electron paramagnetic resonance (EPR) and electron spin-echo envelope modulation (ESEEM) spectroscopic analyses were exchanged into 25 mM MOPS (pH 6.75) by repeated concentration and dilution in Centricon 30 (Amicon) centrifugal concentrators. The final subunit concentration was 0.5 mM for the non-fusion forms of TfdA and 0.4 mM for the MBP-TfdA proteins. $CuCl_2$ was added to a concentration of 450 and 350 μM, respectively. Buffered solutions of α-KG and 2,4-D were added to final concentrations of 5 mM. Glycerol was present at 40% in all samples.

X-band EPR spectra were obtained at 77 K on a Bruker ESP-300E spectrometer. ESEEM data were collected on a home-built spectrometer; the microwave bridge of this instrument has been previously described in detail (25). Data collection and analyses were controlled by a Power Computing model 200 Power PC using software written with LabView version 5.01 (National Instruments). Electron spin echoes were digitized, averaged, and integrated by a Tektronix model 620B digital oscilloscope interfaced to the spectrometer computer via an IEEE-488 bus. Two four-channel delay and gate generators (Stanford Research Systems model DG535), a Bruker BH-15 magnetic field controller, and a Hewlett-Packard model 8656B radiofrequency synthesizer were also interfaced using IEEE-488 protocol. Data were collected using a reflection cavity that employed a folded microstrip resonator (26). A three-pulse stimulated echo sequence (90-τ-90°-*T*-90°) was used. ESEEM spectra were generated by Fourier transformation of the time domain data using dead time reconstruction (27). Simulations of the experimental data were performed on a Sun SparcII work station. Simulation programs were written in FORTRAN and based on the density matrix formalism developed by Mims (28). Software for the frequency analysis of the experimental and simulated data was written in Matlab (Mathworks, Natick, MA).

Sequence Comparisons—Related sequences were initially detected by BLAST (29) and PSI-BLAST (20) analyses. Alignments were generated with the CLUSTAL algorithm (30), and the figure was prepared using Genedoc (31).

RESULTS

Production of the Mutant TfdAs—Initially, all of the mutant genes were expressed from their pUC19-based plasmids except for those encoding H113A, H167A, and H200A TfdA, which were in pBC KS$^-$-derived plasmids. By using the standard protocol to produce soluble, wild-type TfdA (growth at 30 °C to early stationary phase), only the H8A, H113A, D115A, H216A, and H235A variants existed as soluble proteins. All of the other TfdA variants were present as inclusion bodies even when grown at lower temperatures (22 °C), in M9 minimal medium, or in LB broth containing 660 mM sorbitol and 2.5 mM betaine (32). In addition, isopropyl-1-thio-β-D-galactopyranoside-controlled production of H167A and H262A proteins from mutant genes cloned into pET23a did not yield soluble samples even when the harvested cell pellets were suspended in buffer containing 20% glycerol to limit protein aggregation.

To overcome the solubility problems for the five TfdA variants, MBP-TfdA fusion proteins were created. Wild-type TfdA and the MBP-TfdA fusion protein had essentially identical k_{cat} and very similar K_m values for α-KG and 2,4-D (Table III). A slight increase in the apparent K_D for Fe(II) may reflect some metal binding capacity of MBP. Since the presence of the fusion protein did not appear to greatly affect the kinetic parameters of wild-type enzyme, similar fusion proteins were created for the H167A, H200A, H213A, H245A, and H262A TfdA variants.

TABLE III
Summary of the kinetic parameters for active TfdA variants

TfdA sample	k_{cat}	K_m αKG	K_m 2,4-D	K_D Fe(II)
	min^{-1}	μM	μM	μM
Wild type	442 ± 33	4.9 ± 0.73	19.3 ± 3.7	2.0 ± 0.5
MBP fusion	411 ± 23	9.9 ± 1.8	33.7 ± 2.5	15.2 ± 5.4
H8A[a]	284 ± 6.9	6.5 ± 1.8	17.7 ± 3.8	1.9 ± 0.7
MBP-H213A	22.1 ± 2.9	8.3 ± 2.9	318 ± 44	27.7 ± 9.8
H216A	474 ± 47	6.05 ± 2.6	52 ± 5	2.4 ± 1.7
H235A	284 ± 25	9.6 ± 1.6	34 ± 8	1.4 ± 1.7

[a] More than 75% of the protein was present as the degradation product. The k_{cat} was estimated from the active, full-length fraction.

Kinetic Analyses of Altered TfdAs—Results from kinetic analyses of the four active mutant proteins are summarized in Table III. H8A TfdA was soluble and active but was rapidly proteolyzed to an inactive form. By electrophoretic comparisons, the cleavage site appeared to be the same as in wild-type TfdA (between Arg-77 and Phe-78) (21). The rate of proteolysis of H8A TfdA was enhanced compared with that seen for the wild-type enzyme despite the presence of EDTA and protease inhibitors in the purification buffer. Because purified H8A TfdA was more than 75% degraded, the catalytic rate constant was calculated with the estimated amount of intact enzyme. These calculations indicate rates and K_m values similar to those for the wild-type enzyme. Similarly, the kinetic parameters for H235A TfdA were comparable to the native enzyme. In contrast, two variants exhibited differences from wild-type enzyme in their kinetic parameters. The H213A MBP-TfdA variant exhibited a 20-fold reduction in k_{cat} and a 10-fold increase in K_m for 2,4-D. In addition, H216A TfdA had a modest (2.5-fold) increase in the K_m for 2,4-D and no change in catalytic rate. The other kinetic parameters for H213A MBP-TfdA and H216A TfdA (K_m for α-KG and K_D for ferrous ion) did not differ significantly from the wild-type values. Six soluble TfdA variants (H113A, D115A, MBP-H167A, MBP-H200A, MBP-H245A, and MBP-H262A) exhibited no activity even when assayed with elevated substrate and cofactor concentrations (10 mM α-KG, 5 mM 2,4-D, and 250 μM Fe(II)).

Evaluation of the Structural Consequences of the Mutations—To assess whether the inactive mutant proteins assumed conformations similar to the wild-type enzyme, their apparent molecular weights were estimated by gel filtration analysis. The observed size of wild-type TfdA was found to be 51 kDa by comparison to protein standards, suggesting that TfdA forms a compact dimer or an elongated monomer. The elution volume for both H113A and D115A corresponded exactly to wild-type TfdA indicating that these proteins are not significantly altered in their quaternary structure. MBP-TfdA eluted both in the void volume (approximately 25% of the protein) and at a position corresponding to 216 kDa (roughly 75% of the protein), suggesting that MBP-TfdA forms at least a dimer. Because each MBP-TfdA subunit is comprised of two domains separated by a 13-amino acid linker, the resultant protein may migrate with a larger apparent molecular weight. MBP-H167A and MBP-H200A samples demonstrated the same two-peak profile as MBP-TfdA but with larger proportions eluting in the void volume. MBP-H245A and MBP-H262A proteins were soluble; however, gel filtration analysis indicated the presence of only highly aggregated material eluting in the void volume. Because these mutant proteins exhibited aberrations in their folding properties, the catalytic role of His-245 and His-262, if any, could not be assessed.

Downloaded from http://www.jbc.org/ by guest on September 3, 2020

COR-AAD1-00002574
Bayer EX1008 (Part 5 of 9)

EPR Spectroscopic Characterization of Variants with Altered Metal Sites—The metallocenter properties for selected TfdA variants were probed by EPR spectroscopy. To circumvent the problems that arise in EPR measurements of integer spin paramagnetic centers, Fe(II) was substituted with cupric ion. Although the Cu(II) form of TfdA is inactive, Cu(II) binds competitively with respect to Fe(II) (K_i = 1–3 μM), and copper-substituted TfdA has been used previously to study the metal coordination environment of this enzyme in the presence and absence of substrates (22–24). Spectral parameters of wild-type Cu(II)-TfdA, Cu(II)-TfdA + α-KG, and Cu(II)-TfdA + α-KG + 2,4-D (Fig. 2A and Table IV), agreed well with those reported previously (23, 24). Earlier studies of copper-substituted wild-type TfdA indicated that the metal is bound in a type 2 environment with a mixture of O and N ligands in the equatorial plane. Upon addition of α-KG and 2,4-D to the enzyme, the spectral parameters are altered to a more rhombic signal with accompanying resolution of ligand hyperfine coupling (Fig. 2A). These results suggest that binding of the co-substrates to the enzyme leads to a better defined copper site with α-KG binding directly to the metallocenter (23, 24). The small $A_{\parallel}$ (less than 14 mT) for the α-KG- and 2,4-D-bound sample indicates a significant distortion from planarity.

The four inactive mutant forms of TfdA with quaternary structures similar to the corresponding wild-type protein (H113A, D115A, MBP-H167A, and MBP-H200A) were analyzed by EPR spectroscopy to assess the metal coordination environments. No significant differences between the spectra of MBP-TfdA and the non-fusion wild-type TfdA were observed (data not shown). EPR spectra of the copper-substituted samples, in all cases, showed contributions from multiple copper sites indicating a mixture of copper centers, most likely resulting from copper binding in multiple conformations or at sites other than the active site. The presence of alternative copper-binding sites is not surprising in an enzyme with nine histidines.

The EPR spectra for Cu-H113A TfdA alone and in the presence of α-KG and 2,4-D (Fig. 2*B* and Table IV) differ significantly from spectra of wild-type enzyme and show modest changes in Cu(II) g values and hyperfine tensor principal values upon substrate additions. The broadening of the EPR signal in the $g_{\parallel}$ region upon addition of α-KG again suggests a mixture of copper site conformations. Thus, it appears that alteration of His-113 significantly affects the metal binding properties for TfdA such that copper is no longer constrained to a single active site configuration.

The EPR spectrum of D115A-TfdA (Fig. 2*C*) has parameters similar to those observed in the copper-substituted wild-type protein (Table IV), although with less resolution of $A_{\parallel}$. Addition of α-KG (in the presence or absence of 2,4-D) has a dramatic effect on the appearance of the D115A data, enhancing resolution of the Cu(II) hyperfine peaks at $g_{\parallel}$ and the ligand hyperfine structure in the $g_{\perp}$ region (Fig. 2*C*). The appearance of these superhyperfine interactions may result from a subtle shift in the orientation of the principal g tensor such that the imidazole ligands occupy an increasingly equatorial position (33). These results are consistent with the formation of a tighter or more regular copper-binding site upon addition of the co-substrate.

The EPR spectrum for MBP-H167A TfdA (Fig. 2*D*), like that for the H113A variant, is poorly resolved, probably due to binding of copper in multiple configurations instead of formation of one major conformation. Additionally, few significant changes are seen upon addition of either α-KG or 2,4-D. The MBP-H200A EPR spectrum (Fig. 2*E*) is better resolved than that of H113A or MBP-H167A and clearly shows a second set of resonances of lower amplitude with parameters identical to those observed for the copper-substituted wild-type enzyme

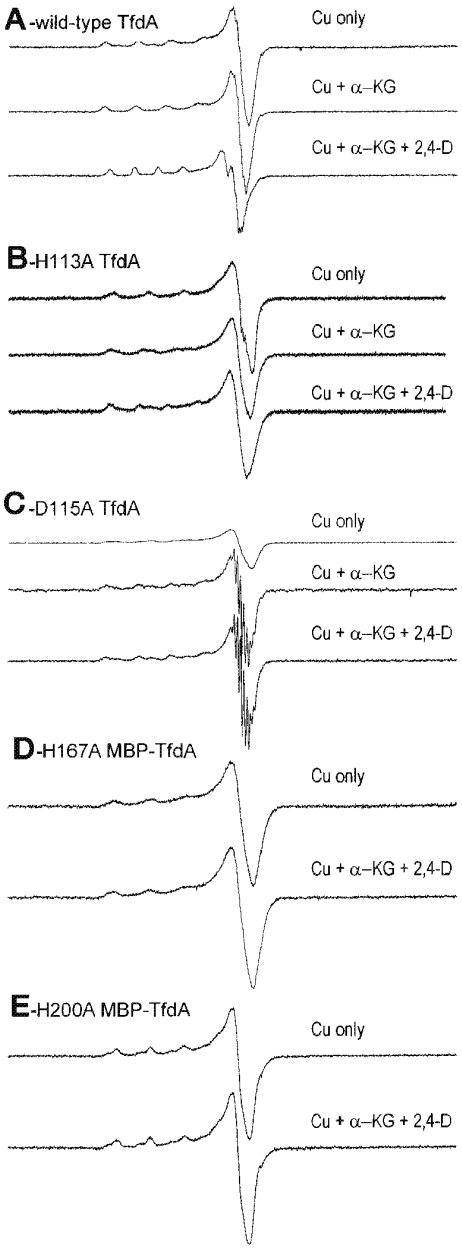


FIG. 2. **X-band CW-EPR spectra of Cu(II)-substituted TfdA variants.** EPR spectra were obtained at 77 K for the following samples (substrate concentrations were 5 mM, when present). *Top to bottom,* wild-type Cu-TfdA in the absence of substrates, with α-KG, and with α-KG + 2,4-D (*A*). H113A Cu-TfdA in the absence of substrates, with α-KG, and with α-KG + 2,4-D (*B*). D115A Cu-TfdA in the absence of substrates, with α-KG, and with α-KG + 2,4-D (*C*). MBP-H167A Cu-TfdA in the absence of substrates, with α-KG, and with α-KG + 2,4-D (*D*). MBP-H200A Cu-TfdA in the absence of substrates and in the presence of α-KG + 2,4-D (*E*). Spectral parameters are listed in Table IV.

(Table IV). The presence of this wild-type signal suggests that His-200 is most likely not a copper-binding ligand in TfdA. As found for H113A and MBP-H167A, addition of α-KG and/or 2,4-D has little effect on the spectrum.

ESEEM Spectroscopic Characterization of Variants with Altered Metal Sites—Pulsed EPR (ESEEM) spectroscopy has proven useful for determining the number of histidines bound to copper in proteins. This approach has been previously used to determine that copper-substituted wild-type TfdA binds cop-

Downloaded from http://www.jbc.org/ by guest on September 3, 2020

COR-AAD1-00002575
Bayer EX1008 (Part 5 of 9)

TABLE IV
Summary of the EPR spectral parameters for Cu(II)-substituted TfdA variants

	$g_\parallel$	$A_\parallel$	$g_\perp$
		mT	
Wild-type TfdA	2.34	16.3	2.07
Wild-type TfdA/α-KG	2.36	15.1	2.07
Wild-type TfdA/α-KG/2,4-D	2.38	12.0	2.09
H113A	2.30	16.6	2.07
H113A/α-KG	2.33	15.8	2.07
H113A/α-KG/2,4-D	2.35	14.0	2.08
D115A	2.30	17.0	2.06
D115A/α-KG	2.30	16.2	2.06
	2.34	16.8	2.06
D115A/α-KG/2,4-D	2.30	16.2	2.06
	2.34	16.8	2.06
MBP-H167A	2.30	17.1	2.07
MBP-H167A/α-KG/2,4-D	2.30	17.1	2.07
MBP-H200A	2.30	17.1	2.07
	2.34	16.1	2.07
MBP-H200A/α-KG/2,4-D	2.30	17.1	2.07
	2.34	16.1	2.07

per in a site with two histidyl residues directly coordinated to the metal. As previously reported (23), three-pulse ESEEM spectra collected in the $g_\parallel$ region for wild-type TfdA exhibit sharp peaks at 0.6, 0.9, and 1.5 MHz and a broad feature at 3.5 MHz (Fig. 3*B*). This signature is typical of imidazole bound in an equatorial position to copper. The additional appearance of narrow combination bands at 2.1, 2.5, and 3.1 MHz in these spectra indicated the presence of at least two such imidazole ligands bound to the copper (34–36). Spectral simulations using the density matrix approach of Mims (28) were used to analyze these data further including determination of the number of histidyl ligands coordinated to copper. The $g_\parallel$ ESEEM of Cu(II)-substituted wild-type TfdA was simulated with magnetic parameters for copper equatorially coordinated to two identical histidines with a simulation program using the angle selection scheme developed for ENDOR analysis (37, 38). For each simulation, a background decay function was applied to allow the amplitudes of the initial 1.5 μs of the simulations to match the data. The resulting simulated data sets (*dashed curves*) are superimposed on the experimental data in Fig. 3. Further analysis of these data suggested that formation of the ternary complex with α-KG and 2,4-D results in the probable loss or reorientation of one of these imidazole ligands, as evidenced by a substantial decrease in the modulation intensity and disappearance of the combination bands (23).

Three-pulse ESEEM patterns for the H113A (*trace A*), MBP-H167A (*trace B*), and D115A (*trace C*) variants of TfdA are shown in Fig. 4. Each data set was collected under identical conditions and normalized so that the integrated echo amplitudes range from zero, determined by shifting the integration window off of the signal at the end of a scan, to one which marks the largest measured echo amplitude. Low frequency modulations indicative of equatorially bound histidyl ligand(s) are observed for all four mutant TfdAs. The ESEEM from H113A (*trace A*) and MBP-H200A (not shown) variants are nearly identical and show modulations that are considerably weaker than those measured for MBP-H167A (*trace B*) and D115A (*trace C*). Each of these data contains a large unmodulated or DC component (well over 80% of the total signal intensity in the case of H113A), contrasting sharply with the ESEEM for copper-substituted wild-type TfdA, where the DC component constituted less than 40% of the total signal intensity (Fig. 3*A*).

The frequency spectra, obtained by Fourier transformation (FT) of the data shown in Fig. 4, are characterized by major

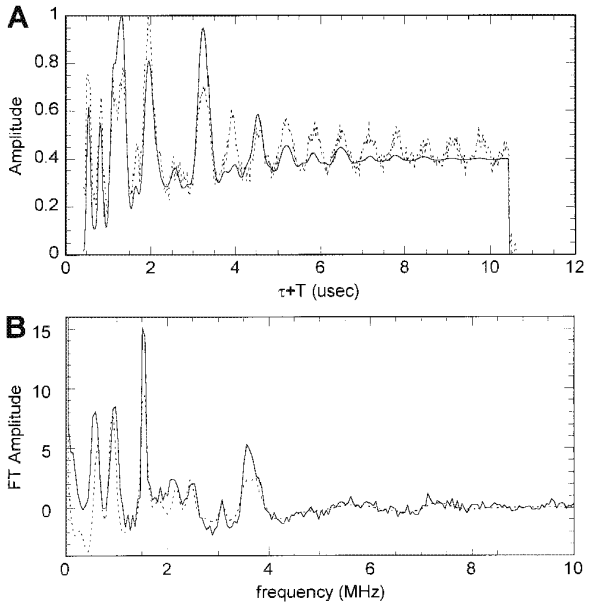


FIG. 3. **Three-pulse ESEEM spectrum and Fourier transformation of Cu(II)-substituted wild-type TfdA with 2-histidine simulation data.** ESEEM spectrum of wild-type Cu(II)-TfdA + α-KG (*solid*) and computer-simulated data for Cu(II) bound by two identical histidines (*dashed*) (*A*) and the corresponding frequency domain spectrum (*B*). Parameters for data collections were magnetic field = 2800 G, τ = 375 ns, T = 50 ns, ν = 8.98 GHz; 4.2 K. Cu(II) hyperfine parameters: g_{xy} = 2.05, g_z = 2.34, $A_{xx} = A_{yy}$ = 20 MHz, A_{zz} = 487 MHz; Superhyperfine parameters: g_N = 0.40347, A_{iso} = 1.7 MHz, radius = 2.75 Å [θ,ϕ] = [2.37,2.07] radians, e^2qQ = 1.60 MHz, η = 0.75, NQI [α,β,γ] = [0.50,1.1,0.1] radians. The simulated data were treated with an exponential decay function to give $y_{ij} = (y_{ij} - 0.17)\cdot\exp((\tau + T)/3500)^{1.5}) + 0.17$. For each simulation, a background decay function was applied to allow the amplitudes of the initial 1.5 μs of the simulations to match the data.

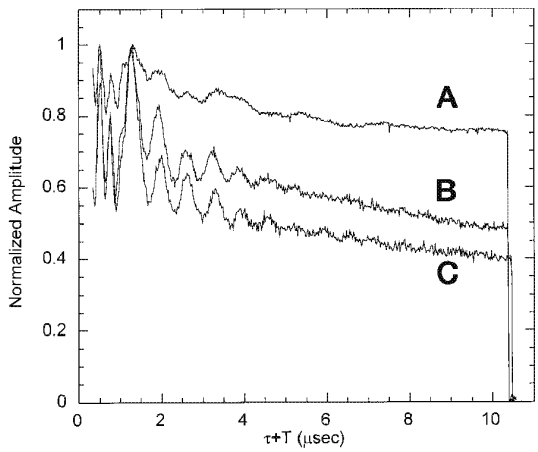


FIG. 4. **Three-pulse ESEEM time domain spectra of TfdA variants.** H113A Cu-TfdA (*A*), magnetic field = 3050 G, τ = 300 ns, T = 40 ns. MBP-H167A Cu-TfdA (*B*), magnetic field = 3100 G, τ = 300 ns, T = 40 ns. D115A Cu-TfdA (*C*), magnetic field = 3050 G, τ = 385 ns, T = 55 ns, ν = 8.8 GHz; 4.2 K.

features at 0.7, 1.5, and 4.0 MHz that are indicative of histidyl imidazole equatorially coordinated to Cu(II) (36). The spectra obtained for D115A and MBP-H167A variants are shown in Figs. 5*B* and 6*B* (*solid lines*), respectively. The resolution in these spectra is poor when compared with similar data obtained for rigid Cu(II) proteins or model complexes (39, 40). In Fig. 5*A*, the normalized three-pulse ESEEM data for D115A TfdA (*solid line*) are shown with the computer-simulated data

Downloaded from http://www.jbc.org/ by guest on September 3, 2020

COR-AAD1-00002576
Bayer EX1008 (Part 5 of 9)

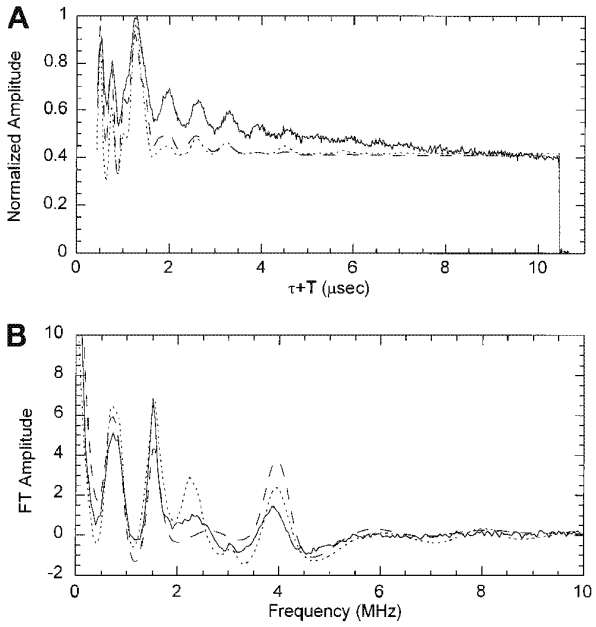


FIG. 5. **Spectral simulation of ESEEM data for D115A-Cu-TfdA.** Experimental (*solid line*), computer-simulated 1-His (*dashed line*), and simulated 2-His (*dotted line*) time domain spectra (*A*) and the corresponding Fourier-transformed data (*B*) for copper-substituted D115A TfdA are shown. Magnetic field = 3050 G, τ = 230 ns, T = 50 ns G, ν = 8.8 GHz, 4.2 K, g_N = 0.40347, e^2qQ = 1.55 MHz, η = 0.87, A_{xx} = 1.6 MHz, A_{yy} = 1.9 MHz, A_{zz} = 2.2 MHz. The simulated data were treated with an exponential decay function to give $y_{ij} = (y_{ij} - 0.05)\cdot\exp((\tau + T)/600)^{0.8}) - 0.05$.

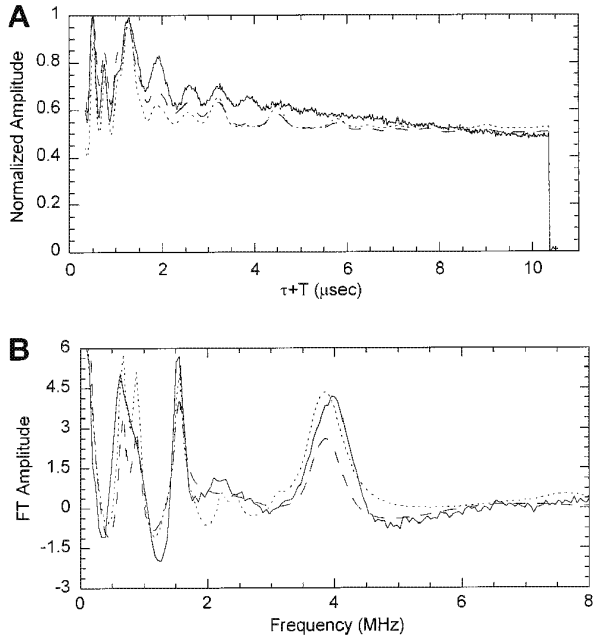


FIG. 6. **Spectral simulation of ESEEM data for MBP-H167A-Cu-TfdA.** Experimental (*solid line*), computer-simulated 1-His (*dashed line*), and 2-His (*dotted line*) time domain spectra (*A*) and the corresponding Fourier-transformed data (*B*) are shown. Magnetic field = 3100 G, τ = 300 ns, T = 40 ns, ν = 8.8 GHz, 4.2 K, g_N = 0.40347, e^2qQ = 1.60 MHz, η = 0.82, A_{xx} = 1.55 MHz, A_{yy} = 1.9 MHz, A_{zz} = 2.0 MHz. The simulated data were treated with an exponential decay function to give $y_{ij} = (y_{ij} - 0.03)\cdot\exp((\tau + T)/350)^{0.5}) - 0.03$.

for one (*dashed line*) and two (*dotted line*) coordinated histidyl ligands obtained using spin Hamiltonian parameters typical for the remote nitrogen of imidazole equatorially bound to Cu(II). To compare the amplitudes of the ESEEM simulations with those obtained experimentally, the simulated ESEEM patterns of Fig. 5*A* were multiplied by background decay functions characterized by an e^{-1} time of 600 ns. This decay time constant is a factor of 6 faster than that used to make the comparison between simulation and experiment for wild-type Cu-TfdA in Fig. 3. Unfortunately, the severity of this decay impairs our ability to distinguish whether 1 or 2 nitrogen nuclei are giving rise to the ESEEM of D115A based on modulation depths.

The Fourier transforms of the experimental and simulated ESEEM functions of Fig. 5*A* are shown in Fig. 5*B*. Although the combination lines are weaker in the data for D115A (*solid line*) than for wild-type TfdA, the combination line at ~3.0 MHz is observed, and its frequency is predicted nicely by the 2-His simulation. The broader line widths of the FT spectra found for D115A TfdA, and the subsequent difficulty in observing the combination lines most likely reflects a distribution of ^{14}N superhyperfine couplings for the Cu(II) sites of the variant. To account for the observed line widths and relative peak amplitudes in our simulations, it was necessary to average several calculated data sets obtained with ^{14}N isotropic hyperfine coupling constants that ranged from 1.6 to 1.8 MHz. This assumption of a distribution of hyperfine couplings results in better agreement between experiment and theory for our ESEEM simulations and is in accord with the poor resolution observed in the cw-EPR spectrum of Cu(II)-D115A TfdA in the absence of substrates.

A parallel analysis was undertaken for the MBP-H167A data, and the results are provided in Fig. 6. The *dash* and *dot* patterns of Fig. 6*A* are simulation results for one and two equatorially bound histidyl ligands, respectively. The broadness of the lines at 0.6 and 0.9 MHz results in these frequencies being unresolved in the experimental data. This effect could be simulated using a higher asymmetry parameter, η, for the nuclear quadrupole interaction but not without significant deficiencies in the prediction of the double quantum peak at 4 MHz. A more satisfactory method of accounting for this coalescence in the simulations was through the averaging of calculation results obtained using a distribution of isotropic hyperfine coupling constants, as in the simulations for D115A. The simulations in Fig. 6 are the result of averaging five such data sets where the ^{14}N isotropic hyperfine coupling ranged from 1.6 to 1.9 MHz. This method resulted in the broadening of the low frequency peaks to the point where they began to overlap, without reducing the magnitude of the double quantum feature at 4 MHz. As in the analysis of D115A, different background decay functions were applied to these simulations to provide the best match to the modulation intensities for the initial 1.5 μs of the ESEEM data (*solid line*). The background decay required to reduce the initial amplitudes of both one and two imidazole simulations was a factor of 10 faster than that used to simulate wild-type Cu(II)-TfdA ESEEM. This problem, combined with the lack of resolved combination peaks in the data, makes it difficult to determine the number of bound histidines. Although the modulation intensities are best accounted for by the one-histidine model, the features of the ESEEM spectrum are better simulated assuming two coupled nitrogens. The ESEEM patterns associated with the H113A and MBP-H200A mutants were too shallow to be consistent with single histidyl coordination, and it is likely that these mutant proteins have multiple Cu(II)-binding sites, some with equatorially coordinated histidine ligand(s) and some without.

The Cu(II)-substituted forms of H113A, D115A, MBP-H167A, and MBP-H200A were also analyzed by ESEEM spec-

Downloaded from http://www.jbc.org/ by guest on September 3, 2020

COR-AAD1-00002577
Bayer EX1008 (Part 5 of 9)

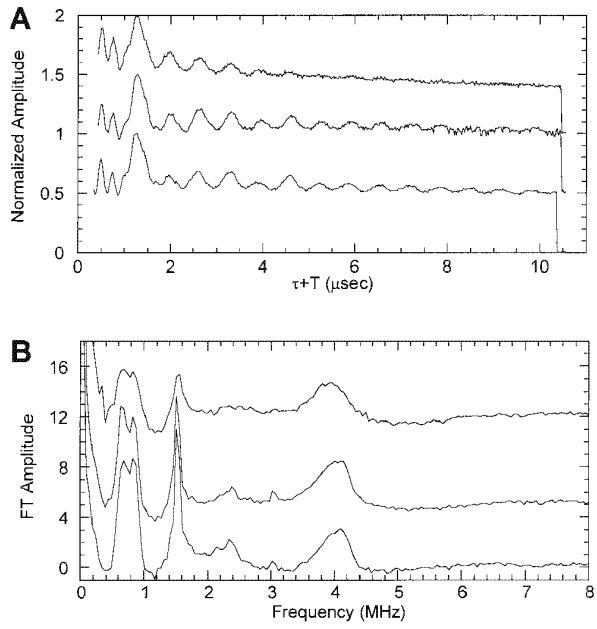


FIG. 7. **Three-pulse ESEEM of D115A TfdA (4.2K).** *Top to bottom,* D115A Cu-TfdA in the absence of substrate, with 5 mM α-KG, and with 5 mM α-KG + 5 mM 2,4-D (*A*) and the corresponding frequency domain spectra (*B*). Conditions for these measurements were identical to those of Fig. 3.

troscopy in the presence of α-KG and 2,4-D. Only slight variations in the line shape of the higher frequency peak at ~4.0 MHz were observed for the three histidine mutants. This result contrasts sharply with those for copper-substituted wild-type TfdA where addition of the co-substrates resulted in data that suggested a shift from two equatorially bound histidyl ligands to only one. The lack of similar changes in the ESEEM of these mutants upon addition of the co-substrates supports the conclusion that alteration of these key histidyl residues significantly effects the metal binding properties of the TfdA enzyme. Three-pulse ESEEM spectra for D115A TfdA in the presence of α-KG and α-KG + 2,4-D (Fig. 7) show that addition of co-substrates leads to improved resolution in the ESEEM spectra without significant changes in the amount of unmodulated intensity. These results mirror the improved resolution observed in the cw-EPR spectra. For the ternary complex with both co-substrates bound to the D115A variant, all three combination lines from the electron spin manifold that gives rise to the intense low frequency peaks are resolved (Fig. 7*B*). Furthermore, the cw-EPR spectra of D115A treated with co-substrates show well resolved ligand hyperfine structure at $g_\perp$. Taken together, these data indicate that two histidyl ligands remain equatorially bound during addition of the co-substrates and support our proposal that the differences between theory and experiment found for the two-histidine simulation of Fig. 5 most likely stem from a distribution of structures present prior to substrate addition.

DISCUSSION

EPR, ESEEM, and extended x-ray absorption fine structure spectroscopies of both the Fe(II)- and Cu(II)-forms of wild-type TfdA had previously indicated that the resting enzyme has two imidazoles and a mixture of bound nitrogens and oxygens as ligands to the metal (22–24). ESEEM and x-ray absorption data indicated that both imidazole ligands are retained upon addition of αKG, whereas addition of 2,4-D leads to the displacement or g tensor reorientation of a histidine out of the equatorial plane (22–24). Our present results confirm the importance of multiple histidines and one aspartate for TfdA activity and allow us to assign functions to selected residues.

Mutation of His-113 or Asp-115 to alanine both eliminates activity and alters the structure of Cu(II) metallocenter site. Both variants show EPR spectra consistent with at least two distinct Cu(II)-binding sites. Substrate binding perturbs these spectra giving rise to better resolution of $g_\parallel$ features associated with each metal site suggesting that the copper is likely present at the same binding site as in the wild-type enzyme. His-113 and Asp-115 comprise the HX(D/E) motif that is strictly conserved in enzymes related to TfdA (Fig. 8) and more distantly related α-KG-dependent dioxygenases (Table I) (7). Site-directed mutagenesis studies analogous to those described here demonstrated the importance of this motif in a number of Group I enzymes including asparyl, lysyl, prolyl, and flavanone hydroxylases (8, 10–13). Furthermore, crystal structures of IPNS and DAOCS established these residues as ligands to the Group I metal centers. Our studies support the proposal that residues in the HX(D/E) motif are ligands to the metal in TfdA and, most likely, other Group II enzymes.

Cu(II)-D115A TfdA ESEEM and EPR spectra (particularly for the case where substrates are bound) indicate the presence of two imidazole ligands at one of the Cu(II) sites. The intensity of the non-modulated echo signal was greater for this variant, as compared with that found for the wild-type enzyme, providing evidence for another copper binding environment that lacks equatorially bound histidines. The absence of the aspartate ligand alters the chemistry that occurs at the active site upon addition of the co-substrates. The geometry of the Cu(II) site shows less dispersion when α-KG and 2,4-D are bound as evidenced by the increased resolution in the EPR spectrum and ESEEM pattern. These observations are consistent with those made for the wild-type Cu(II) TfdA; however, the structural rearrangement triggered by formation of the Cu(II)-αKG-2,4-D ternary complex in wild-type TfdA is not observed for D115A TfdA. Together, these data indicate that Asp-115 is very likely a metal-binding residue and may also be involved in formation of the proper catalytic conformation. Because these observations pertain to the Cu(II) form of TfdA, it is difficult to draw conclusions about the specific electronic role of Asp-115 in the native Fe(II) TfdA based on these observations.

The identity of the second metal-binding histidine, predicted by various spectroscopic studies, is less clear. Spectral simulations of H167A are consistent with the presence of two imidazole nitrogens per copper in this protein. Furthermore, His-167 is replaced with an arginine in the TfdA sequence encoded *tfdA* on pJJB in *Burkholderia cepacia* (GenBank™ accession number AAB47567). Thus, even though this residue most closely matches the spacing observed in the Group I sequences, it is unlikely that His-167 is the third metal ligand to the TfdA iron metallocenter. EPR and ESEEM analyses of H200A TfdA suggest that His-200 is important for creation of the metallocenter. Although His-200 is conserved among the enzymes with high identities to TfdA, such as TauD from *E. coli* and sulfonate/α-KG dioxygenase from yeast, a corresponding histidine is not found in more distantly related Group II enzymes such as γ-butyrobetaine hydroxylase or clavaminate synthase (Fig. 8). Mutational analysis of prolyl 4-hydroxylase (10) provided evidence for a non-ligand histidine at the active site that is important for α-KG binding and for controlling the decarboxylation of α-KG in the absence of substrate. Perhaps His-200 serves a similar function in TfdA, providing an explanation for the changes in active site structure upon its alteration. Sequence comparisons of all Group II enzymes, including several putative dioxygenases with overall similarity to TfdA, reveal that His-262 in TfdA is the only other invariant histidine (Fig.

Downloaded from http://www.jbc.org/ by guest on September 3, 2020

COR-AAD1-00002578
Bayer EX1008 (Part 5 of 9)

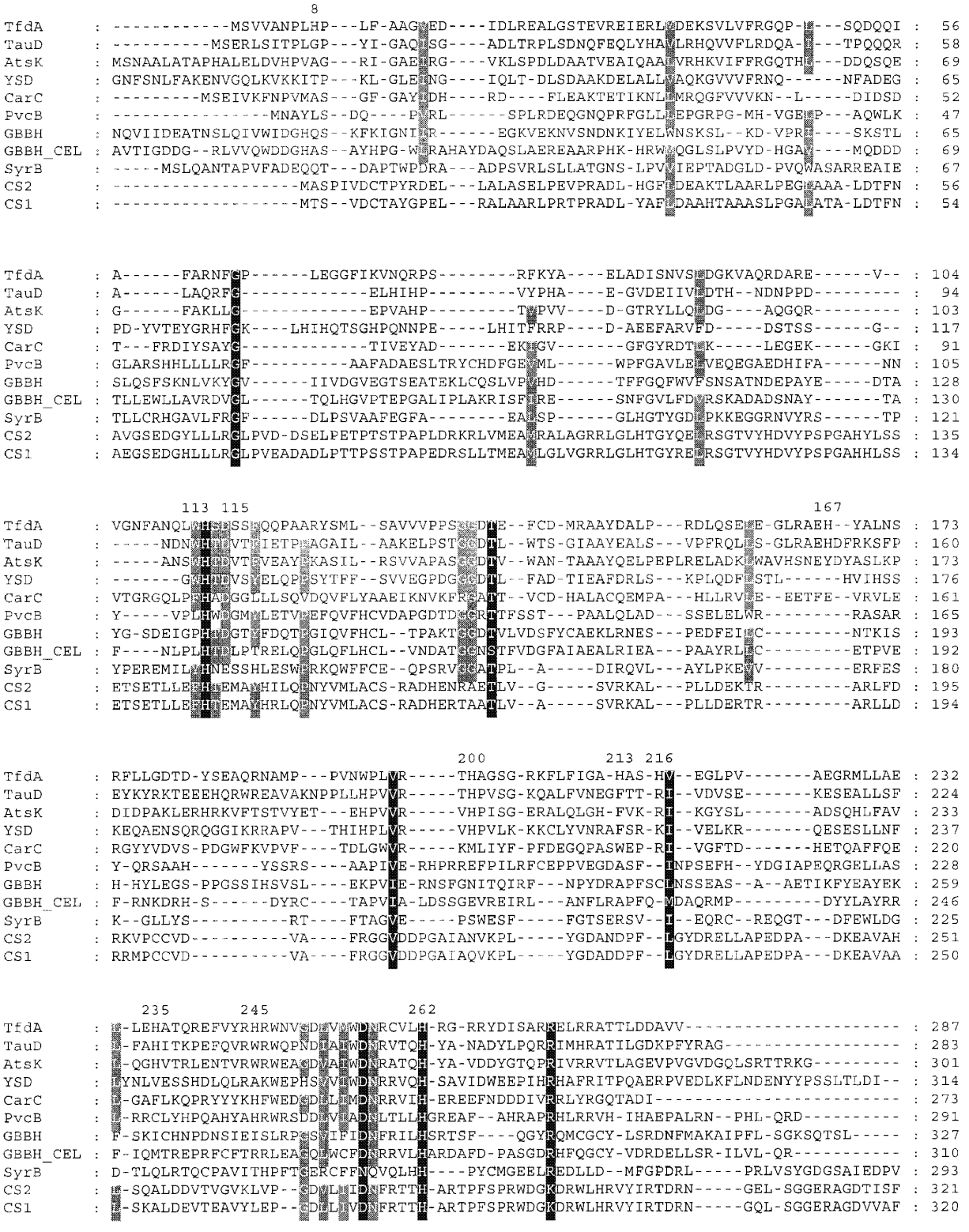


FIG. 8. **Sequence comparison of TfdA and other Group II α-KG-dependent dioxygenases.** The accession numbers and sequence identifiers are shown in parentheses for the following Group II sequences: *R. eutropha* 2,4-D/α-KG dioxygenase (TfdA, M16730); *E. coli* taurine/α-KG dioxygenase (TauD, P37610); putative α-KG dioxygenase from sulfate-ester transport gene cluster in *Pseudomonas putida* (AtsK, AF126201); *S. cerevisiae* sulfonate/α-KG dioxygenase (YSD, Q12358); *Erwinia carotovora* carbapenem biosynthesis enzyme C (CarC, AAD38231); *Pseudomonas aeruginosa* pyoverdine biosynthesis enzyme (PvcB, AF002222); *Pseudomonas syringae* SyrI, syringomycin biosynthesis enzyme I (SyrB, AAB63253); *Pseudomonas* sp. γ-butyrobetaine hydroxylase (GBBH, P80193); *Caenorhabditis elegans* γ-butyrobetaine hydroxylase (GBBH_CE, Z66523); *Streptomyces clavuligerus* clavaminate synthase 1 and 2 (CS1, A44241; CS2, L06214). Highly conserved residues (*black boxes*) and residues conserved in more than 75% of the sequences (*dark gray boxes*) are *highlighted*. Amino acid numbers for each sequence are shown at the *right* of each line; mutated TfdA residues are *numbered* above.

Downloaded from http://www.jbc.org/ by guest on September 3, 2020

COR-AAD1-00002579
Bayer EX1008 (Part 5 of 9)

8); thus, we suggest that this is most likely the third metal-binding residue. In support of our assignment of His-262 as a metal ligand, this residue is 10 amino acids away from Arg-273 creating an $HX_{10}R$ motif similar to that in DAOCS and related enzymes (8). This arginine is conserved in the other Group II enzymes (Fig. 8). Together, these data suggest a more general motif for α-KG-dependent dioxygenases, $HX(D/E)X_nHX_{10-15}R$ where X_n varies with the different subgroups within the superfamily (Group I, n = 44–65; Group II n = 123–153; and Group III, n = 74–104) (4).

His-213 and His-216 may also be present at or near the TfdA active site. MBP-H213A and H216A TfdA variants exhibited increased 2,4-D K_m values, and the former enzyme also demonstrated a decreased catalytic rate. These data may indicate that His-213 (perhaps also assisted by His-216) facilitates 2,4-D binding by electrostatic interactions between the imidazole nitrogen and the substrate carboxylate group; however, additional studies are required to test this hypothesis. The importance of the 2,4-D carboxylate for binding to TfdA is indicated by the inability of phenoxyethanol to serve as a substrate (21). Neither His-213 nor His-216 are conserved among other related α-KG-dependent dioxygenases. The divergence of sequences in this region may reflect differences in the residues required to bind substrates unique to each enzyme.

Our results provide no evidence to indicate that His-8, His-235, or His-245 are critical for catalysis. The H8A variant exhibits enhanced protease sensitivity, but the full-length protein possesses near wild-type activity. Similarly, the H235A protein is nearly unaffected in its activity. Neither of these residues is conserved in homologous sequences. As described for the H262A TfdA variant, His-245 appears to be structurally important. Because H262A and H245A derivatives of TfdA exist in non-native, highly aggregated conformations, we were unable to assess directly whether these residues may also play a catalytic role. Although His-245 is not conserved in these sequences, it is in the C-terminal half of the protein which in other α-KG-dependent dioxygenases show a higher level of similarity than the overall sequence comparisons (41). This region might be more constrained for structural reasons.

The $HX(D/E)X_nH$ motif, which is found in all known α-KG dependent dioxygenases, is an example of the more general structural arrangement (2-His-1-carboxylate) found in non-heme Fe(II) enzymes including extradiol dioxygenases and pterindependent hydroxylases (42). It is proposed that these three ligands anchor the iron in the active site of the enzyme while leaving three open coordination sites available for the binding of substrate, cofactor, and oxygen. Several studies suggest that O_2 reacts much more readily with such iron centers after the displacement of solvent molecules by more electronegative substrate molecules (42). In addition, it is the diversity of exogenous ligands that enable non-heme Fe(II)-dependent oxygenases to catalyze such a wide range of reactions.

Our proposed model of the active site of TfdA is shown in Fig. 9. His-113, Asp-115, and a third residue tentatively identified as His-262 are shown as ligands to the metal. As in the crystal structures of both DAOCS and IPNS, water molecules are thought to occupy the three remaining coordination sites in substrate-free enzyme. The model includes a likely binding mode for α-KG based on the DAOCS crystal structure (17). Recent spectroscopic studies of clavaminate synthase (43), TauD (44), and TfdA (24) are consistent with a similar mode of α-KG binding in these enzymes. We have no evidence to suggest direct binding of 2,4-D to the metal center and indicate the presence of a separate 2,4-D-binding site adjacent to the metal in the model. Mutation of His-213 affects both substrate binding and the rate of catalysis and therefore is shown to be present near the active site to indicate potential substrate interactions, but the precise role of the residue is still to be defined. In the absence of a crystal structure, the site-directed mutagenesis, metallocenter spectroscopy, and kinetic analysis studies described here provide the most complete working model of the TfdA active site. This model begins to define the necessary elements for catalysis in Group II α-KG-dependent dioxygenases and finds similarities between these enzymes and other well studied representatives of this superfamily.

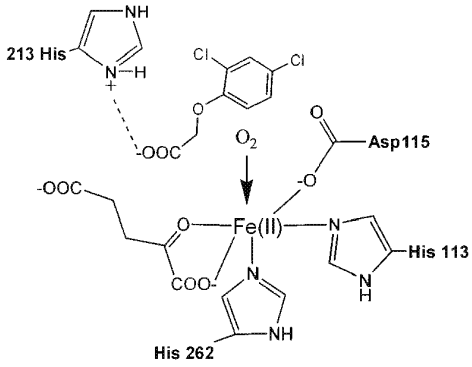


FIG. 9. **Model for the active site of TfdA.** The three residues proposed to ligate the ferrous ion of TfdA are shown along with a possible coordination mode for the substrates, α-KG and 2,4-D. His-213, implicated in catalysis and/or binding of 2,4-D, is also illustrated.

Note Added in Proof—The recently reported structure of clavaminate synthase (45) confirms our proposed roles for residues in the $Hx(D/E)x_{138-207}Hx_{15}$ (R/K) motif for the Group II α-KG-dependent dioxygenases.

REFERENCES

1. Fukumori, F., and Hausinger, R. P. (1993) *J. Bacteriol.* **175,** 2083–2086
2. De Carolis, E., and De Luca, V. (1994) *Phytochemistry* **36,** 1093–1107
3. Prescott, A. G., and John, P. (1996) *Annu. Rev. Plant Physiol. Plant Mol. Biol.* **47,** 245–271
4. Hogan, D. A. (1999) *Characterization and Function of 2,4-Dichlorophenoxyacetic Acid/α-Ketoglutarate Dioxygenase and Related Enzymes.* Ph.D. thesis, Michigan State University, East Lansing, MI
5. Kivirikko, K. I., and Pihlajaniemi, T. (1998) *Adv. Enzymol. Relat. Areas Mol. Biol.* **72,** 328–398
6. Hedden, P. (1992) *Biochem. Soc. Trans.* **20,** 373–377
7. Borovok, I., Landman, O., Kreisberg-Zakarin, R., Aharonowitz, Y., and Cohen, G. (1996) *Biochemistry* **35,** 1981–1987
8. Lukacin, R., and Britsch, L. (1997) *Eur. J. Biochem.* **248,** 748–757
9. Kreisberg-Zakarin, R., Borovok, I., Yanko, M., Aharonowitz, Y., and Cohen, G. (1999) *Antonie Van Leeuwenhoek* **75,** 33–39
10. Myllyharju, J., and Kivirikko, K. I. (1997) *EMBO J.* **16,** 1173–1180
11. Lamberg, A., Pihlajaniemi, T., and Kivirikko, K. I. (1995) *J. Biol. Chem.* **270,** 9926–9931
12. Pirskanen, A., Kaimio, A.-M., Myllylä, R., and Kivirikko, K. I. (1996) *J. Biol. Chem.* **271,** 9398–9402
13. McGinnis, K., Ku, G. M., VanDusen, W. J., Fu, J., Garsky, V., Stern, A. M., and Friedman, P. A. (1996) *Biochemistry* **35,** 3957–3962
14. Lloyd, M. D., Lee, H. J., Harlos, K., Zhang, Z. H., Baldwin, J. E., Schofield, C. J., Charnock, J. M., Garner, C. D., Hara, T., Terwisscha van Scheltinga, A. C., Valegard, K., Viklund, J. A., Hajdu, J., Andersson, I., Danielsson, A., and Bhikhabhai, R. (1999) *J. Mol. Biol.* **287,** 943–960
15. Roach, P. L., Clifton, I. J., Fülöp, V., Harlos, K., Barton, G. J., Hajdu, J., Andersson, I., Schofield, C. J., and Baldwin, J. E. (1995) *Nature* **375,** 700–704
16. Roach, P. L., Clifton, I. J., Hensgens, C. M. H., Shibata, N., Schofield, C. J., Hajdu, J., and Baldwin, J. E. (1997) *Nature* **387,** 827–830
17. Valegård, K., van Scheltinga, A. C. T., Lloyd, M. D., Hara, T., Ramaswamy, S., Perrakis, A., Thompson, A., Lee, H.-J., Baldwin, J. E., Schofield, C. J., Hajdu, J., and Andersson, I. (1998) *Nature* **394,** 805–809
18. Eichhorn, E., van der Ploeg, J. R., Kertesz, M. A., and Leisinger, T. (1997) *J. Biol. Chem.* **272,** 23031–23036
19. Hogan, D. A., Auchtung, T. A., and Hausinger, R. P. (1999) *J. Bacteriol.* **181,** 5876–5879
20. Altschul, S. F., Madden, T. L., Schäffer, A. A., Zhang, J., Zhang, Z., Miller, W., and Lipman, D. J. (1997) *Nucleic Acids Res.* **25,** 3389–3402
21. Fukumori, F., and Hausinger, R. P. (1993) *J. Biol. Chem.* **268,** 24311–24317
22. Cosper, N. J., Stålhandske, C. M. V., Saari, R. E., Hausinger, R. P., and Scott, R. A. (1999) *J. Biol. Inorg. Chem.* **4,** 122–129
23. Whiting, A. K., Que, L., Jr., Saari, R. E., Hausinger, R. P., Fredrick, M. A., and McCracken, J. (1997) *J. Am. Chem. Soc.* **119,** 3413–3414
24. Hegg, E. L., Whiting, A. K., McCracken, J., Hausinger, R. P., and Que, J., L. (1999) *Biochemistry* **38,** 16714–16726

Downloaded from http://www.jbc.org/ by guest on September 3, 2020

COR-AAD1-00002580
Bayer EX1008 (Part 5 of 9)

25. McCracken, J., Shin, D.-H., and Dye, J. L. (1992) *Appl. Mag. Res.* **3,** 305–316
26. Lin, C. P., Bowman, M. K., and Norris, J. R. (1985) *J. Magn. Reson.* **65,** 369–374
27. Mims, W. B. (1984) *J. Magn. Reson.* **59,** 291–306
28. Mims, W. B. (1972) *Phys. Rev. B: Solid State* **5,** 2409–2419
29. Altschul, S. F., Gish, W., Miller, W., Myers, E. W., and Lipman, D. J. (1990) *J. Mol. Biol.* **215,** 403–10
30. Thompson, J. D., Higgins, D. G., and Gibson, T. J. (1994) *Nucleic Acids Res.* **22,** 4673–4680
31. Nicholas, K. B., Jr., Nicholas, H. B., Jr., and Deerfield, D. W., II (1997) *EMB News* **4,** 14
32. Blackwell, J. R., and Horgan, R. (1991) *FEBS Lett.* **295,** 1–12
33. Rotilio, G., Agrò, A. F., Calabrese, L., Bossa, F., Guerrieri, P., and Mondovì, B. (1971) *Biochemistry* **10,** 616–621
34. McCracken, J., Cornelius, J. B., and Peisach, J. (1989) in *Pulsed EPR: A New Field of Applications* (Keijzers, C. P., Reijerse, E. J., and Schmidt, J., eds) pp. 155–161, Elsevier/North-Holland Biomedical Press, Amsterdam
35. McCracken, J., Pember, S., Benkovic, S. J., Villafranca, J. J., Miller, R. J., and Peisach, J. (1988) *J. Am. Chem. Soc.* **110,** 1069–1074
36. Mims, W. B., and Peisach, J. (1978) *J. Chem. Phys.* **69,** 4921–4930
37. Hoffman, B. M., Martinsen, J., and Venters, R. A. (1984) *J. Magn. Reson.* **59,** 110–123
38. Hurst, G. C., Henderson, T. A., and Kreilick, R. W. (1985) *J. Am. Chem. Soc.* **107,** 7294–7299
39. McCracken, J., Peisach, J., and Dooley, D. M. (1987) *J. Am. Chem. Soc.* **109,** 4064–4072
40. Jiang, F., Peisach, J., Ming, L.-J., Que, L., Jr., and Chen, V. J. (1991) *Biochemistry* **30,** 11437–11445
41. Jia, S., McGinnis, K., VanDusen, W. J., Burke, C. J., Kuo, A., Griffin, P. R., Sardana, M. K., Elliston, K. O., Stern, A. M., and Friedman, P. A. (1994) *Proc. Natl. Acad. Sci. U. S. A.* **91,** 7227–7231
42. Hegg, E. L., and Que, L., Jr. (1997) *Eur. J. Biochem.* **250,** 625–629
43. Pavel, E. G., Zhou, J., Busby, R. W., Gunsior, M., Townsend, C. A., and Solomon, E. I. (1998) *J. Am. Chem. Soc.* **120,** 743–753
44. Ryle, M. J., Padmakumar, R., and Hausinger, R. P. (1999) *Biochemistry* **38,** 15278–15286
45. Zhang, Z., Ren, J., Stammers, D. K., Baldwin, J. E., Harlos, K., and Schofield, C. J. (2000) *Nat. Struct. Biol.* **7,** 127–133

Downloaded from http://www.jbc.org/ by guest on September 3, 2020

COR-AAD1-00002581
Bayer EX1008 (Part 5 of 9)

Site-directed Mutagenesis of 2,4-Dichlorophenoxyacetic Acid/α-Ketoglutarate Dioxygenase: IDENTIFICATION OF RESIDUES INVOLVED IN METALLOCENTER FORMATION AND SUBSTRATE BINDING

Deborah A. Hogan, Sheila R. Smith, Eric A. Saari, John McCracken and Robert P. Hausinger

J. Biol. Chem. 2000, 275:12400-12409.
doi: 10.1074/jbc.275.17.12400

Access the most updated version of this article at http://www.jbc.org/content/275/17/12400

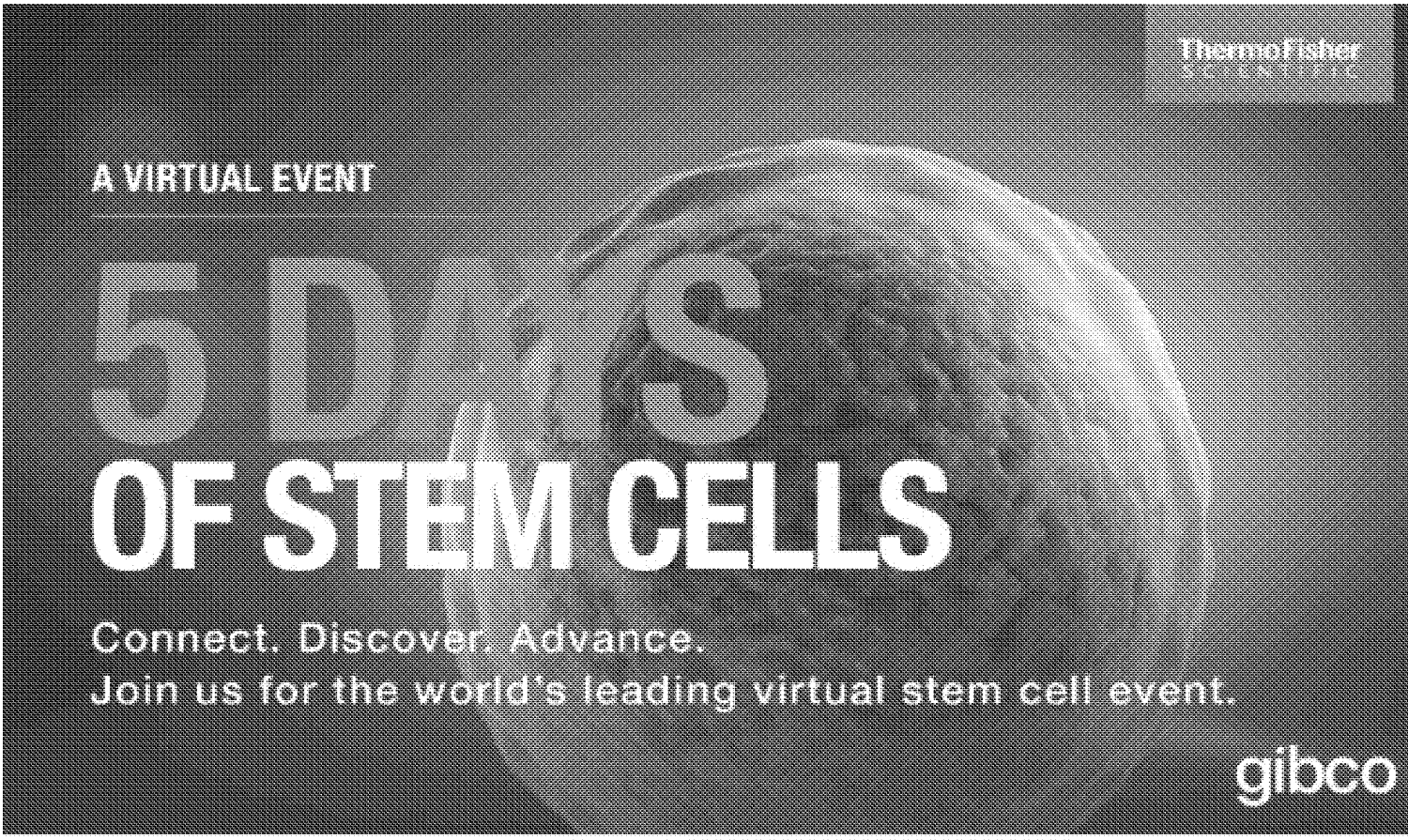
Alerts:
- When this article is cited
- When a correction for this article is posted

Click here to choose from all of JBC's e-mail alerts

This article cites 43 references, 9 of which can be accessed free at
http://www.jbc.org/content/275/17/12400.full.html#ref-list-1

Downloaded from http://www.jbc.org/ by guest on September 3, 2020

COR-AAD1-00002582
Bayer EX1008 (Part 5 of 9)



Stay on the leading edge of stem cell research

The Gibco™ 5 Days of Stem Cells virtual event connects you to the latest stem cell techniques, research breakthroughs, and esteemed scientists from around the world–all from the comfort of anywhere.

The 5-day virtual agenda is packed full of incredible insights in the form of:

- Leading scientific presentations from thought leaders around the world
- Behind-the-scenes virtual training demos
- Scientific poster sessions
- Hundreds of key stem cell tools and resources
- A global network of researchers including our stem cell experts and technical support

We'll share developments, discoveries, and cutting-edge content connected to a wide variety of stem cell applications, including disease modeling, cell and gene therapy, 3D modeling, and much more.

It's all happening October 12–16, 2020.

CURRENT PROTOCOLS

Register for free at **thermofisher.com/5daysofstemcells**

ThermoFisher SCIENTIFIC

For Research Use Only. Not for use in diagnostic procedures. © 2020 Thermo Fisher Scientific Inc. All rights reserved. All trademarks are the property of Thermo Fisher Scientific and its subsidiaries unless otherwise specified. COL012782 0920

Electrokinetic Movement and Biodegradation of 2,4-Dichlorophenoxyacetic Acid in Silt Soil

Simon A. Jackman,[1] Giacomo Maini,[2] Ajay K. Sharman,[2] Garry Sunderland,[3] Christopher J. Knowles[1]

[1]Oxford Centre for Environmental Biotechnology, Department of Engineering Science, University of Oxford, Parks Road, Oxford OX1 3PJ; and Natural Environment Research Council, Centre for Ecology & Hydrology, Mansfield Road, Oxford OX1 3SR, UK; telephone: +44-1865-281630; fax.: +44-1865-281696; e-mail: simon.jackman@eng.ox.ac.uk
[2]Viridian EHC Ltd., 114-116 John Wilson Business Park, Thanet Way, Whitstable, Kent CT5 3QT, UK
[3]Capenhurst Tech. Ltd., Capenhurst Technology Park, Capenhurst, Chester CH1 6ES, UK

Received 10 September 2000; accepted 30 December 2000

Abstract: The coupling of electrokinetic movement of an organic contaminant, 2,4-dichlorophenoxyacetic acid (2,4-D), through soil and its biodegradation in situ has been demonstrated. In a first experiment, the direction and rate of movement of 2,4-D were determined using homogeneously contaminated soil (864 mg 2,4-D/kg dry weight soil) compacted into six individual compartments, 6 cm long, 3 cm wide, and 4 cm deep. Each compartment was bordered by a carbon felt anode and a stainless steel cathode. The application of a current density of 3.72 A/m^2 led to migration of 2,4-D towards the anode at a rate of approximately 4 cm/day. In a second experiment, electrokinetic movement and biodegradation were combined in situ. Sterilized silt soil contaminated with ring-labeled ^{14}C-2,4-D (811 mg 2,4-D/kg dry weight soil) was compacted into a single soil compartment, 22 cm long, 7 cm wide, and 4 cm deep, in a 4.5 cm region adjacent to the cathode. The remainder of the compartment was filled with sterilized soil (to a total weight of 1,015 g). *Burkholderia spp. RASC c2* (1.88 × 10^{11} cells), a tetracycline-resistant bacterium with chromosomally encoded degradative genes for 2,4-D, was inoculated into the soil at a position 14–16 cm from the cathode. The reactor was placed within a sealed perspex box, with a constant air flow connected to sodium hydroxide traps. Under an applied current density of 0.89 A/m^2, the pollutant moved towards the bacteria. As it reached the inoculated region, its concentration decreased in the soil and $^{14}CO_2$ was recovered in the traps. At the end of the experiment, 87.1% of radiolabel had been removed from the soil, 5.8% of which was recovered as $^{14}CO_2$. A third, control, experiment showed a significant contrast in the absence of an electric current, where a slow rate of diffusion controlled the movement of both 2,4-D and bacteria in the soil and biodegradation occurred at the interface between the diffusing fronts. © 2001 John Wiley & Sons, Inc. *Biotechnol Bioeng* **74:** 40–48, 2001.
Keywords: biodegradation; bioremediation; 2,4-dichlorophenoxyacetic acid; electrokinetics; electromigration

INTRODUCTION

Bioremediation is an attractive technology for the cleanup of contaminated land as it is based upon the use of natural processes to degrade organic pollutants to carbon dioxide and water. It also has the potential to be cost-competitive, with estimations of 10–80 £/m^3 contaminated soil compared to 30–75 £/m^3 for landfill and 100–400 £/m^3 for incineration (IAL Consultants, Market Opportunities for Environmental Biotechnology, Contaminated Land in the United Kingdom, 1998). As a result, the overall market in the UK is growing at 10% per year. During the last few decades there have been enormous advances in understanding the microbiology and genetics of bioremediation (Head, 1998). However, it has proved difficult to use bacteria to treat real contaminated sites. This is because the degradative effectiveness of microorganisms can be affected by environmental factors such as temperature, pH, and moisture levels and then can be inhibited by high concentrations of the pollutants themselves or of other organics or metal ions within the soil matrix. Pollutants can also have reduced bioavailability due to sequestration within micropores, binding to soil matrices, and partitioning/dissolution in soil organic matter (Hatzinger and Alexander, 1995).

Electrokinetics, the application of direct electric current to soil, is an emerging engineering technique for the remediation of contaminated soil (Acar and Alshawabkeh, 1993). It has been applied to both metal and organic contamination. An electric current between electrodes inserted into the soil generates hydrogen ions at the anode and hydroxyl ions at

Correspondence to: S. A. Jackman
Contract grant sponsors: Engineering and Physical Sciences Research Council; Department of Trade and Industry

© 2001 John Wiley & Sons, Inc.

COR-AAD1-00002584
Bayer EX1008 (Part 5 of 9)

the cathode, which move into the soil by electromigration, forming a pH gradient (Probstein and Hicks, 1993). When hydroxyl ions are titrated with acid at the cathode and hydrogen ions acidify the soil, cationic metal species can be eluted from their interactions with soil particles. These metals move by electromigration towards the cathode, where they are removed and collected. Anionic metal complexes, inorganic anions, and negatively charged organics will migrate towards the anode. Dipolar interactions between water molecules and soil surfaces lead to an electroosmotic flow of water towards the cathode, which is able to transport uncharged organics.

The application of electrokinetics to the remediation of organic-contaminated soil has focused upon electroosmotic approaches for uncharged molecules such as coal tar constituents, including PAHs (Bruell et al., 1992). The incorporation of surfactants (Kim and Lee, 1999) or cyclodextrins (Ko et al., 2000) has proved to be effective in solubilizing more hydrophobic organics. In situ biodegradation of organics has been enhanced by electrokinetic supply of nutrients (Budhu et al., 1997; Electorowicz and Boeva, 1996). The coupling of electrokinetic movement with degradation of organics has been demonstrated by a US government/industry consortium, using a process termed Lasagna™, to move nonaqueous phase liquids, such as trichloroethylene (TCE) into an area containing zerovalent iron for catalytic remediation (Ho et al., 1999a,b) or methanotrophic bacteria for biodegradation (Davis-Hoover et al., 1999). Phenol-contaminated soil has also been treated by moving the contaminant into treatment zones containing iron (Yang and Long, 1999) and degradative bacteria (Ho et al., 1995). Patents have been granted for similar processes in which the biodegradation of organics is enhanced by the electrokinetic processes alone (Clarke et al., US Patent 5,846,393) and in combination with the use of Fenton's reagent to perform oxidative reactions (Clarke et al., US Patent 5,861,090). Furthermore, DeFlaun and Condee (1997) have demonstrated that bacteria can be moved through aquifer material, towards a polluted area, by electrokinetic transport, leading to the degradation of the organic pollutant TCE.

The concept of moving an organic contaminant into an area containing degradative microorganisms is attractive because of the potential for movement into an inoculated degradative zone, dispersion from areas of high contamination, and release from sequestration in soil micropores. The work presented in this article is aimed at gaining a greater understanding of the movement and degradation of organic compounds under electrokinetic conditions. Using a standardized soil and an electrokinetic apparatus that has been utilized successfully for the remediation of metal-contaminated soil (Maini et al., 2000b) and historic metal and organic contamination (Maini et al., 2000a), the organic contaminant 2,4-dichlorophenoxyacetic acid (2,4-D) was selected as an appropriate model. This contaminant is widespread in the environment and its interactions with soil and its bioavailability have been studied extensively (Shelton and Doherty, 1997). Furthermore, bacteria capable of degrading 2,4-D have been isolated and the metabolic pathways elucidated (Matheson et al., 1996; Singh et al., 1999). These bacteria have been marked with antibiotic resistance and the *lux* cassette, enabling their detection in the environment (Beaton, et al., 1999).

MATERIALS AND METHODS

Two separate experiments were performed. The first was to measure the movement of 2,4-D through soil and the second was to combine movement with biodegradation in situ. The apparatus for both experiments is shown in Figure 1.

The specific details of the conditions used in these two experiments, in terms of soil quantities, soil compartment sizes, electrode conditions, and timescales, are shown in Table I. Anode and cathode were connected to a power pack (IsoTech IPS 601A; RS Components, Leics., UK) capable of delivering a direct electric current of 0–1 A at up to 60 V. The carbon felt anode (Osaka Gas Donocarb S-221, supplied by Ashland Sudchemie, Germany) was fed with anolyte (sodium phosphate solution) via a peristaltic pump. This was to replace soil water which was moved towards the cathode by electroosmosis and to maintain a neutral pH at this electrode. The stainless steel cathode was contained within a chamber bordered by a semipermeable membrane (Daramic, Industrial profile 707, supplied by Grace GmbH, Germany). The catholyte solution was circulated by means of a peristaltic pump from the cathode into a chamber containing a pH electrode. The solution in this chamber was maintained at pH 6.5 by addition of acid from a reservoir to titrate hydroxyl ions which were constantly produced at the cathode. A sealed perspex box, together with sodium hydroxide traps and an air pump, was incorporated around the central soil reactor in order to trap $^{14}CO_2$ produced from biodegradation of radiolabeled 2,4-D. The details of the soil used for all experiments are displayed in Table II. Conventional soil textural classification places it between a silty clay loam and silt loam.

Experiment 1: Movement of 2,4-D in an Electric Field in Soil

The first experiment was performed to determine the rate of movement of 2,4-D in soil under a DC electric field. Nonsterile soil was homogeneously contaminated with 2,4-D (100 mg/ml solution in 1 M KOH) by mixing the solution into dried soil with a spatula and adjusting the soil to 30% (w/w) moisture. The final concentration of 2,4-D in the soil was determined by extraction in 0.01 M $CaCl_2$ and analysis by high-performance liquid chromatography (HPLC) using a C18 reverse phase column and 69% methanol, 31% water mobile phase adjusted to pH 2.5 with orthophosphoric acid (Shaw and Burns, 1998). The concentration of 2,4-D was 864 mg per kg dry weight soil. The soil was packed into the electrokinetic reactor, which contained six separate compartments, 6 cm long, 3 cm wide, and 4 cm deep, and compressed by hand. The sealed perspex box and associated

COR-AAD1-00002585
Bayer EX1008 (Part 5 of 9)

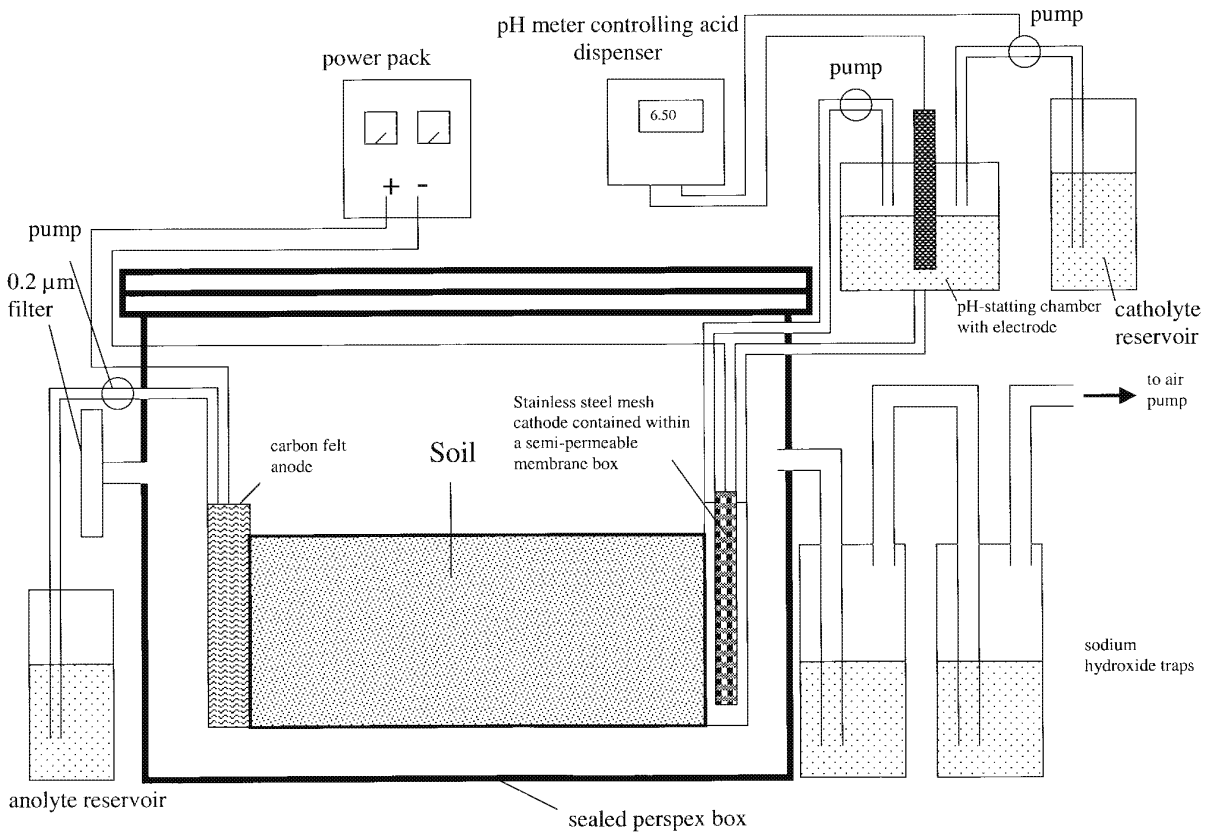


Figure 1. Schematic diagram of electrokinetic apparatus.

air pump and sodium hydroxide traps were not used for this experiment. A current density of 3.72 A/m^2 was applied for 4 days with sampling at time points shown in Table I. Individual soil cells were destructively sampled by taking six sections between the anode and cathode using a cork borer and spatula. Two sets of samples were taken at 92 h to investigate the reproducibility between different cells.

Information on the rate of 2,4-D movement derived from this experiment was used to determine an appropriate electric current for a second experiment in which 2,4-D movement was coupled to biodegradation in situ.

Experiment 2: Combining Electrokinetic Movement with Biodegradation of 2,4-D

In order to combine electrokinetic movement of 2,4-D with its degradation by introduced bacteria in situ, several changes were made to the approach detailed above. Most

Table I. Experimental conditions for electrokinetic experiments.

	Experiment 1 Electrokinetic movement of 2,4-D	Experiment 2 Electrokinetic movement and degradation of ^{14}C-2,4-D
Quantity of soil, g dry weight	888	710.5
Number and size of soil compartments	Six compartments, 6 cm long, 3 cm wide, 4 cm deep	One compartment, 22 cm long, 7 cm wide, 4 cm deep
Catholyte pH	6.5	6.5
Catholyte amendment solution	4 M acetic acid	0.5 M nitric acid
Anolyte	0.2 M Na_2HPO_4	0.5 M Na_2HPO_4
Anolyte flow rate (mL/day)	60	10
Applied current (A/m^2)	3.72	0.89
Sampling times (days)	0, 0.125, 1, 2, 4	0, 3, 6, 9, 14, 22
Total duration (days)	4	22

COR-AAD1-00002586
Bayer EX1008 (Part 5 of 9)

Table II. Soil properties of silt soil used in all electrokinetic experiments.

Parameter	Value
PH	8.1
Soil density (kg/dm^3)	1.350
Extractable phosphorus (mg/L)	24
Cation exchange capacity (me/100 g)	21.7
Particle size 2000–600 μm (%)	1
600–212 μm (%)	4
212–63 μm (%)	7
63–20 μm (%)	43
20–2 μm (%)	19
<2 μm (%)	26
Soil buffering capacity (g/kg) (calculated as the amount of H^+ from sulfuric acid required to acidify the soil to pH 2)	0.52
Hydraulic permeability, k (m/s)	1.81×10^{-11}
Calcium carbonate (%)	2
Total sulphur (%)	0.08
Total nitrogen (%)	0.25
Organic matter (%)	3.40
Organic carbon (%)	1.97
C:N ratio	7.9:1

This is an agricultural soil obtained from Wye College, University of London.

importantly, the soil was sterilized for this experiment. 2,4-D was added to a region of the soil next to the cathode and bacteria capable of mineralizing 2,4-D were added to the soil at a specific location closer to the anode. The aim of the experiment was that the applied electric current would move the 2,4-D into the position where the bacteria were located. An apparatus of 22 cm in length, between the anode and cathode, 7 cm width, and 4 cm depth (as opposed to six separate compartments of 6 cm length, 3 cm width, and 4 cm depth) was used to enable a maximum initial distance to be used between contaminant and bacteria. Radiolabeled 2,4-D (ring-labeled with ^{14}C) was incorporated so that complete mineralization of the compound could be detected by production of $^{14}CO_2$. The trapping of $^{14}CO_2$ necessitated enclosure of the soil apparatus in a sealed perspex box. Anolyte and catholyte connections and current delivery were via specific connections through the sides of the box. Two further ports were present, one of which was fitted with a 0.22 μm air filter and the other was attached to two traps (1 M NaOH; 100 mL total volume) in series together with an air pump to ensure constant movement of air through the apparatus to allow for the trapping of $^{14}CO_2$. A digital humidity and temperature meter, displaying real-time readings, was also placed in this box.

For soil contamination, ring-labeled ^{14}C-2,4-D (Sigma Chemical Co., Poole, UK) was mixed with cold 2,4-D to give a specific activity of 20,600 cpm/mg. Soil was prepared at 30% (w/w) moisture (70% of water-holding capacity; a water content thought to be optimal for aerobic microbial metabolism (Eweis et al., 1998)) by addition of water containing cycloheximide (50 mg/L; an inhibitor of fungal metabolism) and sterilized (by spreading to a depth of 1 cm and autoclaving three times at 121°C for 20 min with a 24-h period between two autoclavings) prior to contamination with 2,4-D to ensure that the presence of other microorganisms did not interfere with the behavior of the introduced organism. Sterilized soil (213 g wet weight, 30% w/w moisture) was contaminated with 2,4-D to 811 mg/kg dry weight soil and packed into the electrokinetic reactor adjacent to the cathode. The remainder of the soil, to a total amount of 1,015 g (wet weight; 30% w/w moisture), was packed into the reactor up to the anode with compaction by hand.

The bacterium used in this experiment was *Burkholderia* spp. *RASC* c2, which is able to mineralize 2,4-D (Suwa et al., 1996). It had been marked with tetracycline antibiotic resistance such that it can be detected in a mixed population of bacteria by plating onto agar containing tetracycline. For experiments involving this bacterium, it was grown overnight in 1/10 strength peptone, tryptone, yeast, glucose (PTYG) medium at 30°C, 160 rpm. PTYG medium (full strength) contained (per liter) 2.5 g peptone, 2.5 g tryptone, 5.0 g yeast extract, 5.0 g glucose, 0.3 g $MgSO_4$. $7H_2O$, 0.035 g $CaCl_2$. Cells (1.88×10^{11}) were harvested by centrifugation and washed twice in quarter strength Ringers (QSR) solution, resuspended in 500 μL QSR, and inoculated directly into soil between 14 and 16 cm from the cathode. Inoculation was performed using a pipette to deliver 50 μL aliquots of the highly concentrated cell suspension at approximately 0.6 cm intervals across the width of the soil. The pipette tip was inserted into the compacted soil such that its end was 0.5 cm below the surface and the cell suspension was expelled. The small perturbation in moisture content was not significant for the bulk of the soil at this location over the course of the experiment.

From the results of the first experiment, in which 2,4-D moved at a rate of 4 cm per day, a current of 8 mA (0.89 A/m^2) was chosen for the second experiment to give an approximate rate of movement of 2,4-D of 1 cm per day. This current was applied across the soil and the voltage, temperature, and humidity were recorded. Experimental conditions are shown in Table II. When the conductivity of the catholyte solution exceeded 20 mS, it was diluted or replaced with deionized water. Voltage profiles across the soil were measured at regular intervals using a hand-held voltmeter.

Soil samples were taken by dividing the soil into 12 equal sections, of 1.83 cm length, between anode and cathode. For each of the time points, 12 samples were taken, removing one-sixth of the soil across the width of the compartment. Individual samples were therefore 1.83 cm long, 1.15 cm wide, and 4 cm deep. Removal of the soil in this manner, without its replacement, exposed increasing areas of the anode and cathode to air. To compensate for the reduced surface area of the electrodes, the current was reduced accordingly and the amount of anolyte added to the anode was also reduced. The amount of soil in the electrokinetic reactor was also compensated for in calculations of total 2,4-D and radiolabel. All analyses of soil samples were performed

COR-AAD1-00002587
Bayer EX1008 (Part 5 of 9)

in triplicate and each result calculated as average ±SEM. Soil samples were analyzed for moisture content by measuring dry weights using crucibles and drying at 105°C for 24 h. Soil pH was determined by resuspending the soil in deionized water (1 g in 1 ml), pelleting the soil by centrifugation, and measurement of the supernatant using a standard laboratory pH meter. Concentrations of chloride, nitrate, phosphate, and sulphate in the soil were determined by ion chromatography using a Metrosep Anion Dual 2 column with a mobile phase comprising 2.4 mM Na_2CO_3, 2 mM $NaHCO_3$, and 10% (v/v) acetone. Analysis of radioactivity and 2,4-D concentration was performed on soil extracted in 0.01 M $CaCl_2$. Counting of radioactivity in soil extracts, sodium hydroxide traps, and catholyte was performed following direct addition of scintillation fluid (Ready Value scintillation cocktail; Beckman, Fullerton, CA, USA) and mixing. 2,4-D concentration was also determined by HPLC, as described above. Total bacterial cell numbers were determined by preparing serial dilutions of soil suspensions in QSR and plating onto *Pseudomonas* selective agar (Oxoid, UK) containing 12.5 μg/L tetracycline. Colonies were counted after incubation at 30°C for 3 days. The presence of other contaminating organisms, which were present in very small numbers in some soil samples, was clearly identifiable by the different colony morphologies that they demonstrated.

RESULTS

Experiment 1: Electrokinetic Movement of 2,4-D.

The electrokinetic movement of 2,4-D through 6 cm-long cells of silt soil was determined by sampling of soil sections (six sections between anode and cathode), extraction of 2,4-D, and analysis by HPLC (Fig. 2).

2,4-D concentration decreased in the cathode region, while its concentration remained high in the anode region

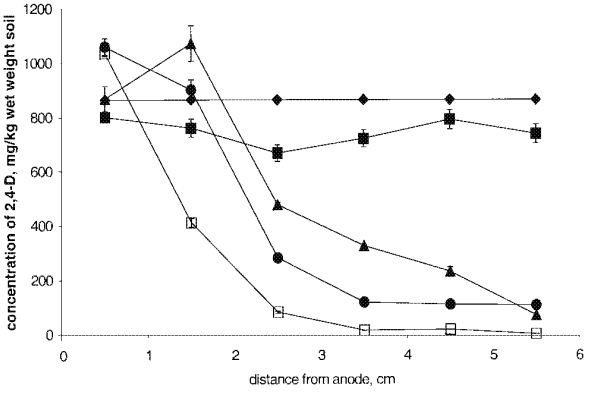


Figure 2. Electrokinetic movement of 2,4-D through silt soil. Concentrations of 2,4-D (±SEM), determined by HPLC, are displayed for time zero (solid diamonds) and following sampling at 3 (solid squares), 24 (solid triangles), 48 (solid circles), and 92 (open squares) h time points.

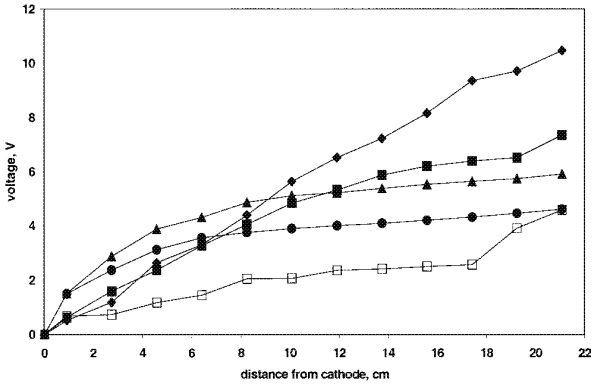


Figure 3. Voltage profile across soil during electrokinetic treatment. Individual voltage measurements were conducted with a hand-held voltmeter, inserting the electrodes into the soil to a depth of 1 cm. Results are shown for measurements after 1 day (closed diamonds), 3 days (closed squares), 9 days (closed triangles), 14 days (closed circles), and 22 days (open squares).

and it was also detected in the anode compartments. These results demonstrate movement towards the anode. 2,4-D has a pKa of 2.64 and therefore is negatively charged at neutral pH values. Its movement towards the anode was therefore by electromigration, which was the dominant process during the application of the electric current. It was not possible to quantify the concentrations of 2,4-D within the anode compartments as these were shared between different soil sections. Concentrations of 2,4-D at positions 4, 5, and 6 cm from the anode were reduced to 1.5% of the starting concentration within 92 h. The measurements are reproducible between different soil cells as analysis of two separate soil cells at the 92-h time point demonstrated no significant difference between the 2,4-D profiles. Approximately 45% of the 2,4-D migrated a distance of 4 cm or more in a 24-h period. The remainder of the 2,4-D migrated between 1 and 3 cm during this time period. Some acidification of the soil occurred during electrokinesis, to between pH 3.5 and pH 4 in the 1-cm region nearest to the anode.

Experiment 2: Combining Electrokinetic Movement with Biodegradation of 2,4-D

Contaminated soil was packed into the electrokinetic reactor and bacteria introduced. A direct electric current of 0.89 A/m^2 led to an initial voltage of 10.5 V across the soil. Complete voltage profiles across the soil during the course of the experiment are shown in Figure 3.

The voltage profiles in Figure 3 show approximately linear voltage curves for all time points, indicating the absence of any significantly resistive zones within the soil matrix.

The temperature within the sealed perspex box surrounding the soil compartment was 21°C and the humidity was 69% at the start of the experiment. The temperature remained at 21°C for the duration of the experiment and the humidity of the air rose to 94% after day 1 and thereafter remained at 91 ± 7%.

COR-AAD1-00002588
Bayer EX1008 (Part 5 of 9)

For the first 14 days of the experiment, soil moisture levels remained between 28–38% (w/v) across the central area of the soil cell, with some drying after 22 days, to a minimum of 23% (w/v). Moisture contents were higher at each side of the soil cell. This may be explained by addition of phosphate solution to the anode region and movement of water into the cathode region by electroosmosis from the anode and diffusion across the semipermeable housing of the cathode compartment.

The pH of the soil remained between pH 7–8.8 for the duration of the experiment, except for acidification in the 3.6 cm region closest to the anode. Figure 4 shows that phosphate, added at the anode, moved into the soil over the 22-day period, reaching a distance of 8 cm from the cathode. Over the same time period, nitrate anions migrated into the soil from the catholyte chamber, being distributed throughout the soil after 22 days. Chloride and sulphate migrated rapidly toward the anode, with removal of the majority of both anions from the soil within 14 days (data not shown). It was not possible to observe an increase in chloride levels in the soil resulting from the mineralization of 2,4-D.

2,4-D movement and biodegradation was determined by extraction of soil samples collected after 3, 6, 9, 14, and 22 days and HPLC/radioactivity estimations. The results of these analyses are displayed as soil profiles in Figure 5.

The analytical data presented in Figure 5 were identical, as determined directly by HPLC analysis or by calculation from radioactivity measurements. HPLC analyses yielded a single peak for 2,4-D, with no evidence of breakdown products such as chlorophenols or chlorocatechols. *Burkholderia* spp. *RASC c2* is capable of complete mineralization of 2,4-D, with degradation proceeding via 2,4-dichlorophenol and 3,5-dichlorocatechol. The conversion of dichlorophenol to dichlorocatechol is known to be the rate-limiting step of the pathway (Daugherty and Karel, 1994). Incomplete metabolism would therefore most likely result in a buildup of dichlorophenol. Extraction of soil with 0.5 N sodium hydroxide (to solubilize organic matter) and with 6 N HCl did not yield significant radiolabel, indicating that a negligible amount of the carbon from 2,4-D was incorporated into soil organic matter, biomass, or bound residues. This is further corroborative evidence for the complete conversion of 2,4-D to carbon dioxide and water.

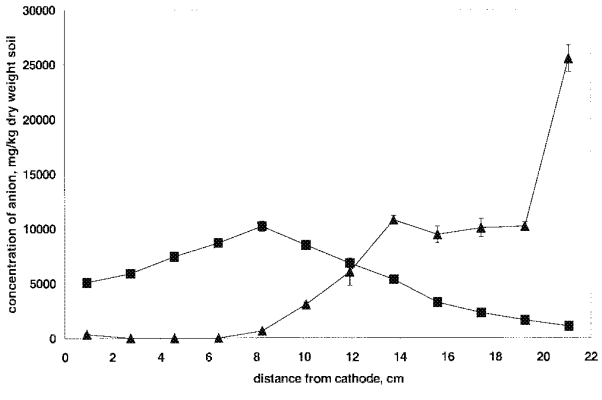


Figure 4. Distribution (±SEM) of nitrate (closed squares) and phosphate (closed triangles) anions across soil following 22 days of electrokinetic treatment. Determinations were performed by extraction with water and analysis by ion chromatography.

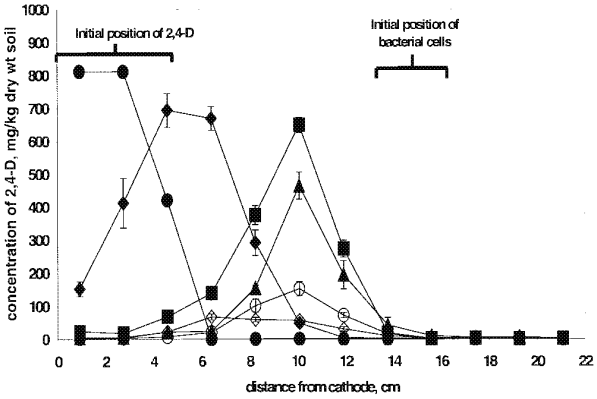


Figure 5. Distribution of 2,4-D across soil during electrokinetic treatment. Results (±SEM) are shown for time 0 (closed circles), 3 days (closed diamonds), 6 days (closed squares), 9 days (closed triangles), 14 days (open circles), and 22 days (open diamonds). The positions of 2,4-D and bacterial cells at the start of the experiment is shown.

Total soil recovery of radiolabeled 2,4-D over time is shown, together with cumulative recovery of $^{14}CO_2$, in Figure 6.

Figure 6 shows a decrease in radiolabel present within the soil from 6 days onwards and the appearance of radiolabel in the sodium hydroxide traps. Total recovery of radiolabel within the traps was 5.8% of the radioactivity lost from the soil. The sealed perspex box was opened for five time periods of approximately 2 h during the experiment and this may have led to as much as 2.3% of $^{14}CO_2$ being lost to the atmosphere. Recovery of radiolabeled 2,4-D in the catholyte was 3.2% of 2,4-D added to the soil. The detection of 2,4-D in the catholyte was presumably due to its transport with the electroosmotic flow of water. The formation of $^{14}CO_2$ is evidence of bacterial mineralization of 2,4-D.

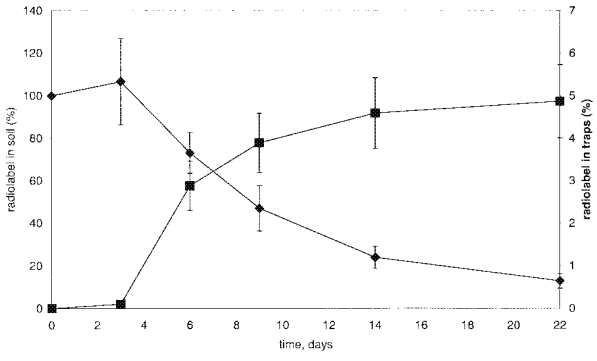


Figure 6. Disappearance of radiolabel from soil and appearance in traps during the electrokinetic treatment of soil. Results (±SEM) are shown for soil percentage (diamonds) and cumulative trap percentage (squares).

COR-AAD1-00002589
Bayer EX1008 (Part 5 of 9)

The bacteria present in the soil were analyzed in terms of cell numbers (Fig. 7). Of the 1.88×10^{11} cells added to the soil at the start of the experiment, the cell recovery, as determined by plate-counting, was 29 ± 11% after 3 days, 55 ± 33% after 6 days, 50 ± 37% after 9 days, 49 ± 18% after 14 days, and 23 ± 11% recovery after 22 days. These recoveries, together with the results for individual soil sections, contain significant variations between triplicate analyses. This may be because the soil was inoculated 1 cm below the surface, whereas the soil samples were taken from the top, middle, and bottom of each section.

The movement and degradation of 2,4-D in the soil is shown in Figures 5, 6, and 7. Figure 7 indicates that there was movement of 2,4-D towards the anode within 3–6 days. From 6 days onwards there was also a reduction in the 2,4-D concentration in the region 6–15 cm from the cathode, which was accompanied by an overall disappearance of 2,4-D from the soil (Fig. 6). There was no appearance of 2,4-D between 15–22 cm from the cathode, indicating that, despite electromigration towards the anode, the 2,4-D was not reaching this area. Figure 7 shows that the region around 15 cm from the cathode contained the 2,4-D-degrading bacteria. It appears that when 2,4-D, migrating towards the anode, reached the region containing the degradative bacteria it was degraded in situ, resulting in a decrease in soil 2,4-D levels and the appearance of $^{14}CO_2$ in sodium hydroxide traps.

A third, control, experiment was performed under identical conditions to the second experiment (i.e., sterilized soil with 2,4-D contamination and microbial inoculation in separate regions) except that no electric current was applied and therefore no anolyte or catholyte solutions were required. 2,4-D diffused only slowly over a short distance from the region where it had been added to the soil into the neighboring, uncontaminated soil region. Bacteria also gradually diffused from their point of inoculation. Some degradation of 2,4-D was observed within the soil, with 39% recovery of 2,4-D in the soil after 24 days. This degradation appeared to occur in the region of overlap between the bacteria and 2,4-D, in which an increase in bacterial numbers was observed, although it is also possible that there may have been some degradation by indigenous organisms due to incomplete sterilization of the soil. This result strongly contrasted with the studies in the presence of electric current, in which 2,4-D migrated through the soil and was no longer found in its starting location after 6 days. 2,4-D remained largely in its original location after 24 days and significantly less degradation was observed.

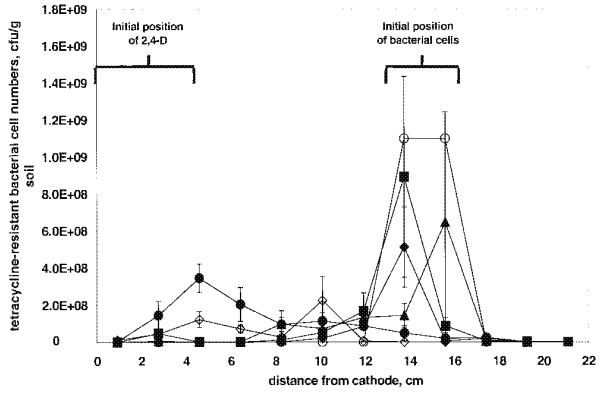


Figure 7. Distribution of tetracycline-resistant *Burkholderia* cells across the soil during electrokinetic treatment. Results (±SEM) are shown for time 0 (open circles), 3 days (closed diamonds), 6 days (closed squares), 9 days (closed triangles), 14 days (closed circles), and 22 days (open diamonds). An initial inoculum of 1.875×10^{11} cells was added between 14 and 16 cm from the cathode. The position of 2,4-D and added bacterial cells at the start of the experiment are shown.

DISCUSSION

The application of bioremediation technologies to contaminated sites requires microorganisms with the necessary metabolic capabilities to be present, that pollutants are in a bioavailable form, and that environmental conditions, in terms of moisture levels, pH, and redox, are suitable for biodegradation to occur (Eweis et al., 1998). In practice, the heterogeneity of many contaminants and soils and the presence of other inhibitory contaminants often reduces the effectiveness of bioremediation. Multidisciplinary approaches, incorporating the skills of engineers, microbiologists, chemists, and hydrogeologists, may be required for the implementation of a combination of techniques in order to achieve successful remediation. The use of electrokinetics together with bioremediation has been proposed as an effective tool for remediation of organic contamination (Chillingar et al., 1997). The choice of a well-characterized pollutant, 2,4-D, a bacterium with known degradative capability and a standardized system in terms of the soil used and the electrokinetic apparatus, as presented in this article, has been used to enable elucidation of the potential for this combined approach.

The electromigration of 2,4-D towards the anode under neutral pH conditions would be anticipated from the negative charge on the molecule. Similar movements of anions such as chromate, nitrate, and sulphate have been shown by other workers (Budhu et al., 1997; Reddy et al., 1997). Studies on the movement of charged species by electromigration have shown this to be at least an order of magnitude greater than movement by electroosmosis (Acar and Alshawabkeh, 1993). It should also be noted that 2,4-D is mobile under the applied electric current. Electrokinetics is therefore effective in disrupting the interactions (e.g., ionic and van der Waals' forces) between a charged pollutant and the soil matrix under unsaturated conditions. The electromigration of 2,4-D towards the anode is more rapid than the comparative movements of PAHs (Maini et al., 2000a) and phenol (Yang and Long, 1999) by electroosmosis towards the cathode.

In combining electromigration towards the anode with biodegradation, it has been possible to demonstrate that the introduced bacteria were metabolically active under the electric current conditions employed. This finding is of im-

COR-AAD1-00002590
Bayer EX1008 (Part 5 of 9)

portance for future use of the technique and agrees with our preliminary studies into DC effects upon bacteria in solution and soil slurries (Jackman et al., 1999) and the results from the Lasagna™ process in which *p*-nitrophenol was initially used as a model contaminant (Ho et al., 1995) and TCE biodegradation was subsequently demonstrated (Davis-Hoover et al., 1999). The ability to maintain an active microbial population also resulted from adequate control of pH and moisture levels in the presence of the electrokinetic processes. The location of the bacteria within the soil followed a narrow distribution over the first 9 days, leading to a broader distribution closer to the cathode over the subsequent 13 days. A range of potential forces may have been acting upon the bacteria in the soil. Natural spreading of the inoculum, chemotaxis towards the 2,4-D, growth of new organisms, reaction to different pH and ionic conditions in the soil may have all contributed to the overall effect. At the microscopic scale, the locations of the bacteria and contaminant in relation to soil pore size classes and the levels of moisture present would also affect their interactions and the degradation process. Electrokinetic forces of electroosmosis, towards the cathode, and electrophoresis, towards the anode (bacterial cells possess a net negative cell surface charge under the majority of environmental conditions (Collins and Stotzky, 1992)) would have been acting upon the bacteria. However, DeFlaun and Condee (1997) demonstrated that electrophoresis of bacteria required an electric field in the range of 5–10 volts per centimeter of soil to achieve relatively slow movement of *Burkholderia* cells through silt soil. When no current was applied, as in the third (control) experiment, initial diffusive processes were followed by degradation and bacterial growth at the position of the overlapping diffusional fronts of contaminant and bacteria.

This study has also demonstrated the mineralization of a pollutant, as evidenced by the production of $^{14}CO_2$. The calculated recovery of ^{14}C, taking into account $^{14}CO_2$ which was trapped and that which may have been lost when the apparatus was opened, together with 2,4-D recovered in the catholyte, was 11.3%. The absence of any evidence for metabolic intermediates or soil-bound residues would suggest that the losses may be due to inadequate sealing and trapping within the apparatus and possible absorption of $^{14}CO_2$ to other sinks within the apparatus. Recoveries of $^{14}CO_2$ have been shown previously to vary considerably, with defined radiorespirometric studies yielding 10–80% recoveries, depending on the apparatus materials used (e.g., rubber bungs absorbed $^{14}CO_2$) and the chemistry of the trapping solutions (Coveney and Wetzel, 1984; McKinley et al., 1983). A larger headspace and a greater depth of soil is also known to affect recovery of $^{14}CO_2$ (Knaebel and Vestal, 1988).

In summary, the findings in this study demonstrate that it is possible to move an organic contaminant into a biodegradative zone for mineralization in situ. There is a potential for the use of specially designed degradative zones, as described previously, or for pollutants to be moved from areas of high concentration or co-contamination into areas where microorganisms are active. By altering environmental conditions, the bioavailability of pollutants may also increase as interactions with soil particles, including sequestration in micropores or ionic binding to surfaces, are affected. The continued use and development of a controlled, engineered apparatus together with well-characterized pollutants and marked bacteria should enable these advances to be made.

We thank Professor Ken Killham, University of Aberdeen, UK, for the provision of *Burkholderia* spp. *RASC* c2 for these studies.

References

Acar YB, Alshawabkeh AN. 1993. Principles of electrokinetic remediation. Environ Sci Technol 27:2638–2647.

Beaton Y, Shaw LJ, Glover LA, Meharg AA, Killham K. 1999. Biosensing 2,4-dichlorophenol toxicity during biodegradation by Burkholderia sp. RASC c2 in soil. Environ Sci Technol 33:4086–4091.

Bruell CJ, Segall BA, Walsh MT. 1992. Electroosmotic removal of gasoline hydrocarbons and TCE from clay. J Environ Eng ASCE 118: 68–83.

Budhu M, Rutherford M, Sills G, Rasmussen W. 1997. Transport of nitrates through clay using electrokinetics. J Environ Eng ASCE 123: 1251–1253.

Chillingar GV, Loo WW, Khilyuk LF, Katz SA. 1997. Electrobioremediation of soils contaminated with hydrocarbons and metals: progress report. Energ Source 19:129–146.

Collins YE, Stotzky G. 1992. Heavy metals alter the electrokinetic properties of bacteria, yeasts and clay minerals. Appl Environ Microbiol 58:1592–1600.

Coveney MF, Wetzel RG. 1984. Improved double-vial radiorespirometric technique for mineralization of 14C-labeled substrates. Appl Environ Microbiol 47:1154–1157.

Daugherty DD, Karel SF. 1994. Degradation of 2,4-dichlorophenoxyacetic acid by Pseudomonas-cepacia DB01(PRO101) in a dual substrate chemostat. Appl Environ Microbiol 60:3261–3267.

Davis-Hoover WJ, Bryndzia LT, Roulier MH, Murdoch LC, Kemper M, Cluxton P, Al-Abed S, Slack WW, Vesper SJ. 1999. In situ bioremediation utilizing horizontal Lasagna. In: Leeson A, Alleman BC. Engineered approaches for in-situ bioremediation of chlorinated solvent contamination. Columbus, OH: Battelle Press. p 263–267.

DeFlaun MF, Condee CW. 1997. Electrokinetic transport of bacteria. J Hazard Mater 55:263–277.

Electorowicz M, Boeva V. 1996. Electrokinetic supply of nutrients in soil bioremediation. Environ Technol 17:1339–1349.

Eweis JB, Ergas SJ, Chang DPY, Schroeder ED. 1998. Bioremediation principles. In: Tchobanoglous G, editor. McGraw-Hill Series in Water Resources and Environmental Engineering. Boston: McGraw-Hill. p 296.

Hatzinger PB, Alexander M. 1995. Effect of aging of chemicals in soil on their biodegradability and extractability. Environ Sci Technol 29: 537–545.

Head IM. 1998. Bioremediation: towards a credible technology. Microbiol-UK 144:599–608.

Ho SV, Sheridan PW, Athmer CJ, Heitkamp MA, Brackin JM, Weber D, Brodsky PH. 1995. Integrated in-situ soil remediation technology: the Lasagna process. Environ Sci Technol 29:2528–2534.

Ho SV, Athmer C, Sheridan PW, Hughes BM, Orth R, McKenzie D, Brodsky PH, Shapiro A, Thornton R, Salvo J, Schultz D, Landis R, Griffith R, Shoemaker S. 1999a. The Lasagna technology for in situ soil remediation. 1. Small field test. Environ Sci Technol 33: 1086–1091.

Ho SV, Athmer C, Sheridan PW, Hughes BM, Orth R, McKenzie D,

COR-AAD1-00002591
Bayer EX1008 (Part 5 of 9)

Brodsky PH, Sivavec TM, Salvo J, Schultz D, Landis R, Griffith R, Shoemaker S. 1999b. The Lasagna technology for in situ soil remediation. 2. Large field test. Environ Sci Technol 33:1092–1099.

Jackman SA, Maini G, Sharman AK, Knowles CJ. 1999. The effects of direct electric currents upon the viability and metabolism of acidophilic bacteria. Enzyme Microb Technol 24:316–324.

Kim J, Lee K. 1999. Effects of electric field directions on surfactant enhanced electrokinetic remediation of diesel-contaminated sand column. J Environ Sci Health A 34:863–877.

Knaebel DB, Vestal JR. 1988. A comparison of double vial to serum bottle radiorespirometry to measure microbial mineralization in soils. J Microbiol Meth 7:309–317.

Ko S-O, Schlautman MA, Carraway ER. 2000. Cyclodextrin-enhanced electrokinetic removal of phenanthrene from a model clay soil. Environ Sci Technol 34:1535–1541.

Maini G, Sharman AK, Knowles CJ, Sunderland G, Jackman SA. 2000a. Electrokinetic remediation of metals and organics from historically contaminated soil. J Chem Technol Biotechnol 75:657–664.

Maini G, Sharman AK, Sunderland G, Knowles CJ, Jackman SA. 2000b. An integrated method incorporating sulfur-oxidizing bacteria and electrokinetics to enhance removal of copper from contaminated soil. Environ Sci Technol 34:1081–1087.

Matheson VG, Forney LJ, Suwa Y, Nakatsu CH, Sexstone AJ, Holben WE. 1996. Evidence for acquisition in nature of a chromosomal 2,4-dichlorophenoxyacetic acid/a-ketoglutarate dioxygenase gene by different Burkholderia spp. Appl Environ Microbiol 62:2457–2463.

McKinley VL, Federle TW, Vestal JR. 1983. Improvements in and environmental applications of double-vial radiorespirometry for the study of microbial mineralization. Appl Environ Microbiol 45:255–259.

Probstein RF, Hicks RE. 1993. Removal of contaminants from soils by electric fields. Science 260:498–503.

Reddy KR, Parupudi US, Devulapalli SN, Xu CY. 1997. Effects of soil composition on the removal of chromium by electrokinetics. J Hazard Mater 55:135–158.

Shaw LJ, Burns RG. 1998. Biodegradation of 2,4-D in a noncontaminated grassland soil profile. J Environ Qual 27:1464–1471.

Shelton DR, Doherty MA. 1997. A model describing pesticide bioavailability and biodegradation in soil. Soil Sci Soc Am J 61:1078–1084.

Singh BK, Kuhad RC, Singh A, Lal R, Tripathi KK. 1999. Biochemical and molecular basis of pesticide degradation by microorganisms. Crit Rev Biotechnol 19:197–225.

Suwa Y, Wright AD, Fukimori F, Nummy KA, Hausinger RP, Holben WE, Forney LJ. 1996. Characterization of a chromosomally encoded 2,4-dichlorophenoxyacetic acid/a-ketoglutarate dioxygenase from Burkholderia sp. strain RASC. Appl Environ Microbiol 62:2464–2469.

Yang GCC, Long YW. 1999. Removal and degradation of phenol in a saturated flow by in-situ electrokinetic remediation and Fenton-like process. J Hazard Mater 69:259–271.

COR-AAD1-00002592
Bayer EX1008 (Part 5 of 9)

JOURNAL OF BACTERIOLOGY, Sept. 1994, p. 5284–5289
0021-9193/94/$04.00+0
Copyright © 1994, American Society for Microbiology
Vol. 176, No. 17

Integration and Excision of a 2,4-Dichlorophenoxyacetic Acid-Degradative Plasmid in *Alcaligenes paradoxus* and Evidence of Its Natural Intergeneric Transfer

J. O. KA† AND J. M. TIEDJE*

Center for Microbial Ecology and Departments of Microbiology and of Crop and Soil Sciences, Michigan State University, East Lansing, Michigan 48824

Received 14 February 1994/Accepted 24 June 1994

A self-transmissible 2,4-dichlorophenoxyacetic acid (2,4-D)-degradative plasmid, pKA2, has been identified in a new 2,4-D-degrading strain, *Alcaligenes paradoxus* 2811P, isolated from agricultural soil. pKA2 occurred as a 42.9-kb plasmid in strain 2811P. A derivative strain, 2811C, was isolated from a stock culture in which the entire pKA2 plasmid was apparently integrated into the host chromosome without loss of the 2,4-D$^+$ phenotype. This interpretation is based on the disappearance of a free plasmid DNA band, a shift in the *tfdA*-hybridizing band to the chromosome, loss of transmissibility of the 2,4-D$^+$ trait, and appropriate shifts in Southern hybridization bands of plasmid DNA compared with whole-cell DNA. The integrated plasmid of strain 2811C was excised either precisely or imprecisely after continued transfer on 2,4-D-containing medium. This suggests that a chromosome-free plasmid cycle may occur to optimize fitness under conditions of specific resource fluctuation. Another new 2,4-D-degrading strain, *Pseudomonas pickettii* 712, which was isolated from the same field plot but at a different time, was found to carry a plasmid that is nearly identical to pKA2. The plasmid of this strain, pKA4, is 40.9 kb long and has features in common with pKA2, such as high self-transmissibility, hybridization only to the *tfdA* gene among the 2,4-D-metabolic genes of 2,4-D-degradative plasmid pJP4, and similar restriction endonuclease-generated fragments. Furthermore, the genetic homology between the two plasmids was high since all fragments of pKA2 hybridized to pKA4. These results suggest that these two plasmids are closely related and thus their occurrence in two genera in nature is the result of natural horizontal gene transfer.

A number of catabolic plasmids which enable host microorganisms to utilize xenobiotic compounds as carbon and energy sources have been isolated and described. Most catabolic plasmids exist as extrachromosomal genetic elements that replicate autonomously. However, there are reports that catabolic gene recombination occurs between the chromosome and plasmids under selective conditions. This is well documented for aromatic hydrocarbon-degradative genes on the *Pseudomonas* TOL plasmid; these are excised occasionally by reciprocal recombination between the direct repeats (15) and integrated into the host chromosome (10, 20). The integrated genes can be rescued by plasmids R2 and pMG18 to form novel recombinants (10).

Most of the genes coding for herbicide 2,4-dichlorophenoxyacetic acid (2,4-D-degradative enzymes have been reported to be contained on plasmids (3, 4, 16, 17). Unlike the toluene-degradative genes in pseudomonads (1, 10, 20) and the 3-chlorobenzoate-degradative genes in *Alcaligenes* sp. strain BR60 (23), 2,4-D-degradative genes have not been shown to move either between chromosomal DNA and plasmid DNA or between plasmids. Furthermore, there have been no reports that the entire catabolic plasmid can be integrated into the host chromosome and then excised to form a free plasmid. This phenomenon could play an important role in gene persistence and enhanced expression of operons in environments where resources fluctuate.

The increasing use of xenobiotic compounds may stimulate a more widespread dissemination of the corresponding degradative plasmids among microbial populations in nature. The transfer of catabolic plasmids, such as 2,4-D-degradative plasmid pJP4 (5), on agar media is well known. However, naturally occurring horizontal gene transfer between bacterial populations is difficult to detect because of the absence of the appropriate means for investigating such low-frequency events in open environments. The horizontal transfer of genes responsible for 3-chlorobenzoate degradation in a natural aquatic community was suggested in a microcosm study that stimulated conditions in a shallow bay (6). Physically and genetically indistinguishable 2,4-D-degradative plasmids were detected in different *Alcaligenes* species isolated independently from soil (3), which provides indirect evidence of natural gene transfer. Nonetheless, there have been few reports that support degradative gene exchange between different genera in open environments.

In this report, we present evidence of chromosomal integration of an entire 2,4-D-degradative plasmid and demonstrate that it can be excised either precisely or imprecisely during growth on 2,4-D. In addition, we present evidence of natural intergeneric transfer of this plasmid between *Alcaligenes paradoxus* and *Pseudomonas pickettii* strains that were isolated from the same soil at two different times.

MATERIALS AND METHODS

Bacterial strains. Strains 2811P and 712 were isolated from the gene flow plot at the long-term ecological research site at the W. K. Kellogg Biological Station (Hickory Corners, Mich.) by enrichment for growth on 2,4-D as the sole source of carbon. These strains were identified as belonging to *A. paradoxus* and *P. pickettii*, respectively (11). Strain 2811C was

* Corresponding author.
† Present address: Department of Agricultural Biology, Seoul National University, Suwon, Korea.

Downloaded from http://jb.asm.org/ on September 3, 2020 at Corteva Agriscience

COR-AAD1-00002593

Bayer EX1008 (Part 5 of 9)

isolated from a glycerol stock culture of strain 2811P kept at −20°C for 2 years (except when occasionally thawed) and was reconfirmed as *A. paradoxus*. *P. cepacia* DBO1, which was obtained from R. Olsen (University of Michigan), contains transposon Tn*5* and is resistant to kanamycin (75 μg/ml), bacitracin (50 μg/ml), and carbenicillin (50 μg/ml).

Media and growth conditions. Peptone-tryptone-yeast extract-glucose broth consisted of 0.25 g of peptone (Difco Laboratories, Detroit, Mich.), 0.25 g of tryptone (Difco), 0.5 g of yeast extract (Difco), 0.5 g of glucose, 0.03 g of magnesium sulfate, and 0.003 g of calcium chloride. Solid medium containing 1.5% (wt/vol) agar was used for strain purification. Bacterial strains were cultured in Luria broth (14) (to produce cells not induced to metabolize 2,4-D), harvested, and prepared in sodium phosphate buffer as described previously (12). MMO mineral medium (21) plus 2,4-D at 500 ppm was used for the axenic culture studies and cultivation of 2,4-D-degrading strains to detect and isolate plasmid DNA. All cultures were incubated at 30°C. Liquid cultures were aerated by shaking at 200 rpm in a G24 environmental incubator shaker (New Brunswick Scientific Co., New Brunswick, N.J.).

DNA isolation. Plasmid DNA was isolated by using the procedure of Hirsch et al. (8). Chromosomal DNA was isolated by the procedure of Watson et al. (19) and subsequently purified by cesium chloride-ethidium bromide ultracentrifugation (14). For detection of plasmid DNA, cells were lysed by using a modified form (2) of the procedure of Kado and Liu (13). 2,4-D-degrading bacteria were cultivated at 30°C in 5 ml of MMO mineral medium containing 2,4-D at 500 ppm. When cells reached maximum density, they were harvested by microcentrifugation (16,000 × *g* for 1 min), washed with 1 ml of sterilized distilled water, and repelleted in a 1.5-ml Eppendorf microcentrifuge tube. The pellet was resuspended in 30 μl of distilled water and lysed by adding 120 μl of lysing solution (50 mM Tris base, 3% sodium dodecyl sulfate, pH 12.6). The solution was incubated at room temperature for 15 min, heated at 80°C for 1 min in a water bath, and extracted with 1 volume of a phenol-chloroform solution (1:1, vol/vol) saturated with TE buffer (10 mM Tris base, 1 mM EDTA, pH 8.0). The lysate was incubated overnight at room temperature. After microcentrifugation (14,000 rpm for 15 min), the aqueous phase was transferred into a new Eppendorf tube and mixed with 1/5 of a volume of 5× loading dye (14). Samples of 110 μl were subjected to electrophoresis in 0.7% (wt/vol) agarose in Tris-acetate buffer (40 mM Tris-acetate, 1 mM Na_2-EDTA). Gels were photographed on a DNA Transilluminator (Fotodyne Inc.) with type 55 positive-negative film (Polaroid Corp.).

Southern hybridization. To study hybridization patterns with 2,4-D-metabolic genes (*tfdA*, *tfdB*, *tfdC*, and *tfdD*), plasmid and chromosomal DNAs were prepared in crude lysate as described above, separated in a horizontal 0.7% agarose gel, transferred to nitrocellulose hybridization membranes (14), and hybridized with *tfd* gene probes. To analyze the restriction fragment profile, purified plasmid DNA and chromosomal DNA were digested with appropriate restriction endonucleases, size fractionated, and hybridized as described above. The probes were internal segments of the *tfd* metabolic genes (9) and 23S rRNA gene (18) that had been labeled with ^{32}P with a Random Primed DNA Labeling Kit (Boehringer Mannheim, Indianapolis, Ind.). The plasmid DNA probe was labeled with ^{32}P with a Nick Translation Kit (Boehringer Mannheim). The prehybridization, hybridization, and posthybridization washes used have been previously described (11). Hybridization signals were detected by autoradiography with X-Omat AR film (Kodak, Rochester, N.Y.) exposed at −70°C with a Quanta III (Sigma, St. Louis, Mo.) intensifying screen. If necessary, the bound probe was stripped from the membranes prior to rehybridization by washing three times for 15 min each time with boiled distilled water containing 0.1% (wt/vol) sodium dodecyl sulfate.

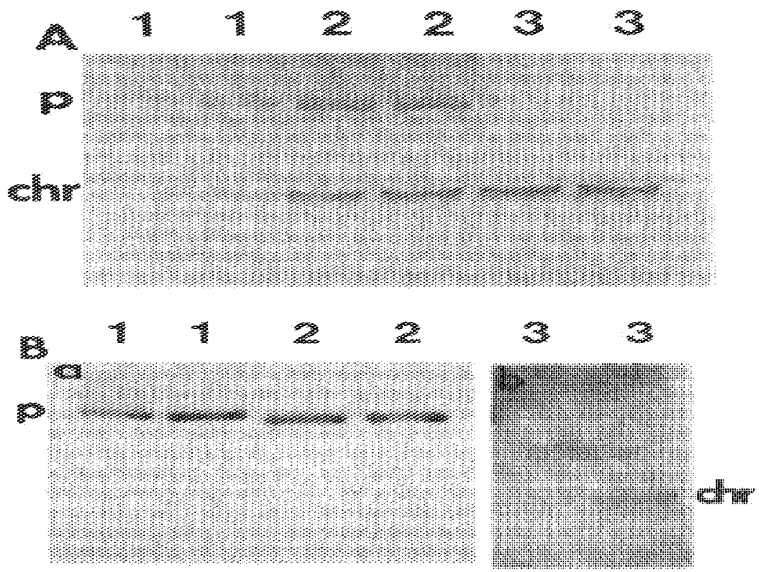


FIG. 1. Resolution of plasmids of 2,4-D-degrading strains. Agarose gel (A) and autoradiogram (B) of the gel after hybridization with the *tfdA* gene as the probe. Lanes: 1, *P. pickettii* 712 containing plasmid pKA2; *A. paradoxus* 2811P containing plasmid pKA2; 2, *A. paradoxus* 2811P containing plasmid pKA4; 3, *A paradoxus* 2811C not containing plasmid DNA. The positions of plasmid and chromosomal and linear (chr) DNAs are shown. The films in panel B were exposed for 20 min (a) and 2 days (b).

Conjugation. Matings were performed on membrane filters as described by Willetts (22). Transconjugants were selected on 2,4-D minimum medium containing MMO mineral medium, 2,4-D at 500 ppm, kanamycin (75 μg/ml), bacitracin (50 μg/ml), carbenicillin (50 μg/ml), and 1.5% Noble agar, and then their plasmid content was analyzed by agarose gel electrophoresis of crude lysates. The donor viable count was measured by plating dilutions on peptone-tryptone-yeast extract-glucose plates and counting the distinctive colonies of the donor. The frequency of transfer was calculated as the number of exconjugants per donor cell.

RESULTS

Properties of strains 2811P, 2811C, and 712. Strains 2811P and 712 were isolated from the same field subplot at different times; they contained 2,4-D-degradative plasmids pKA2 and PKA4 (Fig. 1A), respectively, and grew with 2,4-D as the sole carbon source. Strain 2811C, a derivative of strain 2811P, appeared not to have any free plasmid (Fig. 1A, lane 3). The presence of a free plasmid in 2811C could not be demon-

Downloaded from http://jb.asm.org/ on September 3, 2020 at Corteva Agriscience

COR-AAD1-00002594

Bayer EX1008 (Part 5 of 9)

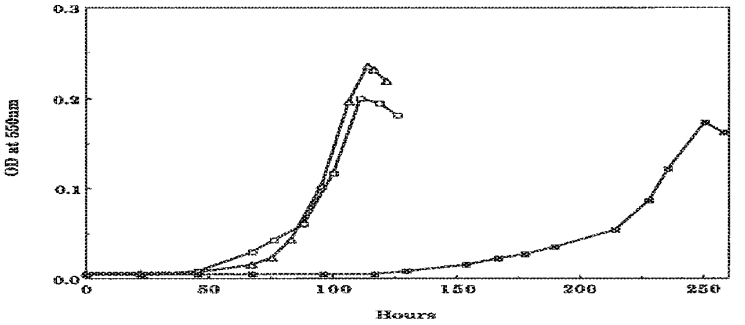


FIG. 2. Growth characteristics of 2,4-D-degrading strains in 2,4-D-containing mineral medium under uninduced conditions. Symbols: △, *P. pickettii* 712; □, *A. paradoxus* 2811P; ■, *A. paradoxus* 2811C. Each point is the mean of replicate cultures. OD, optical density.

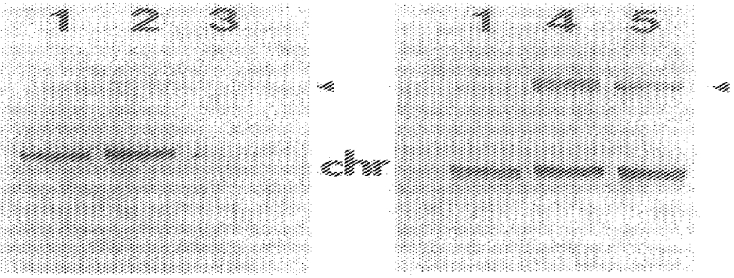


FIG. 3. Agarose gel showing plasmids in the donors, transconjugants, and recipient. Lanes: 1, recipient *P. cepacia* DBO1; 2, transconjugant from 712 × DBO1; 3, donor *P. pickettii* 712; 4, transconjugant from 2811P × DBO1; 5, donor *A. paradoxus* 2811P. The arrowheads show the plasmid conferring the 2,4-D$^+$ phenotype. A cryptic plasmid was also present in the recipient strain.

strated, even by pulsed-field gel electrophoresis (13a). Southern blots of plasmid DNA and chromosomal DNA of these three strains hybridized to only the *tfdA* gene (and not *tfdB*, *tfdC*, or *tfdD*), and the homologous sequence was located on plasmid DNA in strains 2811P and 712, whereas it was located on the chromosomal DNA in strain 2811C (Fig. 1B). This suggested that the plasmid DNA not detected in the agarose gel was integrated into the host chromosome in strain 2811C. A universal probe of the 23S rRNA gene (18) was used as a probe to check whether strains 2811P and 2811C are the same strain. When the total DNAs of strains 2811P and 2811C were digested with two different restriction enzymes (*Eco*RI and *Hin*dIII) and compared on a Southern blot, matching band patterns were observed between these two DNA samples, confirming that these were identical strains.

These three strains showed a relatively long lag time (>50 h) and slow growth in 2,4-D minimal medium when not previously induced to grow on 2,4-D (Fig. 2). Strain 2811C had a much longer lag time than strain 2811P in 2,4-D-containing medium, perhaps because of different gene expression resulting from the chromosomal location of the 2,4-D operon. In contrast, strains 2811P and 712, which were identified as different genera but had nearly identical 2-4-D-degradative plasmids, showed similar and more rapid growth patterns in 2,4-D-containing medium.

Plasmid transfer. The possibility of transfer of the 2,4-D-degradative genes was tested by filter mating. In three independent experiments, transfer of pKA2 from strain 2811P to *P. cepacia* DBO1 was obtained at an average frequency of 7.7×10^{-5} per donor colony formed. Under similar conditions, the 2,4-D$^+$ phenotype was not transferred at a detectable frequency ($<10^{-9}$) from strain 2811C, supporting the interpretation that the 2,4-D genes were not contained on a free conjugative plasmid in this strain. Plasmid pKA4 of strain 712 was transferred at an average frequency of 1.0×10^{-2} per donor cell. Plasmid bands exhibiting identical electrophoretic mobilities were observed in agarose gels containing the transconjugants and their respective donors (Fig. 3).

Physical evidence of integration of the plasmid into the chromosome. To investigate the fate of pKA2 in strain 2811C, plasmid pKA2 and total DNAs of strains, 2811P and 2811C were digested with two different restriction enzymes and analyzed on Southern blots hybridized with ^{32}P-labeled pKA2 plasmid DNA (Fig. 4). As expected, all of the seven hybridized fragments of pKA2 (Fig. 4) were also observed in the *Eco*RI-digested total DNA of strain 2811P, which contained the same plasmid, in addition to an unexpected novel fragment (CA; Fig. 4A). The novel fragment was not observed in the digested plasmid DNA but was observed in the digested total DNAs of both strains 2811P and 2811C. For this reason, we believed it to be derived from the digested host chromosomal DNA. This was further supported by the fact that its radioactive signal was much weaker than the signal obtained with the plasmid DNA fragment of a similar size because of its lower copy number. In *Eco*RI-digested total DNA of strain 2811C, one fragment (ED) disappeared with concomitant appearance of three extra hybridized fragments (arrowheads in Fig. 4A). This observation indicates that the whole pKA2 plasmid was integrated into the host chromosomal DNA without loss of the 2,4-D$^+$ phenotype, although normally the appearance of only two additional bands is expected with the loss of one band with chromosome integrations. The loss of one hybridized fragment (HB) with concomitant appearance of three novel fragments (arrowheads) was also observed in *Hin*dIII digests (Fig. 4).

Excision of plasmid pKA2. The existence of plasmid pKA2 as both an independent plasmid in strain 2811P and a chromosomally integrated plasmid in strain 2811C, together with the observed difference in their growth patterns on 2,4-D-containing medium (Fig. 2), suggested that the population containing a free plasmid might be derived from strain 2811C and that it could be preferably amplified under selection imposed by growth on 2,4-D. To investigate this hypothesis, strain 2811C was cultivated in 2,4-D-containing broth with repeated transfers into fresh medium. After the seventh transfer, a weak plasmid band was detected on the agarose gel. The intensity of this band increased with the increasing number of transfers. Southern hybridization of the gel with *tfdA* exhibited a clear hybridized plasmid band from the seventh transfer, and the radioactive intensity was much increased after the 9th and the 11th transfers (Fig. 5). After longer film exposure, weak hybridized bands were observed in the chromosomal DNA band area on Southern blots of the original culture and in cultures after the 7th, 9th, and 11th transfers (data not shown). After further transfers on 2,4-D-containing medium, a second

Downloaded from http://jb.asm.org/ on September 3, 2020 at Corteva Agriscience

COR-AAD1-00002595

Bayer EX1008 (Part 5 of 9)

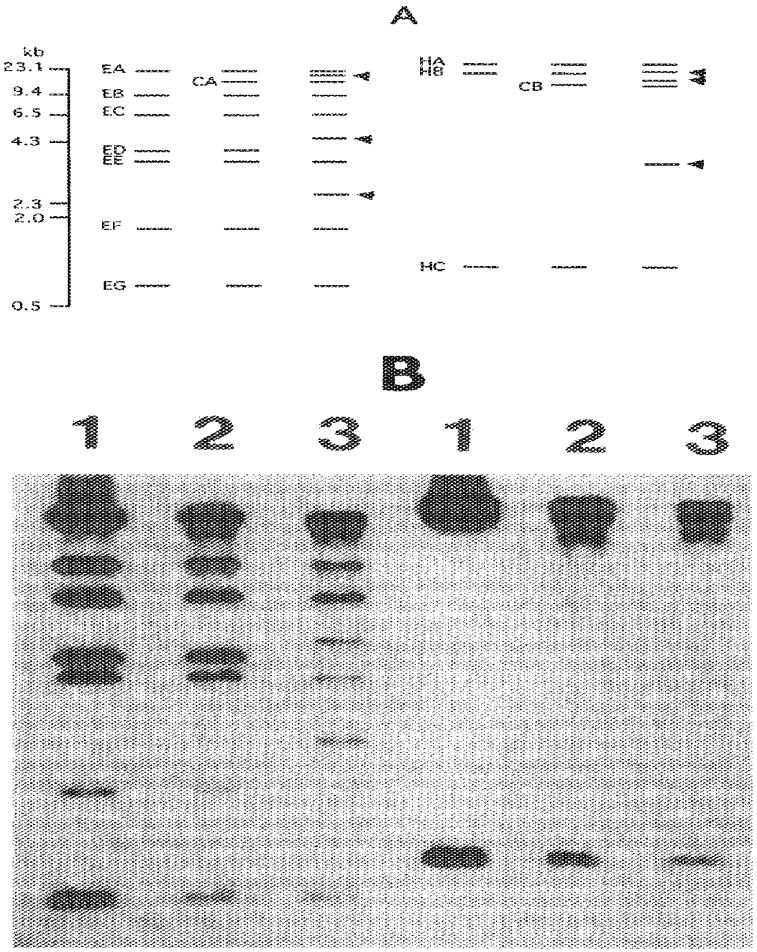


FIG. 4. Line drawing (A) and autoradiogram (B) of a Southern blot hybridization of labeled plasmid pKA2 with *Eco*RI (left) and *Hin*dIII (right) restriction enzyme digests of pKA2 plasmid DNA (lanes 1), total DNA of strain 2811P (lanes 2), and total DNA of strain 2811C (lanes 3). Novel extra bands presumably resulting from the integration process are indicated by the arrowheads in panel A.

plasmid band was detected from the culture of the 20th transfer, suggesting that the integrated plasmid could also be excised in a different way. These results indicated that the initial culture of strain 2811C became a mixed culture of 2811C and at least two other plasmid-containing variants that are probably more fit for growth on 2,4-D.

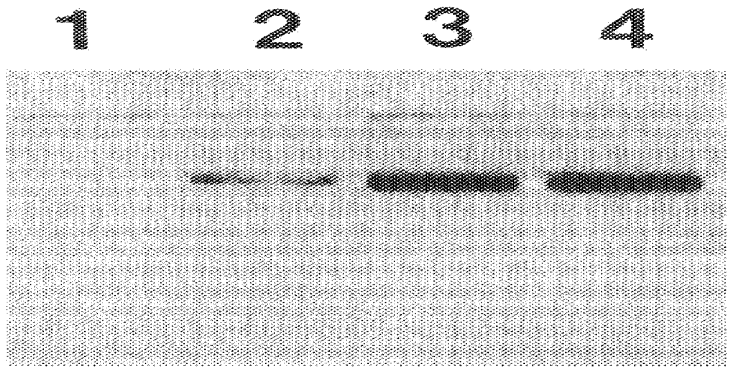


FIG. 5. Excision of plasmid DNA in strain 2811C during continuous growth on 2,4-D-containing medium. Samples (5 ml) of the culture grown initially (lane 1) and after the 7th (lane 2), 9th (lane 3), and 11th (lane 4) transfers were subjected to the Kado procedure and then plasmid and chromosomal DNAs in the lysate were gel separated and analyzed on Southern blots hybridized with the labeled *tfdA* probe. The film was exposed for 4 h.

To estimate the ratio of the 2811C population to the population of the excised-plasmid-containing strains, colonies from cultures after the 8th and 14th transfers were randomly selected, purified on peptone-tryptone-yeast extract-glucose plates, and subjected to the modified Kado procedure. Whereas no plasmid DNA band was detected in the 30 colonies examined from the 8th transfer, clear plasmid DNA bands were observed in 5 of 28 colonies examined from the 14th transfer. This result suggested that the mixed population was composed mainly of strain 2811C, even at the 8th transfer, while plasmid-containing strains gradually became more predominant and made up approximately 18% of the population after the 14th transfer. Plasmid DNAs were isolated from three colonies selected randomly from the five colonies to analyze the fragment profiles of restriction endonuclease digests. Two of the three plasmids showed restriction profiles identical to that of plasmid pKA2 in *Eco*RI and *Hin*dIII digests (Fig. 6), while the third plasmid revealed deletion of four fragments as well as the appearance of an extra, novel fragment (arrowhead) in *Eco*RI digests (Fig. 6). The derivative plasmid may have come from an alternative excision event of the integrated pKA2 plasmid in strain 2811C because the 3.5-kb fragment (the fifth band in the *Eco*RI digest in Fig. 6), which contained the sequences homologous to the *tfdA* gene, remained in the chromosome (data not shown).

Comparison of pKA2 of *A paradoxus* with pKA4 of *P. pickettii*. As stated above, plasmid pKA2 of *A. paradoxus* has properties similar to those of plasmid pKA4 of *P. pickettii* in regard to size, high transmissibility, and hybridization pattern with *tfd* probes. In addition to that, restriction enzyme analysis with *Eco*RI and *Hin*dIII revealed similar restriction patterns for these two plasmids (Fig. 7A). In *Eco*RI digests, only two of the seven fragments (EB and EC) showed altered mobilities in agarose gel electrophoresis while one of the three fragments (HB) revealed different mobility in *Hin*dIII digests (Fig. 7A). When fragments EA, ED, and EE of both plasmids (pKA2 and pKA4) were isolated from the agarose gel and digested with

Downloaded from http://jb.asm.org/ on September 3, 2020 at Corteva Agriscience

COR-AAD1-00002596

Bayer EX1008 (Part 5 of 9)

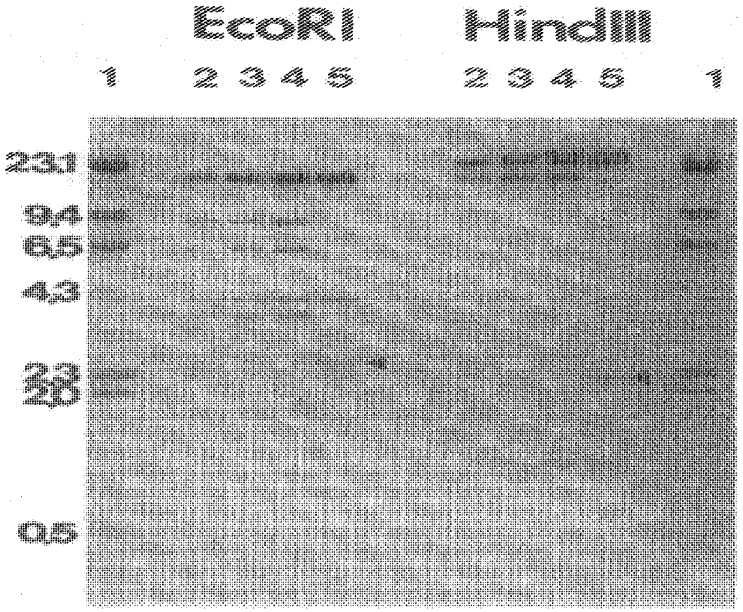


FIG. 6. Agarose gel containing restriction enzyme-digested plasmid DNA. Lanes: 1, lambda DNA digested with *Hin*dIII as size markers; 2, plasmid pKA2; 3, 4, and 5, plasmids isolated from three independent colonies derived from strain 2811C after 14 serial transfers on 2,4-D. The numbers on the left are molecular sizes in kilobases. The arrowheads indicate novel extra bands.

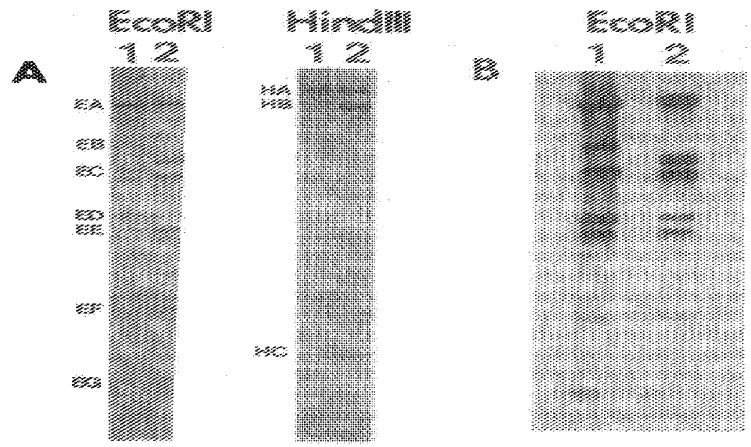


FIG. 7. (A) Agarose gel containing plasmids digested with restriction endonucleases. Lanes: 1, plasmid pKA2; 2, plasmid pKA4. (B) Autoradiogram of Southern blot hybridization of labeled plasmid pKA4 with *Eco*RI-digested pKA2 (lanes 1) and pKA4 (lanes 2).

*Bgl*II, the fragments were identical for each plasmid (data not shown). To determine whether all of the DNA fragments of plasmids pKA2 and pKA4 generated by restriction endonuclease *Eco*RI are homologous to one another, the fragments were analyzed on Southern blots hybridized with pKA4 DNA as the probe (Fig. 7B). All of the fragments of pKA2 were shown to be hybridizable with pKA4. The identical restriction profiles and hybridization patterns demonstrate that pKA2 of *A. paradoxus* and pKA4 of *P. pickettii* are genetically homologous, suggesting that intergeneric gene transfer between these two strains has occurred in nature.

DISCUSSION

The data demonstrate that 2,4-D-degradative plasmid pKA2 can exist as both a plasmid integrated into the host chromosome and a free plasmid. Since most of the 2,4-D-degradative genes have been reported to be carried on plasmids (3, 4, 16, 17), the observation of its chromosomal location was surprising. The integrated plasmid could be precisely excised, reforming the original pKA2 plasmid. The growth advantage of strain 2811P over strain 2811C in 2,4-D minimal medium (Fig. 2) may result from excision of plasmid DNA from the chromosome, with subsequent selection enhancing the plasmid-containing population. The detection of strain 2811C in the stock culture of 2811P and the creation of 2811P from 2811C in 2,4-D-containing medium suggest that the entire pKA2 plasmid can move into and out of the host chromosome. We have been unable to study the integration of the plasmid into the chromosome because of the absence of any selection for this variant.

The dynamics of the excision were more easily observed. The population containing the excised pKA2 plasmid appeared at an early stage of 2,4-D selection. A different population containing a smaller form of the pKA2 subsequently emerged at a late stage with continual transfers. In the smaller derivative plasmid, a 19.6-kb region corresponding to four fragments of *Eco*RI digests was deleted, with the concomitant appearance of a novel fragment (Fig. 6). It is interesting that the *tfdA* gene remained in the chromosome in this derivative population. This mode of variable gene excision could be explained with a "gene cassette" model (7), in which site-specific recombination of a gene cassette with an ancestral integron could lead to a new integron. According to this model, plasmid pKA2 would have at least two specific conserved sites, which recombine either with each other or with the specific site on the chromosome during the insertion and excision events. The observation that a fragment of the digested chromosomal DNA was hybridizable with pKA2 DNA indicates that these two DNA elements shared some conserved sequences.

The location of pKA2 in the chromosome not only resulted in loss of the freedom of its conjugal transfer but also led to slower growth of the host. While chromosomally located plasmid pKA2 seemed to have been excised at an early stage in the serial transfers, the plasmid-containing strain did not rapidly become the dominant type. This result suggests that 2811P could not competitively overcome 2811C within several transfers, although the former grew much more rapidly than the latter in the axenic culture. This observation could be explained by our previous finding that the exchange of cell

Downloaded from http://jb.asm.org/ on September 3, 2020 at Corteva Agriscience

COR-AAD1-00002597

Bayer EX1008 (Part 5 of 9)

products in the mixed-culture environment reduced the lag period of the slowly growing and noncompetitive strain, making it more competitive (12).

We isolated two different 2,4-D-degrading bacteria belonging to the genera *Alcaligenes* and *Pseudomonas* from the same soil at two different times. The observation that plasmid pKA2 of *A. paradoxus*, isolated in 1989, showed a restriction profile nearly identical to that of pKA4 of *P. pickettii*, isolated in 1990, together with their similar physical properties and genetic homology, strongly suggests that intergeneric gene transfer followed by plasmid modification, or vice versa, has occurred between these two species in nature.

While it is not clear how pKA2 is integrated into and excised from the chromosome, our results show that a conjugative plasmid can be integrated in its entirety into the host chromosome and that the chromosomally located plasmid can be excised either precisely or imprecisely. Additionally, we found evidence that intergeneric gene transfer between *Alcaligenes* and *Pseudomonas* species occurred in nature. Future research on the physiological differences between strains 2811P and 2811C on 2,4-D-containing medium, the specific integration sites on pKA2 and the chromosome, and the mechanism of integration and excision should reveal the mechanism and benefit of this genetic flexibility.

ACKNOWLEDGMENTS

This work was supported by National Science Foundation grants from the Long-Term Ecological Research Program (NSF-DEB 9211771) and the Center for Microbial Ecology (NSF-BIR 9120006).

We thank William Holben, Larry Snyder, and Cathy McGowan for valuable suggestions on this study.

REFERENCES

1. **Carney, B. F., and J. V. Leary.** 1989. Novel alterations in plasmid DNA associated with aromatic hydrocarbon utilization by *Pseudomonas putida* R5-3. Appl. Environ. Microbiol. **55**:1523–1530.
2. **Demezas, D.** Oklahoma State University. Personal communication.
3. **Don, R. H., and J. M. Pemberton.** 1981. Properties of six pesticide degradation plasmids isolated from *Alcaligenes paradoxus* and *Alcaligenes eutrophus*. J. Bacteriol. **145**:681–686.
4. **Fisher, P. R., J. Appleton, and J. M. Pemberton.** 1978. Isolation and characterization of the pesticide-degrading plasmid pJP1 from *Alcaligenes paradoxus*. J. Bacteriol. **135**:798–804.
5. **Friedrich, B., M. Meyer, and H. G. Schlegel.** 1983. Transfer and expression of the herbicide-degrading plasmid pJP4 in aerobic autotrophic bacteria. Arch. Microbiol. **134**:92–97.
6. **Fulthorpe, R. R., and R. C. Wyndham.** 1989. Survival and activity of a 3-chlorobenzoate-catabolic genotype in a natural system. Appl. Environ. Microbiol. **55**:1584–1590.
7. **Hall, R. M., D. E. Brookes, and H. W. Stokes.** 1991. Site-specific insertion of genes into integrons: role of the 59-base element and determination of the recombination cross-over point. Mol. Microbiol. **5**:1941–1959.
8. **Hirsch, P. R., M. VanMontagu, A. W. B. Johnston, N. J. Brewin, and J. Schell.** 1980. Physical identification of bacteriocinogenic, nodulation and other plasmids in strains of *Rhizobium leguminosarum*. J. Gen. Microbiol. **120**:404–412.
9. **Holben, W. E., B. M. Schroeter, V. G. M. Calabrese, R. H. Olsen, J. K. Kukor, V. O. Biederbeck, A. E. Smith, and J. M. Tiedje.** 1992. Gene probe analysis of soil microbial populations selected by amendment with 2,4-dichlorophenoxyacetic acid. Appl. Environ. Microbiol. **58**:3941–3948.
10. **Jeenes, D. J., and P. A. Williams.** 1982. Excision and integration of degradative pathway genes from TOL plasmid pWWO. J. Bacteriol. **150**:188–194.
11. **Ka, J. O., W. E. Holben, and J. M. Tiedje.** 1994. Genetic and phenotypic diversity of 2,4-dichlorophenoxyacetic acid (2,4-D)-degrading bacteria isolated from 2,4-D-treated field soils. Appl. Environ. Microbiol. **60**:1106–1115.
12. **Ka, J. O., W. E. Holben, and J. M. Tiedje.** 1994. Analysis of competition in soil among 2,4-dichlorophenoxyacetic acid-degrading bacteria. Appl. Environ. Microbiol. **60**:1121–1128.
13. **Kado, C. I., and S.-T. Liu.** 1981. Rapid procedure for detection and isolation of large and small plasmids. J. Bacteriol. **145**:1365–1373.
13a. **Kuritz, T., E. Anneliese, A. B. Todd, and C. P. Wolk.** High resolution mapping of the chromosome of *Anabaena* sp. strain PCC 7120 required for photosynthesis and nitrogen fixation. Mol. Microbiol. **8**:101–110.
14. **Maniatis, T., E. F. Fritsch, and J. Sambrook.** 1982. Molecular cloning: a laboratory manual. Cold Spring Harbor Laboratory, Cold Spring Harbor, N.Y.
15. **Meulien, P., and P. Broda.** 1982. Identification of chromosomally integrated TOL DNA in cured derivatives of *Pseudomonas putida* PAW1. J. Bacteriol. **152**:911–914.
16. **Pemberton, J. M., B. Corney, and R. H. Don.** 1979. Evolution and spread of pesticide degrading ability among soil microorganisms, p. 287–299. *In* K. N. Timmis and A. Publer (ed.), Plasmids of medical, environmental and commercial importance. Elsevier/North-Holland Biomedical Press, Amsterdam.
17. **Pemberton, J. M., and P. R. Fisher.** 1977. 2,4-D plasmids and persistence. Nature (London) **268**:732–733.
18. **Regensburger, A., W. Ludwig, and K. H. Schleifer.** 1988. DNA probes with different specificities from a cloned 23S rRNA gene of *Micrococcus luteus*. J. Gen. Microbiol. **134**:1197–1204.
19. **Schofield, P. R., M. A. Djordjevic, B. G. Rolfe, J. Shine, and J. M. Watson.** 1983. A molecular linkage map of nitrogenase and nodulation genes in *Rhizobium trifolii*. Mol. Gen. Genet. **192**:459–465.
20. **Sinclair, M. I., P. C. Maxwell, B. R. Lyon, and B. W. Holloway.** 1986. Chromosomal location of TOL plasmid DNA in *Pseudomonas putida*. J. Bacteriol. **168**:1302–1308.
21. **Stanier, R. Y., N. J. Palleroni, and M. Doudoroff.** 1966. The aerobic pseudomonads: a taxonomic study. J. Gen. Microbiol. **43**:159–271.
22. **Willetts, N. S.** 1988. Conjugation. Methods Microbiol. **21**:49–77.
23. **Wyndham, R. C., R. K. Singh, and N. A. Strauss.** 1988. Catabolic instability, plasmid gene deletion and recombination in *Alcaligenes* sp. BR60. Arch. Microbiol. **150**:237–243.

Downloaded from http://jb.asm.org/ on September 3, 2020 at Corteva Agriscience

COR-AAD1-00002598

Bayer EX1008 (Part 5 of 9)

APPLIED AND ENVIRONMENTAL MICROBIOLOGY, Apr. 1994, p. 1116–1120
0099-2240/94/$04.00+0
Copyright © 1994, American Society for Microbiology
Vol. 60, No. 4

Use of Gene Probes To Aid in Recovery and Identification of Functionally Dominant 2,4-Dichlorophenoxyacetic Acid-Degrading Populations in Soil

J. O. KA†, W. E. HOLBEN‡, AND J. M. TIEDJE*

Center for Microbial Ecology and Departments of Microbiology and of Crop and Soil Sciences, Michigan State University, East Lansing, Michigan 48824

Received 15 June 1993/Accepted 16 December 1993

The herbicide 2,4-dichlorophenoxyacetic acid (2,4-D) was applied to soils in microcosms, and degradation was monitored after each of five repeated additions. Total DNAs were isolated from soil bacterial communities after each 2,4-D treatment. The DNA samples were analyzed on slot blots and Southern blots by using a *tfdA* gene probe subcloned from plasmid pJP4 and a *Spa* probe derived from a different 2,4-D-degrading isolate, a *Sphingomonas paucimobilis* strain. 2,4-D applied to soil was quickly degraded by indigenous microbial populations. As determined by slot blot analyses of DNA from a Michigan soil, the increase in hybridization signal in response to 2,4-D treatments was greater with the *Spa* probe than with the *tfdA* probe. In contrast, the DNA from a Saskatchewan soil exhibited an increase in hybridization signal with the *tfdA* probe. This indicated that a population with 2,4-D-degradative gene sequences different from the *tfdA* gene sequence was dominant in the Michigan site, but not in the Saskatchewan site. A Southern blot analysis of DNA from Michigan soil showed that the dominant 2,4-D-degrading population was *S. paucimobilis* 1443. A less dominant 2,4-D-degrading population was detected with the *tfdA* probe; further analysis revealed that this population was a *Pseudomonas pickettii* 712. These gene probe analyses revealed that an important population carrying out 2,4-D degradation was not detected when the canonical *tfdA* gene probe was used. After a series of new strains were isolated, we identified a probe to detect and identify the dominant members of this new group.

In the past, in soil microbiology studies workers typically either measured a process or studied model isolates, but rarely was a connection between these two approaches established. We have explored the use of nucleic acid-based methods involving total bacterial community DNA extracted from soil to identify populations that grow in response to a new carbon addition. We used 2,4-dichlorophenoxyacetic acid (2,4-D) as a model carbon source because probes for structural genes (*tfdA*, *tfdB*, *tfdC*, *tfdD*, and *tfdE*) which detect some 2,4-D-degrading populations have been identified (9) and this chemical serves as a growth substrate for a moderate number of indigenous soil organisms (4, 5). In a previous study performed with a Canadian soil, we showed that an increase in the population of 2,4-D degraders in response to 2,4-D addition corresponded to an increase in hybridization of the soil bacterial community DNA to the *tfdA* and *tfdB* gene probes (9). The correspondence between hybridization signal and population density and the simple band pattern observed in Southern blot analyses suggested that a single population with sequences homologous to the *tfdA* and *tfdB* genes had accounted for 2,4-D degradation. This may not be typical, however, as more diversity in natural populations would be expected. In this study we examined a Michigan soil with a dominant 2,4-D-degrading population that does not exhibit sequence homology with the *tfd* probes and used the gene probe method to help identify a novel dominant 2,4-D degrader, as well as to study the response of a secondary 2,4-D-degrading population.

* Corresponding author. Mailing address: Center for Microbial Ecology, Michigan State University, East Lansing, MI 48824. Fax: (517) 353-2917. Electronic mail address: 21394JMT@msu.edu.

† Present address: Department of Agricultural Biology, Seoul National University, Suwon, Korea.

‡ Present address: The Agouron Institute, La Jolla, CA.

MATERIALS AND METHODS

Bacterial strains and media. Strains of *Pseudomonas pickettii* and *Sphingomonas paucimobilis* capable of utilizing 2,4-D as a sole source of carbon were isolated from the Gene Flow plots at the Long-Term Ecological Research site at the Kellogg Biological Station (KBS) in Hickory Corners, Mich. (11). *Escherichia coli* JM83 has been described elsewhere (2). *S. paucimobilis* and *P. pickettii* strains were cultivated in MMO mineral medium (14) containing 2,4-D at a concentration of 500 ppm (500 μg/ml) at 30°C. *E. coli* JM83 was cultivated in Luria broth (12) at 37°C. Plasmid DNA was isolated by using the method of Hirsch et al. for large plasmids (7) or the method of Maniatis et al. for small plasmids (12).

Soil treatment. Stock solutions (20 mg/ml) of analytical grade 2,4-D (Sigma Chemical Co., St. Louis, Mo.) were prepared by dissolving 2,4-D in 0.1 M NaH_2PO_4 buffer (pH 7.0) and were stored at 4°C until they were used. Soil (Typic Hapludalfs, fine loamy, mixed, mesic) (13) with no history of 2,4-D treatment was obtained from the untreated control plot within the Gene Flow study area at the KBS Long-Term Ecological Research site. The soil was stored at field moisture levels at 4°C until it was used. Soil samples (500 g) which had been sifted through a 2-mm-pore-size sieve were transferred to sterile polyethylene wide-mouth bottles. The soil water content was adjusted to 25% (wt/wt) by adding sterile, distilled water. 2,4-D in phosphate buffer was added to a concentration of 250 ppm and thoroughly mixed in two bottles; two control bottles received only phosphate buffer. The disappearance of 2,4-D from soil was monitored as described below, and when 2,4-D was degraded, the soil was respiked with 2,4-D for each of five

Downloaded from http://aem.asm.org/ on September 3, 2020 by guest

COR-AAD1-00002599

Bayer EX1008 (Part 5 of 9)

cycles of degradation. At the end of each degradation cycle, 50-g subsamples were taken from both the 2,4-D treated and control soils. Total soil bacterial DNA was extracted by the bacterial fractionation method, which involves the separation of bacterial cells from soil particles by differential centrifugation followed by lysis of the recovered cells (8). DNA from Saskatchewan soils that had been treated with 2,4-D and extracted by the same procedure (9) was used for comparison.

Measurement of 2,4-D in soil. The 2,4-D in soil was analyzed by vortexing soil with an equal volume of sterile distilled water and then centrifuging the preparation. The supernatant was filtered through a Millipore Millex-GS syringe filter and analyzed for 2,4-D with a Hewlett-Packard series 1050 high-performance liquid chromatography equipped with a Lichrosorb RP-18 column (Anspec Co., Ann Arbor, Mich.) and a UV detector set at 230 nm; methanol–0.1% phosphoric acid (60:40) was used as the eluant.

Hybridization analysis. To analyze 2,4-D-degrading microbial populations, the *tfdA* gene was chosen from among the five structural genes (*tfdA*, *tfdB*, *tfdC*, *tfdD*, and *tfdE*) of plasmid pJP4 (1, 3) because it appears to be more specific to the 2,4-D degradation pathway of plasmid pJP4 than the other genes (6, 9, 11). The *tfdA* and *Spa* (*S. paucimobilis*) probes are described in an accompanying paper (11). All restriction enzymes and T4 DNA ligase were purchased commercially and were used according to the manufacturer's specifications. Cloned plasmids in *E. coli* JM83 were amplified and isolated by the method of Maniatis et al. (12). The cloned probe fragments were isolated as restriction fragments from the pUC19 vector sequences on a 0.7% agarose gel, purified with a Geneclean kit (Bio 101, Inc., La Jolla, Calif.), and labelled with ^{32}P by using a random primed DNA labeling kit (Boehringer Mannheim, Indianapolis, Ind.) or a nick translation kit (Boehringer Mannheim) according to the manufacturer's specifications. Labelled probes were separated from unincorporated nucleotides prior to use with a spun column (12). The probes were used at a concentration of approximately 10^6 cpm/ml of hybridization fluid.

For slot blot experiments, total soil bacterial DNA (0.25 μg) dissolved in TE (10 mM Tris-Cl, 1 mM EDTA) was denatured for 10 min at 100°C, chilled on ice, and then transferred onto nitrocellulose hybridization membranes by using a Bio-Dot SF manifold (Bio-Rad Laboratories, Richmond, Calif.). The membranes were then placed DNA side up on a piece of (Whatmann 3MM) filter paper soaked in denaturing solution (1.5 M NaCl, 0.5 M NaOH) for 5 min and then neutralized by transfer to a piece of filter paper soaked with a solution containing 1.5 M NaCl, 0.5 M Tris-Cl, and 1 mM EDTA for 1 min. The DNA was then fixed to the membranes with a UV cross-linker (Stratagene, La Jolla, Calif.).

For Southern blot experiments, soil community DNA (1.5 μg) was digested with appropriate restriction endonucleases according to the manufacturer's specifications, size fractionated by electrophoresis through horizontal 0.7% agarose gels, and transferred to nitrocellulose hybridization membranes by the capillary technique (12). The DNA was fixed to the membrane with a UV cross-linker.

Prehybridization, hybridization, and posthybridization washes were performed as described in an accompanying paper (11). Hybridization signals were visualized with a Betascope radioactive blot analyzer (Betagen Corp., Waltham, Mass.) or by autoradiography with X-Omat AR film (Kodak, Rochester, N.Y.) exposed at −70°C, using a Quanta III intensifying screen (Sigma). The exposure times were 1 to 7 days depending on the intensity of the radioactive signal.

RESULTS

Degradation of 2,4-D in soil. The first treatment of KBS soil with 2,4-D resulted in slow 2,4-D degradation, and it took 3 to 4 weeks for the added 2,4-D to be degraded completely (data not shown). The rates of degradation for subsequent additions of 2,4-D were much higher; it took 1 week or less for complete degradation for each of the four additional 2,4-D amendments.

Gene probe hybridization. When soil bacterial community DNA was probed with the *tfdA* gene probe in slot blot analyses, no significant hybridization was observed with KBS soil DNA except for a weak signal obtained after the fifth treatment of KBS soil (Fig. 1A, lane a), while a strong hybridization signal was observed with DNA from the Saskatchewan soil (Fig. 1A, lanes c and d). Apparently, 2,4-D-degrading microbial populations with DNA sequences very different from the *tfdA* sequence had become dominant in the KBS soil. Thus, we sought to identify the successful new 2,4-D degraders in the KBS soil. Since we had isolated a group of predominant 2,4-D degraders that did not hybridize to *tfd* genes (11), we used the *Spa* probe for this group to analyze the KBS soil DNA. We observed significant hybridization of this probe to DNA from KBS soils treated one to five times with 2,4-D (Fig. 1B, lanes a and b), while no increase in hybridization signal was observed after repeated 2,4-D treatments with the Saskatchewan soil DNA (Fig. 1B, lanes c and d).

To confirm that the hybridization signals observed in slot blot analyses were due to 2,4-D-degrading microbial populations and to identify specific 2,4-D-degrading isolates responsible for the hybridization signals, soil DNA from KBS soil was hybridized to the *Spa* probe after restriction endonuclease digestion (Fig. 2). After a single treatment and after four additional treatments of soil with 2,4-D, two hybridization bands (5.0 and 11.3 kb) were detected with this probe only in 2,4-D-treated samples. The positions of the hybridization bands remained constant throughout the experiment, indicating that these bands represent a single, stably maintained population.

Since each lane in Fig. 2 contained the same amount of total bacterial community DNA (1.5 μg), the intensity of the hybridization at each time point was proportional to the amount of target DNA in each sample. A quantitative hybridization analysis revealed that the size of this population increased about twofold between the first and fifth 2,4-D treatments.

Soil community DNA obtained after the fifth treatment with 2,4-D and DNA isolated from *S. paucimobilis* 1443 produced identical hybridization band patterns when three different restriction endonucleases were used (Fig. 3). This suggests that *S. paucimobilis* 1443 was one of the dominant 2,4-D degraders throughout the experiment.

Since there was also hybridization with the *tfdA* probe (albeit weak) (Fig. 1), we tried to identify the responsible *tfdA*-hybridizing strain(s). A single band of hybridization to *tfdA* (8.8 kb) was detected on Southern blots of bacterial community DNA after the second through the fifth additions of 2,4-D (Fig. 4). The DNA from soils not treated with 2,4-D and the DNA from soils after the first 2,4-D treatment exhibited no significant hybridization to the *tfdA* gene probe (Fig. 4). Of 47 2,4-D-degrading strains isolated from the test plot, 15 hybridized to the *tfdA* probe (14). Since the KBS soil community DNA did not hybridize to the *tfdB*, *-C*, or *-D* probe (data not shown), the *tfdA* probe hybridization signal observed on Southern blots might represent one or more of the strains belonging to group II (11), which comprises the KBS isolates that exhibit sequence homology only to the *tfdA* probe. Plasmid DNA from

Downloaded from http://aem.asm.org/ on September 3, 2020 by guest

COR-AAD1-00002600

Bayer EX1008 (Part 5 of 9)

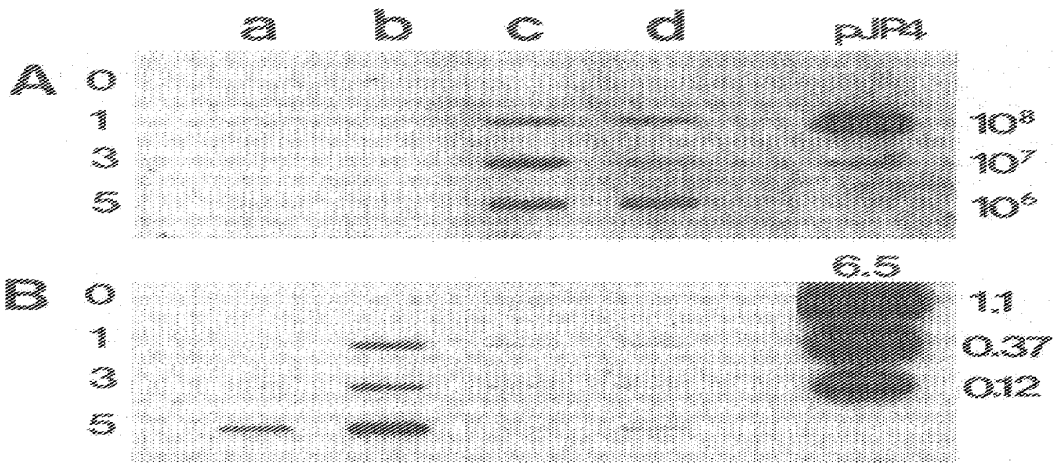


FIG. 1. Hybridization of DNAs from KBS (lanes a and b) and Saskatchewan (lanes c and d) soils to the *tfdA* probe (A) and the *Spa* probe (B). Lanes a through d contained 0.25 μg portions of soil DNA extracted after zero, one, three, and five additions of 2,4-D, respectively. The following positive controls were included: KBS control soil DNA containing 10^6, 10^7, and 10^8 cells of *Pseudomonas cepacia* DBO1(pJP4) per g of soil (lane pJP4); 1.1, 0.37, and 0.12 ng of the *Spa* probe (lane 6.5).

P. pickettii 712, one of the group II isolates, was compared with total soil bacterial DNA obtained after the fifth 2,4-D treatment in Southern blot analyses by using the *tfdA* gene probe (Fig. 5). Matching band patterns were obtained for these two DNA samples when the samples were digested with three different restriction endonucleases, suggesting that *P. pickettii* was the dominant *tfdA*-homologous 2,4-D-degrading organism in the soils after the second through fifth treatments.

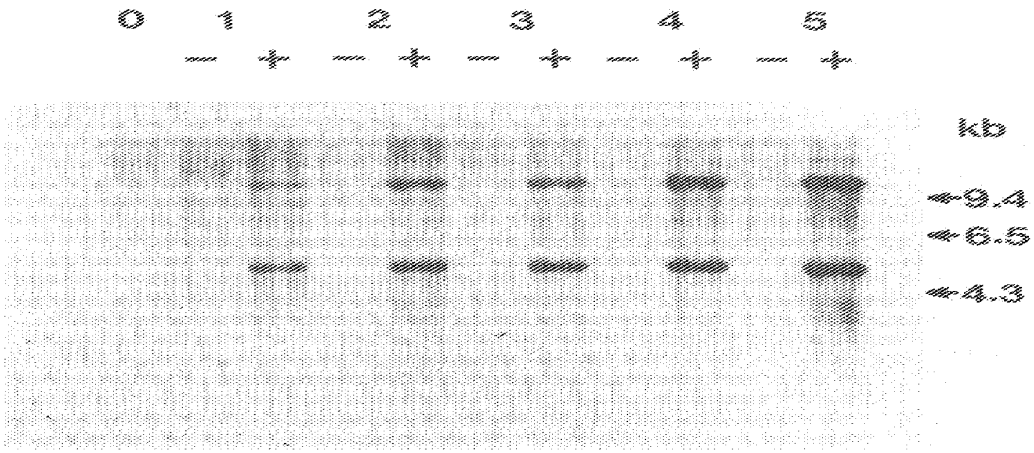


FIG. 2. Detection of indigenous 2,4-D-degrading microbial populations in soil by Southern blot analysis with the *Spa* probe. Soil DNA samples (1.5 μg) were digested with *Hin*dIII, size fractionated by agarose gel electrophoresis, and then transferred to nitrocellulose membranes. 0, 1, 2, 3, 4, and 5, DNA samples from soils after zero, one, two, three, four, and five treatments with 2,4-D, respectively. +, 2,4-D treated; –, no 2,4-D treatment (controls).

Downloaded from http://aem.asm.org/ on September 3, 2020 by guest

COR-AAD1-00002601

Bayer EX1008 (Part 5 of 9)

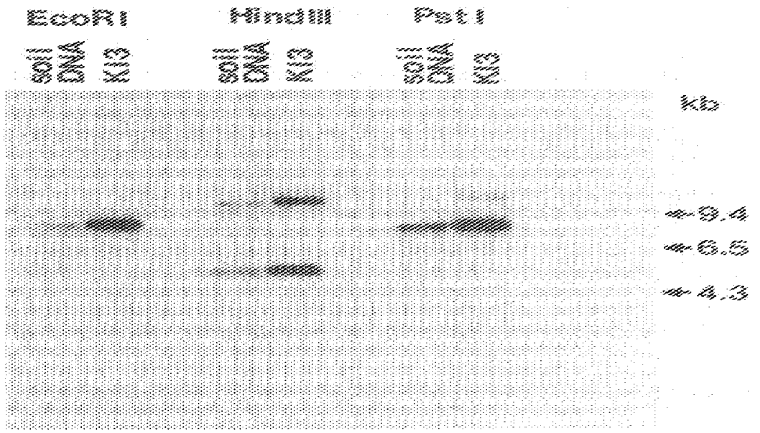


FIG. 3. Hybridization bands obtained from soil bacterial community DNA and *S. paucimobilis* 1443 DNA (KI3) digested with three different restriction endonucleases, size fractionated by agarose gel electrophoresis, and hybridized with the *Spa* probe. The DNA used was the DNA isolated after five 2,4-D treatments.

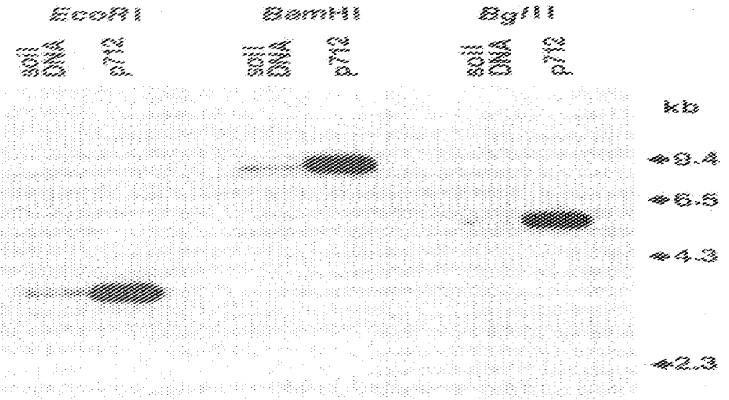


FIG. 5. Hybridization bands obtained from soil bacterial community DNA and *P. picketii* 712 plasmid DNA (p712) digested with three different restriction endonucleases, size fractionated by electrophoresis, and hybridized with the *tfdA* gene probe. The soil DNA used was the DNA isolated after five 2,4-D treatments.

DISCUSSION

The DNA from the 2,4-D-treated KBS soils exhibited no or only weak hybridization to the *tfdA* gene, while the DNA from the Saskatchewan soil exhibited the expected strong hybridization to *tfdA*. The population densities of the 2,4-D degraders estimated by the most-probable-number method were similar (ca. 5.0×10^7 organisms per g of soil) in the two soils (9, 10), indicating that there was no difference in the densities of the populations probed. Hence, organisms with different DNA sequences for 2,4-D degradation must exist in the Michigan soil. We tried to resolve the discrepancy between the high most-probable-number counts and the weak hybridization signal with *tfdA* by using the *Spa* probe for the group III isolates from the test site, since these organisms exhibited no hybridization to *tfdA* genes (11). The *Spa* probe that defines this group exhibited increasing hybridization to the soil DNA in response to 2,4-D treatment and therefore could be used to detect and identify the missing 2,4-D degraders. We do not know yet what genes are encoded by the *Spa* fragment, but the hybridization response following 2,4-D addition shows that this probe does track an important population with this function.

Our results also illustrate that a single probe often may not be sufficient to monitor populations with a specific function unless the target genes have highly conserved sequences. The KBS soil contains at least three different groups of 2,4-D degraders (11); thus, even the two probes which we used (the *tfdA* gene probe and the *Spa* probe) may not completely monitor all of the indigenous 2,4-D-degrading microbial pop-

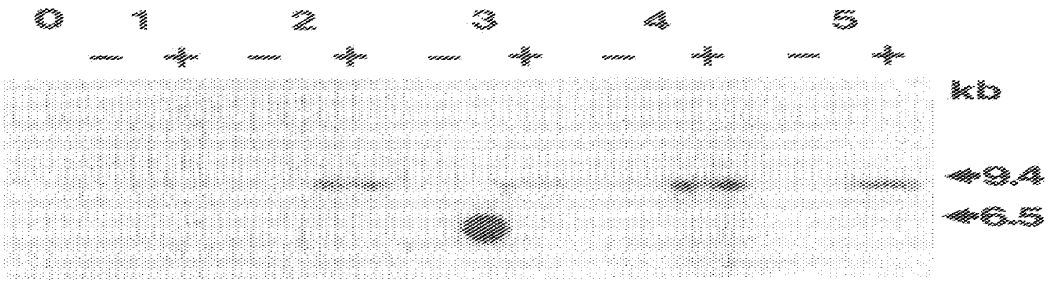


FIG. 4. Detection of indigenous 2,4-D-degrading populations in soil by Southern blot analysis with the *tfdA* probe. 0, 1, 2, 3, 4, and 5 total soil bacterial community DNA isolated after zero, one, two, three, four, and five treatments with 2,4-D, respectively. +, 2,4-D treated; —, no 2,4-D treatment (controls). DNA samples (1.5 μg) were digested with *Bam*HI, size fractionated by agarose gel electrophoresis, and then transferred to nitrocellulose membranes.

Downloaded from http://aem.asm.org/ on September 3, 2020 by guest

COR-AAD1-00002602

Bayer EX1008 (Part 5 of 9)

ulation. Divergence of sequences has been observed for other functional genes in ecological studies (e.g., the *mer* gene) (15).

S. paucimobilis 1443 was identified by the Southern blot analysis as the dominant 2,4-D degraders in the Michigan soil examined. This strain was more dominant than *P. pickettii* 712 on the basis of the strength of its hybridization signal. These two apparently dissimilar strains seemed to coexist in similar proportions after the second to fifth 2,4-D additions.

The DNA probe method used in conjunction with measurements of community activity can reveal whether very different populations are missing from the data base. Once a probe is developed for these populations, it can be used to help isolate and identify which members of the missing group are dominant.

ACKNOWLEDGMENTS

This work was supported by the following National Science Foundation grants: grant NSF-DEB 9211771 from the Long-Term Ecological Research Program, grant BSR 870547, and grant BIR 9120006 to the Center for Microbial Ecology.

We thank Cathy McGowan for valuable comments concerning the manuscript.

REFERENCES

1. **Amy, P. S., J. W. Schulke, L. M. Frazier, and R. J. Seidler.** 1985. Characterization of aquatic bacteria and cloning of genes specifying partial degradation of 2,4-dichlorophenoxyacetic acid. Appl. Environ. Microbiol. **49:**1237–1245.
2. **Bethesda Research Laboratories.** 1985. BRL M13 cloning/dideoxy sequencing instruction manual. Bethesda Research Laboratories, Gaithersburg, Md.
3. **Don, R. H., and J. M. Pemberton.** 1985. Genetic and physical map of the 2,4-dichlorophenoxyacetic acid-degradative plasmid pJP4. J. Bacteriol. **161:**466–468.
4. **Fournier, J. C.** 1980. Enumeration of the soil microorganisms able to degrade 2,4-D by metabolism or co-metabolism. Chemosphere **9:**169–174.
5. **Fournier, J. C., P. Codaccioni, and G. Soulas.** 1981. Soil adaptation to 2,4-D degradation in relation to the application rates and the metabolic behaviour of the degrading microflora. Chemosphere **8:**977–984.
6. **Harker, A. R., R. H. Olsen, and R. J. Seidler.** 1989. Phenoxyacetic acid degradation by the 2,4-dichlorophenoxyacetic acid (TFD) pathway of plasmid pJP4: mapping and characterization of the TFD regulatory gene, *tfdR*. J. Bacteriol. **171:**314–320.
7. **Hirsch, P. R., M. Van Montagu, A. W. B. Johnston, N. J. Brewin, and J. Schell.** 1980. Physical identification of bacteriocinogenic, nodulation and other plasmids in strains of *Rhizobium leguminosarum*. J. Gen. Microbiol. **120:**403–412.
8. **Holben, W. E., J. K. Jansson, B. K. Chelm, and J. M. Tiedje.** 1988. DNA probe method for the detection of specific microorganisms in the soil bacterial community. Appl. Environ. Microbiol. **54:**703–711.
9. **Holben, W. E., B. M. Schroeter, V. G. Matheson, R. H. Olsen, J. K. Kuker, V. O. Biederbeck, A. E. Smith, and J. M. Tiedje.** 1992. Gene probe analysis of soil microbial populations selected by amendment with 2,4-dichlorophenoxyacetic acid. Appl. Environ. Microbiol. **58:**3941–3948.
10. **Ka, J. O., P. Burauel, J. A. Bronson, W. E. Holben, and J. M. Tiedje.** Unpublished data.
11. **Ka, J. O., W. E. Holben, and J. M. Tiedje.** 1994. Genetic and phenotypic diversity of 2,4-dichlorophenoxyacetic acid (2,4-D)-degrading bacteria isolated from 2,4-D-treated field soils. Appl. Environ. Microbiol. **60:**1106–1115.
12. **Maniatis, T., E. F. Fritsch, and J. Sambrook.** 1982. Molecular cloning: a laboratory manual. Cold Spring Harbor Laboratory, Cold Spring Harbor, N.Y.
13. **Robertson, G. P., K. M. Klingensmith, M. J. Klug, and E. A. Paul.** 1990. Spatial variability of soil properties and microbial activity as related to primary productivity in an agricultural landscape. Bull. Ecol. Soc. Am. **71:**305.
14. **Stanier, R. Y., N. J. Palleroni, and M. Doudoroff.** 1966. The aerobic pseudomonads: a taxonomic study. J. Gen. Microbiol. **43:**159–271.
15. **Tsai, Y.-L., and B. H. Olsen.** 1990. Effects of Hg^{2+}, CH_3-Hg^+, and temperature on the expression of mercury resistance genes in environmental bacteria. Appl. Environ. Microbiol. **56:**3266–3272.

Downloaded from http://aem.asm.org/ on September 3, 2020 by guest

COR-AAD1-00002603

Bayer EX1008 (Part 5 of 9)

JOURNAL OF BACTERIOLOGY, Jan. 2002, p. 509–518 Vol. 184, No. 2
0021-9193/02/$04.00+0 DOI: 10.1128/JB.184.2.509–518.2002
Copyright © 2002, American Society for Microbiology. All Rights Reserved.

Novel 2,4-Dichlorophenoxyacetic Acid Degradation Genes from Oligotrophic *Bradyrhizobium* sp. Strain HW13 Isolated from a Pristine Environment

Wataru Kitagawa,[1] Sachiko Takami,[1] Keisuke Miyauchi,[1] Eiji Masai,[1] Yoichi Kamagata,[2] James M. Tiedje,[3] and Masao Fukuda[1]*

Department of Bioengineering, Nagaoka University of Technology, Nagaoka, Niigata 940-2188,[1] and Research Institute of Biological Resources, National Institute of Advanced Industrial Science and Technology, Tsukuba, Ibaraki 305-8566,[2] Japan, and Center for Microbial Ecology, Michigan State University, East Lansing, Michigan 48824[3]

Received 30 July 2001/Accepted 9 October 2001

The *tfd* genes of *Ralstonia eutropha* JMP134 are the only well-characterized set of genes responsible for 2,4-dichlorophenoxyacetic acid (2,4-D) degradation among 2,4-D-degrading bacteria. A new family of 2,4-D degradation genes, *cadRABKC*, was cloned and characterized from *Bradyrhizobium* sp. strain HW13, a strain that was isolated from a buried Hawaiian soil that has never experienced anthropogenic chemicals. The *cadR* gene was inferred to encode an AraC/XylS type of transcriptional regulator from its deduced amino acid sequence. The *cadABC* genes were predicted to encode 2,4-D oxygenase subunits from their deduced amino acid sequences that showed 46, 44, and 37% identities with the TfdA and TfdB subunits of 2,4,5-trichlorophenoxyacetic acid (2,4,5-T) oxygenase of *Burkholderia cepacia* AC1100 and with a putative ferredoxin, ThcC, of *Rhodococcus erythropolis* NI86/21, respectively. They are thoroughly different from the 2,4-D dioxygenase gene, *tfdA*, of *R. eutropha* JMP134. The *cadK* gene was presumed to encode a 2,4-D transport protein from its deduced amino acid sequence that showed 60% identity with the 2,4-D transporter, TfdK, of strain JMP134. *Sinorhizobium meliloti* Rm1021 cells containing *cadRABKC* transformed several phenoxyacetic acids, including 2,4-D and 2,4,5-T, to corresponding phenol derivatives. Frameshift mutations indicated that each of the *cadRABC* genes was essential for 2,4-D conversion in strain Rm1021 but that *cadK* was not. Five 2,4-D degraders, including *Bradyrhizobium* and *Sphingomonas* strains, were found to have *cadA* gene homologs, suggesting that these 2,4-D degraders share 2,4-D degradation genes similar to those of strain HW13 *cadABC*.

2,4-Dichlorophenoxyacetic acid (2,4-D) is a manufactured herbicide that has been widely used for the control of broadleaf weeds since its introduction in the 1940s. Many 2,4-D-degrading microorganisms have been isolated from agricultural, urban, and industrial soils and sediments (2, 3, 9, 22, 30, 50), and the catabolic pathway of 2,4-D mineralization in *Ralstonia eutropha* JMP134 has been extensively characterized (8–10, 14, 19, 25, 26, 32–35, 38, 41–43, 48). In JMP134, 2,4-D is transformed to 2,4-dichlorophenol (2,4-DCP) by α-ketoglutarate-dependent 2,4-D dioxygenase encoded by *tfdA*, and 2,4-DCP is subsequently hydroxylated by 2,4-DCP hydroxylase encoded by *tfdB* to form 3,5-dichlorocatechol (3,5-DCC). 3,5-DCC is further metabolized through an intradiol ring cleavage pathway encoded by *tfdCDEF* (Fig. 1). These genes are located on plasmid pJP4.

Most 2,4-D-degrading bacteria isolated from human-disturbed sites contain *tfdA* gene homologs. They include various copiotrophic, fast-growing genera in the β and γ subdivisions of the *Proteobacteria* and have been classified as class I 2,4-D degraders (24). Ka et al. reported another group of 2,4-D degraders (class II) that were also isolated from disturbed sites but have neither *tfdA* gene homologs nor α-ketoglutarate-dependent 2,4-D dioxygenase activity (21–23). This group is composed of copiotrophic, fast-growing strains in the α subdivision of the *Proteobacteria*, mostly belonging to the genus *Sphingomonas*. Fulthorpe et al. (17) and Kamagata et al. (24) isolated 2,4-D degraders from noncontaminated, pristine soils, degraders which have neither *tfdA* gene homologs nor α-ketoglutarate-dependent 2,4-D dioxygenase activity and, in contrast to those of the other two classes, grow slowly. This group of 2,4-D degraders (class III) is affiliated with the *Bradyrhizobium-Agromyces-Nitrobacter-Afipia* cluster (A. Saitou, H. Mitsui, and T. Hattori, Abstr. 11th Meet. Jpn. Soc. Microb. Ecol., p. 26, 1995) of oligotrophic bacteria in the α subdivision of the *Proteobacteria*. The existence of three distinct ecological and genetic classes of 2,4-D degraders indicates a diversity of 2,4-D degradation genes and perhaps of pathways among 2,4-D degraders. However, the 2,4-D degradation genes of class II and III 2,4-D degraders have not been characterized.

In this report, we describe the cloning and characterization of the new 2,4-D catabolic genes *cadRABKC*, which are responsible for the degradation of 2,4-D in a class III 2,4-D degrader, *Bradyrhizobium* sp. strain HW13. This strain was isolated from a buried, pristine soil from within Hawaii Volcanoes National Park, Hawaii. This soil was covered 4,800 years ago by a lava flow which has separated that soil from human impact since before the colonization of Hawaii (24). We also examined the distribution of *cadA* gene homologs among other class II and class III 2,4-D degraders. Our results reveal a second family of genes capable of 2,4-D degradation and show that these genes exist in communities previously unexposed to manufactured chlorinated chemicals.

* Corresponding author. Mailing address: Department of Bioengineering, Nagaoka University of Technology, Kamitomioka, Nagaoka, Niigata 940-2188, Japan. Phone: 81-258-47-9405. Fax: 81-258-47-9450. E-mail: masao@vos.nagaokaut.ac.jp.

Downloaded from http://jb.asm.org/ on September 3, 2020 at Corteva Agriscience

COR-AAD1-00002604
Bayer EX1008 (Part 5 of 9)

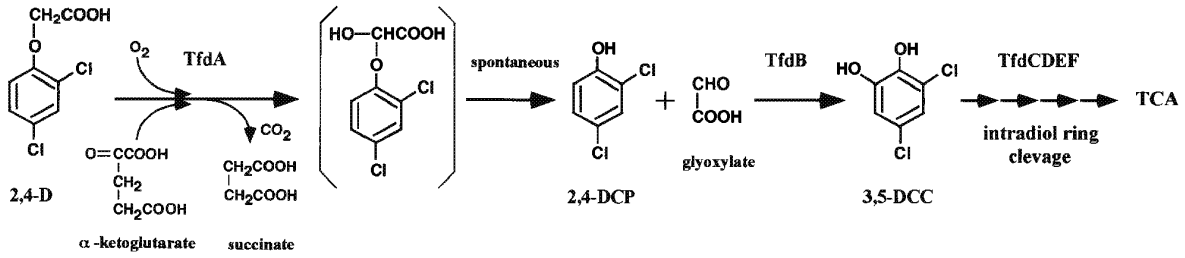


FIG. 1. Proposed 2,4-D degradation pathway encoded by *tfd* genes in *R. eutropha* JMP134. The TfdA enzyme, α-ketoglutarate-dependent 2,4-D dioxygenase, catalyzes the simultaneous oxidation of both 2,4-D and α-ketoglutarate to generate 2,4-DCP. 2,4-DCP is transformed to 3,5-DCC by TfdB, and 3,5-DCC is further metabolized through an intradiol ring cleavage pathway encoded by *tfdCDEF*. TCA, tricarboxylic acid cycle.

MATERIALS AND METHODS

Bacterial strains, plasmids, and culture conditions. The plasmids and bacterial strains used are listed in Table 1. *Bradyrhizobium* strains were grown at 30°C in CPTYM (1.25 g of Bacto Tryptone, 1.25 g of Bacto Peptone, 1.25 g of Casamino Acids, 2.5 g of yeast extract, 1.5 g of mannitol, 0.03 g of $MgSO_4 \cdot 7H_2O$, and 0.0035 g of $CaCl_2 \cdot 2H_2O$, each per liter). Minimal salt medium W (W medium) (37) was used for the growth on 2,4-D or other phenoxyacetic acid substrates. *Sphingomonas* strains, *Sinorhizobium meliloti* Rm1021 (12), and *Pseudomonas putida* PpY101 (13) were used as host strains for the strain HW13 gene library and were grown at 30°C in Luria-Bertani (LB) medium. *Escherichia coli* HB101 was grown in LB medium at 37°C. Antibiotics were used at final concentrations of 50 μg/ml for ampicillin, 10 μg/ml for tetracycline, 50 μg/ml for kanamycin, and 100 μg/ml for nalidixic acid.

DNA and RNA manipulations, nucleotide sequencing, and sequence analysis. DNA and RNA manipulations were carried out essentially as described elsewhere (1, 46). A Kilosequence kit (Takara Shuzo, Kyoto, Japan) was used to construct a series of deletion derivatives whose nucleotide sequences were determined by the dideoxy termination method with an ALFexpress DNA sequencer (Amersham Pharmacia Biotech, Piscataway, N.J.). The nucleotide sequence analysis was carried out with GeneWorks software (Intelligenetics, Inc., Mountain View, Calif.) and the FASTA and ClustalW programs provided by the National Institute of Genetics, Shizuoka, Japan. Southern and Northern slot blot hybridization analyses were performed as described previously (52). Total RNAs were extracted from HW13 cells grown on CPTYM followed by incubation in W medium containing 1 mM 2,4-D or in another potentially inducing substrate. RNA was blotted onto a nylon membrane, and hybridization was performed with a DNA probe specific to *cadA*. In the case of strain Rm1021 harboring plasmid pVBC, cells grown in LB medium were incubated in W medium containing 1 mM substrate. A frameshift mutant of the *cadR* gene in pVBC was constructed by digestion with *Bam*HI followed by treatment with T4 DNA polymerase and ligation. The resultant plasmid, pVBC1, was recovered from a transformant, and the absence of a *Bam*HI site in pVBC1 was verified. Frameshift mutants of *cadA* (pVBC2), *cadB* (pVBC3), and *cadK* (pVBC4) were constructed in the same manner; *Sse*8387I, *Xho*I, and *Eco*RI were used for the restriction enzyme cleavages respectively.

TABLE 1. Strains and plasmids used in this study

Strain or plasmid	Relevant characteristic(s)	Reference or origin
Strains		
Bradyrhizobium sp. strains		
HW13	Wild type, class III 2,4-D degrader	24
HWK12	Wild type, class III 2,4-D degrader	24
BTH	Wild type, class III 2,4-D degrader	24
Sphingomonas sp. strains		
B6-5	2,4-D conversion ability lost, originally isolated as a class II 2,4-D degrader	16
B6-10	Wild type, class II 2,4-D degrader	16
TFD26	Wild type, class II 2,4-D degrader	16
TFD44	Wild type, class II 2,4-D degrader	16
Ralstonia eutropha JMP134	Wild type, class I 2,4-D degrader	9
Sinorhizobium meliloti Rm1021	Host strain; Nal^r Sm^r	12
Sinorhizobium meliloti 22-10	Rm1021 harboring p22-10	This study
Pseudomonas putida PpY101	Host strain; *met* Nal^R	13
Escherichia coli HB101	*supE44 hsdS20*(r_B^- m_B^-) *recA13 ara-14 proA2 lacY1 galK2 rpsL20 xyl-5 mtl-1 leuB6 thi-1*	Takara Shuzo
Plasmids		
pVK100	Cosmid vector; Km^r Tc^r RK2 *ori* Mob^+	29
p22-10	2,4-D conversion-positive clone of HW13 gene library in pVK100	This study
pVBC	pVK100 with 6-kb *Bgl*II-*Hin*dIII fragment of HW13 carrying *cadRABKC*	This study
pVBC1	*cadR* frameshift mutant of pVBC	This study
pVBC2	*cadA* frameshift mutant of pVBC	This study
pVBC3	*cadB* frameshift mutant of pVBC	This study
pVBC4	*cadK* frameshift mutant of pVBC	This study
pVBCΔ5	*cadC* deletion mutant of pVBC	This study
pBluescript II KS(+)	Cloning vector; Ap^r	
pBHS1	pBluescript II KS with 3.6-kb *Hin*cII-*Spe*I fragment of HW13 carrying *cadABK*; direction of *cadABK* is identical to that of the *lac* promoter of pBluescript II KS	This study
pRK2013	Helper plasmid for triparental mating; Km^r Tra^+	45

Downloaded from http://jb.asm.org/ on September 3, 2020 at Corteva Agriscience

COR-AAD1-00002605
Bayer EX1008 (Part 5 of 9)

Construction and transfer of HW13 gene library. HW13 total DNA was partially digested with *Eco*RI, and the fragments obtained were inserted into a broad-host-range cosmid vector, pVK100 (29). The average size of the DNA inserts was approximately 25 kb. The resultant DNA library was introduced into *E. coli* HB101 by in vitro packaging and transfection by using Gigapack II plus gold packaging extract (Stratagene, La Jolla, Calif.). The gene library was conjugally transferred from *E. coli* to *P. putida* PpY101 and *S. meliloti* Rm1021 by triparental mating with a helper plasmid, pRK2013 (11, 45).

Screening for 2,4-D-converting clones. Approximately 2,500 clones of each host strain harboring the HW13 gene library were screened as follows. Five clones were inoculated and cultured together in 3 ml of LB medium. The harvested cells were washed and incubated with shaking for 2 days at 30°C in 3 ml of W medium supplemented with 50 μM 2,4-D. A 1-ml aliquot was centrifuged (10,000 × *g*, 10 min), the supernatant was filtered through a membrane filter (pore size, 0.45 μm; Advantec, Tokyo, Japan), and the filtrate was analyzed for disappearance of 2,4-D by high-performance liquid chromatography (HPLC) as described below. When 2,4-D conversion activity was observed in the culture, the five individual clones were cultured separately, and each culture filtrate was analyzed for 2,4-D disappearance.

Detection of phenoxyacetic acid conversion activity. (i) 2,4-D conversion activity assay. HPLC analysis of a culture filtrate was performed at room temperature with an Alliance 2690 system (Waters, Milford, Mass.) equipped with a TSKgel ODS-80TM column (6 mm [internal diameter] by 150 mm; Tosoh, Tokyo, Japan). The mobile phase was a mixture of water (49.5%), acetonitrile (49.5%), and phosphate (1.0%), run at a flow rate of 1.0 ml/min. 2,4-D and the metabolite, 2,4-DCP, were detected at 280 nm by a UV spectrophotometric detector. The metabolite was subjected to gas chromatography-mass spectrometry analysis as described previously (47).

(ii) Conversion activity of phenoxyacetic acids. Conversion activity of phenoxyacetic acids, including 2,4-D, was examined as follows. Strain Rm1021 harboring pVBC was grown in 50 ml of LB medium with 50 μM 2,4-D. The cells were resuspended at an optical density at 660 nm (OD_{660}) of 2.0 in 10 ml of W medium containing 50 μM 2,4-D and other phenoxyacetic acids and were incubated with shaking for 3.5 h at 30°C. At appropriate intervals, a 1-ml aliquot was withdrawn and analyzed by HPLC as described above.

(iii) Conversion activity in crude cell extract. Crude cell extract of strain Rm1021 harboring pVBC was prepared, and an enzyme reaction was performed as described by Danganan et al. (6). 2,4-D was added at a final concentration of 50 μM. The resulting reaction solution was subjected to HPLC analysis.

Detection of gene products. The *cadABK* genes in plasmid pBSH1 were induced under the control of the *lac* promoter in *E. coli* HB101, and the whole cellular protein was subjected to sodium dodecyl sulfate-polyacrylamide gel electrophoresis (SDS-PAGE) analysis as described previously (36). In the case of HB101 harboring pVBC, cells grown in LB medium containing 100 μM 2,4-D were incubated in W medium containing 100 μM 2,4-D for 3.5 h at 30°C, and their protein was subjected to SDS-PAGE analysis. The expression of the *cad* genes in strain Rm1021 was also examined. Rm1021 cells harboring pVBC were grown in LB medium containing 50 μM 2,4-D and were incubated in W medium containing 50 μM 2,4-D for 3.5 h at 30°C. The whole cellular protein was then subjected to SDS-PAGE.

Nucleotide sequence accession number. The nucleotide sequence determined in this study has been deposited in the DDBJ, EMBL, and GenBank databases under accession no. AB062679.

RESULTS

Cloning of 2,4-D degradation genes of *Bradyrhizobium* sp. strain HW13. We constructed a gene library of HW13 in *E. coli* HB101 by using a cosmid vector, pVK100, which can be mobilized from *E. coli* to other gram-negative host strains by triparental mating. When *E. coli* HB101 cells harboring the HW13 gene library were grown in LB medium and incubated in 2,4-D minimal medium, no 2,4-D-degrading activity was seen among approximately 2,500 clones. We then conjugally transferred the HW13 gene library by triparental mating to *P. putida* PpY101 (13), which was derived from the host strain of the toluene degradation plasmid, TOL, and hence was expected to express degradation genes more efficiently than *E. coli*. In this case, we also examined about 2,500 clones but did not detect any positive clones of *P. putida* PpY101. Since there could be some difficulty in expressing HW13 genes in these distantly related hosts, we employed a closely related host, *S. meliloti* strain Rm1021, for screening 2,4-D degradation genes of HW13. Sutton et al. (49) succeeded in inducing the expression of root curling genes of *Bradyrhizobium japonicum* by using *S. meliloti* as the host strain. The HW13 gene library was transferred by triparental mating to *S. meliloti* Rm1021, and the clones were screened for 2,4-D degradation activity. Among approximately 2,500 clones screened, one transconjugant, 22-10, showed 2,4-D degradation activity. 2,4-D disappeared in the culture broth of 22-10, a phenomenon which was accompanied by the appearance of a metabolite with a retention time identical to that of authentic 2,4-DCP. Gas chromatography-mass spectrometry analysis of the metabolite revealed a fragment spectrum that matched that of 2,4-DCP (data not shown). No other metabolite was detected in the culture broth, and further degradation of 2,4-DCP was not observed. These results indicate that clone 22-10 metabolized 2,4-D to 2,4-DCP, as has been found for strain JMP134.

A plasmid containing fragment 22-10 was extracted, recovered in *E. coli*, and designated p22-10. p22-10 has an insertion length of about 22 kb. Subclones of p22-10 were constructed by using vector pVK100 as shown in Fig. 2. These subclones were conjugally transferred to the host strain Rm1021, and 2,4-D degradation by each conjugant was examined. 2,4-D degradation activity was conferred by pVBGP and pVBC. The insertion fragment of pVBC completely overlapped that of pVBGP. The 0.4-kb left-terminal and 1.3-kb right-terminal deletions of the pVBC insert resulted in a loss of 2,4-D degradation activity, as shown in pVBM5 and pVE42, respectively, suggesting that most of the pVBC insert (a 6.0-kb *Bgl*II-*Hin*dIII fragment) is required for 2,4-D metabolism. *E. coli* HB101 and *P. putida* PpY101 containing pVBC, however, showed no 2,4-D degradation.

We also examined the 2,4-D degradation activity of crude cell extracts prepared from pVBC-containing cells of *E. coli* HB101, *P. putida* PpY101, and *S. meliloti* Rm1021. None of these crude extracts exhibited 2,4-D degradation activity.

Nucleotide sequence analysis of the DNA insert in pVBC. The entire 6-kb DNA insert of pVBC was sequenced and found to consist of 6,040 nucleotides. As shown in Fig. 2, it contained five open reading frames (ORFs) whose deduced amino acid sequences are similar to those of the gene products involved in the degradation of other aromatic chemicals (Table 2). The ORF1 product showed the highest identity with NitR, an AraC/XylS type of transcriptional regulator of *Rhodococcus rhodochrous* J1 (21%) (31). The ORF2 and ORF3 products showed 46 and 44% identities with TftA and TftB of *Burkholderia cepacia* AC1100, which correspond to large and small subunits of 2,4,5-trichlorophenoxyacetic acid (2,4,5-T) oxygenase, respectively (7). The ORF2 and ORF3 products also have identities exceeding 30% with the large and small subunits of benzoate dioxygenase, BenA and BenB, respectively, of *Acinetobacter* sp. strain ADP1 (40) and *Rhodococcus* sp. strain RHA1 (28). The ORF4 product showed 60% identity with the 2,4-D transport protein, TfdK, of pJP4 (35). The ORF5 product showed 37 and 35% identities with the [2Fe-2S] ferredoxin protein, ThcC, of thiocarbamate-herbicide-degrading *Rhodococcus erythropolis* NI86/21 (39) and with the putidaredoxin protein, CamB, of camphor-degrading *P. putida* ATCC 17453,

Downloaded from http://jb.asm.org/ on September 3, 2020 at Corteva Agriscience

COR-AAD1-00002606
Bayer EX1008 (Part 5 of 9)

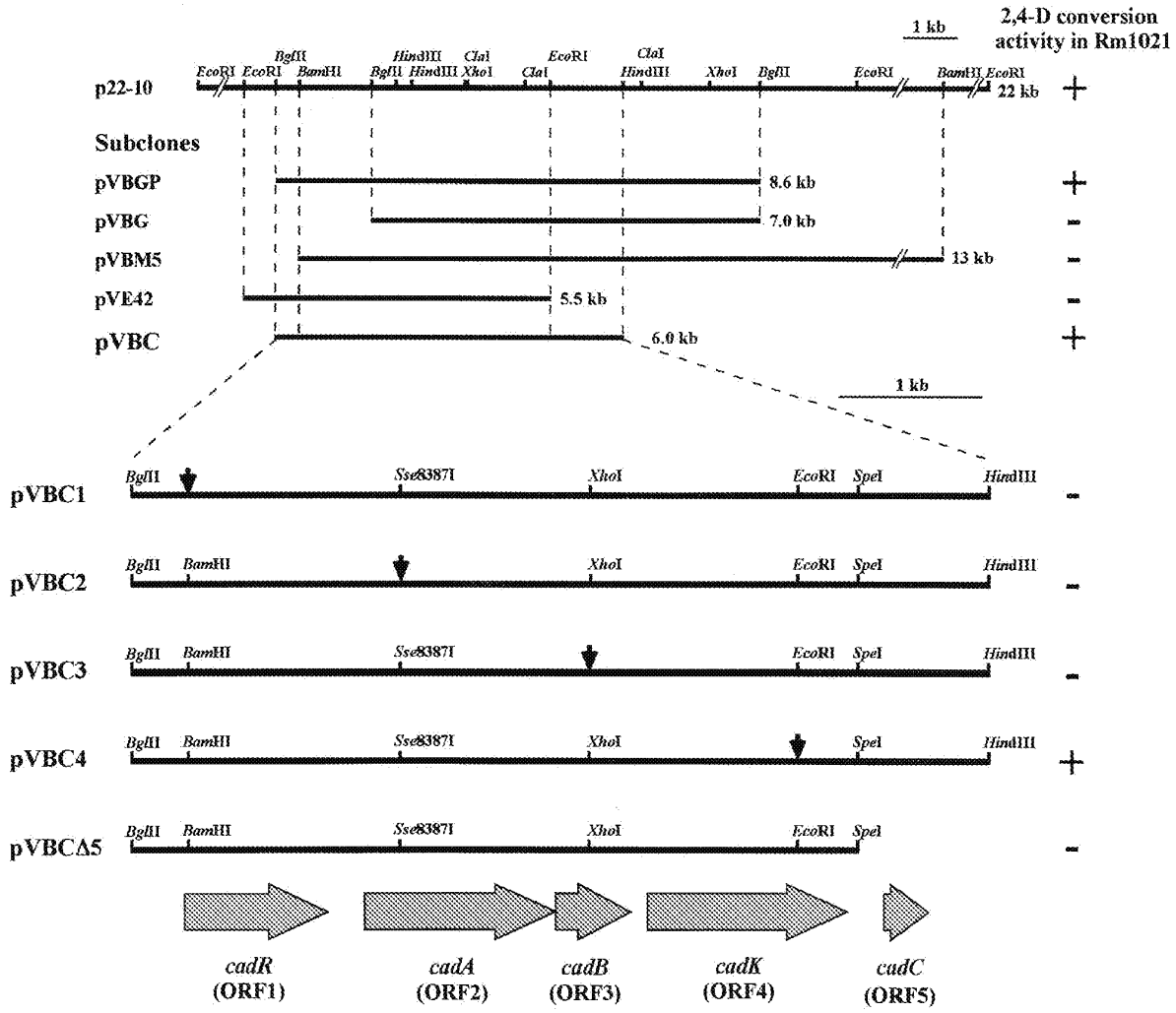


FIG. 2. Subcloning and identification of 2,4-D degradation genes. The spanning region of inserts in subclones of p22-10 (top), the positions of frameshift mutations (vertical arrows), and the region of a deletion in mutant derivatives of pVBC (bottom) are illustrated. The 2,4-D degradation activity of each clone is summarized on the right. The ORFs containing *cad* genes are represented by large horizontal arrows at the bottom which correspond to the physical maps of mutant derivatives of pVBC.

respectively, proteins which mediate electron transfer from NADH to cytochrome P-450cam monooxygenase (44). Based on these results, we infer these ORFs to be chloroaryl ether degradation genes and designate ORF1 to ORF5 as *cadR*, *cadA*, *cadB*, *cadK*, and *cadC*, respectively.

Expression of *cad* genes in *E. coli*. To identify the gene products in *E. coli*, a 3.6-kb *Hin*cII-*Spe*I fragment containing *cadABK* was subcloned into pBluescript II KS to construct pBHS1. The molecular sizes of the *cadABK* products were estimated to be 49.8, 19.8, and 48.9 kDa, respectively, on the basis of their nucleotide sequences. However, the induction of polypeptides with sizes corresponding to putative *cadABK* gene products was not observed (data not shown). Similar SDS-PAGE analysis was also performed with *S. meliloti* Rm1021 harboring pVBC, which showed 2,4-D degradation, but the polypeptides expected for *cadRABKC* gene products were not detected. We also could not detect these gene products in HB101 harboring pVBC (data not shown).

***cadR*, *cadA*, *cadB*, and *cadC* were essential for 2,4-D transformation in *S. meliloti* Rm1021.** To examine whether each of the *cadRABKC* genes is essential for 2,4-D conversion activity, frameshift and deletion mutants of pVBC were constructed as illustrated in Fig. 2. pVBC1, pVBC2, pVBC3, and pVBC4 contained frameshift mutations in *cadR*, *cadA*, *cadB*, and *cadK*, respectively, and pVBCΔ5 had a deletion of the 825-bp *Spe*I-*Hin*dIII fragment, including the entire *cadC* gene. These plasmids were introduced into *S. meliloti* Rm1021 by triparental mating. Each conjugant was grown in LB medium and incubated in W medium containing 50 μM 2,4-D to determine 2,4-D degradation activity. As summarized in Fig. 2, pVBC1,

Downloaded from http://jb.asm.org/ on September 3, 2020 at Corteva Agriscience

COR-AAD1-00002607
Bayer EX1008 (Part 5 of 9)

TABLE 2. Proteins homologous to ORFs found in pVBC (deduced amino acid sequence)

ORF (protein encoded)	Homolog (% identity)	Origin (plasmid)	Function or enzyme	Accession no.
ORF1 (CadR)	NitR (21)	*Rhodococcus rhodochrous* J1	Regulator for nitrilase	D67026
	FeaR (18)	*Escherichia coli* K-12	Regulator for 2-phenylethylamine catabolism	AE000235
ORF2 (CadA)	TftA (46)	*Burkholderia cepacia* AC1100	2,4,5-T oxygenase large subunit	U11420
	BenA (34)	*Acinetobacter* sp. strain ADP1	Benzoate 1,2-dioxygenase terminal oxygenase large subunit	AF009224
	BenA (34)	*Rhodococcus* sp. strain RHA1	Benzoate 1,2-dioxygenase terminal oxygenase large subunit	AB055706
ORF3 (CadB)	TftB (44)	*Burkholderia cepacia* AC1100	2,4,5-T oxygenase small subunit	U11420
	BenB (32)	*Acinetobacter* sp. strain ADP1	Benzoate 1,2-dioxygenase terminal oxygenase small subunit	AF009224
	BenB (31)	*Rhodococcus* sp. strain RHA1	Benzoate 1,2-dioxygenase terminal oxygenase small subunit	AB055706
ORF4 (CadK)	TfdK (60)	*Ralstonia eutropha* JMP134(pJP4)	2,4-D transporter	U16782
	PcaK (28)	*Acinetobacter* sp. strain ADP1	4-Hydroxybenzoate transporter	L05770
	BenK (27)	*Acinetobacter* sp. strain ADP1	Benzoate transporter	AF009224
ORF5 (CadC)	ThcC (37)	*Rhodococcus erythropolis* NI86/21	Putative ferredoxin	U17130
	FdVI (37)	*Rhodobacter capsulatus* B10	Putative ferredoxin	Y11304
	CamB (35)	*Pseudomonas putida* ATCC 17453	Putidaredoxin for cytochrome P-450cam monooxygenase	J05406

pVBC2, pVBC3, and pVBCΔ5 lost the ability to transform 2,4-D. In contrast, pVBC4 retained the ability to convert 2,4-D to 2,4-DCP. These results indicate that *cadA*, *cadB*, *cadC*, and *cadR* are essential for 2,4-D conversion in Rm1021 but that *cadK* is not.

Substrate preference of *cad* gene products in Rm1021. In order to examine the substrate preference of *cad* gene products, the conversion rates of phenoxyacetic acids, including 2,4-D, phenoxyacetic acid (PAA), 2-chlorophenoxyacetic acid (2-CPAA), 4-chlorophenoxyacetic acid (4-CPAA), 2,3-dichlorophenoxyacetic acid (2,3-D), 3,4-dichlorophenoxyacetic acid (3,4-D), and 2,4,5-T, were examined by using resting cells of pVBC-containing Rm1021. Strain Rm1021, which contained the vector pVK100, showed no transformation activity against any of these substrates. The cells grown in LB medium with 50 μM 2,4-D were incubated in W medium with a 50 μM concentration of each of the phenoxyacetic acids mentioned above, and the concentrations of the phenoxyacetic acids were determined periodically. As shown in Fig. 3, PAA, 4-CPAA, 3,4-D, 2,4,5-T, and 2,4-D were transformed efficiently at the initial conversion rate of 10 to 12.5 μM/h at an OD_{660}. 2-CPAA was transformed less effectively at an initial rate of 6.3 μM/h at an OD_{660}. 2,3-D was not transformed at all. These results indicate that the *cad* gene products can metabolize a variety of phenoxyacetic acids. Benzoate was not metabolized, although *cadAB* have similarity to the benzoate dioxygenase genes *benAB* (data not shown).

***cadA* gene transcription induction.** To determine the induction profiles of *cadA* gene transcription, Northern hybridization was performed with HW13 and pVBC-containing *S. meliloti* Rm1021. No *cadA* transcription was observed in HW13 cells or in pVBC-containing Rm1021 cells pregrown in CPTYM or in LB medium in the absence of phenoxyacetic acids. When phenoxyacetic acids were added, only 2,4-D and 4-CPAA induced *cadA* gene transcription, and this occurred in both strain HW13 and strain Rm1021 (Table 3). We also examined the growth of HW13 on these phenoxyacetic acids and found that the assimilation profiles were consistent with the

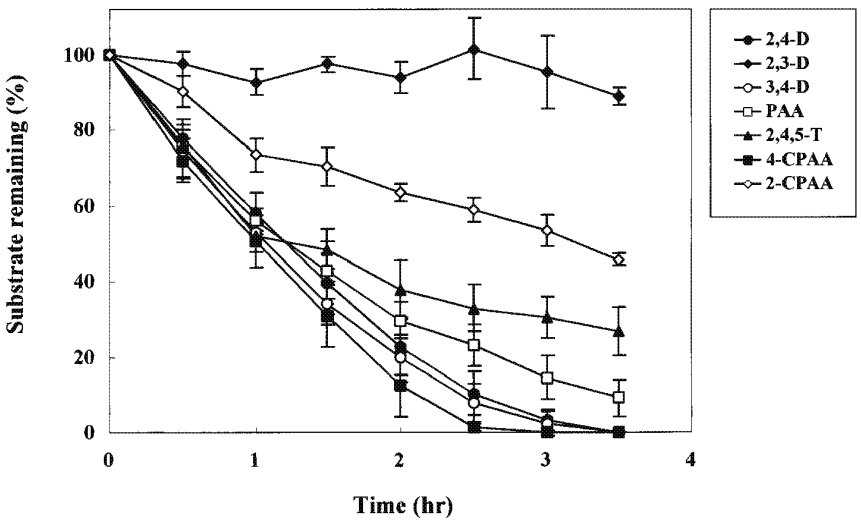


FIG. 3. Transformation of phenoxyacetic acids by Rm1021 harboring pVBC. The cells grown in the presence of 2,4-D were incubated in W medium containing a 50 μM concentration of each substrate. The remaining substrates were analyzed by HPLC. The data are the averages of three independent experiments. Standard deviations are indicated by error bars.

Downloaded from http://jb.asm.org/ on September 3, 2020 at Corteva Agriscience

COR-AAD1-00002608
Bayer EX1008 (Part 5 of 9)

TABLE 3. Induction substrate specificity of *cadABC*

Substrate	Northern hybridization with the *cadA* gene		Growth of HW13
	HW13	Rm1021 (pVBC)	
2,4-dichlorophenoxyacetic acid	+	+	+
2,3-dichlorophenoxyacetic acid	–	–	–
3,4-dichlorophenoxyacetic acid	–	–	–
2,4,5-trichlorophenoxyacetic acid	–	–	–
2-chlorophenoxyacetic acid	–	–	–
4-chlorophenoxyacetic acid	+	+	+
phenoxyacetic acid	–	–	–

cadA transcription profiles (Table 3). These results suggest that *cad* gene expression is strictly regulated at the transcriptional level.

***cadA* gene in class II and class III 2,4-D degraders.** To examine the distribution of *cad* gene homologs among class II and class III 2,4-D degraders, Southern hybridization analysis was performed with the HW13 *cadA* gene probe on *Sal*I digests of total DNAs prepared from a class I 2,4-D degrader, *R. eutropha* JMP134; class II 2,4-D degraders, *Sphingomonas* sp. strains B6-5, B6-10, TFD26, and TFD44 (16); and class III 2,4-D degraders, including *Bradyrhizobium* sp. strains HWK12 and BTH (24). As shown in Fig. 4, all of the class II and III 2,4-D degraders tested, except for the class II degrader B6-5, showed evidence of *cadA* gene homologs. Strain B6-5 originally grew on 2,4-D but had lost this ability before the hybridization experiments were performed. The class I 2,4-D degrader *R. eutropha* JMP134 did not show evidence of any *cadA* gene homologs. These results suggest that many class II and III 2,4-D degraders could employ *cad* gene homologs for 2,4-D degradation.

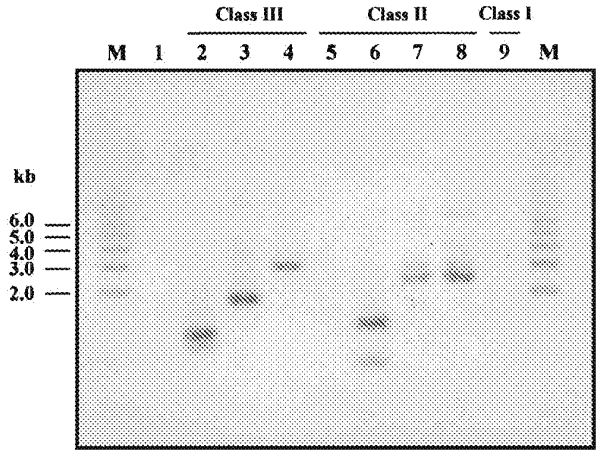


FIG. 4. Southern hybridization analysis of 2,4-D degraders. Hybridization was performed with the HW13 *cadA* gene probe on *Sal*I-digested total DNAs from 2,4-D degraders. Lane 1, *S. meliloti* Rm1021; lane 2, HW13; lanes 3 and 4, class III degraders (*Bradyrhizobium* sp. strains HWK12 and BTH); lanes 5 to 8, class II degraders (*Sphingomonas* sp. strains B6-5, B6-10, TFD26, and TFD44); lane 9, class I degrader (*R. eutropha* JMP134). Lanes M, DNA size marker.

Downloaded from http://jb.asm.org/ on September 3, 2020 at Corteva Agriscience

COR-AAD1-00002609
Bayer EX1008 (Part 5 of 9)

DISCUSSION

New 2,4-D degradation genes have been cloned from *Bradyrhizobium* sp. strain HW13, which was recovered from a buried Hawaiian soil that has been isolated from 2,4-D and other anthropogenic chemicals by lava flows since before human colonization of the islands. These lava layers formed solid, 2- and 5-m-thick rock caps over the soil from which the strain was isolated. Furthermore, neither 2,4-D nor 2,4,5-T was ever used in this region of the park (T. Tunison, U.S. National Park Service, personal communication). The degradation genes were entirely different from the well-known *tfd* genes that encode the 2,4-D degradation pathway of *R. eutropha* JMP134, suggesting that at least the initial 2,4-D degradation step of HW13 has a totally distinct evolutionary origin from that of JMP134.

The new 2,4-D degradation genes were designated *cadRABKC*. With the exception of *cadK*, they have no similarity to *tfd* genes. The *cadR* gene may encode a positive transcriptional regulator, because its sequence is somewhat similar to that of *nitR*, which an AraC/XylS codes for type of positive transcriptional regulator (31), and the deletion and frameshift mutations within *cadR* resulted in the loss of 2,4-D conversion activity in *S. meliloti* Rm1021 (Fig. 2). This gene seems to be essential for the expression of *cadABKC* genes in Rm1021. The *cadA* and *cadB* genes are predicted to encode large and small subunits, respectively, of 2,4-D oxygenase, based on sequence similarity to the *tftAB* 2,4,5-T oxygenase genes of *B. cepacia* AC1100 (7) and the *benAB* benzoate dioxygenase genes of *Acinetobacter* sp. strain ADP1 (40) and *Rhodococcus* sp. strain RHA1 (28). The *cadC* gene is deduced to encode a ferredoxin subunit of 2,4-D oxygenase based on its identity with the *camB* ferredoxin (putidaredoxin) gene of *P. putida* ATCC 17453, which is involved in the oxidation of camphor. Frameshift mutations in each of the *cadABC* genes resulted in the loss of conversion activity of 2,4-D to 2,4-DCP, indicating that the respective gene encodes a functional subunit of a multicomponent 2,4-D oxygenase. The *cadK* gene is thought to encode a 2,4-D transporter because of its high sequence similarity to *tfdK*, the 2,4-D transporter gene of JMP134 (35). The frameshift mutation of *cadK* did not affect 2,4-D conversion activity expressed in Rm1021. However, this result does not establish whether *tfdK* is involved in 2,4-D transport, because transporters are not indispensable for 2,4-D and benzoate uptake. For example, growth of strain JMP134 on 2,4-D and strain ADP1 on benzoate was not prevented by mutations in *tfdK* (35) or the benzoate transporter gene, *benK* (4), respectively. Also, Rm1021 may itself have an equivalent 2,4-D transporter that conceals the defect of the *cadK* frameshift mutation in Rm1021. Resolving the role of *cadK* in 2,4-D degradation requires the disruption of *cadK* in HW13, but all of the attempts to disrupt *cadK* in HW13 were unsuccessful.

The *cadABC*-encoded 2,4-D oxygenase of HW13 seems to be included in the family of aromatic ring-hydroxylation dioxygenases, that is, Rieske nonheme iron oxygenases (18). The enzymes of this family are composed of a terminal oxygenase component and one or two electron transport components. In the case of HW13 2,4-D oxygenase, the terminal oxygenase and electron transport components are encoded by *cadAB* and *cadC*, respectively.

As indicated in Fig. 5A and B, the subunits of 2,4-D oxygenase encoded by *cadAB* could be classified in the benzoate subfamily of two-component ring-hydroxylation dioxygenases because of their identity with *benAB*-encoded subunits of benzoate dioxygenase. On the other hand, the *cadC*-encoded ferredoxin subunit of 2,4-D oxygenase seems to be a member of the P-450 ferredoxin subfamily, as illustrated in Fig. 5C. These results suggest that *cadABC*-encoded 2,4-D oxygenase employs very unique electron transfer components distinct from those of the two-component benzoate dioxygenases. Thus, the *cadABC* region encoding 2,4-D oxygenase is suggested to have three components. *cadAB* and *cadC* are thought to encode the terminal oxygenase and ferredoxin components, respectively. The gene encoding the ferredoxin reductase component remains unidentified. From our conjugation experiments, the *cadABC* genes were sufficient to confer 2,4-D conversion activity to Rm1021, suggesting that Rm1021 provided a protein equivalent to a ferredoxin reductase component for the *cadABC*-encoded 2,4-D oxygenase. In contrast, *cadABC* genes on the pVBC plasmid did not confer 2,4-D conversion activity to the *E. coli* or *P. putida* host strains. When we used *E. coli* and *P. putida* as host strains, no positive clones having 2,4-D conversion activity were obtained from the HW13 genomic library. The expression of *cadABC* genes in these hosts might be too poor to show 2,4-D conversion activity, or these hosts might not have equivalents to a ferredoxin reductase component for the gene of *cadABC* that encodes 2,4-D oxygenase. No promoter consensus sequences were found in the preceding upstream sequences of *cadR* and *cadA*, a finding that supports the former possibility. The latter possibility can be proposed based on the case of *tftAB*-encoded 2,4,5-T oxygenase. In contrast to HW13 *cadABC*, *tftAB* genes from *B. cepacia* AC1100 conferred 2,4,5-T conversion activity to *Pseudomonas aeruginosa* PAO1. Four polypeptides, including two oxygenase subunits encoded by *tftAB* and polypeptides of 15 and 29 kDa, are required for the activity of 2,4,5-T oxygenase in AC1100 (6, 7). The 15- and 29-kDa polypeptides are thought to constitute a reductase component. *P. aeruginosa* PAO1 seems to have the substitute for the reductase component of *tftAB*-encoded 2,4,5-T oxygenase. The putative molecular sizes of putidaredoxin and putidaredoxin reductase for cytochrome P-450cam monooxygenase encoded by *camB* and *camA* are estimated to be 11.5 and 45.5 kDa, respectively, based on their amino acid sequences (44). The predicted molecular size of *cadC*-encoded ferredoxin is 11.2 kDa, which is in good agreement with the size of *camB*-encoded putidaredoxin. Thus, the subunits of the *tftAB*-encoded 2,4,5-T oxygenase that are predicted to constitute a reductase component seem to be distinct from those of the *cadABC*-encoded 2,4-D oxygenase.

Although the amino acid sequence identities of the *cadAB* and *tftAB* products are not very high (around 45%), the substrate preferences of *cadAB*-encoded 2,4-D and *tftAB*-encoded 2,4,5-T oxygenases on phenoxyacetic acids are very similar. Both oxygenases transformed a variety of phenoxyacetic acids to similar extents (6). Both of them readily degraded 4-CPAA, 2,4-D, and 2,4,5-T. In addition, *cadAB*-encoded 2,4-D oxygenase transformed 3,4-D. The chlorine substitution at the *para* position seems to be important for their catalytic activity against chlorinated phenoxyacetic acids. On the other hand, *tftAB*-encoded 2,4,5-T oxygenase transformed 2,4,5-T rela-

Downloaded from http://jb.asm.org/ on September 3, 2020 at Corteva Agriscience

COR-AAD1-00002610
Bayer EX1008 (Part 5 of 9)

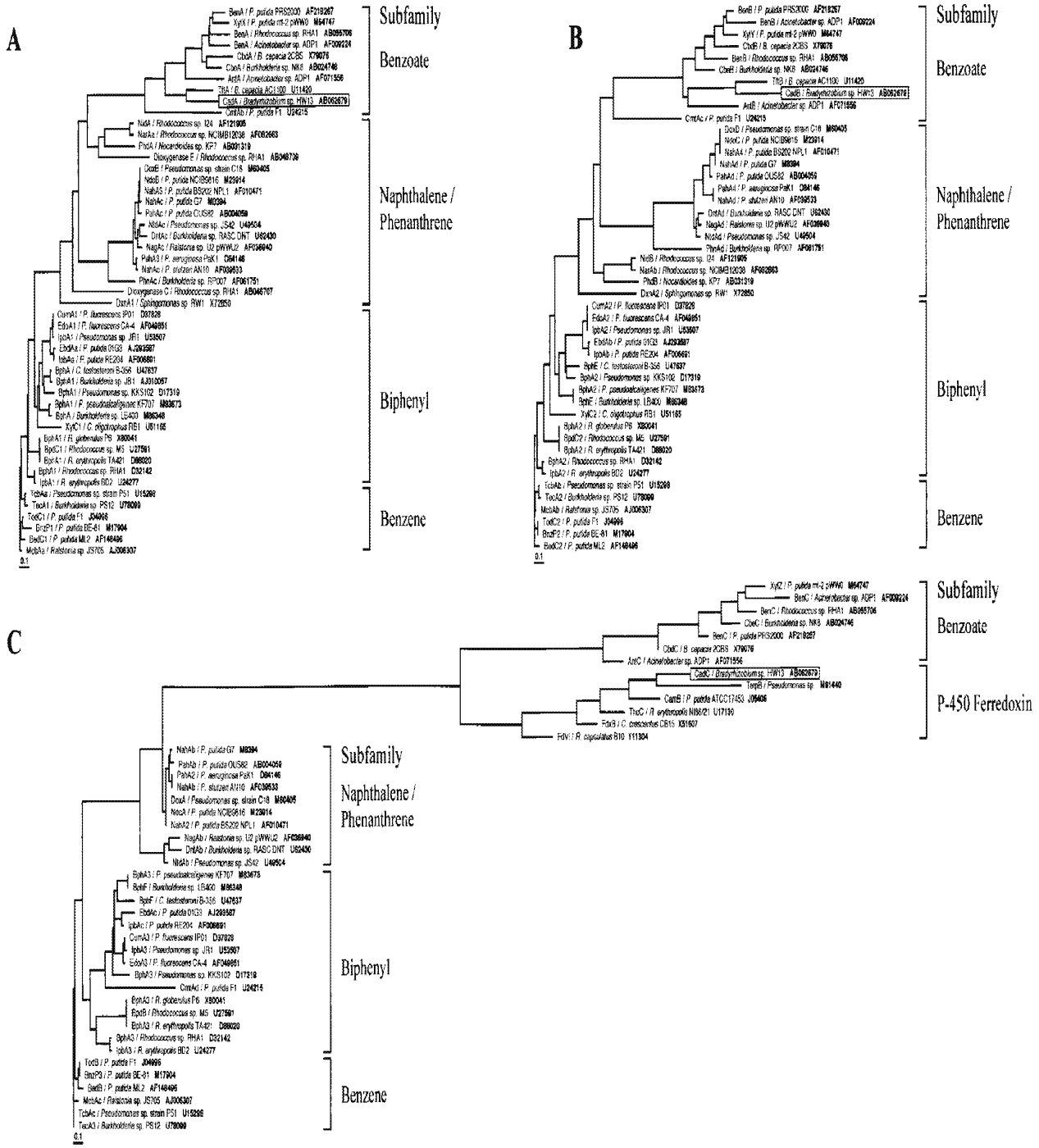


FIG. 5. Phylogenetic trees of CadABC subunits of strain HW13 2,4-D oxygenase and the related oxygenase subunits. The phylogenetic trees of *cadA* product and large (α) subunits of aromatic ring hydroxylation dioxygenases (A), *cadB* product and small (β) subunits of aromatic ring hydroxylation dioxygenases (B), and *cadC* product and ferredoxin subunits of ring hydroxylation dioxygenases and cytochrome P-450cam monooxygenases (C) are shown. In panel C, ferredoxin reductase component protein sequences were used in the case of the two-component dioxygenase system (benzoate subfamily). The deduced amino acid sequences were aligned by using the ClustalW program. CadA, CadB, and CadC subunits of HW13 2,4-D oxygenase are boxed. The accession numbers are shown to the right of each enzyme. The representative substrate for each subfamily is indicated to the right of the figure.

Downloaded from http://jb.asm.org/ on September 3, 2020 at Corteva Agriscience

COR-AAD1-00002611
Bayer EX1008 (Part 5 of 9)

tively more rapidly than it transformed 2,4-D. The degradation activities of 2,4,5-T and 2,4-D by *cadAB*-encoded 2,4-D oxygenase were almost the same. It is very likely that *tftAB*-encoded 2,4,5-T oxygenase is more specific to 2,4,5-T than is *cadAB*-encoded 2,4-D oxygenase, because *tftAB*-containing strain AC1100 was isolated after long-term selection for growth on 2,4,5-T in which a chemostat community of microorganisms from waste dump sites plus those harboring the degradative plasmids CAM, TOL, SAL, and pAC25 experienced a gradual shift from substrates for the degradative plasmids to 2,4,5-T, with the latter eventually becoming the sole carbon source (27). The substrate specificity on phenoxyacetic acids of *tfdA*-encoded dioxygenase of JMP134 apparently differs from those of *cadAB*-encoded 2,4-D and *tftAB*-encoded 2,4,5-T oxygenases. *tfdA*-encoded dioxygenase degraded 2,4-D at a high rate, degraded 4-CPAA less rapidly, and degraded 2,4,5-T and PAA very slowly (15). In contrast to the case for *tfdA*, whose encoded 2,4-D dioxygenase catalyzes simultaneous dioxygenation of 2,4-D and α-ketoglutarate, Xun and Wagnon proposed that *tftAB*-encoded 2,4,5-T oxygenase catalyzes monooxygenation of 2,4,5-T (51). On the basis of the similarities of amino acid sequences and substrate preferences between *tftAB*-encoded 2,4,5-T and *cadAB*-encoded 2,4-D oxygenases, we suggest that *cadAB*-encoded 2,4-D oxygenase also catalyzes the monooxygenation of 2,4-D.

The gene organization of the *tftAB* region in strain AC1100 is very different from that of *cadAB*. The *cadAB* region consists of *cadRABKC*, which encodes a positive regulator, oxygenase subunits, and a putative transporter. In contrast, the *tftAB* region contains only *tftAB*, which encodes oxygenase subunits (7, 20). DNA rearrangements may have occurred during the long-term selection for 2,4,5-T growth, a process that may have selected variants with the *tftAB* segment excised from the region that originally had had a gene organization similar to that of *cadRABKC*. The loss of a positive regulator gene equivalent to *cadR* might have been restored by the acquisition of an alternate constitutive promoter sequence or by some other means of removing the obstacle to improved growth on 2,4,5-T.

The deletion of *cadR* in a *cad* gene plasmid resulted in the loss of 2,4-D conversion activity in strain Rm1021. The transcription of *cadA* was induced only by 2,4-D and 4-CPAA in both strain Rm1021 and strain HW13. These results strongly suggest that *cadR* is primarily responsible for the transcription induction of *cadA* by 2,4-D and 4-CPAA in both Rm1021 and HW13. Of the several phenoxyacetic acids tested, 2,4-D and 4-CPAA were found to support the growth of HW13 and to induce *cadA* gene transcription, suggesting that the growth of HW13 on phenoxyacetic acids is governed by the induction of *cadA* transcription regulated by *cadR*.

Although the *cadRABKC* genes conferred 2,4-D conversion activity to *S. meliloti* Rm1021, we are not sure whether they are solely responsible for 2,4-D degradation in strain HW13. We made several attempts to inactivate the *cadA* gene by a gene replacement, but all of the inserts were localized outside *cadA*. However, the following evidence strongly suggests that at least the *cadRABC* genes are responsible for 2,4-D degradation in HW13. (i) Genes other than *cadAB* were not obtained from the HW13 gene library (which contained about 2,500 clones), which is enough to cover the HW13 chromosome with 99.9% probability. (ii) *cadAB* gene products showed good identity with *tftAB*-encoded 2,4,5-T oxygenase subunits that catalyze degradation of 2,4,5-T and 2,4-D. (iii) *cadA* transcription was induced by 2,4-D. (iv) The substrates which induced *cadA* transcription in HW13 were consistent with the substrates that supported growth. (v) HW13 does not have identifiable *tfd* gene homologs. (vi) *cadA* gene homologs were shared by class II and class III 2,4-D degraders that have no *tfd* gene homologs. In addition, we recently obtained two independent mutant strains of HW13 that had been irradiated with UV light, were deficient in their growth on 2,4-D, and accumulated 2,4-DCP (unpublished results). These results suggest that the conversion of 2,4-D to 2,4-DCP that can be conducted by *cadABC* is a part of the 2,4-D degradation pathway in HW13.

In this study, we isolated new 2,4-D oxygenase genes, *cadRABKC*, from a class III 2,4-D degrader, *Bradyrhizobium* sp. strain HW13. This set of 2,4-D oxygenase genes appears to be responsible for 2,4-D transformation in HW13 and may be involved in 2,4-D transformation in at least some class II and III 2,4-D degraders. If *cadABC*-encoded 2,4-D oxygenase is primarily responsible for 2,4-D catabolism in 2,4-D degraders of both class II and class III, then the difference between these classes may have originated not from the difference in 2,4-D degradation genes but from the difference in the degraders' intrinsic growth rates. The *Bradyrhizobium* strain we studied is apparently able to call on an existing oxygenase complex to attack a new chlorinated chemical not experienced in its natural evolutionary history. This strain seems to have recruited and adapted the oxygenase components to catabolize 2,4-D in addition to having the existing chlorophenol catabolic pathway, as suggested in the pentachlorophenol degradation pathway (5). The unique ferredoxin component encoded by *cadC* and the terminal oxygenase component encoded by *cadAB* may suggest the independent recruitment of these two components from separate origins. The organism's slow growth on 2,4-D suggests that its enzymes are not optimized for growth on this substrate, but it shows nonetheless that a native soil community can have genetic resources to degrade at least some anthropogenic chemicals.

ACKNOWLEDGMENT

We thank Hisayuki Mitsui for the kind gift of *S. meliloti* Rm1021.

REFERENCES

1. **Ausubel, F. M., R. Brent, E. Kingston, D. D. Moore, J. G. Seidman, J. A. Smith, and K. Struhl.** 1990. Current protocols in molecular biology. John Wiley & Sons, Inc., New York, N.Y.
2. **Bhat, M. A., M. Tsuda, K. Horiike, M. Nozaki, C. S. Vaidyanathan, and T. Nakazawa.** 1994. Identification and characterization of a new plasmid carrying genes for degradation of 2,4-dichlorophenoxyacetate from *Pseudomonas cepacia* CSV90. Appl. Environ. Microbiol. **60**:307–312.
3. **Chaudhry, G. R., and G. H. Huang.** 1988. Isolation and characterization of a new plasmid from a *Flavobacterium* sp. which carries the genes for degradation of 2,4-dichlorophenoxyacetate. J. Bacteriol. **170**:3897–3902.
4. **Collier, L. S., N. N. Nichols, and E. L. Neidle.** 1997. *benK* encodes a hydrophobic permease-like protein involved in benzoate degradation by *Acinetobacter* sp. strain ADP1. J. Bacteriol. **179**:5943–5946.
5. **Copley, S. D.** 2000. Evolution of a metabolic pathway for degradation of a toxic xenobiotic: the patchwork approach. Trends Biochem. Sci. **25**:261–265.
6. **Danganan, C. E., S. Shankar, R. W. Ye, and A. M. Chakrabarty.** 1995. Substrate diversity and expression of the 2,4,5-trichlorophenoxyacetic acid oxygenase from *Burkholderia cepacia* AC1100. Appl. Environ. Microbiol. **61**:4500–4504.
7. **Danganan, C. E., R. W. Ye, D. L. Daubaras, L. Xun, and A. M. Chakrabarty.** 1994. Nucleotide sequence and functional analysis of the genes encoding 2,4,5-trichlorophenoxyacetic acid oxygenase in *Pseudomonas cepacia* AC1100. Appl. Environ. Microbiol. **60**:4100–4106.

Downloaded from http://jb.asm.org/ on September 3, 2020 at Corteva Agriscience

COR-AAD1-00002612
Bayer EX1008 (Part 5 of 9)

8. **Don, R. H., and J. M. Pemberton.** 1985. Genetic and physical map of the 2,4-dichlorophenoxyacetic acid-degradative plasmid pJP4. J. Bacteriol. **161:** 466–468.
9. **Don, R. H., and J. M. Pemberton.** 1981. Properties of six pesticide degradation plasmids isolated from *Alcaligenes paradoxus* and *Alcaligenes eutrophus*. J. Bacteriol. **145:**681–686.
10. **Don, R. H., A. J. Weightman, H. J. Knackmuss, and K. N. Timmis.** 1985. Transposon mutagenesis and cloning analysis of the pathways for degradation of 2,4-dichlorophenoxyacetic acid and 3-chlorobenzoate in *Alcaligenes eutrophus* JMP134(pJP4). J. Bacteriol. **161:**85–90.
11. **Figurski, D. H., and D. R. Helinski.** 1979. Replication of an origin-containing derivative of plasmid RK2 dependent on a plasmid function provided in *trans*. Proc. Natl. Acad. Sci. USA **76:**1648–1652.
12. **Finan, T. M., B. Kunkel, G. F. De Vos, and E. R. Signer.** 1986. Second symbiotic megaplasmid in *Rhizobium meliloti* carrying exopolysaccharide and thiamine synthesis genes. J. Bacteriol. **167:**66–72.
13. **Fukuda, M., and K. Yano.** 1985. Construction of broad host range vectors for gram-negative bacteria. Agric. Biol. Chem. **49:**2719–2724.
14. **Fukumori, F., and R. P. Hausinger.** 1993. *Alcaligenes eutrophus* JMP134 "2,4-dichlorophenoxyacetate monooxygenase" is an α-ketoglutarate-dependent dioxygenase. J. Bacteriol. **175:**2083–2086.
15. **Fukumori, F., and R. P. Hausinger.** 1993. Purification and characterization of 2,4-dichlorophenoxyacetate/alpha-ketoglutarate dioxygenase. J. Biol. Chem. **268:**24311–24317.
16. **Fulthorpe, R. R., C. McGowan, O. V. Maltseva, W. E. Holben, and J. M. Tiedje.** 1995. 2,4-Dichlorophenoxyacetic acid-degrading bacteria contain mosaics of catabolic genes. Appl. Environ. Microbiol. **61:**3274–3281.
17. **Fulthorpe, R. R., A. N. Rhodes, and J. M. Tiedje.** 1996. Pristine soils mineralize 3-chlorobenzoate and 2,4-dichlorophenoxyacetate via different microbial populations. Appl. Environ. Microbiol. **62:**1159–1166.
18. **Gibson, D. T., and R. E. Parales.** 2000. Aromatic hydrocarbon dioxygenases in environmental biotechnology. Curr. Opin. Biotechnol. **11:**236–243.
19. **Harker, A. R., R. H. Olsen, and K. J. Seidler.** 1989. Phenoxyacetic acid degradation by the 2,4-dichlorophenoxyacetic acid (TFD) pathway of plasmid pJP4: mapping and characterization of the TFD regulatory gene, *tfdR*. J. Bacteriol. **171:**314–320.
20. **Hübner, A., C. E. Danganan, L. Xun, A. M. Chakrabarty, and W. Hendrickson.** 1998. Genes for 2,4,5-trichlorophenoxyacetic acid metabolism in *Burkholderia cepacia* AC1100: characterization of the *tftC* and *tftD* genes and locations of the *tft* operons on multiple replicons. Appl. Environ. Microbiol. **64:**2086–2093.
21. **Ka, J. O., W. E. Holben, and J. M. Tiedje.** 1994. Analysis of competition in soil among 2,4-dichlorophenoxyacetic acid-degrading bacteria. Appl. Environ. Microbiol. **60:**1121–1128.
22. **Ka, J. O., W. E. Holben, and J. M. Tiedje.** 1994. Genetic and phenotypic diversity of 2,4-dichlorophenoxyacetic acid (2,4-D)-degrading bacteria isolated from 2,4-D-treated field soils. Appl. Environ. Microbiol. **60:**1106–1115.
23. **Ka, J. O., W. E. Holben, and J. M. Tiedje.** 1994. Use of gene probes to aid in recovery and identification of functionally dominant 2,4-dichlorophenoxyacetic acid-degrading populations in soil. Appl. Environ. Microbiol. **60:**1116–1120.
24. **Kamagata, Y., R. R. Fulthorpe, K. Tamura, H. Takami, L. J. Forney, and J. M. Tiedje.** 1997. Pristine environments harbor a new group of oligotrophic 2,4-dichlorophenoxyacetic acid-degrading bacteria. Appl. Environ. Microbiol. **63:**2266–2272.
25. **Kaphammer, B., J. J. Kukor, and R. H. Olsen.** 1990. Regulation of *tfdCDEF* by *tfdR* of the 2,4-dichlorophenoxyacetic acid degradation plasmid pJP4. J. Bacteriol. **172:**2280–2286.
26. **Kaphammer, B., and R. H. Olsen.** 1990. Cloning and characterization of *tfdS*, the repressor-activator gene of *tfdB*, from the 2,4-dichlorophenoxyacetic acid catabolic plasmid pJP4. J. Bacteriol. **172:**5856–5862.
27. **Kellogg, S. T., D. K. Chatterjee, and A. M. Chakrabarty.** 1981. Plasmid-assisted molecular breeding: new technique for enhanced biodegradation of persistent toxic chemicals. Science **214:**1133–1135.
28. **Kitagawa, W., K. Miyauchi, E. Masai, and M. Fukuda.** 2001. Cloning and characterization of benzoate catabolic genes in the gram-positive polychlorinated biphenyl degrader *Rhodococcus* sp. strain RHA1. J. Bacteriol. **183:** 6598–6606.
29. **Knauf, V. C., and E. W. Nester.** 1982. Wide host range cloning vectors: a cosmid clone bank of an *Agrobacterium* Ti plasmid. Plasmid **8:**45–54.
30. **Kolv, V., R. Marits, and A. Heinaru.** 1996. Sequence analysis of the 2,4-dichlorophenol hydroxylase gene *tfdB* and 3,5-dichlorocatechol 1,2-dioxygenase gene *tfdC* of 2,4-dichlorophenoxyacetic acid degrading plasmid pEST4011. Gene **174:**293–297.
31. **Komeda, H., Y. Hori, M. Kobayashi, and S. Shimizu.** 1996. Transcriptional regulation of the *Rhodococcus rhodochrous* J1 *nitA* gene encoding a nitrilase. Proc. Natl. Acad. Sci. USA. **93:**10572–10577.
32. **Laemmli, C. M., J. H. J. Leveau, A. J. B. Zehnder, and J. R. van der Meer.** 2000. Characterization of a second *tfd* gene cluster for chlorophenol and chlorocatechol metabolism on plasmid pJP4 in *Ralstonia eutropha* JMP134(pJP4). J. Bacteriol. **182:**4165–4172.
33. **Leveau, J. H., F. Konig, H. Fuchslin, C. Werlen, and J. R. van der Meer.** 1999. Dynamics of multigene expression during catabolic adaptation of *Ralstonia eutropha* JMP134 (pJP4) to the herbicide 2,4-dichlorophenoxyacetate. Mol. Microbiol. **33:**396–406.
34. **Leveau, J. H., and J. R. van der Meer.** 1997. Genetic characterization of insertion sequence ISJP4 on plasmid pJP4 from *Ralstonia eutropha* JMP134. Gene **202:**103–114.
35. **Leveau, J. H. J., A. J. B. Zehnder, and J. R. van der Meer.** 1998. The *tfdK* gene product facilitates uptake of 2,4-dichlorophenoxyacetate by *Ralstonia eutropha* JMP134(pJP4). J. Bacteriol. **180:**2237–2243.
36. **Masai, E., K. Sugiyama, N. Iwashita, S. Shimizu, J. E. Hauschild, T. Hatta, K. Kimbara, K. Yano, and M. Fukuda.** 1997. The *bphDEF* meta-cleavage pathway genes involved in biphenyl/polychlorinated biphenyl degradation are located on a linear plasmid and separated from the initial *bphACB* genes in *Rhodococcus* sp. strain RHA1. Gene **187:**141–149.
37. **Masai, E., A. Yamada, J. M. Healy, T. Hatta, K. Kimbara, M. Fukuda, and K. Yano.** 1995. Characterization of biphenyl catabolic genes of gram-positive polychlorinated biphenyl degrader *Rhodococcus* sp. strain RHA1. Appl. Environ. Microbiol. **61:**2079–2085.
38. **Matrubutham, U., and A. R. Harker.** 1994. Analysis of duplicated gene sequences associated with *tfdR* and *tfdS* in *Alcaligenes eutrophus* JMP134. J. Bacteriol. **176:**2348–2353.
39. **Nagy, I., G. Schoofs, F. Compernolle, P. Proost, J. Vanderleyden, and R. De Mot.** 1995. Degradation of the thiocarbamate herbicide EPTC (*S*-ethyl dipropylcarbamothioate) and biosafening by *Rhodococcus* sp. strain NI86/21 involve an inducible cytochrome P-450 system and aldehyde dehydrogenase. J. Bacteriol. **177:**676–687.
40. **Neidle, E. L., C. Hartnett, L. N. Ornston, A. Bairoch, M. Rekik, and S. Harayama.** 1991. Nucleotide sequences of the *Acinetobacter calcoaceticus benABC* genes for benzoate 1,2-dioxygenase reveal evolutionary relationships among multicomponent oxygenases. J. Bacteriol. **173:**5385–5395.
41. **Pérez-Pantoja, D., L. Guzmán, M. Manzano, D. H. Pieper, and B. González.** 2000. Role of $tfdC_ID_IE_IF_I$ and $tfdD_{II}C_{II}E_{II}F_{II}$ gene modules in catabolism of 3-chlorobenzoate by *Ralstonia eutropha* JMP134(pJP4). Appl. Environ. Microbiol. **66:**1602–1608.
42. **Perkins, E. J., G. W. Bolton, M. P. Gordon, and P. F. Lurquin.** 1988. Partial nucleotide sequence of the chlorocatechol degradative operon *tfdCDEF* of pJP4 and similarity to promoters of the chlorinated aromatic degradative operons *tfdA* and *cleABD*. Nucleic Acids Res. **16:**7200.
43. **Perkins, E. J., M. P. Gordon, O. Caceres, and P. F. Lurquin.** 1990. Organization and sequence analysis of the 2,4-dichlorophenol hydroxylase and dichlorocatechol oxidative operons of plasmid pJP4. J. Bacteriol. **172:**2351–2359.
44. **Peterson, J. A., M. C. Lorence, and B. Amarneh.** 1990. Putidaredoxin reductase and putidaredoxin. Cloning, sequence determination, and heterologous expression of the proteins. J. Biol. Chem. **265:**6066–6073.
45. **Ruvkun, G. B., and F. M. Ausubel.** 1981. A general method for site-directed mutagenesis in prokaryotes. Nature **289:**85–88.
46. **Sambrook, J., E. F. Fritsch, and T. Maniatis.** 1989. Molecular cloning: a laboratry manual, 2nd ed. Cold Spring Harbor Laboratory Press, Cold Spring Harbor, N.Y.
47. **Seto, M., K. Kimbara, M. Shimura, T. Hatta, M. Fukuda, and K. Yano.** 1995. A novel transformation of polychlorinated biphenyls by *Rhodococcus* sp. strain RHA1. Appl. Environ. Microbiol. **61:**3353–3358.
48. **Streber, W. R., K. N. Timmis, and M. H. Zenk.** 1987. Analysis, cloning, and high-level expression of 2,4-dichlorophenoxyacetate monooxygenase gene *tfdA* of *Alcaligenes eutrophus* JMP134. J. Bacteriol. **169:**2950–2955.
49. **Sutton, B. C. S., J. Stanley, M. G. Zelechowska, and D. P. S. Verma.** 1984. Isolation and expression of *Rhizobium japonicum* cloned DNA encoding an early soybean nodulation function. J. Bacteriol. **158:**920–927.
50. **Suwa, Y., A. D. Wright, F. Fukimori, K. A. Nummy, R. P. Hausinger, W. E. Holben, and L. J. Forney.** 1996. Characterization of a chromosomally encoded 2,4-dichlorophenoxyacetic acid/α-ketoglutarate dioxygenase from *Burkholderia* sp. strain RASC. Appl. Environ. Microbiol. **62:**2464–2469.
51. **Xun, L., and K. B. Wagnon.** 1995. Purification and properties of component B of 2,4,5-trichlorophenoxyacetate oxygenase from *Pseudomonas cepacia* AC1100. Appl. Environ. Microbiol. **61:**3499–3502.
52. **Yamada, A., H. Kishi, K. Sugiyama, T. Hatta, K. Nakamura, E. Masai, and M. Fukuda.** 1998. Two nearly identical aromatic compound hydrolase genes in a strong polychlorinated biphenyl degrader, *Rhodococcus* sp. strain RHA1. Appl. Environ. Microbiol. **64:**2006–2012.

Downloaded from http://jb.asm.org/ on September 3, 2020 at Corteva Agriscience

COR-AAD1-00002613
Bayer EX1008 (Part 5 of 9)

Extremophiles (2001) 5:375–384
Digital Object Identifier (DOI) 10.1007/s007920100202
© Springer-Verlag 2001

ORIGINAL PAPER

Sabine Kleinsteuber · Roland H. Müller · Wolfgang Babel

Expression of the 2,4-D degradative pathway of pJP4 in an alkaliphilic, moderately halophilic soda lake isolate, *Halomonas* sp. EF43

Received: October 16, 2000 / Accepted: April 20, 2001 / Published online: October 6, 2001

Abstract The broad host range plasmid pJP4, which carries genes for the degradation of 2,4-dichlorophenoxyacetic acid (2,4-D), 2-methyl-4-chlorophenoxyacetic acid, and 3-chlorobenzoic acid, was used in conjugation experiments with mixed cultures enriched from water and sediment samples from an alkaline pond in the area of Szegedi Fehértó, a soda lake in south Hungary. pJP4-encoded mercury resistance was used as a selection marker. One of the transconjugants, the alkaliphilic, moderately halophilic strain EF43, stably maintained the plasmid and was able to degrade 2,4-D and 3-chlorobenzoate under alkaline conditions in the presence of an additional carbon source such as pyruvate, benzoate, or α-ketoglutarate, indicating that the degradative genes of pJP4 were expressed in this strain. However, it was unable to grow on these chloroaromatic substrates when the substrate was the sole source of carbon and energy. Chemostat cultivation experiments revealed that the 2,4-D degradation rate during growth on benzoate or pyruvate was limited by the low activity of chlorocatechol-degrading enzymes, particularly chloromuconate cycloisomerase. Strain EF43 was identified as *Halomonas* sp. on the basis of 16S rRNA sequencing and additional taxonomic studies. 16S rRNA sequence analysis revealed that strain EF43 is closely related to typical soda lake isolates belonging to the genus *Halomonas*.

Key words Alkaliphiles · Halophiles · *Halomonas* · 2,4-D · Degradation of chloroaromatic compounds · Conjugative transfer · pJP4

Communicated by W.D. Grant

S. Kleinsteuber (✉) · R.H. Müller · W. Babel
UFZ Centre for Environmental Research, Department of Environmental Microbiology, Permoserstrasse 15, D-04318 Leipzig, Germany
Tel. +49-341-2352191; Fax +49-341-2352247
e-mail: kleinst@umb.ufz.de

Introduction

Alkaliphilic bacteria have been extensively studied with regard to their biotechnologically relevant extracellular enzymes (for reviews, see Grant et al. 1990; Horikoshi 1996) and as model organisms to solve bioenergetic problems (for reviews, see Krulwich et al. 1988; Krulwich and Guffanti 1992; Hicks and Krulwich 1995; Krulwich 1995). However, little is known about their capabilities of detoxifying xenobiotics. One special problem in this context is toxic residues in pesticide factories and microbial decontamination of building rubble after their demolition, since aqueous eluates from building rubble are highly alkaline. Microbes degrading xenobiotics in such inhospitable environments must be adapted both to extreme pH values and toxic substrates. There are a few examples of bacterial strains isolated from contaminated building rubble that are capable of degrading xenobiotics such as phenoxyalkanoic acid herbicides (Hoffmann et al. 1996; Ehrig et al. 1997; Mertingk et al. 1998; Müller et al. 1999) or chlorophenols (Müller et al. 1998) under alkaline conditions. However, bacteria isolated from naturally occurring alkaline environments and degrading xenobiotics have rarely been described (Maltseva et al. 1996; Kanekar et al. 1999). The most stable naturally occurring alkaline environments are soda lakes with pH values up to 11.5. They are located in areas characterized by a unique combination of geological, geographical, and climatic conditions that diminish the significant buffering capacity of atmospheric CO_2 by the evaporative concentration of sodium carbonate (Grant and Tindall 1986; Grant 1992).

Genes for the degradation of xenobiotics are often located on transmissible plasmids. Whereas the horizontal intergeneric exchange of degradative genes and the dissemination of catabolic plasmids as a means of enhancing the degradative potential of microbial communities are well described for soil ecosystems (Short et al. 1991; Neilson et al. 1994; Hong et al. 1995; Ingham et al. 1995; DiGiovanni et al. 1996; Top et al. 1998; Newby et al. 2000), little is known about these mechanisms in alkaline environments or about the taxa with degradative capabilities in such ecosystems. One of the best characterized catabolic plasmids is the broad host range

COR-AAD1-00002614
Bayer EX1008 (Part 5 of 9)

IncP1 plasmid pJP4 from *Ralstonia eutropha* JMP134, which encodes the pathway for the degradation of the chlorinated aromatic compounds 2,4-dichlorophenoxyacetate (2,4-D), 2-methyl-4-chlorophenoxyacetate (MCPA), and 3-chlorobenzoate, and confers resistance to mercury ions (Pemberton et al. 1979; Don and Pemberton 1981). Although it is known to be transmissible in bacteria of various genera, the taxonomic range on which pJP4 confers the ability to grow on 2,4-D or 3-chlorobenzoate is narrower than its host range (Don and Pemberton 1981; Friedrich et al. 1983; Neilson et al. 1994; Feng et al. 1994; DiGiovanni et al. 1996; Newby et al. 2000). The 2,4-D degradation pathway of pJP4 is well understood, the enzymes participating in the pathway have been purified and characterized (Pieper et al. 1988; Kuhm et al. 1990; Fukumori and Hausinger 1993; Seibert et al. 1993; Farhana and New 1997), the genes encoding these enzymes (*tfd* genes) have been localized, cloned, and sequenced (Don et al. 1985; Streber et al. 1987; Perkins et al. 1990; Matrubutham and Harker 1994; Kasberg et al. 1995; Leveau et al. 1998), and the regulatory mechanisms of *tfd* gene expression have been elucidated (You and Ghosal 1995; Leveau and van der Meer 1996; Filer and Harker 1997; Leveau et al. 1999; Pérez-Pantoja et al. 2000; Laemmli et al. 2000).

We used the plasmid pJP4 as a model system to elucidate the adaptive potential of bacteria from pristine alkaline environments to toxic substrates such as 2,4-D. Our objective was to ascertain whether conjugative transfer of plasmid pJP4 into soda lake isolates enables the 2,4-D degradative trait to be established in these isolates under alkaline conditions.

Materials and methods

Sample collection and enrichment

Water and sediment samples were collected from an alkaline pond in the area of Szegedi Fehértó, a soda lake near Szeged in south Hungary. The chemical parameters of the water sample were as follows: pH 9.1; conductivity 6.34 mS/cm; Na^+ 1,499 mg/l; HCO_3^- 1,371 mg/l; CO_3^{2-} 393 mg/l; Cl^- 470 mg/l.

Alkaline mineral medium (AMM), pH 10 (modified according to Maltseva et al. 1996) was prepared by mixing sterile component A (20 g Na_2CO_3 and 20 g $NaHCO_3$ in 300 ml H_2O), component B [10 g NaCl, 3 g KCl, 0.5 g NH_4NO_3, 0.3 g $(NH_4)_2SO_4$, 0.4 g $MgSO_4$, 0.3 g NaH_2PO_4, and trace elements (Imhoff and Trüper 1977) in 700 ml H_2O], and the vitamin solution DSM 141. Enrichment cultures for 2,4-D-degrading bacteria were grown in AMM supplemented with 100 mg/l yeast extract or 5 mM α-ketoglutarate, and 0.5 mM 2,4-D. 2,4-D concentration was measured by HPLC. Aerobic chemoorganotrophic bacteria were enriched in AMM supplemented with 10 mM succinate as a carbon source. Cultivation was performed in 500 ml shaking flasks on a rotary shaker at 200 rpm and 30°C.

Mating and screening of transconjugants

Equal volumes of the succinate-grown enrichment cultures and LB-grown cultures of *Escherichia coli* HB101 harboring pJP4 were harvested, washed in 100 mM Tris-HCl, pH 8.5, and spread together on R2A agar plates buffered with 100 mM Tris-HCl, pH 8.5, and containing 1% (w/v) NaCl. Control plates were inoculated with either the donor or the recipient. After overnight incubation at 30°C, cells were harvested from the plates, diluted in AMM, and spread on AMM agar plates containing 10 mM succinate and 0.1 mM $HgCl_2$. After 2–3 days' incubation at 30°C, the resulting mercury-resistant colonies were picked and transferred onto fresh selection plates. The biomass of the presumptive transconjugants was boiled in sterilized water and centrifuged, and then 5 µl of the supernatants was transferred onto a nylon membrane together with control DNA from *Ralstonia eutropha* JMP134 (pJP4) and *R. eutropha* JMP222 (a plasmid-free derivative of JMP134). A pJP4-specific *tfdC* probe was prepared and digoxygenin-labeled as described by Kleinsteuber et al. (1998). Dot blot hybridization with the *tfdC* probe was performed at 55°C, and hybridization and detection were done as described elsewhere (Kleinsteuber et al. 1998). *tfdC*-positive clones were further screened for the presence of plasmid pJP4 using the plasmid minipreparation method described by Müller et al. (1998). Plasmid DNA was separated in 0.6% agarose gels, blotted onto nylon membrane using standard procedures (Sambrook et al. 1989), and hybridized at 60°C to a digoxygenin-labeled *tfdB* probe, which had been prepared by polymerase chain reaction (PCR) from pJP4 DNA by applying *tfdB*-specific primers (Vallaeys et al. 1996). PCR, purification, and labeling of the PCR products, as well as hybridization and detection, were performed as described by Kleinsteuber et al. (1998).

Degradation tests

To screen the degradation properties of transconjugants, cells grown on succinate overnight were harvested by centrifugation, washed in AMM, and resuspended in 3 ml fresh AMM (pH 10) with 0.5 to 1 mM 2,4-D, 50 mg/l yeast extract, and, additionally, 5 µg/l ferrous sulfate. For degradation tests at pH 8.5, component A of AMM was omitted and Tris-HCl, pH 8.5, was added to a final concentration of 100 mM, and NaCl was added to an equimolar sodium ion concentration. After 6–10 days' incubation at 30°C, the decrease in 2,4-D concentration in comparison to a sterile control was determined by HPLC.

Further degradation tests with strain EF43 were performed in 100-ml batch cultures at 30°C and 200 rpm with alkaline R2A medium (buffered with 20 g/l Na_2CO_3 and 20 g/l $NaHCO_3$) or AMM, supplemented with 0.5 mM 2,4-D or 3-chlorobenzoate, respectively. Additional carbon sources were added to a final concentration of 5 mM. The concentration of 2,4-D or 3-chlorobenzoate was measured by HPLC and compared with the sterile controls.

COR-AAD1-00002615
Bayer EX1008 (Part 5 of 9)

Chemostat cultivation and growth analysis

Continuous cultivation was performed in a 1-l laboratory fermenter under aerobic conditions at 30°C and pH 9.0. AMM without component A but containing 35 g/l NaCl instead was used. Either 10 mM sodium benzoate or 15 mM sodium pyruvate was supplied as the growth substrate, and for each growth substrate, experiments were done both with and without 5 mM 2,4-D and with and without 5 mM 3-chlorobenzoate. The biomass concentration was determined by measuring the optical density at 700 nm (OD_{700}) and by the dry mass determination of washed cells. Off-gas was monitored by a Maihak UNOR 6N and OXOR 6N analyzer (Maihak, Hamburg, Germany) at a gas flow rate of 70 l/h. Total inorganic carbon (TIC) and organic carbon (TOC) were determined from the cell-free supernatant of the culture broth by a high-TOC analyzer (Elementar, Hanau, Germany) at 1,050°C in TIC/nonpurgeable organic carbon mode. The carbon content of biomass was obtained from a CHN-1000 analyzer (Leco, St. Joseph, MI, USA) from washed cells dried overnight at 105°C.

The pH-dependency of growth was determined from continuous cultivation using the method of Esener et al. (1981). The culture was chemostatically precultivated on benzoate at a rate of 0.35 h^{-1} at pH 8.5. Maximum growth rates were derived from biomass decay characteristics at supercritical dilution rates. The maximum rates at the various pH values were consecutively determined after having exposed the culture to the individual pH values for about 2 h by continuously feeding the growth medium at appropriate rates.

The stability of plasmid pJP4 during chemostatic cultivation was verified by plasmid preparation using the Nucleobond AX100 kit (Macherey-Nagel, Düren, Germany), applying the protocol for the isolation of low copy number plasmids.

Determination of enzyme activities

2,4-D/α-ketoglutarate dioxygenase was determined according to Fukumori and Hausinger (1993) by colorimetrically measuring the liberation of 2,4-dichlorophenol after reaction with 4-aminoantipyrin. Catechol 1,2-dioxygenases I and II were determined using the method of Nakazawa and Nakazawa (1970) by determining the formation of the *cis,cis*-muconic acid derivatives using catechol or 3,5-dichlorocatechol, respectively, as the substrate. Catechol 2,3-dioxygenase was determined by the method of Nozaki (1970) by monitoring the formation of 2-hydroxymuconic acid semialdehyde. *cis,cis*-Muconate cycloisomerase was assayed according to Schmidt and Knackmuss (1980) by applying 3,5-dichlorocatechol and the partially purified type II catechol 1,2-dioxygenase (kindly provided by M. Schlömann, University of Stuttgart) in order to generate the 2,4-dichloro-*cis,cis*-muconic acid derivative in a precultivation phase; the activity was calculated by using an extinction coefficient of 9,700 l/mol cm (Dorn and Knackmuss 1978). Benzoate dioxygenase and 2,4-dichlorophenol hydroxylase were measured respirometrically in the presence of 1 mM substrate. The enzyme activities were measured at 30°C and are given in μmol/min mg protein (U/mg).

Microbiological characterization and identification

Gram behavior was determined by the KOH test (Ryu 1938). The GC content of DNA was measured by HPLC according to Mesbah et al. (1989). Cellular fatty acids were determined after methylation by gas chromatography as described by Loffhagen et al. (1995) using the MIS automated microbial identification system (MIDI, Barksdale Professional Center, Newark, NJ, USA) after growth of the strain on R2A agar (3.5% NaCl) at 28°C. Substrate utilization patterns and additional metabolic characteristics were determined using the Biolog automated microbial identification system (Biolog, Hayward, CA, USA), and the API 20 identification kit (Biomérieux, Marcy-l'Ecole, France) according to the suppliers' recommendations with the difference that the cells were resuspended in 3% (w/v) NaCl solution.

The salt dependency of growth was determined in R2A medium containing various concentrations of NaCl in the range of 0%–25% (w/v), corresponding to 0.02–4.3 M total sodium ion concentration. Specific growth rates under various salt concentrations were analyzed during exponential growth in batch cultures by linear regression of the logarithm of OD_{700} with time.

Sequencing of the 16S rDNA was performed as described by Müller et al. (1999). The BLASTN program (http://www.ncbi.nlm.nih.gov/blast/; version 2.0; Altschul et al. 1990) was used to search for similar sequences in the nucleotide sequence databases, and the Sequence Match tool (version 2.7) was used to search for similar sequences in the Ribosomal Database Project II (http://rdp.cme.msu.edu/html/; Maidak et al. 1999). The sequence of the 16S rDNA of strain EF43 will appear in the GenBank, EMBL, and DDBJ nucleotide sequence databases under accession No. AF280796. Phylogenetic analysis was performed using the ARB package (http://www.arb-home.de/). A phylogenetic tree was reconstructed from the 16S rRNA sequences of strain EF43, its 38 closest relatives within the ARB database, and two additional 16S rRNA sequences from GenBank (Acc. Nos. AJ133761, AF140007). The sequences of strain EF43 and the two additional sequences were aligned to the 16S rRNA sequences of the ARB database by the ARB editor, the alignment was corrected manually, and a tree was reconstructed from all 41 sequences using the fastDNAml tool.

Results

Conjugative transfer of pJP4 into soda lake alkaliphiles and characterization of transconjugants

Aerobic chemoorganotrophic bacteria growing on succinate as the sole source of carbon and energy were enriched

COR-AAD1-00002616
Bayer EX1008 (Part 5 of 9)

from the water and sediment samples under alkaline conditions (pH 10). Direct enrichments of 2,4-D-degrading bacteria did not even succeed in the presence of α-ketoglutarate as an additional carbon source. The succinate-grown mixed bacterial cultures were mated with *E. coli* HB101 as donor of the plasmid pJP4 using the plasmid-encoded mercury resistance as the selection marker. Transconjugants were selected on mercury-containing AMM agar (pH 10), where *E. coli* is unable to grow. Although mercury-resistant bacteria were already present in the recipient mixed cultures as indicated by control plating, the number of colonies growing on the transconjugant selection plates was significantly higher. In order to confirm that mercury-resistant colonies were actually transconjugants, they were screened by dot blot hybridization with a pJP4-specific *tfdC* probe. In total, 842 clones were tested, of which 762 clones were *tfdC*-positive.

Plasmid profiles of 454 transconjugants were analyzed by isolating the plasmid DNA from succinate-grown cultures, agarose gel electrophoresis, and Southern hybridization with a pJP4-derived *tfdB* probe to detect homology of plasmid bands to pJP4. Of the 454 transconjugants, 403 clones carried a plasmid of about 80 kb, which corresponds to the size of pJP4. All these plasmids hybridized to the *tfdB* probe under stringent conditions. No plasmid was detected in 27 clones, and 24 clones showed plasmid bands smaller than 80 kb. One of these plasmids hybridized to the *tfdB* probe under stringent conditions, indicating that it was a deletion derivative of pJP4. However, with the other smaller plasmids no *tfdB* signals were detected, indicating that they were not pJP4 derivatives. Nevertheless, it cannot be ruled out that the catabolic region of pJP4 was deleted in these clones. Thirty-five isolates exhibited multiple plasmid bands of various sizes, not hybridizing even to the entire pJP4, indicating that these isolates carry indigenous plasmids.

Only with 32 of the 762 transconjugants tested was a decrease of at least 10 mg/l 2,4-D, in comparison with the sterile control, detected after 6–10 days' incubation at 30°C. No significant differences in the degradative behavior of the isolates were detected at pH 10 or pH 8.5. None of the transconjugants was able to degrade the 2,4-D completely or to grow on 2,4-D as the sole carbon source, although no toxic intermediates such as 2,4-dichlorophenol were detected. However, a significant decrease in 2,4-D was observed with a few isolates during growth on α-ketoglutarate or pyruvate. One of these isolates, strain EF43, was further investigated regarding its degradative properties as well as its microbiological and physiological characteristics.

Taxonomic characterization of strain EF43

After growth on alkaline R2A agar, strain EF43 forms round convex colonies of 1–2 mm diameter, faintly bright and white to cream-colored. The cells are strongly motile, straight rods and have a length of 1.4–1.7 µm and a diameter of 0.8 µm. They are Gram-negative and show positive reactions for oxidase, catalase, and nitrate reduction. The following composition of cellular fatty acids was determined: 10:0 (4.7%), 12:0 (4.8%), 12:0 3OH (9.4%), 16:1 ω7c (12.8%), 16:0 (12.5%), 17:0 cyclo (2.7%), 18:1 ω7c (49.9%), and 19:0 cyclo ω8c (3.2%). The GC content of the DNA was 67.5 mol%. Concerning the substrate utilization pattern, the Biolog automated microbial identification system identified strain EF43 as *Halomonas aquamarina* with a similarity index of 0.550. Positive reactions were obtained with respect to the utilization of α-ketoglutaric acid, DL-lactic acid, succinamic acid, mono-methylsuccinic acid, succinic acid, β-hydroxybutyric acid, L-glutamic acid, L-proline, L-serine, and L-alanine.

Strain EF43 is able to grow over a wide range of salt concentrations: growth was observed in R2A medium containing 1%–15% (w/v) NaCl. No growth was observed above 20% NaCl. Sodium ions are required for growth. The optimal sodium ion concentration for growth was 0.4–0.8 M. The influence of pH on the growth of strain EF43 was determined in mineral medium at optimal sodium ion concentration (about 0.6 M NaCl) and with benzoate as the growth substrate. The strain has a broad pH optimum (8.5–10). Although the specific growth rate significantly decreases below pH 8 and above pH 10.6, in rich medium (R2A) it also grows at neutral pH. According to its growth characteristics with respect to salt content and pH value, strain EF43 is an alkaliphilic, moderately halophilic bacterium.

The nucleotide sequence of the nearly complete 16S rRNA gene (1488 bp) was determined. As calculated by BLAST, the 16S rRNA sequence of strain EF43 shows 97% similarity to the 16S rRNA sequences of Crater Lake isolate 12C1 (Acc. No. X92135) and of Lake Elmenteita isolate WE5 (Acc. No. X92140), two soda lake isolates from the East African Rift Valley (Duckworth et al. 1996), and 97% similarity to the 16S rRNA sequences of *Halomonas* sp. isolate Co12 (Acc. No. AJ133761), a marine isolate, and of *Halomonas* sp. ML-185 (Acc. No. AF140007), a soda lake isolate from Mono Lake, California. The closest relative in the Ribosomal Database Project was *Halomonas salina*^{T} ATCC 49509 with a similarity score of 0.848. A phylogenetic tree was reconstructed by the maximum likelihood method from the 16S rRNA sequences of strain EF43 and its 38 closest relatives from the ARB database and of strains *Halomonas* sp. isolate Co12 and *Halomonas* sp. ML-185 (Fig. 1). The tree clearly shows that strain EF43 clusters within the genus *Halomonas* and that it is closely related to the soda lake isolates *Halomonas* sp. ML-185 (Mono Lake isolate), Crater Lake isolate 12C1 and Lake Elmenteita isolate WE5, as well as to some other East African soda lake isolates (Duckworth et al. 1996). The 16S rRNA sequence of strain EF43 contains all 15 signature features characteristic of the family *Halomonadaceae* and the additional 4 signature features characteristic of the genus *Halomonas* (Dobson and Franzmann 1996). By virtue of its taxonomic characteristics and the phylogenetic analysis, strain EF43 was identified as *Halomonas* sp.

Degradative properties and physiological characteristics of strain EF43

Degradation tests in batch cultures revealed that strain EF43 is able to degrade 2,4-D and 3-chlorobenzoate during

COR-AAD1-00002617
Bayer EX1008 (Part 5 of 9)

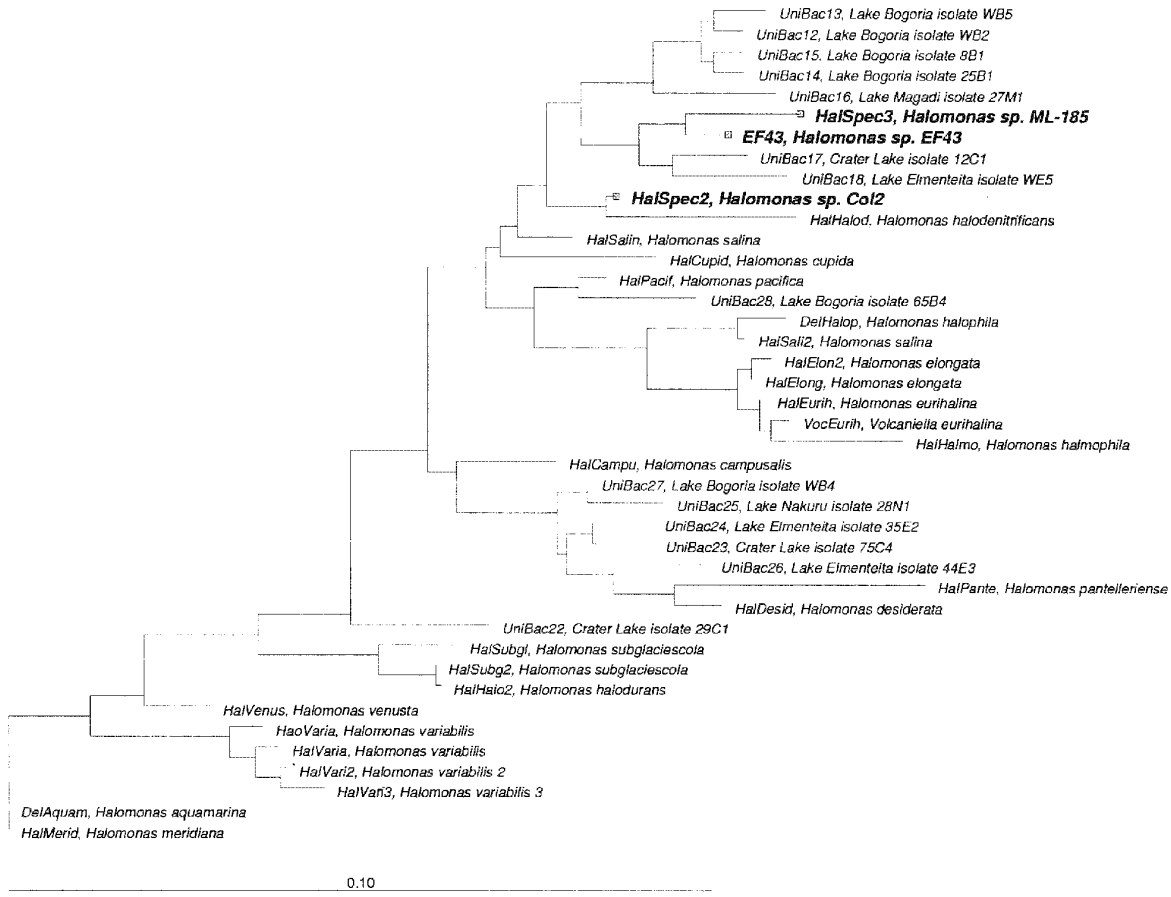


Fig. 1. Phylogenetic tree showing the relationship between strain EF43 and its closest relatives. The 16S rRNA sequences added to the ARB database are shown in *bold*

growth on pyruvate, α-ketoglutarate, or benzoate (Figs. 2A, 3A). In the presence of pyruvate as growth substrate, the degradation of 0.5 mM 3-chlorobenzoate was virtually complete within 24 h (Fig. 3A). By contrast, during growth on acetate or succinate as well as in the absence of an additional carbon source, only slight or no degradation was measured (Figs. 2B, 3B). Degradation of 3-chlorobenzoate was completely inhibited when the strain grew on succinate (Fig. 3B). Although no intermediates such as 2,4-dichlorophenol were detected during the degradation of 2,4-D, during the degradation of 3-chlorobenzoate, the media became brown colored, which might have been due to the accumulation of an oxidized polymer of the intermediate 3-chlorocatechol.

The results obtained with batch incubation were confirmed by chemostat cultivation of strain EF43 on 2,4-D or 3-chlorobenzoate with benzoate or pyruvate as the growth substrates. A considerable amount of the chloroaromatics was utilized under these conditions in the presence of either of the substrates. In the case of benzoate, the amount was 77% of the carbon from 2,4-D as follows from the carbon balances, i.e., from the difference between the total carbon fed during growth on benzoate or benzoate + 2,4-D (2.0 mMolC/h) and the difference between the TOC values during growth on benzoate or benzoate + 2,4-D (0.46 mMolC/h) (Table 1). The utilization of 2,4-D had little effect on the biomass gain; moreover, the overall growth yield on the basis of C-moles was significantly diminished in the presence of 2,4-D as compared with that on growth substrate alone (Table 1). Utilization of the growth substrates proceeded with rather low efficiency: from the biomass yield, the efficiency of energy transduction with benzoate and pyruvate was calculated to have an apparent P/O coefficient of 1.29 and 1.15, respectively (for more details on the calculations see Müller and Babel 1994).

Steady states were characterized by rather high stationary 2,4-D concentrations even at comparatively low growth rates (the maximum growth rate was $\mu_{max} = 0.45\ h^{-1}$ for benzoate at pH 9). In addition, a product appeared in HPLC measurements with both UV and RI (refractive index) detection, which coeluted in HPLC measurements with the product formed by incubating 3,5-dichlorocatechol with catechol 1,2-dioxygenase type II. However, whether this compound is identical to 2,4-dichloro-*cis,cis*-muconate remains

COR-AAD1-00002618
Bayer EX1008 (Part 5 of 9)

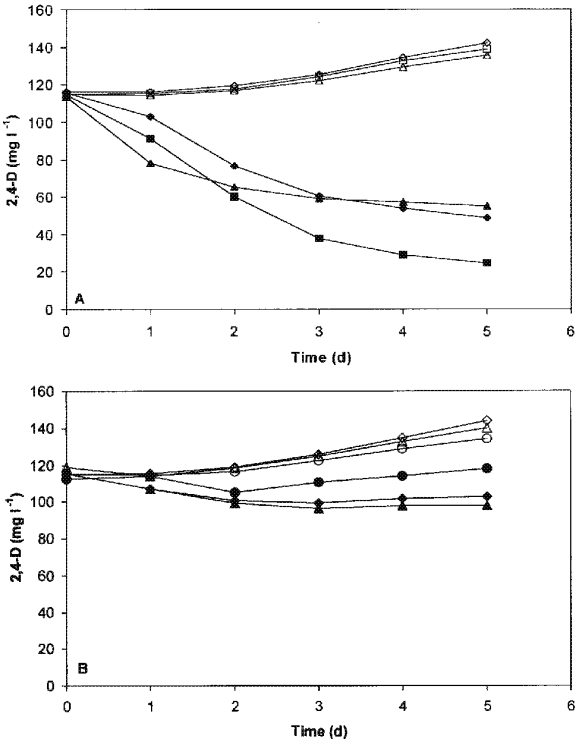


Fig. 2A,B. Degradation of 2,4-dichlorophenoxyacetate (*2,4-D*) by strain EF43 in alkaline mineral medium (pH 10) in the presence of various carbon sources (*open symbols*: sterile control; *filled symbols*: strain EF43). **A** 2,4-D degradation during growth on 5 mM α-ketoglutarate (*solid triangles*), 5 mM benzoate (*solid diamonds*), and 5 mM pyruvate (*solid squares*). **B** 2,4-D degradation without an additional carbon source (*solid circles*), during growth on 5 mM succinate (*solid diamonds*), and during growth on 5 mM acetate (*solid triangles*)

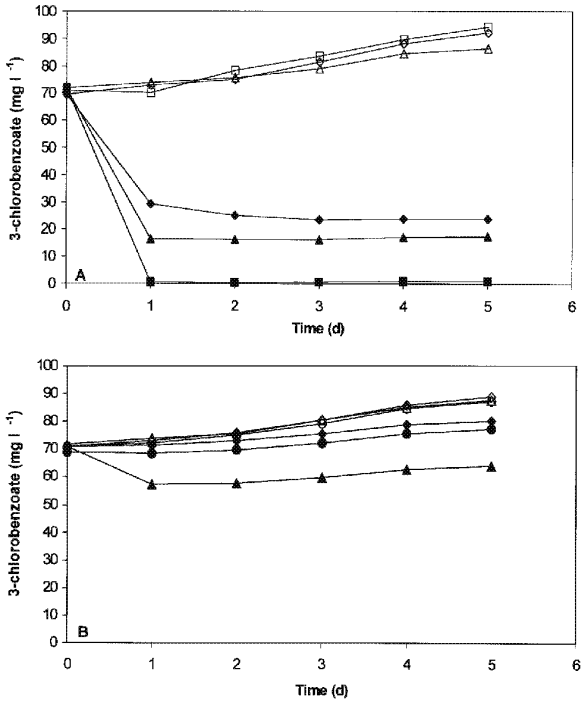


Fig. 3A,B. Degradation of 3-chlorobenzoate by strain EF43 in alkaline mineral medium (pH 10) in the presence of various carbon sources (*open symbols*: sterile control; *filled symbols*: strain EF43). **A** 3-chlorobenzoate degradation during growth on 5 mM α-ketoglutarate (*solid triangles*), 5 mM benzoate (*solid diamonds*), and 5 mM pyruvate (*solid squares*). **B** 3-chlorobenzoate degradation without an additional carbon source (*solid circles*), during growth on 5 mM succinate (*solid diamonds*), and during growth on 5 mM acetate (*solid triangles*)

Table 1. Growth parameters and distribution of carbon during chemostat cultivation of strain EF43 on heterotrophic substrates and substrate mixtures

Substrate(s)	D (h^{-1})	Dry wt (g/l)	Y (Cmol/Cmol)	2,4-D (mM)	DCP	C_{feed} (mMolC/h)	$C_{Dry\ wt}$ (mMolC/h)	CO_2	TOC	TIC	Σ	%
10 mM Benzoate	0.05	0.623	0.313	–	–	3.5	1.06	1.81	0.12	0.46	3.45	98.6
10 mM Benzoate+5 mM 2,4-D	0.05	0.648	0.215	1	→ 0	5.5	1.06	2.25	0.58	1.38	5.27	95.8
15 mM Pyruvate	0.05	0.426	0.27	–	–	2.25	0.5	0.68	0.4	0.5	2.08	92.4
15 mM Pyruvate+5 mM 2,4-D	0.035	0.519	0.182	0.55	→ 0	2.975	0.46	1.475	0.45	0.49	2.875	96.6

Y, growth yield coefficient; C_{feed}, substrate carbon fed; 2,4-D, 2,4,-dichlorophenoxyacetate; TOC, organic carbon in cell-free supernatant of fermentation broth; TIC, inorganic carbon in cell-free supernatant of fermentation broth, corrected by concentrations of carbonate trapped from atmospheric CO_2 at pH 9; DCP, 2,4-dichlorophenol

to be proved by more detailed analyses. No accumulation of 2,4-dichlorophenol nor β-ketoadipate was detected by the application of references in HPLC analyses. A possible accumulation of chlorodienlactone or chloromaleylacetate was not investigated because these compounds were not available for application. The liberation of products during growth on substrate mixtures was supported by TOC measurements in the supernatants, which showed that the amount of carbon derived from stationary 2,4-D levels was lower than the total amount found in the culture broth (Table 1). The concentrations of benzoate and pyruvate themselves were below the detection limits in these cultures.

Enzyme activities with regard to 2,4-D metabolism were determined from chemostat cultures. From the results

COR-AAD1-00002619
Bayer EX1008 (Part 5 of 9)

Table 2. Enzyme activities (in µmol/min mg protein) for aromate degradation during growth on individual substrates and substrate mixtures

Enzyme	Assay substrate	Growth substrate(s) benzoate/2,4-D	Benzoate/ 3-CBA	Benzoate	Pyruvate/ 2,4-D	Pyruvate	JMP134[b]
2,4-D/α-ketoglutarate dioxygenase	2,4-D	0.127	0.06	<0.02	0.658	<0.02	0.105
Phenol hydroxylase	Phenol	0[a]	n.d.	n.d.	0[a]	0[a]	0.13
	2,4-Dichlorophenol	0.114	n.d.	n.d.	0.034	0.002	0.23
Catechol 1,2- dioxygenase	Catechol	12.1	6.145	5.0	4.9	0	0.49
	3,5-Dichlorocatechol	0.066	0.145	0	0.742	0	0.45
cis-cis-Muconate cycloisomerase	*cis,cis*-Muconate	0.195	0.6	0.475	0.26	n.d.	0.008
	2,4-Dichloro-*cis,cis*-muconate	0.046	0.03	0.0075	0.11	n.d.	0.39
Catechol 2,3- dioxygenase	Catechol	0	0	0	0	0	<0.001
Benzoate dioxygenase	Benzoate	0.322	0.12	0.124	n.d.	n.d.	

n.d., not determined; 3-CBA, 3-chlorobenzoic acid
[a] Inhibition of endogenous respiration after adding phenol
[b] After growth on 2,4-D (data from Pieper et al. 1988)

shown in Table 2, it is evident that high 2,4-D/α-ketoglutarate dioxygenase activities were expressed during cultivation in the presence of 2,4-D. In combination with benzoate, this activity was similar to that found in the natural host of pJP4, *R. eutropha* JMP134, during growth on 2,4-D, but was more than fivefold that after growth on pyruvate. High chlorocatechol 1,2-dioxygenase activity was found for growth on pyruvate in the presence of 2,4-D. By contrast, the enzyme for the next metabolic step of the modified *ortho* pathway, i.e., chloromuconate cycloisomerase, was expressed at a low level, the activity during growth on benzoate and 2,4-D being reduced to about 10% in comparison with *R. eutropha* JMP134 growing on 2,4-D. Catechol 2,3-dioxygenase activity initiating the *meta* cleavage pathway was not detected in strain EF43 (Table 2).

The stability of pJP4 was regularly verified by plasmid preparation during all chemostat cultivation experiments. The plasmid was shown to be stably maintained by strain EF43 in both the presence or the absence of 2,4-D or 3-chlorobenzoate.

Discussion

Taxonomic status

Based on its 16S rRNA sequence and additional taxonomic characteristics, strain EF43 was assigned to the genus *Halomonas*. This identification is supported by the presence of the 19 16S rRNA signature features characteristic of the genus *Halomonas* (Dobson and Franzmann 1996) and by the composition of the major fatty acids 18:1 plus 19:0 cyclo (53.1%), 16:1 plus 17:0 cyclo (15.5%), and 16:0 (12.5%), which is consistent with the major fatty acid composition of the genus *Halomonas* (Dobson and Franzmann 1996). This identification is further confirmed by physiological characteristics (sodium ion requirement, salt tolerance up to 20% NaCl and growth optimum at 0.6 M sodium ion concentration, nitrate reduction) and by the substrate utilization pattern. Strain EF43 grows on acetate, succinate, β-hydroxybutyrate, DL-lactate, and L-α-alanine, which were described as characteristic substrates of the genus *Deleya* (Balows et al. 1992), a genus which was unified with the genus *Halomonas* by Dobson and Franzmann (1996).

As indicated by the phylogenetic analysis, the closest relatives of strain EF43 are soda lake alkaliphiles (Duckworth et al. 1996) such as Crater Lake isolate 12C1 (Acc. No. X92135; 97% similarity) and Lake Elmenteita isolate WE5 (Acc. No. X92140; 97% similarity), which should also be assigned to the genus *Halomonas*, and the Mono Lake isolate *Halomonas* sp. ML-185 (Acc. No. AF140007; 97% similarity). 2,4-D degradation under alkaline conditions by members of the *Halomonadaceae* has been described previously (Maltseva et al. 1996). From these findings and our results, we conclude that the *Halomonadaceae* are potential degraders of chloroaromatic compounds in alkaline and saline environments, as was recently confirmed by conjugation experiments with a *gfp*-tagged pJP4 and soda lake isolates as recipients (Kleinsteuber et al. 2000).

Expression of the 2,4-D degradative pathway

The broad host range plasmid pJP4 encoding the 2,4-D degradative pathway of the neutrophilic bacterium *Ralstonia eutropha* JMP134 was successfully transferred into bacteria isolated from an alkaline environment and was shown to be stably maintained in the majority of transconjugants, indicating that the host range of this IncP1 plasmid also includes alkaliphiles. The degradative genes were expressed in at least some of the transconjugants, enabling them to degrade 2,4-D and 3-chlorobenzoate under alkaline conditions, as demonstrated with isolate EF43. However, the significant degradation of 2,4-D or 3-chlorobenzoate was observed only if an additional carbon source was provided. A similar

COR-AAD1-00002620
Bayer EX1008 (Part 5 of 9)

effect was previously observed with other pJP4 transconjugants (Feng et al. 1994).

2,4-D and 3-chlorobenzoate degradation was observed during growth on benzoate, pyruvate, or α-ketoglutarate, or in R2A medium. Only slight or no degradation occurred during growth on succinate or acetate. Remarkably, the degradation of 3-chlorobenzoate was completely inhibited during growth on succinate. This effect might be due to transcriptional repression of the chlorocatechol catabolic operon, since succinate has been described as a catabolite repressor specific to the modified *ortho* cleavage pathway encoded by the *clcABD* operon in *Pseudomonas putida* (McFall et al. 1997a).

The plasmid pJP4 encodes the entire degradative pathway down to β-ketoadipate (Streber et al. 1987; Perkins et al. 1990; Matrubutham and Harker 1994; Kasberg et al. 1995; Pérez-Pantoja et al. 2000; Laemmli et al. 2000) including a 2,4-D transport protein (Leveau et al. 1998) and the two identical transcriptional activators TfdR and TfdS (Matrubutham and Harker 1994; You and Ghosal 1995; Leveau and van der Meer 1996). The *tfd* genes are expressed in concert due to the TfdR/S-regulated promoters (Leveau et al. 1999; Laemmli et al. 2000) which are induced by the metabolites 2,4-dichloromuconate (Filer and Harker 1997) or 2-chloromuconate (McFall et al. 1997b). Consequently, the complete degradation of 2,4-D and 3-chlorobenzoate and the funneling of metabolites into the tricarboxylic acid cycle should be possible in bacteria possessing the β-ketoadipate pathway (Harwood and Parales 1996), provided that the *tfd* genes generally are expressed. Since strain EF43 degrades benzoate via the *ortho* cleavage pathway, the lack of β-ketoadipate coenzyme A transferase and/or β-ketoadipyl coenzyme A thiolase cannot be the reason for the inability to grow on 2,4-D or 3-chlorobenzoate. Although during growth on benzoate the enzymes of the β-ketoadipate pathway are induced, benzoate shows no enhancing effect on the 2,4-D degradation rate in comparison with nonaromatic growth substrates such as pyruvate or α-ketoglutarate. However, the presence of an additional carbon source enables strain EF43 to significantly degrade 2,4-D or 3-chlorobenzoate, whereas these chloroaromatic compounds are not sufficient as sole sources of carbon and energy for the strain, indicating a biochemical bottleneck.

In the case of 2,4-D, this bottleneck may result from the fact that the initial step of assimilating 2,4-D is catalyzed by an α-ketoglutarate-dependent dioxygenase. α-Ketoglutarate must be supplied and — because it is oxidatively decarboxylated to succinate in this step — regenerated in order to initiate and maintain the cleavage reaction; otherwise 2,4-D will not be utilized despite the presence of 2,4-D/α-ketoglutarate-dioxygenase (Müller and Babel 2000). This supply requirement might result from the fact that, in contrast to the activity of the initial reaction, the activity of consecutive enzymatic steps in 2,4-D degradation, and finally the formation of acetylCoA and succinate from the phenolic intermediate, is rather low in strain EF43. The 2,4-D/α-ketoglutarate dioxygenase might catalyze a futile reaction under these conditions by wasting carbon from the pool of metabolites as CO_2, which would result in a shortage of carbon and energy and thus prevent the balancing of assimilatory and dissimilatory routes.

This explanation is not as obvious in the case of 3-chlorobenzoate. The enzymatic profile is similar in that it is characterized by a high rate of activity in the initial step followed by strongly reduced rates in consecutive parts of the pathway. However, the requirement of two substrates is not the reason for the bottleneck in this case. The metabolism of 3-chlorobenzoate into tricarboxylic acid cycle intermediates is balanced, including the expenditure and gain of reduction equivalents in the initial metabolic steps. However, whether the availability of reduction equivalents in stoichiometric proportion is guaranteed is questionable, bearing in mind that conversion of substrate via this sequence is the only source of energy to satisfy maintenance requirements. The role of reduction equivalents is suggested by the results of batch experiments, which showed that the degradation of 3-chlorobenzoate proceeded much better when NADH emerged early from the auxiliary substrates, such as was the case for pyruvate, α-ketoglutarate, and, to a lesser extent, benzoate.

The rate-limiting step in 2,4-D degradation by strain EF43 appears to be chlorocatechol conversion, since the activity of at least the chloromuconate cycloisomerase is very low compared with that of the natural host of pJP4, and the accumulation of 2,4-dichloro-*cis,cis*-muconate during 2,4-D degradation is likely. Activities of (chloro)dienlactone hydrolase (TfdE) and (chloro)maleylacetate reductase (TfdF) were not determined, and the possible accumulation of the metabolites chlorodienlactone or chloromaleylacetate has not yet been examined. As a consequence, it cannot be excluded that one of the further chlorocatechol converting enzymes (TfdE or TfdF) causes the bottleneck in 2,4-D degradation by strain EF43. The reasons for this imbalance must be further elucidated by mRNA and protein analyses. The genes *tfdC*, *tfdD*, *tfdE*, *tfdF*, and *tfdB* are organized in one operon as well as $tfdD_{II}$, $tfdC_{II}$, $tfdE_{II}$, $tfdF_{II}$, and $tfdB_{II}$ (Leveau et al. 1999; Laemmli et al. 2000). Although both modules I (*tfdCDEFB*) and II ($tfdD_{II}C_{II}E_{II}F_{II}B_{II}$) are expressed and are required for efficient degradation (Laemmli et al. 2000), the activity of TfdD and TfdE is primarily supplied by module I, whereas the TfdF activity is likely to be supplied by module II (Pérez-Pantoja et al. 2000). As demonstrated by Pérez-Pantoja et al. (2000), *Ralstonia eutropha* JMP222 derivatives containing cloned modules I or II grew on 3-chlorobenzoate, whereas in the case of *Pseudomonas putida* KT2440, only the derivative containing module I was able to grow on 3-chlorobenzoate. These results suggest a different transcriptional efficiency of the TfdR-regulated promoters of modules I and II, leading to an insufficient activity of the chlorocatechol-converting enzymes in those host strains not efficiently transcribing both modules, and consequently to the accumulation of metabolites during the degradation of 2,4-D or 3-chlorobenzoate.

Acknowledgements The authors would like to thank H. Borsdorf for the determination of carbon content, C. Härtig for fatty acid determination, and L. Wünsche for the determination of the GC content and the Biolog analyses.

COR-AAD1-00002621
Bayer EX1008 (Part 5 of 9)

References

Altschul SF, Gish W, Miller W, Myers EW, Lipman, DJ (1990) Basic local alignment search tool. J Mol Biol 215:403–410

Balows A, Trüper HG, Dworkin M, Harder W, Schleifer K-H (eds) (1992) The prokaryotes. 2nd edn. Springer, Berlin Heidelberg New York

DiGiovanni GD, Neilson JW, Pepper IL, Sinclair NA (1996) Gene transfer of *Alcaligenes eutrophus* JMP134 plasmid pJP4 to indigenous soil recipients. Appl Environ Microbiol 62:2521–2526

Dobson SJ, Franzmann PD (1996) Unification of the genera *Deleya* (Baumann et al. 1983), *Halomonas* (Vreeland et al. 1980), and *Halovibrio* (Fendrich 1988) and the species *Paracoccus halodenitrificans* (Robinson and Gibbons 1952) into a single genus, *Halomonas*, and placement of the genus *Zymobacter* in the family *Halomonadaceae*. Int J Syst Bacteriol 46:550–558

Don RH, Pemberton JM (1981) Properties of six pesticide degradation plasmids isolated from *Alcaligenes paradoxus* and *Alcaligenes eutrophus*. J Bacteriol 145:681–686

Don RH, Weightman AJ, Knackmuss H-J, Timmis KN (1985) Transposon mutagenesis and cloning analysis of the pathways for degradation of 2,4-dichlorophenoxyacetic acid and 3-chlorobenzoate in *Alcaligenes eutrophus* JMP134(pJP4). J Bacteriol 161:85–90

Dorn E, Knackmuss KH (1978) Chemical structure and biodegradability of halogenated aromatic compounds. Two catechol 1,2-dioxygenases from a 3-chlorobenzoate grown pseudomonad. Biochem J 174:73–84

Duckworth AW, Grant WD, Jones BE, van Steenbergen R (1996) Phylogenetic diversity of soda lake alkaliphiles. FEMS Microbiol Ecol 19:181–191

Ehrig A, Müller RH, Babel W (1997) Isolation of phenoxy herbicide-degrading *Rhodoferax* species from contaminated building material. Acta Biotechnol 17:351–356

Esener AA, Roels JA., Kossen NWF, Roozenburg JWH (1981) Description of microbial growth behaviour during wash-out phase; determination of the maximum specific growth rate. J Appl Microbiol Biotechnol 13:141–144

Farhana L, New PB (1997) The 2,4-dichlorophenol hydroxylase of *Alcaligenes eutrophus* JMP134 is a homotetramer. Can J Microbiol 43:202–205

Feng L, Rolfe BG, Gartner E, Van Zwielen L, Kennedy IR (1994) Expression of the 2,4-D degrading plasmid pJP4 of *Alcaligenes eutrophus* in *Rhizobium trifolii*. Acta Biotechnol 14:119–129

Filer K, Harker AR (1997) Identification of the inducing agent of the 2,4-dichloro-phenoxyacetic acid pathway encoded by plasmid pJP4. Appl Environ Microbiol 63:317–320

Friedrich B, Meyer M, Schlegel HG (1983) Transfer and expression of the herbicide-degrading plasmid pJP4 in aerobic autotrophic bacteria. Arch Microbiol 134:92–97

Fukumori F, Hausinger RP (1993) Purification and characterization of 2,4-dichloro-phenoxyacetate/α-ketoglutarate dioxygenase. J Biol Chem 268:24311–24317

Grant WD (1992) Alkaline environments. In: Lederberg J (ed) Encyclopedia of microbiology. Academic, London, pp 73–80

Grant WD, Tindall BJ (1986) The alkaline saline environment. In: Herbert RA, Codd GA (eds) Microbes in extreme environments. Academic, London, pp 25–54

Grant WD, Mwatha WE, Jones BE (1990) Alkaliphiles: ecology, diversity and applications. FEMS Microbiol Rev 75:255–270

Harwood CS, Parales RE (1996) The β-ketoadipate pathway and the biology of self-identity. Annu Rev Microbiol 50:553–590

Hicks DB, Krulwich TA (1995) The respiratory chain of alkaliphilic bacteria. Biochim Biophys Acta 1229:303–314

Hoffmann D, Müller RH, Kiesel B, Babel W (1996) Isolation and characterization of an alkaliphilic bacterium capable of growing on 2,4-dichlorophenoxyacetic acid and 4-chloro-2-methylphenoxyacetic acid. Acta Biotechnol 16:121–131

Hong SM, Ahn YJ, Park YK, Min K-H, Kim C-K, Ka J-O (1995) Effects of genetically different 2,4-D-degradative plasmids on degradation phenotype and competitiveness of soil microorganisms. J Microbiol 33:208–214

Horikoshi K (1996) Alkaliphiles – from an industrial point of view. FEMS Microbiol Rev 18:259–270

Imhoff JF, Trüper HG (1977) *Ectothiorhodospira halochloris* sp. nov. A new extremely halophilic phototrophic bacterium containing bacteriochlorophyll b. Arch Microbiol 114:115–121

Ingham ER, Doyle JD, Hendricks CW (1995) Assessing interactions between the soil foodweb and a strain of *Pseudomonas putida* genetically engineered to degrade 2,4-D. Appl Soil Ecol 2:263–274

Kanekar PP, Sarnaik SS, Kelkar AS (1999) Bioremediation of phenol by alkaliphilic bacteria isolated from alkaline lake of Lonar, India. J Appl Microbiol Symp Suppl 85:128S-133S

Kasberg T, Daubaras DL, Chakrabarty AM, Kinzelt D, Reineke W (1995) Evidence that operons *tcb*, *tfd*, and *clc* encode maleylacetate reductase, the fourth enzyme of the modified *ortho* pathway. J Bacteriol 177:3885–3889

Kleinsteuber S, Hoffmann D, Müller RH, Babel W (1998) Detection of chlorocatechol 1,2-dioxygenase genes in proteobacteria by PCR and gene probes. Acta Biotechnol 18:231–240

Kleinsteuber S, Kiesel B, Müller RH, Babel W (2000) Assessing the adaptive potential of alkaliphilic bacteria to chloroaromatic substrates by using the green fluorescent protein as a marker for monitoring plasmid transfer. In: Biotechnology 2000. Abstracts of the world congress on biotechnology, Berlin, September 3–8, 2000, 1:329–331

Krulwich TA (1995) Alkaliphiles: 'basic' molecular problems of pH tolerance and bioenergetics. Mol Microbiol 15:403–410

Krulwich TA, Guffanti AA (1992) Proton-coupled bioenergetic processes in extremely alkaliphilic bacteria. J Bioenerg Biomembr 24:587–599

Krulwich TA, Hicks DB, Seto-Young D, Guffanti AA (1988) The bioenergetics of alkaliphilic bacilli. Crit Rev Microbiol 16:15–36

Kuhm AE, Schlömann M, Knackmuss, H-J, Pieper DH (1990) Purification and characterization of dichloromuconate cycloisomerase from *Alcaligenes eutrophus* JMP134. Biochem J 266:877–883

Laemmli CM, Leveau JHJ, Zehnder AJB, van der Meer, JR (2000) Characterization of a second gene cluster for chlorophenol and chlorocatechol metabolism on plasmid pJP4 in *Ralstonia eutropha* JMP134(pJP4). J Bacteriol 182:4165–4172

Leveau JHJ, van der Meer JR (1996) The *tfdR* gene product can successfully take over the role of the insertion element-inactivated TfdT protein as a transcriptional activator of the *tfdCDEF* gene cluster, which encodes chlorocatechol degradation in *Ralstonia eutropha* JMP134(pJP4). J Bacteriol 178:6824–6832

Leveau JHJ, Zehnder AJB, van der Meer JR (1998) The *tfdK* gene product facilitates uptake of 2,4-dichlorophenoxyacetate by *Ralstonia eutropha* JMP134(pJP4). J Bacteriol 180:2237–2243

Leveau JHJ, König F, Füchslin H, Werlen C, van der Meer JR (1999) Dynamics of multigene expression during catabolic adaptation of *Ralstonia eutropha* JMP134 (pJP4) to the herbicide 2,4-dichlorophenoxyacetate. Mol Microbiol 33:396–406

Loffhagen N, Härtig C, Babel W (1995) Fatty acid patterns of *Acinetobacter calcoaceticus* 69-V indicate sensitivity against xenobiotics. Appl Microbiol Biotechnol 44:526–531

Maidak BL, Cole JR, Parker CT, Garrity GM, Larsen N, Li B, Lilburn TG, McCaughey MJ, Olsen GJ, Overbeek R, Pramanik S, Schmidt TM, Tiedje JM, Woese CR (1999) A new version of the RDP (Ribosomal Database Project). Nucleic Acids Res 27:171–173

Maltseva O, McGowan C, Fulthorpe R, Oriel P (1996) Degradation of 2,4-dichlorophenoxyacetic acid by haloalkaliphilic bacteria. Microbiol-UK 142:1115–1122

Matrubutham U, Harker AR (1994) Analysis of duplicated gene sequences associated with *tfdR* and *tfdS* in *Alcaligenes eutrophus* JMP134. J Bacteriol 176:2348–2352

McFall SM, Abraham B, Narsolis CG, Chakrabarty AM (1997a) A tricarboxylic acid cycle intermediate regulating transcription of a chloroaromatic biodegradative pathway: fumarate-mediated repression of the *clcABD* operon. J Bacteriol 179:6729–6735

McFall SM, Parsek MR, Chakrabarty AM (1997b) 2-chloromuconate and ClcR-mediated activation of the *clcABD* operon: in vitro transcriptional and DNase I footprint analyses. J Bacteriol 179:3655–3663

Mertingk H, Müller RH, Babel W (1998) Etherolytic cleavage of 4-(2,4-dichloro-phenoxy)butyric acid and 4-(4-chloro-2-methylphe-

COR-AAD1-00002622
Bayer EX1008 (Part 5 of 9)

noxy)butyric acid by species of *Rhodococcus* and *Aureobacterium* isolated from an alkaline environment. J Basic Microbiol 38:257–267

Mesbah M, Premachandran U, Whitman WB (1989) Precise measurement of the G+C content of deoxyribonucleic acid by high-performance liquid chromatography. Int J Syst Bacteriol 39:159–167

Müller RH, Babel W (1994) Phenol and its derivatives as heterotrophic substrates – an energetic comparison. Appl Microbiol Biotechnol 42:446–451

Müller RH, Babel W (2000) A theoretical study on the metabolic requirements resulting from α-ketoglutarate-dependent cleavage of phenoxyalkanoates. Appl Environ Microbiol 66:339–344

Müller RH, Jorks S, Kleinsteuber S, Babel W (1998) Degradation of various chlorophenols under alkaline conditions by Gram-negative bacteria closely related to *Ochrobactrum anthropi*. J Basic Microbiol 38:269–281

Müller RH, Jorks S, Kleinsteuber S, Babel W (1999) *Comamonas acidovorans* strain MC1: a new isolate capable of degrading the chiral herbicides dichlorprop and mecoprop and the herbicides 2,4-D and MCPA. Microbiol Res 154:241–246

Nakazawa T, Nakazawa A (1970) Pyrocatechase (*Pseudomonas*). In: Tabor H, Tabor CW (eds) Methods in Enzymology vol. 17A. Academic, London, pp 518–522

Neilson JW, Josephson KL, Pepper IL, Arnold RB, DiGiovanni GD, Sinclair NA (1994) Frequency of horizontal gene transfer of a large catabolic plasmid (pJP4) in soil. Appl Environ Microbiol 60:4053–4058

Newby DT, Josephson KL, Pepper, IL (2000) Detection and characterization of plasmid pJP4 transfer to indigenous soil bacteria. Appl Environ Microbiol 66:290–296

Nozaki M (1970) Metapyrocatechase (*Pseudomonas*). In: Tabor H, Tabor CW (eds) Methods in Enzymology vol. 17A. Academic, London, pp 522–525

Pemberton JM, Corney B, Don RH (1979) Evolution and spread of pesticide degrading ability among soil micro-organisms. In: Timmis KN (ed) Plasmids of medical, environmental and commercial importance. Elsevier/North-Holland, Amsterdam, pp 287–299

Pérez-Pantoja D, Guzmán L, Manzano M, Pieper DH, González B (2000) Role of $tfdC_ID_IE_IF_I$ and $tfdD_{II}C_{II}E_{II}F_{II}$ gene modules in catabolism of 3-chlorobenzoate by *Ralstonia eutropha* JMP134(pJP4). Appl Environ Microbiol 66:1602–1608

Perkins EJ, Gordon MP, Caceres O, Lurquin PF (1990) Organization and sequence analysis of the 2,4-dichlorophenol hydroxylase and dichlorocatechol oxidative operons of plasmid pJP4. J Bacteriol 172:2351–2359

Pieper DH, Reineke W, Engesser KH, Knackmuss HJ (1988) Metabolism of 2,4-dichlorophenoxyacetic acid, 4-chloro-2-methylphenoxyacetic acid, and 2-methyl-phenoxyacetic acid by *Alcaligenes eutrophus* JMP134. Arch Microbiol 151:365–371

Ryu E (1938) On the Gram-differentiation of bacteria by the simplest method. J Jpn Soc Vet Sci 17:31

Sambrook J, Maniatis T, Fritsch EF (1989) Molecular cloning — a laboratory manual, 2nd edn. Cold Spring Harbor Laboratory, Cold Spring Harbor, New York

Schmidt E, Knackmuss KH (1980) Chemical structure and biodegradability of halogenated aromatic compounds. Conversion of chlorinated muconic acids into maleoylacetic acid. Biochem J 192:339–347

Seibert V, Stadler-Fritzsche K, Schlömann M (1993) Purification and characterization of maleylacetate reductase from *Alcaligenes eutrophus* JMP134(pJP4). J Bacteriol 175:6745–6754

Short KA, Doyle JD, King RJ, Seidler RJ, Stotzky G, Olsen RH (1991) Effects of 2,4-dichlorophenol, a metabolite of a genetically engineered bacterium, and 2,4-dichloro-phenoxyacetate on some microorganism-mediated ecological processes in soil. Appl Environ Microbiol 57:412–418

Streber WR, Timmis KN, Zenk MH (1987) Analysis, cloning, and high level expression of 2,4-dichlorophenoxyacetate monooxygenase gene *tfdA* of *Alcaligenes eutrophus* JMP134. J Bacteriol 169:2950–2955

Top EM, Van Daele P, De Saeyer N, Forney LJ (1998) Enhancement of 2,4-dichlorophenoxyacetic acid (2,4-D) degradation in soil by dissemination of catabolic plasmids. Anton Leeuw Int J G 73:87–94

Vallaeys T, Fulthorpe RR, Wright AM, Soulas G (1996) The metabolism of 2,4-dichlorophenoxyacetic acid degradation involves different families of *tfdA* and *tfdB* genes according to PCR-RFLP analysis. FEMS Microbiol Ecol 20:163–172

You IS, Ghosal D (1995) Genetic and molecular analysis of a regulatory region of the herbicide 2,4-dichlorophenoxyacetate catabolic plasmid pJP4. Mol Microbiol 16:321–331

COR-AAD1-00002623
Bayer EX1008 (Part 5 of 9)

Arch Microbiol (2004) 181 : 112–121
DOI 10.1007/s00203-003-0634-4

ORIGINAL PAPER

Caroline Laemmli · Christoph Werlen
Jan Roelof van der Meer

Mutation analysis of the different *tfd* genes for degradation of chloroaromatic compounds in *Ralstonia eutropha* JMP134

Received: 1 September 2003 / Revised: 6 November 2003 / Accepted: 19 November 2003 / Published online: 16 December 2003
© Springer-Verlag 2003

Abstract *Ralstonia eutropha* JMP134 possesses two sets of similar genes for degradation of chloroaromatic compounds, *tfdCDEFB* (in short: tfd_I cluster) and $tfdD_{II}C_{II}E_{II}F_{II}B_{II}$ (tfd_{II} cluster). The significance of two sets of *tfd* genes for the organism has long been elusive. Here, each of the *tfd* genes in the two clusters on the original plasmid pJP4 was replaced by double recombination with a gene fragment in which a kanamycin resistance gene was inserted into the respective *tfd* gene's reading frame. The insertion mutants were all tested for growth on 2,4-dichlorophenoxyacetic acid (2,4-D), 2-methyl-4-chlorophenoxyacetic acid (MCPA), and 3-chlorobenzoate (3-CBA). None of the $tfdD_{II}C_{II}E_{II}F_{II}B_{II}$ genes appeared to be essential for growth on 2,4-D or on 3-CBA. Mutations in *tfdC*, *tfdD* and *tfdF* also did not abolish but only retarded growth on 2,4-D, indicating that they were redundant to some extent as well. Of all *tfd* genes tested, only *tfdE* and *tfdB* were absolutely essential, and interruption of those two reading frames abolished growth on 2,4-D, 3-CBA (*tfdE* only), and MCPA completely. Interestingly, strains with insertion mutations in the tfd_I cluster and those in $tfdD_{II}$, $tfdC_{II}$, $tfdE_{II}$ and $tfdB_{II}$ were severely effected in their growth on MCPA, compared to the wild-type. This indicated that not only the tfd_I cluster but also the tfd_{II} cluster has an essential function for *R. eutropha* during growth on MCPA. In contrast, insertion mutation of $tfdD_{II}$ resulted in better growth of *R. eutropha* JMP134 on 3-CBA, which is most likely due to the prevention of toxic metabolite production in the absence of $TfdD_{II}$ activity.

Keywords *Ralstonia eutropha* JMP134 · *tfd* genes · Insertion mutagenesis · 2,4-Dichlorophenoxyacetic acid · 2-Methyl-4-chlorophenoxyacetic acid · 3-Chlorobenzoate

C. Laemmli · C. Werlen · J. R. van der Meer
Swiss Federal Institute for Environmental Science and Technology (EAWAG),
8600 Duebendorf, Switzerland

Present address:
C. Laemmli
Department of Molecular Biology,
University of Geneva,
30 Quai Ernest-Ansermet, 1211 Genève 4, Switzerland

Present address:
J. R. van der Meer (✉)
Institut de Microbiologie Fondamentale,
University of Lausanne,
Bâtiment de Biologie, 1015 Lausanne, Switzerland
Tel.: +41-21-6925630, Fax: + 41-21-6925635
e-mail: janroelof.vandermeer@imf.unil.ch

Introduction

Ralstonia eutropha JMP134 (pJP4) was originally isolated from an unspecified soil sample based on its ability to use the herbicide 2,4-dichlorophenoxyacetic acid (2,4-D) as sole carbon and energy source (Don and Pemberton 1981; Don et al. 1985). The strain can grow on various other haloaromatic compounds, such as 3-chlorobenzoate (3-CBA) (Don et al. 1985) and 2-methyl-4-chlorophenoxyacetic acid (MCPA) (Pieper et al. 1988). The initial degradation steps of 2,4-D and MCPA involve an oxidation at the ether bond by means of an α-ketoglutarate dependent dioxygenase (encoded by *tfdA*), which leads to the release of glyoxylate and the formation of 2,4-dichlorophenol and 2-methyl-4-chlorophenol, respectively (Streber et al. 1987; Pieper et al. 1988) (Fig. 1). The chlorophenols from 2,4-D and MCPA are then oxidized by a hydroxylase (encoded by *tfdB* and possibly also by $tfdB_{II}$) to form 3,5-dichloro- and 3-methyl-5-chlorocatechol, respectively. 3-CBA is oxidized at the 1,2- or 1,6-position by a benzoate dioxygenase and then dehydrogenated to form approximately two-thirds 3-chloro- and one-third 4-chlorocatechol (Pieper et al. 1993). *tfdA* and *tfdB* are located on the plasmid pJP4 (Streber et al. 1987; Perkins et al. 1990), whereas the genes for conversion of 3-CBA to chlorocatechol are presumed to be chromosomally located (Laemmli et al. 2002). Although different enzymes are used in the initial degradation steps, metabolism of 2,4-D, MCPA, and 3-CBA all proceeds via chloro- (methyl-) substituted catechols (Fig. 1). The chloro- (methyl-) catechols are transformed by the so-called modified *ortho*-cleavage pathway enzymes, which

COR-AAD1-00002624
Bayer EX1008 (Part 5 of 9)

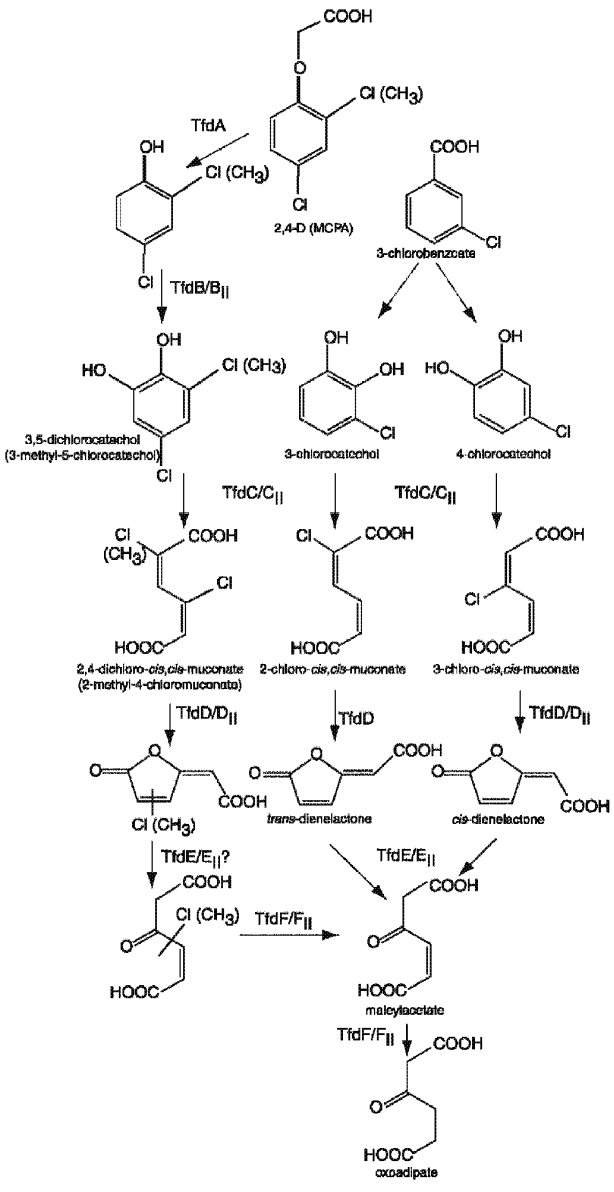


Fig. 1 Metabolic pathways for 2,4-dichlorophenoxyacetic acid (2,4-D), 2-methyl-4-chlorophenoxyacetic acid (MCPA) and 3-chlorobenzoate by *Ralstonia eutropha* JMP134 (pJP4). Individual intermediates in each of the pathways are displayed as far as known, with assignment of the respective Tfd-enzymes catalyzing the reaction. For simplicity, not all intermediate steps in muconate conversion are drawn. The pathway for MCPA degradation follows that of 2,4-D and the position of the methyl group in MCPA and its intermediates is shown within *parentheses*. Details of the reactions catalyzed by TfdE and $TfdE_{II}$ with chloro- or methyldienelactones are not known. *TfdA* α-Ketoglutarate-dependent dioxygenase, *TfdB*(B_{II}) chlorophenol hydroxylase, *TfdC*(C_{II}) chlorocatechol 1,2-dioxygenase, *TfdD*(D_{II}) chloromuconate cycloisomerase, *TfdE*(E_{II}) dienelactone hydrolase, *TfdF*(F_{II}) maleylacetate reductase

are also encoded on plasmid pJP4. Interestingly, pJP4 harbors two homologous sets of genes encoding the transformation of chloro- (methyl-) phenol via chloro- (methyl-) catechols through the modified *ortho*-cleavage pathway. These genes are called *tfdCDEFB* (in short, the tfd_I cluster) and $tfdD_{II}C_{II}E_{II}F_{II}B_{II}$ (in short, tfd_{II}).

Initially, only the *tfdCDEFB* genes had been identified through transposon mutagenesis to be responsible for growth on 2,4-D (Don et al. 1985). Long afterwards, the $tfdD_{II}C_{II}E_{II}F_{II}B_{II}$ cluster was identified by DNA sequencing (Laemmli et al. 2000). Both gene clusters lay in a 22-kb region on plasmid pJP4 (Fig. 2), and it was proposed that the second cluster had been more recently inserted on pJP4 by the action of a transposable element formed by one intact and one partial copy of IS*JP4* (Leveau and van der Meer 1997). The potential role of the second gene cluster for *R. eutropha* has become subject of a debate (Laemmli et al. 2000; 2002; Pérez-Pantoja et al. 2000; Plumeier et al. 2002; Schlömann 2002). Heterologous expression studies showed that all genes from the tfd_{II} cluster produce active enzymes in *Escherichia coli*, with enzymatic activities expected based on sequence similarities to their counterparts in the tfd_I cluster (Laemmli et al. 2000). Transcription studies indicated that the genes from the tfd_I and from the tfd_{II} cluster are actively transcribed during growth on 2,4-D (Leveau et al. 1999). More recently, Plumeier et al. (2002) separated and partially purified the enzyme fractions from *R. eutropha* JMP134 grown on 2,4-D and demonstrated that the cluster II enzymes were indeed synthesized, except perhaps $TfdE_{II}$, the dienelactone hydrolase, which contributed to only 5% of dienelactone hydrolase activity in cell extracts. The relative activities of the chlorocatechol 1,2-dioxygenase $TfdC_{II}$ compared to TfdC, and of the chloromuconate cycloisomerase $TfdD_{II}$ compared to TfdD in 2,4-D grown cells amounted to 20%, and that of $TfdF_{II}$ compared to TfdF even to 50% (Plumeier et al. 2002). No hydroxylase activity (by TfdB or $TfdB_{II}$) was purified in this study. These data allowed the conclusion that *R. eutropha* JMP134 uses both *tfd* clusters during growth on 2,4-D, even though one or more 2,4-D-degrading enzymes may actually be redundant. To draw more conclusive evidence about the necessity, specificity, and differences between the two *tfd* clusters, each of the *tfd* clusters was cloned individually in a *R. eutropha* strain devoid of plasmid pJP4, such as JMP222 (Pérez-Pantoja et al. 2000) and JMP289 (Laemmli et al. 2002). Since these *R. eutropha* strains lack *tfdA* and *tfdB*, they cannot grow on 2,4-D, but can convert 3-CBA to 3-chloro- and 4-chlorocatechol (CC) (Fig. 1), and CC metabolism could thus be tested by introducing the tfd_I or tfd_{II} cluster. The results of those studies showed that *R. eutropha* JMP222 and 289 carrying a plasmid containing the tfd_I cluster under control of *tfdR* could grow on 3-CBA (Leveau and van der Meer 1996; Pérez-Pantoja et al. 2000; Laemmli et al. 2002). However, *R. eutropha* JMP289 with the tfd_{II} cluster did not grow on 3-CBA as sole carbon source (Laemmli et al. 2002). This was attributed to an inability of $TfdD_{II}$ to convert 2-chloromuconate, to the formation of possible toxic intermediates, and to a very low activity of $TfdE_{II}$ (Laemmli et al. 2002; Plumeier et al. 2002; Pérez-Pantoja et al. 2003). Others have reported that *R. eutropha* JMP222 provided with the tfd_{II} cluster could grow on 3-CBA (Pérez-Pantoja et al. 2000), but no

COR-AAD1-00002625
Bayer EX1008 (Part 5 of 9)

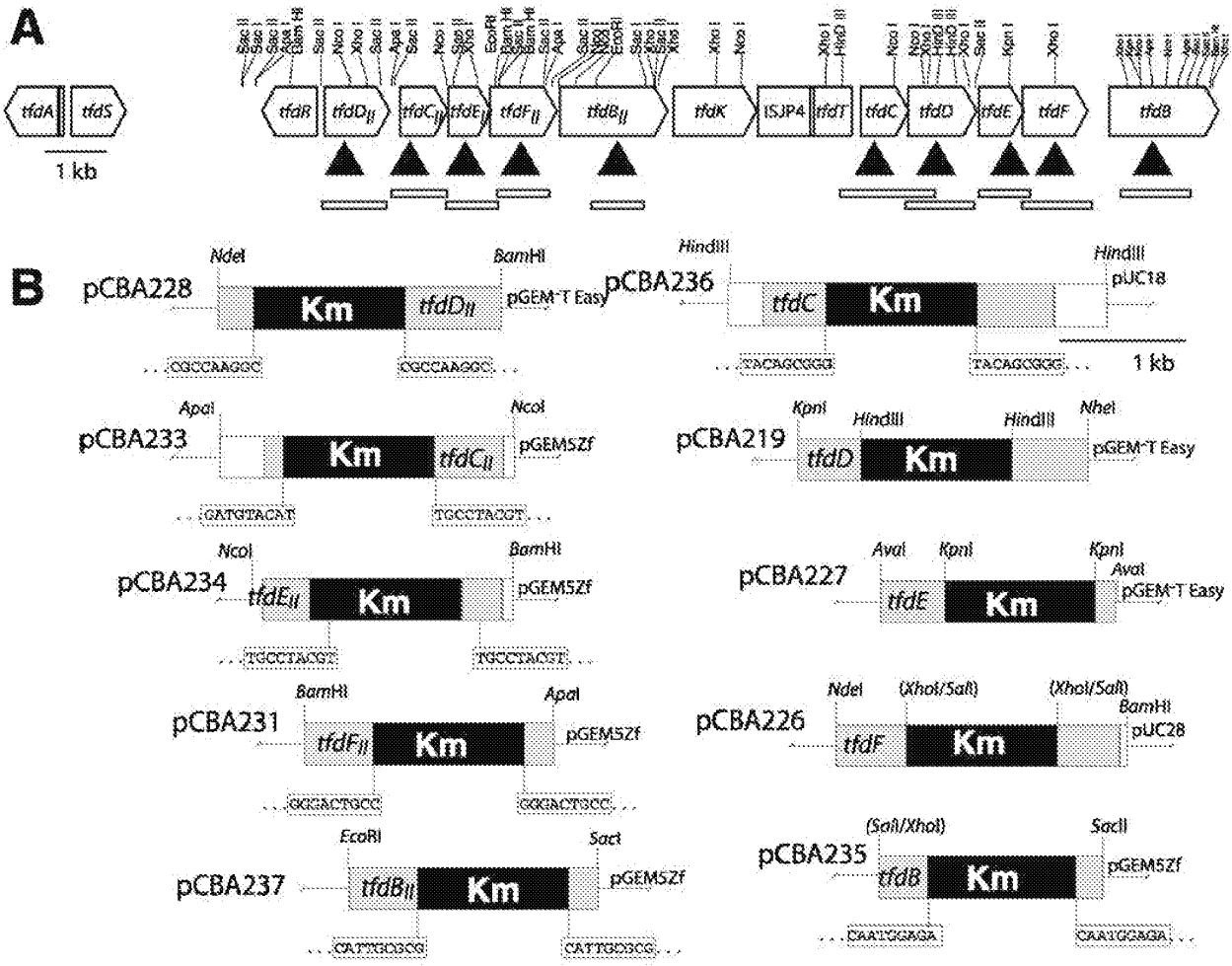


Fig. 2 **A** The location, orientation, and size of all known *tfd* genes on plasmid pJP4, including relevant restriction sites and fragments used for cloning (depicted as white *bars*). *Black triangles* indicate the approximate kanamycin gene insertion sites. **B** Maps and designation of the plasmids used in this study for construction of the *tfd* knockout mutants, and the exact insertion sites of the kanamycin gene (exemplified as a *black box*). *Gray zones* indicate coding area of the target gene, *white zones* that of non-target coding areas present on the same cloned fragment. Nucleotides duplicated by the kanamycin gene in vitro insertion are *boxed*

satisfactory explanation has been given for the different behavior of strains JMP222 and JMP289.

One disadvantage of the studies with separately cloned *tfd* clusters in *R. eutropha* was that only functional differences with respect to 3-CBA and its central intermediates 3-CC and 4-CC could be investigated. The objective of the present study was to analyze the function of each *tfd* gene in either gene cluster with respect to metabolism of 2,4-D and MCPA. This would reveal whether functional differences exist between the gene products of the two *tfd* clusters with respect to metabolism of chlorophenols, 3,5-dichloro- and 3-methyl-5-chlorocatechol. In order to achieve this, mutants of *R. eutropha* JMP134 were constructed by directly inactivating each gene of the tfd_I and tfd_{II} cluster on the original pJP4 plasmid. The growth behavior of these mutants on 2,4-D, 3-CBA and MCPA was determined and further confirmed by expression analysis of the *tfd* genes in the knockout mutants through RNA hybridizations and by enzyme activity measurements.

Materials and methods

Bacterial strains and cultivation conditions

R. eutropha JMP134 (pJP4) uses 2,4-D, 3-CBA, and MCPA as sole carbon and energy sources (Don and Pemberton 1981; Don et al. 1985). *Escherichia coli* DH5α (Sambrook et al. 1989) was used for cloning purposes. *E. coli* cultures were grown in Luria-Bertani (LB) medium supplemented with ampicillin (100 µg/ml), kanamycin (100 µg/ml), or tetracycline (10 µg/ml).

R. eutropha JMP134 and mutant cultures were grown at 30 °C in nutrient broth (Biolife, Milan, Italy), one-tenth strength nutrient broth, or in *Pseudomonas* type 21C mineral medium (Gerhardt et al. 1981) supplemented with either 10 mM fructose, 2.5 mM 2,4-D, 3 mM 3-CBA, or 3 mM MCPA, and kanamycin (100 µg/ml) if necessary. Growth experiments were carried out in triplicate in 200-ml Erlenmeyer flasks. Growth was monitored by measuring the turbidity of a culture sample at 546 nm (OD_{546}) against medium, or in 96-well microtiter plates. In case of colorization of the medium after growth on chloroaromatic compounds, the OD_{546} of the spent

COR-AAD1-00002626
Bayer EX1008 (Part 5 of 9)

Table 1 Plasmids used in this study

Plasmid	Relevant characteristics	Reference
pUC28		
pGEM-T-Easy		Promega
pGEM5Zf		Promega
pRME1	Kanamycin resistance gene of Tn*903*, flanked by symmetrical restriction sites	(Harayama et al. 1986)
pCBA10	1.4-kb *Hin*dIII fragment of pCBA4 containing *tfdC* and part of *tfdD*	This work
pCBA83III	1 kb *Apa*I-*Nco*I fragment of pCBA83 (Leveau et al. 1999) in pGEM5Zf, containing $tfdC_{II}$	(Laemmli et al. 2000)
pCBA83IV	0.8-kb *Nco*I-*Bam*HI fragment of pCBA83 in pGEM5Zf, containing $tfdE_{II}$ and a small part of $tfdF_{II}$	(Laemmli et al. 2000)
pCBA84III	0.5-kb *Bam*HI-*Apa*I fragment of pCBA84 in pGEM5Zf, containing an internal piece of $tfdF_{II}$	(Laemmli et al. 2000)
pCBA96	0.85-kb *Eco*RI-*Sac*I fragment of pCBA84 in pGEM7Zf, containing an interal $tfdB_{II}$ fragment	(Leveau et al. 1999)
pCBA102	0.4-kb *Dra*I-*Xho*I fragment of *tfdB* in pGEM5Zf	(Leveau et al. 1999)
pCBA127	$tfdD_I$ in pGEM-T-Easy	(Laemmli et al. 2002)
pCBA219	1.2-kb *Hin*dIII fragment of pRME1 into the internal *Hin*dIII site in *tfdD* of pCBA127	This work
pCBA221	$tfdF_I$ ORF amplified by PCR into pGEM-T-Easy	This work
pCBA225	Open reading frame of *tfdE* amplified by PCR and cloned into pGEM-T-Easy	This work
pCBA226	1.2-kb *Kpn*I fragment of pRME1 into the internal *Kpn*I site in *tfdE* of pCBA225	This work
pCBA227	1.2-kb *Sal*I fragment of pRME1 into the internal *Xho*I site in *tfdF* of pCBA221	This work
pCBA231	EZ::TN <KAN-2>insertion into $tfdF_{II}$ on pCBA84III	This work
pCBA233	EZ::TN <KAN-2>insertion into $tfdC_{II}$ on pCBA83III	This work
pCBA234	EZ::TN <KAN-2>insertion into $tfdE_{II}$ on pCBA83IV	This work
pCBA235	EZ::TN <KAN-2>insertion into *tfdB* on pCBA102	This work
pCBA236	EZ::TN <KAN-2>insertion into *tfdC* on pCBA10	This work
pCBA237	EZ::TN <KAN-2>insertion into $tfdB_{II}$ on pCBA96	This work

medium was measured separately. These growth experiments were repeated four times with independently grown precultures. Growth of *R. eutropha* mutants on the various substrates was also determined in 96-well polystyrene plates. Five µl of a preculture grown on nutrient broth with kanamycin was diluted in 250 µl medium in a plate well. Cultures were inoculated in six-fold repetition on each of the four growth substrates (one-tenth strength nutrient broth, minimal medium plus 2,4-D, MCPA, or 3-CBA) or on minimal medium alone, and on three different plates, which were started with an 8-h time difference. The 96-well plates were closed with a lid that was taped extensively with Parafilm to avoid evaporation and were incubated at 30 °C with 200 rpm rotation. Growth of the cultures was followed by measuring the OD_{546} in a Rainbow Microwell plate reader. Growth experiments in 96-well plates were repeated at least twice for each mutant independently. After growth in 96-well plates, the cultures were checked by PCR for the correct insertion mutation (see below).

DNA and RNA manipulations

Plasmid isolations from *E. coli* DH5α, genomic DNA isolation, transformations, and other DNA manipulations were carried out according to established procedures (Sambrook et al. 1989). Restriction enzymes and other DNA modifying enzymes were obtained from Amersham Life Science (Cleveland, Ohio, USA), Sigma, or GIBCO/BRL Life Technologies (Gaithersburg, Md., USA) and used according to the specifications of the manufacturer. Oligonucleotides for the PCR were obtained from Microsynth GmbH (Balgach, Switzerland). The PCR mixtures contained 200 pmol of each primer per ml, 20 mM Tris-HCl (pH 8.4), 50 mM KCl, 0.05% (v/v) W-1, 2 mM $MgCl_2$, 0.25 mM of each deoxynucleoside triphosphate, and 30 U *Taq* DNA polymerase (Sigma) per ml. DNA was sequenced as described previously (Ravatn et al. 1998), and nucleotide sequences were analyzed with the DNASTAR software (DNASTAR Inc., Madison, Wis., USA). Genomic DNA isolated from *R. eutropha* JMP134 and its mutants was blotted by hydrochloric acid depurination and vacuum-transferred as described by the manufacturer of the VacuGene XL blotting system (Pharmacia, Uppsala, Sweden).

In order to test for polar effects of the inserted kanamycin resistance gene, RNA was isolated from cell pellets of *R. eutropha* JMP134 and its mutants as described previously (Baumann et al. 1996). Cultures for RNA isolation were grown on 10 mM fructose at 30 °C to an OD_{546} of between 0.8 and 0.9, and induced by adding 3-CBA to a final concentration of 1 mM. Induction continued for 2 h, after which the cells were immediately recovered by centrifugation. DNase I-treated RNA samples were spotted on Hybond N+ membranes (Amersham) and hybridized with biotin-labeled antisense RNAs for each of the *tfd* ORFs, except *tfdA* and $tfdD_{II}$, as described elsewhere (Leveau et al. 1999).

Plasmids

For each of the *tfdCDEFB* or $tfdD_{II}C_{II}E_{II}F_{II}B_{II}$ genes, a gene displacement plasmid was constructed containing the gene to be interrupted and the kanamycin resistance gene within it. Since the genes were interrupted with the kanamycin resistance gene only and not by classical transposon mutagenesis, the risk for polar effects was minimized. The plasmids used for construction of the *tfd* gene fragments are listed in Table 1. The location of the different insertions is depicted in Fig. 2. At least 300 bp of the target gene were included on each side of the inserted kanamycin resistance gene in order to facilitate recombination in *R. eutropha* JMP134.

In three cases (*tfdD*, *tfdE*, and *tfdF*) the kanamycin gene was inserted through directional cloning. The kanamycin resistance gene was recovered as a 1.2-kb *Hin*dIII fragment from plasmid pRME1

COR-AAD1-00002627
Bayer EX1008 (Part 5 of 9)

and inserted into an internal *Hin*dIII restriction site of *tfdD* (in plasmid pCBA127, yielding pCBA219). Similarly, a 1.2-kb *Kpn*I fragment of pRME1 was used to interrupt *tfdE* at its internal *Kpn*I site (in pCBA225, yielding pCBA226). The *tfdF* gene was interrupted by using the internal *Xho*I site, into which the 1.2-kb *Sal*I fragment of pRME1 was inserted (in pCBA221, yielding pCBA227). For the other *tfd* genes, plasmids containing specific gene fragments were in vitro mutagenized using the EZ::TN <KAN-2>insertion kit (Epicentre Technologies, Madison, Wis., USA). After transformation into *E. coli* and subsequent plasmid isolations, the insertion sites of the kanamycin resistance gene were verified on agarose gel and by DNA sequencing, using primers facing outwards from the kanamycin gene (according to instructions of the supplier). This resulted in plasmids pCBA231, 233, 234, 235, 236, and 237 (Fig. 2, Table 1).

Construction of gene displacement mutants of *R. eutropha* JMP134

All *tfd* knockout plasmids were transformed individually into *R. eutropha* JMP134 by electroporation. To obtain electrocompetent *R. eutropha* JMP134, the strain was inoculated (1:50) from a freshly grown culture on 2,4-D in 5 ml nutrient broth and grown overnight. From this culture, 0.25 ml were used to inoculate 50 ml nutrient broth. The latter culture was grown at 30 °C to an OD_{546} of 0.5. Subsequently, the cells were placed on ice for 30 min and centrifuged for 15 min at 4,300×*g* and 4 °C. The cell pellet was resuspended with 40 ml of 10% (v/v) ice-cold glycerol/demineralized water solution and the cells were again centrifuged. The pellet was then resuspended in 20 ml of 10% ice-cold glycerol solution, the cells again centrifuged, and the cell pellet resuspended in 200 µl ice-cold 10% glycerol. Prior to electroporation, 40 µl competent cells were mixed with 2 µl plasmid DNA (containing approximately 200 ng DNA) and placed on ice for 1 min. The settings for the electroporation were 25 µF, 200 Ω, and 2.3 kV. Immediately following the pulse, 1 ml nutrient broth was added to the cells, and the cell suspension was removed from the cuvette, transferred to a 12-ml sterile vial, and incubated at 30 °C with shaking. One third of this cell suspension was plated on nutrient agar containing kanamycin for selection after 2 h and the rest after overnight incubation. Typically, between 10 and 50 kanamycin-resistant *R. eutropha* colonies appeared from 200 ng plasmid DNA after 36 h at 30 °C. Single and double recombinants were differentiated by checking for the presence or absence of vector DNA by screening for ampicillin resistance (at 50 µg/ml) or sensitivity. All suspected double recombinants were checked by Southern blotting and by PCR with relevant primers (sequences available on request).

Induction of *tfd* gene expression in *R. eutropha* JMP134 and mutants

R. eutropha JMP134 and a few selected mutants were grown at 30 °C in *Pseudomonas* minimal medium supplemented with 10 mM fructose to an OD_{546} of 0.8–0.9. Induction was achieved by adding 3-CBA, 2,4-D, or MCPA to a final concentration of 1 mM, and strains were incubated for an additional 2 h at 30 °C. Cells were then centrifuged for 15 min at 4,300×*g* (4 °C), washed with 40 ml washing buffer (20 mM Tris-HCl, pH 7) and resuspended in 1 ml washing buffer. The cell suspensions was disrupted by sonication (Branson Sonifer 450; SCAN AG, Basel, Switzerland). One-ml cell suspensions were sonicated (eight times for 5 s each) at an output of 30–40 W, with at least a 1-min pause between pulses. Cell suspensions were then centrifuged for 30 min (4 °C) at 15,000×*g*. The resulting supernatants, referred to as cell extracts, were transferred to a fresh tube and used in enzyme activity assays. Protein concentrations in the cell extracts were determined as described by Bradford (1976), using bovine serum albumin as standard. The enzyme assays were carried out by spectrophotometric methods as described previously (Laemmli et al. 2000). The substrates tested included 3-chloro- (3-CC) and 3,5-dichlorocatechol (3,5-DCC) for chlorocatechol 1,2-dioxygenase, 3-chloromuconate (3-CM) for chloromuconate cycloisomerase, *cis*-dienelactone for dienelactone hydrolase, and maleylacetate for maleylacetate reductase.

Chemicals

3-CC (purity 99%) and 3,5-DCC (purity 99%) were purchased from Promochem (Wesel, Germany). 3-Chloromuconate, *cis*- and *trans*-dienelactone were the kind gift of Dr. Walter Reineke (Bergische Universität-Gesamthochschule Wuppertal, Wuppertal, Germany). Maleylacetate was prepared by alkaline hydrolysis of *cis*-dienelactone (Evans et al. 1971) by mixing 1 ml of 5 mM *cis*-dienelactone with 7.5 µl of 2 N NaOH and incubating for 15 min at room temperature. 2,4-D, 3-CBA and MCPA were purchased from Fluka Chemie (Buchs, Switzerland).

Results

Transcription of *tfd* in the insertion mutants

In order to study possible differences and redundancies in the enzymes of the two modified *ortho*-cleavage pathways encoded by the *tfd* gene clusters I and II, the genes were inactivated individually on plasmid pJP4 in *R. eutropha* JMP134 by insertion mutagenesis with a kanamycin resistance gene. Recombination onto plasmid pJP4 in *R. eutropha* was relatively effective, and for all targeted *tfd* genes double recombinants were obtained at an approximate frequency of 20% of all primary kanamycin resistant transformants. Correct insertion of the kanamycin gene was verified by PCR and Southern hybridization (data not shown). In order to determine whether expression of the *tfd* genes within the JMP134 mutants was impaired by the insertion of the kanamycin gene (polar effects), the abundance of *tfd* mRNA in the different mutants after induction with 3-CBA was analyzed by dot-blot hybridization of total RNA using anti-sense RNA probes for each of the *tfd* genes, except $tfdD_{II}$, *tfdA* and *tfdR/S*. Hybridization signals of different RNA dilutions and after different exposure times revealed that insertion of the kanamycin gene did not largely effect expression of the *tfd* genes and that, upon induction with 3-CBA, expression of nearly all of the *tfd* genes in the knockout mutants resembled that of the wild-type (not shown). Except for the relatively poor expression of *tfdF* in strain JMP134 (*tfdD*::Km), there were very few clear differences in expression. However, the difference in strain JMP134 (*tfdD*::Km) could not directly be attributed to insertion of the kanamycin resistance gene, since the expression of *tfdE* in strain JMP134 (*tfdD*::Km) did not seem to be influenced. Thus, it was concluded that the effects of gene displacement by insertion of the kanamycin resistance gene were due to inactivation of that particular *tfd* gene and not to polar effects on other *tfd* genes.

Growth on 3-CBA, 2,4-D and MCPA by *tfd* knockout mutants of strain JMP314 (pJP4)

All insertion mutants were analyzed for growth on fructose (not shown), 3-CBA, 2,4-D, or MCPA as sole carbon and energy source (Fig. 3, Table 2). Growth of the wild-type strain JMP134 (pJP4), which uses all three compounds as sole carbon and energy source, was used as reference. In-

COR-AAD1-00002628
Bayer EX1008 (Part 5 of 9)

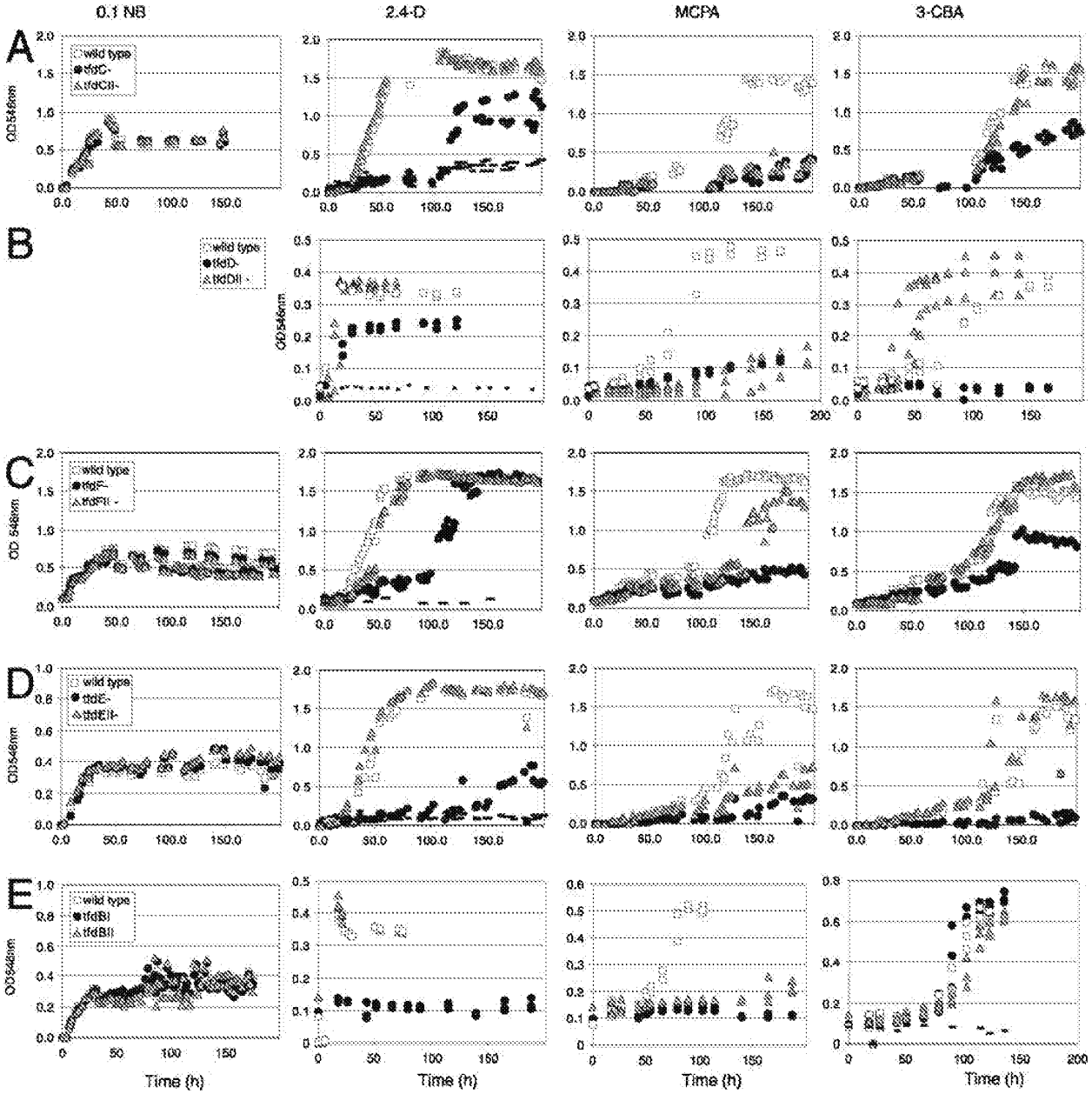


Fig. 3A–E Growth of *R. eutropha* JMP134 (pJP4) and the *tfd* insertion mutants on one-tenth strength nutrient broth or minimal medium supplemented with either 2.5 mM 2,4-D, 3 mM MCPA, or 3 mM 3-CBA. Growth was measured as turbidity at 546 nm, but cannot be compared between **A**, **C**, **D** and **E** NB (experiment in microwell plates), and **B** and **E** 2,4-D/MCPA/3-CBA (Erlenmeyer flasks), due to differences in the optical translucence of the microwell plates and cuvettes used to measure samples from the Erlenmeyer flasks and the different lengths of the optical paths. Data points are means from triplicate measurements of the same incubation series (shown without error bar), but plotted for all independent incubations simultaneously, thus resulting in a 'stuttering' curve. *Open squares* Wild-type JMP134, *closed circles* mutation in tfd_I cluster, *gray triangles* mutation in tfd_{II} cluster gene, *stripes* control incubation with minimal medium only. **A** *tfdC* and $tfdC_{II}$; **B** *tfdD* and $tfdD_{II}$; **C** *tfdF* and $tfdF_{II}$; **D** *tfdE* and $tfdE_{II}$; **E** *tfdB* and $tfdB_{II}$

sertion of the kanamycin gene did not lead to measurable growth retardation in any of the mutants on one-tenth strength nutrient broth in batch cultures (Fig. 3). All mutants also grew well on fructose, indicating that no auxotrophy was generated by accident. The effect of the mutations was different for each of the three chlorinated carbon sources. None of the mutations in *tfd* cluster II genes affected growth of *R. eutropha* on 2,4-D. By contrast, mutations in *tfdC*, *tfdD*, and *tfdF* resulted in growth retardation on 2,4-D, but the cells recovered after a longer lag phase and/or to a lower yield, indicating that the activities of the TfdC, TfdD, and TfdF enzymes can be partially exchanged by $TfdC_{II}$, $TfdD_{II}$, and $TfdF_{II}$, respectively. Mutations in *tfdE* and *tfdB*, however, completely prevented

COR-AAD1-00002629
Bayer EX1008 (Part 5 of 9)

Table 2 Phenotype of *tfd* mutants in *Ralstonia eutropha* JMP134, summarized for all independent growth experiments. *2,4-D* 2,4-Dichlorophenoxyacetic acid, *MCPA* 2-methyl-4-chlorophenoxyacetic acid, *3-CBA* 3-chlorobenzoate. +++ Faster than wild-type growth, ++ equally fast and equal yield, + less fast and less yield, ± very slight growth, – non-significant growth, *E* essential for growth, *NE* non-essential, *R* redundant (function can partially be fulfilled by counterpart), *I* inhibitory

Mutant	Substrate					
	2,4-D		MCPA		3-CBA	
	Phenotype	Character	Phenotype	Character	Phenotype	Character
$tfdD_{II}$	++	N.E.	±	E	+++	I
$tfdC_{II}$	++	N.E.	–	E	++	N.E.
$tfdE_{II}$	++	N.E.	±	E	++	N.E.
$tfdF_{II}$	++	N.E.	+	R	++	N.E.
$tfdB_{II}$	++	N.E.	±	E	++	N.E.
tfdC	+	R	–	E	+	R
tfdD	+	R	±	E	–	E
tfdE	–	E	–	E	–	E
tfdF	+	R	±	E	+	R
tfdB	–	E	–	E	++	N.E.

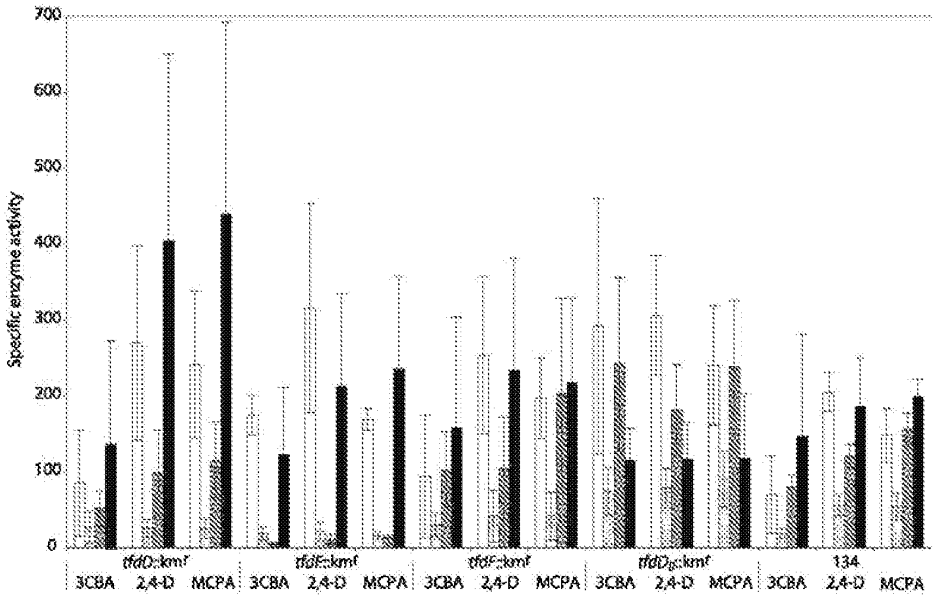


Fig. 4 Specific enzyme activities encoded by the tfd_I and tfd_{II} genes measured in cell extracts of *R. eutropha* JMP134 and several insertion mutants. 1 mU corresponds to 1 nmol of substrate disappearance or product formation per min. *Open bars* Chlorocatechol 1,2-dioxygenase, *stippled bars* chloromuconate cycloisomerase, *hatched bars* dienelactone hydrolase, *black bars* maleylacetate reductase

growth on 2,4-D. In comparison to a minimal medium only control, these mutants did not grow significantly or consistently on 2,4-D. Therefore, *tfdE* and *tfdB* appear to be essential for growth of *R. eutropha* on 2,4-D (Table 2).

A very different behavior was found when *R. eutropha* mutants were incubated with MCPA. Compared to growth of the wild-type strain on MCPA, the growth rates and yields of all of the mutants, except for $tfdF_{II}$, were severely retarded (about 20% of wild-type turbidity after 200 h incubation). The mutant with the $tfdF_{II}$ insertion could still grow on MCPA, but with a considerably longer lag phase, at a slightly lower rate, and with a lower yield (80% of the turbidity of the wild-type culture after 200 h). This was surprising and suggests that either the gene copy number or subtle differences in substrate range between the Tfd enzymes encoded by cluster I and cluster II are important for growth on MCPA. The effect of the different mutations for growth on 3-CBA was more variable. In general, even wild-type *R. eutropha* grew slower and after a longer lag-phase with 3-CBA than with 2,4-D or MCPA. Most mutations in *tfd* cluster II genes did not affect growth rate and yield on 3-CBA, except for $tfdD_{II}$. The $tfdD_{II}$ mutant of *R. eutropha* JMP134 (pJP4) actually grew more consistently and faster on 3-CBA compared to the wild-type strain. Mutations in *tfdC* and *tfdF* did not completely abolish growth on 3-CBA, whereas those in *tfdD* and *tfdE* did. Mutations in *tfdB* or $tfdB_{II}$ did not affect growth on 3-CBA.

Activity of the gene products from the *tfdI* and *tfdII* cluster in mutants of strain JMP134

The activities of the chlorocatechol pathway enzymes were measured in cell extracts of several mutant *R. eutropha* strains as well as of wild-type JMP134 upon induction with 3-CBA, 2,4-D, or MCPA. The three induction substrates were chosen for comparison to the substrates used in the growth experiments. No significant differences in induction level were observed with respect to the induc-

COR-AAD1-00002630
Bayer EX1008 (Part 5 of 9)

tion substrate (3-CBA, 2,4-D, or MCPA) (Fig. 4), although 3-CBA tended to be the least efficient inducer. However, differences were observed between the strains. In all cell extracts tested, chlorocatechol 1,2-dioxygenase activity (TfdC and $TfdC_{II}$) varied between 100 and 300 mU·(mg·protein)$^{-1}$ and maleylacetate reductase activity (TfdF and $TfdF_{II}$) between 150 and 400 mU·(mg·protein)$^{-1}$ depending on the strain and the induction substrate used. *R. eutropha* strain *tfdD$_{II}$*::Km had the overall highest chloromuconate cycloisomerase (TfdD) and dienelactone hydrolase (TfdE) activities – around 80 mU·(mg·protein)$^{-1}$ and 200–250 mU·(mg·protein)$^{-1}$, respectively, but maleylacetate reductase activity was somewhat reduced. In contrast, *R. eutropha* with an insertion in *tfdE* displayed surprisingly low chloromuconate cycloisomerase (TfdD and $TfdD_{II}$) and dienelactone hydrolase activity ($TfdE_{II}$). Cell extracts of this strain contained chloromuconate cycloisomerase activities ranging between 16 and 21 mU·(mg·protein)$^{-1}$ and no significant dienelactone hydrolase activities (at the level of our detection limit). The absence of dienelactone hydrolase activity ($TfdE_{II}$) would imply that *tfdE$_{II}$* was either not translated or produced a dysfunctional or very unstable protein, since $TfdE_{II}$-activity was measured before in *E. coli* (Laemmli et al. 2000).

Discussion

In terms of its evolution, it was convincingly shown that the *tfd$_{II}$* gene cluster had been inserted into an ancestor *tfd$_{I}$* cluster by means of transposition (Leveau and van der Meer 1997). Hence, the remaining problem has been to demonstrate that the *tfd$_{II}$* gene cluster has a specific value for the strain in terms of chloroaromatic degradation, or else it would have disappeared or genetically changed. Several different approaches, i.e. heterologous cloning in *E. coli*, enzyme purification, transposon mutagenesis, and cloning in *R. eutropha*, were previously taken and it was concluded that the genes from the *tfd$_{II}$* cluster are expressed in *R. eutropha* JMP134 (pJP4) (Leveau et al. 1999; Plumeier et al. 2002), but without obvious selective advantage for the microorganism. Several possible advantages were postulated, such as double gene dosage and thus a higher expression level of the chlorocatechol degradative enzymes (Pérez-Pantoja et al. 2000, 2003; Plumeier et al. 2002), the presence of a 2,4-D uptake system in the *tfd$_{II}$* cluster (Leveau et al. 1998), and of the regulatory genes *tfdR* and *tfdS* (Leveau and van der Meer 1996; Laemmli et al. 2002). Clear negative effects of the *tfd$_{II}$* cluster were also found. For example, the $TfdD_{II}$ enzyme appeared to be incapable of converting 2-CM, one of the possible intermediates in the metabolism of 3-CC (Laemmli et al. 2000; Pérez-Pantoja et al. 2000; Laemmli et al. 2002; Plumeier et al. 2002), which limits growth of *R. eutropha* strains carrying the *tfd$_{II}$* gene cluster on a plasmid on 3-CBA (Laemmli et al. 2002). It could also be shown that 3-CC and 4-CC exert toxic effects on *R. eutropha* when not metabolized rapidly enough (Pérez-Pantoja et al. 2003). Hence, too low expression levels of the chlorocatechol-1,2-dioxygenase TfdC or $TfdC_{II}$ leading to higher than normal 3-CC and 4-CC metabolite production will inhibit growth.

In order to further study the function of each of the *tfd* genes for *R. eutropha* JMP134 (pJP4), we did not use the previously practiced approach of cloning either the *tfd$_{I}$* or *tfd$_{II}$* cluster (or hybrid clusters) on a plasmid in a pJP4-free strain of *R. eutropha*. With these strains it was only possible to test intracellular conversion of chlorocatechols, which would be formed by growing the cells on 3-CBA. Therefore, we constructed mutants of the wild-type strain JMP134 by interrupting each of the *tfd* genes on pJP4 (except *tfdA*, *tfdR*, and *tfdS*) by homologous recombination and gene replacement with a kanamycin resistance gene. The knockout strains were tested for their ability to grow on 2,4-D, 3-CBA, or MCPA as sole carbon and energy source. Compared to the growth behavior of the wild-type strain JMP134, four distinct phenotypes were observed for the knockout mutants: (1) no or very slight growth, (2) less optimal growth than the wild-type strain, (3) growth equal to that of the wild-type strain, and (4) more optimal growth than the wild-type. Based on these phenotypes, all of the *tfd* genes were categorized with respect to their function for metabolism of 2,4-D, 3-CBA and MCPA into essential, not essential, inhibitory, and redundant genes (Table 2). The outcome of these studies was that *tfdE* and *tfdB* are the only essential genes in the *tfd* clusters, since their disruption abolished growth on all three substrates (for *tfdE*) or on 2,4-D and MCPA (for *tfdB*, since TfdB activity is not required for growth on 3-CBA). Apparently, the "counterparts" of *tfdE* and *tfdB* (*tfdE$_{II}$* and *tfdB$_{II}$*) do not replace their functions in *R. eutropha*. No dienelactone hydrolase activity could be measured in induced cell extracts of *R. eutropha* with the *tfdE* interruption, which is in agreement with the lack of observed growth of this strain. Very low $TfdE_{II}$ activity had also been detected in cell extracts of *R. eutropha* JMP134 (pJP4) pregrown on 2,4-D (Plumeier et al. 2002). Since *tfdE$_{II}$* mRNA could be detected at normal levels in *R. eutropha* with the *tfdE*::Km insertion, and since we had previously shown that expression of *tfdE$_{II}$* in *E. coli* (from an optimal promoter and translational fusion system) results in a functional dienelactone hydrolase able to catalyze the conversion of *cis*- and *trans*-dienelactone (Laemmli et al. 2000), we conclude that for some reason the *tfdE$_{II}$* mRNA is either not or very weakly translated in *R. eutropha* or results in a very unstable protein. In this respect, it was surprising to find that the *tfdE$_{II}$* insertion mutant was not able to grow on MCPA, suggesting that weak $TfdE_{II}$ activity is still important for growth on that substrate.

In contrast to the results obtained for *tfdE* and *tfdB*, the *tfdC*, *tfdD* and *tfdF* gene products were not absolutely essential for chloroaromatic growth. For example, *tfdD* expression was only essential for growth on 3-CBA, which can be explained by the fact that the counterpart enzyme, $TfdD_{II}$, is unable to catalyze the conversion of 2-CM, an intermediate in 3-CBA metabolism (Fig. 1), to *trans*-dienelactone (Laemmli et al. 2002; Plumeier et al. 2002). When tested on 2,4-D, the *tfdD* gene was not essential for

COR-AAD1-00002631
Bayer EX1008 (Part 5 of 9)

growth, but led only to growth retardation and lower yield. Apparently, the *tfdD*$_{II}$ gene product is sufficiently active with 2,4-dichloromuconate (Fig. 1) to allow growth on 2,4-D. The *tfdC* and *tfdF* genes turned out to be redundant for growth on 2,4-D as well, and insertion mutants grew with a significantly longer lag phase, but not with a slower growth rate. However, both insertion mutants did have difficulties in growing on 3-CBA. This demonstrates that, depending on the growth substrate, the *tfdC*$_{II}$ and *tfdF*$_{II}$ gene products can take over the role of their counterparts TfdC and TfdF.

On MCPA, all *tfd*$_{I}$ cluster mutants were essentially unable to grow or grew only very slightly. However, also cells carrying an insertion mutations in the *tfd*$_{II}$ gene cluster, except for the *tfdF*$_{II}$ insertion mutant, grew at best very slowly on MCPA. Since the wild-type strain grew well on MCPA, and since all mutants displayed different phenotypes on 2,4-D and 3-CBA, their growth behavior on MCPA cannot be an artifact. Hence, this demonstrated that the gene products of *tfd* cluster II play an important role in growth on MCPA and is thus a clear indication for a positive effect for *R. eutropha* JMP134 of carrying the *tfd*$_{II}$ gene cluster for chloroaromatic degradation: a widening of the substrate range. While several hypotheses can be raised for the behavior of the mutants of MCPA, they are not completely satisfactory at this moment. First of all, the expression level of the *ortho*-cleavage pathway enzymes could become too low with only one of the gene copies present. This, however, does not seem to be the case, since the level of enzyme activities in mutant *R. eutropha* cultures induced with MCPA were not particularly different from those induced with 3-CBA or 2,4-D, nor from the wild-type (Fig. 4). The second hypothesis is that different substrate specificities of the enzymes from both clusters are needed for MCPA degradation. This, however, would imply that MCPA metabolism follows different pathways, which is not impossible but for which no further evidence exists at the moment (Pieper et al. 1988).

The most pressing problem for *R. eutropha* JMP134 (pJP4) is that expression of *tfdD*$_{II}$ is not favorable for growth on 3-CBA. We conclude this from the finding that *tfdD*$_{II}$ knockouts grew even more consistently than the wild-type strain on 3-CBA, which indicates that TfdD$_{II}$ activity during metabolism of 3-CBA is inhibitory to the cells, even when TfdD is active. Our results with the *tfdF*$_{II}$ insertion mutant are slightly in contrast to those obtained by others. For example, Ledger et al. (2002) constructed a *tfdF*$_{II}$ insertion mutant in a strain of *R. eutropha* JMP134 (pJP4) with the additional *xylXYZ* genes. This mutant could not grow on 3,5-dichlorobenzoate, which was taken as an indication for the necessity of *tfdF*$_{II}$ in the conversion of 3,5-dichlorocatechol. 3,5-Dichlorocatechol is also an intermediate in 2,4-D degradation. We presently cannot explain this difference. Seibert et al. (1993) purified the chloromaleylacetate reductase activity from *R. eutropha* JMP134 which consisted of the TfdF$_{II}$ protein, suggesting that the TfdF$_{II}$ protein was solely responsible for this activity and thus essential for growth on chloroaromatic compounds. However, more recently, Plumeier et al. (2002) purified both TfdF and TfdF$_{II}$ from *R. eutropha* JMP134 (pJP4) grown on 2,4-D, and showed that each enzyme contributes to about half of the total maleylacetate reductase activity. Hence, insertion mutants in either *tfdF* or *tfdF*$_{II}$ would still be able to grow on 2,4-D.

The results of the present study have helped to elucidate further subtle differences in the role of the *tfd*$_{I}$ and *tfd*$_{II}$ gene clusters for chloroaromatic degradation by *R. eutropha* JMP134 (pJP4). From an evolutionary standpoint, the presence of two orthologous gene clusters on plasmid pJP4 is interesting and exemplary for various other microbial systems, and is always assumed to have some selective advantage. Summarizing all previous data, would lead to the conclusion that indeed some functional differences exist, but they also mostly argue against keeping the *tfd*$_{II}$ cluster. Our previous hypothesis had therefore been that maintaining the configuration of two *tfd* clusters on plasmid pJP4 must somehow provide a selective disadvantage of deleting the *tfd*$_{II}$ part (Laemmli et al. 2002). Deletion of the *tfd*$_{II}$ cluster (most easily envisioned through recombination between the ends of the IS*JP4* elements) would result in loss of the *tfdR* and *tfdS* regulatory genes, which would affect efficient chloroaromatic degradation. However, as was discovered in the present study, there is another clear metabolic advantage for keeping the *tfd*$_{II}$ cluster genes, namely, the degradation of MCPA.

Acknowledgements The authors gratefully acknowledge the financial support rendered by the Swiss National Science Foundation through grant 31-49222 to CL.

References

Baumann B, Snozzi M, Zehnder AJB, van der Meer JR (1996) Dynamics of denitrification activity of *Paracoccus denitrificans* in continuous culture during aerobic-anaerobic changes. J Bacteriol 178:4367–4374

Bradford MM (1976) A rapid and sensitive method for the quantification of microgram quantities of protein utilizing the principle of protein-dye binding. Anal Biochem 72:248–254

Don RH, Pemberton JM (1981) Properties of six pesticide degradation plasmids isolated from *Alcaligenes paradoxus* and *Alcaligenes eutrophus*. J Bacteriol 145:681–686

Don RH, Weightman AJ, Knackmuss H-J, Timmis KN (1985) Transposon mutagenesis and cloning analysis of the pathways for degradation of 2,4-dichlorophenoxyacetic acid and 3-chlorobenzoate in *Alcaligenes eutrophus* JMP134(pJP4). J Bacteriol 161:85–90

Evans WC, Smith BSW, Fernley HN, Davies JI (1971) Bacterial metabolism of 2,4-dichlorophenoxyacetate. Biochem J 122:543–551

Gerhardt P, Murray RGE, Costilow RN, Nester EW, Wood WA, Krieg NR, Briggs Phillips G (eds) (1981) Manual of methods for general bacteriology. American Society for Microbiology, Washington, D.C.

Harayama S, Leppik RA, Rekik M, Mermod N, Lehrbach PR, Reineke W, Timmis KN (1986) Gene order of the TOL catabolic plasmid upper pathway operon and oxidation of both toluene and benzyl alcohol by the *xylA* product. J Bacteriol 167: 455–461

Laemmli CM, Leveau JHJ, Zehnder AJB, van der Meer JR (2000) Characterization of a second *tfd* gene cluster for chlorophenol and chlorocatechol metabolism on plasmid pJP4 in *Ralstonia eutropha* JMP134(pJP4). J Bacteriol 182:4165–4172

COR-AAD1-00002632
Bayer EX1008 (Part 5 of 9)

Laemmli CM, Schönenberger R, Suter MJ-F, Zehnder AJB, van der Meer JR (2002) TfdDII, one of the two chloromuconate cycloisomerases of *Ralstonia eutropha* JMP134 (pJP4), cannot efficiently convert 2-chloro-*cis*,*cis*-muconate to *trans*-dienelactone to allow growth on 3-chlorobenzoate. Arch Microbiol 178:13–25

Ledger T, Pieper DH, Pérez-Pantoja D, Gonzalez B (2002) Novel insights into the interplay between peripheral reactions encoded by *xyl* genes and the chlorocatechol pathway encoded by *tfd* genes for the degradation of chlorobenzoates by *Ralstonia eutropha* JMP134. Microbiology 148:3431–3440

Leveau JHJ, van der Meer JR (1996) The *tfdR* gene product can successfully take over the role of the insertion element-inactivated TfdT protein as a transcriptional activator of the *tfdCDEF* gene cluster, which encodes chlorocatechol degradation in *Ralstonia eutropha* JMP134(pJP4). J Bacteriol 178:6824–6832

Leveau JHJ, van der Meer JR (1997) Genetic characterization of insertion sequence IS*JP4* on plasmid pJP4 from *Ralstonia eutropha* JMP134. Gene 202:103–114

Leveau JH, Zehnder AJ, van der Meer JR (1998) The *tfdK* gene product facilitates uptake of 2,4-dichlorophenoxyacetate by *Ralstonia eutropha* JMP134(pJP4). J Bacteriol 180:2237–2243

Leveau JHJ, König F, Füchslin H-P, Werlen C, van der Meer JR (1999) Dynamics of multigene expression during catabolic adaptation of *Ralstonia eutropha* JMP134 (pJP4) to the herbicide 2, 4-dichlorophenoxyacetate. Mol Microbiol 33:396–406

Pérez-Pantoja D, Guzman L, Manzano M, Pieper DH, Gonzalez B (2000) Role of $tfdC_ID_IE_IF_I$ and $tfdD_{II}C_{II}E_{II}F_{II}$ gene modules in catabolism of 3-chlorobenzoate by *Ralstonia eutropha* JMP134(pJP4). Appl Environ Microbiol 66:1602–1608

Pérez-Pantoja D, Ledger T, Pieper DH, Gonzalez B (2003) Efficient turnover of chlorocatechols is essential for growth of *Ralstonia eutropha* JMP134 (pJP4) in 3-chlorobenzoic acid. J Bacteriol 185:1534–1542

Perkins EJ, Gordon MP, Caceres O, Lurquin PF (1990) Organization and sequence analysis of the 2,4-dichlorophenol hydroxylase and dichlorocatechol oxidative operons of plasmid pJP4. J Bacteriol 172:2351–2359

Pieper DH, Reineke W, Engesser K-H, Knackmuss H-J (1988) Metabolism of 2,4-dichlorophenoxyacetic acid, 4-chloro-2-methylphenoxyacetic acid and 2-methylphenoxyacetic acid by *Alcaligenes eutrophus* JMP134. Arch Microbiol 150:95–102

Pieper DH, Knackmuss H-J, Timmis KN (1993) Accumulation of 2-chloromuconate during metabolism of 3-chlorobenzoate by *Alcaligenes eutrophus* JMP134. Appl Microbiol Biotechnol 39: 563–567

Plumeier I, Pérez-Pantoja D, Heim S, Gonzalez B, Pieper DH (2002) Importance of different *tfd* genes for degradation of chloroatomatics by *Ralstonia eutropha* JMP134 (pJP4) on 3-chlorobenzoate. J Bacteriol 184:4054–4064

Ravatn R, Studer S, Springael D, Zehnder AJB, van der Meer JR (1998) Chromosomal integration, tandem amplification, and deamplification in *Pseudomonas putida* F1 of a 105-kilobase genetic element containing the chlorocatechol degradative genes from *Pseudomonas* sp. strain B13. J Bacteriol 180:4360–4369

Sambrook J, Frisch EF, Maniatis T (1989) Molecular cloning: a laboratory manual, 2nd edn. Cold Spring Harbor Laboratory, Cold Spring Harbor, New York

Schlömann M (2002) Two chlorocatechol catabolic gene modules on plasmid pJP4. J Bacteriol 184:4049–4053

Seibert V, Stadler-Fritzsche K, Schlömann M (1993) Purification and characterization of maleylacetate reductase from *Alcaligenes eutrophus* JMP134(pJP4). J Bacteriol 175:6745–6754

Streber WR, Timmis KN, Zenk MH (1987) Analysis, cloning, and high-level expression of 2,4-dichlorophenoxyacetate monooxygenase gene *tfdA* of *Alcaligenes eutrophus*. J Bacteriol 169: 2950–2955

COR-AAD1-00002633
Bayer EX1008 (Part 5 of 9)

2,4-Dichlorophenoxyacetic Acid Metabolism in Transgenic Tolerant Cotton (*Gossypium hirsutum*)

F. Laurent,* L. Debrauwer, E. Rathahao, and R. Scalla

Laboratoire des Xénobiotiques, INRA, B.P. 3, 180 chemin de Tournefeuille, 31931 Toulouse Cedex 9, France

The metabolic fate of 2,4-dichlorophenoxyacetic acid (2,4-D) was studied in leaves of transgenic 2,4-D-tolerant cotton (*Gossypium hirsutum*), which is obtained by transfer of the *tfdA* gene from the bacterium *Alcaligenes eutrophus*. The *tfdA* gene codes for a dioxygenase catalyzing the degradation of 2,4-D to 2,4-dichlorophenol (2,4-DCP). [*phenyl*-^{14}C]-2,4-D was administered by petiolar absorption followed by an 18 h water chase or converted to the isopropyl ester and sprayed onto the leaf surface; the leaves were harvested 48 h later. The herbicide was degraded to 2,4-DCP by the bacterial enzyme expressed in the plants. 2,4-DCP was rapidly converted to more polar metabolites and was never found in detectable amounts. Metabolite structures were deduced from enzymatic hydrolysis studies and mass spectrometric analyses. The first metabolite was the glucoside conjugate of 2,4-DCP (2,4-DCP−*β*-*O*-glucoside). The major terminal metabolites were two more complex glucosides: 2,4-DCP−(6-*O*-malonyl)glucoside and 2,4-DCP−(6-*O*-sulfate)glucoside.

Keywords: *Gossypium hirsutum; herbicide metabolism; transgenic plant; 2,4-dichlorophenoxyacetic acid; glucosyl−sulfate conjugate*

Downloaded via CORTEVA AGRISCIENCE on September 3, 2020 at 19:09:49 (UTC).
See https://pubs.acs.org/sharingguidelines for options on how to legitimately share published articles.

INTRODUCTION

The development of new herbicides meets with increasing costs and more and more stringent toxicological and environmental requirements. In these conditions, an alternative strategy consists of creating herbicide-resistant crop varieties. The introduction of genes for herbicide degradation is an attractive method to reach that goal because it can be applied to herbicides the biochemical target of which is not known or to herbicides with several sites of action, such as auxinic herbicides.

Transgenic cotton or tobacco plants ~100-fold more tolerant to 2,4-dichlorophenoxyacetic acid (2,4-D) have been obtained by transfer of the *tfdA* gene from the bacterium *Alcaligenes eutrophus* (Streber and Willmitzer, 1989; Bayley et al., 1992; Lyons et al., 1993). That transformation extends the use of 2,4-D to dicotyledonous crops, whereas its use was originally restricted to grasses.

Phenoxyalkanoic acids such as 2,4-D are usually metabolized in plants mainly by the formation of glucose esters and amino acid amides or by ring hydroxylation followed by glucose conjugation (Feung et al., 1978). In transgenic plants, the bacterial *tfdA* gene codes for a dioxygenase catalyzing the degradation of 2,4-D to 2,4-dichlorophenol (2,4-DCP) (Fukumori and Hausinger, 1993), which is much less phytotoxic than the parent compound (Llewellyn and Last, 1996). Degradation of the 2,4-D side chain normally takes place in some plants (Loos, 1976; Aizawa, 1989), but the precise nature of the reaction involved is not fully understood (Owen, 1975). Moreover, that pathway is often of minor importance, and, except for red currant (*Ribes sativum* Syme) (Luckwill and Lloyd-Jones, 1960), it does not seem to play any significant role in the tolerance to 2,4-D.

2,4-DCP is potentially harmful to animal populations and to the environment (Jensen, 1996). It is converted to a glucoside conjugate in the aquatic angiosperm *Lemna gibba* (Ensley et al., 1994). However, contrary to other chlorophenol derivatives such as pentachlorophenol (Schmitt et al., 1985), its metabolism in crop plants has been little studied.

The biochemical fate of 2,4-DCP in resistant, transgenic plants has thus to be clarified. The lack of knowledge in that domain prompted us to examine the metabolism of 2,4-D in transgenic tolerant cotton.

MATERIALS AND METHODS

Chemicals. [U-*phenyl*-^{14}C]-2,4-dichlorophenoxyacetic acid (specific activity = 18.2 *μ*Ci/mmol; radiochemical purity > 97% as determined by HPLC), nonlabeled 2,4-D, and 2,4-DCP were purchased from Sigma (St. Quentin Fallavier, France). The isopropyl ester of 2,4-D was prepared as described by Sánchez-Brunete et al. (1991). 2,4-DCP−*β*-D-glucoside was synthesized according to the procedure of Koenigs-Knorr (Conchie and Levvy, 1963). 2,4-DCP−(6-*O*-malonyl)-*β*-D-glucopyranoside was prepared following the one-step method developed by Roscher et al. (1996). 2,4-DCP−(6-*O*-sulfate)-*β*-D-glucopyranoside was synthesized by mole to mole reaction of synthetic 2,4-DCP−*β*-D-glucoside with pyridine−sulfur trioxide in anhydrous dimethylformamide (Whistler et al., 1963). Glucosides were purified by HPLC as described below (see Chromatography).

Without other specifications, all other chemicals were of analytical grade.

Plant Material and 2,4-D Applications. Transgenic 2,4-D-tolerant cotton (*Gossypium hirsutum* cv. Cooker 315) was kindly provided by Dr. D. J. Llewellyn (CSIRO). Seeds were individually sown in 300 mL plastic pots containing a compost/vermiculite mixture (2:1) and grown for 5 weeks in a climate-controlled cabinet set at 30/25 °C (day/night) with a 16 h photoperiod.

Two methods of herbicide administration were used. First, leaves of intact cotton plants were sprayed with [^{14}C]-2,4-D-isopropyl ester (300 mg/L, 2.24 *μ*Ci/mmol), dissolved in a 0.1% Tween 80/50% acetone solution, until dripping wet. That herbicide concentration was half the lowest concentration inducing damage to the transgenic cotton (Llewellyn, 1996).

* Author to whom correspondence should be addressed [fax (33) 05 61 28 52 44; e-mail flaurent@toulouse.inra.fr].

10.1021/jf990672c CCC: $19.00 © 2000 American Chemical Society
Published on Web 10/13/2000

COR-AAD1-00002634
Bayer EX1008 (Part 5 of 9)

Treated leaves were harvested 48 h after the spray application. In other experiments, fully expanded leaves were excised and their petioles inserted in vials containing 1 mL of a solution of [^{14}C]-2,4-D (18 μCi/mmol, 0.5 μCi, without unlabeled 2,4-D). The labeled 2,4-D solution was absorbed in ~2 h and was replaced by distilled water. The treatment was continued for 18 h prior to metabolite extraction.

Preparation of Plant Extracts. When 2,4-D was absorbed from the upper surface of leaves of intact plants, the leaves were rinsed with acetone to remove surface residues of treatments. In all experiments, the tissues were frozen at −80 °C and then ground with a ball grinder for 5 min. The resulting powders were extracted with water (5 mL/g of fresh weight) and then with a methanol/dichloromethane mixture (2:1, v/v). The surface washings and the aqueous and organic extracts were concentrated and then directly analyzed by radio-HPLC or further purified.

In some experiments, metabolites were purified by solid phase extraction (SPE). Water extracts were acidified (pH 3), loaded on C18 SPE cartridges (Supelco, France), and eluted with increasing methanol concentrations. Eluates from 0 to 50% methanol were dried and solubilized with 10 mM $NaHCO_3$ and then transferred to anionic exchange cartridges (Chromabond SB, Macherey-Nagel). Metabolites were eluted with a formic acid/methanol mixture (1:9, v/v) and then with 0.3 M H_3PO_4.

Chemical or Enzymatic Metabolite Hydrolyses. Hydrolyses were carried out in 200 μL of reaction media, according to the method of Schmitt et al. (1986). Samples containing at least 4000 dpm of the compound under investigation were evaporated to dryness.

Acid Hydrolysis. Samples were dissolved in 2 N HCl and heated at 100 °C for 2 h.

Alkaline Hydrolysis. Samples were incubated with 0.1 N NaOH for 1 h at 50 °C.

β-Glucosidase Hydrolysis. Samples were incubated during 2 h at 30 °C with almond β-glucosidase (2 units) (G-0395, Sigma) in 0.1 M, pH 5.0, sodium acetate buffer.

Esterase Hydrolysis. Samples were incubated for 10 min at 30 °C with rabbit liver esterase (2.5 units) (E-9636, Sigma) in 0.05 M, pH 7.5, potassium phosphate buffer or with 60 μL of crude esterase preparation from parsley stems (Matern, 1983) in 0.1 M, pH 5.0, sodium succinate buffer. After hydrolysis, alkaline samples were acidified to pH 3 with HCl. Then acid and acidified alkaline hydrolysates were extracted three times with ethyl ether and analyzed by HPLC. Enzymatic hydrolysates were acidified with HCl to pH 3 and directly analyzed by HPLC.

Chromatography. HPLC separations were performed on a Spectra-Physics P4000 liquid chromatograph equipped with a P1000 Spectra-Physics UV detector set at 216 nm. Radioactivity was monitored with an on-line Canberra-Packard Flow-One\beta scintillation detector, operated with Flow-Scint II scintillation counting cocktail (Canberra-Packard). The binary mobile phase was A = H_2O plus 2% acetic acid and B = acetonitrile plus 2% acetic acid. Separations were carried out on a C18, 6 μm Bischoff column (4.6 mm × 250 mm) at ambient temperature with a flow rate of 1 mL min^{-1}. Two-step elution was as follows: step 1, 25% B, 12 min; step 2, 40% B, 18 min.

2,4-D and its metabolites were compared to synthesized standards on the basis of their retention times: 2,4-D, 20.8 min; 2,4-DCP, 22.6 min; 2,4-DCP glucoside, 6.8 min; 2,4-DCP (malonyl) glucoside, 11.9 min; 2,4-DCP (sulfate) glucoside, 3.8 min.

Mass Analysis. Mass spectra were obtained with a Finnigan LCQ quadrupole ion trap mass spectrometer (Thermo Quest, Les Ulis, France) equipped with an electrospray or an APCI ionization source and operating under negative ionization conditions. For ESI/MS experiments, a typical needle voltage of 5 kV and a heated capillary temperature of 220 °C were used. Sample solutions (5−10 ng/μL in methanol/water, 50:50) were infused at a flow rate of 3 μL/min into the ESI source. Sheath gas flow rate was adjusted in each case to obtain a stable spray and a maximum signal level. No auxiliary gas was used. In the case of APCI-MS experiments, the vaporizer and heated capillary temperatures were set to 450 and 150 °C, respectively. The source voltage and current were 1.90 kV and 5 μA, respectively. The gas flow rate was adjusted for good spraying conditions. Metabolites were analyzed by direct flow injection (typically 20−50 ng per injection) using methanol/water (50:50) at a flow rate of 1 mL/min. All analyses were performed in normal scan mode (unit resolution) under automatic gain control conditions. Helium was used as the collision gas for MS-MS experiments. Ion isolation and collision conditions were optimized separately for each metabolite to gain maximal structural information.

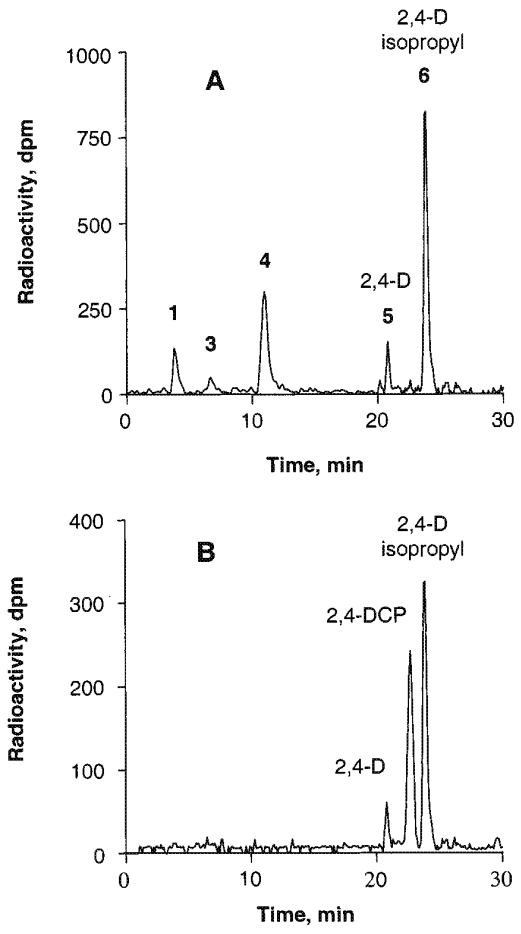


Figure 1. HPLC radiochromatograms of extracts from 2,4-D-tolerant cotton leaves sprayed with [^{14}C]-2,4-D isopropyl ester: (A) aqueous extract; (B) aqueous extract after acid hydrolysis [half level of radioactivity of (A)].

RESULTS AND DISCUSSION

After transgenic cotton plants had been sprayed with [^{14}C]-2,4-D isopropyl ester, five radioactive peaks were observed in HPLC chromatograms of aqueous extracts (Figure 1A). Peaks 5 and 6 were identified as 2,4-D and 2,4-D isopropyl ester, respectively. The three other peaks (1, 3, and 4) were more polar. In organic extracts, only the parent compound and its de-esterified product, 2,4-D, were observed. 2,4-DCP was absent from both extracts, even though they accounted for 97% of the total radioactivity.

After acid hydrolysis of water extracts, all of the radioactivity of polar compounds was found under a 2,4-DCP peak (Figure 1B). No increase of the 2,4-D radioactivity was detected. Therefore, as expected, 2,4-DCP

COR-AAD1-00002635
Bayer EX1008 (Part 5 of 9)

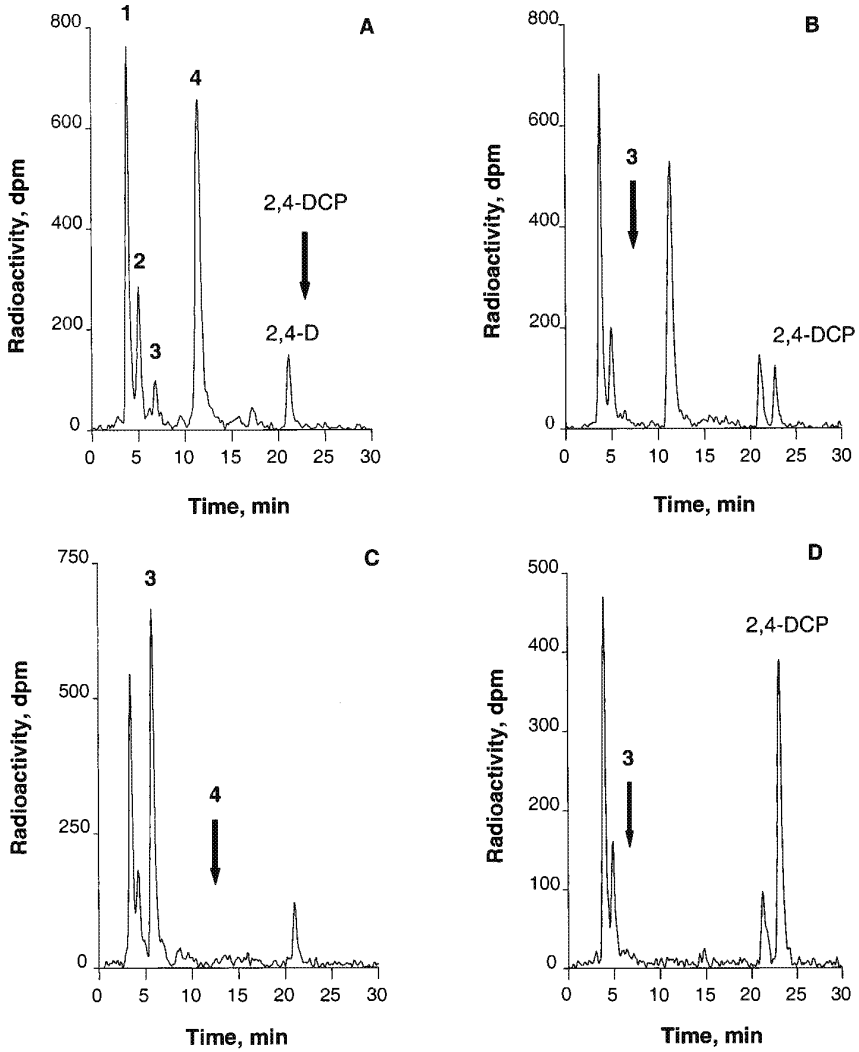


Figure 2. HPLC radiochromatogram of water extracts from excised, 2,4-D-tolerant cotton leaves after petiolar absorption of [^{14}C]-2,4-D: (A) water extract; (B) water extract after treatment with β-glucosidase; (C) water extact after treatment with a crude esterase preparation from parsley stems; (D) same extract as in (C), after a further treatment with β-glucosidase.

was formed in transgenic cotton but as an apparently transient intermediate that is rapidly metabolized to more polar compounds.

When loaded on SPE columns, 2,4-D and the components of peaks 1 and 4 were retained by the anion exchanger, contrary to peak 3. Peak 4 and 2,4-D were eluted in weakly acidic conditions (formic acid/methanol, 1:9), whereas elution of peak 1 required a strong acid (0.3 M H_3PO_4). These results indicated that peaks 1 and 4 were acidic compounds, with different acidic functions.

The structures of the three metabolites were next examined by enzymatic hydrolysis studies and mass spectrometric analyses. To increase the amounts of metabolites, excised leaves were allowed to metabolize 2,4-D for 18 h, after an initial absorption period of 2 h. In these conditions, the same polar metabolites as above were detected, with in addition a new peak representing <10% of the total polar metabolites (Figure 2A; peak 2). The identity of that compound was not determined, but it was identified as a 2,4-DCP metabolite by acid hydrolysis and mass spectrometry (negative mode APCI-MS).

Digestion of water extracts by β-glucosidase converted metabolite **3** to 2,4-DCP (Figure 2B). In addition, metabolite **3** coeluted in HPLC with authentic 2,4-DCP–β-*O*-glucoside and yielded by ESI-MS-MS the same mass spectrum as the authentic 2,4-DCP–β-*O*-glucoside with a base peak quasi-molecular ion at *m/z* 323, a characteristic dichlorine isotopic pattern, and a diagnostic *m/z* 161 fragment ion corresponding to dichlorophenol moiety of the molecule.

The other metabolites were not degraded by β-glucosidase or other glycosidases (results not shown). Metabolite **4** (Figure 2A) was hydrolyzed by 0.1 N NaOH to yield a product coeluting with the β-glucoside, suggesting the presence of an ester linkage in a complex glucoside conjugate. As this metabolite was acidic, it was tentatively identified as a 2,4-DCP–(6-*O*-malonyl)glucoside. Upon treatment with a parsley esterase preparation, specific to the hemiester of malonic acid (Matern, 1983), metabolite **4** was hydrolyzed to yield the glucoside, which could be further hydrolyzed with β-glucosidase to give 2,4-DCP (Figure 2C,D).

As shown by its retention characteristics on an anion exchanger, metabolite **1** was a strongly acidic compound.

COR-AAD1-00002636
Bayer EX1008 (Part 5 of 9)

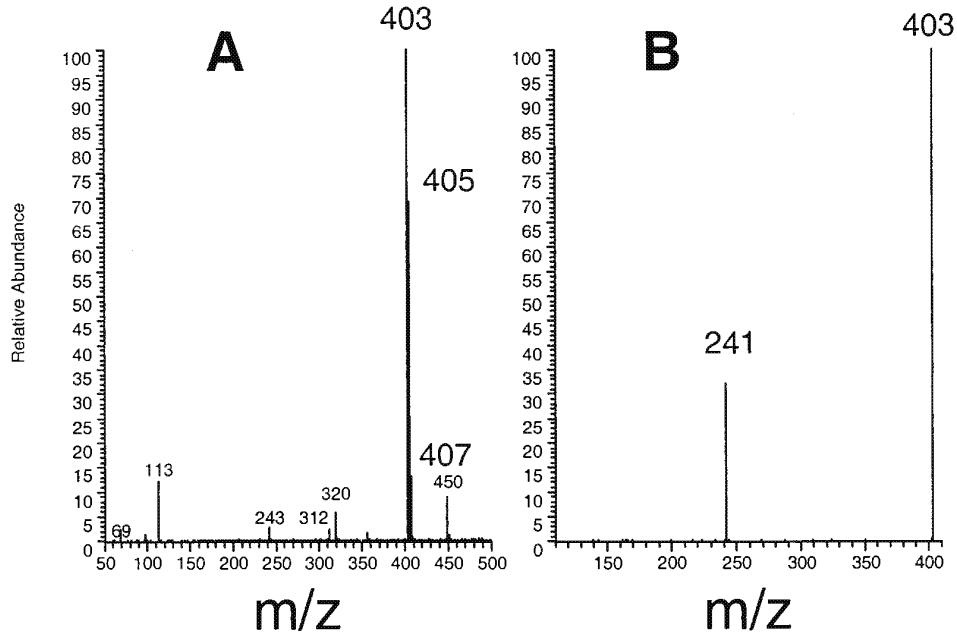


Figure 3. Negative ESI/MS spectra of metabolite **1** isolated from an aqueous extract of 2,4-D-treated tolerant cotton plant: (A) full scan mass spectrum; (B) CAD mass spectrum of $(M - H)^-$ ions (*m/z* 403).

Its ESI mass spectrum showed a quasi-molecular ion cluster at *m/z* 403/405/407 (Figure 3A), characteristic of a molecule with two chlorine atoms. The MS-MS decomposition of the *m/z* 403 parent ion gave a fragment ion at *m/z* 241 corresponding to a loss of 2,4-DCP (Figure 3B). The same *m/z* 241 daugther ion was observed from the selected *m/z* 405 quasi-molecular ion, showing that the *m/z* 241 ion did not contain any chlorine atom. Thus, this ion was tentatively identified as a complex glucoside with a hydroxyl subtituted by an acidic function. The mass increase of 80 th compared to the unchanged glucoside was compatible with a sulfate derivative. A synthesized 2,4-DCP−(6-*O*-sulfate)glucoside yielded the same CAD mass spectrum and coeluted with metabolite **1** in HPLC. Sulfate ester conjugates are generally bound to the aglycon moiety of secondary metabolites—mainly on aryl compounds (Paulson, 1976; Fenwick et al., 1983). Direct carbohydrate sulfating is less frequent. Some sulfate ester glucosides of natural metabolites, such as brucinium, have been described (Whistler et al., 1963), but such derivatives are relatively rare among pesticide metabolites. In a recent study (Capps et al., 1996), a 6-*O*-sulfate glucoside conjugate was described as a unique conjugate for a dihalogenated molecule in cotton, too. The other reported case concerns the metabolism of phemedipham in sugar beet, in which 2-*O*-sulfate glucosides are formed (Lamoureux, 1989).

In conclusion, a metabolic pathway of 2,4-D in transgenic 2,4-D-tolerant cotton is proposed (Figure 4). The main metabolites in transgenic cotton were complex derivates of 2,4-DCP−glucoside, malonyl, and sulfate, conjugates. These conjugates were not described in wild plants treated with 2,4-D, even in plants in which 2,4-D dealkylation is the major degradative pathway, such as black currant (Luckwill and Lloyd-Jones, 1960), because the 2,4-D used is labeled on the alkyl chain.

The metabolism of 2,4-D in wild cotton has been scarcely described. Only one study shows that alkyl-labeled 2,4-D undergoes some side-chain degradation,

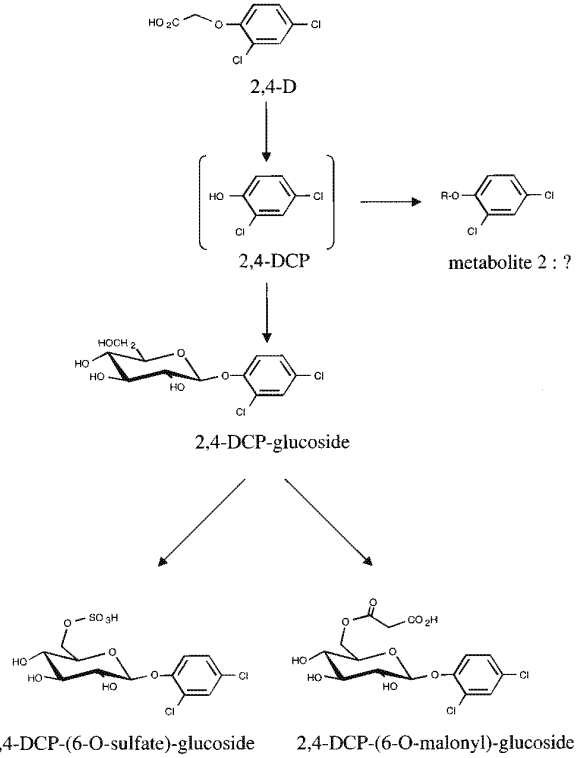


Figure 4. Proposed metabolic pathway of 2,4-D degradation in transgenic cotton.

but the degradation is slow, and the metabolites have not been identified (Morgan and Wayne, 1963). We have examined that point by supplying wild cotton with [^{14}C]-2,4-DCP, to avoid the phytotoxic effect of 2,4-D. In these conditions, wild cotton synthesizes the same three glucosylated metabolites as transgenic cotton (results not shown). Hence, transgenesis does not modify the native metabolism of 2,4-DCP in cotton.

COR-AAD1-00002637
Bayer EX1008 (Part 5 of 9)

The effect of 2,4-DCP on health depended on the subconjugate items. Malonyl conjugate and glucoside, like the natural glucosides such as isoflavone conjugates, could be hydrolyzed in the gastrointestinal tract and liberate free 2,4-DCP. The latter, like the other polychlorophenols, is directly toxic for humans (Jensen, 1996), and its toxicity should be increased by its transformation to dioxin-like compounds in the organism (Wittsiepe et al., 2000). On the other hand, greater chemical or enzymatic stability of the sulfate glucoside should decrease the health hazard.

Generally, chlorophenols were degraded by soil microorganisms. However, it seems that 2,4-DCP was less rapidly mineralized than the parent compound, 2,4-D. For this reason, the use of transgenic plants, tolerant for 2,4-D, could increase the environmental contamination by chlorophenols due to the use of phenoxy acid herbicides. Nevertheless, the 2,4-D-tolerant cotton has been developed to protect sensitive cottons from the 2,4-D spray drift from applications to wild tolerant crops (Lyon et al., 1993) and not to widen the use of the 2,4-D to the sensitive crops.

ABBREVIATIONS USED

2,4-D, 2,4-dichlorophenoxyacetic acid; 2,4-DCP, 2,4-dichlorophenol; SPE, solid phase extraction; HPLC, high-performance liquid chromatography; ESI/MS, electrospray ionization/mass spectrometry; MS-MS, mass spectrometry−mass spectrometry; APCI, atmospheric pressure chemical ionization.

ACKNOWLEDGMENT

We thank Dr. D. Llewellyn from CSIRO, Division of Plant Industry (Canberra City, Australia), for providing the transgenic cotton seeds.

LITERATURE CITED

Aizawa, H. Phenoxyacetic acids. In *Metabolic Maps of Pesticides*; Coulston, F., Korte, F., Eds.; Academic Press: San Diego, CA, 1989; pp 102−107.

Bayley, C.; Trolinder, C.; Morgan, M.; Quisenberry, J. E.; Ow, D. W. Engineering 2,4-D resistance into cotton. *Theor. Appl. Genet.* **1992**, *83*, 645−649.

Capps, T. M.; Barringer, V. M.; Eberle, W. J.; Brown, D. R.; Sanson, D. R. Identification of a unique glycosyl sulfate conjugate metabolite of Profenofos in cotton. *J. Agric. Food Chem.* **1996**, *44*, 2408−2411.

Conchie, J.; Levvy, G. A. Aryl glycopyranosides by the Koenigs-Knorr method. In *Methods in Carbohydrate Chemistry*; Whistler, R. L., Wolfrom, M. L., BeMiller, J. N., Eds.; Academic Press: New York, 1963; Vol. II, pp 335−337.

Ensley, H. E.; Barber, J. T.; Polito, A.; Oliver, A. I. Toxicity and metabolism of 2,4-dichlorophenol by the aquatic angiosperm *Lemna gibba*. *Environ. Toxicol. Chem.* **1994**, *13*, 325−331.

Fenwick, G. R.; Heaney, R. K.; Mullin, N. J. Glucosinolates and their breakdown products in food and food plants. *CRC Crit. Rev. Food Sci. Nutr.* **1983**, *18*, 123−201.

Feung, C.-S.; Loerch, S. L.; Hamilton, R. H.; Mumma, R. O. Comparative metabolic fate of 2,4-dichlorophenoxyacetic acid in plants and plant tissue culture. *J. Agric. Food Chem.* **1978**, *26*, 1064−1067.

Fukumori, F.; Hausinger, R. P. *Alcaligenes eutrophus* JMP134 "2,4-dichlorophenoxyacetate monooxygenase" is an α-keto-glutarate-dependent dioxygenase. *J. Bacteriol.* **1993**, *175*, 2083−2086.

Jensen, J. Chlorophenols in the terrestrial environment. *Rev. Environ. Contam. Toxicol.* **1996**, *146*, 25−51.

Lamoureux, G. L. Plant metabolism of herbicides in relation to detoxification, selectivity, antidoting, and synergism. In *Xenobiotic Metabolism and Disposition*; Kato, R., Estabrook, R. W., Gayen, M. N., Eds.; Taylor and Francis: Bristol, PA, 1989; pp 267−274.

Llewellyn, D.; Last, D. Genetic engineering of crops for tolerance to 2,4-D. In *Herbicide Resistant Crops*; Duke, S. O., Ed.; Lewis Publishers, CRC Press: Boca Raton, FL, 1996; pp 159−174.

Loss, M. A. Phenoxyalkanoic acids. In *Herbicides: Chemistry, Degradation and Mode of Action*; Kearney, P. C., Kaufman, D. D., Eds.; Dekker: New York, 1976; Vol. 1, pp 1−128.

Luckwill, L. C.; Lloyd-Jones, C. P. Metabolism of plant growth regulators. I. 2,4-dichlorophenoxyacetic acid in leaves of red and black currant. *An. Appl. Biol.* **1960**, *48*, 613−625.

Lyon, B. R.; Cousins, Y. L.; Llewellyn, D. J.; Dennis, E. S. Cotton plant transformed with a bacterial degradation gene are protected from accidental spray drift damage by the herbicide 2,4-dichlorophenoxyacetic acid. *Transgenic Res.* **1993**, *2*, 162−169.

Matern, U. Acylhydrolase from parsley (*Petroselinum hortense*). Relative distribution and properties of four hydrolyzing malonic acid hemiesters of flavonoid glucosides. *Arch. Biochem. Biophys.* **1983**, *224*, 261−271.

Morgan, P. W.; Wayne, C. H. Metabolism of 2,4-D by cotton and grain sorghum. *Weeds* **1963**, *11*, 130−135.

Owen, W. J. Metabolism of herbicides−detoxification as a basis of selectivity. In *Herbicides and Plant Metabolism*; Dodge, A. D., Ed.; Seminar Series 38; Society for Experimental Biology: Cambridge, U.K., 1989; pp 171−198.

Paulson, G. D. Sulfate ester conjugates−Their synthesis, purification, hydrolysis, and chemical spectral properties. In *Bound and Conjugated Pesticide Residues*; Kaufman, D. D., Still, G. G., Paulson, G. D., Bandal, K. B., Eds.; ACS Symposium Series 29; American Chemical Society: Washington, DC, 1976; pp 86−102.

Roscher, R.; Steffen, J.-S.; Herderich, M.; Schwab, W.; Schreier, P. Synthesis of 6′-*O*-malonyl-β-D-glucopyranoside. Facile preparation of malonylated glycoconjugates. *J. Agric. Food Chem.* **1996**, *44*, 1626−1629.

Sànchez-Brunete, C.; Pérez, S.; Tadeo, J. L. GC and HPLC of phenoxy-ester herbicides. *J. Chromatogr.* **1991**, *552*, 235−240.

Schmitt, R.; Kaul, J.; von der Trenk, T.; Schaller, E.; Sandermann, H., Jr. β-D-glucosyl and *O*-malonyl-β-D-glucosyl conjugates of pentachlorophenol in soybean and wheat: identification and enzymatic synthesis. *Pestic. Biochem. Physiol.* **1985**, *24*, 77−85.

Streber, W. R.; Willmitzer, L. Transgenic tobacco plants expressing a bacterial detoxifying enzyme are resistant to 2,4-D. *Bio/Technology* **1989**, *7*, 811−816.

Whistler, R. L.; Spencer, W. W.; BeMiller, J. N. Sulfates. In *Methods in Carbohydrate Chemistry*; Whistler, R. L., Wolfrom, M. L., BeMiller, J. N., Eds.; Academic Press: New York, 1963; Vol. II, pp 298−303.

Wittsiepe, J.; Kullmann, Y.; Schrey, P.; Selenka, F.; Wilhelm, M. Myeloperoxidase-catalyzed formation of PCDD/F from chlorophenols. *Chemosphere* **2000**, *40*, 963−968.

Received for review June 21, 1999. Revised manuscript received July 18, 2000. Accepted July 28, 2000.

JF990672C

COR-AAD1-00002638
Bayer EX1008 (Part 5 of 9)

HAL
archives-ouvertes.fr

Enhanced activity of several herbicide-degrading enzymes: a suggested mechanism responsible for multiple resistance in blackgrass (Alopecurus myosuroides Huds.)

Anne Letouzé, Jacques Gasquez

To cite this version:

Anne Letouzé, Jacques Gasquez. Enhanced activity of several herbicide-degrading enzymes: a suggested mechanism responsible for multiple resistance in blackgrass (Alopecurus myosuroides Huds.). Agronomie, EDP Sciences, 2003, 23 (7), pp.601-608. 10.1051/agro:2003036 . hal-00886214

HAL Id: hal-00886214
https://hal.archives-ouvertes.fr/hal-00886214

Submitted on 1 Jan 2003

HAL is a multi-disciplinary open access archive for the deposit and dissemination of scientific research documents, whether they are published or not. The documents may come from teaching and research institutions in France or abroad, or from public or private research centers.

L'archive ouverte pluridisciplinaire **HAL**, est destinée au dépôt et à la diffusion de documents scientifiques de niveau recherche, publiés ou non, émanant des établissements d'enseignement et de recherche français ou étrangers, des laboratoires publics ou privés.

COR-AAD1-00002639
Bayer EX1008 (Part 5 of 9)

Agronomie 23 (2003) 601–608
© INRA, EDP Sciences, 2003
DOI: 10.1051/agro:2003036

Original article

Enhanced activity of several herbicide-degrading enzymes: a suggested mechanism responsible for multiple resistance in blackgrass (*Alopecurus myosuroides* Huds.)

Anne LETOUZÉ[a], Jacques GASQUEZ[b]

[a] Institut Universitaire de Technologie (IUT), Département "Génie Biologique", 39 rue Paul Mazy, 24019 Périgueux Cedex, France
[b] Institut National de la Recherche Agronomique (INRA), Unité de Malherbologie et Agronomie, 17 rue Sully, BP 86510, 21065 Dijon Cedex, France

(Received 6 August 2002; accepted 25 March 2003)

Abstract – Experiments were carried out to analyse enhanced herbicide metabolism mediated by cytochrome P450 monooxygenases (P450(s)) or glutathione-S transferases (GST(s)) as a possible mechanism responsible for multiple resistance in three blackgrass populations. The RA population is resistant to aryloxyphenoxypropionates (fops) and flupyrsulfuron, the RB to fenoxaprop-P, flupyrsulfuron and ureas and the RC to fenoxaprop-P, haloxyfop and clodinafop. Based on the coleoptile length, growth responses of seedlings to the herbicide responsible for resistance and to combined treatments of the herbicide plus P450(s) or GST(s), inhibitors were compared. Growth of the RA seedlings was significantly reduced with flupyrsulfuron plus malathion, suggesting that P450(s) activity may be involved in the resistance. In contrast, none of the four inhitors tested had an effect on the fop resistance. Fenoxaprop-P plus tridiphane, flupyrsulfuron plus malathion and ureas plus PBO or ABT significantly reduced the RB coleoptiles' growth. Therefore, multiple resistance in this population may be due to an elevation of P450(s) and GST(s) activity. In the RC population, PBO, ABT and tridiphane synergised clodinafop, haloxyfop and fenoxaprop-P effects, suggesting that the two enzymatic systems may also be involved in the RC resistances.

multiple herbicide resistance / enhanced herbicide detoxification / P450(s)/GST(s) / *Alopecurus myosuroides* Huds.

Résumé – L'amplification d'enzymes de détoxication des herbicides : un mécanisme possible responsable des résistances multiples chez le vulpin (*Alopecurus myosuroides* Huds.). Cette expérimentation a pour but d'analyser l'éventuelle implication de monooxygénases à cytochrome P450 (P450(s)) et de glutathione S-transférases (GST(s)) dans les résistances multiples observées chez trois populations de vulpin. La population RA résiste aux aryloxyphenoxypropionates (fops) et au flupyrsulfuron, la RB au fénoxaprop-P, au flupyrsulfuron et aux urées et la RC au fénoxaprop-P, à l'haloxyfop et au clodinafop. Les croissances de la première feuille des plantules exposées à l'herbicide seul et à un mélange "herbicide + inhibiteur" ont été analysées. La croissance des plantules RA est fortement réduite en présence de flupyrsulfuron associé au malathion. Ainsi, des P450(s) pourraient être impliquées dans la résistance de cette population. En revanche, les quatre inhibiteurs sont sans effet sur la résistance aux fops. Comparées à l'effet des herbicides utilisés seuls, les combinaisons fénoxaprop-P plus tridiphane, flupyrsulfuron plus malathion et urées plus PBO ou ABT réduisent significativement la croissance des plantules RB. Ces résultats suggèrent donc que des P450(s) et des GST(s) pourraient être responsables des résistances multiples de cette population. Pour finir, les résistances de la population RC pourraient là aussi résulter de l'activité des deux systèmes enzymatiques puisque la croissance des plantules est significativement inhibée par les herbicides utilisés en association avec l'ABT, le PBO et le tridiphane.

résistances multiples / détoxication / P450(s)/GST(s) / *Alopecurus myosuroides* Huds.

1. INTRODUCTION

The impact of herbicides on our modern agricultural technology has been phenomenal and their usage now exceeds that of fungicides and insecticides combined [18]. The use of herbicides has increased as more selective herbicides have become available and as they replace mechanical tillage as a method of weed control. Nevertheless, an undesirable outcome of widespread use of herbicides for weed control has been the appearance and rapid proliferation of resistant weeds [32]. The 1999 international survey of herbicide-resistant weeds recorded more than 200 resistant biotypes in 45 countries all over the world [18] and herbicide resistance is now posing a major threat to current agricultural practices [20].

Communicated by Gérard Guyot (Avignon, France)

* Corresponding author: anne.letouze@wanadoo.fr

COR-AAD1-00002640
Bayer EX1008 (Part 5 of 9)

Herbicide resistance can be defined as the natural inherited ability of some biotypes within a population to survive and reproduce following a herbicide treatment that would, under normal conditions of use, effectively control that weed population [18]. A herbicide is a selection agent for any heritable traits within a population that enable survival of individuals in the presence of herbicide. Therefore, the survival mechanism need only be sufficiently efficacious to confer survival at the rate of herbicide used. As herbicide treatments are nearly always at relatively low doses, this ensures survival of individuals expressing both strong and relatively weak resistance mechanisms. Plants with any genetically derived resistance mechanisms will survive and contribute to the subsequent gene pool. When a very large number of a highly variable weed species are treated, there can be survivors with quite different resistance mechanisms [43]. The allogamous nature of a weed species contributes to the development of such multiple resistance. In allogamous species, resistant individuals carrying different resistance genes may cross-pollinate and progeny may then carry both resistance genes. Successive selections may thus accumulate resistance mechanisms within individuals. Multiple resistance is defined as the expression (within individuals or populations) of more than one resistance mechanism, endowing the ability to withstand herbicides from different chemical classes [16]. Multiple resistance is best documented in the weed species *Lolium rigidum* Gaud (rye grass) [4] and, to a small extent, in *Alopecurus myosuroides* Huds. (blackgrass), which exhibit many of the characteristics that favour the accumulation of herbicide resistance mechanisms [3]. These characteristics include a high reproductive capacity, an allogamous reproduction and a genetic plasticity [16]. Such populations that have developed multiple mechanisms, conferring resistance not only to the challenging herbicide but to other herbicide groups, are difficult to control by chemical means. Therefore, elucidation of the mechanisms endowing herbicide multiple resistance in such populations is of prime importance.

Herbicide resistance in weed species may be conferred by two major mechanisms: (I) a mutation of the gene encoding the herbicide target site that confers a high level of resistance, or (II) an enhanced herbicide detoxification by non-specific enzymes that confers a slighter level of resistance [14, 15, 25, 40]. Higher plants are frequently able to metabolise the xenobiotics that they absorb and the phytotoxicity of a herbicide is often closely associated with the rate at which it is metabolised. Most resistant species rapidly metabolise herbicide while susceptible species are unable to do it, or at rates too slow to prevent herbicide from reaching its site of action [23]. Resistance involving herbicide detoxification may be conferred by an elevated expression of cytochrome P450 monooxygenases (P450(s)), a super enzyme family. The existence of P450(s) in higher plants was first proven in the early 1970s [36]. Accumulating evidence indicates that there is a multiplicity of P450(s) in plants [19] and they are best known and most studied for their oxygenase activity [1, 16, 36]. P450(s) have the capacity to attack a vast range of structurally unrelated chemicals to transform them into more polar, soluble products, diminishing or suppressing their toxicity [10]. Another method of detoxification involves the glutathione-S transferases (GST(s)) [12, 23, 24], a group of multiple isozymes which catalyse the conjugation of electrophilic xenobiotics with the tripeptide glutathione (GSH) to form polar, non-toxic peptide conjugates [5, 17]. Consequently, the water solubility, reactivity and biological properties of the electrophile are altered. Conjugation is often followed by sequestration of the conjugate metabolite in a physiologically inactive compartment such as a vacuole [7]. GST(s) are important in detoxifying major classes of herbicides, including chloro-s-triazines, chloroacetanilides, sulfoxide derivatives of thiocarbamates, diphenyl ethers and several aryloxyphenoxypropionates.

In this study, enhanced herbicide metabolism was analysed as a possible mechanism responsible for multiple resistance observed in three blackgrass populations. Inhibitors known to antagonise metabolism-based resistance in plants were used to determine whether resistance in these populations is the result of one or more herbicide-degrading enzymes. Growth responses of seedlings to combined treatments of inhibitors and herbicides responsible for the resistance were analysed.

2. MATERIALS AND METHODS

2.1. Plant material

Three herbicide-resistant populations (RA, RB and RC) and one standard susceptible population (S) of *Alopecrurus myosuroides* Huds. collected in France were used in this study. The RA population is made up of 100% of individuals resistant to three aryloxyphenoxypropionates (fenoxaprop-P, haloxyfop and clodinafop) and flupyrsulfuron, a sulfonylurea herbicide. The RB population is 100% resistant to fenoxaprop P, flupyrsulfuron and two ureas (isoproturon and chlorotoluron). The RC population is made up of 30% of individuals resistant to fenoxaprop-P, haloxyfop and clodinafop. These resistance patterns were first determined using a herbicide laboratory sprayer [27] and then confirmed with a resistance screening bioassay previously developed [28].

2.2. Chemical products

2.2.1. Detoxifying-enzyme Inhibitors

The inhibitors were chosen according to their reported effect on detoxifying enzymes in plants. Piperonyl butoxide (PBO) (Loveland Industries, USA), 1-aminobenzotriazole (ABT) (Sigma, France) and malathion (Cluzeau, France) were used as cytochrome P450 monooxygenase inhibitors [2, 13, 41, 44]. Tridiphane (AGR 280959, Dowelanco, USA) was used as a preferential inhibitor of glutathione-S transferases [23].

To determine for each inhibitor the concentration to use in combination with each herbicide, we selected from among a range of doses the highest one that had no phytotoxic effect on its own on the coleoptile growth of the susceptible seedlings. Inhibitor solutions containing 2.5, 5, 10, 20, 40 and 80 $mg \cdot L^{-1}$ ABT, PBO, malathion and 0.15625, 0.3125, 0.625, 1.25, 2.5 and 5 $mg \cdot L^{-1}$ tridiphane were prepared by serial dilutions in distilled water.

COR-AAD1-00002641
Bayer EX1008 (Part 5 of 9)

2.2.2. Herbicides

The experiments were carried out with the acid or technical forms of the herbicides rather than the commercial formulations. The advantage of these forms compared with the commercial formulations is a higher solubility in water (e.g.: fenoxaprop-P acid, 61 $g \cdot L^{-1}$; fenoxaprop-P-P-ethyl, 0.7 $mg \cdot L^{-1}$). Therefore, these forms allow preparation of "true" aqueous solutions of active ingredients.

The herbicide concentrations were previously determined as reliable concentrations to discriminate between the resistant and susceptible individuals with a seedling bioassay based on the coleoptile length (28, 29, 31 and see below). Herbicide solutions containing 6 $mg \cdot L^{-1}$ fenoxaprop-P acid, 2.5 $mg \cdot L^{-1}$ haloxyfop acid (AgrEvo, Germany), 5 $mg \cdot L^{-1}$ clodinafop propargyl (Novartis, France), 6 $mg \cdot L^{-1}$ flupyrsulfuron (Dupont, France) and 8 $mg \cdot L^{-1}$ isoproturon and chlorotoluron (Aventis, France) were prepared by serial dilutions. Each herbicide had been dissolved previously in 0.1% (V/V) dimethylsulphoxide (DMSO). The pH of the herbicide solutions was adjusted to pH 7 with a Tris[hydroxymethyl]aminomethane (Tris) buffer.

2.3. Dose-response experiments

Except for ureas, the herbicide and inhibitor effects were determined using the herbicide resistance screening bioassay previously developed and based on the coleoptile length of pre-germinated seeds exposed for six days to the discriminating herbicide concentration that provided the largest difference in coleoptile length of the susceptible and resistant seedlings [28]. According to this seedling test, the lengths of the susceptible (S) and resistant (R) coleoptiles were always shorter and longer than 10 mm long, respectively. As isoproturon and chlorotoluron inhibit photosynthesis, it was shown that coleoptile length was not the best discriminative parameter for assessing resistance to ureas [28, 29]. Thus, for these two herbicides, resistance was screened based on the complete bleaching of the coleoptiles within two weeks. At the discriminating concentration selected, all the S coleoptiles were bleached while the R ones were still green like the control [26, 28].

To conduct all the dose-response experiments, seeds of each population were pre-germinated in 15-cm-diameter glass petri-dishes lined with small glass tubes supporting one sheet of blotting paper (Germaflor No. 55, 160 $g \cdot m^{-2}$, Müller). To stimulate seed germination, the petri-dishes were filled with 30 mL of 2 g $KNO_3 \cdot L^{-1}$ and placed in a controlled environment room (12 h, 20 °C light/12 h, 15 °C dark). After 4 days, pre-germinated seeds with rootlets 3–4 mm long were transferred onto one sheet of blotting paper (Germaflor No. 55, 160 $g \cdot m^{-2}$, Müller) laid on two layers of 6-mm-diameter glass marbles in a plastic box (9 cm × 9 cm × 9 cm). Each box was filled with 25 mL growth medium, closed and placed for six days in a controlled environment room (18 h, 22 °C light/6 h, 20 °C dark).

Pre-germinated seeds of the three resistant populations (RA, RB and RC) were exposed to a control medium (without herbicide and inhibitor), to the selective dose of each herbicide responsible for the resistance and to all the combinations of herbicide plus inhibitor. For all experiments, 100 pre-germinated seeds were used (25 seeds per box). Except for the two ureas, the herbicide and inhibitor effects were assessed after six days' growth by measuring the coleoptile length (from the point of seed attachment to the coleoptile tip). For ureas we estimated, two weeks later, the degree of bleaching.

The inhibitor concentration used in association with the herbicide was the highest one among a range of doses that had no phytotoxic effect on its own. Then, when the growth (or colouring) of a resistant coleoptile was affected by a combination of herbicide plus inhibitor, it only resulted from the inhibition of the herbicide detoxifying enzyme. To determine the reliable concentration of each inhibitor, 100 pre-germinated seeds of the S population (25 seeds per box) were exposed to the range of doses (see above). From among the range of inhibitor doses tested, we selected the highest one that still allowed a coleoptile growth at least equal to 95% of the control.

The effect of each treatment was assessed by measuring the coleoptile length, which was expressed as a percentage of the control.

The control medium was made of distilled water and the pH was adjusted to pH 7 with a Tris buffer.

2.4. Statistical analysis

For each experiment, data were subjected to an analysis of variance (ANOVA) and the mean coleoptile lengths were separated with a Duncan's multiple range test ($P < 0.05$) [37].

3. RESULTS

3.1. Dose-response to the herbicides

When the S seedlings were exposed for six days to the three aryloxyphenoxypropionate herbicides and flupyrsulfuron, they were strongly inhibited by the concentration selected, as they were shorter than 5 mm (Fig. 1A). According to the seedling bioassay, none of the RA coleoptiles were inhibited by the herbicides tested, compared with the S coleoptiles, and they were always longer than 10 mm (Fig. 1B). In the same way, all the RB coleoptiles were longer than 10 mm in the presence of the discriminating dose of fenoxaprop-P and flupyrsulfuron. In contrast, they were strongly inhibited by clodinafop and haloxyfop (4 and 3 mm long, respectively) (Fig. 1C). When exposed to the three aryloxyphenoxypropionate herbicides some RC coleoptiles were always longer than 10 mm (Fig. 1D). For this population, about 30% of seedlings were longer than 10 mm in the presence of these three herbicides (results not shown). In contrast, all the RC coleoptiles were strongly inhibited by flupyrsulfuron (Fig. 1D). In the presence of the two ureas, all the S and R coleoptiles tested were bleached, except for the RB coleoptiles (Tab. I).

Therefore, according to the seedling bioassay previously developed (see materials and methods section), the RA population was resistant to the three aryloxyphenoxypropionates and flupyrsulfuron, the RB population was resistant to fenoxaprop-P, flupyrsulfuron and ureas and the RC population was resistant to the three aryloxyphenoxypropionates. All these results confirm what is observed in the field.

COR-AAD1-00002642
Bayer EX1008 (Part 5 of 9)

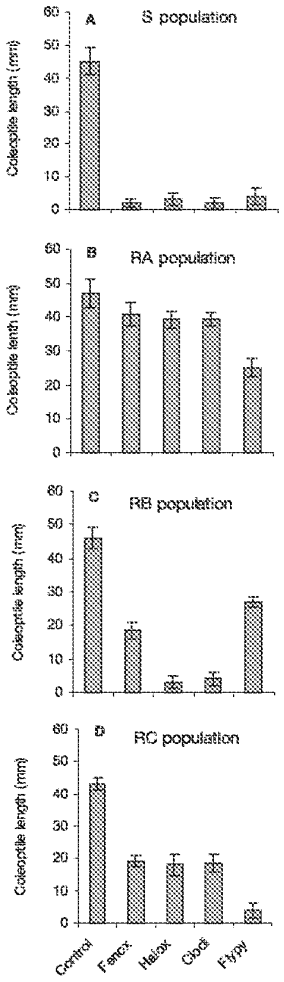


Figure 1. Mean coleoptile length of 100 seedlings for the four blackgrass populations (S, RA, RB and RC) exposed for six days to 6 mg·L^{-1} fenoxaprop-P acid (Fenox), 2.5 mg·L^{-1} haloxyfop acid (Halox), 5 mg·L^{-1} Clodinafop propargyl (Clodi) and 6 mg·L^{-1} flupyrsulfuron (Flupy). S: susceptible – R: resistant. Vertical bars = +/– standard errors.

3.2. Dose-response to the associations herbicide plus inhibitor

3.2.1. RA population

The combined effects of the herbicides responsible for resistance in the RA population and the four inhibitors on the coleoptile length of the seedlings are presented in Figure 2. For fenoxaprop-P, haloxyfop and clodinafop, there were no significant differences between the mean coleoptile lengths of the RA seedlings exposed to the herbicide alone or combined with each inhibitor (Fig. 2A, B and C). In the same way, when compared with the effect of 6 mg·L^{-1} flupyrsulfuron alone, combinations of this herbicide with ABT, PBO or tridiphane did not significantly reduce the RA coleoptiles' length. In contrast, significant reduction of the RA coleoptiles was recorded when flupyrsulfuron was combined with malathion (Fig. 2D). While the RA coleoptiles exposed to flupyrsulfuron were 25 mm long, they were shorter than 5 mm when exposed to the association flupyrsulfuron plus malathion.

Table I. Percentage of bleached coleoptiles for the four blackgrass (S, RA, RB and RC) exposed for 2 weeks in 8 mg·L^{-1} isoproturon and chlorotoluron. One hundred coleoptiles were tested per population. S: susceptible – R: resistant.

Herbicide	Populations	% of bleached coleoptiles
Isoproturon	S	100
	RA	100
	RB	0
	RC	100
Chlorotoluron	S	100
	RA	100
	RB	0
	RC	100

3.2.2. RB population

Addition of ABT, PBO and malathion to fenoxaprop-P did not significantly affect the RB coleoptiles' growth compared with what was observed in the presence of the herbicide alone. In contrast, the combination of fenoxaprop-P plus tridiphane strongly reduced the RB coleoptiles (Fig. 3A). In the presence of fenoxaprop-P, the RB coleoptiles were still 18 mm long, whereas they did not exceed 6 mm with fenoxaprop-P plus tridiphane. For flupyrsulfuron, the addition of ABT, PBO and tridiphane did not significantly reduce the RB coleoptiles' mean length compared with the length measured in the presence of flupyrsulfuron alone (Fig. 3B). In contrast, the addition of malathion to the herbicide solution was significantly effective and strongly inhibited the coleoptile growth of all the RB seedlings, which never exceeded 3.5 mm in length (Fig. 3B). For isoproturon and chlorotoluron, Table II shows that the addition of ABT and PBO to the herbicide solution induced bleaching of the RB coleoptiles, whereas malathion and tridiphane were without effect on the large majority of the coleoptiles.

3.2.3. RC population

For population C, when compared with the effect of fenoxaprop-P alone, combination with ABT, PBO or malathion did not significantly reduce the length of the R coleoptiles (Fig. 4A). Among the 100 seedlings tested, 28 were not affected (results not shown). In contrast, the addition of tridiphane to the herbicide solution strongly inhibited the growth of all the RB coleoptiles compared with what was observed when seedlings were exposed to fenoxaprop-P alone (Fig. 4A). Indeed, with fenoxaprop-P the RC coleoptiles that were not affected were still 19 mm long, while they were all shorter than 5 mm with the combination. Compared with haloxyfop alone, the RC coleoptiles' growth was significantly inhibited by both ABT and PBO, while malathion and tridiphane were not effective on the R coleoptiles' growth (Fig. 4B). Indeed, these two last inhibitors were without any

COR-AAD1-00002643
Bayer EX1008 (Part 5 of 9)

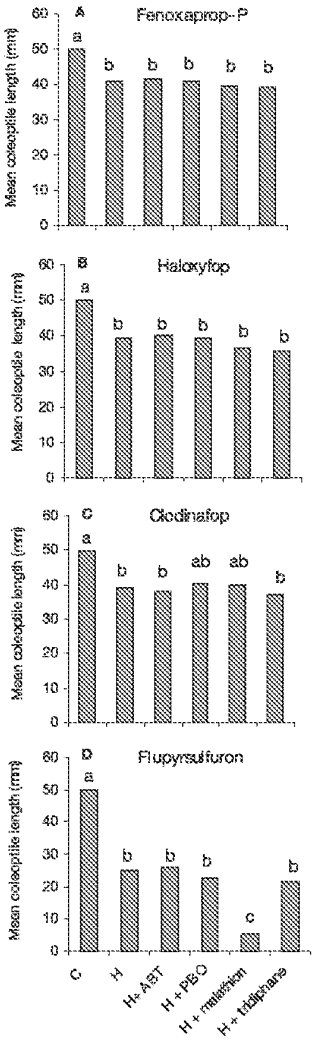


Figure 2. Mean coleoptile length of 100 RA seedlings exposed for six days to 6 $mg \cdot L^{-1}$, 2.5 $mg \cdot L^{-1}$ haloxyfop, 5 $mg \cdot L^{-1}$ diclofop and 6 $mg \cdot L^{-1}$ flupyrsulfuron alone or in combination with the four detoxifying-enzyme inhibitors. C: control, H: herbicide, ABT: 1-aminobenzotriazole, PBO: piperonyl-butoxide. Different letters indicate significant difference between coleoptile lengths (Duncan's multiple range test at the 0.05 level).

effect on 30 RB seedlings among the 100 seedlings tested (result not shown). In the same way, combinations of clodinafop with ABT or PBO significantly reduced all the RC coleoptiles compared with what was observed with the herbicide alone. As for haloxyfop, the two other combinations did not cause a significant reduction in the coleoptile length compared with the herbicide alone (Fig. 4C). Still, 30 RC seedlings were not affected by these combinations (results not shown).

All these results are summarised in Table III.

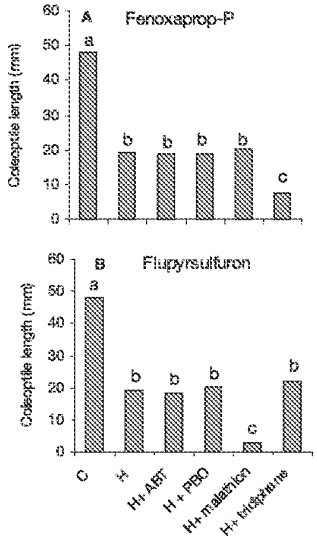


Figure 3. Mean coleoptile length of 100 RB seedlings exposed for six days to 6 $mg \cdot L^{-1}$ and flupyrsulfuron alone or in combination with the four detoxifying-enzyme inhibitors. C: control, H: herbicide, ABT: 1-aminobenzotriazole, PBO: piperonyl-butoxide. Different letters indicate significant difference between coleoptile lengths (Duncan's multiple range test at the 0.05 level).

Table II. Percentage of bleached coleoptiles for the RB population exposed for 2 weeks to 8 $mg \cdot L^{-1}$ isoproturon and chlorotoluron alone or in combination with the four detoxifying-enzyme inhibitors. One hundred coleoptiles were tested per treatment. ABT: a-aminobenzotriazole, PBO: piperonyl-butoxide.

Herbicide	Inhibitor	% of bleached coleoptiles
Isoproturon	-	0
	ABT	100
	PBO	100
	malathion	2
	tridiphane	1
Chlorotoluron	-	0
	ABT	100
	PBO	100
	malathion	1
	tridiphane	1

4. DISCUSSION

This experiment was conducted to analyse whether enhanced herbicide metabolism was a possible mechanism responsible for multiple resistance in the three blackgrass populations studied. Four inhibitors, ABT, PBO, malathion and tridiphane, known to antagonise metabolism-based resistance by inhibiting herbicide-detoxifying enzymes such as P450(s) and GST(s), were used in combination with the herbicides responsible for resistance.

In addition to their role in herbicide detoxification, P450(s) and GST(s) are also involved in important physiological

COR-AAD1-00002644
Bayer EX1008 (Part 5 of 9)

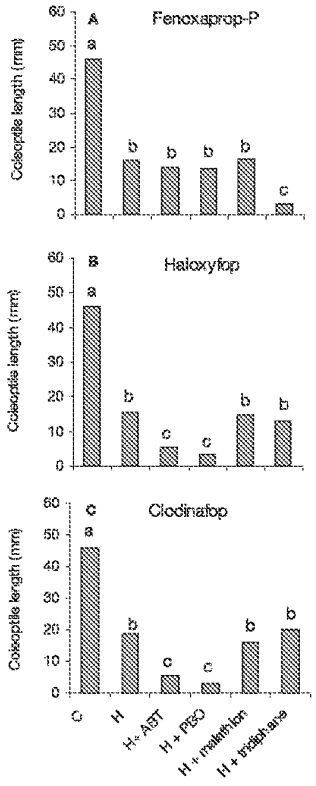


Figure 4. Mean coleoptile length of 100 RC seedlings exposed for six days to 6 mg·L^{-1}, 2.5 mg·L^{-1} and 5 mg·L^{-1} clodinafop alone or in combination with the four detoxifying-enzyme inhibitors. C: control, H: herbicide, ABT: 1-aminobenzotriazole, PBO: piperonyl-butoxide. Different letters indicate significant difference between coleoptile lengths (Duncan's multiple range test at the 0.05 level).

reactions in plants such as protection during oxidative stress, transport and regulation of certain metabolites or detoxification of endogenous compounds [33]. This is why increasing concentrations of each inhibitor used alone are not without effect on S coleoptiles' growth (results not shown). Thus, for each inhibitor we selected the highest concentration that did not reduce coleoptile growth (see Material and Methods).

The results shown in Figure 2 indicate that the RA seedlings became susceptible to flupyrsulfuron when malathion was used. As malathion is described as a potential P450(s) inhibitor [33], these results suggest that P450(s) activity may be responsible for flupyrsulfuron resistance in the RA population. This result is consistent with a previous study where malathion was shown to synergise the action of another sulfonylurea herbicide, chlorsulfuron, in *Lolium rigidum* [33]. This biochemical study revealed that malathion increased chlorsulfuron toxicity by inhibiting the herbicide metabolism mediated by P450(s). On the other hand, none of the four inhibitors tested affected the coleoptile growth when the three aryloxyphenoxypropionates were used (Fig. 2). Thus, we may suppose that

Table III. Summary of the action of the four inhibitors on herbicide effects in the three resistant blackgrass populations. Cross means that the inhibitors synergises the herbicide effect. ABT: a-aminobenzotriazole, PBO: piperonyl-butoxide. R: resistant.

Populations	Herbicides	P450(s) inhibitors			GST(s) inhibitor
		ABT	PBO	malathion	tridiphane
RA	Fenoxaprop-P				
	Haloxyfop				
	Clodinafop propargyl				
	Flupysulfuron			X	
RB	Fenoxaprop-P				X
	Isoproturon	X	X		
	Chloroproturon	X	X		
	Flupysulfuron			X	
RC	Fenoxaprop-P				X
	Haloxyfop	X	X		
	Clodinafop propargyl	X	X		

either none of the herbicide-detoxifying enzymes investigated in this study are responsible for resistance to aryloxyphenoxypropionates of the RA population, or another mechanism is involved in the resistance. A previous study, conducted with the same blackgrass population, had suggested that this population may contain a mutated acetyl CoA carboxylase (ACCAse) [3, 30], the target-site of aryloxyphenoxypropionates [22, 35, 38, 40]. Target site-based resistance is the most commonly reported mechanism of resistance to ACCase-inhibiting herbicides [9, 39]. Therefore, in addition to possessing a probably resistant ACCase, the RA biotype may show an enhanced metabolism of flupyrsulfuron, endowed by P450(s). As 100% of the RA seedlings are resistant to the three aryloxyphenoxypropionates and to flupyrsulfuron, we may speculate that all the RA seedlings may possess both a mutated ACCase and an increased activity of P450(s) susceptible to malathion.

Moreover, an experiment conducted to investigate the inheritance of fenoxaprop-P resistance within the RA population has suggested that the RA individuals may also resist this herbicide due to an enhanced activity of P450(s) inhibited by malathion [31]. This mechanism of resistance to fenoxaprop-P was identified thanks to the segregation genes in the F2 generation. But here, as we only investigated the mechanism of fenoxaprop-P resistance within the F1 generation, the possible implication of P450(s) susceptible to malathion in the resistance could not be identified because it may be disguised by the presence of a mutated ACCase.

Fenoxaprop-P phytotoxicity was increased in the RB biotype in the presence of tridiphane (Fig. 3), a potential GST inhibitor [23]. Thus, this result suggests that increased activity of GST(s) may be responsible for fenoxaprop-P degradation and therefore for herbicide resistance in this population. Glutathione conjugation was first suggested as a possible pathway of fenoxaprop-p detoxification in barley, crabgrass, oat and wheat [11, 42]. These in vitro metabolism studies revealed that

COR-AAD1-00002645
Bayer EX1008 (Part 5 of 9)

fenoxaprop-P underwent rapid displacement of the phenyl group by glutathione (GSH). In blackgrass, the involvement of GST in fenoxaprop-P resistance was first demonstrated in the English population "Peldon" where the GST activity was significantly increased in the presence of the herbicide [7, 34]. The role of GST(s) in resistance to multiple herbicides in blackgrass was more recently confirmed by Cummins et al. [8]. This work has suggested that GST(s) may function as glutathione peroxiades to prevent oxidative injury caused as a primary or secondary effect of herbicide action.

Malathion synergised the effect of flupyrsulfuron on RB seedlings, whereas PBO and ABT synergised the effects of isoproturon and chlorotoluron (Fig. 3 and Tab. II). Malathion, ABT and PBO are all P450 inhibitors. Therefore, we may suppose that the RB seedlings are resistant to flupyrsulfuron and ureas, probably due to an increased activity of two different isoenzymes of P450(s). A previous study conducted to investigate chlorotoluron metabolism in leaves of resistant and susceptible biotypes of blackgrass demonstrated the implication of P450(s) in the resistance to ureas [21]. According to our results, we may therefore speculate that at least three different herbicide-metabolising enzymes have increased activity in the RB population: GST(s), P450(s) inhibited by malathion and P450(s) affected by both ABT and PBO. Moreover, as the entire population is resistant to fenoxaprop-P, flupyrsulfuron and ureas, all the seedlings could show an increased activity of the three enzymatic systems. We suggest that malathion inhibits the P450s responsible for metabolising flupyrsulfuron, but not those responsible for metabolising urea herbicides. In contrast, PBO and ABT inhibit the P450s responsible for metabolising urea herbicides, but not flupyrsulfuron. Thus, even though the large majority of the P450(s) are known to show a broad and partially overlapping substrate specificity [6], this experiment revealed that some of them might be specific for one herbicide family.

As for the RB population, tridiphane antagonises fenoxaprop-P resistance in the RC population, suggesting that an enhanced activity of GST(s) may also be involved in this resistance (Fig. 4). Figure 4 also shows that the RC seedlings became susceptible to haloxyfop and clodinafop in the presence of ABT and PBO. Thus, in addition to the GST activity, the RC population may show an enhanced activity of P450(s). Contrary to the RA and RB populations, 100% resistant, the RC population is only made up of about 30% resistant individuals to fenoxaprop-P, haloxyfop and clodinafop (results not shown). Thus, either the same 30% of plants may show an enhanced activity of both GST(s) and P450(s) or either 30% possess an amplification of GST(s) and another 30% an amplification of P450(s). As blackgrass is an allogamous species, the most probable hypothesis is that some resistant individuals effectively show an enhanced activity of both GST(s) and P450(s) while some others may only possess an amplification of one of the two enzymatic systems.

Based on both the differential patterns of herbicide resistance and inhibition of herbicide metabolism by cytochrome P450 inhibitors (Tab. III), we may suggest that at least three metabolic systems involving different isoenzymes of cytochrome P450 monooxygenases may contribute to enhanced detoxification in blackgrass. At least one isoenzyme might be responsible for resistance to flupyrsulfuron, a second for resistance to haloxyfop and clodinafop and a third isoenzyme may give enhanced metabolism of ureas. While malathion appears to be specific for the P450(s) involved in flupyrsulfuron degradation, this study revealed that ABT and PBO may possess a broad spectrum of substrates, as they both inhibited at least two different isoenzymes of P450(s): one responsible for the detoxification of the two ureas and another responsible for detoxification of haloxyfop and clodinafop. Moreover, we cannot exclude the hypothesis that three or even four isoenzymes of P450(s) may be specifically involved in the detoxification of these four herbicides, all inhibited by ABT and PBO.

Even though the rigorous proof of involvement of detoxifying enzymes in the resistance responses requires the detection of the catalysed herbicide breakdown products and the demonstration that the biotypes have different capacities to produce these compounds, this study strongly suggests that the multiple resistance observed in the three blackgrass populations may be the result of an enhanced metabolism of herbicide involving P450(s) and, more rarely, GST(s). Moreover, this work shows the possible accumulation of different resistance mechanisms in a single population and even in a single plant. This phenomena has already been observed in rye grass populations [33] and in the resistant blackgrass population from the UK, Peldon [3]. The out-crossing nature of blackgrass in combination with the extensive and varied herbicide applications provide ideal conditions for accumulation of multiple resistance mechanisms. In addition, it appears that populations such as the ones studied in this experiment would be resistant to herbicide families yet to be marketed or even discovered, particularly where such herbicide chemistries can be metabolised by P450(s). While blackgrass and rye grass share common biological elements, they are not unique. Multiple herbicide resistance is predicted to develop in other weed species. This phenomena complicates the chemical management of these resistant weed populations. For such a population that accumulates several mechanisms of resistance, the use of mixtures of herbicides and cultural methods appears to be the most effective resistance management strategy.

Acknowledgments: This study was partially supported by funds provided by Aventis. We thank Annick Matejicek for technical assistance.

REFERENCES

[1] Bolwell G.P., Bozak K., Zimmerlin A., Plant cytochrome P450, Phytochemistry 37 (1994) 1491–1506.

[2] Christopher J.T., Preston C., Powles S.B., Malathion antagonizes metabolism-based chlorosulfuron resistance in *Lolium rigidum*, Pest. Biochem. Phys. 49 (1994) 172–182.

[3] Cocker K.M., Moss S.R., Coleman J.O.D., Multiple mechanisms of resistance to fenoxaprop-p-ethyl in UK and other European population of herbicide-resistant *Alopecurus myosuroides*, Pest. Biochem. Phys. 65 (1999) 169–180.

[4] Cocker K.M., Northcroft D.S., et al., Resistance to ACCase inhibiting herbicides and isoproturon in UK populations of *Lolium multiflorum*: mechanisms of resistance and implication for control, Pest. Manage. Sci. 57 (2001) 587–597.

[5] Cole D.J., Detoxification and activation of agrochemicals in plants, Pest. Sci. 42 (1994) 209–222.

COR-AAD1-00002646
Bayer EX1008 (Part 5 of 9)

[6] Cole D.J., Cummins I., Hatton P.J., et al., Glutathione transferases in crops and major weeds, in: Hatzio K. (Ed.), Regulation of enzymatic systems detoxifying xenobiotics in plants, Kluwer Academic Publishers, Netherlands, 1997, pp. 139–154.

[7] Cummins I., Moss S., Cole D.J., et al., Gluthatione transferases in herbicide-resistance and herbicide-susceptible black-grass (*Alopecurus mysosuroides)*, Pest. Sci. 51 (1997) 244–250.

[8] Cummins I., Cole D.J., Edwards R.A., Role for glutathione transferases functioning as glutathione peroxidases in resistance to multiple herbicides in black-grass, Plant J. 18 (1999) 285–292.

[9] Devine M.D., Shimabukuro R.H., Resistance to acetyl coenzyme A carboxylase inhibiting herbicides, in: Powles S.B., Holtum J.A.M. (Eds.), Herbicide resistance in plants – biology and biochemistry, Lewis Publishers, USA, 1994, pp. 141–169.

[10] Durst F., Salun J.P., Werck-Reichart D., et al., Cytochrome P450 endowed herbicide metabolism, in: De Prado R., Jorrin J., Garcia-Torres L. (Eds.), Weed and crop resistance to herbicides, Kluwer Academic Publishers, Dordrecht, Netherlands, 1997, pp. 101–108.

[11] Edwards R., Cole D.J., Glutathione transferases in wheat (*Triticum*) species with activity towards fenoxaprop-P-ethyl and other herbicides, Pest. Biochem. Phys. 54 (1996) 96–101.

[12] Edwards R., Glutathione transferases in plants involved in herbicide detoxification, in: Proc. Brighton Crop Prot. Conf. – Weeds, Brighton, 1995, pp. 823–832.

[13] Gaillardon P., Cabanne F., Scalla R., et al., Effect of mixed function oxydase inhibitors on the toxicity of chlorotoluron and isoproturon to wheat, Weed Res. 25 (1985) 397–402.

[14] Gasquez J., État de la résistance aux herbicides en France, in: Xe Colloque international sur la biologie des mauvaises herbes, Dijon, 1996, pp. 173–180.

[15] Gasquez J., Les graminées adventices résistantes aux herbicides antigraminées en France, in: Compte rendu de la dix-septième conférence du Columa, Journées Internationales sur la Lutte contre les Mauvaises Herbes – ANPP, Dijon, 1998, pp. 133–140.

[16] Hall L.M., Holtum J.A.M., Powles S.B., Mechanims responsible for cross resistance and multiple resistance, in: Powles S.B., Holtum A.M.M. (Eds.), Herbicide resistance in plants – biology and biochemistry, Lewis Publishers, USA, 1994, pp. 141–169.

[17] Hatton P.J., Edwards R., Cole D.J., Glutathione transferases in major weed species, Pest. Sci. 43 (1995) 173–178.

[18] Heap I., International survey of herbicide-resistant weeds: lessons and limitations, in: Proc. 1999 Brighton Crop Prot. Conf. – Weeds, Brighton, 1999, pp. 769–776.

[19] Hendry G., Why do plant have cytochrome P-450? Detoxification versus defence, New Phytol. 102 (1986) 239–247.

[20] Holt J.S., Holtum J.A.M., Powles S.B., Mechanisms and agronomic aspects of herbicide resistance, Annu. Rev. Plant Phys. 44 (1993) 3203–3209.

[21] Hyde R.J., Hallahan D.L., Bowyer J.R, Chlorotoluron metabolism in leaves of resistant and susceptible biotype of the grass weed *Alopecurus myosuroides*, Pest. Sci. 47 (1996) 185–190.

[22] Köcher H., Kellner H.M., Lötzshk K., et al., Mode of action and metabolic rate of the herbicide Fenoxaprop-P-ethyl, in: Proc. 1982 British Crop Prot. Conf. – Weeds, Brigthon, 1982, pp. 341–347.

[23] Lamoureux G.L., Rusness D., Tridiphane [2-(3,5-dichlorophenyl)-2-(2,2,2-trichloroethyl)oxirane] an atrazine synergist: enzymatic conversion to a potent glutathione S-transferase inhibitor, Pest. Biochem. Phys. 26 (1986) 323–342.

[24] Lamoureux G.L., Shimabukuro R.H., Frears S., Glutathione and glucoside conjugation in herbicide selectivity, in: Caseley J.C., Cussans G.W., Atkin R. (Eds.), Herbicide resistance in weeds and crops, Butterworth-Heinemann Ltd, Oxford, UK, 1991, pp. 227–250.

[25] Lebaron H.M., McFarland J., Herbicide resistance in weeds and crops – an overview and prognosis, in: Green M.B., Lebaron H.M., Moberg W.K. (Eds.), Managing Resistance to Agrochemicals – from fundamental research to practical strategies, American Chemical Society, Washington, DC, US, 1990, pp. 336–352.

[26] Letouzé A., Détection et caractérisation des résistances aux herbicides antigraminées chez le vulpin (*Alopecurus myosuroides* huds), Thesis, France, 1999, 132 p.

[27] Letouzé A., Gasquez J., Développement d'un standardisé pour la recherche de résistances croisées, in: Dix-septième conférence du Columa, Journées Internationales contre les Mauvaises Herbes, Dijon, 1998, pp. 141–148.

[28] Letouzé A., Gasquez J., A reliable test for screening aryloxyphenoxypropic acid resistance within *Alopecurus myosuroides* and *Lolium* spp. populations, Weed Res. 39 (1999) 37–48.

[29] Letouzé A., Matéjicek A., Henry A., et al., Rapid determination of herbicide resistance pattern in blackgrass (*Alopecurus myosuroides*), in: Proc. 1999 Brighton Crop Prot. Conf. – Weeds, Brighton, 1999, pp. 557–558.

[30] Letouzé A., Gasquez J., A pollen test to detect ACCase target-site resistance within *Alopecurus myosuroides* populations, Weed Res. 40 (2000) 151–162.

[31] Letouzé A., Gasquez J., Inheritance of fenoxaprop-P-ethyl resistance in a blackgrass (*Alopecurus myosuroides* Huds.) population, Theor. Appl. Genet. 103 (2001) 288–296.

[32] Powles S.B., Holtum J.A.M., Mattews J.M., et al., Herbicide cross-resistance in annual rygrass (*Lolium rigidum* Gaud.), The search for a mechanism, in: Green M.B., Lebaron H.M., Moberg W.K. (Eds.), Managing Resistance to Agrochemicals – from fundamental research to practical strategies, American Chemical Society, Washington, USA, 1990, pp. 336–352.

[33] Preston C., Tardif F.J., Christopher J.T., et al., Multiple resistance to dissimilar herbicide chemistries in Biotype of *Lolium rigidum* due to enhanced activity of several herbicide degrading enzymes, Pest. Biochem. Phys. 54 (1996) 123–134.

[34] Reade J.P.H., Hull M.R., Cobb A.H., A role for glutathione-S-transferase in herbicide resistance in blackgrass (*Alopecurus myosuroides*), in: Proc. 1997 Brighton Crop Prot. Conf. – Weeds, Brighton, 1997, pp. 777–782.

[35] Rendina A.R., Felts J.M., Cyclohexanediones herbicides are selective and potent inhibitors of acetyl-CoA carboxylase from grasses, Plant Physiol. 86 (1988) 983–986.

[36] Rivière J.L., Cabanne F., Animal and plant cytochrome P-450 systems, Biochimie 69 (1987) 743–752.

[37] Scherrer B., "Biostatistique", Eska S.A.R.L., 1984.

[38] Secor J., The discovery of the selective inhibition of acetyl coenzyme A carboxylase activity by two classes of graminicides, in: Proc. Brighton Crop Prot. Conf., Brighton, 1989, pp. 145–154.

[39] Shukla A., Leach G.E., Devine M.D., High-level resistance to sethoxydim conferred by an alteration in the enzyme acetyl CoA carboxylase in *Setaria faberi* and *Setaria veridis*, Plant Physiol. Biochem. 35 (1997) 803–807.

[40] Shukla A., Dupont S., Devine M.D., Resistance to ACCase-inhibitor herbicides in wild oat: evidence for target site-based resistance in two biotypes from Canada, Pest. Biochem. Phys. 57 (1997) 147–155.

[41] Singh S., Kirkwood R.C., Marshall G., Effect of the monooxygenase inhibitor piperonyl butoxide on the herbicide activity and metabolism of isoproturon in herbicide resistant and susceptible biotype of *Phalaris minor* and wheat, Pest. Biochem. Phys. 59 (1998) 143–153.

[42] Tal A., Romano M.L., Stephenson G.R., Glutathione conjugation: a detoxication pathway for fenoxaprop-P-ethyl in barley, crabgrass, oat and wheat, Pest. Biochem. Phys. 46 (1993) 190–199.

[43] Tardif F.J., Powles S.B., Herbicide multiple-resistance in a *Lolium rigidum* biotype is endowed by multiple mechansims: isolation of a subset with resistant acetyl-CoA carboxylase, Physiol. Plant. 91 (1994) 488–495.

[44] Zimmerlin A., Durst F., Aryl hydroxylation of herbicide diclofop by wheat cytochrome P-450 monooxygenase, Plant Phytol. 100 (1992) 874–881.

COR-AAD1-00002647
Bayer EX1008 (Part 5 of 9)

related to the optical performances and to the energy at which the optical device is designed to work. In Table 1, the energy region from 500 eV to 50 keV is divided into three parts: low, medium and high energies.

At low energies, the material thickness needed to provide a π-phase shift becomes smaller (200–300 nm), but it is still necessary to achieve high aspect ratios of about 10 if one wishes to fabricate zones at the current lithographic spatial resolution limit[15,16]. With the latest generation of electron-beam machines and nano-structuring technologies[17,18], zone plates with a resolution of 20–50 nm have been fabricated for 200–500 eV X-rays, and alignment accuracy of ~10 nm has already been demonstrated[8]. Working at the lithographic limit, the outermost zone width of a quaternary FZP becomes twice as large as that of a binary FZP, thus doubling the optical resolution $\delta_{r,m}$. Therefore, at low energy, quaternary FZPs are complementary to binary FZPs, providing a good trade-off between the reduction of the optical resolution and the increase of the efficiency.

At medium energy, the typical phase-shifter thickness is of the order of one micrometre. Practical aspect ratios of 5–10, that can be achieved by today's very-large-scale integration (VLSI) technology, limit the minimum spatial resolution to 150 nm. At high energy, the phase-shifter thickness further increases to a few micrometres (see Table 1) and, accordingly, the minimum feature size reaches about 1 μm. In this range, where other optical devices are somewhat limited (although refractive lenses could improve in the future), quaternary FZPs show some unique advantages, especially with respect to their efficiency and optical resolution (see Table 1). Also, multilevel FZPs are compatible at high energy with microdiffraction, where the high focusing length matches the necessary low angular divergence.

With the consolidation of third-generation synchrotrons, multilevel FZPs could be used as focusing elements in research fields where high efficiency and high signal-to-noise ratio are needed at X-ray wavelengths. □

Received 2 June; accepted 9 September 1999.

1. Dhez, P., Chevallier, P., Lucatorto, T. B. & Tarrio, C. Instrumental aspects of X-ray microbeams in the range above 1 keV. *Rev. Sci. Instrum.* **70**, 1907–1920 (1999).
2. Snigirev, A., Kohn, V., Snigireva, I. & Lengeler, B. A compound refractive lens for focusing high-energy X-rays. *Nature* **384**, 49–51 (1996).
3. Kirz, J., Jacobsen, C. & Howells, M. Soft X-ray microscopes and their biological applications. *Q. Rev. Biophys.* **28**, 33–130 (1995).
4. Wang, J. *et al.* X-ray fluorescence correlation spectroscopy: a method for studying particle dynamics in condensed matter. *Phys. Rev. Lett.* **80**, 1110–1113 (1998).
5. Rodrigues, W. *et al.* X-ray microdiffraction studies of an integrated laser-modulator system in *Proc. 6th Conf. on Synchrotron Radiation Instrumentation (SRI97)* (Himeji Citizen Hall, Hyogo, Japan, 1997).
6. Tatchyn, R. O. in *X-ray Microscopy* Vol. 43 (eds Smah, G. & Rudolph, D.) 40–50 (Springer Series in Optical Sciences, Springer, Berlin, 1990).
7. Lai, B. *et al.* Hard X-ray phase zone plate fabricated by Lithographic techniques. *Appl. Phys. Lett.* **1**, 1877–1880 (1992).
8. Di Fabrizio, E. *et al.* High-performance multilevel blazed X-ray microscopy Fresnel zone plates fabricating using X-ray lithography. *J. Vac. Sci. Technol. B.* **12**, 3979 (1994).
9. Yun, W. *et al.* Nanometer focusing of hard X-rays by phase zone plates. *Rev. Sci. Instrum.* **70**, 2238–2241 (1999).
10. Michette, A. G. *Optical Systems for Soft X-rays* (Plenum, New York, 1986).
11. Schelokob, I. A. *et al.* Second generation of grazing-incidence-phase Fresnel zone plates. *Opt. Commun.* **159**, 278–284 (1999).
12. Kirz, J. Phase zone plates for X-rays and extreme UV. *J. Opt. Soc. Am.* **64**, 301–309 (1974).
13. Barrett, R., Kaulich, B., Oestreich, S. & Susini, J. The scanning microscopy end-station at the ESRF X-ray microscopy beamline. *Proc. SPIE* **3499**, 80–90 (1998).
14. Nieman, B. in *X-ray Microscopy and Spectromicroscopy* (eds Thieme, J., Schmahl, G., Rudolph, D. & Umbach, E.) 44–55 (Springer, Chernogolovka, Russia, 1998).
15. Spector, S. J., Jaconsen, C. J. & Tennant, D. M. Process optimization for production of sub-20 nm soft X-ray zone plate. *J. Vac. Sci. Technol. B* **15**, 2872–2876 (1997).
16. David, C. *et al.* Low-distortion electron-beam lithography for fabrication of high-resolution germanium and tantalum phase zone plates. *J. Vac. Sci. Technol. B* **13**, 2762–2766 (1995).
17. Schneider, G., Schliebe, T. & Aschoff, H. Cross linked polymers for nanofabrication of high resolution zone-plates in nickel and germanium. *J. Vac. Sci. Technol. B* **13**, 2809–2812 (1995).
18. Weiss, D., Peuker, M. & Schneider, G. Radiation enhanced network formation in copolymer galvanoforms for diffractive nickel X-ray optics with high aspect ratios. *Appl. Phys. Lett.* **72**, 1805–1807 (1998).

Correspondence and requests for materials should be addressed to E.D.F. (e-mail: difabriz@sci.area.trieste.it).

Influence of environmental changes on degradation of chiral pollutants in soils

David L. Lewis*†, A. Wayne Garrison*, K. Eric Wommack*†, Alton Whittemore*, Paul Steudler‡ & Jerry Melillo‡

* *US Environmental Protection Agency, Ecosystems Research Division, National Exposure Research Laboratory, Athens, Georgia 30605, USA*
† *Department of Marine Sciences, University of Georgia, Athens, Georgia 30602, USA*
‡ *The Ecosystems Center, Marine Biological Laboratory, Woods Hole, Massachusetts 02542, USA*

Numerous anthropogenic chemicals of environmental concern—including some phenoxy acid herbicides, organophosphorus insecticides, polychlorinated biphenyls, phthalates, freon substitutes and some DDT derivatives—are chiral. Their potential biological effects, such as toxicity, mutagenicity, carcinogenicity, and endocrine disrupter activity, are generally enantiomer-selective, and different enantiomers are preferentially degraded (transformed) by micro-organisms in various environments[1–8]. Here we use field and laboratory experiments to demonstrate that environmental changes in soils can alter these preferences, and to suggest that the preferences shift owing to different groups of related microbial genotypes being activated by different environmental changes. In Brazilian soils, almost all pasture samples preferentially transformed the non-herbicidal enantiomer of dichlorprop ((*RS*)-2-(2,4-dichlorophenoxy)propionic acid), while most forest samples either transformed the herbicidal enantiomer more readily or as rapidly as the non-herbicidal enantiomer. Organic nutrient enrichments shifted enantioselectivity for methyl dichlorprop ((*RS*)-methyl 2-(2,4-dichlorophenoxy)propionic acid) strongly towards preferentially removing the non-herbicidal enantiomer in soils from Brazil and North America, potentially increasing phytotoxicity of its residues relative to that of the racemate. Assessments of the risks chemical pollutants pose to public health and the environment need to take into account the chiral selectivity of microbial transformation processes and their alteration by environmental changes, especially for pesticides as up to 25 per cent are chiral[9].

Enantiospecific biological effects associated with chiral chemicals are well recognized in the pharmaceutical industry where 50 of the top 100 most widely sold drugs, including barbiturates, ibuprofen, albuterol, and Ritalin, are marketed as single enantiomers to avoid adverse side effects[8,10]. The high cost of separating enantiomers

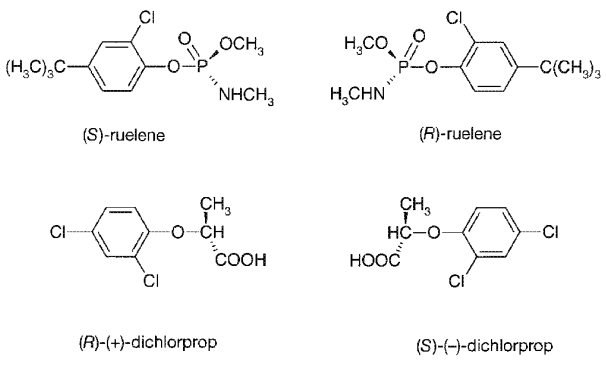


Figure 1 Enantiomers of ruelene and dichlorprop.

© 1999 Macmillan Magazines Ltd

COR-AAD1-00002648
Bayer EX1008 (Part 5 of 9)

Table 1 Effect of deforestation on dichlorprop enantioselectivity in Brazilian soils

	n	$t_{1/2}$ (days)	c.v. (%)	(+) (%)	(–) (%)	(+/–) (%)
Methyl dichlorprop						
Forest	52	0.77	62	7.7	1.9	90
Pasture	75	0.63	49	11	1.7	87
Dichlorprop						
Forest	16	11	36	13	38	50
Pasture	37	16	57	6.7	93	0.0

Soil samples were collected from a forest in Rondonia, Brazil and from six deforested areas (pastures) nearby, ranging 9–47 years in age. Soil samples (1 gram) were amended with herbicides and incubated overnight for methyl dichlorprop and over ~6 months for dichlorprop. Selectivity for different enantiomers ((+) or (–)) was quantified as percentages of soil samples in which differences in the amounts transformed of each enantiomer were ≥15%. Non-selective samples (+/–) had concentration differences between (+) and (–) enantiomers of <15%. Transformation half-lives ($t_{1/2}$) of herbicide racemates were calculated ± a coefficient of variation (c.v.) among a number (*n*) of replicate soil samples. Almost all (93%) of the pasture samples preferentially transformed the non-herbicidal (–) enantiomer, while most forest samples either preferentially transformed the herbicidal enantiomer (13%) or transformed it as rapidly as the (–) enantiomer (50%).

Table 2 Effect of nutrient enrichment on enantioselectivity for methyl dichlorprop

	n	(+) (%)	(–) (%)	(+/–) (%)	Net preference (%)
Rondonia, Brazil					
Soil	127	9.0	2.0	88	7.0 (+)
Enrichment	340	15	50	35	35 (–)
Harvard Forest, Massachusetts, USA					
Soil	29	45	48	7.0	3.0 (–)
Enrichment	207	3.0	80	17	77 (–)
Risdalsheia, Norway					
Soil	16	0.0	88	13	88 (–)
Enrichment	80	15	74	11	59 (–)

Methods for testing soil were the same as Table 1, except that the soil samples contained beef extract and peptone. Net preferences, which indicated the extent to which soil (or soil + organic nutrients) preferentially transformed an enantiomer, were calculated as the absolute values of differences in percentage of soil samples preferring (+) or (–) enantiomers.

currently prohibits applying this technology to the commercial production of most pesticides and other industrial chemicals to reduce the unwanted effects of racemates as environmental pollutants. Notable exceptions include two herbicides, dichlorprop and mecoprop, in which a limited portion of the total worldwide production includes single enantiomers[11].

In the case of chiral pollutants, environmental studies have historically neglected to determine the adverse effects associated with particular enantiomers, and which enantiomers may persist in the environment. Consequently, much of the environmental data that has been collected for chiral pollutants, including many of the chemicals raising the greatest public concern, may have represented only the presence of relatively innocuous enantiomers.

To assess the persistence of different pollutant enantiomers across a wide latitudinal transect, and the possible influence of large-scale environmental changes on that persistence, we investigated enantioselectivity in soils collected from three areas after amending them with ruelene ((*RS*)-4-tert-butyl-2-chlorophenylmethyl-*N*-methyl phosphoramidate), dichlorprop, and methyl dichlorprop (Fig. 1). The sites included an upland plateau in Risdalsheia, Norway about 20 km inland of the North Sea, an 80-year-old mixed deciduous forest (Harvard Forest) in the northeastern US, and an area of the Fazenda Nova Vida about 250 km south of the city of Porto Velho in Rondonia, Brazil. Only the (+) enantiomers of dichlorprop and methyl dichlorprop are herbicidal[11] (see Methods). Both enantiomers of ruelene were insecticidal; however, the (+) enantiomer was four times more toxic.

Table 1 shows that tropical deforestation (conversion to pastures) had little or no effect on enantioselectivity or demethylation rates of the racemate of methyl dichlorprop. Demethylation was the first and most rapid step in the transformation process, which quantitatively produced dichlorprop as the reaction product. Soil warming in North America and Norway also had no measurable effect on racemate demethylation rates or enantioselectivity for methyl dichlorprop where field plots were heated 5 °C above ambient temperatures for ~7 years in North America and ~4 years in Norway[12,13]. Transformation of dichlorprop began after a 6-month lag period and proceeded 20 times more slowly (half-life of ~14 days compared with ~0.7 days for methyl dichlorprop).

Addition of inorganic fertilizers to forest and pasture plots in Brazil had no measurable effect on enantioselectivity for methyl dichlorprop (tested at 2 weeks and at 5 months after fertilization), or to plots in North America fertilized since May 1988. Laboratory enrichments with organic nutrients, which caused soils preferentially transforming the (+) enantiomer to shift to strongly preferentially transforming the inactive (–) enantiomer in samples from North America and Brazil (Table 2), did not have the same effect in samples from Norway where soils already preferentially removed the (–) enantiomer. There, microorganisms preferring the (+) enantiomer may have increased in activity somewhat after nutrient amendments, but most samples (74%) still preferred the (–) enantiomer. Preferential removal of (–) methyl dichlorprop would render residues more phytotoxic than the same concentrations of the racemate, as long as demethylation is a prerequisite step and the (+) dichlorprop enantiomer is not preferentially removed after nutrient enrichment.

Ruelene, like dichlorprop, was transformed by microbial populations only after about a 6-month lag period. The half-life, once transformation began, was ~40 days in Brazilian soils and 20 days in Norwegian soils. Ruelene racemate transformation rates were unaffected by deforestation or soil warming. Enantioselectivity, however, was affected in both cases. In Brazil, deforestation caused soils to shift from preferentially removing the less toxic ruelene (–) enantiomer (22% (+), 67% (–), 11% (+/–), $n = 17$) to exclusively transforming the (+) enantiomer. Soil warming in Norway, on the other hand, caused soils to shift from all samples preferentially removing the ruelene (+) enantiomer to some (22%) preferentially removing the less toxic enantiomer ($n = 13$). Technical obstacles to separating ruelene enantiomers were greater than those faced with dichlorprop; therefore, fewer soil samples were successfully analysed (17 from Brazil and 13 from Norway). Nevertheless, results were consistent with the behaviour of dichlorprop, where environmental changes affected enantioselectivity when long lag periods were required for adaptation.

Delayed microbial transformation of chemical residues is commonly observed and is often assumed to represent the amount of time required for low concentrations of microorganisms responsible for the transformation process to attain significant numbers after using the chemicals as substrates or energy sources. Hollibaugh[14], however, investigated enantioselectivity for D- and L-amino acids metabolized by marine bacteria and found that lag periods could not be explained by growth of sub-populations. Instead, they were consistent with times required for activating metabolically quiescent microbial populations or inducing enzymes for enantiomer-specific uptake or transformation processes.

As environmental changes in this study affected only the two chemicals with long lag periods, sorption, a more rapid process, probably did not play a role. Enantioselective sorption has been ruled out elsewhere as well[7]. Nevertheless, many soils have their genesis with living matter and their organic components may retain chiral centres capable of selectively binding specific enantiomers. Enantioselective sorption to soil organics, if it occurs, could affect the availability of various enantiomers for microbial transformation.

To investigate the diversity and biogeography of bacteria capable of demethylating methyl dichlorprop, small-subunit (16S) ribosomal

© 1999 Macmillan Magazines Ltd

COR-AAD1-00002649
Bayer EX1008 (Part 5 of 9)

RNA (rRNA) genes of 50 soil bacterial isolates were compared using amplified ribosomal DNA restriction analysis (ARDRA)[15] (Fig. 2). ARDRA has proved useful in taxonomic assessments of bacterial culture collections[16] and 16S rDNA clone libraries[17] at genus and species levels.

In general, isolates from Norway and North America formed three large clusters and appeared to be more closely related to one another than to isolates from Brazil. Conversely, Brazilian isolates formed smaller clusters that were more distantly related to one another and to Norwegian and North American clusters. It is plausible that these relationships among bacterial isolates reflect ecological differences between these geographical regions. ARDRA patterns that indicated taxonomic identity between two or more isolates were, in every comparison examined except one (Norway isolates 409-1 versus 416-4), supported by 16S rDNA sequence data demonstrating gene-sequence identity. Furthermore, isolates with identical ARDRA patterns exhibited the same enantioselectivity phenotype regardless of their geographical origins, except in the case of the two isolates noted above.

Although the ARDRA banding pattern was virtually the same for Norway isolates 409-1, which preferentially transformed the (−) enantiomer, and 416-4, which was non-enantioselective, 16S rDNA sequence data varied by several base pairs. Isolate 409-1 did metabolize the (+) enantiomer, but at a much slower rate than the (−) enantiomer. In fact, with all soil samples and bacterial isolates, both enantiomers for each test chemical were transformed simultaneously, but at different rates. This behaviour is consistent with what has been observed by others where enantioselectivity has been detected in environmental samples.

Our data suggest that microbial enantioselectivity with environmental pollutants is controlled by the activation of metabolically quiescent microbial populations or the induction of enantiomer-specific enzymes, as was the case with amino acids, and that this selectivity follows lines of genetic similarity where different groups of related microbes are activated by different kinds of environmental changes.

With one exception (Norway 409-1), only isolates from Brazil exhibited enantioselectivity with methyl dichlorprop. Among those isolates, 58% were enantioselective and their preferences roughly reflected those observed with soil incubations (Table 2). However, Norwegian and North American isolates did not reflect the (−) enantiomer preference observed in soil incubations from these locations. Most of these isolates were non-enantioselective, but the relatively few genotypes that were enantioselective tended to

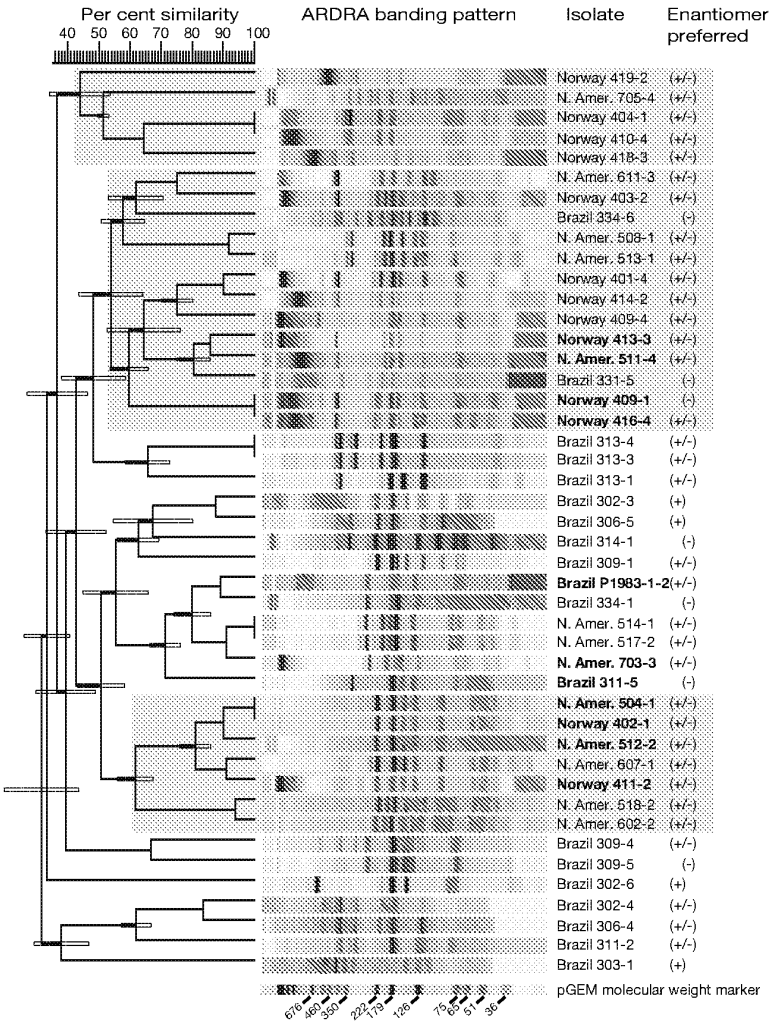


Figure 2 Amplified ribosomal DNA restriction analysis of bacterial isolates. Confidence limits for the placement of nodes are shown with error bars. Molecular weight marker (pGEM) to which band positions were normalized is shown at the bottom. Numbers indicate size in base pairs of DNA. In general, isolates that enantioselectively transformed methyl dichlorprop from North American and Norwegian soils formed three large clusters (grey boxes) whereas Brazilian isolates formed smaller, more distantly related, clusters.

© 1999 Macmillan Magazines Ltd

COR-AAD1-00002650
Bayer EX1008 (Part 5 of 9)

dominate transformation processes such that soil samples from North America preferred either (+) or (−) enantiomers while almost all of the soil samples from Norway preferred the (−) enantiomer.

These results have important implications for public health and environmental protection. The differing effects of inorganic and organic nutrients on enantioselectivity (Tables 1, 2), for example, raise new questions with respect to land application of processed sewage sludge (biosolids), which transforms pollutants enantioselectively[18]. Under a regulation first promulgated by the US Environmental Protection Agency in 1993 (ref. 19), biosolids are used as a commercial fertilizer for agricultural lands heavily treated with pesticides. In the USA, Europe, and elsewhere, governments are promoting the agricultural use of biosolids to replace ocean dumping of municipal wastes. Substituting organic-rich biosolids for inorganic fertilizers may increase microbial transformation rates of some of the active enantiomers of pesticides and thus diminish their effectiveness in the field. On the other hand, persistence may be enhanced for some enantiomers posing a risk to public health and the environment.

This study demonstrates that significant environmental changes, such as tropical deforestation and global warming, may substantially alter the relative persistence of enantiomers of chiral pollutants, exacerbating the adverse effects of some while ameliorating the effects of others. It calls into question the accuracy and future relevance of current risk assessments for numerous pollutants, and underscores the need to better incorporate science in efforts aimed at protecting public health and the environment[20]. □

Methods

Dichlorprop and ruelene were microbially transformed rapidly enough to process numerous samples, and could also be adequately separated from extracts of soils and microbiological media. Dichlorprop, one of the most widely used herbicides, is applied as the acid and various esters that are readily attacked by common bacterial esterases. Ruelene has been banned in the USA but is still used elsewhere. Chiral Technologies (Exton, Pennsylvania, USA) separated the enantiomers from racemates and methylated the dichlorprop enantiomers.

Brazilian soil samples were collected in March and August 1998 from a forest and an adjacent 11-year-old pasture. Plots in both areas were treated with inorganic fertilizers (~33 kg N per hectare and 13 kg P per hectare). Additional samples were collected from 9-, 15-, 19-, 26- and 47-year-old pastures. Soil-warming samples with corresponding control (unheated) samples were collected in October 1998 from field plots in Harvard Forest, Massachusetts where buried, computer-controlled electrical cables heated soil 5 °C above ambient temperatures, beginning in July 1991. Samples were also collected in September 1998 from field plots in Risdalsheia, Norway that had been similarly heated since May 1994.

Soil samples of 1-gram each were treated with 10-ml aqueous racemic herbicide or insecticide solutions containing ~25 mg l^{-1} of each enantiomer and incubated at 25 °C overnight for methyl dichlorprop and ~6 months for dichlorprop and ruelene. Half-lives were estimated from changes in pollutant concentrations after transformation began, assuming first-order kinetics. Enantiomer concentrations usually decreased >80%.

Methyl dichlorprop enantiomers were detected by flame ionization (FID) after separation with a 25 m × 0.25 mm wall coated, open tubular fused silica column coated with a 0.25-μm layer of CP ChirasilDex CB (Chrompack, Ravitan, New Jersey, USA). Dichlorprop enantiomers were separated by capillary electrophoresis (CE) (15 kV with 25 mM tetraborate buffer and 25 mM trimethyl-β-cyclodextrin) and detected by ultraviolet absorption at 230 nm. Ruelene enantiomers were also separated by CE in the micellar electrokinetic chromatography mode (20 kV with 20 mM tetraborate buffer at pH 8.5 containing 100 mM sodium dodecyl sulphate, 20% acetonitrile, and 40 mM 2-hydroxypropyl-β-cyclodextrin) and detected at 200 nm.

Only samples demonstrating a decrease of ≥15% in racemates (two standard deviations of the experimental error for determining concentrations) were analysed for enantioselectivity. Samples exhibiting enantioselectivity generally had a ≥50% difference between concentrations of the two enantiomers at the final sampling time; non-enantioselective samples (+/−) generally showed no significant differences.

For soils enriched with organic nutrients, the 10-ml volume of added liquid contained various concentrations (undiluted, and diluted by factors of 100 and 10,000 of beef extract plus peptone (Difco Laboratories, Detroit, Michigan, USA), a standard source of complex organic nutrients for culturing a wide variety of microorganisms. Net preferences, which indicated the extent to which soil (or soil + organic nutrients) preferentially degraded an enantiomer, were absolute values of differences in percentage of samples preferentially degrading (+) or (−) enantiomers. All dilutions of the organic nutrients affected enantioselectivity similarly; therefore, these results were pooled in Table 2. Because Brazilian forest and pasture samples exhibited almost identical degrees of preference for methyl dichlorprop enantiomers, results from these samples were also combined in Table 1.

To operationally determine the taxonomic relationships between bacterial isolates, restriction banding patterns of the 16S rDNA of each isolate were compared. Phenol/chloroform-extracted DNA from each bacterial isolate was used as the template in a polymerase chain reaction (PCR) to amplify 16S rDNA. The primers used in the PCR (27f (5′-AGAGTTTGATCCTGGCTCAG-3′) and 1492r (5′-GGTTACCTTGTTACG ACTT-3′)) yielded an amplicon corresponding to bases 8 through 1492 (*Escherichia coli* numbering) of the bacterial 16s rDNA. After the PCR, the 16S rDNA amplicon was purified by phenol/chloroform extraction and digested with two restriction enzymes, *Rsa*I and *Alu*I. Restriction products were separated by electrophoresis on a highly resolving 3% agarose gel (Metaphor, FMC, Rockland, Maine, USA) and visualized using a laser gel scanner and the double-stranded DNA fluorescent stain SYBR Gold (Molecular Probes, Portland, Oregon, USA). Gel lanes were normalized to a single molecular weight standard and analysed using the computer software program Molecular Analyst. Banding patterns were compared based on constituent band positions. The cluster diagram, based on differences in ARDRA banding patterns, was produced by UPGMA (unweighted pair group method using arithmetic averages) of a Jaccard similarity matrix. The cophenetic correlation was 77%. To investigate the reliability of ARDRA relationships a portion (~720 base pairs) of the 16S rDNA was sequenced from the isolates shown in bold-faced type in Fig. 2. In general, isolates with similar or identical banding patterns also had similar or identical 16S rDNA sequences.

Mortality rates with ruelene were determined by exposing North American forest tent caterpillars (*Malacosoma disstria*). Forty larvae from a single nest were divided into two equal groups and fed equal amounts of native black cherry leaves coated with either the (+) or (−) enantiomer. The insecticide was dissolved in acetone (200 mg ml^{-1}), thinly spread over the surface of the leaves and allowed to air dry. Similar tests, in which plantains (*Plantago* sp.) were treated with 700 mg l^{-1} of separate enantiomers of methyl dichlorprop, showed that, as with dichlorprop, only the (+) enantiomer is herbicidal.

Received 18 May; accepted 14 September 1999.

1. Falconer, R. L., Bidleman, T. F., Gregor, D. J., Semkin, R. & Teixeira, C. Enantioselective breakdown of α-hexachlorocyclohexane in a small arctic lake and its watershed. *Environ. Sci. Technol.* **29,** 1297–1302 (1995).
2. Jantunen, L. M. & Bidleman, T. F. Air-water gas exchange of hexachlorocyclohexanes (HCHs) and the enantiomers of α-HCH in arctic regions. *Geophys. Res.* **108,** 28837–28846 (1996).
3. Aigner, E. J., Leone, A. D. & Falconer, R. I. Concentrations and enantiomeric ratios of organochlorine pesticides in soils from the U.S. corn belt. *Environ. Sci. Technol.* **32,** 1162–1168 (1998).
4. Wiberg, K. *et al.* Enantioselective gas chromatography/mass spectrometry of methylsulfonyl PCBs with application to arctic marine mammals. *Anal. Chem.* **70,** 3845–3852 (1998).
5. Garrison, A. W., Schmitt, P., Martens, D. & Kettrup, A. Enantiomeric selectivity in the environmental degradation of dichlorprop as determined by high-performance capillary electrophoresis. *Environ. Sci. Technol.* **30,** 2449–2455 (1996).
6. Tett, V. A., Willetts, A. J. & Lappin-Scott, H. M. Enantioselective degradation of the herbicide mecoprop [2-(2-methyl-4-chlorophenoxy) propionic acid] by mixed and pure bacterial cultures. *Microbial Ecol.* **14,** 191–200 (1994).
7. Zipper, C., Suter, M. J.-F., Haderlein, M. G. & Kohler, H.-P. E. Changes in the enantomeric ratio of (*R*) to (*S*)-mecoprop indicate in situ biodegradation of this chiral herbicide in a polluted aquifer. *Environ. Sci. Technol.* **32,** 2070–2076 (1998).
8. Kohler, H.-P. E. *et al.* Environmental fate of chiral pollutants—the necessity of considering stereochemistry. *Chimia* **51,** 947–95 (1997).
9. Williams, A. Opportunities for chiral chemicals. *Pestic. Sci.* **46,** 3–9 (1996).
10. *Counting on Chiral Drugs. Chem. Eng. News* **76**(38), 83 (1998).
11. Buser, H. P. & Francotte, E. in *Chiral Separations* (ed. Ahuja, S.) Ch. 5 (American Chemical Society, Washington DC, 1997).
12. Peterjohn, W. T. *et al.* Responses of trace gas fluxes and N availability to experimentally elevated soil temperatures. *Ecol. Appl.* **4,** 617–625 (1994).
13. Lukewille, A. & Wright, R. F. Experimentally increased soil temperature causes release of nitrogen at a boreal forest catchment in southern Norway. *Glob. Change Biol.* **3,** 13–21 (1997).
14. Hollibaugh, J. T. Metabolic adaptation in natural bacterial populations supplemented with amino acids. *Estuar. Coast. Mar. Sci.* **9,** 215–230 (1979).
15. Akkermans, A. D. L., van Elsas, J. D. & de Bruijn, F. J. *Molecular Microbial Ecology Manual* 1–488 (Kluwer Academic, Dordrecht, 1995).
16. Fulthorpe, R. R., Rhodes, A. N. & Tiedje, J. M. High levels of endemicity of 3-chlorobenzoate-degrading soil bacteria. *Appl. Environ. Microbiol.* **64,** 1620–1627 (1998).
17. Moyer, C. L., Dobbs, F. C. & Karl, D. M. Estimation of diversity and community structure through restriction fragment length polymorphism distribution analysis of bacterial 16S rRNA genes from a microbial mat at an active, hydrothermal vent system. Loihi Seamount, Hawaii. *Appl. Environ. Microbiol.* **60,** 871–879 (1994).
18. Müller, M. D. & Buser, H.-R. Environmental behavior of acetamide pesticide stereoisomers. 2. Stereo- and enantioselective degradation in sewage sludge and soil. *Environ. Sci. Technol.* **29,** 2031–2037 (1995).
19. Standards for the use or disposal of sewage sludge. In *Code of Federal Regulations,* Title 40, Part 503, Subpart B, *Land Application* (US Government Printing Office, revised 1 July 1998).
20. Lewis, D. L. EPA science: casualty of election politics. *Nature* **381,** 731–732 (1996).

Acknowledgements

We thank R. Wright and C. Cerri for collecting soil samples, R. E. Hodson and J. T. Hollibaugh and S. Karickhoff for suggestions, and J. Avants, G. Chapman, and L. Howell for performing chiral analyses. J. Maudsley and D. Gattie assisted with bioassays. K.E.W. was supported by a National Research Council post-doctoral fellowship.

Correspondence and requests for materials should be addressed to D.L.L. (e-mail: LewisDaveL@aol.com).

© 1999 Macmillan Magazines Ltd

COR-AAD1-00002651
Bayer EX1008 (Part 5 of 9)

Phenoxyacetate Herbicide Detoxication by Bacterial Enzymes

M. A. Loos, J.-M. Bollag, and M. Alexander

Extracts of an *Arthrobacter* sp. contained enzymes dehalogenating 2,4-dichloro-, 2-methyl-4-chloro-, and 2- and 4-chlorophenoxyacetates. From the phenoxyacetates, these enzyme preparations produced compounds with the chromatographic characteristics of the corresponding phenols. The bacterial extracts further metabolized the phenols as well as several chloro- and methylcatechols. The enzyme acting on the phenoxy compounds was separated from the enzyme metabolizing the chlorophenols.

Downloaded via CORTEVA AGRISCIENCE on September 3, 2020 at 19:21:47 (UTC).
See https://pubs.acs.org/sharingguidelines for options on how to legitimately share published articles.

The phenoxyacetates are one of the major groups of herbicides used for selective control of weeks, and the vast amounts that are used annually are degraded ultimately to yield nontoxic products. Despite the significance of microorganisms for the detoxication of pesticides in the environment, little is known of the microbial mechanisms of degradation. Hydroxylation of the aromatic ring has been reported to occur in microorganisms as well as in plants (Evans and Smith, 1954; Faulkner and Woodcock, 1961; Thomas *et al.*, 1964), and evidence has been obtained which indicates that certain bacteria are capable of removing the acetate moiety following ring hydroxylation (Evans and Smith, 1954; Gaunt and Evans, 1961). By contrast, the present authors' work with intact cells of an *Arthrobacter* sp. indicated that the side chain of 2,4-dichlorophenoxyacetate (2,4-D) was removed without prior hydroxylation of the benzene ring (Loos *et al.*, 1967a, b).

Detailed studies of the mechanisms of breakdown of the chlorinated phenoxyacetate herbicides have been hampered by the lack of an enzyme preparation able to decompose these compounds. The preparation and some properties of a bacterial enzyme system which catalyzes the degradation of 2,4-D, 2- and 4-chlorophenoxyacetates (2-CPA and 4-CPA), and 2-methyl-4-chlorophenoxyacetate (MCPA) are here described.

MATERIALS AND METHODS

The phenoxyacetate-degrading *Arthrobacter* sp. described previously (Loos *et al.*, 1967a) was cultured with aeration at 25° C. in the following medium: 2,4-D or MCPA (neutralized with NaOH), 3.0 grams as the free acid; KH_2PO_4, 1.2 grams; K_2HPO_4, 4.8 grams; NH_4NO_3, 0.5 gram; $MgSO_4 \cdot 7H_2O$, 0.2 gram; $CaCl_2 \cdot 2H_2O$, 25 mg.; $FeCl_3 \cdot 6H_2O$, 2.5 mg.; and distilled water, 1.0 liter. The bacteria were collected by centrifugation, the cells were washed twice with 0.01*M* phosphate buffer, pH 7.2, and resuspended in the same buffer. The cell suspension was passed twice through a cooled French pressure cell operated at 20,000-p.s.i. pressure. Whole cells and the larger components of broken cells were removed by centrifuging the suspension at 20,000 × G for 30 minutes to yield the crude extract. The soluble fraction was obtained by centrifuging the crude extract at 144,000 × G for 1 hour.

Solutions containing 0.5 ml. of extract (14.7 to 23.0 mg. of protein) 0.5 ml. of 0.01*M* phosphate buffer, pH 7.2, and 1.0 μmole of substrate were incubated with shaking at either 30° or 25° C. The reactions were stopped, and protein was precipitated by adding 10 ml. of the tungstic acid reagent of Van Slyke and Hawkins (Hawk *et al.*, 1954). The tungstic acid-treated reaction mixtures were analyzed for chloride using the method of Bergmann and Sanik (1957). Corrections were made for chloride introduced with the extract, in substrate solutions, and in the tungstic acid solution. No chloride was released from any of the substrates, in the absence of extract, by the addition of tungstic acid. Metabolism of phenol or catechol was assessed by measuring the extent of disappearance of the substrates (Lacoste *et al.*, 1959; Mitchell, 1924). In the catechol assay, 0.05% osmic acid was added to a solution buffered at pH 7.8.

RESULTS AND DISCUSSION

Both the crude extract and the soluble fraction derived from it metabolized 2,4-D with the release of 92 and 80% of the organic chlorine, respectively, in a 3-hour incubation period. Extracts of 2,4-D- or MCPA-grown cells also produced chloride when incubated with other phenoxyacetates as well as with several phenols and catechols (Table I). Enzymes in the preparation apparently are capable of metabolizing several phenoxyacetate herbicides, including not only 2,4-D but also MCPA and 4-CPA. The failure of the extract to dehalogenate 6-hydroxy-2,4-dichlorophenoxyacetate suggests that it is not an intermediate in the degradation of 2,4-D by this microorganism, in contrast with the findings of Evans and Smith (1954) with pseudomonads.

Phenols and catechols were also metabolized by the crude bacterial extracts, as indicated by phenol or catechol disappearance (Table I). Activity was noted with 2,4-dichlorophenol and 2-methyl-4-chlorophenol, the compounds which would be formed upon cleavage of the ether linkage of 2,4-D and MCPA, respectively, as well as with 2- and 4-chlorophenol. By measuring the rate of chloride formation at regular intervals, it was shown that the rate of dehalogenation of the chlorophenols was essentially the same whether the extracts were prepared from cells cultured on 2,4-D or MCPA. The 4-chloro- and the 3,5-dichlorocatechols, possible subsequent intermediates in the degradation of the herbicides, were also enzymatically dechlorinated. During the course of the reaction, the phenol or catechol was destroyed. The extent of degradation was similar whether chloride release or phenol or catechol disappearance was used to assay enzymatic action.

Laboratory of Soil Microbiology, Department of Agronomy, Cornell University, Ithaca, N.Y.

COR-AAD1-00002652
Bayer EX1008 (Part 5 of 9)

Table I. Metabolism of Phenoxyacetates, Phenols, and Catechols by Extracts of an *Arthrobacter* sp.

Substrate	Incubation Time, Hours	Chloride Release, %	Substrate Disappearance, %
2,4-Dichlorophenoxyacetate	3	92[a]	
2-Methyl-4-chlorophenoxyacetate	4	39	
2-Chlorophenoxyacetate	4	72[a]	
4-Chlorophenoxyacetate	4	70[a]	
6-Hydroxy-2,4-dichlorophenoxyacetate	3	0[a]	
2-Hydroxy-4-chlorophenoxyacetate	3	28[a]	
2,4-Dichlorophenol	4	100[a]	
2-Methyl-4-chlorophenol	4	72	65
2-Chlorophenol	4	65	82
4-Chlorophenol	4	68	80
4-Chlorocatechol	4	77[a]	63
3,5-Dichlorocatechol	4	90[a]	
3-Methylcatechol	4		84
4-Methylcatechol	4		81
Catechol	4		100

[a] Extract prepared from 2,4-D-grown cells and incubated at 30° C. In all other instances, extracts were prepared from MCPA-grown cells and incubated at 25° C.

With the exception of 3,5-dichlorocatechol, from which 16% of the bound chlorine was liberated, no halide was formed when these chlorine-containing phenoxyacetates, phenols, and catechols were incubated for 4 hours with an extract heated for 5 minutes at 80° C.

If the first step in 2,4-D decomposition is a decarboxylation, the product would be 2,4-dichloroanisole. To determine whether the anisole is an intermediate in the degradation, 0.5 ml. of the crude extract prepared from 2,4-D grown cells was incubated with 0.5 ml. of 0.01*M* phosphate buffer, pH 7.2, and approximately 2 μmoles of 2,4-dichloroanisole. Although some 2,4-dichloroanisole remained undissolved throughout the incubation period, gas chromatographic analysis showed the presence in the aqueous solution of small amounts of the substrate (less than 10 μg. per ml.). The amount of chloride detected in the reaction mixture at the end of a 3-hour incubation period was equivalent to only about 7% of the bound chlorine supplied. The inability of the extract to metabolize 2,4-dichloroanisole at a significant rate, if at all, suggests that it is not an intermediate in 2,4-D breakdown by the bacterium.

Phenolic intermediates were produced by the soluble fraction during the degradation of 2,4-D, 4-CPA, and 2-CPA. The reaction mixture contained 11.2 mg. of extract-protein when 2,4-D was the substrate or 12.4 mg. of extract-protein when 4-CPA or 2-CPA was provided. At regular intervals, tungstic acid was added to individual tubes containing the reaction mixtures, and aliquots were extracted with ether. The ether extract was dried with anhydrous Na_2SO_4, concentrated where necessary, and chromatographed using an Aerograph Model A-700 gas chromatograph fitted with a flame ionization detector. The column was a coiled glass tube, 10 feet long × 3/8-inch I.D., containing DC 200 silicone oil (12,500 centistokes) on 80- to 100-mesh, acid-washed Chromosorb W, in a 1 to 9 ratio by weight. N_2 (flow rate, 190 ml. per minute) was the carrier gas. The operating temperatures were: column, 200°; injector, 250°; and detector, 260° C. Compounds with retention times of 187, 116, and 170 seconds had accumulated after incubation of the soluble fraction with 2,4-D, 2-CPA, and 4-CPA. These retention times are identical to those of authentic 2,4-dichlorophenol and 2- and 4-chlorophenol, respectively (Figure 1).

The soluble fraction was concentrated by lyophilization, and the concentrated preparation was placed on a column of Sephadex G-150 equilibrated with 0.02*M* phosphate buffer, pH 7.0. The column was eluted with the same buffer, and activity of the fractions which were collected was tested using MCPA, 2-methyl-4-chlorophenol, and 4-chlorocatechol as substrates. No activity on 2-methyl-4-chlorophenol, as measured by phenol destruction or chloride release, was found in any of the fractions, but the enzyme (or enzymes) catalyzing the conversion of MCPA to a phenol was demonstrable in certain fractions. This enzyme did not release halide from MCPA. By contrast, chloride was liberated by preparations containing the enzyme acting upon 4-chlorocatechol (Figure 2). Thus, dehalogenation of MCPA apparently occurs after removal of the aliphatic moiety from the molecule.

Because the eluate from the Sephadex column was devoid of phenol-metabolizing activity, it was possible to isolate and characterize the phenol generated enzymatically from MCPA. The phenol was collected from the reaction mixture and identified on the basis of its retention time in the gas chromatograph as 2-methyl-4-chlorophenol.

The phenoxyacetate-cleaving enzyme of this bacterium is labile, and its activity is lost after several days. The reaction appears to be enzymatic, inasmuch as activity is abolished upon heating at 80° C. for 5 minutes. Gas chromatographic analysis showed that solutions containing either the enzyme preparations or the substrates alone did not contain compounds corresponding to the metabolites observed.

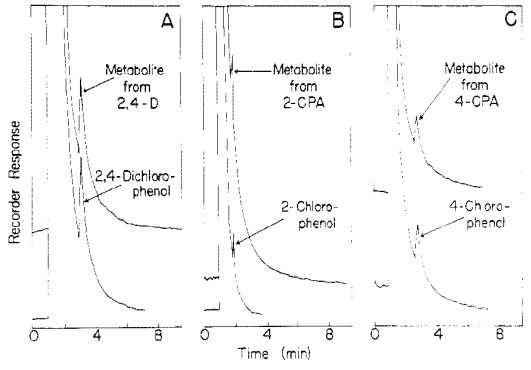


Figure 1. Gas chromatograms of authentic chlorophenols and metabolites

The metabolites were produced by the soluble fraction after incubation with 2,4-D for 1 hour (*A*) and with 2-CPA (*B*) and 4-CPA (*C*) for 2 hours. The volume of sample injected into the chromatograph was 15, 5, and 5 μl., respectively

COR-AAD1-00002653
Bayer EX1008 (Part 5 of 9)

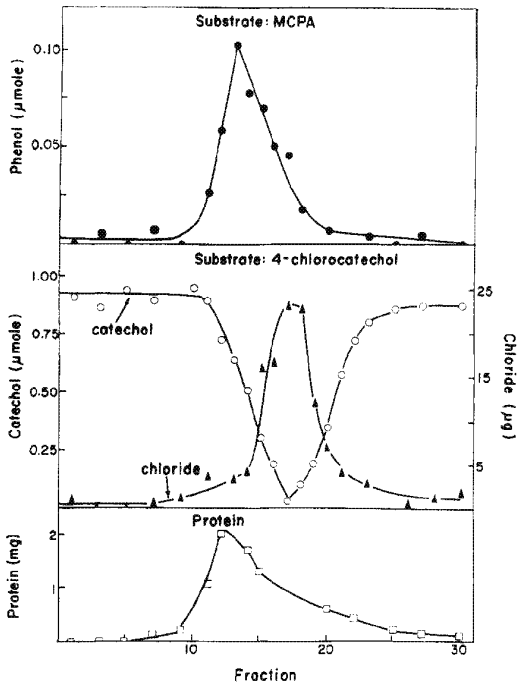


Figure 2. Enzymatic activity of Sephadex G-150 eluate on MCPA and 4-chlorocatechol

Fractions of 3.5 ml. were collected, and the reactions were measured using 1.0 μmole of substrate and 1.0 ml. of the eluate. Values for protein represent protein content of the fraction

Intact cells of the *Arthrobacter* sp. convert phenoxyacetates to their corresponding phenols (Loos *et al.*, 1967b). The finding that enzymes in extracts of this bacterium convert 2,4-D, 2-CPA, 4-CPA, and MCPA to the corresponding phenols and also further degrade these compounds not only shows unequivocally the intermediary role of phenols in the biological decomposition but also makes it possible to study the individual enzymatic steps in the metabolism of phenoxyacetate herbicides.

The conversion of phenoxyacetates to phenols has been reported to occur in plants (Chkanikov *et al.*, 1956). The elucidation of the enzymatic mechanism involved in degradation of phenoxyacetates and phenols by the *Arthrobacter* sp. should provide a basis for understanding how plant tissues as well as microorganisms act upon these compounds.

ACKNOWLEDGMENT

The authors thank C. S. Helling for advice and assistance in the chromatographic analysis and J. E. Maurer for able technical assistance.

LITERATURE CITED

Bergmann, J. G., Sanik, J., Jr., *Anal. Chem.* **29,** 241 (1957).
Chkanikov, D. I., Pavlova, N. N., Gertsuskii, D. F., *Khim. v Sel'skom Khoz.* **3**(4), 56 (1956).
Evans, W. C., Smith, B. S. W., *Biochem. J.* **57,** XXX (1954).
Faulkner, J. K., Woodcock, D., *J. Chem. Soc.* **1961,** p. 5397.
Gaunt, J. K., Evans, W. C., *Biochem. J.* **79,** 25P (1961).
Hawk, P. B., Oser, B. L., Summerson, W. H., "Practical Physiological Chemistry," p. 544, Blakiston, New York, 1954.
Lacoste, R. J., Venable, S. H., Stone, J. C., *Anal. Chem.* **31,** 1246 (1959).
Loos, M. A., Roberts, R. N., Alexander, M., *Can. J. Microbiol.*, **8** (1967a).
Loos, M. A., Roberts, R. N., Alexander, M., *Can. J. Microbiol.*, **8** (1967b).
Mitchell, C. A., *Analyst* **49,** 162 (1924).
Thomas, E. W., Loughman, B. C., Powell, R. G., *Nature* **204,** 884 (1964).

Received for review March 9, 1967. Accepted May 18, 1967. Work supported in part by Public Health Service Research Grant EF-00547 from the Division of Environmental Engineering and Food Protection.

COR-AAD1-00002654
Bayer EX1008 (Part 5 of 9)

Chemosphere, Vol.24, No.10, pp 1423-1429, 1992
Printed in Great Britain

0045-6535/92 $5.00 + 0.00
Pergamon Press Ltd.

CHROMATOGRAPHIC SEPARATION OF THE ENANTIOMERS OF MARINE POLLUTANTS. PART 5: ENANTIOSELECTIVE DEGRADATION OF PHENOXYCARBOXYLIC ACID HERBICIDES BY MARINE MICROORGANISMS

Peter Ludwig [1], Wilfried Gunkel [2] and Heinrich Hühnerfuss [1] *

1 Institut für Organische Chemie, University of Hamburg, Martin-Luther-King-Platz 6, W-2000 Hamburg 13, F.R.G.

2 Biologische Anstalt Helgoland, Notkestr. 31, W-2000 Hamburg 52, F.R.G.

ABSTRACT

The degradation of the racemate of the herbicide 2-(2,4-dichlorophenoxy)propionic acid [Dichlorprop; DCPP] by a marine microbial community was investigated by High-performance liquid chromatography [HPLC] using α_1-AGP as chiral stationary phase. The microorganisms degraded exclusively the R-enantiomer, while the S-enantiomer remained unaffected. 2,4-Dichlorophenol was identified as the first degradation product of the R-enantiomer, which implies an increase in toxicity by about an order of magnitude according to the MICROTOX-test.

INTRODUCTION

Recently Faller et al. reported results on the degradation of (±)-α-HCH by marine microorganisms for all significant North Sea areas (1, 2). The authors determined the enantiomeric ratios by capillary gas chromatography [CGC] using heptakis(3-*O*-butyryl-2,6-di-*O*-pentyl)-β-cyclodextrin as chiral stationary phase. In the plume of the river Elbe, the Skagerrak and the Norwegian coastal current an excess of (-)-α-HCH was found (average value of (+)-α-HCH/(-)-α-HCH about 0.85 ± 0.1), while off the east British coast and in the central North Sea an

* To whom correspondence should be addressed

COR-AAD1-00002655
Bayer EX1008 (Part 5 of 9)

excess of (+)-α-HCH was determined ((+)-α-HCH/(-)-α-HCH about 1.15 ± 0.1). Enantiomeric ratios of (+)-α-HCH/(-)-α-HCH = 1 in the North Sea areas of the Atlantic inflow suggested the importance of non-enzymatic degradation processes in ocean areas far away from the sources of pollutants. Ludwig et al. (3) were able to simulate the microbial degradation of (±)-α-HCH in the laboratory by a marine microbial community sampled off the island of Heligoland, which is representative at least for the German Bight. It turned out that the transformation processes observed in the laboratory experiments were very comparable to those occurring *in-situ*. The same conclusions were drawn by Hühnerfuss et al. (4) who investigated water samples from various parts of the Baltic Sea.

In all experiments summarized above the microbial marine community was able to degrade both (+)-α-HCH and (-)-α-HCH, however, the degradation rate was different thus giving rise to an excess of one enantiomer.

In addition to the unpolar chlorinated hydrocarbons several more polar organic pesticides play an important role in the marine ecosystem. As recently shown by Ludwig (5), phenoxyalkanoic acid herbicides may achieve considerable concentrations in the German Bight, e.g., 2,4-dichlorophenoxyacetic acid [2,4-D] of the order of 10 ng/l, 2-(2,4-dichlorophenoxy)-propionic acid [DCPP] of the order of 2 ng/l, 2-(4-chloro-2-methylphenoxy)propionic acid [MCPP] of the order of 11 ng/l, and another isomer of MCPP of the order of 7 ng/l were found. In the case of the chiral phenoxyalkanoic acid derivatives, only the R-enantiomer is an active herbicide. In some commercially available mixtures, however, the racemate is prevailing. As a consequence, both the R- and the S-enantiomer are transported into the North Sea thus potentially influencing the marine ecosystem. Therefore, this work focuses upon the question, whether or not a microbial marine culture is able to degrade the two enantiomers of chiral phenoxyalkanoic acid derivatives or , rather one enantiomer is being accumulated in the marine ecosystem. Polar organic compounds of this kind cannot be investigated directly by CGC, however, the application of High-performance liquid chromatography [HPLC] using α_1-AGP as chiral stationary phase turned out to be an elegant method both for the clean-up step and for the separation of the enantiomers of the chiral phenoxyalkanoic acid derivatives.

EXPERIMENTAL

Media and Cultural Conditions

Aerobic sediment (0.4 g) and 200 ml seawater obtained from the North Sea area off the island Heligoland were shaken in the dark for four weeks at room temperature with 0.4 mg 2,4-D thus giving an enrichment culture which was used for the degradation experiments of the phenoxyalkanoic acid derivatives 2,4-D, DCPP, and MCPP reported.

The following sterile medium was inoculated with 0.2 ml of the enrichment culture: 150 ml aged seawater (Station 8; 25 m depth; see Hühnerfuss et al. (6)), 50 ml distilled water, 0.2 g glucose, 2 mg $FeSO_4$, 20 mg $MgSO_4$, 50 mg $(NH_4)_2SO_4$, 2.7 g $Na_2HPO_4 \cdot 2\,H_2O$, and 50 mg DCPP were adjusted to pH=8.0 with 10 %-NaOH solution. The resulting inoculated mixture was shaken under the same conditions as described above for three weeks.

COR-AAD1-00002656
Bayer EX1008 (Part 5 of 9)

Analytical procedure

The HPLC analysis of the phenoxyalkanoic acid derivatives was performed with a L-6200 pump of Merck-Hitachi according to the procedure described by Blessington et al. (7) using α_1-AGP as chiral stationary phase (CHROMTECH/ICT, Frankfurt, FRG; 100 x 4 mm) and a mobile phase consisting of water/2-propanol 96:4 with 10 mmol phosphate buffer (pH 4.85; 0.9 ml/min; UV-detection at 240 nm). In general, 0.1 ml of the centrifuged medium was diluted 1 : 20 with the mobile phase, and then 20 µl of this solution was injected into the HPLC system.

RESULTS AND DISCUSSION

Microbial degradation of DCPP

Typical HPLC chromatograms obtained from a sterile control and a mixed microbial culture after a period of three weeks are shown in Figures 1A and 1B, respectively, for DCPP . It is obvious that the R-enantiomer was degraded by the microbial culture, while the S-enantio-

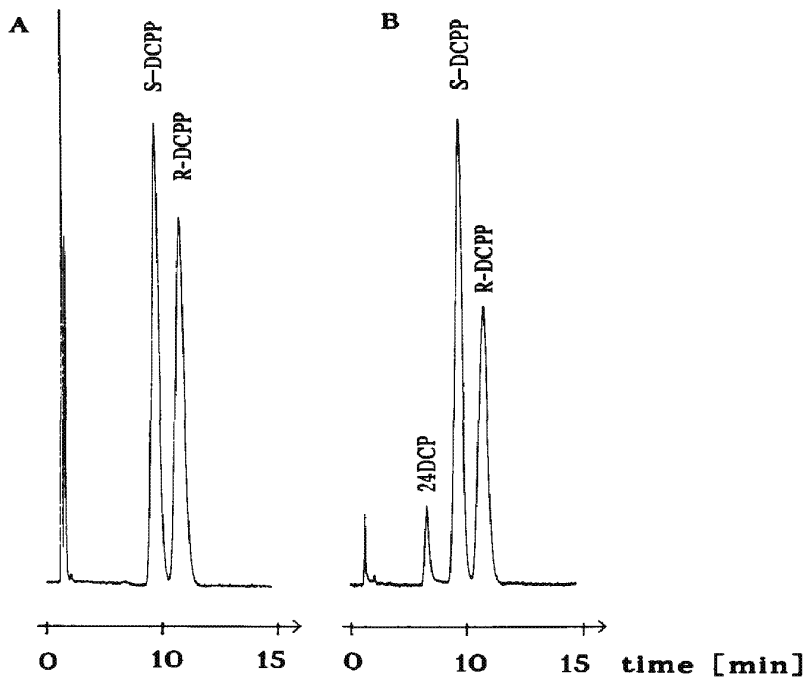


Figure 1A, 1B: HPLC chromatograms of the enantiomers of 2-(2,4-di-chlorophenoxy)propionic acid [DCPP] of a sterile control (A) and after degradation by marine microorganisms (21 days; B); α_1-AGP-column 100 mm x 4 mm; water/2-propanol 96:4 with 10 mmol phosphate buffer; pH=4.85; velocity 0.9 ml/min; UV-detection at 240 nm.

COR-AAD1-00002657
Bayer EX1008 (Part 5 of 9)

mer appears to be largely unaffected. The exclusive degradation product identified during the first period of the experiment is 2,4-dichlorophenol [24DCP]. This implies that as a first step the ether bond of the phenoxy group is broken thus giving the respective halogenated phenol, similar to results reported for the degradation of 2,4-D by terrestric microorganisms (8, 9).

Quantitative insight into the temporal development of the concentrations of the DCPP enantiomers was gained during experiments of three weeks duration each. The average concentration values of the respective sterile control (same media but not inoculated) and the two DCPP enantiomers of two degradation experiments are summarized in Figures 2A and 2B, respectively. These results confirm the assumption stated above that the microbial marine culture which represents at least the southeastern part of the North Sea (German Bight) is able to degrade exclusively the R-enantiomer while the concentration of the S-enantiomer remains constant within the error of this method. The statistical error is assumed to be at maximum 2 to 3 percent , because the only preparation step prior to injection into the HPLC

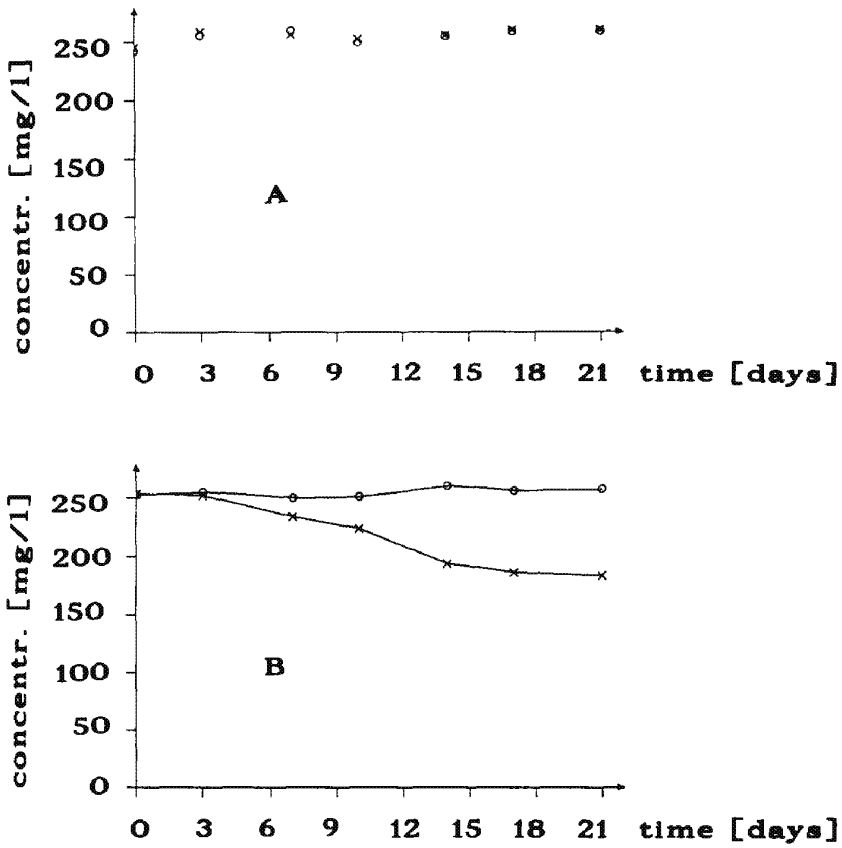


Figure 2: Temporal development of the concentrations of the S-enantiomer (circles) and the R-enantiomer (crosses) of 2-(2,4-dichlorophenoxy)propionic acid [DCPP] in a sterile control (A) and in the presence of a culture of marine microorganisms (B).

COR-AAD1-00002658
Bayer EX1008 (Part 5 of 9)

system comprises a dilution of the medium which has no effect on the ratio of the enantiomers. As a consequence of the exclusive degradation of the R-enantiomer, considerable shifts of the enantiomeric ratios S-/R-enantiomer were observed during the experimental period of three weeks. The results, which are given for two experiments and the sterile control in Table 1, illustrate the good reproducibility of this method. Whether or not the exclusive degradation of the R-enantiomer leads to an accumulation of the S-enantiomer in the marine ecosystem has to be investigated by additional *in-situ* measurements.

Table 1: Enantiomeric ratios (S/R) of 2-(2,4-dichlorophenoxy)propionic acid [DCPP] during a period of 3 weeks as encountered in the presence of a mixed culture of marine microorganisms and in a sterile control. The values, which were determined by HPLC using a chiral α_1 -AGP column, are averages of two injections.

time [days]	enantiomeric ratios (S/R)		
	experiment 1	experiment 2	steril control
0	0.99	1.00	0.99
3	1.02	1.01	0.99
7	1.08	1.05	1.01
10	1.14	1.11	0.99
14	1.34	1.35	1.00
17	1.37	1.39	1.00
21	1.41	1.41	1.00

The temporal development of the 24DCP formation as measured by the same HPLC method as described above is depicted in Figure 3. During the first two weeks the concentration of the 24DCP exactly corresponds with the loss of the DCPP R-enantiomer. Then, an additional degradation of the 24DCP appears to begin which is expressed by a maximum in the curve shown in Figure 3.

The formation of halogenated phenols as a first microbial degradation product of phenoxyalkanoic acid derivatives may cause considerable problems to the marine ecosystem. Ludwig (5) determined the toxic levels of both DCPP and 24DCP by means of the MICROTOX-test in the course of which the influence of toxic organic compounds on the light emission of luminescent marine bacteria is measured (for experimental details see (5, 10)). It is well-known that this test correlates well with fish- (11) and daphniae-tests (12), but is much faster and simpler than the latter test procedures. As a result, so-called "effective concentration" [EC_{50}] values are obtained which correspond with the concentrations showing a decrease in the light emission of 50 percent. In this case, Ludwig (5) obtained EC_{50} values of 0.130 ± 0.013 mmol/l and 0.013 ± 0.002 mmol/l for DCPP and 24DCP, respectively. These values imply that degradation of DCPP by marine microorganisms gives rise to an increase in toxicity by about one order of magnitude during the first degradation step (formation of

COR-AAD1-00002659
Bayer EX1008 (Part 5 of 9)

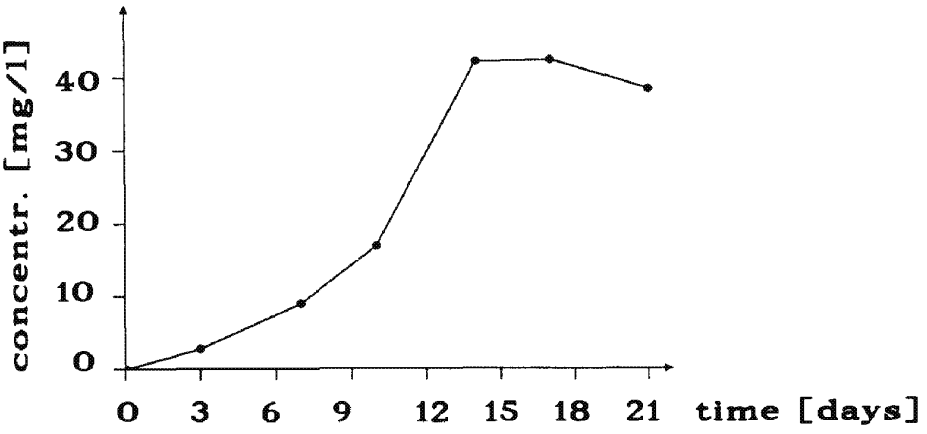


Figure 3: The formation of 2,4-dichlorophenol [24DCP] during the degradation of the R-enantiomer of DCPP.

the halogenated phenol). This in turn may have a severe impact on the marine ecosystem, in particular, if the meteorological and oceanographic conditions are unfavorable and lead to additonal increases in the concentrations of the halogenated phenols as observed, e.g., for pentachlorophenol [PCP] in the German Bight (6).

Microbial degradation of 2,4-D and MCPP

Basically, the degradation of 2,4-D by the marine microbial culture was accomplished by the same mechanism as found for DCPP. As a first step the ether bond is broken and 24DCP is formed. Since the EC_{50} value for 2,4-D is 0.121 ± 0.009 mmol/l (5), i.e., very comparable with the value for DCPP, the same toxicological implications are given as discussed above.

With regard to MCPP , the present marine microbial culture was not able to degrade this compound. Therefore, is has to be assumed that MCPP may be more persistent in the marine environment. Further investigations must show whether this leads to accumulation effects of the latter phenoxyalkanoic acid derivative in the marine ecosystem.

Comparison with other chiral pollutants

The most notable difference between the results presented and those reported for the microbial degradation of other chiral pollutants is as following: In the case of (±)-α-HCH, β-PCCH, and γ-PCCH the mixed culture of marine microorganisms was able to degrade the two enantiomers of these pollutants, although this was achieved at different rates (1-5). As a consequence a shift of the enantiomeric ratios was observed. DCPP is being degraded also

COR-AAD1-00002660
Bayer EX1008 (Part 5 of 9)

enantioselectively, however, in contrast to these earlier results, the marine microbial community exclusively degrades the R-enantiomer, while the S-enantiomer appears to be persistent. This has the fatal consequence that application of a racemate of DCPP in agriculture instead of the pure R-enantiomer, which is exclusively active as herbicide, may give rise to enrichment of the S-enantiomer in the marine environment.

ACKNOWLEDGMENTS

This work has been supported by the Ministry of Science and Technology of the Federal Republic of Germany (BMFT- project MFU 0620 "Prozesse im Schadstoffkreislauf Meer-Atmosphäre: Ökosystem Deutsche Bucht").

References

1. Faller, J., Hühnerfuss, H., König, W.A., Krebber, R., and Ludwig, P.; Environ.Sci.Technol. **25,** 676-678 (1991).
2. Faller, J., Hühnerfuss, H., König, W.A., and Ludwig, P.; Mar.Pollut.Bull. **22**, 82-86 (1991).
3. Ludwig, P., Hühnerfuss, H., König, W.A., and Gunkel, W.; Mar. Chem. (1992), in press.
4. Hühnerfuss, H., Faller, J., König, W.A., and Ludwig, P.; Environ. Sci.Technol. (1992), submitted for publication.
5. Ludwig, P.; "Untersuchungen zum enantioselektiven Abbau von polaren und unpolaren chlorierten Kohlenwasserstoffen durch marine Mikroorganismen", Ph.D. thesis, University of Hamburg, Hamburg (F.R.G.), 135 pp. (1991).
6. Hühnerfuss, H., Dannhauer, H., Faller, J., and Ludwig, P.; Dt.hydrogr. Z. **43 (5)**, in press (1990).
7. Blessington, B., and Crabb, N.; J.Chromatogr. **483**, 349-358 (1989).
8. Oh, K.H., and Tuovinen, O.H.; FEMS Microbiol.Lett. **79**, 141-146 (1991).
9. Horvath, M., Ditzelmüller, G., Loidl, M., and Streichsbier, F.; Appl. Microbiol.Biotechnol. **33**, 213-216 (1990).
10. Trevors, J.T., "Bacterial growth and activity as indicators of toxicity, in: Toxicity testing using microorganisms", **Vol. 1**, Bitton, G., and Dutka, B.J., eds., CRC Press, Inc., Boca Raton, Florida (1986).
11. Indorato, A.M., Snyder, K.B., and Usinowicz, P.J.; "Toxicity screening using Microtox, in: Toxicity screening tests", Symp.Abstr., Dutka, B.J., and Liu, D., eds., Canada Centre for Inland Waters, Burlington (1983).
12. Vasseur, P., Ferard, J.F., Rast, C., and Larbaigt, G.; "Luminescent marine bacteria in acute toxicity testing, in: Ecotoxicological testing for the marine environment", **Vol. 2**, Persoone, G., Jaspers, E., and Claus, C., eds., State University Ghent & Inst.Mar.Scient. Res., Belgium (1984).

(Received in Germany 6 February 1992; accepted 6 March 1992)

COR-AAD1-00002661
Bayer EX1008 (Part 5 of 9)

Plant Molecular Biology **13**: 533–540, 1989.
© 1989 *Kluwer Academic Publishers. Printed in Belgium.*

Expression of a bacterial gene in transgenic tobacco plants confers resistance to the herbicide 2,4-dichlorophenoxyacetic acid

Bruce R. Lyon, Danny J. Llewellyn, John L. Huppatz, Elizabeth S. Dennis and W. James Peacock
CSIRO Division of Plant Industry, GPO Box 1600, Canberra City, ACT 2601, Australia

Received 1 June 1989; accepted 15 June 1989

Key words: 2,4-dichlorophenoxyacetic acid (2,4-D), detoxification, herbicide resistance, transgenic plants

Abstract

Plants resistant to the herbicide 2,4-dichlorophenoxyacetic acid (2,4-D) were produced through the genetic engineering of a novel detoxification pathway into the cells of a species normally sensitive to 2,4-D. We cloned the gene for 2,4-D monooxygenase, the first enzyme in the plasmid-encoded 2,4-D degradative pathway of the bacterium *Alcaligenes eutrophus*, into a cauliflower mosaic virus 35S promoter expression vector and introduced it into tobacco plants by *Agrobacterium*-mediated transformation. Transgenic tobacco plants expressing the highest levels of the monooxygenase enzyme exhibited increased tolerance to 2,4-D in leaf disc and seed germination assays, and young plants survived spraying with levels of herbicide up to eight times the usual field application rate. The introduction of the gene for 2,4-D monooxygenase into broad-leaved crop plants, such as cotton, should eventually allow 2,4-D to be used as an inexpensive post-emergence herbicide on economically important dicot crops.

Introduction

The introduction of novel traits such as herbicide resistance into agronomically important crop plants is one promising aspect of the application of genetic engineering to plant breeding. Herbicide-tolerant transgenic plants have been produced in a variety of ways, including over-expressing a sensitive target gene product or supplementing the sensitive plant cells with mutant, herbicide-resistant copies of the target gene. Detoxification strategies, in which bacterial genes for herbicide detoxification or degradation have been used (e.g. degradative genes for phosphinothricin [3] and bromoxynil [19] detoxification), are an alternate and more straightforward means of creating herbicide-resistant plants since it is unnecessary to first identify the biochemical target of the herbicide. This is particularly important where the effect of the herbicide may be pleiotrophic, as in the case of 2,4-dichlorophenoxyacetic acid (2,4-D), a compound which mimics the action of the plant hormone auxin.

Soil organisms that degrade 2,4-D were identified more than thirty years ago [20] and multienzyme pathways for 2,4-D degradation have subsequently been demonstrated in several bacterial genera [4, 8, 22]. In the most intensively studied organism, *Alcaligenes eutrophus*, the 2,4-D degradative pathway comprises six specialized enzymes, encoded by a 75 kb plasmid designated pJP4, which convert 2,4-D to chloromaleylacetic

COR-AAD1-00002662
Bayer EX1008 (Part 5 of 9)

acid, a compound subsequently metabolized to succinic acid [5]. The genes for these six enzymes (*tfdA-F*) have been mapped by transposon insertion and the sequences of three of the genes (*tfdA*, *tfdC* and *tfdD*) have been determined [5, 11, 21].

The first gene in the 2,4-D degradation pathway (*tfdA*) encodes a 2,4-D monooxygenase which converts 2,4-D into 2,4-dichlorophenol by cleavage of the aliphatic side chain [21]. Preliminary evidence on the biological effects of 2,4-dichlorophenol suggests that this degradation product is less toxic to plants than the herbicide [18]. Accordingly, we cloned the gene for the 2,4-D monooxygenase (*tfdA*), transferred it into tobacco plants and demonstrated that transgenic plants expressing this enzyme exhibit tolerance to the herbicide 2,4-D.

Materials and methods

Manipulation of the 2,4-D monooxygenase gene (tfdA)

Alcaligenes eutrophus strain JMP134 carrying the 2,4-D degradative plasmid pJP4 was generously provided by R.H. Don (University of Queensland, Australia). Following conjugative transfer to *Escherichia coli* MC1061, plasmid DNA was isolated, cleaved with *Hin*d III and cloned into the *Hin*d III site of pUC119 by standard techniques [16]. A transformant bearing the 21 kb *Hin*d III B fragment of pJP4 cloned in pUC119 then served as the source of DNA for further manipulation of the *tfdA* gene. The *Hin*d III fragment was reduced by successive digestion with *Bam* HI, *Sal* I, *Xba* I and *Nco* I to give a 980 bp fragment bounded by *Bam* HI linkers (GGGATCCC, Boehringer Mannheim) at the filled-in *Xba* I and *Nco* I sites (Fig. 1A). Analysis of the *tfdA* sequence [21] had revealed the presence of an out-of-frame ATG codon 95 bp upstream from the GTG translational start codon, and this sequence was removed by BAL-31 digestion [16] of 20 bp from the 5′ end of the subclone. Finally, oligomutagenesis was

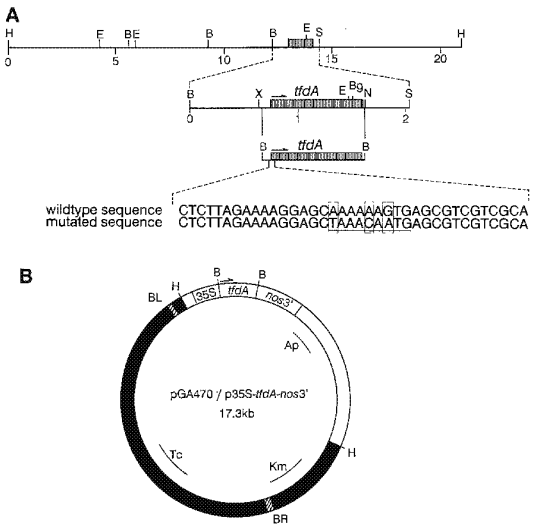


Fig. 1. Cloning of the gene for 2,4-D monooxygenase (*tfdA*) from *Alcaligenes eutrophus* strain JMP134. A. The 960 bp *Bam* HI-*Bam* HI fragment was produced from the 21 kb *Hin*d III B fragment of plasmid pJP4 by successive subcloning and BAL-31 digestion as described in Materials and methods. This clone was subjected to oligomutagenesis in the vicinity of the bacterial GTG translational start codon (base changes are boxed) to produce a plant consensus sequence and ATG translational start codon (underlined). The scale beneath each map is in kilobase pairs. Restriction endonuclease sites are: B, *Bam* HI; Bg, *Bgl* II; E, *Eco* RI; H, *Hin*d III; N, *Nco* I; S, *Sal* I; X, *Xba* I. The arrow indicates the direction of translation of *tfdA*. B. Schematic representation of the *tfdA* gene cloned between the cauliflower mosaic virus 35S promoter and the nopaline synthase (*nos*) 3′ polyadenylation signal of pJ35SN and inserted into the binary vector plasmid pGA470. Km designates the neomycin phosphotransferase gene which mediates kanamycin resistance in transformed plants; Ap and Tc designate the bacterial genes for ampicillin and tetracycline resistance, respectively. B_L and B_R designate the left and right borders of the T-DNA, respectively.

conducted using an adaptation of an oligonucleotide deletion method [6] to convert the GTG start codon to an ATG and to produce a sequence which matches a published plant consensus for the region adjacent to the translation start [14]. The 37 base oligonucleotide CTCTTAGAA AAGGAGCTAAACA*ATG*AGCGTCGTC GCA was synthesized using an Applied Biosystems 380A DNA synthesizer and correct mutagenesis of the start codon region confirmed by dideoxy sequencing.

COR-AAD1-00002663
Bayer EX1008 (Part 5 of 9)

Construction of gene fusions

The *tfdA* gene was excised as a 960 bp *Bam* HI fragment and cloned into the unique *Bam* HI sites of three plant expression vectors based on the cauliflower mosaic virus (CaMV) 35S promoter and the nopaline synthase (*nos*) 3′ polyadenylation signal. Plasmid pJ35SN was constructed by replacing the *Hin*d III-*Bam* HI *nos* promoter-chloramphenicol acetyltransferase coding sequences of pNCAT4 (obtained from L. Herrera-Estrella and M. Van Montagu, Rijksuniversiteit, Gent, Belgium), with a *Hin*d III-*Bam* HI fragment containing the 35S promoter of p35SCN [23], and subcloning a *Sca* I-*Hin*d III fragment derived from this construct (comprising 35S promoter and *nos* 3′ separated by *Bam* HI, *Sma* I and *Eco* RI sites) into *Sca* I-*Hin*d III cleaved pUC19. Plasmid p3x35SN was constructed by cloning two additional copies of the 35S promoter upstream enhancer region [15], bounded by *Sal* I and *Eco* RV sites, 5′ to the 35S promoter of pJ35SN. All three enhancer regions were in the same orientation. Plasmid p35SAMVN was constructed by cloning a synthesized 44 base oligonucleotide equivalent to the alfalfa mosaic virus (AMV) leader [10] and bounded by *Bgl* II and *Bam* HI sites into the *Bam* HI site of pJ35SN. The unmodified GTG containing *tfdA* coding sequence was also cloned into pJ35SN in both orientations.

Construction of binary vectors and plant transformation

As illustrated in Fig. 1B, the 35S-*tfdA-nos* constructs were cleaved with *Hin*d III and cloned into the *Hin*d III site of the binary vector plasmid pGA470 [1]. Triparental mating with selection as described [7] was employed to transfer the binary vector constructs from *E. coli* to the avirulent *Agrobacterium tumefaciens* strain LBA 4404 Rif^r [12]. Constructions in *Agrobacterium* were verified by restriction and DNA blotting analysis. Leaves of *Nicotiana tabacum* cv. Wisconsin 38 were transformed by these *Agrobacterium* strains and shoots were regenerated on kanamycin medium essentially as described [7]. Transgenic kanamycin-resistant plants transformed by these promoter constructs were designated TFD 1, 5 or 8 (corresponding to *tfdA* in the coding orientation in pJ35SN, p3x35SN or p35SAMVN, respectively), or TFD 3 (corresponding to *tfdA* in the inverse orientation in pJ35SN). Transgenic plants were maintained under antibiotic selection in aseptic containers and young leaves were periodically harvested for analysis. Selected transgenic plants were transferred to soil in a biosafety containment glasshouse and propagated for seed.

2,4-D monooxygenase assay

Bacterial enzyme extracts were prepared by sonication of cultures suspended in 0.02 M potassium phosphate buffer (pH 7.3), while plant enzyme extracts were prepared by grinding tissue with sand in the presence of 0.02 M potassium phosphate buffer, 2% insoluble polyvinylpyrrolidone and 10 mM dithiothreitol. Extracts were equilibrated for protein content and assayed for 2,4-D monooxygenase activity in the presence of 0.01–0.03 μCi 2,4-dichloro[*ring*-U-^{14}C]phenoxyacetic acid (Amersham; purified by ethyl acetate extraction), 1 mM cysteine and 20 mM NADH. After being flushed with O_2, the assay mixes were incubated with shaking at 30 °C for 1–3 h. The reaction products were extracted into chloroform and separated by thin-layer chromatography (TLC) using benzene-methanol (19 : 1, v/v) as solvents [9]. Phenolic compounds were detected on the chromatogram by staining with diazotized *p*-nitroaniline followed by $NaHCO_3$ [2] or by autoradiography with Fuji X-ray film for 1–14 days.

2,4-D toxicity tests

Tobacco leaf discs of approximately 1 cm in diameter were punched aseptically from fresh leaves and plated on shoot regeneration media [17] containing 0.2, 0.8, 3.2 or 12.8 mg/l 2,4-D

COR-AAD1-00002664
Bayer EX1008 (Part 5 of 9)

and incubated for 60 days before shoot and callus tissue was weighed for comparison. Leaf discs from wild-type plants were routinely plated as internal controls on test plates. F_1 seeds generated by self-pollination from wild-type and transgenic plants were surface-sterilized and plated on modified Murashige and Skoog media (no vitamins, 10 g/l sucrose) containing 0, 0.1, 0.2, 0.4, 0.8, 1.6, 3.2 and 6.4 mg/l 2,4-D or 200 mg/l kanamycin and incubated for 14 days before relative germination rates were determined. At 4–8 weeks after germination, seedlings were sprayed until dripping wet with a range of 2,4-D (isopropyl ester in 50% acetone) concentrations (0, 10, 30, 100, 300, 1000 and 3000 mg/l) and were observed for detrimental effects over a period of three weeks.

Results

Cloning and expression of tfdA in bacteria and plants

The 2,4-D monooxygenase gene (*tfdA*) of *A. eutrophus* plasmid pJP4 possesses an 861-nucleotide open reading frame [21]. We cloned in *E. coli* a 960 bp segment comprising the complete *tfdA* gene bounded by 5′ and 3′ non-coding sequences of approximately 90 bp and 10 bp, respectively (Fig. 1A). Oligomutagenesis of three bases in the 5′ region of the gene converted the GTG translational start codon of the native gene to an ATG and produced a plant consensus sequence [TAAACA] immediately upstream of this codon (Fig. 1A).

Both unmodified (GTG) and modified (ATG) *tfdA* genes were fused to the β-galactosidase promoter of pUC plasmids and expression of 2,4-D monooxygenase in *E. coli* was induced by culture in the presence of isopropylthiogalactoside (IPTG). In order to confirm that the cloned and mutated *tfdA* fragment did encode a fully active 2,4-D monooxygenase, bacterial cell extracts were assayed for their ability to convert ^{14}C-labelled 2,4-D into 2,4-dichlorophenol (Materials and methods). An abundant radiolabelled product was detected in extracts from bacteria harbouring either the unmodified or modified *tfdA* gene (Fig. 2, lanes 2 and 3), but was not observed in the enzyme-free control (Fig. 2, lane 5), nor in extracts of *E. coli* containing pUC118 or the modified *tfdA* gene cloned in the inverse orientation (Fig. 2, lanes 1 and 4). This product exhibited a TLC R_F value of approximately 0.46 for the benzene-methanol solvent system and co-migrated with authentic 2,4-dichlorophenol (BDH). Sufficient quantities of the enzymic product were present to demonstrate the characteristic purple colour of 2,4-dichlorophenol by direct staining with diazotized p-nitroaniline.

Assays for 2,4-D monooxygenase activity were conducted on up to thirty different plants produced by transformation with each of the constructs and on the untransformed wild-type tobacco W-38. Unlike the *E. coli* extracts, the extracts from control tobacco plants were able to slowly metabolize 2,4-dichlorophenol by an, as yet, unknown mechanism. This assay was therefore not an accurate measure of the level of 2,4-D monooxygenase present in plant extracts, but did give a qualitative indication of the level of expression. Transgenic plants showing the highest level of 2,4-dichlorophenol were analysed further.

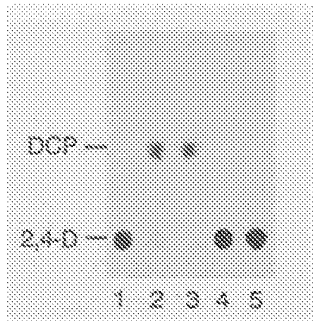


Fig. 2. Chromatogram of 2,4-D monooxygenase assay. Bacterial extracts were assayed for 2,4-D monooxygenase activity and the chromatogram was exposed to X-ray film as described in Materials and methods. Bands due to 2,4-dichlorophenoxyacetic acid (2,4-D) and 2,4-dichlorophenol (DCP) are marked. Lanes are: 1, *E. coli* (pUC118); 2, *E. coli* (unmodified *tfdA* cloned in pUC118); 3, *E. coli* (modified *tfdA* cloned in pUC119); 4, *E. coli* (modified *tfdA* cloned in incorrect orientation in pUC119); 5, enzyme-free control.

COR-AAD1-00002665
Bayer EX1008 (Part 5 of 9)

Leaf disc assay for resistance to 2,4-D

The increase in tolerance to 2,4-D *in vivo* was determined by assaying the ability of leaf discs from transgenic plants to regenerate shoots in the presence of the herbicide. Wild-type Wisconsin 38 tobacco leaf discs generated shoots on levels of 2,4-D up to 0.2 mg/l but were inhibited by more than 0.4 mg/l of the herbicide. At these higher levels of 2,4-D, large quantities of undifferentiated callus were produced, presumably as a response to the presence of the auxin analogue. In similar tests conducted with 2,4-dichlorophenol, W-38 tobacco-generated shoots at levels as high as 45–50 mg/l (above which tissue was bleached and killed), implying that 2,4-dichlorophenol is 100-fold less toxic to tobacco than the herbicide 2,4-D when applied externally.

A 2,4-D concentration of 0.8 mg/l, too toxic for the formation of shoots by wild-type tobacco, was used to test for transgenic plants tolerant to high levels of 2,4-D. This level of herbicide prevented the growth of shoots from explants of the non-transformed wild-type, inverse orientation of the ATG construction (TFD 3-1 plants), both orientations of the GTG constructions, together with at least one of the tested transgenic plants expressing low levels of monooxygenase (TFD 8-24). This level of 2,4-D did not adversely affect the formation of shoots by a number of transgenic plants, from all three different promoter constructs containing the ATG modified *tfdA* coding region, that expressed high levels of monooxygenase activity in the *in vitro* assay. Those plants containing the AMV leader region construction appeared marginally better, e.g. TFD 8-1, 8-2, 8-6 and 8-14 (Fig. 3), and these were analysed in most detail. Some of these transgenic plants generated shoots on levels of 2,4-D as high as 12.8 mg/l, representing a 32-fold increase in tolerance to the herbicide compared with the inverse orientation control TFD 3 and wild-type plants. Attempts to select directly for 2,4-D-resistant plants in transformation experiments were, however, unsuccessful.

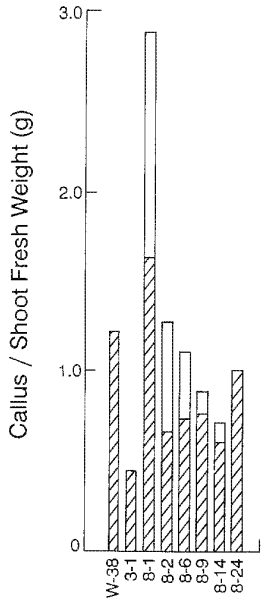


Fig. 3. Tobacco callus and shoot formation on media containing 2,4-D. Tobacco leaf discs were plated on shoot-inducing media containing 0.8 mg/l 2,4-D. Wild-type and transgenic callus (hatched) and shoot (open) formation is expressed as average fresh weight (g).

Seed germination assay for resistance to 2,4-D

Table 1 presents the germination data for seed derived by self-pollination of wild-type and transgenic plants. Germination of wild-type and control TFD 3 seed was affected by concentrations

Table 1. Germination of seed derived from wild-type and transgenic plants on 2,4-D and kanamycin expressed as a percentage of viable seed (50 seeds/treatment).

Plant	2,4-D (mg/l)						Kanamycin 200 mg/l
	0.1	0.2	0.4	0.8	1.6	3.2	
W-38	69	0	0	0	0	0	
TFD 3-1	57	0	0	0	0	0	60
TFD 1-1	85	54	62	52	4	0	80
TFD 5-2	86	41	0	0	0	0	96
TFD 5-10	90	78	68	40	0	0	68
TFD 5-27	89	73	64	73	9	0	80
TFD 8-1	92	67	63	69	33	0	94
TFD 8-6	92	92	81	65	22	10	92
TFD 8-14	80	74	66	50	4	0	60
TFD 8-24	52	10	0	0	0	0	96

COR-AAD1-00002666
Bayer EX1008 (Part 5 of 9)

of 2,4-D as low as 0.1 mg/l and was completely inhibited at 0.2 mg/l. In contrast, some transgenic seed was able to germinate on levels of 2,4-D up to 3.2 mg/l, an increase in tolerance to the herbicide of approximately 30-fold.

The seed germination assay was further employed to investigate cross resistance to other phenoxyacetic acid herbicides, including 2 methyl-4-chlorophenoxyacetic acid (MCPA) and 2,4,5 trichlorophenoxyacetic acid (2,4,5-T). Seed from TFD 8-6, the most resistant in the plate assays, showed more resistance than wild-type seed to MCPA in the range 0.025–0.1 mg/l, and 20% of the transgenic seed was able to germinate at 0.2 mg/l, a level which prevented germination of the wild type. Transgenic seed was no more tolerant to 2,4,5-T than the wild-type seed.

2,4-D resistance in young plants

Progeny germinated from wild type, TFD 8-1 and TFD 8-6 seed were transferred to soil and grown for 4–8 weeks before being sprayed with concentrations of herbicide ranging from 0–3000 mg/l. Wild-type plants were affected by levels as low as 10 mg/l and were killed by levels of 300 mg/l or more (Fig. 4A). Transgenic plants were much more tolerant to the herbicide, being unaffected by 300 mg/l 2,4-D (Fig. 4A), only slightly affected by 1000 mg/l (data not shown), and even surviving 3000 mg/l 2,4-D (Fig. 4B).

An estimate of the field application rate corresponding to our experimental spraying regime suggests that 1000 mg/l is approximately equivalent to 1–2 kg of 2,4-D per hectare. For weed control, fields are normally sprayed with 0.25–0.5 kg/ha, hence, the transgenic tobacco F_1 progeny can survive spraying with 2,4-D concentrations 4–8 times the normal field application of the herbicide.

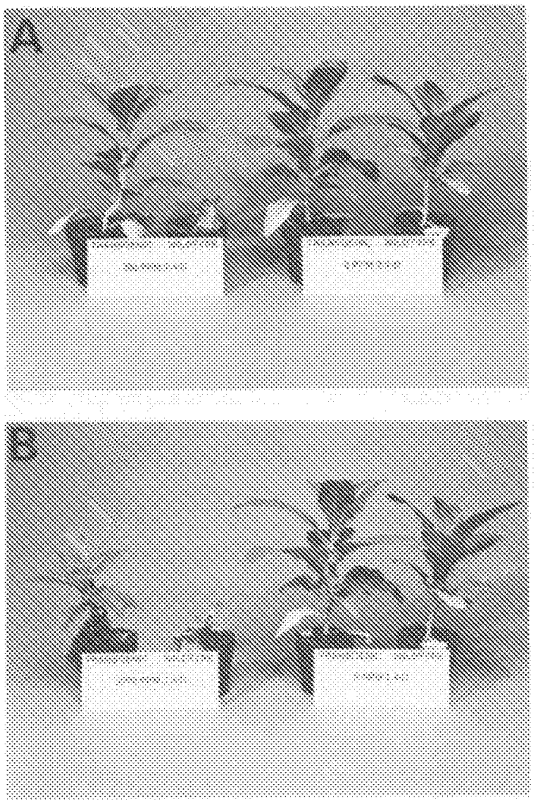


Fig. 4. Spraying of young tobacco plants with 2,4-D. Wild-type (W-38) and transgenic (TFD 8-6) plants were sprayed with (A) 300 mg/l 2,4-D, or (B) 3000 mg/l 2,4-D.

Discussion

The first gene in the 2,4-D degradative pathway of the bacterium *Alcaligenes eutrophus* (*tfdA*) was cloned into three different CaMV 35S promoter-nopaline synthase 3′ expression vectors, and introduced into tobacco plants by *Agrobacterium*-mediated transformation. The bacterial gene had been modified by oligomutagenesis to produce a plant consensus translation start sequence upstream of the translation initiation codon, changed from a GTG to ATG. Many of the transgenic plants demonstrated increased tolerance to 2,4-D as determined by the generation of shoots from leaf discs in the presence of high levels of the herbicide, while plants transformed with an unmodified *tfdA* gene did not exhibit improved tolerance to 2,4-D, indicating that this gene is not expressed efficiently in plants. Resistant plants were produced from all three promoter constructs. One of the most resistant contained the AMV leader region, purported to increase trans-

COR-AAD1-00002667
Bayer EX1008 (Part 5 of 9)

lational efficiencies of mRNAs containing this sequence [13]. More intensive studies will be required to fully evaluate the effectiveness of the different promoter constructs in transgenic plants.

A TLC assay for 2,4-D monooxygenase activity in bacterial extracts was not suitable for the accurate determination of enzyme activity in plant extracts, but did enable the initial selection of potential 2,4-D-resistant transgenic plants. A strong correlation was observed between this assay and the three *in vivo* methods (leaf disc, seed germination and spray toxicity) of assessing resistance to 2,4-D. An alternative assay, using antibodies to 2,4-D monooxygenase, is being developed for the early detection of enzyme in transformed tissue from cotton and other plants.

The seed germination assays suggest that high levels of resistance to the herbicide are dependent on both the possession of multiple copies of the *tfdA* gene and the site of integration of the T-DNA in the genome. Seed segregation ratios in the presence of discriminating doses of 2,4-D give some indication of the number of gene insertions in each transgenic plant and support Southern blot analyses of genomic DNA from the parental plants. These results indicate that more than one copy of the *tfdA* gene is present in the most resistant plants such as TFD8-6.

Transgenic seed was found to be slightly resistant to the herbicide MCPA, a result consistent with the observation that *A. eutrophus* can slowly metabolize this compound, which is structurally similar to 2,4-D. The fact that there was no cross-resistance to the closely related herbicide 2,4,5-T implies a high degree of substrate specificity for the 2,4-D monooxygenase. We are currently testing a wide variety of phenoxyacetate herbicides in order to establish the full herbicide resistance spectrum mediated by the 2,4-D monooxygenase and to gain insight into the protein-substrate interactions involved.

Although the level of resistance to 2,4-D in tobacco is adequate, with transgenic progeny able to survive spraying with 2,4-D concentrations some 4–8-fold higher than the usual field application rate, we expect that further improvement in gene expression will be required to obtain adequate protection in other species which are often more sensitive to 2,4-D than tobacco. Despite using a strong promoter linked to the 2,4-D monooxygenase gene, we were unable to detect *tfdA* transcripts by Northern blot hybridization. It may be possible to increase expression by improving transcript stability, perhaps by shortening the non-translated leader sequence of the *tfdA* coding region fragment (currently 90 bp) or substituting new 3′ ends in the expression vectors. These are strategies that have been effective with other gene constructs. The level of resistance in the current transgenic plants will be improved by selecting progeny carrying multiple copies of the *tfdA* gene and sequentially increasing the gene dosage by judicious crossing. This will be important to establish the upper limit of resistance possible with this enzymic detoxification system.

2,4-D is highly active against many species of broad-leaved weeds and is widely employed as a weed control agent on cereal crops. Broad-leaved crop plants, such as cotton, are sensitive to this herbicide, and accidental drift damage from the aerial spraying of neighbouring grain fields can devastate a crop. We are interested in engineering herbicide-resistant cotton that will firstly be resistant to 2,4-D drift damage, and secondly, will enable the post-emergence spraying of cotton with 2,4-D for the control of broad-leaved weeds. The result with the tobacco system suggests that the introduction and expression of the *tfdA* gene in cotton and other broad-leaved crops should provide the necessary level of herbicide tolerance to achieve these objectives.

Acknowledgements

This work was funded in part by Cotton Seed Distributers, Ltd. and the Australian Cotton Research Council. We thank Yvonne Cousins, Alan Downie and Hal Hatch for helpful suggestions, T.J. Higgins, Phil Larkin and Don Spencer for critical reading of the manuscript, and Jenny Thistleton and Les McCaffery for expert technical assistance.

COR-AAD1-00002668
Bayer EX1008 (Part 5 of 9)

References

1. An G, Watson BD, Stachel S, Gordon MP, Nester EW: New cloning vehicles for transformation of higher plants. EMBO J 4: 277–284 (1985).
2. Bray HG, Thorpe WV, White K: The fate of certain organic acids and amides in the rabbit. 10. The application of paper chromatography to metabolic studies of hydroxybenzoic acids and amides. Biochem J 46: 271–275 (1950).
3. De Block M, Botterman J, Vandewiele M, Dockx J, Thoen C, Gossele V, Rao Movva N, Thompson C, Van Montagu M, Leemans J: Engineering herbicide resistance in plants by expression of a detoxifying enzyme. EMBO J 6: 2513–2518 (1987).
4. Don RH, Pemberton JM: Properties of six pesticide degradation plasmids isolated from *Alcaligenes eutrophus* and *Alcaligenes paradoxus*. J Bact 145: 681–686 (1981).
5. Don RH, Weightman AJ, Knackmuss H-J, Timmis KN: Transposon mutagenesis and cloning analysis of pathways for degradation of 2,4-dichlorophenoxyacetic acid and 3-chlorobenzoate in *Alcaligenes eutrophus* JMP134 (pJP4). J Bact 161: 85–90 (1985).
6. Eghtedarzadeh MK, Henikoff S: Use of oligonucleotides to generate large deletions. Nucl Acids Res 14: 5115 (1986).
7. Ellis JG, Llewellyn DJ, Dennis ES, Peacock WJ: Maize Adh-1 promoter sequences control anaerobic regulation: addition of upstream promoter elements from constitutive genes is necessary for expression in tobacco. EMBO J 6: 11–16 (1987).
8. Evans WC, Smith BSW, Fernley HN, Davies JI: Bacterial metabolism of 2,4-dichlorophenoxyacetate. Biochem J 122: 543–551 (1971).
9. Gamar Y, Gaunt JK: Bacterial metabolism of 4-chloro-2-methylphenoxyacetate. Formation of glyoxylate by side-chain cleavage. Biochem J 122: 527–531 (1971).
10. Gehrke L, Auron PE, Quigley GJ, Rich A, Sonenberg N: 5′-Conformation of capped alfalfa mosaic virus ribonucleic acid 4 may reflect its independence of the cap structure or of cap-binding protein for efficient translation. Biochemistry 22: 5157–5164 (1983).
11. Ghosal D, You I-S: Nucleotide homology and organization of chlorocatechol oxidation genes of plasmids pJP4 and pAC27. Mol Gen Genet 211: 113–120 (1988).
12. Hoekema A, Hirsch PR, Hooykaas PJJ, Schilperoort RA: A binary plant vector strategy based on separation of vir and T-region of the *Agrobacterium tumefaciens* Ti-plasmid. Nature 303: 179–181 (1983).
13. Jobling, S and Gerhke, L: Enhanced translation of chimeric mRNAs containing plant viral untranslated leader sequences. Nature 325: 622–625 (1987).
14. Joshi CP: An inspection of the domain between putative TATA box and translation start site in 79 plant genes. Nucl Acids Res 15: 6643–6653 (1987).
15. Kay R, Chan A, Daly M, McPherson J: Duplication of CaMV 35S promoter sequences creates a strong enhancer for plant genes. Science 236: 1299–1302 (1987).
16. Maniatis T, Fritsch TE, Sambrook J: Molecular Cloning: A Laboratory Manual. Cold Spring Harbor Laboratory Press, Cold Spring Harbor, NY (1982).
17. Murashige T, Skoog F: A revised medium for rapid growth and bioassays with tobacco tissue cultures. Physiol Plant 15: 473–497 (1962).
18. Perkins EJ, Stiff CM, Lurquin PF: Use of *Alcaligenes eutrophus* as a source of genes for 2,4-D resistance in plants. Weed Sci 35 (Suppl. 1): 12–18 (1987).
19. Stalker DM, McBride KE, Malyj LD: Herbicide-resistance in transgenic plants expressing a bacterial detoxification gene. Science 242: 419–423 (1988).
20. Steenson TI, Walker N: The pathway of breakdown of 2:4-dichloro- and 4-chloro-2-methyl-phenoxyacetic acid by bacteria. J Gen Microbiol 16: 146–155 (1957).
21. Streber WR, Timmis KN, Zenk MH: Analysis, cloning and high-level expression of 2,4-dichlorophenoxyacetate monooxygenase gene *tfdA* of *Alcaligenes eutrophus* JMP134. J Bact 169: 2950–2955 (1987).
22. Tiedje JM, Duxbury JM, Alexander M, Dawson JE: 2,4-D metabolism pathway of degradation of chlorocatechols by *Arthrobacter* species. J Agric Food Chem 17: 1021–1026 (1969).
23. Walker JC, Howard EA, Dennis ES, Peacock WJ: DNA sequences required for anaerobic expression of maize alcohol dehydrogenase 1 gene. Proc Natl Acad Sci USA 84: 6624–6628 (1987).

COR-AAD1-00002669
Bayer EX1008 (Part 5 of 9)

Transgenic Research **2**, 162–169 (1993)

Cotton plants transformed with a bacterial degradation gene are protected from accidental spray drift damage by the herbicide 2,4-dichlorophenoxyacetic acid

BRUCE R. LYON, YVONNE L. COUSINS, DANNY J. LLEWELLYN* and ELIZABETH S. DENNIS

CSIRO Division of Plant Industry, GPO Box 1600, Canberra City, ACT 2601, Australia (Fax: +61 624 650 00)

Received 30 April 1992; revised 6 July 1992; accepted 7 July 1992

The agronomic performance of broad leaved crop plants such as cotton would be greatly improved if genetically-engineered resistance to broadleaf herbicides could both protect the plants from accidental spray drift damage and allow the suppression of problem broadleaf weeds by chemical means. Following *in vitro* modification and the addition of plant expression signals, the gene for 2,4-*D* monooxygenase, a bacterial enzyme that degrades the broadleaf herbicide 2,4-dichlorophenoxyacetic acid (2,4-*D*), was introduced into cotton plants by *Agrobacterium*-mediated transformation. First generation homozygous progeny of regenerated transgenic cotton plants carrying this gene exhibited up to a 50–100 fold increase in tolerance to 2,4-*D* compared with untransformed controls, and glasshouse trials suggest that the genetically-engineered plants would be completely protected from spray drift of 2,4-*D*, at least up to the normal field application rates commonly used on neighbouring cereal crops.

Keywords: transgenic cotton plants; 2,4-*D* herbicide tolerance; herbicide detoxification

Introduction

There are many situations in modern agriculture where herbicides cannot be efficiently employed because of the lack of suitable chemicals that can differentiate between crop plants and weeds. Within a dicotyledonous (broadleaf) crop such as cotton, for example, broadleaf weeds such as Noogoora burr (*Xanthium occidentale*), which have a similar herbicide sensitivity spectrum to cotton, must be removed by mechanical or hand cultivation. Difficulties have consistently arisen in multi-cropping systems where monocotyledonous crops such as wheat or sorghum, which can tolerate a range of herbicides directed at broadleaf weeds, are grown in rotation with sensitive dicotyledonous crops. Thus in Australia, cotton plants can be severely damaged by the inadvertent drift of the volatile herbicide 2,4-dichlorophenoxyacetic acid (2,4-*D*) initially applied to adjacent cereal crops or by trace contaminants of 2,4-*D* left in the tanks of aerial spray rigs.

One possible solution to these problems in areas where multi-cropping is practised, lies in the development by genetic engineering of crops which are tolerant to herbicides that cause spray drift damage. Numerous genes for herbicide tolerance have been developed over the past five years (reviewed by Schulz *et al.*, 1990) and used to produce transgenic plants tolerant to herbicides such as glyphosate, sulfonylureas, glufosinate (De Block *et al.*, 1987) and bromoxynil (Stalker *et al.*, 1988). The latter two conferred resistance through the genetic engineering of a herbicide detoxification pathway in the plant cells. A major advantage of this detoxification strategy is that it removes the need to first identify the site(s) of action of the herbicide in the plant, since the aim is to intercept the chemical before it reaches its target(s). Also, if the herbicide has multiple sites of action each of the susceptible targets can be protected simultaneously with a single detoxification mechanism. This strategy is particularly appropriate to developing plants tolerant to the synthetic plant auxin 2,4-*D* and we recently validated this strategy in transgenic tobacco as described below.

*To whom correspondence should be addressed.

0962–8819 © 1993 Chapman & Hall

COR-AAD1-00002670

Bayer EX1008 (Part 5 of 9)

Transgenic tobacco plants with increased tolerance to 2,4-*D* (Lyon *et al.*, 1989; Streber and Willmitzer, 1989) have been produced by employing an appropriately modified gene for a 2,4-*D* monooxygenase from the bacterium *Alcaligenes eutrophus.* This enzyme catalyzes the first step in the bacterial degradation of 2,4-*D* and cleaves the acetate side chain of 2,4-*D* to give glyoxylate and 2,4-dichlorophenol (Don *et al.*, 1985). The latter compound is between 50 and 100 times less toxic to tobacco plants than 2,4-*D*, as measured by leaf disc regeneration and seed germination assays (Lyon *et al.*, 1989). In this paper we report the successful adoption of the 2,4-*D* detoxification strategy to a commercially important broadleaf crop with the production of transgenic cotton plants that should be completely protected from any accidental damage by this herbicide.

Materials and methods

Construction of the binary vector

In vitro manipulation of the 2,4-*D* monooxygenase gene (*tfdA*) from *A. eutrophus* strain JMP134 and the construction of plant expression fusions using the Cauliflower Mosaic Virus (CaMV) 35S promoter, Alfalfa Mosaic virus coat protein gene leader region and the nopaline synthase (*nos*) 3′ polyadenylation signal was described in Lyon *et al.* (1989). Although we could assay the expression of the *tfdA* gene phenotypically in regenerated transgenic plants by their resistance to 2,4-*D*, we previously had difficulty in assaying 2,4-*D* monooxygenase activity enzymatically in plant tissues using an *in vitro* assay that performed well with extracts of bacteria expressing the enzyme. Since the transformation of cotton is a slow and laborious process taking up to a year, an easily assayable marker gene linked to the 35S-*tfdA* gene was considered valuable for use in screening calli at early stages in the transformation process. A binary transformation vector carrying both a plant-selectable kanamycin resistance gene (*Npt* II) marker and a screenable histochemical marker was therefore constructed from pGA470 (An *et al.*, 1985) by blunt end ligation of the filled *Hin* *d*III-*Eco* RI35S-GUS (β-glucuronidase encoded by the *GusA* gene from *Eschericia coli* (Jefferson *et al.*, 1987)) gene of p35SGN100 (Bogusz *et al.*, 1990) into the filled *Eco* RI site of pGA470. The orientation containing the 35S-GUS gene transcribed in the opposite direction to the selectable marker gene was arbitrarily selected. The 35S-*tfdA*-*nos* construct was then cleaved with *Hin* *d*III and introduced into the binary vector at its unique *Hin* *d*III site such that the *tfdA* gene would be transcribed in the same direction as the *npt* II gene and opposite to that of the GUS gene. A schematic representation of the final binary vector plasmid is presented in Fig. 1. Triparental mating was employed to transfer the binary vector construct to the super-virulent disarmed

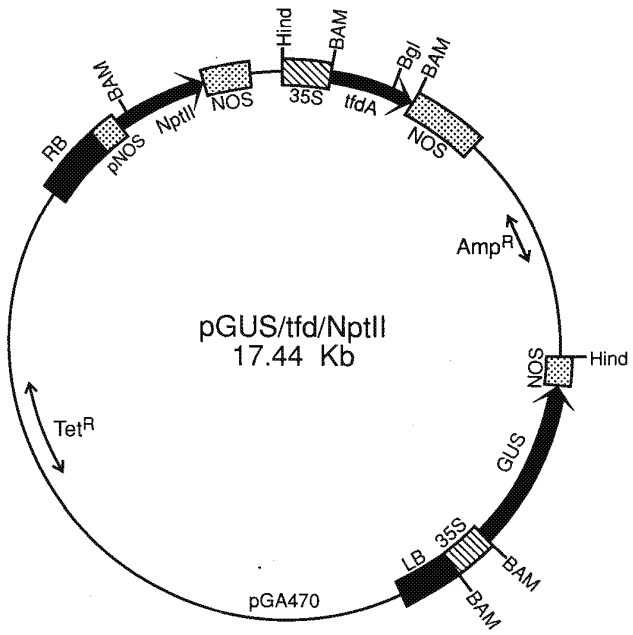


Fig. 1. Schematic representation of the pGUS-*tfdA*-*Npt* II binary vector plasmid used in this study. The GUS and *tfdA* genes were cloned between cauliflower mosaic virus 35S promoters and nopaline synthase (*Nos*) 3′ polyadenylation signals and inserted into the binary vector plasmid pGA470 as described in the Materials and methods section. Restriction endonuclease sites are *Bam*, *Bam* HI; *Bgl*, *Bgl* II; *Hin* d, *Hin* *d*III. The arrows indicate the directions of gene transcription. *Npt* II designates the neomycin phosphotransferase gene which mediates kanamycin resistance in transformed plant, pNOS, the promoter of the nopaline synthase gene; Amp^R and Tet^R designate the bacterial genes for ampicillin and tetracycline resistance, respectively. LB and RB designate the left and right borders of the T-DNA, respectively.

Agrobacterium tumefaciens strain AGL1 (Lazo *et al.*, 1991) and constructions were verified by restriction and DNA blotting analysis.

Transformation and regeneration of cotton plants

Cotton seedling explants were transformed by *A. tumefaciens* infection and transgenic plantlets regenerated by somatic embryogenesis essentially as described by Firoozabody *et al.* (1987). Cotyledons from 12-day seedlings of *Gossypium hirsutum* cv Coker 315 were transformed by co-cultivation with *Agrobacterium* AGL1 containing the GUS-*tfdA*-*npt II* binary vector construct. Transgenic kanamycin-resistant callus was selected on 35 mg l^{-1} kanamycin for six weeks, then numbered and tested for GUS activity after 2–3 months. Selected GUS positive callus was cultured on embryogenesis medium until globular embryos developed and germinated (4–6 months). Plantlets were developed from these embryos

COR-AAD1-00002671
Bayer EX1008 (Part 5 of 9)

over the next 2–3 months using the procedure reported by Cousins *et al.* (1991) and were hardened off in a growth cabinet before being placed in soil pots and transferred to a biosafety containment glasshouse for seed propagation.

Analysis of plant tissue for the presence of introduced genes

Colonies of cotton callus growing on antibiotic selection media and small leaf samples of regenerated plants were asssayed for GUS activity using 4-methyl-umbelliferyl glucuronide as the enzyme substrate (Jefferson *et al.*, 1987) and were scored relative to the level of UV fluorescence of control non-transformed tissues. Globular embryos were analysed for GUS activity using X-glucuronide as the enzyme substrate and were scored on the basis of the development of a blue colour. Selected callus and leaf material was assayed for neomycin phosphotransferase activity according to the method of Reiss *et al.* (1984). DNA from floral buds and young leaves was purified by a modification (K. Jacobsen, personal communication) of a previously published technique for the extraction of nucleic acids from cotton (Hughes and Galau, 1988) or using the CTAB method of Taylor and Powell (1982). The DNA samples were employed as templates in polymerase chain reactions (PCR) using primers selected from each end of the *tfdA* coding sequence and a kit supplied by Perkin-Elmer or cleaved with restriction endonucleases and analysed by Southern blotting as described in Mitchell *et al.* (1989).

2,4-D toxicity tests

F_1 seeds generated by self-pollination of wildtype and transgenic plants were germinated in soil in a biosafety containment glasshouse. At four to eight weeks post germination, young plants were sprayed to run-off using a pump-action garden sprayer with a range of 2,4-*D* (isopropyl ester in 50% acetone and 0.1% Tween 80) concentrations (*0, 10, 30, 100, 300, 600, 900* and 1200 ppm). Plants were observed for detrimental effects over a period of three weeks.

Results

Transformation, regeneration and propagation of Coker 315 cotton

Fully expanded cotyledons from over 100 Coker 315 seedlings were cut into 4–6 pieces, co-cultivated with *Agrobacterium* and cultured for callus production under kanamycin selection. Cotyledon pieces from each seedling were kept separate in case individual seedlings were of a more regenerable genotype. Most cotyledon pieces developed some degree of callusing along the cut edges and foci of more prolific callus, each of which was believed to represent an independent transformation event, were subcultured onto selective media. After further subculture, the darker green, less friable callus material was assayed for GUS activity. From a total of 267 such samples, 83 were found to give strong GUS reactions while most of the remainder were clearly not expressing GUS enzyme and were discarded. This result was unexpected as all the tissues would presumably have to be transformed with the *npt* II gene (and therefore also the GUS gene) in order to proliferate on the kanamycin-containing medium over a number of subcultures.

Callus samples (49) were eventually selected for transfer onto embryogenesis medium and incubated for extended periods with limited subculture. During this time, 24 of them developed a cream-coloured granular appearance and, in 11 cases, subsequently produced globular embryos which were seen to germinate and grow cotyledon- and root-like structures. Embryos were trans-

Table 1. Regenerated cotton plants transformed with the GUS–*tfdA*–*npt II* gene construct

Transformation event	*Plantlets* in vitro	*Plants in bud*	*Flower mutants*	*Dead*	*Infertile*	*Fertile*
1	1	1	–	–	1	–
34	3	2	–	–	2	–
71	1	1	–	–	–	1
72	15	4	–	–	–	4
75	50	6	–	2	3	1
100	24	3	1	1	1	–
108	12	3	–	1	2	–
112	18	4	–	2	2	–
165	50	10	2	1	1	6
177	9	1	–	–	1	–
193	18	7	3	1	3	–
Total	201	42	6	8	16	12

COR-AAD1-00002672
Bayer EX1008 (Part 5 of 9)

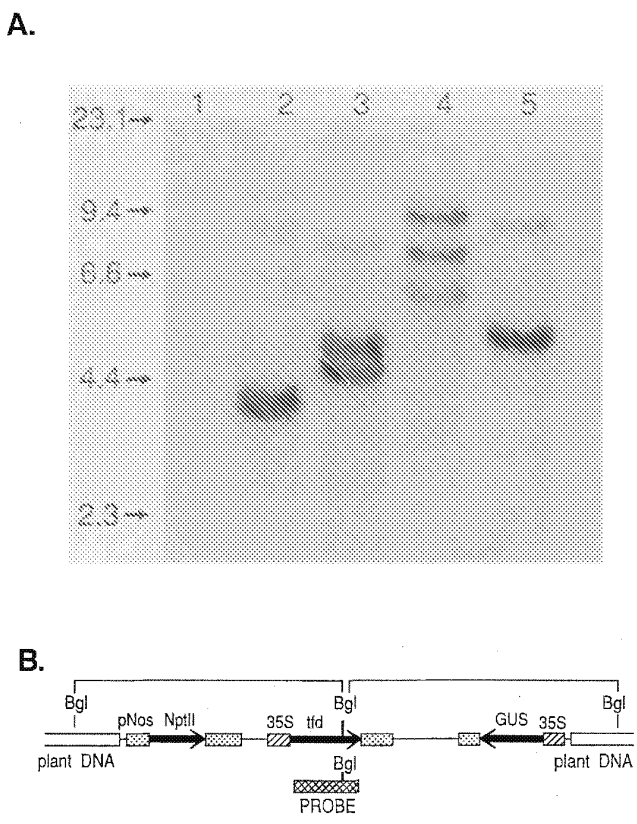


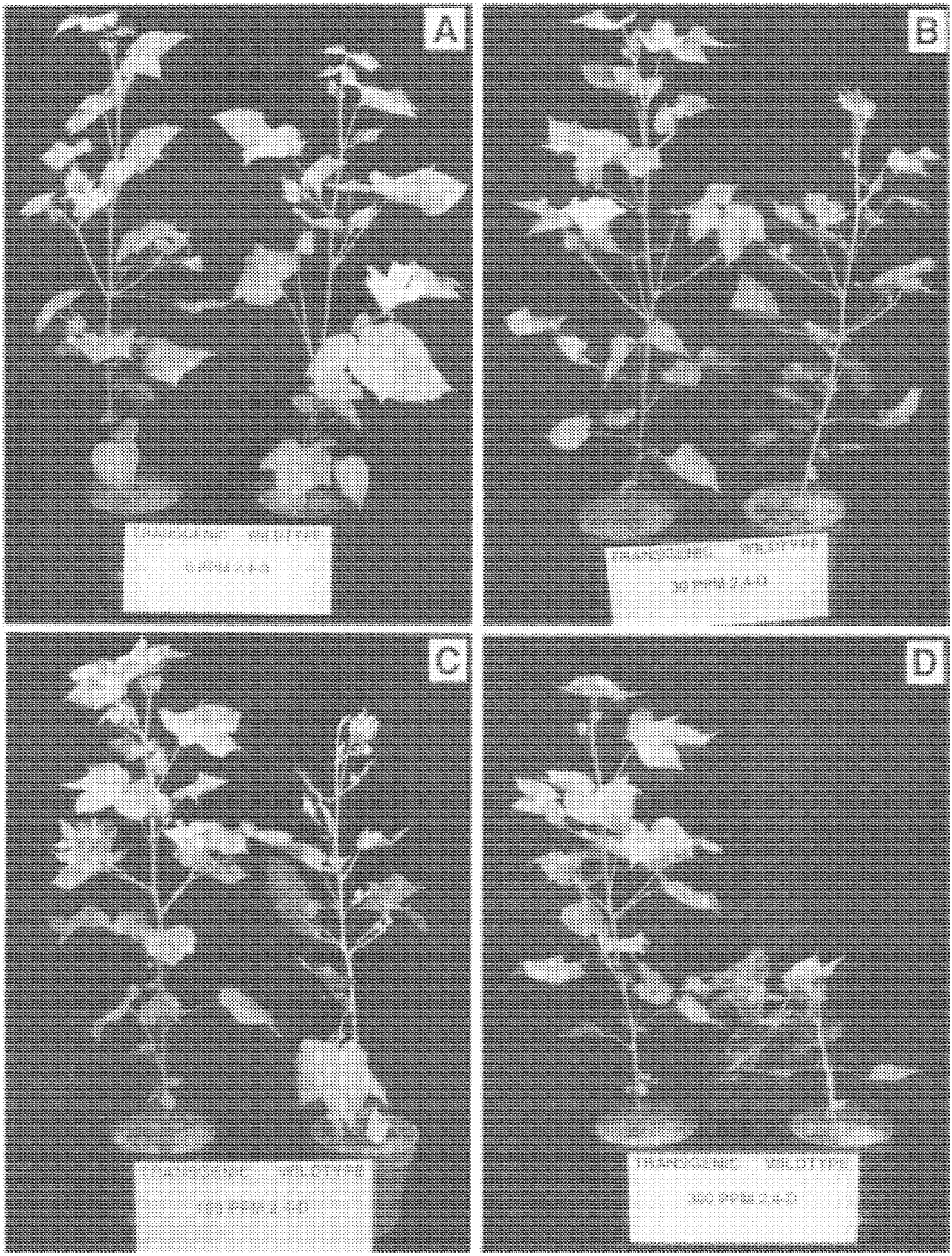
Fig. 2.(A) Genomic Southern blot analysis of 2,4-*D* tolerant cotton plants. Of the total genomic DNA, 10 µg from selected progeny plants of the four transgenic cotton lines were digested with *Bgl* II, separated on 0.7% agarose, transferred to Hybond N-membrane and probed with the *tfdA* coding region probe. Lane 1, Coker 315 control; lane 2, 71–1 progeny plant No. 5; lane 3, 72–11 progeny plant No. 4; lane 4, 75–24 progeny plant No. 16; lane 5, 165–5 progeny plant No. 29. Molecular markers in kilobase pairs are indicated at the side of lanes. **(B)** Schematic outline of the expected structure of the T-DNA inserted into the plant genome. The predicted fragments generated by *Bgl* II digestion and the position of the *tfdA* probe used in the Southern blot are indicated. (Not to scale.)

ferred onto germination medium and grown until true leaves and substantial root systems were present, at which time they were hardened-off and transplanted to soil in pots. Of 201 germinating embryos that were treated in this manner, 42 plants (derived from 11 different transformation events) survived long enough in the glasshouse to form floral bud or bud-like structures (Table 1). Twelve of these plants (from four different transformation events: 71, 72, 75 and 165) were found to be self-fertile, being able to set bolls and produce viable seed. Only one member of each of these groups was analysed further as plants derived from the same embryogenic callus lines were assumed to be derived from a single transformation event. The remaining plants failed to develop seed as they were not self-fertile (16), possessed critical mutations in floral morphology (6), or died before setting bolls (8) (Table 1) and were discarded. GUS and NPT II *in situ* assays on young leaves indicated that all the fertile plants were expressing both the GUS and NPT II gene products at high levels (not shown).

Analysis for transgenic plants for the presence of tfdA

Evidence for the presence of *tfdA* in transgenic plants and their progeny was provided by Southern blotting, PCR analysis and (ultimately) phenotypic expression. In most primary transformants, there was, as expected, a strong correlation between the presence of the *tfdA* gene and the detection of GUS and NPT II enzyme activities, suggesting that the transformants had received an entire copy of the T-DNA and that this was stably inherited in the fertile plants. Southern blotting of DNA from progeny of the four fertile transformants (Fig. 2) revealed that the *tfdA* gene was inserted at different genomic positions in all of them, confirming that they were the result of independent transformation events. The T-DNA insert contains a single *Bgl* II site near the 3′ end of the *tfdA* coding region. Southern blots of DNA digested with this enzyme should therefore contain two bands (whose size would be determined by the positions of flanking *Bgl* II sites in the plant DNA), one (containing over 90% of the *tfdA* coding region) hybridizing more strongly than the other. Multiple independent insertions should have more than one pair of these bands. Only one of the fertile transformants (71–1) contained a single T-DNA insertion (lane 2) while the other three transformants (72–11 and 75–24 and 165–5) appear to have received multiple (probably two) copies of the T-DNA (lanes 3–5). The faint upper band in Lane 2 is the result of partial digestion of the DNA and was not present in other blots of DNA digested with *Bgl* II or other enzymes that cut once within the T-DNA insert (not shown). These findings on T-DNA insert numbers are supported by seed segregation data for both GUS activity and 2,4-*D* tolerance (see below). Plant 165–5 is interesting since the Southern blot only shows a single pair of hybridizing bands, yet the GUS and 2,4-*D* resistance segregate as if there are two or more independent insertions. It is possible that the 5.0 kb band is a doublet and that the other end of the T-DNA is a large fragment that did not transfer efficiently to the membrane. While PCR analysis holds promise as a rapid means for detecting the presence of introduced genes in transgenic plants, we experienced difficulties in obtaining consistent results with cotton DNA using primers internal to the *tfdA* gene, and hence relied on the Southern blotting data to provide confirmation of transformation.

COR-AAD1-00002673
Bayer EX1008 (Part 5 of 9)



COR-AAD1-00002674
Bayer EX1008 (Part 5 of 9)

*Spraying of young cotton plants with 2,4-*D

Progeny seed produced by self-fertilisation of four of the original transformants (71–1, 72–11, 75–24 and 165–5), together with wildtype seed, was germinated in soil and grown for approximately four weeks before small leaf samples from each plant were assayed for GUS activity. As indicated above, segregation of the GUS gene within the selfed progeny suggested that this gene existed as a single site T-DNA insertion 71–1 (21 of the 28 plants tested expressed GUS activity), but as multiple independent insertions in 72–11, 75–24 and 165–5. Provided that the T-DNA was inherited as a stable entity in the transgenic plants, the *tfdA* gene would also segregate in this manner. GUS assays on progeny plants were therefore used to ensure that, where possible, subsequent spraying experiments included GUS negative progeny as internal controls at each of the herbicide concentration steps. This was not possible with 165–5 progeny as all 28 progeny expressed GUS.

Groups of 28 R_1 cotton plants (eight progeny from each of the R_0 transgenic parents 71–1, 72–11 and 165–5 and four wild type Coker 315 plants) were sprayed with one of four concentrations of 2,4-*D* (0 ppm, 30 ppm, 100 ppm and 300 ppm) and observed for detrimental effects over the next three weeks (eg. Fig. 3). Wild type plants and GUS negative transgenic progeny were severely affected even by the lowest level of herbicide (30 ppm) (Fig. 3B), where GUS positive transgenic progeny from all three original transformants showed only slight damage at the highest 2,4-*D* concentration (eg. Fig. 3D for 71–1 progeny plants). At 300 ppm, damage to the transgenic plants comprised browning and eventual loss of some new shoot tips and squares (flower buds), together with slight stem twisting, however, all plants were able to recover quickly, with normal shoots and squares evident after 2–3 weeks (Fig. 3D). There appeared to be no substantial differences in the tolerance at 300 ppm within the GUS positive R_1 progeny of any of the three groups of plants or between the three transformant groups, and all GUS positive plants proved to be tolerant to 2,4-*D* at 300 ppm 2,4-*D*.

In order to determine the effective increase in tolerance to 2,4-*D* accorded through possession of the *tfdA* gene, three GUS expressing R_1 transgenic progeny from 71–1 were sprayed with each of 600 ppm, 900 ppm and 1200 ppm solutions of the herbicide and compared with wild type cotton that had been sprayed with 10 ppm 2,4-*D*. Damage to the transgenic plants at 900 ppm was approximately equivalent to that observed for the wild type plants sprayed with 10 ppm, indicating that the transgenic plants were at least 90-fold more resistant to the herbicide than wild type cotton (data not shown).

R_2 seed was collected from individual 2,4-*D* resistant R_1 plants. Twelve seeds from each were germinated and tested for GUS expression in young leaves using the histochemical stain. Progeny of 71–1–7 were all GUS positive while for plant 71–1–8 only 8 out of 12 were GUS positive. These results are consistent with 71–1–7 being homozygous for the single T-DNA insert and 71–1–8 being hemizygous, designations confirmed by Southern blot analysis (not shown). Progeny from 72–11, 75–24 and 165–5 R_1 plants segregated GUS in various ways, consistent with the multiple inserts present in the original R_0 plants. The R_2 progeny were sprayed at four weeks with 600 ppm 2,4-*D*, a dose that seemed to discriminate between different plants when used against the R_1 progeny. Plants were assessed after one, two and three weeks.

At one week there were distinct differences between the different groups of plants. The 71–1 R_2 progeny were the most tolerant to 600 ppm 2,4-*D* with the homozygous 71–1–7 progeny suffering very little damage, other than some mild burning of the young leaves present at the time of spraying. New leaves generated subsequent to spraying were undamaged. Segregating progeny from 71–1–8 showed three classes of damage. The GUS negative plants (4 out of 12) were badly burnt and twisted and all of the shoots, including axillary buds were dead. Among the GUS positive plants (8 out of 12) there was either very little damage (3 out of 12) similar to the homozygous 71–1–7 plants or moderate damage where the older leaves were burnt and the new leaves were slightly distorted but otherwise green and healthy. The other progeny plants of the independent transformants showed varying degrees of damage, but in all cases the segregating GUS negative plants were killed by 600 ppm 2,4-*D*. In general the 75–24 GUS positive R_2 progeny segregated three phenotypes, from very little damage in a few plants, to moderate damage in some and severe damage in others. The severely damaged plants still contained viable axillary buds and began to recover after two weeks. R_2 progeny of 72–11 and 165–5 plants had similar phenotypes except that there were more of the severely damaged plants at one week. By three weeks most of the GUS positive progeny from all four groups had recovered and were flowering and setting seed.

Discussion

The herbicide 2,4-*D* is active against most dicotyledonous weed species and, although its use has been actively suppressed in some European countries, in Australia and the USA, it is still widely used as a weed control agent on

Fig. 3. Spraying of young cotton plants with 2,4-*D*. Wild type (Coker 315) on the right of each panel and transgenic (71–1) R_1 progeny plants on the left of each panel were sprayed with (**A**) 0 ppm 2,4-*D*, (**B**) 30 ppm 2,4-*D*, (**C**) 100 ppm 2,4-*D* or (**D**) 300 ppm 2,4-*D*. (Photographs were taken three weeks after spraying.)

COR-AAD1-00002675
Bayer EX1008 (Part 5 of 9)

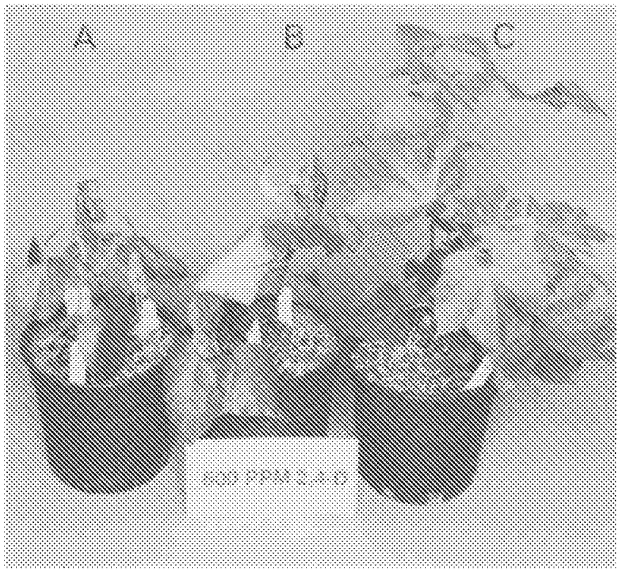


Fig. 4 Spraying of R_2-segregants of plant 71-1-7 with a discriminating dose of 2,4-*D* (600 ppm). **(A)** *tfdA* null segregants, **(B)** segregants hemizygous for the *tfdA* gene and **(C)** segregants homozygous for the *tfdA* gene. (Plants were photographed two weeks after spraying).

monocot crops such as wheat and sorghum. Weed control is a serious issue in many agricultural situations where productivity can be severely limited if weeds are not suppressed by cultivation or treatment with chemical weedicides. In broad-acre crops cultivation can have deleterious effects on soil structure and result in soil loss or degradation, chemical weedicides provide an acceptable alternative provided that they have no long-term environmental or health impacts (Combellack, 1989). 2,4-*D* might be considered an old-fashioned herbicide and has been scorned because of its use with the structurally related, but biologically different, herbicide 2,4,5-trichlorophenoxyacetic acid (2,4,5-T) in Agent Orange in mass forest defoliation in Vietnam, but it does have many of the properties that could be considered desirable in an herbicide. Unlike 2,4,5-T, 2,4-*D* is biodegradable, surviving only five or six weeks in the soil (Noble and Hargreaves, 1992), due to the action of numerous species of bacteria, yeasts and fungi (e.g. Don and Pemberton, 1981). It is relatively safe for humans (Mullison, 1988) and does not contain the contaminating dioxins that caused the banning of 2,4,5 -T when a link with specific human cancers was discovered. No such link has been clearly demonstrated for 2,4-*D* (Mullison, 1988 and references therein). 2,4-*D* has been carefully assessed by Australian authorities and registered for use as an herbicide. It will continue to remain a component of Australian cropping systems and problems with spray drift damage to dicot crops, such as cotton, will remain a problem in multi-cropping systems, unless tolerant varieties can be developed.

We are interested in engineering 2,4-*D* resistant cotton that will be tolerant to drift damage caused by 2,4-*D* to make multi-cropping strategies more effective and allow greater flexibility in herbicide usage. In earlier work we demonstrated the potential of the gene (*tfdA*) for the first enzyme in the 2,4-*D* degradative pathway of the bacterium *A. eutrophus* (Streber *et al.*, 1987) to detoxify 2,4-*D* when expressed in transgenic tobacco. This result suggested that the introduction of the *tfdA* gene into a commercial species such as cotton should also allow 2,4-*D* detoxification and protect the plants from accidental spray drift damage.

A relatively efficient transformation frequency for cotton cotyledons was achieved by employing the super virulent *A. tumefaciens* strain AGL1 and screening putative transformed callus tissue for GUS activity at an early stage. GUS positive reactions were recorded from a high percentage of the kanamycin resistant callus recovered after *Agrobacterium* infection, giving a transformation frequency (transformants/seedling) of 60%. We have assumed that T-DNA transfer proceeds from the right border to the left border and that the presence of the GUS gene indicates the successful transfer of the entire T-DNA. We have not yet determined why many of the remaining callus cultures failed to produce a GUS positive reaction, despite being capable of surviving on kanamycin-containing media, but presume it was because of incomplete transfer of the T-DNA (e.g. van Lijsebettens *et al.*, 1986), rather than 'escapes' from selection on kanamycin. About 50% of the callus lines produced embryogenic callus when subcultured onto embryo development media and eleven of these (46%) produced germinating embryos that eventually developed into whole plants. Thus a quite workable regeneration rate of approximately 22% was achieved for the transformed callus lines using our screening strategy for a co-transferred screenable marker gene (GUS). Once in the glasshouse, however, only plants from four of the callus lines were able to produce fully fertile flowers, set fruit and produce acceptable yields of viable seed. This indicates that cells from the majority of callus lines may have undergone deleterious mutations, or other forms of somaclonal variation whilst in culture, that prevented the regeneration of normal fertile plants. Such a result is not unexpected given the length of time (over twelve months in some instances) that the cells spent in culture. We have observed similar abnormalities in plants regenerated using auxins other than 2,4-*D* in the culture medium, so cannot directly attribute these effects to toxicity by this specific compound. More rapid turnaround in tissue culture through more intensive subculture regimes and/or induction of embryogenesis in liquid culture has subsequently reduced the frequency of abnormal plants by significantly reducing the time needed for plant regeneration. Although some of our transgenic

COR-AAD1-00002676
Bayer EX1008 (Part 5 of 9)

plants may have had partial fertility (e.g. Cousins *et al.*, 1991), we did not attempt to recover seed from any male sterile transgenic plants by cross-pollination with pollen from fertile non-transgenic plants.

The level of herbicide resistance obtained in our transgenic cotton is promising, with engineered plants able to survive spraying with 2,4-*D* at concentrations more than 90-fold higher than that tolerated by wild type cotton. Following calibration trials with the commercial 2,4-*D* herbicide, Nufarm Estercide 800, on wild type tobacco in the field and transgenic tobacco (Lyon *et al.*, 1989) in the glasshouse, we estimate that the minimum effective field application rate of 280 grams 2,4-*D* per hectare would be approximately equivalent to the 300 ppm rate used in this and our previous work in tobacco (data not shown). This would mean that the transgenic cotton would suffer no damage if it were accidentally exposed in a spray drift situation to the minimum weed control rate of 2,4-*D*. 2,4-*D* can, however be used at much higher rates for some problem weeds and unintentional exposure to these higher doses of the herbicide could cause significant damage and loss in crop productivity. The 2,4-*D* tolerance gene is currently being transferred into all of our existing commercial cotton varieties from our best transformant (71–1) by traditional breeding techniques with recurrent back-crosses and this material should be ready for commercial release as 2,4-*D* drift tolerant cultivars within the next five years.

Acknowledgments

This work was funded in part by Cotton Seed Distributors, Ltd and the Australian Cotton Research and Development Corporation. We thank Ms M. Brown and J. Thistleton for their assistance with plant regeneration DNA isolation and GUS assays, and Drs J. Huppatz and C. Jenkins for critically reading the manuscript. We would also thank Dr W.J. Peacock for his continued support and enthusiasm for this project from its inception.

References

An, G., Watson, B.D., Stachel, S., Gordon, M.P. and Nester, E.W. (1985) New cloning vehicles for transformation of higher plants. *EMBO J.* **4**, 277–84.

Bogusz, D., Llewellyn, D.J., Craig, S., Dennis, E.S., Appleby, C.A. and Peacock, W.J. (1990) Non-legume haemoglobin genes retain organ-specific expression in heterologous transgenic plants. *Pl. Cell* **2**, 633–41.

Combellack, J.H. (1989) The importance of weeds and the advantages and disadvantages of herbicide use. *Pl. Prot. Quart.* **4**, 14–32.

Cousins, Y.L., Lyon, B.R. and Llewellyn, D.J. (1991) Transformation of an Australian cotton cultivar: prospects for cotton improvement through genetic engineering. *Aust. J. Pl. Physiol.* **18**, 481–94.

De Block, M., Botterman, J., Vandewiele, M., Dockx, J., Thoen, C., Gossele, V., Rao Movva, N., Thompson, C., van Montagu, M. and Leemans, J. (1987) Engineering herbicide resistance in plants by expression of a detoxifying enzyme. *EMBO J.* **6**, 2513–8.

Don, R.H. and Pemberton, J. (1981) Properties of six pesticide degradation plasmids isolated from *Alcaligenes eutrophus* and *Alcaligenes paradoxus*. *J. Bacteriol.* **145**, 681–6.

Don, R.H., Weightman, A.J., Knackmuss, H.-J. and Timmis, K.N. (1985) Transposon mutagenesis and cloning analysis of pathways for degradation of 2,4-dichlorophenoxyacetic acid and 3-chlorobenzoate in *Alcaligenes eutrophus* JMP134(pJP4). *J. Bacteriol.* **161**, 85–90.

Firoozabody, E., DeBoer, D., Merlo, D., Halk, E., Amerson, L., Rashka, K. and Murray, E. (1987) Transformation of cotton (*Gossypium hirsutum* L.) by *Agrobacterium tumefaciens* and regeneration of transgenic plants. *Pl. Mol. Biol.* **10**, 105–16.

Hughes, D.W. and Galau, G. (1988) Preparation of RNA from cotton leaves and pollen. *Pl. Mol. Biol. Rep.* **6**, 253–7.

Jefferson, R.A., Kavanagh, T.A. and Bevan, M.W. (1987) GUS fusions: β-glucuronidase as a sensitive and versatile gene fusion marker in higher plants. *EMBO J.* **6**, 3901–7.

Lazo, G.R., Stein, P.A. and Ludwig, R.A. (1991) A DNA transformation competent *Arabidopsis* genomic library in *Agrobacterium*. *Bio/Technology* **9**, 963–7.

Lyon, B.R., Llewellyn, D.J., Huppatz, J.L., Dennis, E.S. and Peacock, W.J. (1989) Expression of a bacterial gene in transgenic tobacco plants confers resistance to the herbicide 2,4-dichlorophenoxyacetic acid. *Pl. Mol. Biol.* **13**, 533–40.

Mitchell, L.E., Dennis, E.S. and Peacock, W.J. (1989) Molecular analysis of an alcohol dehydrogenase (*Adh*) gene from chromosone 1 of wheat. *Genome* **32**, 349–58.

Mullison, W.R. (1988) A 2,4-D toxicological update. *Proc. West. Soc. Weed Sci.* **41**, 20–30.

Noble, R. and Hargreaves, P. (1992) Are herbicide residues accumulating in our soils. Austral. *Grain* **2**, 10.

Reiss, B., Sprengel, R., Will, H. and Schaller, H. (1984) A new sensitive method for qualitative and quantitative analysis of neomycin phosphotransferase in crude cell extracts. *Gene* **30**, 217–23.

Schulz, A., Wengenmayer, F. and Goodman, H. (1990) Genetic engineering of herbicide resistance in plants. *CRC Crit. Rev. Pl. Sci.* **9**, 1–15.

Stalker, D.M., McBride, K.E. and Malyj, L.D. (1988) Herbicide-resistance in transgenic plants expressing a bacterial detoxification gene. *Science* **242**, 419–23.

Streber, W.R., Timmis, K.N. and Zenk, M.H. (1987) Analysis, cloning and high-level expression of 2,4-dichlorophenoxyacetate monooxygenase gene *tfdA* of *Alcaligenes eutrophuas* JMP134. *J. Bact.* **169**, 2950–5.

Streber, W.R. and Willmitzer, L. (1989) Transgenic tobacco plants expressing a bacterial detoxifying enzyme are resistant to 2,4-*D*. *Bio/Technology* **7**, 811–6.

Taylor, B. and Powell, A. (1982) Isolation of plant DNA and RNA. *Focus* **4**, 4–6.

van Lijsebettens, M., Inze, D., Schell, J. and van Montagu, M. (1986) Transformed cell clones as a tool to study T-DNA integration mediated by *Agrobacterium tumefaciens*. *J. Mol. Biol.* **188**, 129–45.

COR-AAD1-00002677
Bayer EX1008 (Part 5 of 9)

Characterization of a new 2,4-dichlorophenoxyacetic acid degrading plasmid pEST4011: physical map and localization of catabolic genes

ANDRES A. MÄE,* REET O. MARITS, NORA R. AUSMEES, VIIA M. KÔIV and AIN L. HEINARU

Institute of Molecular and Cell Biology at Tartu University, Estonian Biocentre, Vanemuise 46-127, Tartu EE2400, Republic of Estonia

(*Received 6 April 1992; revised 12 July 1993; accepted 26 July 1993*)

Plasmid pEST4011 enables *Pseudomonas putida* PaW85 to degrade 2,4-dichlorophenoxyacetic acid (2,4-D) and 3-chlorobenzoate (3-CBA). This new 2,4-D degradative plasmid has considerable homology with the regions of pJP4 containing the 2,4-D degradative genes (*tfd*). Restriction fragment *Bam*HI-B of plasmid pEST4011, which has homology with this region, was cloned into the broad-host-range vector pKT240 and studied in *P. putida* PaW85. Restriction mapping, hybridization analysis and enzyme assays established the location of the genes for 2,4-D monooxygenase (*tfdA*), 2,4-dichlorophenol hydroxylase (*tfdB*), chlorocatechol 1,2-dioxygenase (*tfdC*) and the *tfdR* and *tfdS* regulatory genes on this fragment. Plasmid pEST4012 is a derivative of pEST4011 derived through the spontaneous deletion of a 42 kbp DNA fragment, which results in the loss of the 2,4-D$^+$ and 3-CBA$^+$ phenotype. We present here the physical maps of pEST4011 and pEST4012. In spite of the similarities in functions, the size (70 kbp), order of catabolic genes and restriction pattern of pEST4011 are clearly different from those of pJP4.

Introduction

Plasmids involved in the degradation of 2,4-dichlorophenoxyacetic acid (2,4-D) have been under considerable investigation (Pemberton & Fisher, 1977; Pierce *et al.*, 1981; Amy *et al.*, 1985; Chaudhry & Huang, 1988). The 2,4-D degradative plasmid pJP4 from *Alcaligenes eutrophus* JMP134 (isolated in Australia) has become a model for the investigation of 2,4-D degradation (Don & Pemberton, 1985; Don *et al.*, 1985; Ghosal & You, 1988, 1989; Harker *et al.*, 1989; Kaphammer & Olsen, 1990; Kaphammer *et al.*, 1990; Perkins *et al.*, 1990). A second plasmid, pRC10, present in a 2,4-D-degrading *Flavobacterium* sp. isolated in the USA, has also been characterized in detail (Chaudhry & Huang, 1988). Little information is, however, available on the nature and physical structure of other 2,4-D degradative plasmids.

Despite differences in the size and restriction pattern of 2,4-D plasmids there is considerable homology between the 2,4-D degradative genes (Don & Pemberton, 1981; Amy *et al.*, 1985; Chaudhry & Huang, 1988; Ditzelmüller *et al.*, 1989). Comparison of other plasmids which determine the degradation of chlorinated compounds with pJP4 would be of great value in understanding the evolutionary process by which enzymes with novel specificities are evolved by bacteria and how they have spread amongst bacteria.

Recently, we isolated from 2,4-D-pretreated soils in Estonia several plasmid-containing strains with the ability to degrade 2,4-D. Restriction analysis revealed that they all harboured an identical 78 kbp plasmid, designated pEST4002 (Ausmees & Heinaru, 1990).

In this paper, we present the physical maps of the 70 kbp plasmid pEST4011, a derivative of pEST4002 which encodes enzymes for the catabolism of 2,4-D, and pEST4012, a spontaneous 2,4-D$^-$ derivative of pEST4011, which has 42 kbp deleted. DNA–DNA hybridization showed extensive homology between the catabolic regions of pJP4 and pEST4011. The structural genes 2,4-D monooxygenase (*tfdA*), chlorocatechol 1,2-dioxygenase (*tfdC*), 2,4-dichlorophenol hydroxylase (*tfdB*) and the regulatory genes *tfdR* and *tfdS* have been cloned and localized on pEST4011.

*Author for correspondence. Present address: Department of Molecular Genetics, Uppsala Genetic Centre, Swedish University of Agricultural Sciences, Box 7010, S-750 07 Uppsala, Sweden. Fax +46 18 67 32 79.

Abbreviations: 2,4-D, 2,4-dichlorophenoxyacetic acid; 3-CBA, 3-chlorobenzoate.

0001-7506 © 1993 SGM

COR-AAD1-00002678
Bayer EX1008 (Part 5 of 9)

Methods

Bacterial strains and plasmids. Bacterial strains and plasmids used or constructed in this study are described in Table 1.

Media and culture conditions. The complete medium was Luria broth (LB) and the minimal medium (MS) was M9 salts solution (Maniatis *et al.*, 1982) supplemented with trace elements (Bauchop & Elsden, 1960). Concentrated stock solution (20 mg ml^{-1}) of 2,4-D was prepared as the sodium salt and added to MS medium at a final concentration of from 4·0 to 20·0 mM. Antibiotics were incorporated into LB medium at the following concentrations: 30 μg amplicillin (Ap) ml^{-1}, 1000 μg carbenicillin (Cb) ml^{-1}, 1000 μg streptomycin (Sm) ml^{-1} and 25 μg kanamycin (Km) ml^{-1}. *Pseudomonas* strains were incubated at 30 °C and *Escherichia coli* strains at 37 °C, respectively. Cultures (30 ml) for enzyme assays were grown in MS medium supplemented with Casamino acids (0·3 %, w/v). 2,4-D and 2,4-dichlorophenol (2,4-DCP) were added to final concentrations of 0·025 % (w/v) and 0·007 % (w/v), respectively. After 4 h growth, a 30 ml culture was used to inoculate 70 ml of the same medium and allowed to grow to mid-exponential phase.

Table 1. *Bacterial strains and plasmids*

Strain or plasmid	Relevant markers*	Source or reference
E. coli		
HB101	*hsdS20 recA13 ara-14 proA2 lacY1 galK2 rpsL20 xyl-5 mtl-1 supE44*	Maniatis *et al.* (1982)
TG1		Gibson (1984)
P. putida		
PaW85	Prototroph; Tn*4652* in chromosome	Bayley *et al.* (1977)
PaW340	Sm^r Trp^-; Tn*4652* in chromosome	Bayley *et al.* (1977)
EST4021	Prototroph; 2,4-D^+	This study
EST4022	Prototroph; 2,4-D^-	This study
A. eutrophus		
JMP134	Prototroph; 2,4-D^+	Dr H.-J. Knackmuss†
Pseudomonas sp.		
EST4002	Prototroph; 2,4-D^+	Ausmees & Heinaru (1990)
Plasmids		
pUC18	Cloning vector (Ap^r)	Yanisch-Perron *et al.* (1985)
pKT240	Cloning vector (Cb^r Km^r)	Bagdasarian *et al.* (1983)
pJP4	Plasmid from JMP134 (2,4-D^+ Hg^r 3-CBA^r)	Don & Pemberton (1981)
pEST4002	Plasmid from EST4002 (2,4-D^+; wild-type 2,4-D plasmid)	Ausmees & Heinaru (1990)
pEST4011	Del. mutant of pEST4002 (2,4-D^+)	This study
pEST4012	Del. mutant of pEST4002 (2,4-D^-)	This study
pEST4013	pKT240 carrying 10·5 kbp *Bam*HI fragment of pEST4011	This study
pEST4014	pKT240 carrying 7·8 kbp *Bam*HI–*Eco*RI fragment of pEST4013	This study
pEST4015	pKT240 carrying 4·5 kbp *Bam*HI–*Kpn*I fragment of pEST4013	This study
pEST4016	pKT240 carrying 2·5 kbp *Xho*I fragment of pEST4013	This study

*Abbreviations: Ap, ampicillin; Cb, carbenicillin; Km, kanamycin; Sm, streptomycin; Hg, mercury; Trp^-, requirement for tryptophan; 2,4-D^+, ability to grow on 2,4-dichlorophenoxyacetic acid; 3-CBA^+, ability to grow on 3-chlorobenzoate.

† Institut für Mikrobiologie der Universität Stuttgart, Germany.

DNA transformation. For transformation of *P. putida* cells with plasmid DNA, we followed the method described by Bagdasarian & Timmis (1982). Transformation of *E. coli* cells was as described by Hanahan (1983).

DNA isolation, analysis and manipulation. Plasmid DNA was isolated by the procedures of Hansen & Olsen (1978) and Connors & Barnsley (1982) and purified by ethidium bromide–CsCl density gradient centrifugation. DNA cleavage by restriction endonucleases, agarose gel electrophoresis and isolation of restriction fragments from low-melting agarose gels were performed as described by Maniatis *et al.* (1982). The DNA fragments were cloned in *E. coli* into pUC18 (Yanisch-Perron *et al.*, 1985) and in *P. putida* into pKT240 (Bagdasarian *et al.*, 1983). The sizes of DNA fragments in agarose gels were calculated by comparing their mobilities with fragments of plasmid pWW0 of known size (Downing & Broda, 1979).

Southern blotting and hybridization. DNA fragments were separated on 1·0 % (w/v) agarose gels and transferred to nitrocellulose filters according to Southern (1975). DNA probes were labelled to a specific activity of $1–3 \times 10^7$ c.p.m. (μg DNA)$^{-1}$ by nick-translation (Maniatis *et al.*, 1982).

Oxygen uptake assay. Activities of 2,4-D monooxygenase were measured by monitoring oxygen uptake in the presence of 2,4-D using a Clark oxygen electrode (Yellow Springs Instruments Co.) and the YSI model 5300 biological oxygen monitor. Reaction mixtures contained approximately 10^8 washed cells ml^{-1} and 2·5 mM-2,4-D in 100 mM-potassium phosphate buffer (pH 7·6). The endogenous oxygen uptake was measured for 4 min in the absence of substrate and the reaction was started by injecting 20 μl of 2,4-D into the chamber. The oxygen uptake was monitored for 5 min.

Extract preparation and enzyme assays. Cell extracts for 2,4-dichlorophenol hydroxylase (*tfdB*) and chlorocatechol 1,2-dioxygenase (*tfdC*) assay were prepared by harvesting mid-exponential phase cultures by centrifugation at 8000 *g* for 10 min. The cell pellets were washed with 10 ml 100 mM-potassium phosphate buffer (pH 7·6), centrifuged again and suspended in 5 ml 100 mM-potassium phosphate buffer (pH 7·6) containing 1 mM-2-mercaptoethanol, 0·1 mM-EDTA and 2 μM-flavin adenine nucleotide. Cell-free extracts were prepared and 2,4-DCP hydroxylase activity was determined by the procedure of Kaphammer & Olsen (1990).

Chlorocatechol 1,2-dioxygenase assays were performed as described by Hageman (1966) using 3-methylcatechol as the substrate instead of chlorocatechols. *P. putida* PaW85 did not express catechol 1,2-dioxygenase activity at detectable levels when grown in MS medium containing 0·3 % Casamino acids with or without 2,4-D or 2,4-DCP.

Protein concentrations were determined by the method of Bradford (1976).

Results

Characterization of Pseudomonas putida EST4021(pEST4011)

We have previously reported the isolation of a new 2,4-D degradative plasmid pEST4002 in *Pseudomonas*

COR-AAD1-00002679
Bayer EX1008 (Part 5 of 9)

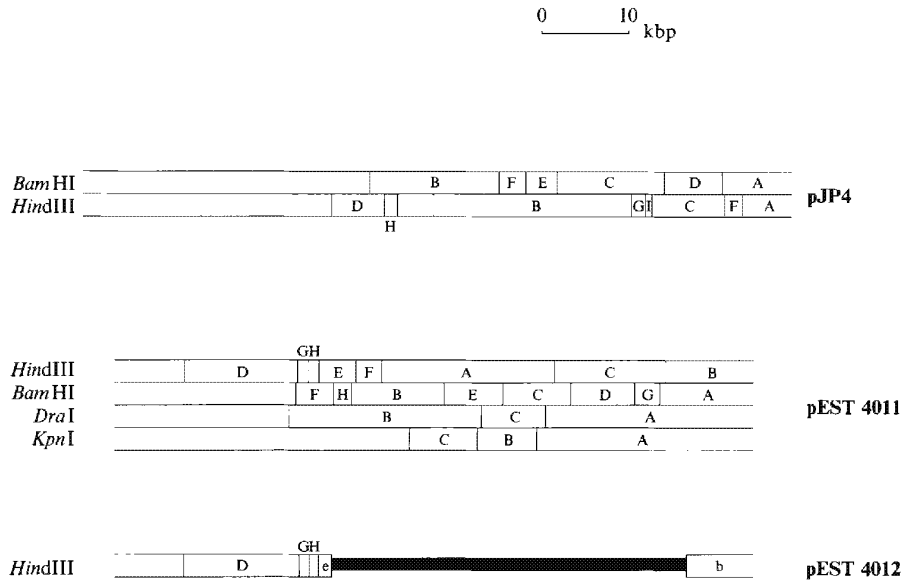


Fig. 1. Restriction digest map of plasmids pJP4 (Kaphammer *et al.*, 1990; Perkins *et al.*, 1990), pEST4011 and pEST4012. The black box in plasmid pEST4012 shows the deleted region.

sp. EST4002 (Ausmees & Heinaru, 1990), which could also utilize 3-CBA in addition to 2,4-D as a sole source of carbon. The growth characteristics are similar to those of *A. eutrophus* (Don & Pemberton, 1981) which harbours plasmid pJP4 (Don & Pemberton, 1985; Don *et al.*, 1985). The 2,4-D$^+$ phenotype was very unstable in EST4002 and similar isolates (results not presented). In EST4002, 80% of the cells had lost their ability to grow on 2,4-D after growth in a non-selective LB medium for 4 h. In most cases the 2,4-D$^-$ clones were either plasmid-free or contained a smaller plasmid, derived from pEST4002 by a deletion of 20–30 kbp (Ausmees & Heinaru, 1990). Due to the instability of the 2,4-D$^+$ phenotype and the difficulties with DNA extraction from the wild-type strains the exact location and size of the deletion was not determined.

To overcome the above difficulties pEST4002 was transferred by conjugation from EST4002 into the plasmid-free recipient strain *P. putida* PaW340. Restriction analysis showed that 2,4-D$^+$ transconjugants of PaW340 contained a 70 kbp plasmid pEST4011, which had lost a 7·8 kbp *Eco*RI fragment present in pEST4002 (78 kbp).

P. putida strain PaW85 was transformed with pEST4011 and subcultured to obtain stable 2,4-D$^+$ 3-CBA$^+$ transformants. A single plasmid, pEST4011 in strain EST4021 was detected. In batch cultures the growth rates of EST4021(pEST4011) were the same at 2,4-D concentrations between 4·0–20·0 mM; 4 mM-2,4-D (1 mg ml^{-1}) was degraded within 14 h after a lag period of 1–3 h.

In spite of its similar functions, the size (70 kbp) and restriction pattern of plasmid pEST4011 (Fig. 1) are considerably different from those of pJP4 (80 kbp).

In contrast to pEST4002 in EST4002, pEST4011 was relatively stable in EST4021. However, growth of EST4021 in LB medium for 30 generations resulted in a putative cured strain which had simultaneously lost its ability to grow on 2,4-D and 3-CBA. One 2,4-D$^-$ strain. EST4022 did not revert to the 2,4-D$^+$ phenotype at detectable levels (< 1 in 10^{10}) and contained a 28 kbp plasmid pEST4012. Five such 2,4-D$^-$ 3-CBA clones, isolated in separate experiments after prolonged growth of EST4021 in LB medium, contained plasmids with the same restriction patterns as pEST4012.

2,4-D monooxygenase, 2,4-DCP hydroxylase and chlorocatechol 1,2-dioxygenase activities were detected in EST4021(pEST4011), but not in EST4022(pEST4012). This suggests that the catabolic genes are located on the excised DNA segment.

Physical maps of the plasmids pEST4011 and pEST4012

By using restriction analysis, gene cloning and Southern hybridization a physical map of pEST4011 and pEST4012 was determined with restriction endonucleases *Bam*HI, *Dra*I, *Hin*dIII and *Kpn*I (Fig. 1). Comparison of pEST4012 with pEST4011 indicates the excision of a 42 kbp fragment and the restriction mapping reveals that the excised region is a continuous segment of the 2,4-D plasmid pEST4011.

COR-AAD1-00002680
Bayer EX1008 (Part 5 of 9)

Homology between pJP4 and pEST4011

The homology between pEST4011 and the 2,4-D$^+$ plasmid pJP4 was investigated by Southern hybridization. pEST4011 hybridized to all of the restriction fragments of pJP4 except fragments *Bam*HI-D, *Hin*dIII-A and E to H. This indicated that pEST4011 had homology with the regions of pJP4 encoding 2,4-D degradative enzymes (Fig. 2*a*, *b*). Subsequently, we cloned *Bam*HI-C, *Bam*HI-F and *Hin*dIII-B fragments from pJP4 into pUC18. The preliminary location of the degradative genes on plasmid pEST4011 was determined by preparing three probes using isolated pJP4 fragments *Bam*HI–*Cla*I (from *Bam*HI-C), *Bam*HI–*Xho*I (from *Bam*HI-E) and *Bam*HI–*Eco*RI (from *Hin*dIII-B). Those fragments contain *tfdC–tfdB* (chlorocatechol 1,2-dioxygenase, 2,4-DCP hydroxylase) genes, *tfdR* (regulator), *tfdC* (chlorocatechol 1,2-dioxygenase) genes and *tfdA* (2,4-D monooxygenase), *tfdS* (regulator) genes respectively (Perkins *et al.*, 1990). All of these fragments of pJP4 hybridized with the *Bam*HI-B restriction fragment of pEST4011, thus indicating that catabolic genes for 2,4-D degradation are located on pEST4011 in the 10·5 kbp *Bam*HI-B fragment.

Localization of tfd genes in pEST4011

Plasmid pEST4013 was constructed by cloning the *Bam*HI-B fragment of pEST4011 into the *Bam*HI site of the vector plasmid pKT240.

Strain PaW85, containing pEST4013 showed inducible expression of the *tfdA* (2,4-D monooxygenase), *tfdB* (2,4-DCP hydroxylase) and *tfdC* (chlorocatechol 1,2-dioxygenase) genes when 2,4-D and 2,4-dichlorophenol were used as inducers (Fig. 2*b*).

Further hybridization experiments are summarized in Fig. 2*a*, *b*. The hybridization of the 2·1 kbp *Sal*I–*Bam*HI (*tfdB*, 2,4-DCP hydroxylase) and the 1·6 kbp *Hin*dIII fragment of pJP4, which contains the *tfdC* (chlorocatechol 1,2-dioxygenase) and a part of the *tfdD* (chloromuconate cycloisomerase) gene only with the same 2·5 kbp *Xho*I fragment of pEST4013 shows that the *tfdB* and *tfdC* genes in pEST4011 are more closely located as compared with the corresponding genes of pJP4. The 1·0 kbp *Bam*HI–*Xho*I fragment of pJP4, which contains the *tfdR* (regulator) gene hybridized only to the 1·0 kbp *Bam*HI–*Xho*I fragment of pEST4013. Hybridization was also detected between the cloned 1·5 kbp *Eco*RI–*Bam*HI fragment of pJP4, which contains the *tfdA* (2,4-D monooxygenase) and part of the *tfdS* (regulator) gene and the 2·7 kbp *Hin*dIII fragment of pEST4013.

The 7·8 kbp *Eco*RI–*Bam*HI fragment from *Bam*HI-B of pEST4011 was subcloned into the vector plasmid pKT240 to give pEST4014. The *tfdA* locus is either absent or defective in this plasmid as no 2,4-D monooxygenase (*tfdA*) activity could be detected in PaW85 (pEST4014). However, 2,4-DCP hydroxylase (*tfdB*) and chlorocatechol 1,2-dioxygenase (*tfdC*) activities were inducible in this strain (Fig. 2*b*). This revealed that the regulatory genes *tfdR* and *tfdS* are present on the 7·8 kbp *Eco*RI–*Bam*HI fragment.

The 4·5 kbp *Kpn*I–*Bam*HI fragment from pEST4013 was subcloned into pKT240 to give pEST4015. Chlorocatechol 1,2-dioxygenase (*tfdC*) was inducible in PaW85 (pEST4015) when 2,4-DCP was used as an inducer, whereas no 2,4-DCP hydroxylase (*tfdB*) activities was detected (Fig. 2*b*). The regulatory gene, *tfdS*, must therefore be located somewhere left from *Kpn*I–*Bam*HI (4·5 kbp) in the *Eco*RI–*Bam*HI (7·8 kbp) fragment.

The 2·5 kbp *Xho*I fragment from pEST4013 was subcloned into pKT240 to give pEST4016. Strain PaW85(pEST4016) exhibited uninducible expression of chlorocatechol 1,2-dioxygenase (*tfdC*) activity and no 2,4-DCP hydroxylase (*tfdB*) activity (Fig. 2*b*). This suggests that the regulatory gene, *tfdR*, is located at the right-end of the 10·5 kbp *Bam*HI fragment in pEST4013.

Discussion

In this report we have characterized a new 2,4-D plasmid pEST4002 determining catabolism of 2,4-D and 3-CBA. This plasmid originated from *Pseudomonas* sp. EST4002 isolated from soil in Estonia (Ausmees & Heinaru, 1990). The size (70 kbp) and restriction pattern of the derived plasmid pEST4011 (Fig. 1) differed considerably from those of pJP4 previously reported in *Alcaligenes eutrophus* JMP134 (Don & Pemberton, 1985; Harker *et al.*, 1989).

Loss of the 2,4-D$^+$ and 3-CBA$^+$ phenotype in EST4011 occurred at a high frequency and spontaneously by the deletion of approximately 42 kbp of DNA (Fig. 1). One possible mechanism for specific excision is reciprocal recombination between two DNA sequences present as direct repeats at the end of the excised region. If there are more than two repeats present on the plasmid molecules, the deleted sequence will be determined by the recombination switch points between specific repeats. pJP4 contains three such direct repeats (Ghosal *et al.*, 1985) and undergoes deletions of a 15 to 18 kbp segment when selected for growth on 3-CBA alone (Ghosal *et al.*, 1985), and about 40 kbp are deleted with the loss of growth on 2,4-D$^+$ and 3-CBA$^+$ (Don & Pemberton, 1985). A similar situation may be the case for pEST4011, in which the loss of the 2,4-D$^+$ and 3-CBA$^+$ phenotypes occurs by the excision of a 42 kbp sequence.

It is interesting to note that pEST4011 showed homology only with the regions coding for the degradative genes (*tfdA–F*) and regulatory genes *tfdS* and *tfdR*

COR-AAD1-00002681
Bayer EX1008 (Part 5 of 9)

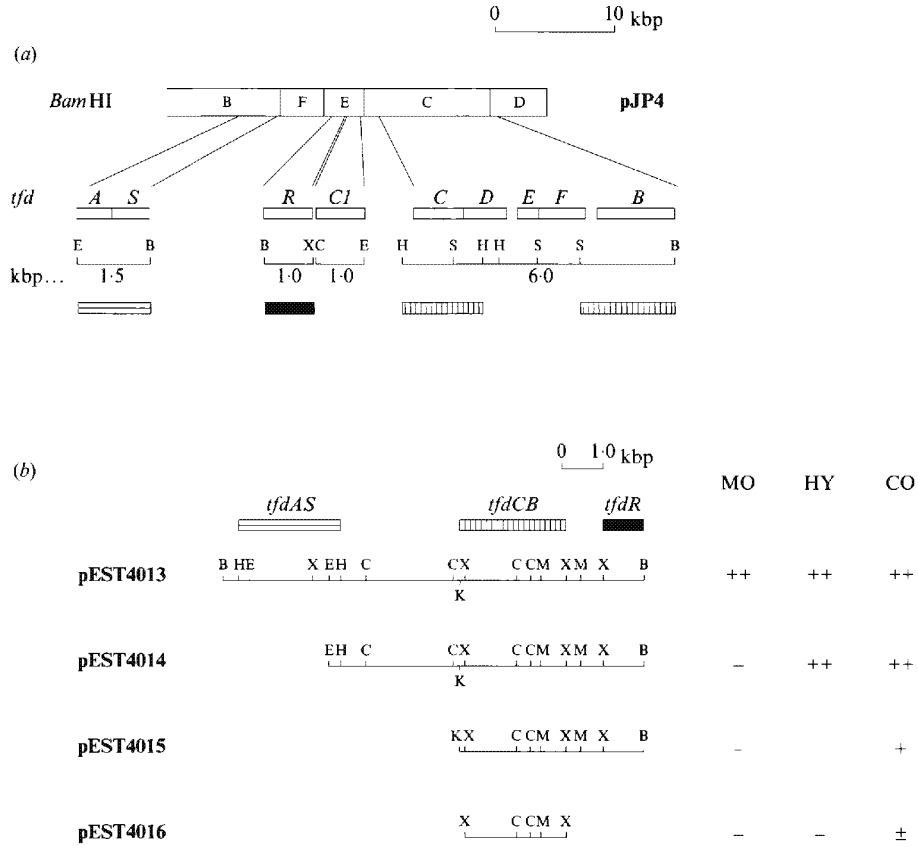


Fig. 2. (*a*) Map of pJP4 based on data from Kaphammer *et al.* (1990) and Perkins *et al.* (1990). The approximate locations of *tfdA*, *tfdS*, *tfdR*, *tfdCDEF* and *tfdB* are shown. (*b*) Cloning of DNA fragments of pEST4011 in *P. putida* PaW85 using the broad-host-range vector pKT240. Relevant restriction sites of pEST4011 DNA fragments used for cloning are shown for the 10·5 kbp *Bam*HI fragment (B, *Bam*HI; C, *Cla*I; E, *Eco*RI; H, *Hin*dIII; K, *Kpn*I; M, *Mlu*I; S, *Sal*I; X, *Xho*I). Each plasmid listed on the left was subcloned from pEST4013 (pKT240 carrying the 10·5 kbp *Bam*HI-B fragment of pEST4011). The fragments of pEST4013 hybridizing with the pJP4 fragments containing *tfdA* and *tfdS* (⊟), *tfdR* (■), and *tfdC,D,B* (▥) are shown. Expression of *tfd* genes in *P. putida* PaW85 is shown on the right: MO, 2,4-dichlorophenoxyacetic acid monooxygenase activity; HY, 2,4-dichlorophenol hydroxylase activity; CO, chlorocatechol 1,2-dioxygenase activity. ++, strong inducible activity; +, inducible activity; ±, uninducible activity; –, no activity. By the terms 'inducible' and 'uninducible' we mean the following: in an inducible system the enzyme activities differ at least fivefold when an inducer compound is used or not; in the uninducible system the enzymes exhibit a low constitutive level of expression independent of the presence or absence of the inducer.

of pJP4. This supports other evidence that 2,4-D degradative plasmids demonstrate appreciable homology between the genes encoding enzymes that catalyse the same steps in breakdown of 2,4-D and related compounds (Chaudhry & Huang, 1988).

By using DNA–DNA hybridization, DNA cloning techniques and enzyme assays we established the location of at least three catabolic genes encoding the first three steps in the 2,4-D degradation pathway: 2,4-D monooxygenase (*tfdA*), 2,4-D dichlorophenol hydroxylase (*tfdB*) and chlorocatechol 1,2-dioxygenase (*tfdC*) on the 10·5 kbp *Bam*HI-B fragment of pEST4011. On the basis of hybridization with the *tfdR* probe from pJP4 and the results of gene expression from pEST4015 and pEST4016, we have assigned the *tfdR* gene to the right-hand of the *Bam*HI-B fragment of plasmid pEST4011 (Fig. 2*b*). Testing enzyme activities in pEST4014 and pEST4015 verified the location of the second regulatory gene, *tfdS* needed for the inducible expression of 2,4-DCP hydroxylase, the product of gene *tfdB*. It is possible that this regulator could be an analogue for *tfdS* present in pJP4.

In spite of the strong homology between catabolic and regulatory genes of 2,4-D pathways in pJP4 and pEST4011, the order of these genes on the two plasmids is completely different (Fig. 2*a*, *b*). A further comparative study of the nucleotide sequence of catabolic genes in pEST4011, pJP4 and related plasmids would widen our understanding of the unique differences and evolutionary relationship between different 2,4-D degradative plas-

COR-AAD1-00002682
Bayer EX1008 (Part 5 of 9)

mids in strains isolated from different geographical regions of the world.

We thank P. A. Broda and P. A. Williams for critical reading of the manuscript. *A. eutrophus* JMP134(pJP4) was the gift of H.-J. Knackmuss.

References

AMY, P. S., SCHULKE, J. W., FRAZIER, L. M. & SEIDLER, R. J. (1985). Characterization of aquatic bacteria and cloning of genes specifying partial degradation of 2,4-dichlorophenoxyacetic acid. *Applied and Environmental Microbiology* **49**, 1237–1245.

AUSMEES, N. R. & HEINARU, A. L. (1990). New plasmids of herbicide 2,4-D degradation. *Genetika* **26**, 770–772 (in Russian).

BAGDASARIAN, M. & TIMMIS, K. N. (1982). Host vector systems for gene cloning in *Pseudomonas*. *Current Topics of Microbiology and Immunology* **96**, 46–67.

BAGDASARIAN, M. M., AMANN, E., LURZ, R., RUECKERT, B. & BAGDASARIAN, M. (1983). Activity of the hybrid *trp.lac(tac)* promotor of *Escherichia coli* in *Pseudomonas putida*. Construction of broad-host-range controlled-expression vectors. *Gene* **26**, 273–282.

BAUCHOP, T. & ELSDEN, S. R. (1960). The growth of microorganisms in relation to their energy supply. *Journal of General Microbiology* **23**, 469–495.

BAYLEY, S. A., DUGGLEBY, C. J., WORSEY, M. J., WILLIAMS, P. A., HARDY, K. G. & BRODA, P. (1977). Two modes of loss of the TOL function from *Pseudomonas putida* mt-2. *Molecular and General Genetics* **154**, 203–204.

BRADFORD, M. (1976). A rapid and sensitive method for the quantitation of microgram quantities of protein utilizing the principle of protein-dye binding. *Analytical Biochemistry* **72**, 248–254.

CHAUDHRY, G. R. & HUANG, G. H. (1988). Isolation and characterization of a new plasmid from *Flavobacterium* sp. which carries the genes for degradation of 2,4-dichlorophenoxyacetate. *Journal of Bacteriology* **170**, 3897–3902.

CONNORS, M. A. & BARNSLEY, E. A. (1982). Naphthalene plasmids in *Pseudomonas*. *Journal of Bacteriology* **91**, 1140–1154.

DITZELMÜLLER, G., MICHAEL, L. & STREICHSBIER, F. (1989). Isolation and characterization of a 2,4-dichlorophenoxyacetic acid-degrading soil bacterium. *Applied Microbiology and Biotechnology* **31**, 93–96.

DON, R. H. & PEMBERTON, J. M. (1981). Properties of six pesticide degradation plasmids isolated from *Alcaligenes eutrophus* and *Alcaligenes paradoxus*. *Journal of Bacteriology* **145**, 681–686.

DON, R. H. & PEMBERTON, J. M. (1985). Genetic and physical map of the 2,4-dichlorophenoxyacetic acid-degradative plasmid pJP4. *Journal of Bacteriology* **161**, 466–468.

DON, R. H., WEIGHTMAN, A. J., KNACKMUSS, H. J. & TIMMIS, K. N. (1985). Transposon mutagenesis and cloning analysis of the pathways for degradation of 2,4-dichlorophenoxyacetic acid and 3-chlorobenzoate in *Alcaligenes eutrophus* JMP134(pJP4). *Journal of Bacteriology* **161**, 85–90.

DOWNING, R. & BRODA, P. A. (1979). Cleavage map of the TOL plasmid of *Pseudomonas putida* mt-2. *Molecular and General Genetics* **177**, 189–191.

GHOSAL, D. & YOU, I.-S. (1988). Nucleotide homology and organization of chlorocatechol oxidation genes of plasmid pJP4 and pAC27. *Molecular and General Genetics* **211**, 113–120.

GHOSAL, D. & YOU, I.-S. (1989). Operon structure and nucleotide homology of the chlorocatechol oxidation genes of plasmids pJP4 and pAC27. *Gene* **83**, 225–232.

GHOSAL, D., YOU, I.-S., CHATTERJEE, D. K. & CHAKRABARTY, A. M. (1985). Plasmids in the degradation of chlorinated aromatic compounds. In *Plasmids in Bacteria*, pp. 667–686. Edited by D. R. Helinski, S. N. Cohen, D. B. Clewell, D. A. Jackson & A. Hollaender. New York: Plenum Press.

GIBSON, T. J. (1984). *Studies on the Epstein–Barr virus genome*. PhD thesis, Cambridge University, Cambridge (UK).

HAGEMAN, G. D. (1966). Synthesis of the enzymes of the mandelate pathway by *Pseudomonas putida*. I. Synthesis of the enzymes by the wild-type. *Journal of Bacteriology* **91**, 1140–1154.

HANAHAN, D. (1983). Studies on transformation of *E. coli* with plasmids. *Journal of Molecular Biology* **166**, 577–580.

HANSEN, J. E. & OLSEN, R. H. (1978). Isolation of large bacterial plasmids and characterization of the P2 incompatibility group plasmids pGM1 and pGM5. *Journal of Bacteriology* **135**, 227–238.

HARKER, A. R., OLSEN, R. H. & SEIDLER, R. J. (1989). Phenoxyacetic acid degradation by the 2,4-dichlorophenoxyacetic acid (TFD) pathway of plasmids pJP4: mapping and characterization of the TFD regulatory gene *tfdR*. *Journal of Bacteriology* **171**, 314–320.

KAPHAMMER, B. & OLSEN, R. H. (1990). Cloning and characterization of *tfdS*, the repressor–activator gene of *tfdB*, from the 2,4-dichlorophenoxyacetic acid catabolic plasmid pJP4. *Journal of Bacteriology* **172**, 5856–5862.

KAPHAMMER, B., KUKOR, J. J. & OLSEN, R. H. (1990). Regulation of *tfd* CDEF by *tfdR* of 2,4-dichlorophenoxyacetic acid degradation plasmid pJP4. *Journal of Bacteriology* **172**, 2280–2286.

MANIATIS, T., FRITSCH, E. F. & SAMBROOK, J. (1982). *Molecular Cloning. A Laboratory Manual. Cold Spring Harbor, NY: Cold Spring Harbor Laboratory.*

PEMBERTON, J. M. & FISHER, P. R. (1977). 2,4-D plasmids and persistence. *Nature, London* **268**, 732–733.

PERKINS, E. J., GORDON, M. P., CACERES, D. & LURQUIN, P. F. (1990). Organization and sequence analysis of the 2,4-dichlorophenol hydroxylase and dichlorocatechol oxidative operons of plasmid pJP4. *Journal of Bacteriology* **172**, 2351–2359.

PIERCE, G. E., FACKLAM, T. J. & RICE, J. M. (1981). Isolation and characterization of plasmids from environmental strains of bacteria capable of degrading the herbicide 2,4-D. *Developments in Industrial Microbiology* **22**, 401–408.

SOUTHERN, E. M. (1975). Detection of specific sequences among DNA fragments separated by gel electrophoresis. *Journal of Molecular Biology* **98**, 503–517.

YANISCH-PERRON, C., VIEIRA, J. & MESSING, J. (1985). Improved M13 phage cloning vectors and host strains: nucleotide sequences of the M13 mp18 and pUC19 vectors. *Gene* **33**, 103–119.

COR-AAD1-00002683
Bayer EX1008 (Part 5 of 9)

Microbiology (1996), **142**, 1115–1122 Printed in Great Britain

Degradation of 2,4-dichlorophenoxyacetic acid by haloalkaliphilic bacteria

Olga Maltseva, Catherine McGowan, Roberta Fulthorpe† and Patrick Oriel

Author for correspondence: Olga Maltseva. Tel: +1 517 353 7858. Fax: +1 517 353 2917. e-mail: 23142ovm@msu.edu

Center for Microbial Ecology and Department of Microbiology, Michigan State University, East Lansing, Michigan 48824, USA

Three 2,4-dichlorophenoxyacetic acid (2,4-D)-degrading bacterial isolates were obtained from the highly saline and alkaline Alkali Lake site in southwestern Oregon contaminated with 2,4-D production wastes. While similar in most respects, the three isolates differed significantly in 2,4-D degradation rates, with the most active strain, I-18, demonstrating an ability to degrade up to 3000 mg 2,4-D l^{-1} in 3 d. This strain was well adapted to the extreme environment from which it was isolated, growing optimally on 2,4-D at pH 8·4–9·4 and at sodium ion concentrations of 0·6–1·0 M. According to its optimum salt concentration and pH for growth, this isolate was a moderately halophilic, alkaliphilic bacterium. The 16S RNA gene sequence (303 nt) was identical for all three isolates and most closely resembled those of the moderately halophilic eubacteria of the family *Halomonadaceae* (91% identity). Biochemical and genetic examination revealed strain I-18 utilizes the same 2,4-D degradation pathway as most of the 2,4-D-degrading bacteria from non-extreme environments. Hybridization data and comparison of the partial sequences of the *tfdA* gene from the Alkali Lake isolates with those of bacteria from non-extreme environments suggested a common genetic origin of the 2,4-D degradation pathway in the two groups of micro-organisms.

Keywords: *Halomonadaceae*, 2,4-dichlorophenoxyacetic acid, degradation of chloroaromatic compounds, halophilic bacteria, alkaliphilic bacteria

INTRODUCTION

The critical role of micro-organisms in the degradation of organic pollutants is well known. Although the micro-organisms capable of degradation of organic pollutants and their catabolic pathways have been investigated intensively, information on the microbial degradation of xenobiotics in environments of high salinity and alkalinity is still very limited (Oren *et al.*, 1992). Comparison of analogous catabolic enzymes and pathways of phylogenetically diverse bacteria isolated from extreme and moderate environments should provide information regarding their metabolic diversity. The study of xenobiotic-degrading extremophiles may also help in evaluating their use in bioremediation of contaminated saline and/or alkaline environments.

The 2,4-dichlorophenoxyacetic acid (2,4-D) degradation pathway is one of the best understood, and provides a good model for such investigations. This herbicide has been released into the environment for more than 40 years, and is degraded in soils fairly rapidly. Many bacteria of different genera are able to completely degrade 2,4-D (Don & Pemberton, 1981; Chaudhry & Chapalamadugu 1991; Häggblom, 1992). Degradation of 2,4-D via oxidative cleavage of the ether bond with subsequent chlorophenol hydroxylation followed by the modified *ortho*-cleavage pathway of chlorocatechols has been demonstrated for most of these isolates. This pathway has been most extensively studied using *Alcaligenes eutrophus* strain JMP134(pJP4) (Don & Pemberton, 1981, 1985). The enzymes participating in the 2,4-D degradation pathway

†**Present address:** Division of Physical Sciences Scarborough Campus, University of Toronto, 1265 Military Trail, Scarborough, Ontario M1C 1A4, Canada.

Abbreviation: 2,4-D, 2,4-dichlorophenoxyacetic acid.

The GenBank accession numbers for the partial nucleotide sequences of the *tfdA* gene and 16S ribosomal RNA from the Alkali Lake isolates reported in this paper are U22499 and U22836, respectively. (The two sequences were identical in the three isolates studied.)

COR-AAD1-00002684
Bayer EX1008 (Part 5 of 9)

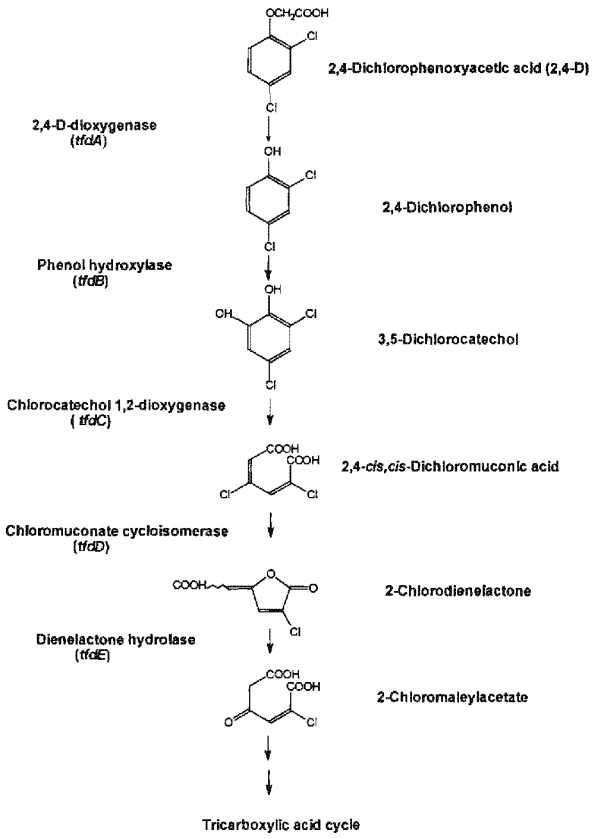


Fig. 1. Pathway for the degradation of 2,4-D in *A. eutrophus* strain JMP134.

have been purified and characterized, and genes that code for these enzymes (*tfdA*, *tfdB*, *tfdCDEF*) have been sequenced (Ghosal & You, 1988, 1989; Perkins *et al.*, 1990; Kuhm *et al.*, 1990; Schlömann *et al.*, 1990; Häggblom, 1992; Fukumori & Hausinger, 1993; Seibert *et al.*, 1993). The pathway is summarized in Fig. 1.

We now report on the isolation and characterization of 2,4-D-degrading bacteria of the family *Halomonadaceae* as a first example of moderately halophilic bacteria capable of complete mineralization of chloroaromatic compounds.

METHODS

Site description and sample collection. Alkali Lake and West Alkali Lake are hypersaline alkaline lakes in the high desert of southwestern Oregon. The groundwater in the vicinity of the lakes has a salinity near 10 % due to sodium chloride and sodium carbonate, and a pH of 9·5–10 (Pankow *et al.*, 1984). Between 1969 and 1971 the area separating Alkali Lake and West Alkali Lake was used as a waste storage area. In 1976 approximately 6000 tonnes 2,4-D herbicide production waste were released into the site by the crushing of waste drums in shallow covered trenches. The groundwater in this site is within about 1 m of the surface and is now contaminated with high levels of monochloro-, dichloro- and trichlorophenols, and also with 2,4-D, 4-methyl-2-chlorophenoxyacetic acid and related halo-aromatic compounds (Pankow *et al.*, 1984; Johnson *et al.*, 1985). Samples used in this study were taken from soil just above groundwater level across the contaminant plume gradient in April 1993 in cooperation with the State of Oregon Department of Environmental Quality.

Medium. The alkaline mineral medium 1 (AMM1), pH 9·5, was prepared by mixing sterile component A (20 g Na_2CO_3 and 20 g $NaHCO_3$ in 300 ml H_2O), component B [40 g NaCl, 3 g KCl, 0·5 g NH_4NO_3, 0·3 g $(NH_4)_2SO_4$, 0·4 g $MgSO_4$, 0·3 g NaH_2PO_4 and trace elements (Imhoff & Trüper, 1977) in 700 ml H_2O] and vitamins (Wolin *et al.*, 1963). $MgSO_4$, NaH_2PO_4 and vitamins were made as 1000 × stock solutions and sterilized separately. Alkaline mineral medium 2, pH 9·4, with decreased carbonate concentration (AMM2) was used in some experiments. It contained 5 g Na_2CO_3 and 5 g $NaHCO_3$ in component A. AMM agar was prepared by adding 20 g agar to component B before sterilization. Prior to mixing, all solutions were cooled to room temperature or, in the case of AMM agar media, at least to about 45 °C. The carbon sources and their concentrations were 2,4-D (50–3000 mg l^{-1}) and yeast extract (50–500 mg l^{-1}).

Enrichment. Soil samples collected at six points across the contaminant plume gradient were combined. Subsamples (5 g) of the mixture was added to 200 ml AMM1 in Erlenmeyer flasks and incubated aerobically at 30 or 37 °C. Cultures were grown statically or on a rotary shaker at 200 r.p.m. 2,4-D (50 mg l^{-1}) was used as the only carbon source. In the case of complete disappearance of 2,4-D from enrichment cultures, repeated additions (from two to five) were used to supply micro-organisms with growth substrate. The ability to degrade 2,4-D was evaluated by HPLC and by measurement of the $^{14}CO_2$ evolution from ^{14}C-labelled 2,4-D (see below). Enrichments demonstrating 2,4-D degradation (5 ml) were transferred to fresh AMM1 (50 ml) containing 50 mg yeast extract l^{-1} and 200 mg 2,4-D l^{-1}. These enriched samples were plated onto AMM1 agar plates containing 500 mg 2,4-D l^{-1}. For purification of isolates, single colonies were selected and transferred onto AMM1 plates containing 500 mg 2,4-D l^{-1}. Confirmation of 2,4-D degradation was carried out by inoculating each isolate into liquid AMM1 containing 50 mg yeast extract l^{-1} and 200 mg 2,4-D l^{-1} and determination of both increase of OD_{550} and disappearance of herbicide. Liquid AMM1 with the same concentrations of yeast extract and 2,4-D, but without microbial cultures, was used as a control.

Catabolism of ^{14}C-labelled 2,4-D. For isotopic experiments, the reaction mixture contained in a 1·5 ml microcentrifuge tube 0·25 ml AMM1, 0·25 ml enrichment cultures and 50 mg l^{-1} ring-labelled 2,4-D [Sigma, specific activity 20·2 mCi $mmol^{-1}$ (747 MBq $mmol^{-1}$), 0·05 μCi per sample]. A control tube contained only labelled 2,4-D and AMM1 without enrichment cultures. The tubes were inserted into scintillation vials containing on the bottom 1 ml phenethylamine as a trapping agent. Vials were closed with caps and incubated on a rotary shaker at 150 r.p.m. for 3 d. At the end of the incubation period the microcentrifuge tubes were removed from the scintillation vials and 10 ml of the Bio-Safe II scintillation cocktail was added to the trapping agent. Radioactivity was measured using an LKB 1211 Rackbeta liquid scintillation counter with appropriate correction for quenching.

High performance liquid chromatography (HPLC). This was performed with a Hewlett-Packard series 1050 chromatograph equipped with a multiple wavelength detector set at 230 nm. Separation was achieved on a reversed-phase Lichrosorb RP-18 column (Merck) of internal diameter 4 mm and length 250 mm.

COR-AAD1-00002685
Bayer EX1008 (Part 5 of 9)

The flow rate was 1·5 ml min^{-1}. Compounds were detected at 230 nm. The mobile phase was an aqueous solution of 40 % (v/v) methanol and 0·1 % (w/v) H_3PO_4.

Utilization of other aromatic compounds as sources of carbon and energy. Growth on aromatic compounds was measured in AMM with benzoic, 3-hydroxy- and 4-hydroxybenzoic acids supplied at 300 mg l^{-1}; 2-chloro-, 3-chloro- and 4-chlorobenzoic acids, and 2-methyl-4-chlorophenoxyacetic acid supplied at 150 mg l^{-1}; and monochlorophenols, 2,4-dichloro-, 2,6-dichloro- and 2,4,6-trichlorophenol, and 2,4,5-trichlorophenoxyacetic acid supplied at 30 mg l^{-1}. Cultures were analysed for increase in OD and removal of the aromatic compound from the medium.

Determination of optimal growth conditions. The specific growth rates under various conditions were analysed during exponential growth by linear regression of the logarithm of OD_{550} with time. Salt dependency of growth was determined in AMM1 and AMM2 containing various concentrations of NaCl (0 1·8 M) in component B. To determine the pH optima for growth, media pH was varied by mixing component B of AMM with various buffer systems: 40 mM HEPES, pH 6·8–7·5; 40 mM Tris, pH 7·1–8·9; and 200 mM $Na_2CO_3/NaHCO_3$ buffer, pH 8·6–10·6. The pH values reported here are the initial ones, but they varied less then 0·2 units during growth of the culture. All media were supplemented with NaCl to keep the sodium ion concentration near 0·8 M.

Fatty acid analysis. The fatty acid methyl ester analysis of lipids was performed by MIDI Laboratories (Newark, DE). Isolate I-18 was precultured on AMM1 agar supplemented with 2 g 2,4-D l^{-1} and streaked onto plates of tryptic soy agar (TSA) containing 10 % (w/v) NaCl. Plates were incubated for 4 d. Saponification, methylation and extraction were performed as described by Sasser & Wichman (1991).

Preparation of cell-free extracts and enzyme assay. Strain I-18 was grown on AMM1 containing 2000 mg 2,4-D l^{-1} and 50 mg yeast extract l^{-1} for 36 h, then harvested by centrifugation and washed twice with 50 mM Tris/HCl buffer, pH 8·0 containing 0·1 mM dithiothreitol and 2 mM $MnSO_4$. After disruption of the cells by sonication for 2 min at 0 °C, cell-free extracts were separated from whole cells and cell debris by centrifugation at 25000 ***g*** for 40 min at 5 °C.

Activities of the modified *ortho*-cleavage pathway enzymes were measured spectrophotometrically using a Perkin-Elmer Coleman 124 instrument (USA). One unit of enzyme activity was defined as the amount of enzyme that catalysed the formation of 1 μmol product min^{-1} at room temperature. Activities of chlorocatechol 1,2-dioxygenase (EC 1.13.11.1), chloromuconate cycloisomerase (EC 5.5.1.7) and dienelactone hydrolase (EC 3.1.1.45) were determined as described previously (Dorn & Knackmuss, 1978; Maltseva *et al.*, 1994).

Protein concentrations were determined using a Bio-Rad Protein Assay Kit with bovine serum albumin as a standard.

DNA extraction and Southern hybridization. Strain I-18 was cultured with 2,4-D as growth substrate as described above. Strains P-3 and I-17 were grown on AMM1 containing 1 g sodium pyruvate l^{-1} and 200 mg 2,4-D l^{-1}. The miniprep method of Ausubel *et al.* (1987) was used to extract total genomic DNA. *Eco*RI-digested DNA was separated by gel electrophoresis on an 0·8 % (w/v) agarose gel and blotted onto Hybond-N nylon membranes (Amersham). The probes were internal segments of the *tfdA*, *tfdB*, *tfdC* and *tfdD* genes of *A. eutrophus* JMP134(pJP4) (Holben *et al.*, 1992). All probes were labelled with digoxigenin dUTP using a DNA labelling kit (Boehringer-Mannheim) according to the manufacturer's instructions. Hybridizations were performed at three different stringencies as described by Fulthorpe *et al.* (1995).

PCR amplification and sequencing of PCR products. The 16S ribosomal RNA genes were amplified using rD1 and fD1 primers (Weisburg *et al.*, 1991). The *tfdA* genes were amplified using primers TV1 and TV2 designed by Tatiana Vallaeys and Alice Wright and synthesized at the Macromolecular Facility, Michigan State University (Vallaeys *et al.*, 1996). The PCR reaction mixtures were prepared according to the manufacturer's protocol (Perkin Elmer Cetus). Thermal cycling was done in a Perkin Elmer 9700 Thermal Cycler using the following conditions: melting at 92 °C for 1 min; cycling 35 times at 92 °C for 1 min 10 s, 55 °C for 30 s and 72 °C for 2 min 10 s; followed by a final extension at 72 °C for 6 min 10 s. Amplified products were purified using a Gene Clean kit (BIO 101). Sequencing was carried out at Michigan State University Sequencing Facility using the Applied Biosystems Model 373A automatic sequencer (Perkin Elmer Cetus) and fluorescently labelled dye termination. The sequencing primer used for 16S was 519R (5′-GTA TTA CCG CGG CTG CTG G-3′) (Lane *et al.*, 1985). Partial sequences were compared to data in GenBank using the Basic Local Alignment Search Tool (BLAST) from the National Center for Biotechnology Information (Altschul *et al.*, 1990) and also the database of the Ribosomal Database Project (Larsen *et al.*, 1993).

Chemicals. Catechol was purchased from Sigma and 4-chlorocatechol from Helix Biotech Corporation. 3-Chlorocatechol and 3,5-dichlorocatechol, and *cis*-dienelactone were kind gifts from M. Schlömann, Universität Stuttgart, and W. Reineke, Bergische Universität-Gesamthochschule Wuppertal, respectively. Chloromuconic acids were prepared as described by Kuhm *et al.* (1990) using partially purified chlorocatechol dioxygenase kindly supplied by M. Schlömann and M. Vollmer, Universität Stuttgart.

RESULTS

Characterization of isolates

Three strains able to degrade 2,4-D were isolated from the enrichments and designated P-3, I-17 and I-18. On AMM1 agar supplemented with 1 g yeast extract l^{-1} and 1 g Casamino acids l^{-1} these bacteria initially produced small transparent colonies, progressing into yellow colonies with tan pigmentation in the centre and a lobate edge. The isolates grew well at 30 °C, but no growth was observed at 37 °C. All strains were Gram-negative, motile rods. Electron microscopy revealed cells of isolate I-18 to be about 1·7–1·9 μm in length and about 0·6–0·7 μm in diameter (data not shown).

The sequences of approximately 303 nucleotides, corresponding to the *E. coli* 16S RNA gene sequence from nt 211 to 513, were identical for all three isolates and showed strong similarity to 16S RNA sequences of the moderately halophilic eubacteria. The highest identity was found with *Halomonas elongata* ATCC 33173 (91·4 %), *Halovibrio variabilis* DSM 3051 (91·1 %), *Deleya halophila* DSM 4770 (89·8 %), *Halomonas meridiana* DSM 5425 (89·8 %) and *Deleya marina* ATCC 25374 (89·8 %).

The major fatty acids of isolate I-18 and their concentration ranges were 10:0 (3·56–4·52 %), 12:0 3-OH (2·81–3·58 %), 14:0 (1·94–2·40 %), 16:0 (8·46–9·06 %), 16:1 cis 9 (12·24–15·48 %), 17:0 cyclo (4·90–5·90 %) and

COR-AAD1-00002686
Bayer EX1008 (Part 5 of 9)

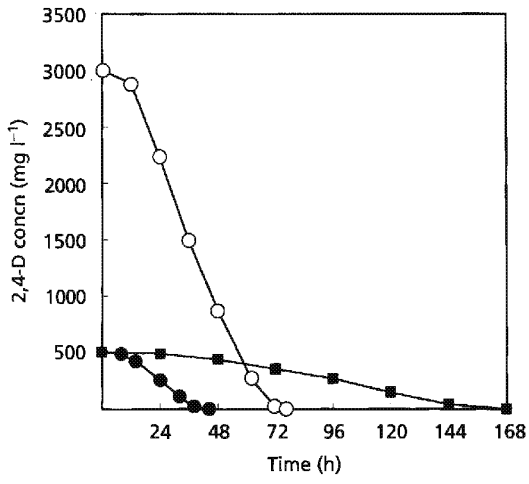


Fig. 2. Influence of yeast extract on 2,4-D degradation by strain I-18. Cells were grown on AMM1, pH 9·5, containing 2,4-D (500 mg l^{-1}) (■) or 2,4-D (500 or 3000 mg l^{-1}) plus yeast extract (50 mg l^{-1}) (●, ○).

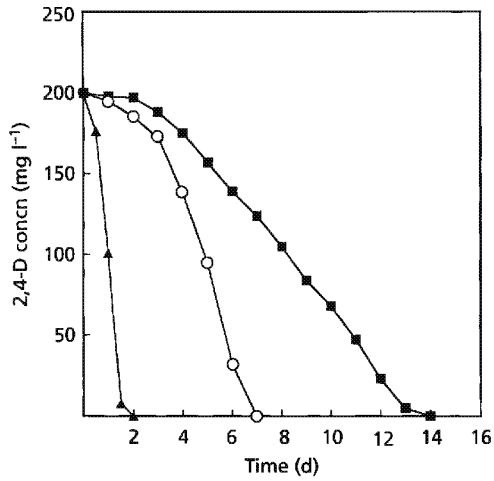


Fig. 3. Degradation of 2,4-D by Alkali Lake isolates I-18 (▲), P-3 (○) and I-17 (■) in AMM1, pH 9·5, supplemented with 50 mg yeast extract l^{-1}.

an unresolved mixture of 18:1 (54·54–56·57 %) and 19:0 cyclo 11-12 (4·41–6·38 %).

Dynamics of 2,4-D degradation

Although the Alkali Lake isolates were able to grow on minimal alkaline medium with 2,4-D as single carbon and energy source, addition of a trace of yeast extract greatly increased the rate of 2,4-D degradation (Fig. 2; data for isolates I-17 and P-3 not shown). While similar in appearance and colony morphology, the three isolates demonstrated significant differences in ability to metabolize 2,4-D (Fig. 3). The growth range and degradation ability of the most active isolate I-18 were examined in more detail. When supplemented with 50 mg yeast extract l^{-1}, strain I-18 demonstrated an ability to degrade 3000 mg 2,4-D l^{-1} over a 3 d period. This strain was able to utilize other aromatic compounds including benzoic acid, *m*-hydroxy- and *p*-hydroxybenzoic acid, 3-chlorobenzoic acid and, less efficiently, 4-chlorophenol and 2,4-dichlorophenol (data not shown). Growth was not observed with 2-chloro- or 4-chlorobenzoic acid, 2-chloro- or 3-chlorophenol or 2,4,5-trichlorophenoxyacetic acid.

Salt effects on the growth of strain I-18

Different NaCl optima were observed during growth of isolate I-18 in AMM1 and AMM2 containing different amounts of sodium carbonates (Fig. 4a). When specific growth rates were plotted against total sodium ion concentration, however, almost coincident curves were obtained, indicating the strong growth response to sodium ions and lesser dependence of growth on carbonate or chloride concentration (Fig. 4b). This organism was able to grow over a wide range of salt concentrations on both yeast extract and 2,4-D. However, the use of complex media supported growth over a wider range of NaCl concentrations than did defined media. The optimal sodium ion concentration for growth was the same on both defined and complex media (0·6–1·0 M), and no growth was observed below 0·1 M.

pH effects on the growth of strain I-18

This was studied in media of different pH and a sodium ion concentration of approximately 0·8 M. The bacterium was able to grow on yeast extract over a wide pH range (6·5–10·5) and had a broad pH optimum (8·2–9·6) (Fig. 5). When grown on defined medium with 2,4-D, a more narrow pH range of the growth was found (7·4–9·8) with the optimum between 8·4 and 9·4.

Degradation pathway of isolate I-18

High activities of catechol 1,2-dioxygenase, muconate cycloisomerase and dienelactone hydrolase were detected in cell-free extracts of isolate I-18 grown on 2,4-D (Table 1). Activities of catechol 1,2-dioxygenase and muconate cycloisomerase were higher with chlorinated than with unsubstituted substrates. The data suggest that haloalkaliphilic strain I-18, like the well-studied strain *A. eutrophus* JMP134(pJP4), uses the modified *ortho*-cleavage pathway for 2,4-D degradation.

Genetic comparison of the 2,4-D degradation pathway in bacteria from extreme and non-extreme environments

No hybridization of the DNA from the Oregon isolate I-18 with the pJP4 genes *tfdA*, *tfdB*, *tfdC* and *tfdD* encoding the first four steps of the 2,4-D degradation pathway in *A. eutrophus* JMP134 was found at high stringency, but positive signals were observed with *tfdA*, *tfdB* and *tfdD* probes at medium stringency and very weak hybridization

COR-AAD1-00002687
Bayer EX1008 (Part 5 of 9)

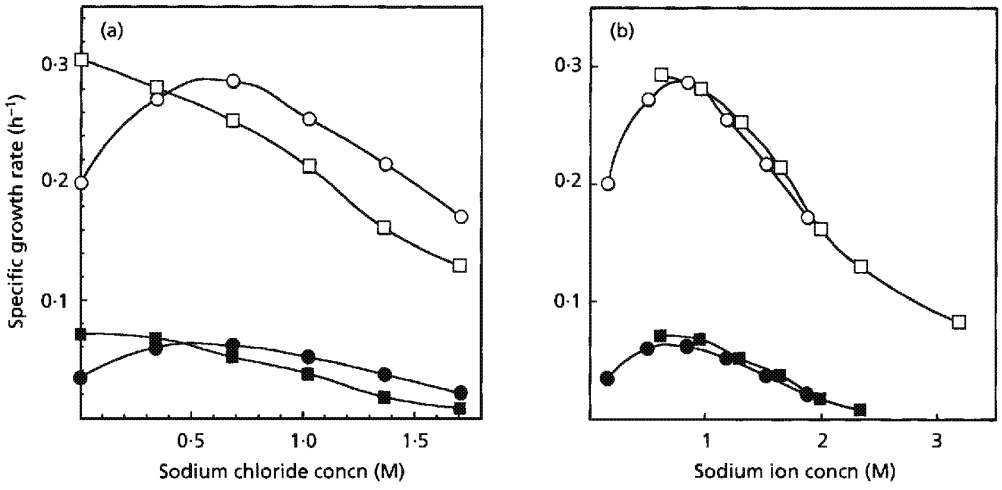


Fig. 4. Influence of sodium chloride (a) and sodium ion concentration (b) on growth of isolate I-18 on yeast extract (500 mg l^{-1}; open symbols) and on 2,4-D (500 mg l^{-1}) plus yeast extract (50 mg l^{-1}) (filled symbols). Cells were grown in AMM1, pH 9·5, containing 20 g Na_2CO_3 l^{-1} and 20 g $NaHCO_3$ l^{-1} (□, ■) or in AMM2, pH 9·4, containing 5 g Na_2CO_3 l^{-1} and 5 g $NaHCO_3$ l^{-1} (○, ●). Both media were supplemented with different concentations of sodium chloride.

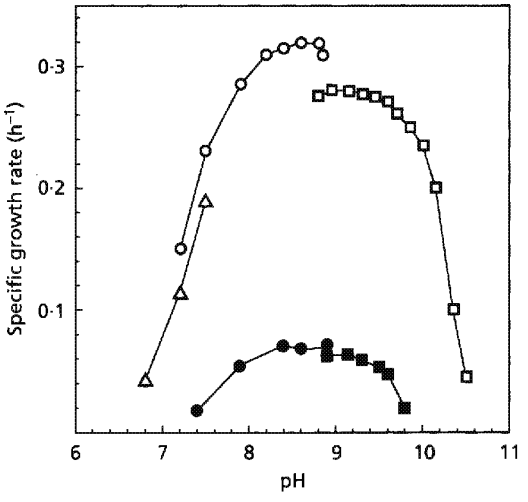


Fig. 5. Influence of pH on growth of isolate I-18 on yeast extract (500 mg l^{-1}; open symbols) or on 2,4-D (500 mg l^{-1}) plus yeast extract (50 mg l^{-1}) (filled symbols). The pH values of the media were adjusted with the following buffer systems: 40 mM HEPES/NaOH (pH 6·8–7·5) (△), 40 mM Tris/HCl (pH 7·1–8·9) (○, ●), and 200 mM Na_2CO_3/$NaHCO_3$ (pH 8·6–10·6) (□, ■). All media were supplemented with NaCl to keep the sodium ion concentration near 0·8 M.

Table 1. Enzyme activities in cell extracts of 2,4-D-grown cells of isolate I-18

Enzyme	Substrate	Specific activity [mU (mg protein)$^{-1}$]	Relative activity (%)*
Catechol 1,2-dioxygenase	Catechol	110	100
	3-Chlorocatechol	61	55
	4-Chlorocatechol	81	74
	3,5-Dichlorocatechol	188	171
Muconate cycloisomerase	*cis, cis*-Muconate	17	100
	2-Chloro-*cis, cis*-muconate	43	252
	3-Chloro-*cis, cis*-muconate	56	329
	2,4-Dichloro-*cis, cis*-muconate	33	194
Dienelactone hydrolase	*cis*-Dienelactone	65	

*Relative activities of catechol 1,2-dioxygenase and muconate cycloisomerase are expressed as a percentage of the value with catechol and muconate, respectively.

with *tfdC* was found at low stringency (Fig. 6). Hybridization patterns for all three Alkali Lake isolates were identical (data for isolates I-17 and P-3 not shown). The sizes of all DNA restriction fragments of these isolates hybridizing with *tfdA–D* differed from those of pJP4.

The *tfdA* genes from the Alkali Lake isolates were PCR-amplified and the products sequenced. The sequences of approximately 317 nucleotides, corresponding to the *A. eutrophus* JMP134 *tfdA* gene sequence from nt 449–765, were identical for all three isolates. The partial sequences of these isolates showed strong similarity to *tfdA* sequences of *Burkholderia* sp. strain RASC (formerly *Pseudomonas* sp. TFD3) and *A. eutrophus* JMP134 (94% and 77% identity, respectively) (Perkins *et al.*, 1990; Suwa

COR-AAD1-00002688
Bayer EX1008 (Part 5 of 9)

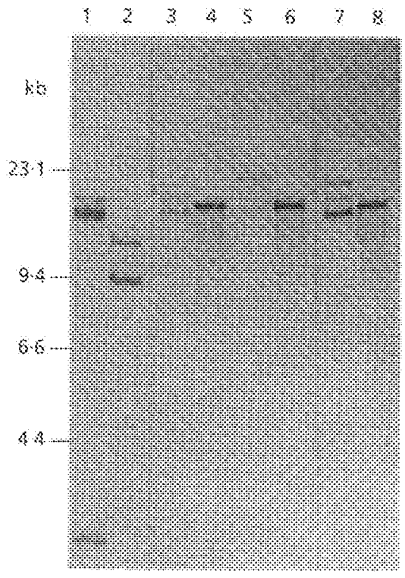


Fig. 6. Low stringency hybridization of pJP4-derived probes *tfdA* (lanes 1 and 2), *tfdB* (lanes 3 and 4), *tfdC* (lanes 5 and 6) and *tfdD* (lanes 7 and 8) with DNA from Alkali Lake isolate I-18 (lanes 1, 3, 5 and 7) and *A. eutrophus* JMP134(pJP4) (lanes 2, 4, 6 and 8) digested with *Eco*RI.

et al., 1994) and were identical to that of strains B6-9 and TFD31 (nucleotide accession number U43196) which were tentatively identified as *Rhodoferax fermentans* (Fulthorpe *et al.*, 1995).

DISCUSSION

Three bacterial isolates capable of complete mineralization of 2,4-D were obtained from the highly saline and alkaline Alkali Lake site. The most active strain, I-18, was well-adapted to the extreme environment from which it was isolated, growing optimally at a sodium ion concentration near 0·6–1·0 M and at pH 8·4–9·4. According to the classification of Kushner & Kamekura (1988), this isolate is a moderately halophilic bacterium. Since micro-organisms with pH optima for growth in excess of pH 8 are defined as alkaliphiles (Grant & Tindall, 1986), strain I-18 should be regarded as a moderately halophilic, alkaliphilic bacterium.

The partial 16S RNA sequences of the three 2,4-D degrading isolates from the Alkali Lake site indicate that they are members of the gamma subdivision of the *Proteobacteria* and belong to the family *Halomonadaceae*, which unifies moderately halophilic eubacteria (Dobson *et al.*, 1993; Franzmann & Tindall, 1990; Franzmann *et al.*, 1988). The 16S RNA sequences obtained for the Alkali Lake isolates had cytosine at position 486 (*Escherichia coli* numbering), as have all the other members of this family examined so far, which is an extremely rare attribute among the prokaryotes (Dobson *et al.*, 1993). It has been shown recently that the three genera of the family *Halomonadaceae* (*Halomonas*, *Deleya* and *Halovibrio*) cannot be resolved on the basis of phylogenetic, chemotaxonomic or phenotypic data and unification of these genera in a single genus has been proposed (Dobson *et al.*, 1993). Until the taxonomy of this group is clarified it is not feasible to assign these bacteria to a species or genus. The close taxonomic relationship of the Alkali Lake isolates and the *Halomonadaceae* indicated by the 16S RNA sequencing data is consistent with the finding that isolate I-18 is a moderately halophilic bacterium. In addition the major fatty acids of isolate I-18 (16:0, 16:1, 17:0 cyc, 18:1 and 19:0 cyc), representing 90% of the total fatty acids, are the same as for other members of the *Halomonadaceae* (Franzmann & Tindall, 1990).

The alkaliphilicity of *Halomonadaceae* strain I-18 is not surprising as it is known that some bacteria of this family are capable of growth at pH 9 and even pH 10 (Del Moral *et al.*, 1988; Vreeland *et al.*, 1980). Recently, it was shown that two groups of alkaliphilic isolates from Kenyan Soda Lakes also belong to the *Halomonadaceae* (Jones *et al.*, 1994).

The Alkali Lake isolates are the first known aerobic, halophilic bacteria able to use chloroaromatic compounds as sources of carbon and energy. Enzyme activities of strain I-18 suggest that it utilizes the same pathway of 2,4-D degradation as the majority of 2,4-D-degrading bacteria from non-extreme environments (Häggblom, 1992). Since the contamination of the Alkali Lake site with chloro-aromatic compounds is recent, the origin of the 2,4-D degradation pathway in the haloalkaliphilic bacteria is of interest. The DNA from all three Alkali Lake isolates hybridized to pJP4 genes *tfdA*, *tfdB*, *tfdC* and *tfdD*, responsible for 2,4-D degradation in the well-known 2,4-D-degrading bacterium *A. eutrophus* JMP134. Moreover, the partial sequences of the *tfdA* genes from the Alkali Lake isolates were only slightly different from the sequence of the *tfdA* gene of *A. eutrophus* JMP134 and identical to that of the 2,4-D-degrading strains *R. fermentans* B6-9 and TFD31 isolated from non-extreme environments in Ontario and Southern Saskatchewan, respectively (Fulthorpe, 1991; Tonso *et al.*, 1995). These data suggest a common origin of the genes encoding 2,4-D degradation in the haloalkaliphilic bacteria and bacteria from non-extreme environments.

An interesting characteristic of moderately halophilic eubacteria is their mode of osmoadaptation. In contrast to the extremely halophilic Archaea that have high intracellular potassium and sodium ion concentrations and enzymes adapted to this environment (Hochstein, 1988), moderately halophilic bacteria can extensively accumulate organic osmolytes called 'compatible solutes' which do not interfere with cell metabolism and may even contribute to enzyme stability (Galinski, 1993). It is not clear whether the enzymes of moderately halophilic eubacteria have special adaptive changes to function optimally in an environment of high osmolarity (Kushner & Kamekura, 1988). The data obtained in this investigation indicate that very similar TfdA enzymes can function efficiently in both halophilic and non-halophilic eubacteria. Complete

COR-AAD1-00002689
Bayer EX1008 (Part 5 of 9)

sequencing of the genes encoding 2,4-D degradation in strain I-18, and study of catabolic gene transfer between halophilic and non-halophilic eubacteria should more firmly establish the compatibility of the enzymes from both groups of micro-organisms and the requirements for engineering xenobiotic-degrading halophilic eubacteria.

ACKNOWLEDGEMENTS

This work was supported by National Science Foundation Science and Technology Center Grant No. BIR 9120006.
We wish to thank Brian McClure of the Oregon Department of Environmental Quality for assistance in sample collection. We are grateful to Helen Gorlew for performing the FAME analysis and to Jacqueline Wood of the MSU Center for Electron Optics for the scanning electron microscopy. We thank Tatiana Vallaeys and Alice Wright for designing the primers used to amplify DNA from *tfdA* genes. We are grateful to M. Schlömann and M. Vollmer for supplying 3-chlorocatechol, 3,5-dichlorocatechol and partially purified chlorocatechol 1,2-dioxygenase and to W. Reineke for *cis*-dienelactone. We also thank Eva Top and Cindy Nakatsu for helpful advice.

REFERENCES

Altschul, S. F., Gish, W., Miller, M., Myers, E. W. & Lipman, D. J. (1990). Basic local alignment search tool. *J Mol Biol* **215**, 403–410.

Ausubel, F. M., Brent, R., Kingston, R. E., Moore, D. D., Smith, J. A., Seidman, J. G. & Struhl, K. (1987). *Current Protocols in Molecular Biology*. New York: John Wiley.

Chaudhry, G. R. & Chapalamadugu, S. (1991). Biodegradation of halogenated organic compounds. *Microbiol Rev* **55**, 59–79.

Del Moral, A., Prado, B., Quesada, E., García, T., Ferrer, R., & Ramos-Comenzana, A. (1988). Numerical taxonomy of moderately halophilic Gram-negative rods from an inland saltern. *J Gen Microbiol* **134**, 733–741.

Dobson, S. J., McMeekin, T. A. & Franzmann, P. D. (1993). Phylogenetic relationships between some members of the genera *Deleya*, *Halomonas*, and *Halovibrio*. *Int J Syst Bacteriol* **43**, 665–673.

Don, R. H. & Pemberton, J. M. (1981). Properties of six pesticide degradation plasmids isolated from *Alcaligenes eutrophus* and *Alcaligenes paradoxus*. *J Bacteriol* **145**, 681–686.

Don, R. H. & Pemberton, J. M. (1985). Genetic and physical map of the 2,4-dichlorophenoxyacetic acid-degradative plasmid pJP4. *J Bacteriol* **161**, 466–468.

Dorn, E. & Knackmuss, H.-J. (1978). Chemical structure and biodegradability of halogenated aromatic compounds. Two catechol 1,2-dioxygenases from a 3-chlorobenzoate grown pseudomonad. *Biochem J* **174**, 73–84.

Franzmann, P. D. & Tindall, B. J. (1990). A chemotaxonomic study of the members of the family *Halomonadaceae*. *Syst Appl Microbiol* **13**, 142–147.

Franzmann, P. D., Wehmeyer, U. & Stackebrandt, E. (1988). *Halomonadaceae* fam. nov., a new family of the class *Proteobacteria* to accommodate the genera *Halomonas* and *Deleya*. *Syst Appl Microbiol* **11**, 16–19.

Fukumori, F. & Hausinger, R. P. (1993). Purification and characterization of 2,4-dichlorophenoxyacetate/α-ketoglutarate dioxygenase. *J Biol Chem* **268**, 24311–24317.

Fulthorpe, R. R. (1991). *Survival, activity and transfer of a bacterial catabolic transposon in an aquatic ecosystem*. PhD thesis, Carleton University, Ottawa.

Fulthorpe, R. R., McGowan, C., Maltseva, O. V., Holben, W. H., & Tiedje, J. M. (1995). 2,4-Dichlorophenoxyacetic acid degrading bacteria are mosaics of catabolic genes. *Appl Environ Microbiol* **61**, 3274–3281.

Galinski, E. A. (1993). Compatible solutes of halophilic eubacteria: molecular principles, water–solute interaction, stress protection. *Experientia* **49**, 487–496.

Ghosal, D. & You, I.-S. (1988). Nucleotide homology and organization of chlorocatechol oxidation genes of plasmids pJP4 and pAC27. *Mol Gen Genet* **211**, 113–120.

Ghosal, D. & You, I.-S. (1989). Operon structure and nucleotide homology of the chlorocatechol oxidation genes of plasmids pJP4 and pAC27. *Gene* **83**, 225–232.

Grant, W. D. & Tindall, B. J. (1986). The alkaline saline environment. In *Microbes in Extreme Environments*, pp. 25–54. Edited by R. A. Herbert & G. A. Cood. London: Academic Press.

Häggblom, M. M. (1992). Microbial breakdown of halogenated aromatic pesticides and related compounds. *FEMS Microbiol Rev* **103**, 29–72.

Hochstein, L. I. (1988). The physiology and metabolism of the extremely halophilic bacteria. In *Halophilic Bacteria*, vol. 2, pp. 67–79. Edited by F. Rodriguez-Valera. Boca Raton, FL: CRC Press.

Holben, W. E., Schroeter, B. M., Calabrese, V. G. M., Olsen, R. H., Kukor, J. K., Biederbeck, V. O., Smith, A. E. & Tiedje, J. M. (1992). Gene probe analysis of soil microbial populations selected by amendment with 2,4-dichlorophenoxyacetic acid. *Appl Environ Microbiol* **58**, 3941–3948.

Imhoff, J. F. & Trüper, H. G. (1977). *Ectothiorhodospira halochloris* sp. nov. a new extremely halophilic phototrophic bacterium containing bacteriochlorophyll b. *Arch Microbiol* **114**, 115–121.

Johnson, R. L., Brillante, S. M., Isabelle, L. M., Houck, J. E. & Pankow, J. F. (1985). Migration of chlorophenolic compounds at the chemical waste disposal site at Alkali Lake, Oregon. 2. Contaminant distribution, transport, and retardation. *Ground Water* **23**, 652–666.

Jones, B. E., Grant, W. D., Collins, N. C. & Mwatha, W. E. (1994). Alkaliphiles: diversity and identification. In *Bacterial Diversity and Sytematics*, pp. 195–230. Edited by F. G. Priest, A. Ramos-Cormenzana & B. J. Tindall. New York & London: Plenum Press.

Kuhm, A. E., Schlömann, M., Knackmuss, H.-J. & Pieper, D. (1990). Purification and characterization of dichloromuconate cycloisomerase from *Alcaligenes eutrophus* JMP134. *Biochem J* **266**, 877–883.

Kushner, D. J. & Kamekura, M. (1988). Physiology of halophilic bacteria. In *Halophilic Bacteria*, vol. 1, pp. 109–138. Edited by F. Rodriguez-Valera. Boca Raton, FL: CRC Press.

Lane, D. J., Pace, B., Olsen, G. J., Stahl, D. A., Sogin, M. L. & Pace, N. R. (1985). Rapid determination of 16S ribosomal RNA sequences for phylogenetic analyses. *Proc Natl Acad Sci USA* **82**, 6955–6959.

Larsen N., Olsen, G. J., Madak, B. L., McCaughey, M. J., Overbeek, R., Make, T. J., Marsh, T. L. & Woese, C. R. (1993). The ribosomal database project. *Nucleic Acids Res* **21**, 3021–3023.

Maltseva, O. V., Solyanikova, I. P., Golovleva, L. A., Schlömann, M. & Knackmuss, H.-J. (1994). Dienelactone hydrolase from *Rhodococcus erythropolis* 1CP: purification and properties. *Arch Microbiol* **162**, 368–374.

Oren, A., Gurevich, P., Azachi, M. & Henis, Y. (1992). Microbial degradation of pollutants at high salt concentration. *Biodegradation* **3**, 387–398.

Pankow, J. F., Johnson, R. L., Houck, J. E., Brillante, S. M. & Bryan, W. J. (1984). Migration of chlorophenolic compounds at the

COR-AAD1-00002690
Bayer EX1008 (Part 5 of 9)

chemical waste disposal site at Alkali Lake, Oregon. 1. Site description and ground-water flow. *Ground Water* **22**, 593–601.

Perkins, E. J., Gordon, M. P., Caceres, O. & Lurquin, P. F. (1990). Organization and sequence analysis of the 2,4-dichlorophenol hydroxylase and dichlorocatechol oxidative operons of plasmid pJP4. *J Bacteriol* **172**, 2351–2359.

Sasser, M. & Wichman, M. D. (1991). Identification of microorganisms through use of gas chromatography and high performance liquid chromatography. In *Manual of Clinical Microbiology*, pp. 11–118. Edited by W. J. Hausler, K. L. Herrmann, H. D. Isenberg & H. J.Shadony. Washington, DC: American Society for Microbiology.

Schlömann, M., Pieper, D. H. & Knackmuss, H.-J. (1990). Enzymes of haloaromatics degradation: Variations of *Alcaligenes* on a theme by *Pseudomonas*. In *Pseudomonas: Biotransformation, Pathogenesis, and Evolving Biotechnology*, pp. 185–196. Edited by S. Silver, A. M. Chakrabarty, B. Iglevsky & S. Kaplan. Washington, DC: American Society for Microbiology.

Seibert V., Stadler-Fritzsche, K. & Schlömann, M. (1993). Purification and characterization of maleylacetate reductase from *Alcaligenes eutrophus* JMP 134 (pJP4). *J Bacteriol* **175**, 6745–6754.

Suwa, Y., Holben, W. E. & Forney, L. J. (1994). Cloning of a novel 2,4-D catabolic gene isofunctional to *tfdA* from *Pseudomonas* sp. TFD3. In *Abstracts of the 94th General Meeting of the American Society for Microbiology*. Washington, DC: American Society for Microbiology.

Tonso, N. L., Matheson, V. G. & Holben, W. E. (1995). Polyphasic characterization of a suite of bacterial isolates capable of degrading 2,4-D. *Microb Ecol* **30**, 1–22.

Vallaeys, T., Fulthorpe, R. R., Wright, A. M. & Soulas, G. (1996). The metabolic pathway of 2,4-dichlophenoxyacetic acid degradation involves different families of *tfdA* and *tfdB* genes according to PCR-RFLP analysis. *FEMS Microbiol Ecol* (in press).

Vreeland, R. H., Litchfield, C. D., Martin, E. L. & Elliot, E. (1980). *Halomonas elongata*, a new genus and species of extremely salt-tolerant bacteria. *Int J Syst Bacteriol* **30**, 485–495.

Weisburg, W. G., Barns, S. M., Pelletier, D. A. & Lane, D. J. (1991). 16S ribosomal DNA amplification for phylogenetic study. *J Bacteriol* **173**, 697–703.

Wolin, E. A., Wolin, M. J. & Wolfe, R. S. (1963). Formation of methane by bacterial extracts. *J Biol Chem* **238**, 2882–2886.

Received 12 September 1995; revised 22 December 1995; accepted 10 January 1996.

COR-AAD1-00002691
Bayer EX1008 (Part 5 of 9)

Journal of Industrial Microbiology & Biotechnology (2000) 25, 255–259
© 2000 Society for Industrial Microbiology 1367-5435/00 $15.00
www.nature.com/jim

Biodegradation of mixtures of chlorophenoxyalkanoic acid herbicides by *Alcaligenes denitrificans*

MW Marriott, CW Smejkal and HM Lappin-Scott

School of Biological Sciences, University of Exeter, Hatherly Laboratories, Prince of Wales Road, Exeter, Devon EX4 4PS, UK

An *Alcaligenes denitrificans* strain able to degrade (*R*)-2-(2-methyl-4-chlorophenoxy)propionic acid [(*R*)-MCPP, mecoprop] was assessed for its ability to utilise a range of chlorophenoxyalkanoic acid herbicides in single, binary, tertiary and quaternary combinations in batch culture. Degradation rates were rapid with single growth substrates; complete degradation occurred within 29 h for 2,4-dichlorophenoxyacetic acid (2,4-D), 43 h for 4-chloro-2-methylphenoxyacetic acid (MCPA) and 50 h for (*R*)-MCPP, respectively. After 20 h, the degradation of (*RS*)-2-(2,4-dichlorophenoxy)propionic acid [(*RS*)-2,4-DP] had ceased, with only the (*R*)-enantiomer being degraded. In binary combination, 2,4-D and MCPP degraded within 55 h. Degradation rates decreased when herbicides were added in tertiary and quaternary combinations. Thus, at the whole cell level, catalysis of closely related herbicides is likely to be facilitated by diverse enzymatic activity in *A. denitrificans*. *Journal of Industrial Microbiology & Biotechnology* (2000) **25,** 255–259.

Keywords: *Alcaligenes denitrificans*; biodegradation; mecoprop; 2,4-D; dichlorprop

Introduction

The phenoxyalkanoic acid herbicides are xenobiotic analogues of the endogenous plant growth regulator, indole acetic acid (IAA). They are widely used in agriculture as they increase crop yields [5]. It is important to investigate the microbial degradation of this group of herbicide [7]. This progressive increase in application has resulted in many soil and aquifer microflora capable of degrading a wide variety of chlorinated aromatic compounds [2,9,27,30] including the phenoxyalkanoic acid herbicides [15,16,18,31,35].

The degradation of individual phenoxy herbicides is well documented, especially for 2,4-dichlorophenoxyacetic acid (2,4-D) [3,8,13,21]. This has been facilitated by the diversity of organisms able to utilise 2,4-D as the sole carbon source thus providing axenic cultures to elucidate the involvement of the *tfd* genes in the assemblage of the degradative pathway [6,33,34]. Similar studies on (*R*)-2-(2-methyl-4-chlorophenoxy)propionic acid (MCPP) degradation have been hampered by the limited number of equivalent pure cultures. More recently bacterial strains have been isolated with the ability to degrade MCPP (Refs. [18,31,35]; Smejkal *et al.*, unpublished) and the MCPP degradation pathway has been elucidated [32,35].

Many phenoxyalkanoic herbicides are applied to cereal crops as mixed formulations to increase the spectrum of weeds killed. Similar mixtures of these herbicides are also found in herbicide manufacturing plant effluents. Therefore, understanding the dynamics of mixed herbicide biodegradation is of great importance. Simultaneous degradation of 2,4-D and mecoprop occurs using mixed bacterial cultures derived from soil [10,22,23]. Reports have suggested that bacterial strains degrading the phenoxyacetic acid herbicides 2,4-D and 4-chloro-2-methylphenoxyacetic acid (MCPA) are unable to degrade the phenoxypropionic acids MCPP and 2-(2,4-dichlorophenoxy)propionic acid (2,4-DP) [11,24]. Some strains were even constrained to the degradation of 2,4-D as a sole carbon source [14]. The selection of mecoprop degrading strains is extremely useful as they have the ability to utilise and degrade both the phenoxypropionic and phenoxyacetic herbicides [4,12,18,31,35]. Although utilisation of alternative phenoxy herbicides by prominent strains has been investigated [11,24], there are limited studies on the biodegradation of combinations of two or more phenoxyalkanoic herbicides [29,30]. This study investigates the ability of *Alcaligenes denitrificans* to utilise a broad spectrum of the phenoxyalkanoic acid herbicides in single, binary, tertiary and quaternary mixtures. This is of extreme importance when assessing the capability of soil bacteria to facilitate degradation of mixtures of these herbicides and can also be a measure of relative persistence in soils.

Correspondence: Dr HM Lappin-Scott, School of Biological Sciences, University of Exeter, Hatherly Laboratories, Prince of Wales Road, Exeter, Devon EX4 4PS, UK
Received 16 April 2000; accepted 7 August 2000

Materials and methods

Chemicals

Technical grade (*R*)-MCPP and MCPA were purchased from Lancaster Synthesis (Morecambe, Lancashire, UK). MSS Optica, the potassium salt of (*R*)-MCPP, was donated by Pennine Chemical Services Ltd. (Huddersfield, West Yorkshire, UK). Technical grade 2,4-D and (*RS*)-2,4-DP were obtained from Sigma Chemicals (Poole, Dorset, UK). Analytical grade (*R*)-MCPP, 2,4-D, MCPA and (*RS*)-2,4-DP were obtained from Promochem Ltd. (St. Albans, Hertfordshire, UK).

COR-AAD1-00002692
Bayer EX1008 (Part 5 of 9)

Herbicide stock solutions

(*R*)-MCPP, MCPA and (*RS*)-2,4-DP were made as stock solutions of 100 g l^{-1}. For this 10.0 g herbicide was added to 100 ml of 0.5 M sodium hydroxide (NaOH) solution and stirred until dissolved, the pH was then adjusted to 7.0. To prevent thermal dechlorination that may occur during conventional autoclaving, the solutions were filter sterilised, using a 0.2-μm pore size Sartorious minisart filter. The 2,4-D stock solution was prepared in the same manner but using 1.0 g of herbicide to give a concentration of 10.0 g l^{-1}.

Growth conditions

The axenic culture of *A. denitrificans* was maintained in 100 ml of minimal medium containing (g l^{-1} of distilled water): $MgSO_4$, 0.2; $(NH_4)_2SO_4$, 0.5; KH_2PO_4, 0.5; K_2HPO_4, 1.5. To this growth medium 1.0 ml of trace element (TES) was added, which contained (g l^{-1} distilled water): Na_2EDTA, 12.0; $FeSO_4$, 2.0; $CaCl_2$, 1.0; $NaSO_4$, 10.0; $ZnSO_4$, 0.4; $MnSO_4$, 0.4; $CuSO_4$, 0.1; Na_2MoO_4, 0.1; and 0.5 ml of concentrated H_2SO_4. The pH of the solution was adjusted to 7.0. The appropriate herbicide was added to give a concentration of 1.0 g l^{-1}.

Herbicide biodegradation

For biodegradation experiments four flasks, each containing 100 ml of minimal medium, 1.0 ml of TES and 1.0 g l^{-1} of the appropriate herbicides were pre-warmed at 28°C for 1–2 h. A 2.0% inoculum of a 24-h culture of *A. denitrificans* was added to three of the flasks, the fourth flask remained uninoculated as a control. *A. denitrificans* cells used in all of the experiments had prior exposure for 24 h to a growth medium containing a combination of 1.0 g l^{-1} of (*R*)-MCPP and 2,4-D. The culture was aerated by shaking it in an orbital shaker at 120 rpm. The temperature was kept at 28°C, the optimum temperature for growth of *A. denitrificans*. Growth of the cells was measured by culture absorbance at 420 nm using a Cecil spectrophotometer. Herbicide degradation was monitored indirectly by chloride ion release and directly by HPLC. Herbicide combinations used were: (a) binary: (*R*)-MCPP and 2,4-D, (b) tertiary: (*R*)-MCPP, 2,4-D and MCPA, (c) quaternary: (*R*)-MCPP, 2,4-D, MCPA and (*RS*)-2,4-DP.

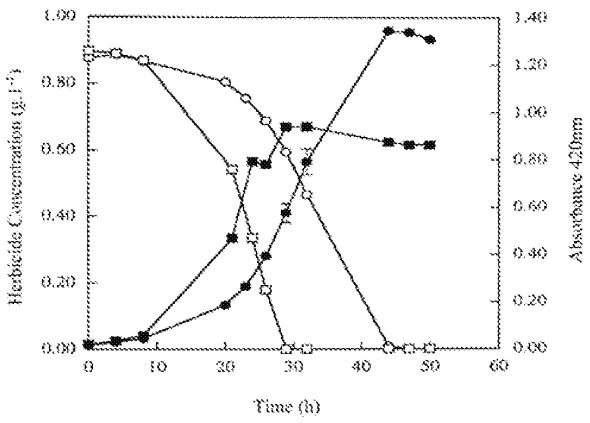


Figure 1 Decrease in concentration of 2,4-D (□) and MCPA (○) in monosubstrate cultures and the concomitant increase in absorbance of 2,4-D (■) and MCPA (●) cultures. Bars = SE, $n = 3$.

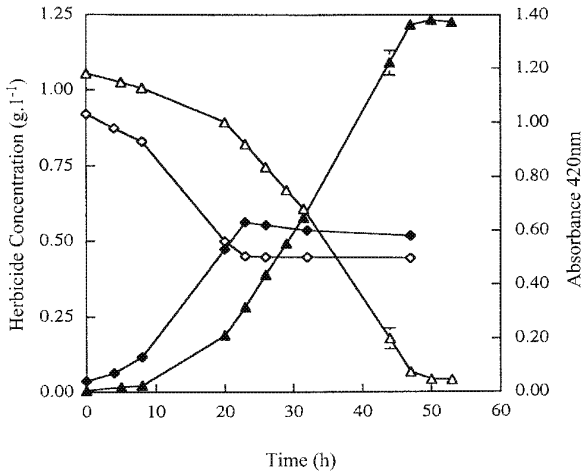


Figure 2 Decrease in concentration of (*R*)-MCPP (△) and (*RS*)-2,4-DP (◇) in monosubstrate cultures and the concomitant increase in absorbance of (*R*)-MCPP (▲) and (*RS*)-2,4-DP (◆) cultures. Bars = SE, $n = 3$.

HPLC analysis

The HPLC system consisted of a pump (Altex), an injector with a 20-μl loop (Rheodyne 7125), and LC-UV detector (Pye Unicam), and an integrator (Shimadzu C-R6A Chromatopac). A 5.0 μm Phenomenex ODS 1 column was eluted with a mobile phase of acetonitrile and phosphate buffer (50:50 v/v) at a flow rate of 1.0 ml min^{-1}, the phosphate buffer of 6.0 g K_2HPO_4 and 3.0 ml of concentrated orthophosphoric acid per litre of HPLC-grade water. The detection signal for all herbicides was monitored at 229 nm. For standard stock solutions of (*R*)-MCPP, 2,4-D, MCPA, and (*RS*)-2,4-DP the compounds were dissolved in 10.0 ml of 0.5 M NaOH before making up the volume to 100 ml with HPLC-grade water. Samples (1.5 ml) of culture were removed from each flask and transferred to an Eppendorf tube, which was centrifuged at 13,000 rpm for 10 min using a Micro Centaur centrifuge; 1.0 ml of the supernatant phase was filter sterilised, using a 0.2-μm Sartorius ministart, into a 5.0-ml vial. The samples were diluted with 1.0 ml 0.5 M NaOH, 1.0 ml HPLC-grade water and 2.0 ml 1.0 M acetic acid. To identify peaks, the retention times recorded with the experimental samples were compared with those of known reference samples. Standard curves were plotted using peak area versus concentrations of standards. HPLC data was used to determine biodegradation rates (milligrams per hour, mg h^{-1}) and percentage biodegradation (%BD) of single and mixed herbicides. Recovery of the parent compounds was estimated to be 60%.

Statistical analysis

All experiments were undertaken in triplicate and the means and standard errors calculated. When appropriate data were compared using ANOVA and considered significant if $P<0.05$ and a comparison between means was performed using a Tukey test.

COR-AAD1-00002693
Bayer EX1008 (Part 5 of 9)

Table 1 Time taken for the biodegradation of each phenoxy acid herbicide in both single- and mixed-formulation batch cultures

Herbicide	Herbicide combination							
	Single		Binary		Tertiary		Quaternary	
	%BD	Hours	%BD	Hours	%BD	Hours	%BD	Hours
(*R*)-(+)-MCPP	97	50	97	50	97	55	90	70
2,4-D	100	29	100	50	99	55	90	70
MCPA	100	43	ND	ND	60	75	40	95
(±)-2,4-DP	50	20	ND	ND	ND	ND	50	70

%BD = percentage biodegradation, ND = not determined.
Single = one herbicide present; binary = (*R*)-MCPP and 2,4-D; tertiary = (*R*)-MCPP, 2,4-D and MCPA; quaternary = (*R*)-MCPP, 2,4-D, MCPA and 2,4-DP.

Correlations were calculated using the Pearson linear correlation coefficient. All statistical calculations were carried out using the Student SYSTAT 1.0 computer package.

Results

Single-substrate biodegradation

A. denitrificans was tested for the ability to degrade 2,4-D, MCPA, (*R*)-MCPP, and (*RS*)-2,4-DP as single substrates (Figures 1 and 2). The degradation of 2,4-D was rapid and complete degradation was reached after 29 h (Figure 1, Table 1). MCPA was also rapidly degraded with complete mineralization after 43 h (Figure 1, Table 1). The overall degradation rates for 2,4-D and MCPA were 33 and 28 mg h^{-1}, respectively (Table 2). After 50 h, 97% of (*R*)-MCPP was degraded (Figure 2, Table 1) at a rate of 22 mg h^{-1}. (*RS*)-2,4-DP was degraded at a significantly faster rate (26 mg h^{-1}) than (*R*)-MCPP (Table 2); however, at 20 h only 50% of the racemic compound had been degraded (Figure 2, Table 1).

Binary-substrate biodegradation

A. denitrificans was tested for the ability to degrade a binary mixture of (*R*)-MCPP and 2,4-D with 97% and 100% mineralization at 55 h (Figure 3, Table 1), respectively. The degradation rate for (*R*)-MCPP was not significantly affected by the presence of 2,4-D; however, the rate of 2,4-D degradation was significantly slower (Table 2).

Table 2 Biodegradation rates of four phenoxy herbicides as single- and mixed-formulation batch cultures

Herbicide	Herbicide combination and biodegradation rate (mg h^{-1})			
	Single	Binary	Tertiary	Quaternary
(*R*)-(+)-MCPP	22	20	18	13
2,4-D	33	18	15	15
MCPA	28	ND	13	5
(±)-2,4-DP	26	ND	ND	6

ND = not determined.
Single = one herbicide present; binary = (*R*)-MCPP and 2,4-D; tertiary = (*R*)-MCPP, 2,4-D and MCPA; quaternary = (*R*)-MCPP, 2,4-D, MCPA and 2,4-DP.

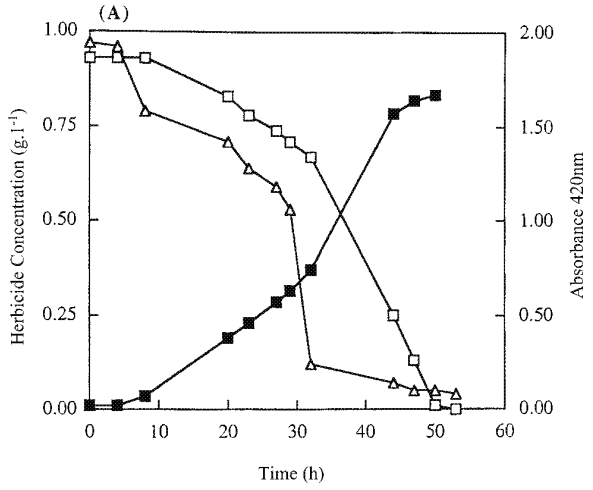


Figure 3 Binary substrate culture biodegradation of (*R*)-MCPP (△) and 2,4-D (□) with the associated increase in absorbance (■). Bars = SE, $n = 3$.

Tertiary-substrate biodegradation

Degradation of the tertiary mixture containing (*R*)-MCPP, 2,4-D and MCPA was assessed (Figure 4). The degradation patterns observed for (*R*)-MCPP and 2,4-D were approximately the same as when incorporated into a binary mixture (Tables 1 and 2). Conversely, MCPA degradation was affected by the presence of both 2,4-D and (*R*)-MCPP as only 60% was degraded as opposed to 100% when utilised as a single substrate. The rate was also significantly reduced from 28 to 13 mg h^{-1} (Table 2).

Quaternary-substrate biodegradation

The degradation of the quaternary mixture of (*R*)-MCPP, 2,4-D, MCPA and (*RS*)-2,4-DP by *A. denitrificans* was also assessed

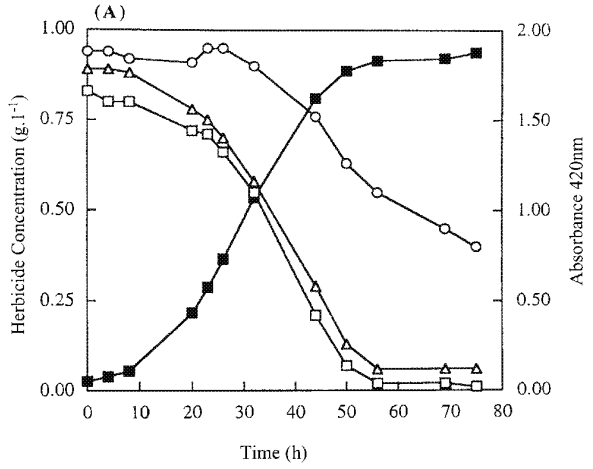


Figure 4 Biodegradation of a tertiary herbicide mixture containing (*R*)-MCPP (△), 2,4-D (□), and MCPA (○) showing associated increase in growth as absorbance at 420 nm (■). Bars = SE, $n = 3$.

COR-AAD1-00002694
Bayer EX1008 (Part 5 of 9)

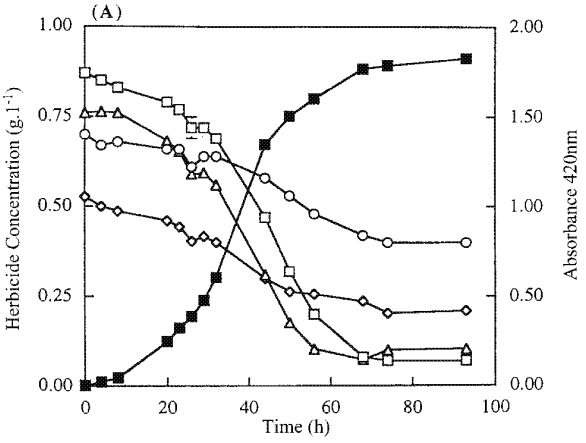


Figure 5 Biodegradation of a quaternary herbicide mixture containing (*R*)-MCPP (△), 2,4-D (□), MCPA (○), and (RS)-2,4-DP (◇) with the associated increase in absorbance (■). Bars = SE, $n = 3$.

(Figure 5). The degradation rate of (*R*)-MCPP and 2,4-D remained relatively unchanged (Table 2) with 90% biodegradation of these compounds being achieved at maximum growth (70 h). The rate of MCPA was significantly reduced to 5 mg h^{-1} with only 40% of the compound being degraded. As with single-substrate degradation, only 50% (*RS*)-2,4-DP was utilised in a quaternary mixture; however, the rate was reduced from 26 to 6 mg h^{-1} (Table 2).

Discussion

In this study we report the ability of *A. denitrificans* to degrade chlorophenoxyalkanoic acid herbicides in single and mixed combinations. It has been reported that this strain has specificity for the (*R*)-enantiomer of MCPP and is unable to degrade the (*S*)-enantiomer [31]. Further work has demonstrated that this strain also has enantiomeric specificity for the (*R*)-enantiomer of 2,4-DP [26] and is supported by the results of this study where only 50% of the racemic mixture was degraded. Many reports have encompassed the study of enantioselective uptake and degradation of chiral compounds [17,28,31,35,36] and it is believed that this is controlled by activation of enantiomer-specific enzymes [20,26]. Such discrimination between the (*R*) and (*S*)-enantiomers is often determined by the initial step of the catabolic pathway [28] where enantiomer- and substrate-specific degradative enzymes are involved. An (*RS*)-MCPP-degrading *Sphingomonas herbicidovorans* MH, was found to carry two distinct α-ketoglutarate dependent dioxygenases, one being specific for the (*R*)-enantiomer and the other for the (*S*), providing this strain with the ability to utilise both MCPP enantiomers [20].

The rate of (*RS*)-2,4-DP degradation was greater than (*R*)-MCPP despite the culture being enriched on the latter. This may be explained by the additional methyl substituent found on the aromatic ring [1]. Single substrate degradation of both 2,4-D and MCPA was achieved after 1–2 days and this is in accordance with data presented for other MCPP-degrading strains [18]. These compounds are achiral and possess a two-, rather than a three-carbon carboxylic acid side chain, thus increasing their susceptibility to degradation.

A. denitrificans effectively degraded 2,4-D and (*R*)-MCPP in binary, tertiary and quaternary combinations and this can be explained by similarities in the *tfdA* gene that encodes α-ketoglutarate-dependent dioxygenase in both MCPP- and 2,4-D-degrading strains (Ref. [26]; Smejkal *et al.*, unpublished). Additionally, in this study *A. denitrificans* had prior exposure to these compounds leading to activation of enzymes with the ability to utilise both 2,4-D and (*R*)-MCPP. The degradation of MCPA was significantly affected in tertiary and quaternary combinations and it is difficult to postulate a feasible explanation for this. Changes in pH has been shown to effect degradation [19,25] by reducing available phosphates.

A. denitrificans has the ability to degrade a wide range of phenoxy herbicides in single and mixed combinations. In biotechnological terms this is extremely useful because effluents containing mixtures of these herbicides can be treated.

The molecular profile of *A. denitrificans* is currently being investigated in our laboratory to determine the role of the *tfd* genes in the assemblage of the mecoprop metabolic pathway. Further studies will determine the levels of enzyme expression when *A. denitrificans* is exposed to varying substrates, providing valuable information on substrate preference in this strain.

Acknowledgements

We thank A.J. Willetts and J.D. Boyle for helpful discussions. We also gratefully acknowledge the award of a NERC studentship to M.W.M.

References

1 Alexander M and MIH Aleem. 1961. Effect of chemical structure on microbial decomposition of aromatic herbicides. *J Agric Food Chem* 9: 44–47.
2 Chaudry GR and S Chapalamadugu. 1991. Biodegradation of halogenated organic compounds. *Microbiol Revs* 55: 59–79.
3 Daugherty DD and SF Karel. 1994. Degradation of 2,4-dichlorophenoxyacetic acid by *Pseudomonas cepacia* DBO1 (pRO101) in a dual-substrate chemostat. *Appl Environ Microbiol* 60: 3261–3267.
4 Ehrig A, RH Müller and W Babel. 1997. Isolation of phenoxy herbicide-degrading *Rhodoferax* species from contaminated building material. *Acta Biotechnol* 17: 351–356.
5 Fletcher WW and RC Kirkwood. 1982. Herbicides as Plant Growth Regulators. Granada, London, pp. 21–24.
6 Fulthorpe RR, C McGowan, OV Maltseva, WE Holben and JM Tiedje. 1995. 2,4-Dichlorophenoxyacetic acid-degrading bacteria contain mosaics of catabolic genes. *Appl Environ Microbiol* 61: 3274–3281.
7 Gevao B, KT Semple and KC Jones. 2000. Bound pesticide residues in soils: a review. *Environ Pollut* 108: 3–14.
8 Greer LE, JA Robinson and DR Shelton. 1992. Kinetic comparison of seven strains of 2,4-dichlorophenoxyacetic acid degrading bacteria. *Appl Environ Microbiol* 58: 1027–1030.
9 Häggblom MM. 1992. Microbial breakdown of halogenated aromatic pesticides and related compounds. *FEMS Microbiol Rev* 103: 29–72.
10 Hallberg KB, MP Kelly and OH Tuovinen. 1991. Simultaneous degradation of the herbicides 2,4-dichlorophenoxyacetic acid and 2-(2-methyl-4-chlorophenoxy)propionic acid by mixed bacterial cultures. *Curr Microbiol* 23: 65–69.
11 Hoffmann D, RH Müller, B Kiesel and W Babel. 1996. Isolation and characterization of an alkaliphilic bacterium capable of growing on 2,4-dichlorophenoxyacetic acid and 4-chloro-2-methylphenoxyacetic acid. *Acta Biotechnol* 16: 212–131.
12 Horvath M, M Dietzelmüller, M Loidl and F Streichsbier. 1990. Isolation and characterization of a 2-(2,4-dichlorophenoxy)propionic acid-degrading soil bacterium. *Appl Microbiol Biotechnol* 33: 213–216.

COR-AAD1-00002695
Bayer EX1008 (Part 5 of 9)

13 Jacobsen CS and JC Pederson. 1992. Growth and survival of *Pseudomonas cepacia* DBO1 (pRO101) in soil amended with 2,4-dichlorophenoxyacetic acid. *Biodegradation* 2: 245–252.
14 Ka JO, WE Holben and JM Tiedje. 1994. Genetic and phenotypic diversity of 2,4-dichlorophenoxyacetic acid (2,4-D)-degrading bacteria isolated from 2,4-D-treated field soils. *Appl Environ Microbiol* 60: 1106–1115.
15 Kilpi S. 1980. Degradation of some phenoxy acid herbicides by mixed cultures of bacteria isolated from soil treated with 2-(2-methyl-4-chloro)phenoxypropionic acid. *Microb Ecol* 6: 261–270.
16 Lappin HM, MP Greaves and JH Slater. 1985. Degradation of the herbicide mecoprop [2-(2-methyl-4-chlorophenoxy)propionic acid] by a synergistic microbial community. *Appl Environ Microbiol* 49: 429–433.
17 Lewis DL, AW Garrison, KE Wommack, A Whittemore, P Steudler and J Melillo. 1999. Influence of environmental change on degradation of chiral pollutants in soils. *Nature* 401: 898–901.
18 Müller RH, S Jorks, S Kleinsteuber and W Babel. 1999. *Comamonas acidovorans* strain MC1: a new isolate capable of degrading the chiral herbicides dichlorprop and mecoprop and the herbicides 2,4-D and MCPA. *Microbiol Res* 145: 241–246.
19 Neilson AH. 1990. The biodegradation of halogenated organic compounds. *J Appl Bacteriol* 69: 445–470.
20 Nickel K, MJ-F Suter and H-PE Kohler. 1997. Involvement of two α-ketoglutarate-dependent dioxygenases in enantioselective degradation of (*R*)- and (*S*)-mecoprop by *Sphingomonas herbicidovorans* MH. *J Bacteriol* 179: 6674–6679.
21 Oh KH and OH Tuovinen. 1990. Degradation of 2,4-dichlorophenoxyacetic acid by mixed cultures of bacteria. *J Ind Microbiol* 6: 275–278.
22 Oh KH and OH Tuovinen. 1991. Bacterial degradation of phenoxy herbicide mixtures 2,4-D and MCPP. *Bull Environ Contam Toxicol* 47: 222–229.
23 Oh KH and OH Tuovinen. 1994. Biodegradation of the phenoxy herbicides MCPP and 2,4-D in fixed film column reactors. *Int Biodeterior Biodegrad* 33: 93–99.
24 Pieper DH, W Reineke, KH Engesser and HJ Knackmuss. 1988. Metabolism of 2,4-dichlorophenoxyacetic acid, 4-chloro-2-methylphenoxyacetic acid and 2-methylphenoxyacetic acid by *Alcaligenes eutrophus* JMP134. *Arch Microbiol* 150: 95–102.
25 Robertson BK and M Alexander. 1992. Influence of calcium, iron and pH on phosphate availability for microbial mineralization of organic chemicals. *Appl Environ Microbiol* 58: 38–41.
26 Saari RE, DA Hogan and RP Hausinger. 1999. Stereospecific degradation of the phenoxypropionate herbicide dichlorprop. *J Mol Catal B: Enzym* 6: 421–428.
27 Sahasrabudhe SR and VV Modi. 1987. Microbial degradation of chlorinated aromatic compounds. *Microbiol Sci* 4: 300–303.
28 Simoni S, S Klinke, C Zipper, W Angst and H-PE Kohler. 1996. Enantioselective metabolism of chiral 3-phenylbutyric acid, an intermediate of linear alkylbenzene degradation, by *Rhodococcus rhodochrous* PB1. *Appl Environ Microbiol* 62: 749–755.
29 Smith AE and BJ Hayden. 1981. Relative persistence of MCPA, MCPB and mecoprop in Saskatchewan soils, and the identification of MCPA in MCPB-treated soils. *Weed Res* 21: 179–183.
30 Smith AE and AJ Aubin. 1991. Effects of long term 2,4-D and MCPA field applications on the soil breakdown of 2,4-D, MCPA, mecoprop and 2,4,5-T. *J Environ Qual* 20: 436–438.
31 Tett VA, AJ Willetts and HM Lappin-Scott. 1994. Enantioselective degradation of the herbicide mecoprop [2-(2-methyl-4-chlorophenoxy) propionic acid] by mixed and pure bacterial cultures. *FEMS Microbiol Ecol* 14: 191–200.
32 Tett VA, AJ Willetts and HM Lappin-Scott. 1997. Biodegradation of the chlorophenoxy herbicide (*R*)-(+)-mecoprop by *Alcaligenes denitrificans*. *Biodegradation* 8: 43–52.
33 Vallaeys T, RR Fulthorpe, AM Wright and G Soulas. 1996. The metabolic pathway of 2,4-dichlorophenoxyacetic acid degradation involves different families of *tfd*A and *tfd*B genes according to PCR-RFLP analysis. *FEMS Microbiol Ecol* 20: 163–172.
34 Vallaeys T, L Courde, C McGowan, AD Wright and RR Fulthorpe. 1999. Phylogenetic analyses indicate independent recruitment of diverse gene cassettes during assemblage of the 2,4-D catabolic pathway. *FEMS Microbiol Ecol* 28: 373–382.
35 Zipper C, K Nickel, W Angst and H-PE Kohler. 1996. Complete microbial degradation of the chiral herbicide mecoprop [(*RS*)-2-(4-chloro-2-methylphenoxy)propionic acid] in an enantioselective manner by *Sphingomonas herbicidovorans* sp. Nov. *Appl Environ Microbiol* 62: 4318–4322.
36 Zipper C, M Bunk, AJB Zehnder and H-PE Kohler. 1998. Enantioselective uptake and degradation of the chiral herbicide dichlorprop [(*RS*)-2-(2,4-dichlorophenoxy)propanoic acid] by *Sphingomonas herbicidovorans* MH. *J Bacteriol* 180: 3368–3374.

COR-AAD1-00002696
Bayer EX1008 (Part 5 of 9)

APPLIED AND ENVIRONMENTAL MICROBIOLOGY, July 1996, p. 2457–2463 Vol. 62, No. 7
0099-2240/96/$04.00+0
Copyright © 1996, American Society for Microbiology

Evidence for Acquisition in Nature of a Chromosomal 2,4-Dichlorophenoxyacetic Acid/α-Ketoglutarate Dioxygenase Gene by Different *Burkholderia* spp.

V. GRACE MATHESON,[1,2] LARRY J. FORNEY,[2]* YUICHI SUWA,[2]† CINDY H. NAKATSU,[2]‡ ALAN J. SEXSTONE,[1] AND WILLIAM E. HOLBEN[2]§

Department of Plant Pathology and Environmental Microbiology, West Virginia University, Morgantown, West Virginia 26506,[1] and Center for Microbial Ecology, Michigan State University, East Lansing, Michigan 48824[2]

Received 9 August 1995/Accepted 28 December 1995

We characterized the gene required to initiate the degradation of 2,4-dichlorophenoxyacetic acid (2,4-D) by the soil bacterium *Burkholderia* sp. strain TFD6, which hybridized to the *tfdA* gene of the canonical 2,4-D catabolic plasmid pJP4 under low-stringency conditions. Cleavage of the ether bond of 2,4-D by cell extracts of TFD6 proceeded by an α-ketoglutarate-dependent reaction, characteristic of TfdA (F. Fukumori and R. P. Hausinger, J. Bacteriol. 175:2083–2086, 1993). The TFD6 *tfdA* gene was identified in a recombinant plasmid which complemented a *tfdA* transposon mutant of TFD6 created by chromosomal insertion of Tn*5*. The plasmid also expressed TfdA activity in *Escherichia coli* DH5α, as evidenced by enzyme assays with cell extracts. Sequence analysis of the *tfdA* gene and flanking regions from strain TFD6 showed 99.5% similarity to a *tfdA* gene cloned from the chromosome of a different *Burkholderia* species (strain RASC) isolated from a widely separated geographical area. This chromosomal gene has 77.2% sequence identity to *tfdA* from plasmid pJP4 (Y. Suwa, W. E. Holben, and L. J. Forney, abstr. Q-403, *in Abstracts of the 94th General Meeting of the American Society for Microbiology 1994*.). The *tfdA* homologs cloned from strains TFD6 and RASC are the first chromosomally encoded 2,4-D catabolic genes to be reported. The occurrence of highly similar *tfdA* genes in different bacterial species suggests that this chromosomal gene can be horizontally transferred.

The herbicide 2,4-dichlorophenoxyacetic acid (2,4-D) is metabolized by a variety of microorganisms (1, 20, 25, 52). Previous studies suggest that 2,4-D catabolic genes are usually encoded on conjugative plasmids (1, 3, 7, 8, 12, 34, 39, 40). The 2,4-D catabolic genes of *Alcaligenes eutrophus* JMP134(pJP4) have been extensively characterized (9, 21, 29, 30, 39, 41, 42, 49). Plasmid pJP4 is an 80-kb, broad-host-range, self-transmissible plasmid encoding *tfdA*, *tfdB*, *tfdC*, *tfdD*, *tfdE*, and *tfdF*—six of seven genes required for the conversion of 2,4-D to products of intermediary metabolism (9). These genes are organized into three transcriptional units. Both the 2,4-dichlorophenol (2,4-DCP) hydroxylase operon encoding *tfdB* and the dichlorocatechol oxidation operon composed of *tfdCDEF* are contained within a 7,954-bp *Hin*dIII-*Sst*I fragment (41). TfdB hydroxylates 2,4-DCP to form 3,5-dichlorocatechol, and the *tfdB* gene is similar in sequence to the phenol monooxygenase gene, *pheA*, of *Pseudomonas* sp. strain EST1001 (38, 41). The *tfdCDEF* genes encode enzymes that convert 3,5-dichlorocatechol to chloromaleylacetate, which enters the tricarboxylic acid cycle after dechlorination by the chromosomal chloromaleylacetate reductase gene (32). The *tfdCDE* gene sequences (41) are similar to those of the chlorocatechol degradation genes, *clcABD* (13) and *tcbCDE* (57).

The *tfdA* gene, which encodes the first enzyme of the known 2,4-D degradation pathway encoded on pJP4, is located 13 kb away from the *tfdCDEFB* gene cluster (49). This enzyme transforms α-ketoglutarate to succinate and carbon dioxide concomitant with conversion of 2,4-D to 2,4-DCP and glyoxylate (14). In contrast to the *tfdB*, *tfdC*, *tfdD*, *tfdE*, and *tfdF* genes, the *tfdA* gene exhibits no significant similarity to other known gene sequences in chloroaromatic metabolism, and the reaction catalyzed by the 2,4-D/α-ketoglutarate (α-KG) dioxygenase (TfdA) appears to be unique to 2,4-D catabolism (14).

Studies from our group have shown that genetic diversity exists among genes required for 2,4-D degradation by soil bacterial populations (5, 25–27, 37, 52, 53). Soil bacteria able to degrade 2,4-D have been isolated from widely separated geographical locations, including Michigan, Oregon, Canada, and Australia. Samples of total genomic DNA from 53 such isolates were tested for homology to plasmid pJP4 of *A. eutrophus* JMP134. Of the 53 isolates, 32 did not have strong homology to pJP4 in colony hybridization experiments (52). The probe included *tfdA*, *tfdB*, *tfdC*, *tfdD*, *tfdE*, and *tfdF* of the canonical pJP4-encoded 2,4-D catabolic pathway, as well as the plasmid backbone of pJP4. The lack of strong homology to pJP4 indicates that substantial differences exist among gene sequences encoding 2,4-D catabolic enzymes.

In this paper, we report the characterization of a gene that is isofunctional but not highly homologous to the *tfdA* gene of plasmid pJP4. We demonstrate that the gene is chromosomally encoded, not carried on a conjugative plasmid. However, dissemination of this chromosomal DNA fragment occurs in nature, as indicated by isolation of the gene from two different species of *Burkholderia*, one originating in Michigan and the other originating in Oregon. These findings indicate that transfer of chromosomally encoded as well as plasmid-encoded genes contributes to the evolution of microbial 2,4-D catabolic capabilities.

* Corresponding author.
† Present address: National Institute for Resources and Environment, Tsukuba, Japan.
‡ Present address: Department of Agronomy, Purdue University, West Lafayette, IN 47906.
§ Present address: Division of Biological Sciences, The University of Montana, Missoula, MT 59812.

MATERIALS AND METHODS

Transposon mutagenesis of strain TFD6. *Burkholderia* sp. strain TFD6 is a gram-negative, rod-shaped, 2,4-D-degrading bacterium that was isolated from soil with a history of 2,4-D application at Kellogg Biological Station, Hickory

Downloaded from http://aem.asm.org/ on September 3, 2020 at Corteva Agriscience

COR-AAD1-00002697
Bayer EX1008 (Part 5 of 9)

Corners, Mich. (52). Strain TFD6 was identified to the genus level by 16S rDNA sequence analysis (24, 35). Strain 1B is a 2,4-D-negative mutant of strain TFD6 in which the *tfdA* gene was insertionally inactivated by transposon Tn*5* by using plasmid pRL1062a, a suicide vector for the delivery of Tn*5* (58). This vector has a narrow host range and can be used to mobilize Tn*5* into recipient strains by selecting for kanamycin resistance, which is encoded by Tn*5*. Plasmid pRL1062a was introduced into strain TFD6 via electroporation with a Gene Pulser (Bio-Rad Laboratories, Richmond, Calif.) at 1.5 kV for approximately 4.5 ms. The manufacturer's recommendations were followed for growth phase and preparation of competent cells, concentration of cells and DNA, and recovery media following electroporation. The growth and recovery temperature was 30°C for TFD6 and its derivatives. For growth of competent cells, strain TFD6 was cultured in MSC2 medium, a mineral salts medium supplemented with 0.3% Difco Casamino Acids and 250 μg of 2,4-D (Sigma Chemical Co., St. Louis, Mo.) per ml. The mineral base consisted of 10 mM Na_2HPO_4, 10 mM KH_2PO_4, 2.5 mM $(NH_4)_2SO_4$, 0.2 mM $MgSO_4 \cdot 7H_2O$, 50 μM $CaCl_2 \cdot 2H_2O$, 8.6 μM disodium EDTA, 10 μM $FeSO_4 \cdot 7H_2O$, 4 μM $ZnSO_4 \cdot 7H_2O$, 10 μM $MnSO_4 \cdot H_2O$, 1.5 μM $CuSO_4 \cdot 5H_2O$, 8 μM $Co(NO_3)_2 \cdot 6H_2O$, and 1 μM $(NH_4)_6Mo_7O_{24} \cdot 4H_2O$. For solid medium, 1.5% (wt/vol) Bacto Agar (Difco, Detroit, Mich.) was added.

Screening of Tn*5* mutants. Transformants were plated on nitrocellulose filters (Schleicher & Schuell, Keene, N.H.) placed on MSC2K agar (MSC2 supplemented with 100 μg of kanamycin [Sigma] ml^{-1} to select for Tn*5*) and incubated at room temperature. Mutants that had lost the ability to incorporate 2,4-D into biomass were identified by the method of Dunbar et al. (10) as follows. When colonies were clearly visible, replicate filters were prepared and placed on the same medium, also containing 0.5 μCi of ring-labeled [^{14}C]2,4-D per 25 ml of agar medium. Master filters were transferred to fresh MSC2K agar. Replicate filters were incubated overnight on the radiolabeled substrate and then transferred for 20 min onto phosphate-buffered agar with 750 μg of unlabeled 2,4-D per ml to remove unincorporated [^{14}C]2,4-D. The filters were then air dried and placed under X-Omat film (Kodak, Rochester, N.Y.) overnight. Autoradiograms were superimposed on the dried filters, and 2,4-D^- mutants were identified as colonies that were visible on filters but failed to incorporate the label into biomass (i.e., they were unable to metabolize 2,4-D) as indicated by lack of signal on autoradiograms. Those colonies were purified from the master filters and confirmed to be 2,4-D^- by incubation in MSC2K broth and subsequent measurement of residual 2,4-D by high-pressure liquid chromatography (HPLC) as described previously (23).

Complementation of the 2,4-D^- mutant with the *tfdA* gene from pJP4. The 2,4-D^- mutant designated 1B was shown to be deficient in TfdA function by complementation with *tfdA* carried on plasmid pYS11 (50). This plasmid was constructed by cloning the 1.2-kb *Sph*I fragment of pUS311 (14), containing the *tfdA* gene of pJP4, into the *Sph*I site of the broad-host-range plasmid pSP329. Plasmid pSP329 was constructed by Ksenzenko (31) by cloning the *Hae*II fragment of pUC18 into pTJS75 (45). Transformation of 1B by electroporation with pYS11 occurred at a frequency of 10^{-2} per recipient. Transformants were selected on MSC2KT (MSC2K supplemented with 20 μg of tetracycline ml^{-1} to select for pSP329 and its derivatives) and then screened for restored 2,4-D degradation ability by the [^{14}C]2,4-D assay described above. Complementation of 1B was confirmed by incubation of transformants in MSC2KT broth and subsequent HPLC analysis of residual 2,4-D.

Molecular biology techniques. Restriction endonucleases and DNA-modifying enzymes were purchased from Gibco BRL, Gaithersburg, Md., Boehringer Mannheim Corp., Indianapolis, Ind., and New England Biolabs, Inc., Beverly, Mass., and used as specified by the manufacturers. Alkaline lysis and isolation of plasmid DNA, agarose gel electrophoresis, and Southern transfer were all performed by standard techniques (43). Total genomic DNA was purified as described by Ausubel et al. (2). Probes for hybridization experiments and fragments to be subcloned were gel purified from SeaPlaque low-melting-point agarose (FMC BioProducts, Rockland, Maine) with the Gene Clean Kit (BIO 101, Inc., La Jolla, Calif.).

Localization of the Tn*5* insertion site in mutant 1B. Purified plasmid and total genomic DNA from mutant 1B and wild-type TFD6 were digested with *Eco*RI. The resulting restriction fragments were size fractionated on a 0.8% agarose gel, blotted onto a Hybond N nylon membrane (Amersham) by capillary transfer (47), and hybridized with a probe to the 1.1-kb *Hin*dIII-*Sma*I internal fragment of Tn*5* (22).

Southern blot hybridizations. Probe DNA was labeled with digoxigenin-dUTP by using a nonradioactive DIG DNA labeling and detection kit (Boehringer Mannheim Corp.) as recommended by the manufacturer. Prehybridization and hybridization solutions were also as recommended for the digoxigenin kit and contained 5× SSC (1× SSC is 0.15 M NaCl plus 0.015 M sodium citrate) (2), 0.1% *N*-lauroylsarcosine, 0.02% sodium dodecyl sulfate (SDS), 5% blocking reagent, and 50% formamide. The filters were prehybridized for at least 1 h and hybridized overnight with a solution containing denatured digoxigenin-dUTP-labeled probe. Incubation temperatures for prehybridization and hybridization were increased from the recommended 42°C to 62°C to achieve very high stringency conditions (90 to 100% homology). For low-stringency (60% homology) hybridization reactions, formamide was omitted from the prehybridization and hybridization solutions. The filters were washed twice for 5 min each at room temperature in 2× SSC–0.1% SDS and then twice for 15 min each at 68°C in 0.1× SSC–0.1% SDS. Color development of digoxigenin-dUTP-labeled probes was performed by following the instructions enclosed with the kit.

Cloning of the *tfdA* gene of strain TFD6. The *tfdA* gene of strain TFD6 was cloned from a *Bam*HI partial digest of total genomic DNA. Restriction fragments were ligated into pSP329 which had been digested with *Bam*HI and dephosphorylated with calf intestinal alkaline phosphatase (Bethesda Research Laboratories). Dephosphorylation and ligation reactions were performed by following standard protocols (43). Mutant 1B was transformed with the ligation mixture by electroporation, and transformants were selected on MSC2KT agar. Clones containing the *tfdA* gene from TFD6 were identified by the complementation assay with [^{14}C]2,4-D as described above. A recombinant plasmid (pGC3) containing the cloned *tfdA* gene from TFD6 was extracted from a complemented mutant 1B and transformed into *Escherichia coli* DH5α for propagation and maintenance. *E. coli* DH5α was cultured on Luria broth (LB) and LB agar (43) at 37°C. *E. coli* strains transformed with pSP329 or pGC3 were selected on LB supplemented with 20 μg of tetracycline per ml. Plasmid DNA was purified from this *E. coli* host and transformed into mutant 1B to confirm complementation. Complementation of mutant 1B by pGC3 was assayed by incorporation of [^{14}C]2,4-D from MSC2KT agar containing [^{14}C]2,4-D and by degradation of 2,4-D in MSC2KT broth as detected by HPLC analysis of culture fluid after incubation with the complemented mutant.

Restriction fragments from pGC3 were subcloned into the high-copy-number plasmid pGEM3Zf(+) (Promega Corp., Madison, Wis.) for more detailed restriction mapping and DNA sequencing. Subclones constructed with pGEM3Zf(+) were transformed into *E. coli* DH5α and selected on LB with 300 μg of ampicillin per ml. For blue-white selection, 5-bromo-4-chloro-3-indolyl-β-D-galactopyranoside (X-Gal) and isopropyl-β-D-thiogalactopyranoside (IPTG) (Boehringer Mannheim) were added to the agar plates as described previously (43).

Comparison of *tfdA* homologs in wild-type strains, mutants, and clones. Southern (capillary) blots were prepared from restriction digests of total genomic DNA extracted from strains JMP134 (which includes plasmid pJP4), TFD6, 1B, and RASC, as well as plasmids pGC3 and pYC6. Strain RASC is a 2,4-D-degrading bacterium isolated from sewage sludge in Oregon and kindly provided by Penny Amy. This strain carries a chromosomal *tfdA* gene (51). It is also a species of *Burkholderia*, although it is phylogenetically distinct from strain TFD6 as judged by 16S rDNA partial-sequence analysis (35). Plasmid pYC6 is a 7.2-kb *Eco*RI fragment that contains the *tfdA* gene from strain RASC cloned into pGEM3Zf(+) (50). Replicate blots of these DNA samples were hybridized to probes specific for the *tfdA* gene of pJP4 and to a *tfdA* probe derived from a 1-kb *Xba*I-*Pst*I chromosomal DNA fragment from strain RASC. This fragment was adjacent to the Tn*5* insert in a TfdA$^-$ mutant of RASC and includes part of the coding region for the *tfdA* gene in this strain (50). Hybridizations were performed under high-stringency conditions (90 to 100% homology between probe and target) and under low-stringency conditions (60% homology).

Enzyme assays for TfdA activity. The activity of 2,4-D/α-KG dioxygenase (TfdA) was assayed in cell extracts of strains TFD6 and 1B, as well as *E. coli* DH5α containing recombinant plasmids pGC9 and pGC97. The plasmids were constructed by cloning a 3.4-kb *Hin*dIII fragment containing the *tfdA* gene of TFD6 into pGEM3Zf(+) in both orientations. *E. coli* DH5α harboring pGEM3Zf(+) was included as a negative control. The enzyme assay was performed as described by Fukumori and Hausinger (15). The conditions of this assay were optimized for TfdA activity and resulted in accumulation of the product, 2,4-DCP, which is quantified colorimetrically. Briefly, 1-liter cultures of TFD6 and 1B (in MSC2 and MSC2K, respectively) and 200-ml cultures of *E. coli* harboring each recombinant plasmid or the vector (in LB–300 μg of ampicillin per ml) were grown to late log phase at 30°C, with aeration provided by shaking at 200 rpm. The cultures were harvested by centrifugation and resuspended in 2.5 ml of 10 mM Tris (pH 7). The cell suspensions were passed through a French pressure cell at 120 MPa three times for strains TFD6 and 1B and once for *E. coli* strains. For each lysate, 1 ml was transferred to a 1.5-ml microcentrifuge tube and clarified by centrifugation at top speed in a microcentrifuge for 10 min at 4°C.

The enzyme assay mixture contained 1 mM α-KG, 50 μM ascorbate, 50 μM $(NH_4)_2Fe(SO_4)_2$, 1 mM 2,4-D, and either 2, 20, or 100 μl of crude enzyme extract in 10 mM imidazole buffer (pH 6.75). The volume was adjusted to 1 ml with Milli Q water. A control reaction mixture that contained 5 mM EDTA to inhibit enzyme activity was included for each sample. After 30 min at 30°C, 5 mM EDTA was added to each reaction. The 2,4-DCP produced by the dioxygenase activity was quantified by addition of 100 μl of pH 10 buffer solution (15), 10 μl of 2% 4-aminoantipyrine, and 10 μl of 8% potassium ferricyanide. The reactions were allowed to develop for 20 min at room temperature, and the A_{510} was determined on a Hewlett-Packard model 8452A diode array spectrophotometer. The A_{510} was corrected for background phenol production by subtracting the absorbance of the control reaction mixture corresponding to each sample. The concentration of 2,4-DCP was determined by comparison with a standard curve. Total protein in each crude cell extract was measured with the Bio-Rad protein assay dye reagent (4) as recommended by the manufacturer, with bovine serum albumin as a standard. The specific activity of 2,4-D/α-KG dioxygenase was defined as the number of micromoles of 2,4-DCP produced per minute per milligram of protein under the assay conditions.

Sequence analysis. Sequencing was performed at the Michigan State University Sequencing Facility with an Applied Biosystems model 373A DNA sequenc-

Downloaded from http://aem.asm.org/ on September 3, 2020 at Corteva Agriscience

COR-AAD1-00002698
Bayer EX1008 (Part 5 of 9)

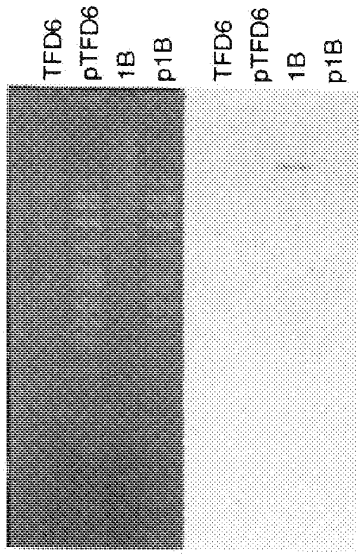


FIG. 1. Localization of the Tn*5* insertion to the chromosome of mutant 1B. (Left panel) Agarose gel electrophoresis of *Eco*RI digests of plasmids pTFD6 and p1B and genomic DNA from strain TFD6 and mutant 1B. (Right panel) Capillary blot of agarose gel hybridized to an internal fragment of Tn*5*. Each lane contains approximately 1 μg of DNA.

ing system and −21m13 and m13 reverse primers. Gaps between the sequences obtained from subclones were filled in by using 18-bp primers homologous to regions flanking the gaps. These primers were synthesized at the Macromolecular Structure Facility, Department of Biochemistry, Michigan State University.

RESULTS

Transposon mutagenesis of strain TFD6. Insertion of Tn*5* into the genome of *Burkholderia* sp. strain TFD6 occurred at a frequency of about 10^{-5} per recipient. Approximately 0.03% of the transposon mutants were unable to metabolize 2,4-D as determined by their inability to incorporate radioactive label from [^{14}C]2,4-D into the biomass. A 2,4-D$^-$ mutant designated 1B was purified from the replicate master plate and confirmed to be 2,4-D$^-$ by incubation in MSC2K broth (containing 250 μg of 2,4-D per ml) and subsequent HPLC analysis of residual 2,4-D. While TFD6 degraded 250 μg of 2,4-D per ml to undetectable levels within 2 days, none of the added 2,4-D was depleted in cultures of mutant 1B incubated for 14 days.

Complementation of mutant 1B with the *tfdA* gene of pJP4. Transformation of the 2,4-D$^-$ mutant 1B with pYS11 (which contains the *tfdA* gene of pJP4) restored the ability of this mutant to degrade 2,4-D. The resulting transformants incorporated label from [^{14}C]2,4-D into biomass, while mutant 1B cells transformed with the vector pSP329 as a control did not (data not shown). This result suggested that the Tn*5* insertion in mutant 1B inactivated the expression of a *tfdA* gene. Incubation of complemented mutants in MSC2KT broth with subsequent analysis of residual 2,4-D by HPLC confirmed the 2,4-D$^+$ phenotype of the complemented mutant.

Localization of the chromosomal *tfdA* gene. The Tn*5* insertion which inactivated the *tfdA* gene in mutant 1B was classified as chromosomal by hybridization of purified plasmid and total genomic DNA to the *nptII* probe (22) from an internal region of Tn*5*. The probe hybridized to total DNA but not to the purified plasmid fraction, suggesting that the interrupted gene was located on a large replicon and not on a typical catabolic plasmid (Fig. 1).

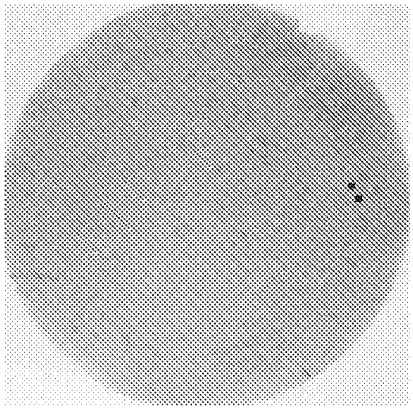


FIG. 2. Identification of clones with the 2,4-D/α-KG dioxygenase gene of strain TFD6. Mutant 1B transformed with a mixture of TFD6 genomic DNA fragments ligated into pSP329 was plated on nitrocellulose filters and incubated on ring-labeled [^{14}C]2,4-D. The autoradiogram is superimposed on the dried filter, demonstrating incorporation of radioactive label by two putative clones.

Cloning of the chromosomal *tfdA* gene of strain TFD6. The *tfdA* gene of strain TFD6 was cloned by ligation of *Bam*HI-digested DNA into an expression vector. The ligation mixture was transformed by electroporation into mutant 1B at a frequency of 10^{-2} per recipient. Approximately 0.15% of transformed colonies screened on MSC2KT agar containing ring-labeled [^{14}C]2,4-D incorporated the label into biomass, as shown in Fig. 2. The colony producing the most intense signal on the autoradiogram was designated GC3 and purified for further analysis. Mutant 1B was transformed with the recombinant plasmid pGC3 to confirm its ability to complement the mutation in *tfdA*. Transformants able to metabolize 2,4-D were screened by demonstrating incorporation of ^{14}C from [^{14}C]2,4-D as described above. The 2,4-D$^+$ phenotype was further confirmed by incubation in MSC2KT broth and subsequent HPLC analysis. Plasmid pGC3 was maintained in *E. coli* DH5α.

A restriction site map of the 4.4-kb *Bam*HI fragment in pGC3 which contains the *tfdA* gene of TFD6 is shown in Fig. 3. To localize the *tfdA* gene, several subclones were constructed, transformed into mutant 1B, and subjected to complementation analysis with [^{14}C]2,4-D incorporated into MSC2KT agar (Fig. 3). The results indicated that the *tfdA* gene is encoded on the 3.4-kb *Hin*dIII fragment of pGC7.

Comparison of *tfdA* homologs. The restriction maps of pGC3 and its derivatives showed that the *tfdA* gene of strain TFD6 was dissimilar to *tfdA* of pJP4, in that the latter contains an *Eco*RI site. The map of pGC3 was identical to the corresponding chromosomal fragment cloned from *Burkholderia* sp. strain RASC into plasmid pYC6 (50). The similarity of the cloned fragments was striking, since strains TFD6 and RASC are different species according to 16S rDNA sequence analysis (35) and have different DNA fingerprints and carry different plasmids (52). The two strains were also isolated from very different environments in widely separated geographical locations. Strain TFD6 was isolated from a mid-Michigan agricultural soil previously treated with 2,4-D (52), and strain RASC was isolated from sewage sludge in Oregon, similar to other isolates described by Amy et al. (1).

The *tfdA* gene of strain TFD6 exhibited homology to *tfdA* from pJP4 when hybridized under low-stringency conditions but hybridized to the *tfdA* gene of strain RASC under high-stringency conditions (Fig. 4). Under high-stringency condi-

Downloaded from http://aem.asm.org/ on September 3, 2020 at Corteva Agriscience

COR-AAD1-00002699
Bayer EX1008 (Part 5 of 9)

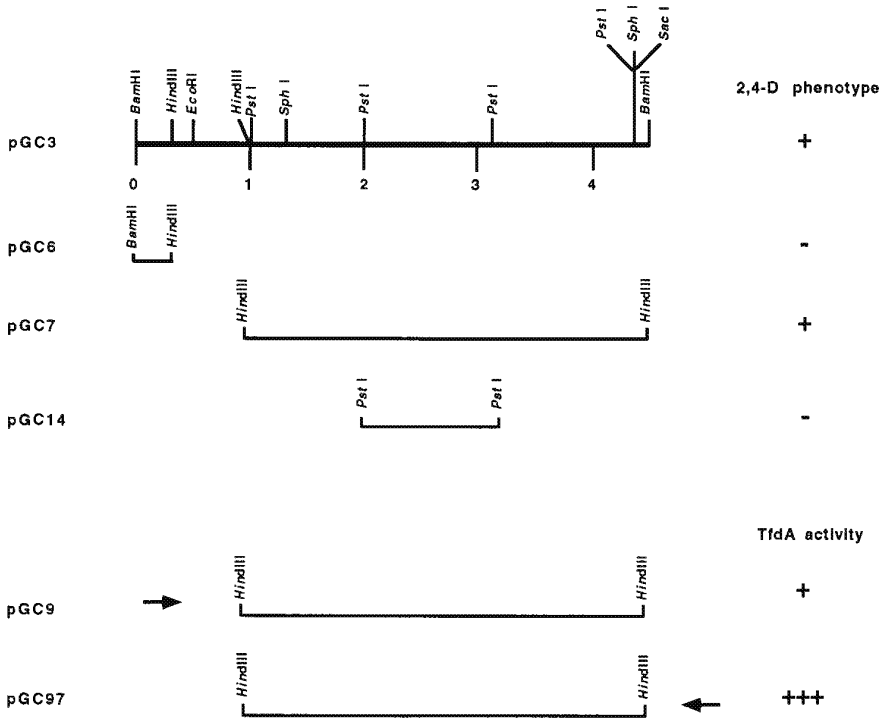


FIG. 3. Cloning of DNA fragments of TFD6 by using the broad-host-range plasmid vector pSP329 or the high-copy plasmid vector pGEM3Zf(+). The 2,4-D phenotype of subclones constructed with pSP329 and propagated in mutant 1B was determined by uptake of radioactive label from agar containing ring-labeled [^{14}C]2,4-D and by HPLC analysis after incubation in 2,4-D broth. Enzyme activity analogous to that of TfdA was assayed in subclones constructed in pGEM3Zf(+) and propagated in *E. coli*. Numbers indicate distances from zero in kilobases.

tions, *tfdA* from pJP4 hybridized only to JMP134 genomic DNA. In contrast, *tfdA* from strain RASC hybridized to TFD6, 1B, and RASC genomic DNA as well as to pGC3 and pYC6 plasmid DNA, but not to genomic DNA from strain JMP134. Under low-stringency conditions, the *tfdA* gene of pJP4 hybridized to all the strains, indicating that the cloned *tfdA* (TFD6) gene shares at least 60% sequence homology with *tfdA* (pJP4).

Insertion of Tn*5* into the genome of mutant 1B caused the 4.4-kb *Bam*HI fragment (containing the *tfdA* gene in TFD6) to shift to a position equivalent to 5.3 kb. When hybridized to *tfdA* (pJP4) at low stringency, a second band appeared in the same lane at around 1.9 kb. A probe specific for Tn*5* also hybridized under high-stringency conditions to both the 5.3- and 1.9-kb bands in *Bam*HI-digested DNA from mutant 1B (data not shown). These results corroborate the position of Tn*5* within the *tfdA* gene of mutant 1B.

Enzyme assays for TfdA activity. Functional evidence for the presence of a gene isofunctional to *tfdA* in strain TFD6 and interruption of the gene in mutant 1B is provided by the results of the TfdA enzyme assay (Table 1). Activity analogous to that of TfdA was detected in a crude cell extract of strain TFD6 but was negligible in an extract of mutant 1B. The protein was expressed in *E. coli* from recombinant plasmids pGC9 and pGC97, constructed by ligating the 3.4-kb *Hin*dIII fragment of pGC3 in both orientations into the high-copy-number cloning vector pGEM3Zf(+) (Table 1; Fig. 3). A dramatic orientation effect was observed, which strongly suggests that transcription of the gene is from the *lac* promoter in pGC97.

Sequence analysis. The smallest fragment of pGC3 which hybridized to *tfdA* of strain RASC was the *Pst*I fragment subcloned into pGC14 (data not shown). Thus, sequencing was initiated within this fragment. The sequence of the entire *tfdA* gene was obtained, plus 51 nucleotides upstream of the translation start codon and 167 nucleotides downstream of the stop codon. Comparative analysis revealed 99.5% homology to the coding region and flanking regions of the *tfdA* gene of strain RASC (GenBank accession number U25717 [50]). Single base substitutions occur between the TFD6 and RASC sequences, and there is an apparent GC inversion at nucleotide 346. Amino acid translations of the *tfdA* sequences from strains TFD6 and RASC were identical, with the exception of one nonconserved replacement of an Arg codon (CGC) in TFD6 for an Ala codon (GCC) in RASC at nucleotide 346. Interestingly, the G+C content of the sequence shown is 60%, slightly lower than the published value of 66% for *Burkholderia* spp. (59), suggesting that this DNA segment may have been acquired by horizontal gene transfer.

DISCUSSION

Previous studies of 2,4-D degradation described or assumed the existence of 2,4-D catabolic genes on plasmids (1, 3, 7, 8, 34), suggesting that conjugative spread of a few ancestral plasmids accounts for the widespread occurrence of 2,4-D catabolic ability among environmental microorganisms. Suwa et al. (51) were the first to report the chromosomal location of a gene isofunctional to the *tfdA* gene of plasmid pJP4. This study provides evidence of mobility of that chromosomal gene between bacteria in the environment.

Several lines of evidence indicate that the chromosomal *tfdA*

Downloaded from http://aem.asm.org/ on September 3, 2020 at Corteva Agriscience

COR-AAD1-00002700
Bayer EX1008 (Part 5 of 9)

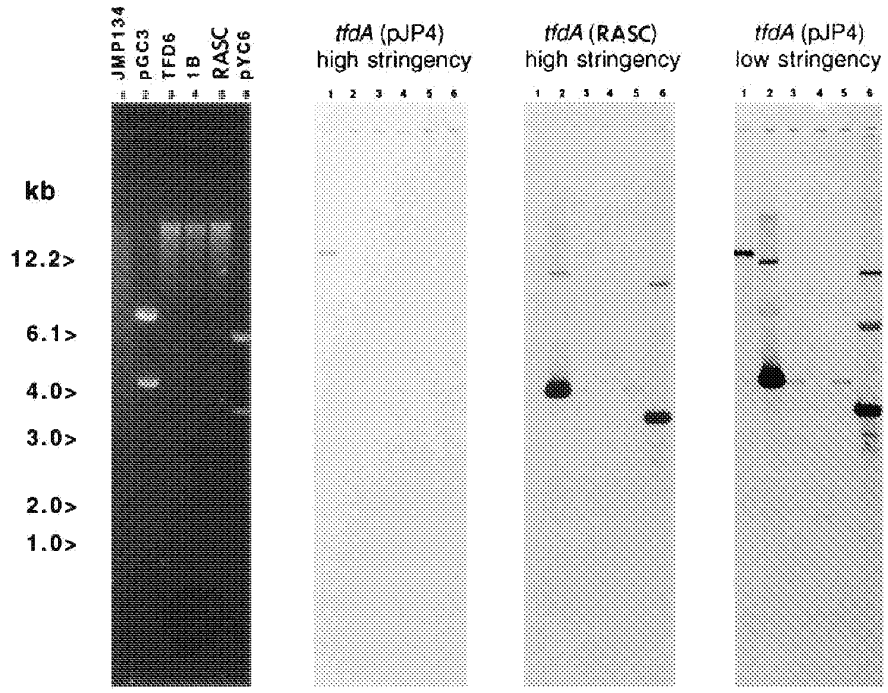


FIG. 4. Homology of the 2,4-D/α-KG dioxygenase gene from strain TFD6 to *tfdA* from pJP4 and *tfdA* from strain RASC. Each lane contains approximately 1 μg of DNA digested with *Bam*HI. Lanes: 1, *A. eutrophus* JMP134; 2, pGC3; 3, strain TFD6; 4, Tn*5* mutant 1B; 5, strain RASC; 6, pYC6.

gene of *Burkholderia* sp. strain TFD6 may reside on a mobile element that has been transferred between microbes in the environment. First, the *tfdA* gene of strain TFD6 exhibits 99.5% sequence similarity to the *tfdA* gene cloned from *Burkholderia* sp. strain RASC, although these two strains are phylogenetically distinct on the basis of partial 16S rDNA sequence analyses (35). Second, a congruency analysis revealed that the 16S rDNA sequences, which are known to be highly conserved, have diverged more between the two strains than have the *tfdA* sequences (35). This suggests that the two strains acquired the *tfdA* gene after differentiating into distinct species at the level of rRNA (11). Third, the G+C content of the chromosomal *tfdA* sequence is about 6% lower than the reported value for *Burkholderia* spp. (59), also suggesting acquisition of foreign DNA. Fourth, the chromosomal *tfdA* genes in the two strains are carried on identical 4.4-kb *Bam*HI restriction fragments but different *Eco*RI restriction fragments (16). Strain RASC contains a 7.2-kb *Eco*RI fragment encoding *tfdA*, while the hybridizing band from strain TFD6 measured 9.5 kb. The *Eco*RI site shown on the restriction map of pGC3 (Fig. 3) corresponds to one end of the 7.2-kb *Eco*RI fragment cloned from strain RASC into pYC6 (50). This polymorphism demonstrates that differences in the restriction maps of the two strains occur within 7.2 kb of the *Eco*RI site shown on the map of pGC3. In addition, the two strains yielded different patterns of hybridization to gene probes derived from the *tfdB* and *tfdC* genes of plasmid pJP4 (16). The DNA from strain TFD6 hybridized at high stringency to both *tfdB* and *tfdC* probes derived from pJP4, while strain RASC DNA hybridized to *tfdB* under low-stringency conditions only and did not hybridize at all to *tfdC*. While hybridization data alone do not confirm the presence or absence of functional genes, these differences support the speculation that the chromosomal *tfdA* gene was recruited for assembly of a 2,4-D catabolic pathway.

TABLE 1. 2,4-D/α-ketoglutarate activity in cell extracts

Strain	Sp act $(10^{-2})^a$
TFD6	0.36
1B	0.021
DH5α(pGEM)	0.00
DH5α(pGC9)	1.70
DH5α(pGC97)	116.0

[a] Specific activity is defined as micromoles of 2,4-dichlorophenol produced per minute per milligram of protein under the assay conditions.

Mechanisms contributing to acquisition of genes by microorganisms for the catabolism of xenobiotic substrates such as 2,4-D have been reviewed (56). In addition to conjugation, transduction and transformation can mediate chromosomal and plasmid DNA transfer in the environment (33, 44). The foreign DNA must be integrated into the host DNA before it can be maintained. Some catabolic genes reside on transposable elements and are thus flanked by insertion sequences which facilitate their mobilization and recombination. Six different transposons have been shown to encode aromatic or haloaromatic catabolic genes, and mobilization of these elements between chromosomal and plasmid DNA has been observed (6, 17, 18, 36, 46, 48, 54, 55, 57).

Reports of 2,4-D catabolic genes with different degrees of similarity arranged differently on diverse plasmids and in different hosts suggest that assembly of these genes takes place by recombination mechanisms (3, 7, 34, 37, 53). The dynamic nature of plasmid pJP4 and other 2,4-D catabolic plasmids has been observed and may contribute to pathway assembly in nature. Ghosal and You (19) reported repeated sequences in pJP4, the occurrence of duplications in response to selection

Downloaded from http://aem.asm.org/ on September 3, 2020 at Corteva Agriscience

COR-AAD1-00002701
Bayer EX1008 (Part 5 of 9)

for 3-chlorobenzoate function, and deletions in the absence of selective pressure, indicating the dynamic nature of this plasmid. Ka and Tiedje (28) recently reported integration of a self-transmissible 2,4-D degradative plasmid into the chromosome of its host. The 2,4-D^+ phenotype was retained by the host, but transmissibility was lost. The plasmid later excised from the chromosome and was again transmissible. Plasmids pEST4011 from *P. putida* PaW85 and pMAB1 from *Pseudomonas cepacia* (*Burkholderia cepacia*) CSV90 both contain 2,4-D catabolic sequences highly similar to those of pJP4 (3, 34). These plasmids each undergo spontaneous deletions, resulting in loss of the 2,4-D^+ phenotype from the host bacterium. These examples suggest the occurrence of recombination events which could potentially facilitate the dissemination of both plasmid-borne and chromosomally encoded 2,4-D catabolic genes followed by recruitment and reassembly in recipient organisms.

We have established that chromosomal *tfdA* genes sharing 99.5% sequence identity occur in bacterial hosts of different species. It is therefore likely that transmission of this gene in nature involves one or more recombination events, perhaps mediated by a transposon. Analysis of the chromosomal sequences flanking the *tfdA* gene of strains TFD6 and RASC may reveal clues to the mechanism of transfer of this region of DNA.

ACKNOWLEDGMENTS

This work was supported by a research assistantship through the division of Plant and Soil Sciences, West Virginia University; National Science Foundation grant BSR 8705407; National Science Foundation Science and Technology Center grant BIR 9120006; the Michigan State University Agricultural Experiment Station; and the Japan Research and Development Corporation.

Strain RASC was kindly provided by Penny Amy, plasmid pRL1062a was provided by Peter Wolk, and pSP329 was provided by Tamara Tsoi. We thank Alice Wright for assistance with sequence analysis, Yoichi Kamagata for help with enzyme assays, John Dunbar for instruction on the [^{14}C]2,4-D screening technique, and Cathy McGowan for 16S sequence analysis.

REFERENCES

1. **Amy, P. S., J. W. Schulke, L. M. Frazier, and R. J. Seidler.** 1985. Characterization of aquatic bacteria and cloning of genes specifying partial degradation of 2,4-dichlorophenoxyacetic acid. Appl. Environ. Microbiol. **49:**1237–1245.
2. **Ausubel, F. M., R. Brent, R. E. Kingston, D. D. Moore, J. G. Seidman, J. A. Smith, and K. Struhl.** 1987. Current protocols in molecular biology. John Wiley & Sons, Inc., New York.
3. **Bhat, M. A., M. Tsuda, K. Horiike, M. Nozaki, C. S. Vaidyanathan, and T. Nakazawa.** 1994. Identification and characterization of a new plasmid carrying genes for degradation of 2,4-dichlorophenoxyacetate from *Pseudomonas cepacia* CSV90. Appl. Environ. Microbiol. **60:**307–312.
4. **Bradford, M. M.** 1976. A rapid and sensitive method for the quantitation of microgram quantities of protein utilizing the principle of protein-dye binding. Anal. Biochem. **72:**248–254.
5. **Calabrese, V. G. M., N. L. Tonso, A. J. Sexstone, and W. E. Holben.** 1992. Characterization and classification of diverse 2,4-dichlorophenoxyacetic acid (2,4-D) degrading populations using whole plasmid probes in colony hybridization analyses, abstr. Q-37, p. 341. *In* Abstracts of the 92nd General Meeting of the American Society for Microbiology 1992. American Society for Microbiology, Washington, D.C.
6. **Carney, B. F., L. Krockel, J. V. Leary, and D. D. Focht.** 1989. Identification of *Pseudomonas alcaligenes* chromosomal DNA in the plasmid DNA of the chlorobenzene-degrading recombinant *Pseudomonas putida* CB1-9. Appl. Environ. Microbiol. **55:**1037–1039.
7. **Chaudry, G. R., and G. H. Huang.** 1988. Isolation and characterization of a new plasmid from a *Flavobacterium* sp. which carries the genes for degradation of 2,4-dichlorophenoxyacetate. J. Bacteriol. **170:**3897–3902.
8. **Don, R. H., and J. M. Pemberton.** 1981. Properties of six pesticide degradation plasmids isolated from *Alcaligenes paradoxus* and *Alcaligenes eutrophus*. J. Bacteriol. **145:**681–686.
9. **Don, R. H., A. J. Weightman, H. J. Knackmuss, and K. N. Timmis.** 1985. Transposon mutagenesis and cloning analysis of the pathways for degradation of 2,4-dichlorophenoxyacetic acid and 3-chlorobenzoate in *Alcaligenes eutrophus* JMP134(pJP4). J. Bacteriol. **161:**85–90.
10. **Dunbar, J., A. Rhodes, D. C. L. Wong, M. J. Yarou, and L. Forney.** Unpublished data.
11. **Dykhuizen, D. E., and L. Green.** 1991. Recombination in *Escherichia coli* and the definition of biological species. J. Bacteriol. **173:**7257–7268.
12. **Fisher, P. R., J. Appleton, and J. M. Pemberton.** 1978. Isolation and characterization of the pesticide-degrading plasmid pJP1 from *Alcaligenes paradoxus*. J. Bacteriol. **135:**798–804.
13. **Frantz, B., and A. M. Chakrabarty.** 1987. Organization and nucleotide sequence determination of a gene cluster involved in 3-chlorocatechol degradation. Proc. Natl. Acad. Sci. USA **84:**4460–4464.
14. **Fukumori, F., and R. P. Hausinger.** 1993. *Alcaligenes eutrophus* JMP134 "2,4-dichlorophenoxyacetate monooxygenase" is an α-ketoglutarate-dependent dioxygenase. J. Bacteriol. **175:**2083–2086.
15. **Fukumori, F., and R. P. Hausinger.** 1993. Purification and characterization of 2,4-dichlorophenoxyacetate/α-ketoglutarate dioxygenase. J. Biol. Chem. **268:**24311–24317.
16. **Fulthorpe, R. R., C. McGowan, O. V. Maltseva, W. E. Holben, and J. M. Tiedje.** 1995. 2,4-Dichlorophenoxyacetic acid-degrading bacteria contain mosaics of catabolic genes. Appl. Environ. Microbiol. **61:**3274–3281.
17. **Fulthorpe, R. R., and R. C. Wyndham.** 1992. Involvement of a chlorobenzoate-catabolic transposon, Tn*5271*, in community adaptation to chlorobiphenyl, chloroaniline, and 2,4-dichlorophenoxyacetic acid in a freshwater ecosystem. Appl. Environ. Microbiol. **58:**314–325.
18. **Fulthorpe, R. R., and R. C. Wyndham.** 1991. Transfer and expression of the catabolic plasmid pBRC60 in wild bacterial recipients in a freshwater ecosystem. Appl. Environ. Microbiol. **57:**1546–1553.
19. **Ghosal, D., and I.-S. You.** 1988. Gene duplication in haloaromatic degradative plasmids pJP4 and pJP2. Can. J. Microbiol. **34:**709–715.
20. **Greer, L. E., J. A. Robinson, and D. R. Shelton.** 1992. Kinetic comparison of seven strains of 2,4-dichlorophenoxyacetic acid-degrading bacteria. Appl. Environ. Microbiol. **58:**1027–1030.
21. **Harker, A. R., R. H. Olsen, and R. J. Seidler.** 1989. Phenoxyacetic acid degradation by the 2,4-dichlorophenoxyacetic acid (TFD) pathway of plasmid pJP4: mapping and characterization of the TFD regulatory gene, *tfdR*. J. Bacteriol. **171:**314–320.
22. **Holben, W. E., J. K. Jansson, B. K. Chelm, and J. M. Tiedje.** 1988. DNA probe method for the detection of specific microorganisms in the soil bacterial community. Appl. Environ. Microbiol. **54:**703–711.
23. **Holben, W. E., B. M. Schroeter, V. G. M. Calabrese, R. H. Olsen, J. K. Kukor, V. O. Biederbeck, A. E. Smith, and J. M. Tiedje.** 1992. Gene probe analysis of soil microbial populations selected by amendment with 2,4-dichlorophenoxyacetic acid. Appl. Environ. Microbiol. **58:**3941–3948.
24. **International Journal of Systematic Bacteriology.** 1993. List no. 45. Validation of the publication of new names and new combinations previously effectively published outside the IJSB. Int. J. Syst. Bacteriol. **43:**398–399.
25. **Ka, J. O., W. E. Holben, and J. M. Tiedje.** 1994. Genetic and phenotypic diversity of 2,4-dichlorophenoxyacetic acid (2,4-D)-degrading bacteria isolated from 2,4-D-treated field soils. Appl. Environ. Microbiol. **60:**1106–1115.
26. **Ka, J. O., W. E. Holben, and J. M. Tiedje.** 1994. Use of gene probes to aid in recovery and identification of functionally dominant 2,4-dichlorophenoxyacetic acid-degrading populations in soil. Appl. Environ. Microbiol. **60:**1116–1120.
27. **Ka, J. O., W. E. Holben, and J. M. Tiedje.** 1994. Analysis of competition in soil among 2,4-dichlorophenoxyacetic acid-degrading bacteria. Appl. Environ. Microbiol. **60:**1121–1128.
28. **Ka, J. O., and J. M. Tiedje.** 1994. Integration and excision of a 2,4-dichlorophenoxyacetic acid degradative plasmid in *Alcaligenes paradoxus* and evidence of its natural intergeneric transfer. J. Bacteriol. **176:**5284–5289.
29. **Kaphammer, B., J. J. Kukor, and R. H. Olsen.** 1990. Regulation of *tfdCDEF* by *tfdR* of the 2,4-dichlorophenoxyacetic acid degradation plasmid pJP4. J. Bacteriol. **172:**2280–2286.
30. **Kaphammer, B., and R. H. Olsen.** 1990. Cloning and characterization of *tfdS*, the repressor-activator gene of *tfdB*, from the 2,4-dichlorophenoxyacetic acid catabolic plasmid pJP4. J. Bacteriol. **172:**5856–5862.
31. **Ksenzenko, V.** Unpublished data.
32. **Kukor, J. J., R. H. Olsen, and J.-S. Siak.** 1989. Recruitment of a chromosomally encoded maleylacetate reductase for degradation of 2,4-dichlorophenoxyacetic acid by plasmid pJP4. J. Bacteriol. **171:**3385–3390.
33. **Lorenz, M. G., D. Gerjets, and W. Wackernagel.** 1991. Release of transforming plasmid and chromosomal DNA from two cultured soil bacteria. Arch. Microbiol. **156:**319–327.
34. **Mae, A. A., R. O. Marits, N. R. Ausmees, V. M. Koiv, and A. L. Heinaru.** 1993. Characterization of a new 2,4-dichlorophenoxyacetic acid degrading plasmid pEST4011: physical map and localization of catabolic genes. J. Gen. Microbiol. **139:**3165–3170.
35. **McGowan, C.** 1994. Ph.D. thesis. Michigan State University, East Lansing.
36. **Nakatsu, C., N. G. James, R. Singh, N. Straus, and C. Wyndham.** 1991. Chlorobenzoate catabolic transposon Tn*5271* is a composite class I element with flanking class II insertion sequences. Proc. Natl. Acad. Sci. USA **88:**8312–8316.

Downloaded from http://aem.asm.org/ on September 3, 2020 at Corteva Agriscience

COR-AAD1-00002702
Bayer EX1008 (Part 5 of 9)

37. **Nakatsu, C. H.** 1994. Genetic organization and molecular evolution of the 2,4-D catabolic pathway, p. 51–73. *In* Japanese Research and Development Corporation–Michigan State University Workshop on Microbial Evolution and Biodegradation.
38. **Nurk, A., L. Kasak, and M. Kivisaar.** 1991. Sequence of the gene (*pheA*) encoding phenol monooxygenase from *Pseudomonas* sp. EST1001: expression in *Escherichia coli* and *Pseudomonas putida*. Gene **102:**13–18.
39. **Pemberton, J. M., B. Carney, and R. H. Don.** 1979. Evolution and spread of pesticide degrading ability among soil microorganisms, p. 287–299. *In* K. N. Timmis and A. Puhler (ed.), Plasmids of medical, environmental and commercial importance. Elsevier/North-Holland Biomedical Press, Amsterdam.
40. **Pemberton, J. M., and P. R. Fisher.** 1977. 2,4-D plasmids and persistence. Nature (London) **268:**732–733.
41. **Perkins, E. J., M. P. Gordon, O. Caceres, and P. F. Lurquin.** 1990. Organization and sequence analysis of the 2,4-dichlorophenol hydroxylase and dichlorocatechol oxidative operons of plasmid pJP4. J. Bacteriol. **172:**2351–2359.
42. **Perkins, E. J., and P. F. Lurquin.** 1988. Duplication of a 2,4-dichlorophenoxyacetic acid monooxygenase gene in *Alcaligenes eutrophus* JMP134-(pJP4). J. Bacteriol. **170:**5669–5672.
43. **Sambrook, J., E. F. Fritsch, and T. Maniatis.** 1989. Molecular cloning: a laboratory manual, 2nd ed. Cold Spring Harbor Laboratory, Cold Spring Harbor, N.Y.
44. **Saye, D. J., O. A. Ogunseitan, G. S. Sayler, and R. V. Miller.** 1990. Transduction of linked chromosomal genes between *Pseudomonas aeruginosa* strains during incubation in situ in a freshwater habitat. Appl. Environ. Microbiol. **56:**140–145.
45. **Schmidhauser, T. J., and D. R. Helinski.** 1985. Regions of broad-host-range plasmid RK2 involved in replication and stable maintenance in nine species of gram-negative bacteria. J. Bacteriol. **164:**446–455.
46. **Sinclair, M. I., P. C. Maxwell, B. R. Lyon, and B. W. Holloway.** 1986. Chromosomal location of TOL plasmid DNA in *Pseudomonas putida*. J. Bacteriol. **168:**1302–1308.
47. **Southern, E. M.** 1975. Detection of specific sequences among DNA fragments separated by gel electrophoresis. J. Mol. Biol. **98:**503–517.
48. **Springael, D., S. Kreps, and M. Mergeay.** 1993. Identification of a catabolic transposon, Tn*4371*, carrying biphenyl and 4-chlorobiphenyl degradation genes in *Alcaligenes eutrophus* A5. J. Bacteriol. **175:**1674–1681.
49. **Streber, W. R., K. N. Timmis, and M. H. Zenk.** 1987. Analysis, cloning, and high-level expression of 2,4-dichlorophenoxyacetate monooxygenase gene *tfdA* of *Alcaligenes eutrophus* JMP134. J. Bacteriol. **169:**2950–2955.
50. **Suwa, Y., A. D. Wright, F. Fukimori, K. A. Nummy, R. P. Hausinger, W. E. Holben, and L. J. Forney.** 1996. Characterization of chromosomally encoded 2,4-dichlorophenoxyacetic acid–α-ketoglutarate dioxygenase from *Burkholderia* sp. strain RASC. Appl. Environ. Microbiol. **62:**2464–2469.
51. **Suwa, Y., W. E. Holben, and L. J. Forney.** 1994. Cloning of a novel 2,4-D catabolic gene isofunctional to *tfdA* from *Pseudomonas* sp. strain TFD3, abstr. Q-403, p. 459. *In* Abstracts of the 94th General Meeting of the American Society for Microbiology 1994. American Society for Microbiology, Washington, D.C.
52. **Tonso, N. L., V. G. Matheson, and W. E. Holben.** 1995. Polyphasic characterization of a suite of bacterial isolates capable of degrading 2,4-D. Microb. Ecol. **30:**1–22.
53. **Top, E. M., W. E. Holben, and L. J. Forney.** 1995. Characterization of diverse 2,4-dichlorophenoxyacetic acid degradative plasmids isolated from soil by complementation. Appl. Environ. Microbiol. **61:**1691–1698.
54. **Tsuda, M., and T. Iino.** 1990. Naphthalene degrading genes on plasmid NAH7 are on a defective transposon. Mol. Gen. Genet. **223:**33–39.
55. **Tsuda, M., K. I. Minegishi, and T. Iino.** 1989. Toluene transposons Tn*4651* and Tn*4653* are class II transposons. J. Bacteriol. **171:**1386–1393.
56. **van der Meer, J. R., W. M. de Vos, S. Harayama, and A. J. B. Zehnder.** 1992. Molecular mechanisms of genetic adaptation to xenobiotic compounds. Microbiol. Rev. **56:**677–694.
57. **van der Meer, J. R., A. J. B. Zehnder, and W. M. de Vos.** 1991. Identification of a novel composite transposable element, Tn*5280,* carrying chlorobenzene dioxygenase genes of *Pseudomonas* sp. strain P51. J. Bacteriol. **173:**7077–7083.
58. **Wolk, C. P., Y. Cai, and J.-M. Panoff.** 1991. Use of a transposon with luciferase as a reporter to identify environmentally responsive genes in a cyanobacterium. Proc. Natl. Acad. Sci. USA **88:**5355–5359.
59. **Yabuuchi, E., Y. Kosako, H. Oyaizu, I. Yano, H. Hotta, Y. Hashimoto, T. Ezaki, and M. Arakawa.** 1992. Proposal of *Burkholderia* gen. nov. and transfer of seven species of the genus *Pseudomonas* homology group II to the new genus, with the type species *Burkholderia cepacia* (Palleroni and Holmes 1981) comb. nov. Microbiol. Immunol. **36:**1251–1275.

Downloaded from http://aem.asm.org/ on September 3, 2020 at Corteva Agriscience

COR-AAD1-00002703
Bayer EX1008 (Part 5 of 9)

APPLIED AND ENVIRONMENTAL MICROBIOLOGY, Oct. 1998, p. 4089–4092 Vol. 64, No. 10
0099-2240/98/$04.00+0
Copyright © 1998, American Society for Microbiology. All Rights Reserved.

Evidence for Interspecies Gene Transfer in the Evolution of 2,4-Dichlorophenoxyacetic Acid Degraders

CATHERINE MCGOWAN,† ROBERTA FULTHORPE,* ALICE WRIGHT, AND J. M. TIEDJE
Center for Microbial Ecology, Michigan State University, East Lansing, Michigan 48823-1101

Received 6 April 1998/Accepted 3 August 1998

Small-subunit ribosomal DNA (SSU rDNA) from 20 phenotypically distinct strains of 2,4-dichlorophenoxyacetic acid (2,4-D)-degrading bacteria was partially sequenced, yielding 18 unique strains belonging to members of the alpha, beta, and gamma subgroups of the class *Proteobacteria*. To understand the origin of 2,4-D degradation in this diverse collection, the first gene in the 2,4-D pathway, *tfdA*, was sequenced. The sequences fell into three unique classes found in various members of the beta and gamma subgroups of *Proteobacteria*. None of the α-Proteobacteria yielded *tfdA* PCR products. A comparison of the dendrogram of the *tfdA* genes with that of the SSU rDNA genes demonstrated incongruency in phylogenies, and hence 2,4-D degradation must have originated from gene transfer between species. Only those strains with *tfdA* sequences highly similar to the *tfdA* sequence of strain JMP134 (*tfdA* class I) transferred all the 2,4-D genes and conferred the 2,4-D degradation phenotype to a *Burkholderia cepacia* recipient.

Bacteria capable of mineralizing 2,4-dichlorophenoxyacetic acid (2,4-D), a commonly used herbicide, are found in many different phylogenetic groups (2, 3, 7, 11, 22, 23). Evidence suggests that numerous variants of 2,4-D catabolic genes exist and that catabolic operons consist of a near-random mixing of these variants (7). Interspecies gene transfer is a well-documented phenomenon (13), and horizontal gene transfer of the 2,4-D-degrading plasmid pJP4 has been shown (3, 5). However, not all 2,4-D catabolic operons are found on plasmids (10, 11, 16, 20). The extent to which other 2,4-D genes have been exchanged in nature is unknown. The aim of this research was to assess the role of horizontal gene transfer in the evolution of 2,4-D-degrading strains. This article summarizes the results of two aspects of this work—the study of the transfer of the entire 2,4-D pathway by using standard mating experiments and a phylogenetic study of the *tfdA* gene. The *tfdA* gene codes for an α-ketoglutarate-dependent 2,4-D dioxygenase which converts 2,4-D into 2,4-dichlorophenol and glyoxylate (6). This 861-bp gene was first sequenced from *Ralstonia eutropha* JMP134 (19). Two more *tfdA* genes were cloned from chromosomal locations in *Burkholderia* strain RASC and *Burkholderia* strain TFD6 (16, 20). These proved to be identical to each other and 78.5% similar to the original. An alignment of the two variants allowed conserved areas to be identified and primers to be designed for the amplification of *tfdA*-like genes from other sources (24). Sequence analysis of putative *tfdA* fragments and the small-subunit ribosomal DNA (SSU rDNA) of the strains carrying them allowed us to construct phylogenies of the genes and their hosts and to look for congruency between them.

Mating experiments. A collection of 2,4-D degraders containing 15 unique strains as determined by genomic fingerprinting (7) was used as a source of donors in a series of mating experiments (Table 1). *Burkholderia cepacia* D5, lacking the ability to grow on 2,4-D and not hybridizing to any *tfd* genes, was used as a recipient in mating experiments. Strain D5 contains neomycin phosphotransferase genes (*nptII*) carried on transposon Tn*5* and is resistant to 50 μg each of kanamycin, carbenicillin, and bacitracin per ml. All of the 2,4-D strains used were sensitive to these antibiotics. Filter matings were performed with a donor-to-recipient ratio of 1:10. Colonies which grew on selective medium (500 ppm of 2,4-D in mineral salts agar [MMO] [23] including 50 μg of kanamycin, carbenicillin, and bacitracin per ml) were subjected to further tests. Their ability to catabolize 2,4-D was tested in liquid medium (same composition as that described above).

The disappearance of 2,4-D from the culture medium was monitored by high-performance liquid chromatography. Cells were removed by centrifugation, and the supernatant was filtered through 0.2-μm-pore-size filters. These samples were then analyzed on a Lichrosorb Rp-18 column (Anspec Co., Ann Arbor, Mich.) with 60% methanol–40% 0.1% H_3PO_4 as the eluant. 2,4-D was detected by measuring light absorption at 230 nm. The presence of *tfd* genes was detected by hybridizing colony blots with a DNA probe derived from the entire pJP4 plasmid. The identity of the colonies was confirmed by probing with the *nptII* gene of Tn*5* (found in *B. cepacia* D5). Probes were labeled with random hexanucleotides incorporating [^{32}P]dCTP (3,000 Ci/mmol; New England Nuclear, Boston, Mass.). Hybridizations were done under high-stringency conditions by using 50% formamide and Denhardt's solution (18) at 42°C. Of the 15 unique strains tested, 9 transferred 2,4-D degradation abilities to D5. This transfer was confirmed by hybridization with pJP4 for eight of these strains. *B. cepacia* RASC could transfer degradative abilities, but neither it nor the transconjugant hybridized to the pJP4 probe. Work subsequent to this study has confirmed that the genes carried by RASC do not hybridize to those found on pJP4 under high-stringency conditions (7).

Phylogenetic analyses. Total genomic DNA was isolated from 20 unique 2,4-D-degrading strains (including all 15 used for mating experiments) grown on 500 ppm of 2,4-D mineral salts medium amended with 50 ppm of yeast extract. SSU rDNA was amplified by using fD1 and rD1 as primers (25). Putative *tfdA* fragments were amplified by using primers TVU and TVL as previously described (24). PCR products were purified with a Gene Clean kit (Bio 101, La Jolla, Calif.). Sequencing was done with an Applied Biosystems model 373A

* Corresponding author. Present address: University of Toronto at Scarborough, 1265 Military Trail, Scarborough, Ontario, Canada M1C 1A4. Phone: (416) 287-7221. Fax: (416) 287-7279. E-mail: fulthorpe@scar.utoronto.ca.
† Present address: 1798 Colorado Drive, East Lansing, MI 48823.

Downloaded from http://aem.asm.org/ on September 3, 2020 at Corteva Agriscience

COR-AAD1-00002704
Bayer EX1008 (Part 5 of 9)

TABLE 1. 2,4-D-degrading strains, geographic origins, and GenBank accession numbers

Strain	GenBank accession no. (SSU rDNA)	Origin	Most similar to genus and/or species[a]	Transfer[b]	*tfdA* type[c]	GenBank accession no. (*tfdA* gene)	Reference or source
JMP134	AF049542	Australia	*Ralstonia eutropha*	+	I	M16730	3
EML1549	AF049546	Oregon	*Burkholderia* sp.	+	I		2
TFD39	AF049539	Saskatchewan	*Burkholderia* sp.	+	I	U43197	23
K712	AF049543	Michigan	*Burkholderia* sp.	+	I	U43276	11
TFD9	AF049537	Saskatchewan	*Alcaligenes xylosoxidans*	+	I	U43276	23
TFD41	AF049541	Michigan	*Ralstonia eutropha*	+	I		23
TFD38	AF049540	Michigan	*Ralstonia eutropha*	+	ND[c]		23
TFD23	AF049536	Michigan	*Rhodoferax fermentans*	+	I	U43276	23
RASC	AF049544	Oregon	*Burkholderia* sp.	(+)	II	U25717	2
TFD6	AF049546	Michigan	*Burkholderia* sp.	−	II		23
TFD2	AF049545	Michigan	*Burkholderia* sp.	−	II		23
TFD31	AF049536	Saskatchewan	*Rhodoferax fermentans*	−	III		23
B6-9	AF049538	Ontario	*Rhodoferax fermentans*	ND	III	U43196	9
I-18	U22836	Oregon	*Halomonas* sp.	ND	III	U22499	15
K1443	AF049531	Michigan	*Sphingomonas* sp.	−		—[d]	11
2,4-D1	AF049535	Montana	*Sphingomonas* sp.	−		—	R. Sanford
B6-5	AF049533	Ontario	*Sphingomonas* sp.	ND		—	9
B6-10	AF049534	Ontario	*Sphingomonas* sp.	ND		—	9
EML146	AF049532	Oregon	*Sphingomonas* sp.	−		—	2
M1	AF049530	French Polynesia	*Rhodospeudomonas* sp.	ND			R. Fulthorpe

[a] The generus and/or species most similar to the strain is given based on similarities of SSU rDNA sequences.
[b] Symbols: +, able to transfer 2,4-D degradation to *B. cepacia* D5; (+), able to transfer at very low frequency; −, no transfer detected.
[c] ND, not determined.
[d] —, no amplificate was obtained.

automatic sequencer (Perkin-Elmer Cetus) by using fluorescently labeled dye termination at the Michigan State University Sequencing Facility. The sequencing primer used for SSU rDNA fragments was 519R (5′ GTA TTA CCG CGG CTG CTG G-3′). For *tfdA* fragments, the sequencing primers were the same as the amplification primers. GenBank accession numbers for these sequences are given in Table 1.

The SSU rDNA sequences were compared to sequences in GenBank by using the Basic Local Alignment Search Tool (BLAST) (1), and those strains with the highest maximal segment

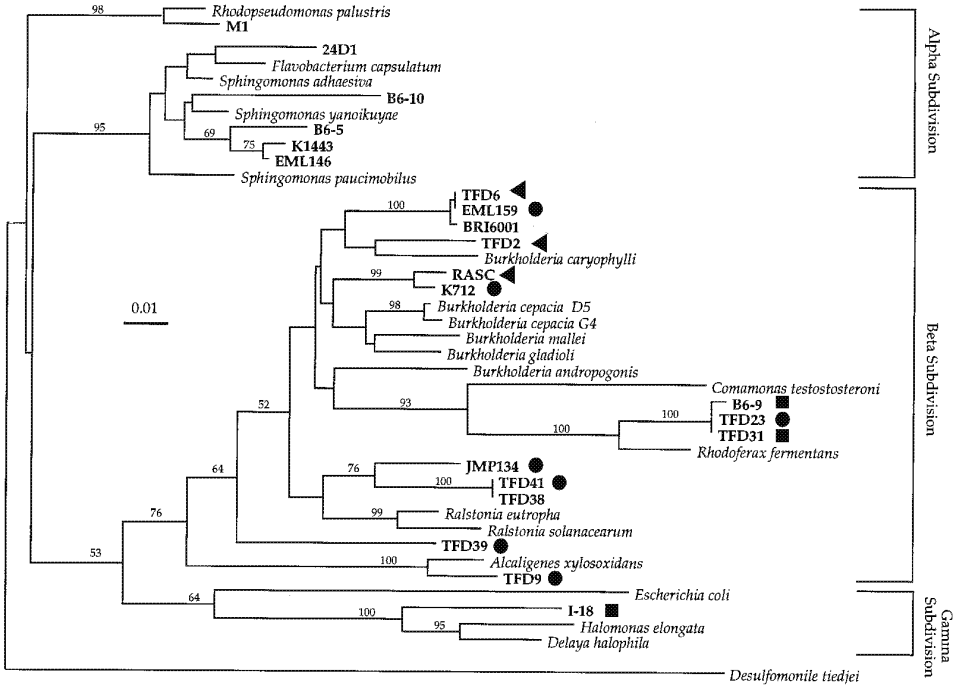


FIG. 1. Neighbor-joining dendrogram (Jukes-Cantor distances) of SSU rDNA from 2,4-D-degrading bacteria (indicated in boldface type) and reference strains (indicated in italic type). Class I (●), class II (▲), and class III (■) types of *tfdA* genes are indicated. Bootstrap confidence limits (percentages) are indicated above each branch. Scale bar represents a Jukes-Cantor distance of 0.01.

Downloaded from http://aem.asm.org/ on September 3, 2020 at Corteva Agriscience

COR-AAD1-00002705
Bayer EX1008 (Part 5 of 9)

pair scores were retrieved from GenBank and included in the phylogenetic analysis. Sequences were aligned manually with the software SeqEd (Applied Biosystems) and with MacClade (14). Sites where nucleotides were not resolved for all sequences were deleted from the alignment, as were those nucleotides corresponding to the small loop in this region that is absent in the alpha subgroup of the class *Proteobacteria*. These deletions left 283 unambiguous sites for the construction of the SSU rDNA phylogenies. Phylogenetic trees were constructed by using the neighbor-joining analysis of pairwise Jukes-Cantor distances (4), and the topology was confirmed by using the maximum parsimony method PAUP (21). *Desulfomonile tiedjei* of the δ-Proteobacteria was used as an outgroup. Bootstrap analysis based on 100 replicates was used to place confidence estimates on the tree. Only bootstrap values of greater than 50 were used.

2,4-D degrader diversity. The 2,4-D degraders in this study were distributed throughout the alpha, beta, and gamma subgroups of the *Proteobacteria* (Fig. 1). The lack of representation of gram-positive bacteria is likely a reflection of isolation methods, not of the lack of gram-positive 2,4-D degraders. The majority of these strains were members of the beta subgroup of *Proteobacteria*, five of which were most closely related to the genus *Burkholderia*, having at least 92% sequence similarity with each other. Three were closely related to *Rhodoferax fermentans* (close to the class *Comamonadaceae*), three were related to *Ralstonia eutropha*, and one was related to *Alcaligenes xylosoxidans*. TFD39 falls outside any clear cluster. One member of the γ-Proteobacteria, strain I-18, a haloalkaliphile, was found to be closely related to the salt-loving genus *Halomonas* (15). The remaining six strains all clustered in the alpha branch of *Proteobacteria* (Fig. 1). Of this subgroup, five were most closely related to the genus *Sphingomonas*. One member of the α-Proteobacteria, strain M1, which is the most oligotrophic and slow growing of all the strains used in this study, is 97% similar to *Rhodopseudomonas palustris*. The character of strain M1 correlates well with its phylogenetic placement near the slow-growing genus *Bradyrhizobium*.

***tfdA* gene fragments.** *tfdA* gene fragments were successfully amplified and sequenced from 10 strains of β-Proteobacteria and 1 strain of γ-Protobacteria. None of the strains from the α-Proteobacteria gave any amplificates with these primers. These 313 contiguous nucleotides were aligned with additional *tfdA* sequences from JMP134 and from strain RASC (Fig. 2). Three distinct classes of *tfdA* gene sequences with slight variations in each class were found. Class I included fragments from JMP134, TFD39, TFD23, K712, and TFD9 that differed from each other by 2 bp at the most. Class I *tfdA* genes are probably plasmid encoded. All strains with a class I *tfdA* gene examined so far contained broad-host-range, self-transmissible plasmids containing 2,4-D genes (2, 3, 11, 17). All of the strains with a class I *tfdA* gene were able to transfer the 2,4-D phenotype in the mating studies reported above. The class II *tfdA* sequences included identical fragments amplified from RASC, TFD6, and TFD2 which were 76% similar to those in class I. Class III included identical fragments from strains TFD31, B6-9, and I-18 which were 77% similar to class I genes and 80% similar to class II genes. Both class II and III *tfdA* genes differed from each other and from class I genes in the same nine sites corresponding to the third base pair of the codons. The *tfdA* phylogenetic tree is a simple one, with three distinct branches that are incongruent with the SSU rDNA-derived phylogeny (Fig. 3). Class I *tfdA* sequences were found in *Burkholderia*-like strains, in strains related to the *Comamonas-Rhodoferax* group, and in the *Ralstonia-Acaligenes* group, all in the β-Proteobacteria. Class II sequences are less widely distributed, found only in *Burkholderia*-like branches. However,

```
[                10        20        30        40        50]
[                .         .         .         .         .]
JMP134     CATCACCAGATCTCCCACGTTCCAGCGATGCCGGTACACGAATTCCCGCT    [50]
TFD39      ..................................................    [50]
TFD23      ..................................................    [50]
B69        ......G........G..T.......T......A.....A..C.T..T.    [50]
RASC       ......A.....C..G..T.......T......A..G..A..C.T.G.T.    [50]

[                60        70        80        90       100]
[                .         .         .         .         .]
JMP134     GTGTCGCGTGCTCGAGAAGCTCCGCAAGCAGCATCCGGCCTTCGGCCACC    [100]
TFD39      ..................................................    [100]
TFD23      ..................................................    [100]
B69        .C.....................A..C........G..A........G..G    [100]
RASC       .C.....A..............T...........G..A........G..G    [100]

[                110       120       130       140       150]
[                .         .         .         .         .]
JMP134     GGAAGGCCTTCGACGTGGCTCGCGTGCGCGCCGATGAAGAGAAACTTGCG    [150]
TFD39      ..................................................    [150]
TFD23      ..................C...............................    [150]
B69        ...C....C....T...A.C...A..A..C.....A..A............    [150]
RASC       ...C.........T...A..A..A..A..C.....A..A............    [150]

[                160       170       180       190       200]
[                .         .         .         .         .]
JMP134     CCCGGAGCCGGCGTGGGTTCGAACCAGCGGCCAGTTGACCGGCGGCATGG    [200]
TFD39      ..............................A...................    [200]
TFD23      ..............................A...................    [200]
B69        T..A..T..C........G..G.....T.....AC.C.....A.....C.    [200]
RASC       T..A..T..C........G..G.T..........C.C.....A.....C.    [200]

[                210       220       230       240       250]
[                .         .         .         .         .]
JMP134     CATTGCGTTGCGCTTCCGAATAGTCGGTGTCGCCGAGCAGGAAGCGGGAG    [250]
TFD39      ..................................................    [250]
TFD23      ..................................................    [250]
B69        ..........ACT...A........C..A.....A..A.T.........A    [250]
RASC       ..........ACT...A.....C..T........A..A.TA........A    [250]

[                260       270       280       290       300]
[                .         .         .         .         .]
JMP134     TTCAGTGCGTAGTGCTCGGCACGCAGCCCTTCCAACTCGGATTGGAGGTC    [300]
TFD39      ..................................................    [300]
TFD23      ...................................T..............    [300]
B69        .....C...........T..G....AT..C.G..GT..CTTC.T..AA..    [300]
RASC       .G...C...........T.......AT..C.G..GT..CTTC.T..AA..    [300]

[                310 ]
[                .   ]
JMP134     CCGAGGCAGCGCG    [313]
TFD39      .............    [313]
TFD23      .............    [313]
B69        .TCG..G..AT..    [313]
RASC       .TCG..A..AT..    [313]
```

FIG. 2. Alignment of 313 nucleotides of internal fragments of *tfdA* genes from representative strains. Nucleotides identical to *tfdA* from pJP4 are represented by periods.

even in this subgroup, this *tfdA* variant is found in strains that differ by 7% at the SSU rDNA level (RASC and TFD2). However, the class III sequences were most interesting, being found both in the *Comamonas-Rhodoferax* group and in a strain of the γ-Proteobacteria, I-18, strains that differ by 24% at the SSU rDNA level. Class III genes have since been found in a collection of randomly isolated non-2,4-D degraders, including gram-positive bacilli, as well as in various gram-negative bacteria, even though the gene is not expressed (10).

An interesting result was the detection of two different *tfdA* gene variants in sibling strains. TFD23 and TFD31 are identical at the ribosomal gene level, but one harbors a class I gene and the other harbors a class III gene. Similarly, TFD6 and

Downloaded from http://aem.asm.org/ on September 3, 2020 at Corteva Agriscience

COR-AAD1-00002706
Bayer EX1008 (Part 5 of 9)

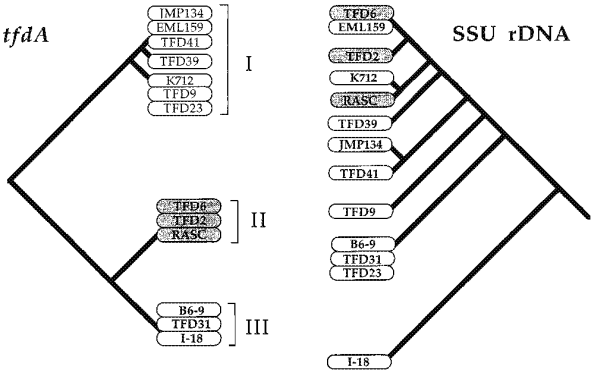


FIG. 3. Phylogenetic incongruency of *tfdA* genes and SSU rDNA from diverse 2,4-D-degrading bacteria. Dendrograms for *tfdA* and SSU rDNA are indicated. Shading indicates the type of *tfdA* sequence, either class I, II, or III. Note that branch lengths are not drawn to scale.

EML159 are rRNA siblings that carry a class II and class I gene, respectively.

None of the α-Proteobacteria yielded a PCR product when amplified with the conserved *tfdA* primers. This finding complements our observation that none of these bacteria hybridized to the *tfdA* gene, even under conditions of low stringency, indicating that any *tfdA*-like genes in the α-Proteobacteria are likely to be more divergent from the ones sequenced here (7, 11). In addition, none of the *Sphingomonas* strains in the study hybridized with a whole pJP4 probe, and similarly, no *Sphingomonas* strains scored positive for transfer of 2,4-D-degrading ability to recipient *B. cepacia* D5. Together these results suggest a reduced gene flow between members of the α- and β- or γ-Proteobacteria or poor gene expression of β- or γ-derived genes by α-Proteobacteria. Although plasmid pJP4 is a broad-host-range plasmid and has been known to transfer to α-Proteobacteria such as *Rhizobium* and *Agrobacterium* species and to γ-Proteobacteria such as *Pseudomonas putida*, *Pseudomonas fluorescens*, and *Pseudomonas aeruginosa*, the 2,4-D pathway is not expressed in these strains of the α- or γ-Proteobacteria (3). Phylogenetically limited expression of plasmid-borne 3-chlorobenzoate-degradative genes has also been noted for the pseudomonads (8). Subsequent studies have found divergent but related sequences for the *tfdB* and *tfdC* genes in 2,4-D-degrading *Sphingomonas* strains (7, 12, 24).

With the exceptions of the minor differences within the class I pJP4-like *tfdA* sequences, there were no intermediate *tfdA* sequences. The most likely explanation of this is that the rate of horizontal transfer of the *tfd* genes is high relative to the rate at which mutations can accumulate. Examination of sequences of *tfdA* genes from a greater variety of organisms may turn up more intermediate variation.

ACKNOWLEDGMENTS

We thank Arturo Massol-Deya and Jizhong Zhou for primers and Tom Schmidt, Bonnie Bratina, and Jim Smith for advice and assistance with sequence analysis. We thank William Holben, Jong-Ok Ka, Nancy Tonso, Penny Amy, and Charles Greer for the use of their strains and Richard Lenski for valuable discussions in comparing phylogenies of *tfdA* and SSU rDNA. We also thank the people in the Research on Microbial Evolution Laboratory for their support.

This work was supported by the National Science Foundation (grant DEB9120006), a part of the Joint Project on Microbial Evolution with the Research and Development Corporation of Japan (JRDC).

REFERENCES

1. **Altschul, S. F., W. Gish, W. Miller, E. W. Myers, and D. J. Lipman.** 1990. Basic local alignment search tool. J. Mol. Biol. **215**:403–410.
2. **Amy, P. S., J. W. Schuike, L. M. Frazier, and R. J. Seidler.** 1985. Characterization of aquatic bacteria and cloning of genes specifying partial degradation of 2,4-dichlorophenoxyacetic acid. Appl. Environ. Microbiol. **49**:1237–1245.
3. **Don, R. H., and J. M. Pemberton.** 1981. Properties of six pesticide degradation plasmids isolated from *Alcaligenes paradoxus* and *Alcaligenes eutrophus*. J. Bacteriol. **145**:681–686.
4. **Feisenstein, J.** 1988. Phylogenies from molecular sequences: inference and reliability. Annu. Rev. Genet. **22**:521–565.
5. **Friedrich, B., M. Meyer, and B. Schlegel.** 1983. Transfer and expression of the herbicide-degrading plasmid pJP4 in aerobic autotrophic bacteria. Arch. Microbiol. **134**:92–97.
6. **Fukumori, F., and R. P. Hausinger.** 1993. *Alcaligenes eutrophus* JMP134 "2,4-dichlorophenoxyacetate monooxygenase" is an α-ketoglutarate-dependent dioxygenase. J. Bacteriol. **175**:2083–2086.
7. **Fulthorpe, R. R., C. McGowan, O. V. Maltseva, W. H. Holben, and J. M. Tiedje.** 1995. 2,4-Dichlorophenoxyacetic acid-degrading bacteria contain mosaics of catabolic genes. Appl. Environ. Microbiol. **61**:3274–3281.
8. **Fulthorpe, R. R., and R. C. Wyndham.** 1991. Transfer and expression of the catabolic plasmid pBRC60 in wild bacterial recipients in a freshwater ecosystem. Appl. Environ. Microbiol. **57**:1546–1553.
9. **Fulthorpe, R. R., and R. C. Wyndham.** 1992. Involvement of a chlorobenzoate catabolic transposon, Tn*5271*, in community adaptation to chlorobiphenyl, chloroaniline, and 2,4-dichlorophenoxyacetic acid in a freshwater ecosystem. Appl. Environ. Microbiol. **58**:314–325.
10. **Hogan, D. A., D. B. Buckley, C. B. Nakatsu, T. M. Schmidt, and R. P. Hausinger.** 1997. Distribution of the *tfdA* gene in soil bacteria that do not degrade 2,4-dichlorophenoxyacetic acid, 2,4-D. Microb. Ecol. **34**:90–96.
11. **Ka, J. O., W. E. Holben, and J. M. Tiedje.** 1994. Genetic and phenotypic diversity of 2,4-dichlorophenoxyacetic acid (2,4-D)-degrading bacteria isolated from 2,4-D-treated field soils. Appl. Environ. Microbiol. **60**:1106–1115.
12. **Leander, M., T. Vallaeys, and R. R. Fulthorpe.** 1998. Amplification of putative chlorocatechol dioxygenase fragments from alpha and beta proteobacteria. Can. J. Microbiol. **44**:482–486.
13. **Levy, S. B., and R. V. Miller.** 1989. Gene transfer in the environment. McGraw Hill Publishing Company, New York, N.Y.
14. **Maddison, W. P., and D. R. Maddison.** 1992. MacClade: analysis of phylogeny and character evolution, version 3.0. Sinauer Associates, Sunderland, Mass.
15. **Maltseva, O., C. McGowan, R. Fulthorpe, and P. Oriel.** 1996. Degradation of 2,4-dichlorophenoxyacetic acid by haloalkaliphilic bacteria. Microbiology **142**:1115–1122.
16. **Matheson, V. G., L. J. Forney, Y. Suwa, C. Nakatsu, A. J. Sexstone, and W. E. Holben.** 1996. Evidence for acquisition in nature of a chromosomal 2,4-dichlorophenoxyacetic acid/α-ketoglutarate dioxygenase gene by different *Burkholderia* spp. Appl. Environ. Microbiol. **62**:2457–2463.
17. **Nakatsu, C. H., F. Fukumori, R. Fulthorpe, R. Hausinger, W. Holben, Y. Kamagata, R. Korona, R. Lenski, O. Maltseva, V. G. Matheson, C. McGowan, Y. Suwa, J. Tiedje, N. Tonso, E. Top, A. Wright, and L. Forney.** 1997. Genetic diversity of 2,4-dichlorophenoxyacetic acid (2,4-D) catabolic genes, p. 197–206. *In* K. Horikoshi, M. Fukuda, and T. Kudo (ed.), Microbial diversity and genetics of biodegradation. Japan Scientific Societies Press, Tokyo, Japan.
18. **Sambrook, J., E. F. Fritsch, and T. Maniatis.** 1989. Molecular cloning: a laboratory manual, 2nd ed. Cold Spring Harbor Laboratory Press, Cold Spring Harbor, N.Y.
19. **Streber, W. R., K. N. Timmis, and M. H. Zenk.** 1987. Analysis, cloning, and high-level expression of 2,4-dichlorophenoxyacetate monooxygenase gene *tfdA* of *Alcaligenes eutrophus* JMP134. J. Bacteriol. **169**:2950–2955.
20. **Suwa, Y., A. D. Wright, F. Fukumori, K. A. Nummy, R. P. Hausinger, W. E. Holben, and L. J. Forney.** 1996. Characterization of a chromosomally encoded 2,4-dichlorophenoxyacetic acid/α-ketoglutarate dioxygenase from *Burkholderia* sp. strain RASC. Appl. Environ. Microbiol. **62**:2464–2469.
21. **Swofford, D. L.** 1993. PAUP: Phylogenetic Analysis Using Parsimony, version 3.1. Computer program distributed by the Illinois Natural History Survey, Champaign, Ill.
22. **Tiedje, J. M., J. M. Duxbury, M. Alexander, and J. E. Dawson.** 1969. 2,4-D metabolism: pathway of degradation of chlorocatechols by Arthrobacter sp. J. Agric. Food Chem. **17**:1021–1025.
23. **Tonso, N. L., V. G. Matheson, and W. E. Holben.** 1995. Polyphasic characterization of a suite of bacterial isolates capable of degrading 2,4-D. Microb. Ecol. **30**:3–24.
24. **Vallaeys, T., R. R. Fulthorpe, A. M. Wright, and G. Soulas.** 1996. The metabolic pathway of 2,4-dichlorophenoxyacetic acid degradation involves different families of *tfdA* and *tfdB* genes according to PCR-RFLP analysis. FEMS Microb. Ecol. **20**:163–172.
25. **Weisburg, W. G., S. M. Barns, D. A. Pelletier, and D. J. Lane.** 1991. 16S ribosomal DNA amplification for phylogenetic study. J. Bacteriol. **173**:697–703.

Downloaded from http://aem.asm.org/ on September 3, 2020 at Corteva Agriscience

COR-AAD1-00002707
Bayer EX1008 (Part 5 of 9)

Environ. Sci. Technol. 2004, 38, 6625−6632

Influence of Frozen Storage on Herbicide Degradation Capacity in Surface and Subsurface Sandy Soils

SARAH K. MORTENSEN AND CARSTEN S. JACOBSEN*

Geological Survey of Denmark and Greenland (GEUS), Department of Geochemistry, Øster Voldgade 10, DK-1350 Copenhagen K, Denmark

The degradation of MCPA and metribuzin was investigated in laboratory batch experiments using fresh and frozen-stored soil samples from the unsaturated zone of a sandy soil. Mineralization potentials measured in fresh and frozen-stored soils were similar, and mineralization kinetics in surface and subsurface soils could be fitted using the same kinetic models. MCPA mineralization data from all three horizons were best described with the exponential growth form of the three-half-order model. During the mineralization of MCPA, growth in MCPA-degrading microbial populations was confirmed by increases in the abundance of *tfdA* genes following MCPA exposure. In contrast to MCPA, metribuzin mineralization followed zero-order kinetics, and very little metribuzin was mineralized (<1%) in all three of the investigated soil horizons. In addition, metribuzin dissipation and metabolite formation were also measured in surface and subsurface soils using LC-MS/MS. Differences in metribuzin dissipation were observed in the A-horizon at the beginning of the experiment and resulted in substantially different 50% disappearance time, DT_{50}, values for frozen-stored (36 days) and fresh (<15 days) soil samples. However, the % of metribuzin remaining in fresh and frozen-stored surface soils was comparable from day 37 and thereafter.

Downloaded via CORTEVA AGRISCIENCE on September 3, 2020 at 19:39:37 (UTC).
See https://pubs.acs.org/sharingguidelines for options on how to legitimately share published articles.

Introduction

The widespread use of herbicides during the past 50 years has resulted in numerous reports of groundwater contamination (*1*−*3*). In fact, herbicide leaching to water resources beneath the unsaturated zone of soils poses a serious risk to the drinking water supply in Denmark, as almost 100% of Danish drinking water is provided by groundwater reserves. Knowledge of the parameters controlling pesticide transport through the unsaturated zone of soils (e.g., microbial degradation or sorption characteristics) is required to protect groundwater resources. In this study, MCPA (4-chloro-2-methylphenoxyacetic acid) and metribuzin (4-amino-6-*tert*-butyl-3-methylthio-1,2,4-triazin-5(4*H*)-one) degradation were investigated in the unsaturated zone of a sandy soil.

MCPA has been used in Denmark to control broad-leaf weeds primarily in cereal crops since the late 1940s. As with some of the other phenoxyalkanoic acid herbicides used in Denmark, MCPA has been detected in the Danish groundwater at concentrations exceeding 0.1 $\mu g\ L^{-1}$ (*4*), that is, the maximum allowable concentration for drinking water in the European Union (*5*). Metribuzin is a selective herbicide used in Denmark for pre- and post-emergence control of grasses and broad-leaf weeds in potato crops. Although metribuzin has not yet been detected in Danish groundwater, the Danish Pesticide Leaching Assessment Program (PLAP) reported groundwater to be contaminated with two of its degradation products (*6*). Both of the herbicides investigated in this study are weakly sorbed to sandy soils with organic carbon contents <1.7% (*7*, *8*), and so knowledge of their degradation in surface and subsurface soils is essential for predicting leaching risks.

Various kinetic models have been used to describe the degradation of xenobiotic compounds in soil environments [for review, see Fomsgaard (*9*)]. The three-half-order model was developed by Brunner and Focht (*10*) to describe mineralization kinetics in soil and has previously been used to describe the mineralization of phenoxyalkanoic acid herbicides (*9*, *11*) as well as metribuzin (*12*). This kinetic model is able to describe the mineralization of organic compounds in instances involving either growth-linked or co-metabolic biodegradation. Thus, the parameter estimates from modeling with the three-half-order model were used in the present study as indicators of degradation type (metabolic vs cometabolic). In addition, MCPA-degrading populations were monitored for growth using DNA-based techniques. Specifically, the abundance of *tfdA*-homologous genes, which are commonly carried by phenoxyalkanoic acid degraders (*13*−*16*), was determined at different stages during the mineralization of MCPA.

Although freshly collected soil samples should be used when studying processes that involve soil microorganisms (*17*), various practicalities often make soil storage necessary. In general, drying soil samples is not recommended as a means to preserve soil for such studies (*17*, *18*). However, there is less agreement on whether freezing is an acceptable method in which to preserve soil samples. For example, Stenberg et al. (*19*) recommended storing soil samples at −20 °C for up to 13 months in a study comparing the effects of cold (+2 °C) and frozen storage on microbial biomass and activities in 12 agricultural soils, whereas the ISO standard (*20*) on soil storage for studies assessing aerobic microbial processes warns against freezing as a storage method. In fact, several studies have shown that freezing soil samples causes damage to indigenous microbial communities (*21*−*23*). Such effects could possibly alter the degradation potentials of soils later used in degradation studies. Nevertheless, a few studies have reported that storing soils in a frozen state prior to herbicide degradation studies did not significantly affect the results of these studies (*19*, *24*). However, both of these studies only investigated herbicide degradation in surface soils originating from areas with cold winters.

To our knowledge, all of the literature concerning the effects of freezing soil samples is comprised of studies using surface soils. As microorganisms in the vadose zone of subsurface soils in temperate regions are rarely ever exposed to the stress factors associated with freeze/thaw events, such events might be even more consequential for these populations than for the microbial populations of surface soils. Therefore, the main objective of this study was to investigate the degradation of MCPA and metribuzin after artificial freeze/thaw events in the A-, B-, and C-horizons of a sandy soil.

Materials and Methods

Soil. The soil used in the experiments was a sandy, agricultural soil from Southern Jutland, Denmark (55°1.65′ N, 9°7.70′ E;

* Corresponding author phone: +45-38142313; e-mail: csj@geus.dk.

10.1021/es049542x CCC: $27.50 © 2004 American Chemical Society
Published on Web 11/02/2004

COR-AAD1-00002708
Bayer EX1008 (Part 5 of 9)

TABLE 1. Soil Characteristics

horizon	depth (cm)	clay (%)	silt (%)	sand (%)	C (%)	pH (H_2O)
A	21−35	5.2	9.8	82.8	1.3	5.5
B	40−55	5.0	2.8	91.7	0.3	6.1
C	80−90	2.5	2.0	95.2	0.1	6.3

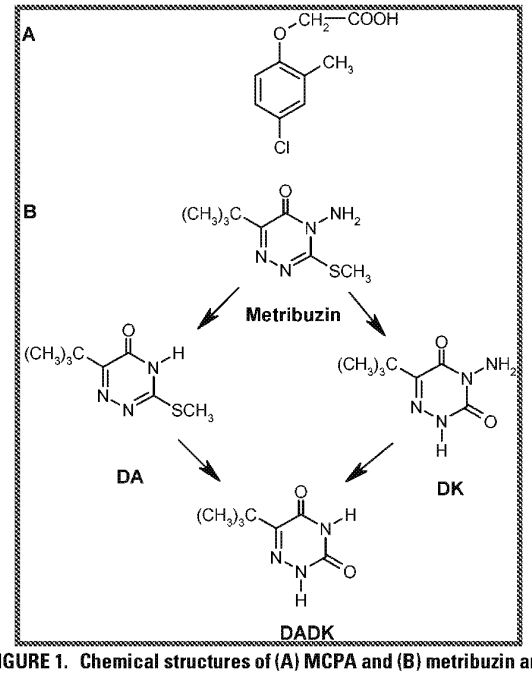


FIGURE 1. Chemical structures of (A) MCPA and (B) metribuzin and its primary metabolites (*25*).

WGS84). Samples were collected in January 2002 from three different soil horizons above the groundwater table (Table 1). The soil was stored in the dark at 5 °C until the day after collection and thereafter sieved (4 mm mesh). Half of the samples were then stored in the dark at −18 °C for a period of 52 h and thereafter allowed to defrost in the dark for a period of 5 days at 10 °C. The other half of the soil samples were kept in the dark at 10 °C for a total of 7 days. All of the samples were stored at their natural moisture content.

Chemicals. Ring-6-^{14}C-labeled metribuzin with a specific activity of 5.2 MBq/mg and a radiochemical purity of 96.6% was obtained from Internationale Isotope (Munich, Germany). Unlabeled metribuzin, desaminometribuzin (DA), diketometribuzin (DK), and desaminodiketo-metribuzin (DADK) were purchased from Dr. Ehrenstorfer (Augsburg, Germany). Metribuzin had a purity of 99.5%, DA a purity of 99%, and the remaining two degradation products a purity of 98%. Uniformly ring ^{14}C-labeled MCPA with a specific activity of 5.9 MBq/mg and a radiochemical purity of 95% was obtained from Izotop (Budapest, Hungary). Unlabeled MCPA with a purity of 99.1% was also obtained from Dr. Ehrenstorfer.

Stock solutions of radiolabeled and unlabeled herbicides were made using HPLC grade acetonitrile from Romil (Cambridge, UK). Prior to addition of metribuzin and MCPA to soils, the acetonitrile from adequate amounts of the stock solutions was allowed to evaporate before redissolving the compounds in Milli-Q water. Chemical structures of the herbicides and some degradation products are shown in Figure 1.

Mineralization Studies. Soil (20 g dw) was transferred to 100 mL flasks with airtight glass stoppers and left overnight in the dark at 10 °C. The soil in each microcosm was then spiked with 1 mL of a 20 mg/L solution (50 000 dpm/mL) of MCPA or metribuzin in Milli-Q water, thereby giving a final concentration of 1 mg/kg of dry soil. The solution was carefully mixed into the soil with a sterile pipet. All of the soil systems had a pressure potential corresponding to pF = 1.4, after their amendment with aqueous solution. All microcosms were set up in triplicate and incubated in darkness at 10 °C. The $^{14}CO_2$ released due to soil respiration was trapped in NaOH (2 mL, 0.5 M) placed in small test tubes inside the flasks. The microcosms were aerated each time NaOH was removed (at least once a week). NaOH was transferred to 20 mL scintillation vials containing 10 mL of scintillation fluid (OpTiPhase HiSafe 3). The vials were shaken, stored still >24 h, and then counted for 10 min using a Wallac 1409 Liquid Scintillation System (Perken Elmer Life Sciences, Wallac Oy, Turku, Finland).

Degradation of Metribuzin. Soil (20 g dw) was transferred to 250 mL blue cap flasks and left overnight in the dark at 10 °C. The soil in each microcosm was then spiked with 1 mL of a 20 mg/L solution of unlabeled metribuzin in Milli-Q water. As a result, each soil system had a metribuzin concentration of 1 mg/kg dry soil. The solution was carefully mixed into the soil with a sterile pipet, and the microcosms were incubated at 10 °C in darkness. The final water content of the soils was the same as in the mineralization experiments. To prevent anaerobic conditions from developing in the soil systems, they were aerated for 10 min in a sterile hood every 14 days. On days 15, 37, 50, 64, and 85, three replicate blue cap flasks of each soil type (A-fresh, A-frozen, C-fresh, C-frozen) were sacrificed. In addition, triplicate control samples that were spiked (as described above) on the day of sampling were also sacrificed. Results from the controls were later used to calculate the recovery % of metribuzin, and metribuzin dissipation calculations were adjusted accordingly.

Pressurized liquid extraction was performed using an ASE 200 system from Dionex (Sunnyvale, CA). The extraction conditions were similar to those described by Henriksen et al. (*26*), except that a purge time of 300 s was used. Isocratic separation of metribuzin and its metabolites was obtained using a 100 × 2.1 mm Xterra RP_{18} column (3.5 μm particle size) from Waters (Milford, MA) and a Waters model 2690 HPLC system. The mobile phase was composed of methanol:water:0.2% acetic acid (50:25:25) and had a flow rate of 180 μL/min. The injected volume was 10 μL, and the temperature in the autosampler chamber was set to 5 °C. A Quattro Ultima triple quadropole mass spectrometer from Micromass (Manchester, UK) equipped with electrospray ionization (ESI) was used to detect metribuzin, DA, DK, and DADK. Nitrogen was used at the desolvation gas at a flow rate of 600 L/h, and the capillary voltage was set to 2.8 kV for the detection of all four compounds. All of the other MS-MS settings were the same as those used by Henriksen et al. (*26*). Soil extracts were diluted six times with a methanol: water (75:25; v/v) solution for the detection of metribuzin, while DA, DK, and DADK were detected using undiluted soil extracts.

Bacteria and Growth Conditions. The MCPA-degrading *Burkholderia cepacia* DBO1 with pRO101 (*27*) was used to create a ^{32}P-labeled probe and as a positive control for hybridization. A small amount of the frozen stored culture (50% glycerol) was spread on Luria Bertani (LB) agar supplemented with 15 ppm tetracycline and incubated for 48 h at 30 °C. A single colony was transferred to 20 mL of LB medium and shaken at 150 rpm for 19 h at 30 °C. The late log phase was harvested, washed twice in phosphate buffer (0.015 M, pH = 7.4), and resuspended in 20 mL of buffer. DNA was then extracted from 1 mL of this suspension.

COR-AAD1-00002709
Bayer EX1008 (Part 5 of 9)

TABLE 2. Primers Used for *tfdA* Amplification

primer	position in *tfdA* gene (pJP4)	sequence (5′ → 3′)
TVU	1168–1185	ACG-GAG-TTC-TG(C/T)-GA(C/T)-ATG
TVL	1513–1530	AAC-GCA-GCG-(G/A)TT-(G/A)TC-CCA
SM-extF	1141–1157	GTG-GTG-GTT-CCG-CCG-TC
SM-extR	1543–1560	CGA-GAT-GTC-GTA-CCT-GCG

DNA Extraction and *tfdA* Gene Analysis. On days 0, 3, 7, 13, 18, and 30, 0.35 g of soil was removed from each of the mineralization flasks containing ^{14}C-labeled MCPA. (Soil from control flasks was removed on days 12 and 31.) DNA was extracted from 0.10 g of wet sediment using the FastDNA SPIN Kit for soil (BIO 101; Carlsbad, CA). The manufacturer's instructions were slightly modified to obtain an increased extraction efficiency (*28*) by bead beating the samples in a FastPrep FP 120 instrument (BIO 101) for 3 × 30 s at speed 5.0 instead of 1 × 30 s at speed 5.5. The DNA was eluted in 100 μL of DES (DNase/pyrogen free water) and stored at −20 °C. DNA from 1 mL of a *B. cepacia* DBO1 suspension was extracted in the same manner.

Primers for *tfdA* analysis, TVU and TVL (Table 2), were derived from conserved regions of the *tfdA* gene sequences of pJP4 and *Burkholderia* strain RASC (*29*). Each 50 μL PCR mixture contained 1 × GeneAmp PCR-buffer (Applied Biosystems; Foster City, CA), 1 mg/mL DNase-free bovine serum albumin (Amersham Pharmacia; Uppsala, Sweden), 100 μM of each dNTP (Applied Biosystems), 0.5 μM of TVU and TVL, 1.25 U AmpliTaq Gold DNA polymerase (Applied Biosystems), and 1.0 μL of DNA template. DNA extracted from soil samples was diluted 10 times in DNase/RNase free water (BIO 101) to titrate PCR inhibiting substances (e.g., humic acids) present in the DNA extractions. A dilution series (10^{-1}–10^{-8}) of the DNA extracted from DBO1 cells was also amplified to use as internal standards for the hybridization blots, and PCR mixtures containing 1 μL of dH_2O instead of a DNA template were used as negative controls. PCR was performed on a Genius thermal cycler (Techne; Cambridge, England) using the protocol described by Vallaeys et al. (*29*). All PCR products were purified using the QIAquick PCR Purification Kit (QIAGEN, Hilden, Germany).

A double-stranded *tfdA* gene probe was generated by nested PCR. The PCR mixture for the first PCR reaction contained (per 50 μL) 1 × GeneAmp PCR-buffer (Applied Biosystems), 1 mg/mL DNase-free BSA (Amersham Pharmacia), 100 μM of each dNTP (Applied Biosystems), 0.5 μM of SM-extF and SM-extR (Table 2), 1.25 U AmpliTaq Gold DNA polymerase (Applied Biosystems), and 1.0 μL of DNA extracted from *P. cepacia* DBO1 and diluted 1000 times in DNase/RNase free water (BIO 101). The first PCR program was as follows: 10 min at 95 °C; 30 cycles of 30 s at 95 °C, 30 s at 58 °C, and 1 min at 72 °C; with a final extension of 6 min at 72 °C. The PCR product was purified using the QIAquick PCR Purification Kit (QIAGEN).

Radiolabeling the DNA probe was accomplished in the second PCR reaction according to a protocol described by Sambrook and Russell (*30*). The PCR mixture for 50 μL probe contained 1× GeneAmp PCR-buffer (Applied Biosystems), 200 μM of dATP, dGTP, and dTTP (Promega; Madison, WI), 2 μM dCTP (Promega), 1 μM of TVU and TVL primers, 2.5 U AmpliTaq Gold DNA polymerase (Applied Biosystems), 370 MBq/mL [α-^{32}P]dCTP (Amersham Biosciences, England; specific activity, 110 TBq/mmol), and 5 μL double-stranded DNA template (purified PCR product from the first PCR reaction). The radiolabeled probe was purified with the QIAquick PCR Purification Kit (QIAGEN).

Denatured PCR products were vacuum blotted onto a 0.45 μm positively charged nylon membrane (Boehringer Mannheim; Mannheim, Germany) and UV cross-linked to the membrane with a UV Stratalinker 2400 (Stratagene; La Jolla, CA). DNA blots were prehybridized at 68 °C for 5 h in 25 mL of hybridization buffer (5× SSC (pH = 7.0), 0.02% SDS (pH = 7.2), 1% Boehringer Mannheim blocking reagent, 0.1% *N*-lauroylsarcosine, 1.25 mg of salmon sperm). After the denatured ^{32}P-labeled probe was added to the hybridization buffer, the DNA blots were hybridized at 68 °C for 18 h. Post-hybridization washes were performed under the following high-stringency conditions: (1) 2 × 5 min at room temperature with 2× SSC + 0.1% SDS, (2) 2 × 15 min at 68 °C with prewarmed 0.1× SSC + 0.1% SDS. DNA blots were placed in plastic wrap and exposed to a MP Cyclone phosphor storage screen (Packard; Meriden, CT) for 24 h. Hybridization signals were visualized and quantified using the Cyclone storage phosphor system (Packard).

Data Analysis. Calculated cumulative mineralization values were corrected for background radioactivity, and *t*-tests ($P < 0.05$) were performed on the averages of triplicates. Cumulative MCPA mineralization results were also corrected for the removal of 0.35 g of [^{14}C]-MCPA-amended soil on days 3, 7, 13, 18, and 30.

Nonlinear regression analysis was performed on $^{14}CO_2$ data using the curve-fitting program in SigmaPlot (for Windows, version 5.00, SPSS). This program fits curves using the Marquardt–Levenberg algorithm. Mineralization curves were fitted with zero-order, first-order, and three-half-order kinetic models. The three-half-order model developed by Brunner and Focht (*10*) has a linear form, which assumes either linear- or zero-growth of the biomass:

$$P = S_0[1 - \exp(-k_1 t - {}^1/_2 k_2 t^2)] + k_0 t \quad (1)$$

as well as an exponential growth form:

$$P = S_0\{1 - \exp[-k_1 t - E_0/\mu(\exp(\mu t) - 1)]\} + k_0 t \quad (2)$$

where P is product formation (CO_2), S_0 is the initial substrate concentration, k_0 is the zero-order rate, k_1 is an initial exponential rate constant, k_2 is the rate of increase of the first-order rate constant with time, μ is the growth rate constant, and E_0 is the initial cell concentration. The three-half-order model was proposed to describe CO_2 evolution during mineralization in soil. In addition, the following first-order model can also be used to describe mineralization kinetics in soil:

$$P = S_0[1 - \exp(-k_1 t)] \quad (3)$$

The dissipation of metribuzin in soil samples was described using first-order kinetics:

$$C_t = C_1 \exp(-k_1 t) \quad (4)$$

as well as the following two-compartment model (*31*):

$$C_t = C_1 \exp(-k_1 t) + C_2 \exp(-k_2 t) \quad (5)$$

where C_t is the amount of herbicide remaining at time t, C_1 is the initial amount of herbicide dissipated through the first-order process, k_1 is the dissipation rate constant for the first-order process, C_2 is the initial amount of herbicide dissipated through a second first-order process, and k_2 is the dissipation rate constant for the second first-order process.

F-tests ($P < 0.05$), as described by Robinson (*32*), along with an evaluation of the degree of correlation between

COR-AAD1-00002710
Bayer EX1008 (Part 5 of 9)

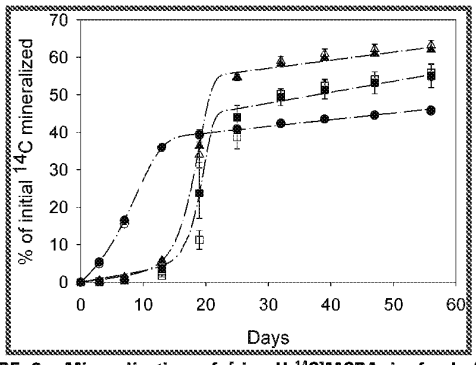


FIGURE 2. Mineralization of [ring-U-^{14}C]MCPA in fresh (solid symbols) and frozen-stored (empty symbols) soil samples from the A- (circles), B- (triangles), and C-horizons (squares). For clarity, only the modeled curves of fresh soil samples using the exponential growth form of the three-half-order model (dash−dot lines) are shown.

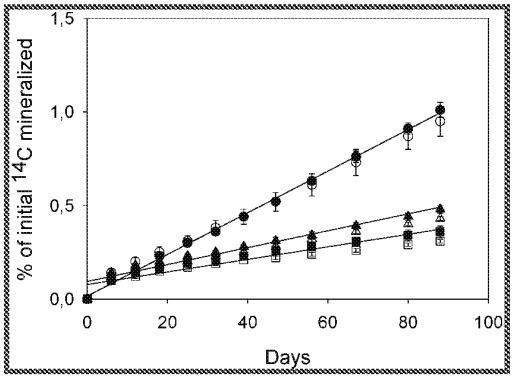


FIGURE 3. Mineralization of [ring-6-^{14}C]metribuzin in fresh (solid symbols) and frozen-stored (empty symbols) soil samples from the A- (circles), B- (triangles), and C-horizons (squares). The solid lines are modeled curves of fresh soil samples using zero-order kinetics.

parameters, the standard deviation of parameter estimates, how realistic the parameter estimates were, and the distribution of residuals around the model's curve were all used to deem which models best fit the data sets.

Results

Mineralization Studies. All of the MCPA mineralization curves were sigmoidal (Figure 2), although the lag-phases in the B- and C-horizons were significantly longer than that in the A-horizon. The relationship between soil depth and the total amount of $^{14}CO_2$ recovered after 56 days followed no apparent trend. The maximum amount of total accumulated $^{14}CO_2$, 63.4%, was seen in the B-horizon, and the least amount of [ring-U-^{14}C]MCPA was mineralized in the A-horizon.

The mineralization of metribuzin did not exceed 1.0% after 88 days in any of the soil horizons (Figure 3). As the level of radiochemical impurities in [ring-6-^{14}C]metribuzin was 3.4%, the mineralization seen may be attributed to mineralization of impurities rather than the herbicide. All of the mineralization curves were linear, but the mineralization rates in A-horizon samples (0.01% ^{14}C day^{-1}) were slightly higher than those in samples from the B- and C-horizons (0.004% and 0.003% ^{14}C day^{-1}, respectively). Furthermore, there were no significant differences between the mineralization rates in fresh and frozen samples.

Kinetic Modeling. According to performed F-tests ($P < 0.05$) as well as the residual sum of squares (Tables 3 and 4), the exponential form of the three-half-order model best described the MCPA mineralization data in all three horizons. As Focht and Brunner (*33*) deemed the k_1-term insignificant in cases where the exponential growth model gives a better fit than the linear growth model, we have simplified the exponential form of the three-half-order model by dropping the k_1-term (Table 3). The estimated E_0 values of 0.0000–0.0001 day^{-1} in the B- and C-horizons indicate lower initial population densities in the two subsurface horizons.

A comparison of the residual sum of squares (RSS) listed in Table 3 reveals that the exponential three-half-order model gives a more satisfactory description of MCPA mineralization in the A- and B-horizons than in the C-horizon. Because the standard error of the growth rate constant (μ) estimated for the C-horizon is quite high, the MCPA mineralization potentials of the three soil horizons were compared using the first-order model (eq 3). First-order rate constants (k_1) were calculated from the slope of the linear segment in a plot of $\ln(1 - P/S_0)$ versus time, where $0.94 < r^2 < 0.96$ (data not shown). The resulting k_1-values were 0.246 day^{-1} (A-horizon), 0.226 day^{-1} (B-horizon), and 0.177 day^{-1} (C-horizon).

Finally, the mineralization curves of metribuzin were best described by zero-order kinetics (Figure 3); RSS < 0.04.

Metribuzin Dissipation. In the A-horizon, first-order kinetics sufficiently described the dissipation of metribuzin in frozen-stored soil samples ($R^2 = 0.96$), but according to Robinson's F-test (*32*) metribuzin dissipation in fresh soil samples was best described by the biphasic two-compartment model ($R^2 = 0.99$). The initial disappearance of metribuzin in fresh soil samples was rapid, and less than 50% was left after only 15 days (Figure 4). Even so, the dissipation rate decreased with time, and approximately 20% of the metribuzin added was still present after 85 days. The initial metribuzin dissipation rate in frozen-stored soil samples was not as fast as in the fresh samples, but similar amounts of metribuzin were detected in the two sample types by the end of the experiment. A 50% dissipation time (DT_{50}) of 36 days for metribuzin in frozen-stored soil from the A-horizon was calculated using first-order kinetics.

In accordance with the faster dissipation of metribuzin in fresh soil samples during the first 2 weeks of the experiment, the formation of DK after 15 days was only detected in fresh soil samples, whereas DK formation was similar in both fresh and frozen samples after 30 days (Figure 5).

Toward the end of the experiment, an increase in the formation of DADK was observed in both sample types and coincided with a fall in the amount of DK. The greatest total amount of metabolites was detected on day 50, where 20.5% of the metribuzin added to fresh soil samples was present in the form of DK, DA, or DADK. However, no clear correlation between the total formation of metabolites and the dissipation of metribuzin in the A-horizon was observed. For example, a total metabolite formation of 4.8% in fresh soil samples after 15 days does not account for the disappearance of 58.6% of the metribuzin added.

Metribuzin was much more persistent in the C-horizon than in the A-horizon, and the average amount of metribuzin remaining in fresh soils from the C-horizon after 15 days did not significantly differ from the amount remaining after 85 days ($P < 0.05$). In fact, more than 70% of the added metribuzin was still present in both fresh and frozen-stored soils after 85 days (Figure 4). Using first-order kinetics, the DT_{50} values for fresh and frozen-stored soil samples were 178 and 151 days, respectively. Furthermore, the formation of metabolites in the C-horizon was almost nonexistent. The greatest total amount of metabolites was detected on day 85 and had a value of under 5% (data not shown). In addition, no DADK was detected whatsoever.

Abundance of *tfdA* Genes. Changes in the relative *tfdA* gene abundance in MCPA-exposed soil samples and non-

COR-AAD1-00002711
Bayer EX1008 (Part 5 of 9)

TABLE 3. Fresh Soil Parameter Estimates and Their Standard Errors Using a Simplified Exponential Form of the Three-Half-Order Kinetics Model (Eq 2)

chemical	soil horizon	residual sum of squares	μ (day^{-1})	$\mathcal{E}_0$ (day^{-1})	S_0 (%)	k_0 (%·day^{-1})
MCPA	A	1.93	0.227 ± 0.005	0.0321 ± 0.0009	36.24 ± 0.20	0.178 ± 0.005
	B	48.7	0.472 ± 0.052	0.0001 ± 0.0001	50.56 ± 1.30	0.216 ± 0.031
	C	204	0.634 ± 0.560	0.0000 ± 0.0000	38.92 ± 2.63	0.294 ± 0.064

TABLE 4. Fresh Soil Parameter Estimates and Their Standard Errors Using the Linear Form of the Three-Half-Order Kinetics Model (Eq 1)

chemical	soil horizon	residual sum of squares	K_1 (day^{-1})	k_2 (day^{-2})	S_0 (%)	k_0 (%·day^{-1})
MCPA	A	15.9	−0.0003 ± 0.006	0.024 ± 0.002	37.23 ± 0.61	0.155 ± 0.016
	B	397	−0.032 ± 0.010	0.008 ± 0.002	63.95 ± 8.24	−0.048 ± 0.174
	C	389	−0.031 ± 0.013	0.007 ± 0.002	52.77 ± 10.15	0.031 ± 0.013

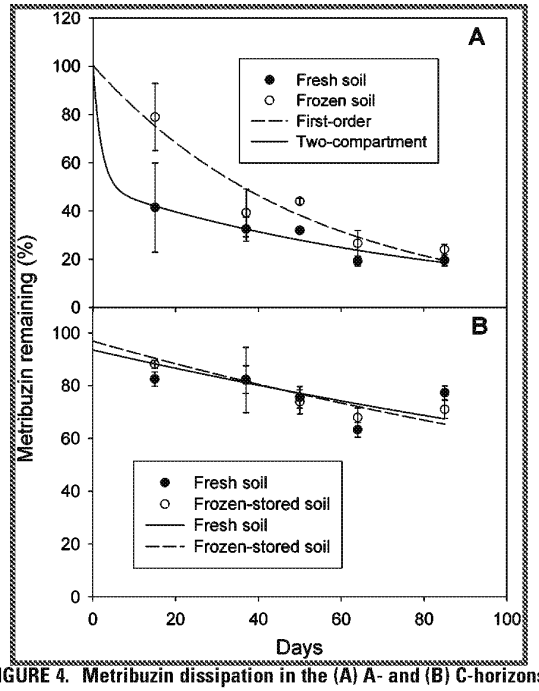


FIGURE 4. Metribuzin dissipation in the (A) A- and (B) C-horizons. Two-compartment model parameter estimates for describing dissipation in fresh soil were $C_1 = 50.00$, $k_1 = 0.500$, $C_2 = 50.00$, and $k_2 = 0.012$; when $0 < k_1 < 0.5$ and $0 < k_2 < 1$. First-order parameter estimates for frozen-stored soil were $C_1 = 100.3$ and $k_1 = 0.019$, when $k_1 < 0$.

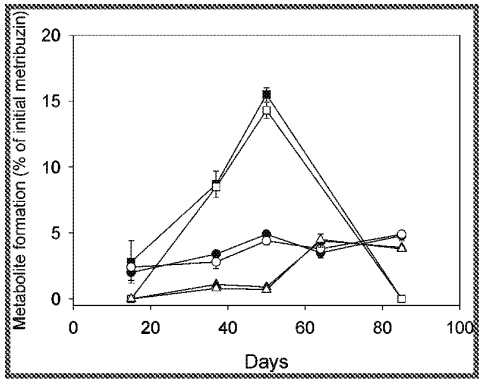


FIGURE 5. Formation of DA (circles), DK (squares), and DADK (triangles) in fresh (solid symbols) and frozen-stored (empty symbols) samples from the A-horizon. Error bars show the standard error of metabolite formation in triplicate samples.

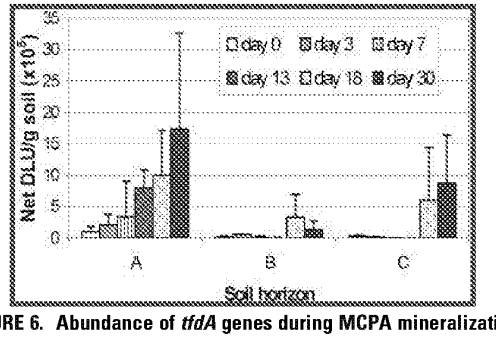


FIGURE 6. Abundance of *tfdA* genes during MCPA mineralization. Error bars show the standard error of signal intensities in triplicate samples.

exposed controls were monitored using quantitative hybridization analysis of PCR products. The relative abundance of *tfdA* genes in soil DNA extracts increased in the A- and C-horizons during MCPA mineralization. In both horizons, the initial increase in average signal intensity coincided with the exponential phase of mineralization (Figures 2 and 6). Furthermore, *tfdA* gene levels remained elevated throughout the remainder of the experiment, even though MCPA mineralization rates decreased. The abundance of *tfdA genes* at time 0 was highest in the A-horizon, which supports the lack of lag time in this horizon (Figures 2 and 6).

In the B-horizon, a slight increase in the abundance of *tfdA* genes was also observed during the exponential phase of mineralization (Figures 2 and 6). However, *tfdA* gene levels in this horizon did not remain elevated, and a decrease in signal intensity was seen at the end of the experiment (day 30). The signal intensities from MCPA-exposed samples in the B-horizon were lower than those in the A- and C-horizons, even though a higher % of added [^{14}C]MCPA was mineralized in the B-horizon.

Meanwhile, there were no significant increases in the average signal intensities of the nonexposed controls ($P < 0.05$) from any of the soil horizons during the course of the experiment (data not shown). For example, the nonexposed controls from the A-horizon had a signal intensity average of only 1.0×10^3 Digital Light Units (DLU)/g of soil on day 31.

The detection limit of the PCR hybridization method used in this study was determined for a pure *B. cepacia* DBO1(pJP4) culture. Assuming a DNA extraction efficiency of 100%, as few as 3 CFU DBO1 per sample could be detected using the constructed ^{32}P-labeled probe.

COR-AAD1-00002712
Bayer EX1008 (Part 5 of 9)

Discussion

Mineralization Studies. Freezing soil samples from the A-, B-, and C-horizons of a sandy soil prior to mineralization studies with MCPA, metribuzin, or acetate (data for acetate not shown) did not cause significant changes in the mineralization data obtained. Similar observations have also been reported for herbicides such as linuron, atrazine, and TCA in surface soil samples (*19, 24*). Thus, it seems that both MCPA and metribuzin degradation are equally unaffected by a single freeze/thaw episode. On the other hand, the lack of difference between mineralization curves in frozen-stored and fresh soils might also be due to the fact that any changes caused by freeze/thaw events were masked by the 5-day conditioning period prior to soil amendment. We have chosen the 5-day conditioning period, as previous studies have shown that bursts in CO_2 evolution or O_2-uptake rates following freeze/thaw events only last for a period of 1−4 days (*34, 35*).

In the present study, the mineralization of MCPA was greatest in the subsurface soils. Willems et al. (*36*) similarly observed higher values of total mineralization in subsurface soils with 2,4-dichlorophenoxyacetic acid (2,4-D), a phenoxyalkanoic acid herbicide with a chemical structure similar to MCPA, and proposed that degrading microorganisms in surface soils might prefer to degrade the relatively large amounts of available soil organic C instead of 2,4-D, whereas in subsurface soils, there are limited amounts of available C sources other than the added substrate, and the addition of compounds such as 2,4-D or MCPA is likely to result in a burst of microbial activity.

The low amount of MCPA mineralization observed in the A-horizon might also be the result of a reduction in the bioavailability of MCPA and/or its degradation products. Bolan and Baskaran (*37*) showed that the adsorption of 2,4-D (K_d-values) increased as the organic matter content increased in soils with an organic C % ranging from 1.4% to 9.8%. In addition, decreases in 2,4-D degradation rates also coincided with increases in organic matter content. Furthermore, soil humus in surface soils may serve as a sink for intermediate MCPA degradation products such as 4-chloro-2-methylphenol (*38*−*41*), and thus decrease the % of total MCPA mineralized to CO_2.

The amount of metribuzin mineralized in this study was less than the amount of impurities in the radiolabeled compound. Other studies have similarly shown that metribuzin's ring structure is not easily degraded by soil microorganisms, reporting the amount of metribuzin mineralization in soil to be less than 10% of the applied amount (*42*−*44*).

Kinetic Modeling of Mineralization Data. MCPA mineralization was best described in all three horizons by the exponential form of the three-half-order model. Reffstrup et al. (*11*) likewise used this model to fit the mineralization of mecoprop at a slightly higher concentration (5 ppm) in both surface and subsurface sandy loam soils. In studies using similar soil types, other types of phenoxyalkanoic acid mineralization curves have also been observed and can probably be explained by differences in initial concentrations (*9, 11, 45, 46*). In the present study, growth-linked biodegradation was directly confirmed by monitoring MCPA-degrading populations with DNA-based techniques. Very little metribuzin was mineralized in the surface soils of the present study (≤1%), and the observed mineralization was best described by zero-order kinetics. Similarly, low amounts of metribuzin mineralization (<3%) have also been reported in other surface and subsurface soil horizons (*44*).

Metribuzin Dissipation. Even though only negligible amounts of metribuzin were mineralized in all of the investigated soil horizons, significant metribuzin removal was observed in the A-horizon. The dissipation of metribuzin in frozen-stored soil samples followed first-order kinetics, which is in accordance with results published in several earlier studies using different soil types (*47*−*49*). However, metribuzin dissipation in fresh soil samples was best described using a two-compartment kinetic model, as the initial fast disappearance rate (first compartment) was followed by substantially slower dissipation processes (second compartment). The slower degradation observed in frozen-stored soil samples at the beginning of the experiment is likely due to damage suffered by indigenous microbial populations during freeze/thaw episodes. A similar explanation was used by Thorstensen and Lode (*50*) to account for a 35% decrease in bentazone degradation after 28 days in an organic-rich soil that had been stored frozen. However, because no damage was seen in the C-horizon soil, the effect might be solely related to the organic content of the soils.

The faster initial formation of diketometribuzin (DK) in fresh surface soil samples was in agreement with the faster metribuzin dissipation rate measured in these samples at the beginning of the experiment. However, DK levels were practically identical in fresh and frozen-stored surface soils by day 37. The concentration of DK (15.5% of the initial metribuzin concentration) peaked in the A-horizon at day 50 and was the highest amount recovered for any of the metabolites during the course of the experiment. In addition, DADK levels increased as DK levels fell, and the amount of DA recovered was relatively constant throughout the experiment. Similar metabolite dynamics have also been observed in other surface soils (*12, 51*).

Several observations lead us to the conclusion that the metribuzin dissipation measured in surface soils is not entirely due to its degradation. As very little metribuzin was mineralized and metabolite accumulation was relatively low after 3 months of incubation, the metribuzin disappearance observed is probably also the result of an increase in unextractable metribuzin with time, otherwise referred to as aging. In contrast to surface soils, the recovery of metribuzin and its metabolites in subsurface soils was relatively stable (in the range of 77−87%) throughout the experiment. This also supports the notion that an aging-induced loss of extraction efficiency influenced dissipation results in the A-horizon, as aging via incorporation of metribuzin into the soil organic matter would only occur in surface soils. Increases in the unextractable amount of metribuzin with time have previously been reported in other studies (*43, 52*). In fact, the nonbiological degradation of metribuzin reported in studies where metabolite formation is not measured (*48, 53*) could also be the result of aging. In a study by Sharom and Stephenson (*8*), no increases in metabolite formation were observed during a 6 month period in soil that was initially sterilized, and so the authors proposed that the measured degradation in these samples was due to the extraction efficiency. Even so, the formation of unidentified metabolites could also have contributed to the loss of metribuzin recovery in the A- as well as the C-horizon. Moorman and Harper (*12*) found that up to 14% of applied metribuzin was extracted in the form of metabolites other than DA, DK, and DADK. In addition, Locke et al. (*43*) detected practically equal amounts of unidentifiable and known metabolites in their study of metribuzin degradation.

In subsurface soils, little metribuzin dissipation was observed in both frozen-stored and fresh soil samples, and DT_{50} values in both sample types were >150 days. Furthermore, hardly any metabolites were detected during 85 days of incubation. Thus, it seems likely that the metribuzin metabolites previously detected in groundwater wells (*6, 25*) are products of surface soil degradation.

Abundance of *tfdA* Genes. The sigmoidal shapes of MCPA mineralization curves and the estimated growth parameters from kinetic modeling both indicate growth in MCPA-

COR-AAD1-00002713
Bayer EX1008 (Part 5 of 9)

degrading microbial populations following MCPA exposure. As increases in the population densities of culturable phenoxyacid-herbicide degraders have previously been shown to coincide with increases in *tfdA* gene frequencies (*54*), changes in the size of MCPA-degrading populations were monitored in the present study by measuring *tfdA* gene levels. In all three horizons, the PCR signal of *tfdA* genes increased as mineralization rates increased (during the exponential phase). However, the PCR signal of *tfdA* genes in the B-horizon did not follow the same pattern as in the A- and C-horizons, and the PCR signal fell as the mineralization of MCPA started to level off. This decline in the recorded signal of *tfdA* genes might be due to factors such as predation by protozoa. The greatest increase in the *tfdA* gene signal was observed in the A-horizon, which was also the soil horizon with the greatest mineralization rate constant (k_1). In contrast, the relative *tfdA* gene levels in the B- and C-horizons did not positively correlate with the calculated MCPA mineralization rates. This might be the result of the lacking presence of any *tfdA*-homologous genes in some of the indigenous MCPA degraders of this sandy soil profile. Phenoxyacid-degrading strains without any *tfdA*-homologous catabolic genes have been described in several studies (*13*−*16*). It should also be noted that the PCR analysis is not quantified using Real Time PCR analysis or competitive PCR so the exact data can be influenced by minor PCR errors.

This research is the first to show that frozen storage of soil samples that are not normally subjected to freeze−thaw cycles is acceptable for the assessment of pesticide degradation. Complete degradation, as measured by the mineralization of ^{14}C-ring-labeled pesticides, is practically unaffected by frozen storage, while mother compound removal, as measured by LC-MS/MS analysis, is initially higher in fresh soil when compared with frozen-stored soil.

Acknowledgments

This research was supported by the Danish Research Council through the SOUND project (Molecular Tools for Sustainable Land Use). We thank Bo Svensmark and Trine Henriksen for their valuable advice. Thanks are also due to Lasse Gudmundson for skilled technical assistance in the field.

Literature Cited

(1) Spliid, N. H.; Køppen, B. Occurrence of pesticides in Danish shallow ground water. *Chemosphere* **1998**, *37*, 1307−1316.
(2) Barbash, J. E.; Thelin, G. P.; Kolpin, D. W.; Gilliom, R. J. Major herbicides in ground water: Results from the National Water-Quality Assessment. *J. Environ. Qual.* **2001**, *30*, 831−845.
(3) Cerejeira, M. J.; Viana, P.; Batista, S.; Pereira, T.; Silva, E.; Valério, M. J.; Silva, A.; Ferreira, M.; Silva-Fernandes, A. M. Pesticides in Portuguese surface and ground waters. *Water Res.* **2003**, *37*, 1055−1063.
(4) *Groundwater Monitoring 2002*; Jørgensen, L. F., Ed.; Geological Survey of Denmark and Greenland, Ministery of the Environment: Copenhagen, Denmark, 2002 (in Danish).
(5) EEC council directive on drinking water (80/778/EEC). *Off. J. Eur. Communities* **1980**, *229*, August 30th.
(6) Kjær, J.; Ullum, M.; Olsen, P.; Sjelborg, P.; Helweg, A.; Mogensen, B.; Plauborg, F.; Jørgensen, J. O.; Iversen, B. V.; Fomsgaard, I.; Lindhardt, B. In *The Danish Pesticide Leaching Assessment Programme: Monitoring Results May 1999*−*June 2001*; Kjær, J., Ed.; Geological Survey of Denmark and Greenland, Ministery of the Environment: Copenhagen, Denmark, 2002.
(7) Helweg, A. Degradation and adsorption of ^{14}C-MCPA in soil-influence of concentration, temperature and moisture content on degradation. *Weed Res.* **1987**, *27*, 287−296.
(8) Sharom, M. S.; Stephenson, G. R. Behavior and fate of metribuzin in eight Ontario soils. *Weed Sci.* **1976**, *24*, 153−160.
(9) Fomsgaard, I. S. Modelling the mineralization kinetics for low concentrations of pesticides in surface and subsurface soil. *Ecol. Modell.* **1997**, *102*, 175−208.
(10) Brunner, W.; Focht, D. D. Deterministic three-half-order kinetic model for microbial degradation of added carbon substrates in soil. *Appl. Environ. Microbiol.* **1984**, *47*, 167−172.
(11) Reffstrup, T. K.; Sørensen, H.; Helweg, A. Degradation of mecoprop at different concentrations in surface and sub-surface soil. *Pestic. Sci.* **1998**, *52*, 126−132.
(12) Moorman, T. B.; Harper, S. S. Transformation and mineralization of metribuzin in surface and subsurface horizons of a Mississippi delta soil. *J. Environ. Qual.* **1989**, *18*, 302−306.
(13) Ka, J. O.; Holben, W. E.; Tiedje, J. M. Genetic and phenotypic diversity of 2,4-dichlorophenoxyacetic acid (2,4-D)-degrading bacteria isolated from 2,4-D treated field soils. *Appl. Environ. Microbiol.* **1994**, *60*, 1106−1115.
(14) Fulthorpe, R. R.; McGowan, C.; Maltseva, O. V.; Holben, W. E.; Tiedje, J. M. 2,4-Dichlorophenoxyacetic acid-degrading bacteria contain mosaics of catabolic genes. *Appl. Environ. Microbiol.* **1995**, *61*, 3274−3281.
(15) Müller, R. H.; Kleinstueber, S.; Babel, W. Physiological and genetic characteristics of two bacterial strains utilizing phenoxypropionate and phenoxyacetate herbicides. *Microbiol. Res.* **2001**, *156*, 121−131.
(16) Smejkal, C. W.; Vallaeys, T.; Burton, S. K.; Lappin-Scott, H. M. Substrate specificity of chlorophenoxyalkanoic acid-degrading bacteria is not dependent upon phylogenetically related *tfdA* gene types. *Biol. Fertil. Soils* **2001**, *33*, 507−513.
(17) Anderson, J. P. E. In *Pesticide Effects on Soil Microflora*; Sommerville, L., Greaves, M. P., Eds.; Taylor and Francis: London, 1987; pp 45−60.
(18) Zelles, L.; Adrian, P.; Bai, Q. Y.; Stepper, K.; Adrian, M. V.; Fischer, K.; Maier, A.; Ziegler, A. Microbial activity measured in soils stored under different temperature and humidity conditions. *Soil Biol. Biochem.* **1991**, *23*, 955−962.
(19) Stenberg, B.; Johansson, M.; Pell, M.; Sjödahl-Svensson, K.; Stenström, J.; Torstensson, L. Microbial biomass and activities in soil as affected by frozen and cold storage. *Soil Biol. Biochem.* **1998**, *30*, 393−402.
(20) ISO/TC 190/SC 2 (International Organization for Standardization/Technical Committee 190/Sub-committee 2). *Soil Quality-Sampling Part 6: Guidance on collection, handling and storage of soil for assessment of aerobic microbial processes in the laboratory (ISO 10381-6: 1993E)*; International Organization for Standardization: Geneva, Switzerland, 1993.
(21) Soulides, D. A.; Allison, F. E. Effect of drying and freezing soils on carbon dioxide production, available mineral nutrients, aggregation, and bacterial population. *Soil Sci.* **1961**, *91*, 291−298.
(22) Christ, M.; David, M. B. Fractionation of dissolved organic carbon in soil water: effects of extraction and storage methods. *Commun. Soil Sci. Plant Anal.* **1994**, *25*, 3305−3319.
(23) Shishido, M.; Chanway, C. P. Storage effects on indigenous soil microbial communities and PGPR efficacy. *Soil Biol. Biochem.* **1998**, *30*, 939−947.
(24) Rugbjerg, D.; Helweg, A. *6th Danish Plant Protection Conference/ Pesticides and Environ-ment*; Statens Planteavlsforsøg: Lyngby, Denmark, 1989; pp 23−31 (in Danish).
(25) Lawrence, J. R.; Eldan, M.; Sonzogni, W. C. Metribuzin and metabolites in Wisconsin (U.S.A.) well water. *Water Res.* **1993**, *27*, 1263−1268.
(26) Henriksen, T.; Svensmark, B.; Juhler, R. K. Analysis of metribuzin and transformation products in soil by pressurized liquid extraction and liquid chromatographic-tandem mass spectrometry. *J. Chromatogr., A* **2002**, *957*, 79−87.
(27) Harker, A. R.; Olsen, R. H.; Seidler, R. J. Phenoxyacetic acid degradation by the 2,4-diclorophenoxyacetic acid (tfd) pathway of plasmid pJP4 − mapping and characterization of the tfd regulatory gene, tfdR. *J. Bacteriol.* **1989**, *171*, 314−320.
(28) de Liptbay J. R. Ph.D. Thesis. University of Copenhagen, Copenhagen, Denmark, 2001.
(29) Vallaeys, T.; Fulthorpe, R. R.; Wright, A. M.; Soulas, G. The metabolic pathway of 2,4-dichlorophenoxyacetic acid degradation involves different families of *tfdA* and *tfdB* genes according to PCR-RFLP analysis. *FEMS Microbiol. Ecol.* **1996**, *20*, 163−172.
(30) Sambrook, J.; Russell, D. W. In *Molecular Cloning: A laboratory manual*; Cold Spring Harbor Laboratory Press: Cold Spring Harbor, NY, 2001; Vol. 1, pp 9.14−9.17.
(31) Scow, K. M.; Simkins, S.; Alexander, M. Kinetics of mineralization of organic compounds at low concentrations in soil. *Appl. Environ. Microbiol.* **1986**, *51*, 1028−1035.
(32) Robinson, J. A. Determining microbial kinetic parameters using nonlinear regression analysis: advantages and limitations in microbial ecology. *Adv. Microb. Ecol.* **1985**, *8*, 61−114.
(33) Focht, D. D.; Brunner, W. Kinetics of biphenyl and polychlorinated biphenyl metabolism in soil. *Appl. Environ. Microbiol.* **1985**, *50*, 1058−1063.

COR-AAD1-00002714
Bayer EX1008 (Part 5 of 9)

(34) Ross, D. J. Effects of freezing and thawing of some grassland topsoils on oxygen uptakes and dehydrogenase activities. *Soil Biol. Biochem.* **1972**, *4*, 115−117.
(35) Skogland, T.; Lomeland, S.; Goksøyr, J. Respiratory burst after freezing and thawing of soil: experiments with soil bacteria. *Soil Biol. Biochem.* **1988**, *20*, 851−856.
(36) Willems, H. P. L.; Lewis, K. J.; Dyson, J. S.; Lewis, F. J. Mineralization of 2,4-D and atrazine in the unsaturated zone of a sandy loam soil. *Soil Biol. Biochem.* **1996**, *28*, 989−996.
(37) Bolan, N. S.; Baskaran, S. Biodegradation of 2,4-D herbicide as affected by its adsorption−desorption behaviour and microbial activity of soils. *Aust. J. Soil Res.* **1996**, *34*, 1041−1053.
(38) Pieper, D. H.; Reineke, W.; Engesser, K.-H.; Knackmuss, H.-J. Metabolism of 2,4-dichlorophenoxyacetic acid, 4-chloro-2-methylphenoxyacetic acid and 2-methylphenoxyacetic acid by *Alcaligenes eutrophus* JMP 134. *Arch. Microbiol.* **1988**, *150*, 95−102.
(39) Stevenson, F. J. Organic matter reactions involving herbicides in soil. *J. Environ. Qual.* **1972**, *1*, 333−343.
(40) Gaunt, J. K.; Evans, W. C. Metabolism of 4-chloro-2-methylphenoxyacetate by a soil pseudomonad. *Biochem. J.* **1971**, *122*, 519−526.
(41) Smith, A. E. Identification of 4-chloro-2-methylphenol as a soil degradation product of ring-labelled [14C]mecoprop. *Bull. Environ. Contam. Toxicol.* **1985**, *34*, 656−660.
(42) Ladlie, J. S.; Meggitt, W. F.; Penner, D. Role of pH on metribuzin dissipation in field soils. *Weed Sci.* **1976**, *24*, 508−511.
(43) Locke, M. A.; Harper, S. S.; Gaston, L. A. Metribuzin mobility and degradation in undisturbed soil columns. *Soil Sci.* **1994**, *157*, 279−288.
(44) Mallawatantri, A. P.; McConkey, B. G.; Mulla, D. J. Characterization of pesticide sorption and degradation in macropore linings and soil horizons of Thatuna silt loam. *J. Environ. Qual.* **1996**, *25*, 227−235.
(45) Helweg, A. Degradation and adsorption of ^{14}C-mecoprop (MCPP) in surface soils and in subsoil. Influence of temperature, moisture content, sterilization and concentration on degradation. *Sci. Total Environ.* **1993**, *132*, 229−241.
(46) Larsen, L.; Sørensen, S. R.; Aamand, J. Mecoprop, isoproturon and atrazine in and above a sandy aquifer: vertical distribution of mineralization potential. *Environ. Sci. Technol.* **2000**, *34*, 2426−2430.
(47) Hyzak, D. L.; Zimdahl, R. L. Rate of degradation of metribuzin and two analogs in soil. *Weed Sci.* **1974**, *22*, 75−79.
(48) Savage, K. E. Metribuzin persistence in soil. *Weed Sci.* **1977**, *25*, 55−59.
(49) Di, H. J.; Aylmore, L. A. G.; Kookana, R. S. Degradation rates of eight pesticides in surface and subsurface soils under laboratory and field conditions. *Soil Sci.* **1998**, *163*, 404−411.
(50) Thorstensen, C. W.; Lode, O. Organic compounds in the environment: Laboratory degradation studies of bentazone, dichlorprop, MCPA, and propiconazole in Norwegian soils. *J. Environ. Qual.* **2001**, *30*, 947−953.
(51) Henriksen, T.; Svensmark, B.; Juhler, R. K. Degradation and sorption of metribuzin and primary metabolites in a sandy soil. *J. Environ. Qual.* **2004**, *33*, 619−627.
(52) Sha'ato, R.; Buncel, E.; Gamble, D. G.; vanLoon, G. W. Kinetics and equilibria of metribuzin sorption on model soil components. *Can. J. Soil Sci.* **2000**, *80*, 301−307.
(53) Webster, G. R. B.; Sarna, L. P.; Macdonald, S. R. Nonbiological degradation of the herbicide metribuzin in Manitoba soils. *Bull. Environ. Contam. Toxicol.* **1978**, *20*, 401−408.
(54) Holben, W. E.; Schroeter, B. M.; Calabrese, V. G. M.; Olsen, R. H.; Kukor, J. K.; Biederbeck, V. O.; Smith, A. E.; Tiedje, J. M. Gene probe analysis of soil microbial populations selected by amendment with 2,4-dichlorophenoxyacetic acid. *Appl. Environ. Microbiol.* **1992**, *58*, 3941−3948.

Received for review March 25, 2004. Revised manuscript received September 16, 2004. Accepted September 16, 2004.

ES049542X

COR-AAD1-00002715
Bayer EX1008 (Part 5 of 9)

Acta Biotechnol. **21** (2001) 3, 227–242

Pseudo-recalcitrance of Chlorophenoxyalkanoate Herbicides – Correlation to the Availability of α-Ketoglutarate

MÜLLER*, R. H., BABEL, W.

UFZ – Umweltforschungszentrum Leipzig–Halle GmbH
Sektion Umweltmikrobiologie
Permoserstraße 15
04318 Leipzig, Germany

* Corresponding author
Phone: + 49 341 235 2248
Fax: + 49 341 235 2247
E-mail: rmueller@umb.ufz.de

Summary

Cleavage of the ether bond of chlorophenoxyalkanoate herbicides is catalyzed by an α-ketoglutarate-linked dioxygenase (TfdA). In this step, α-ketoglutarate is decarboxylated to succinate and must be regenerated for continual substrate cleavage. Limitations in herbicide degradation are to be expected in the case of a shortage of α-ketoglutarate. Such a situation was simulated and studied with *Delftia* (formerly *Comamonas) acidovorans* MC1 and *Rhodoferax* sp. P230, which constitutively express etherolytic dioxygenase activity by excreting 2,4-dichlorophenol (DCP) as a dead-end product. The results showed that 2,4-dichlorophenoxyacetate (2,4-D) could hardly be cleaved under these conditions which is attributed to the inability to regenerate α-ketoglutarate from the cleavage products, i.e. succinate and glyoxylate [1]. With pyruvate, in contrast, liberated as the oxidized alkanoic acid from the cleavage of (*RS*)-2-(2,4-dichlorophenoxy)propionate (2,4-DP), the regeneration of α-ketoglutarate seems to be guaranteed from succinate as resulted from the utilization of 2,4-DP to a considerable amount under these conditions. The extent was limited, however, which was apparently caused by the accumulation of DCP. Continual cleavage of 2,4-DP could be demonstrated in the presence of *Ochrobactrum* sp. K2-14, which functions as a DCP-consuming strain. Addition of extra metabolites, i.e. α-ketoglutarate or other readily metabolizable substrates, improved the cleavage of the herbicides. This was most pronounced with 2,4-D that was found now to be also utilized to a considerable extent. Conversely, the cleavage of the herbicides (2,4-DP) was reduced and ultimately ceased with cells depleted by starvation of the pool of metabolites. Again, this deficit could be restored by adding α-ketoglutarate. The limitations in utilizing phenoxyalkanoate herbicides are discussed in terms of pseudo-recalcitrance owing to deficits in metabolites (α-ketoglutarate) rather than enzyme activity (TfdA).

Introduction

The initial step of the degradation of 2,4-D encoded by the gene *tfdA* from *Ralstonia eutropha* JMP134 has been elucidated and shown to follow an α-ketoglutarate-depend-

© WILEY-VCH Verlag Berlin GmbH, 13086 Berlin, 2001 0138-4988/01/0308-0227 $ 17.50+.50/0

COR-AAD1-00002716
Bayer EX1008 (Part 5 of 9)

ent dioxygenase mechanism [2, 3]. As a result of this catalytic step, the phenoxyalkanoates are cleaved into the phenolic derivative and the oxidized alkanoic acid, whereas α-ketoglutarate yields succinate and CO_2. Further metabolism of the chlorophenolic intermediate proceeds via a modified *ortho* cleavage pathway [4, 5]. TfdA-like activity is widespread in nature [6–8]. Moreover, etherolytic activity being catalyzed by an α-ketoglutarate-dependent dioxygenase has been shown to also function with other phenoxyalkanoates, such as the enantiomeric phenoxypropionates. This holds true with *Sphingomonas herbicidovorans* MH [9] or *Delftia acidovorans* MC1 and *Rhodoferax* sp. P230 [10]. The specificity of the degradation of the different phenoxyalkanoates is based accordingly on the specificity of the enzymes initiating the metabolic route of decomposing the various phenoxyalkanoates. The fact that the cleavage of these herbicides requires α-ketoglutarate (which is oxidatively decarboxylated to succinate in this reaction) necessitates its regeneration. In the case of complete degradation of the ring structure, no limitations should arise in view of the fact that C2 (acetyl-CoA) and C4 (succinate) compounds were derived in the primary assimilatory route besides succinate and the oxidized alkanoic acid (glyoxylate, pyruvate) resulting from the etherolytic cleavage reaction. In the case of incomplete degradation, by contrast, in which the phenolic intermediate may form a dead-end product, restrictions concerning continual cleavage are to be expected [1]. Thus despite the expression of TfdA or analogous enzymes, substrate turnover via these enzymes may be limited. Consequently, this property should influence and decide the fate of chlorophenoxy herbicides in biotopes in which, for example, consortia are responsible for the complete degradation of these compounds, i.e., in which the individual enzymatic steps or partial sequences are harboured in different strains.

In this investigation, the ability to attack the phenoxyalkanoate herbicides under such conditions and the limitations resulting from the necessity of regenerating α-ketoglutarate are considered. Such strains were used which exhibit constitutive expression of TfdA-like cleavage activity without further metabolizing the phenolic intermediates. Effects resulting from DCP accumulation were taken into account

Materials and Methods

Strains and Cultivation

The investigations were carried out with *Rhodoferax* sp. P230, which was isolated from herbicide-contaminated building rubble [11], and *Delftia acidovorans* MC1 obtained from a fixed-bed reactor operated for the degradation of a mixture of chlorophenoxy herbicides [12].

The mineral salt solution (MM) used for growth under minimal conditions contained [in mg/l]: NH_4Cl, 760; KH_2PO_4, 340; K_2HPO_4, 485; $CaCl_2 \times 6\ H_2O$, 27; $MgSO_4 \times 7\ H_2O$, 71.2; $FeSO_4 \times 7\ H_2O$, 4.98; $CuSO_4 \times 5\ H_2O$, 0.785; $MnSO_4 \times 4\ H_2O$, 0.81; $ZnSO_4 \times 7\ H_2O$, 0.44; $Na_2MoO_4 \times 2\ H_2O$, 0.25. Strain MC1 is able to grow prototrophically; in the case of Strain P230, the medium was supplemented with either 0.1 g/l yeast extract or a vitamin mixture containing biotin (3.8 mg/l), thiamine (9 mg/l) and vitamin B12 (0.14 mg/l). For growth on complex carbon source, the medium contained 3 g/l of each peptone and yeast extract and 10 mM fructose (PYE + F) or 1 g/l of each peptone, yeast extract and α-ketoglutarate (PYE + α-KG). The pH values were adjusted to 8.5.

Ochrobactrum sp. K2-114 [13] was grown chemostatically on 2 g/l dichlorophenol at a dilution rate of 0.04 h^{-1}. The cells were harvested, washed and resuspended into MM containing 50% [v/v] glycerol at an $OD_{700} = 30$ and stored at – 20 °C. Before use, the cells were centrifuged and washed two times with MM.

COR-AAD1-00002717
Bayer EX1008 (Part 5 of 9)

Degradation Experiments

The strains were routinely grown as an overnight culture on complex medium. Strain MC1 was inoculated from colonies grown under selective conditions on (*RS*)-2-(2,4-dichlorophenoxy)propionate; Strain P230 was obtained from a sequentially transferred culture grown on PYE+F or PYE+α-KG. The cells were collected by centrifugation, washed in nitrogen-free MM and routinely re-suspended into nitrogen-free MM to an optical density of OD_{700} = 0.25. Streptomycin was routinely added to the suspensions at a concentration of 50 mg/l if not otherwise indicated. At respective times, samples were withdrawn, the biomass separated by centrifugation and the supernatant used for analysis.

Analyses

The chlorophenoxyalkanoate compounds and the chlorophenols were determined by HPLC using a SHIMADZU chromatograph with diode array detection according to a method described elsewhere [14]. The biomass concentration was determined by using the optical density at 700 nm (OD_{700}). An OD_{700} of 1 corresponds to a bacterial dry mass of 0.54 g/l with Strain MC1 and to 0.46 g/l with Strain P230.

Chemicals

(*R*)-2,4-DP was procured from RIEDEL-DEHAEN. (*S*)-2,4-DP was prepared following the method of ZIPPER [15]. (*R*)-2-(4-chloro-2-methylphenoxy)propionate and (*S*)-2-(4-chloro-2-methylphenoxy)propionate (MCPP) were synthesized according to MATELL [16]. The other phenoxyalkanoates were obtained from SIGMA with the highest purity available.

Results

Cleavage Pattern

Application of 0.45 mM (*RS*)-2,4-DP to non-induced cells of *Rhodoferax* sp. P230 resulted in etherolytic cleavage of this compound the extent being limited. DCP resulting from this reaction behaved as a dead-end product in the presence of streptomycin and was excreted into the medium (Fig. 1). The degradation pattern was completely paralleled by supplying pure (*R*)-2,4-DP which is in accordance with a constitutive expression of *R*-specific cleavage activity: 0.15–0.17 mM of this enantiomer were converted under these conditions leading to the accumulation of approximately equimolar concentrations of DCP (Fig. 1). Applying lower initial substrate concentrations (0.18 mM), again about 0.15 mM of (*R*)-2,4-DP were cleaved, whereas only half of the molar concentration of the racemic substrate disappeared (Fig. 1). This was attributed to the *S*-enantiomer that was not utilized by the non-induced cells of this strain [10]. 2,4-D was also not degraded to a significant extent under these conditions (not shown). The presence of streptomycin did not essentially influence the cleavage pattern of the herbicides as was derived from the data obtained after different periods of pre-incubation with this antibiotic.

In contrast, Strain MC1 shows constitutive activity for the cleavage of both (*R*)- and (*S*)-2,4-DP. The cleavage activity of the *R*-enantiomer was high with cells grown overnight on complex medium. The substrate routinely supplied (0.45 mM) was completely utilized with the given concentration of biomass of 0.1–0.15 g/l. In contrast, some of

COR-AAD1-00002718
Bayer EX1008 (Part 5 of 9)

the substrate remained unutilized after incubation with the racemic mixture under these conditions (Fig. 2). This was probably caused by the *S*-enantiomer, which was utilized to only a limited extent under the prevailing conditions, and at a lower rate. In general, the extent of cleavage was found to be a function of the biomass concentration with the various herbicides. The graphs of concentration vs. extent, obtained after 24 h of incubation (substrate consumption characteristics almost followed the progress curves as shown in Fig. 2) exhibited approximate linearity (Fig. 3). This means that the specific conversion rate is a constant with the various substrates, i.e., substrate consumption was not dependent on the concentration of DCP accumulated in the time run. 2,4-D, again, was hardly degraded by Strain MC1 under these conditions (Fig. 2). Nevertheless, the disappearance of a very small but distinct amount of this substrate was observed in most experiments. The significance of this property became obvious from the data in Fig. 3 according to which this behaviour became more evident the higher the initial biomass concentration was. Due to these data, 2,4-D was cleaved to an extent of about 3% in comparison to (*R*)-2,4-DP.

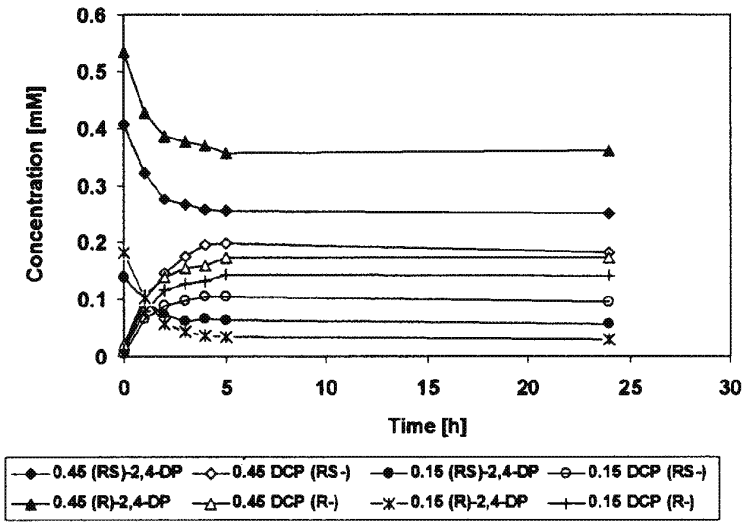


Fig. 1. Degradation of various phenoxyalkanoates by non-induced cells of *Rhodoferax* sp. P230
The samples contained 0.15 to 0.45 ± 0.04 mM of the respective herbicides (see legend). The references regarding DCP in the legend correspond to the original substrate used.

Influence of α-Ketoglutarate

The data shown above revealed essential differences in the cleavage characteristics of the different herbicides. Whereas 2,4-D remained almost inert by these cultures, the enantiomers of 2,4-DP were utilized to a considerable extent in accordance with the expression profile of the respective etherolytic dioxygenases [10].

COR-AAD1-00002719
Bayer EX1008 (Part 5 of 9)

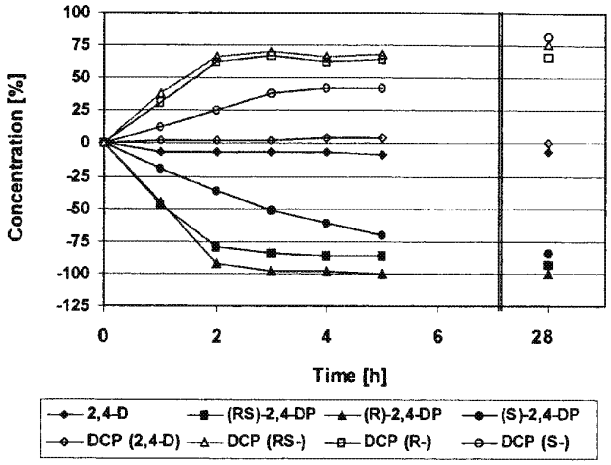


Fig. 2. Degradation of various phenoxyalkanoates by non-induced cells of *Delftia acidovorans* MC1
The samples contained 0.45 ± 0.04 mM of the respective herbicides; the biomass concentration corresponded to $OD_{700} = 0.1$.

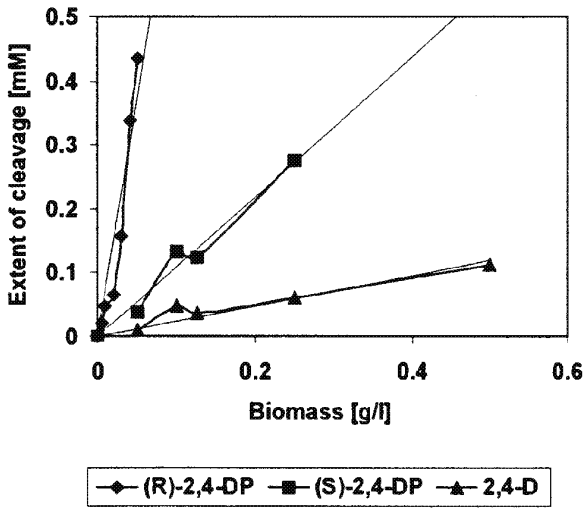


Fig. 3. Influence of the biomass concentration on the extent of cleavage of various phenoxyalkanoates by non-induced cells of Strain MC1
Strain MC1 was grown overnight on PYE + F. The cells were harvested and re-suspended to the respective biomass concentrations. The degradation experiments were performed in the presence of 0.45 ± 0.05 mM of the various phenoxyalkanoates.

COR-AAD1-00002720
Bayer EX1008 (Part 5 of 9)

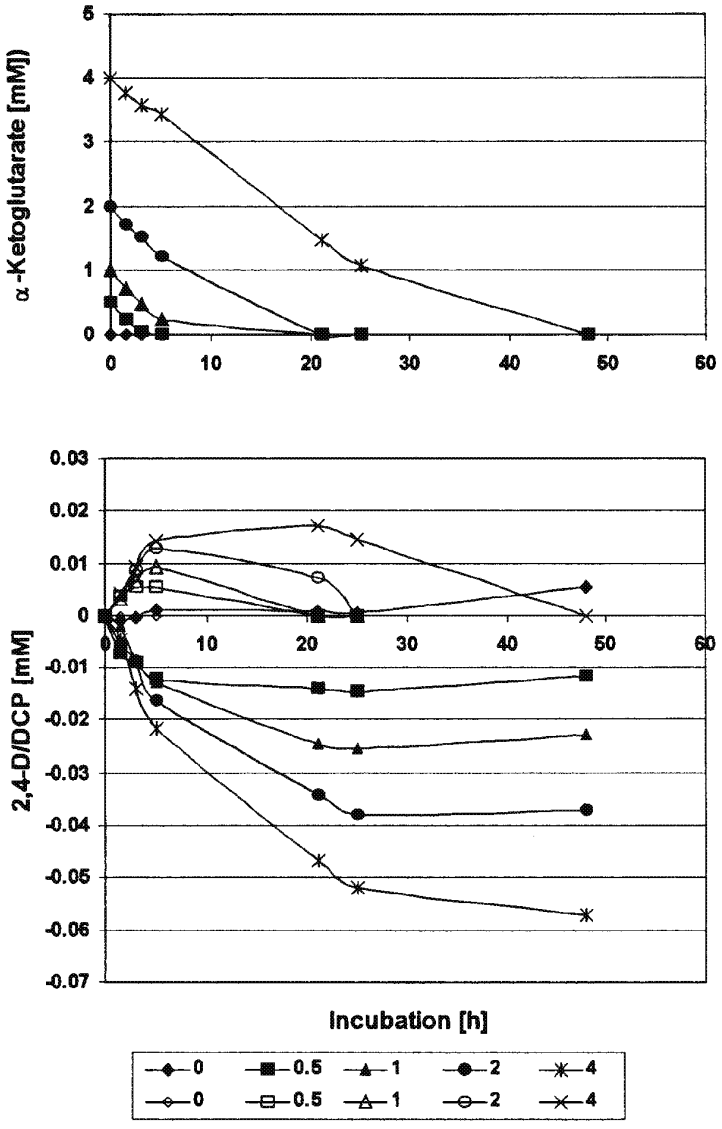


Fig. 4. Degradation of 2,4-D by non-induced cells of *Rhodoferax* sp. P230
The strain was grown on PYE + α-KG medium. Washed cells were incubated in nitrogen-free medium containing 0.4–0.45 mM 2,4-D in the absence and presence of different concentrations of α-ketoglutarate (see figures in the legend [in mM]. Streptomycin was omitted.
Full symbols: 2,4-D concentration; open symbols: DCP concentration.

COR-AAD1-00002721
Bayer EX1008 (Part 5 of 9)

The consumption of the latter substrates, however, proceeded at different rates and showed limitations in the extent under the respective conditions. Different effects, described as follows, were shown to be responsible for this behaviour.

The availability of α-ketoglutarate as the second oxygen acceptor is a pre-requisite for continual herbicide utilization initiated by this special dioxygenase mechanism. Consequently, the supply of α-ketoglutarate should stimulate the cleavage of the herbicides by this two-substrate reaction. This, indeed, holds true. Stimulation was most pronounced with 2,4-D (Fig. 4). The extent of cleavage of this herbicide was dependent on the α-ketoglutarate concentration, after exhaustion of this compound no further consumption of 2,4-D was observed (Fig. 4). As the decrease of 2,4-D was faint in the absence of α-ketoglutarate, this compound plays the role of "start assistance" [17] under these conditions. In contrast, the phenoxypropionates served as suitable substrates for non-induced cells, i.e. these herbicides were also remarkably degraded without any addition. Nevertheless, the presence of α-ketoglutarate drastically increased the rate of herbicide consumption (Fig. 5). This was the case – referring to the lower α-ketoglutarate concentrations – as long as α-ketoglutarate was present. After its depletion, the rate decreased and attained such a value as observed in the initial phase of herbicide conversion in the absence of α-ketoglutarate. A further characteristic of herbicide consumption under these conditions was that the cleavage rate was drastically decreased to about 20% of its initial value after about 5 h. It is a remarkable fact that this property did apply also to the sample that yet contained α-ketoglutarate. It is another remarkable fact that substrate cleavage continued with a constant rate (irrespective of the actual DCP concentration) in the various samples.

This abrupt shift in the degradation rate should be caused by the accumulation of DCP known to be an inhibitor (uncoupler) and may consequently interfere with substrate uptake. An inhibitory pattern of this compound was demonstrated by pre-incubating with DCP Strains MC1 and P230; this affected substrate consumption (Fig. 6). According to these characteristics, extracellular application of DCP reduced the initial cleavage activity of the herbicides immediately. The effect was dependent on the DCP concentration and was even enforced with time, especially in the presence of 0.3 mM of DCP. In the presence of 0.06 mM of DCP, inhibition was moderate and paralleled more or less the shape of the activity profile observed in the absence of DCP. Similar inhibition was obtained by adding dinitrophenol: An incubation of 4 h in the presence of 1 mM completely prevented cleavage of (*R*)-2,4-DP by Strain MC1 (not shown). The inhibition characteristics observed when extracellular DCP was used, however, were in contrast to the behaviour of the decline of activity when DCP was accumulated due to the action of the dioxygenases. Here inhibitory effects were noticed only after a period of approx. 5 hours irrespective of the concentration of DCP accumulated during this time (Fig. 5). This means that the cells suffer from DCP derived from intracellular or extracellular sources in a different manner. Referring to the activity/DCP-accumulation properties, the cleavage pattern should be altered by avoiding the accumulation of DCP. Consequently, the picture was completely changed by incubating Strain P230 in the presence of *Ochrobactrum* sp. K2-14, the latter being induced for the complete degradation of DCP [13]. In the presence of this strain that did not carry etherolytic activities [13], the amount of (*R*)-2,4-DP supplied was completely converted (Fig. 7).

COR-AAD1-00002722
Bayer EX1008 (Part 5 of 9)

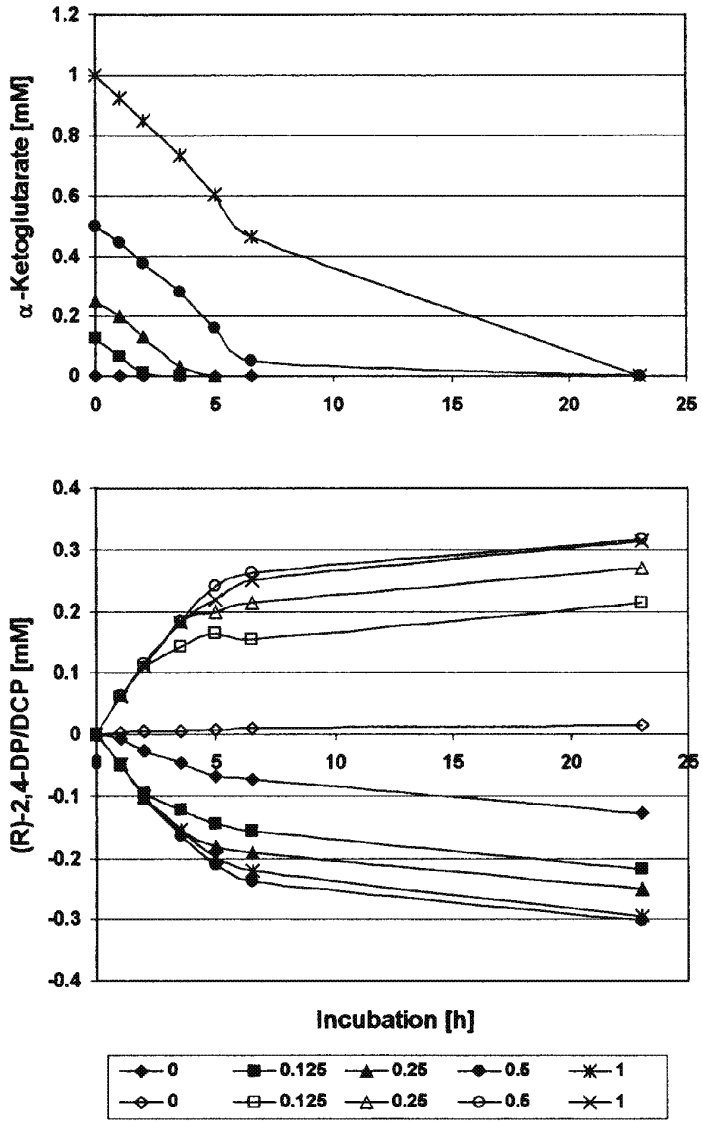
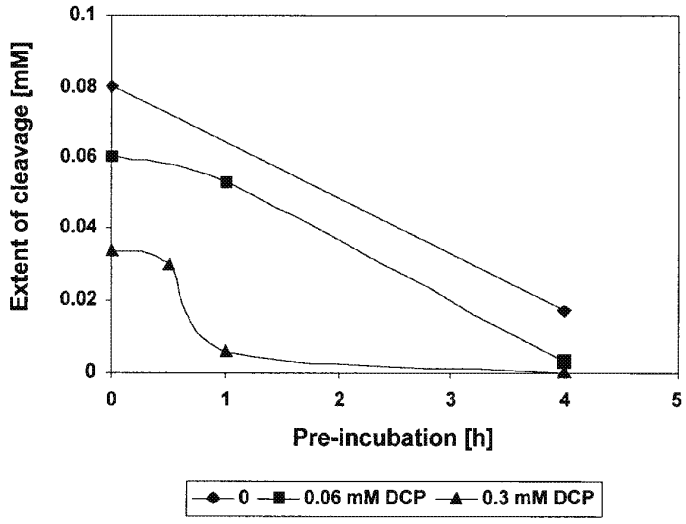


Fig. 5. Degradation of (*R*)-2,4-DP by non-induced cells of *Rhodoferax* sp. P230
The strain was grown on PYE + α-KG medium. Washed cells were incubated in nitrogen-free medium containing 0.4–0.45 mM (*R*)-2,4-DP in the absence and presence of different concentrations of α-ketoglutarate (see figures in the legend [in mM]). Streptomycin was omitted.
Full symbols: (*R*)-2,4-DP concentration; open symbols: DCP concentration.

COR-AAD1-00002723
Bayer EX1008 (Part 5 of 9)



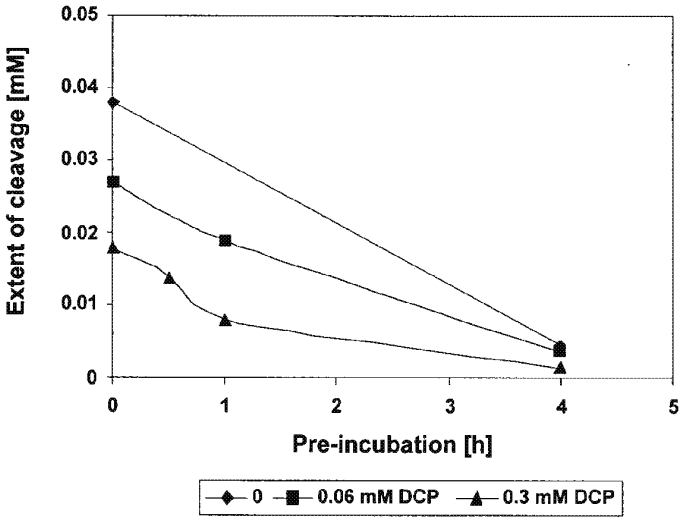


Fig. 6. Effect of pre-incubation with DCP on the cleavage of herbicides
Strains MC1 (upper part) and P230 (lower part) were pre-incubated in the absence and presence of different concentrations of DCP. After a respective time of pre-incubation, (*S*)-2,4-DP (Strain MC1) or (*R*)-2,4-DP (Strain P230) were added and the progress of herbicide consumption was recorded. The values correspond to the final amounts of substrate cleaved after 24 h of incubation. For both strains, the cell density corresponded to $E_{700} = 0.1$.

COR-AAD1-00002724
Bayer EX1008 (Part 5 of 9)

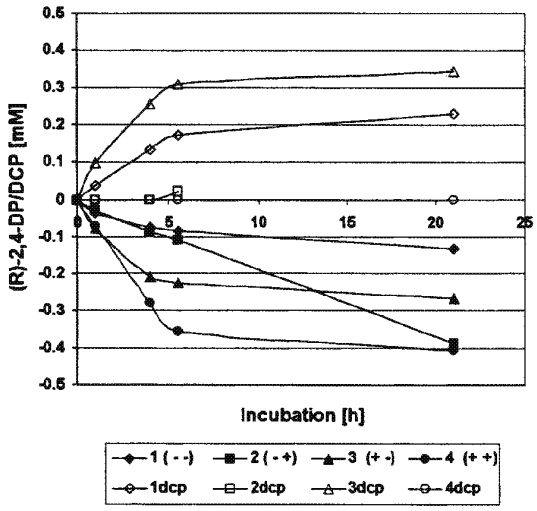


Fig. 7. Effect of *Ochrobactrum* sp. K2-14 on the degradation of R-2,4-DP by *Rhodoferax* sp. P230
The cells were prepared as shown in the legend to Fig. 5. The incubation was performed in the absence or presence of α-ketoglutarate (– or +, first position in the brackets of the legend) and in the absence or presence of *Ochrobactrum* sp. P230 (– or +, second position in the brackets of the legend). The cells of this strain induced for DCP degradation were added to the suspension to give a final density of $E_{700} = 0.1$.

The presence of α-ketoglutarate stimulated the rate of herbicide consumption by a factor of 5, in a manner similar to the results shown in Fig. 5 regarding the initial phases. Even the absolute rates of substrate consumption were similar in these two experiments (Fig. 5 and Fig. 7). This means that DCP accumulated during the first 5 hours did not essentially influence the cleavage properties. This fact was supported by directly comparing the initial rates shown in Fig. 7, which are almost identical over the first 5 hours, but suddenly declined in those cases where DCP accumulated. The further rates of substrate consumption were again nearly identical irrespective of the concentration of DCP (Curve 1 vs. 3).
The results in Fig. 6 indicated that cleavage activity decreased during incubation also in those cases where DCP was absent during pre-incubation. This should be attributed to starvation effects as is shown in more detail in Fig. 8. According to these data, cleavage activity declined over time and was almost nil already after 4 hours of incubation in the absence of any carbon source. This effect could be raised by supplying α-ketoglutarate: In the presence of an amount of 100 mg/l, the effect as provoked after 4 hours of starvation could completely be restored. Some additive behaviour in the extent of the effect became evident when feeding α-ketoglutarate immediately or subsequently to starvation or both (Fig. 8). The stimulation of cleavage of phenoxy herbicides was, however, not solely dependent on α-ketoglutarate but was also found when

COR-AAD1-00002725
Bayer EX1008 (Part 5 of 9)

using other substrates, some of these results are listed in Tab. 1. Again, the effect was most pronounced with 2,4-D. In addition to the effects concerning the extent of cleavage, the presence of these substrates increased also the rate of cleavage by a factor of up to 3 (not shown).

Tab. 1. Influence of various carbon/energy sources on the cleavage of phenoxyalkanoates in non-induced cells

Substrate	Degradation (-fold)		
	Strain MC1		Strain P230
	2,4-D	(*S*)-2,4-DP	(*R*)-2,4-DP
Without	1 (42)[1)]	1 (240)[1)]	1 (48)[1)]
α-Ketoglutarate	4.6	1.2	1.9
Pyruvate	3.3	1.3	1.3
Fructose	5.9	1.35	1.15
Yeast extract	2.2	1.2	3.3

The cells were derived from overnight cultures on PYE + F medium. The incubation was performed in nitrogen-free minimal medium in the presence of streptomycin. The substrates were supplied (as the sodium salts with the organic acids) at a concentration of 100 mg/l.

[1)] The values show the relative extent of the increase in cleavage by adding various substrates; at a value of 1, obtained in the absence of an additional carbon source, the total amounts of substrate (μM) cleaved within 24 h are given in the brackets.

Discussion

Various effects may cause phenoxyalkanoate herbicides to behave recalcitrant. At a first glance and as an experience made already formerly [18, 19], the presence of DCP, the first intermediate in the degradation of these compounds, is one factor that seems to interfere with utilization of phenoxyalkanoates despite the expression of the respective degradative enzymes. This may be attributed to DCP function as an uncoupler [20] and may interfere with the uptake of the herbicides shown to a large extent to be an energy-dependent process [21, 22]. Such effects accompanying the accumulation of DCP were considered, but on the basis of the present results only as secondary. This especially holds true as some substrate turnover may be obtained also in the presence of (uncoupling) DCP concentrations due to passive substrate uptake (Fig. 7; cf. [22]).

The primary effect causing recalcitrance is attributed to the α-ketoglutarate dependent nature of the initial cleavage reaction and might be caused by a shortage of intracellular carbon metabolites, finally α-ketoglutarate. Cleavage of phenoxyalkanoates by an α-ketoglutarate-linked dioxygenase is a two-substrate reaction. One component, i.e. the phenoxyalkanoate herbicide, is externally offered as the proper substrate, whereas the other component, α-ketoglutarate, must be replenished by the cell's metabolism itself. No limitations are to be expected in this reaction if the phenoxyalkanoates are

COR-AAD1-00002726
Bayer EX1008 (Part 5 of 9)

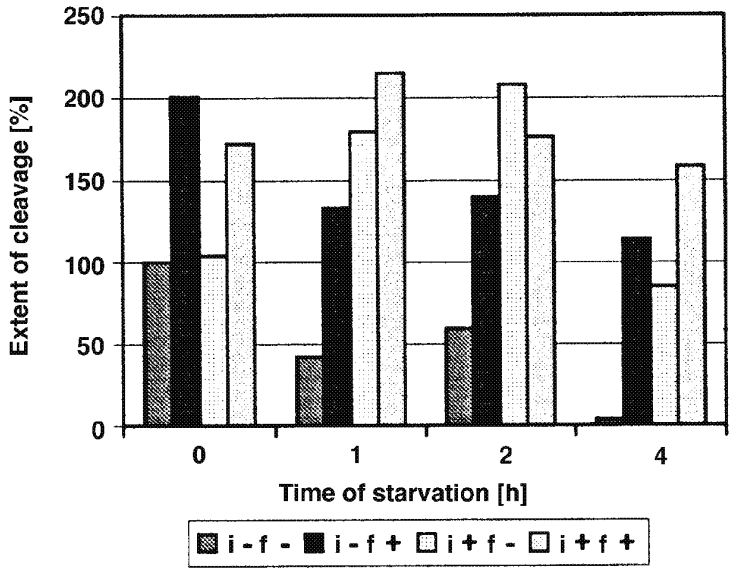


Fig. 8. Effect of starvation and addition of α-ketoglutarate on the extent of cleavage of (*S*)-2,4-DP with non-induced cells of Strain MC1
Strain MC1 was grown overnight on PYE + α-KG. The cells were harvested, washed and resuspended into MM to an $OD_{700} = 0.25$.
i: Addition of (*S*)-2,4-DP after the time of starvation without (–) or with (+) 0.5 mM α-ketoglutarate.
f: Pre-incubation of 4 h on 0.5 mM α-ketoglutarate after the time of starvation before adding (*S*)-2,4-DP without (–) or with (+) a second quantity of α-ketoglutarate.

completely degraded. The primary substrate assimilation of the various phenoxyalkanoate herbicides results in a pool of C2, C3 and C4 intermediates [4, 23] that are suitable precursors for the regeneration of α-ketoglutarate [1]. With incomplete degradation, however, releasing DCP or any further intermediate as a dead-end product, difficulties may arise because a potential source of α-ketoglutarate (i.e. acetyl-CoA and succinate) connecting the modified *ortho* pathway to the central metabolism will not become available. The flow of carbon considered under these conditions makes it plain that, with phenoxyacetate herbicides, the regeneration of α-ketoglutarate would not be possible (taking into account succinate and glyoxylate as the available metabolites in this case) and no continual cleavage would proceed [1]. This was the predominant feature in the present experiments, which showed that 2,4-D resided almost unutilized under the given conditions. The application of a second carbon source ought to substitute for the depletion of the intracellular pool of metabolites relaxing the constraints with respect to the availability of α-ketoglutarate. As a result, both the rate and extent of cleavage were increased indeed. With 2,4-D, this additive may even provide start assistance [17]. Considered from another angle, the TfdA-like reactions

COR-AAD1-00002727
Bayer EX1008 (Part 5 of 9)

may waste intracellular metabolites under these conditions. Consequently, these cells might suffer not only from an accumulation of DCP but also from a shortage of energy impairing maintenance effort and thus endangering survivability [24].

By contrast, the same cultures showed a significant degree of degradation in the case of phenoxypropionates. Here, the regeneration of α-ketoglutarate from succinate, implying pyruvate as the cleavage product from these herbicides, is more easily enabled for stoichiometric reasons [1]. This finding became evident from the pattern in Fig. 5. A high initial rate of herbicide cleavage was observed which indicates a self-sufficient regeneration of α-ketoglutarate. The presence of external α-ketoglutarate nevertheless behaved stimulatory. Remarkably, the initial rate suddenly declined to 1/5 after about 5–6 hours, an effect not dependent on the presence of α-ketoglutarate; rather an almost constant rate was finally observed, independently of the presence of this metabolite. This shift should be caused by DCP being accumulated (as it was prevented in the presence of a DCP-consuming strain; cf. Fig. 7). The consecutive substrate consumption characteristics should be an expression of the rate of (passive) transport of the herbicide across the membrane. Besides, non-specific uptake of phenoxy herbicides was found to occur as was shown with non-induced cells of *S. herbicidovorans* [22] or with mutants of *Ralstonia eutropha* JMP134(pJP4) lacking the specific transport protein [21].

Properties of recalcitrance should be of significance to natural biotopes. 2,4-D degradation is most often found to be associated with consortia; this follows from a global survey on pristine biotopes [25]. It is interesting to note that indications of 2,4-D degradation became evident in this study only after at least 2 weeks' incubation, whereas 3-chlorobenzoate utilization proceeded immediately. Localization of the degradative capabilities on different strains is one explanation although the respective genes were often found to be harboured on the same plasmid. Consequently, and in accordance with our results, however, it will be harder to spot strains exhibiting incomplete degradation, as this potential is masked due to the metabolic peculiarities. With the same consequence, a range of strains has been isolated in the past that shows complete degradation of 2,4-D [23, 26, 27]. For this, the strains applied in this paper represent a suitable model for studying this property due to the constitutive expression of cleavage activities. In contrast, but not unexpectedly from the present results (for further details see [1]), complete degradation by pure cultures has been questioned in the past for phenoxypropionate herbicides because this property was exclusively found to be associated with consortia [28–30]; complete degradation has only recently been attributed to individual strains. Besides the two bacterial species considered in this publication [11, 12], a third strain, *Sphingomonas herbicidovorans* MH, has been reported as being capable to perform the complete degradation of these compounds [31, 32]. The experience that phenoxypropionate degradation is more likely to be found in consortia might be caused by the fact that the cleavage reaction could be detected more easily in these cases.

Due to the metabolic peculiarities, the phenoxyalkanoate herbicides may prove apparently inert despite the existence of TfdA activity. The present experiments should contribute to an understanding of the fate of these compounds in natural habitats. If consortia play a role in degradation, especially with phenoxyacetates, the cleavage reaction requires the presence of a carbon source in addition to the herbicides or the

COR-AAD1-00002728
Bayer EX1008 (Part 5 of 9)

interspecies exchange of carbon compounds in order to proceed; induction and repression mechanisms may modulate the effects. Under selective conditions, however, genetic information can rather easily be acquired to complete the degradative performances. Localization on plasmids of these genes is one aspect of ease distribution. Another aspect, the modular arrangement of the complete degradative pathway of phenoxyalkanoates found in various strains by separating the genes encoding for TfdA (phenoxyalkanoate/α-ketoglutarate dioxygenase), TfdB (chlorophenol hydroxylase) and TfdC-F (enzymes of the modified *ortho* cleavage pathway) into separate operons [33], should be favourable. Capture of respective genes has indeed been demonstrated [34]. Sometimes such mechanisms might be correlated to the effects observed in enrichment cultures in which, after a rather long period of incubation, degradability suddenly started, freeing the culture (strain) from metabolic limitations as discussed here. These observations were also made by TIEDJE *et al.* [25] because most samples obtained from pristine environments revealed 2,4-D degradation only after a long time of incubation.

In conclusion, these results have shown that recalcitrance observed with phenoxyalkanoate herbicides need not necessarily originate from deficits in degradative enzymes, particularly in the initial etherolytic enzymes, but can be caused by gaps or shortages in metabolism, affecting the α-ketoglutarate dependency of this initial degradative step. This property has to be taken into account when describing the phenoxy herbicide degradation potential in natural biotopes and when treating them in technical systems.

Received 10 May 2000
Received in revised form 6 March 2001
Accepted 28 March 2001

References

[1] MÜLLER, R. H., BABEL, W.: A theoretical study on the metabolic requirements resulting from α-ketoglutarate-dependent cleavage of phenoxyalkanoates. Appl. Environ. Microbiol. **66** (2000), 339–344.

[2] FUKUMORI, F., HAUSINGER, R. P.: *Alcaligenes eutrophus* JMP 134 "2,4-dichlorophenoxyacetate monooxygenase" is an α-ketoglutarate-dependent dioxygenase. J. Bacteriol. **175** (1993), 2083–2086.

[3] FUKUMORI, F., HAUSINGER, R. P.: Purification and characterization of 2,4-dichlorophenoxyacetate/α-ketoglutarate dioxygenase. J. Biol. Chem. **268** (1993), 24311–24317.

[4] REINEKE, W., KNACKMUSS, H. J.: Microbial degradation of haloaromatics. Annu. Rev. Microbiol. **42** (1988), 263–287.

[5] PIEPER, D. H., REINEKE, W., ENGESSER, K. H., KNACKMUSS, H. J.: Metabolism of 2,4-dichlorophenoxyacetic acid, 4-chloro-2-methylphenoxyacetic acid, and 2-methylphenoxyacetic acid by *Alcaligenes eutrophus* JMP 134. Arch. Microbiol. **151** (1988), 365–371.

[6] VALLAEYS, T., FULTHORPE, R. R., WRIGHT, A. M., SOULAS, G.: The metabolic pathway of 2,4-dichlorophenoxyacetic acid degradation involves different families of *tfd*A and *tfd*B genes according to PCR-RFLP analysis. FEMS Microbiol. Ecol. **20** (1996), 163–172.

[7] HOGAN, D. A., BUCKLEY, D. H., NAKATSU, C. H., SCHMIDT, T. M., HAUSINGER R. P.: Distribution of the *tfdA* gene in soil bacteria that do not degrade 2,4-dichlorophenoxyacetic acid (2,4-D). Microbial Ecol. **34** (1997), 90–96.

COR-AAD1-00002729
Bayer EX1008 (Part 5 of 9)

[8] MCGOWAN, C., FULTHORPE, R., WRIGHT, A., TIEDJE, J. M.: Evidence for interspecies gene transfer in the evolution of 2,4-dichlorophenoxyacetic acid degraders. Appl. Environ. Microbiol. **64** (1998), 4089–4092.

[9] NICKEL, K., SUTER, M. J. F., KOHLER, H. P. E.: Involvement of two α-ketoglutarate dependent dioxygenases in enatioselective degradation of *(R)*- and *(S)*-mecoprop by *Sphingomonas herbicidovorans* MH. J. Bacteriol. **179** (1997), 6674–6679.

[10] MÜLLER, R. H., KLEINSTEUBER, S., BABEL, W.: Physiological and genetic characterization of two bacterial strains exhibiting phenoxyacetate- and phenoxypropionate-utilizing activity. Microbiol. Res. (2001), in press.

[11] EHRIG, A., MÜLLER, R. H., BABEL, W.: Isolation of phenoxy herbicide-degrading *Rhodoferax* species from contaminated building material. Acta Biotechnol. **17** (1997), 351–356.

[12] MÜLLER, R. H., JORKS, S., KLEINSTEUBER, S., BABEL, W.: *Comamonas acidovorans* MC1: a new isolate capable of degrading the chiral herbicides dichlorprop and mecoprop and the herbicides 2,4-D and MCPA. Microbiol. Res. **154** (1999), 241–246.

[13] MÜLLER, R. H., JORKS, S., KLEINSTEUBER, S., BABEL, W.: Degradation of various chlorophenols under alkaline conditions by GRAM-negative bacteria closely related to *Ochrobactrum anthropi*. J. Basic Microbiol. **38** (1998), 269–281.

[14] OH, K. H., TUOVINEN, O. H.: Degradation of 2,4-dichlorophenoxyacetic acid by mixed cultures of bacteria. J. Ind. Microbiol. **6** (1990), 275–278.

[15] ZIPPER, C.: Microbial degradation and environmental fate of chiral phenoxyalkanoic acid herbicides. Dissertation ETH Zurich No. 12543 (1998).

[16] MATELL, M.: Stereochemical studies on plant growth regulators. VII. Optical active α-(2-methyl-4-chlorophenoxy)-propionic acid and α-(2,4-dichlorophenoxy)-*n*-butyric acid and their steric relations. Arkiv Kemi **6** (1953), 365–373.

[17] BABEL, W., MÜLLER, R. H.: In: Microorganisms as catalysts for the decontamination of ecosystems. Encyclopedia of Life Support Systems. Oxford: EOLSS Publishers: 2001, in press.

[18] KNACKMUSS, H. J.: Xenobiotic degradation of industrial sewage: haloaromatics as target substrates. Biochem. Soc. Symp. **48** (1983), 173–190.

[19] MILNER C. R., GOULDER, R.: Comparative toxicity of chlorophenols, nitrophenols, and phenoxyalkanoic acids to freshwater bacteria. Bull. Environ. Contam. Toxicol. **37** (1986), 714–718.

[20] LOFFHAGEN, N., HÄRTIG, C., BABEL, W.: The toxicity of substituted phenolic compounds to a detoxifying and an acetic acid bacterium. Ecotoxicol. Environ. Saf. **36** (1997), 269–274.

[21] LEVEAU, J. H., ZEHNDER, A. J., van der MEER, J. R.: The *tfd*K gene product facilitates uptake of 2,4-dichlorophenoxyacetate by *Ralstonia eutropha* JMP134(pJP4). J. Bacteriol. **180** (1998), 2237–2243.

[22] ZIPPER, C., BUNK, M., ZEHNDER, A. J., KOHLER, H.-P. E.: Enantioselective uptake and degradation of the chiral herbicide dichlorprop [(*RS*)-2-(2,4-dichlorophenoxy)propanoic acid] by *Sphingomonas herbicidovorans* MH. J. Bacteriol. **180** (1998), 3368–3374.

[23] HÄGGBLOM, M. M.: Microbial breakdown of halogenated aromatic pesticides and related compounds. FEMS Microbiol. Rev. **103** (1992), 29–72.

[24] MÜLLER, R. H., BABEL, W.: Measurement of growth at very low rates ($\mu \geq 0$), an approach to study the energy requirement for the survival of *Alcaligenes eutrophus* JMP 134. Appl. Environ. Microbiol. **62** (1996), 147–151.

[25] TIEDJE, J. M., FULTHORPE, R., KAMAGATA, Y., MCGOWAN, C., RHODES, A., TAKAMI, H.: What is the global pattern of chloroaromatic degrading microbial populations? In: HORIKOSHI, K., FUKUDA, M., KUDO, T. eds.: Microbial Diversity and Genetics of Biodegradation. Basel: S. Karger, 1997, 65–74.

[26] DON, R. H., PEMBERTON, J. M.: Properties of six pesticide degradation plasmids isolated from *Alcaligenes paradoxus* and *Alcaligenes eutrophus*. J. Bacteriol. **145** (1981), 681–686.

[27] SINTON, G. L., FAN, L. T., ERICKSON, L. E., LEE, S. M.: Biodegradation of 2,4-D and related compounds. Enzyme Microb. Technol. **8** (1986), 395–403.

COR-AAD1-00002730
Bayer EX1008 (Part 5 of 9)

[28] KILPI, S.: Degradation of some phenoxy acid herbicides by mixed cultures of bacteria isolated from soil treated with 2-(2-methyl-4-chloro)phenoxypropionic acid. Microbial Ecol. **6** (1980), 261–270.

[29] PFARL, C., DIETZELMÜLLER, G., LOIDL, M., STREICHSBIER, F.: Microbial degradation of xenobiotic compounds in soil columns. FEMS Microbiol. Ecol. **73** (1990), 255–265.

[30] KELLY, M. P., HENIKEN, M. R., TUOVINEN, O. H.: Dechlorination and the spectral changes associated with bacterial degradation of 2-(2-methyl-4-chlorophenoxy)propionic acid. J. Ind. Microbiol. **7** (1991), 137–146.

[31] HORVATH, M., DIETZELMÜLLER, M., LOIDL, M., STREICHSBIER, F.: Isolation and characterization of a 2-(2,4-dichlorophenoxy)propionic acid-degrading soil bacterium. Appl. Microbiol. Biotechnol. **33** (1990), 213–216.

[32] ZIPPER, C., NICKEL, K., ANGST, W., KOHLER, H.-P. E.: Complete microbial degradation of both enantiomers of the chiral herbicide mecoprop [(*RS*)-2-(4-chloro-2-methylphenoxy)propionic acid] in an enantioselective manner by *Sphingomonas herbicidovorans* sp. nov. Appl. Environ. Microbiol. **62** (1996), 4318–4322.

[33] FULTHORPE, R. R., MCGOWAN, C., MALTSEVA, O. V., HOLBEN, W. E., TIEDJE, J. M.: 2,4-Dichlorophenoxyacetic acid-degrading bacteria contain mosaics of catabolic genes. Appl. Environ. Microbiol. **61** (1995), 3274–3281.

[34] TOP, E. M., MALTSEVA, O. V., FORNEY, L. J.: Capture of a catabolic plasmid that encodes only 2,4-dichlorophenoxyacetic acid:α-ketoglutaric acid dioxygenase (TfdA) by genetic complementation. Appl. Environ. Microbiol. **62** (1996), 2470–2476.

COR-AAD1-00002731
Bayer EX1008 (Part 5 of 9)

Acta Biotechnol. 19 (1999) 4, 349–355

Short Communication

Separation of Two Dichlorprop/α-Ketoglutarate Dioxygenases with Enantiospecific Properties from *Comamonas acidovorans* MC1

MÜLLER, R. H., BABEL, W.

UFZ – Umweltforschungszentrum Leipzig–Halle GmbH
Sektion Umweltmikrobiologie
Permoserstraße 15
04318 Leipzig, Germany

Summary

Comamonas acidovorans MC1, which is capable of degrading the chiral phenoxypropionate herbicides 2-(2,4-dichlorophenoxy)propionate [dichlorprop, (*RS*)-2,4-DP] and 2-(4-chloro-2-methylphenoxy)propionate [mecoprop, (*RS*)-MCPP] and of degrading the phenoxyacetate herbicides 2,4-dichlorophenoxyacetate (2,4-D) and 4-chloro-2-methylphenoxyacetate (MCPA), was investigated with respect to the enzymatic basis of this broad substrate specificity. The initial steps of the degradation pathway of (*RS*)-2,4-DP and 2,4-D were studied. By applying either ion exchange chromatography or hydrophobic interaction chromatography it was possible to separate two enzyme fractions with etherolytic activity, which exhibited pronounced substrate specificity. One enzyme fraction was highly specific for the degradation of the *R*-enantiomer of 2,4-DP and did not essentially attack the *S*-configuration. The other enzyme fraction showed pronounced activity toward the cleavage of the *S*-enantiomer and additionally utilized 2,4-D with almost equal velocity; (*R*)-2,4-DP was even cleaved at a low rate by this enzyme. These results confirm the existence of phenoxyalkanoate-degrading enzymes with enantiospecific properties in strain MC1.

Introduction

Bacterial degradation of phenoxyalkanoates is initiated by cleaving the ether bond resulting in the liberation of chlorophenols. This initial step, encoded by the gene *tfdA*, is catalyzed by an α-ketoglutarate-dependent dioxygenase, as shown with 2,4-D and the purified enzyme derived from the gene harboured on plasmid pJP4 [1, 2]. The gene *tfdA* was found to be widespread in nature [3–5]. Besides the degradation of phenoxyacetates, α-ketoglutarate-dependent degradation has been described as being involved in the degradation of phenoxypropionates, i.e. (*RS*)-2-(2,4-dichlorophenoxy)propionate [(*RS*)-2,4-DP, dichlorprop] and (*RS*)-2-(4-chloro-2-methylphenoxy)propionate [(*RS*)-MCPP, mecoprop]. This holds true for *Sphingomonas herbicidovorans* MH [6], *Rhodoferax* sp. P230 [7] and *Comamonas acidovorans* MC1 [8]. Whereas in the first two cases TfdA-like activities could be demonstrated by applying primers from the conserved region of this gene [5], these primers did not give amplification products by

COR-AAD1-00002732
Bayer EX1008 (Part 5 of 9)

PCR with strain MC1 (S. KLEINSTEUBER, personal communication). Nevertheless, the reaction proved to be α-ketoglutarate-dependent. Moreover, as dichlorprop and mecoprop are chiral compounds, we expected two distinct enzymes with specificity for the cleavage of the *R*- and *S*-enantiomer, respectively [9, 10]. Besides phenoxypropionates, the latter three strains are capable of degrading phenoxyacetate herbicides (2,4-D, MCPA). In order to elucidate the enzymatic basis of this broad substrate consumption pattern, we looked for enzymes with distinct substrate specificity. The present investigations were performed with *C. acidovorans* MC1.

Materials and Methods

Cultivation

Strain MC1 was grown in a mineral salt solution which was balanced for 2 grams of biomass and contained [in mg/l]: NH_4Cl, 760; KH_2PO_4, 340; K_2HPO_4, 485; $CaCl_2 \times 6\ H_2O$, 27; $MgSO_4 \times 7\ H_2O$, 71.2; $FeSO_4 \times 7\ H_2O$, 4.98; $CuSO_4 \times 5\ H_2O$, 0.785; $MnSO_4 \times 4\ H_2O$, 0.81; $ZnSO_4 \times 7\ H_2O$, 0.44; $Na_2MoO_4 \times 2\ H_2O$, 0.25. (*RS*)-2,4-DP was supplied as the sole source of carbon and energy. Growth was performed under fed-batch conditions in such a way that the actual substrate concentration in the fermentation broth did not exceed 0.2 g/l. The cells were grown in an INFORS ISF 205 fermenter with a working volume of 5 l under aerobic conditions with a pH value of 8.0 and at 30 °C. After reaching the respective biomass concentrations, aliquots of the concentrated mineral salt solution were added, and the fed-batch supply of (*RS*)-2,4-DP continued. The growth process was stopped after a final biomass concentration of about 5 g/l had been obtained. The cells were harvested, washed and resuspended in 0.01 M Tris buffer (pH 7.5) and stored at – 20 °C for further use.

Enzyme Preparation

The cell suspension was thawed at room temperature. The cells were disintegrated in the presence of 0.25 mM α-ketoglutarate and 10 µM ammonium iron (II) sulphate by three passages through a precooled French pressure cell press at 18,000 psi. One part of protamine sulphate (1 % w/v, pH 7.0) was added to nine parts of the disintegrate and chilled on ice for 20 min. Particle free supernatants were obtained from these disintegrates by centrifugation at 23,000 × g (15 min, 4 °C).

The supernatants were applied to chromatographic separations performed either by ion exchange chromatography on *Q*-sepharose (Fast Flow, PHARMACIA) or by hydrophobic interaction chromatography on butyl sepharose (4 Fast Flow, PHARMACIA) at 12 °C in columns with a dimension of 50 × 25 mm. In the first case, the column was equilibrated with 0.01 M Tris buffer (pH 7.5) containing 1 mM α-ketoglutarate and 50 µM ammonium iron (II) sulphate (buffer A); the elution was performed by linearly increasing gradients of sodium chloride. Some elution steps were performed using constant salt concentrations as indicated in the figures. In the second case, the column was equilibrated by buffer A containing 1 M ammonium sulphate; the elution was carried out by linearly decreasing gradients of ammonium sulphate using buffer A. The columns were loaded with about 25 mg of protein. The total volumes of the various gradients were 120 ml with IEX and 180 ml with HIC. The eluates were collected in fractions of 6 ml.

Measurement

The activity of phenoxyalkanoate/α-ketoglutarate dioxygenase using (*RS*)-2,4-DP, (*R*)-2,4-DP, (*S*)-2,4-DP or 2,4-D as the substrates was determined according to FUKUMORI and HAUSINGER [1, 2] by colorimetrically measuring (at 510 nm) the liberation of the phenolic intermediate (2,4-dichloro-

COR-AAD1-00002733
Bayer EX1008 (Part 5 of 9)

phenol) after the reaction with potassium ferricyanide and 4-aminoantipyrin. The assay was performed in 0.01 M imidazole buffer (pH 6.75) which contained 1 mM of α-ketoglutarate ascorbic acid and the respective phenoxyalkanoate as well as 0.2 mM of ammonium iron (II) sulphate. The reaction was started by adding enzyme solution (0.01–0.1 mg/ml). The reaction was monitored for 10 min by sequentially taking samples and halted by adding 1 mM EDTA. During this period, the progress curves were almost linear with the amount of enzyme applied. The specific enzyme activity of one unit corresponds to the liberation of one µmole of DCP/min mg protein. In order to determine the enzymatic activity after chromatographic separation, 0.1 ml of the respective fractions was added to 0.7 ml of the assay mixture. The activity was indicated as arbitrary units referring to the optical density ($\times 10^3$) at 510 nm developed after 10 min of incubation; the values were corrected for blanks. Protein was determined using the BRADFORD reagent (Bioquant protein, MERCK). The enantiomers of 2,4-DP were synthesized, as described in [10] and [11].

Results and Discussion

The fractionation of crude extract by ion exchange chromatography on *Q*-sepharose, applying a gradient of NaCl ranging from 0 to 0.5 M (V_{total} = 120 ml), resulted in the elution of two peaks of activity, one appearing in the vicinity of unbound protein and one appearing at the end of the gradient. Applying more adapted gradients showed a reasonable resolution of protein bands carrying the respective phenoxyalkanoate-degrading activities (Fig. 1) after screening the fractions with both (*RS*)-2,4-DP and 2,4-D. Usage of the different enantiomers of 2,4-DP resulted in the detection of the respective substrate specificity. The enzyme responsible for the cleavage of the *S*-enantiomer of 2,4-DP was eluted at very low salt concentrations (around 0.02 M NaCl) and could be separated from various other proteins by using a very flat gradient (Fig. 2 a). In addition, these enzyme fractions showed similar activities for the degradation of 2,4-D and, at a low rate, of (*R*)-2,4-DP. A second peak of activity was found by using gradients with higher salt concentrations. The protein eluted at about 0.22 M NaCl under these conditions showed high specificity for the degradation of (*R*)-2,4-DP and did not essentially degrade (*S*)-2,4-DP and 2,4-D (Fig. 2 b).

Activities with such substrate specificity could also be separated by applying hydrophobic interaction chromatography on butyl sepharose (Fig. 3). Two peaks of activity with distinct specificity were again clearly separated. The fractions which eluted at around 0.5 M ammonium sulphate showed high specificity for the degradation of (*R*)-2,4-DP. The *S*-enantiomer and 2,4-D were barely cleaved by the proteins eluted in these fractions. On the contrary, the protein fractions which appeared at the end of this gradient showed high specificity for the degradation of both (*S*)-2,4-DP and 2,4-D. In addition, (*R*)-2,4-DP was attacked to a certain extent (Fig. 3).

The results show that there are two enzyme fractions which exhibit distinct affinities for the degradation of the two enantiomers of (*RS*)-2,4-DP. The enzyme responsible for the cleavage of the *R*-enantiomer is highly specific and hardly accepted the *S*-enantiomer. The enzyme exhibiting pronounced activity for the *S*-enantiomer has a wider spectrum: it degrades 2,4-D at a similar rate and even utilizes (*R*)-2,4-DP at a low rate. The fact that these enzymatic characteristics were observed using two different techniques of protein separation suggests that no additional enzyme with specificity for the degradation of 2,4-D is present. This is supported by screening the fractions which

COR-AAD1-00002734
Bayer EX1008 (Part 5 of 9)

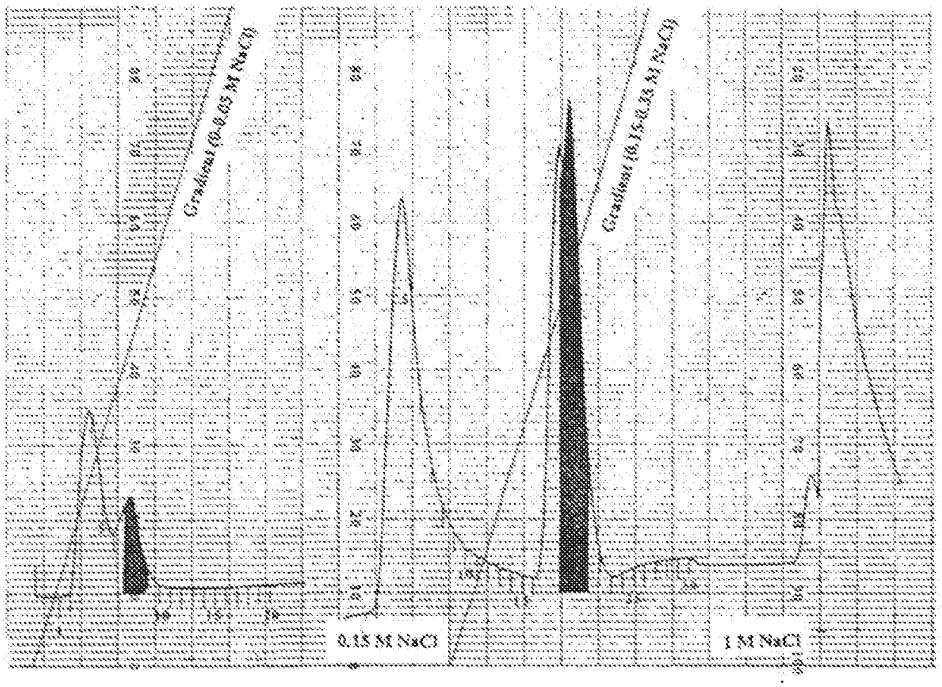


Fig. 1. Characteristics of protein absorption (278 nm) during the chromatography of crude extract on *Q*-sepharose and rough screening of phenoxyalkanoate-cleaving activity
The elution was performed with 0.01 M Tris buffer (pH 7.5) containing 1 mM α-ketoglutarate and 50 μM ammonium iron (II) sulphate. Sodium chloride at a constant concentration or via gradients was used, as indicated in the figure. The total volume of the individual gradients was 120 ml. Fractions of 6 ml were collected. The cleaving activity in the fractions was determined by applying both (*RS*)-2,4-DP and 2,4-D as the substrates. Fractions which responded positively in the assays are indicated by shadowed areas.

appeared in the elution profile for activity, as shown in Fig. 1. The latter was confirmed by the stability characteristics of the two enzymes. The protein responsible for the cleavage of (*R*)-2,4-DP was relatively stable, and the specific activity was increased by this separation step on *Q*-sepharose from 0.027 U/mg to 0.135 U/mg. This activity was maintained over 24 h and decreased to about 75% after 4 days of storage at 4 °C. By way of contrast, the activity of the *S*-enantiomer specific enzyme was almost completely lost within 5 h after elution including the loss of activity with regard to the cleavage of 2,4-D. Indications of the presence of two different enzymes were derived from electrophoretic separations of the crude extract of *S. herbicidovorans* MH [12]. The present results are taken as a basis for the purification and characterization of the individual enzymes involved in the degradation of phenoxyacetate and phenoxypropionate herbicides, including the solution of the stability problems.

COR-AAD1-00002735
Bayer EX1008 (Part 5 of 9)

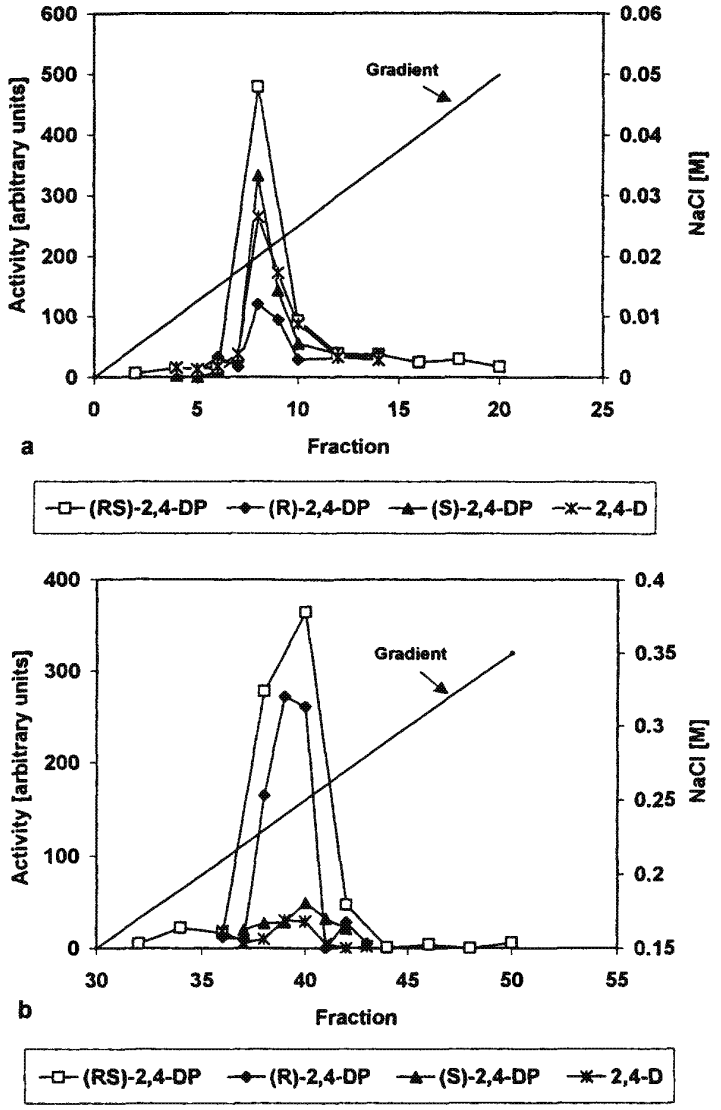


Fig. 2. Pattern of distribution of the phenoxyalkanoate-degrading activity after fractionation on *Q*-sepharose

a) The elution proceeded via a linear gradient of sodium chloride ranging from 0–0.05 M in a total volume of 120 ml, solubilized in 0.01 M Tris puffer (pH 7.5) containing 1 mM α-ketoglutarate and 50 µM ammonium iron(II) sulphate (buffer A).

b) The elution proceeded with buffer A via a linear gradient of sodium chloride ranging from 0.15–0.35 M in a total volume of 120 ml; before starting this gradient, the column was eluted with 60 ml buffer A containing 0.15 M sodium chloride.

For symbols see insert to the figure.

COR-AAD1-00002736
Bayer EX1008 (Part 5 of 9)

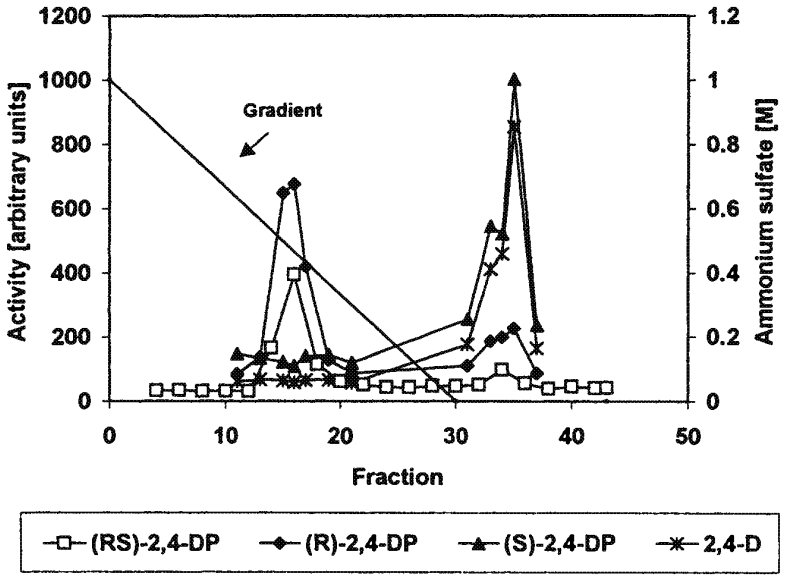


Fig. 3. Pattern of distribution of the phenoxyalkanoate degrading activity after fractionation on butyl sepharose
The elution proceeded via a linear gradient (V_{total} = 180 ml) of ammonium sulphate ranging from 1 M to zero, solubilized in 0.01 M Tris buffer (pH 7.5) containing 1 mM α-ketoglutarate and 50 µM ammonium iron (II) sulphate.
For symbols see insert to the figure.

Received 18 August 1999
Received in revised form 1 October 1999
Accepted 18 October 1999

References

[1] FUKUMORI, F., HAUSINGER, R. P.: *Alcaligenes eutrophus* JMP 134 "2,4-dichlorophenoxyacetate monooxygenase" is an α-ketoglutarate-dependent dioxygenase. J. Bacteriol. **175** (1993), 2083–2086.

[2] FUKUMORI, F., HAUSINGER, R. P.: Purification and characterization of 2,4-dichlorophenoxyacetate/α-ketoglutarate dioxygenase. J. Biol. Chem. **268** (1993), 24311–24317.

[3] FULTHORPE, R. R., MCGOWAN, C., MALTSEVA, O. V., HOLBEN, W. E.; TIEDJE, J. M.: 2,4-Dichlorophenoxyacetic acid-degrading bacteria contain mosaics of catabolic genes. Appl. Environ. Microbiol. **61** (1995), 3274–3281.

[4] TOP, E. M., HOLBEN, W. E., FORNEY, L. J.: Characterization of diverse 2,4-dichlorophenoxyacetic acid-degradative plasmids isolated from soil by complementation. Appl. Environ. Microbiol. **61** (1995), 1691–1698.

[5] VALLAEYS, T., FULTHORPE, R. R., WRIGHT, A. M., SOULAS, G.: The metabolic pathway of 2,4-dichlorophenoxyacetic acid degradation involves different families of *tfd*A and *tfd*B genes according to PCR-RFLP analysis. FEMS Microbiol. Ecol. **20** (1996), 163–172.

COR-AAD1-00002737
Bayer EX1008 (Part 5 of 9)

[6] ZIPPER, C., NICKEL, K., ANGST, W., KOHLER, H. P. E.: Complete microbial degradation of both enantiomers of the chiral herbicide mecoprop [(*RS*)-2-(4-chloro-2-methylphenoxy)propionic acid] in an enantioselective manner by *Sphingomonas herbicidovorans* sp. nov. Appl. Environ. Microbiol. **62** (1996), 4318–4322.

[7] EHRIG, A., MÜLLER, R. H., BABEL, W.: Isolation of phenoxy herbicide-degrading *Rhodoferax* species from contaminated building material. Acta Biotechnol. **17** (1997), 351–356.

[8] MÜLLER, R. H., JORKS, S. KLEINSTEUBER, S., BABEL, W.: *Comamonas acidovorans* MC1: A new isolate capable of degrading the chiral herbicides dichlorprop and mecoprop and the herbicides 2,4-D and MCPA. Microbiol. Res. **154** (1999), in press.

[9] ARMSTRONG, D. W., REID III, G. L., HILTON, M. L., CHANG, C. D.: Relevance of enantiomeric separations in environmental science. Environ. Pollut. **79** (1993), 51–58.

[10] ZIPPER, C.: Microbial degradation and environmental fate of chiral phenoxyalkanoic acid herbicides. Diss. ETH Zurich No. 12543 (1998).

[11] MATELL, M.: Stereochemical studies on plant growth regulators. VII. Optical active α-(2-methyl-4-chlorophenoxy)-propionic acid and α-(2,4-dichlorophenoxy)-*n*-butyric acid and their steric relations. Arkiv Kemi **6** (1953), 365–373.

[12] NICKEL, K., SUTER, M. J. F. KOHLER, H. P. E.: Involvement of two α-ketoglutarate dependent dioxygenases in enatioselective degradation of *(R)*- and *(S)*-mecoprop *by Sphingomonas herbicidovorans* MH. J. Bacteriol. **179** (1997), 6674–6679.

COR-AAD1-00002738
Bayer EX1008 (Part 5 of 9)

Microbiol. Res. (1999) **154**, 241–246
http://www.urbanfischer.de/journals/microbiolres

© Urban & Fischer Verlag

Comamonas acidovorans strain MC1: a new isolate capable of degrading the chiral herbicides dichlorprop and mecoprop and the herbicides 2,4-D and MCPA

Roland H. Müller, Siegfried Jorks, Sabine Kleinsteuber, Wolfgang Babel

UFZ Centre for Environmental Research, Dept. of Environmental Microbiology, Permoserstr. 15, D-04318 Leipzig, Germany

Accepted: August 5, 1999

Abstract

A gram-negative prototrophic bacterial species, strain MC1, was isolated from the vicinity of herbicide-contaminated building rubble and identified by 16S rDNA sequence analysis, its physiological properties, GC content, and fatty acid composition as *Comamonas acidovorans*. This strain displays activity for the productive degradation of the two enantiomers of dichlorprop [(RS)-2-(2,4-dichlorophenoxy-)propionate; (RS)-2,4-DP] and mecoprop [(RS)-2-(4-chloro-2-methyl-) phenoxypropionate; (RS)-MCPP] in addition phenoxyacetate herbicides, i.e. 2,4-dichlorophenoxyacetate (2,4-D) and 4-chloro-2-methylphenoxyacetate (MCPA), and various chlorophenols were utilized. Rates amounted to 1.2 mmoles/h g dry mass (2,4-D) and 2.7 mmoles/h g dry mass [(RS)-2,4-DP]. Degradation of (RS)-2,4-DP was not inhibited up to concentrations of 500 mg/l, nor of 2,4-D up to 200 mg/l. The optimum pH value of (RS)-2,4-DP degradation was around 8. The application of respective primers for PCR amplification revealed the presence of *tfdB* and *tfdC* genes.

Key words: *Comamonas acidovorans* – degradation – mecoprop – dichlorprop – 2,4-D

Introduction

Bacterial strains selected for the degradation of phenoxyacetic acid herbicides were found to be restricted to productively utilize only those compounds of the range of phenoxyalkanoic acid herbicides, including phenoxypropionate and phenoxybutyrate derivatives. This holds for the most prominent strain *Ralstonia eutropha (Alcaligenes eutrophus)* JMP 134 (Don and Pemberton 1981, Pieper *et al.* 1988) or for example for *Comamonas acidovorans* P4 a (Hoffmann *et al.* 1996) which only utilize phenoxyacetate derivatives (i.e. 2,4-D, MCPA or similar compounds) as the carbon and energy source for growth. In some cases this was even restricted to the utilization of 2,4-D (Ka *et al.* 1994). In addition, by employing phenoxybutyrates for enrichment, strains were obtained which only cleaved these derivatives but did not attack phenoxypropionates or phenoxyacetates (Mertingk *et al.* 1998). In contrast, the supply of phenoxypropionate herbicides as the selective substrate resulted in the enrichment of strains which productively utilized a broader spectrum of phenoxyalkanoic acids comprising phenoxypropionate and phenoxyacetate herbicides. This was described for strain MH (Horvath *et al.* 1990) now identified as *Sphingomonas herbicidovorans* (Zipper *et al.* 1996) and for *Rhodoferax* sp. strain P230 (Ehrig *et al.* 1997). The selection of pure cultures able to completely degrade phenoxypropionates was not obvious and has been questioned in the past as many cases have been described in which this activity was associated with consortia (Kilpi 1980; Lappin *et al.* 1985; Pfarl *et al.* 1990; Kelly *et al.* 1991). Here we report on a prototrophic bacterium capable of completely utilizing (productively mineralizing) the racemic compounds 2-(2,4-dichlorophenoxy-)propionate [(RS)-2,4-DP; dichlorprop] and 2-(4-chloro-2-methylphenoxy-)propionate [(RS)-MCPP; mecoprop]. In addition, this strain exhibits activity for the degradation of phenoxyacetates (2,4-D, MCPA) and utilizes various chlorophenols.

Corresponding author: R. H. Müller,
E-Mail: rmueller@umb.ufz.de

0944-5013/99/154/03-241 $12.00/0

COR-AAD1-00002739
Bayer EX1008 (Part 5 of 9)

Materials and methods

Strains and cultivation. Strain MC1 was isolated from a fixed-bed reactor operated for several months under aerobic conditions to degrade a herbicide mixture containing (RS)-2,4-DP and 4-(2,4-dichlorophenoxy-) butyrate (M. Millitzer, unpublished; cf. Müller *et al.* 2000). The microorganisms were derived from the biofilm grown on the surface of the fixed-bed matrix particles (concrete debris 10 mm in diameter), resuspended in growth medium and streaked onto agar plates containing various phenoxyalkanoic acid herbicides at concentrations of 50–200 mg/l. Colonies were subsequently transferred into liquid medium containing herbicide at a concentration of 20–200 mg/l and yeast extract (100 mg/l). Degradation of the herbicides was followed by aerobic treatment at 30 °C. Passages on solid and liquid medium were repeated several times. Strain MC1 was obtained from this selection procedure, and grown and stored under selective conditions using 200 mg/l of (RS)-2,4-DP.

Strain MC1 was grown on a mineral salt solution containing (in mg/l): NH_4Cl, 760; KH_2PO_4, 340; K_2HPO_4, 485; $CaCl_2 \cdot 6\,H_2O$, 27; $MgSO_4 \cdot 7\,H_2O$, 71.2; $FeSO_4 \cdot 7\,H_2O$, 4.98; $CuSO_4 \cdot 5\,H_2O$, 0.785; $MnSO_4 \cdot 4\,H_2O$, 0.81; $ZnSO_4 \cdot 7\,H_2O$, 0.44; $Na_2MoO_4 \cdot 2\,H_2O$, 0.25. Batch cultivation in the presence of 200 mg/l of herbicide was performed in 100 and 500 ml shaking flasks on a rotary shaker at 200 rpm and a temperature of 30 °C. Fed-batch and continuous cultivation of the strain were performed in a 1-litre laboratory fermenter under aerobic conditions, 30 °C and pH 8.5. The herbicides were supplied as the sole source of carbon and energy at a concentration of 2 g/l. For auxanographic tests, the strain was precultivated up to stationary conditions on mineral salt solution containing 2 g/l sodium pyruvate. A 10% (v/v) inoculum was supplied to the mineral salt solution containing the carbon sources to be tested at a concentration of 1 g/l.

Microbial characterization. Gram-staining was performed using Hucker's method and the L-alanine aminopeptidase test (Burkhardt 1992). Investigations by the BIOLOG Automated Microbial Identification System (BIOLOG Inc., Hayward, USA) were performed as described by Wünsche and Babel (1996); the API 20 NE identification kit (Biomérieux, Marcy-l'Ecole, France) was applied as per the technical instructions. Cellular fatty acids were determined after methylation by gas chromatography as specified in the instructions for the MIDI Inc. automatic identification system (Barksdale Professional Center, Newark DE, USA) (cf. Loffhagen *et al.* 1995) after growth of the strain on trypticase soy broth agar (Becton Dickinson, Cockeysville MD, USA). The GC content was determined by HPLC measurement as indicated by Mesbah *et al.* (1989).

16S rDNA analysis. A small colony of strain MC1 was resuspended in 50 µl sterile A. dest., boiled in a water bath for 10 min, and centrifuged for 5 min at 23,000 × g at 4 °C. The supernatant was used for polymerase chain reaction (PCR). Amplification reaction was performed in a 100 µl solution containing 2 µl supernatant, 50 µl *Taq* PCR Master Mix (QIAGEN GmbH), and 20 pmol each of primers 27F and 1525R (Lane 1991). The PCR was carried out in an Eppendorf Mastercycler® 5330 with a denaturation step at 95 °C for 5 min, 30 cycles at 95 °C for 45 sec, 58 °C for 45 sec, and 72 °C for 75 sec, and a final extension step at 72 °C for 5 min. After checking by electrophoresis on an 0.8% (w/v) agarose gel (Sambrook *et al.* 1989) the PCR product was purified with NucleoSpin Extract 2 in 1 (Macherey-Nagel GmbH & Co. KG) and the DNA concentration was measured spectrophotometrically at 260 nm.

The ABI PRISM™ BigDye™ Terminator Cycle Sequencing Ready Reaction kit (PE Applied Biosystems) and sequencing primers 27F, 357F, 519R, 530F, 926F, 1100R, 1114F and 1525R (Lane 1991) were used to sequence the 16S rDNA. Sequencing reactions were performed using 4.0 µl terminator ready reaction mix, 100 ng PCR product, 10 pmol sequencing primer in a total volume of 20 µl. The reactions were carried out in a Thermocycler PTC200 (MJ Research, Inc.) with denaturation at 94 °C for 5 min, 25 cycles consisting of 30 sec at 94 °C, 30 sec at 60 °C, and 4 min at 60 °C. The sequencing products were purified by Centri-Sep™ spin columns (Princeton Separations). 4 µl of purified product were mixed with template suppression reagent (TSR, PE Applied Biosystems) by vortexing. The samples were heated at 90 °C for 2 min and chilled on ice. Electrophoresis of the samples was carried out on an ABI PRISM™ 310 Genetic Analyzer. Data were analyzed using ABI PRISM™ DNA Sequencing Analysis and ABI PRISM™ Autoassembler™ software.

The 16S rDNA sequence of strain MC1 was manually aligned using ABI PRISM™ Sequence Navigator software with the 16S rDNA sequences of representatives of the genus *Comamonas* obtained from the Ribosomal Database Project (Maidak *et al.* 1999) and GenBank database (National Centre for Biotechnology Information, Bethesda, Md.). Gaps at the 5' and 3' ends of the alignment were omitted from further analysis including 1462 bases. A dendrogram was constructed by the Unweighted Pair Group Method using Averages (UPGMA) using the MicroSeq™ Microbial Identification and Analysis software (PE Applied Biosystems).

Nucleotide sequence accession numbers. The sequence of the 16S rDNA of MC1 has been deposited in GenBank under the accession number AF149849. The ac-

COR-AAD1-00002740
Bayer EX1008 (Part 5 of 9)

cession numbers of sequences used for alignment are as follows: *C. acidovorans* (IAM 12409^T): AB021417, *C.* sp. (isolate 158) AJ002803, *C. terrigena* (IAM 12052^T): AB021418, *C. terrigena* (IMI 359870): AF078772, *C. testosteroni* (ATCC 11996): M11224, *C. testosteroni* (MBIC3841): AB007997, and *C. testosteroni* (MBIC3840): AB007996.

Analyses. Chlorinated phenols and phenoxyalkanoic acids were determined by HPLC according to Oh and Tuovinen (1990). Chloride was determined by ion chromatography on an IonPak AS 14 column with 3.5 mM Na_2CO_3/1.0mM $NaHCO_3$ as the mobile phase (2.5 ml/min) using a DIONEX DX-100 configuration. Biomass concentration was obtained by measuring the optical density at 700 nm and by dry mass determination.

Results and discussion

Taxonomic characterization

After growth on PYE agar, strain MC1 forms round convex colonies of 2–3 mm, faintly bright and beige in colour, exhibiting an undulatory edge after 2–3 days of incubation. The cells are strongly motile and have a variable length of 3–12 µm and a diameter of 0.7–1.0 µm. They are gram-negative and show positive reaction for oxidase and catalase. For further taxonomic description, substrate utilization patterns and characteristics of cell composition were applied. Positive reactions were obtained with respect to the utilization of nitrate (reduction), mannitol, gluconate, caprate, adipate, malate and phenylacetate, according to which the strain was assigned to *Comamonas acidovorans* with no contradicting reaction by using the Biomérieux API 20 NE kit. This was confirmed by the BIOLOG system, which identified strain MC1 as *C. acidovorans* with a SIM value of 0.841. Characteristics differentiating the various species of *Comamonas* due to their substrate utilization pattern are summarized in Table 1. According to these results, strain MC1 matches the characteristics of *C. acidovorans* and clearly distinguishes from *C. terrigena* and *C. testosteroni.* This is further confirmed by the analysis of fatty acids of this strain which comprised (in %): 10:0 3 OH (2.4), 12:0 (2.37), 16:0 (35.33), 17:0 cyclo (10.41), 18:1 w7c (15.72) and a summed feature including 16:1 w7c/15 iso 2 OH and 15:0 iso 2 OH/16:1 w7c (30.41); any other compounds were less than 1%. According to these pattems, the MIDI automated system assigned strain MC1 to *C. acidovorans* with a similarity index of 0.693. The GC content of strain MC1 was 65.2%. This figure is between those found with *C. testosteroni* and *C. acidovorans* [(62.5–64.5) and (66.6–68.5) respectively (De Vos *et al.* 1985); (61.1–61.9) and (66.2–67.0) respectively (Tamaoka and Komagata 1987)] but matches those of *C. terrigena.* Assignment of strain MC1 to this species is ruled out due to the fact that it grows prototrophically and the differences in various auxanographic results as shown in Table 1. Strain MC1 exhibited a level of 16S rDNA sequence similarity with *C. testosteroni* ATCC 11996, MBIC3840, and MBIC3841 of 95.4% to 95.5%, 93.8% with *C. terrigena* IAM 12052^T and *C. terrigena* IMI 359870. The 16S rDNA of strain MC1 exhibited a level of sequence similarity of 99.1% with the strain *C. acidovorans* IAM 12409^T (type strain) and 99.7% with *C.* sp. isolate 158. A dendrogram constructed by the Unweighted Pair Group Method using Averages (UPGMA) is shown in Fig. 1. In conclusion of all of these results strain MC1 was assigned to *C. acidovorans.*

Table 1. Auxanographic characteristics of strain MC1.[1]

Compound	*C. terrigena*	*C. testosteroni*	*C. acidovorans*	Strain MC1[2]		
				B	A	G
D-Fructose	–	–	+	–		+
D-Mannitol	–	–	+	+	+	+
Phenylacetate	–	–	+		+	
DL-Tartrate	–	–	+			+
L-Histidine	–	+	+	+		
L-Phenylalanine	–	+	+	+		
Benzoate	–	+	–			–
β-Alanine	+	–	+			–
Testosterone	–	+	–			–
DL-β-Hydroxybutyrate	–	+	–			–
Supplements (L-methionine, nicotinamid)	+	–	–			–

[1] Differentiating characteristics were taken from De Vos *et al.* (1985) and Willems *et al.* (1991).
[2] Results obtained from BIOLOG (B), API (A) and growth (G) characteristics.

COR-AAD1-00002741
Bayer EX1008 (Part 5 of 9)

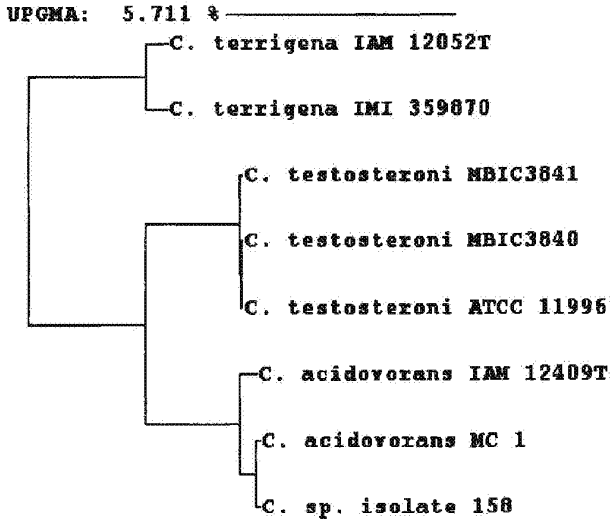


Fig. 1. Dendrogram showing phylogenetic relationships of strain MC1 and representatives of the genus *Comamonas*

Degradative properties

The degradative capabilities of strain MC1 with respect to a range of phenoxyalkanoic acid herbicides and chlorinated phenols are shown in Table 2. The strain evidently degraded the phenoxyacetate and the enantiomeric phenoxypropionate herbicides within one day of incubation with respect to both the 2,4-dichlorinated and 4-chloro-2-methylated derivatives. The respective chlorophenols (DCP, MCP) were likewise utilized, as were 2-CP and 4-CP. By contrast, phenoxybutyrate derivatives were not attacked within several days of incubation, which was also the case with 3-CP. Phenol was not utilized either. Quantitative evaluations in the presence of 200 mg/l of substrate revealed (RS)-2,4-DP and 2,4-D degradation rates of 2.4–2.7 mmoles/h g dry mass and 1.0–1.2 mmoles/h g dry mass respectively after precultivation on either (RS)-2,4-DP or 2,4-D. Concentration-dependent activity pattern showed highest rates at around 500 mg/l of (RS)-2,4-DP; higher concentrations inhibited activity, which was nevertheless still 30% of the maximum at 1,000 mg/l of (RS)-2,4-DP after short-term incubation (Fig. 2). With 2,4-D, optimum activity was found at a substrate concentration of 200 mg/l. Both curves exhibit a certain complexity. The influence of the pH is shown in Fig. 3. Accordingly, strain MC1 shows (RS)-2,4-DP utilization ranging from slightly acidic up to alkaline conditions. Highest activity was found around pH 8; at pH 10 about 10% of the maximum activity persisted. Utilization of the herbicides was considered quantitative depending on the liberation of chloride from the respective substrates (Table 3), resulting in a molar concentration approximately twice as high as the initial substrate concentration after the complete

Table 2. Degradation of chlorinated aromatic compounds and phenol with strain MC1.

Compound (Abbreviation)	Degradation
2,4-dichlorophenoxyacetate (2,4-D)	+ (1)
4-chloro-2-methylphenoxyacetate (MCPA)	+ (1)
(RS)2-(2,4-dichlorophenoxy-)propionate [(RS)-2,4-DP]	+ (1)
(RS)2-(4-chloro-2-methylphenoxy-)propionate [(RS)-MCPP]	+ (1)
4-(2,4-dichlorophenoxy-)butyrate (2,4-DB)	– (4)
4-(4-chloro-2-methylphenoxy-)butyrate (MCPB)	– (4)
2,4-dichlorophenol (DCP)	+ (1)
4-chloro-2-methylphenol (MCP)	+ (2)
2-chlorophenol (2-CP)	+ (4)
3-chlorophenol (3-CP)	– (4)
4-chlorophenol (4-CP)	+ (1)
Phenol	– (4)

Strain MC1 was pregrown on agar plates containing minimal salt solution and 200 mg/l (RS)-2,4-DP and 100 mg/l of yeast extract. One loop of biomass was transferred into 40 ml of mineral salt solution containing 20 mg/l of the respective compounds +100 mg/l yeast extract and incubated aerobically at 30 °C over the time (in brackets) indicated. +, degradation within the time (days) indicated, –, no degradation within the time indicated.

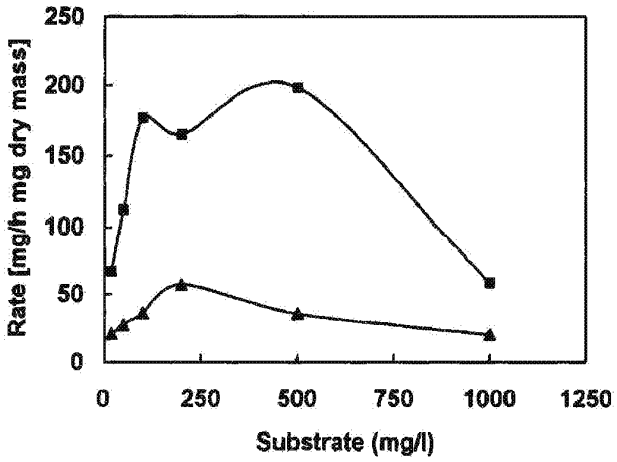


Fig. 2. Dependence of the degradation rate on substrate concentration. Strain MC1 was continuously cultivated on (RS)-2,4-DP. Cells were harvested under sterile conditions, washed and resuspended at a concentration of 0.1 g/l into mineral salt solution, pH 8.5, and incubated in the presence of (RS)-2,4-DP at the concentrations indicated. Cells used for the investigation of the influence of 2,4-D concentration were obtained from the continuous cultivation on this substrate, harvested and stored in the presence of 50% glycerol until measurement. The cells were washed before application with the respective medium. Samples were taken at appropriate times and rates of substrate disappearance calculated via linear regression, ▲ 2,4-D; ■ (RS)-2,4-DP.

COR-AAD1-00002742
Bayer EX1008 (Part 5 of 9)

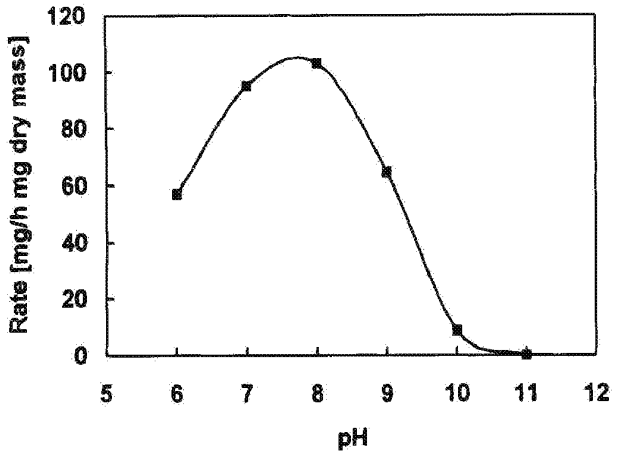


Fig. 3. Influence of the pH on substrate degradation. Strain MC1 was continuously cultivated on (RS)-2,4-DP at a dilution rate of 0.05 h^{-1}. Cells were harvested, washed and resuspended at a concentration of 0.1 g/l into 0.1 M Bis-Trispropane buffer of the respective pH value and measured in the presence of 100 mg/l of substrate.

Table 3. Stoichiometry of herbicide degradation.

Substrate	Substrate consumption (mM)	Chloride formation
2,4-D	0.91	2.18
(RS)-2,4-DP	0.83	2.08
(RS)-MCPP	0.685	0.625

Strain MC1 was continuously cultivated on (RS)-2,4-DP. Cells were harvested, washed and resuspended in chloride-free mineral salt solution (exchange of chloride by sulphate in the salts of the medium) and incubated at 30 °C on the substrates indicated until their complete disappearance (HPLC measurement).

disappearance of the substrates with the dichlorinated compounds [(RS)-2,4-DP, 2,4-D], and about equimolar concentration with the 4-chloro-2-methyl-substituted derivatives [(RS)-MCPP].

Genetic and enzymatic investigations.

Preliminary investigations as to the enzymatic and genetic background of herbicide utilization applying the primers derived from conserved regions of the respective genes *tfdA* and *tfdB* (Vallaeys *et al.* 1996) and *tfdC* (Kleinsteuber *et al.* 1998) revealed PCR products indicating the presence of *tfdB* (encoding chlorophenol hydroxylase) and *tfdC* (encoding chlorocatechol 1,2-dioxygenase), whereas the respective primers did not result in any amplification product with respect to *tfdA* [encoding 2,4-D(phenoxyalkanoate)/α-ketoglutarate dioxygenase] after growth on LB medium. Nevertheless, enzyme activity catalyzing the primary step of phenoxyalkanoate degradation proved to be a TfdA-analogous reaction as it was obligatorily dependent on Fe^{2+} and α-ketoglutarate (cf. Fukumori and Hausinger 1993); enzyme activities were less than 3% in the absence of these compounds in comparison to the complete assay [0.07–0.12 µmole (RS)-2,4-DP/min mg crude extract protein].

Comamonas acidovorans MC1 is a further example of a strain exhibiting substrate specificity for the degradation of both phenoxyacetate and phenoxypropionate herbicides. Moreover, as the latter is a racemic mixture of the two optical active stereoisomers, complete utilization of these compounds indicates specificities for the degradation of both the (R)- and (S)-enantiomer. In general, the enantiomers of a given compound should be considered to be individual substrates from a physiological viewpoint (Armstrong *et al.* 1993; Zipper 1998) requiring defined enzyme activities. The requirement of individual enzymes was indicated by the fact that *Alcaligenes denitrificans* for instance was only able to degrade the R-enantiomer (Tett *et al.* 1994). The molecular basis of this substrate specificity is likely to be attributed to the initial step of degradation, i.e. the phenoxyalkanoate(2,4-D)/α-ketoglutarate dioxygenase. In the case of *R. eutropha* JMP134 it was shown that k_{cat} and K_m values were one order of magnitude lower and higher respectively with respect to phenoxypropionates as compared to the proper phenoxyacetate (2,4-D) substrates (Fukumori and Hausinger 1993); this probably holds for the enzyme from *C. acidovorans* P4a (P. Reinhold and R. H. Müller, unpublished). Turnover rates of phenoxypropionates might be too low under these conditions to support growth due to a shortage of energy (Müller and Babel 1996). The molecular basis of the broad substrate utilization profile of strain MC1 is not yet evident and calls for further investigations on an enzymatic and genetic level.

Acknowledgement

The authors are indepted to C. Härtig for fatty acid determination and to L. Wünsche for the determination of the GC content.

References

Armstrong, D. W., Reid III, G. L., Hilton, M. L., Chang, C. D. (1993): Relevance of enantiomeric separations in environmental science. Environ. Poll. **79,** 51–58.

Burkhardt, F. (1992): Färbeverfahren. In: Mikrobiologische Diagnostik (Ed.: Burkhardt, F.), Georg Thieme Verlag, Stuttgart, New York, 680–682.

DeVos, P., Kerstens, K., Falsen, E., Pot, B., Gillis, M., Segers, P., DeLey, J. (1985): *Comamonas* Davis and Park 1962 gen.

COR-AAD1-00002743
Bayer EX1008 (Part 5 of 9)

nov., nom. rev. emend., and *Comamonas terrigena* Hugh 1962 sp. nov., nom. rev. Int. J. System. Bacteriol. **35,** 443–453.

Don, R. H., Pemberton, J. M. (1981): Properties of six pesticide degradation plasmids isolated from *Alcaligenes paradoxus* and *Alcaligenes eutrophus*. J. Bacteriol. **145,** 681–686.

Ehrig, A., Müller, R. H., Babel, W. (1997): Isolation of phenoxy herbicide-degrading *Rhodoferax* species from contaminated building material. Acta Biotechnol. **17,** 351–356.

Fukumori, F., Hausinger, R. P. (1993): Purification and characterization of 2,4-dichlorophenoxyacetate/α-ketoglutarate dioxygenase. J. Biol. Chem. **268,** 24311–24317.

Hoffmann, D., Müller, R. H., Kiesel, B., Babel, W. (1996): Isolation and characterization of an alkaliphilic bacterium capable of growing on 2,4-dichlorophenoxyacetic acid and 4-chloro-2-methylphenoxyacetic acid. Acta Biotechnol. **16,** 121–131.

Horvath, M., Dietzelmüller, M., Loidl, M., Streichsbier, F. (1990): Isolation and characterization of a 2-(2,4-dichlorophenoxy)propionic acid-degrading soil bacterium. Appl. Microbiol. Biotechnol. **33,** 213–216.

Ka, J. O., Holben, W. E., Tiedje, J. M. (1994): Genetic and phenotypic diversity of 2,4-dichlorophenoxyacetic acid (2,4-D)-degrading bacteria isolated from 2,4-D-treated field soils. Appl. Environ. Microbiol. **60,** 1106–1115.

Kelly, M. P., Heniken, M. R., Tuovinen, O. H. (1991): Dechlorination and the spectral changes associated with bacterial degradation of 2-(2-methyl-4-chlorophenoxy)propionic acid. J. Ind. Microbiol. **7,** 137–146.

Kilpi, S. (1980): Degradation of some phenoxy acid herbicides by mixed cultures of bacteria isolated from soil treated with 2-(2-methyl-4-chloro)phenoxypropionic acid. Microbiol. Ecol. **6,** 261–270.

Kleinsteuber, S., Hoffmann, D., Müller, R. H., Babel, W. (1998): Detection of chlorocatechol 1,2-dioxygenase genes in proteobacteria by PCR and gene probes. Acta Biotechnol. **18,** 231–240.

Lane, D. J. (1991): 16S/23S rRNA sequencing. In: Nucleic acid techniques in bacterial systematics (Eds.: Stackebrandt, E., Goodfellow, M.), Wiley, Chichester, 177–203.

Lappin, H. M., Greaves, M. P., Slater, J. H. (1985): Degradation of the herbicide [2-(2-methyl-4-chlorophenoxy)]propionic acid by a synergistic microbial community. Appl. Environ. Microbiol. **49,** 429–433.

Loffhagen, N., Härtig, C., Babel, W. (1995): Fatty acid patterns of *Acinetobacter calcoaceticus* 69-V indicate sensitivity against xenobiotics. Appl. Microbiol. Biotechnol. **44,** 526–531.

Maidak, B. L., Cole J. R., Parker, C. T., Jr., Garrity, G. M., Larsen, N., Li, B., Lilburn, T. G., McCaughey, M. J., Olsen, G. J., Overbeek, R., Pramanik, S., Schmidt, T. M., Tiedje, J. M., Woese, C. R. (1999): A new version of the RDP (Ribosomal Database Project). Nucleic Acids Res. **27,** 171–173.

Mertingk, H., Müller, R. H., Babel,W. (1998): Etherolytic cleavage of 4-(2,4-dichlorophenoxy)butyric acid and 4-(4-chloro-2-methylphenoxy)butyric acid by species of *Rhodococcus* and *Aureobacterium* isolated from an alkaline environment. J. Basic Microbiol. **38,** 257–267.

Mesbah, M., Premachandran, U., Whitman, W. B. (1989): Precise measurement of the G+C content of deoxyribonucleic acid by high-performance liquid chromatography. Int. J. System. Bacteriol. **39,** 159–167.

Müller, R. H., Babel, W. (1996): Measurement of growth at very low rates ($\mu \geq 0$), an approach to study the energy requirement for the survival of *Alcaligenes eutrophus* JMP 134. Appl. Environ. Microbiol. **62,** 147–151.

Müller, R. H., Müller, R. A., Jahn, Y., Babel, W. (2000): Bioremediation of building material contaminated with herbicides. In: Remediation of hazardous waste contaminated soils (Eds.: Wise, D. L., Trantolt, D. J., Cichon, E. J.),. 2nd edition, Marcel Dekker, New York, (in press).

Oh, K. H., Tuovinen, O. H. (1990): Degradation of 2,4-dichlorophenoxyacetic acid by mixed cultures of bacteria. J. Ind. Microbiol. **6,** 275–278.

Pfarl, C., Dietzelmüller, G., Loidl, M., Streichsbier, F. (1990): Microbial degradation of xenobiotic compounds in soil columns. FEMS Microbiol. Ecol. **73,** 255–265.

Pieper, D. H., Reineke, W., Engesser, K. H., Knackmuss, H. J. (1988): Metabolism of 2,4-dichlorophenoxyacetic acid, 4-chloro-2-methylphenoxyacetic acid, and 2-methylphenoxyacetic acid by *Alcaligenes eutrophus* JMP 134. Arch. Microbiol. **151,** 365–371.

Sambrook, J., Fritsch, E. F., Maniatis, T. (1989): Molecular cloning: a laboratory manual. 2nd edition, Cold Spring Harbor Laboratory Press, Cold Spring Harbor, NY.

Tamaoka, J., Komagata, K. (1987): Reclassification of *Pseudomonas acidovorans* den Dooren de Jong 1926 and *Pseudomonas testosteroni* Marcus and Talalay 1956 as *Comamonas acidovorans* comb. nov. and *Comamonas testosteroni* comb. nov., with an emended description of the genus *Comamonas*. Int. J. System. Bacteriol. **37,** 52–59.

Tett, V. A., Willets, A. J., Lappin-Scott, H. M. (1994): Enantioselective degradation of the herbicide mecoprop [2-(2-methyl-4-chlorophenoxy)propionic acid] by mixed and pure cultures. FEMS Microbiol. Ecol. **14,** 191–200.

Vallaeys, T., Fulthorpe, R. R., Wright, A. M., Soulas, G. (1996): The metabolic pathway of 2,4-dichlorophenoxyacetic acid degradation involves different families of *tfdA* and *tfdB* genes according to PCR-RFLP analysis. FEMS Microbiol. Ecol. **20,** 163–172.

Willems, A., Pot, B., Falsen, E., Vandamme, P., Gillis, M., Kerstens, K., DeLey, J., (1991): Polyphasic taxonomic study of the emended genus *Comamonas:* Relationship to *Aquaspirillum aquaticum,* E. Falsen group 10, and other clinical isolates. Int. J. System. Bacteriol. **41,** 427–444.

Wünsche, L., Babel, W., (1996): The suitability of the BIOLOG automated microbial identification system for assessing the taxonomic compositions of terrestrial bacterial communities. Microbiol Res. **151,** 133–143.

Zipper, C., Nickel, K., Angst, W., Kohler, H.-P. E. (1996): Complete microbial degradation of both enantiomers of the chiral herbicide mecoprop [(RS)-2-(4-chloro-2-methylphenoxy)propionic acid] in an enantioselective manner by *Sphingomonas herbicidovorans* sp. nov. Appl. Environ. Microbiol. **62,** 4318–4322

Zipper, C. (1998): Microbial degradation and environmental fate of chiral phenoxyalkanoic acid herbicides. PhD thesis Zurich No. 12543.

COR-AAD1-00002744
Bayer EX1008 (Part 5 of 9)

JOURNAL OF BACTERIOLOGY, Nov. 1997, p. 6674–6679 Vol. 179, No. 21
0021-9193/97/$04.00+0
Copyright © 1997, American Society for Microbiology

Involvement of Two α-Ketoglutarate-Dependent Dioxygenases in Enantioselective Degradation of (*R*)- and (*S*)-Mecoprop by *Sphingomonas herbicidovorans* MH

KATHRIN NICKEL, MARC J.-F. SUTER, AND HANS-PETER E. KOHLER*

Swiss Federal Institute for Environmental Science and Technology (EAWAG), CH-8600 Dübendorf, Switzerland

Received 18 June 1997/Accepted 15 August 1997

Cell extracts of *Sphingomonas herbicidovorans* MH grown on (*R*)-mecoprop contained an enzyme activity that selectively converted (*R*)-mecoprop to 4-chloro-2-methylphenol, whereas extracts of cells grown on (*S*)-mecoprop contained an enzyme activity selective for the *S* enantiomer. Both reactions were dependent on α-ketoglutarate and ferrous ions. Besides 4-chloro-2-methylphenol, pyruvate and succinate were detected as products of the reactions. Labeling experiments with $^{18}O_2$ revealed that both enzyme activities catalyzed a dioxygenation reaction. One of the oxygen atoms of pyruvate and one of the oxygen atoms of succinate were derived from molecular oxygen. Analysis of cell extracts obtained from cells grown on different substrates by sodium dodecyl sulfate-polyacrylamide gel electrophoresis showed that growth on (*R*)-mecoprop and (*S*)-mecoprop caused the appearance of prominent protein bands at 34 and 32 kDa, respectively. Both protein bands were present when cells grew on the racemic mixture. The results demonstrate that *S. herbicidovorans* initiated the degradation of each enantiomer of mecoprop by a specific α-ketoglutarate-dependent dioxygenase. By comparing conversion rates of various phenoxy herbicides, we confirmed that the two enzyme activities were distinct from that of TfdA, which catalyzes the first step in the degradation of 2,4-dichlorophenoxyacetic acid in *Ralstonia eutropha* JMP134.

Substituted phenoxyalkanoic acid herbicides are widely used in weed control. 2,4-Dichlorophenoxyacetic acid (2,4-D) and the chiral compounds (*R,S*)-2-(4-chloro-2-methylphenoxy)propionic acid (mecoprop) and (*R,S*)-2-(2,4-dichlorophenoxy)propionic acid (dichlorprop) are members of this class of herbicides. The herbicidal activities of the last two compounds are exclusively associated with the *R* enantiomers. Today, the pure *R* enantiomers of mecoprop and of dichlorprop are commercially available as mecoprop-P and dichlorprop-P, respectively. Yet many commercial formulations contain the racemic mixtures and not the pure *R* enantiomers (27). In order to understand the environmental fate of the chiral compound mecoprop, it is important to study the degradation of the enantiomers independently, as has been recently emphasized (1, 2, 9, 22, 29).

Studies concerning the fate and the persistence of phenoxyalkanoic acids in soil revealed that degradation of these herbicides is caused mainly by microorganisms (17, 23). The breakdown of 4-chloro-2-methylphenoxyacetic acid (MCPA) and 2,4-D starts with the removal of the alkanoic acid side chain to yield the corresponding phenol (17). Consequently, a great deal of research effort was put into unravelling the subsequent degradation of 2,4-dichlorophenol and 4-chloro-2-methylphenol, the metabolites of 2,4-D and MCPA, respectively (10). In soil, the microbial metabolism of mecoprop leads to the appearance of 4-chloro-2-methylphenol (24). This metabolite is also formed in a mixed bacterial culture with mecoprop as the sole source of carbon and energy (14). So far, only two pure bacterial strains have been isolated for their ability to degrade mecoprop and dichlorprop (12, 26). One of them, *Alcaligenes denitrificans*, degrades only the *R* enantiomer of mecoprop (26), whereas the other, *Sphingomonas herbicidovorans* MH (formerly *Flavobacterium* sp. strain MH), completely degrades both enantiomers of mecoprop in an enantioselective manner (29). The pathway for the degradation of 2,4-dichlorophenol in *S. herbicidovorans* MH seems to correspond to the one in 2,4-D-grown *Ralstonia eutropha* JMP134, i.e., via *ortho* cleavage of the aromatic ring (12, 19).

In contrast to the ample knowledge of the biochemistry of the degradation of the phenolic metabolites, little is known of the biochemistry of the initial steps in the degradation of phenoxyalkanoic acid herbicides. Recently, it has been shown that *R. eutropha* JMP134 does not initiate metabolism of 2,4-D by a monooxygenase but by an α-ketoglutarate-dependent dioxygenase which is encoded by the *tfdA* gene of plasmid pJP4 (7). The enzyme was purified from *Escherichia coli* cells that overexpressed the *tfdA* gene, and its properties were described (8). In contrast, the initial attack on 2,4,5-trichlorophenoxyacetic acid in *Burkholderia cepacia* AC1100 is catalyzed by an oxygenase, TftAB, which shows homology to two multicomponent dioxygenases involved in benzoate and toluate degradation and is not dependent on α-ketoglutarate (4, 5, 28). Horvath et al. (12) deduced from their studies that a side-chain-cleaving activity must be crucial for the ability to degrade dichlorprop and mecoprop, but they could not detect the initial enzyme activity of the degradation pathways in cell extracts of *S. herbicidovorans* MH.

We recently described the ability of *S. herbicidovorans* MH to use both enantiomers of mecoprop as the sole source of carbon and energy (29). We now report that *S. herbicidovorans* MH initiates degradation of mecoprop by two α-ketoglutarate-dependent dioxygenase activities: one that is specific for (*R*)-mecoprop and one that is specific for (*S*)-mecoprop.

* Corresponding author. Mailing address: Department of Microbiology, EAWAG, Ueberlandstrasse 133, CH-8600 Dübendorf, Switzerland. Phone: 41 1 823 5521. Fax: 41 1 823 5547. E-mail: kohler@eawag.ch.

Downloaded from http://jb.asm.org/ on September 3, 2020 by guest

COR-AAD1-00002745
Bayer EX1008 (Part 5 of 9)

MATERIALS AND METHODS

Bacterial strains and culture conditions. *S. herbicidovorans* MH (DSM 11019) (29) was grown on mineral salts medium with different phenoxyalkanoic acids as the carbon and energy sources. The mineral salts medium consisted of 20 mM phosphate buffer (Na_2HPO_4-KH_2PO_4, pH 6.5), $(NH_4)_2SO_4$ (0.24 g/liter), $MgSO_4 \cdot 7H_2O$ (0.15 g/liter), $Ca(NO_3)_2 \cdot 4H_2O$ (2 mg/liter), and a trace element solution (0.4 ml/liter) that contained the following compounds: $FeSO_4 \cdot 7H_2O$ (2.50 g/liter), $MnSO_4 \cdot H_2O$ (0.75 g/liter), $ZnSO_4 \cdot 7H_2O$ (1.30 g/liter), $CuSO_4 \cdot 5H_2O$ (0.25 g/liter), $Co(NO_3)_2 \cdot 6H_2O$ (0.30 g/liter), $Na_2MoO_4 \cdot 2H_2O$ (0.15 g/liter), $NiSO_4 \cdot 7H_2O$ (0.01 g/liter), H_3BO_3 (0.10 g/liter), and H_2SO_4 (5.0 ml/liter). Carbon sources were supplied at 200 mg/liter. After being autoclaved, the medium was supplemented with peptone (40 mg/liter; Biolife, Milano, Italy) and with a vitamin solution (1 ml/liter containing pyridoxin-HCl [0.1 g/liter], biotin [20 mg/liter], folic acid [20 mg/liter], thiamine-HCl [50 mg/liter], riboflavin [50 mg/liter], nicotinic acid [50 mg/liter], Ca-pantothenate [50 mg/liter], 4-aminobenzoic acid [50 mg/liter], nicotinamide [50 mg/liter], and vitamine B_{12} [50 mg/liter]). Strain MH was maintained for several months at 4°C in liquid mineral salts medium with 2,4-D or racemic mecoprop as the carbon source, as well as on nutrient broth agar plates. For long-term storage at −80°C, cells grown on nutrient broth, which consisted of Standard I nutrient broth (5 g/liter; Merck, Darmstadt, Germany) in 20 mM phosphate buffer (pH 6.5), were incubated with 15% (vol/vol) glycerol for 2 h at room temperature prior to being frozen. *R. eutropha* JMP134(pJP4) was cultivated like *S. herbicidovorans* MH with 2,4-D (200 mg/liter) as the sole carbon and energy source.

Precultures (50 ml) were grown in mineral salts medium with the appropriate carbon source in 250-ml Erlenmeyer flasks at 25°C on a rotary shaker (100 rpm). Cells used for preparing cell extracts were cultivated in 2-liter Erlenmeyer flasks equipped with magnetic stirring bars in 800 ml of mineral salts medium with the appropriate carbon source. Cells were grown at room temperature, with stirring being held constant at 370 rpm.

Chemicals. Racemic mecoprop (98%) was obtained from Rhône-Poulenc, Paris, France. The pure (*S*)-mecoprop and (*R*)-mecoprop were prepared as described in reference 29. (*R*)-Dichlorprop and (*S*)-dichlorprop were kindly provided by C. Bolliger and C. Zipper, Swiss Federal Institute for Environmental Science and Technology (3). 2,4-D, 4-(4-chloro-2-methylphenoxy)butyric acid (MCPB), and 4-chloro-2-methylphenol were obtained from Aldrich-Chemie, Steinheim, Germany. MCPA as well as high-performance liquid chromatography (HPLC)-grade methanol was bought from Fluka Chemicals, Buchs, Switzerland. $^{18}O_2$ was obtained from Eurisotop, Centre d'Etudes de Saclay, Gif-sur-Yvette, France. L-Lactate dehydrogenase from rabbit muscle was bought from Boehringer Mannheim, Rotkreuz, Switzerland. All other chemicals were purchased from Merck and Fluka Chemicals.

Preparation of cell extracts. At the end of the exponential growth phase, cells were harvested by centrifugation (15 min at 7,500 × *g*) at 4°C and washed with an excess of mineral salts medium. One gram of wet cells was resuspended in 3 ml of a 20 mM Tris-HCl buffer (pH 7.5) containing 5 mM $MgCl_2$, 1 mM dithiothreitol, and 3 μg of DNase I. This cell suspension was passed three times through a French press (Hypramag, Zurich, Switzerland) at 1 MPa. After DNA digestion for 1 h at 4°C, the crude extract was centrifuged at 16,000 × *g* to remove cellular particles and membranes. The protein contents of cell extracts varied from 8 to 15 mg/ml. Protein was determined with the Bio-Rad protein assay kit (Bio-Rad, Munich, Germany). Cell extracts were stored for several months at −20°C without significant loss of enzyme activities. In cell extracts stored at 4°C for 1 day, the enzyme activities decreased.

Enzyme assays. The enzyme assays were performed in 50 mM imidazole buffer (pH 6.75) at 23°C. The assay mixture (total volume, 0.5 ml), if not stated otherwise, contained 1 mM ascorbate, 100 μM $(NH_4)_2Fe(SO_4)_2 \cdot 6H_2O$ (the stock solution was acidified to a pH of 2), 1 mM α-ketoglutarate, and 1 mM (*R*)-, (*S*)-, or racemic mecoprop. The assays were started by the addition of 50 μl of cell extract, and during the incubation the reaction mixture was gently stirred in order to assure oxygen saturation. Samples were taken at the appropriate time intervals and boiled for 2 min to stop the reaction. Denatured protein was removed by centrifugation at 16,000 × *g* for 10 min. Standards of reference substances were treated in the same manner.

Labeling with $^{18}O_2$. Incorporation of ^{18}O into the products of the enzyme reactions was measured in order to confirm the dioxygenation reactions. The enzyme assays in the presence of $^{18}O_2$ were carried out in 14-ml serum flasks, which were closed with gas-tight rubber septa and equipped with small magnetic stirring bars. The incubation mixture (total volume, 0.5 ml) consisted of 1 mM ascorbate, 100 μM ferrous ions, 1 mM α-ketoglutarate, 1 mM NADH, 50 μl of cell extract, 1.4 U of L-lactate dehydrogenase, and 50 mM 1,3-bis[tris-(hydroxymethyl)-methylamino]propane (pH 6.75). A 1:1 mixture of $^{18}O_2$ and $^{16}O_2$ was obtained by displacing 2.6 ml of $^{18}O_2$ into the head space of the flask with a gas-tight syringe (Dynatech, Baton Rouge, La.). After addition of the appropriate enantiomer of mecoprop (1 mM), the reaction mixture was gently stirred for 20 min. The reaction was stopped, and the reaction mixture treated as described above. The metabolites were subsequently analyzed by HPLC-mass spectrometry (MS). Analogous experiments with $^{16}O_2$ were carried out with open vials.

Analytical procedures. (i) HPLC. Quantitation of the mecoprop enantiomers and of 4-chloro-2-methylphenol was achieved by HPLC with a Nucleodex-α-PM column (200 by 4 mm; Macherey-Nagel, Düren, Germany) under isocratic conditions. The mobile phase consisted of a 70/30 (vol/vol) mixture of methanol and 50 mM NaH_2PO_4 (pH 3.0), and the flow rate was 0.7 ml/min. Phenoxyalkanoic acids and the substituted phenols were detected with a photodiode array detector (Waters-Millipore, Milford, Mass.) at a wavelength of 230 nm. By this method, detection limits of 4 μM for the mecoprop enantiomers and 11 μM for 4-chloro-2-methylphenol could be achieved. Typical retention times were 7.0, 8.3, and 13.0 min for (*R*)-mecoprop, (*S*)-mecoprop, and 4-chloro-2-methylphenol, respectively.

TABLE 1. Dependence on cofactors and on supplements of the initial conversion reactions of cell extracts from (*R*)- and (*S*)-mecoprop-grown *S. herbicidovorans* MH during incubation with racemic mecoprop

Cofactor(s) and supplement(s)	% Conversion of (*R*)-mecoprop by crude cell extract of (*R*)-mecoprop-grown cells[a]	% Conversion of (*S*)-mecoprop by crude cell extract of (*S*)-mecoprop-grown cells[a]
Fe^{2+}, ascorbate, α-ketoglutarate, L-cysteine, catalase, O_2	100 (65.5)	100 (68.0)
−Fe^{2+}[b]	10	33
−Ascorbate[b]	56	26
−α-Ketoglutarate[b]	0	0
−L-Cysteine[b]	114	101
−Catalase[b]	113	100
−Active protein[b,c]	0	0

[a] Specific activity in nanomoles of substrate consumed per milligram of protein per minute is given in parentheses.
[b] Complete assay minus the specified component.
[c] Proteins were denatured by boiling the cell extract prior to the assay.

(ii) Colorimetric assay for phenolic compounds. Alternatively, phenolic compounds formed during the enzyme assay were determined by the method of King et al. (15), except that the absorption of the resulting red antipyrine dye was measured at its specific maximum of 510 nm. This method was valid for 4-chloro-2-methylphenol as well as for 2,4-dichlorophenol in the range of 1 to 50 μM. If necessary, samples were diluted with 50 mM imidazole buffer (pH 6.75) prior to incubation with the dye reagents.

(iii) GC-MS. Gas chromatography (GC)-MS analysis of metabolites and their trimethylsilyl (TMS) derivatives was performed as described elsewhere (16).

(iv) HPLC-MS. Pyruvate, lactate, and succinate were analyzed by HPLC-MS. The samples were applied to a Nucleosil-C_{18} column (250 by 4 mm; Macherey-Nagel). Reversed-phase chromatography was performed isocratically with H_2SO_4 (pH 2.65) as the mobile phase at a flow rate of 0.5 ml/min and at 10°C by means of an HP1100 series HPLC system (Hewlett-Packard, Urdorf, Switzerland). Typical retention times for pyruvate, lactate and succinate were 6.5, 8.0, and 20.0 min, respectively. The HPLC was coupled to an MS (Micromass, Manchester, Great Britain) equipped with an electrospray ion source. Mass spectra were acquired with the negative ion mode, a needle voltage of 3.5 kV, a cone voltage of 30 V, nitrogen as the nebulizer and drying gas, and an ion source temperature of 150°C. The mass range of 50 to 500 Da was scanned once per second.

Electrophoresis and molecular weight determinations. Proteins of the crude cell extracts were separated under denaturing and reducing conditions by sodium dodecyl sulfate-polyacrylamide gel electrophoresis (SDS-PAGE). Slab gels (100 by 60 by 0.75 mm) were prepared with 12.5% acrylamide. A mixture of the following proteins (molecular weights in parentheses; Pharmacia Biotech, Uppsala, Sweden) served as a molecular weight marker: phosphorylase *b* (94,000), bovine serum albumin (67,000), ovalbumin (43,000), carbonic anhydrase (30,000), soybean trypsin inhibitor (20,100), and α-lactalbumin (14,400). Gels were stained with Coomassie brilliant blue G-250. The destaining solution consisted of 30% methanol, 1.5% acetic acid, and 68.5% water.

RESULTS

Mecoprop transformation with cell extracts. Cell extracts of (*S*)-mecoprop-grown cells of *S. herbicidovorans* MH effected the selective transformation of (*S*)-mecoprop to 4-chloro-2-methylphenol upon incubation with a racemic mixture of mecoprop (Table 1). On the other hand, cell extracts of (*R*)-mecoprop-grown cells contained an enzyme activity that specifically transformed the *R* enantiomer. The product of this reaction was also 4-chloro-2-methylphenol. In both cases, disappearance of the substrate was coupled to the concomitant

Downloaded from http://jb.asm.org/ on September 3, 2020 by guest

COR-AAD1-00002746
Bayer EX1008 (Part 5 of 9)

stoichiometric formation of the phenolic product. Both reactions strictly required α-ketoglutarate, and the rates of conversion were dependent on ferrous ions and L-ascorbic acid. Omission of these two components from the reaction mixture led to a decrease of the reaction rates, whereas omission of L-cysteine and catalase did not (Table 1). Addition of NADH and NADPH to the reaction mixture did not have a significant effect on the conversion rates. Boiling of the cell extracts for 2 min completely abolished the activities. Decreases in the turnover rates observed during the reactions were probably due to the oxidation of the ferrous ions in the reaction mixture. Addition of fresh ferrous ion solution to the reaction mixture at 5-min intervals guaranteed a constant conversion rate for at least 20 min. Optimal assay conditions were as follows: 50 mM imidazole buffer (pH 6.75), 0.1 mM ferrous ions, 1 mM L-ascorbic acid, 1 mM α-ketoglutarate, and 1 mM substrate. The enzyme activities were lost at pH values of 6.5 and lower.

Identification of the reaction products. The products of the reactions catalyzed by the two enzyme activities were identical. In both instances, the oxidative cleavage of the ether bond yielded 4-chloro-2-methylphenol and pyruvate. 4-Chloro-2-methylphenol was identified by HPLC. It cochromatographed with an authentic standard, and its UV spectrum (diode array) was identical to that of the standard. Additionally, the compound was identified by GC-MS of its TMS derivative. Its mass spectrum was identical to that of the TMS derivative of the authentic standard. Both TMS derivatives had identical retention times on the GC column under the conditions employed. Pyruvate was identified by HPLC-MS. It cochromatographed with authentic pyruvate and produced an identical mass spectrum. The cosubstrate α-ketoglutarate was oxidatively decarboxylated to succinate and presumably CO_2 during the course of the reactions. We did not measure CO_2, but succinate was identified by GC-MS. Its TMS derivative cochromatographed with the TMS derivative of authentic succinate, and both compounds produced identical mass spectra. We also identified succinate by HPLC-MS. The retention time and the mass spectrum of authentic succinate and those of the metabolite produced by the enzyme reaction were identical.

Incorporation of ^{18}O into succinate and pyruvate. In order to confirm the dioxygenation reaction for the formation of 4-chloro-2-methylphenol and pyruvate from (*R*)- and (*S*)-mecoprop by the two α-ketoglutarate-dependent dioxygenase activities, the incubations were carried out in the presence of $^{18}O_2$. As the oxygen atom of the keto group of pyruvate readily exchanges with water by the reversible formation of pyruvate hydrate (25), we fixed the incorporated ^{18}O label by the lactate dehydrogenase-catalyzed reduction of pyruvate to lactate (18). The *R*-enantiomer-specific and the *S*-enantiomer-specific activities produced identical products with identical isotope patterns. Results are shown only for the transformation of (*R*)-mecoprop by the *R*-enantiomer-specific enzyme activity (Fig. 1). 4-Chloro-2-methylphenol was isolated, derivatized, and analyzed by GC-MS. Lactate and succinate were directly analyzed by HPLC-MS. Figure 1 shows the mass spectra (segment around the signal of the molecular ion) of lactic acid (Fig. 1A and D), succinic acid (Fig. 1B and E), and the TMS derivative of 4-chloro-2-methylphenol (Fig. 1C and F) from incubations with $^{16}O_2$ from air (Fig. 1A to C) and with a one-to-one mixture of $^{16}O_2$ and $^{18}O_2$ (Fig. 1D to F). The isotope patterns unequivocally show that one atom of molecular oxygen was incorporated into lactate and succinate but that none was incorporated into 4-chloro-2-methylphenol.

Transformation of related substrates. Cell extracts from *S. herbicidovorans* MH grown on different substrates were examined for their ability to transform mecoprop and other phenoxyalkanoic acid herbicides to the corresponding phenols. The activities of the cell extracts were highly dependent on the growth substrate (Table 2). Growth on the *R* enantiomer of mecoprop effected high activity in the extract for the transformation of the *R* enantiomer of mecoprop and of the *R* enantiomer of dichlorprop. When the cells grew with (*S*)-mecoprop as the carbon and energy source, the prevalent enzyme activity in the extract was specific for the *S* enantiomers of those two herbicides. Cell extract of cells grown on complex medium also contained an enzyme activity that preferentially turned over the *S* enantiomers of mecoprop and dichlorprop. Cell extract of cells grown on 2,4-D exhibited an activity for the *S* enantiomers and did not appear to contain an activity specific for 2,4-D. This is in contrast to cell extract of *R. eutropha* JMP134 grown on 2,4-D. This extract acted on 2,4-D, MCPA, and (*S*)-dichlorprop but not on (*S*)-mecoprop. These data indicate that the two α-ketoglutarate-dependent dioxygenase activities in *S. herbicidovorans* MH are distinct from the activity of TfdA, the α-ketoglutarate-dependent dioxygenase that initiates the degradation of 2,4-D in *R. eutropha* JMP134. All cell extracts of *S. herbicidovorans* MH converted MCPA. Activities for

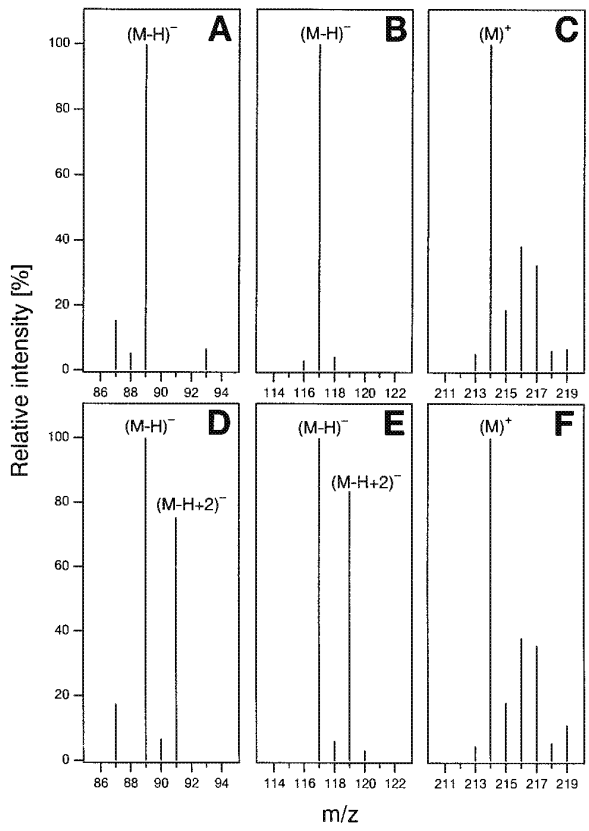


FIG. 1. Mass spectral analysis of the products from (*R*)-mecoprop and α-ketoglutarate by cell extracts of (*R*)-mecoprop-grown cells of *S. herbicidovorans* MH in the presence of $^{18}O_2$. The assay mixture contained ascorbate (1 mM), ferrous ions (100 μM), α-ketoglutarate (1 mM), NADH (1 mM), (*R*)-mecoprop (1 mM), and L-lactate dehydrogenase (1.4 U). L-Lactate dehydrogenase effected the quick conversion of the direct reaction product pyruvate to lactate necessary for trapping the ^{18}O label. Segments of the mass spectra of lactic acid (A and D), succinic acid (B and E), and the TMS derivative of 4-chloro-2-methylphenol (C and F) from incubations with $^{16}O_2$ (A to C) and with a 1:1 mixture of $^{18}O_2$ and $^{16}O_2$ (D to F) are shown.

Downloaded from http://jb.asm.org/ on September 3, 2020 by guest

COR-AAD1-00002747
Bayer EX1008 (Part 5 of 9)

TABLE 2. Enzyme activities in cell extracts of *S. herbicidovorans* MH grown on different substrates and in cell extracts of *R. eutropha* JMP134 grown on 2,4-D

Assay substrate	% Enzyme activity[a] in cell extracts of:				
	S. herbicidovorans MH grown on:				*R. eutropha* JMP134 grown on 2,4-D
	(*R*)-Mecoprop	(*S*)-Mecoprop	CM	2,4-D	
(*R*)-Mecoprop	100 (19.3)	19	20	41	0
(*S*)-Mecoprop	26	100 (25.1)	100 (42.9)	100 (24.2)	2
(*R*)-Dichlorprop	84	11	10	16	0
(*S*)-Dichlorprop	13	106	97	56	25
MCPA	10	39	29	24	73
MCPB	5	4	2	9	0
2,4-D	11	15	10	15	100 (120.7)

[a] Specific activities in nanomoles of phenolic compound produced per milligram of protein per minute are given in parentheses. CM, complex medium.

MCPA were highest in those cell extracts that were active with the *S* enantiomer of mecoprop.

Protein patterns of different cell extracts on SDS-polyacrylamide gels. The protein compositions of crude extracts of cells grown on different substrates were compared after separation of the proteins by SDS-PAGE. The cell extract from (*S*)-mecoprop-grown cells contained a large amount of a protein with a molecular mass of 32 kDa, while the predominant protein in cell extract from (*R*)-mecoprop-grown cells had a molecular mass of 34 kDa (Fig. 2). When a racemic mixture of mecoprop served as the growth substrate, both proteins were present in approximately equal amounts. A 32-kDa protein was present in cell extract from cells grown on complex medium as well as on 2,4-D. Cell extract of *R. eutropha* JMP134 showed a prominent protein band of 32 kDa on the SDS gel, as was described for TfdA (8).

DISCUSSION

S. herbicidovorans MH is able to use both enantiomers of the herbicide mecoprop as the sole source of carbon and energy. However, the enantiomers are selectively degraded, with the *S* enantiomer disappearing much faster from the culture medium than the *R* enantiomer when strain MH grows on the racemic mixture (29). The cause of the selective metabolism of the two enantiomers of mecoprop may be the presence of enantioselective enzyme activities, the presence of a specific transport system for each enantiomer, or both. The results presented in this study reveal the existence of an enantioselective initial step in the degradation of each enantiomer.

The enzyme activity of cell extracts obtained from cells grown on the pure enantiomers selectively acted on the growth enantiomer. Both enzyme activities depended on α-ketoglutarate and ferrous ions, and for both, the first intermediates were the achiral compounds 4-chloro-2-methylphenol and pyruvate. Succinate was produced from α-ketoglutarate during the course of both reactions. Experiments with $^{18}O_2$ confirmed that both enzyme activities catalyzed a dioxygenation reaction. The appearance of the ^{18}O label in pyruvate and not in phenol suggests that the oxidative cleavage of the ether bond proceeded via hydroxylation at the C-2 carbon of the propionic acid side chain. The resulting unstable intermediate could decompose to 4-chloro-2-methylphenol and pyruvate. A similar process was proposed for the oxidation of diethyl ether by the toluene 2-monooxygenase enzyme system (13). This suggestion is also consistent with a general reaction mechanism for α-ketoglutarate-dependent dioxygenases which is thought to start with the formation of a ferryl oxidant (Fe^{IV}=O) by the binding of oxygen to the iron cofactor, a process that is linked to the oxidative decarboxylation of α-ketoglutarate to succinate (6, 11, 20, 21). We therefore propose a degradation scheme based on two distinct α-ketoglutarate-dependent dioxygenases for the initial transformation of (*R*)- and (*S*)-mecoprop to 4-chloro-2-methylphenol and pyruvate (Fig. 3) by *S. herbicidovorans* MH. Both enzymes seem to share their overall chemistries with TfdA, the enzyme catalyzing the first step of the degradation of 2,4-D by *R. eutropha* JMP134 (7, 8), but not their substrate specificities (Table 2). Whereas TfdA preferentially transforms 2,4-D, the enzyme activities present in cell extracts of *S. herbicidovorans* MH specifically turned over either the *R* or the *S* enantiomers of mecoprop and of dichlorprop. They showed only small activities with 2,4-D as the substrate (Table 2).

Nevertheless, degradation of other phenoxyalkanoic acid herbicides might be effected by these enzyme activities. After growth of *S. herbicidovorans* MH on 2,4-D, we observed the presence of (*S*)-mecoprop-degrading activity in the cell extract (Table 2 and Fig. 2). Strain MH grew as fast on 2,4-D as it grew on (*S*)-mecoprop, although in such cell extracts the activity for 2,4-D was only 15% of that for (*S*)-mecoprop. A reasonable explanation for these findings is the existence of specific transport systems. We also found that the enzyme activity for the conversion of (*S*)-mecoprop was present in *S. herbicidovorans* MH when the cells grew on complex medium (Table 2 and Fig. 2) and on succinate (data not shown). This indicates that the enzyme activity specific for the *S* enantiomer is constitutively expressed. As experiments with washed-cell suspensions showed that cells grown on complex medium did not take up oxygen when they were incubated with (*S*)-mecoprop (29), we suggest the existence of an inducible transport system for (*S*)-mecoprop. After growth on (*R*)-mecoprop, the prevailing enzyme activity is specific for the *R* enantiomer (Table 2). Figure 2 clearly shows that in such cell extracts no prominent protein band that corresponds to the *S*-enantiomer-specific enzyme activity is present. We therefore conclude that the otherwise constitutively expressed *S*-enantiomer-specific enzyme activity was repressed under these conditions. A closer examination of the induction and repression processes will be necessary to

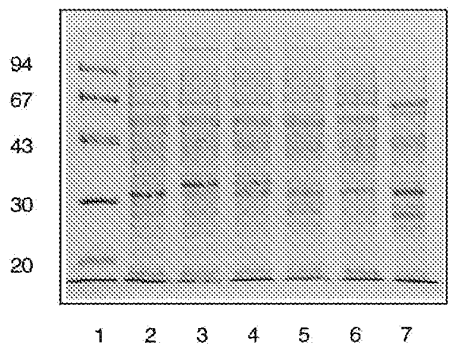


FIG. 2. SDS-PAGE of cell extracts from *S. herbicidovorans* MH grown with various growth substrates and of cell extract from *R. eutropha* JMP134 grown on 2,4-D. Lane 1, molecular mass markers (subunit sizes are given in kilodaltons on the left); lanes 2 to 6, cell extracts of *S. herbicidovorans* MH grown with (*S*)-mecoprop (lane 2), (*R*)-mecoprop (lane 3), racemic mecoprop (lane 4), complex medium (lane 5), and 2,4-D (lane 6); lane 7, cell extract of *R. eutropha* JMP134 grown on 2,4-D. Ten micrograms of protein per lane was applied.

Downloaded from http://jb.asm.org/ on September 3, 2020 by guest

COR-AAD1-00002748
Bayer EX1008 (Part 5 of 9)

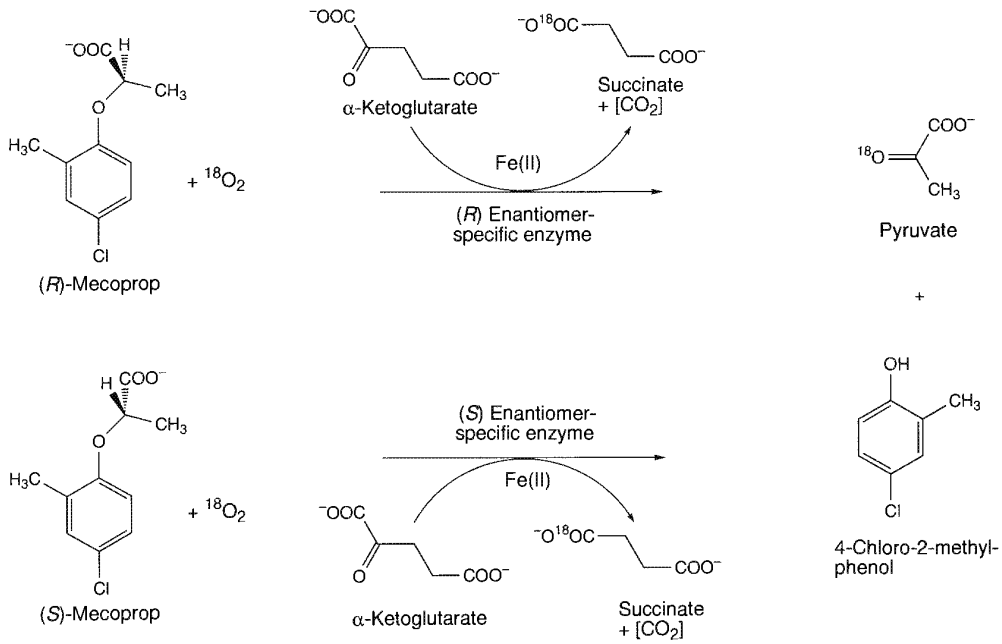


FIG. 3. Proposed scheme for the initial steps in the degradation of both enantiomers of mecoprop in *S. herbicidovorans* MH.

better understand how strain MH regulates degradation of (*R*)- and (*S*)-mecoprop.

Although the results of the experiments with cell extracts grown on different carbon sources need confirmation by additional experiments with pure enzymes, the data presented in Table 2 comprise some interesting aspects of the substrate specificities of the three proposed enzyme activities. TfdA-containing cell extract of *R. eutropha* JMP134 showed highest activity with 2,4-D followed by MCPA (73%) and (*S*)-dichlorprop (25%). This sequence is in agreement with data for purified TfdA, for which the k_{cat} values for MCPA and (*R*,*S*)-dichlorprop were 44 and 12%, respectively, of that for 2,4-D (8). However, (*S*)-mecoprop was a poor substrate of TfdA and (*R*)-dichlorprop and (*R*)-mecoprop were not substrates of TfdA at all (Table 2). Therefore, substrate specificity of TfdA seems to depend on two parts of the substrate molecule: on the aromatic moiety and on the substitution and configuration of the C-2 carbon atom of the alkanoic acid side chain. TfdA apparently accepted only 2-phenoxy-propionic acid derivatives with an *S* configuration at the C-2 carbon of the side chain. It would be very interesting to examine the kinetic parameters of purified TfdA with the pure dichlorprop enantiomers. The two mecoprop-degrading enzyme activities of *S. herbicidovorans* MH were highly active with the phenoxypropionic acid derivatives but also acted on 2,4-D (11 to 15%), MCPA (10 to 39%), and MCPB (4 to 5%). Each enzyme activity strongly depended on the substitution and the configuration at the C-2 carbon of the alkanoic acid side chain. The substitution on the aromatic part of the molecule did not seem to play such an important role in substrate specificity.

ACKNOWLEDGMENTS

This work was supported by Swiss National Science Foundation grant 21-44303.95.

We thank Christian Zipper and Christof Bolliger for providing the pure enantiomers of mecoprop and dichlorprop.

REFERENCES

1. **Ariëns, E. J.** 1989. Racemates—an impediment in the use of drugs and agrochemicals, p. 31–68. *In* A. M. Krstulovic (ed.), Chiral separations by HPLC. Ellis Horwood Ltd., Chichester, Great Britain.
2. **Armstrong, D. W., G. L. Reid, M. L. Hilton, and C.-D. Chang.** 1993. Relevance of enantiomeric separations in environmental science. Environ. Pollut. **79:**51–58.
3. **Bolliger, C.** 1996. Master's thesis. Swiss Federal Institute of Technology (ETHZ), Zurich, Switzerland.
4. **Danganan, C. E., S. Shankar, R. W. Ye, and A. M. Chakrabarty.** 1995. Substrate diversity and expression of the 2,4,5-trichlorophenoxyacetic acid oxygenase from *Burkholderia cepacia* AC1100. Appl. Environ. Microbiol. **61:**4500–4504.
5. **Daubaras, D. L., C. D. Hershberger, K. Kitano, and A. M. Chakrabarty.** 1995. Sequence analysis of a gene cluster involved in metabolism of 2,4,5-trichlorophenoxyacetic acid by *Burkholderia cepacia* AC1100. Appl. Environ. Microbiol. **61:**1279–1289.
6. **Feig, A. L., and S. J. Lippard.** 1994. Reactions of non-heme iron(II) centers with dioxygen in biology and chemistry. Chem. Rev. **94:**759–805.
7. **Fukumori, F., and R. P. Hausinger.** 1993. *Alcaligenes eutrophus* JMP134 "2,4-dichlorophenoxyacetate monooxygenase" is an α-ketoglutarate-dependent dioxygenase. J. Bacteriol. **175:**2083–2086.
8. **Fukumori, F., and R. P. Hausinger.** 1993. Purification and characterization of 2,4-dichlorophenoxyacetate/α-ketoglutarate dioxygenase. J. Biol. Chem. **268:**24311–24317.
9. **Garrison, A. W., P. Schmitt, D. Martens, and A. Kettrup.** 1996. Enantiomeric selectivity in the environmental degradation of dichlorprop as determined by high performance capillary electrophoresis. Environ. Sci. Technol. **30:**2449–2455.
10. **Häggblom, M. M.** 1992. Microbial breakdown of halogenated aromatic pesticides and related compounds. FEMS Microbiol. Rev. **103:**29–72.
11. **Hanauske-Abel, H. M., and V. Günzler.** 1982. A stereochemical concept for the catalytic mechanism of prolylhydroxylase. Applicability to classification and design of inhibitors. J. Theor. Biol. **94:**421–455.
12. **Horvath, M., G. Ditzelmüller, M. Loidl, and F. Streichsbier.** 1990. Isolation and characterization of a 2-(2,4-dichlorophenoxy)propionic acid-degrading bacterium. Appl. Microbiol. Biotechnol. **33:**213–216.
13. **Hur, H.-G., L. M. Newman, L. P. Wackett, and M. J. Sadowsky.** 1997. Toluene 2-monooxygenase-dependent growth of *Burkholderia cepacia* G4/PR1 on diethyl ether. Appl. Environ. Microbiol. **63:**1606–1609.
14. **Kelly, M. P., M. R. Heniken, and O. H. Tuovinen.** 1991. Dechlorination and spectral changes associated with bacterial degradation of 2-(2-methyl-4-chlorophenoxy)propionic acid. J. Ind. Microbiol. **7:**137–146.
15. **King, R. J., K. A. Short, and R. J. Seidler.** 1991. Assay for detection and enumeration of genetically engineered microorganisms which is based on the

Downloaded from http://jb.asm.org/ on September 3, 2020 by guest

COR-AAD1-00002749
Bayer EX1008 (Part 5 of 9)

activity of a deregulated 2,4-dichlorophenoxyacetate monooxygenase. Appl. Environ. Microbiol. **57:**1790–1792.
16. **Kohler, H. P. E., A. Schmid, and M. van der Maarel.** 1993. Metabolism of 2,2′-dihydroxybiphenyl by *Pseudomonas* sp. strain HBP1: production and consumption of 2,2′,3-trihydroxybiphenyl. J. Bacteriol. **175:**1621–1628.
17. **Loos, M. A.** 1975. Phenoxyalkanoic acids, p. 1–128. *In* P. C. Kearney and D. D. Kaufman (ed.), Herbicides. Chemistry, degradation and mode of action, 2nd ed., vol. 1. Marcel Dekker, Inc., New York, N.Y.
18. **Merkler, D. J., R. Kulathila, A. P. Consalvo, S. D. Young, and D. E. Ash.** 1992. ^{18}O isotopic ^{13}C NMR shift as proof that bifunctional peptidylglycine α-amidating enzyme is a monooxygenase. Biochemistry **31:**7282–7288.
19. **Pieper, D. H., W. Reineke, K.-H. Engesser, and H.-J. Knackmuss.** 1988. Metabolism of 2,4-dichlorophenoxyacetic acid, 4-chloro-2-methylphenoxyacetic acid and 2-methylphenoxyacetic acid by *Alcaligenes eutrophus* JMP 134. Arch. Microbiol. **150:**95–102.
20. **Prescott, A. G.** 1993. A dilemma of dioxygenases (or where biochemistry and molecular biology fail to meet). J. Exp. Bot. **44:**849–861.
21. **Roach, P. L., I. J. Clifton, V. Fülöp, K. Harlos, G. Barton, J. Hajdu, I. Andersson, C. J. Schofield, and J. E. Baldwin.** 1995. Crystal structure of isopenicillin *N* synthase is the first from a new structural family of enzymes. Nature **375:**700–704.
22. **Simoni, S., S. Klinke, C. Zipper, W. Angst, and H.-P. E. Kohler.** 1996. Enantioselective metabolism of chiral 3-phenylbutyric acid, an intermediate of linear alkylbenzene degradation, by *Rhodococcus rhodochrous* PB1. Appl. Environ. Microbiol. **62:**749–755.
23. **Smith, A. E.** 1989. Degradation, fate, and persistence of phenoxyalkanoic acid herbicides in soil. Rev. Weed Sci. **4:**1–24.
24. **Smith, A. E.** 1985. Identification of 4-chloro-2-methylphenol as a soil degradation product of ring-labelled [^{14}C]mecoprop. Bull. Environ. Contam. Toxicol. **34:**656–660.
25. **Strehlow, H.** 1962. Die Kinetik der Hydratation von α-Ketosäuren. Z. Elektrochem. **66:**392–396.
26. **Tett, V. A., A. J. Willets, and H. M. Lappin-Scott.** 1994. Enantioselective degradation of the herbicide mecoprop [2-(2-methyl-4-chlorophenoxy)propionic acid] by mixed and pure bacterial cultures. FEMS Microbiol. Ecol. **14:**191–200.
27. **Worthing, C. R., and R. J. Hance.** 1991. The pesticide manual—a world compendium, 9th ed. The British Crop Protection Council, Farnham, Great Britain.
28. **Xun, L., and K. B. Wagnon.** 1995. Purification and properties of component B of 2,4,5-trichlorophenoxyacetate oxygenase from *Pseudomonas cepacia* AC1100. Appl. Environ. Microbiol. **61:**3499–3502.
29. **Zipper, C., K. Nickel, W. Angst, and H.-P. E. Kohler.** 1996. Complete microbial degradation of both enantiomers of the chiral herbicide mecoprop [(*RS*)-2-(4-chloro-2-methylphenoxy)propionic acid] in an enantioselective manner by *Sphingomonas herbicidovorans* sp. nov. Appl. Environ. Microbiol. **62:**4318–4322.

Downloaded from http://jb.asm.org/ on September 3, 2020 by guest

COR-AAD1-00002750
Bayer EX1008 (Part 5 of 9)

Check for updates

Cloning and expression of DL-2-haloacid dehalogenase gene from *Burkholderia cepacia*

Y. Ohkouchi*, H. Koshikawa* and Y. Terashima*

*Department of Environmental Engineering, Kyoto University, Yoshida-Honmachi, Sakyo, Kyoto, Japan

Abstract *Burkholderia cepacia* strain KY, which can utilize a herbicide 2,4-D as a sole carbon and energy source, catalyzes the hydrolytic dehalogenation of both D- and L-2-haloalkanoic acids. We have cloned the gene encoding DL-2-haloacid dehalogenase, and obtained a recombinant plasmid (pUCDEXL) containing approximately 4.5 kbp insert. In both of *B. cepacia* strain KY and this clone *E. coli* JM109/pUCDEXL, DL-2-haloacid dehalogenase was induced significantly with monohalogenated acetic acids, such as chloroacetate, bromoacetate and iodoacetate. This dehalogenase was also overexpressed in *E. coli* using three different promoters. In pET vector systems with T7 *lac* promoter, a large amount of dehalogenase was selectively expressed, but some parts of the protein were accumulated in the form of inclusion bodies. This problem was overcome to carry on growth and induction at 22°C, and at the same time, the maximum specific activity of dehalogenase was reached at 12.6 U/mg, 500-fold higher activity than in wild strain, *B. cepacia* strain KY grown with 2,4-D.

Keywords Activity; cloning; 2,4-D; 2-haloacid dehalogenase; monohalogenated acetate; overexpression

Water Science and Technology Vol 42 Nos 7–8 pp 261–268 © IWA Publishing 2000

Introduction

Modern industrial and agricultural processes require the consumption of many synthetic halogenated compounds, and release them continuously as pollutants into the environment. In many cases, these xenobiotic compounds show high toxicity and persistence, and cause the contamination of soils and groundwaters. Haloaromatics such as chlorinated phenols and PCBs, and haloaliphatics such as trichloroethylene (TCE) are major pollutants. In both cases, dehalogenation step plays an important role in detoxification of these halogenated compounds. Several enzymatic dehalogenations involved in microbial degradation of halogenated compounds have been reported, and their dehalogenation mechanisms are further being investigated (Janssen *et al.*, 1994). Especially, halidehydrolases which catalyze hydrolytic dehalogenation from 2-halocarboxylic acids or haloalkane, monooxygenases which catalyze oxidative dehalogenation from halogenated phenols and TCE (Orser *et al.*, 1993; Schenk *et al.*, 1989; Wackett, 1995), and reductive dehalogenation from haloaromatics which were predominantly proceeding under anaerobic conditions (Neumann *et al.*, 1994) have been expected for application in the field of environmental engineering, cleanup and bioremediation technology. These useful enzymes are, however, generally unstable and show low productivity and activity. Therefore, it is very important to increase production of these enzymes through genetic engineering (Liu *et al.*, 1995; Widersten, 1998) for modification of catalytic function by protein engineering techniques, chemical modification (Jiang *et al.*, 1996), immobilization (Diez *et al.*, 1996), mutagenesis and so on (Asmara *et al.*, 1993; Kurihara *et al.*, 1995).

Burkholderia cepacia, named strain KY, was isolated from soil with herbicide 2,4-dichlorophenoxyacetic acid (2,4-D) as a sole carbon and energy source, in our laboratory. This strain KY can release chloride ion from 2,4-D in the degradation process (Koshikawa *et al.*, 1995). The enzyme extracted from *B. cepacia* strain KY catalyzed the hydrolytic dehalogenation of both D- and L-2- haloalkanoic acids (Reaction 1), however, not for

Downloaded from https://iwaponline.com/wst/article-pdf/42/7-8/261/29263/261.pdf
by ppv@rpdesk.com

COR-AAD1-00002751
Bayer EX1008 (Part 5 of 9)

2,4-D directly. This dehalogenating enzyme was purified and characterized, and was classified into DL-2-haloacid dehalogenase on its reaction characteristics (Ohkouchi *et al.*, 1996).

$$RCHXCOOH+OH^{-}\rightarrow RCHOHCOOH+X^{-},$$

R=H or methyl group, X=halogen atom: (Reaction 1)

In this investigation, we have isolated and cloned the structural gene encoding this DL-2-haloacid dehalogenase from *B. cepacia* strain KY, and identified the induction factors necessary to its expression in both *B. cepacia* strain KY and *E. coli*. Furthermore, to obtain more efficient expression, the overexpression systems of this DL-2-haloacid dehalogenase in *E. coli* have been constructed using three different promoters, and conditions of dehalogenase expression in these systems have been examined and optimized. We also have discussed and demonstrated the availability of these expression systems.

Materials and methods

Growth and culture conditions

Burkholderia cepacia strain KY was grown at 30°C in basic medium containing 0.1% Yeast extract, 0.5% $(NH_4)_2SO_4$, 0.1% KH_2PO_4, 0.1% $Na_2HPO_4 \cdot 12H_2O$ and 0.01% $MgSO_4$ and appropriate halogenated compounds. Recombinant *Escherichia coli* JM109 was grown at 37°C in LB medium, if necessary, ampicillin (final concentration=100 mg/L) and isopropyl-1-thio-β–D-galactoside (IPTG, final concentration=0.5 mM) was added. For *E. coli* BL21 (DE3)pLysS, LB medium was used in small scale culture (5 mL), and SB medium which is more rich than LB medium containing 0.1% Tryptone, 0.2% Yeast extract, 0.5 v/v% Glycerol, 0.13% KH_2PO_4 and 0.04% KH_2PO_4 in large scale culture (3 L) were also used to enhance cell growth.

Dehalogenase activity assay

The harvested cells were disrupted with ultrasonic homogenizer (UltraS Homogenizer VP-5S, TITEC or Vibra cell, Sonics and Materials), and the supernatant after centrifugation served as an enzyme solution. The reaction (total volume 90 µL) was carried out with 100 mM Tris-sulphate buffer (pH 9.5), 25 mM DL-2-chloropropionic acid (DL-2-CPA) as a substrate, and the enzyme solution. Enzyme reaction was stopped by adding of 10 µL of 3 M H_2SO_4. The released chloride ions were analyzed spectrophotometrically (UV-2500, Shimadzu) (Iwasaki *et al.*, 1956). One unit of dehalogenase activity was defined as the amount of enzyme that catalyzes the dehalogenation of 1-µmol of a substrate per minute. The specific activity was also defined as dehalogenase activity per 1 mg-protein. Protein was assayed by Bio-Rad Protein Asay (Bio-Rad Laboratories).

DNA manipulations

Chromosomal DNA extracted and purified from *B. cepacia* strain KY was digested with EcoRI completely. The *Eco*RI fragments were ligated with a vector pUC118 (TAKARA SHUZO, 3.2 kbp) at *Eco*RI site, and transformed into *E. coli* JM109. Transformant, which showed dehalogenase activity, was screened on LB plate containing 0.2% bromoacetate (Liu *et al.*, 1995). Recombinant plasmids were checked by 0.4% agarose gel electrophoresis. Plasmids were extracted using GFX Micro Plasmid Prep Kit (Amersham Pharmacia Biotech).

Dehalogenase expression

B. cepacia strain KY and obtained transformant were cultivated in basic medium and LB medium described above respectively, with bromoacetate (0 to 200 mg/L), and the

Downloaded from https://iwaponline.com/wst/article-pdf/42/7-8/261/29263/261.pdf
by ppv@rpdesk.com

COR-AAD1-00002752
Bayer EX1008 (Part 5 of 9)

dehalogenase activities were determined. Also in transformed *E. coli*, the effect on dehalogenase induction was examined by addition of ten halogenated compounds (1 mM) instead of bromoacetate. Chloroacetate, iodoacetate, dichloroacetate, trichloroacetate, 2-chloropropionate (2-CPA), 3-chloroacetate, 2,2-dichloroacetate, 2,3-dichloroacetate as haloaliphatic acids, and 2,4-dichlorophenol and 2,4-D as haloaromatics were used. The amount of induced dehalogenase was checked visually by SDS-PAGE.

Overexpression in *E. coli*

Preparation of insert fragments by PCR amplification. Oligonucleotide primers were designed based on the open reading frame region of known DL-2-haloacid dehalogenase from *Pseudomonas* sp. Strain 113 (Nardi-Dei *et al.*, 1997). Oligonucleotide primers were ordered and synthesized by Biologica co. The nucleotide sequences of primers used in PCR reaction are as follows. (The italic sequences indicate the recognition site of restriction enzymes added for ligation):

Forward primers: 5'-*GAATT*CGGAGGAGACACAAATGTC-3' (24mer, Italic; *Eco*RI site)

5'-*CATAT*GTCCCATCGACCGATAC-3' (22mer, Italic; *Nde*I site)

Reverse primer: 5'-*GAATTC*TCAGCCCTTCTCTGTTGG-3' (24mer, Italic; *Eco*RI site)

PCR reaction was performed on Programmable Thermal Controller with Hot Bonnet (PTC-100-60-HB, MJ Research) under mineral oil free conditions. A 50 µL reaction mixture contained 0.5µM of each designated primer, 50 ng chromosomal DNA extracted from *B. cepacia* strain KY as templates and 25 µl Premix Taq (Ex Taq version, TAKARA SHUZO). The DNA templates were first denatured at 95°C for 4 minutes. The subsequent 25 cycles consisted of a 1-min denaturation step at 94°C, a 1-min annealing step at 62°C and a 2-min primer extention step at 72°C. The amplified fragments were checked by 1.2% agarose gel electrophoresis. These fragments were digested with restriction enzymes described as below.

Construction of plasmids for dehalogenase overexpression. Three plasmids, pUC118, pKK223-3 (Amersham Pharmacia Biotech., 4.6 kbp) and pET-21a (Novagen, 5.4 kbp) were used as vectors. The PCR fragments prepared previously were digested with EcoRI for ligation to pUC118 and pKK223-3. For ligation to pET-21a, the fragments were digested with two restriction enzymes, *Nde*I and *Eco*RI. These *Eco*RI-*Eco*RI fragments were ligated with vectors, pUC118 and pKK223-3 at the *Eco*RI site, and also *Nde*I-*Eco*RI fragments were ligated with pET-21a vector at the corresponding restriction site.

Conditions for dehalogenase overexpression. For pUC and pKK vectors, *E. coli* JM109 was used as host strain for expression as well as for subcloning. Only a pET vector was transformed into *E. coli* BL21 (DE3)pLysS which carries the gene for T7 RNA polymerase for target enzyme expression. Dehalogenase was induced by addition of IPTG to a final concentration 0.5 mM. IPTG was added at culture start when dehalogenase was expressed in *E. coli* JM109, and cells were incubated at 37°C for 15 hours. On the other hand, *E. coli* BL21(DE3)pLysS was incubated until OD_{660} reached approximately 0.6 at 37, 30, 25, 22°C. Then, IPTG was added and the incubation and expression were continued. The time for the expression at each temperature was optimized experimentally. The amount of induced dehalogenase was checked visually by SDS-PAGE.

Downloaded from https://iwaponline.com/wst/article-pdf/42/7-8/261/29263/261.pdf
by ppv@rpdesk.com

COR-AAD1-00002753
Bayer EX1008 (Part 5 of 9)

Results and discussion

Cloning of 2-haloacid dehalogenase gene

In many transformant grown on LB plates containing 0.2% bromoacetate, one clone which showed the highest activity was selected. The recombinant plasmid isolated from this clone was found to contain an insert of approximately 4.5 kb-DNA. This recombinant plasmid was designated as pUCDEXL, and was shown in Figure 1. This clone showed approximately 3.5 U/mg-dehalogenase activity in the presence of 0.2% bromoacetate added for selection of dehalogenase clones. In the absence of bromoacetate, however, the dehalogenase activity was decreased to a level of 0.3 U/mg. This suggests that bromoacetate can play a role as an inducer for this DL-2-haloacid dehalogenase.

Dehalogenase expression

In both *B. cepacia* strain KY and JM109/pUCDEXL, by addition of bromoacetate to medium, dehalogenase activities were raised dramatically as shown in Figure 2. In the range of 0 to 1.0 mM, the activities were increased depending on concentration of bromoacetate. This result suggests that DL-2-haloacid dehalogenase from *B. cepacia* strain KY was inducible enzyme, which has been observed in some other dehalogenases, for example, fluoroacetate dehalogenase H-I from *Moraxella* sp. Strain B (Motosugi *et al.*, 1982), haloacid dehalogenase BhlB from *Xanthobacter autotrophicus* GJ10 (van der Ploeg *et al.*, 1995). These dehalogenases were reported as inducible enzymes with fluoroacetate and bromoacetate, respectively.

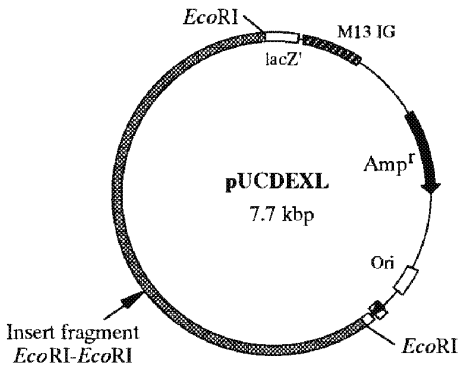


Figure 1 Structure of the recombinant plasmid, pUCDEXL for the dehalogenase expression. a pUCDEXL contained approximately 4.5 kbp insert fragment encoding DL-2-haloacid dehalogenase at *Eco*RI restriction site of pUC118

Table 1 Effect of various halogenated compounds on the dehalogenase activity in *E. coli* JM109/pUCDEXL

Halogenated compounds	Specific activity (U/mg)	Relative activity (%)
Control	0.30	100
Chloroacetate	0.65	217
Bromoacetate	1.79	597
Iodoacetate	3.10	1033
Dichloroacetate	0.35	117
Trichloroacetate	0.34	113
DL-2-Chloropropionate (2-CPA)	0.38	127
3-Chloropriopionate	0.34	113
2,2-Dichloropropionate	0.36	120
2,3-Dichloropropionate	0.25	83.3
2.,4-Dichlorophenol	N.D.	–
2,4-Dichlorophenoxy acetate (2,4-D)	0.42	140

Control: No halogenated compounds were added to LB medium.
N.D.: The cell growth was completely inhibited

Downloaded from https://iwaponline.com/wst/article-pdf/42/7-8/261/29263/261.pdf
by ppv@rpdesk.com

COR-AAD1-00002754
Bayer EX1008 (Part 5 of 9)

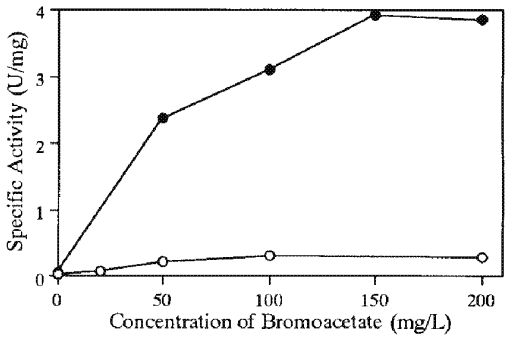


Figure 2 Effect of bromoacetate concentration on the dehalogenase activity in *B. cepacia* and *E. coli* JM109/pUCDEXL. ○: The specific activity of *B. cepacia* cultivated in basic medium. ●: The specific activity of *E. coli* JM109/pUCDEXL in LB medium containing ampicillin and IPTG. (bromoacetate 1 mM=139.0mg/L)

The effect of various halogenated compounds on dehalogenase activity in JM109/pUCDEXL was also shown in Table 1. Only monohalogenated acetates, chloroacetate, bromoacetate and iodoacetate showed significant increase in the dehalogenase activity. The wild strain *B. cepacia* strain KY was also grown with 2-CPA very well, and the dehalogenase activity was higher than that with 2,4-D (with 2,4-D, 0.025 U/mg; with 2-CPA, 0.28 U/mg). Against our expectation, however, 2-CPA could not act as dehalogenase inducer. This suggests that *B. cepacia* strain KY can catalyze the transformation of 2-CPA to chloroacetate, and dehalogenase was induced by chloroacetate accumulated in culture medium. On the other hand, *E. coli* JM109/pUCDEXL could not grow with 2-CPA as a sole carbon and energy source. So, it could not catalyze this transformation; the dehalogenase induction with 2-CPA had not occurred consequently. In the presence of 1 mM 2,4-dichlorophenol, the cell growth of JM109/pUCDEXLwas completely inhibited.

Each crude extract (15 μg-protein/each lane) was applied to SDS-PAGE, and it was found that the amount of dehalogenase increased with monohalogenated acetates (data not shown). These results demonstrate the effect of monohalogenated acetates as inducers on this dehalogenase expression. In JM109/pUCDEXL, IPTG did not function as inducer of the dehalogenase. These results also suggest that intrinsic promoter on this dehalogenase gene from *B. cepacia* strain KY regulates the dehalogenase expression instead of *lac* promoter on pUC vector.

Overexpression of dehalogenase in *E. coli*

Construction of plasmids for dehalogenase overexpression. DL-2-haloacid dehalogenase from *B. cepacia* strain KY showed a high similarity to DL-DEX 113 from *Pseudomonas* sp. Strain 113 in its enzyme characteristics and molecular weight (Motosugi *et al.*, 1982; Ohkouchi *et al.*, 1996). The PCR amplification with designed primer pairs and chromosomal DNA from *B. cepacia* strain KY as template DNA was successful. The amplified PCR fragments had length approximately 1.0 kbp. The constructed plasmids for overexpression were shown in Figure 3, which were designated pUCDEXs, pKKDEX and pETDEXa, respectively. The *lac* promoter in pUCDEXs, the *tac* promoter in pKKDEX, and the T7 *lac* promoter in pETDEXa regulate the expression of the dehalogenase, respectively. Only in pETDEXa, the ribosome-binding site on pET-21a vector was used for expression, and the initiation codon (ATG; Met) was located at *Nde*I recognition site. In pUCDEXs and pKKDEX, the sequences of ribosome-binding site and initiation codon from *B. cepacia* strain KY were contained in the insert *Eco*-RI-*Eco*RI fragments amplified by PCR. The termination codon on this dehalogenase gene, which was located on the insert fragments was used in all vector systems.

Downloaded from https://iwaponline.com/wst/article-pdf/42/7-8/261/29263/261.pdf
by ppv@rpdesk.com

COR-AAD1-00002755
Bayer EX1008 (Part 5 of 9)

Table 2 Effect of incubation and induction temperature on the dehalogenase activity in *E. coli* BL21(DE3)pLysS/pETDEXa

Temperature (°C)	Induction times (hours)	Specific activity in soluble fraction (U/mg)
37	3.0	2.64
30	5.0	4.49
25	10.0	7.47
22	12.0	12.5

Table 3 The dehalogenase expression in overexpression systems with three promoters

Vector	Promoter	Host *E. coli* strain	Inducer	Induction conditions	Specific activity (U/mg)
pUC118	*lac*	JM109	IPTG	37°C, 15hours	3.98
pKK223-3	*tac*	JM109	IPTG	37°C, 15hours	4.27
pET-21a	T7 *lac*	BL21(DE3)pLysS	IPTG	22°C, 12hours	12.6

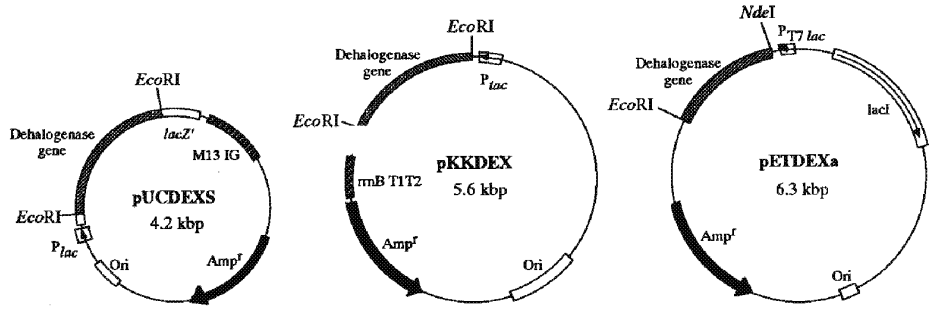


Figure 3 Physical maps of plasmids pUCDEXS, PKKDEX and pETDEXa constructed for overexpression of the dehalogenase in *E. coli*. Each plasmid contains the ampicillin resistance gene (Amp^r) and origins of replicon for *E. coli* (Ori). The dehalogenase gene was located understream of each promoter, P_{lac}, P_{tac} and $P_{T7\,lac}$

Overexpression of DL-2-haloacid dehalogenase. The dehalogenase activity in soluble fraction extracted from BL21(DE3)pLysS/pETDEXa grown at each temperature was compared in Table 2. The growth and induction at 37°C showed poor cell growth and caused decrease of dehalogenase activity. Because the amounts of dehalogenase in both soluble and insoluble fractions had not diminished dramatically in SDS-PAGE (data not shown), so many part of the producd dehalogenase seemed to be accumulated in the form of an inclusion body (Noguchi *et al.*, 1998).

The inclusion body has a merit of protein stability against proteases, but it is insoluble and biologically inactive. The reactivation of protein in the form of the inclusion body is generally difficult because it is very experimental and varies for each protein. Therefore, the dehalogenase may be transferred to the soluble fraction from the insoluble fraction. Incubation of the cells at lower temperature improved the dehalogenase specific activity in soluble fraction. Finally, when the growth and induction were carried out slowly at 22°C, the dehalogenase activity was up to 12.5 U/mg. An explanation for this could be that the speed of dehalogenase synthesis was slower and the folding of protein could proceed more completely (Ishii *et al.*, 1995).

The maximum expressions of pUCDEXs, pKKDEX and pTDEXa were compared in Table 3. The expression of pETDEXa at 22°C had reached the highest specific activity,

Downloaded from https://iwaponline.com/wst/article-pdf/42/7-8/261/29263/261.pdf
by ppv@rpdesk.com

COR-AAD1-00002756
Bayer EX1008 (Part 5 of 9)

12.6 U/mg. The measured tendency of dehalogenase activity corresponded well for the transcription ability of each promoter. In pUCDEXs and pKKDEX, the cell growth was very good. Therefore, it was expected that various protein syntheses following the cell growth were proceeding at the same time, which causes the decrease of dehalogenase specific activity.

But in pETDEXa, the cell growth was slow and poor, and the many other proteins co-existing in cells could be inhibited slightly of their synthesis. These results demonstrate that the target protein of dehalogenase was expressed selectively in *E. coli* cells. This over-expression system using a pETDEXa will become very useful for enzyme purification and further studies. In addition, it has the advantage that the product, DL-2-haloacid dehalogenase can retain natural characteristics and the structure of a wild type enzyme, because expressed dehalogenase in this pETDEXa has no tag sequences, but specific affinity purification using tag sequences cannot be applied for its purification.

Conclusions

The following conclusions were obtained in this investigation.

1. The structural gene encoding DL-2-haloacid dehalogenase from 2,4-D degrading microorganism, *B. cepacia* strain KY, has been cloned, and cloned *E. coli* showed the specific activity, approximately 3.5 U/mg.
2. This dehalogenase was induced with monohalogenated acetate in *E. coli* significantly. Bromoacetate induced the dehalogenase successfully also in *B. cepacia* strain KY.
3. Overexpression systems of DL-2-haloacid dehalogenase with three different promoters, *lac*, *tac* and T7 *lac* promoter were constructed. When the dehalogenase was expressed in *E. coli* using pETDEXa at 37°C, some parts of the dehalogenase were taken in the form of inclusion body, and as a result, the dehalogenase activity in the soluble fraction was decreased. But this phenomenon was improved to carry out growth and induction slowly at 22°C, and the maximum activity was reached at 12.6 U/mg in the pETDEXa system.

References

Asmara, W., Murdiyatmo, U., Baines, A.J., Bull, A.T. and Harman, D.J. (1993). Protein engineering of the 2-haloacid halidohydrolase IVa from *Pseudomonas cepacia* MBA4. *Biochem. J.*, **292**(Pt 1), 69–74.

Diez, A., Prieto, M.I., Alvarez, M.J., Bautista, J.M., Garrido, J. and Puyet, A. (1996). Improved catalytic performance of a 2-haloacid dehalogenase from *Azotobacter* sp. by ion-exchange immobilisation. *Biochem. Biophys. Res. Commun.*, **220**(3), 828–833.

Ishii, Y., Fujimura, T., Sasaki, H., Nuguchi, Y., Yamada, H., Niwa, M. and Shimomura, K. (1995). High-level production, chemical modification and site-directed mutagenesis of a cephalosporin Cacylase from *Pseudomonas* strain N176. *Eur. J. Biochem.*, **230**(2), 773–778.

Iwaaki, I., Utsumi, S., Hagin, K. and Ozawa, T. (1956). A new spectrophotometric method for the determination of small amount of chloride using the mercuric thiocyanate method. *Bull. Chem. Soc. Japan*, **29**(6), 860–864.

Janssen, D.B., Pries, F. and van der Ploeg, J.R. (1994). Genetics and biochemistry of dehalogenating enzymes. *Annu. Rev. Microbiol.*, **48,** 163–191.

Jiang, N., Liu, J. and Soda, K. (1996). Chemical modification of dehalogenase. *Chin. J. Biotechnol.*, **12**(3), 189–193.

Koshikawa, H., Ohkouchi, Y., Ozaki, H. and Terashima, Y. (1995). Dehalogenation catalyzed by soil bacteria utilizing organo halide herbicides. *Proc. of Environmental Engineering Research*, **32**, 121–127.

Kurihara, T., Liu, J.Q., Nardi-Dei, V., Koshikawa, H., Esaki, N. and Soda, K. (1995). Comprehensive site-directed mutagenesis of L-2-halo acid dehalogenase to probe catalytic amino acid residues. *J. Biochem. (Tokyo)*, **117**(6), 1317–1322.

Liu, J.Q., Kurihara, T., Hardi-Dei, V., Okamura, T., Esaki, N. and Soda, K. (1995). Overexpression and feasible purification of thermostable L-2-halo acid dehalogenase of *Pseudomonas* sp. YL. *Biodegradation*, **6**(3), 223–227.

Downloaded from https://iwaponline.com/wst/article-pdf/42/7-8/261/29263/261.pdf
by ppv@rpdesk.com

COR-AAD1-00002757
Bayer EX1008 (Part 5 of 9)

Motosugi, K., Esaki, N. and Soda, K. (1982). Purification and properties of a new enzyme, DL-2-haloacid dehalogenase, from *Pseudomonas* sp. *J. Bacteriol.*, **150**(2) 522–527.

Nardi-Dei, V., Kurihara, T., Park, C., Esaki, N. and Soda, K. (1997). Bacterial DL-2-haloacid dehalogenase from *Pseudomonas* sp. strain 113: gene cloning and structural comparison with D- and L-2-haloacid dehalogenases. *J. Bacteriol,* **179**(13), 4232–4238.

Neumann, A., Scholz-Muramatsu, H. and Dickert, G. (1994). Tetrachloroethene metabolism of *Dehalospirillum multivorans*. *Arch. Microbiol.*, **162**(4), 295–301.

Noguchi, Y., Yamada, H., Yamaguchi, M., Watanabe, K., Fujimura, T., Ishii, Y. and Saito, Y. (1998). An approach to high-level production of cephalosporin acylase from *Pseudomonas* strain N176 in *Escherichia coli*. *J. Ferment. Bioeng.*, **85**(6), 634–637.

Ohkouchi, Y., Koshikawa, H., Nishijima, M., Ozaki, H. and Terashima, Y. (1996). Purification and characterization of 2-haloacid dehalogenase produced by 2,4-D degrading strain. *Proc. of Environmental Engineering Research*, **33**, 185–193.

Orser, C.S., Lange, C.C., Xun, L., Zahrt, T.C. and Schenider, B.J. (1993). Cloning, sequence analysis, and expression of the *Fravobacterium* pentachlorophenol-4-monooxygenase gene in *Escherichia coli*. *J. Bacteriol.*, **175**(2), 411–416.

Schenk, T., Muller, R., Morsberger, F., Otto, M.K. and Lingens, F. (1989). Enzymatic dehalogenation of pentachlorophenol by extracts from *Arthrobacter* sp. Strain ACTCC 33790. *J. Bacteriol.*, **171**(10), 5487–5491.

van der Ploeg, J., Willemsen, M., van Hall, G. and Janssen, D.B. (1995). Adaptation of *Xanthobacter autotrophicus* GJ10 to bromoacetate due to activation and mobilization of the haloacetate dehalogenase gene by insertion element IS1247. *J. Bacteriol*, **177**(5), 1348–1356.

Wackett, L.P. (1995). Bacterial co-metabolism of halogenated organic compounds. *Microbial Transformation and Degradation of Toxic Organic Chemicals*. L.Y. Young and C.E. Cerniglia (eds.). Wiley-Liss, New York, pp. 217–241.

Widersten, M. (1998). Heterologous expression in *Escherichia coli* of soluble active-site random mutants of haloalkane dehalogenase from *Xanthobacter autotrophicus* GJ10 by coexpression of molecular chaperonins GroEL/ES. *Protein Expr. Purif*, **13**(3), 389–395.

Downloaded from https://iwaponline.com/wst/article-pdf/42/7-8/261/29263/261.pdf
by ppv@rpdesk.com

COR-AAD1-00002758
Bayer EX1008 (Part 5 of 9)

Published October, 1982

Kinetics of Microbial Decomposition of 2,4-D in Soil: Effects of Herbicide Concentration[1]

L. W. PARKER AND K. G. DOXTADER[2]

ABSTRACT

The kinetics of the degradation of (2,4-dichlorophenoxy) acetic acid (2,4-D) in Ascalon fine sandy loam (Typic Ustoll) under laboratory conditions was studied in relation to herbicide concentration to test the feasibility of employing either the first-order or Michaelis-Menten equation to model the degradation of 2,4-D. At 27°C, the herbicide degraded through two first-order reactions: an initial slow rate (slow phase) followed by a fast rate (fast phase). The first-order rate constants (k values) for the slow phase decreased as 2,4-D concentrations were increased from 1.3 to 10.2 $\mu g\ g^{-1}$ soil, and remained constant above the latter concentration. The k values for the fast phases of decomposition were independent of herbicide concentration. The duration of the slow phase increased linearly from 11 to 28 d as the herbicide concentration was increased from 1.3 to 25 $\mu g\ g^{-1}$ soil.

When 2,4-D degradation was measured during short incubation periods (instantaneous rates) to preclude growth of 2,4-D-decomposing organisms, the rates conformed to the Hane's linearization of the Michaelis-Menten equation ($r^2 = 0.93$). Apparent substrate inhibition occurred above herbicide concentrations of 40 $\mu g\ g^{-1}$ soil. Instantaneous rates were measured for soil samples previously incubated for various times with 2,4-D. Two significant peaks in activity (rate) were observed, one between concentrations of 4 and 9 $\mu g\ g^{-1}$ soil, and the other between 20 and 40 $\mu g\ g^{-1}$ soil. These data suggest the presence of two enzyme systems, differing with respect to the concentration at which substrate inhibition occurred.

Additional Index Words: **(2,4-dichlorophenoxy)acetic acid, pesticide, persistence.**

Parker, L. W., and K. G. Doxtader. 1982. Kinetics of microbial decomposition of 2,4-D in soil: effects of herbicide concentration. J. Environ. Qual. 11:679-684.

A number of studies have provided information indicating that (2,4-dichlorophenoxy)acetic acid (2,4-D) persistence in soil is affected by herbicide concentration (Mitchell and Marth, 1946; DeRose and Newman, 1947; Altom and Stritzke, 1973). Hurle (1973) observed a linear increase in the duration of the lag phase with an increase in the initial concentration of 2,4-D. The lag phase is the time after the addition of 2,4-D to soil during which no significant degradation of the herbicide is detected (Audus, 1949). Burschel and Freed (1960) analyzed results presented by Audus (1952) and concluded that after an initial lag, 2,4-D decomposition followed first-order kinetics, that is

$$-dc/dt = kc, \qquad [1]$$

where dc/dt is the change in concentration (c) with respect to time (t), and k is the first-order rate constant. Hemmett and Faust (1969) assumed 2,4-D degradation followed zero-order kinetics in aquatic systems. They incorporated initial numbers of active microorganisms into a rate equation as follows:

$$-dc/dt = k'(AM)c, \qquad [2]$$

where k' is a zero-order rate constant, AM is the initial number of activated microorganisms, and c is the herbicide concentration. In actuality, they probably observed first-order kinetics, since the rate was dependent on the concentration of 2,4-D (Hamaker, 1972).

With first-order kinetics, the concentration of herbicide affects how often collisions occur between the herbicide and a catalyst (microbial enzyme). In some cases, an equilibrium exists between herbicide and catalyst and the complex formed between the two is the reacting agent. The rate then depends on the concentration of herbicide (c) and catalyst and on the rate of complex formation (k_2). The maximum rate (k_1) would depend on the breaking of the complex to regenerate the catalyst and release the degradation products. This relationship is expressed by the hyperbolic rate equation (Hamaker, 1972):

$$-dc/dt = k_1c/(k_2 + c). \qquad [3]$$

The Michaelis-Menten rate equation has been used to model herbicide degradation (Hamaker et al., 1967; Hamaker et al., 1968; Youngson et al., 1967) as follows:

$$v = (V_{max}c)/(k_m + c), \qquad [4]$$

where v is the velocity of rate of decomposition, V_{max} is the maximum rate of decomposition for a given enzyme concentration and k_m is the half-saturation constant. Structurally, the Michaelis-Menten equation is similar to the hyperbolic rate equation. Hamaker et al. (1967) found the Michaelis-Menten equation to fit the data for picloram degradation in the laboratory but not for degradation in the field. Miekle et al. (1973), while reporting that the Michaelis-Menten rate equation fit the pattern of picloram disappearance, concluded that fractional order kinetics were more useful.

The objectives of this study were to: (i) determine the effect of herbicide concentration on degradation kinetics, (ii) test the feasibility of employing either the first-order or Michaelis-Menten equation to model the degradation of 2,4-D, and (iii) determine the response of the 2,4-D degrading enzyme systems to differing concentrations of 2,4-D.

MATERIALS AND METHODS

Degradation of 2,4-D was measured using triplicate samples of Ascalon fine sandy loam (Typic Ustoll) incubated at 0.1 bar moisture tension and temperatures of 27 or 30 ± 0.5°C in a flow-through respiration system. Carbon dioxide evolved during the decomposition of ^{14}C-carboxyl-labeled 2,4-D was trapped and its radioactivity determined using scintillation counting. Details concerning soil characteristics and analytical procedures are given in Parker and Doxtader (1983). Cumulative herbicide degradation was measured in time-

[1] Contribution of the Dep. of Agronomy, Colorado State University, Ft. Collins, CO 80523. Published with the approval of the Colorado State Exp. Stn. as Sci. Paper Ser. no. 2724. Received 21 May 1981.

[2] Research Associate/Assistant Professor, Dep. of Biology, Box 3AF, New Mexico State University, Las Cruces, NM 88003; and Associate Professor, Dep. of Agronomy, Colorado State Univ.; respectively.

COR-AAD1-00002759
Bayer EX1008 (Part 5 of 9)

Table 1—Effects of 2,4-D concentration and temperature on the slow and fast phases of decomposition.*

Temperature	2,4-D concentration	Slow phase duration	Slow phase: Decomposition rate	Slow phase: Rate constant	Fast phase: Decomposition rate	Fast phase: Rate constant
.C	$\mu g\ g^{-1}$	d	$\mu g\ g^{-1}\ d^{-1} \times 10^3$	$d^{-1} \times 10^3$	$\mu g\ g^{-1}\ d^{-1} \times 10^3$	$d^{-1} \times 10^3$
27	1.3	11 a	0.080 a	61.77 d	0.134 a	102.8 a
	2.5	13 ab	0.125 b	48.17 c	0.246 b	94.4 a
	5.1	15 b	0.157 b	30.77 b	0.364 b	71.30 a
	10.2	19 c	0.209 c	20.47 ab	0.704 c	68.98 a
	20.4	24 d	0.229 c	11.22 a	1.826 d	80.5 a
30	1.0	0 a	--	--	0.071 a	70.80 a
	2.6	0 a	--	--	0.111 a	42.97 a
	4.2	0 a	--	--	0.148 a	35.33 a
	16.8	63	0.189 c	11.25 e	--	--
	33.6	63	0.246 d	7.32 d	--	--
	67.2	63	0.091 b	1.36 b	--	--
	134.4	63	0.073 b	0.55 a	--	--

* Values followed by the same letter in a column for a given temperature are not significantly different at the 0.05 level.

course experiments. Instantaneous rates of degradation were determined using incubation times that were short enough to preclude growth of 2,4-D-decomposing organisms.

Decomposition at 27°C

Cumulative degradation was measured by incubating soil samples with up to 20.4 μg 2,4-D g^{-1} soil. First-order rate constants were calculated by the following relationships:

$$\log c = mt + b, \text{ and} \quad [5]$$

$$k = 2.303\ m, \quad [6]$$

where c is the concentration of 2,4-D remaining ($\mu g\ g^{-1}$ soil): t is time in days; b is the intercept ($\mu g\ g^{-1}$ soil); and m is the slope. Instantaneous degradation rates were measured by amending soil samples with 2,4-D; after a 24-h period that allowed soil equilibration, the CO_2 evolved was trapped for a 20-h interval.

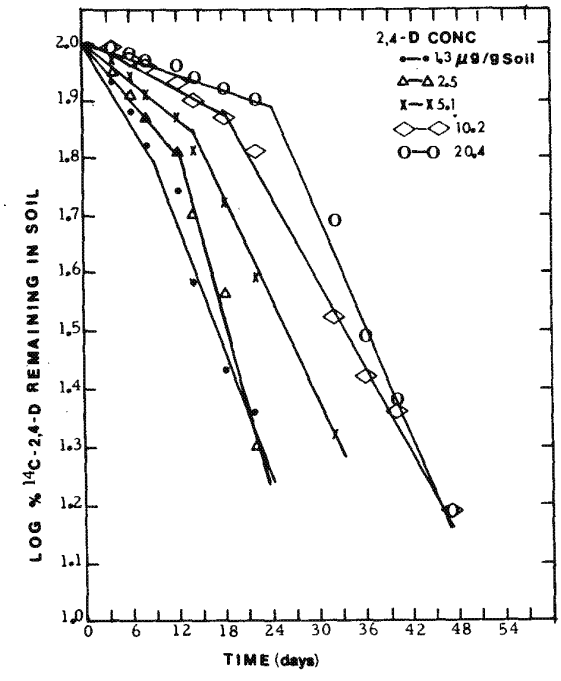


Fig. 1—Effects of initial 2,4-D concentration on the kinetics of 2,4-D decomposition at 27°C.

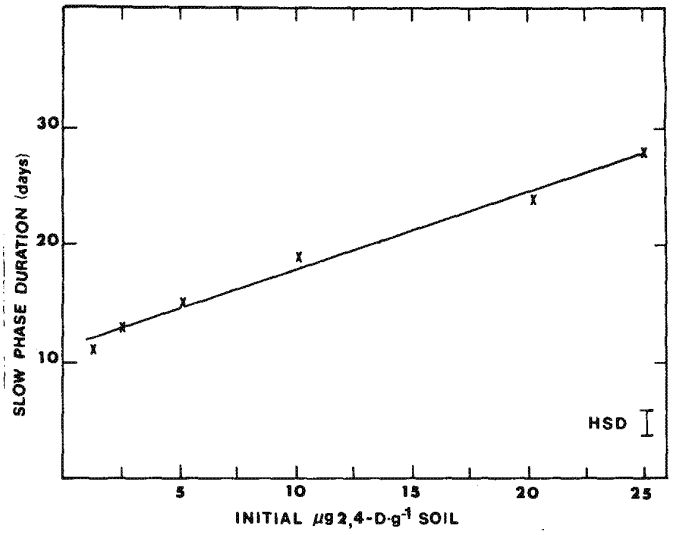


Fig. 2—Effect of initial 2,4-D concentration on length of the slow decomposition phase at 27°C.

Decomposition at 30°C

Cumulative degradation was measured by incubating soil samples with up to 134 μg 2,4-D g^{-1} soil. Instantaneous degradation rates were measured by two methods. The first method was the one used by studies at 27°C. A second method was employed to obtain instantaneous rate data at various times during the course of decomposition. Soil samples were amended with nonlabeled 2,4-D (5 $\mu g\ g^{-1}$) and, after various incubation times, were treated with varying amounts of labeled 2,4-D; $^{14}CO_2$ involved for a 6-h period was collected and assayed. The concentration of the nonlabeled 2,4-D remaining in the soil at the time of the instantaneous rate measurements was estimated from separate soil samples that had been incubated with the same concentration of 2,4-D (labeled).

Statistical Analyses

Differences between first-order rate constants, degradation rates (instantaneous), and slow-phase durations were tested by analysis of variance. When significance was observed at the $P = 0.05$ level, Tukey's Q (Honestly Significant Difference [HSD]) values were calculated for mean separation (Sokal and Rohlf, 1969). Significance between V_{max} values for the instantaneous rate data were determined by t-tests of a Hane's linearization of the data (Sokal and Rohlf, 1969).

RESULTS

Cumulative Degradation

For soils incubated at 27°C, two first-order reactions were observed for each concentration, an initial slow reaction rate followed by a more rapid one (Fig. 1). The rate of 2,4-D decomposition during the slow phase increased with increasing initial concentration (Table 1) as did the duration of the slow phase (Table 1; Fig. 2). There was no effect of the initial concentrations on the k values for the fast phase (Fig. 3). However, k values for the slow phase were reduced as 2,4-D concentration was increased.

The pattern of 2,4-D degradation at 30°C was different from that at 27°C. For 2,4-D concentrations >16.8 $\mu g\ g^{-1}$ soil, no fast phase was measured for the

COR-AAD1-00002760
Bayer EX1008 (Part 5 of 9)

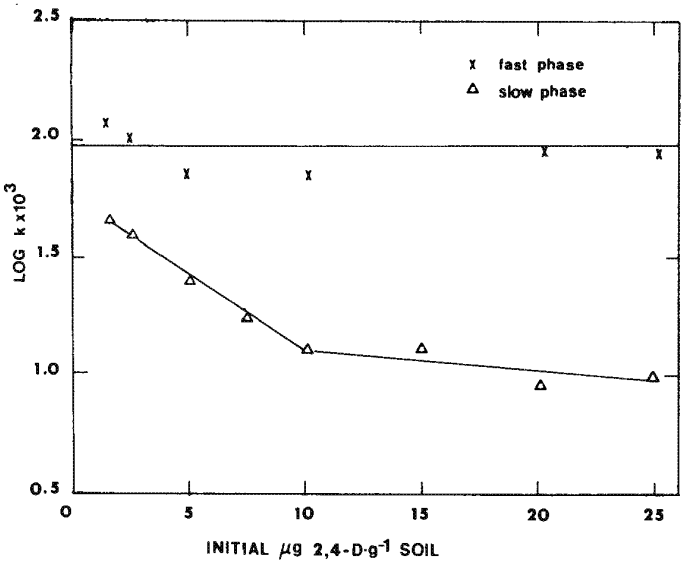


Fig. 3—Effects of the initial 2,4-D concentration on rate constant (k) values at 27°C.

duration of the experiment, and for herbicide concentrations <4.2 μg g^{-1} soil, no slow phase was observed (Table 1).

Instantaneous Degradation Rates

Degradation rates at 27 and 30°C were plotted as a function of initial substrate concentration according to a Michaelis-Menten presentation (Fig. 4). The V_{max} values for 2,4-D degradation at the two temperatures were estimated from Hanes plots in which the initial 2,4-D concentration divided by the rate of decomposition (c/v) was regressed against c. The Hanes relationship was chosen because it gives the best distribution of data along the x (concentration) axis and, therefore, provides a good estimate of slope ($1/V_{max}$) values (Cornish-Bowden, 1976). For the data collected at 27°C, a deviation from linearity occurred at 100 μg 2,4-D g^{-1} soil, so these values were not used in the calculations. The V_{max} and k_m values were 0.0128 μg 2,4-D g^{-1} soil h^{-1} and 12.3 μg 2,4-D g^{-1} soil, respectively.

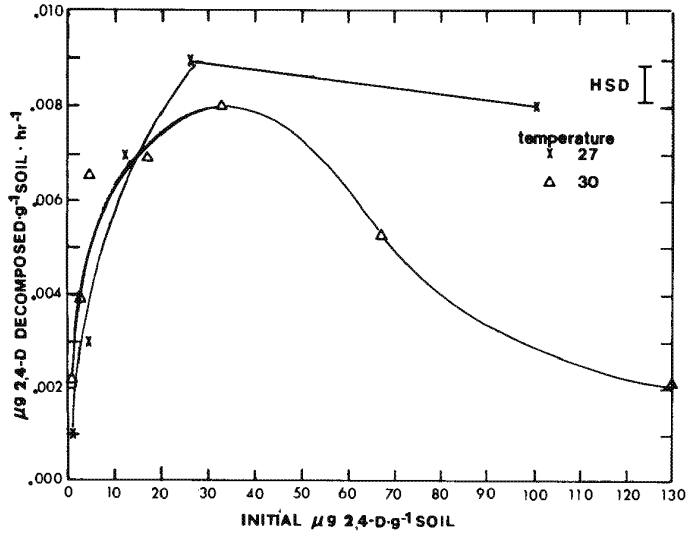


Fig. 4—Effects of initial 2,4-D concentration on rate of 2,4-D decomposition at two temperatures (2-d incubation).

The effect of herbicide concentration on degradation rates at 30°C was consistent with Michaelis-Menten kinetics for concentrations <33.6 μg g^{-1} soil (Fig. 4), with apparent substrate inhibition occurring at higher 2,4-D concentrations. Only the data for samples having less then this concentration were used for the Hanes plot. The values for V_{max} and k_m were 0.0085 μg 2,4-D g^{-1} soil h^{-1} and 2.37 μg 2,4-D g^{-1}, respectively.

The effect of 2,4-D concentration on instantaneous rates was measured at selected times during the decomposition of 5 μg 2,4-D g^{-1} soil at 30°C. A peak ($P = 0.05$) in the rate of decomposition was observed within the concentration range of 4.4–7.3 μg 2,4-D g^{-1} soil after 14, 21, and 28 d of incubation (Fig. 5). A slower degradation rate as a result of a higher 2,4-D concentration was measured following this peak in activity for the above sample dates, which on days 14 and 21 was followed by a second peak in the degradation rate as a result of increasing herbicide concentration. This second peak in activity was higher than the first peak on day 14, but was lower on sample dates 21 and 28. On day 35, there was a trend showing the first peak in activity, however, this was not significant.

If the deviations in linearity of the Hanes relationships resulting from the first peak and apparent substrate inhibition are ignored, the V_{max} and k_m values can be estimated (Table 2). These values for day 14 were higher than for day 2 (Fig. 4). Data characterizing the rapid increase in degradation for 2,4-D concentrations <10 μg g^{-1} soil were inadequate for determining possible k_m and V_{max} values.

The effects of apparent substrate inhibition on V_{max} and k_m were analyzed using nonlinear regression assuming that the first peak in activity represents one enzyme system or population and the second peak represents another population. Enzyme system 2 (the second population) was best described by the following relationship:

$$v_2 = \frac{V_{max2}c}{(k_{m2} + c)(1 + c/k_i)}, \quad [7]$$

where k_i (μg g^{-1}) is a constant for substrate inhibition, and enzyme system 2 is represented by subscript 2. Enzyme system 1, however, could not be modeled using this relationship and required the following inhibition-threshold concentration modification of the Michaelis-Menten equation to adequately predict herbicide degradation.

$$\text{If } c < c_o \text{ then } I(c - c_o) = 0 \quad [8]$$

$$v_1 = \frac{V_{max1}c}{k_{m1} + c} - I(c - c_o) \quad [9]$$

$$\text{If } v_1 < 0 \text{ then } v_1 = 0 \quad [10]$$

where c_o is the threshold concentration when inhibition first occurs, I is a constant, and enzyme system 1 is represented by subscript 1. The observed velocity is thus

COR-AAD1-00002761
Bayer EX1008 (Part 5 of 9)

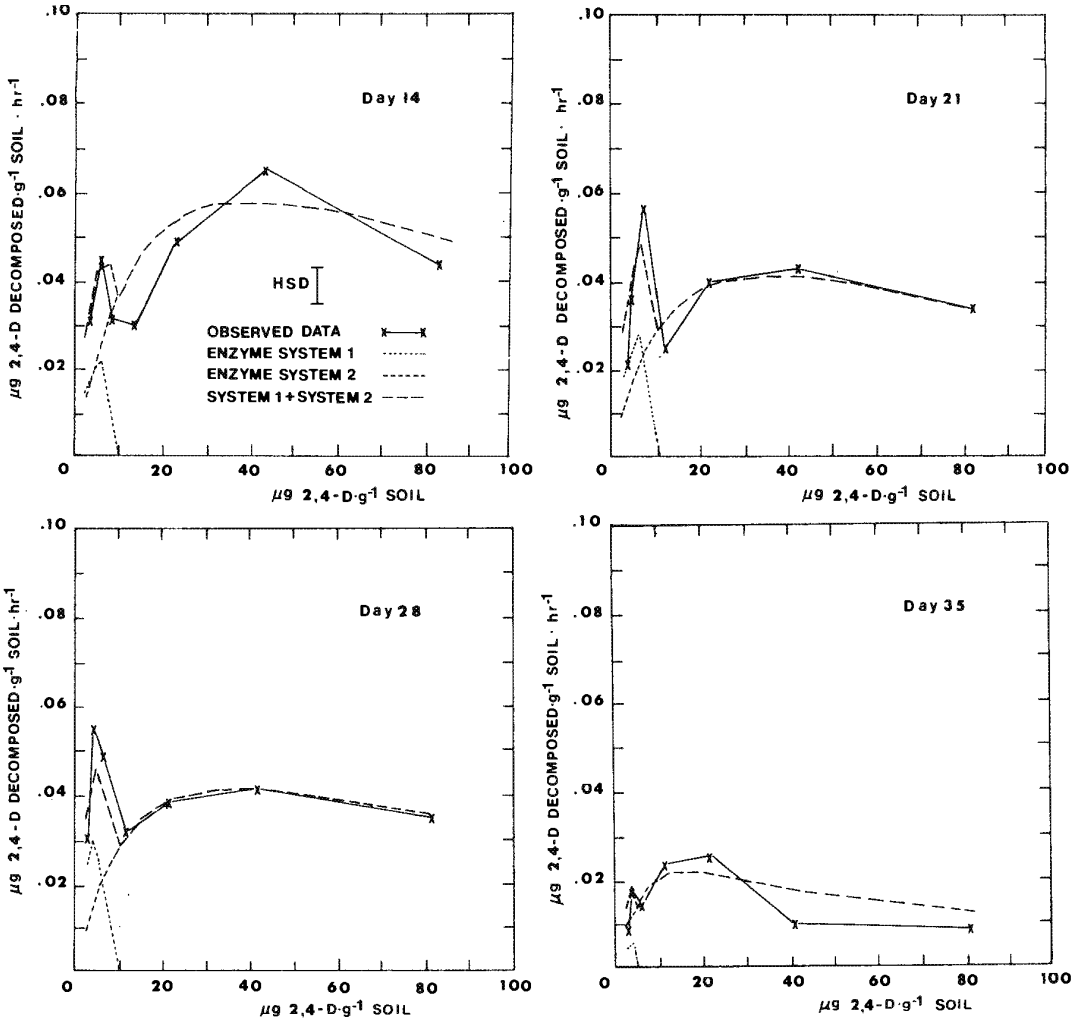


Fig. 5—Effects of 2,4-D concentration on the observed and predicted instantaneous rates of 2,4-D decomposition for soil samples previously incubated for varying times with 5 μg 2,4-D g^{-1} soil at 30°C. The r^2 values for the respective dates were 0.72, 0.78, 0.82, and 0.65.

the sum of v_1 and v_2. The model's estimates of V_{max} and k_m values are presented in Table 2 and the model's output in Fig. 5. The regression coefficients for the model are given in Fig. 5.

DISCUSSION

The instantaneous-rate data, as opposed to data from time-course studies, should be better suited for analysis in terms of classical enzyme kinetics, since the measurements were taken at short enough intervals to preclude microbial growth and enzyme production. The response to the presence of the substrate in relation to varying initial 2,4-D concentrations is described by the Michaelis-Menten equation (Eq. [4]). The Michaelis-Menten rate law functions between first- and zero-order kinetics (Williams and Williams, 1973). At low substrate concentrations relative to the k_m value, the Michaelis-Menten equation reduces to the form of a first-order reaction:

$$v = v_{max}/k_m c, \qquad [11]$$

where $k_m >>> c$.

When c is much greater than k_m, the Michaelis-Menten equation approaches a zero-order reaction:

$$v = V_{max}, \qquad [12]$$

when $c >>> km$. The rate of 2,4-D degradation at high substrate concentrations for 27°C showed a zero-order response (Fig. 4).

When applying enzyme kinetics to processes involving microbial cells in soil, caution must be taken because microorganisms are complex systems of linked reactions, and the soil is a complex physical environment composed of many microhabitats. Therefore, V_{max} and k_m values that are estimated for the degradation of organic substrates in soil are empirical and may not have the same significance as those for pure enzyme systems.

The effect of varying 2,4-D concentrations on instantaneous degradation rates was measured at various times throughout the degradation process in order to determine possible changes in the 2,4-D-degrading enzyme system(s) of the decomposer population (Fig. 4 and 5).

COR-AAD1-00002762
Bayer EX1008 (Part 5 of 9)

Table 2—The effect of substrate inhibition on the estimation of V_{max} and k_m values for 2,4-D decomposition in soil originally incubated with 5 μg 2,4-D g^{-1} soil at 30°C.*

Incubation time†	2,4-D remaining‡	With inhibition							Without inhibition	
		System 1				System 2			System 2	
		V_{max}	k_m	I	c_o	V_{max}	k_m	k_i	V_{max}	k_m
d	%	μg g^{-1} h^{-1}	μg g^{-1}		μg g^{-1}	μg g^{-1} h^{-1}	μg g^{-1}	μg g^{-1}	μg g^{-1} h^{-1}	μg g^{-1}
2	94	0.003	1.50	0.007	6	0.037	34.4	22.0	0.009 a	2.37 a
14	58	0.035	3.75	0.007	6	0.240	42.0	39.0	0.092 d	21.20 c
21	38	0.045	3.74	0.007	6	0.140	30.0	42.0	0.064 c	21.01 c
28	25	0.050	2.54	0.007	4	0.132	28.0	46.7	0.051 c	8.67 b
35	20	0.008	2.00	0.007	4	0.085	17.0	17.0	0.033 b	5.76 b

* Values followed by the same letter in a column are not significantly different at the 0.05 level.
† Days after amending soil with 5 μg 2,4-D soil.
‡ Percentage of the 5 μg 2,4-D g^{-1} soil remaining at the start of the instantaneous-rate measurement.

Evidence for the involvement of more than one type of enzyme system in 2,4-D degradation is suggested by the results of instantaneous-rate studies at 30°C. At 2,4-D concentrations > 10 μg g^{-1} soil, degradation rate data were consistent with Michaelis-Menten kinetics with apparent substrate inhibition (Fig. 5). However, at herbicide concentrations less than this value, deviations were observed (Fig. 5). The presence of these activity peaks can be explained by the presence of two enzyme systems displaying different k_m values. Equations [7-10] are a theoretical model for a mixture of two enzyme systems, one exhibiting greater affinity for 2,4-D, and thus a lower k_m value than the other. Park (1976) suggested that in nutritionally poor environments, those organisms having a low maximum specific growth rate but a high substrate affinity (k_s) may be the most successful. In the present study, organisms possessing low k_m values might have a competitive advantage over those possessing high k_m values because of the low concentrations of 2,4-D supporting the growth of the decomposer population.

Since 2,4-D decomposer activity is proportional to decomposer biomass,[3] V_{max} values are indicative of decomposer population dynamics. Enzyme system 1 or popualtion 1 did not peak until day 28, while enzyme system 2 was highest on day 14 and decreased on subsequent sample dates. This indicates a shift in the decomposer population during the decomposition process at 30°C.

A reduction in activity that occurred at 2,4-D concentrations above 40 μg g^{-1} soil for enzyme system 2 and > 10 μg g^{-1} soil for enzyme system 1 was explained in terms of substrate or product inhibition (Fig. 4 and 5). Substrate inhibition has been observed for a pseudomonad growing on 2,4-dichlorophenol in pure culture (Tyler and Finn, 1974). Reduction in 2,4-D decomposition rate due to high substrate concentration has also been observed by Ou et al. (1978). Enzyme system 1 could only be modeled by an inhibition-threshold concentration modification of the Michaelis-Menten equation. This type of inhibition has been observed for yeast on alcohols (Tseng and Wayman, 1975). Enzyme system 2 was best modeled by Eq. [7]. This modification of the Michaelis-Menten equation has been shown to be the best for describing the effects of substrate inhibition (Edwards, 1970).

The V_{max} and k_m values estimated by the model incorporating substrate inhibition were considerably higher than the V_{max} and k_m values estimated when substrate inhibition was ignored. This indicated a higher potential for 2,4-D degradation than that observed. If the decomposer population were to become adapted to the herbicide during subsequent applications higher rates would be expected as has been observed by Audus (1964).

Cumulative Decomposition at 27°C

Two first-order reactions were observed for each 2,4-D concentration. An initial slow rate (slow phase), which corresponds to the lag phase observed by Audus (1949), was followed by a rapid rate (fast phase) of herbicide disappearance. As expected for first-order reactions, the k values were independent of 2,4-D concentration above an initial 2,4-D level of 10 μg g^{-1} soil (Table 1). At lower concentrations, the k value decreased with increasing 2,4-D levels. This deviation from classical first-order kinetics could have resulted from the activity of two enzyme systems. Enzyme system 1 dominated the degradation process at low 2,4-D concentrations (< 10 μg^{-1}), while enzyme system 2 was dominant at concentrations > 10 μg g^{-1} (Fig. 5). This pseudo-first-order kinetic pattern will be referred to as first-order kinetics in the context of this discussion.

First-order rate constants are convenient for predicting the persistence of a compound in soil since the product of k and the initial concentration of the compound gives the rate at which it will be degraded under a given set of environmental conditions. However, the shift from a slow to a rapid degradation rate as a result of 2,4-D decomposer growth makes the use of one rate constant to model the degradation of this herbicide infeasible. If the shift from slow to fast phases occurred at the same time for all herbicide concentrations, then the degradation process could be modeled by two first-order equations. However, the duration of the slow phase increased linearly with increasing herbicide concentration. Therefore, the mechanisms involved in this shift must be taken into allowance. Hurle (1973) also reported a linear increase in lag time with increasing initial

[3] L. W. Parker, 1979. The kinetics of the microbial decomposition of 2,4-D in soil. Ph.D. Thesis. Colorado State University, Fort Collins (Diss. Abstr. 40/04B:181-184).

COR-AAD1-00002763
Bayer EX1008 (Part 5 of 9)

2,4-D concentration. This increase in slow-phase duration was a result of a decrease in decomposer growth at high concentrations.[3] The transition from slow to fast phase occurred when the decomposer population reached a sufficient size so that a doubling in decomposers resulted in significant increase in degradation rate.

Cumulative Degradation at 30°C

The decomposition pattern observed for soils incubated at 30°C differed from that at 27°C in two respects. At 2,4-D concentrations <5 $\mu g\ g^{-1}$ soil degradation occurred by a single fast first-order reaction while for concentrations >16 $\mu g\ g^{-1}$ soil, only a slow first-order reaction was found (Table 1). These results indicate that the 2,4-D decomposer population active at lower herbicide concentration (enzyme system 1) has an optimum temperature $\geq 30°C$, while the population active at higher 2,4-D concentrations has an optimum temperature of 27°C or less.

Applications for Modeling 2,4-D Degradation

The use of the first-order equation to describe 2,4-D degradation was satisfactory only when degradation occurred by a single first-order reaction at a particular initial concentration. Since first order rate constants were dependent on substrate concentration and there was more than one population of 2,4-D decomposers involved, the first-order equation including a function of microbial biomass would be unsatisfactory for modeling the decomposition process that sifted from a slow to fast reaction rate over a variety of herbicide concentrations.

The Michaelis-Menten equation was unsatisfactory due to the involvement of more than one enzyme system and substrate inhibition. However, two Michaelis-Menten equations incorporating substrate-inhibition functions could adequately model 2,4-D degradation when the time step was short enough to preclude growth of the active organisms. Since the shift from slow to fast phase was a function of decomposer growth,[3] relationships between decomposer population on dynamics and herbicide concentration need to be incorporated into the model to predict herbicide degradation across time.

LITERATURE CITED

1. Altom, J. D., and J. F. Stritzke. 1973. Degradation of dicamba, picloram, and four phenoxy herbicides in soils. Weed Sci. 21: 556–560.
2. Audus, L. J. 1949. The biological detoxication of 2,4-D in soil. Plant Soil 2:31–36.
3. Audus, L. J. 1952. Decomposition of 2,4-dichloraphenoxyacetic acid and 2-methyl-4-chlorophenoxy acetic acid in the soil. J. Sci. Food Agric. 3:268–279.
4. Audus, L. J. 1964. Herbicide behavior in the soil. p. 163–206. *In* L. J. Audus (ed.) The physiology and biochemistry of herbicides. Academic Press, New York.
5. Burschel, P., and V. H. Freed. 1960. The decomposition of herbicides in soils. Weeds 7:157–161.
6. Cornish-Bowden. 1976. Principles of enzyme kinetics. Butterworths, London.
7. DeRose, H. R., and A. S. Newman. 1947. Comparison of the persistence of certain plant growth-regulators when applied to soil. Soil Sci. Soc. Am. Proc. 12:222–226.
8. Edwards, V. H. 1970. The influence of high substrate concentrations on microbial kinetics. Biotechnol. Bioeng. 12:679–712.
9. Hamaker, J. W. 1972. Decomposition: quantitative aspects. p. 253–340. *In* C. A. I. Goring and J. W. Hamaker (ed.) Organic chemicals in the soil environment. Marcel-Dekker Inc., New York.
10. Hamaker, J. W., C. R. Youngson, and C. A. I. Goring. 1967. Prediction of the presistence and activity of TORDON herbicide in soils under field conditions. Down Earth 23:30–36.
11. Hamaker, J. W., C. R. Youngson, and C. A. I. Goring. 1968. Rate of detoxification of 4-amino-3,5,6-trichloropicoplinic acid in soil. Weed Res. 8:46–57.
12. Hemmett, R. B., Jr., and S. D. Faust. 1969. Biodegradation kinetics of 2,4-D by aquatic microorganisms. Residue Rev. 29: 191–207.
13. Hurle, K. 1973. Lag-phase studien mit DNOC und 2,4-D im boden. p. 151–162. *In* Proc. Symp. on Herbicides and the Soil. 1973. European Weed Research Council, Versailles, France.
14. Meikle, R.W., C. R. Youngson, R. T. Hedlund, C. A. I. Goring, J. W. Hamaker, and W. W. Addington. 1973. Measurement and prediction of picloram disappearance rates from soil. Weed Sci. 21:549–555.
15. Mitchell, J. W., and P. C. Marth. 1946. Germination of seeds in soil containing 2,4-dichlorophenoxy acetic acid. Botan. Gaz. 107: 408–416.
16. Ou, Li-Tse, D. Rothwell, W. B. Wheeler, and J. M. Davidson. 1978. The effect of high 2,4-D concentrations on degradation and carbon dioxide evolution in soils. J. Environ. Qual. 7:241–246.
17. Park, D. 1976. Carbon and nitrogen levels as factors influencing fungal decomposers. p. 41–59. *In* J. M. Anderson and A. Macfadyen (ed.) The role of terrestrial and aquatic organisms in decomposition processes. 17th Symp. of the British Ecol. Soc. Blackwell Scientific Publishing Co., Oxford.
18. Parker, L. W., and K. G. Doxtader. 1983. Kinetics of the microbial degradation of 2,4-D in soil: effects of temperature and moisture. J. Environ. Qual. Vol. 12 (in press).
19. Sokal, R. R., and F. J. Rohlf. 1969. Biometry: the principles and practices of statistics in biological research. W. H. Freeman and Co., San Francisco.
20. Tseng, M. M., and M. Wayman. 1975. Kinetics of yeast growth: inhibition-threshold substrate concentrations. Can. J. Microbiol. 21:994–1003.
21. Tyler, J. E., and R. K. Finn. 1974. Growth rates of a pseudomonad on 2,4-dichlorophenoxy acetic acid and 2,4-dichlorophenol. Appl. Microbiol. 28:181–184.
22. Williams, V. R., and H. B. Williams. 1973. Basic physical chemistry for the life sciences. W. H. Freeman and Co., San Francisco.
23. Youngson, C. R., C. A. I. Goring, R. W. Meikle, H. H. Scott, and J. D. Griffith. 1967. Factors influencing the decomposition of TORDON herbicide in soils. Down Earth 23:3–11.

COR-AAD1-00002764
Bayer EX1008 (Part 5 of 9)

Weed Science. 1987. Volume 35 (Suppl. 1):12–18

Use of *Alcaligenes eutrophus* as a Source of Genes for 2,4-D Resistance in Plants

E. J. PERKINS, C. M. STIFF, and P. F. LURQUIN[1]

Abstract. **The soil bacterium *Alcaligenes eutrophus* is able to degrade phenoxy herbicides such as 2,4-D [(2,4-dichlorophenoxy)acetic acid]. It has been shown that several degradative genes are located on a large plasmid harbored by this organism. We have demonstrated by HPLC and gas chromatography that 2,4-dichlorophenol is a major metabolite resulting from 2,4-D degradation by *A. eutrophus*. A portion of the large plasmid carrying the 2,4-D catabolic genes has been cloned and mapped by restriction endonuclease digestion. Overlapping subclones have been produced and were used in conjugation experiments in order to identify the first gene involved in 2,4-D detoxification. Once sequenced, this gene will be transferred to dicotyledonous plant cells using available vector systems.**

Additional index words. **2,4-D monooxygenase gene, plant cell transformation, gas chromatography, 2,4-dichlorophenol toxicity.**

INTRODUCTION

Phenoxy herbicides, such as 2,4-D and MCPA [(4-chloro-2-methylphenoxy)acetic acid] show high selectivity between broadleaf and grass species, enabling them to be used in the control of many broadleaf weeds in cereal and grass crops. A substituted benzoic acid such as dicamba (3,6-dichloro-2-methoxybenzoic acid) also shows high selectivity against broadleaf weeds and is used in barley (*Hordeum vulgare* L.), maize (*Zea mays* L.), oats (*Avena sativa* L.), and wheat (*Triticum aestivum* L.).

Considerable attention has been given to the possibility of generating dicotyledonous crop plants resistant to one or several of the herbicides mentioned above. If such plants could be produced, weed control in broadleaf crops would be facilitated and the effects of contamination by spraying neighboring fields would be minimized.

Various attempts to isolate mutants or variants resistant or tolerant to 2,4-D, for example, have met with limited success. Breeding herbicide-tolerant crop cultivars by conventional methods has not yet led to the production of major crops resistant to 2,4-D. Similarly, successful breeding for benzoic herbicides and MCPA resistance has not been reported (9). A few herbicide-tolerant variants have been selected in plant tissue culture (for review, see 15), but in only one case [carrot (*Daucus carota* L.) cells] did the variants stably retain the ability to tolerate 2,4-D. No resistance or tolerance to MCPA or dicamba was reported.

This absence of success is certainly due in part to our poor understanding of the molecular mechanisms involved in the metabolism (detoxification) of phenoxy acid and benzoic acid compounds in plants. It is generally assumed that benzoics, such as dicamba, are first hydroxylated and subsequently conjugated with glucose. Decarboxylation has also been reported (1). Interestingly, 5-OH dicamba was found to be nontoxic (1). In the case of 2,4-D ring hydroxylation, side chain cleavage as well as conjugation with glucose or amino acids all seem to participate in the detoxification process, whereas ring cleavage, which seems to occur in bacteria, has not been described in plants (1). Needless to say, genes coding for the above enzymatic functions has not been identified and characterized.

Another approach to the production of 2,4-D-resistant dicotyledonous plants would be to identify, clone, and transform into plant cells a bacterial gene known to code for the metabolization of 2,4-D into a less toxic compound. Genes coding for the degradation of Cba (chlorobenzoic acid), 2,4-D, and MCPA has been described in the bacteria *A. eutrophus* and was shown to be carried by a 77 kbp broad host range plasmid, pJP4, of the IncPl incompatibility group[2] (6, 10, 16). In addition, key functions involved in the degradative pathway have been identified by transposon insertion mutagenesis (7). Indeed, insertion of Tn1771 at several locations in two adjacent Hind III fragments of pJP4 inhibits either Cba degradation alone, or both Cba and 2,4-D degradation (5). This observation shows that 2,4-D and Cba are degraded via convergent pathways. Fragments of pJP4 known to be involved in 2,4-D degradation were cloned in pBR322 (recombinant designated JMP470)[2] and in pKT231 (recombinant designated pRD25)[3] and were made available to us by these authors.

Plasmid-coded bacterial degradation of 2,4-D and presumably MCPA seems to occur via cleavage of the side chain followed by ring hydroxylation and ring cleavage (10). Presumably, Cba could also be hydroxylated and subsequently cleaved. Finally, the aromatic ring is converted into succinic acid. *A. eutrophus* harboring pJP4 can use Cba, 2,4-D, or MCPA as sole carbon sources. Once a key plasmid-borne gene is identified, it will be possible to transfer it to dicotyledonous plants.

This paper reports our preliminary results on the biological effects of a major 2,4-D metabolite, 2,4-DCP (2-4 dichlorophenol), as well as the strategy used to isolate the first *Alcaligenes* gene involved in the 2,4-D degradative pathway. Finally, we will briefly describe and exemplify the strategy used to transfer a bacterial gene into a legume, cowpea [*Vigna sinensis* (L.) Walp. 'Black Eye'].

MATERIALS AND METHODS

A. eutrophus (pJP4) and *E. coli* (pJMP470) were obtained from J. M. Pemberton. *E. coli* (pRD25) was obtained from R. H. Don. The latter plasmids were subcloned into pUC9

[1] Grad. Res. Asst., Res. Assoc. and Assoc. Prof., Program in Genetics and Cell Biology, Washington State Univ., Pullman, WA 99164-4350 U.S.A.

[2] J. M. Pemberton. Personal communication.

[3] R. H. Don. Personal communication.

Downloaded from https://www.cambridge.org/core. Reprints Desk, on 04 Sep 2020 at 15:39:18, subject to the Cambridge Core terms of use, available at https://www.cambridge.org/core/terms. https://doi.org/10.1017/S0043174500060987

COR-AAD1-00002765
Bayer EX1008 (Part 5 of 9)

or pUC19 and transformed into *E. coli* JM83 using the Xgal selection system (17). Metabolization of 2,4-D by *A. eutrophus* was analyzed by HPLC using the conditions derived from Drinkwine et al. (8) and by gas chromatography and electron capture detection. Cowpea leaf fragments were transformed in vitro by inoculation with *Agrobacterium tumefaciens* C59 carrying the disarmed pGV 3850 Ti plasmid (4). An *A. tumefaciens* C58 strain with a Ti plasmid harboring the dominant selectable marker *neo* gene (kanamycin resistance) was constructed by first cloning the Eco RI cassette from pMON213 containing the *neo* gene under the control of the *nos* T-DNA promoter (11) into the single Eco RI site of the intermediate vector pLGV2385 (18). The resulting recombinant DNA was introduced into *A. tumefaciens* (pGV3850) by a triparental cross. Exconjugants carrying a recombinant Ti plasmid pGV3850/*nos-neo* were selected and one of them, *A. tumefaciens* pGV3850 K2, was used to transfer the kanamycin resistance gene to cowpea cells. Selection of transformed plant cells was performed on Murashige and Skoog medium containing 1 mg/L 2,4-D, 100 μg/ml kanamycin, and 0.2 mg/ml cefoxitin in order to kill residual *A. tumefaciens* cells (3).

HPLC conditions. The mobile phase used was HPLC grade methanol with 0.01 M KH_2PO_4:K_2HPO_4, pH 6.7, both filtered through a 0.45-μM Millipore filter. Analysis was performed with a programmed gradient, at ambient temperature, with a 0 to 10% methanol gradient over 7 min, hold 1 min, then a 10 to 40% methanol gradient over 15 min at a flow rate of 2 ml per min. Separations were performed with a Whatman Partisil PXS 10/25 00S reverse-phase column with a Rainin 5-μm reverse-phase guard column on a Beckman modular HPLC system with ultraviolet detection at 280 nm.

Gas chromatography conditions. Analysis was performed on a Perkin-Elmer Sigma 3B gas chromatograph equipped with a ^{63}Ni-electron capture detector. The column used was SPB-5 nonpolar fused silica column 0.25-μm filter, 0.25-mm internal diameter, 30 m long, with a 1-m deactivated 0.25-mm internal diameter fused silica guard column joined with a capillary butt end connector. The carrier gas was 95% argon:5% methane or helium with 95% argon:5% methane makeup gas. Samples were analyzed on a linear temperature gradient; 95 C for 4 min, 4 C per min to 250 C. Injector port temperature was 250 C and detector temperature was 350 C.

Sample analysis. HPLC analysis was performed on 1-ml overnight cultures of *E. coli* JM83 containing pJMP470 in a succinate-Luria broth liquid medium containing 100 μg/ml 2,4-D free acid. The culture was pelleted at 1000 × *g* for 5 min and washed two times with 5 ml distilled water. Washed pellets were resuspended in 1 ml distilled water. Ten milliliter cultures of *A. eutrophus* 134 containing pJP4 were grown in 2,4-D medium[2] at 29 C for approximately 48 h. The *A. eutrophus* cultures were pelleted at 1000 × *g* for 5 min and resuspended in 1 ml distilled water. Cultures were extracted as described in Guerrant et al. (12). Samples were filtered with a 0.45-μm Millipore filter before analysis.

Gas chromatographic analysis was performed on 40 ml overnight culture of *A. eutrophus* 134 harboring pJP4 at 29 C in rich media (yeast extract and bactopeptone) with 300 μg/ml 2,4-D or 2,4-D media. Cells were removed by centrifugation at 20 000 × *g* and the supernatant pH adjusted to 9 with NaOH. Samples were then extracted with two 20-ml volumes of anhydrous ether. The ether phase was dried with nitrogen gas. Dried samples were then derivatized with 100 μl bis-trimethyl silyltrifluoroacetamide and 100 μl glass-distilled pyridine in a 5-ml reaction vessel at 68 C for 20 min. Sample volume was then brought up to 5 ml with hexane and analyzed by gas chromatography.

RESULTS

Metabolization of 2,4-D by *A. eutrophus*. It has been proposed that the degradation of 2,4-D in soil bacteria proceeds first via the conversion of 2,4-D into 2,4-DCP by side chain cleavage (10). Figure 1 shows that indeed 2,4-DCP is a major metabolite produced by *A. eutrophus* JMP134 (pJP4) grown in minimal medium containing 2,4-D as sole carbon source. In fact, 2,4-DCP is excreted in large amounts into the culture medium whether the cells are grown in minimal or rich medium in the presence of 2,4-D (Figures 2 and 3). We have also observed that at a concentration of 0.3 mg/ml 2,4-DCP completely prevents growth of *A. eutrophus* JMP134 (pJP4)

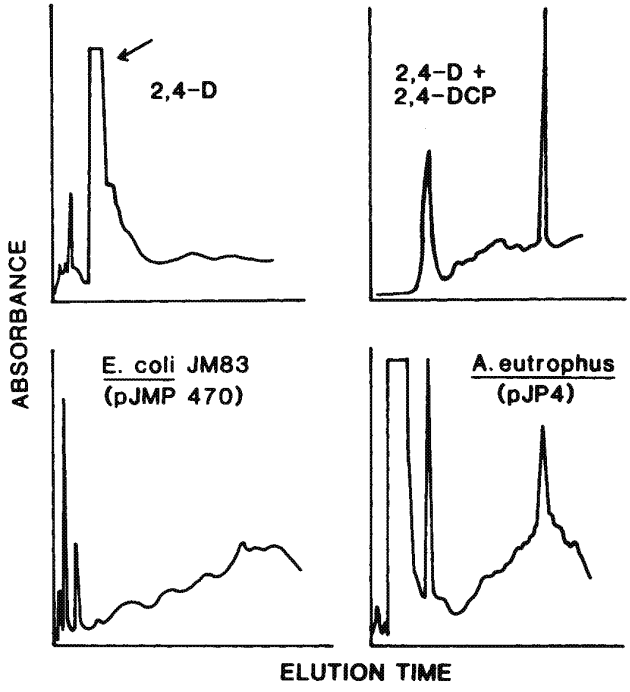


Figure 1. HPLC analysis of 2,4-D and 2,4-DCP in *E. coli* and *A. eutrophus*. Top left, 2,4-D standard; top right, 2,4-D plus 2,4-DCP standards. Bottom left, *E. coli* JM83 (pJMP470) grown in the presence of 2,4-D; bottom right, *A. eutrophus* (pJP4) grown in the presence of 2,4-D.

Downloaded from https://www.cambridge.org/core. Reprints Desk, on 04 Sep 2020 at 15:39:18, subject to the Cambridge Core terms of use, available at https://www.cambridge.org/core/terms. https://doi.org/10.1017/S0043174500060987

COR-AAD1-00002766
Bayer EX1008 (Part 5 of 9)

in rich medium. This observation strongly suggests that *A. eutrophus* possesses a system that precisely regulates the rate of uptake and degradation of 2,4-D as well as 2,4-DCP excretion. However, 2,4-DCP at 0.1 mg/ml was nontoxic. Figure 1 also shows that *E. coli* harboring pJMP470 (pBR322 containing some of the cloned 2,4-D degradation genes) does not take up 2,4-D. Similarly, *E. coli* 397 carrying pJP4 is unable to take up 2,4-D. This observation explains the failure of this *E. coli* strain to grow on 2,4-D medium (10).

Liu and Chapman (14) have reported that 2,4-DCP conversion into 2,4-dichlorocatechol is also plasmid encoded in *A. eutrophus*. This result, together with the above observa-

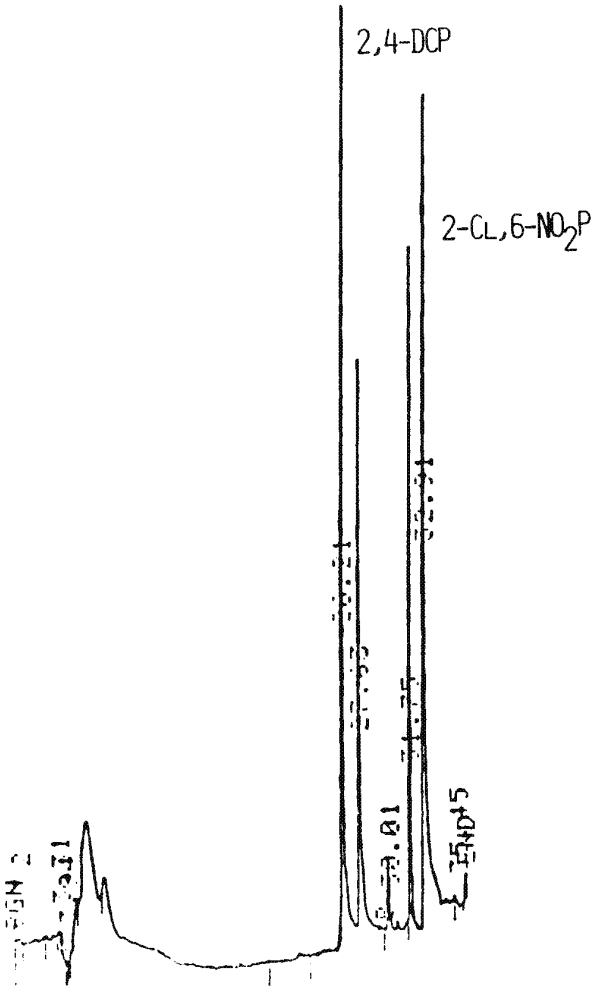


Figure 2. Gas chromatographic analysis of *A. eutrophus* minimal 2,4-D medium after bacterial growth. Labeled peaks are 2,4-DCP and the 2-chloro-6-nitrophenol internal standard. Carrier gas: 95% argon, 5% methane at 10 cm/min linear velocity; chart speed, 2 cm/min. Temperature gradient, 4 min at 95 C, 4 C/min to 200 C. Column, Supelco fused silica SPB-5, 0.25-mm internal diameter, 30 m with a 1-m guard column. Injector, 250 C; detector, 350 C.

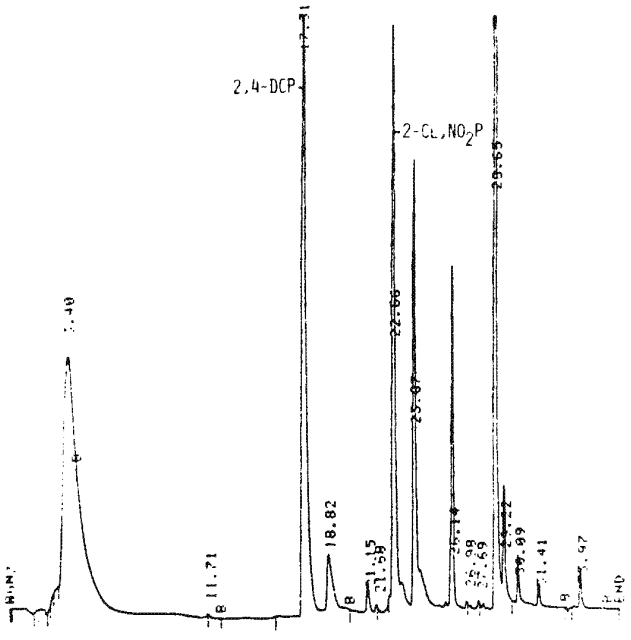


Figure 3. Gas chromatographic analysis of *A. eutrophus* rich medium with 2,4-D after bacterial growth. Labeled peaks are as in Figure 2. Carrier gas, helium at 22 cm/min linear velocity; chart speed, 5 cm/min. Other conditions as in Figure 2.

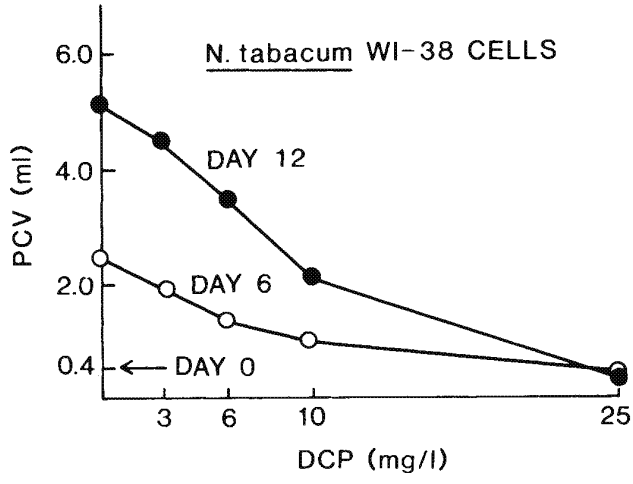


Figure 4. Growth of tobacco WI-38 cells in suspension in the presence of increasing amounts of 2,4-DCP. Arrow indicates inoculum size. Growth of cultures supplemented with 0 to 25 mg/l 2,4-DCP was followed for 16 days with samples removed for PCV measurement at 3-day intervals. For clarity, only PCV values for 0, 6, and 12 days are shown. The errors on PCV values are ± 0.1 ml for measurements up to 1 ml and ± 0.25 ml above ml.

Downloaded from https://www.cambridge.org/core. Reprints Desk, on 04 Sep 2020 at 15:39:18, subject to the Cambridge Core terms of use, available at https://www.cambridge.org/core/terms. https://doi.org/10.1017/S0043174500060587

COR-AAD1-00002767
Bayer EX1008 (Part 5 of 9)

tion, strongly suggests that, indeed, the first gene in the 2,4-D degradation pathway codes for an enzyme (a monooxygenase) which converts 2,4-D into 2,4-DCP.

Biological effects of 2,4-DCP on plants and plant cells. Assuming that the 2,4-D monooxygenase gene can be cloned from pJP4 and transferred into plant cells, it is expected that these plant cells will produce significant amounts of 2,4-DCP. Therefore, it is of paramount importance to determine 2,4-DCP toxicity levels in plant cells. Growth of tobacco (*Nicotiana tobacum* L.) WI-38 cells in suspension culture was inhibited by increasing concentration of 2,4-DCP, 50% inhibition being observed at 10 mg/L 2,4-DCP (Figure 4). We also noted that 2,4-DCP did not exercise any hormonal action at lower concentrations.

The effect of 2,4-DCP on germinating WI-38 tobacco seeds was also investigated. We observed that 2,4-DCP had

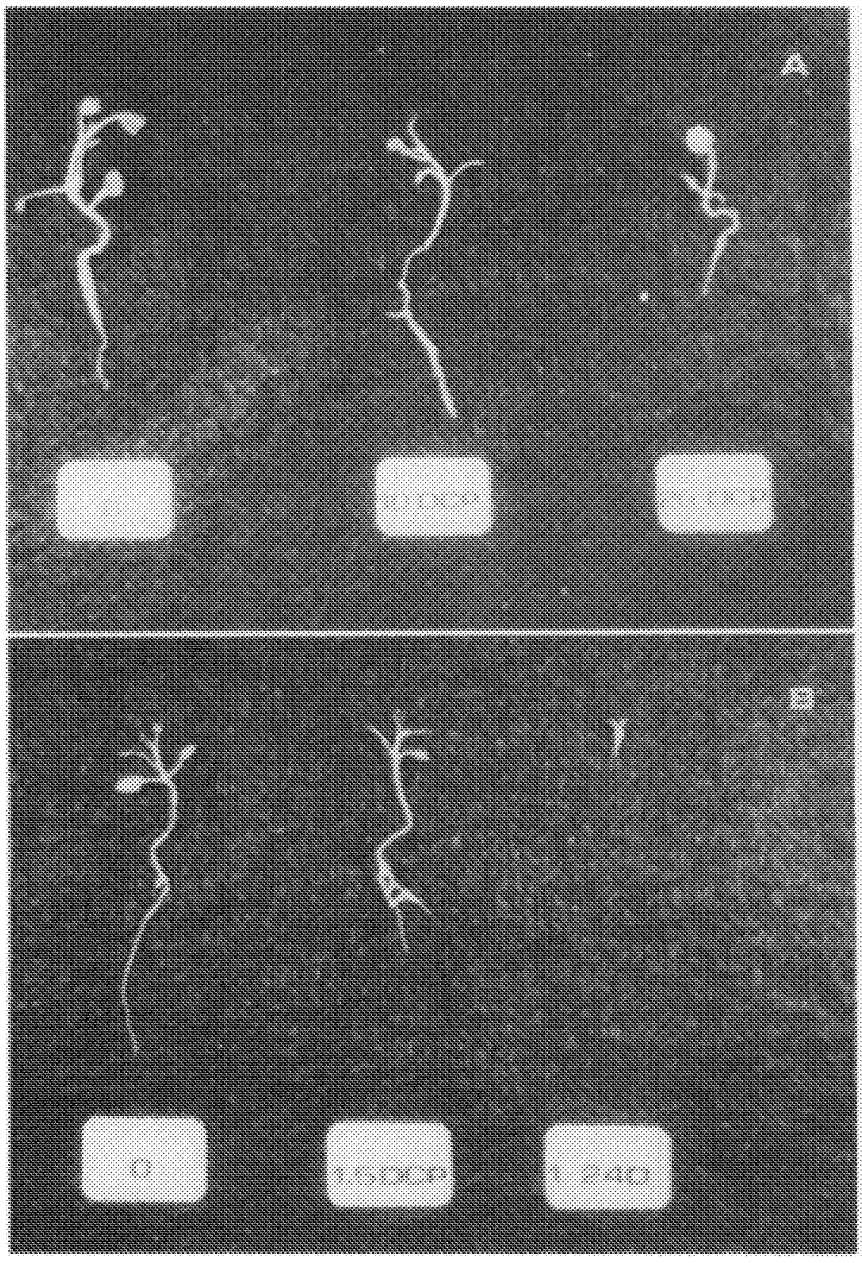


Figure 5. Effect of 2,4-D and 2,4-DCP on germinating tobacco WI-38 seeds. A. 0, control; 10, 10 mg/L 2,4-DCP; 25, 25 mg/L 2,4-DCP. B. 0, control; 1.5, 1.5 mg/L 2,4-DCP; 1, 1.0 mg/L 2,4-D.

Downloaded from https://www.cambridge.org/core. Reprints Desk, on 04 Sep 2020 at 15:39:18, subject to the Cambridge Core terms of use, available at https://www.cambridge.org/core/terms. https://doi.org/10.1017/S0043174500060587

COR-AAD1-00002768
Bayer EX1008 (Part 5 of 9)

Table 1. Tobacco WI-38 radicle and leaf length 10 days after germination as affected by either 2,4-D or 2,4-DCP[a].

2,4-D			2,4-DCP		
Concentration	Radicle	Leaf	Concentration	Radicle	Leaf
(mg/L)	(mm)		(mg/L)	(mm)	
0	24.3 ± 3.2	6.2 ± 0.6	0	23.1 ± 3.0	6.1 ± 0.6
1.0	2.1 ± 0.2	2.5 ± 0.2	1.5	24.1 ± 3.2	5.5 ± 0.5
2.0	...[b]	1.3 ± 0.1	3.0	19.3 ± 2.5	4.5 ± 0.5
4.0	...[c]	1.0 ± 0.1	10.0	19.5 ± 2.5	5.1 ± 0.5
10.0[d]	...	...	50.0[d]	...	...

[a]Data are means ± standard deviations.

[b]Rounded radicle; no measurements were made.

[c]Callus at radicle.

[d]No germination at this concentration.

a much lower toxicity than 2,4-D as measured by leaf and root development as a function of 2,4-D and 2,4-DCP concentration (Figure 5). Table 1 shows that a pronounced toxic effect of 2,4-DCP is exhibited at a concentration of 10 mg/L. A 2,4-D concentration of 1.0 mg/L virtually blocks plant development. The same results were obtained with turnip (*Brassica napus* L.) seeds (not shown). In fact, we also observed that the toxic effect of 2,4-DCP is a transient one. It appeared that 3 weeks after germination, the inhibited plantlets resumed normal growth rate. Whether this is due to detoxification of 2,4-DCP or degradation in the medium is unknown.



Figure 6. Effect of painting 2,4-DCP on cowpea primary leaves. Left, control plant; right, painted plant, 10 mg/L 2,4-DCP.

The postgermination effect of 2,4-DCP application was tested in cowpea plants. For this, cowpea primary leaves were painted twice at a 13-day interval with a solution of aqueous 2,4-DCP (10 mg/L). Application of 2,4-DCP retarded the development of trifoliate leaves compared with control (Figure 6). Here also, this effect was transient.

Germinating wheat seeds are more sensitive to 2,4-D than to 2,4-DCP (Figure 7). However, the absence of a transformation system in economically important monocots,

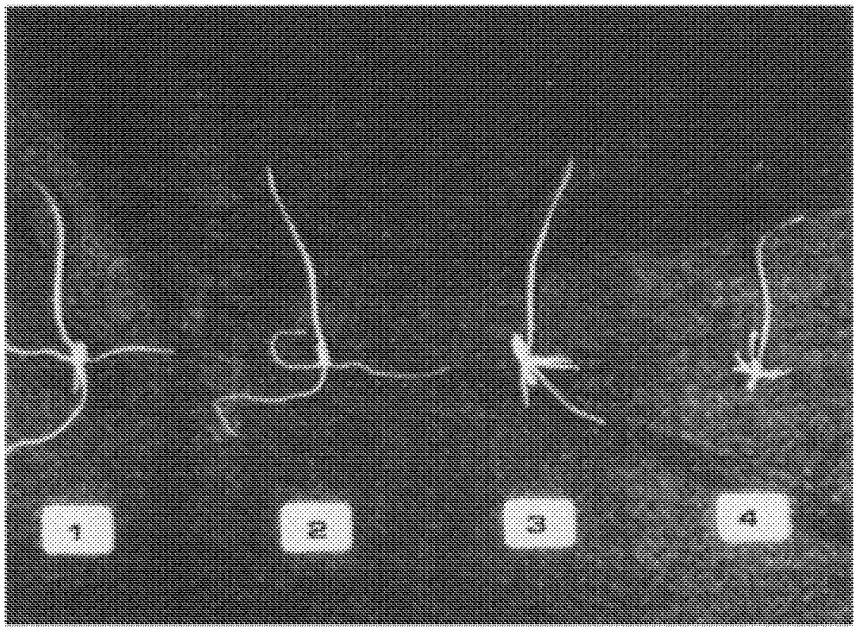


Figure 7. Effect of 2,4-DCP and 2,4-D on germinating wheat seeds: 1, control; 2, 1.5 mg/L 2,4-DCP; 3, 1.0 mg/L 2,4-D; 4, 1.5 mg/L 2,4-DCP + 1.0 mg/L 2,4-D.

Downloaded from https://www.cambridge.org/core. Reprints Desk, on 04 Sep 2020 at 15:39:18, subject to the Cambridge Core terms of use, available at https://www.cambridge.org/core/terms. https://doi.org/10.1017/S0043174500060587

COR-AAD1-00002769
Bayer EX1008 (Part 5 of 9)

with the possible exception of asparagus (*Asparagus officinalis* L.) (13), presently precludes the transfer of the 2,4-D monooxygenase gene into these plants.

Isolation of the 2,4-D monooxygenase gene. Don et al. (5) have demonstrated that the 2,4-D degradative pathway is clustered in a defined region of the *A. eutrophus* plasmid pJP4. This region has been cloned in various vectors and we have established an extensive restriction endonuclease map of these clones. In addition, we have subcloned the 2,4-D region (Figure 8). These subclones (designated pEPs) have been introduced into plasmidless *A. eutrophus* 228 rif via recloning into the wide host range mobilizable plasmid pUCD2. *A. eutrophus* exconjugants which became able to convert 2,4-D into 2,4-DCP have been identified by gas chromatography as described above. These experiments have shown that the 2,4-D monooxygenase gene is located on the subclones designated pEP109 through 111. The coding region of the 2,4-D monooxygenase gene will be identified by sequencing pEP111, and this gene will then be cloned next to a promoter recognizable by plant RNA polymerase II and transformed into plant cells as explained in the next section.

Transfer of a 2,4-D catabolic gene into plant cells. Recent progress in the knowledge of *A. tumefaciens*-mediated tumorigenesis has allowed the construction of disarmed Ti plasmids from which all oncogenes have been deleted and substituted by pBR322. Such Ti plasmids can be used to introduce foreign genes into the truncated T-DNA via homologous recombination with pBR322. It has been shown that bacterial genes under the control of an adequate promoter such as *nos* can be transferred to plant cells via T-DNA integration and are expressed in plants regenerated from these transformed cells (4).

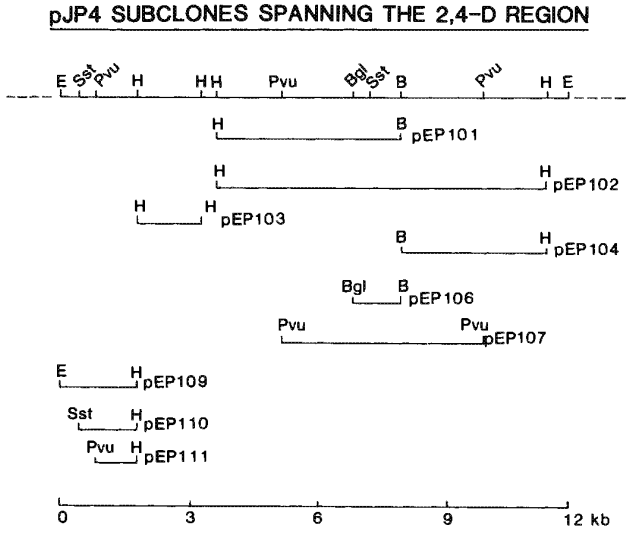


Figure 8. Map of the pJP4 2,4-D degradation region and subcloning scheme of the 2,4-D region. Top line: Eco RI fragment of pJP4 carrying the 2,4-D degradation genes. Restriction sites are as follows: E, EcoRI; Sst, Sst I; Pvu, Pvu II; H, Hind III; Bgl, Bgl II; B, Bam HI.

GENERAL STRATEGY FOR GENE TRANSFER

1. GENE A ISOLATED FROM pEP111
2. CLONE DOWNSTREAM FROM nos PROMOTER IN pLGV2385
3. CONJUGATE INTO A. TUMEFACIENS C58(pGV3850)
4. COCULTIVATE WITH LEAF DISKS
5. TEST TISSUE FOR 2,4-DCP PRODUCTION AND 2,4-D TOLERANCE

Figure 9. General strategy for the transfer of the 2,4-D monooxygenase gene (gene A) into plant cells.

The general cloning strategy is outlined in Figure 9. Briefly, a gene, preferably of known sequence, has to be cloned next to the T-DNA nopaline synthase promoter region in an intermediate vector such as pLGV2385. This molecule is then conjugated or transformed into *A. tumefaciens* pGV3850 whose T-DNA consists of the left and right borders flanking pBR322. Recombinants containing the foreign gene can then be used to infect plant cells which can in turn be used to assay for the presence and expression of this gene.

To exemplify this strategy, we have cloned an Eco RI cassette from pMON213 containing the *neo* gene under *nos* promoter control into the single Eco RI site of pLGV2385. The *nos-neo* hybrid gene has been used to confer kanamycin resistance to tobacco and petunia (*Petunia hybrida* Vilm.) cells (2, 11, 18).

After conjugation into *A. tumefaciens* pGV3850, recombinants containing this hybrid gene were selected and used to infect pieces of cowpea primary leaves in vitro. Callus cells actively proliferated on the leaf pieces infected with *A. tumefaciens* containing the *nos-neo* gene in the presence of 100 μg/ml kanamycin (Figure 10). Control leaf pieces incubated with *A. tumefaciens* pGV3850 not containing the *nos-neo* hybrid gene did not show callus cell proliferation, turned brown, and died on kanamycin-containing medium.

Once the *A. eutrophus* 2,4-D monooxygenase gene is identified and sequenced, a similar strategy will be used to transfer it into plant cells (Figure 9).

DISCUSSION

Catabolic plasmids have been shown to detoxify chemicals ranging from heavy metal salts to complex organic molecules. Thanks to the development of dicotyledonous plant transformation systems, it has become theoretically possible to transfer and express any prokaryotic gene in such plants.

Plasmid-borne genes coding for the degradation of chlorinated herbicides such as 2,4-D and MCPA have attracted attention since they offer the potential to produce herbicide-resistant plants. A prerequisite for the production of such plants is that the early degradation product(s) of 2,4-D be less toxic than 2,4-D itself. We have shown that 2,4-

Downloaded from https://www.cambridge.org/core. Reprints Desk, on 04 Sep 2020 at 15:39:18, subject to the Cambridge Core terms of use, available at https://www.cambridge.org/core/terms. https://doi.org/10.1017/S0043174500060987

COR-AAD1-00002770
Bayer EX1008 (Part 5 of 9)

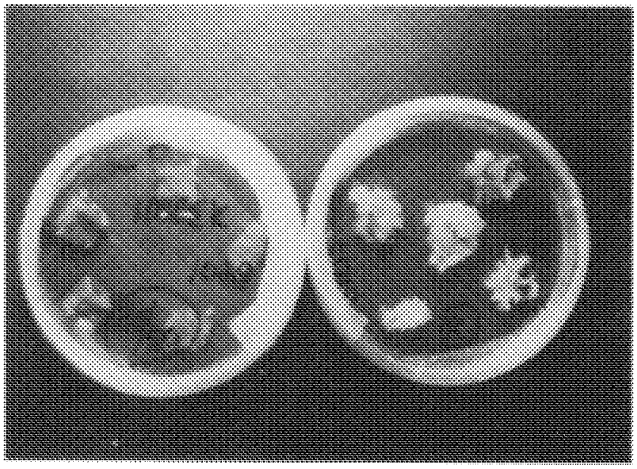


Figure 10. Result of a cocultivation experiment between cowpea primary leaf pieces and control *A. tumefaciens* pGV3850 (left) or *A. tumefaciens* pGV3850 containing a *mos-neo* hybrid gene in the T-DNA.

DCP, the first metabolite of 2,4-D in *A. eutrophus*, is indeed much less toxic than 2,4-D. Therefore, it appears justified to attempt the cloning and transfer of the 2,4-D monooxygenase gene into plants. In cases where it has been clearly demonstrated that the plant cells themselves can actively cleave the side chain of 2,4-D, it might be worthwhile to transfer the next two genes of the pathway which code for the two subunits of 2,4-DCP hydroxylase. These particular genes have been precisely mapped on the *A. eutrophus* plasmid pJP4 (5). In fact, one can even envision the transfer of all three genes into plant cells if it turned out that 2,4-dichlorocatechol was even less toxic than 2,4-DCP.

The above strategy represents an interesting alternative to the search for plant mutants resistant to chlorinated or other herbicides. Therefore, it would be of importance to search for plasmids able to degrade herbicides that do not belong to the phenoxy class.

ACKNOWLEDGMENTS

We thank Dr. A. Kleinhofs and M. Fredrickson for introducing the Eco RI *nos-neo* cassette into pLGV2835 and recombination with pGV3850. We also thank M. Young for technical assistance and Dr. E. G. Perkins for the loan of HPLC columns and advice. Supported by NSF grant DMB-8410058 and the State of Washington High Technology Center.

LITERATURE CITED

1. Ashton, F. M. and A. S. Crafts. 1981. Molecular fate of herbicides in plants. Pages 40–48 *in* Mode of Action of Herbicides. John Wiley-Interscience, New York.
2. Bevan, M. W., R. B. Flavell, and M. -D. Chilton. 1983. A chimeric antibiotic resistance gene as a selectable marker for plant cell transformation. Nature 304:184–187.
3. Christen, A. A., M. A. Kirkpatrick, and P. F. Lurquin. 1984. Antibiotics and bacterial auxotrophic mutants in the co-cultivation of plant protoplasts and bacterial cells or spheroplasts. Z. Pflanzenphysiol. 113:213–221.
4. De Block, M., L. Herrera-Estrella, M. Van Montagu, J. Schell, and P. Zambryski. 1984. Expression of foreign genes in regenerated plants and their progeny. EMBO J. 3:1681–1689.
5. Don, R. H. and J. M. Pemberton. 1985. Genetic and physical map of the 2,4-D degradative plasmid pJP4. J. Bacteriol. 161: 466–468.
6. Don, R. H. and J. M. Pemberton. 1981. Properties of six pesticide degradation plasmids isolated from *Alcaligenes eutrophus* and *Alcaligenes paradoxus*. J. Bacteriol. 145:681–686.
7. Don, R. H., A. J. Weightman, H. -J. Knackmuss, and K. N. Timmis. 1985. Transposon mutagenesis and cloning analysis of the pathways for degradation of 2,4-D and 3-Cba in *Alcaligenes eutrophus* JMP134 (pJP4). J. Bacteriol. 161:85–90.
8. Drinkwine, A. D., D. W. Bristol, and J. R. Fleeker. 1979. Separation of 2,4-D and its phenolic derivatives by reversed-phase high-performance chromatography. J. Chromatogr. 174:264–268.
9. Faulkner, J. S. 1982. Breeding herbicide-tolerant crop cultivars by conventional methods. Pages 235–256 *in* H. M. Le Baron and J. Gressel, eds. Herbicide Resistance in Plants. John Wiley and Sons, New York.
10. Fisher, P. R., J. Appleton, and J. M. Pemberton. 1978. Isolation and characterization of the pesticide-degrading plasmid pJP1 from *Alcaligenes paradoxus*. J. Bacteriol. 135:798–804.
11. Fraley, R. T., S. G. Rogers, R. Horsch, P. R. Sanders, J. S. Flick, S. P. Adams, M. L. Bittner, L. A. Brand, C. L. Fink, J. S. Fry, G. R. Galuppi, S. B. Goldberg, N. L. Hoffmann, and S. C. Woo. 1983. Expression of bacterial genes in plant cells. Proc. Nat. Acad. Sci. U.S.A. 80:4803–4807.
12. Guerrant, G. O., M. A. Lambert, and C. W. Moss. 1982. Analysis of short-chain amino acids from anaerobic bacteria by high-performance liquid chromatography. J. Clin. Microbiol. 16:355–360.
13. Hernalsteens, J. P., L. Thia-Toong, J. Schell, and M. Van Montagu. 1984. An *Agrobacterium*-transformed cell culture from the monocot *Asparagus officinalis*. EMBO J. 3:3039–3041.
14. Liu, T. and P. J. Chapman. 1984. Purification and properties of a plasmid-encoded 2,4-dichlorophenol hydroxylase. FEBS Lett. 173:314–318.
15. Meredith, C. P. and P. S. Carlson. 1982. Herbicide resistance in plant cell cultures. Pages 275–291 *in* H. M. Le Baron and J. Gressel, eds. Herbicide Resistance in Plants. John Wiley and Sons, New York.
16. Pemberton, J. M., B. Corney, and R. H. Don. 1979. Evaluation and spread of pesticide degrading ability among soil microorganisms. Pages 287–299 *in* K. N. Timmis and A. Pukler, eds. Plasmids of Medical, Environmental and Commercial Importance. North-Holland Biomedical Press.
17. Vieira, J. and J. Messing. 1982. The pUC plasmids, an M13mp7-derived system for insertion mutagenesis and sequencing with synthetic universal primers. Gene 19:259–268.
18. Zambryski, P., H. Joos, C. Genetello, M. Van Montagu, and J. Schell. 1983. Ti plasmid vector for the introduction of DNA into plant cells without alteration of their normal regeneration capacity. EMBO J. 2:2143–2150.

Downloaded from https://www.cambridge.org/core. Reprints Desk, on 04 Sep 2020 at 15:39:18, subject to the Cambridge Core terms of use, available at https://www.cambridge.org/core/terms. https://doi.org/10.1017/S0043174500060987

COR-AAD1-00002771
Bayer EX1008 (Part 5 of 9)

JOURNAL OF BACTERIOLOGY, Aug. 2002, p. 4054–4064 Vol. 184, No. 15
0021-9193/02/$04.00+0 DOI: 10.1128/JB.184.15.4054–4064.2002
Copyright © 2002, American Society for Microbiology. All Rights Reserved.

Importance of Different *tfd* Genes for Degradation of Chloroaromatics by *Ralstonia eutropha* JMP134†

Iris Plumeier,[1] Danilo Pérez-Pantoja,[2] Sabina Heim,[1] Bernardo González,[2] and Dietmar H. Pieper[1]*

Department of Environmental Biotechnology, GBF-German Research Center for Biotechnology, D-38124 Braunschweig, Germany,[1] and Departamento de Genética Molecular y Microbiología, Facultad de Ciencias Biológicas, Pontificia Universidad Católica de Chile, Santiago, Chile[2]

Received 26 December 2001/Accepted 18 March 2002

The $tfdC_ID_IE_IF_I$ and $tfdD_{II}C_{II}E_{II}F_{II}$ gene modules of plasmid pJP4 of *Ralstonia eutropha* JMP134 encode complete sets of functional enzymes for the transformation of chlorocatechols into 3-oxoadipate, which are all expressed during growth on 2,4-dichlorophenoxyacetate (2,4-D). However, activity of tfd_I-encoded enzymes was usually higher than that of tfd_{II}-encoded enzymes, both in the wild-type strain grown on 2,4-D and in 3-chlorobenzoate-grown derivatives harboring only one *tfd* gene module. The $tfdD_{II}$-encoded chloromuconate cycloisomerase exhibited special kinetic properties, with high activity against 3-chloromuconate and poor activity against 2-chloromuconate and unsubstituted muconate, thus explaining the different phenotypic behaviors of *R. eutropha* strains containing different *tfd* gene modules. The enzyme catalyzes the formation of an equilibrium between 2-chloromuconate and 5-chloro- and 2-chloromuconolactone and very inefficiently catalyzes dehalogenation to form *trans*-dienelactone as the major product, thus differing from all (chloro)muconate cycloisomerases described thus far.

Ralstonia eutropha JMP134, isolated by its capability to mineralize 2,4-dichlorophenoxyacetate (2,4-D) (7), is one of the most intensively studied chloroaromatic-degrading organisms. 2,4-D, 4-chloro-2-methylphenoxyacetate (MCPA) (37), 3-chlorobenzoate (3CB) (16), 2,4,6-trichlorophenol (4), and 4-fluorobenzoate (43) as well as various other aromatic substrates (11, 35, 37, 42) are growth substrates for this strain. The genes necessary for the metabolism of 2,4-D and MCPA are localized on a 22-kb DNA fragment of plasmid pJP4 (24). The first genes encoding enzymes involved in 2,4-D degradation, identified more than 10 years ago (8, 47), include the *tfdA* gene, encoding a 2,4-D/α-ketoglutarate dioxygenase (15), the *tfdB* gene, encoding a 2,4-dichlorophenol hydroxylase (13), and the chlorocatechol *tfdCDEF* gene cluster. Two identical regulatory genes, *tfdR* and *tfdS*, whose products belong to the LysR family of transcriptional regulators and which are positioned as inverted repeats, have been localized (18, 27), with *tfdS* being positioned divergently from *tfdA* (Fig. 1). A third putative regulator gene, *tfdT*, localized directly upstream of *tfdC*, is interrupted by insertional sequence ISJP4, which renders it inactive (25). Therefore, it has been proposed that the *tfdR* and *tfdS* genes are the master regulators, which control the activity of *tfd* genes (25). Downstream and positioned divergently from *tfdR*, an open reading frame with significant similarities to *tfdD* was observed (27), and a whole new set of *tfd* genes between *tfdR* and *tfdT* (i.e., $tfdD_{II}C_{II}E_{II}F_{II}$, $tfdB_{II}$, and *tfdK*) has recently been localized. More recently, both *tfdCDEF-B* and $tfdD_{II}C_{II}E_{II}F_{II}$-$B_{II}$, as well as *tfdA* and *tfdK*, have been shown to be expressed upon exposure to 2,4-D (24). However, the contributions of the different *tfd*-encoded enzymes to the complete metabolism of pathway intermediates have not yet been determined, nor has it been shown that all genes encode functional enzymes. Pérez-Pantoja et al. (34), by evaluating the function of the *tfdCDEF* ($tfdC_ID_IE_IF_I$ module I) and $tfdD_{II}C_{II}E_{II}F_{II}$ (module II) genes in *R. eutropha* JMP222 for growth on 3CB, have shown that both modules encode functional enzymes for chlorocatechol metabolism. Similarly, Laemmli et al. (22) reported that all genes carried by *tfd* module II code for functional enzymes. However, a low level of dienelactone (4-carboxymethylenebut-2-ene-4-olide) hydrolase activity and an even lower activity against 2-chloromuconate were observed in strains containing module II genes, whereas a very poor maleylacetate reductase activity was found in strains containing only module I (34). Therefore, despite its high similarity to genes encoding functional maleylacetate reductases (19), $tfdF_I$ has been said to encode a poor or nonfunctional enzyme. Moreover, attempts to purify maleylacetate reductase from *R. eutropha* JMP134 yielded a protein with an N-terminal sequence matching that of $TfdF_{II}$ (45), indicating a critical role of $TfdF_{II}$ for growth of strain JMP134 on 2,4-D. In addition to $TfdF_I$ and $TfdF_{II}$, yet another maleylacetate reductase was evident in strain JMP134 by the induction of such an activity during growth of pJP4-cured derivative JMP222 on 4-fluorobenzoate (43). The possibility that the low maleylacetate reductase activity observed in strain JMP222 containing module I is due to recruitment of the chromosomally encoded gene cannot, therefore, be excluded. A chromosomally encoded dienelactone hydrolase, which converts *trans*-dienelactone much faster than *cis*-dienelactone, is also present in strain JMP222 (43) and probably is responsible for the poor activity observed in strain JMP222 containing module II with *cis*-dienelactone (34). Thus, the contributions of the different *tfd* gene modules to chloroaromatic degradation in strain JMP134 are not yet clear. Interestingly, interruption of $tfdC_I$, -D_I, or -E_I

* Corresponding author. Mailing address: Bereich Mikrobiologie, AG Biodegradation, Gesellschaft für Biotechnologische Forschung mbH, Mascheroder Weg 1, D-38124 Braunschweig, Germany. Phone: 49/(0)531/6181-467. Fax: 49/(0)531/6181-411. E-mail: dpi@gbf.de

† For a commentary on this article, see page 4049 in this issue.

Downloaded from http://jb.asm.org/ on September 3, 2020 at Corteva Agriscience

COR-AAD1-00002772
Bayer EX1008 (Part 5 of 9)

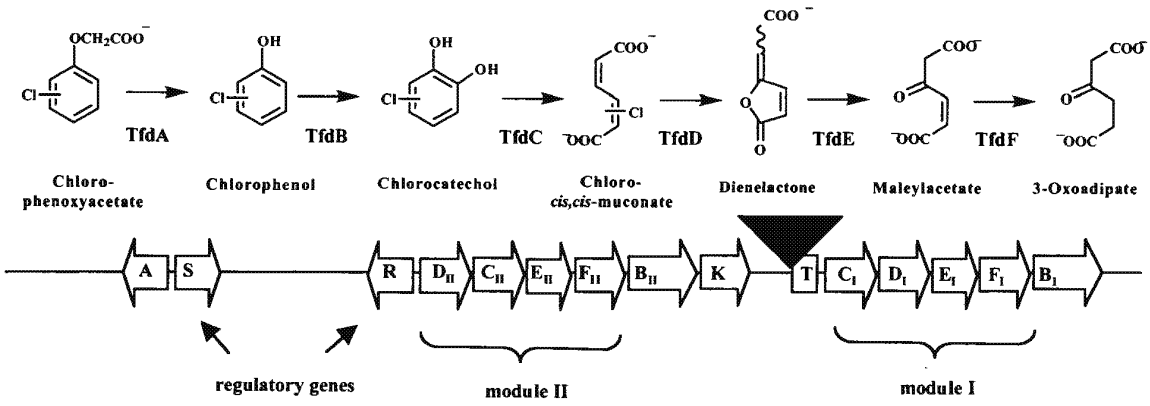


FIG. 1. Overview of genes and enzymes involved in the degradation of chloroaromatics by *R. eutropha* JMP134. The enzymes catalyzing the indicated catabolic steps are TfdA, 2,4-D/α-ketoglutarate dioxygenase, TfdB, chlorophenol hydroxylase, TfdC, chlorocatechol dioxygenase, TfdD, chloromuconate cycloisomerase, TfdE, dienelactone hydrolase, and TfdF, maleylacetate reductase. The *tfd* genes in *R. eutropha* are localized on plasmid pJP4. Arrows, orientations of the *tfd* genes described thus far; black triangle, insertion element ISJP4.

by transposon mutagenesis resulted in mutants no longer capable of growing on 2,4-D (8), suggesting that the products of these genes play a major role in the metabolism of this substrate. In contrast, interruption of $tfdF_I$ resulted in only a slight retardation of growth. The critical importance of the $tfdD_I$-encoded chloromuconate cycloisomerase is supported by the fact that diverse attempts to purify chloromuconate cycloisomerase from strain JMP134 resulted in purification of only $TfdD_I$ (17, 21). In the present investigation, the importance of the different *tfd*-encoded enzymes, chlorocatechol 1,2-dioxygenase, chloromuconate cycloisomerase, dienelactone hydrolase, and maleylacetate reductase, for growth of *R. eutropha* on chloroaromatics was characterized biochemically.

MATERIALS AND METHODS

Bacterial strains. The 2,4-D-degrading organism *R. eutropha* JMP134 was isolated by Don and Pemberton (7). *R. eutropha* JMP222 is a derivative of strain JMP134, cured of plasmid pJP4. *R. eutropha* JMP222(pBBR1M-I) and *R. eutropha* JMP222(pBBR1M-II) are derivatives of strain JMP222 containing either module I (pBBR1M-I) or module II chlorocatechol genes as described recently (34).

Culture conditions and preparation of cell extracts. Growth in liquid culture was performed in the mineral salts medium described by Dorn et al. (9) containing 50 mM phosphate buffer (pH 7.4). The medium was supplemented with a carbon source, usually at 2.5 or 5 mM. Cells were grown in fluted Erlenmeyer flasks, incubated at 30°C on a rotary shaker at 150 rpm. Growth was monitored spectrophotometrically. Harvested cells were resuspended in Tris-HCl buffer (100 mM, pH 7.5) supplemented with 2 mM $MnCl_2$ and disrupted with a French press (Aminco, Silver Spring, Md.). Cell debris was removed by centrifugation at 100,000 × *g* for 1 h at 4°C.

Enzyme assays. Muconolactone isomerase (EC 5.3.3.4) was assayed as described by Prucha et al. (40) in 50 mM sodium phosphate (pH 7.5) with 0.1 mM (4*S*,5*S*/4*R*,5*R*)-5-chloro-3-methylmuconolactone as the substrate. Accumulation of 3-methylidienelactone was analyzed spectrophotometrically at 270 nm ($\varepsilon_{3\text{-methyl }trans\text{-dienelactone}}$ = 15,200 M^{-1} cm^{-1}). Catechol 1,2-dioxygenase (EC 1.13.11.1), chlorocatechol dioxygenase, muconate cycloisomerase (EC 5.5.1.1), chloromuconate cycloisomerase (EC 5.5.1.7), and dienelactone hydrolase (EC 3.1.1.45) were measured as previously described (10, 43, 44) with catechol, 3-chlorocatechol, muconate, 3-chloromuconate, or *cis*-dienelactone as the substrate. Substrate concentrations in the enzymatic tests were usually 0.05 mM, except for catechols and substituted catechols, which were added at initial concentrations of 0.2 mM. 3-Chloromuconate, as the substrate for chloromuconate cycloisomerase, was prepared in situ from 4-chlorocatechol by using $TfdC_{II}$ that was partially purified by anion-exchange chromatography and that was free of any interfering enzyme activity. Activity of partially purified chloromuconate cycloisomerases was determined in the presence of an excess of dienelactone hydrolase. Generally, $TfdE_I$, partially purified by hydrophobic interaction chromatography and free of any interfering enzyme activity, was used. Maleylacetate reductase (EC 1.3.1.32) was measured as described by Seibert et al. (45) by using 0.05 mM maleylacetate freshly prepared by alkaline hydrolysis of *cis*-dienelactone or through transformation by $TfdE_I$ partially purified by hydrophobic-interaction chromatography. For determination of the kinetic properties of $TfdD_{II}$, the formation of *cis*-dienelactone was recorded at 305 nm. A reaction coefficient of 5,300 M^{-1} cm^{-1} was calculated after complete transformation of 3-chloromuconate (20 to 50 μM) into *cis*-dienelactone.

Specific activities are expressed as micromoles of substrate converted or product formed per minute per gram of protein at 25°C. Protein concentrations were determined by the Bradford procedure (2).

Chromatographic separation of enzyme activities. Cells were harvested during late-exponential growth, and the cell extract (usually containing between 8 and 20 mg of protein per ml) was applied directly to a MonoQ HR5/5 column (Amersham Pharmacia Biotech) or mixed with an equal volume of 2 M $(NH_4)_2SO_4$ and, after centrifugation, applied to a phenyl-Superose HR5/5 column (Amersham Biosciences, Freiburg, Germany). At least three independent experiments were performed for each type of growth condition to verify the reproducibility of the method. Elution of the respective activities was highly reproducible and varied between independent experiments by only ±1 fraction, which corresponds to differences of 0.01 M NaCl or 0.02 M $(NH_4)_2SO_4$. Proteins were eluted from the MonoQ HR5/5 column by a linear gradient of NaCl (0 to 0.5 M) in Tris-HCl (50 mM, pH 7.5, supplemented with 2 mM $MnCl_2$) in a total volume of 25 ml or by a stepwise gradient of 0 to 0.14 M over 2 ml, 0.14 to 0.29 M over 17 ml, and 0.25 to 0.5 M over 6 ml. Proteins were eluted from the phenyl-Superose HR5/5 column by a linear gradient of $(NH_4)_2SO_4$ (1 to 0 M) in Tris-HCl (50 mM, pH 7.5, supplemented with 2 mM $MnCl_2$) over 25 ml or by a stepwise gradient of 1 to 0.8 M over 2 ml, 0.8 to 0.5 M over 8 ml, 0.5 to 0.3 M over 2 ml, 0.3 to 0.2 M over 6 ml, and 0.2 to 0 M over 10 ml. For chromatographic separation of maleylacetate reductases, proteins were eluted from the MonoQ HR5/5 column by the gradients described above, with Tris-HCl buffer exchanged for phosphate buffer. The flow rate was always 1 ml/min, and the fraction volume was 0.5 ml. Partial purification of $TfdD_{II}$ was achieved by successive separation using hydrophobic interaction and gel filtration. The two fractions from the phenyl-Superose HR5/5 chromatography containing the most $TfdD_{II}$ activity were pooled, concentrated by ultrafiltration to a final volume of 0.5 ml, applied to a Superose 12 column (HR10/30) (Amersham Biosciences), and eluted with 50 mM Tris-HCl, pH 7.5, at a flow rate of 0.3 ml/min (fraction volume, 0.5 ml). Similarly, fractions from MonoQ HR5/5 chromatography containing TfdFI activity were pooled, concentrated, and subjected to gel filtration.

Electrophoretic methods. Sodium dodecyl sulfate-polyacrylamide gel electrophoresis (SDS-PAGE) was performed on a Bio-Rad Miniprotein II essentially as described by Laemmli (23). The acrylamide concentrations for the concentrating and separating gels were 5 and 10% (wt/vol), respectively. The proteins were

Downloaded from http://jb.asm.org/ on September 3, 2020 at Corteva Agriscience

COR-AAD1-00002773
Bayer EX1008 (Part 5 of 9)

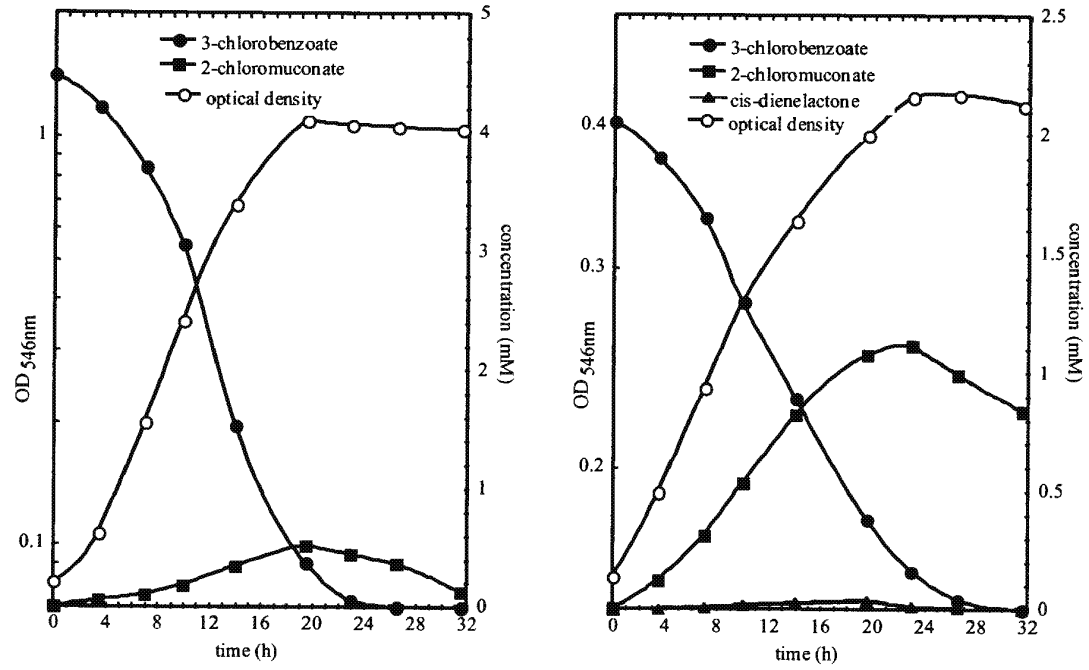


FIG. 2. Growth of *R. eutropha* JMP222(pBBR1M-I) (left) and *R. eutropha* JMP222(pBBR1M-II) (right) on 3CB. Substrate depletion and product formation were monitored by HPLC.

stained by Coomassie brilliant blue R250. Molecular mass standards (Bio-Rad, Munich, Germany) were lysozyme (14.4 kDa), trypsin inhibitor (21.5 kDa), carbonic anhydrase (31.0 kDa), albumin (45.0 kDa), bovine serum albumin (66.2 kDa), and phosphorylase b (97.4 kDa). For quantification of $TfdD_{II}$ in partially purified fractions, gels were stained with the fluorescent dye Sypro Ruby (Molecular Probes Inc., MoBiTec GmbH, Göttingen, Germany). Gels were scanned with a Fujifilm LAS-1000 charge-coupled device camera. The relative amount of the $TfdD_{II}$ protein band was determined with the AIDA, version 2.1, software package (Raytest Isotopenmessgeräte GmbH, Straubenhardt, Germany).

For two-dimensional gel electrophoresis, a 250-μl aliquot of a $TfdF_I$-containing fraction obtained by anion-exchange chromatography was precipitated with 10% trichloroacetic acid, and then the precipitate was washed with ice-cold acetone. The protein was dissolved in 300 μl of reswelling solution containing 7.4 M urea, 2 M thiourea, 4% CHAPS (3-[{3-cholamidopropyl}dimethylammonio]-1-propanesulfonate), 20 mM Tris base, 30 mM dithiothreitol (DTT), one-half tablet of protease inhibitor (MiniComplete; Roche Applied Biosciences, Mannheim, Germany), 5% IPG buffer, pH 4 to 7 (Amersham Biosciences) and applied to isoelectric focusing (IEF) ReadyStrips (Bio-Rad). After 100 kV · h focusing time in the first dimension (IEF), the gel strip was equilibrated for the second dimension (SDS-PAGE) twice for 15 min by using 5 ml of equilibration solution consisting of 6 M urea, 30% glycerol, 2% SDS, 0.06 mM bromophenol blue, 50 mM Tris base, pH 8.8, 65 mM DTT, and 260 mM iodoacetamide. The strip was applied then to an SDS–10 to 15% PAGE gel (1.5 mm thick) and developed overnight in an IsoDALT chamber (Amersham Biosciences).

N-terminal amino acid sequencing. Proteins were electroblotted onto a polyvinylidene difluoride membrane, and the membrane was stained with Coomassie brilliant blue R250. N-terminal amino acid sequencing was performed with an Applied Biosystems model 494A Procise HT sequencer.

Analytical methods. High-performance liquid chromatography (HPLC) of low-molecular-weight compounds was performed with a Lichrospher SC 100 RP8 reverse-phase column (125 by 4.6 mm; Bishoff, Leonberg, Germany). Methanol-H_2O containing 0.1% (vol/vol) H_3PO_4 was used as the eluant at a flow rate of 1 ml/min. The column effluent was monitored simultaneously at 210, 260, and 270 nm by a diode array detector (Shimadzu). Typical retention volumes using 25% (vol/vol) methanol were 7.7 (2-chloro-*cis,cis*-muconate), 2.5 (2-chloromuconolactone), 1.1 (5-chloromuconolactone), 4.1 (*cis*-dienelactone), and 1.8 ml (*trans*-dienelactone); those using 40% (vol/vol) methanol were 2.1 (2-chloro-*cis,cis*-muconate) and 1.4 ml (*cis*-dienelactone); those using 50% (vol/vol) methanol were 4.4 (3CB) and 0.7 ml (2-chloro-*cis,cis*-muconate). Kinetic measurements were recorded on an UV 2100 spectrophotometer (Shimadzu Corporation, Kyoto, Japan).

Transformation of 2-chloromuconate by chloromuconate cycloisomerase. Transformation of 2-chloromuconate was usually performed in 50 mM Tris-HCl, pH 8. The reaction mixtures contained 500 μM 2-chloromuconate and 20 to 100 mU (as determined with 50 μM 3-chloromuconate as the substrate) of chloromuconate cycloisomerase per ml. Substrate transformation was monitored by HPLC.

Chemicals. Chemicals were purchased from Sigma-Aldrich Chemie GmbH, Taufkirchen, Germany; Baker Chemikalien, Griesheim, Germany; and Merck AG, Darmstadt, Germany. 3-Chlorocatechol was obtained from Promochem, Wesel, Germany. 2-Chloro-*cis,cis*-muconate and (4*R*,5*R*/4*S*,5*S*)-5-chloro-3-methylmuconolactone were prepared as described by Pieper et al. (36, 38). (4*R*,5*S*)-5-Chloromuconolactone and (4*S*)-2-chloromuconolactone were prepared as described by Prucha et al. (40). *cis*-Dienelactone was a generous gift from Stefan Kaschabek and Walter Reineke (Bergische Universität-Gesamthochschule, Wuppertal, Germany).

RESULTS

Growth of *R. eutropha* JMP222 derivatives containing pBBR1M-I or pBBR1M-II on 3CB and expression of Tfd gene products. Differences in the growth of *R. eutropha* JMP222 derivatives harboring *tfd* module I or II on 3CB have been reported previously (34). Accordingly, *R. eutropha* JMP222(pBBR1M-I) exhibited significantly higher growth rates (0.19/h) and higher growth yields (0.22 units of optical density at 546 nm (OD_{546})/mM 3CB) during growth on 3CB than did *R. eutropha* JMP222(pBBR1M-II) (0.06/h and 0.13 OD_{546} units/mM 3CB), as indicated by the turbidity of the culture obtained after complete transformation of the 3CB growth substrate (Fig. 2). The observed differences in growth yield seem to be due to the significantly different amounts of

Downloaded from http://jb.asm.org/ on September 3, 2020 at Corteva Agriscience

COR-AAD1-00002774
Bayer EX1008 (Part 5 of 9)

TABLE 1. Specific activities of catechol and chlorocatechol catabolic enzymes of 2,4-D- or 3-CB-grown cells of *R. eutropha* JMP134, JMP222(pBBR1M-I), and JMP222(pBBR1M-II)

Enzyme activity	Assay substrate	Sp act (U/g of protein)[a] for indicated strain/substrate			
		JMP134(pJP4)/ 5 mM 2,4-D	JMP134(pJP4)/ 5 mM 3CB	JMP222(pBBR1M-I)/ 5 mM 3CB	JMP222(pBBR1M-II)/ 2 mM 3CB
(Chloro) catechol 1,2-dioxygenase	Catechol	430 ± 90	840 ± 120	550 ± 90	540 ± 90
	3-Chlorocatechol	420 ± 90	380 ± 80	540 ± 90	290 ± 70
	4-Chlorocatechol	410 ± 80	370 ± 80	520 ± 90	260 ± 50
(Chloro) muconate cycloisomerase	Muconate	<5	120 ± 20	<5	90 ± 30
	2-Chloromuconate	25 ± 5	15 ± 5	35 ± 10	<5
	3-Chloromuconate	270 ± 40	180 ± 40	360 ± 40	140 ± 50
Dienelactone hydrolase	*cis*-Dienelactone	1,050 ± 120	980 ± 110	1,200 ± 400	55 ± 15
Maleylacetate reductase	Maleylacetate	750 ± 170	510 ± 150	470 ± 150	1,520 ± 300

[a] Values are averages of at least three independent experiments.

intermediates produced during growth of the two strains. Thus, whereas *R. eutropha* JMP222(pBBR1M-I) accumulated 15% ± 5% of added 3CB as 2-chloromuconate, more than 50% of added 3CB appeared as 2-chloromuconate in the culture supernatant during growth of *R. eutropha* JMP222(pBBR1M-II).

Whereas 2-chloromuconate was the only intermediate excreted during the growth of *R. eutropha* JMP222(pBBR1M-I), *R. eutropha* JMP222(pBBR1M-II) also excreted minute amounts of *cis*-dienelactone, corresponding to 2% of the substrate transformed. The accumulation of large amounts of 2-chloromuconate in strain JMP222 expressing module II, compared to the amounts accumulated in strain JMP222 expressing module I, can be explained by the recently reported very low activity of $TfdD_{II}$ chloromuconate cycloisomerase with this substrate (34). Accumulation of *cis*-dienelactone can be assumed to have been due to the observed low activity of $TfdE_{II}$ dienelactone hydrolase in *R. eutropha* JMP222(pBBR1M-II) (Table 1).

Maleylacetate, produced by the activity of dienelactone hydrolase on *cis*- or *trans*-dienelactone, was never observed in the culture supernatants, indicating that maleylacetate reductase did not constitute a pathway bottleneck in *R. eutropha* JMP222(pBBR1M-II) or in *R. eutropha* JMP222(pBBR1M-I), despite the fact that only poor maleylacetate reductase activities have been recently reported to be induced during growth of strain JMP222 expressing *tfd* module I (34). This discrepancy can be explained by the fact that the former enzyme activity measurements were performed with maleylacetate produced in situ by cell extracts. However, by using maleylacetate freshly prepared from *cis*-dienelactone by alkaline hydrolysis or purified dienelactone hydrolase and by measuring the enzymatic activity immediately after the preparation of a cell extract containing at least 5 mg of protein per ml, it was possible to reproducibly detect significant maleylacetate reductase activities in *R. eutropha* JMP222(pBBR1M-I) (Table 1). All other enzyme activities were as previously reported (Table 1) (34).

Levels of Tfd activity during growth of *R. eutropha* JMP134 on chloroaromatics. Due to the fact that all four enzymes involved in the chlorocatechol degradation of *tfd* modules I and II were obviously active and based on detection of the respective mRNAs, which showed that both gene modules were expressed during growth on 2,4-D (22, 24), the importance of each gene module for the degradation of chloroaromatics in wild-type strain *R. eutropha* JMP134(pJP4) was investigated. Chromatographic methods were applied to partially purify and separate the respective isoenzymes from cell extracts without significant loss of activity. Strains *R. eutropha* JMP222(pBBR1M-I) and R. *eutropha* JMP222(pBBR1M-II) were used for the establishment of an optimized purification scheme.

Anion-exchange chromatography of cell extracts of 3CB-grown *R. eutropha* JMP222(pBBR1M-I) or JMP(pBBR1M-II) resulted in high recoveries of $TfdC_I$ (60% ± 10% of applied activity), $TfdC_{II}$ (80% ± 10%), $TfdD_I$ (70% ± 10%), $TfdD_{II}$ (60% ± 10%), $TfdE_I$ (90% ± 10%), and $TfdE_{II}$ (90% ± 10%) activity (Fig. 3A and B), although only low activities of maleylacetate reductase (activity of $TfdF_I$ eluting at 0.21 ± 0.02 M NaCl was usually lower than 5% of the applied activity, and activity of $TfdF_{II}$ eluting at 0.16 ± 0.01 M NaCl was usually lower than 10%) could be recovered. However, $TfdC_I$ (eluting at 0.29 M NaCl) showed a distinctly different retention behavior than did $TfdC_{II}$ (eluting at 0.19 M NaCl). $TfdD_I$ and $TfdD_{II}$ also exhibited different properties (eluting at 0.43 and 0.17 M NaCl, respectively). $TfdE_I$ and $TfdE_{II}$ could not be separated by such a chromatographic method (eluting at 0.16 M NaCl). Optimization of the applied NaCl gradient did not result in a significant enhancement of separation.

Resolution of soluble enzymes by anion-exchange chromatography clearly indicated that two peaks of activity against catechol (Fig. 3B) were recovered from *R. eutropha* JMP222(pBBR1M-II). Thus, the high level of catechol 1,2-dioxygenase activity with catechol, compared to that with 3-chlorocatechol in 3CB-grown cells of strain JMP222(pBBR1M-II) (Table 1), is due to the induction of the chromosomally encoded catechol 1,2-dioxygenase (eluting at 0.22 M NaCl) in addition to $TfdC_{II}$. Whereas $TfdC_{II}$ exhibited similar activities against both catechol and 3-chlorocatechol, transformation of 3-chlorocatechol by fractions containing catechol 1,2-dioxygenase was negligible. A chromosomally encoded muconate cycloisomerase (exhibiting significant activity only with *cis,cis*-muconate and eluting at 0.22 M NaCl) was also induced under these conditions (Fig. 3B). A similar induction of enzymes of the 3-oxoadipate pathway has previously

Downloaded from http://jb.asm.org/ on September 3, 2020 at Corteva Agriscience

COR-AAD1-00002775
Bayer EX1008 (Part 5 of 9)

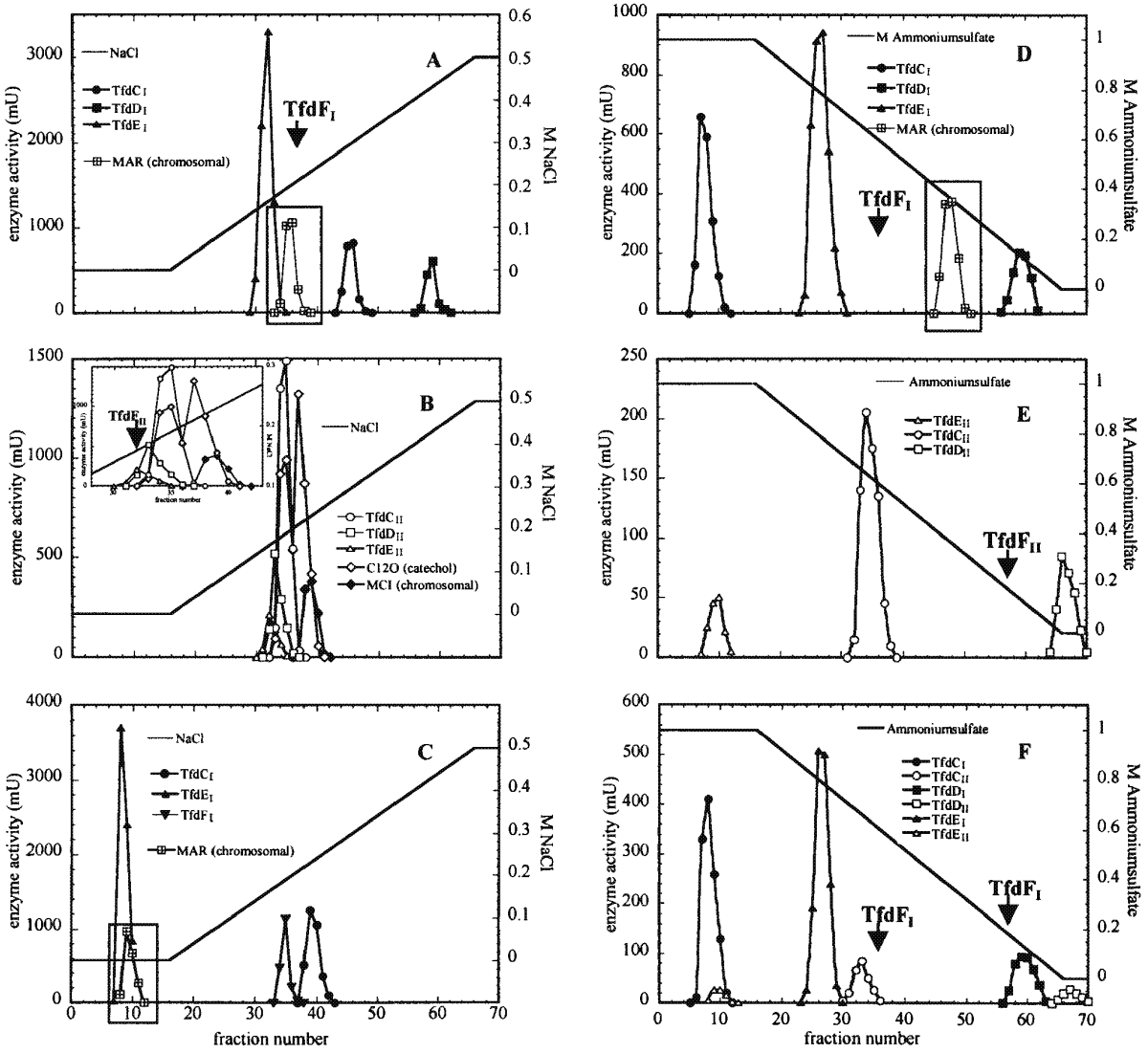


FIG. 3. Separation of proteins from cell extracts of *R. eutropha* JMP134, JMP222, and derivatives by means of a MonoQ HR5/5 anion-exchange (A to C) or a phenyl-Superose HR5/5 hydrophobic-interaction column (D to F). Cell extracts were either directly applied (A to C) or applied after addition of ammonium sulfate (final concentration of 1 M) (D to E), and proteins were eluted with a linear gradient of NaCl (0 to 0.5 M) or $(NH_4)_2SO_4$ (1 to 0 M). The eluted fractions (0.5 ml) were analyzed for activities against the respective assay substrates (usually applied at a concentration of 50 μM, except for catechol and 3-chlorocatechol, which were added at a concentration of 200 μM). Enzymes eluting with a yield of >40% are shown. Arrows, enzymes eluting with a low yield (>20%; $TfdF_I$ and $TfdF_{II}$). Elution was performed in Tris-HCl buffer, except for panel C, where phosphate buffer was used. (A) Separation of a cell extract of 3CB-grown cells of JMP222(pBBR1M-I) (6.1 mg of protein). (Inset) Activity of chromosomally encoded maleylacetate reductase after separation of a cell extract of 4-fluorobenzoate (4FB)-grown cells of JMP222 (7.9 mg of protein). (B) Separation of a cell extract of 3CB-grown cells of JMP222(pBBR1M-II) (11.6 mg of protein). (Inset) Detailed view of the activities observed in fractions 30 to 41. (C) Separation of a cell extract of 3CB-grown cells of JMP222(pBBR1M-I) (5.6 mg of protein). (Inset) Activity of chromosomally encoded maleylacetate reductase after separation of a cell extract of 4FB-grown cells of JMP222 (6.5 mg of protein). Muconate cycloisomerase activities could not be recovered after elution with phosphate buffer, as phosphate completely inhibited those enzymes. (D) Separation of a cell extract of 3CB-grown cells of JMP222(pBBR1M-I) (4.7 mg of protein). (Inset) Activity of chromosomally encoded maleylacetate reductase after separation of a cell extract of 4FB-grown cells of JMP222 (8.1 mg of protein). (E) Separation of a cell extract of 3CB-grown cells of JMP222(pBBR1M-II) (4.5 mg of protein). (F) Separation of a cell extract of 2,4-D-grown cells of JMP222(pBBR1M-I) (3.6 mg of protein).

been observed in 3CB-grown cells of *R. eutropha* JMP134 (36), whereas those enzymes were not induced during growth of this strain on 2,4-D (21). However, neither catechol 1,2-dioxygenase nor muconate cycloisomerase was induced during growth of strain JMP222(pBBR1M-I) with 3CB. The observed dienelactone hydrolase activity in strain JMP222(pBBR1M-II) was not identical to that of chromosomally encoded dienelactone hydrolase of strain JMP222 observed during growth on

Downloaded from http://jb.asm.org/ on September 3, 2020 at Corteva Agriscience

COR-AAD1-00002776
Bayer EX1008 (Part 5 of 9)

4-fluorobenzoate (43), as the enzyme induced in strain JMP222(pBBR1M-II) exhibited similar activities against both *cis*- and *trans*-dienelactone (activity with *trans*-dienelactone was 60% of that with *cis*-dienelactone at substrate concentrations of 50 to 100 μM). The chromosomally encoded enzyme, in contrast, has been shown to exhibit activity only against *trans*-dienelactone (43).

Hydrophobic interaction chromatography was observed to be superior to anion-exchange chromatography, allowing separation of the different chlorocatechol dioxygenases and chloromuconate cycloisomerases, as well as the dienelactone hydrolases (Fig. 3D and E). However, the yields (50% ± 10% for $TfdD_I$ and $TfdD_{II}$; 60% ± 10% for $TfdE_I$, $TfdE_{II}$, and $TfdC_{II}$; and 70% ± 10% for $TfdC_I$) were usually slightly lower than those obtained by anion-exchange chromatography, and hydrophobic-interaction chromatography also failed to give highly active preparations of maleylacetate reductase. Although a reasonable maleylacetate reductase activity, corresponding to less than 20% of the applied activity (eluting at 0.16 M $[NH_4]_2SO_4$), could be observed after hydrophobic-interaction chromatography of a cell extract of 3CB-grown strain JMP222(pBBR1M-II), only negligible activity (corresponding to less than 5% of the applied activity and eluting at 0.60 ± 0.04 M $[NH_4]_2SO_4$) could be recovered from a cell extract of strain JMP222(pBBR1M-I) grown on 3CB.

Neither TfdCI nor $TfdE_{II}$ interacted with the column material under the applied conditions (i.e., an initial ammonium sulfate concentration of 1 M; Fig. 3D and E). Further increases in the initial ammonium sulfate concentration resulted in precipitation of dienelactone hydrolase activities. However, no catechol 1,2-dioxygenase activity against 3-chlorocatechol was observed in the initially eluting fractions during separation of the JMP222(pBBR1M-II)-derived extract. Furthermore, no activity against *cis*-dienelactone could be found in the respective fractions after separation of a JMP222(pBBR1M-I)-derived extract, indicating that the activities assigned to $TfdC_I$ or $TfdE_{II}$ were not due to chromatographic artifacts.

R. eutropha JMP134 was grown on 2,4-D, and, subsequently, the soluble proteins were separated by means of hydrophobic-interaction chromatography (Fig. 3F). The activities of tfd_I-encoded enzymes $TfdC_I$, $TfdD_I$, and $TfdE_I$ were approximately 40 to 70% of those induced during growth of strain JMP222(pBBR1M-I) on 3CB, and those of tfd_{II}-encoded enzymes $TfdC_{II}$, $TfdD_{II}$, and $TfdE_{II}$ were approximately 25 to 50% of those induced during growth of strain JMP222(pBBR1M-II) on 3CB. As the yields of the respective isoenzymes after chromatographic separation were always similar, the comparison of total activities in the respective fractions indicates the actual importance of the respective enzymes for the degradation process. As shown in Fig. 3F, in 2,4-D-grown cells of *R. eutropha* JMP134, the Tfd_{II}-derived enzyme activities comprised 20% ± 5% of the observed total activity against 3-chlorocatechol and 3-chloromuconate but only approximately 5% of the observed activity against *cis*-dienelactone.

Characterization of maleylacetate reductases induced during growth of *R. eutropha* JMP134 and derivatives on chloroaromatics. *R. eutropha* JMP222 is capable of growth on 4-fluorobenzoate, and induction of a chromosomally encoded maleylacetate reductase under these conditions has been reported (43). Therefore, the possibility that the maleylacetate reductase activities observed during growth of strain JMP222(pBBR1M-I) or JMP222(pBBR1M-II) on 3CB (Table 1) are, at least partially, due to recruitment of this chromosomally encoded maleylacetate reductase cannot be excluded. Partial purification of this enzyme activity, which was usually induced at levels of 300 ± 50 U/g of protein in 4-fluorobenzoate-grown cells of strain JMP222, showed that this enzyme, in contrast to the activities induced in strains JMP222(pBBR1M-I) and JMP222(pBBR1M-II), exhibits high stability. Approximately 50% of the applied activity could be recovered by hydrophobic-interaction chromatography; the activity eluted at 0.38 M ammonium sulfate (Fig. 3D, inset). As no significant activity was observed in the respective fractions after separation of JMP222(pBBR1M-I)- or JMP222(pBBR1M-II)-derived cell extracts, it can be concluded that the chromosomally encoded maleylacetate reductase activity was not recruited in these strains for growth on 3CB. Similarly, as no significant activity was observed in the respective fractions after separation of a cell extract of 2,4-D-grown cells of strain JMP134 (Fig. 3F), it seems that the chromosomally encoded maleylacetate reductase does not play a major role in the degradation of this substrate in the wild-type strain.

Approximately 90% of the applied maleylacetate reductase activity of 4-fluorobenzoate-grown cells of *R. eutropha* JMP222 was recovered by anion-exchange chromatography; the activity eluted at 0.2 M NaCl (Fig. 3A, inset), a condition similar to those under which the activities of JMP222(pBBR1M-I) and JMP222(pBBR1M-II) eluted. However, the yields of the latter maleylacetate preparations were <5 and 10% ± 5%, respectively, again indicating that the chromosomally encoded maleylacetate reductase plays no significant role during 3CB degradation by strain JMP222(pBBR1M-I) or JMP222(pBBR1M-II).

As neither hydrophobic-interaction chromatography nor anion-exchange chromatography resulted in sufficient resolution of the three maleylacetate reductase activities or in reasonable yields of $TfdF_{II}$ or, particularly, $TfdF_I$, anion-exchange chromatography was applied and Tris-HCl buffer in the eluant was replaced by phosphate buffer. This simple change had a marked effect on the retention behavior of the chromosomally encoded maleylacetate reductase, as well as on the $TfdE_I$ enzyme, as their interactions with the column material were nearly abolished (Fig. 3C). Moreover, the use of phosphate buffer dramatically increased the yield of $TfdF_I$. In a typical separation run, after application of a cell extract of strain JMP222(pBBR1M-I) containing 15 mg of protein, the two most active fractions contained, together, 7,050 mU of $TfdF_I$ activity and 0.48 mg of protein (corresponding to a specific activity of 14,700 U/g of protein) in a complete volume of 1 ml. Further purification by gel filtration resulted in a significant loss of activity. Less than 10% of the applied activity was recovered, with specific activities of up to only 800 U/g of protein. To further demonstrate that the maleylacetate reductase induced in 3CB-grown strain JMP222(pBBR1M-I) is identical to $TfdF_I$, an aliquot of a highly active fraction obtained by anion-exchange chromatography, containing 240 μg of protein, was subjected to two-dimensional gel electrophoresis and blotted onto a polyvinylidene difluoride membrane and a major protein spot corresponding to the estimated molecular mass of

Downloaded from http://jb.asm.org/ on September 3, 2020 at Corteva Agriscience

COR-AAD1-00002777
Bayer EX1008 (Part 5 of 9)

the $TfdF_I$ subunit (37.9 kDa) was analyzed by N-terminal sequencing. The amino-terminal sequence was identified as MKKFTLDYLSPR; this sequence was identical to the sequence deduced from the *tfdF*$_I$ gene. Therefore, it can be assumed that the maleylacetate reductase activity present in 3CB-grown cells of strain JMP222(pBBR1M-I) is, in fact, due to expression of *tfdF*$_I$.

Thus, the use of anion-exchange chromatography with phosphate buffer has enabled the characterization of the expression of $TfdF_I$, as well as of the different dienelactone hydrolases and catechol 1,2-dioxygenases, during growth of *R. eutropha* JMP134 and JMP222 derivatives.

2,4-D-grown cells of strain JMP134 induce significant levels of $TfdF_I$, comprising roughly half of the total maleylacetate reductase activity. Calculations of the levels of $TfdC_I$ versus $TfdC_{II}$ and of $TfdE_I$ versus $TfdE_{II}$ in those cells confirmed the results obtained above by hydrophobic interaction chromatography, with 20% of the total chlorocatechol 1,2-dioxygenase activity due to $TfdC_{II}$ and 5% of the total dienelactone hydrolase activity due to $TfdE_{II}$.

Characterization of chloromuconate cycloisomerase $TfdD_{II}$. Compared to the previously described chloromuconate cycloisomerases from gram-negative microorganisms (21, 51) the chloromuconate cycloisomerase activity encoded by *tfdD*$_{II}$ exhibited very poor activity against 2-chloromuconate, possibly resembling chloromuconate cycloisomerase of *Rhodococcus opacus* 1CP (46). Therefore, this enzyme activity was further characterized. $TfdD_{II}$ was partially purified from 3CB-grown cells of strain JMP222(pBBRM1-II) by anion-exchange chromatography and gel filtration. A total of 2.1 U (calculated for a substrate concentration of 50 μM 3-chloromuconate) of chloromuconate cycloisomerase (specific activity of 185 U/g) was applied to a MonoQ column. The three most active fractions eluting from the column were pooled (1.8 U with a specific activity of 650 U/g) and subjected to gel filtration. A total of 0.8 U was recovered in four fractions, with specific activities as high as 3,800 U/g. Kinetics experiments were performed by quantification of *cis*-dienelactone formation at 305 nm, and a K_m value of 190 ± 15 μM was calculated. For quantification of $TfdD_{II}$ in active fractions, aliquots were separated by PAGE (40 to 300 ng of protein per fraction) and stained with Sypro Ruby. A major band with a molecular mass of 41 ± 1 kDa, which contained 30 to 60% of the total protein in the respective fractions, was observed. The N-terminal sequence of this protein (MLTEKAIADSPN) was identical to that expected for $TfdD_{II}$. Thus, maximal transformation rates calculated during kinetics experiments could be related to the amount of $TfdD_{II}$ present. Taking into account the predicted subunit molecular mass of 36.9 kDa, a k_{cat} value of 1,950 ± 150 min^{-1} was calculated.

By the photometric test (depletion in the presence of an excess of dienelactone hydrolase as measured at λ = 260 nm), $TfdD_{II}$ exhibited significant activity only against 3-chloromuconate and poor activity against 2-chloro-substituted muconate, as well as against unsubstituted muconate. At a substrate concentration of 0.1 mM, the activity with muconate was only 0.4% ± 0.1% of that with 3-chloromuconate and the activity with 2-chloromuconate was 0.8% ± 0.2%.

This substrate spectrum significantly resembles that reported for chloromuconate cycloisomerase of *Rhodococcus opacus* (46). This cycloisomerase differs from those of previously described gram-negative organisms in that it lacks the ability to convert 2-chloromuconolactone and to form *trans*-dienelactone from 2-chloromuconate. Thus, the kinetic properties of the $TfdD_{II}$ chloromuconate cycloisomerase were assessed by using the partially purified enzyme fractions described above. These fractions were free of any muconate cycloisomerase (capable of transforming 2-chloromuconolactone), muconolactone isomerase (capable of dehalogenating intermediate 5-chloromuconolactone), or dienelactone hydrolase activities. As shown in Fig. 4, the predominant products formed from 2-chloromuconate were identified as 2- and 5-chloromuconolactone. The ratio between 2-chloromuconate, 5-chloromuconolactone, and 2-chloromuconolactone, after a short incubation period, was about 20:4:3, as previously reported for the equilibrium between those compounds after addition of muconate cycloisomerases (50). Further incubation resulted in the formation of mainly *trans*-dienelactone and minor amounts of *cis*-dienelactone. A control incubation using partially purified muconate cycloisomerase resulted in the formation of a similar equilibrium between 2-chloromuconate and 5- and 2-chloromuconolactone. However, the rate of *trans*-dienelactone formation was negligible in those assays (less than 2 μM h^{-1} in the presence of 100 mU of muconate cyc-

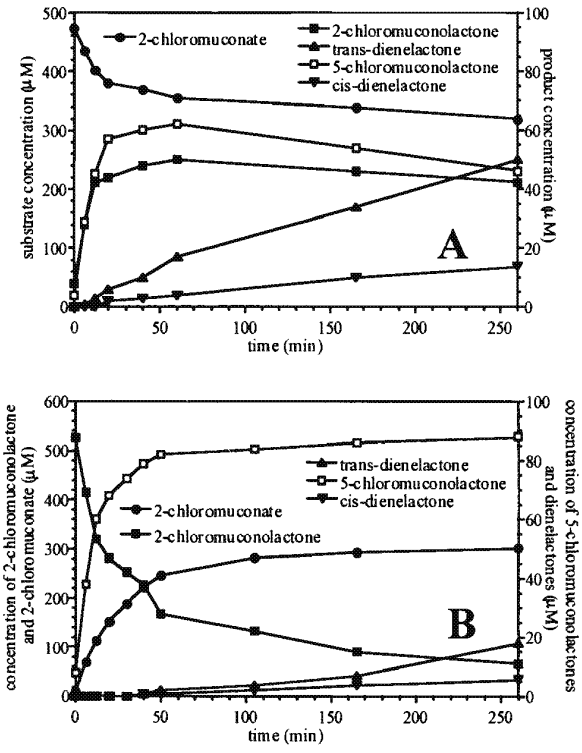


FIG. 4. HPLC analyses of the conversion of 2-chloro-*cis,cis*-muconate (A) and 2-chloromuconolactone (B) by $TfdD_{II}$ chloromuconate cycloisomerase *of R. eutropha* JMP222. Reaction mixtures (0.2 ml) contained 50 mM Tris-HCl (pH 8) supplemented with 1 mM $MnCl_2$, 0.5 mM 2-chloro-*cis,cis*-muconate (A) or 0.5 mM 2-chloromuconolactone (B) and 20 (as determined with 3-chloromuconate as the substrate) (A) or 10 mU (B) of $TfdD_{II}$.

Downloaded from http://jb.asm.org/ on September 3, 2020 at Corteva Agriscience

COR-AAD1-00002778
Bayer EX1008 (Part 5 of 9)

loisomerase per ml, compared to 12 μM h^{-1} in the presence of 100 mU of Tfd_{II} per ml).

Incubation of $TfdD_{II}$ with 2-chloromuconolactone resulted in formation of the equilibrium between 2-chloromuconate and 2- and 5-chloromuconolactone described above, demonstrating that $TfdD_{II}$, in contrast to the *Rhodococcus* enzyme, can transform 2-chloromuconolactone. Considerable levels of *trans*-dienelactone formation were visible only after significant accumulation of 5-chloromuconolactone.

DISCUSSION

Chloroaromatic degradation by *R. eutropha* JMP134 has been the subject of investigations for decades. The recently discovered $tfdD_{II}$, $tfdC_{II}$, $tfdE_{II}$, $tfdF_{II}$, and $tfdB_{II}$ genes have elucidated a new layer of complexity for chloroaromatic degradation by this strain. It had been shown that tfd_{II} genes are transcribed in *R. eutropha* JMP134 upon exposure to 2,4-D (22, 24). Moreover, *R. eutropha* JMP222 strains containing tfd_{II} genes were capable of growing on 3CB (34), and expression in *Escherichia coli* showed that tfd_{II} genes encode functional enzymes (22). We have demonstrated here that, besides $tfdF_{II}$ (45), at least $tfdD_{II}$, $tfdC_{II}$, and $tfdE_{II}$ are translated into functional enzymes in *R. eutropha* JMP134. We have also shown that $tfdF_I$, which was previously thought to be nonfunctional or poorly functional (34, 45), is transcribed and translated into a functional enzyme. Thus, tfd_I, as well as tfd_{II}, gene modules encode a complete set of functional and active enzymes for the transformation of chlorocatechols into 3-oxoadipate. However, whereas significant activities of $TfdD_{II}$, $TfdC_{II}$, and $TfdF_{II}$ were obvious during the growth of strain JMP134 on 2,4-D and also of strain JMP222 containing tfd_{II} genes, activities of $TfdE_{II}$ were negligible compared with those of $TfdE_I$. The basis for this poor activity remains to be elucidated. A second obvious difference between tfd_I- and tfd_{II}-encoded proteins lies in the TfdD proteins. On the first view, both $TfdD_I$ (21, 51) and $TfdD_{II}$ are characterized by their poor activity with 2-chloromuconate and muconate, compared to that with 3-chloromuconate and thus differ only slightly in substrate specificity. However, whereas the relative $TfdD_I$ activity with 2-chloromuconate at substrate concentrations between 10 and 100 μM is 6 to 9% of that with 3-chloromuconate (51), the relative activity of $TfdD_{II}$ is less than 1%. This poor activity with 2-chloromuconate is reflected in the higher accumulation of this intermediate and lower growth yield of strain JMP222 containing tfd_{II} genes, compared to those of strain JMP222 containing tfd_I genes, when the strain is grown on 3CB.

However, the most striking difference between $TfdD_I$ and $TfdD_{II}$ is the poor capability of $TfdD_{II}$ to dechlorinate during cycloisomerization of 2-chloromuconate. In contrast to what was found for other gram-negative bacterium chloromuconate cycloisomerases, where only small amounts of 2- and 5-chloromuconolactone accumulated during 2-chloromuconate turnover (52), dehalogenation to form *trans*-dienelactone by $TfdD_{II}$ is slow compared to cycloisomerization. Thus, $TfdD_{II}$ seems to be specifically dedicated to the transformation of 3-chloro-substituted muconates, a feature recently described for chloromuconate cycloisomerase of *Rhodococcus opacus* 1CP (46). However, whereas the *Rhodococcus* enzyme neither transforms 2-chloromuconolactone nor dehalogenates 2-chloromuconate or 5-chloromuconolactone during cycloisomerization, $TfdD_{II}$ exhibits both capabilities. $TfdD_{II}$ thus appears to be only distantly related, by sequence homology (12) as well as by kinetic properties, to all chloromuconate cycloisomerases described to date (Fig. 5). With respect to biochemical properties, $TfdD_{II}$ is intermediate to muconate and chloromuconate cycloisomerases of gram-negative bacteria, making $TfdD_{II}$ an interesting subject for evolutionary study. Regarding 3-chloromuconate turnover, no differences between $TfdD_{II}$ and other chloromuconate cycloisomerases described so far (e.g., a k_{cat}/K_m value of 10 $\mu M^{-1}min^{-1}$ compared to 7 to 38 $\mu M^{-1}min^{-1}$ for the *Pseudomonas* sp. strain P51- and *Pseudomonas* sp. strain B13-derived and $TfdD_I$ chloromuconate cycloisomerases) were evident.

It has been speculated recently (22) that the main reason for maintenance the tfd_{II} gene cluster, other than as a mechanism for supplying auxiliary functions, such as the facilitated uptake of 2,4-D mediated by TfdK (26), is the supply of a functional transcriptional activator (TfdR) (25). Furthermore it has been assumed that $TfdF_{II}$ is the major maleylacetate reductase complementing a nonfunctional or poorly functional $TfdF_I$ gene product. However, we can demonstrate now that $TfdF_I$ is, in fact, functional and induced at a high level during growth on 2,4-D.

However, besides these observations, the tfd_{II} genes definitely increase the dosage of chlorocatechol genes and of active gene products in strain JMP134 when the strain is grown on chloroaromatics. As has been recently shown, a duplication of the *tfd* gene modules results in an increased growth rate on 3CB (5). It can be proposed that the number of *tfd* genes present in the wild-type strain is limiting for growth on 3CB. As $TfdD_{II}$, $TfdC_{II}$, and $TfdF_{II}$ enzymes constitute more than 20% of the total activity during growth on chloroaromatics, it is evident that maintenance of the tfd_{II} genes would be advantageous for the strain. The fact that an elevated number of chlorocatechol genes is necessary to achieve growth on chloroaromatics has been reported in various cases. The transfer of single copies of chlorocatechol genes (*tcbR* and *tcbCDEF*) originating from *Pseudomonas* sp. strain P51 (48) into *Pseudomonas putida* KT2442 did not result in the expected 3CB-degrading derivatives; multiple chromosomal copies (at least two) were needed to achieve this phenotype (20). Similarly, the transfer of single copies of tfd_I or tfd_{II} genes into the chromosome of *R. eutropha* JMP222 did not result in a 3CB-degrading phenotype, in contrast to the situation where those genes were introduced on a medium-copy-number vector (34). *P. putida* F1 transconjugants containing two copies of the *Pseudomonas* sp. strain B13-derived *clc* element were unable to grow on chlorobenzene, and characterization of chlorobenzene-degrading transconjugants revealed that three to eight copies of the *clc* element were required for growth, with a larger number of *clc* elements being associated with increasingly vigorous growth (41). Moreover, the currently available genetic evidence suggests that gene amplification plays an important role in the adaptation of bacteria to chloroaromatic degradation in contaminated environments (31, 32, 49).

High levels of catechol 1,2-dioxygenase and muconate cycloisomerase were observed in 3CB-grown cells of strain JMP222 harboring tfd_{II} genes and of strain JMP134 but not in 3CB-grown cells of strain JMP222 harboring tfd_I genes or 2,4-

Downloaded from http://jb.asm.org/ on September 3, 2020 at Corteva Agriscience

COR-AAD1-00002779
Bayer EX1008 (Part 5 of 9)

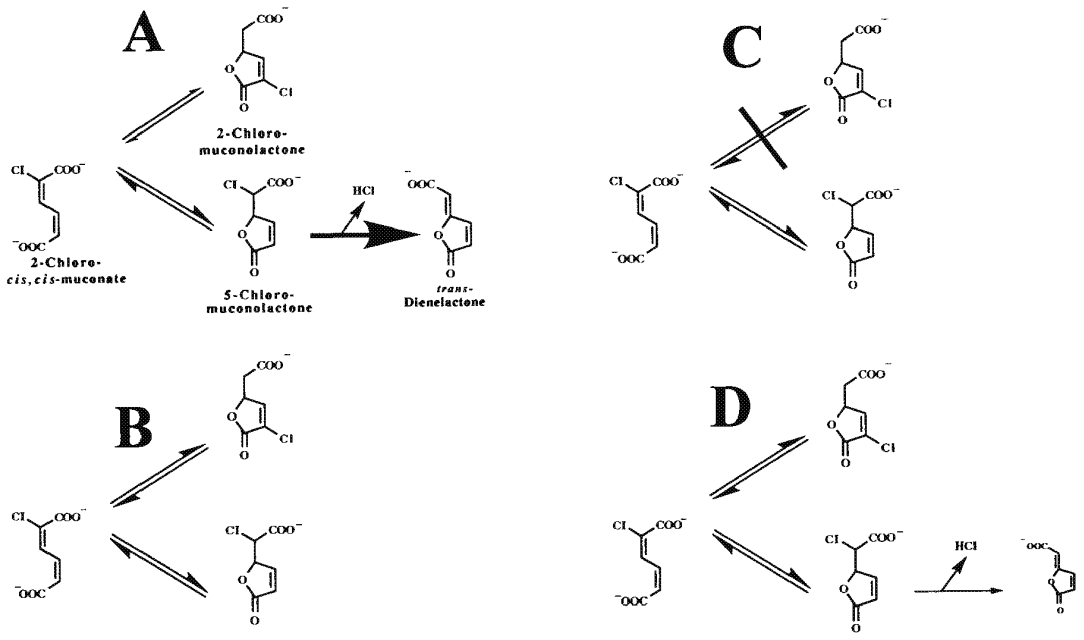


FIG. 5. Reactions involved in 2-chloro-*cis,cis*-muconate conversion by muconate and chloromuconate cycloisomerases. (A) Reactions catalyzed by chloromuconate cycloisomerases such as $TfdD_I$. These enzymes are supposed to preferentially catalyze a 3,6-cycloisomerization, followed by a fast dehalogenation to form *trans*-dienelactone. (B) Reactions catalyzed by muconate cycloisomerases such as the chromosomally encoded enzyme of *R. eutropha* JMP134. These enzymes catalyze the formation of an equilibrium between 2-chloro-*cis,cis*-muconate and 2- and 5-chloromuconolactone. (C) Reactions catalyzed by muconate and chloromuconate cycloisomerase of *Rhodococcus opacus* 1CP. These enzymes catalyze exclusively a 3,6-cycloisomerization and are not capable of transforming 2-chloromuconolactone. (D) Reactions catalyzed by chloromuconate cycloisomerase $TfdD_{II}$. This enzyme catalyzes the formation of an equilibrium between 2-chloro-*cis,cis*-muconate and 2- and 5-chloromuconolactone and is capable of a slow dehalogenation to form *trans*-dienelactone. Minor amounts of *cis*-dienelactone were also observed as products.

D-grown cells of strain JMP134 (Table 1). Expression of catechol and chlorocatechol operons usually requires LysR-type transcriptional activators and inducer muconate (catechol operons) or 2-chloromuconate (chlorocatechol operons) (28). In strain JMP134, the *tfdR* gene product is responsible for expression of the *tfd* operons (25) and it is activated by chloromuconates (14). It has been proposed that, even in the absence of *tfdR*, low-level expression of *tfdCDEF* occurs, implying a cross-activation by chromosomally encoded regulatory elements (14). In *P. putida* it has been shown that CatR, the regulator of the *catBC* operon (for catechol degradation), interacts with the *clcABD* promoter region and, likewise, *clc*R, the regulator of the *clcABD* operon (for chlorocatechol degradation), was shown to interact with the *catBC* promoter region. CatR could even complement a ClcR$^-$ mutant *P. putida* strain harboring the *clcABD* operon for growth on 3CB (29, 33). Moreover, it was recently demonstrated that the LysR-type regulator of the *cbn* operon of *R. eutropha* NH9 is activated by both muconate and 2-chloromuconate (30), implying the presence of significant cross talk among the homologous transcriptional activators. Consequently, it seems likely that the accumulated 2-chloromuconate may drive expression of the catechol pathway genes by acting on a putative *catR*-like element in the chromosomes of strains JMP134 and JMP222. However, induction was observed only in a subset of growth conditions or genetic backgrounds, specifically those that resulted in accumulation of a high level of 2-chloromuconate during growth. Thus, evidently, highly elevated levels of intracellular 2-chloromuconate are necessary to achieve expression of catechol catabolic genes. This agrees with observations of Cosper et al. (6), who proposed that versions of *Acinetobacter* sp. strain ADP1 containing variants of the muconate cycloisomerase with reduced catalytic properties have increased intracellular levels of muconate available, which are responsible for the activation of LysR-type regulator CatM, which is, in turn, capable of activating the expression of genes encoding enzymes for benzoate degradation.

On one hand, the activation of the catechol pathway genes in *R. eutropha* can be regarded as a burden for the strain. However, an induction of this type can be proposed to have advantageous effects, as well, specifically for strains such as JMP222(pBBR1M-II). Catechol 1,2-dioxygenase and muconate cycloisomerase have some activity on chlorinated substrate analogues (21, 37) and thus to a certain extent can be responsible for transformation of pathway intermediates. 2-Chloro- and 3-chloromuconate will, thereby, be transformed into chloromuconolactones (50) and protoanemonin (1), respectively. Protoanemonin accumulation, when this compound is produced at low rates, can be prevented by dienelactone hydrolase (3), and muconolactone isomerase can support the dehalogenation of any 5-chloromuconolactone (39) formed during cycloisomerization of 2-chloromuconate by muconate cycloisomerase or $TfdD_{II}$. Thus, it can be assumed that part of 3CB in strain JMP222(pBBR1M-II) is mineralized by a com-

Downloaded from http://jb.asm.org/ on September 3, 2020 at Corteva Agriscience

COR-AAD1-00002780
Bayer EX1008 (Part 5 of 9)

plex metabolic interplay between chromosome- and plasmid-encoded enzymes.

ACKNOWLEDGMENTS

The work was supported by EC grant EVK1-CT-1999-00023. D.P.-P., D.H.P., and B.G. acknowledge support by the collaborative grant BMBF-IB/CONICYT-Chile and FONDECYT 8990004.

We thank Josef Wissing for his support in protein quantification experiments, Rita Getzlaff for N-terminal amino acid sequencing, and Eva Medina and Edward Moore for critical reading of the manuscript.

REFERENCES

1. **Blasco, R., R.-M. Wittich, M. Mallavarapu, K. N. Timmis, and D. H. Pieper.** 1995. From xenobiotic to antibiotic. Formation of protoanemonin from 4-chlorocatechol by enzymes of the 3-oxoadipate pathway. J. Biol. Chem. **270:**29229–29235.
2. **Bradford, M. M.** 1976. A rapid and sensitive method for the quantification of microgram quantities of protein utilizing the principle of protein-dye binding. Anal. Biochem. **72:**248–254.
3. **Brückmann, M., R. Blasco, K. N. Timmis, and D. H. Pieper.** 1998. Detoxification of protoanemonin by dienelactone hydrolase. J. Bacteriol. **180:**400–402.
4. **Clément, P., V. Matus, L. Cárdenas, and B. González.** 1995. Degradation of trichlorophenols by *Alcaligenes eutrophus* JMP134. FEMS Microbiol. Lett. **127:**51–55.
5. **Clément, P., D. H. Pieper, and B. González.** 2000. Molecular characterization of a deletion/duplication rearrangement in *tfd* genes from *Ralstonia eutropha* JMP134 (pJP4) that improves growth on 3-chlorobenzoic acid but abolishes growth on 2,4-dichlorophenoxyacetic acid. Microbiology **147:**2141–2148.
6. **Cosper, N., L. Collier, T. Clark, R. Scott, and E. Neidle.** 2000. Mutations in *catB*, the gene encoding muconate cycloisomerase, activate transcription of the distal *ben* genes and contribute to a complex regulatory circuit in *Acinetobacter* sp. strain ADP1. J. Bacteriol. **182:**7044–7052.
7. **Don, R. H., and J. M. Pemberton.** 1981. Properties of six pesticide degradation plasmids isolated from *Alcaligenes paradoxus* and *Alcaligenes eutrophus*. J. Bacteriol. **145:**681–686.
8. **Don, R. H., A. J. Weightman, H.-J. Knackmuss, and K. N. Timmis.** 1985. Transposon mutagenesis and cloning analysis of the pathways for degradation of 2,4-dichlorophenoxyacetic acid and 3-chlorobenzoate in *Alcaligenes eutrophus* JMP134(pJP4). J. Bacteriol. **161:**85–90.
9. **Dorn, E., M. Hellwig, W. Reineke, and H.-J. Knackmuss.** 1974. Isolation and characterization of a 3-chlorobenzoate degrading pseudomonad. Arch. Microbiol. **99:**61–70.
10. **Dorn, E., and H.-J. Knackmuss.** 1978. Chemical structure and biodegradability of halogenated aromatic compounds. Substituent effects on 1,2-dioxygenation of catechol. Biochem. J. **174:**85–94.
11. **Ecker, S., T. Widmann, H. Lenke, O. Dickel, P. Fischer, C. Bruhn, and H.-J. Knackmuss.** 1992. Catabolism of 2,6-dinitrophenol by *Alcaligenes eutrophus* JMP 134 and JMP 222. Arch. Microbiol. **158:**149–154.
12. **Eulberg, D., E. M. Kourbatova, L. A. Golovleva, and M. Schlömann.** 1998. Evolutionary relationship between chlorocatechol catabolic enzymes from *Rhodococcus opacus* 1CP and their counterparts in proteobacteria: sequence divergence and functional convergence. J. Bacteriol. **180:**1082–1094.
13. **Farhana, L., and P. B. New.** 1997. The 2,4-dichlorophenol hydroxylase of *Alcaligenes eutrophus* JMP134 is a homotetramer. Can. J. Microbiol. **43:**202–205.
14. **Filer, K., and A. R. Harker.** 1997. Identification of the inducing agent of the 2,4-dichlorophenoxyacetic acid pathway encoded by plasmid pJP4. Appl. Environ. Microbiol. **63:**317–320.
15. **Fukumori, F., and R. P. Hausinger.** 1993. *Alcaligenes eutrophus* JMP134 "2,4-dichlorophenoxyacetate monooxygenase" is an α-ketoglutarate-dependent dioxygenase. J. Bacteriol. **175:**2083–2086.
16. **Ghosal, D., I.-S. You, D. K. Chatterjee, and A. M. Chakrabarty.** 1985. Genes specifying degradation of 3-chlorobenzoic acid in plasmids pAC27 and pJP4. Proc. Natl. Acad. Sci. USA **82:**1638–1642.
17. **Hammer, A., T. Hildenbrand, H. Hofer, K.-L. Ngai, M. Schlömann, and J. J. Stezowski.** 1993. Crystallization and preliminary X-ray data of chloromuconate cycloisomerase from *Alcaligenes eutrophus* JMP134 (pJP4). J. Mol. Biol. **232:**305–307.
18. **Harker, A. R., R. H. Olsen, and R. J. Seidler.** 1989. Phenoxyacetic acid degradation by the 2,4-dichlorophenoxyacetic acid (TFD) pathway of plasmid pJP4: mapping and characterization of the TFD regulatory gene, *tfdR*. J. Bacteriol. **171:**314–320.
19. **Kasberg, T., D. L. Danbaras, A. M. Chakrabarty, D. Kinzelt, and W. Reineke.** 1995. Evidence that operons *tcb*, *tfd*, and *clc* encode maleylacetate reductase, the fourth enzyme of the modified *ortho* pathway. J. Bacteriol. **177:**3885–3889.
20. **Klemba, M., B. Jakobs, R. M. Wittich, and D. H. Pieper.** 2000. Chromosomal integration of the *tcb* chlorocatechol degradation pathway genes as a means of expanding the growth substrate range of bacteria to include haloaromatics. J. Bacteriol. **182:**3255–3261.
21. **Kuhm, A. E., M. Schlömann, H.-J. Knackmuss, and D. H. Pieper.** 1990. Purification and characterization of dichloromuconate cycloisomerase from *Alcaligenes eutrophus* JMP134. Biochem. J. **266:**877–883.
22. **Laemmli, C. M., J. H. J. Leveau, A. J. B. Zehnder, and J. R. van der Meer.** 2000. Characterization of a second *tfd* gene cluster for chlorophenol and chlorocatechol metabolism on plasmid pJP4 in *Ralstonia eutropha* JMP134(pJP4). J. Bacteriol. **182:**4162–4172.
23. **Laemmli, U. K.** 1970. Cleavage of structural proteins during the assembly of the head of bacteriophage T4. Nature **227:**680–685.
24. **Leveau, J. H. J., F. Konig, H. Fuchslin, C. Werlen, and J. R. van der Meer.** 1999. Dynamics of multigene expression during catabolic adaptation of *Ralstonia eutropha* JMP134 (pJP4) to the herbicide 2,4-dichlorophenoxyacetate. Mol. Microbiol. **33:**396–406.
25. **Leveau, J. H. J., and J. R. van der Meer.** 1996. The *tfdR* gene product can successfully take over the role of the insertion element-inactivated TfdT protein as a transcriptional activator of the *tfdCDEF* gene cluster, which encodes chlorocatechol degradation in *Ralstonia eutropha* JMP134(pJP4). J. Bacteriol. **178:**6824–6832.
26. **Leveau, J. H. J., A. J. B. Zehnder, and J. R. van der Meer.** 1998. The *tfdK* gene product facilitates uptake of 2,4-dichlorophenoxyacetate by *Ralstonia eutropha* JMP134(pJP4). J. Bacteriol. **180:**2237–2243.
27. **Matrubutham, U., and A. R. Harker.** 1994. Analysis of duplicated gene sequences associated with *tfdR* and *tfdS* in *Alcaligenes eutrophus* JMP134. J. Bacteriol. **176:**2348–2353.
28. **McFall, S. M., S. A. Chugani, and A. M. Chakrabarty.** 1998. Transcriptional activation of the catechol and chlorocatechol operons: variations on a theme. Gene **223:**257–267.
29. **McFall, S. M., T. J. Klem, N. Fujita, A. Ishihama, and A. M. Chakrabarty.** 1997. DNase I footprinting, DNA bending and *in vitro* transcription analyses of ClcR and CatR interactions with the *clc*ABD promoter: evidence of a conserved transcriptional activation mechanism. Mol. Microbiol. **24:**965–976.
30. **Ogawa, N., S. M. McFall, T. J. Klem, K. Miyashita, and A. M. Chakrabarty.** 1999. Transcriptional activation of the chlorocatechol degradative genes of *Ralstonia eutropha* NH9. J. Bacteriol. **181:**6697–6705.
31. **Ogawa, N., and K. Miyashita.** 1999. The chlorocatechol-catabolic transposon Tn*5707* of *Alcaligenes eutrophus* NH9, carrying a gene cluster highly homologous to that in the 1,2,4-trichlorobenzene-degrading bacterium *Pseudomonas* sp. strain P51, confers the ability to grow on 3-chlorobenzoate. Appl. Environ. Microbiol. **65:**724–731.
32. **Ogawa, N., and K. Miyashita.** 1995. Recombination of a 3-chlorobenzoate catabolic plasmid from *Alcaligenes eutrophus* NH9 mediated by direct repeat elements. Appl. Environ. Microbiol. **61:**3788–3795.
33. **Parsek, M. R., S. M. McFall, D. L. Shinabarger, and A. M. Chakrabarty.** 1994. Interactions of two LysR-type regulatory proteins CatR and ClcR with heterologous promoters: functional and evolutionary implications. Proc. Natl. Acad. Sci. USA **91:**12393–12397.
34. **Pérez-Pantoja, D., L. Guzmán, M. Manzano, D. H. Pieper, and B. González.** 2001. Role of $tfdC_ID_IE_IF_I$ and $tfdD_{II}C_{II}E_{II}F_{II}$ gene modules in catabolism of 3-chlorobenzoate by *Ralstonia eutropha* JMP134(pJP4). Appl. Environ. Microbiol. **66:**1602–1608.
35. **Pieper, D. H., K.-H. Engesser, R. H. Don, K. N. Timmis, and H.-J. Knackmuss.** 1985. Modified *ortho*-cleavage pathway in *Alcaligenes eutrophus* JMP134 for the degradation of 4-methylcatechol. FEMS Microbiol. Lett. **29:**63–67.
36. **Pieper, D. H., H.-J. Knackmuss, and K. N. Timmis.** 1993. Accumulation of 2-chloromuconate during metabolism of 3-chlorobenzoate by *Alcaligenes eutrophus* JMP134. Appl. Microbiol. Biotechnol. **39:**563–567.
37. **Pieper, D. H., W. Reineke, K.-H. Engesser, and H.-J. Knackmuss.** 1988. Metabolism of 2,4-dichlorophenoxyacetic acid, 4-chloro-2-methylphenoxyacetic acid and 2-methylphenoxyacetic acid by *Alcaligenes eutrophus* JMP 134. Arch. Microbiol. **150:**95–102.
38. **Pieper, D. H., K. Stadler-Fritzsche, K.-H. Engesser, and H.-J. Knackmuss.** 1993. Metabolism of 2-chloro-4-methylphenoxyacetate by *Alcaligenes eutrophus* JMP 134. Arch. Microbiol. **160:**169–178.
39. **Prucha, M., A. Peterseim, K. N. Timmis, and D. H. Pieper.** 1996. Muconolactone isomerase of the 3-oxoadipate pathway catalyzes dechlorination of 5-chloro-substituted muconolactones. Eur. J. Biochem. **237:**350–356.
40. **Prucha, M., V. Wray, and D. H. Pieper.** 1996. Metabolism of 5-chlorosubstituted muconolactones. Eur. J. Biochem. **237:**355–366.
41. **Ravatn, R., S. Studer, D. Springael, A. J. B. Zehnder, and J. R. van der Meer.** 1998. Chromosomal integration, tandem amplification, and deamplification in *Pseudomonas putida* F1 of a 105-kilobase genetic element containing the chlorocatechol degradative genes from *Pseudomonas* sp. strain B13. J. Bacteriol. **180:**4360–4369.
42. **Schenzle, A., H. Lenke, P. Fischer, P. A. Williams, and H.-J. Knackmuss.** 1997. Catabolism of 3-nitrophenol by *Ralstonia eutropha* JMP 134. Appl. Environ. Microbiol. **63:**1421–1427.
43. **Schlömann, M., E. Schmidt, and H.-J. Knackmuss.** 1990. Different types of

Downloaded from http://jb.asm.org/ on September 3, 2020 at Corteva Agriscience

COR-AAD1-00002781
Bayer EX1008 (Part 5 of 9)

dienelactone hydrolase in 4-fluorobenzoate-utilizing bacteria. J. Bacteriol. **172:**5112–5118.
44. **Schmidt, E., and H.-J. Knackmuss.** 1980. Chemical structure and biodegradability of halogenated aromatic compounds. Conversion of chlorinated muconic acids into maleoylacetic acid. Biochem. J. **192:**339–347.
45. **Seibert, V., K. Stadler-Fritzsche, and M. Schlömann.** 1993. Purification and characterization of maleylacetate reductase from *Alcaligenes eutrophus* JMP134(pJP4). J. Bacteriol. **175:**6745–6754.
46. **Solyanikova, I. P., O. V. Maltseva, M. D. Vollmer, L. A. Golovleva, and M. Schlömann.** 1995. Characterization of muconate and chloromuconate cycloisomerase from *Rhodococcus erythropolis* 1CP: indications for functionally convergent evolution among bacterial cycloisomerases. J. Bacteriol. **177:**2821–2826.
47. **Streber, W. R., K. N. Timmis, and M. H. Zenk.** 1987. Analysis, cloning, and high-level expression of 2,4-dichlorophenoxyacetate monooxygenase gene *tfdA* of *Alcaligenes eutrophus* JMP134. J. Bacteriol. **169:**2950–2955.
48. **van der Meer, J. R., R. I. L. Eggen, A. J. B. Zehnder, and W. M. de Vos.** 1991. Sequence analysis of the *Pseudomonas* sp. strain P51 *tcb* gene cluster, which encodes metabolism of chlorinated catechols: evidence for specialization of catechol 1,2-dioxygenases for chlorinated substrates. J. Bacteriol. **173:**2425–2434.
49. **van der Meer, J. R., C. Werlen, S. F. Nishino, and J. C. Spain.** 1998. Evolution of a pathway for chlorobenzene metabolism leads to natural attenuation in contaminated groundwater. Appl. Environ. Microbiol. **64:**4185–4193.
50. **Vollmer, M. D., P. Fischer, H.-J. Knackmuss, and M. Schlömann.** 1994. Inability of muconate cycloisomerases to cause dehalogenation during conversion of 2-chloro-*cis,cis*-muconate. J. Bacteriol. **176:**4366–4375.
51. **Vollmer, M. D., U. Scheli, V. Seibert, S. Lakner, and M. Schlömann.** 1999. Substrate specificities of the chloromuconate cycloisomerases from *Pseudomonas* sp. B13, *Ralstonia eutropha* JMP134 and *Pseudomonas* sp. P51. Appl. Microbiol. Biotechnol. **51:**598–605.
52. **Vollmer, M. D., and M. Schlömann.** 1995. Conversion of 2-chloro-*cis,cis*-muconate and its metabolites 2-chloro- and 5-chloromuconolactone by chloromuconate cycloisomerases of pJP4 and pAC27. J. Bacteriol. **177:**2938–2941.

Downloaded from http://jb.asm.org/ on September 3, 2020 at Corteva Agriscience

COR-AAD1-00002782
Bayer EX1008 (Part 5 of 9)

ACADEMIC PRESS

Plasmid 48 (2002) 1–12

PLASMID

www.academicpress.com

Complete characterisation of Tn*5530* from *Burkholderia cepacia* strain 2a (pIJB1) and studies of 2,4-dichlorophenoxyacetate uptake by the organism

R.P-C. Poh, A.R.W. Smith, and I.J. Bruce*

Norwood Laboratory, School of Chemical and Life Sciences, University of Greenwich, Wellington St., London SE18 6PF, UK

Received 25 July 2001, revised 29 April 2002

Abstract

The complete genetic characterisation of Tn*5530* in *Burkholderia cepacia* strain 2a (pIJB1) has been accomplished, indicating that it is a Tn*3*-like transposon with a complex structure bearing operons for the catabolism of 2,4-dichlorophenoxyacetate (2,4-D) and malonate. Tn*5530* is terminated at both ends by the IS*1071*::IS*1471* element and the 2,4-D- and malonate-dissimilatory operons are separated by a region encoding a *putA* and *lrp* gene and a gene encoding a chloride channel protein. The chloride channel protein may have a role in the expulsion of chloride ions liberated by the dissimilation of 2,4-D. In addition, a putative transposase with a high level of sequence similarity to those of plasmid pGH1 from *Xanthomonas campestris* pv. *vesicatoria* and *Pseudomonas syringae* pv. *glycinea*, and a transcription factor similar to those of the TetR family with low but significant levels of sequence similarity to those identified in a number of other organisms was observed. The entire Tn*5530* sequence length, including the IS*1071*::IS*1471* elements, was found to be 40,956 bp, and pIJB1 was replicon-typed and otherwise characterised as being of the IncP-1β subgroup, bearing *merA* and *merD* genes conferring resistance to mercuric chloride. The rate of uptake of 2,4-D by *B. cepacia* strain 2a was observed to proceed more readily at acid pH, suggesting involvement of the undissociated form of the compound. Uptake did not show saturation kinetics, was concentration-dependent, and appeared to occur in two stages; an initial accumulation followed by a linear second phase. Uptake could be inhibited by sodium azide but not by arsenate, *N*,*N*′-dicyclohexylcarbodiimide (DCCD) or carbonylcyanide *m*-chlorophenyl-hydrazone (CCCP) suggesting that it is not energy-dependent. © 2002 Elsevier Science (USA). All rights reserved.

Keywords: 2,4-D; Tn*5530*; IS*1071*::*1471*; pIJB

1. Introduction

Burkholderia cepacia strain 2a utilises 2,4-dichlorophenoxyacetate (2,4-D) as a sole carbon source. The organism was isolated from soil by enrichment culture in 2,4-D-salts medium, and was initially identified at the National Collection of Industrial and Marine Bacteria (NCIMB), Aberdeen, UK, as a strain of *Acinetobacter* (Beadle and Smith, 1982), later amended to *Burkholderia cepacia* (Poh et al., 2001). 2,4-D is converted to 2,4-dichlorophenol by 2,4-D/

* Corresponding author. Fax: +(0)20-8331-8405.
E-mail address: i.j.bruce@gre.ac.uk (I.J. Bruce).

0147-619X/02/$ - see front matter © 2002 Elsevier Science (USA). All rights reserved.
PII: S0147-619X(02)00018-5

COR-AAD1-00002783
Bayer EX1008 (Part 5 of 9)

α-ketoglutarate dioxygenase, recently described by Poh et al. (2001) as resembling the isofunctional enzyme produced by *Alcaligenes eutrophus* JMP134 (Fukumori and Hausinger, 1993a,b). The second enzyme, 2,4-dichlorophenol hydroxylase [EC 1.14.13.20], originally described by Beadle and Smith (1982), produces 3,5-dichlorocatechol, which undergoes *ortho*-cleavage by dioxygenase attack to yield 2,4-dichloro-*cis*,*cis*-muconate. The ring-cleavage product is successively converted enzymically to 2-chloro-*cis*,*cis*-muconolactone, and 2-chloro-4-hydroxy-*cis*,*cis*-muconate (Smith, A.R.W.; unpublished work). Strain 2a contains the plasmid pIJB1, which carries the genes for 2, 4-D dissimilation in the resident Tn*3*-like transposon, Tn*5530* (Aathithan, 1992). Tn*5530* is spontaneously lost from pIJB1 to yield the deletion derivative pIJB2, which has also been isolated and characterised (Aathithan, 1992; Xia et al., 1996, 1998). The full structures of pIJB1 and pIJB2, together with that of Tn*5530* and the accompanying unique IS elements IS*1071*::IS*1471*, were reported by Oswiecimska (1994) and Xia et al. (1996, 1998). Besides strain 2a, a number of other bacteria are capable of the complete mineralisation of 2,4-D via succinate and acetyl-CoA, having been described recently elsewhere, e.g., Laemmli et al. (2000), Perez-Pantoja et al. (2000), Vedler et al. (2000a,b), and Bhat et al. (1994).

Burkholderia cepacia strain 2a was the first 2,4-D-utilising organism in which a putative Tn*3*-like structure was proposed which carried the dissimilatory operon, and the first in which a hybrid IS element, IS*1071*::IS*1471*, was identified which potentially allows excision but not reintegration of the intervening gene sequences (Xia et al., 1996, 1998).

Even though it is now known that other 2,4-D-dissimilatory organisms also carry what are likely to be composite transposon-like structures, the complete characterisation of such a structure has not until now been accomplished.

2. Materials and methods

2.1. Bacterial strains, plasmids, and growth conditions

Burkholderia cepacia 2a (pIJB1), mutant strain 2a-1 (pIJB2), and *Ralstonia eutropha* JMP134 (pJP4) were maintained and cultured on minimal-salts medium supplemented with either 2.26 mM 2,4-D or 6 mM sodium succinate (Poh et al., 2001). When required, minimal-salts medium was further supplemented with antibiotics and heavy metals (see Section 3). *Escherichia coli* NCIMB 11963, carrying RP4, was obtained from the NCIMB (Aberdeen, UK) and cultured according to their instructions. *E. coli* strains JM109, DH10B, and TOP10 (Invitrogen BV, Groningen, Netherlands) were routinely employed as cloning hosts and were maintained and cultured on LB medium containing the appropriate antibiotic.

2.2. Uptake assay

Cells were grown to early log phase ($OD_{550\,nm} \approx 0.3$), harvested, washed, and resuspended to a density of 0.3 mg dry cells ml^{-1} in ice-cold phosphate buffer pH 6.5. 2,4-D uptake was initiated by the addition of 2,4-dichloro-[ring-U-^{14}C]-phenoxyacetic acid (specific activity 46 mCi $mmol^{-1}$; Amersham plc, Cardiff, UK) to the pre-warmed cell suspension which was incubated at 25 °C with gentle agitation. Cells were harvested at intervals up to 120 s by vacuum filtration, by transferring 1 ml of suspension onto a sterile 0.2 μm pore size nitrocellulose membrane at specific time intervals in a Millipore sampling manifold (Millipore, Watford, UK). After filtration, membranes bearing cells were immediately washed with 10 aliquots of 1 ml uptake washing buffer (10 mM Tris–HCl, pH 6.8) containing 10 mM sodium azide, and subsequently transferred into liquid scintillation vials containing 10 ml Ultima GOLD MV scintillation cocktail (Packard Instruments, Pangbourne, UK), and scintillation counted for 30 min using a Packard Tricarb 2000-CA liquid scintillation analyser (Packard Instruments).

2.3. Isolation and manipulation of plasmid DNA

Plasmids pIJB1, pIJB2, and pJP4 were isolated as described previously (Xia et al., 1998). Alkaline lysis (Sambrook et al., 1989), in conjunction with a Promega wizard DNA clean-up kit (Promega UK, Southampton, UK), was used to isolate and purify plasmid pUC19, pBluescript II SK(+), and pCR-XL-TOPO from *E. coli* strains for cloning and sequencing experiments. DNAs were otherwise manipulated and analysed using standard methods (Hanahan et al., 1995; Sambrook et al., 1989). Restriction endonucleases obtained from Roche Diagnostics (Basel, Switzerland) were used according to manufacturer's instructions, and

COR-AAD1-00002784
Bayer EX1008 (Part 5 of 9)

DNA fragments resolved in LMP agarose gels were recovered using a Roche High-Pure PCR product purification kit (Roche Diagnostics) according to manufacturer's instructions.

2.4. Strategy for Tn5530 characterisation

Part of the genetic characterisation of Tn*5530* was based upon Southern hybridisation of pIJB1 restriction digested DNA with heterologous probes generated by PCR from pJP4 template DNAs using primers directed to conserved regions of the specific gene sequences, *tfdA*, *B*, and *D*, known to be present on the two plasmids. This was followed by long PCR of regions of Tn*5530* using combinations of the same primers and ones whose target sites lay within the terminal IS*1071*::IS*1471* elements, and degenerate primers designed from the N-terminal amino-acid sequence of 2,4-D/α-ketoglutarate dioxygenase (Poh et al., 2001). Products were cloned, restriction digested, and sequenced.

Specific genes other than those involved in 2,4-D dissimilation were identified by hybridisation and direct amplification using primers/probes derived from the *MerA* and *D* genes (present on pJP4), while replicon typing of pIJB1 was done by the method of Couturier et al. (1988), supplemented by that of Gotz et al. (1996).

Other regions of Tn*5530* were characterised by direct cloning and sequencing restriction digestion fragments of the transposon.

For a full description of the primers used in this part of the study, see Table 1.

2.5. PCR

PCR was routinely performed in a Progene thermal cycler (Techne [Cambridge], Duxford, UK) using the following protocol: initial

Table 1
Oligonucleotide primers and probes

Origin	Sequences (5′ → 3′)	Reference
Gene specific primer for PCR and probe constriction		
TfdA/pJP4	Forward—ATCGCCTTCGCGCGCAATTTC	Accession No. M16730
	Reverse—ATCACCAGATCTCCCACGTTC	
TfdB/pEST4011	Forward—CCGCGCTCGCACATCACCA	Accession No. U32188
	Reverse—GATCGEAGGAAAATCCCCAAG	
TfdD/pJP4	Forward—GTATCTCGCGCCCCACCTCCTC	Accession No. M65097
	Reverse—TTGCTTCCGCGACCGCTGCTATCT	
Long PCR primers		
TfdC/pEST4011	AAGACATACGACAGCGATGACCACAA	
ALα/hdA protein	CCGACGAAAAGTGGATGAAGGTATTC	Poh et al., 2001
AUα/hdA protein	GAATACCTTCATCCACTTTTCGTCGG	Poh et al., 2001
ISL/IS*1071*::IS*1471*	AACGCCGTCTCATCGCCCCAGTGAAT	Accession No. U67938
Incompatibility typing		
KorA	Forward—ATGAAGAAACGGCTAACCGA	Gotz et al., 1996
	Reverse—TTCCTGTTTCCTCTTGGCGTC	
OriT	Forward—CAGCCTCGCAGAGCAGGAT	Gotz et al., 1996
	Reverse—CAGCCGGGCAGGATAGGTGAAGT	
TrfA2	Forward—CGAAATTCGTGTGGGAGAAGTA	Gotz et al., 1996
	Reverse—CGCTTGCAATGCACCAGGTC	
Mercury gene detection		
MerA/pJP4	Forward—CCACCACGCACGGTGAATTGC	Accession No. AF225974
	Reverse—CCAGTTCCTGCACCGTCATGC	
MerD/pJP4	Forward—GTGAGCGTGCATATCGTGCG	Accession No. AF225974
	Reverse—GCCAACTGCACTTCCAGATCG	
Replicon typing		
IncP1 specific probe pULB2420 (750 bp *Hae*II fragment derived from the *inc*/*rep* functions of RP4 by restriction digestion).		Couturier et al., 1988

COR-AAD1-00002785
Bayer EX1008 (Part 5 of 9)

denaturation at 94 °C for 4 min; then 30 cycles of 94 °C for 30 s; 30 s at the annealing temperature (see Section 3), and 72 °C for 1 min. Finally the samples were held at 72 °C for 5 min. A typical amplification reaction consisted of 10 ng template DNA, 1× PCR buffer (10 mM Tris–HCl, pH 8.0, 50 mM KCl, 1.5 mM $MgCl_2$, 0.1% [w/v] Triton), 0.2 μmol of each primer, 0.2 mmol of each dNTP, 2.5 U *Taq* DNA polymerase (Bioline, London, UK) in a total volume of 50 μl molecular biology grade water (Sigma–Aldrich, Poole, UK) in a 0.5-ml thin-walled Eppendorf tube. Reaction mixtures were stored on ice during preparation, and enzyme was added immediately prior to thermal cycling. An Expand Long Template PCR Kit (Roche Diagnostics) was used to amplify DMA fragments larger than 2 kb, and PCR reactions were carried out according to manufacturer's instructions, in a Progene thermal cycler.

2.6. DNA probe synthesis

DIG-labelled probes were synthesised by incorporation of digoxigenin (DIG)-modified dUTP during PCR using a PCR probe synthesis kit (Roche Diagnostics) according to manufacturer's instructions, and were purified by LMP agarose gel electrophoresis prior to their use in hybridisations.

2.7. Southern-blot hybridisation analysis

Plasmids pIJB1, pIJB2, and pJP4 were digested with restriction endonucleases overnight at 37 °C. DNA fragments were resolved by electrophoresis in 0.8% TAE agarose gels and transferred to nylon hybridisation membranes (Roche Diagnostics; Sambrook et al., 1989). Membranes were pre-hybridised for 10 min at 65 °C and subsequently hybridised at 65 °C for 16 h. After hybridisation, the membranes were washed twice with 20 ml of 2× SSC/0.1% (w/v) SDS at 25 °C for 5 min, and twice in 20 ml of pre-warmed 0.1% (w/v) SSC/0.1% (w/v) SDS at 65 °C for 15 min. Detection of probe/target hybrids was performed using a DIG-nucleic acid detection kit (Roche Diagnostics.) according to manufacturer's instructions.

2.8. DNA cloning and sequencing

Either (a) pIJB1 was single- or double-digested with restriction endonucleases *Bam*HI, *Eco*RV and/or *Kpn*I, and DNA fragments within Tn*5530* were separated by 0.8% TAE agarose gel electrophoresis and cloned into pUC19 or pBluescript; or (b) internal Tn*5530* regions were PCR amplified from pIJB1 plasmid DNA using specific primers, and then cloned into pCR-XL-TOPO vector (Invitrogen).

Major clones were then subjected to sub-cloning to produce smaller fragments for sequence analysis.

Alternatively, DNA templates for sequencing were generated using an EZ::TN ⟨Kan-2⟩ insertion kit (Cambio, Cambridge, UK) according to manufacturer's instructions.

DNA sequencing was carried out either manually, using the Sanger dideoxy chain termination method with autoradiographic detection of products, or by cycle sequencing and detection in an ABI7700 automated sequencer (Applied Biosystems, Warrington, UK).

2.9. DNA sequence data analysis

DNA sequence data were analysed using software provided by the National Center for Biotechnology Information (NCBI, Bethesda, USA) and the Swiss Institute of Bioinformatics (SIB, Geneva, Switzerland) via the Internet. Default parameters of the programs were used in analysis.

2.10. B. cepacia strain 2a curing

E. coli bearing the IncP temperature-sensitive RP1 derivative, pMR5 (Robinson et al., 1980), was mated with *B. cepacia* strain 2a using a filter-based method (Maclean, 1997). Transconjugants were selected for pMR5-encoded kanamycin, tetracycline, and ampicillin resistance on both succinate minimal-salts medium and *Pseudomonas* isolation agar (Difco, West Molesey, UK). As negative controls, both donor and recipient strains were also plated on to the media. A number of transconjugants shown to be 2,4-D^- had their total cellular DNA isolated (Marmur, 1961) and probed with a radio-labelled pIJB1 *Eco*RV E9 fragment (1.3 kb—a 'plasmid backbone' fragment). When no signal was observed, indicating pIJB1 was absent in the clones, pMR5 was subsequently removed from the recipient *B. cepacia* strains by culturing at 42 °C for 48 h in LB broth (Robinson et al., 1980).

2.11. Replicon typing

The hybridisation-based replicon typing method of Couturier et al. (1988) was used to

COR-AAD1-00002786
Bayer EX1008 (Part 5 of 9)

classify plasmid pIJB1 with respect to incompatibility type. The IncP specific probe pULB2420 (750 bp *Hae*II fragment from the inc/rep functions of RP4 (Couturier et al., 1988) was radio-labelled using a random prime labelling kit (Amersham plc.) and employed in Southern-blot analysis of restriction digested pIJB1 DNA.

2.12. Heavy-metal minimum inhibitory concentrations

Cell suspensions of *B. cepacia* (strains 2a, 2a-1, and a cured derivative [see Section 3]) were spread on succinate minimal-salts agar plates containing either $HgCl_2$, $CuSO_4$, $ZnCl_2$, $NiCl_2$, K_2CrO_4, or $CoCl_2$. These compounds were made up as 1 M stock solutions, sterilised by autoclaving, and added to partially cooled media. Concentrations used were: 0.1, 0.2, 0.3, 0.4, 0.5, 0.6, 0.7, 0.8, 0.9, 1, and 5 mM for $ZnCl_2$, $NiCl_2$, K_2CrO_4, $CoCl_2$, $CdCl_2$; 0.1, 0.3, 0.5, 1, 2, 3, 4, 5, 6, 7, 8, 9, and 10 mM for $CuSO_4$, and 0.01, 0.02, 0.03, 0.04, 0.05, 0.06, 0.07, 0.08, 0.09, and 0.1 mM for $HgCl_2$.

3. Results and discussion

3.1. Incompatibility group typing of plasmid pIJB2

It was observed that *B. cepacia* strain 2a could be cured with pMR5 and that the resultant strain was unable to dissimilate 2,4-D. The loss of pIJB1 indicates that pMR5 and pIJB1 are incompatible and supports the view that pIJB1 is an IncP plasmid. The IncP specific probe (Couturier et al., 1988) was also observed to hybridise to the K2 (45 kb) fragment of *Kpn*I-digested pIJB1 DNA. Also, when primer pairs specific for IncP group gene sequences (*KorA*, *OriT*, and *TrfA2* [Gotz et al., 1996]) were employed in PCR analysis of pIJB2 (which was used rather than pIJB1 as it was easier to isolate), products were generated possessing the expected size and greater than 86.2% identity with the corresponding RP4 sequences (data not shown).

DIG-labelled *MerA* and *MerD*-specific probes prepared by PCR from pJP4 template DNA were also observed to hybridise to the E1 (7.1 kb) and E3 (33.7 kb) fragments, respectively, of *Eco*RV digested, Southern blotted, pIJB2 DNA (data not shown).

Their presence was confirmed by PCR using specific primer pairs towards *MerA* and *MerD* genes (Table 1). DNA fragments with the expected size were amplified from pIJB2 and when the products were cloned they were observed to be at least 91.7% identical with the corresponding region of the *MerA* and *MerD* genes of pJP4.

These results strongly suggest that pIJB1 is an IncP-1β plasmid.

3.2. Heavy metal resistance

The only resistance which could be associated with pIJB1, and to a lesser extent pIJB2, was that towards mercuric chloride, where there were small but distinct differences between the MICs of strains bearing pIJB1 (0.05 mM) and pIJB2 (0.03 mM), and the cured strain (0.02 mM). Since Tn*5530* bears no genes for mercury resistance, it is puzzling that mercury susceptibility is slightly enhanced when the transposon is eliminated. Possibly the loss of the genes in Tn*5530* perturbs the organism's physiology enough to produce this effect: at least one of the proposed genes present on Tn*5530* is known to encode a protein which is membrane-associated in other organisms. These observations lend weight to the genetic analysis reported above, indicating the presence of *mer* genes on the plasmid backbone.

3.3. 2,4-D uptake characteristics in B. cepacia strain 2a and strain 2a-1

Uptake of 2,4-D by strain 2a followed a curvilinear course at all 2,4-D concentrations tested. A rapid accumulation of 2,4-D occurred within the first 10 s of incubation, which was followed by a slower, linear uptake from 10 to 120 s. Both the degree of initial accumulation and subsequent linear rate of 2,4-D uptake were observed to be dependent on the external 2,4-D concentration (Fig. 1A and B).

A comparison of the 2,4-D uptake profiles for strain 2a cells cultured in minimal-salts medium containing 2,4-D or sodium succinate and strain 2a-1 cells cultured in succinate minimal-salts medium indicated that strain 2a took up 2,4-D whether or not it had previously been grown on that substrate. However, succinate-cultured strain 2a cells took up slightly less 2,4-D than 2,4-D-grown cells. Strain 2a-1 did not take up 2,4-D at all (Fig. 1A and B).

A Lineweaver–Burk plot of kinetic data for the uptake of 2,4-D at different 2,4-D concentrations yielded a line that passed through the origin of both axes, indicating values for V_{max} and K_m of infinity (data not shown), i.e., uptake did not display

COR-AAD1-00002787
Bayer EX1008 (Part 5 of 9)

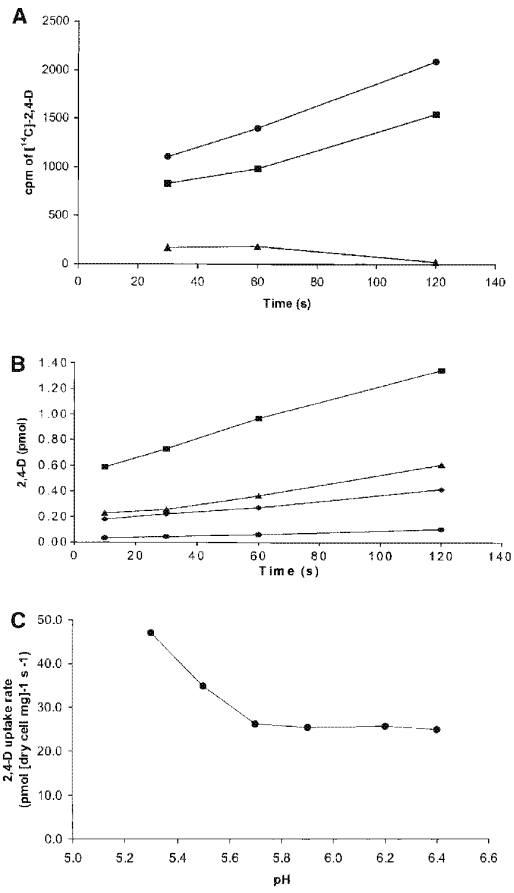


Fig. 1. (A) [^{14}C]2,4-D uptake by *B. cepacia* strain 2a and 2a-1. The 2,4-D uptake profiles of *B. cepacia* 2a and strain 2a-1 were investigated using [^{14}C]2,4-D as described in Sections 2 and 3. Key: (●) Strain 2a—2,4,-D cultured; (■) Strain 2a—succinate cultured; (▲) Strain 2a-1—succinate cultured. (B) Effect of [^{14}C]2,4-D concentration on uptake by *B. cepacia* strain 2a. The effect of 2,4-D concentration on the uptake of [^{14}C]2,4-D was investigated as described in Section 2. Key: (●) 0.66 μM; (◆) 1.96 μM; (▲) 3.26 μM; (■) 6.5 μM. (C) [^{14}C]2,4-D uptake by *B. cepacia* 2a as a function of pH. The influence of pH on 2,4-D uptake by *B. cepacia* 2a was investigated by assay of [^{14}C]2,4-D taken up by cells suspended in phosphate buffer at pH values ranging from 5.3 to 6.4. Cell suspensions were sampled at intervals over 2 min, washed and counted by liquid scintillation (see Materials and methods) and the initial rates of uptake were determined over a period of 10–120 s incubation and plotted against pH.

saturation kinetics and therefore an enzyme/transport protein was unlikely to be involved.

2,4-D uptake by strain 2a cells pre-incubated with various other metabolic inhibitors according to the method of Thayer and Wheelis (1982) showed that CCCP, an effective protonophore which destroys the proton gradient across the cell membrane, reduced the rate of transport by 14%; DCCD, an inhibitor of membrane-bound ATPase, and AsO_4^{3-}, an uncoupler of substrate-level and oxidative phosphorylation, reduced the rate of transport by 16% and 9%, respectively. However 2,4-D uptake was strongly affected by sodium azide, an electron transport inhibitor, where only 10% of the control uptake rate was observed. These results could suggest that 2,4-D uptake is not strictly energy related but rather depends on its own continuous metabolism within the cell and the creation of a metabolic drag effect. A similar mechanism has been suggested for the uptake of other compounds (Wong et al., 1994).

Additionally, pH exerted a significant effect on the rate of 2,4-D uptake by strain 2a, which increased with increasing acidity below pH 5.8 (Fig. 1C). To investigate this effect further, 3,3′-dimethylglutarate, which buffers down to pH 4.0, was used in other experiments, but no uptake was observed at lower pH values, which indicates that this buffer either interferes with 2,4-D uptake or metabolism, or affects cell viability. Although a candidate permease gene has been identified in Tn*5530*, whose analogues in other organisms are believed to be involved in 2,4-D uptake, there is no evidence that the protein is important in 2,4-D uptake by strain 2a. Instead, the data are consistent with a metabolic drag model in which 2,4-D ($pK_a = 2.64$) is taken up through the cell membrane as the free acid, which forms in significant amounts (about 1%) at approximately pH 5. Dissimilation in the cell then constitutes the source of the drag effect. The first two enzymes, oxygenases, require, respectively, α-ketoglutarate and NADPH, regeneration both of which may be inhibited when the electron transport system is inhibited by azide. Strain 2a-1 did not take up 2,4-D because the catabolic genes and the ability to dissimilate 2,4-D are absent.

Finally, 2,4-D grown strain 2a cells pre-incubated with an exogenous carbon source (succinate) to increase their metabolic activity possessed an increased rate of 2,4-D uptake (average factor of 2.7; data not shown).

3.4. Sequence analysis of Tn5530

In total, 29 complete opening reading frames (ORFs) were found to be present within the 36,642 kb of DNA sequenced. Initiation (ATG or GTG) and termination (TGA, TAA, or TAG)

COR-AAD1-00002788
Bayer EX1008 (Part 5 of 9)

codons were identified for all ORFs and most were seen to possess potential ribosome binding sites (rbs). Fourteen were orientated in the same sense whereas the rest were orientated in the opposite sense.

3.5. 2,4-D dissimilatory gene cluster (*tfd*)

A cluster of 2,4-D dissimilatory genes was identified to one end of Tn*5530*. Blast-N and -P analysis indicated that most of these genes and their flanking regions were nearly identical to DNA and protein sequences from *Variovorax paradoxus* TV (Accession No. AB028643) and plasmid pEST4011 from *Achromobacter xylosoxidans* subsp. *denitrificans* EST4002 (Vedler et al., 2000a,b). However neither the entire region covered by the dissimilatory operon nor all the genes involved has yet been completely characterised in the other two organisms. In fact, *V. paradoxus* has only been identified as possessing a cluster of gene sequences involved in 2,4-D dissimilation (location unidentified) whilst *Achromobacter xylosoxidans* possesses plasmid pEST4011 known to encode the ability to degrade 2,4-D. The gene sequences identified in *V. paradoxus* have been reported on GenBank only (*tfdD*, *R*, *C*, *E*, *B*, and *K*) whilst Vedler et al. (2000a,b) have recently identified the locations, organisation, and sequences of the *tfdF*, *A*, *K*, *B*, *C*, and *R* genes on plasmid pEST4011. The characterisation of both strains is incomplete in terms of both gene organisation and sequence related to 2,4-D dissimilation, and in the case of *A. xylosoxidans* the putative composite transposon-like structure resident on pEST4011 has yet to be fully characterised, although a mechanism has recently been published (Clement et al., 2001) for the gene duplication/rearrangement in pJP4.

In *B. cepacia* strain 2a (pIJB1), all the genes involved in the regulation and conversion of 2,4-D to 3-oxoadipate were located and sequenced, and observed to be organised in the following order: *tfdD*, *R*, *C*, *E*, *B*, *K*, *A*, and *F*. A further gene encoding indole acetamide hydrolase, *iaaH*, was observed to lie between the *tfdD* and *R* genes. All 2,4-D dissimilatory genes were orientated in the same sense, apart from *tfdR* that encodes a LysR-type transcription factor which was observed to be orientated in the opposite sense.

In the case of *A. xylosoxidans* pEST4011 it has been noted that the reported *tfdE* gene would be translated to a prematurely terminated protein as a consequence of a dinucleotide deletion (GC) at positions 73 and 74 (Vedler et al., 2000a,b). These researchers consequently decided that the protein product was inactive.

Comparison of the *tfdE* gene sequence from pIJB1 with that of pEST4011 indicates that the initiation codon is likely to be in a different position to that identified by Koiv et al. (1996). If the suggested position for the initiation codon for *tfdE* in the case of pIJB1 is accepted, then a putative rbs site can be observed to be present just upstream for translation of the reading frame. Also, no dinucleotide deletion was observed in the pIJB1 *tfdE* sequence, and the proposed pIJB1 *tfdE* gene is virtually identical to that of *V. paradoxus* (Fig. 2).

Four other ORFs were also identified within or close to the *tfd* gene cluster on Tn*5530*. One, located immediately downstream of *tfdD*, was observed to possess a potential rbs (GA rich) just upstream of the GTG start codon. It is predicted to encode a polypeptide of 337 amino acids, but a Blast-P search has failed to indicate that it possesses any significant similarity to other protein sequences in the databases. The three other candidate ORFs were all located between *tfdA* and *tfdF*, and overlap each other. Two are potentially orientated in the same sense, whilst the third is in the opposite sense. Only the shortest putative ORF was observed to possess a potential rbs, and it encodes a predicted polypeptide of 176 amino acids. None of these putative ORFs showed any similarity to any DNA or amino acid sequences in the databases following Blast-N and -P analysis.

The clustering of chlorocatechol genes into operons has been observed for many other organisms, e.g., *tfd* in pJP4 (as well as pEST4011), *clc* in pAC27, *tcb* in pP51, and *clc* in *Rhodococcus opacus* 1CP (Eulberg et al., 1998; Perkins et al., 1990; Schlomann, 1994; van der Meer et al., 1991). This may suggest that these genes move among bacterial strains as a 'module'.

It seems likely that pIJB1, pEST4011, and pJP4 are related, but possibly that they have evolved differently, as their physical sizes, restriction maps, and gene organisations are considerably different. We have observed that predicted protein translation products from both pJP4 module I and II *tfd* genes bear similarity to those of pIJB1. pIJB1 *tfdC*, *E*, and *B* are more similar to module II pJP4 analogues, whilst *tfdE* is equally similar to both module I and II analogues, and pIJB *tfdD* is more similar to the pJP4 module I analogue. This suggests that individual *tfd* gene sequences from pIJB1 may share a common

COR-AAD1-00002789
Bayer EX1008 (Part 5 of 9)

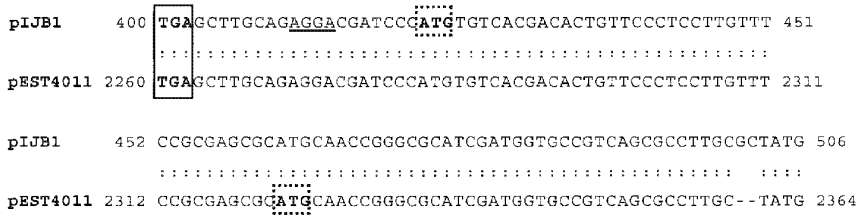


Fig. 2. Comparison of intragenic and immediate upstream nucleotide region of *tfd*C and *tfd*E of pIJB1 to that of pEST4011. □, indicates the location of the termination codons for the putative *tfdC* gene of pIJB1 and *tfdC* of PEST4011, and , indicates the possible locations of start codons for *tfdE* of PEST4011. The rbs site for the purposed *tfdE* gene on PIJB1 is underlined. Dashes in PEST4011 sequences indicate missing bases (pEST4011 position 2361–2362) compared to that of pIJB1.

ancestry with both pJP4 module I and II genes and that the pIJB1 *tfd* gene cluster may have resulted from a 'stitching together' of the module I and II genes (Table 2). The likelihood that pIJB1 and pEST4011 share a common ancestry seems more probable, despite the fact that their physical sizes (117 and 70 kb) and restriction maps are significantly different. Certain *Bam*HI and *Kpn*I pEST4011 digest fragments carrying the 2,4-D dissimilatory genes possess very similar sizes to that of pIJB1 (Mae et al., 1993), and coding sequences are organised in a similar fashion. Also, pEST4011 is relatively unstable, and like pIJB1, undergoes spontaneous deletion and simultaneous loss of 2,4-D dissimilatory ability, and is difficult to isolate from its original *Pseudomonas* sp. host (Mae et al., 1993).

With respect to regulatory genes, the reported location of *tfdS* on pEST4011 was not seen on pIJB1. The location of the *tfdS* gene in pEST4011 had been deduced by hybridisation using a *tfdS* probe derived from pJP4 (Mae et al., 1993), but in a separate hybridisation, using a *tfdR* probe (known to possess an identical sequence to *tfdS*), no hybridisation signal was observed (Mae et al., 1993; Matrubutham and Harker, 1994; You and Ghosal, 1995). Therefore the location of *tfdS* on pEST4011 could be doubtful, and this may explain its apparent absence on pIJB1.

The *tfdA* gene from pIJB1 shares great similarity with the *tfdA* gene of *Burkholderia* sp. RASC (Suwa et al., 1996) and this could suggest that they share a common origin. Biochemical studies of purified 2,4-D/α-ketoglutarate dioxygenase from *B. cepacia* strain 2a indicate that it is more similar structurally and functionally to that from *Burkholderia* sp. RASC than that from *R. eutropha* JMP134 (Poh et al., 2001). A major difference, however, is that the *tfdA* gene in *Burkholderia* sp. RASC is carried on the chromosome rather than the plasmid, pRASC, present in the strain.

See Fig. 3 for a full view of gene organisation, and Accession No. AF029344 for the full sequence.

3.6. Malonate dissimilatory gene cluster

In addition to the 2,4-D gene cluster, the opposite end of Tn*5530* was observed to encode

Table 2
Comparison of pJP4 module I and II and tfdR proteins with Tn*5530 tfd* gene encoded proteins

pIJB1	pJP4			
	Module I Accession No. M35097		Module II Accession No. U16732	
	Region (aa)[a]	Identity	Region (aa)[a]	Identity
TfdC	144/247	58%	224/250	89%
TfdE	No Blast-P result		182/234	77%
TfdB	363/581	62%	523/573	91%
TfdF	171/352	48%	157/352	44%
TfdD	237/638	64%	127/329	38%
TfdR	265/292	90% identity to Accession No. P10086		

COR-AAD1-00002790
Bayer EX1008 (Part 5 of 9)

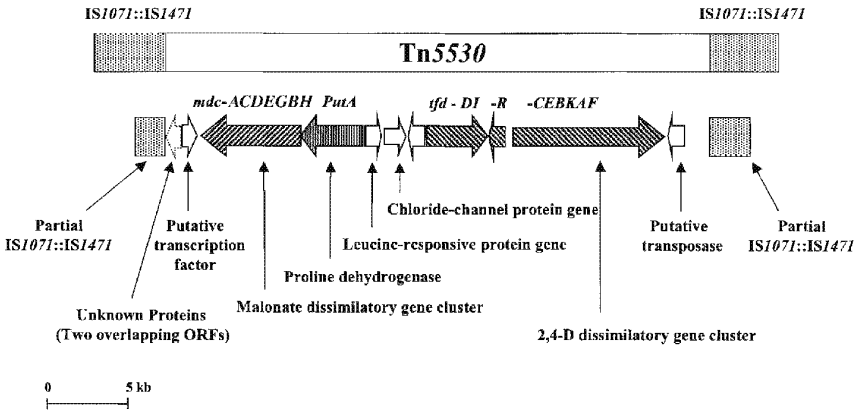


Fig. 3. Transposon Tn*5530*.

another gene cluster potentially concerned with the dissimilation of malonate. This gene cluster was located 7.41 kb upstream and orientated in the opposite sense to the 2,4-D dissimilatory gene cluster. Blast-N of this DNA region indicated that it possessed low degrees of similarity to other malonate dissimilatory gene sequences from *Pseudomonas putida* (Accession No. AB017138), *Klebsiella pneumoniae* (Accession No. U95087), and *Acinetobacter calcoaceticus* (Accession No. AF121266). However, computer-assisted translation of this DNA region and subsequent Blast-P analysis permitted the identification of seven genes that possessed varying degrees of identity (29–68%) to the malonate dissimilatory genes carried by numerous bacteria (Table 3). In fact it was observed that the malonate gene cluster was orientated and organised in an identical manner to that of *A. calcoaceticus* (Koo et al., 1997; Koo and Kim, 1999). However the *mdcI*, *L*, and *M* genes in *A. caloaceticus* encoding proteins involved in uptake, a carrier protein and a transcription factor, were not seen to be present on Tn*5530*. The malonate genes on pIJB were in the order, *mdcA*, *C*, *D*, *E*, *G*, *B*, and *H*.

The strains 2a and 2a-1 were tested for ability to grow on minimal-salts medium supplemented with 0.1% and 0.5% (w/v) malonate. Both strains grew, indicating that even if the Tn*5530* borne *mdc* gene analogues were active, the ability to utilise malonate for growth must also reside on the chromosome.

See Fig. 3 for a full view of gene organisation, and Accession No. AF029344 for the full sequence.

3.7. Proline bifunctional protein (*putA*)

Immediately upstream of the malonate gene cluster, a *putA* gene (3801 bp) was observed to be

Table 3
Blast-P comparison of malonate dissimilatory genes from *B. cepacia* Tn*5530* against those from other bacterial sources

B. cepacia Tn*5530*	Blast-P Score (percentage identity over number of residues); Overall length of protein (aa)			
	A. calcoaceticus (Koo et al., 1997 and Koo and Kim, 1999)	*P. putida* IAM1177 (Chohnan et al., 1999)	*K. pneumoniae* (Hoenke et al., 1997)	*M. rubra* (Berg et al., 1997)
MdcA 560 aa	68%[a]; 378/555	60%; 333/555	60%; 333/555	60%; 333/555
MdcC 108 aa	57%; 45/78	37%; 33/99	36%; 36/99	40%; 41/102
MdcD 297 aa	49%; 145/291	40%; 105/262	43%; 97/225	45%; 110/243
MdcE 233 aa	38%; 93/239	36%; 49/133	29%; 67/226	33%; 61/181
MdcG 230 aa	28%; 52/182	30%; 55/183	—	—
MdcB 290 aa	36%; 99/273	38%; 106/273	35%; 100/280	31%; 81/261
MdcH 302 aa	29%; 90/303	31%; 85/273	31%; 84/270	—

— Blast-P analysis using default parameters failed to indicate a similarity scoring.
[a] % identity, relating to the total number of amino acids in common over the length of sequence compared.

COR-AAD1-00002791
Bayer EX1008 (Part 5 of 9)

present. Blast-P analysis of the entire sequence indicated that it possessed moderately high degrees of similarity to that of *E. coli* strain 0157:H7 (63% identity over 1252 residues; Accession No. AP002554), *Sinorhizobium meliloti* strain GR4 (54% identity over 1256 residues; Accession No. Y08500), *Salmonella typhimurium* strain LT2 (63% over 1254 residues; Accession No. X70843), *Neisseria meningitidis* (50% over 1248 residues; Accession No. AE002396), and *Pseudomonas putida* (61% over 1244 residues; Accession No. AF153207) was observed. The *putA* encoded protein also showed 98.8% (over 340 residues) and 95.7% (over 468 residues) identity with proline dehydrogenase and aldehyde dehydrogenase-conserved domains, when analysed using RPS-Blast.

3.8. Leucine-responsive regulatory factor

A *lrp* gene was identified adjacent to *putA* but orientated in the opposite sense. Blast-P analysis of the translated sequence showed that it possessed a moderately high degree of similarity to the leucine-responsive regulatory proteins of *Bradyrhizobium japonicum* strain USDAI110 (64% identity over 148 residues; Accession No. U85623), *Klebsiella aerogenes* strain W70 (57% identity over 152 residues; Accession No. AF090144), *Salmonella typhimurium* (57% identity over 152 residues; Accession No. U02273), and *E. coli* (57% identity over 152 residues; Accession No. M35869). RPS-Blast analysis of the lrp protein showed that the sequence possessed 99.1% (over 108 residues) and 98.1% (over 104 residues) identity over two regions of the AsnC-type regulatory protein conserved domains.

3.9. Chloride-channel protein

An ORF just downstream of the lrp sequence and orientated in the same sense was identified as encoding a chloride-channelling protein. The predicted protein showed a low but significant degree of similarity to that of *Mesorhizobium loti* strain MAFF30399 (39% identity over 448 residues; Accession No. AP003004) and *Neisseria meningitidis* (36% identity over 431 residues; Accession No. AE002550). RPS-Blast analysis of the chloride channel-like protein also indicated that it possessed 95.4% (over 370 residues) identity to a voltage-gated chloride-channel conserved domain. This protein may have a role to play in the expulsion of Cl^- ions liberated by the dissimilation of 2,4-D.

3.10. Other ORFs

An ORF located downstream of the *mdc* gene cluster, but orientated in opposite sense, was shown to exhibit sequence similarity to a putative TetR-like transcription factor from *Caulobacter crescentus* (29% over 204 residues; Accession No. AE005706) and *Pseudomonas aeruginosa* strain PA01 (30% identity over 210 residues; Accession No. AE004725).

Between the region of the *tfdD* analogue and the ORF encoding the chloride-channel protein, another ORF was identified which exhibited a relatively high degree of similarity at the protein level to a transposase from *Ralstonia metalliduran*s (70% identity over 209 residues; Accession No. AF236817), mainly in the C-terminal region.

A further ORF located downstream from the 2,4-D dissimilatory gene cluster, and orientated in opposite sense, was also observed. A rbs could not be identified for this sequence but the ORF was predicted to encode a protein 327 amino-acids in length. Blast-N analysis identified two regions of the DNA sequence possessing high degrees of similarity to a transposase gene carried on an IS from *Xanthomonas campestris* pv. *vesicatoria* (87% and 85% identity over 125 and 141 bases, respectively; Kousik and Ritchie, 1998), *Xanthomonas campestris* pv. *dieffenbachiae* ([IS*1051*] 84% and 82% identity over 150 and 110 bases; Berthier et al., 1994), plasmid pPGHI (85% and 84% identity over 125 and 121 bases, respectively; Accession No. AF052751) and pEST1226 (84% over 125 and 121 bases; Kallastu et al., 1998). Blast-P of the predicted protein also indicated the same fact with the three most significant matches being plasmid pPGHI (59% identity and 71% similarity over 309 residues; Accession No. AF052751), *Xanthomonas campestris* pv. *vesicatoria* (60% identity and 70% similarity over 319 residues; Kousik and Ritchie, 1998) and *Pseudomonas syringae* pv. *glycinea* (58% identity and 70% similarity over 315 residues; Rangaswamy et al., 1998). This ORF was tentatively designated as a transposase of unknown function.

3.11. IS*1071*::IS*1471*

Both copies of IS*1071*::IS*1471* were partially sequenced. Alignment analysis of the right-partial IS*1071*::IS*1471* sequence showed that several bases were different to the published sequence (Xia et al., 1998). The presence of three extra bases position (IS*1071*::IS*1471* 555–557), a single base deleted

COR-AAD1-00002792
Bayer EX1008 (Part 5 of 9)

(IS*1071*::IS*1471* position 892), and a substitution of adenine for guanine (IS*1071*::IS*1471* position 1159) was observed. Alignment of the left-partial (IS*1071*::IS*1471* sequence indicated that a short sequence of 84 bp was completely different, including a 6-base substitution and 3-base insertions to that of Xia et al. (1998) and this may suggest that the two terminal copies of IS*1071*::IS*1471* on Tn*5530* may not be identical.

References

Aathithan, S., 1992. Molecular genetics of 2,4-dichlorophenoxyacetate (2,4-D) degradation in *Pseudomonas cepacia* 2a. M.Sc. Thesis. University of Greenwich, London.

Beadle, C.A., Smith, A.R.W., 1982. The purification and properties of 2,4-dichlorophenol hydroxylase from a strain of *Acinetobacter* species. Eur. J. Biochem. 123, 323–332.

Berg, M., Hilbi, H., Dimroth, P., 1997. Sequence of a gene cluster from *Malonomonas rubra* encoding components of the malonate decarboxylase Na^+ pump and evidence for their function. Eur. J. Biochem. 245, 103–115.

Berthier, Y., Thierry, D., Lemattre, M., Guesdon, J.L., 1994. Isolation of an insertion sequence (IS*1051*) from *Xanthomonas campestris* pv. *dieffenbachiae* with potential use for strain identification and characterization. Appl. Environ. Microbiol. 60, 377–384.

Bhat, M.A., Tsuda, M., Horiike, K., Nozaki, M., Vaidyanathan, C.S., Nakazawa, T., 1994. Identification and characterization of a new plasmid carrying genes for degradation of 2,4-dichlorophenoxyacetate from *Pseudomonas cepacia* CSV90. Appl. Environ. Microbiol. 60, 307–312.

Chohnan, S., Kurusu, Y., Nishihara, H., Takamura, Y., 1999. Cloning and characterization of *mdc* genes encoding malonate decarboxylase from *Pseudomonas putida*. FEMS Microbiol. Lett. 174, 311–319.

Clement, P., Pieper, D.H., Gonzalez, B., 2001. Molecular characterization of a deletion/duplication rearrangement in *tfd* genes from *Ralstonia eutropha* JMP134 (pJP4) that improves growth in 3–chlorobenzoic acid but abolishes growth on 2,4-dichlorophenoxyacetic acid. Microbiology 147, 2141–2148.

Couturier, M., Bex, F., Bergquist, P.L., Maas, W., 1988. Identification and classification of bacterial plasmids. Microbiol. Rev. 52, 375–395.

Eulberg, D., Kourbatova, E.M., Golovleva, L.A., Schlomann, M., 1998. Evolutionary relationship between chlorocatechol catabolic enzymes from *Rhodococcus opacus* 1CP and their counterparts in proteobacteria: sequence divergence and functional convergence. J. Bacteriol. 180, 1082–1094.

Fukumori, F., Hausinger, R.P., 1993a. *Alcaligenes eutrophus* JMP 134 2,4-dichlorophenoxyacetate monooxygenase is an α-ketoglutarate dependent dioxygenase. J. Bacteriol. 175, 2083–2086.

Fukumori, F., Hausinger, R.P., 1993b. Purification and characterisation of 2,4-dichlorophenoxyacetate/α-ketoglutarate dioxygenase. J. Biol. Chem. 268, 24311–24317.

Gotz, C., Pukhall, R., Smit, E., Tietze, E., Prager, R., Tschape, H., van Elsas, J.D., Smalla, K., 1996. Detection and characterization of broad-host-range plasmids in environmental bacteria by PCR. Appl. Environ. Microbiol. 62, 2621–2628.

Hanahan, D., Jessee, J., Bloom, F.R., 1995. Techniques for transformation of *Escherichia coli*. In: Glover, D.M., Hames, B.D. (Eds.), DNA Cloning: Core Techniques. Oxford University Press, Oxford, pp. 1–35.

Hoenke, S., Schmid, M., Dimroth, P., 1997. Sequence of a gene cluster from *Klebsiella pneumoniae* encoding malonate decarboxylase and expression of the enzyme in *Escherichia coli*. Eur. J. Biochem. 246, 530–538.

Kallastu, A., Horak, R., Kivisaar, M., 1998. Identification and characterization of IS*1411*, a new insertion sequence which causes transcriptional activation of the phenol degradation genes in *Pseudomonas putida*. J. Bacteriol. 180, 5306–5312.

Koiv, V., Marits, R., Heinaru, A., 1996. Sequence analysis of the 2,4-dichlorophenol hydroxylase gene *tfdB* and 3,5-dichlorocatechol 1,2-dioxygenase gene *tfdC* of 2,4-dichlorophenoxyacetic acid degrading plasmid pEST4011. Gene 174, 293–297.

Koo, J.H., Jung, S.B., Byun, H.S., Kim, Y.S., 1997. Cloning and sequencing of genes encoding malonate decarboxylase in *Acinetobacter calcoaceticus*. Biochim. Biophys. Acta 1354, 49–54.

Koo, J.H., Kim, Y.S., 1999. Functional evaluation of the genes involved in malonate decarboxylation by *Acinetobacter calcoaceticus*. Eur. J. Biochem. 266, 683–690.

Kousik, C.S., Ritchie, D.F., 1998. Identification of an insertion sequence (IS*1646*) from *Xanthomonas campestris* pv. *vesicatoria* and its distribution among xanthomonads. Phytopathology 88, S49.

Laemmli, C.M., Leveau, J.H.J., Zehnder, A.J.B., van der Meer, J.R., 2000. Characterisation of a second *tfd* gene cluster for chlorophenol and chlorocatechol metabolism on plasmid pJP4 in *Ralstonia eutropha* JMP134(pJP4). J. Bacteriol. 182, 4165–4172.

Maclean, K.N., 1997. The molecular genetics of 2,4-dichlorophenoxyacetate degradation in *Burkholderia cepacia* strain 2a and *Alcaligenes eutrophus* JMP 134. PhD Thesis. University of Greenwich, London.

Mae, A.A., Marits, R.O., Ausmees, N.R., Koiv, V.M., Heinaru, L.A., 1993. Characterisation of a new 2,4-dichlorophenoxyacetic acid degradating plasmid pEST4011: physical map and localization of catabolic genes. J. Gen. Microbiol. 139, 3165–3170.

Marmur, J., 1961. A procedure for the isolation of deoxyribonucleic acid from microorganisms. J. Mol. Biol. 3, 208–218.

COR-AAD1-00002793
Bayer EX1008 (Part 5 of 9)

Matrubutham, U., Harker, A.R., 1994. Analysis of duplicated gene sequences associated with *tfdR* and *tfdS* in *Alcaligenes eutrophus* JMP134. J. Bacteriol. 176, 2348–2353.

Oswiecimska, K., 1994. Genetic analysis of plasmid pIJB1 in *Pseudomonas cepacia* 2a involved in 2,4-dichlorophenoxyacetate degradation. M.Sc. Thesis. University of Greenwich, London.

Perez-Pantoja, D., Guzman, L., Manzano, M., Pieper, D.H., Gonzalez, B., 2000. Role of *tfdCIDIEIFI* and *tfdDIICIIEIIFII* gene molecules in catabolism of 3-chlorobenzoate by *Ralstonia eutropha* JMP134(pJP4). Appl. Environ. Microbiol. 66, 1602–1608.

Perkins, E.J., Gordon, M.P., Caceres, O., Lurquin, P.F., 1990. Organization and sequence analysis of the 2,4-dichlorophenol hydroxylase and dichlorocatechol oxidative operons of plasmid pJP4. J. Bacteriol. 172, 2351–2359.

Poh, R., Xia, X., Bruce, I.J., Smith, A.R.W., 2001. 2,4-Dichlorophenoxyacetate/alpha-ketoglutarate dioxygenases from *Burkholderia cepacia* 2a and *Ralstonia eutropha* JMP134. Microbios 105, 43–63.

Rangaswamy, V., Mitchell, R., Ullrich, M., Bender, C., 1998. Analysis of genes involved in biosynthesis of coronafacic acid, the polyketide component of the phytotoxin coronatine. J. Bacteriol. 180, 3330–3338.

Robinson, M.K., Bennett, P.M., Falkow, S., Dodd, H.M., 1980. Isolation of a temperature-sensitive derivative of RP1. Plasmid 3, 343–347.

Sambrook, J., Fritsch, E.F., Maniatis, T., 1989. Molecular Cloning: A Laboratory Manual, second ed. Cold Spring Harbor Laboratory Press, New York.

Schlomann, M., 1994. Evolution of chlorocatechol catabolic pathways. Conclusions to be drawn from comparisons of lactone hydrolases. Biodegradation 5, 301–321.

Suwa, Y., Wright, A.D., Fukumori, F., Nummy, K.A., Hausinger, R.P., Holben, W.E., Forney, L.J., 1996. Characterization of a chromosomally encoded 2,4-dichlorophenoxyacetic acid/alpha-ketoglutarate dioxygenase from *Burkholderia* sp. strain RASC. Appl. Environ. Microbiol. 62, 2464–2469.

Thayer, J.R., Wheelis, M.L., 1982. Active transport of benzoate in *Pseudomonas putida*. J. Gen. Microbiol. 128, 1749–1753.

van der Meer, J.R., Eggen, R.I., Zehnder, A.J., de Vos, W.M., 1991. Sequence analysis of the *Pseudomonas* sp. strain P51 *tcb* gene cluster, which encodes metabolism of chlorinated catechols: evidence for specialization of catechol 1,2-dioxygenases for chlorinated substrates. J. Bacteriol. 173, 2425–2434.

Vedler, E., Koiv, V., Heinaru, A., 2000a. Analysis of the 2,4-dichlorophenoxyacetic acid-degradative plasmid pEST4011 of *Achromobacter xylosoxidans* subsp. *denitrificans* strain EST4002. Gene 255, 281–288.

Vedler, E., Koiv, V., Heinaru, A., 2000b. TfdR, the LysR-type transcriptional activator, is responsible for the activation of the *tfdCB* operon of *Pseudomonas putida* 2,4-dichlorophenoxyacetic acid degradative plasmid pEST 4011. Gene 245, 161–168.

Wong, C.M., Dilworth, M.J., Glenn, A.R., 1994. Cloning and sequencing show that 4-hydroxybenzoate hydroxylase (PobA) is required for uptake of 4-hydroxybenzoate in *Rhizobium leguminosarum*. Microbiology 140, 2775–2786.

Xia, X.S., Aathithan, S., Oswiecimska, K., Smith, A.R., Bruce, I.J., 1998. A novel plasmid pIJB1 possessing a putative 2,4-dichlorophenoxyacetate degradative transposon Tn*5530* in *Burkholderia cepacia* strain 2a. Plasmid 39, 154–159.

Xia, X.S., Smith, A.R., Bruce, I.J., 1996. Identification and sequencing of a novel insertion sequence, IS*1471*, in *Burkholderia cepacia* strain 2a. FEMS Microbiol. Lett. 144, 203–206.

You, I.S., Ghosal, D., 1995. Genetic and molecular analysis of a regulatory region of the herbicide 2,4-dichlorophenoxyacetate catabolic plasmid pJP4. Mol. Microbiol. 16, 321–331.

Communicated by A. Chakrabarty

COR-AAD1-00002794
Bayer EX1008 (Part 5 of 9)

PESTICIDE BIOCHEMISTRY AND PHYSIOLOGY **54,** 123–134 (1996)
ARTICLE NO. 0016

Multiple Resistance to Dissimilar Herbicide Chemistries in a Biotype of *Lolium rigidum* Due to Enhanced Activity of Several Herbicide Degrading Enzymes

CHRISTOPHER PRESTON,*,† FRANÇOIS J. TARDIF,† JOHN T. CHRISTOPHER,†,[1] AND STEPHEN B. POWLES*,†,[2]

**Cooperative Research Centre for Weed Management Systems, and †Department of Crop Protection, Waite Campus, The University of Adelaide, PMB 1 Glen Osmond S.A. 5064, Australia*

Received July 17, 1995; accepted January 5, 1996

A biotype of *Lolium rigidum* Gaudin (VLR 69) shows multiple resistance to at least nine dissimilar herbicide chemistries. This biotype has enhanced metabolism to herbicides that inhibit Photosystem II, acetolactate synthase, and acetyl-coenzyme A carboxylase. The potential for malathion and piperonyl butoxide (PBO) to act as synergists for herbicides from five different chemical classes was investigated in potted plants. Of the herbicide/synergist combinations examined, PBO only synergized chlorotoluron, and malathion only synergized chlorsulfuron in this resistant biotype. The ability of PBO, malathion, 1-aminobenzotriazole (ABT), and tetcyclacis to inhibit metabolism of herbicides *in vivo* was also examined. ABT, PBO, and tetcyclacis inhibited metabolism of simazine and chlorotoluron, but malathion did not. Malathion alone inhibited metabolism of chlorsulfuron, ABT inhibited metabolism of diclofop, and none of these compounds affected tralkoxydim metabolism. These results suggest that at least four different herbicide-metabolizing enzymes have increased activity in this resistant biotype. In addition to enhanced metabolism, this biotype also contains a resistant form of acetyl-coenzyme A carboxylase which shows 31-, 4-, and 20-fold resistance to diclofop acid, fluazifop acid, and haloxyfop acid, respectively, but which shows no resistance to sethoxydim or tralkoxydim. Multiple resistance in this biotype of *L. rigidum* is clearly the result of the accumulation of several resistance mechanisms. © 1996 Academic Press, Inc.

INTRODUCTION

The widespread use of herbicides for weed control over the past few decades has resulted in the appearance and rapid proliferation of weeds with resistance to herbicides. Biotypes of numerous previously susceptible species have evolved resistance to one or more herbicides from 16 different herbicide chemistries (1). The most spectacular and serious case of herbicide resistance is in *Lolium rigidum* in Australia, where more than 2000 farms are affected by herbicide-resistant infestations of this species (2). *L. rigidum* is an annual winter-growing grass species that has become naturalized over large areas of the cropping region of southern Australia and herbicides are frequently used to control this weed species. The advent, and widespread adoption, of the grass-selective aryloxyphenoxypropanoate herbicides, such as diclofop-methyl, for control of *L. rigidum* has resulted in the widespread appearance of resistance to these and other herbicides (3). At present *L. rigidum* populations display resistance to 12 classes of herbicide chemistry with 7 modes of action (4). One feature of herbicide-resistant *L. rigidum* populations is that frequently a population is resistant to herbicides from more than one chemical class, often without prior exposure to these chemistries.

There has been an intense effort by our group in recent years to understand the mechanisms of resistance in *L. rigidum* populations. To date we have documented resistant populations with target site changes at acetyl-coenzyme A carboxylase (ACCase)[3] (5, 6) and acetolactate syn-

[1] Present address: Department of Botany and Tropical Agriculture, James Cook University of North Queensland, Townsville QLD. 4711, Australia.

[2] To whom correspondence should be addressed. Fax: 61-8-3037125.

[3] Abbreviations used: ABT, 1-aminobenzotriazole; ACCase, acetyl-coenzyme A carboxylase; ALS, acetolactate syn-

0048-3575/96 $18.00
Copyright © 1996 by Academic Press, Inc.
All rights of reproduction in any form reserved.

COR-AAD1-00002795
Bayer EX1008 (Part 5 of 9)

thase (ALS) (7), as well as enhanced metabolism of ACCase- (8), ALS- (9), and Photosystem II (PS II)-inhibiting herbicides (10, 11). In addition, other mechanisms of resistance have been proposed to account for resistance to ACCase-inhibiting herbicides, such as sequestration of herbicide and resistance associated with recovery of the plasma membrane electrogenic potential following diclofop acid-induced depolarization (12, 13). It is now clear that multiple herbicide resistance in *L. rigidum* is due to multiple resistance mechanisms (14). Individuals within a population may express from one to several resistance mechanisms (6, 15). In this study we examined the possibility that populations of *L. rigidum* that have multiple resistance due to enhanced metabolism of many herbicide classes may contain multiple herbicide-detoxifying enzymes. One such population of *L. rigidum*, biotype VLR 69, is resistant to at least nine herbicide classes (16) and displays enhanced metabolism to some ALS-inhibiting herbicides, such as chlorsulfuron, and PS II-inhibiting herbicides, such as simazine and chlorotoluron (10, 11, 15). The PS II and ALS target sites in this biotype are susceptible to herbicides, except for a small percentage of the population, < 5%, which contains a herbicide-resistant ALS (11, 15). Identification of herbicide metabolites along with studies using inhibitors of cytochrome P450 monooxygenases have indicated that the enhanced herbicide metabolism in this biotype is endowed by increased activity of these oxidative enzymes (10, 11). Here, we have used inhibitors to antagonize metabolism-based resistance to five classes of herbicides in this population to determine whether broad cross-resistance in this population of *L. rigidum* is the result of one or more herbicide-degrading enzymes. In addition we have examined ACCase, the target site for herbicides such as diclofop-methyl and tralkoxydim, for resistance.

thase; DTT, dithiothreitol; EDTA, ethylenediaminetetraacetic acid; I_{50}, concentration of inhibitor required to reduce enzyme activity by 50 %; LD_{50}, concentration of herbicide required to kill 50 % of a population; PBO, piperonyl butoxide; PMSF, phenylmethylsulfonyl fluoride; PS II, Photosystem II; PVP, polyvinylpyrrolidone; Tricine, *N*[tris(hydroxymethyl)methyl]glycine.

MATERIALS AND METHODS

Plant Material

The resistant biotype of *L. rigidum*. VLR 69, was collected from a field used for perennial ryegrass (*L. perenne*) seed production near Mansfield, Victoria, Australia where herbicides had failed to control annual ryegrass. This field had been treated with herbicides at least once annually from 1969 to 1990. In that time this field had received 17 applications of diuron, 5 of atrazine, 6 of chlorsulfuron, 2 of diclofop-methyl, and 3 of a mixture of paraquat and diquat (16). This biotype is resistant to members of at least nine herbicide classes with five modes of action (16). The susceptible biotype, VLR 1, was collected from an area with no history of herbicide application and is susceptible to all herbicides registered for control of *L. rigidum*.

Chemicals

Commercial formulations of herbicides were obtained from AgrEvo (diclofop-methyl), Crop Care Australasia (tralkoxydim), DuPont Australia (chlorsulfuron), and Ciba-Geigy Australia (chlorotoluron and simazine). ^{14}C-Labeled herbicides were gifts from Hoechst AG (Frankfurt, Germany) ([dichlorophenyl-U-^{14}C]diclofop-methyl), Zeneca Agrochemicals (Bracknell, UK) ([cyclohexyl-^{14}C]tralkoxydim), DuPont (Wilmington, DE) ([phenyl-U-^{14}C]chlorsulfuron), and Ciba-Geigy (Basel, Switzerland) ([triazyl-U-^{14}C]simazine and [phenyl-U-^{14}C]chlorotoluron). Malathion and piperonyl butoxide (PBO) were obtained from Incitec (Australia), tetcyclasis from BASF AG (Germany), and 1-aminobenzotriazole (ABT) from Sigma Chemical Co (U.S.A.). $NaH^{14}CO_3$ was purchased from Amersham International plc. Diclofop acid was a gift from Hoechst AG, haloxyfop acid from DowElanco, (South Bend, IN), fluazifop acid and tralkoxydim from Zeneca Agrochemicals, and sethoxydim from Nippon Soda Co. (Odawara, Japan). All other reagents were obtained commercially.

COR-AAD1-00002796
Bayer EX1008 (Part 5 of 9)

Dose Response to Herbicides

Seeds were germinated on 0.6% agar in a germination cabinet set at 19°C and 30 E m^{-2} s^{-1} and one-leaf stage seedlings transplanted to 17-cm pots containing pasteurized potting mix based on a 1:1 mix of sand and peat, with 12 plants per pot. Seedlings were grown outdoors during the normal winter growing season and treated with herbicide at the two-leaf (diclofop-methyl, tralkoxydim, and chlorsulfuron) or three-leaf (simazine and chlorotoluron) stage. Spray treatments were applied using a laboratory sprayer equipped with a twin-nozzle boom moving at 1 m s^{-1} delivering 108 L ha^{-1}. Herbicide rates were chosen to obtain the LD_{50} value for each biotype and therefore higher rates were applied to the resistant biotype than the susceptible biotype. Malathion and PBO were formulated in a mixture of emulsifier and hydrocarbon solvent and applied 30 min to 1 hr prior to herbicide application. Control plants were treated with the mixture of emulsifier and hydrocarbon solvent. Treated plants were returned outdoors and harvested after 21 days, when mortality was assessed. LD_{50} values were assessed and compared by probit analysis using a computer program (POLO PC; LeOra Software, Berkeley, CA; 17). Pot experiments were conducted in a randomized block design containing four replicates. The experiment was conducted twice, in spring 1993 and winter 1994.

Metabolism of Herbicides

Seeds were germinated as described above and transplanted to 1-liter polyethylene trays containing 400 ml black polypropylene beads to support the seedlings. The bases of these trays were perforated and placed in a second tray containing 500 ml nutrient solution (18), which allowed a simple method of changing solutions. Evapo-transpirational losses were replaced by daily addition of distilled H_2O or, every third day, by addition of nutrient solution. Plants were cultured in a growth room with a 12-hr, 20°C, 450 E m^{-2} s^{-1} light/12-hr, 15°C dark regime.

When plants had reached the two-leaf stage about 7 days after transplanting, the nutrient solution was replaced with new solution containing 70 *M* of PBO, ABT, malathion, or tetcyclacis for 24 hr prior to herbicide treatments. Metabolism of simazine and chlorotoluron was determined by transferring the plants to 5 ml of fresh nutrient solution containing either 1.5 *M* [^{14}C]chlorotoluron (3.6 kBq [phenyl-U-^{14}C]chlorotoluron per vial) or 2 *M* [^{14}C]-simazine (3.6 kBq [triazyl-^{14}C]simazine per vial) with 6 plants per vial. Shoots, 6 plants per treatment, were harvested after 24 hr, washed in distilled H_2O and frozen in liquid N_2. Metabolism of chlorsulfuron and tralkoxydim was determined using a cut shoot technique (9, 18). Plants were removed from nutrient solution and the shoots were excised under water. The excised shoots, 6 per vial, were placed in 300 l of 16 *M* [^{14}C]chlorsulfuron (0.75 kBq [phenyl-U-^{14}C]chlorsulfuron per vial) or 30 *M* [^{14}C]tralkoxydim (0.75 kBq [cyclohexyl-^{14}C]-tralkoxydim per vial). Twelve shoots per treatment were harvested after 6 hr, washed in distilled H_2O, and frozen in liquid N_2. Metabolism of diclofop-methyl was determined by transferring plants to fresh nutrient solution and applying a single 1- l drop of 2.5 m*M* [^{14}C]diclofop-methyl (0.58 kBq [chlorophenyl-U-^{14}C]diclofop-methyl per plant, made up in a commercial formulation) to the leaf axil. Shoots were harvested, 8 per sample, after 48 hr, washed thoroughly with 100 ml of 20% methanol and 0.2 % Triton X-100, and frozen in liquid N_2. The effects of the inhibitors on metabolism of each herbicide were subjected to analysis of variance and compared by Fisher's protected LSD.

Extraction and Quantification of Herbicides and Metabolites

Frozen plant material was ground to a paste in liquid N_2, extracted with 3 ml of 80% methanol, and centrifuged at 10,000 *g* for 10 min. The pellet was reextracted in 1 ml of 80% methanol (10,000*g* for 10 min) followed by 1 ml of 50% methanol (10,000*g* for 10 min). The pooled supernatants were concentrated to dryness *in vacuo* and, with the exception of diclofop-

COR-AAD1-00002797
Bayer EX1008 (Part 5 of 9)

methyl samples, resuspended in 50% methanol, centrifuged to remove insoluble material, and filtered prior to injection onto HPLC. Diclofop-methyl samples were resuspended in 200 l 50% methanol and centrifuged to remove insoluble material. The insoluble material was then dissolved in 90 l of methanol and the two fractions were filtered and pooled prior to injection onto HPLC. This technique ensured that <5% of the radioactivity was lost in the insoluble pellet. For all other herbicides this was not a problem as <5% of the total radioactivity remained associated with the insoluble material.

Herbicides and metabolites were separated and quantified by reverse-phase HPLC on an Activon Goldpack 250 × 4.6-mm column (Activon Scientific Products Co., Thornleigh, N.S.W., Australia). Solvents were 9% acetonitrile and 1% acetic acid in H_2O (Solvent A) and 90% acetonitrile and 1% acetic acid in H_2O (Solvent B). The HPLC gradients and flow rates used to elute herbicides and metabolites from the column are listed in Table 1. The column was reequilibrated with the starting conditions prior to injection of each new sample. Radioactivity was detected with an on-line radioactivity detector (Flo-One 1 Beta Model A-140: Radiomatic Instruments and Chemical, Tampa, FL) equipped with a solid Yt-Si cell. Metabolites were quantified as a percentage of the total radioactivity detected.

Extraction and Assay of ACCase

ACCase was extracted, assayed, and herbicide-inhibition kinetics determined as described by Tardif *et al.* (5) with modifications. Three grams of shoot tissue were ground in 10 ml of ice-cold 100 m*M* Tris–HCl, pH 8.0, 2 m*M* isoascorbate, 1 m*M* Na_2EDTA, 10% v/v glycerol, 0.5% w/v PVP-40, 0.5% w/v insoluble PVP, 1 m*M* PMSF, and 20 m*M* DTT. The ground tissue was centrifuged at 27,000*g* for 10 min and the supernatant brought to 60% saturation with $(NH_4)_2SO_4$. The solution was kept stirring at 4°C for 1 hr and then centrifuged at 27,000*g* for 30 min. The pellet was resuspended in 2.6 ml of 50 m*M* Tricine–KOH, pH 8.0, 2.5 m*M* $MgCl_2$, 50 m*M* KCl, and 1 m*M* DTT, loaded onto a column containing Sephadex G-25 (PD-10 column, Pharmacia, Uppsala, Sweden), preequilibrated with 50 m*M* Tricine–KOH, pH 8.0, 2.5 m*M* $MgCl_2$, 50 m*M* KCl, and 1 m*M* DTT and eluted with 2.7 ml of the same buffer. The eluate was stored on ice and assayed immediately for ACCase activity.

ACCase activity was assayed by following acid-stable incorporation of ^{14}C from $NaH^{14}CO_3$ at 30°C (20). Assays were performed in 300 l micro-titer plates (Nunc MicroWell, Roskilde, Denmark) in a final volume of 200 l, containing 50 m*M* Tricine–KOH, pH 8.0, 2.5 m*M* $MgCl_2$, 50 m*M* KCl, 1 m*M* DTT, 1 m*M* ATP, 0.3 m*M* acetyl-coenzyme A, 10 m*M* $NaH^{14}CO_3$, 30 l of enzyme preparation, and herbicides as required. Enzyme was incubated with herbicide for 3 min at 30°C prior to the assay that was initiated by the simultaneous addition of ATP, acetyl-coenzyme A, and $NaH^{14}CO_3$. Assays were run for 5 min and stopped by the addition of 20 l glacial acetic

TABLE 1

Solvent Flow Rates and Solvent Gradient Conditions for Elution of Herbicides and Metabolites by HPLC

Herbicide	Simazine		Chlorotoluron		Chlorsulfuron		Diclofop		Tralkoxydim	
Flow rate (ml min^{-1})	1.2		1.2		1.5		1.5		1.2	
Gradient	Time (min)	Solvent B (%)	Time (min)	Solvent B (%)	Time (min)	Solvent B (%)	Time (min)	Solvent B (%)	Time (min)	Solvent B (%)
	0	0	0	0	0	8	0	30	0	0
	10	13	10	13	26	42	10	70	10	50
	26	75	25	69	33	100	13	100	30	100
	28	100	28	100	38	100	18	100	35	100
	33	100	33	100						

Note. Solvent A consisted of 90:9:1 (by vol) H_2O:acetonitrile:acetic acid and Solvent B consisted of 9:90:1 (by vol) H_2O:acetonitrile:acetic acid. At all times a constant flow rate was maintained.

COR-AAD1-00002798
Bayer EX1008 (Part 5 of 9)

acid. Samples were transferred to 5-ml scintillation vials, a piece of glass filter paper (GF-A; Whatman, Maidstone, Kent, UK) was added to each sample, and the samples were dried under a stream of dry air for 5 hr. Acetyl-coenzyme A-dependent incorporation of radioactivity was determined by liquid scintillation spectroscopy in 3 ml of scintillant (Ultima-Gold XR; Packard, Groningen, The Netherlands).

RESULTS

Dose Response to Herbicides

Whole plant studies have documented that the resistant biotype is resistant to many herbicides including inhibitors of PS II, ALS, and ACCase (16). This was confirmed in the studies conducted here. The dose response experiments were conducted twice, in early spring 1993 and in mid-winter 1994, and there were some differences in the effectiveness of some herbicides between years, probably due to environmental factors. As resistance, and the effects of PBO and malathion on herbicide efficacy were consistent across the two seasons, only data from 1994 are shown (Table 2). As expected the susceptible biotype was controlled by relatively low rates of all herbicides used (Table 2). In contrast, the resistant biotype was resistant to all herbicides examined displaying about 6-fold resistance to simazine, 12-fold resistance to chlorotoluron, 67-fold resistance to chlorsulfuron, more than 270-fold resistance to diclofop-methyl, and about 8-fold resistance to tralkoxydim (Table 2). Where resistance is due to enhanced herbicide metabolism mediated by cytochrome P450 monooxygenases, as appears to be the case for biotype VLR 69 (10, 11), resistance can be reversed by some cytochrome P450 inhibitors. To determine whether a single, broad-spectrum herbicide-metabolizing cytochrome P450 monooxygenase provides multiple resistance in this biotype we examined synergism in potted plants by two cytochrome P450 inhibitors, PBO (reviewed in 21) and malathion (22). In addition, we examined the ability of these inhibitors plus two other cytochrome P450 inhibitors, ABT (reviewed in 23) and tetcyclacis (24), to inhibit herbicide metabolism in this biotype.

Effects of Cytochrome P450 Inhibitors on Dose Response to and Metabolism of PSII Inhibiting Herbicides

PBO has been shown to synergize chlorotoluron action against a *L. rigidum* biotype, WLR 2, resistant to chlorotoluron as a result of enhanced metabolism (10). A similar result was obtained here with biotype VLR 69, where PBO pretreatment reduced the LD_{50} for chlorotoluron by about 3.3-fold (Table 2). PBO was also

TABLE 2

Response of the Susceptible and Resistant Biotypes of L. rigidum, as Determined by LD_{50}, to Simazine, Chlorotoluron, Chlorsulfuron, Diclofop-methyl, and Tralkoxydim

		Herbicide alone	Herbicide plus 2.1 kg ha^{-1} PBO	Herbicide plus 1 kg ha^{-1} malathion
Herbicide	Biotype	LD_{50} (kg ha^{-1})		
Simazine	Susceptible	0.93	0.61	0.81
	Resistant	5.95	6.57	8.03
Chlorotoluron	Susceptible	0.68	0.40*	1.04
	Resistant	8.30	2.51*	10.49
Chlorsulfuron	Susceptible	0.007	0.006	0.001*
	Resistant	0.470	0.497	0.105*
Diclofop-methyl	Susceptible	0.06	0.08	0.08
	Resistant	>16	>16	>16
Tralkoxydim	Susceptible	0.020	0.013*	0.019
	Resistant	0.154	0.078	0.123

Note. Each herbicide was applied alone or in combination with 2.1 kg ha^{-1} PBO or 1 kg ha^{-1} malathion.
*LD_{50}s are significantly different to controls for that herbicide–biotype combination ($P < 0.05$).

COR-AAD1-00002799
Bayer EX1008 (Part 5 of 9)

an effective synergist for chlorotoluron with the susceptible biotype, reducing the LD_{50} by 1.7-fold. In contrast, PBO did not prove to be an effective synergist for simazine with either biotype. Pretreatment of susceptible and resistant biotypes with malathion did not influence phytotoxicity of either simazine or chlorotoluron (Table 2). This agrees with previous studies which demonstrated that malathion is an effective synergist for chlorsulfuron, but not for chlorotoluron in *L. rigidum* (25).

The resistant biotype contains a PS II target site that is sensitive to the PS II-inhibiting herbicides chlorotoluron and simazine and exhibits nontarget site resistance due to enhanced metabolism of both herbicides (10, 11). This was confirmed in this study where after 24 hr of treatment with simazine the resistant biotype had metabolized 65% of the herbicide, whereas the susceptible biotype had only metabolized 18% (Table 3). Pretreatment of the susceptible biotype for 24 hr with ABT and tetcyclacis inhibited metabolism of simazine, whereas malathion and PBO did not significantly inhibit simazine metabolism in the susceptible biotype. Likewise pretreatment of plants of the resistant biotype with ABT or tetcyclacis inhibited metabolism of simazine. PBO pretreatment also inhibited metabolism of simazine in this biotype, but malathion did not. PBO and ABT had equivalent effects on metabolism of simazine by the resistant biotype, however, tetcyclacis was considerably more effective as an inhibitor. Tetcyclacis was the most effective of these inhibitors for both biotypes (Table 3).

Similarly, the resistant biotype had enhanced metabolism of chlorotoluron. Following 24 hr of treatment, the resistant biotype had metabolized 55% of the chlorotoluron in the shoots, compared to 20% metabolized by the susceptible biotype (Table 4). Pretreatment of plants with PBO, ABT, or tetcyclacis, but not malathion, inhibited metabolism of chlorotoluron in both susceptible and resistant biotypes. As for simazine metabolism (Table 3), tetcyclacis was the most effective inhibitor of chlorotoluron metabolism (Table 4). Hence, metabolism of these two PS II-inhibiting herbicides is inhibited by a similar suite of cytochrome P450-inhibiting chemicals in the resistant biotype.

Effects of Cytochrome P450 Inhibitors on Dose Response to and Metabolism of ALS-Inhibiting Herbicides

We have previously documented that malathion is an excellent synergist for chlorsulfuron in the chlorsulfuron-resistant *L. rigidum* biotype SLR 31, but that PBO was ineffective as a synergist (25). A similar result was obtained here where pretreatment of both susceptible and resistant biotypes with malathion dramatically increased the phytotoxicity of chlorsulfuron. The LD_{50} for chlorsulfuron was reduced by 7-fold for the susceptible biotype and 4-fold for the resistant biotype (Table 2). In contrast, PBO

TABLE 3
Metabolism of Simazine by Susceptible and Resistant Biotypes of L. rigidum in 24 h of Treatment with [^{14}C]Simazine

Treatment	Susceptible	Resistant
	Simazine remaining (%)	
Control	82a	35a
PBO	90ab	63b
Malathion	85ab	48ab
ABT	93bc	61b
Tetcyclacis	97c	89c

Note. Treatments within a column followed by different letters are significantly different ($P < 0.05$). Plants were pretreated for 24 hr with PBO, malathion, ABT, or tetcyclacis, each at 70 M, prior to application of [^{14}C]simazine.

TABLE 4
Metabolism of Chlorotoluron by Susceptible and Resistant Biotypes of L. rigidum in 24 hr of Treatment with [^{14}C]Chlorotoluron

Treatment	Susceptible	Resistant
	Chlorotoluron remaining (%)	
Control	80a	45a
PBO	89bc	63b
Malathion	85ab	54ab
ABT	90bc	64b
Tetcyclacis	93c	82c

Note. Treatments within a column followed by different letters are significantly different ($P < 0.05$). Plants were pretreated for 24 hr with PBO, malathion, ABT, or tetcyclacis, each at 70 M, prior to application of [^{14}C]chlorotoluron.

COR-AAD1-00002800
Bayer EX1008 (Part 5 of 9)

pretreatment did not influence chlorsulfuron phytotoxicity in either biotype. Clearly, malathion is a very effective synergist for chlorsulfuron in *L. rigidum* (Table 2; 25).

The target site for chlorsulfuron, ALS, is sensitive to chlorsulfuron in biotype VLR 69, with the exception of about 5% of the population that contain a chlorsulfuron-resistant ALS (15). The remainder of the population is resistant due to enhanced chlorsulfuron metabolism (15). Enhanced chlorsulfuron metabolism was confirmed here, where, in 6 hr of treatment, 22% of the herbicide was metabolized by the resistant biotype compared to 8% metabolized by the susceptible biotype (Table 5). Pretreatment of plants with PBO, ABT, or tetcyclacis did not inhibit chlorsulfuron metabolism by either biotype. In contrast, malathion inhibited the metabolism of chlorsulfuron by both biotypes. This confirms the observations of Christopher *et al.* (25), who demonstrated that malathion, but not other cytochrome P450 inhibitors, inhibited chlorsulfuron metabolism in *L. rigidum* biotype SLR 31. Therefore, it is highly likely that malathion synergizes the action of chlorsulfuron in the resistant biotype by inhibiting chlorsulfuron metabolism.

Effects of Cytochrome P450 Inhibitors on Dose Response to and Metabolism of ACCase-Inhibiting Herbicides

The resistant biotype is resistant to several herbicides that inhibit ACCase, but is not resistant to others, for example sethoxydim (16). Here the resistant biotype proved to be highly resistant to diclofop-methyl, but showed a much lower level of resistance to tralkoxydim (Table 2). Pretreatment of plants with PBO or malathion had no effect on the phytotoxicity of diclofop-methyl for either biotype. Likewise, malathion did not alter phytotoxicity of tralkoxydim. PBO synergized tralkoxydim activity to a small extent. However, the combination of PBO and tralkoxydim was not significantly more effective on the resistant biotype than tralkoxydim alone. Neither PBO nor malathion proved to be effective synergists of ACCase-inhibiting herbicides on the resistant biotype.

TABLE 5
Metabolism of Chlorsulfuron by Susceptible and Resistant Biotypes of L. rigidum in 6 hr of Treatment with [^{14}C]Chlorsulfuron

Treatment	Susceptible	Resistant
	Chlorsulfuron remaining (%)	
Control	92a	78a
PBO	94a	78a
Malathion	99b	91b
ABT	95ab	84ab
Tetcyclacis	92a	83ab

Note. Treatments within a column followed by different letters are significantly different ($P < 0.05$). Plants were pretreated for 24 hr with PBO, malathion, ABT, or tetcyclacis, each at 70 M, prior to application of [^{14}C]chlorsulfuron.

As the resistance status of the target site enzyme for diclofop and tralkoxydim, ACCase, in the resistant biotype has not been previously examined, we partially purified ACCase from both biotypes and assayed with a range of ACCase-inhibiting herbicides. The activity of ACCase extracted from the resistant biotype was markedly less sensitive to inhibition by diclofop acid than was the enzyme from the susceptible biotype (Fig. 1A). In contrast, ACCase from the two biotypes was equally sensitive to tralkoxydim (Fig. 1B). With diclofop acid, the dose of herbicide required for 50% inhibition of isolated enzyme activity was 8.8 M for the resistant biotype compared with 0.3 M for the susceptible biotype. Therefore, the ACCase extracted from the resistant biotype was 29-fold resistant to diclofop acid. The ACCase from the resistant biotype was similarly resistant to other members of the aryloxyphenoxypropanoate group with I_{50} R/I_{50} S ratios of 4.3 for fluazifop acid and 20 for haloxyfop acid. In contrast, no resistance to members of the cyclohexanedione group was observed at the enzyme level with I_{50} R/I_{50} S ratios of 1.2 for sethoxydim and 1 for tralkoxydim (Table 6). A resistant target site clearly accounts for diclofop-methyl resistance in this biotype. In contrast, resistance to tralkoxydim must be endowed by a non-target-site mechanism.

In addition to possessing a resistant ACCase, the resistant biotype also shows enhanced metabolism of diclofop-methyl. The susceptible biotype had metabolized 51% of the herbicide

COR-AAD1-00002801
Bayer EX1008 (Part 5 of 9)

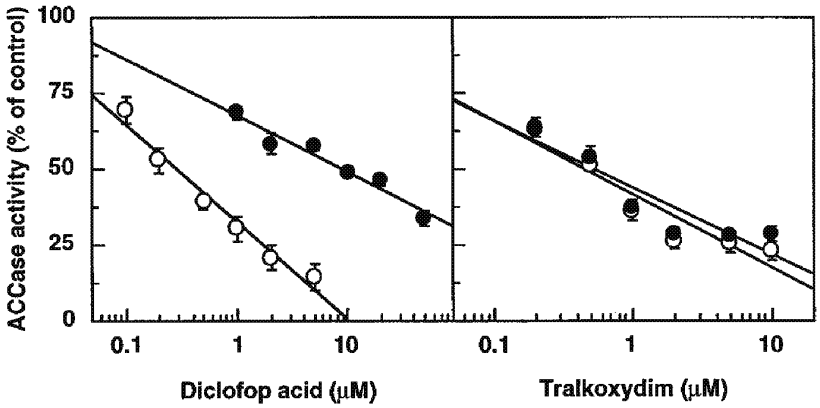


FIG. 1. *Effect of diclofop acid (A) and tralkoxydim (B) on ACCase activity of partially purified extracts from susceptible ( ) and resistant ( ) biotypes of L. rigidum. Each point is the mean ± SE of three extracts with assays performed in duplicate. 100% activities were determined in the absence of herbicide and corresponded to 29.7 ± 6.7 and 24.4 ± 2.7 nmol HCO_3^- fixed min^{-1} mg $protein^{-1}$ for the susceptible and resistant biotypes, respectively.*

to products other than diclofop acid 48 hr after treatment, whereas the resistant biotype had metabolized 62% (Table 7). Pretreatment of plants with ABT reduced metabolism of diclofop in both biotypes. In contrast, pretreatment with malathion, PBO, or tetcyclacis did not inhibit metabolism of diclofop.

The resistant biotype also possesses enhanced metabolism of tralkoxydim. In 6 hr of treatment, the susceptible biotype had metabolized 41% of the tralkoxydim in the shoots, whereas the resistant biotype had metabolized 77% (Table 8). As the target site, ACCase, in the resistant biotype is susceptible to tralkoxydim, this enhanced metabolism of tralkoxydim is probably the mechanism of resistance in this biotype. Pretreatment of plants with PBO, malathion, ABT, or tetcyclacis failed to inhibit metabolism of tralkoxydim in either biotype.

TABLE 6

Concentration of Herbicides Giving 50% Inhibition of ACCase Activity (I_{50}) from Resistant and Susceptible Biotypes of L. rigidum, Calculated from Pooled Data of Three Extracts with Assays Conducted in Duplicate

Herbicide	Susceptible	Resistant	Ratio
	I_{50} (*M*)		(I_{50} S/I_{50} R)
Diclofop acid	0.3	8.8	29
Fluazifop acid	16	68	4.3
Haloxyfop acid	1.1	22	20
Sethoxydim	3.2	3.8	1.2
Tralkoxydim	0.5	0.5	1

Note. Ratios are the values for the resistant biotype divided by the values for the susceptible biotype.

DISCUSSION

L. rigidum biotype VLR 69 shows resistance to herbicides from at least nine chemical classes (16). Cytochrome P450 monooxygenase-mediated enhanced metabolism most likely endows resistance to chlorotoluron (10), simazine (11), and chlorsulfuron (Table 5) in this biotype. It is clear from this study that the specific enzymes involved in detoxification of these three herbicides are not the same. Application of the cytochrome P450 inhibitors PBO (21) and mal-

TABLE 7

Metabolism of Diclofop-methyl by Susceptible and Resistant Biotypes of L. rigidum 48 hr after Treatment with [^{14}C]Diclofop-methyl

Treatment	Susceptible	Resistant
	Diclofop remaining (% as diclofop-methyl plus diclofop acid)	
Control	49a	38a
PBO	48a	44ab
Malathion	53ab	38a
ABT	59b	52b
Tetcyclacis	53ab	45ab

Note. Treatments within a column followed by different letters are significantly different ($P < 0.05$). Plants were pretreated for 24 hr with PBO, malathion, ABT, or tetcyclacis, each at 70 *M*, prior to application of [^{14}C]diclofop-methyl.

COR-AAD1-00002802
Bayer EX1008 (Part 5 of 9)

TABLE 8
Metabolism of Tralkoxydim by Susceptible and Resistant Biotypes of L. rigidum in 6 hr of Treatment with [^{14}C]Tralkoxydim

Treatment	Susceptible	Resistant
	Tralkoxydim remaining (%)	
Control	59ab	23a
PBO	53a	17a
Malathion	67b	26a
ABT	57ab	22a
Tetcyclacis	54ab	18a

Note. Treatments within a column followed by different letters are significantly different ($P < 0.05$). Plants were pretreated for 24 hr with PBO, malathion, ABT, or tetcyclacis, each at 70 M, prior to application of [^{14}C]tralkoxydim.

athion (22) to whole plants of the resistant biotype shows that PBO synergizes chlorotoluron only and malathion synergizes chlorsulfuron only, while neither compound synergized simazine (Table 2). These results are consistent with previous studies where malathion has been shown to synergize chlorsulfuron action on the chlorsulfuron-resistant biotype SLR 31 (25). However, malathion was ineffective as a synergist when resistance was due to a target site modification at ALS (25). Similarly, PBO is an effective synergist for a chlorotoluron-resistant biotype, WLR 2, where resistance is due to enhanced herbicide metabolism (10).

These cytochrome P450 inhibitors as well as ABT (23) and tetcyclacis (24) had differential ability to inhibit metabolism of the five herbicides. The metabolism of simazine and chlorotoluron was inhibited by ABT, PBO, and tetcyclacis, but not by malathion (Tables 3 and 4), chlorsulfuron metabolism was inhibited substantially by malathion only (Table 5), and diclofop metabolism was inhibited by ABT (Table 7). None of the inhibitors substantially reduced metabolism of tralkoxydim (Table 8). We have previously shown that malathion is the only one of these compounds that is an effective inhibitor of chlorsulfuron metabolism in *L. rigidum* biotype SLR 31 (25), and that ABT can inhibit metabolism of both simazine and chlorotoluron in *L. rigidum* biotypes WLR 2 and VLR 69 (10, 11). Based on the different patterns of inhibition of herbicide metabolism by cytochrome P450 inhibitors *in vivo* (Table 9), we suggest that at least four metabolic systems, probably involving different isoenzymes of cytochrome P450 monooxygenases, contribute to enhanced herbicide detoxification in biotype VLR 69. At least one isoenzyme is responsible for resistance to simazine and chlorotoluron, a second isoenzyme is responsible for resistance to chlorsulfuron, a third isoenzyme gives enhanced metabolism of diclofop, and a fourth isoenzyme resistance to tralkoxydim.

With a few exceptions, the effects of synergists on the whole plants correlated well with their ability to inhibit herbicide metabolism. However, PBO inhibits metabolism of simazine (Table 3), but does not synergize the herbicide in whole plants (Table 2). Conversely, PBO synergizes tralkoxydim in the susceptible biotype (Table 2), but does not inhibit metabolism (Table 8). It is possible that the inhibition of simazine metabolism by PBO may be transitory, allowing the plants to recover from the phytotoxic effects. Alternatively, PBO pretreatment may alter either the translocation or distribution of herbicide within the leaf tissue. Similarly, PBO might alter the metabolic pathway for tralkoxydim degradation such that a greater fraction of the metabolites produced are phytotoxic. The metabolites of tralkoxydim in *L. rigidum* are not known; however, in wheat and maize, hydroxymethylphenyl-tralkoxydim, a likely product of a cytochrome P450-mediated reaction is the initial metabolite (26). This metabolite is probably not phytotoxic, but that re-

TABLE 9
Summary of Cytochrome P450 Inhibitors which Inhibit Metabolism of Herbicides in the Resistant Biotype of L. rigidum

Herbicide	Cytochrome P450 inhibitors which inhibit metabolism
Simazine	Tetcyclacis, ABT, PBO
Chlorotoluron	Tetcyclacis, ABT, PBO
Chlorsulfuron	Malathion
Diclofop-methyl	ABT
Tralkoxydim	None

COR-AAD1-00002803
Bayer EX1008 (Part 5 of 9)

mains to be verified. Unlike metabolism in *L. rigidum,* ABT and PBO both inhibit metabolism of tralkoxydim by maize cell cultures (26).

In addition to enhanced metabolism of PS II-, ALS-, and ACCase-inhibiting herbicides, *L. rigidum* biotype VLR 69 contains an ACCase that is insensitive to the aryloxyphenoxypropanoate herbicides. This enzyme is between 4- and 31-fold resistant to the aryloxyphenoxypropanoate herbicides, but shows no resistance to the cyclohexanedione herbicides (Table 6). Target site-based resistance is the most commonly reported mechanism of resistance to the ACCase-inhibiting herbicides (27), and we have documented resistance ACCase in several resistant biotypes of *L. rigidum* (5, 6, 28). The resistant biotype VLR 69 differs from previously reported cases of target site-based resistance to the ACCase-inhibiting herbicides in *L. rigidum* in that the enzyme is not resistant to the cyclohexanedione herbicides. In this respect biotype VLR 69 resembles a resistant biotype of *L. multiflorum* where the ACCase is highly resistant to the aryloxyphenoxypropanoate, but susceptible to the cyclohexanedione herbicides (29). Clearly, resistance to tralkoxydim in biotype VLR 69 is not due to an altered target site (Table 6), but is due to enhanced metabolism of tralkoxydim (Table 8).

A small fraction, about 5%, of the resistant biotype, VLR 69, contains a herbicide-resistant form of ALS (15), whereas the majority of the population is resistant to chlorsulfuron due to enhanced metabolism (Table 4; 15). This biotype of *L. rigidum* therefore contains two target site-based mechanisms of resistance, albeit resistant ALS is present in only a small fraction of the population, as well as enhanced metabolism to a wide range of herbicides, with at least four different metabolic systems contributing to enhanced metabolism. It has been previously demonstrated that more than one mechanism of herbicide resistance can coexist within a population, for example chlorsulfuron resistance in *L. rigidum* due to an altered target site and enhanced metabolism (7), and diclofop-methyl resistance due to an altered target site and a second mechanism in a subset of *L. rigidum* biotype SLR 31 (6). However, the number of mechanisms of resistance documented in biotype VLR 69 is unparalleled.

L. rigidum is an obligate outcrossing species and hence it is not surprising that multiple mechanisms of resistance can appear in this species (see 14). As a result of the outcrossing nature of this species, any mechanisms that provide resistance to herbicides will be mixed among the survivors of herbicide application. This, in combination with the extensive and varied herbicide application history of this population (16), provides ideal conditions for the accumulation of multiple mechanisms of herbicide resistance. As a result of the accumulation of multiple resistance mechanisms in this population, there are few selective herbicides remaining which can control this population. In addition, it appears likely that multiple resistant biotypes such as VLR 69 would be resistant to herbicide chemistries yet to be marketed or discovered, particularly where such herbicide chemistries can be metabolized by cytochrome P450 monooxygenases. We believe that the accumulation of multiple resistance mechanisms in biotypes of *L. rigidum* is not rare and, therefore, the use of selective herbicides as the sole method of control of this species is not a sustainable practice.

ACKNOWLEDGMENTS

This research was supported by grants from the Grains Research and Development Corporation and the Australian Research Council. We thank Hoechst AG (Frankfurt, Germany), Zeneca Agrochemicals (Bracknell, UK), DuPont (Wilmington, U.S.A), and Ciba-Geigy (Basel, Switzerland) for gifts of radiolabeled herbicides.

REFERENCES

1. J. S. Holt, S. B. Powles, and J. A. M. Holtum, Mechanisms and agronomic aspects of herbicide resistance, *Annu. Rev. Plant Physiol Plant Mol. Biol.* **44,** 203 (1993).
2. J. M. Matthews, Management of herbicide resistant weed populations, *in* "Herbicide Resistance in Plants: Biology and Biochemistry" (S. B. Powles and J. A. M. Holtum, Eds.), pp. 317–335, Lewis Publishers, Boca Raton, FL, 1994.

COR-AAD1-00002804
Bayer EX1008 (Part 5 of 9)

3. I. Heap and R. Knight, Variations in herbicide cross-resistance among populations of annual ryegrass (*Lolium rigidum*) resistant to diclofop-methyl, *Aust. J. Agric. Res.* **41,** 121 (1990).
4. L. M. Hall, J. A. M. Holtum, and S. B. Powles, Mechanisms responsible for cross-resistance and multiple resistance, *in* "Herbicide Resistance in Plants: Biology and Biochemistry" (S. B. Powles and J. A. M. Holtum, Eds.), pp. 243–261, Lewis Publishers, Boca Raton, FL, 1994.
5. F. J. Tardif, J. A. M. Holtum, and S. B. Powles, Occurrence of herbicide-resistant acetyl-coenzyme A carboxylase mutant in annual ryegrass (*Lolium rigidum*) selected by sethoxydim, *Planta* **190,** 176 (1993).
6. F. J. Tardif and S. B. Powles, Herbicide multiple-resistance in *Lolium rigidum* biotypes is endowed by multiple mechanisms: Isolation of a subset with resistant acetyl-coenzyme A carboxylase, *Physiol. Plant.* **91,** 488 (1994).
7. J. T. Christopher, S. B. Powles, and J. A. M. Holtum, Resistance to acetolactate synthase-inhibiting herbicides in annual ryegrass (*Lolium rigidum*) involves at least two mechanisms, *Plant Physiol.* **100,** 1909 (1992).
8. J. A. M. Holtum, J. M. Matthews, R. E. Häusler, and S. B. Powles, Cross-resistance to herbicides in annual ryegrass (*Lolium rigidum*). III. On the mechanism of resistance to diclofop-methyl, *Plant Physiol.* **97,** 1026 (1991).
9. J. T. Christopher, S. B. Powles, J. A. M. Holtum, and D. R. Liljegren, Cross-resistance to herbicides in annual ryegrass (*Lolium rigidum*). II. Chlorsulfuron resistance involves a wheat-like detoxification system, *Plant Physiol.* **95,** 1036 (1991).
10. M. W. M. Burnet, B. R. Loveys, J. A. M. Holtum, and S. B. Powles, A mechanism of chlorotoluron resistance in *Lolium rigidum*, *Planta* **190,** 182 (1993).
11. M. W. M. Burnet, B. R. Loveys, J. A. M. Holtum, and S. B. Powles, Increased detoxification is the mechanism of simazine resistance in *Lolium rigidum*, *Pestic. Biochem. Physiol.* **46,** 207 (1993).
12. R. E. Häusler, J. A. M. Holtum, and S. B. Powles, Cross-resistance to herbicides in annual ryegrass (*Lolium rigidum*). IV. Correlation between membrane effects and resistance to graminicides, *Plant Physiol.* **97,** 1034 (1991).
13. J. A. M. Holtum, R. E. Häusler, M. D. Devine, and S. B. Powles, Recovery of transmembrane potentials in plants resistant to aryloxyphenoxypropanoate herbicides: A phenomenon awaiting explanation, *Weed Sci.* **42,** 293 (1994).
14. S. B. Powles and J. M. Matthews, Multiple herbicide resistance in annual ryegrass (*Lolium rigidum*): A driving force for the adoption of integrated weed management, *in* "Resistance '91: Achievements and Developments in Combating Pesticide Resistance" (I. Denholm, A. L. Devonshire and D. W. Hollomon, Eds.), pp. 75–87, Elsevier Applied Science, London, 1991.
15. M. W. M. Burnet, J. T. Christopher, J. A. M. Holtum, and S. B. Powles, Identification of two mechanisms of resistance within one population of rigid ryegrass (*Lolium rigidum*) using a selective germination medium, *Weed Sci.* **42,** 468 (1994).
16. M. W. M. Burnet, Q. Hart, J. A. M. Holtum, and S. B. Powles, Resistance to nine herbicide classes in a population of rigid ryegrass (*Lolium rigidum*), *Weed Sci.* **42,** 369 (1994).
17. R. M. Russell, J. L. Robertson, and N. E. Savin, POLO: A new computer program for probit analysis, *Bull. Entomol. Soc. Amer.* **23,** 209 (1977).
18. D. R. Hoagland and D. I. Arnon, The water culture method of growing plants without soil, Californian Agricultural Experimental Station Circular Number 347, 1938.
19. J. C. Cotterman and L. L. Saari, Rapid metabolic inactivation is the basis for cross-resistance to chlorsulfuron in diclofop-methyl-resistant rigid ryegrass (*Lolium rigidum*) biotype SR4/84, *Pestic. Biochem. Physiol.* **43,** 182 (1992).
20. B. J. Nikolau and J. C. Hawke, Purification and characterization of maize leaf acetyl-coenzyme A carboxylase, *Arch. Biochem. Biophys.* **228,** 86 (1984).
21. E. Hodgson, Microsomal mono-oxygenases, *in* "Comprehensive Insect Physiology, Biochemistry and Pharmacology, Vol III" (G. A. Kerdut and H. Rein, Eds.), pp. 225–2331, Pergamon Press, New York, 1985.
22. K. Kreutz and R. Fonné-Pfister, Herbicide-insecticide interactions in maize: Malathion inhibits cytochrome P450-dependent primisulfuron metabolism, *Pestic. Biochem. Physiol.* **43,** 232 (1992).
23. P. R. Ortiz de Montellano and N. O. Reich, Inhibition of cytochrome P-450 enzymes, in "Cytochrome P-450" (P. R. Ortiz de Montellano, Ed.), pp. 273–314, Plenum Press, New York, 1986.
24. W. Rademacher, H. Fritsch, J. E. Graebe, H. Sauter, and J. Jung, Tetcyclacis and triazole-type plant growth retardants: their influence on the biosynthesis of gibberellins and other metabolic processes, *Pestic. Sci.* **21,** 241 (1987).
25. J. T. Christopher, C. Preston, and S. B. Powles, Malathion antagonizes metabolism-based chlorsulfuron resistance in *Lolium rigidum*, *Pestic. Biochem. Physiol.* **49,** 172 (1994).
26. S. T. Hadfield, A. Wilson, S. F. Kuet, and R. Mason, The metabolism of tralkoxydim in field-grown spring wheat and maize plant cell suspension culture, *Pestic. Sci.* **40,** 193 (1994).
27. M. D. Devine and R. H. Shimabukuro, Resistance to

COR-AAD1-00002805
Bayer EX1008 (Part 5 of 9)

acetyl coenzyme A carboxylase inhibiting herbicides, *in* "Herbicide Resistance in Plants: Biology and Biochemistry" (S. B. Powles and J. A. M. Holtum, Eds.), pp. 141–169, Lewis Publishers, Boca Raton, FL, 1994.

28. F. J. Tardif, C. Preston, J. A. M. Holtum, and S. B. Powles, Resistance to acetyl-coenzyme A carboxylase-inhibiting herbicides endowed by a single major gene encoding a resistant target site in a biotype of *Lolium rigidum*, *Aust. J. Plant Physiol.* **23,** 15 (1996).
29. J. W. Gronwald, C. V. Eberlein, K. J. Betts, R. J. Baerg, N. J. Ehlke, and D. L. Wyse, Mechanism of diclofop resistance in an Italian ryegrass (*Lolium multiflorum* Lam.) biotype, *Pestic. Biochem. Physiol.* **44,** 126 (1992).

COR-AAD1-00002806
Bayer EX1008 (Part 5 of 9)

Electronic Acknowledgement Receipt

EFS ID:	40603998
Application Number:	15288406
International Application Number:	
Confirmation Number:	5402
Title of Invention:	NOVEL HERBICIDE RESISTANCE GENES
First Named Inventor/Applicant Name:	Terry WRIGHT
Customer Number:	107540
Filer:	John P. Breen/Garla Twyman
Filer Authorized By:	John P. Breen
Attorney Docket Number:	14764-258662
Receipt Date:	22-SEP-2020
Filing Date:	07-OCT-2016
Time Stamp:	15:58:45
Application Type:	Utility under 35 USC 111(a)

Payment information:

Submitted with Payment	no

File Listing:

Document Number	Document Description	File Name	File Size(Bytes)/ Message Digest	Multi Part /.zip	Pages (if appl.)
1	Foreign Reference	EP1025250A2.pdf	4349949 2bbce62547d6cc92a33d76ae009c7d5f34ec920c	no	90

Warnings:

Information:					
2	Foreign Reference	EP2535414A1.pdf	10632470 f19b4fac232a16a4e5ac102ac2843b6d61f4 4464	no	143
Warnings:					
Information:					
3	Foreign Reference	JP2005287415A.pdf	771249 e29953c728492176915e8ae058cf000d779 aff31	no	18
Warnings:					
Information:					
4	Foreign Reference	WO9808963A1.pdf	4540269 152a35bf356f82c5f67caf9238d976da3557f 8dd	no	112
Warnings:					
Information:					
5	Foreign Reference	WO9820144A2.pdf	3541672 58665389777945d722392f79a8ceb02789f 91cff	no	91
Warnings:					
Information:					
6	Foreign Reference	WO9838294A1.pdf	1652624 fde13a32feee5c1b0fe4e604d4fddb3be15c e74e	no	39
Warnings:					
Information:					
7	Foreign Reference	WO9838336A1.pdf	4120095 b5c293bba85b19691d7dc15af3b724e1bc1 ba217	no	97
Warnings:					
Information:					
8	Foreign Reference	WO9844139A1.pdf	1765684 cdc4947adc0fb14db4c25b43dd05b51b02f 267cf	no	36
Warnings:					
Information:					

9	Foreign Reference	WO9910513A1.pdf	6707923 b6a9be652f8f56f223052b468d8dea267c1b4acc	no	131
Warnings:					
Information:					
10	Foreign Reference	WO9963092A1.pdf	2658510 40502fbfa23164795f11488956f5b03f5ac1f816	no	56
Warnings:					
Information:					
11	Foreign Reference	WO0006757A1.pdf	2487530 3f38cba4e2c4c355522292429176f78bccab48e4	no	38
Warnings:					
Information:					
12	Foreign Reference	WO0138513A2.pdf	4472273 3f57347430e68305b4e7c32ada0f6c15c9f875f5	no	86
Warnings:					
Information:					
13	Foreign Reference	WO03056904A2.pdf	4252580 a83dbcb92483cd6eaf20496e3f479d2de96b227f	no	76
Warnings:					
Information:					
14	Non Patent Literature	Bayley.pdf	1097444 52fb57769217f5598173c52a8729113b60123f2e	no	5
Warnings:					
Information:					
15	Non Patent Literature	Bhat_Purification_of_3_5-dichlorocatechol.pdf	752977 37011996c72f52db32d0a7ca9127f55e34bdc2dd	no	9
Warnings:					
Information:					

16	Non Patent Literature	Chaudhry_Huang.pdf	3573737 49b6961b2bb1eabcba881e1b43e215dfeddb1c12	no	6
Warnings:					
Information:					
17	Non Patent Literature	Chen_Martin.pdf	957188 001c7a33ee26c2fdf7290bce6caafa5bf3427cca	no	4
Warnings:					
Information:					
18	Non Patent Literature	Cosper.pdf	118914 4cbed88a21f0d5010acbe8d26bb22d2acf50e804	no	8
Warnings:					
Information:					
19	Non Patent Literature	Daane_Haggblom.pdf	119265 0d04cdb7335ba2f9f1fef69445ce6352acb42067	no	6
Warnings:					
Information:					
20	Non Patent Literature	de_Lipthay_Enhanced_degradation.pdf	408884 578f39bd5f16b73288e326a79a20e544cdd3e45b	no	10
Warnings:					
Information:					
21	Non Patent Literature	de_Lipthay_Expression.pdf	535186 7d4f61703e4b9ab7b2dec6ededc1d46892fd2e15	no	10
Warnings:					
Information:					
22	Non Patent Literature	de_Lipthay_In_situ.pdf	210761 a48cff6fb0e1e592ef25fc3669ff24c177d9307e	no	7
Warnings:					
Information:					

23	Non Patent Literature	Dunbar_Genetic_Diversity.pdf	229327 e44263e930c732a51e61234d19cf603191535dcd	no	6
Warnings:					
Information:					
24	Non Patent Literature	Feng_Biodegradation.pdf	327767 841884e89d44492a146669770647c29f97beaf6a	no	7
Warnings:					
Information:					
25	Non Patent Literature	Fuechslin_Effect.pdf	256304 1cf34b2220e0bf412324f43a7601559a3572df3c	no	10
Warnings:					
Information:					
26	Non Patent Literature	Harker_Phenoxyacetic.pdf	1454971 0333c05479947c354574545d833ec732b7c6a066	no	7
Warnings:					
Information:					
27	Non Patent Literature	Hawkins.pdf	500664 2752cbbe4ea3f56103fe4f126aa9dd2f28c1942c	no	5
Warnings:					
Information:					
28	Non Patent Literature	Hegg.pdf	389422 36d29472c268aeb26227bb20834350b3b60c5839	no	13
Warnings:					
Information:					
29	Non Patent Literature	Hoffmann_A_transposon.pdf	241692 9e38b8ca8484fa1818fce979063e9b1086945b0b	no	12
Warnings:					
Information:					

30	Non Patent Literature	Hogan_Distribution.pdf	293326 a86e836ba90448d609e87fdc3a00fdd4a1895e19	no	7
Warnings:					
Information:					
31	Non Patent Literature	Hogan_Site-directed.pdf	408901 e48b3072c54f36a3df35463329733fa7ce517658	no	11
Warnings:					
Information:					
32	Non Patent Literature	Jackman_Electrokinetic.pdf	397707 1a8335b2807a7f52df38c4e6c137840ee25ccc bc	no	10
Warnings:					
Information:					
33	Non Patent Literature	Ka_Integration.pdf	4541593 88b1a905e1337e9c2adca37fba6d83a1e91bb592	no	6
Warnings:					
Information:					
34	Non Patent Literature	Ka_Use_of_Gene_Probes.pdf	3038416 63927a59b42f07991fcd01a2ff824a5853f14df9	no	5
Warnings:					
Information:					
35	Non Patent Literature	Kitagawa_Novel.pdf	469630 cbb6a626c9e57d32ea264333855d9fdf3dadc210	no	10
Warnings:					
Information:					
36	Non Patent Literature	Kleinsteuber.pdf	192892 aee216f155513fec111690bd64d672991a5e080f	no	10
Warnings:					
Information:					

37	Non Patent Literature	Laemmli.pdf	456697 573806d0af0810d5d376fb409d6ce4571f4824f8	no	10
Warnings:					
Information:					
38	Non Patent Literature	Laurent.pdf	417927 6d063237c8b793a8d7b1a805bce98bf46527613c	no	5
Warnings:					
Information:					
39	Non Patent Literature	Letouze.pdf	317520 b1bc39aaeb43f3f3511bfa4313c1f869a2428362	no	9
Warnings:					
Information:					
40	Non Patent Literature	Lewis.pdf	208335 9ce78e2482760143718929 94eba81707f11052b0	no	4
Warnings:					
Information:					
41	Non Patent Literature	Loos.pdf	338446 ad1ae2a2a4771dbc46d6b8a75c61120b6fa8416e	no	3
Warnings:					
Information:					
42	Non Patent Literature	Ludwig.pdf	241361 cdec5c4d3c5a917b183847cfffeca1cb329ace39	no	7
Warnings:					
Information:					
43	Non Patent Literature	Lyon_Expression.pdf	629278 63e37c0ff6bdc280382c6f1a8aeea6e844f37537	no	8
Warnings:					
Information:					

44	Non Patent Literature	Lyon_Cotton.pdf	794983 c514491d348fee56adeaf78d7fded85e6972664b	no	8
Warnings:					
Information:					
45	Non Patent Literature	Mae.pdf	683860 f7c971b6168b7adb48aebbc72a56719a817ba5e7	no	6
Warnings:					
Information:					
46	Non Patent Literature	Maltseva.pdf	1055193 a9aa83cf0f0d97e3a8bca863f0910ca7baedd150	no	8
Warnings:					
Information:					
47	Non Patent Literature	Marriott.pdf	205008 3d41e3dea547bf360fc68a482c71e9203e21ade9	no	5
Warnings:					
Information:					
48	Non Patent Literature	Matheson_Evidence.pdf	326366 19cd78cf9796daa1a1cda2934005756e05db0110	no	7
Warnings:					
Information:					
49	Non Patent Literature	McGowan.pdf	130083 f81afade5ec51b5c1c20b3ec91cc1393056cdc24	no	4
Warnings:					
Information:					
50	Non Patent Literature	Mortensen.pdf	224813 bb646ccc1fb018df97efedb88f39619223175172	no	8
Warnings:					
Information:					

51	Non Patent Literature	Muller_Pseudo.pdf	268197 6da514c9c8913feb678754c51848066b082083a3	no	16
Warnings:					
Information:					
52	Non Patent Literature	Muller_Separation.pdf	414010 0f5f8e4cd3fd98513afa5942739f3fb7224498f6	no	7
Warnings:					
Information:					
53	Non Patent Literature	Muller_Comamonas.pdf	5842254 fd95749e9db884469b7454b274a15f8a7473d2fb	no	6
Warnings:					
Information:					
54	Non Patent Literature	Nickel.pdf	146740 9b05b58657657e9781693408468442684 33a5b1f	no	6
Warnings:					
Information:					
55	Non Patent Literature	Ohkouchi.pdf	426030 6099128d557c57b76e0cc4b7d23024d23dbf0e4f	no	8
Warnings:					
Information:					
56	Non Patent Literature	Parker_Kinetics.pdf	498741 3d17aad5c383a18485fabf2e9b77f4fea57f0f6c	no	6
Warnings:					
Information:					
57	Non Patent Literature	Perkins.pdf	1279394 a54783e042a7215836f96d481262a08625a5c998	no	7
Warnings:					
Information:					

58	Non Patent Literature	Plumeier_Importance.pdf	233405 58e6256a0d10765f234f0048bb617832c21184d0	no	11
Warnings:					
Information:					
59	Non Patent Literature	Poh_Complete.pdf	155435 4dc74440544c54ecb6e6c44bf7d0edaebf8a5331	no	12
Warnings:					
Information:					
60	Non Patent Literature	Preston_Multiple.pdf	246261 79cd82cee9cd314c7a77c1f408e566c5b415d451	no	12
Warnings:					
Information:					
		Total Files Size (in bytes):	88010133		

This Acknowledgement Receipt evidences receipt on the noted date by the USPTO of the indicated documents, characterized by the applicant, and including page counts, where applicable. It serves as evidence of receipt similar to a Post Card, as described in MPEP 503.

New Applications Under 35 U.S.C. 111

If a new application is being filed and the application includes the necessary components for a filing date (see 37 CFR 1.53(b)-(d) and MPEP 506), a Filing Receipt (37 CFR 1.54) will be issued in due course and the date shown on this Acknowledgement Receipt will establish the filing date of the application.

National Stage of an International Application under 35 U.S.C. 371

If a timely submission to enter the national stage of an international application is compliant with the conditions of 35 U.S.C. 371 and other applicable requirements a Form PCT/DO/EO/903 indicating acceptance of the application as a national stage submission under 35 U.S.C. 371 will be issued in addition to the Filing Receipt, in due course.

New International Application Filed with the USPTO as a Receiving Office

If a new international application is being filed and the international application includes the necessary components for an international filing date (see PCT Article 11 and MPEP 1810), a Notification of the International Application Number and of the International Filing Date (Form PCT/RO/105) will be issued in due course, subject to prescriptions concerning national security, and the date shown on this Acknowledgement Receipt will establish the international filing date of the application.

PTO/SB/08a (02-18)
Approved for use through 11/30/2020. OMB 0651-0031
U.S. Patent and Trademark Office; U.S. DEPARTMENT OF COMMERCE

Under the Paperwork Reduction Act of 1995, no persons are required to respond to a collection of information unless it contains a valid OMB control number.

INFORMATION DISCLOSURE STATEMENT BY APPLICANT
(Not for submission under 37 CFR 1.99)

Application Number	15288406
Filing Date	2016-10-07
First Named Inventor	Terry Wright
Art Unit	1663
Examiner Name	KRUSE, David H.
Attorney Docket Number	14764-258662

U.S.PATENTS Remove

Examiner Initial*	Cite No	Patent Number	Kind Code[1]	Issue Date	Name of Patentee or Applicant of cited Document	Pages, Columns, Lines where Relevant Passages or Relevant Figures Appear
	1	5910626		1999-06-08	Haselkorn and Gornicki	
	2	6087563		2000-07-11	DellaPenna and Norris	
	3	6107549		2000-08-22	Feng et al.	
	4	6268547		2001-07-31	Weeks	
	5	7405074		2008-07-29	Castle et al.	
	6	7462481		2008-12-09	Castle et al.	
	7	7659448		2010-02-09	Ahrens et al.	
	8	7863503		2011-01-04	Castle et al.	

INFORMATION DISCLOSURE STATEMENT BY APPLICANT (Not for submission under 37 CFR 1.99)		
	Application Number	15288406
	Filing Date	2016-10-07
	First Named Inventor	Terry Wright
	Art Unit	1663
	Examiner Name	KRUSE, David H.
	Attorney Docket Number	14764-258662

	9	7998703		2011-08-16	Castle et al.	
	10	8222489		2012-07-17	Castle et al.	
	11	9074007		2015-07-07	Danilevskaya et al,	

If you wish to add additional U.S. Patent citation information please click the Add button. Add

U.S.PATENT APPLICATION PUBLICATIONS Remove

Examiner Initial*	Cite No	Publication Number	Kind Code[1]	Publication Date	Name of Patentee or Applicant of cited Document	Pages,Columns,Lines where Relevant Passages or Relevant Figures Appear
	1	20020059659		2002-05-16	Stemmer	
	2	20030056245		2003-03-20	Chatterjee et al.	
	3	20090069182		2009-03-12	Castle et al.	
	4	20120245339		2012-09-27	Castle et al.	
	5	20140325713		2014-10-30	Kovalic et al.	

If you wish to add additional U.S. Published Application citation information please click the Add button. Add

FOREIGN PATENT DOCUMENTS Remove

INFORMATION DISCLOSURE STATEMENT BY APPLICANT (Not for submission under 37 CFR 1.99)		
	Application Number	15288406
	Filing Date	2016-10-07
	First Named Inventor	Terry Wright
	Art Unit	1663
	Examiner Name	KRUSE, David H.
	Attorney Docket Number	14764-258662

Examiner Initial*	Cite No	Foreign Document Number[3]	Country Code[2] ¡	Kind Code[4]	Publication Date	Name of Patentee or Applicant of cited Document	Pages,Columns,Lines where Relevant Passages or Relevant Figures Appear	T[5]
	1	1025250	EP		1999-05-14	Grimm and Tanaka	WO99/23231 and English counterpart US 6624342	☒
	2	2535414	EP		2012-12-19	Castle et al.		☐
	3	2005/287415	JP		2005-10-20	Kamagata et al.	Abstract trans only	☒
	4	9808963	WO		1998-03-05	Gengenback et al.		☐
	5	9820144	WO		1998-05-14	Thompson et al.		☐
	6	9838294	WO		1998-09-03	Kaphammer		☐
	7	9838336	WO		1998-09-03	Elsemore et al.		☐
	8	9844139	WO		1998-10-08	Horn and Hall		☐
	9	9910513	WO		1999-03-04	Daniell		☐
	10	1999/063092	WO		1999-12-06	Luschnig et al.		☐

INFORMATION DISCLOSURE STATEMENT BY APPLICANT (Not for submission under 37 CFR 1.99)		
	Application Number	15288406
	Filing Date	2016-10-07
	First Named Inventor	Terry Wright
	Art Unit	1663
	Examiner Name	KRUSE, David H.
	Attorney Docket Number	14764-258662

	11	2000/006757	WO		2000-02-10	Horn and Hall		☐
	12	2001/038513	WO		2001-05-31	Castle et al.		☐
	13	2003/056904	WO		2003-07-17	Raab		☐

If you wish to add additional Foreign Patent Document citation information please click the Add button | Add

NON-PATENT LITERATURE DOCUMENTS | Remove

Examiner Initials*	Cite No	Include name of the author (in CAPITAL LETTERS), title of the article (when appropriate), title of the item (book, magazine, journal, serial, symposium, catalog, etc), date, pages(s), volume-issue number(s), publisher, city and/or country where published.	T5
	1	BAYLEY et al., Engineering 2,4-D resistance into cotton, Theoretical and Applied Genetics (1992), 83(5), 645-9.	☐
	2	BHAT et al., Purification of 3,5-dichlorocatechol 1,2-dioxygenase, a nonheme iron dioxygenase and a key enzyme in the biodegradation of a herbicide, 2,4-dichlorophenoxyacetic acid (2,4-D), from Pseudomonas cepacia CSV90, Archives of Biochemistry and Biophysics (1993), 300(2), 738-46.	☐
	3	CHAUDHRY and HUANG, Isolation and characterization of a new plasmid from a Flavobacterium sp. which carries the genes for degradation of 2,4-dichlorophenoxyacetate, Journal of Bacteriology (1988), 170(9), 3897-902.	☐
	4	CHEN and MARTIN, Reasons for the acclimation for 2,4-D biodegradation in lake water, Journal of Environmental Quality (1989), 18(2), 153-6.	☐
	5	COSPER et al., X-ray absorption spectroscopic analysis of Fe(II) and Cu(II) forms of a herbicide-degrading ketoglutarate dioxygenase, JBIC, Journal of Biological Inorganic Chemistry (1999), 4(1), 122-129.	☐
	6	DAANE and HAGGBLOM, Earthworm egg capsules as vectors for the environmental introduction of biodegradative bacteria, Applied and Environmental Microbiology (1999), 65(6), 2376-2381.	☐

INFORMATION DISCLOSURE STATEMENT BY APPLICANT (Not for submission under 37 CFR 1.99)		
	Application Number	15288406
	Filing Date	2016-10-07
	First Named Inventor	Terry Wright
	Art Unit	1663
	Examiner Name	KRUSE, David H.
	Attorney Docket Number	14764-258662

	7	DE LIPTHAY et al., Enhanced degradation of phenoxyacetic acid in soil by horizontal transfer of the tfdA gene encoding a 2,4-dichlorophenoxyacetic acid dioxygenase, FEMS Microbiology Ecology (2001), 35(1), 75-84.	☐
	8	DE LIPTHAY et al., Expression of tfdA genes in aquatic microbial communities during acclimation to 2,4-dichlorophenoxyacetic acid, FEMS Microbiology Ecology (2002), 40(3), 205-214.	☐
	9	DE LIPTHAY et al., In situ exposure to low herbicide concentrations affects microbial population composition and catabolic gene frequency in an aerobic shallow aquifer, Applied and Environmental Microbiology (2003), 69(1), 461-467.	☐
	10	DUNBAR et al., Genetic diversity through the looking glass: effect of enrichment bias, Applied and Environmental Microbiology (1997), 63(4), 1326-1331.	☐
	11	FENG and KENNEDY, Biodegradation and plant protection from the herbicide 2,4-D by plant-microbial associations in cotton production systems, Biotechnology and Bioengineering (1997), 54(6), 513-519.	☐
	12	FUECHSLIN et al., Effect of integration of a GFP reporter gene on fitness of Ralstonia eutropha during growth with 2,4-dichlorophenoxyacetic acid, Environmental Microbiology (2003), 5(10), 878-887.	☐
	13	HARKER et al., Phenoxyacetic acid degradation by the 2,4-dichlorophenoxyacetic acid (TFD) pathway of plasmid pJP4: mapping and characterization of the TFD regulatory gene, tfdR, Journal of Bacteriology (1989), 171(1), 314-20.	☐
	14	HAWKINS and HARWOOD, Chemotaxis of Ralstonia eutropha JMP134(pJP4) to the herbicide 2,4-dichlorophenoxyacetate, Applied and Environmental Microbiology (2002), 68(2), 968-972.	☐
	15	HEGG et al., Herbicide-Degrading Keto Acid-Dependent Enzyme TfdA: Metal Coordination Environment and Mechanistic Insights, Biochemistry (1999), 38(50), 16714-16726.	☐
	16	HOFFMANN et al., A transposon encoding the complete 2,4-dichlorophenoxyacetic acid degradation pathway in the alkalitolerant strain Delftia acidovorans P4a, Microbiology (Reading, United Kingdom) (2003), 149(9), 2545-2556.	☐
	17	HOGAN et al., Distribution of the tfdA gene in soil bacteria that do not degrade 2,4-dichlorophenoxyacetic acid (2,4-D), Microbial Ecology (1997), 34(2), 90-96.	☐

INFORMATION DISCLOSURE STATEMENT BY APPLICANT (Not for submission under 37 CFR 1.99)		
	Application Number	15288406
	Filing Date	2016-10-07
	First Named Inventor	Terry Wright
	Art Unit	1663
	Examiner Name	KRUSE, David H.
	Attorney Docket Number	14764-258662

	18	HOGAN et al., Site-directed mutagenesis of 2,4-dichlorophenoxyacetic acid/ketoglutarate dioxygenase. Identification of residues involved in metallocenter formation and substrate binding, Journal of Biological Chemistry (2000), 275(17), 12400-12409.	☐
	19	Poiger et al., J Agic Food Chem. (63)2583-2590 (2015), Environmental Behavior of the Chiral Herbicide Haloxyfop. 1. Rapid and Preferential Interconversion of the Enantiomers in Soil.	☐
	20	KANEKO et al., DNA Research (9)189-197 (2002), Complete Genomic Sequence of Nitrogen-fixing Symbiotic Bacterium Bradyrhizobium japonicum USDA110	☐
	21	JACKMAN et al., Electrokinetic movement and biodegradation of 2,4-dichlorophenoxyacetic acid in silt soil, Biotechnology and Bioengineering (2001), 74(1), 40-48.	☐
	22	KA and TIEDJE, Integration and excision of a 2,4-dichlorophenoxyacetic acid-degradative plasmid in Alcaligenes paradoxus and evidence of its natural intergeneric transfer, Journal of Bacteriology (1994), 176(17), 5284-9.	☐
	23	KA et al., Use of gene probes to aid in recovery and identification of functionally dominant 2,4-dichlorophenoxyacetic acid-degrading populations in soil, Applied and Environmental Microbiology (1994), 60(4), 1116-20.	☐
	24	KITAGAWA et al., Novel 2,4-dichlorophenoxyacetic acid degradation genes from oligotrophic Bradyrhizobium sp. strain HW13 isolated from a pristine environment, Journal of Bacteriology (2002), 184(2), 509-518.	☐
	25	KLEINSTEUBER et al., Expression of the 2,4-D degradative pathway of pJP4 in an alkaliphilic, moderately halophilic soda lake isolate, Halomonas sp. EF43, Extremophiles (2001), 5(6), 375-384.	☐
	26	LAEMMLI et al., Mutation analysis of the different tfd genes for degradation of chloroaromatic compounds in Ralstonia eutropha JMP134, Archives of Microbiology (2004), 181(2), 112-121. (Published online: 16 December 2003).	☐
	27	LAURENT et al., 2,4-Dichlorophenoxyacetic Acid Metabolism in Transgenic Tolerant Cotton (Gossypium hirsutum), Journal of Agricultural and Food Chemistry (2000), 48(11), 5307-5311.	☐
	28	LETOUZE and GASQUEZ, Enhanced activity of several herbicide-degrading enzymes: a suggested mechanism responsible for multiple resistance in blackgrass (Alopecurus myosuroides Huds.), Agronomie (2003), 23(7), 601-608.	☐

INFORMATION DISCLOSURE STATEMENT BY APPLICANT (Not for submission under 37 CFR 1.99)		
	Application Number	15288406
	Filing Date	2016-10-07
	First Named Inventor	Terry Wright
	Art Unit	1663
	Examiner Name	KRUSE, David H.
	Attorney Docket Number	14764-258662

	29	LEWIS et al., Influence of environmental changes on degradation of chiral pollutants in soils, Nature (London) (1999), 401(6756), 898-901.	☐
	30	LOOS et al., Phenoxyacetate herbicide detoxication by bacterial enzymes, Journal of Agricultural and Food Chemistry (1967), 15(5), 858-60.	☐
	31	LUDWIG et al., Chromatographic separation of the enantiomers of marine pollutants. Part 5: enantioselective degradation of phenoxycarboxylic acid herbicides by marine microorganisms, Chemosphere (1992), 24(10), 1423-9.	☐
	32	LYON et al., Expression of a bacterial gene in transgenic tobacco plants confers resistance to the herbicide 2,4-dichlorophenoxyacetic acid, Plant Molecular Biology (1989), 13(5), 533-40.	☐
	33	LYON et al., Cotton plants transformed with a bacterial degradation gene are protected from accidental spray drift damage by the herbicide 2,4-dichlorophenoxyacetic acid, Transgenic Research (1993), 2(3), 162-9.	☐
	34	MAE et al., Characterization of a new 2,4-dichlorophenoxyacetic acid degrading plasmid pEST4011: physical map and localization of catabolic genes, Journal of General Microbiology (1993), 139(12), 3165-70.	☐
	35	MALTSEVA et al., Degradation of 2,4-dichlorophenoxyacetic acid by haloalkaliphilic bacteria, Microbiology (Reading, United Kingdom) (1996), 142(5), 1115-1122.	☐
	36	MARRIOTT et al., Biodegradation of mixtures of chlorophenoxyalkanoic acid herbicides by Alcaligenes denitrificans, Journal of Industrial Microbiology & Biotechnology (2000), 25(5), 255-259.	☐
	37	MATHESON et al., Evidence for acquisition in nature of a chromosomal 2,4-dichlorophenoxyacetic acid/ketoglutarate dioxygenase gene by different Burkholderia spp, Applied and Environmental Microbiology (1996), 62(7), 2457-2463.	☐
	38	MCGOWAN et al., Evidence for interspecies gene transfer in the evolution of 2,4-dichlorophenoxyacetic acid degraders, Applied and Environmental Microbiology (1998), 64(10), 4089-4092.	☐
	39		☐

INFORMATION DISCLOSURE STATEMENT BY APPLICANT (Not for submission under 37 CFR 1.99)		
	Application Number	15288406
	Filing Date	2016-10-07
	First Named Inventor	Terry Wright
	Art Unit	1663
	Examiner Name	KRUSE, David H.
	Attorney Docket Number	14764-258662

	40	MORTENSEN and JACOBSEN, Influence of Frozen Storage on Herbicide Degradation Capacity in Surface and Subsurface Sandy Soils, Environ Sci Technol 2004, 38, 6625-6632.	☐
	41	MULLER and BABEL, Pseudo-recalcitrance of chlorophenoxyalkanoate herbicides - correlation to the availability of ketoglutarate, Acta Biotechnologica (2001), 21(3), 227-242.	☐
	42	MULLER and BABEL, Separation of two dichlorprop/ketoglutarate dioxygenases with enantiospecific properties from Comamonas acidovorans MC1, Acta Biotechnologica (1999), 19(4), 349-355.	☐
	43	MULLER et al., Comamonas acidovorans strain MC1. A new isolate capable of degrading the chiral herbicides dichlorprop and mecoprop and the herbicides 2,4-D and MCPA, Microbiological Research (1999), 154(3), 241-246.	☐
	44	NICKEL et al., Involvement of two ketoglutarate-dependent dioxygenases in enantioselective degradation of (R)- and (S)-mecoprop by Sphingomonas herbicidovorans MH, Journal of Bacteriology (1997), 179(21), 6674-6679.	☐
	45	OHKOUCHI et al., Cloning and expression of DL-2-haloacid dehalogenase gene from Burkholderia cepacia, Water Science and Technology (2000), 42(7-8, Hazard Assessment and Control of Environmental Contaminants (Ecohazard 99)), 261-268.	☐
	46	PARKER and DOXTADER, Kinetics of microbial decomposition of 2,4-D in soil: effects of herbicide concentration, Journal of Environmental Quality (1982), 11(4), 679-84.	☐
	47	PERKINS et al., Use of Alcaligenes eutrophus as a source of genes for 2,4-D resistance in plants, Weed Science (1987), 35(Suppl. 1), 12-18.	☐
	48	PLUMEIER et al., Importance of different tfd genes for degradation of chloroaromatics by Ralstonia eutropha JMP134, Journal of Bacteriology (2002), 184(15), 4054-4064.	☐
	49	POH et al., Complete characterization of Tn5530 from Burkholderia cepacia strain 2a (plJB1) and studies of 2,4-dichlorophenoxyacetate uptake by the organism, Plasmid (2002), 48(1), 1-12.	☐
	50	PRESTON et al., Multiple resistance to dissimilar herbicide chemistries in a biotype of Lolium rigidum due to enhanced activity of several herbicide degrading enzymes, Pesticide Biochemistry and Physiology (1996), 54(2), 123-134.	☐

	51	ROUSSEAUX et al., Isolation and characterisation of new Gram-negative and Gram-positive atrazine degrading bacteria from different French soils, FEMS Microbiology Ecology (2001), 36(2-3), 211-222.	☐
	52	SAARI et al., Stereospecific degradation of the phenoxypropionate herbicide dichlorprop, Journal of Molecular Catalysis B: Enzymatic (1999), 6(4), 421-428.	☐
	53	SCHNEIDERHEINZE et al., Plant and soil enantioselective biodegradation of racemic phenoxyalkanoic herbicides, Chirality (1999), 11(4), 330-337.	☐
	54	SEIFERT et al., Effect of tillage on microbial characteristics and herbicide degradation in a Sharkey clay soil, Weed Science (2001), 49(5), 685-693.	☐
	55	SHAW and BURNS, Enhanced mineralization of [U-14C]2,4-dichlorophenoxyacetic acid in soil from the rhizosphere of Trifolium pratense, Applied and Environmental Microbiology (2004), 70(8), 4766-4774.	☐
	56	SMEJKAL et al., Substrate specificity of chlorophenoxyalkanoic acid-degrading bacteria is not dependent upon phylogenetically related tfdA gene types, Biology and Fertility of Soils (2001), 33(6), 507-513.	☐
	57	STREBER and WILLMITZER, Transgenic tobacco plants expressing a bacterial detoxifying enzyme are resistant to 2,4-D, Bio/Technology (1989), 7(8), 811-16.	☐
	58	SWIEGERS et al., Carnitine biosynthesis in Neurospora crassa: identification of a cDNA coding for N-trimethyllysine hydroxylase and its functional expression in Saccharomyces cerevisiae, FEMS Microbiology Letters (2002), 210(1), 19-23.	☐
	59	TETT et al., Enantioselective degradation of the herbicide mecoprop [2-(2-methyl-4-chlorophenoxy)propionic acid] by mixed and pure bacterial cultures, FEMS Microbiology Ecology (1994), 14(3), 191-200.	☐
	60	TOP and SPRINGAEL, The role of mobile genetic elements in bacterial adaptation to xenobiotic organic compounds, Current Opinion in Biotechnology (2003), 14(3), 262-269.	☐
	61	TOP et al., Capture of a catabolic plasmid that encodes only 2,4-dichlorophenoxyacetic acid:ketoglutaric acid dioxygenase (TfdA) by genetic complementation, Applied and Environmental Microbiology (1996), 62(7), 2470-2476.	☐

INFORMATION DISCLOSURE STATEMENT BY APPLICANT (Not for submission under 37 CFR 1.99)		
	Application Number	15288406
	Filing Date	2016-10-07
	First Named Inventor	Terry Wright
	Art Unit	1663
	Examiner Name	KRUSE, David H.
	Attorney Docket Number	14764-258662

	62	TOP et al., Methane oxidation as a method to evaluate the removal of 2,4-dichlorophenoxyacetic acid (2,4-D) from soil by plasmid-mediated bioaugmentation, FEMS Microbiology Ecology (1999), 28(3), 203-213.	☐
	63	TRAVKIN et al., Characterization of an intradiol dioxygenase involved in the biodegradation of the chlorophenoxy herbicides 2,4-D and 2,4,5-T, FEBS Letters (1997), 407(1), 69-72.	☐
	64	VALLAEYS et al., PCR-RFLP analysis of 16S rRNA, tfdA and tfdB genes reveals a diversity of 2,4-D degraders in soil aggregates, FEMS Microbiology Ecology (1997), 24(3), 269-278.	☐
	65	VALLAEYS et al., The metabolic pathway of 2,4-dichlorophenoxyacetic acid degradation involves different families of tfdA and tfdB genes according to PCR-RFLP analysis, FEMS Microbiology Ecology (1996), 20(3), 163-172.	☐
	66	VEDLER et al., Analysis of the 2,4-dichlorophenoxyacetic acid-degradative plasmid pEST4011 of Achromobacter xylosoxidans subsp. denitrificans strain EST4002, Gene (2000), 255(2), 281-288.	☐
	67	VEDLER et al., TfdR, the LysR-type transcriptional activator, is responsible for the activation of the tfdCB operon of Pseudomonas putida 2,4-dichlorophenoxyacetic acid degradative plasmid pEST4011, Gene (2000), 245(1), 161-168.	☐
	68	VELICER, Pleiotropic effects of adaptation to a single carbon source for growth on alternative substrates, Applied and Environmental Microbiology (1999), 65(1), 264-269.	☐
	69	WHITING et al., Metal Coordination Environment of a Cu(II)-Substituted Keto Acid-Dependent Dioxygenase That Degrades the Herbicide 2,4-D, Journal of the American Chemical Society (1997), 119(14), 3413-3414.	☐
	70	YI et al., Phylogenetic and phenotypic diversity of 4-chlorobenzoate-degrading bacteria isolated from soils, FEMS Microbiology Ecology (2000), 31(1), 53-60.	☐
	71	ZHANG et al., In vitro assay for 2,4-D resistance in transgenic cotton, In Vitro Cellular & Developmental Biology: Plant (2001), 37(2), 300-304.	☐
	72	ZHANG et al., Inheritance and segregation of exogenous genes in transgenic cotton, Journal of Genetics (2000), 79 (2), 71-75.	☐

INFORMATION DISCLOSURE STATEMENT BY APPLICANT (Not for submission under 37 CFR 1.99)		
	Application Number	15288406
	Filing Date	2016-10-07
	First Named Inventor	Terry Wright
	Art Unit	1663
	Examiner Name	KRUSE, David H.
	Attorney Docket Number	14764-258662

	73	ZIPPER et al., Complete microbial degradation of both enantiomers of the chiral herbicide mecoprop [(RS)-2-(4-chloro-2-methylphenoxy)propionic acid] in an enantioselective manner by Sphingomonas herbicidovorans sp. Nov, Applied and Environmental Microbiology (1996), 62(12), 4318-4322.	☐
	74	ZIPPER et al., Enantioselective uptake and degradation of the chiral herbicide dichlorprop [(RS)-2-(2,4-dichlorophenoxy)propanoic acid] by Sphingomonas herbicidovorans MH, Journal of Bacteriology (1998), 180(13), 3368-3374.	☐
	75	CHO ET AL, Agricultural Chemistry and Biotechnology (English Edition) (1999), 42(2), 57-61 , Isolation and characterization of 2-methyl-4-chlorophenoxyacetic acid-degrading bacteria from agricultural soils.	☐
	76	KWON et al J. Kor. Soc. Hort. Sci. (1997), 38(6), 796-799.	☐
	77	LIM ET AL, Journal of Microbiology (Seoul, Republic of Korea) (2004), 42(2), 87-93 Genetic and phenotypic diversity of (R/S)-mecoprop [2-(2-methyl-4-chlorophenoxy)propionic acid]-degrading bacteria isolated from soils	☐
	78	Tamura et al, Nippon Noyaku Gakkaishi (2001), 26(3), 309-314 , Microbial pesticide degradations and evolutionary analysis of degrading enzymes.	☐
	79	PARK ET AL, Journal of Microbiology (Seoul, Republic of Korea) (2003), 41(1), 7-15, Genetic and phenotypic diversity of dichlorprop-degrading bacteria isolated from soils.	☐
	80	VALLAEYS ET AL, Biotechnology Letters (1998), 20(11), 1073-1076 , Isolation and characterization of a stable 2,4-dichlorophenoxyacetic acid degrading bacterium, Variovorax paradoxus, using chemostat culture	☐
	81	(Book, will be provided upon request) Nakatsu CH, Fukumori F, Fulthorpe R, Hausinger R, Holben W, Kamagata Y, Korona R, Lenski R, Maltseva O, Matheson VG, McGowan C. Genetic diversity of 2, 4-dichlorophenoxyacetic acid (2, 4-D) catabolic genes. Microbial diversity and genetics of biodegradation. Japan Scientific Societies Press, Tokyo, Japan. 1997:197-206.	☐
	82	(Same book, will be provided upon request) Hausinger RP, Fukumori F, Hogan DA, Sassanella TM, Kamagata Y, Takami H, Saari RE, Horikoshi K, Fukuda M, Kudo T. Microbial diversity and genetics of biodegradation. by K. Horikoshi, M. Fukuda and T. Kudo, Japan Science Societies Press, Tokyo. 1997:35-51.	☐
	83	Fukamori and Hausinger, JBC (268)24311(1993), Purification and characterization of 2,4-Dichlorophenoxyacetate/a-ketogutarate dioxygenase.	☐

INFORMATION DISCLOSURE STATEMENT BY APPLICANT (Not for submission under 37 CFR 1.99)		
	Application Number	15288406
	Filing Date	2016-10-07
	First Named Inventor	Terry Wright
	Art Unit	1663
	Examiner Name	KRUSE, David H.
	Attorney Docket Number	14764-258662

	84	Fukamori and Hausinger, J Bacterioloogy (175)2083(1993), Alcaligenes eutrophus JMP134 "2,4-Dichlorophenoxyacetate monooxygenase" is an a-Ketoglutarate-dependent dioxygenase.	☐
	85		☐
	86		☐
	87		☐
	88	Ehrig et al., Acta Biotechologica (17)351-356(1997), Isolation of phenoxyherbicidedegrading Rhodoferax species from contaminated building material.	☐
	89	Hausinger, Critical Reviews in Biochemsitry (39)21-68(2004), Fe(II)/α-Ketoglutarate-Dependent Hydroxylases and Related Enzymes.	☐
	90	Kohler et al., J Ind Microbio biotech (23)336(1999), Sphingomonas herbicidovorans MH: a versatile phenoxyalkanoic acid herbicide degrader.	☐
	91	Hausinger and Fukamori, Env Health Perspectives (103)37-39(1995), Characterization of the first enzyme in 2,4-Dichlorphenoxyacetic acid metabolism.	☐
	92	Don et al., J Bacteriol (161)85(1985), Transposon Mutagenesis and Cloning Analysis of the Pathways for Degradation of 2,4-Dichlorophenoxyacetic Acid and 3-Chlorobenzoate in Alcaligenes eutrophus JMP134(pJP4).	☐
	93	Don et al.,J Bacteriol (161)466(1985), Genetic and Physical Map of the 2,4-Dichlorophenoxyacetic Acid-Degradative Plasmid pJP4	☐
	94	Hotopp et al., J. Molec. Catalysis B: Enzymatic (15)155-162(2001), Alternative substrates of 2,4-dichlorophenoxyacetate/-ketoglutarate dioxygenase.	☐

INFORMATION DISCLOSURE STATEMENT BY APPLICANT (Not for submission under 37 CFR 1.99)		
	Application Number	15288406
	Filing Date	2016-10-07
	First Named Inventor	Terry Wright
	Art Unit	1663
	Examiner Name	KRUSE, David H.
	Attorney Docket Number	14764-258662

	95	WESTENDORF ET AL., Microbiol. Res. 157 (4), 317-322 (2002), The two enantiospecific dichlorprop/α-ketoglutarate-dioxygenases from Delftia acidovorans MC1 –protein and sequence data of RdpA and SdpA.	☐
	96	PARK ET AL, Journal of Microbiology and Biotechnology (2003), 13(2), 243-250 , Isolation and characterization of 4-(2,4-dichlorophenoxy)butyric acid-degrading bacteria from agricultural soils.	☐
	97	Mueller RH, Babel W. Degradability and recalcitrance of phenoxyalkanoic acid herbicides- traits of the microbial metabolism. InSecond International Conferen~ce on Remediation of Chlorinated and Racalcitrant Compounds 2000 (pp. 229-236).	☐
	98	TETT, Biodegradation (1997), 8(1), 43-52 , Biodegradation of the chlorophenoxy herbicide (R)-(+)-mecoprop by Alcaligenes denitrificans.	☐
	99	Llewellyn et al, Herbicide-Resistant Crops (1996), 159-74, Genetic engineering of crops for tolerance to 2,4-D.	☐
	100		☐

	101	Baelum et al., Appl. Environ. Microbiol. (72)1476-1486 (2006), Degradation of 4-Chloro-2-Methylphenoxyacetic Acid in Top- and Subsoil Is Quantitatively Linked to the Class III tfdA Gene.	☐
	102	Baelum et al., Appl. Environ. Microbiol. (75)2969-2972 (2009), TaqMan Probe-Based Real-Time PCR Assay for Detection and Discrimination of Class I, II, and III tfdA Genes in Soils Treated with Phenoxy Acid Herbicides.	☐
	103	Griffin et al., J Agric Food Chem (61)6589-6596(2013), Characterization of Aryloxyalkanoate Dioxygenase-12, a Nonheme Fe(II)/α-Ketoglutarate-Dependent Dioxygenase, Expressed in Transgenic Soybean and Pseudomonas fluorescens.	☐
	104	Hausinger, RSC Metallobiology (2015) Chapter 1 of 2-Oxoglutarate-dependent oxygenases, Biochemical diversity of 2-oxoglytarate-dependent oxygenases.	☐
	105	Leibeling et al, Eng Life Sci (13)278(2013), Posttranslational oxidative modification of (R)-2-(2,4-dichlorophenoxy) propionate/α-ketoglutarate-dependent dioxygenases (RdpA) leads to improved degradation of 2,4-dichlorophenoxyacetate (2,4-D).	☐

	106	Muller et al., Applied and Environmental Microbiology (72)4853(2006), Purification and Characterization of Two Enantioselective a-Ketoglutarate-Dependent Dioxygenases, RdpA and SdpA, from Sphingomonas herbicidovorans MH.	☐
	107	Paulin et al., Appl. Environ. Microbiol. (76)2873(2010), Abundance and Expression of Enantioselective rdpA and sdpA Dioxygenase Genes during Degradation of the Racemic Herbicide (R,S)-2-(2,4-Dichlorophenoxy)Propionate in Soil.	☐
	108	Zaprasis et al, Appl. Environ. Microbiol. (76)119(2010), Abundance of Novel and Diverse tfdA-Like Genes, Encoding Putative Phenoxyalkanoic Acid Herbicide-Degrading Dioxygenases, in Soil .	☐
	109	Zhang ET AL. Journal of Agricultural and Food Chemistry (2020), 68(26), 6967-6976 CODEN: JAFCAU; ISSN: 0021-8561 Enantioselective Catabolism of the Two Enantiomers of the Phenoxyalkanoic Acid Herbicide Dichlorprop by Sphingopyxis sp. DBS4.	☐
	110	Krausse et al., 4th biotechnology symposium of the University of Leipzig (abstract) pg 60 (2005), Crystal structure of the 2-oxoglutarate dependent dioxygenase RdpA.	☐
	111	Mueller et al., Un Mich ICBIC 2005 abstract, Insights into the enantiospecificities of (R)- and (S)-dichlorprop/a-ketoglutarate dioxygenases.	☐

INFORMATION DISCLOSURE STATEMENT BY APPLICANT (Not for submission under 37 CFR 1.99)		
	Application Number	15288406
	Filing Date	2016-10-07
	First Named Inventor	Terry Wright
	Art Unit	1663
	Examiner Name	KRUSE, David H.
	Attorney Docket Number	14764-258662

	112	Krausse et al., Freiberg Un Deutschen Gesellschaft fur Kristallographie (2006), (Poster title 72L) Structure of the 2-Oxoglutarate Dependent Dioxygenase RdpA by X-ray Crystallography and Small Angle X-ray Scattering	☐
	113	Gazitua et al., Environ Microbiol (12)2411(2010), Novel α-ketoglutarate dioxygenase tfdA-related genes are found in soil DNA after exposure to phenoxyalkanoic herbicides.	☐
	114	Chekan et al., Proceedings of the National Academy of Sciences (116)13299-13304(2019), Molecular basis for enantioselective herbicide degradation imparted by aryloxyalkanoate dioxygenases in transgenic plants.	☐
	115	Larue et al, Pest Manag Sci (75)2086(2019), Development of enzymes for robust aryloxyphenoxypropionate and synthetic auxin herbicide tolerance traits in maize and soybean crops.	☐
	116	Liu et al., FEMS Microbiol Ecol (86)114-129(2013) , Consumers of 4-chloro-2-methylpheoxyacetic acid from agricultural soil and drilosphere harbor cadA, r/sdpA, and tfdA-like gene encoding oxygenases.	☐
	117	Muller et al., Protein Science (15)prot1356(2006), Structural basis for the enantiospecificities of R- and S-specific phenoxypropionate/a-ketoglutarate dioxygenases.	☐
	118	Muller, Eng Life Sci (7)311-321 (2007), Activity and Reaction Mechanism of the Initial Enzymatic Step Specifying the Microbial Degradation of 2,4-Dichlorophenoxyacetate.	☐
	119	Westendorf, Eng Life Sci (6)552-559(2006), Kinetic Traits and Enzyme Form Patterns of (R)-2-(2,4-Dichlorophenoxy) propionate/a-Ketoglutarate Dioxygenase (RdpA) after Expression in Different Bacterial Strains.	☐
	120	Wright et al., Proc Natl Acad Sci (107)20240(2010), Robust crop resistance to broadleaf and grass herbicides provided by aryloxyalkanoate dioxygenase transgenes.	☐
	121	GenBank accession no. AAA21983.1 tfdA Cupriavidus necator (replaced Ralstonia eutropha), April 23, 1993.	☐
	122	GenBank accession no. AAK81681.1 tfdA Burkholderia cepacia, August 24, 2020, July 23, 2016.	☐

INFORMATION DISCLOSURE STATEMENT BY APPLICANT (Not for submission under 37 CFR 1.99)		
	Application Number	15288406
	Filing Date	2016-10-07
	First Named Inventor	Terry Wright
	Art Unit	1663
	Examiner Name	KRUSE, David H.
	Attorney Docket Number	14764-258662

	123	UniProtKB accession no. Q45423.1 tfdA Burkholderia sp. RASC, Nov 1, 1996.	☐
	124	GenBank accession no. AAS49436 tfdA Achromobacter denitrificans, April 3, 2020.	☐
	125	GenBank accession no. AAB47567.1 tfdABurkholderia cepacia plJB, July 26,2016.	☐
	126	GenBank accession no. AAM76772.1 tfdADelftia acidovorans _-_287 aaProtein_-_NCBI July 26, 2016	☐
	127	GenBank accession no. BAB92965.1 tfdA alpha proteobacterium HWK12, July 2, 2002.	☐
	128	GenBank accession no. BAB92966.1 tfdA alpha proteobacterium HW13, July 2, 2002.	☐
	129	NCBI accession no. WP_011084309.1 tfdA Bradyrhizobium diazoefficiens (replaced B. japonicum), 27-JUL-2019.	☐
	130	UniProtKB accession no. P83309.2 sdpA MC1 Delftia aciovorans, Sep 18, 2019.	☐
	131	UniProtKB accession no. Q700X4.1 sdpA MH Shingobium herbicidovorans, Nov 1, 1996.	☐
	132	GenBank accession no. ABD67501.1 sdpA P230 Rhodoferax sp. P230, March 14, 2006.	☐
	133	UniProtKB accession no. Q8KSC8.2 RdpA Shingobium herbicidovorans, March 1, 2004.	☐

INFORMATION DISCLOSURE STATEMENT BY APPLICANT (Not for submission under 37 CFR 1.99)		
	Application Number	15288406
	Filing Date	2016-10-07
	First Named Inventor	Terry Wright
	Art Unit	1663
	Examiner Name	KRUSE, David H.
	Attorney Docket Number	14764-258662

	134	Muller, Swiss Federal Institute of Technology thesis (Nov2004), Metabolism of phenoxyalkanoic acid herbicides in Sphingomonas herbicidovorans MH cloning and characterization of two enantiospecific α-ketoglutarate-dependent dioxygenases and degradation pathway analysis.	☐
	135	Westendorf Universität Leipzig thesis-German (2005), Enantioselektive Verwertung von Phenoxyalkanoat-Herbiziden durch Bakterien – Eine Charakterisierung der Dioxygenasen des initialen Abbau-Schrittes.	☐
	136	Baelum et al., System Appl Microbiol. (33)67(2010), Supplemental Material to Comparison of 16S rRNA gene phylogeny and functional tfdA gene distribution in thirty-one different 2, 4-dichlorophenoxyacetic acid and 4-chloro-2-methylphenoxyacetic acid degraders.	☐
	137	Zhang et al., J. Agric. Food Chem. (66)12217(2018), Two dcm Gene Clusters Essential for the Degradation of Diclofopmethyl in a Microbial Consortium of Rhodococcus sp. JT-3 and Brevundimonas sp. JT-9.	☐
	138	Jing et al., Ecological indicators (75)126(2017)-Enantioselective toxicity and degradation of chiral herbicidefenoxaprop-ethyl in earthworm Eisenia fetida.	☐
	139	HAN ET AL, World Journal of Microbiology & Biotechnology (2014), 30(10)2567-2576 , 16S rRNA gene phylogeny and tfdA gene analysis of 2,4-D-degrading bacteria isolated in China.	☐
	140	Zhang et al., J. Agric. Food Chem. (58)12878(2010), Enantioselective Environmental Behavior of the Chiral Herbicide Fenoxaprop-ethyl and Its Chiral MetaboliteFenoxaprop in Soil.	☐
	141	Wu et al., J. Agric. Food Chem. (65)3711(2017), Rapid Biodegradation of the Herbicide 2,4-Dichlorophenoxyacetic Acid by Cupriavidus gilardii T-1.	☐
	142	Zabaloy et al., Ann Microbiol (64)969(2014), Isolation and characterization of indigenous 2,4-D herbicide degrading bacteria from an agricultural soil in proximity of Sauce Grande River, Argentina.	☐
	143	Nielsen et al., PLOS One 8(12)e83346(2013), Novel Insight into the Genetic Context of the cadAB Genes from a 4- chloro-2-methylphenoxyacetic Acid-Degrading Sphingomonas.	☐
	144	Mierzejewska et al, Bulletin Env Contam Tox (104)200(2020), Biodegradation Potential and Ecotoxicity Assessment in Soil Extracts Amended with Phenoxy Acid Herbicide (2,4-D) and a Structurally-Similar Plant Secondary Metabolite (Ferulic Acid).	☐

INFORMATION DISCLOSURE STATEMENT BY APPLICANT (Not for submission under 37 CFR 1.99)		
	Application Number	15288406
	Filing Date	2016-10-07
	First Named Inventor	Terry Wright
	Art Unit	1663
	Examiner Name	KRUSE, David H.
	Attorney Docket Number	14764-258662

	145	Shimojo et al., J Biosc Bioengin. (108)56(2009), Analysis of genes encoding the 2,4-dichlorophenoxyacetic acid-degrading enzyme from Sphingomonas agrestis 58-1.	☐
	146	HAN ET AL, World Journal of Microbiology & Biotechnology (2015), 31(7), 1021-1030 , Cloning, expression, characterization and mutational analysis of the tfdA gene from Cupriavidus campinensis BJ71.	☐
	147	Paulin et al., Environ Micriobiol (13)1513-1523(2011), (R,S)-dichlorprop herbicide in agricultural soil induces proliferation and expression of multiple dioxygenase-encoding genes in the indigenous	☐
	148	Muller et al., Protein Science (15)prot1356(2006), Supplemental Table and Figures to Structural basis for the enantiospecificities of R- and S-specific phenoxypropionate/a-ketoglutarate dioxygenases.	☐
	149	Chekan et al., Proceedings of the National Academy of Sciences (116)13299-13304(2019), SUPPLEMENTAL Molecular basis for enantioselective herbicide degradation imparted by aryloxyalkanoate dioxygenases in transgenic plants.	☐
	150	GenBank accession no. BAB92964.1 tfdAa alpha proteobacterium RD5-C2 - NCBI. July 2, 2002.	☐

If you wish to add additional non-patent literature document citation information please click the Add button Add

EXAMINER SIGNATURE

Examiner Signature		Date Considered	

*EXAMINER: Initial if reference considered, whether or not citation is in conformance with MPEP 609. Draw line through a citation if not in conformance and not considered. Include copy of this form with next communication to applicant.

[1] See Kind Codes of USPTO Patent Documents at www.USPTO.GOV or MPEP 901.04. [2] Enter office that issued the document, by the two-letter code (WIPO Standard ST.3). [3] For Japanese patent documents, the indication of the year of the reign of the Emperor must precede the serial number of the patent document. [4] Kind of document by the appropriate symbols as indicated on the document under WIPO Standard ST.16 if possible. [5] Applicant is to place a check mark here if English language translation is attached.

INFORMATION DISCLOSURE STATEMENT BY APPLICANT (**Not for submission under 37 CFR 1.99)**		
	Application Number	15288406
	Filing Date	2016-10-07
	First Named Inventor	Terry Wright
	Art Unit	1663
	Examiner Name	KRUSE, David H.
	Attorney Docket Number	14764-258662

CERTIFICATION STATEMENT

Please see 37 CFR 1.97 and 1.98 to make the appropriate selection(s):

☐ That each item of information contained in the information disclosure statement was first cited in any communication from a foreign patent office in a counterpart foreign application not more than three months prior to the filing of the information disclosure statement. See 37 CFR 1.97(e)(1).

OR

☐ That no item of information contained in the information disclosure statement was cited in a communication from a foreign patent office in a counterpart foreign application, and, to the knowledge of the person signing the certification after making reasonable inquiry, no item of information contained in the information disclosure statement was known to any individual designated in 37 CFR 1.56(c) more than three months prior to the filing of the information disclosure statement. See 37 CFR 1.97(e)(2).

☐

☒ See attached certification statement.

☒ The fee set forth in 37 CFR 1.17 (p) has been submitted herewith.

A certification statement is not submitted herewith.

SIGNATURE

A signature of the applicant or representative is required in accordance with CFR 1.33, 10.18. Please see CFR 1.4(d) for the form of the signature.

Signature	/John P. Breen/	Date (YYYY-MM-DD)	2020-09-22
Name/Print	John P. Breen	Registration Number	38833

This collection of information is required by 37 CFR 1.97 and 1.98. The information is required to obtain or retain a benefit by the public which is to file (and by the USPTO to process) an application. Confidentiality is governed by 35 U.S.C. 122 and 37 CFR 1.14. This collection is estimated to take 1 hour to complete, including gathering, preparing and submitting the completed application form to the USPTO. Time will vary depending upon the individual case. Any comments on the amount of time you require to complete this form and/or suggestions for reducing this burden, should be sent to the Chief Information Officer, U.S. Patent and Trademark Office, U.S. Department of Commerce, P.O. Box 1450, Alexandria, VA 22313-1450. DO NOT SEND FEES OR COMPLETED FORMS TO THIS ADDRESS. **SEND TO: Commissioner for Patents, P.O. Box 1450, Alexandria, VA 22313-1450.**

Privacy Act Statement

The Privacy Act of 1974 (P.L. 93-579) requires that you be given certain information in connection with your submission of the attached form related to a patent application or patent. Accordingly, pursuant to the requirements of the Act, please be advised that: (1) the general authority for the collection of this information is 35 U.S.C. 2(b)(2); (2) furnishing of the information solicited is voluntary; and (3) the principal purpose for which the information is used by the U.S. Patent and Trademark Office is to process and/or examine your submission related to a patent application or patent. If you do not furnish the requested information, the U.S. Patent and Trademark Office may not be able to process and/or examine your submission, which may result in termination of proceedings or abandonment of the application or expiration of the patent.

The information provided by you in this form will be subject to the following routine uses:

1. The information on this form will be treated confidentially to the extent allowed under the Freedom of Information Act (5 U.S.C. 552) and the Privacy Act (5 U.S.C. 552a). Records from this system of records may be disclosed to the Department of Justice to determine whether the Freedom of Information Act requires disclosure of these records.

2. A record from this system of records may be disclosed, as a routine use, in the course of presenting evidence to a court, magistrate, or administrative tribunal, including disclosures to opposing counsel in the course of settlement negotiations.

3. A record in this system of records may be disclosed, as a routine use, to a Member of Congress submitting a request involving an individual, to whom the record pertains, when the individual has requested assistance from the Member with respect to the subject matter of the record.

4. A record in this system of records may be disclosed, as a routine use, to a contractor of the Agency having need for the information in order to perform a contract. Recipients of information shall be required to comply with the requirements of the Privacy Act of 1974, as amended, pursuant to 5 U.S.C. 552a(m).

5. A record related to an International Application filed under the Patent Cooperation Treaty in this system of records may be disclosed, as a routine use, to the International Bureau of the World Intellectual Property Organization, pursuant to the Patent Cooperation Treaty.

6. A record in this system of records may be disclosed, as a routine use, to another federal agency for purposes of National Security review (35 U.S.C. 181) and for review pursuant to the Atomic Energy Act (42 U.S.C. 218(c)).

7. A record from this system of records may be disclosed, as a routine use, to the Administrator, General Services, or his/her designee, during an inspection of records conducted by GSA as part of that agency's responsibility to recommend improvements in records management practices and programs, under authority of 44 U.S.C. 2904 and 2906. Such disclosure shall be made in accordance with the GSA regulations governing inspection of records for this purpose, and any other relevant (i.e., GSA or Commerce) directive. Such disclosure shall not be used to make determinations about individuals.

8. A record from this system of records may be disclosed, as a routine use, to the public after either publication of the application pursuant to 35 U.S.C. 122(b) or issuance of a patent pursuant to 35 U.S.C. 151. Further, a record may be disclosed, subject to the limitations of 37 CFR 1.14, as a routine use, to the public if the record was filed in an application which became abandoned or in which the proceedings were terminated and which application is referenced by either a published application, an application open to public inspections or an issued patent.

9. A record from this system of records may be disclosed, as a routine use, to a Federal, State, or local law enforcement agency, if the USPTO becomes aware of a violation or potential violation of law or regulation.

Electronic Patent Application Fee Transmittal

Application Number:	15288406
Filing Date:	07-Oct-2016
Title of Invention:	NOVEL HERBICIDE RESISTANCE GENES
First Named Inventor/Applicant Name:	Terry WRIGHT
Filer:	John P. Breen/Garla Twyman
Attorney Docket Number:	14764-258662

Filed as Large Entity

Filing Fees for Utility under 35 USC 111(a)

Description	Fee Code	Quantity	Amount	Sub-Total in USD($)
Basic Filing:				
Pages:				
Claims:				
Miscellaneous-Filing:				
Petition:				
Patent-Appeals-and-Interference:				
Post-Allowance-and-Post-Issuance:				
Extension-of-Time:				

Description	Fee Code	Quantity	Amount	Sub-Total in USD($)
Miscellaneous:				
SUBMISSION- INFORMATION DISCLOSURE STMT	1806	1	240	240
		Total in USD ($)		**240**

Electronic Acknowledgement Receipt	
EFS ID:	40625564
Application Number:	15288406
International Application Number:	
Confirmation Number:	5402
Title of Invention:	NOVEL HERBICIDE RESISTANCE GENES
First Named Inventor/Applicant Name:	Terry WRIGHT
Customer Number:	107540
Filer:	John P. Breen/Garla Twyman
Filer Authorized By:	John P. Breen
Attorney Docket Number:	14764-258662
Receipt Date:	22-SEP-2020
Filing Date:	07-OCT-2016
Time Stamp:	16:00:04
Application Type:	Utility under 35 USC 111(a)

Payment information:

Submitted with Payment	yes
Payment Type	CARD
Payment was successfully received in RAM	$240
RAM confirmation Number	E20209LG01319980
Deposit Account	100435
Authorized User	Garla Twyman
The Director of the USPTO is hereby authorized to charge indicated fees and credit any overpayment as follows: 37 CFR 1.16 (National application filing, search, and examination fees) 37 CFR 1.17 (Patent application and reexamination processing fees)	

37 CFR 1.19 (Document supply fees)

37 CFR 1.20 (Post Issuance fees)

37 CFR 1.21 (Miscellaneous fees and charges)

File Listing:

Document Number	Document Description	File Name	File Size(Bytes)/ Message Digest	Multi Part /.zip	Pages (if appl.)
1	Non Patent Literature	Baelum_Degradation.pdf	887196 a45a755a3b17f49883d85a5834e5952e321314a1	no	13
Warnings:					
Information:					
2	Non Patent Literature	Baelum_Taqman.pdf	971811 c45860d78205aabc61306898f1daa1bf2b3a80ee	no	5
Warnings:					
Information:					
3	Non Patent Literature	Griffin_Characterization.pdf	231057 e85303be85ea569df429677004a25538d7a1d57b	no	8
Warnings:					
Information:					
4	Non Patent Literature	Hausinger_Biochemical_diversity.pdf	1125232 dd1c3638a2dc26d2e07e6213ed69c308210dc5a7	no	58
Warnings:					
Information:					
5	Non Patent Literature	Leibeling_Posttranslational.pdf	1033709 3788e92c6fc8af500fba4a53e7092195a42ad54e	no	14
Warnings:					
Information:					
6	Non Patent Literature	Muller_Purification.pdf	1444599 9f64186d8d3ed69dcdf298aa82f87b228a08f5cc	no	10
Warnings:					
Information:					

7	Non Patent Literature	Paulin_Abundance.pdf	1360318 59a50a5e722ffa6e81c68a7dc7cf85329c96a71c	no	12
Warnings:					
Information:					
8	Non Patent Literature	Zaprasis_Abundance.pdf	1513962 63c99d29149084599 0e85780e0da1893c370c780	no	11
Warnings:					
Information:					
9	Non Patent Literature	Zhang_Enantioselective.pdf	834746 0efcb86350ff01b763089566b07d2950b4debc75	no	10
Warnings:					
Information:					
10	Non Patent Literature	Krausse_4th_Biotech_Symposium.pdf	2485337 94478a8748b63d53dd0b16c97e2c772f25347b97	no	234
Warnings:					
Information:					
11	Non Patent Literature	Mueller_Insights.pdf	79370 76c7337654f6f3cfdf45092df288f3e8c8d90f4d	no	1
Warnings:					
Information:					
12	Non Patent Literature	Krausse_poster.pdf	6265782 238255bc4d7086314595f2aba5f3bfd9b86bede5	no	44
Warnings:					
Information:					
13	Non Patent Literature	Gazitua.pdf	792040 ba1bb57d84dbb77e81d341fc226f377129500903	no	15
Warnings:					
Information:					

14	Non Patent Literature	Chekan_Molecular_basis.pdf	1282440 8d3a2254f9df95f11cf637a9ea11c981315ee6f4	no	22
Warnings:					
Information:					
15	Non Patent Literature	Larue_Development.pdf	374988 2a37a0465168152e8065e2a18a1ffdd7877123d0	no	9
Warnings:					
Information:					
16	Non Patent Literature	Liu_Consumers.pdf	267864 527af1a85a15103fd1263f36a74f9e4b637b6983	no	16
Warnings:					
Information:					
17	Non Patent Literature	Mueller_Structural_basis.pdf	454351 ed665f03c933c0c61bca098a06501ec77224a6aa	no	13
Warnings:					
Information:					
18	Non Patent Literature	Muller_Activity_and_reaction.pdf	557476 033ac54db8e5d377b7e1a8a345fed51bbc99159f	no	11
Warnings:					
Information:					
19	Non Patent Literature	Westendorf_Kinetic_traits.pdf	220653 39fd16881ec1244751e4f7ef9ecea6e24fbeec12	no	8
Warnings:					
Information:					
20	Non Patent Literature	Wright_Robust_crop.pdf	250736 3f495d19175ef818ab2ed9426574bb9c71a53282	no	6
Warnings:					
Information:					

21	Non Patent Literature	AAA21983.pdf	61881 dc39352bfce82ab2b60a6410a1f8af4d25af2e9b	no	1
Warnings:					
Information:					
22	Non Patent Literature	AAK81681.pdf	64094 63847d0cc2836fee817a76c0552e705e10c83402	no	2
Warnings:					
Information:					
23	Non Patent Literature	Q45423.pdf	68059 6e53175d72292927444744 3f8295adf6f5ad849c	no	2
Warnings:					
Information:					
24	Non Patent Literature	AAS49436.pdf	61448 8caa797076d13cfdd34475f70732b04c4429626d	no	2
Warnings:					
Information:					
25	Non Patent Literature	AAB47567.pdf	62633 89bebfc1e13f0af910bd01d68cdf7c416d40373d	no	1
Warnings:					
Information:					
26	Non Patent Literature	AAM76772_1_tfdADelftia_acidovorans_-_287_aaProtein_-_NCBI.pdf	64784 2ff9cd1abadc0095bb0b22545e164924a2b8adfa	no	2
Warnings:					
Information:					
27	Non Patent Literature	BAB92965.pdf	64562 91bd7e019dc6433498feba00257d493bbb403b6d	no	1
Warnings:					
Information:					

28	Non Patent Literature	BAB92966.pdf	64869 1ee95eecfff4a242e8cc5e39fa01d7408f4c528c	no	1
Warnings:					
Information:					
29	Non Patent Literature	WP_011084309.pdf	61920 73e598cacd08b35e5379e740fff97361ba34195a	no	1
Warnings:					
Information:					
30	Non Patent Literature	P83309.pdf	70762 d16b4167841c5cdda8687094c67654d0e7c24d70	no	3
Warnings:					
Information:					
31	Non Patent Literature	Q700X4.pdf	74550 c32fcd96bd89d15467346332be9441f1a2dcfd0d	no	4
Warnings:					
Information:					
32	Non Patent Literature	ABD67501.pdf	64943 33b2320c11c7908ed1b74cb7d511b7c7269aeb52	no	2
Warnings:					
Information:					
33	Non Patent Literature	Q8KSC8.pdf	80078 ed08679bae8e28fcd0dea397f791824d78a8b6ff	no	5
Warnings:					
Information:					
34	Non Patent Literature	Muller_Thesis.pdf	1844655 28c640f08947e372a4746f571977112b91be223f	no	182
Warnings:					
Information:					

35	Non Patent Literature	Westendorf_Dissertation.pdf	7412066 962f74117b6b37a6a320dacc47898b95611af01d	no	122
Warnings:					
Information:					
36	Non Patent Literature	Baelum_Compariso.pdf	333928 e4e5a8809ff9aee395aa86ed8471c4a37748ba82	no	10
Warnings:					
Information:					
37	Non Patent Literature	Zhang_Two_dcm.pdf	1966744 72cc5d4b7fa533ae269446440880faad3c4fe362	no	10
Warnings:					
Information:					
38	Non Patent Literature	Jing.pdf	339032 ba3a2bb1fd1317940e218ee960414899d9655087	no	6
Warnings:					
Information:					
39	Non Patent Literature	Han_World_Journal.pdf	449911 0e53db86d95d3517ea89583848f828e1d9f0ac16	no	10
Warnings:					
Information:					
40	Non Patent Literature	Zhang_Enantioselective_environmental.pdf	413550 9b66cd7a18748348edf6a3f96edd25c3a387305f	no	7
Warnings:					
Information:					
41	Non Patent Literature	Wu_Rapid_biodegradation.pdf	1745690 86a259e493ecf72e02560db71a216a4457ad7d39	no	10
Warnings:					
Information:					

42	Non Patent Literature	Zabaloy_Isolation.pdf	604829 1e10cb9fa9379658a0614983f52a16fa8e7555a2	no	9
Warnings:					
Information:					
43	Non Patent Literature	Nielsen_Novel_insight.pdf	507972 f4983e9c7effec23973a2bbbab40c78453f8fd94	no	9
Warnings:					
Information:					
44	Non Patent Literature	Mierzejewska_Biodegradation_potential.pdf	142774 18d88adc8067b0de286f92ff119f3d4bf171b301	no	6
Warnings:					
Information:					
45	Non Patent Literature	Shimojo_Analysis.pdf	419601 fb8daddc2794f4219f4ccfd56c6fd99667b8ad97	no	4
Warnings:					
Information:					
46	Non Patent Literature	Han_Cloning_Expression.pdf	679370 332a4133957bf6f3cf3dfc4aa521543d8acdc62f	no	10
Warnings:					
Information:					
47	Non Patent Literature	Paulin_R_S-Dichlroprop.pdf	404492 2e1f846ceb9bcf9378d853e9865914713dc944ac	no	11
Warnings:					
Information:					
48	Non Patent Literature	Mueller_SupplMaterials.pdf	238242 c6cb7817f44b2c3f4f055cbd26ae2be9cbe620ae	no	5
Warnings:					
Information:					

49	Non Patent Literature	Chekan_Supplemental_Molecular_Basis.pdf	1282440 9d42eab55a3cde0fb91adffbb5742887337e7a32	no	22
Warnings:					
Information:					
50	Non Patent Literature	BAB92964_1_tfdAa_alpha_proteobacterium_RD5-C2_-_NCBI.pdf	64245 f0d199f2904c5641f29effd64832aeb5bd5f812f	no	1
Warnings:					
Information:					
51	Non Patent Literature	Kwon_Expression.pdf	612124 cd3b5c012db3c69732cd9ed548d7668a8a321d7f	no	3
Warnings:					
Information:					
52	Non Patent Literature	Park_Genetic.pdf	782057 11e2ed0f0c4acc00462416afb61ae209c325d351	no	9
Warnings:					
Information:					
53	Information Disclosure Statement (IDS) Form (SB08)	IDS.pdf	190340 6cd89304672348d517308fb7b242856a856e69f1	no	20
Warnings:					
Information:					
This is not an USPTO supplied IDS fillable form					
54	Fee Worksheet (SB06)	fee-info.pdf	30481 3e5223aba68b296aa2abb54e176aff697a7352fc	no	2
Warnings:					
Information:					
		Total Files Size (in bytes):	43762793		

This Acknowledgement Receipt evidences receipt on the noted date by the USPTO of the indicated documents, characterized by the applicant, and including page counts, where applicable. It serves as evidence of receipt similar to a Post Card, as described in MPEP 503.

New Applications Under 35 U.S.C. 111

If a new application is being filed and the application includes the necessary components for a filing date (see 37 CFR 1.53(b)-(d) and MPEP 506), a Filing Receipt (37 CFR 1.54) will be issued in due course and the date shown on this Acknowledgement Receipt will establish the filing date of the application.

National Stage of an International Application under 35 U.S.C. 371

If a timely submission to enter the national stage of an international application is compliant with the conditions of 35 U.S.C. 371 and other applicable requirements a Form PCT/DO/EO/903 indicating acceptance of the application as a national stage submission under 35 U.S.C. 371 will be issued in addition to the Filing Receipt, in due course.

New International Application Filed with the USPTO as a Receiving Office

If a new international application is being filed and the international application includes the necessary components for an international filing date (see PCT Article 11 and MPEP 1810), a Notification of the International Application Number and of the International Filing Date (Form PCT/RO/105) will be issued in due course, subject to prescriptions concerning national security, and the date shown on this Acknowledgement Receipt will establish the international filing date of the application.

Applied and Environmental Microbiology

Degradation of 4-Chloro-2-Methylphenoxyacetic Acid in Top- and Subsoil Is Quantitatively Linked to the Class III *tfdA* Gene

Jacob Bælum, Trine Henriksen, Hans Christian Bruun Hansen and Carsten Suhr Jacobsen
Appl. Environ. Microbiol. **2006, 72(2):1476. DOI: 10.1128/AEM.72.2.1476-1486.2006.**

Updated information and services can be found at:
http://aem.asm.org/content/72/2/1476

These include:

REFERENCES This article cites 56 articles, 27 of which can be accessed free at: http://aem.asm.org/content/72/2/1476#ref-list-1

CONTENT ALERTS Receive: RSS Feeds, eTOCs, free email alerts (when new articles cite this article), more»

CORRECTIONS An erratum has been published regarding this article. To view this page, please click here

Information about commercial reprint orders: http://aem.asm.org/site/misc/reprints.xhtml
To subscribe to to another ASM Journal go to: http://journals.asm.org/site/subscriptions/

Journals.ASM.org

Downloaded from http://aem.asm.org/ on April 30, 2012 by guest

APPLIED AND ENVIRONMENTAL MICROBIOLOGY, Feb. 2006, p. 1476–1486 Vol. 72, No. 2
0099-2240/06/$08.00+0 doi:10.1128/AEM.72.2.1476–1486.2006
Copyright © 2006, American Society for Microbiology. All Rights Reserved.

Degradation of 4-Chloro-2-Methylphenoxyacetic Acid in Top- and Subsoil Is Quantitatively Linked to the Class III *tfdA* Gene

Jacob Bælum,[1,2] Trine Henriksen,[1] Hans Christian Bruun Hansen,[2] and Carsten Suhr Jacobsen[1,2,3]*

Geological Survey of Denmark and Greenland (GEUS), Department of Geochemistry,[1] Royal Veterinary and Agricultural University (KVL), Department of Natural Sciences,[2] and Royal Veterinary and Agricultural University (KVL), Department of Ecology,[3] Copenhagen, Denmark

Received 22 August 2005/Accepted 22 November 2005

The *tfdA* gene is known to be involved in the first step of the degradation of the phenoxy acid herbicide 4-chloro-2-methylphenoxyacetic acid (MCPA) in several soil bacteria, but bacteria containing other *tfdA*-like genes have been isolated as well. A quantitative real-time PCR method was used to monitor the increase in the concentration of *tfdA* genes during degradation of MCPA in sandy topsoil and subsoil over a period of 115 days. Quantitative PCR revealed growth in the *tfdA*-containing bacterial community, from 500 genes g^{-1} soil to approximately 3×10^4 genes g^{-1} soil and to 7×10^6 genes g^{-1} soil for topsoil initially added to 2.3 mg MCPA kg^{-1} (dry weight) soil and 20 mg MCPA kg^{-1} (dry weight) soil, respectively. We analyzed the diversity of the *tfdA* gene during the degradation experiment. Analyses of melting curves of real-time PCR amplification products showed that a shift in the dominant *tfdA* population structure occurred during the degradation period. Further denaturing gradient gel electrophoresis and sequence analysis revealed that the *tfdA* genes responsible for the degradation of MCPA belonged to the class III *tfdA* genes, while the *tfdA* genes present in the soil before the occurrence of degradation belonged to the class I *tfdA* genes. The implications of these results is that the initial assessment of functional genes in soils does not necessarily reflect the organisms or genes that would carry out the degradation of the compounds in question.

Phenoxy acid herbicides have been widely used for agricultural purposes throughout the world since their development in the 1940s. In Denmark, 4-chloro-2-methylphenoxyacetic acid (MCPA) has been among the five top-selling herbicides during the last five decades. The relatively large amounts applied (1,500 to 2,000 g/ha), the weak retention of the compound in soils, and the unrestricted use during cold autumns, when degradation is slow, have resulted in frequent occurrences of MCPA as a groundwater contaminant (50). Groundwater is an important drinking water resource, especially in Denmark, where 99% of the drinking water is provided by groundwater. Hence, studies that explore the fate of potential groundwater-polluting compounds are important.

The degradation of phenoxy herbicides such as 2,4-dichlorophenoxyacetic acid (2,4-D), MCPA, and related compounds has been studied intensively during the last 40 years, with the majority of the work being done on 2,4-D. This, among other studies, has revealed detailed knowledge about the degradation and mineralization kinetics (27, 38), the catabolic pathways (6, 21, 46), the genes and enzymatic systems involved in the degradation (6, 20, 24, 35), and the phylogenetic composition of isolated microbial degraders (25, 53).

Numerous kinetic models have been developed to describe the mineralization of xenobiotic compounds in the environment (for a review, see reference 17). Typically, the models are divided into different forms of degradation kinetics that either take the growth of microorganisms into account or not. Furthermore, different models that take different forms of growth into account, depending on initial cell and substrate concentrations, have been developed (7, 52).

The soil bacterium *Ralstonia eutropha* JMP134, originally isolated from an Australian agricultural soil sample (44), contains genes for the complete pathway of 2,4-D and MCPA degradation. These genes are the ones most extensively studied and have become a model for the study of phenoxy acid degradation (11, 55). This strain harbors plasmid pJP4, which contains all of the structural and regulatory genes needed to convert these compounds to 2-chloromaleylacetic acid, which is further metabolized by chromosomally encoded gene products to finally yield CO_2 and chloride (14, 15, 22, 31, 32, 34). The first step in the degradation pathway is initiated by an α-ketoglutarate-dependent dioxygenase, encoded by the *tfdA* gene, which cleaves the acetate side chain to produce the corresponding phenol 4-chloro-2-methylphenol (MCP) (Fig. 1) (18, 19, 54). Further degradation steps are initiated and regulated by gene products of the genes *tfdB* (45), *tfdCDEF* (35, 45), *tfdR*, and *tfdS* (37, 39).

Numerous strains capable of degrading compounds such as 2,4-D and MCPA have been isolated from various environments and have been found to be distributed over many different phylogenetic groups (4, 13, 24, 25, 33, 35, 55, 57). Itoh et al. (25) suggested classifying the strains into three groups. The first group, which can be further divided into three classes (classes I to III) based on their *tfdA* gene sequence (40), consists of β- and γ-proteobacteria containing *tfdA* genes related to that of *R. eutropha* JMP134. The second group consists of α-proteobacteria that are closely related to *Bradyrhizobium* spp. and contains the *tfdA*-like gene *tfdA*α (60% identical to the canonical *tfdA* gene). The strains in this group were first isolated from pristine environments in Hawaii, Canada, and

* Corresponding author. Mailing address: Department of Geochemistry, Geological Survey of Denmark and Greenland, Øster Voldgade 10, DK-1350 Copenhagen K, Denmark. Phone: 45 3814 2313. Fax: 45 3814 2050. E-mail: csj@geus.dk.

Downloaded from http://aem.asm.org/ on April 30, 2012 by guest

COR-AAD1-00002850
Bayer EX1008 (Part 5 of 9)

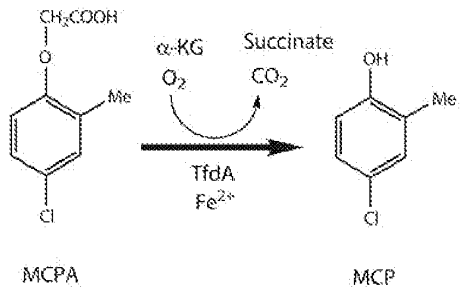


FIG. 1. Catabolic activity of the TfdA enzyme in the degradation of MCPA. α-KG, α-ketoglutarate.

Chile (30) and subsequently from arable soil in Japan (24). Members of the third group are α-proteobacteria belonging to a species of the genus *Sphingomonas*. They are also characterized by using the *tfdA*α gene product during the initial step of the pathway instead of the TfdA enzyme (20). As well as this, several strains in the second and the third groups are known to contain the *cadA* gene, which is related to the *tfdA* gene involved in the degradation of 2,4,5-trichlorophenoxyacetic acid (25).

The main objective of this paper was to describe the functional diversity of MCPA degraders in a profile of MCPA-treated Danish soil. Furthermore, PCR using primers targeting the three groups of phenoxy acid degradation genes was performed to investigate whether the genes were present and which primer set revealed the most specific amplification product. In light of this, one degenerated primer set (this work) targeting the canonical *tfdA* gene for real-time quantitative PCR was chosen. The relative increase in the *tfdA* gene concentration was monitored during a degradation experiment in microcosms. Denaturing gradient gel electrophoresis (DGGE) analyses of the *tfdA* amplification product were used to elucidate whether only one or several homologues of the *tfdA* gene were involved in the MCPA degradation. This revealed a number of clearly separated bands, which were sequenced and compared to known *tfdA* sequences. We further examined the mineralization kinetics of MCPA depending on the effects of the initial substrate and cell concentrations in top- and subsoil. The topsoil was suggested to contain a higher initial cell concentration than the subsoil. The initial cell concentration and the growth of MCPA degraders were determined and monitored during a degradation period by quantitative real-time PCR of the *tfdA* gene. Microbial growth during degradation of MCPA in natural soil has previously been suggested but has only been quantified using less accurate techniques (12, 41).

MATERIALS AND METHODS

Bacteria. *Ralstonia eutropha* JMP134 (13), which carries the *tfdA* gene on the pJP4 plasmid, was used as a positive control and for standard curve preparation in the quantitative real-time PCR assay. Furthermore, it was used as a model organism in the DGGE analysis. DNA from *Burkholderia cepacia* DB01(pRO101), which carries the same *tfdA* gene as pJP4 (22), was used to create a ^{32}P-labeled probe for Southern blot hybridization. Both strains were propagated using standard techniques (27).

Soils. An organic topsoil sample (10 to 25 cm) and a subsoil sample (35 to 50 cm) from a sandy profile were used for the experiments. The profile was taken from the Danish agricultural experimental station in Jyndevad, located on the outwash plain in southern Jutland. The soil has been used for organic farming since 1995, and additionally, it has not been treated with any form of phenoxy acid herbicide since at least 1988. The soils were collected and mixed manually in October 2003 and stored in the dark for 2 months at 5°C before they were passed through a 2-mm sieve. The soils were thereafter stored in the dark at −18°C until 10 days before use. Defrosting and acclimatization were performed in the dark for 10 days at 10°C (41) (for further soil characteristics, see Table 1).

TABLE 1. Soil characteristics

Soil	Depth (cm)	pH	C (%)	Clay (%)	Silt (%)	Sand (%)	WHC[a] (% [vol/vol])
Topsoil	10–25	6.9	2.4	5	3	92	19.25
Subsoil	35–50	6.1	1.0	5	1	94	17.76

[a] WHC, water-holding capacity, measured at a −log water potential of 2.0 cm.

Microcosm setup for degradation experiment. Before experiment setup, stock solutions of MCPA were prepared. To ensure even moistening of the soils to a water content of approximately the water-holding capacity, stock solutions of 20, 174, and 23 mg/liter MCPA were required to obtain concentrations of 2.3 mg MCPA kg^{-1} (dry weight) soil in the topsoil ($Top_{2.3}$), 20 mg MCPA kg^{-1} (dry weight) soil in the topsoil (Top_{20}), and 2.3 mg MCPA kg^{-1} (dry weight) soil in the subsoil ($Sub_{2.3}$), respectively. The stock solutions were prepared by dissolution of MCPA (97.5% purity; Dr. Ehrenstorfer GmbH, Augsburg, Germany) in MilliQ water (Millipore, Birkerød, Denmark). To ensure the complete dissolution of MCPA and to avoid disturbance of the soil pH, the pH in the solutions was adjusted to 6.5 with NaOH.

Subsequently, 20 g (dry weight) of the topsoil and 15 g (dry weight) of the subsoil were transferred to 250-ml Pyrex red cap bottles (airtight). The soils were spiked with 2.3 ml (for the topsoils) and 1.5 ml (for the subsoils) of the respective stock solutions. Stock solutions with MCPA were carefully mixed into the soils with a sterile glass pipette, and the microcosms were incubated at 10°C in the dark. Triplicate bottles were set up for each soil scenario for eight sampling points, and in order to prevent the development of anaerobic conditions in the microcosms, they were aerated by leaving the flasks open for 20 min in a sterile hood every 14 days.

Microcosm setup for mineralization experiment. A mineralization experiment was set up with ^{14}C-labeled MCPA at the same concentrations described above. Stock solutions were prepared as described above for the degradation experiment. [U-^{14}C]MCPA (specific activity of 159.7 μCi/mg, radiochemical purity of >95%; Izotop, Budapest, Hungary) was then added to the stock solutions in trace amounts to achieve an initial radioactivity in each microcosm of 60,000 dpm. The mineralization experiment was performed essentially as described previously by Mortensen and Jacobsen (41), except that 10 g of soil was used and no soil was removed during the experiment. We have previously determined the mass balance for the experimental setup, and recoveries of 93% ± 1.5% were found (5, 9).

MCPA extraction and quantification. On days 0, 6, 12, 22, 33, 50, 68, and 115 after incubation, triplicates of each soil-MCPA degradation series ($Top_{2.3}$, Top_{20}, and $Sub_{2.3}$) were extracted by pressurized liquid extraction for the determination of MCPA amounts. The extractions were performed with an ASE 200 system (Dionex, Sunnyvale, CA). The soils from the degradation assay were packed in 33-ml extraction cells sufficient to contain 40 to 50 g soil. To assist the extractions, Ottawa sand (Fisher scientific, Loughborough, United Kingdom), sufficient to fill out the remaining volume (approximately 1:1 [wt/wt]), was mixed into the soil samples. The entire extraction process was carried out at 50°C. The solvent used for the extractions was a 50:50 (vol/vol) mixture of methanol-water (high-performance liquid chromatography-grade methanol; Fisher Scientific, Loughborough, United Kingdom). Other extraction conditions were as follows: a 40% solvent volume was used for a 10-min static time in one extraction cycle and a 60-s purge time with nitrogen at 1,500 lb/in^2 pressure (1 lb/in^2 = 6,894.76 Pa). The extraction method was optimized for soil samples spiked with MCPA, resulting in extraction efficiencies of 80% ± 2% for the topsoil and 92% ± 4% for the subsoil.

A soil extract of 15 to 20 ml was obtained in 50-ml glass vials. After being thoroughly mixed, an aliquot was filtered through a 0.45-μm polytetrafluoroethylene filter (Titan2; Sun-Sri) to remove particles. To avoid overloading of the liquid chromatography (LC) mass spectrometry system, the filtrates were diluted with a methanol-water (50:50) solution to obtain MCPA concentrations in the range of 50 to 150 μg/liter.

The quantification of MCPA in the soil extracts was performed using an LC tandem mass spectrometry (MS/MS) system. Twenty microliters of the samples

Downloaded from http://aem.asm.org/ on April 30, 2012 by guest

COR-AAD1-00002851
Bayer EX1008 (Part 5 of 9)

TABLE 2. PCR primers

Primer set	Model gene(s)	Primer (5′–3′)[c]	Optimal annealing temp used (°C)[c]	Characteristic[f]	Reference or source
*tfdA**	*R. eutropha* JMP134/ *Burkholderia* sp. strain RASC	F, AACGCAGCGRTTRTCCCA[a] R, ACGGAGTTCTGYGAYATG[a]	58	Unspecific binding; qPCR not possible	59
tfdA-intern	*R. eutropha* JMP134	F, GCATACGACGCGCTGCCTCG R, CTTCGGCCACCGGAAGGCCT	65	Used for probe preperation for Southern blot hybridization	This work
*tfdA***	Sequence alignment of 23 known *tfdA* genes	F, GAGCACTACGCRCTGAAYTCCCG[a,b] R, CTTCGGCCACCGGAAGGCCT	64	One band on agarose gel (approx. 220 bp); qPCR possible	This work
*tfdAα**	Alignment of RD5-C2, HWK12, and HW13 (*tfdAα* genes)	F, CCGGCGTCGATCTGCGCAAG R, GTTGACGACGCGCGCCGA	ND[d]	No clear band on the agarose gel; fluffy PCR products	51
*tfdAα***	Alignment of HW13, HWK12, and BTH (*tfdAα* genes)	F, ACSGAGTTCKSCGACATGCG[a] R, GCGGTTGTCCCACATCAC	65	One band (approx. 350 bp); qPCR may be possible	25
cadA	HW13 (*cadA* gene)	F, AAGCTGCARTTTGARAAY[a] R, MGGATTGAAGAAATCCTGRTA[a]	58	No PCR product	24

[a] R, G/A; Y, T/C; S, G/C; K, G/T; M, A/C.
[b] AGC clamp was added to the 5′ end of the primer for the PCR/DGGE (5′-CGCCCGCCGCGCGCGGCGGGCGGGGCGGGGGCACGGGGGG-3′).
[c] The optimal annealing temperature is based on gradient ramping (58 to 69°C).
[d] ND, no optimal annealing temperature could be determined.
[e] F, forward; R, reverse.
[f] qPCR, quantitative PCR.

was injected, and the compounds were separated on a 100- by 2.1-mm Xterra RP_{18} column (3.5-μm particle size) from Waters (Milford, MA) using a Waters Alliance model 2695 high-performance liquid chromatography system. A mobile phase composed of methanol–water–0.2% acetic acid (78:20:2) at 25°C with a flow rate of 0.18 ml/min was used. For detection and quantification of the MCPA compound, a Quattro Ultima triple quadrupole mass spectrometer from Micromass (Manchester, United Kingdom) equipped with an electrospray ionization unit was used. Electrospray ionization in the negative mode was used, while further conditions were as follows: capillary voltage was 3.20 kV, cone voltage was 80 V, and collision energy for MS/MS was 20 eV. Furthermore, nitrogen was used as the desolvation gas at a flow rate of 600 liters/h. A limit of detection of 1 μg MCPA $liter^{-1}$ was determined for the LC-MS/MS system.

DNA extraction. Soils for DNA extractions were set up parallel to the degradation experiment. Red cap bottles with 20 g (dry weight) of soil amended with 0, 2.3, and 20 mg MCPA kg^{-1} (dry weight) soil for the topsoil (Top_0, $Top_{2.3}$, and Top_{20}) and 0 and 2.3 mg MCPA kg^{-1} (dry weight) soil for the subsoil (Sub_0 and $Sub_{2.3}$) were set up in triplicate. The amount of soil sampled for DNA extractions was 0.5 g (wet weight) to ~0.4 g (dry weight), which was accomplished using a sterile stainless steel sampler designed to collect a composite sample of 0.5 g soil from 5 to 10 distinct spots in the bottle. The same bottle was used throughout the experiment and was aerated parallel to the bottles in the degradation experiment as well as for sample collection on the same days as in the degradation experiment. Whole-community DNA was extracted from the 0.5-g wet soil samples with the FastDNA SPIN kit for soil (Bio101, Inc., Carlsbad, CA). The protocol recommended by the manufacturer was followed, except that the bead-beating step was modified and a freeze-thaw step was included. The beat-beating step was modified to four 30-s pulses at speed 4 instead of one 30-s pulse at speed 5.5 in the FastPrep FP 120 instrument (Bio101), and the freeze-thaw steps were performed for 1 h at −80°C and subsequently for 30 min at 37°C. DNA was finally eluted in 100 μl DNase/RNase-free water (Bio101, Carlsbad, CA) and stored at −80°C.

Primer testing. All PCRs were carried out as real-time PCR assays in an iCycler iQ (Bio-Rad, Hercules, CA). In order to select the most effective primer set, five primer sets were tested (Table 2) using two different commercial PCR master mix kits. *tfdA** and *tfdA*** were the most intensively tested primers. *tfdA** yielded a 307-bp fragment, while the *tfdA*** yielded a 210-bp fragment. *tfdA*** was designed in connection with this work by BLAST alignment analysis (3) of 22 known *tfdA* gene sequences found with *R. eutropha* JMP134 as the search sequence. The GenBank accession numbers for the 22 *tfdA* genes were as follows: M16730, AY238497, AY238496, U43197, U43276, AF439768, AY078159, AF029344, U32188, U25717, U87394, U22499, AF181982, AF182758, AF176240, U65531, U43196, AY238495, AY238494, AY238493, AY238492, and AB074491. Primers were designed to attach to most conserved regions, and since the primer set was designed on the basis of *tfdA* gene sequences belonging to class I and class III, it was expected that it was highly specific for these genes. Primers were obtained from MWG Biotech (Ebersberg, Germany). The first of the two commercial SYBR green PCR master mix kits we tested was iQ SYBR green supermix (Bio-Rad, Hercules, CA) containing PCR buffer, 0.4 mM of each deoxynucleoside triphosphate, 50 U/ml of *iTaq* DNA polymerase, and 6 mM $MgCl_2$. This kit was used mainly with the *tfdA** primer set and through the testing of *tfdAα**, *tfdAα***, and *cadA* primer sets. The other kit we tested was the QuantiTect SYBR green PCR kit (QIAGEN, Crawley, United Kingdom) containing deoxynucleoside triphosphate mix, HotStar *Taq* DNA polymerase, PCR buffer, Rox, and 2.5 mM $MgCl_2$. This kit was only used for PCR with the *tfdA** and *tfdA*** primer sets. The 25-μl reaction mixtures contained 0.4 μM of each primers, 12.5 μl of the respective SYBR green mix, 25.5 μg bovine serum albumin (Amersham Bioscience, Buckinghamshire, United Kingdom), 2.5 μl of 1:10-diluted DNA extract, and RNase/DNase-free water to complete the 25-μl volume. The DNA extracts were diluted 1:10 in RNase/DNase-free water to reduce the influence of PCR-disturbing factors from the soil, such as humic acids.

The conditions for the real-time PCR were as follows: 6 min at 95°C for enzyme activation; 50 cycles of 45 s at 94°C for denaturation, 30 s at the annealing temperature specified in Table 2, and 2 min at 72°C for elongation; and a final 6-min step at 72°C for extension. To obtain a specific melting profile for the real-time PCR product, an 80-cycle protocol of 45 s at 58°C; 30 s at 58°C to 98°C, increasing 0.5°C every cycle; and 45 s at 58°C was used after the real-time PCR. The melting profile was used to determine the presence of the

Downloaded from http://aem.asm.org/ on April 30, 2012 by guest

COR-AAD1-00002852
Bayer EX1008 (Part 5 of 9)

specific product and to determine if the PCR product was composed of DNA sequences of more than one length.

Further investigations of the PCR products were done by gel electrophoresis of 8-μl PCR products on a 1.5% agarose gel in 1× Tris-acetate-EDTA buffer. The gels were stained in ethidium bromide and visualized under UV light.

In case the gels revealed more than one band, a Southern blot hybridization was performed as described previously by Jacobsen (26) and Sambrook and Russell (49), except that the digestion reaction was excluded. The ^{32}P *tfdA* probe for the hybridization was generated using [^{32}P]dCTP (Amersham, United Kingdom) and the Random Primed DNA Labeling kit (Roche Applied Science, Penzberg, Germany) based on the method described previously by Feinberg and Vogelstein (16). A PCR product derived from DNA of the *tfdA*-containing strain *B. cepacia* DB01(pRO101) with the *tfdA*-intern primer set (Table 2) was used as a template.

Quantitative real-time PCR. After optimization of primers, quantitative real-time PCR was performed only with the *tfdA*** primer set as described above on the triplicate samples from days 0, 6, 12, 22, 33, 50, 68, and 115. All quantitative real-time PCRs were set up in triplicate and included three negative control samples in each PCR setup.

Standards for the quantitative PCR were prepared using the well-characterized phenoxy acid degrader *R. eutropha* JMP134. After inoculation into 0.5 g of the topsoil in amounts of 8×10^6, 8×10^5, 8×10^4, 8×10^3, 8×10^2, and 8×10^1 cells g^{-1} soil, the DNA was extracted from the soils as described above, and the extracts were diluted 10-fold to reduce the effect of humic acid disturbances. *R. eutropha* JMP134 was used as the positive control strain as well.

DGGE analysis. PCR for the DGGE analysis was performed as described above with the QuantiTect mastermix kit. The *tfdA*** primer set was used with a GC clamp attached to the 5′ end of the forward primer (Table 2). DGGE analyses were performed on real triplicates of DNA extracts from days 0, 6, 12, 33, and 68 in order to secure enough wells for one data series on one gel. The technique described previously by Muyzer et al. (42) was used for separating and visualizing the *tfdA* PCR products of the DNA extracts. The specific details of the method used are as follows. Gels contained 8% acrylamide and a urea-formamide gradient of 55 to 70% (where 100% denaturant contained 7 M urea and 40% formamide). Electrophoresis was carried out at 70 V for 17 h in 1× Tris-acetate-EDTA buffer using a D-code apparatus (Bio-Rad, Hercules, CA). After electrophoresis, the gels were stained with SYBR gold (Molecular Probes, Eugene, OR) for 45 min, followed by a brief rinse with MilliQ water, and then visualized under UV light and finally photographed. Bands that appeared to have a unique pattern for the soil scenarios were stabbed with sterile pipette tips, which were placed in 20 μl RNase/DNase-free water and rinsed repeatedly. These served as templates in further PCRs using the *tfdA*** primer set (Table 2) without the GC clamp to obtain enough DNA material for sequencing. The nucleotide sequencings were performed by MWG Biotech (Ebersberg, Germany).

Data analysis. The amounts of extracted MCPA were corrected for the extraction efficiency, after which linear regression analyses were performed on the steep segment of the degradation curves to fit it to zero-order kinetics with the following equation:

$$C_t = C_0 - k_0 t \quad (1)$$

where C_t and C_0 are the amounts of herbicide remaining (percentage of initial concentration) at time t and at time zero, respectively; t is the incubation period (days); and k_0 is the zero-order rate constant. The linear regressions were performed only for the steep segment of the degradation curve excluding sampling points from the lag phase and points where MCPA concentrations were below the detection limit.

For the results from the mineralization experiment, the calculated cumulative mineralization values were corrected for background radioactivity. After this, nonlinear regression analyses were performed as described previously by Mortensen and Jacobsen (41).

Nucleotide sequence accession numbers. The GenBank accession numbers for the DNA sequences reported in this study are DQ272405, DQ272406, DQ272407, DQ272408, DQ272409, DQ272410, DQ272411, DQ272412, DQ272413, DQ272414, DQ272415, and DQ272416 for A1, A2, A3, A4, A5, A6, A7, A8, A9, B1, B2, and B3, respectively.

RESULTS

MCPA degradation. The form of the curves for the disappearance of MCPA can be divided into three segments: first, a lag phase, where no or little degradation took place; second, a steep part with relatively fast degradation of MCPA (equation 1); and finally, the last segment, where almost all MCPA (>98%) had disappeared. The lag phases for Top_{20} and $Sub_{2.3}$ both had durations of 12 days, while in $Top_{2.3}$, no lag phase was observed. The steep part of the curve, where MCPA disappeared, shows a large degree of linearity. Therefore, this part was fitted to zero-order kinetics by means of linear regression (Fig. 2), and zero-order rate constants along with DT_{50} values were determined (Table 3). Degradation was fast and resulted in time to 50% degradation (DT_{50}) values of 16, 33, and 37 days for $Top_{2.3}$, Top_{20}, and $Sub_{2.3}$, respectively. However, MCPA could be detected in the soil for rather longer times, until days 33, 50, and 68 for $Top_{2.3}$, Top_{20}, and $Sub_{2.3}$, respectively. In addition to detection and quantification of MCPA, we also detected contents of the first degradation product, MCP. In $Top_{2.3}$ at days 0 to 22 and in Top_{20} at days 22 to 33, we found MCP in concentrations up to 5% of the initial MCPA concentration (data not shown). MCP was not detected in $Sub_{2.3}$ and was not detected after days 22 and 33 for $Top_{2.3}$ and Top_{20}, respectively.

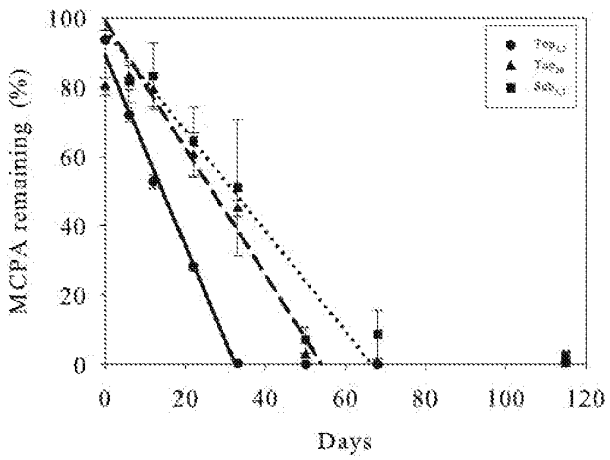


FIG. 2. Degradation of MCPA in the three soil scenarios measured by LC-MS/MS. Linear regression lines of the steep segments are shown. Solid line, $Top_{2.3}$; dashed line, Top_{20}; dotted line, $Sub_{2.3}$. Error bars indicate standard errors.

Mineralization studies. The mineralization curves showing accumulated amounts of $^{14}CO_2$ released from mineralization of ^{14}C-MCPA versus time were all sigmoid, and, like the degradation curves, they could be divided into three segments: a lag phase, a steep segment, and a plateau (Fig. 3A). The lag

TABLE 3. Parameter estimates from the zero-order kinetics model[a] of the steep part of the degradation curves and calculated DT_{50} values

Soil	MCPA (mg/kg)	R^2	k_0 (% × day^{-1})	DT_{50} (days)
Topsoil	2.3	0.990	−2.75	16.2
Topsoil	20	0.941	−1.83	33
Subsoil	2.3	0.711	−1.45	37

[a] See equation 1.

Downloaded from http://aem.asm.org/ on April 30, 2012 by guest

COR-AAD1-00002853
Bayer EX1008 (Part 5 of 9)

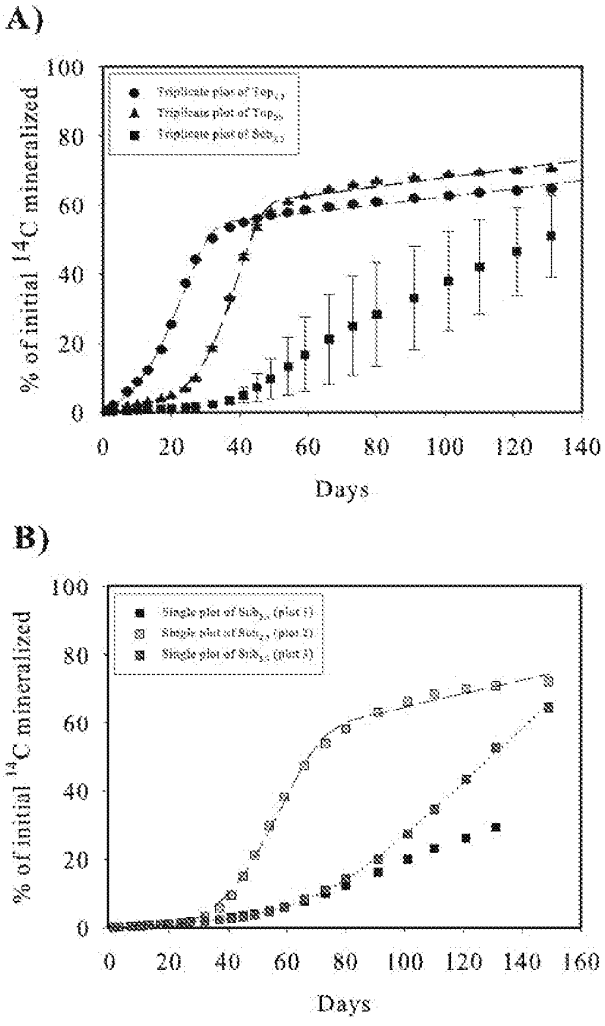


FIG. 3. Mineralization of ^{14}C-MCPA in the three soil scenarios. (A) Curves show triplicate cumulative data from $Top_{2.3}$, Top_{20}, and $Sub_{2.3}$. The dashed line shows a nonlinear fit to the exponential form of the 3/2-order model. Due to the large standard deviation, the plot of the triplicates for $Sub_{2.3}$ was not fitted. (B) Single plots of the $Sub_{2.3}$ replicates. The dotted line shows nonlinear fits to the linear form of 3/2-order model, and the dashed line shows a nonlinear fit to the exponential form of the 3/2-order model (plots 2 and 3). Plot 1 was not satisfactorily fitted to any model. Error bars in A indicate standard errors.

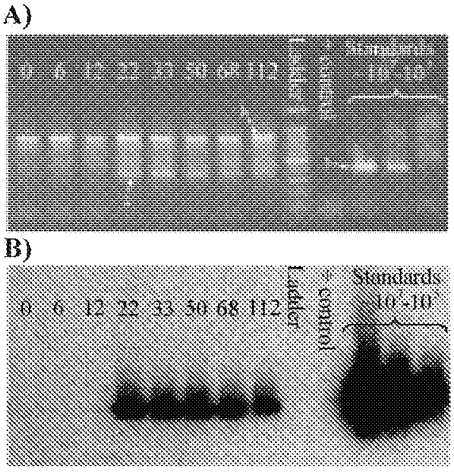


FIG. 4. Primer optimization. (A) Standard agarose gel electrophoresis of real-time PCR amplification products using the *tfdA*∗ primer; the iQ SYBR green supermix and soil DNA from days 0, 6, 12, 33, 50, 68, and 115 of Top_{20} were used as a template. The standard is *R. eutropha* JMP134 inoculated into the soil in concentrations of 8×10^6, 8×10^5, and 8×10^4 cells/g soil, with 8×10^6 cells/g soil shown to the left. Bands 1 and 2 represent the most characteristic bands, as described in the text. Band 3 represents the strain known to contain the *tfdA* gene *R. eutropha* JMP134. The ladder is a 100-bp DNA ladder. (B) Southern hybridization analysis of the agarose gel shown in A using a *tfdA* probe. Similarity can be detected for bands 2 and 3.

phase was significantly longer for Top_{20} and $Sub_{2.3}$ than for $Top_{2.3}$. Furthermore, the lag phase was longer for $Sub_{2.3}$ than for Top_{20}, a pattern similar to that observed in the degradation curves (Fig. 2). An F test ($P < 0.05$) showed that the mineralization curves for $Top_{2.3}$ and Top_{20} were best fitted to the exponential growth form of the 3/2-order model (7) indicating growth during the degradation. The plateau of the curves for $Top_{2.3}$ and Top_{20} occurred after approximately days 37 and 54, respectively, where 55% and 61% of the initially added ^{14}C had been mineralized. Furthermore, the F test and other model parameters (data not shown) showed that Top_{20} fitted better to the model than $Top_{2.3}$.

Due to large standard errors, the average mineralization curve of the triplicates for $Sub_{2.3}$ was not fitted to any kinetic model. The plot of the individual replicates (Fig. 3B) shows three different mineralization curves, only two of which (plots 2 and 3) had sigmoid forms and could be fitted as the topsoil experiments. According to the F test ($P < 0.05$) (48), plot 2 was best fitted to the exponential form of the 3/2-order model as for the topsoil scenario, while plot 3 was best fitted to the linear 3/2-order model (7), indicating no or slight growth. Plot 1 showed no sigmoid curvature and was therefore not fitted to any model.

Primer testing. To make the real-time PCR quantification technique as accurate as possible, the choice of primer set was critical. Therefore, a well-characterized primer set covering a broad range of known *tfdA* sequences was chosen (59). Unfortunately, we found that this primer set was likely to generate diverse bonds, indicating that the PCR product contained genes of more than one length (Fig. 4A). One band (band 2) had the same length, approximately 350 bp, as the positive control strain, *R. eutropha* JMP134 (band 3).

In comparison to the topsoil, the subsoil showed no clear pattern in the bands from the PCR product, even though there were several unspecific bands on the gel (data not shown). To determine which bands were related to the *tfdA* gene, a Southern blot assay was performed with the gels (Fig. 4B). This revealed that only bands 2 and 3 contained DNA that matched the *tfdA* probe designed from the *R. eutropha* JMP134 strain. Several optimization experiments, including increasing annealing temperature, were made to get rid of the unspecific amplification products. Among these, we tried to use another commercial real-time PCR master mix kit, which decreased the

Downloaded from http://aem.asm.org/ on April 30, 2012 by guest

COR-AAD1-00002854
Bayer EX1008 (Part 5 of 9)

unspecific bands (data not shown), but still not satisfactorily, which was expressed by a high detection limit and low R^2 values (<0.90) for the standard curve. Other optimization steps included concentration of $MgCl_2$ and concentration of the primers in the reaction mixture, but we still had no success (data not shown). Therefore, we designed a new set of primers, *tfdA*** (Table 2), which revealed PCR products with no unspecific bindings and a decrease in the cycle threshold values during real-time PCR. Lower cycle threshold values indicate a more specific and effective PCR. The detection limit in the real-time PCR assay for this primer was rather low (800 genes g^{-1} soil). Furthermore, the R^2 values for the standard curves were high (0.999 to 0.990).

Consequently, we used the *tfdA*** primer set for further quantitative real-time PCR assays. Primer testing of primer sets *tfdA*α** (51), *tfdA*α*** (24), and *cadA* (25) were performed as well (Table 2). Only *tfdA*α*** amplified a PCR product that may be possible to use for quantitative real-time PCR (data not shown).

Quantitative real-time PCR analysis. The quantitative real-time PCR analysis indicated that growth occurred in all three soil scenarios during the degradation period (Fig. 5). In $Top_{2.3}$, the *tfdA* concentration increased to a maximum of 3.0×10^4 genes g^{-1} soil at day 12 (Fig. 5A), while the maximum gene concentrations in Top_{20} and $Sub_{2.3}$ were 7.0×10^5 and 2.6×10^4 genes g^{-1} soil, obtained at days 22 to 33 and 50 to 68, respectively (Fig. 5B and C). The number of genes is based on the assumption that *R. eutropha* JMP134(pJP4) grown on rich media and used for real-time PCR standard curve preparation only contains one copy of the *tfdA* gene. The increase in the number of *tfdA* genes is inversely related to the concentration of MCPA in the three soils (Fig. 5A to C). Lag phases were clearly expressed and were shortest for $Top_{2.3}$ and Top_{20} and longest for $Sub_{2.3}$. It is interesting, however, that the increase in the number of *tfdA* genes occurred before the exponential mineralization phases did. It is also interesting that the maximum concentrations of the *tfdA* genes were reached while half of the MCPA remained and that a decrease in concentrations of *tfdA* genes was subsequently observed in the topsoils.

Functional diversity of *tfdA* genes. Two analyses of the functional diversity of the *tfdA* genes were performed, and both indicated a shift during the degradation period. First, an analysis of the melting profiles of the real-time PCR amplification products was performed. A shift in the temperature optimum of the melting profile was observed when the concentration of *tfdA* genes increased. This was observed as a melting optimum of 90°C at day 0 and a melting optimum of 87°C at day 22 (Fig. 6). Therefore, a DGGE analysis of PCR products using the GC-clamped *tfdA*** primer set (Table 2) was performed to obtain more detailed information about the shift in the degrader population with time. This analysis revealed several different bands, which grew up and grew stronger during the degradation experiment. In the $Top_{2.3}$ and Top_{20} analyses, the overall pattern was about the same, with at least five dominating bands (Fig. 7A and B). However, the variation of band intensity differed slightly between treatments. In $Top_{2.3}$, the bands grew up between days 6 and 12, while in Top_{20}, the bands were weak at day 12 and first became strong at day 33, corresponding to the longer lag phase in Top_{20}. For comparison, the melting optimum of the DNA amplified from the

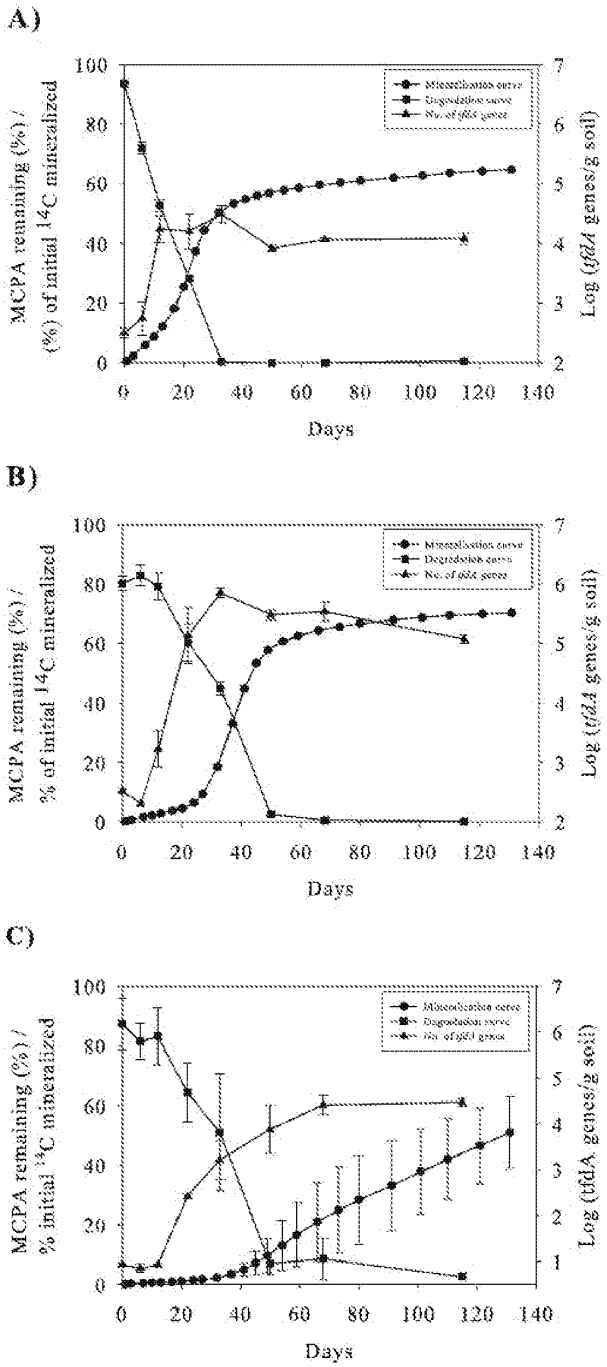


FIG. 5. Nonfitted mineralization and degradation curves compared with the log number of *tfdA* genes using the *tfdA*** primer set in the soil. (A) $Top_{2.3}$; (B) Top_{20}; (C) $Sub_{2.3}$. Error bars indicate standard errors.

standards containing *R. eutropha* strain JMP134 was 90°C. The same changes in melting profiles were observed for all degradation experiments. The melting profile for day 12 in Top_{20}, however, seemed to evolve a double top, which indicated a

Downloaded from http://aem.asm.org/ on April 30, 2012 by guest

COR-AAD1-00002855
Bayer EX1008 (Part 5 of 9)

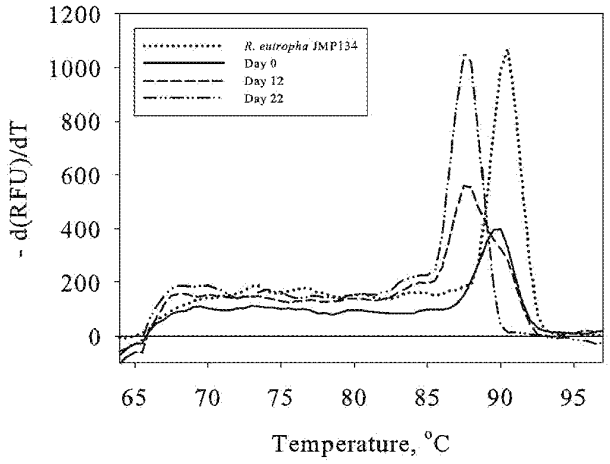


FIG. 6. Melting profiles of real-time PCR amplification products of soil DNA from days 0, 12, and 22 in Top_{20} using the *tfdA*-II primer set and the QuantiTect SYBR green PCR kit. Furthermore, the melting profile of the PCR amplification product from the *tfdA*-containing strain *R. eutropha* JMP134 is shown. The profile displays the negative first derivative of temperature versus relative fluorescence units (RFU) [−d(RFU)/dT] plotted against temperature.

beginning shift in the composition of the degrader population (Fig. 6 and see Fig. 8). Moreover, the intensities of the bands in $Top_{2.3}$ were strongest at day 12, after which the intensity declined throughout the experiment; however, this was not seen in Top_{20}.

The DGGE profiles of $Top_{2.3}$ and Top_{20} from days 0 to 6 and 0 to 12, respectively, were very similar to those of the DNA extracts from the topsoils without MCPA (Fig. 7D). A number of bands were visible on the gel containing the Top_0 DNA extracts, where some of them were common bands that were represented in all lanes throughout the experiment and where some of them were distinct bands represented in only single lanes. The overall pattern in Top_0 was that no change in the population containing the *tfdA* gene occurred over time and that the soil had a natural content of *tfdA* genes that denaturized in the same way as the *tfdA* gene from *R. eutropha* strain JMP134. Interestingly, the organisms represented by this band did not grow up during the experiments when MCPA was applied; however, the intensity of the band remained the same or had a slight decrease (Fig. 7A and B). The DGGE patterns from the subsoil were different from those from the topsoil. First, there were no bands in Sub_0 (Fig. 7E) or on days 0 to 33 for $Sub_{2.3}$ (Fig. 7C). Second, the intensity of the bands from $Sub_{2.3}$ at days 33 and 68 varied between the triplicates, especially for day 33. Furthermore, the intensity of the upper two bands, if any, was weak. Despite this, the other bands were present and had about the same intensity as those for $Top_{2.3}$ (Fig. 7A).

The sequences obtained from the bands stabbed from the DGGE gels were compared to existing sequences encoding α-ketoglutarate-dioxygenase obtained from GenBank, and a phylogenetic tree was constructed (data not shown). The phylogenetic analysis showed that bands A1 to A7, A10, and B1 to B3 (Fig. 7) were located in the same cluster as the class III *tfdA* genes showing 96 to 99% homology to the indigenous genes in this class (Fig. 8). Bands A8 and A9, on the other hand, were located in the same cluster as the class I *tfdA* genes showing 98 and 99% homology, respectively, to the *R. eutropha* JMP134 *tfdA* gene (Fig. 8). Furthermore, the GC content of bands A1 to A7, A10, and B1 to B3 was approximately 63%, while it was 69% for bands A8 and A9.

DISCUSSION

The carbon added in the form of the MCPA substrate should be sufficient to sustain the growth of approximately 10^7 new cells g^{-1} soil in Top_{20} and 1.2×10^6 cells g^{-1} in $Top_{2.3}$ and $Sub_{2.3}$. This is based on the assumption that one new cell requires approximately 1 pg of carbon to evolve (2). In further calculations, we assumed that one cell (JMP134 as well as naturally occurring bacterial populations) only contains a single *tfdA* gene. As the *tfdA* gene is plasmid borne, a single cell can possibly hold more than one *tfdA* gene; this latter assumption may be quite untenable (58). Furthermore, different cells may require different amounts of carbon to evolve, and different substrates may cause populations to grow differently as well (1, 2). When the uncertainties caused by the assumptions described above are taken into account, the maximum concentrations of 3.0×10^4, 7.0×10^5, and 2.6×10^4 genes g^{-1} soil observed in $Top_{2.3}$, Top_{20}, and $Sub_{2.3}$, respectively, correspond to less than 10% of the theoretical numbers. This may be explained in two ways. First, predation by protozoa and amoebae may be responsible for a large decrease of the cell number. This was indicated in a study reported previously by Thirup et al. (56), which showed that the number of culturable microorganisms first increased as a result of amendment with carbon substrate and subsequently decreased as a result of predation. A corresponding pattern was seen in the present study, where numbers of *tfdA* genes, especially in the topsoil experiments, decreased by 0.5 to 1 order of magnitude throughout the experiment after the maximum gene concentration was observed. Second, the primer set used may not have targeted the entire *tfdA* degrader population. Recently, Shaw and Burns (51) found that the canonical *tfdA* gene could not be detected using the *tfdA** primer set on DNA extracted from a 2,4-D degradation experiment for which the soil had not been preexposed to phenoxy acid herbicides but that the *tfdA*α-I primer set yielded a PCR product for the same soil. This indicates that the latter group of phenoxy acid degraders may be involved in the degradation of 2,4-D and probably also in the degradation of MCPA, especially in soils that are not frequently exposed to the herbicide. However, during the test of primers targeting the canonical *tfdA* gene, the *tfdA*α gene, and the *cadA* gene, we observed that PCR products were yielded with the canonical *tfdA* primer and with the *tfdA*α primer but not with the *cadA* primer set. This indicates that organisms that use the *tfdA*α gene product in MCPA metabolism may be present as well.

Growth among bacterial cells and increases in catabolic genes during degradation of phenoxy acids have been reported elsewhere previously (see, e.g., references 12, 28, and 36), but only Lee et al. (36) used a highly accurate quantitative real-time PCR method. They reported concentrations of 2.0×10^7 *tfdA* genes g^{-1} in activated sludge sequentially amended with 300 mg 2,4-D kg^{-1}. Concerning the higher amount of carbon substrate, this corresponds to what was found in the present

Downloaded from http://aem.asm.org/ on April 30, 2012 by guest

COR-AAD1-00002856
Bayer EX1008 (Part 5 of 9)

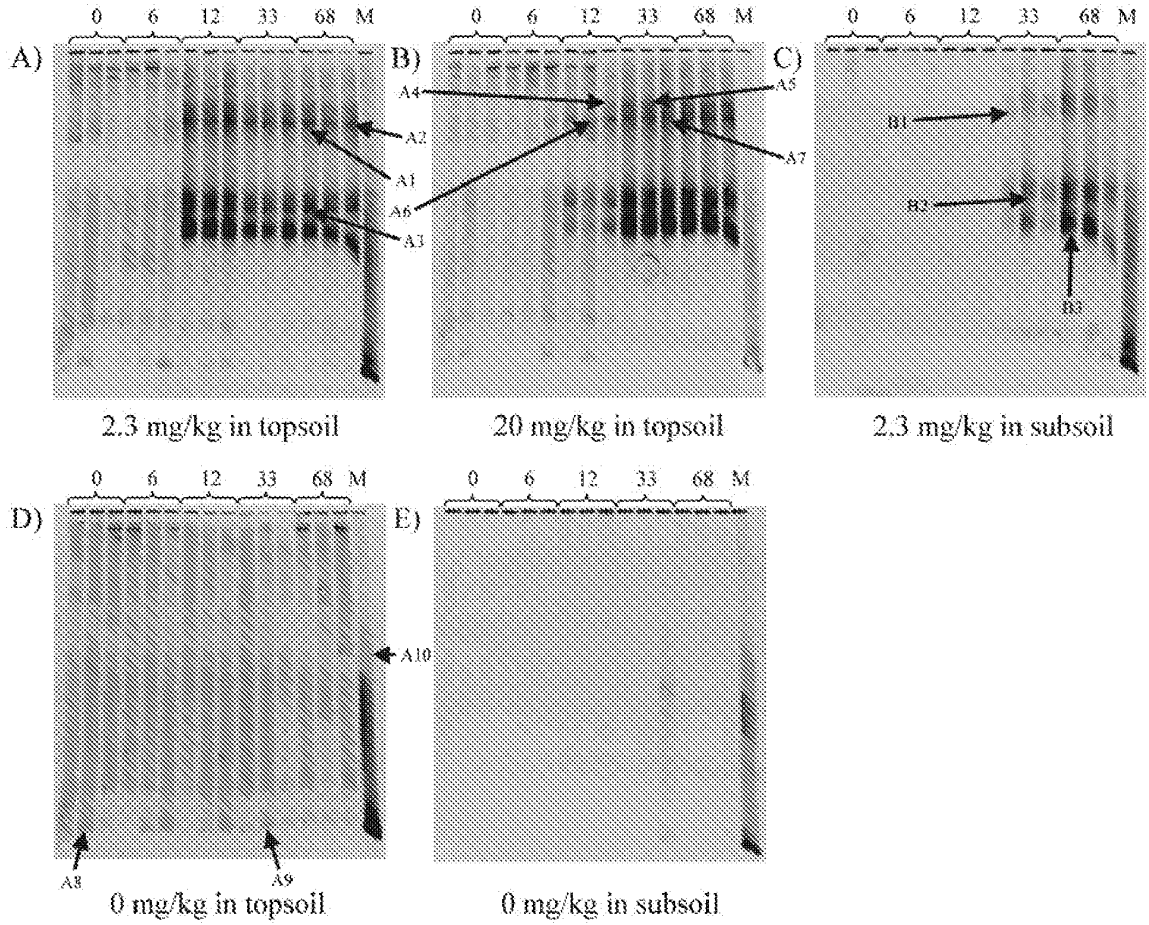


FIG. 7. Functional diversity of MCPA degrader genes using PCR/DGGE analysis with the *tfdA*** primer set. The gene product was separated using 55 to 70% urea gels. DNA extracts from days 0, 6, 12, 33, and 68 were analyzed in real triplicates. For the marker profile (M), DNA extracts from soil samples inoculated with the *tfdA*-containing strain *R. eutropha* JMP134 were used. A1 to A10 indicate bands selected for sequence analysis from topsoil DNA, and B1 to B3 indicate bands selected for sequence analysis from subsoil DNA. A shows the DGGE profile of DNA extracted from $Top_{2.3}$, B shows the DGGE profile of DNA extracted from Top_{20}, and C shows the DGGE profile of DNA extracted from $Sub_{2.3}$. D shows the DGGE profile of DNA extracted from Top_0, and E shows the DGGE profile of DNA extracted from Sub_0.

study. de Lipthay et al. (12), however, reported slightly lower increasing concentrations of the *tfdA* gene in water samples amended with approximately 20 mg 2,4-D $liter^{-1}$, as they observed maximum concentrations of ~10^5 genes ml^{-1}.

Analysis of the functional diversity of the indigenous MCPA degrader community by DGGE on the *tfdA* genes extracted has to our knowledge not previously been published. In this study, results from two different methods both indicated a change in the community of the bacteria containing the *tfdA* gene during a degradation period of 68 days. First, we saw a change in the maximum of the melting profiles of the PCR products from the quantitative PCR assay of the topsoil DNA from 90°C to 87.5°C. This indicates that the *tfdA* PCR products from the organisms grown on MCPA had a lower GC content and therefore were different from the genes present in the soil not exposed to MCPA. This corresponds with the results from the DGGE analyses in which the PCR products from the DNA sampled during the first days of the experiment had a tendency to denaturize at a higher denaturation grade. Interestingly, the maximum of the melting profiles from the first sampling days of the experiment were similar to that of the standard strain *R. eutrophus* JMP134. This was seen on the DGGE gels as well, where a major part of the DNA from the first sampling days seemed to denaturize in the lower part of the gels where DNA from the *R. eutropha* JMP134 also denaturized. The presence of *tfdA* genes in the control topsoil was interesting as well. The soil used for the experiments had not been exposed to phenoxy acid herbicides for at least 15 years; however, a background population of *tfdA* genes is maintained even in the absence of appropriate pesticide substrates. These *tfdA* genes did not increase in numbers during the degradation period, which indicates that they were placed in populations that did not grow actively.

Phylogenetic analyses of nucleotide sequences stabbed from bands on the gels revealed a large degree of homology to what was seen on the melting profiles and on the DGGE gels. All the sequences stabbed from the DGGE gels belonged to the first group of phenoxy acid-degrading organisms. The se-

Downloaded from http://aem.asm.org/ on April 30, 2012 by guest

COR-AAD1-00002857
Bayer EX1008 (Part 5 of 9)

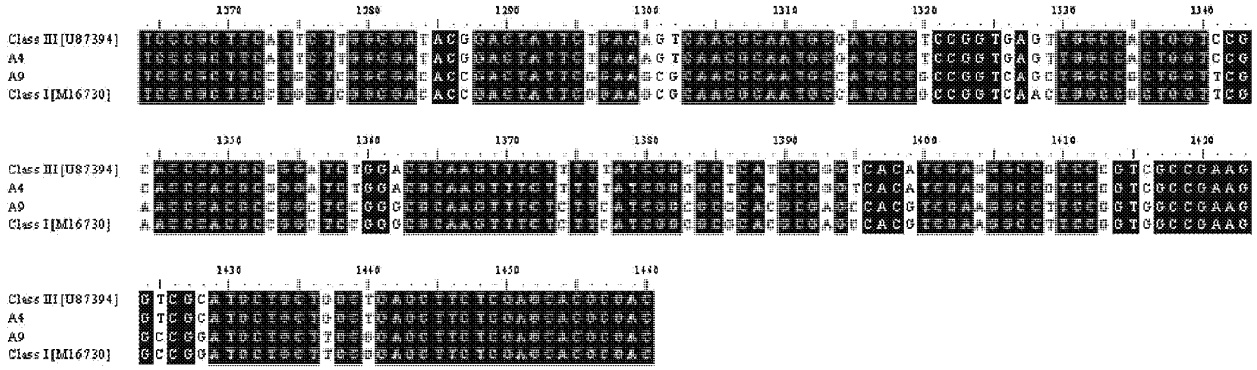


FIG. 8. Sequence alignment of the DNA obtained with the *tfdA*** primer set. The position number relates to GenBank accession number M16730 (*R. eutropha* JMP134). The class I *tfdA* gene sequence represented by *R. eutropha* JMP134 and the class III *tfdA* sequence represented by *Burkholderia cepacia* pIJB were both obtained from GenBank. A2 and A9 correspond to the sequences obtained at day 68 and day 0, respectively. These products were run on a DGGE gel and stabbed prior to sequencing as indicated in the legend of Fig. 7. A2 is highly homologous to bands A1, A3 to A7, A10, and B1 to B3, while A9 and A8 are homologous. Black shading shows highly conserved regions. Designations in brackets are GenBank database accession numbers.

quences stabbed from the bands located at the same denaturation grade as *R. eutropha* strain JMP134 were closely related to this strain and other class I strains as well. In contrast, the sequences stabbed from the bands that increased during the degradation period were related to the class III *tfdA* genes. In general, the role of those organisms containing class I *tfdA* genes in this particular soil remains unclear. A likely and quite interesting explanation may be that they are organisms that can only perform one or a few steps of the degradation pathway, while the class III *tfdA* gene-containing strains are capable of degrading the compound completely. If the class I gene-containing organisms are only capable of degrading the first step, for instance, it may not be likely to grow as a result of the degradation process. If the class III gene-containing bacteria, on the other hand, are capable of degrading MCPA completely, they may be able to grow as a result of the degradation process. This explanation is further supported by the fact that we actually were able to detect the degradation product MCP at days 0 to 22 of the degradation experiment in $Top_{2.3}$ and at days 22 and 33 in Top_{20}. Neither this compound nor the class I *tfdA* gene was found in $Sub_{2.3}$. Until now, the majority of the research on catabolic genes involved in phenoxyacetic acid degradation has been done with respect to 2,4-D, and in general, it has been accepted that organisms containing the class I *tfdA* gene were capable of degrading this particular compound completely. However, it may be suggested that minor differences in the metabolism between MCPA and 2,4-D have made the class I *tfdA* gene-containing bacteria in this particular soil incapable of degrading MCPA completely. Classes I to III were previously defined by Fulthorpe et al. (20) and Itoh et al. (24) based on homology and whether the *tfdA* gene is carried on a plasmid or not. The class III *tfdA* genes are 77% identical to the class I genes, whereas class II only consists of *Burkholderia* sp. strain RASC and a few strains that are 76% identical to the class I strains and 80% identical to the class III strains (24). As is the case for the strains containing the class I gene, the organisms containing the class III gene belong to a broad range of β- and γ-proteobacteria. Even though the diversity of the *tfdA* gene is not yet fully understood, the DGGE analysis indicated that up to five different *tfdA* genes were involved in the degradation of MCPA. However, no clear phylogenetic differences could be determined between those strains represented by the strong bands on the DGGE gels. This is probably due to comigration and other types of bias likely to be observed during DGGE analysis (43). Vallaeys et al. (60) reported that strains isolated from the same soil microcosm containing highly homologous *tfdA* genes were different based on their 16S rRNA genes. This may improve the hypothesis that several different species may contain the catabolic gene and be involved in the degradation and that the five bands sequenced from the DGGE gels represent *tfdA* genes from different strains of MCPA-degrading organisms.

The kinetics of mineralization and degradation observed in this study seem to be slightly slower, especially in the subsoil experiment, than what was reported previously by Caux et al. (8) and Mortensen and Jacobsen (41) but equal to what was reported previously by Helweg (23). This rather slow degradation/mineralization may be partly due to the high MCPA concentrations used, which, as seen in this study, results in a longer lag phase. As adaptation has been shown to increase the rate of mineralization (12), a more likely explanation may be the lack of exposure to MCPA during the last 15 years. Similar results were seen for the soil not previously exposed to phenoxy acid herbicides used by Helweg (23).

For the topsoils, the mineralization curve is shifted towards longer reaction times compared with the degradation curves, indicating metabolite formation during degradation. Even though the delay of mineralization compared to degradation was quite small, we detected the first degradation product, MCP, in $Top_{2.3}$ and Top_{20} but not in $Sub_{2.3}$. However, no proper accumulation of the metabolite was observed, as the compound was not detected after days 22 and 33 in $Top_{2.3}$ and Top_{20}, respectively. It was rather surprising that we did not detect the metabolite in the subsoil, as the delay of the mineralization was more pronounced for this scenario. It is possible that other metabolites evolve in the subsoil, as we only analyzed this particular compound. This indicates that the degradation of MCP may be rate limiting in topsoils. This is

Downloaded from http://aem.asm.org/ on April 30, 2012 by guest

COR-AAD1-00002858
Bayer EX1008 (Part 5 of 9)